Puay Hoon Tan
Aysegul A. Sahin

Atlas of Differential Diagnosis in Breast Pathology

Springer

Atlas of Anatomic Pathology

Series Editor

Liang Cheng
Indianapolis, Indiana
USA

This Atlas series is intended as a "first knowledge base" in the quest for diagnosis of usual and unusual diseases. Each atlas will offer the reader a quick reference guide for diagnosis and classification of a wide spectrum of benign, congenital, inflammatory, nonneoplastic, and neoplastic lesions in various organ systems. Normal and variations of "normal" histology will also be illustrated. Each atlas will focus on visual diagnostic criteria and differential diagnosis. It will be organized to provide quick access to images of lesions in specific organs or sites. Each atlas will adapt the well-known and widely accepted terminology, nomenclature, classification schemes, and staging algorithms. Each volume in this series will be authored by nationally and internationally recognized pathologists. Each volume will follow the same organizational structure. The first Section will include normal histology and normal variations. The second Section will cover congenital defects and malformations. The third Section will cover benign and inflammatory lesions. The fourth Section will cover benign tumors and benign mimickers of cancer. The last Section will cover malignant neoplasms. Special emphasis will be placed on normal histology, gross anatomy, and gross lesion appearances since these are generally lacking or inadequately illustrated in current textbooks. The detailed figure legends will concisely summarize the critical information and visual diagnostic criteria that the pathologist must recognize, understand, and accurately interpret to arrive at a correct diagnosis. This book series is intended chiefly for use by pathologists in training and practicing surgical pathologists in their daily practice. The atlas series will also be a useful resource for medical students, cytotechnologists, pathologist assistants, and other medical professionals with special interest in anatomic pathology. Trainees, students, and readers at all levels of expertise will learn, understand, and gain insights into the complexities of disease processes through this comprehensive resource. Macroscopic and histological images are aesthetically pleasing in many ways. This new series will serve as a virtual pathology museum for the edification of our readers.

More information about this series at http://www.springer.com/series/10144

Puay Hoon Tan • Aysegul A. Sahin

Atlas of Differential Diagnosis in Breast Pathology

Springer

Puay Hoon Tan
Division of Pathology
Singapore General Hospital
Singapore

Aysegul A. Sahin
The University of Texas
M. D. Anderson Cancer Center
Houston, TX
USA

Atlas of Anatomic Pathology
ISBN 978-1-4939-6695-0 ISBN 978-1-4939-6697-4 (eBook)
DOI 10.1007/978-1-4939-6697-4

Library of Congress Control Number: 2017937859

Printed on acid-free paper

This Springer imprint is published by Springer Nature
The registered company is Springer Science+Business Media LLC
The registered company address is: 233 Spring Street, New York, NY 10013, U.S.A.

To my family – Michael, Rebecca, Deborah, Daniel, and Jessica, with much love.

Puay Hoon Tan

To my husband, Toraman, and son, Onur, for their endless love and support, which have shown me what is important in life.

Aysegul Sahin

Series Preface

One Picture Is Worth Ten Thousand Words— Frederick Barnard, 1927

Remarkable progress has been made in anatomic and surgical pathology during the last 10 years. The ability of surgical pathologists to reach a definite diagnosis is now enhanced by immunohistochemical and molecular techniques. Many new clinically important histopathologic entities and variants have been described using these techniques. Established diagnostic entities are more fully defined for virtually every organ system. The emergence of personalized medicine has also created a paradigm shift in surgical pathology. Both promptness and precision are required of modern pathologists. Newer diagnostic tests in anatomic pathology, however, cannot benefit the patient unless the pathologist recognizes the lesion and requests the necessary special studies. An up-to-date Atlas encompassing the full spectrum of benign and malignant lesions, their variants, and evidence-based diagnostic criteria for each organ system is needed. This Atlas is not intended as a comprehensive source of detailed clinical information concerning the entities shown. Clinical and therapeutic guidelines are served admirably by a large number of excellent textbooks. This Atlas, however, is intended as a "first knowledge base" in the quest for definitive and efficient diagnosis of both usual and unusual diseases.

The *Atlas of Anatomic Pathology* is presented to the reader as a quick reference guide for diagnosis and classification of benign, congenital, inflammatory, nonneoplastic, and neoplastic lesions organized by organ systems. Normal and variations of "normal" histology are illustrated for each organ. The Atlas focuses on visual diagnostic criteria and differential diagnosis. The organization is intended to provide quick access to images and confirmatory tests for each specific organ or site. The Atlas adopts the well-known and widely accepted terminology, nomenclature, classification schemes, and staging algorithms.

This book Series is intended chiefly for use by pathologists in training and practicing surgical pathologists in their daily practice. It is also a useful resource for medical students, cytotechnologists, pathologist assistants, and other medical professionals with special interest in anatomic pathology. We hope that our trainees, students, and readers at all levels of expertise will learn, understand, and gain insight into the pathophysiology of disease processes through this comprehensive resource. Macroscopic and histological images are aesthetically pleasing in many ways. We hope that the new Series will serve as a virtual pathology museum for the edification of our readers.

Indianapolis, IN, USA — Liang Cheng, MD

Preface

Breast pathology is key to the diagnosis and management of breast diseases. Interpretation of breast histologic findings constitutes a significant proportion of the daily workload of the surgical pathologist. This task can be challenging and demanding because diagnostic categorization is used to select treatment from a potentially diverse range of options, and the diagnosis of borderline and malignant lesions raises patient anxieties.

In this atlas, we use our collective experience in diagnostic breast pathology to present a pictorial narrative of a wide range of breast conditions that are grouped together along broad themes and histologic patterns, focusing on differential diagnoses and their illustrations. Important morphologic similarities and differences are compared and contrasted through a series of representative photomicrographs, with adjunctive immunohistochemistry used to offer additional support for specific diagnoses. Where relevant, molecular alterations that are characteristic of certain breast lesions are described.

There are many excellent breast pathology textbooks available today that offer encyclopaedic information on a comprehensive list of breast conditions. Our aim in writing this atlas is not to replace or compete with these available textbooks, but to provide a quick visual reference for the practicing surgical pathologist during evaluation of breast lesions. Concise text and explanatory legends accompany the illustrations, many of which are photomicrographs of conditions that could potentially be mistaken for the entity being described; these are arranged together to highlight their differences. Microscopic nuances that help weigh towards certain diagnoses are articulated. Because this is intended to be a working atlas, the list of entities is not exhaustive, including only those that form part of the differential diagnostic spectrum. Some lesions appear in different chapters, illustrating their morphologic heterogeneity.

We hope that this atlas will be a useful microscope tableside companion for the busy surgical pathologist, who could pick it up and have a quick and convenient pictorial guide to differential diagnoses of challenging breast lesions. Pathologists are by nature visual beings, and we trust that the illustrations in this atlas will be enjoyed, much as we delighted in putting them together.

Singapore, Singapore — Puay Hoon Tan
Houston, TX, USA — Aysegul A. Sahin

Acknowledgments

We thank Dr Stuart J Schnitt, Vice Chair for Anatomic Pathology, Beth Israel Deaconess Medical Center, Professor of Pathology, Harvard Medical School, Boston, Massachusetts, for the helpful comments on the contents of this atlas.

We also thank Dr Lester Chee Hao Leong, Senior Consultant, Department of Diagnostic Radiology, Singapore General Hospital, Singapore, for providing the radiological input for the imaging sections.

We are indebted to our colleagues in the breast pathology teams of the Department of Anatomical Pathology, Singapore General Hospital, Singapore, and the MD Anderson Cancer Center, Houston, Texas, for the camaraderie and generous sharing of interesting and challenging breast pathology cases which have contributed to the wealth of material that form, and continue to add to, a great educational resource in breast pathology.

Contents

Normal Breast and Physiological Changes

1

The breast is a modified sweat gland located in the superficial fascia of the anterior chest wall. The mature female breast has a distinctive protuberant, mound-shaped, or conical form and covers the area from the second or third rib to the sixth or seventh rib (Fig. 1.1). The nipple projects from the anterior surface and consists mainly of dense fibrous tissue covered by hyperpigmented skin and contains bundles of smooth muscle fibres. The skin immediately surrounding the nipple, called the areola, is also more pigmented than the rest of the breast skin. The areola contains sebaceous glands and numerous sensory nerve endings but lacks pilosebaceous units and hair (Figs. 1.2 and 1.3).

The breast is made up of glandular and ductal elements embedded within fibrofatty tissue with a ratio of glandular to fibrofatty tissue that varies among individuals (Fig. 1.4) [1]. In addition, with the onset of menopause and decreased oestrogen levels, the relative amount of fatty tissue increases as the glandular tissue diminishes. The breast ductal system consists of 15–20 branching ducts, which radiate from the nipple to continue to the functional units of the breast, the terminal ductal lobular units (TDLUs) (Fig. 1.5). The TDLUs consist of the intralobular ducts and round saccules called ductules, which differentiate into the secretory units or acini during pregnancy and lactation. The terms ductules and acini are often used interchangeably. Individual TDLUs vary greatly in size and typically enlarge to become functional during lactation (Fig. 1.6). The TDLUs are embedded in specialised, hormonally responsive connective tissue stroma called intralobular stroma (Fig. 1.7) [2–8]. The largest amount of breast parenchyma is located in the upper outer quadrant, where the majority of cancers develop. An axillary tail of breast tissue often extends into the axilla. Before puberty, female and male breasts have the same appearance. The structure of the breast is under the influence of hormones, growth, and differentiation factors. When puberty begins in females, mammary ducts branch out, terminal duct buds are formed, and the stromal component (mainly adipose tissue) of the breast proliferates. Both stroma and epithelium undergo changes during the menstrual cycle, pregnancy, lactation, and menopause. During male puberty, breast development is limited to rudimentary large duct development without breast enlargement.

The mammary epithelium is ectodermally derived. Small segments of lactiferous duct orifices at the nipple are lined by

Fig. 1.1 Normal adult female breast. Photograph of a normal female prior to undergoing prophylactic mastectomy

P.H. Tan, A.A. Sahin, *Atlas of Differential Diagnosis in Breast Pathology*, Atlas of Anatomic Pathology,
DOI 10.1007/978-1-4939-6697-4_1

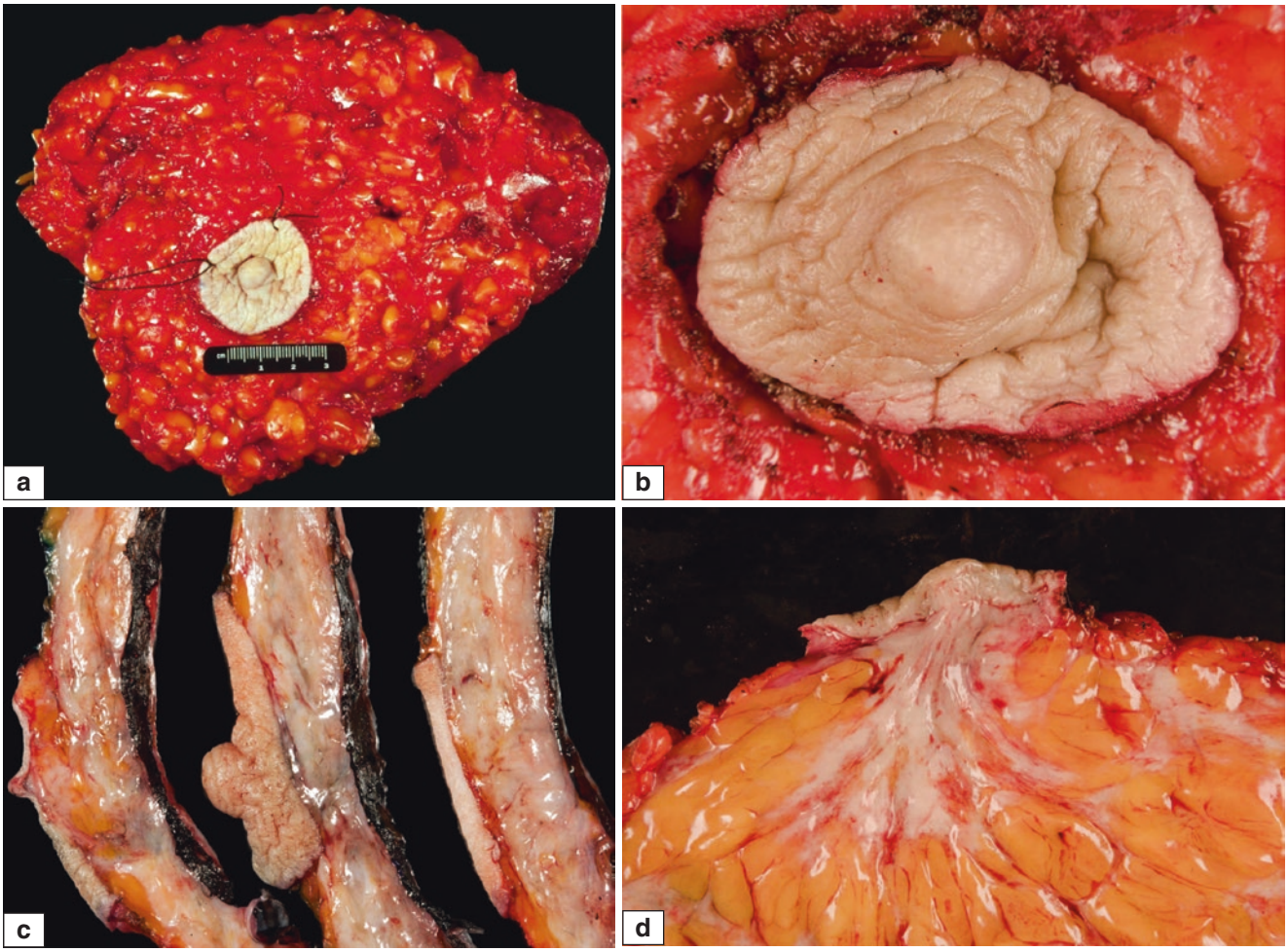

Fig. 1.2 Normal adult female breast. Gross features. (**a**) Skin-sparing total mastectomy specimen showing full extension of breast tissue with the nipple located in the normal central position. (**b**) Higher magnification of the nipple-areolar complex. (**c**) Cut section through the nipple shows dense subareolar fibrous connective tissue. (**d**) Higher magnification of (**c**) showing subareolar fibrous tissue radiating into the fatty breast parenchyma

Fig. 1.3 Normal adult female breast. Gross features. Cut sections of breast mastectomy specimen. The ratio of fat to fibrous tissue is variable and correlates with mammographic density

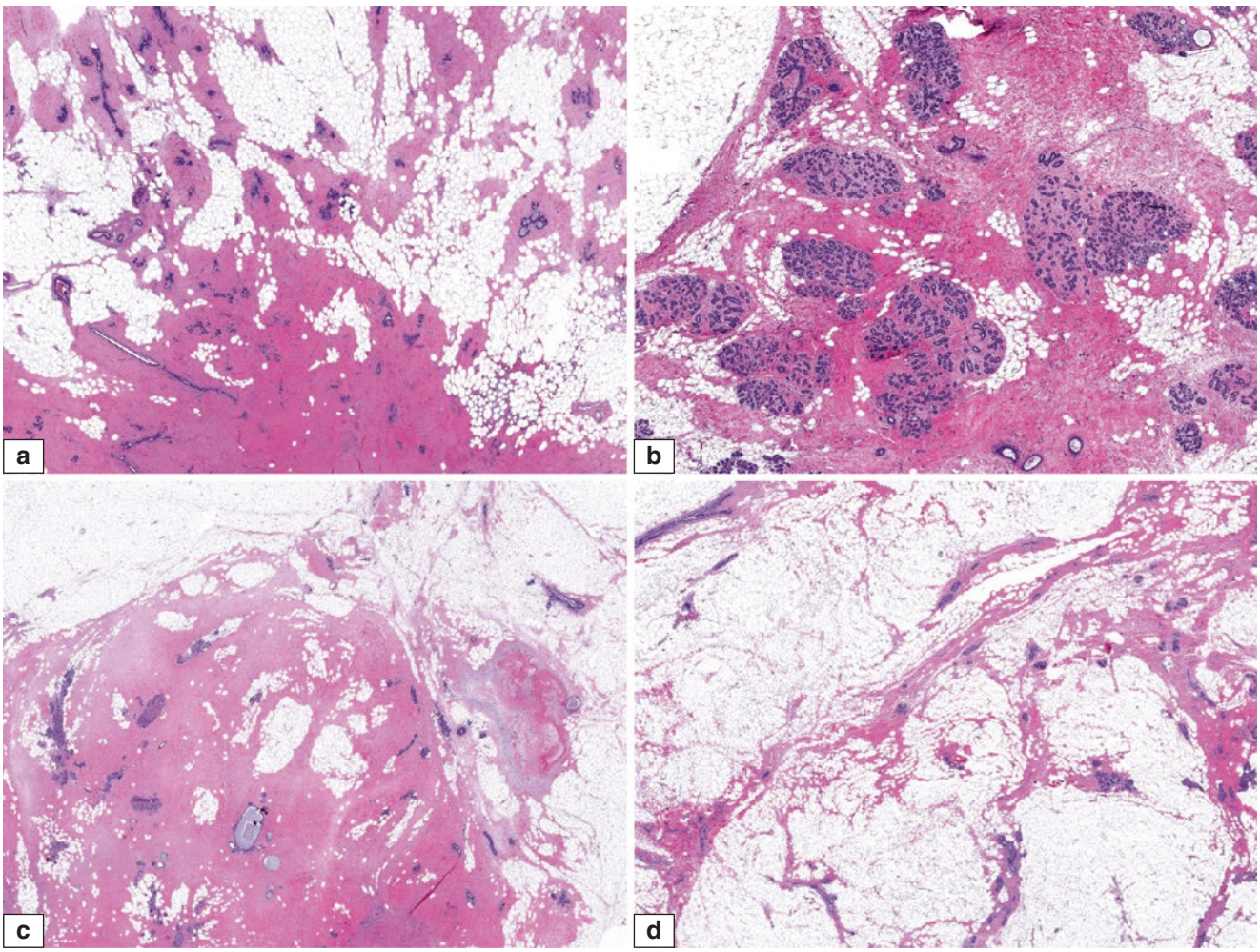

Fig. 1.4 Normal adult female breast. Histologic features. (**a–d**) H&E sections showing varying ratios of fat to fibrous tissue in stroma and various amounts of glandular elements from different cases

squamous epithelium, while the rest of the breast ductal system is lined by two cell layers, inner luminal cells and outer myoepithelial cells, surrounded by the basement membrane (Fig. 1.8). Extension of squamous epithelium beyond lactiferous duct orifices represents squamous metaplasia. The luminal cells are usually low columnar to cuboidal, and myoepthelial cells are located between luminal cells and the basement membrane. The myoepithelial cells are often ovoid to spindle shaped and have scant cytoplasm. The mammary ducts and lobules are embedded in fibrofatty stroma. Interlobular stroma contains adipose tissue, fibroblasts and elastic fibres. Scant inflammatory cells, including lymphocytes, plasma cells, mast cells, and histiocytes, are commonly seen. Rarely, stromal cells show prominent myoid differentiation (Fig. 1.9). The intralobular stroma is usually loose and more cellular than the interlobular stroma, and unlike the interlobular stroma, it usually does not have adipose tissue. Intralobular stroma is hormone sensitive and shows cyclic histologic changes.

Physiological Changes

Menstrual Cyclic Changes

Both stromal and glandular components of the breast undergo histologic changes during the menstrual cycle. However, these changes are not distinct and specific, unlike changes observed in endometrial epithelium during the menstrual cycle [6–8]. In general, during the proliferative phase (days 3–7), the stroma is dense and hypovascular. Crowded and poorly oriented ductal epithelial cells line the acini, and mitoses are easily found, while myoepithelial cells are inconspicuous. Acinar lumens are closed and no secretion is found. In the follicular phase (days 8–14), epithelial cells become columnar, mitotic activity decreases, acinar lumens form but no secretion is evident, and myoepithelial cells become easily identifiable at the periphery of acini. During the secretory phase (days 15–27), myoepithelial cells become

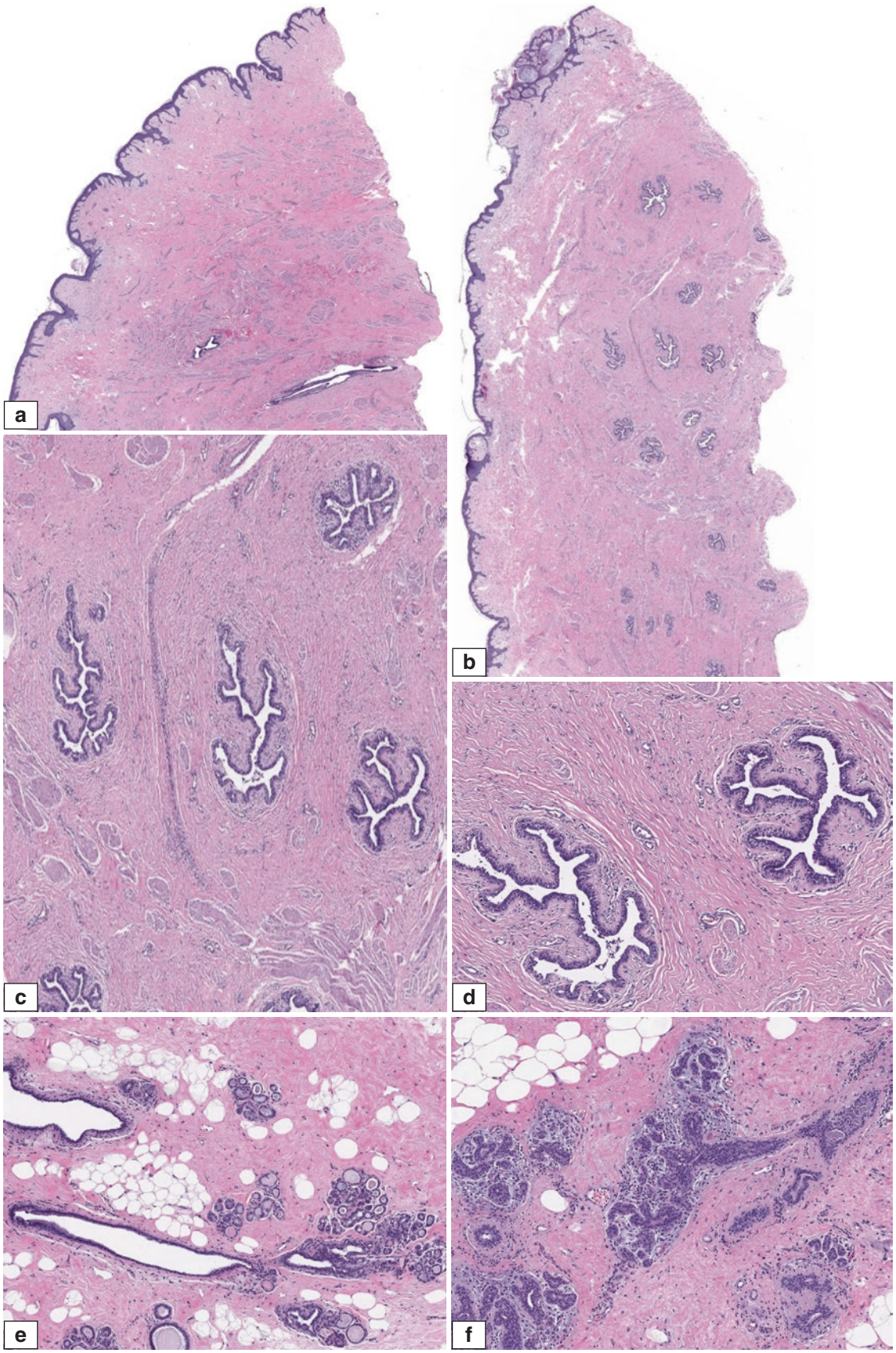

Fig. 1.5 Normal adult female breast. Histologic features. (**a–d**) H&E sections of the nipple-areolar complex showing nipple or lactiferous ducts extending from the skin surface into the breast parenchyma. The lactiferous ducts show a branching shape and are lined by bilayered epithelium (luminal epithelial and outer myoepithelial cells). There may be stromal folds protruding into the ductal lumens which should not be mistaken for a papillary lesion. Smooth muscle bundles are seen among the lactiferous ducts. (**e**, **f**) Terminal ductal lobular unit, which is the functional unit of breast parenchyma, consists of a feeding duct with branching acini embedded in connective tissue

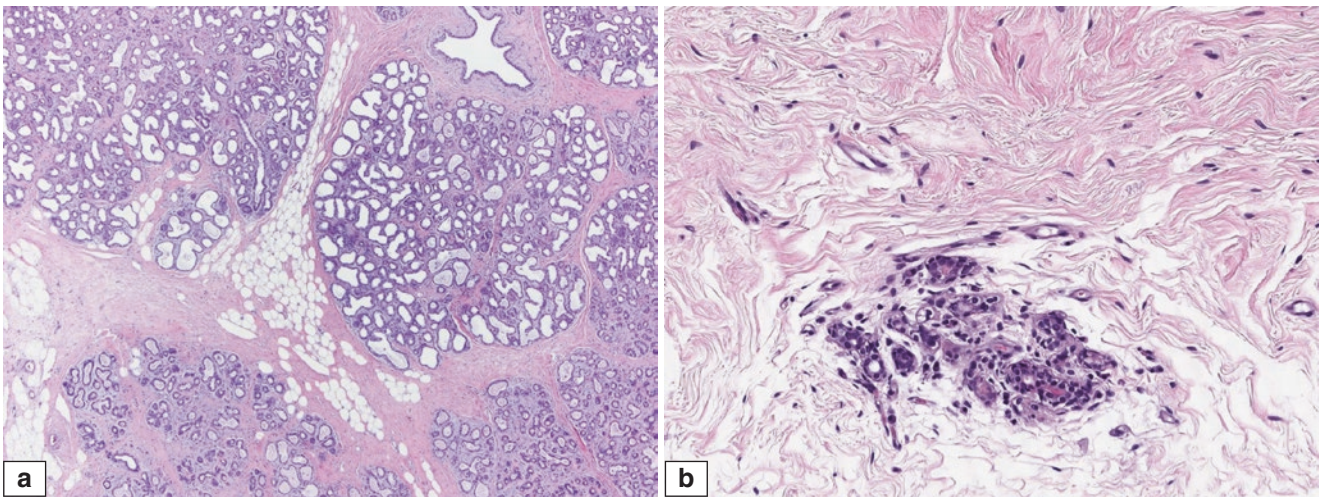

Fig. 1.6 Normal adult female breast with physiological changes. Histologic features. (**a**) Expanded terminal ductal lobular unit of a lactating breast comprises an increased number of acini with luminal secretions. (**b**) Atrophic terminal ductal lobular unit of a postmenopausal female

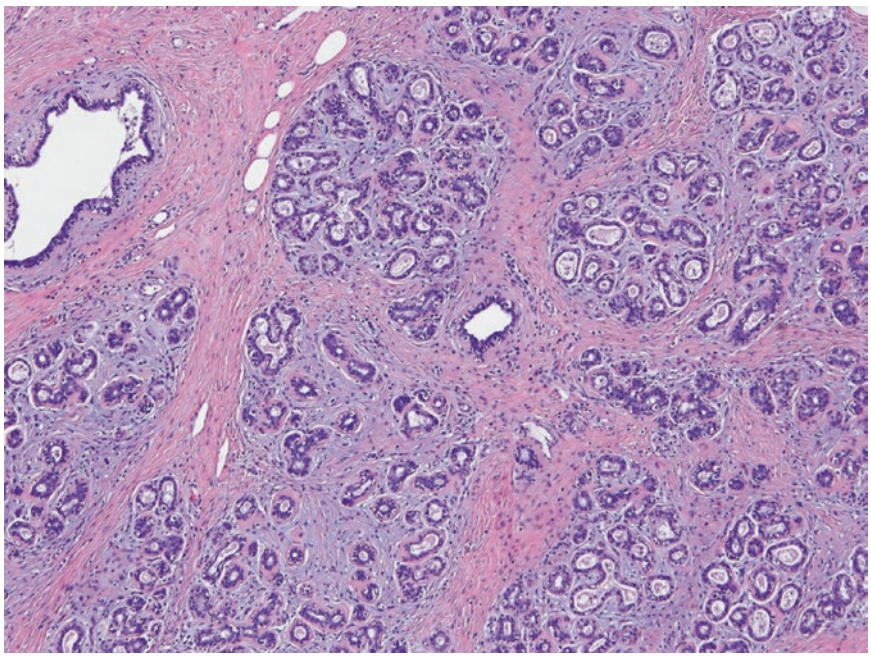

Fig. 1.7 Normal adult female breast. Histologic features. Intralobular stroma shows a loose myxoid appearance, with less collagenisation compared to interlobular fibrous tissue

more prominent with their clear cytoplasm, lumens are open and contain variable amounts of secretions, and the stroma becomes loose and oedematous. The late secretory and early menstrual phase (days 28–2) is characterised by regression of lobules with the stroma becoming compact and may contain inflammatory cells (Fig. 1.10) [9–11].

Pregnancy- and Lactation-Related Changes

As a consequence of hormonal changes, the breast tissue becomes fully mature and functional during pregnancy and lactation. During pregnancy, terminal ducts and lobular acini grow progressively, resulting in lobular enlargement, whereas stromal components decrease (Figs. 1.11 and 1.12). The cytoplasm of acinar cells becomes vacuolated and secretions accumulate in the lumens. During lactation, lobular acinar lumens become distended with abundant secretions. The lobular acinar epithelium contains numerous lipid vacuoles and has a characteristic "hobnail" appearance (Fig. 1.13). The myoepithelial cells become inconspicuous.

Lobular regression happens when lactation ceases. The lobular epithelium becomes flat, interlobular stroma increases and may contain lymphocytes and plasma cells.

The process takes several months to complete and occurs in a heterogeneous fashion. While some lobules show complete involution, others may still show lactational changes for several months and even a year after cessation of lactation.

Menopause-Related Changes

With the onset of menopause, the number and cellularity of lobules decrease (Fig. 1.14). In older women, only ducts may remain. Atrophic acini may become cystic and calcifications are commonly found in these cystic acini. Intralobular stroma becomes fibrocollagenous and generalised fatty replacement of stroma occurs progressively. Postmenopausal hormone replacement therapy stimulates breast epithelium and may increase breast density.

Calcifications

Deposition of calcium salts in breast tissue is called calcifications in the breast. Based on the mammographic appearance of calcifications, they can be categorised into three groups: (1) those typically associated with benign lesions, (2) those that are most likely associated with malignant lesions, and (3) indeterminate ones (Fig. 1.15) [12, 13]. Calcifications associated with benign lesions include eggshell, large, coarse, and rod-like calcifications. In addition, skin and vascular calcifications can be identified as benign on mammograms. There is a high probability that pleomorphic, heterogeneous, linear, or branching (casting) calcifications will be associated with malignant lesions. Amorphous and indistinct calcifications are classified as indeterminate. Calcifications in the breast are also categorised based on their distribution. Grouped or clustered calcifications are small areas of calcifications which are common in many benign proliferations, but are also associated with a moderately increased likelihood of malignancy [14–16]. Diffuse scattered calcifications are randomly distributed in breast parenchyma and are almost always associated with benign lesions or normal breast parenchyma. Segmental calcifications are distributed in a duct and their branches and are frequently associated with intraductal epithelial proliferations. In situ carcinomas associated with comedonecrosis are frequently associated with "castlike" microcalcifications [17–20]. If there is a mass associated with microcalcifications, the imaging appearance of the mass is very important

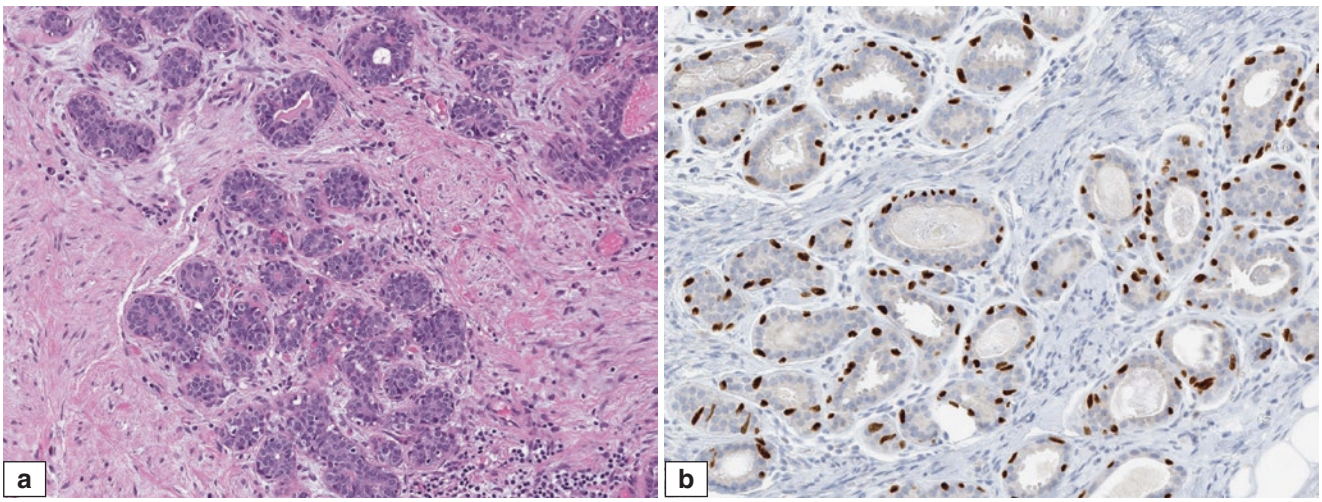

Fig. 1.8 Normal adult female breast. Histologic and immunohistochemical features. (**a**) A lobule composed of multiple acini. The luminal epithelial cells are surrounded by myoepithelial cells, some of which have clear cytoplasm. (**b**) Immunohistochemical staining for p63 highlights myoepithelial cell nuclei

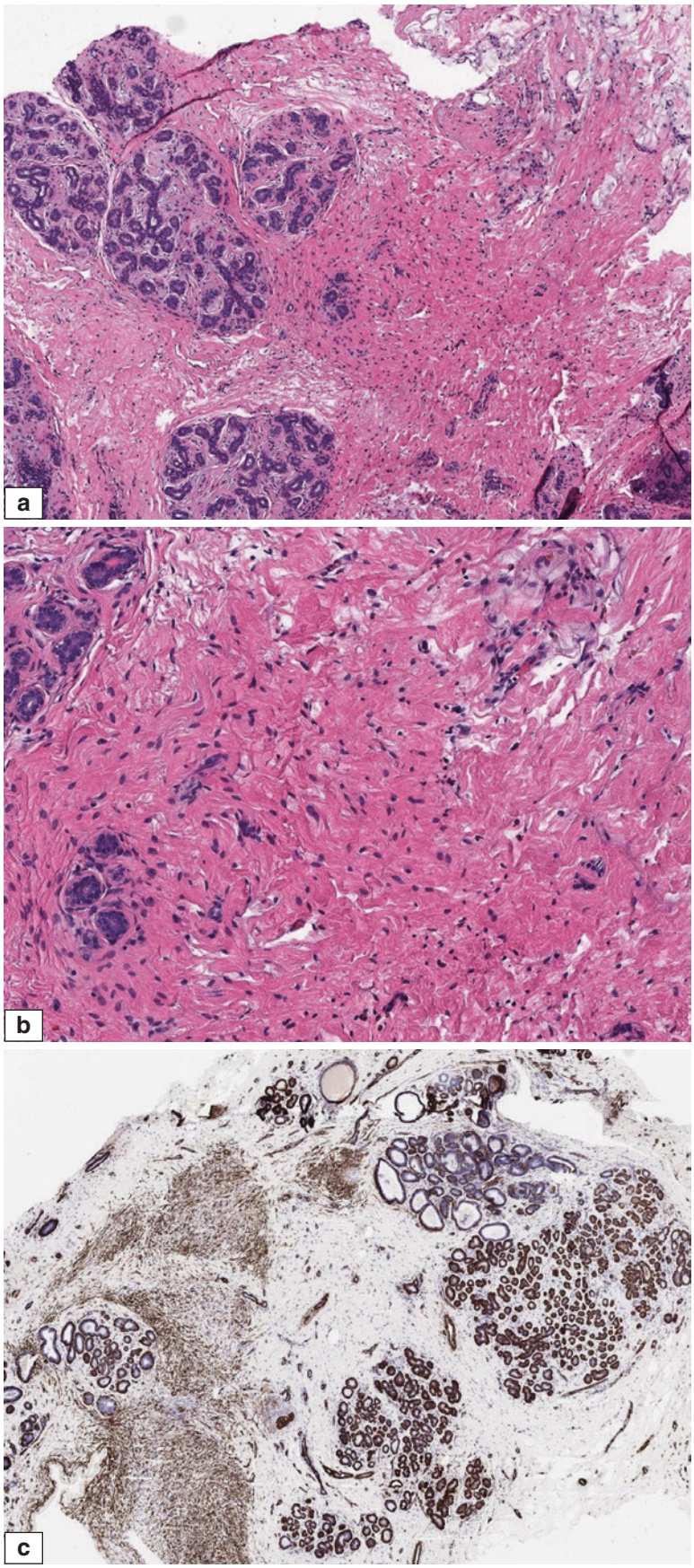

Fig. 1.9 Normal adult female. (**a**, **b**) Stroma shows myoid cells in addition to fibroblasts. (**c**) Spindle cells with myoid differentiation show immunoreactivity for smooth muscle myosin

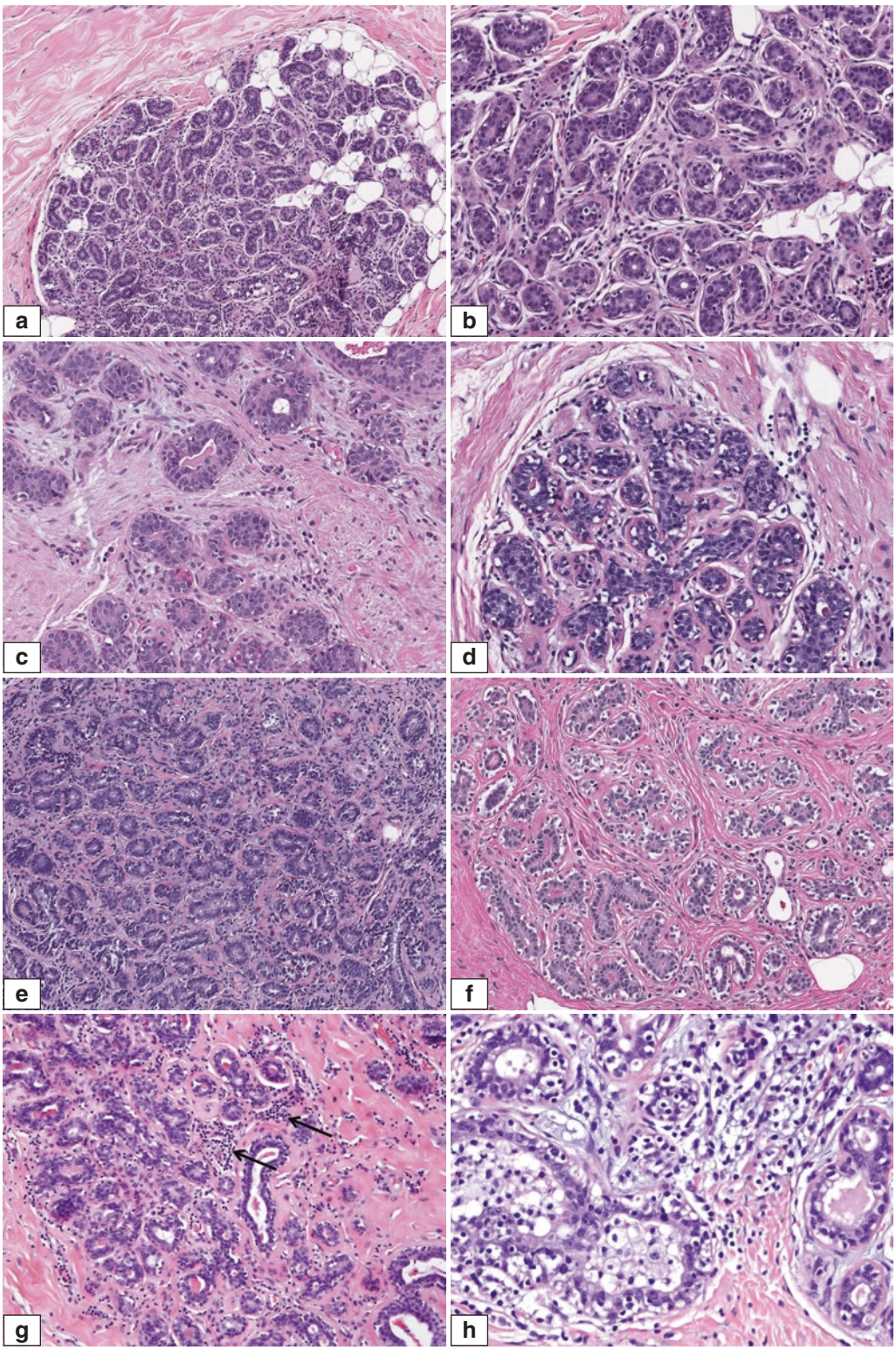

Fig. 1.10 Normal adult female breast. Histologic features of menstrual cycle phases. (**a**) Proliferative phase: H&E section shows lobular unit composed of tightly packed acini. (**b**) Acini are lined by crowded, poorly oriented cells with little or no lumen formation. No secretion is evident. The intralobular stroma is dense and cellular. (**c**) Follicular phase: H&E shows cells lining the acini becoming columnar with central lumens that are apparent. (**d**) Lumens have minimal secretions. (**e**) Secretory phase: Acini have open lumens which contain secretions. (**f**) The lobular stroma is loose. Both epithelial and myoepithelial cells are distinct. (**g**) Closing of the cycle: Small acini associated with dense stroma which contains inflammatory cells (*arrows*). (**h**) Higher magnification shows distinct clear-cell appearances of peripheral myoepithelial cells

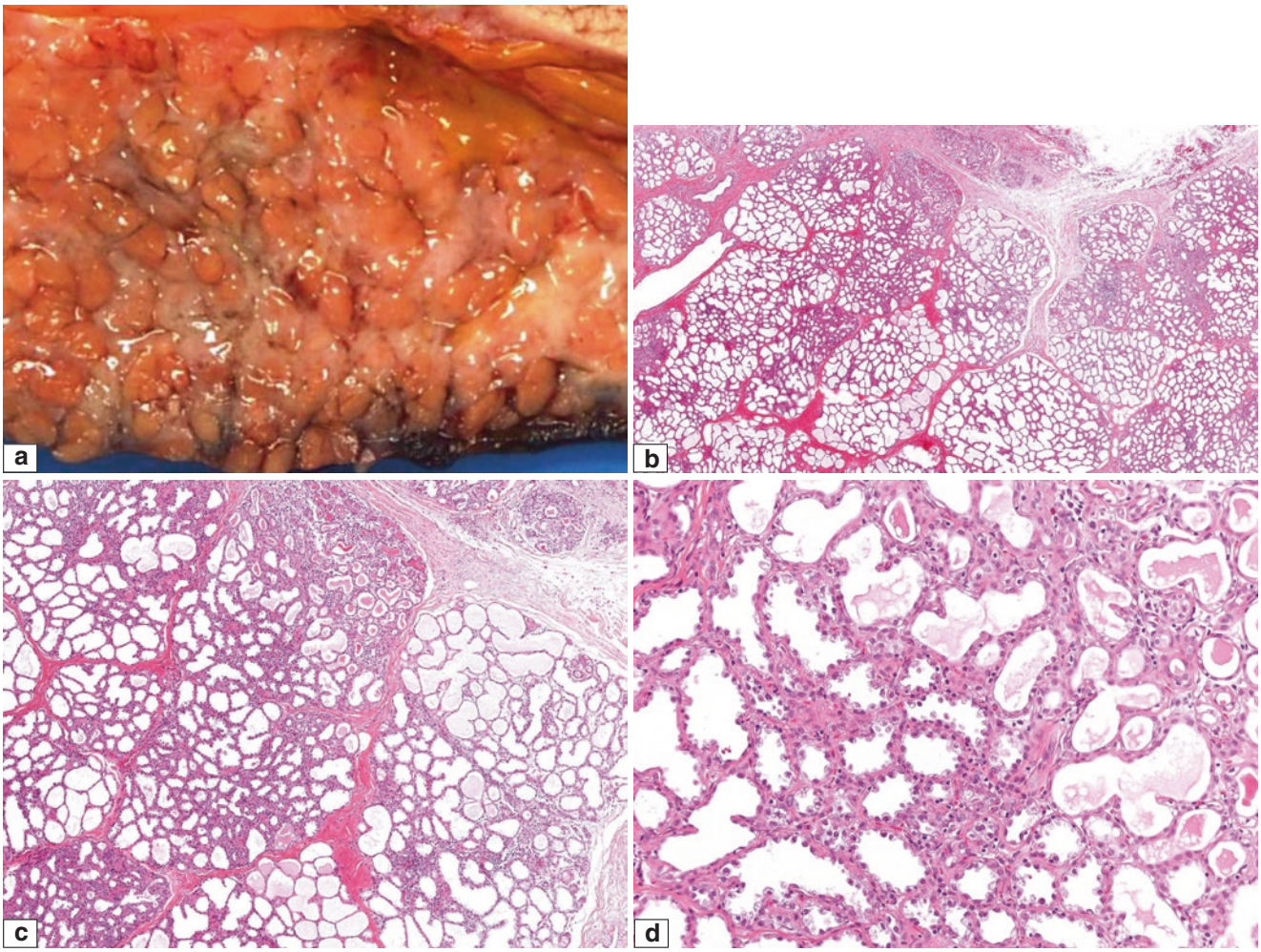

Fig. 1.11 Pregnant adult female breast. Gross and histologic features. (**a**) Breast parenchyma showing distinct tan-brown nodularities corresponding to enlarged lobular units. (**b**, **c**) H&E sections showing enlarged lobules with distended acini replacing the majority of the breast parenchyma. Marked acinar dilatation is evident. (**d**) Higher magnification shows cells lining the acini to have abundant vacuolated cytoplasm. Nuclei are small and round

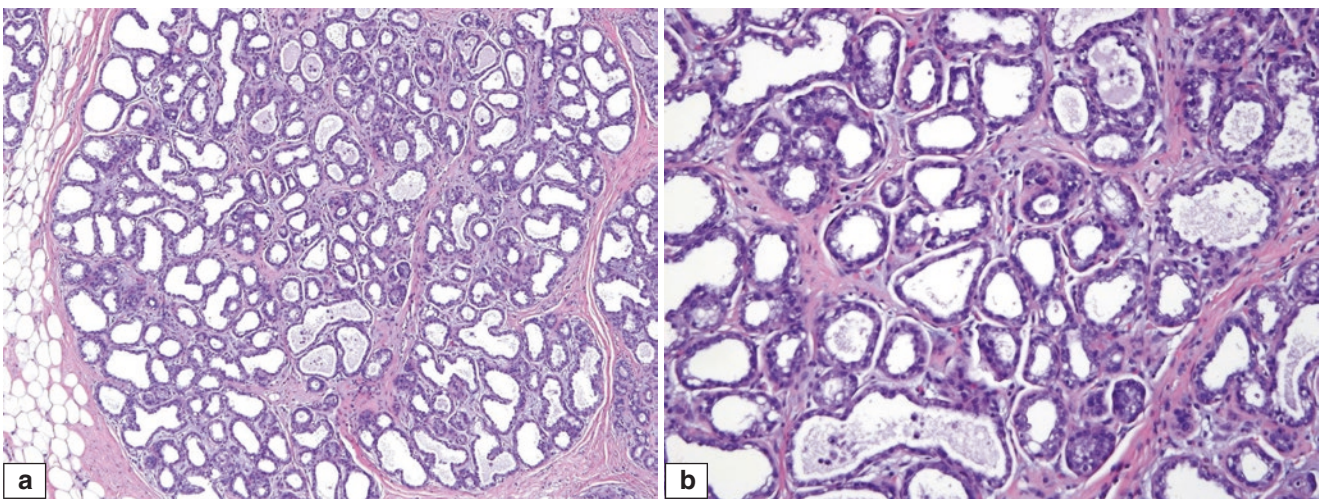

Fig. 1.12 Lactating adult female breast. Histologic features. (**a**, **b**) H&E sections show markedly enlarged lobular unit composed of distended acini with open lumens surrounded by minimal fibromyxoid stroma. The lining epithelial cells have prominent cytoplasmic vacuoles and occasional cytoplasmic snouts

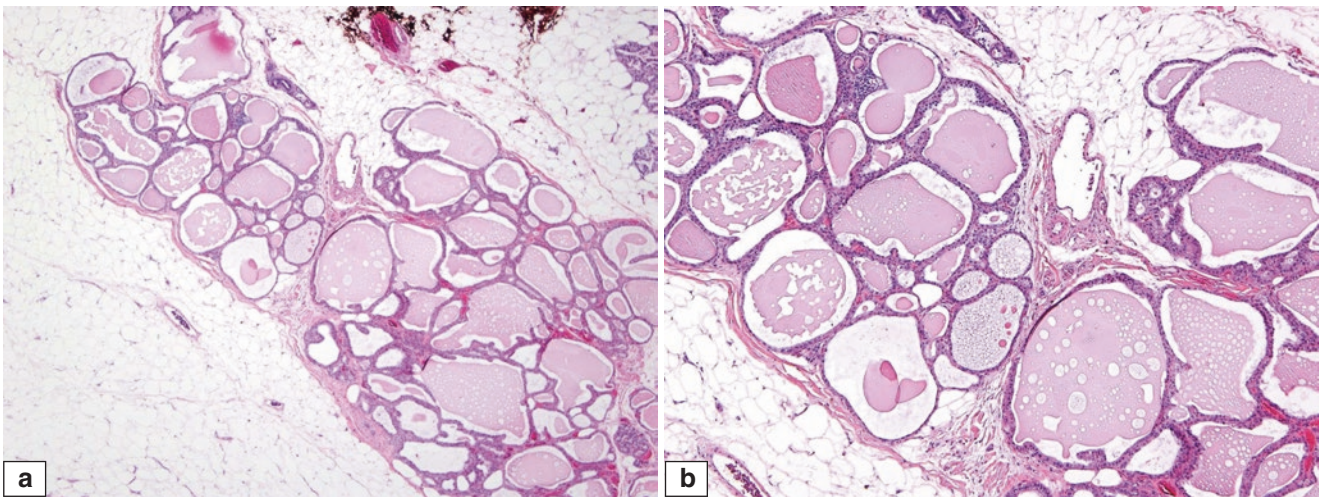

Fig. 1.13 Lactating adult female breast. Histologic features. (**a**, **b**) H&E sections show enlarged lobular units with acini distended by pink secretions. Acini appear to be lined by a single layer of cells, with inconspicuous myoepithelial cells

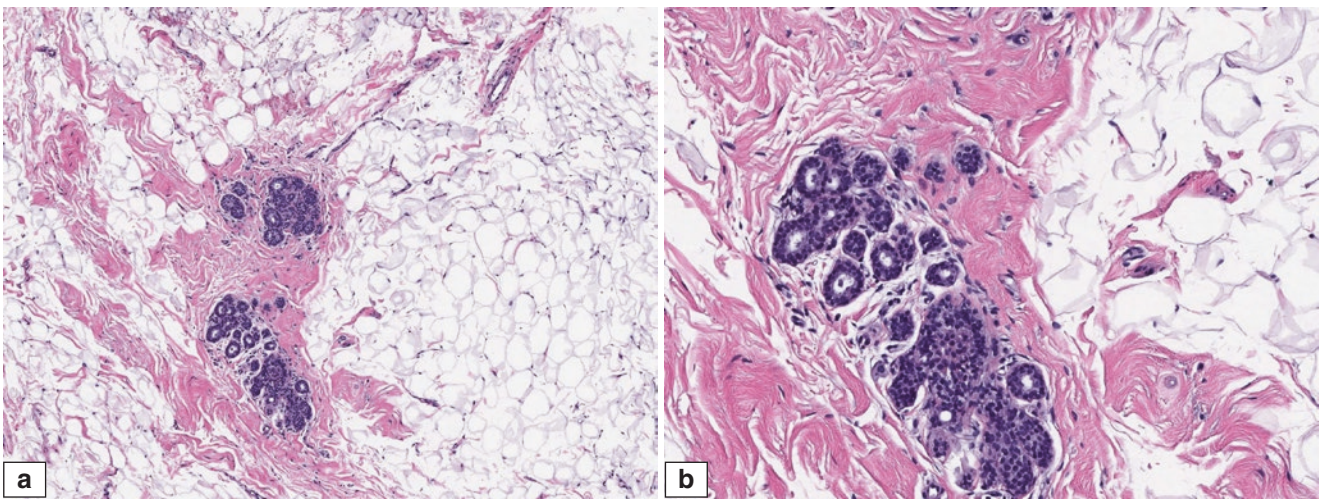

Fig. 1.14 Menopausal adult female breast. Histologic features. (**a**, **b**) H&E sections of breast parenchyma show a significantly reduced number of lobular units along with an increased amount of adipose tissue and stroma

for classification. In order to have uniformity, breast imagers today use the American College of Radiology Breast Imaging Reporting and Data System (BI-RADS) classification. The definitions in this system range from 1 (normal finding) to 6 (biopsy-proven malignancy) [21, 22].

Most of the breast calcifications are calcium phosphate, and they stain darkly basophilic with routine haematoxylin and eosin (H&E)-stained sections (Fig. 1.16a, b). Approximately 10 % of the calcifications that are biopsied are calcium oxalate crystals, which appear to be colourless on H&E sections (Fig. 1.16c, d). They are birefringent under polarised illumination and account for a majority of the calcifications that are reportedly missing on histologic sections. In these situations, sections should be evaluated with polarised light. Both calcium phosphate and oxalate calcifications have similar appearances on mammography. Although rare, cases of ductal carcinoma in situ associated with calcium oxalate crystals have been reported. Calcium oxalate crystals are usually found in benign ducts, most frequently in cystic ducts lined by epithelial cells with apocrine

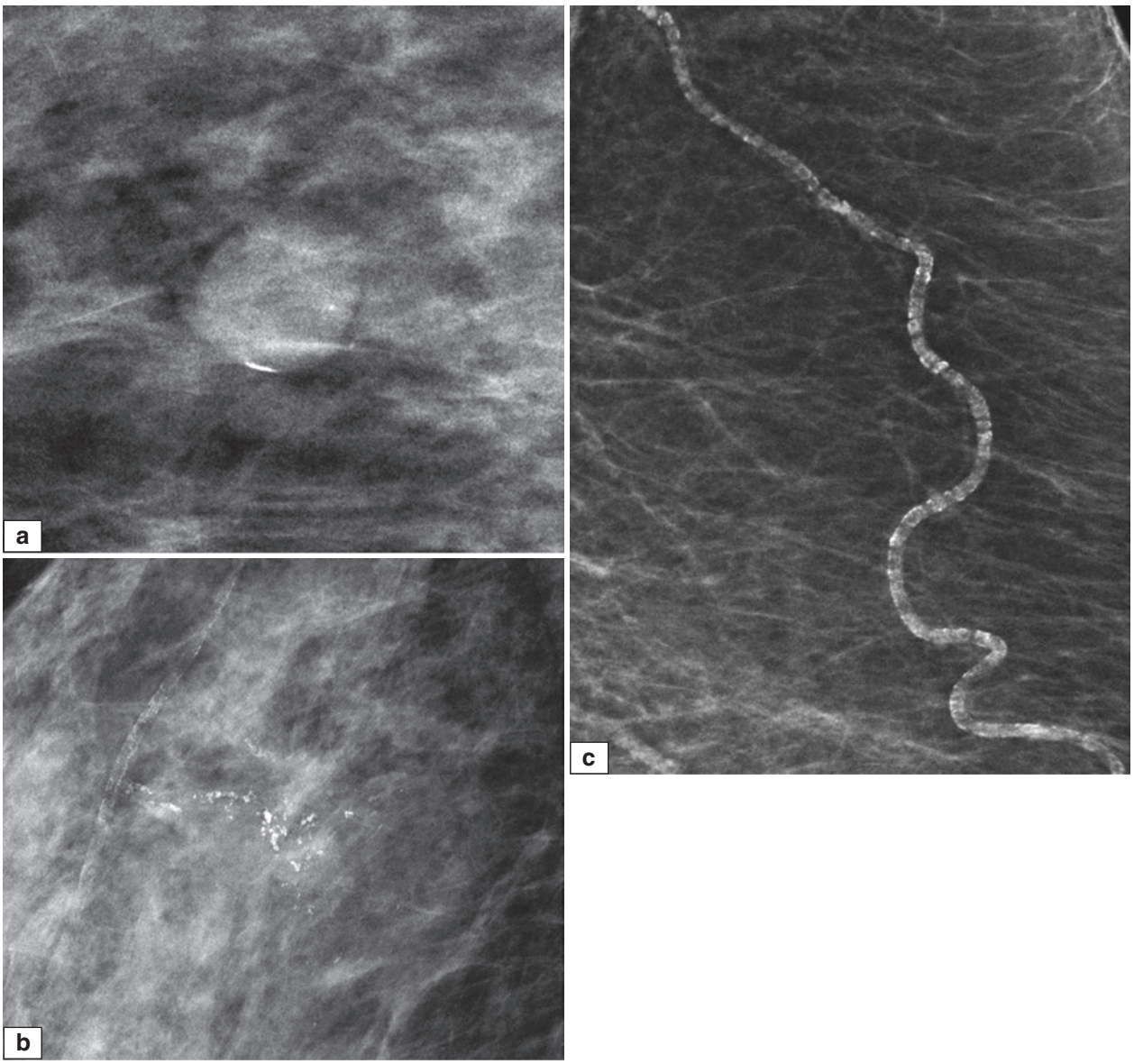

Fig. 1.15 Mammographic appearance of microcalcifications. (**a**) Eggshell calcification associated with benign usual ductal hyperplasia. (**b**) Linear calcifications associated with ductal carcinoma in situ. (**c**) Vascular calcifications

metaplasia. Careful correlation with specimen radiography and calcifications identified on histologic sections is important for accurate diagnosis and verification of completeness of excision of mammographically identified lesions. If no calcifications are demonstrated on tissue sections that are supposed to have microcalcifications, paraffin-embedded tissue blocks can be X-rayed, and if necessary deeper sections can be obtained.

Non-calcified Crystalloids

Variously shaped crystal-like deposits usually associated with proteinaceous secretions can rarely be seen in breast ducts. Since these crystalloids are not calcified, they are not able to be seen on mammograms. Most of them appear as triangular, hexagonal, or rhomboid and stain deeply eosinophilic (Fig. 1.17). They are not birefringent.

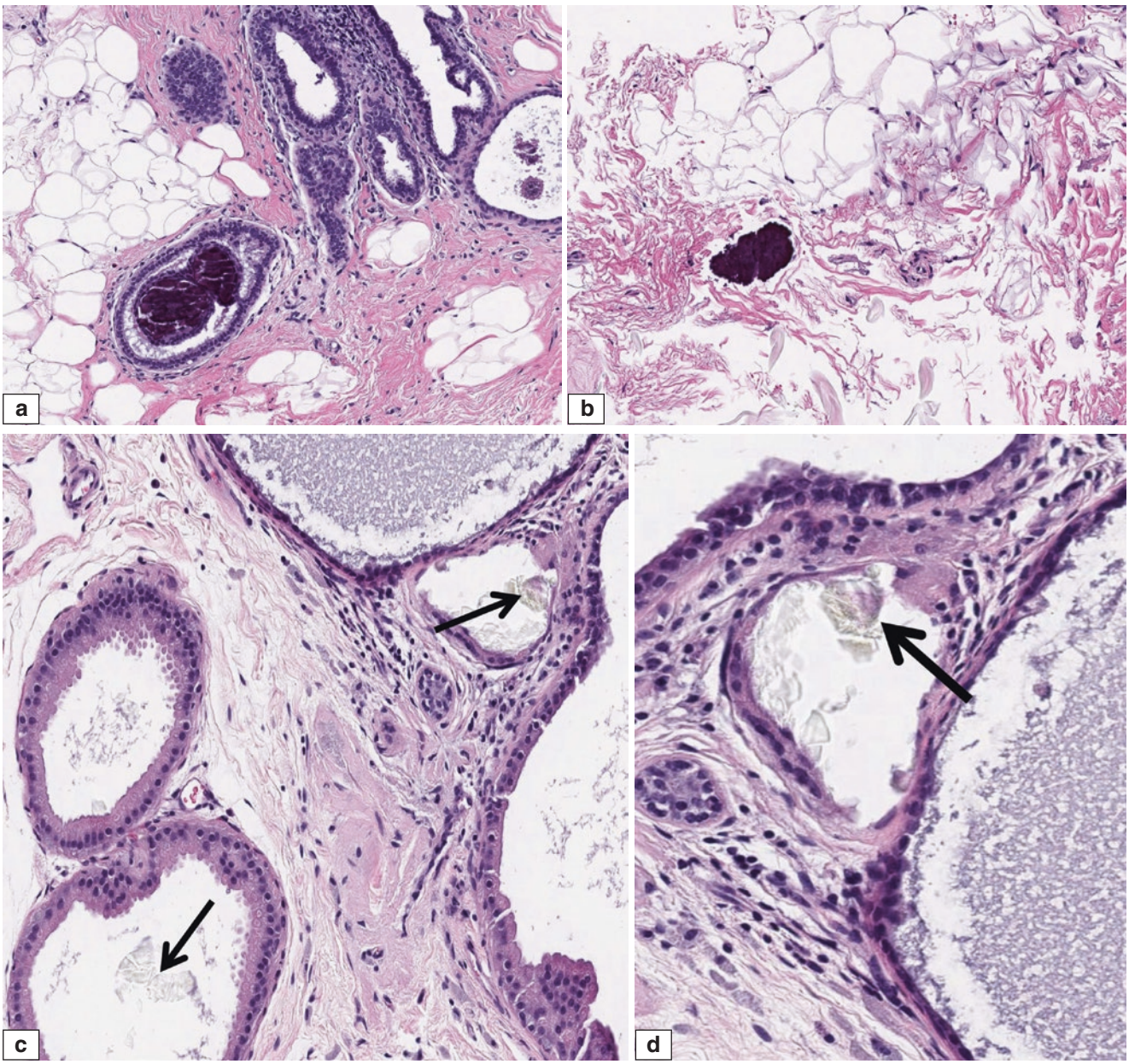

Fig. 1.16 Microcalcifications. Histologic features. (**a**) Calcium phosphate in glandular lumen. (**b**) Calcium phosphate in stroma. (**c**, **d**) Calcium oxalate (*arrows*) in dilated ducts lined by apocrine epithelium

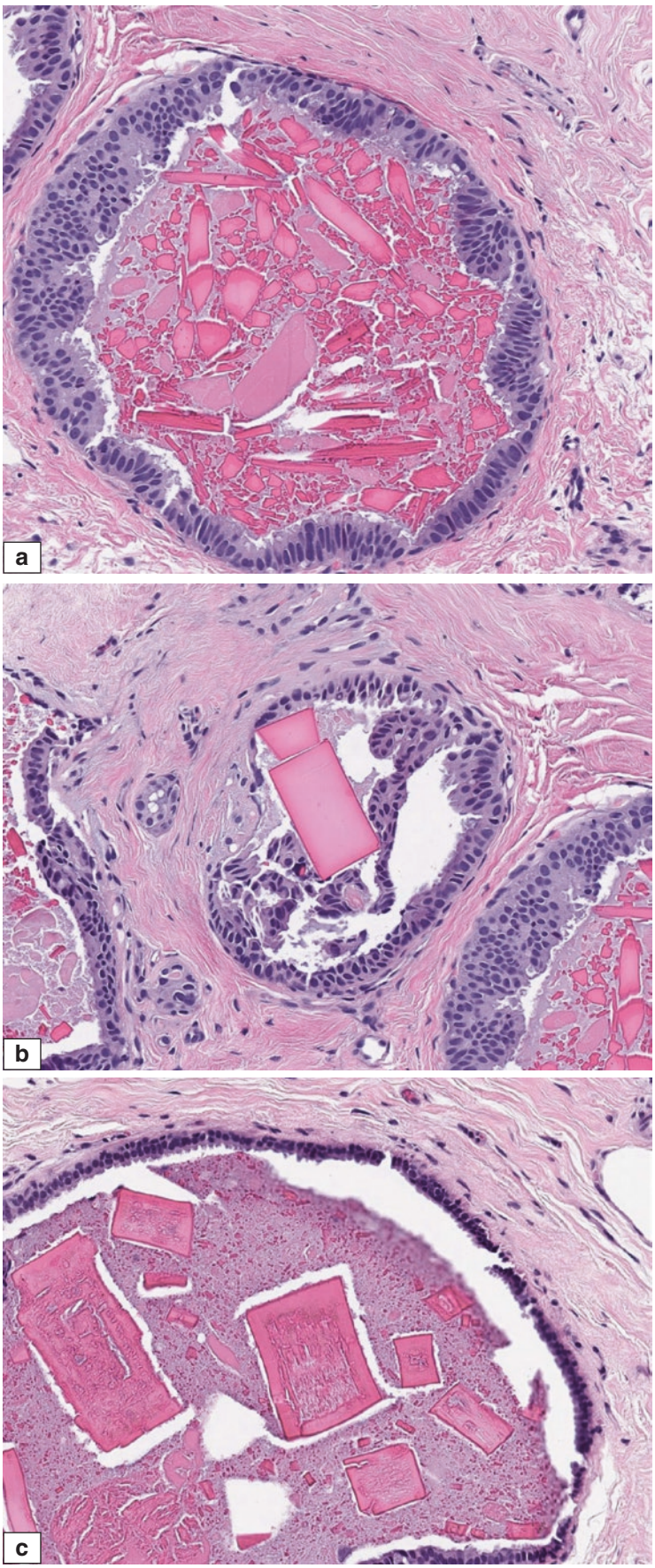

Fig. 1.17 Non-calcified crystalloids. Histologic features. (**a–c**) Crystalloids shown in multiple geometric shapes and sizes. Crystalloids appear as dense eosinophilic deposits

References

1. Anderson TJ. Normal breast: myths, realities, and prospects. Mod Pathol. 1998;11(2):115–9.
2. Sandhu R, Chollet-Hinton L, Kirk EL, Midkiff B, Troester MA. Digital histologic analysis reveals morphometric patterns of age-related involution in breast epithelium and stroma. Hum Pathol. 2016;48:60–8.
3. Ramsay DT, Kent JC, Hartmann RA, Hartmann PE. Anatomy of the lactating human breast redefined with ultrasound imaging. J Anat. 2005;206(6):525–34.
4. Tot T, Tabar L, Dean PB. The pressing need for better histologic-mammographic correlation of the many variations in normal breast anatomy. Virchows Arch. 2000;437(4):338–44.
5. Longacre TA, Bartow SA. A correlative morphologic study of human breast and endometrium in the menstrual cycle. Am J Surg Pathol. 1986;10(6):382–93.
6. Nazário AC, Simões MJ, de Lima GR. Morphological and ultrastructural aspects of the cyclical changes of human mammary gland during the menstrual cycle. Sao Paulo Med J. 1994;112(2):543–7.
7. Ferguson JE, Schor AM, Howell A, Ferguson MW. Changes in the extracellular matrix of the normal human breast during the menstrual cycle. Cell Tissue Res. 1992;268(1):167–77.
8. Ferguson DJ, Anderson TJ. Morphological evaluation of cell turnover in relation to the menstrual cycle in the "resting" human breast. Br J Cancer. 1981;44(2):177–81.
9. Going JJ, Anderson TJ, Battersby S, MacIntyre CC. Proliferative and secretory activity in human breast during natural and artificial menstrual cycles. Am J Pathol. 1988;130(1):193–204.
10. Potten CS, Watson RJ, Williams GT, Tickle S, Roberts SA, Harris M, et al. The effect of age and menstrual cycle upon proliferative activity of the normal human breast. Br J Cancer. 1988;58(2):163–70.
11. Vogel PM, Georgiade NG, Fetter BF, Vogel FS, McCarty Jr KS. The correlation of histologic changes in the human breast with the menstrual cycle. Am J Pathol. 1981;104(1):23–34.
12. Baldwin P. Breast calcification imaging. Radiol Technol. 2013;84(4):383M–404M; quiz 405M–8M.
13. Graf O, Berg WA, Sickles EA. Large rodlike calcifications at mammography: analysis of morphologic features. AJR Am J Roentgenol. 2013;200(2):299–303.
14. Liberman L, Abramson AF, Squires FB, Glassman JR, Morris EA, Dershaw DD. The breast imaging reporting and data system: positive predictive value of mammographic features and final assessment categories. AJR 1998;171:35–40.
15. Burnside ES, Ochsner JE, Fowler KJ, et al. Use of microcalcification descriptors in BI-RADS 4th edition to stratify risk of malignancy. Radiology 2007;242:388–95.
16. Bent CK, Bassett LW, D'Orsi CJ, Sayre JW. The positive predictive value of BI-RADS microcalcification descriptors and final assessment categories. AJR 2010;94:1378–83.
17. Chen PH, Ghosh ET, Slanetz PJ, Eisenberg RL. Segmental breast calcifications. AJR Am J Roentgenol. 2012;199(5):W532–42.
18. Lai KC, Slanetz PJ, Eisenberg RL. Linear breast calcifications. AJR Am J Roentgenol. 2012;199(2):W151–7.
19. Demetri-Lewis A, Slanetz PJ, Eisenberg RL. Breast calcifications: the focal group. AJR Am J Roentgenol. 2012;198(4):W325–43.
20. Henrot P, Leroux A, Barlier C, Génin P. Breast microcalcifications: the lesions in anatomical pathology. Diagn Interv Imaging. 2014;95(2):141–52.
21. American College of Radiology. Breast imaging reporting and data system (BI-RADS). 4th ed. Reston: American College of Radiology; 2003.
22. Bent CK, Bassett LW, D'Orsi CJ, Sayre JW. The positive predictive value of BI-RADS microcalcification descriptors and final assessment categories. AJR Am J Roentgenol. 2010;194(5):1378–83. doi:10.2214/AJR.09.3423.

Developmental, Reactive, and Inflammatory Conditions

2

These are benign lesions and encompass diverse entities that range from ectopic breast tissue to duct ectasia, fat necrosis, mastitis, Rosai–Dorfman disease, diabetic mastopathy, amyloidosis, IgG4-related mastitis, biopsy site changes, reaction to foreign material including implants, and infections.

Ectopic Breast Tissue

Definition

Ectopic breast tissue refers to breast tissue discovered at anatomic locations other than on the anterior chest wall where the normal breasts reside. It appears along the embryological mammary ridges, or milk lines, which extend from the axilla to the upper medial thigh.

Clinical and Epidemiological Features

Ectopic breast tissue is reported to occur in between 1 % and 6 % of women and can be bilateral or unilateral. It is rare in men. Clinically, it may present as an accessory nipple or a lump, commonly in the axilla.

Imaging Features

The imaging appearance of ectopic fibroglandular tissue is similar to that in the breast. On mammography, fibroglandular tissue of higher density is mixed with low-density fatty tissue. On ultrasound examination, the fibroglandular tissue appears hyperechoic relative to adjacent subcutaneous fat. MRI shows physiological background enhancement similar to the breast parenchyma. Fibroadenoma, papilloma, cysts, apocrine metaplasia, epithelial hyperplasia, and carcinoma may arise from ectopic breast tissue with corresponding imaging changes.

Pathologic Features

Macroscopic Pathology

Accessory nipples may appear as brown-coloured skin protuberances. Ectopic breast tissue can be fibrofatty in gross appearance or may be predominantly fatty.

Microscopic Pathology

Histologically, accessory nipples incorporate lactiferous ducts, while ectopic breast tissue displays varying numbers of ducts and lobules (Figs. 2.1, 2.2, 2.3, 2.4, and 2.5). Some cases may be primarily composed of fat. Physiological changes can be observed in ectopic breast tissue, including pregnancy and lactational hyperplasia. Cysts, apocrine metaplasia, epithelial hyperplasia, fibroadenoma (Fig. 2.6), papilloma, and a wide range of lesions occurring in the normally located breast can be encountered in ectopic breast tissue. When ectopic breast tissue is found within axillary lymph nodes, it may be mistaken for metastasis [1, 2].

Differential Diagnosis

Normal Skin Adnexa

Adnexal apocrine glands and sweat ducts of the axilla may mimic breast ducts and lobules of axillary ectopic breast tissue. Whereas adnexal tissue generally occurs in the dermis, breast ducts and lobules are seen deep to the dermis and within adipose tissue. Usually, a terminal duct with surrounding acini or ductules can be observed.

P.H. Tan, A.A. Sahin, *Atlas of Differential Diagnosis in Breast Pathology*, Atlas of Anatomic Pathology,
DOI 10.1007/978-1-4939-6697-4_2

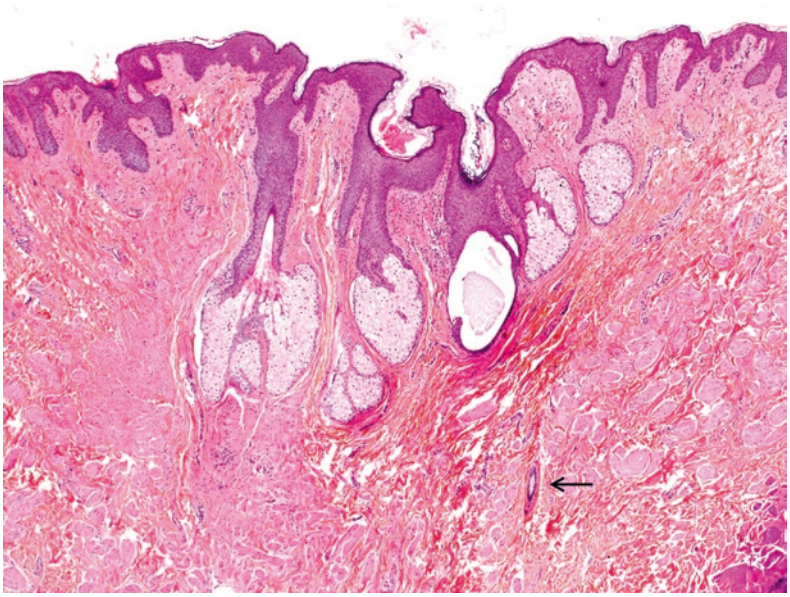

Fig. 2.1 Accessory nipple shows skin with sebaceous glands and bundles of smooth muscle fibres in the dermis. A small duct (*arrow*) is seen among the smooth muscle fibres (Courtesy of Dr. Kenneth Chang)

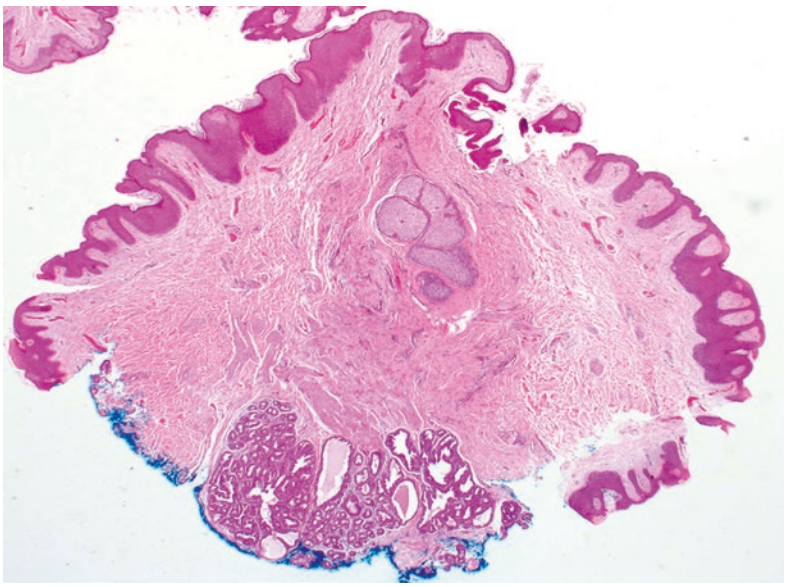

Fig. 2.2 Accessory nipple. A skin "papilloma" removed from the abdominal skin of an adult woman. Histologically, the protuberant skin with sebaceous glands shows a lobular cluster of glands at the resection base

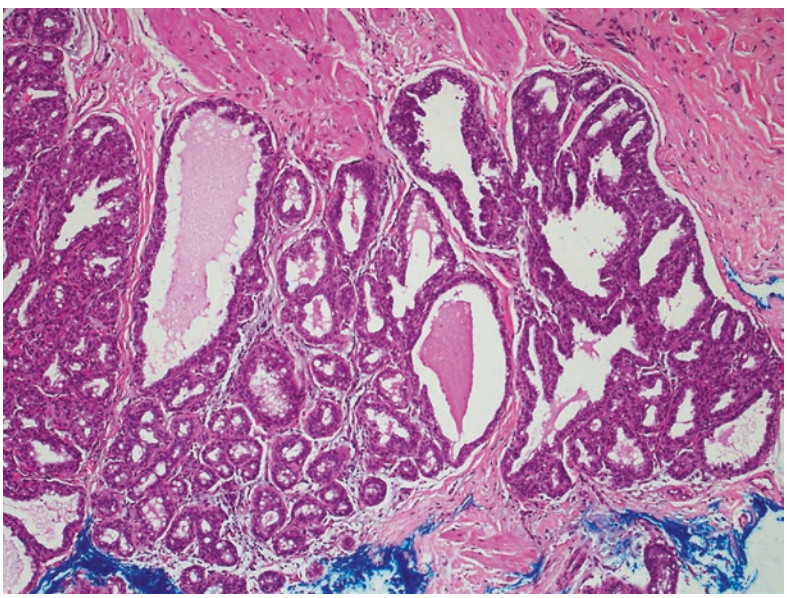

Fig. 2.3 Accessory nipple. High magnification shows crowded glands with dilatation and luminal pink secretions. Some of the lining epithelial cells disclose cytoplasmic vacuolation. These glands are consistent with a breast lobule

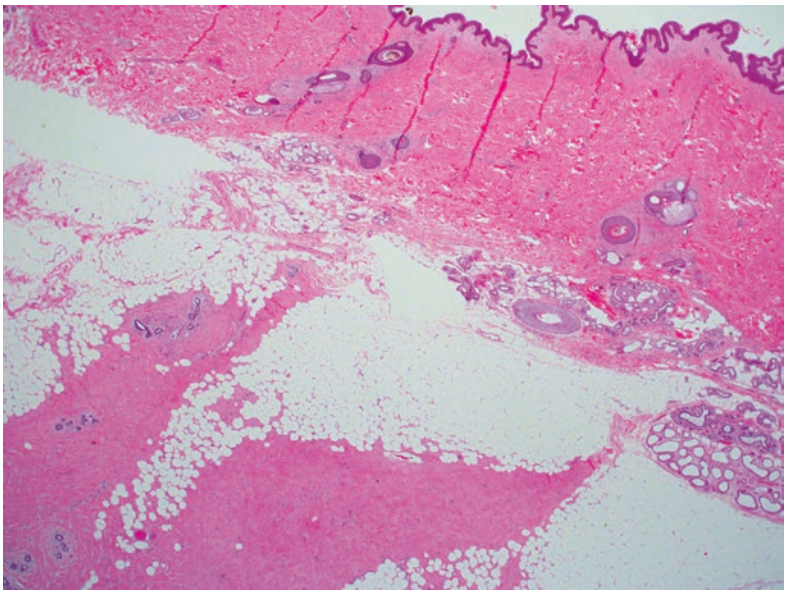

Fig. 2.4 Axillary breast tissue. A few scattered breast lobules are seen deep in the skin and subcutis, embedded within fibrous stroma. Several apocrine glands are also observed in the deep dermis and superficial subcutaneous fat

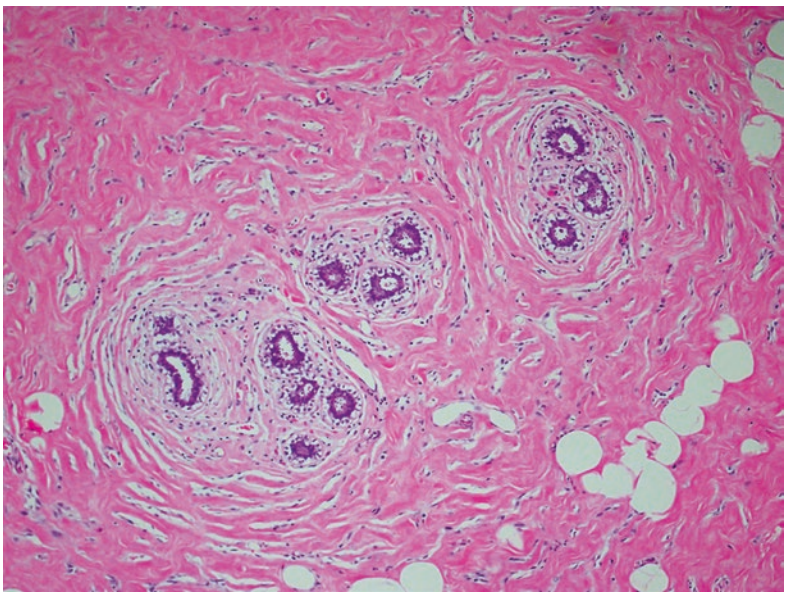

Fig. 2.5 Axillary breast tissue. A few breast ductules are loosely aggregated, forming small lobules. There is pseudoangiomatous stromal hyperplasia

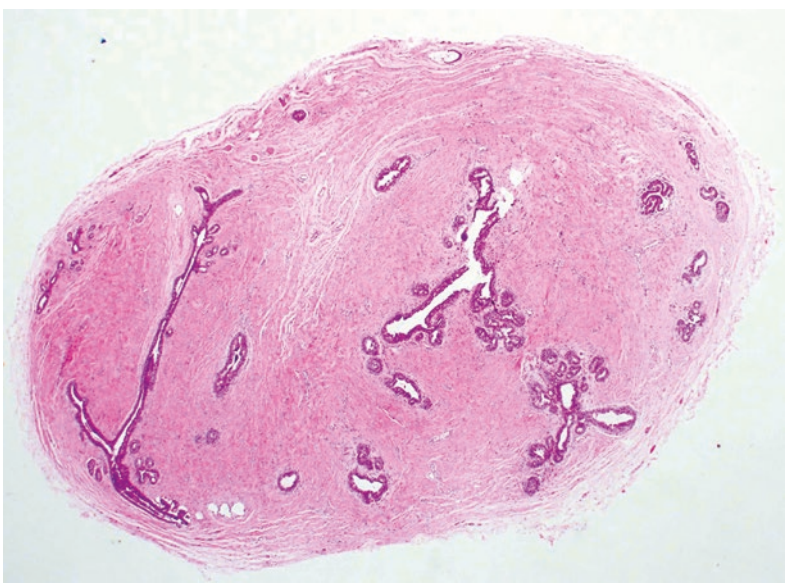

Fig. 2.6 Ectopic breast tissue with a fibroadenoma. Lump in the fourchette that was excised shows a fibroadenoma

Lipoma

When ectopic breast tissue is predominantly fatty, it can resemble a lipoma. The presence of ducts and acini, especially within fibrous areas of the adipose tissue, gives the diagnosis of ectopic breast tissue.

Fibroepithelial Polyp

An accessory nipple may resemble a fibroepithelial polyp, but the finding of lactiferous ducts can be used to make the distinction.

Lymph Node Metastasis

Ectopic breast tissue in axillary lymph nodes may lead to false positive diagnoses of nodal metastases. Clues to the benign nature are the presence of myoepithelial cells around the glands, lack of nuclear atypia, and histological divergence from the corresponding primary breast carcinoma (Fig. 2.7).

Prognosis and Therapy Considerations

Ectopic breast tissue may undergo physiological changes as with the normal breast. Pathologic lesions can also develop for which the management approach will be similar to those occurring in the breast.

Duct Ectasia

Definition

Duct ectasia is a common inflammatory condition of the breast. Many different terms, including plasma cell mastitis, comedomastitis, granulomatous mastitis, and periductal mastitis, have been used to describe the same lesion in the literature. Duct ectasia refers to dilatation of breast ducts with inspissated luminal secretions and accompaniment by inflammatory cells. Luminal histiocytes that spill out into the stroma around the disrupted dilated duct are often present.

Clinical and Epidemiological Features

Duct ectasia most commonly occurs in perimenopausal women, although it has been reported in all age groups. The relatively high frequency of duct ectasia in breast specimens excised for other lesions and in post-mortem evaluations of the breast indicates that many lesions are asymptomatic and never become a clinical problem. The process is usually bilateral and infrequently symptomatic. Nipple discharge, which is usually serous and rarely bloody, is the most common clinical symptom. Nipple retraction or inversion, a palpable mass, or mastalgia can occur. The aetiology of duct ectasia is unknown. Some authors suggest that breast ductal dilatation with involution in postmenopausal women is the initial event in the occurrence of duct ectasia. Others believe that periductal inflammation is the inciting event leading to periductal fibrosis, stasis, and duct ectasia. Cigarette smoking has been linked to the development of periductal mastitis with a higher incidence of lactiferous fistula formation.

Imaging Features

Mammographic findings can mimic cancer, with radiological calcifications, spiculated masses, or lobulated lesions [3]. Duct ectasia can be seen as dilated tubular intramammary ducts filled with fluid that can appear clear or demonstrate mobile internal echoes on real-time sonography due to secretions and cellular debris. On magnetic resonance imaging, duct ectasia may present with a pattern of enhancement that can mimic ductal carcinoma in situ (DCIS).

Pathologic Features

Macroscopic Pathology

Duct ectasia can be seen grossly as cystically dilated spaces that may exude pasty material or as a yellowish firm area due to the collections of foamy histiocytes (Fig. 2.8). Fibrosis related to chronic inflammation may be present.

Microscopic Pathology

Histologically, duct ectasia features cystically dilated ducts with inspissated, luminal proteinaceous secretions. Inflammatory cells are invariably present, mostly composed of foamy histiocytes accompanied by variable numbers of lymphocytes and plasma cells (Fig. 2.9). An acute component with polymorphs can also be seen. Histiocytes in periductal stroma that show an accumulation of ceroid pigment which imparts a brown colour to the cells are commonly referred to as “ochrocytes”. When the duct wall is damaged from inflammation and is disrupted, luminal contents seeping into the surrounding stroma may incite a granulomatous response with epithelioid histiocytes, foreign-body-type multinucleated giant cells, and cholesterol granulomas. The epithelium lining the distended duct wall may be obscured and effaced by the inflammation, to the extent that only a collection of inflammatory cells may be seen on microscopy.

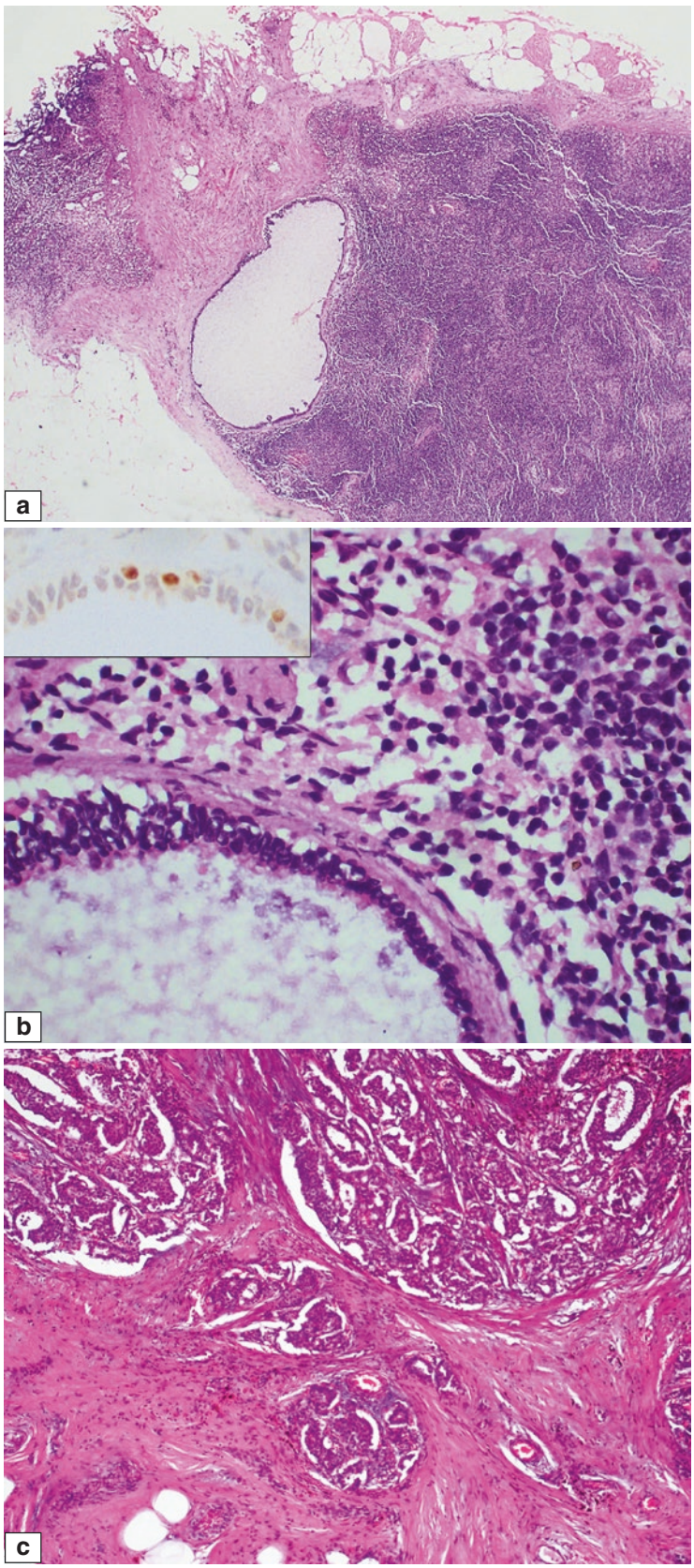

Fig. 2.7 Ectopic breast tissue in a sentinel lymph node. (**a**) The lymph node which was evaluated on frozen section shows a cystically dilated gland lined by flattened epithelium with a few luminal protrusions, within the nodal parenchyma. The primary breast tumour was an invasive ductal carcinoma, grade 1. (**b**) High magnification shows an apparent bilayering of the lining epithelium. Nuclei of the epithelial cells are bland. Inset shows p63 positive myoepithelial cells along the wall of the benign breast gland within the sentinel lymph node. (**c**) Primary breast carcinoma shows invasive grade 1 tumour. The appearances are distinctly different from the cystic glandular inclusion in the sentinel lymph node. Comparison of the histology of both the primary breast tumour and the epithelial inclusions in the lymph node may be helpful in determining if the latter represents a metastasis

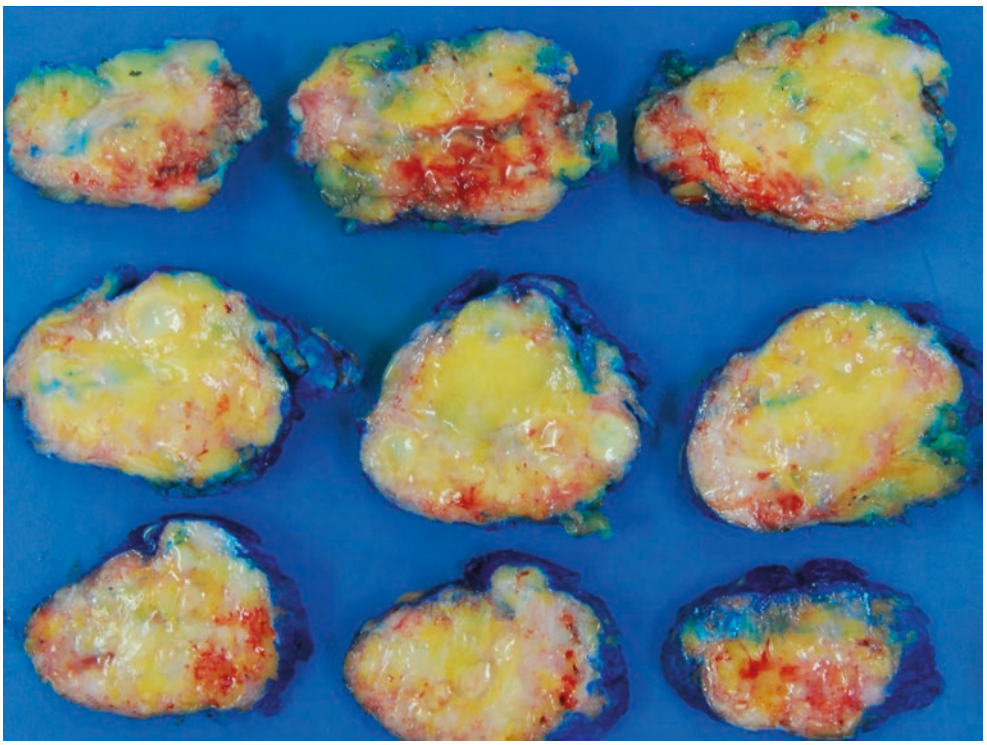

Fig. 2.8 Duct ectasia. Serial gross sections show a fibrofatty appearance with small cysts and surrounding haemorrhage

Residual ductal epithelial cells and elastic fibres around the ectatic duct may be unveiled with keratin immunohistochemistry or elastic stains, respectively (Fig. 2.10). In the later stages of duct ectasia, marked fibrosis of duct walls, sometimes accompanied by elastosis, is the main histologic feature.

Differential Diagnosis

Xanthogranulomatous Mastitis

Xanthogranulomatous mastitis refers to an inflammatory reaction in the breast with a predominance of foamy histiocytes, admixed with granulomas featuring epithelioid histiocytes and multinucleated giant cells. Histologically, the inflammation associated with duct ectasia may be indistinguishable from xanthogranulomatous inflammation, except that the inflammatory process is centred around ectatic ducts in duct ectasia.

Fat Necrosis

Fat necrosis may result from trauma, surgery, and radiation. While the histiocytes and inflammation that accompany necrotic adipocytes are similar to the inflammatory response associated with duct ectasia, fat necrosis primarily occurs within the fatty tissue of the breast, unrelated to ducts. In post-biopsy or postsurgical fat necrosis, there is often a biopsy or surgical cavity rimmed by inflamed granulation tissue, sometimes with sutures or other foreign materials related to the procedure.

Rosai–Dorfman Disease (RDD)

RDD is also known as sinus histiocytosis with massive lymphadenopathy. While it involves predominantly lymph nodes, RDD may be encountered in extranodal sites, including the breast. The sheets of histiocytes with voluminous pale cytoplasm may resemble those seen in duct ectasia, but the hallmark feature of emperipolesis where lymphocytes and plasma cells are found in spaces within histiocytic cytoplasm is an important diagnostic clue of RDD (Fig. 2.11). Extranodal RDD may show fewer histiocytes with more fibrosis. Plasma cells and lymphocytes are frequently seen among the histiocytes. The aetiology remains unknown, with infection and immunologic dysfunction being possibilities.

Pagetoid Spread of Lobular Neoplasia

Histiocytes within the ductal epithelium of duct ectasia may resemble pagetoid extension of lobular neoplasia along the ducts. The presence of histiocytes within the ectatic duct lumen and surrounding stroma supports a histiocytic origin of the cells in the epithelium (Figs. 2.12 and 2.13).

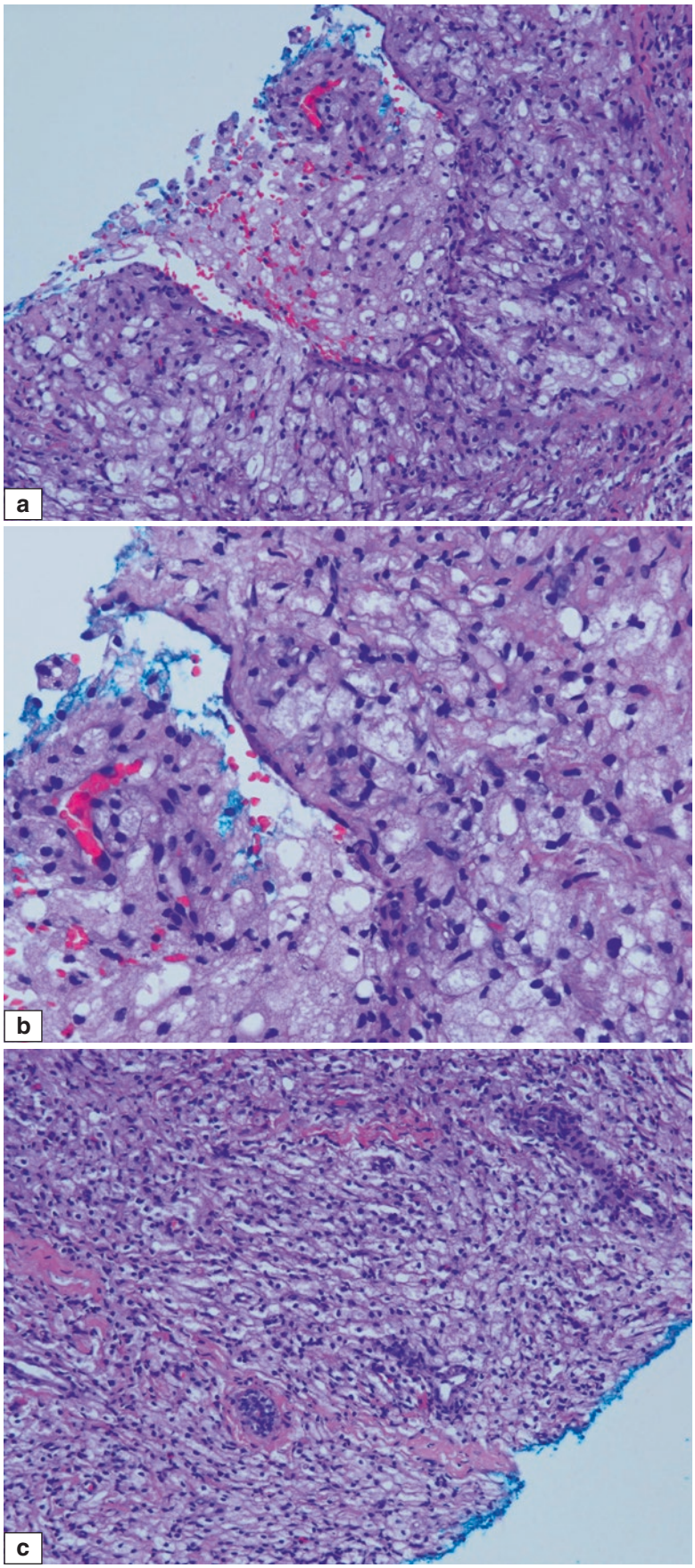

Fig. 2.9 Duct ectasia. (**a**) A distended duct with attenuated epithelial lining shows luminal foamy histiocytes which have spilled out into the surrounding stroma. Scattered lymphocytes are seen among the histiocytes. (**b**) High magnification shows a residual flattened epithelial lining of the effaced duct wall. (**c**) Sheets of foamy histiocytes extend around adjacent ductules

Granular Cell Tumour

Cells of a granular cell tumour show abundant granular eosinophilic cytoplasm that may resemble histiocytes of duct ectasia. However, unlike duct ectasia, where the histiocytes reside within the ductal lumen and around the duct, cells of granular cell tumour are observed within the breast parenchyma and tend to be permeative, with granular cells extending among lobules (Figs. 2.14 and 2.15). Also unlike duct ectasia, where other inflammatory cells accompany histiocytes, granular cell tumour is not usually associated with a significant inflammatory reaction. Immunohistochemistry shows diffuse S100 reactivity in granular cell tumour [4].

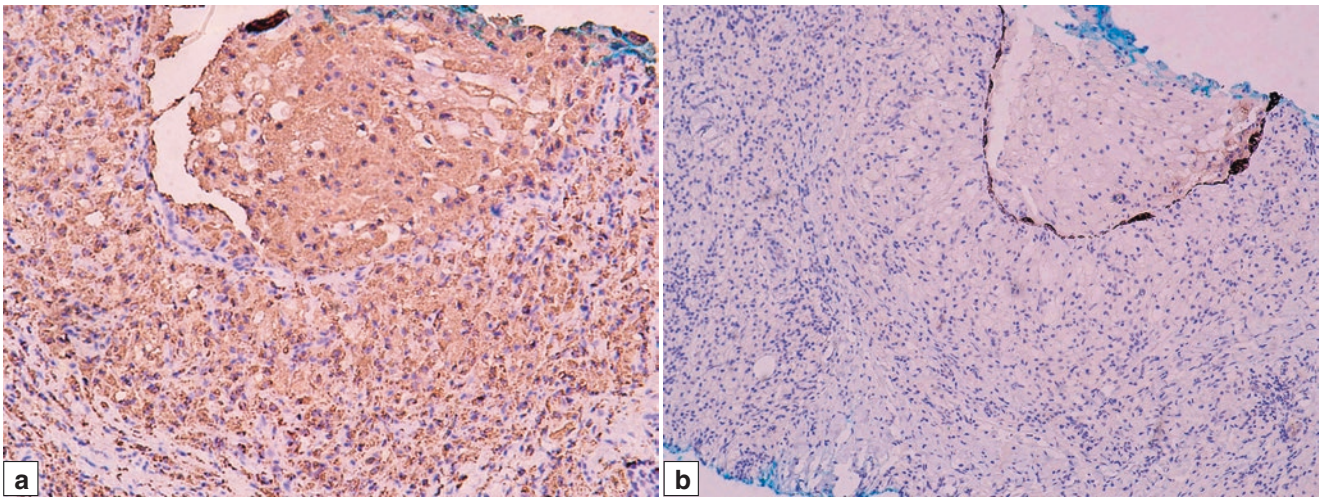

Fig. 2.10 Duct ectasia. (**a**) CD68 immunohistochemistry shows histiocytes that disclose granular cytoplasmic positivity. (**b**) CK7 immunohistochemistry unveils the attenuated epithelial lining of the duct wall which has been obscured by histiocytes

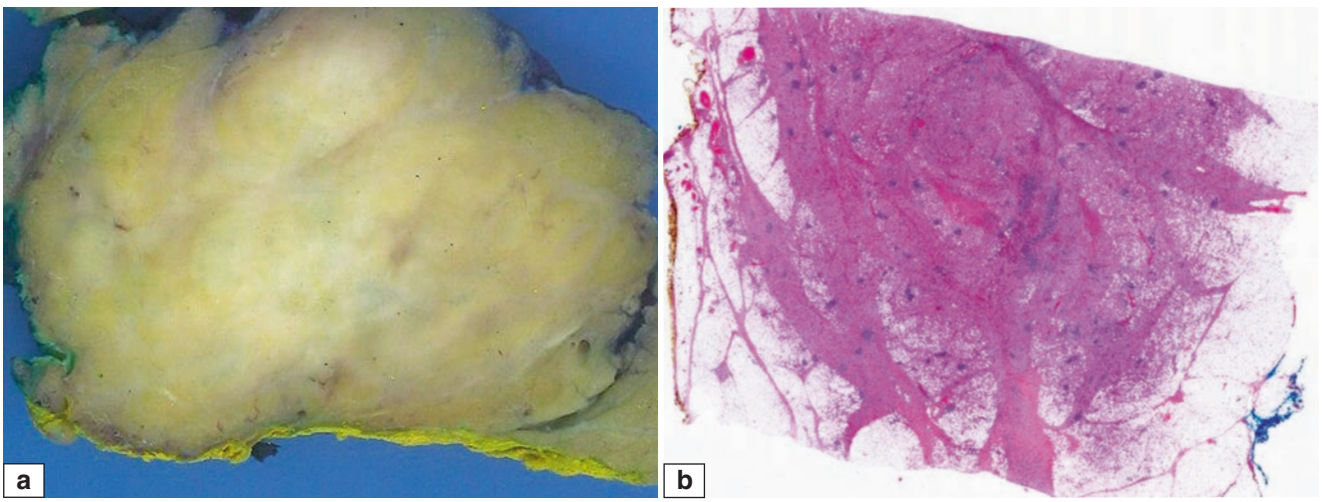

Fig. 2.11 Rosai–Dorfman disease. (**a**) Gross appearance shows an ill-defined whitish-grey and yellowish-brown mass which is of firm consistency, merging with surrounding tissue, without any discrete or well discerned lesional borders. (**b**) Scanning magnification shows fibrous bands within adipose, interspersed with pale zones and scattered lymphocytic aggregates. (**c**) Sheets of pale histiocytes with copious amounts of cytoplasm are found effacing the breast parenchyma. The pale histiocytes may resemble those of duct ectasia. In contrast to RDD, however, the histiocytes accompanying duct ectasia are centred on dilated ducts which often show a disrupted epithelial lining. The histiocytes in duct ectasia are found both within the dilated duct and in the surrounding parenchyma. (**d**) Sheets of pale histiocytes contain vesicular nuclei with abundant pale-to-slightly pink cytoplasm. Within the cytoplasm of some histiocytes, there are lymphocytes and plasma cells in keeping with emperipolesis. Emperipolesis refers to the process in which lymphocytes and plasma cells enter the cytoplasm without undergoing degradation. (**e**) S100 immunohistochemistry decorates the histiocytes which contain inflammatory cells in their cytoplasm. These intracytoplasmic lymphocytes and plasma cells are surrounded by haloes representing spaces enclosed by the histiocytic cytoplasm, as the lymphocytes and plasma cells "wander" through the histiocytes. (**f**) CD68 immunohistochemistry shows granular and clumpy cytoplasmic positivity in histiocytes (*arrows* indicate several positively stained histiocytes)

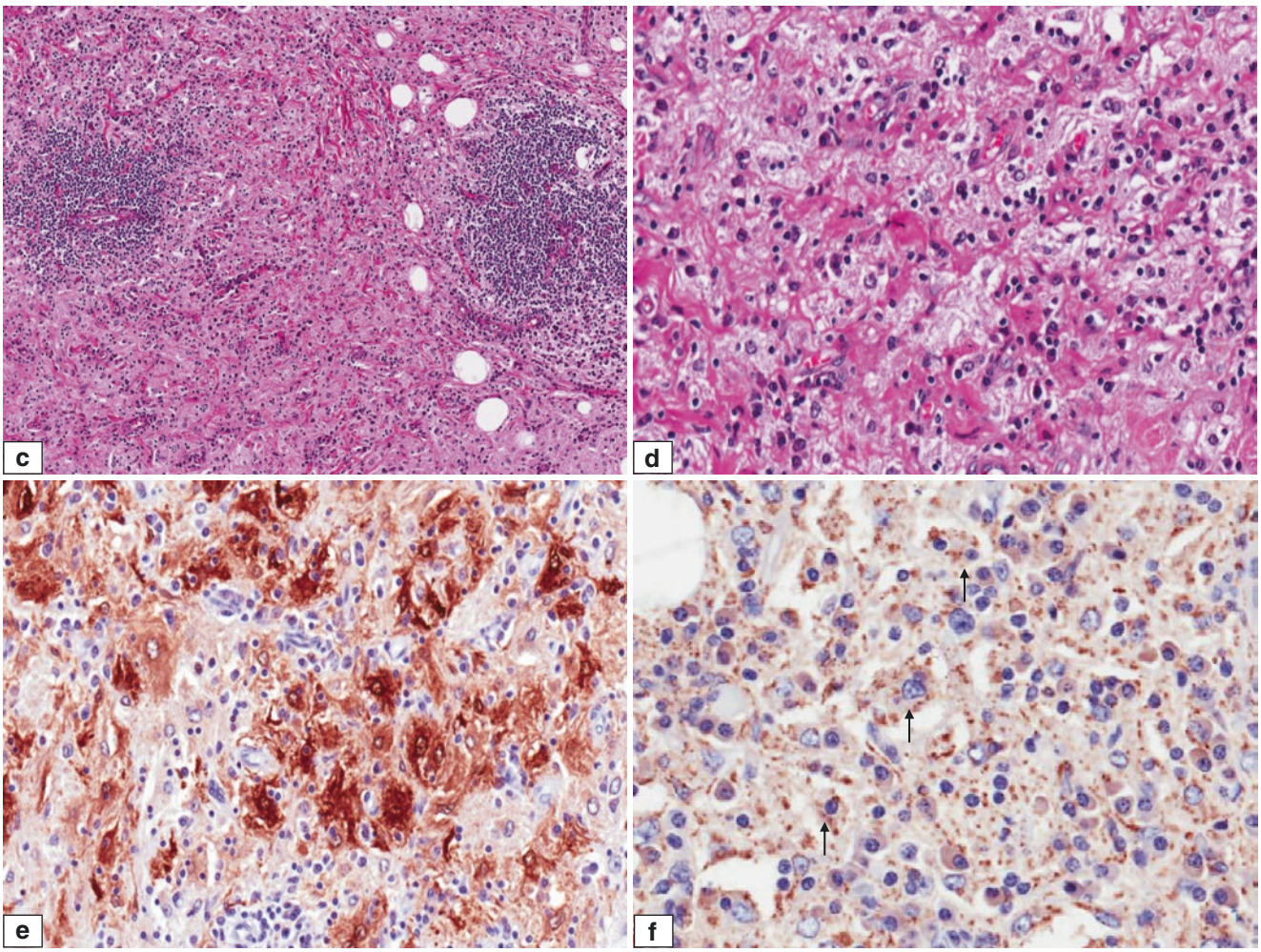

Fig. 2.11 (continued)

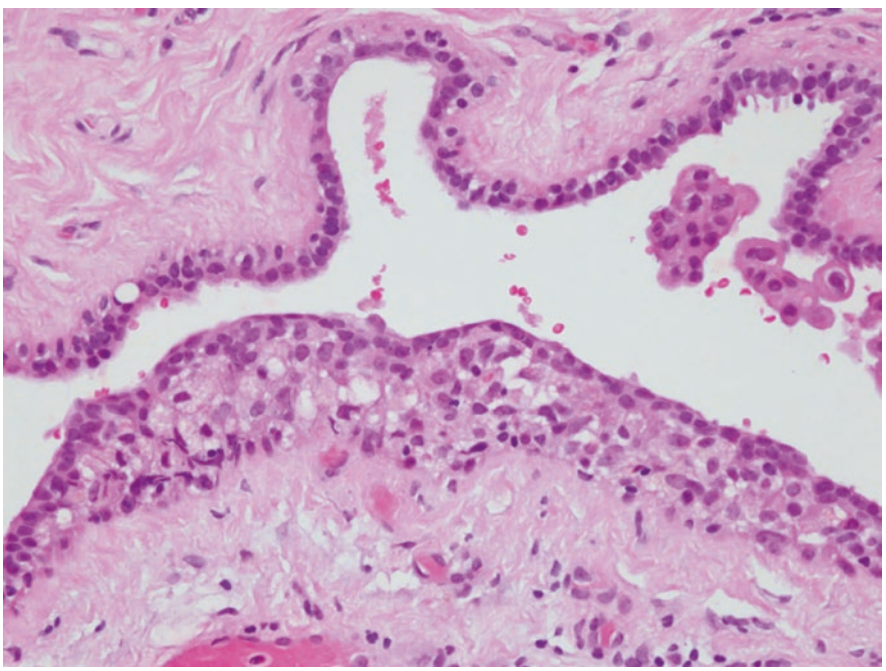

Fig. 2.12 Histiocytes along the duct wall, lying deep to the attenuated luminal epithelium, may mimic lobular neoplasia. In this duct, a few apocrine cells are found in the duct lumen. Several lymphocytes are seen among the foamy histiocytes, which have slightly folded vesicular nuclei with finely vacuolated cytoplasm

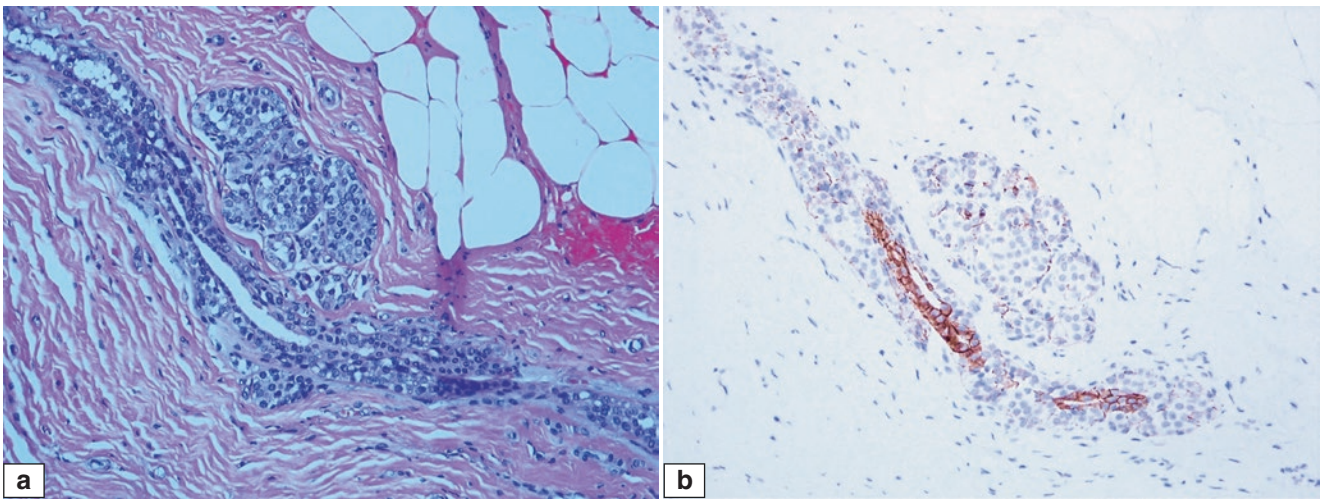

Fig. 2.13 Pagetoid extension of lobular neoplasia along a terminal duct shows rounded cells with pale cytoplasm undermining the luminal epithelium of the terminal duct. Adjacent acini show filling by a similar population of slightly discohesive rounded cells (**a**). E-cadherin immunohistochemistry shows loss of membrane reactivity of the lobular neoplastic cells, with preserved staining of the luminal ductal epithelial cells (**b**)

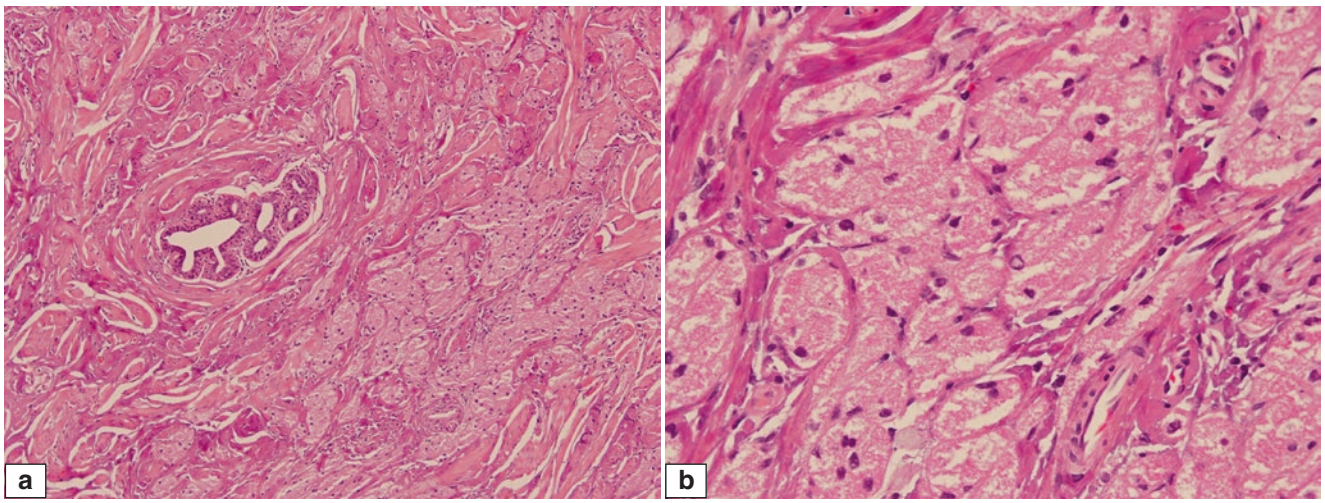

Fig. 2.14 Granular cell tumour. (**a**) Sheets of granular cells with ample granular cytoplasm, ill-defined cytoplasmic borders, and small nuclei are seen extending through stroma among collagen bundles and around a breast lobule. Note the absence of accompanying inflammatory cells, which are usually seen in duct ectasia. (**b**) High magnification shows the granularity of the cytoplasm, with small ovoid nuclei without atypia nor discernible mitoses

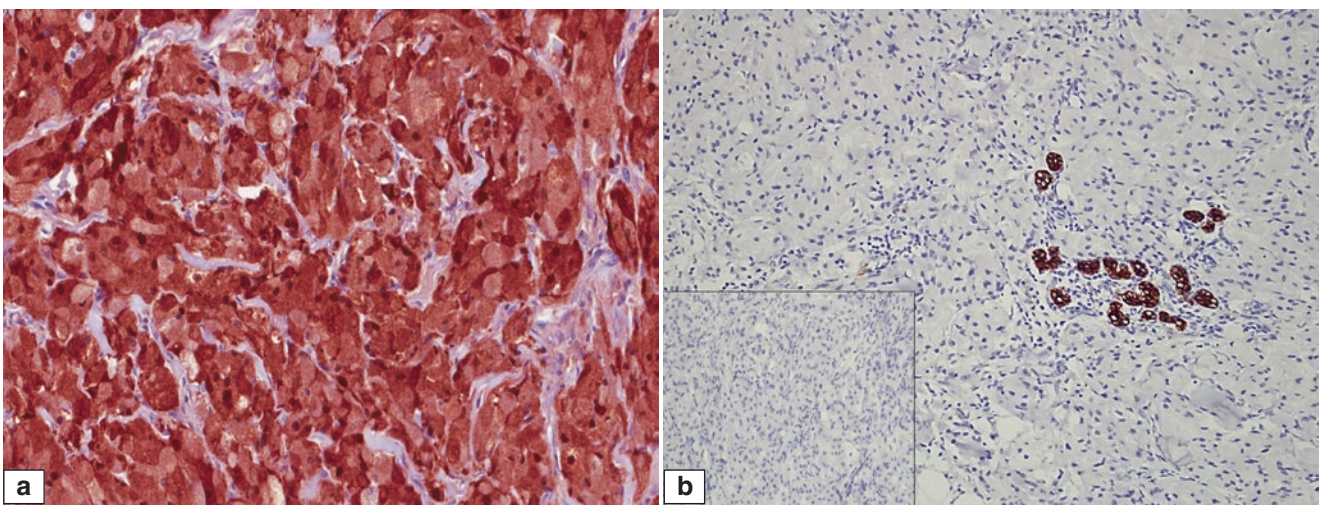

Fig. 2.15 Granular cell tumour. (**a**) S100 immunohistochemistry diffusely decorates the cytoplasm of granular cells. (**b**) CK7 highlights small ducts in the section, whereas tumour cells are negative. MNF116, an epithelial marker, is also negative in the granular cells (inset)

Histiocytoid Invasive Lobular Carcinoma

The histiocytoid variant of invasive lobular carcinoma has a particularly bland appearance on cursory view, with tumour cells mimicking histiocytes (Figs. 2.16, 2.17, 2.18, 2.19, 2.20, and 2.21). Instead of the diffuse sheets of histiocytes that are intermingled with other inflammatory cells frequently observed in duct ectasia, histiocytoid invasive lobular carcinoma often shows areas with more typical linear cords of classical invasive lobular carcinoma as well as lobular neoplasia. Immunohistochemistry shows positive reactivity for epithelial markers, and the tumour cells are also generally ER positive [5].

Invasive Apocrine Carcinoma

The ample cytoplasm of tumour cells of invasive apocrine carcinoma may resemble histiocytes. However, apocrine carcinoma cells have pink cytoplasm and occur in invasive trabeculae and cohesive nests, contrasting against the pale gentle cytoplasm of histiocytes disposed in sheets accompanied by other inflammatory cells. In addition, in apocrine carcinomas, the nuclei tend to be enlarged and round with prominent nucleoli (Figs. 2.22, 2.23, 2.24, 2.25, 2.26, 2.27, and 2.28).

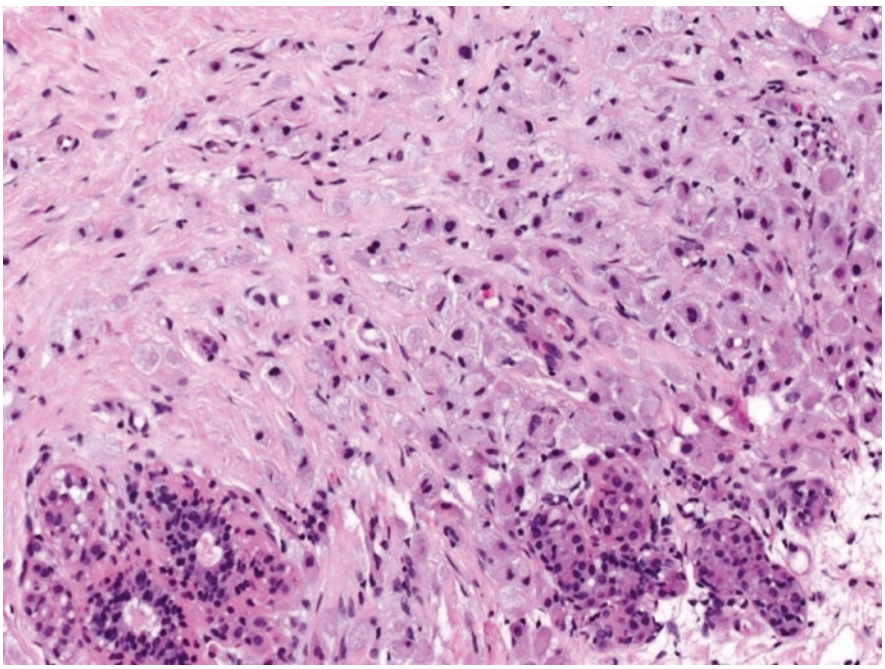

Fig. 2.16 Histiocytoid invasive lobular carcinoma. Histiocyte-like tumour cells percolate through the breast parenchyma. These tumour cells have ample pale-to-pink cytoplasm with hyperchromatic nuclei, some of which are eccentrically placed. Several tumour cells show cytoplasmic vacuoles. Lobular neoplasia (atypical lobular hyperplasia) is present

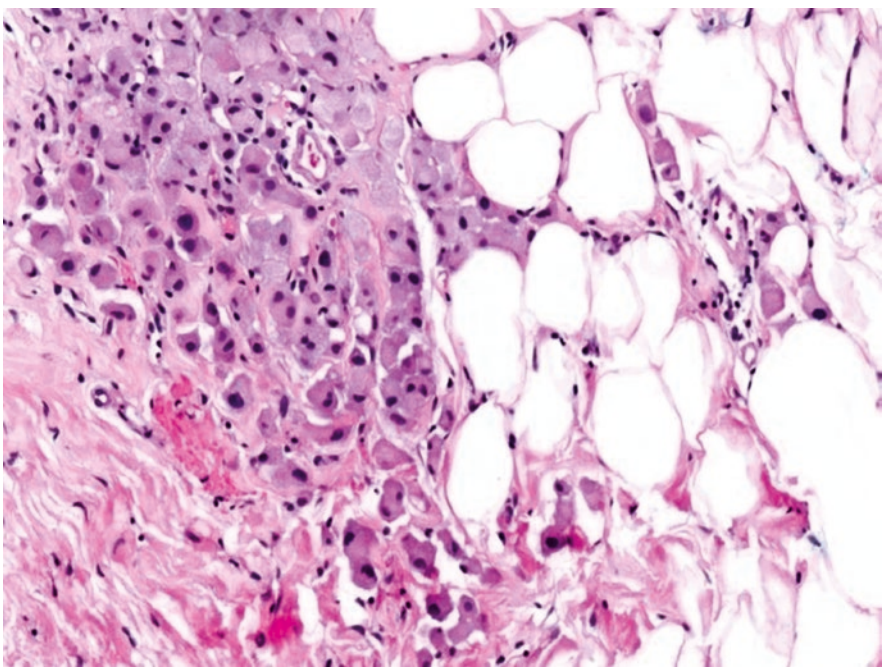

Fig. 2.17 Histiocytoid invasive lobular carcinoma. Histiocyte-like tumour cells with hyperchromatic nuclei and ample pale cytoplasm extend in between the adipocytes, the latter potentially mimicking fat necrosis where histiocytes are seen among degenerate adipocytes. Clues to the malignant nature of histiocytoid invasive lobular carcinoma are the nuclear pleomorphism and hyperchromasia and the absence of accompanying inflammation which is usually observed in an inflammatory histiocytic lesion

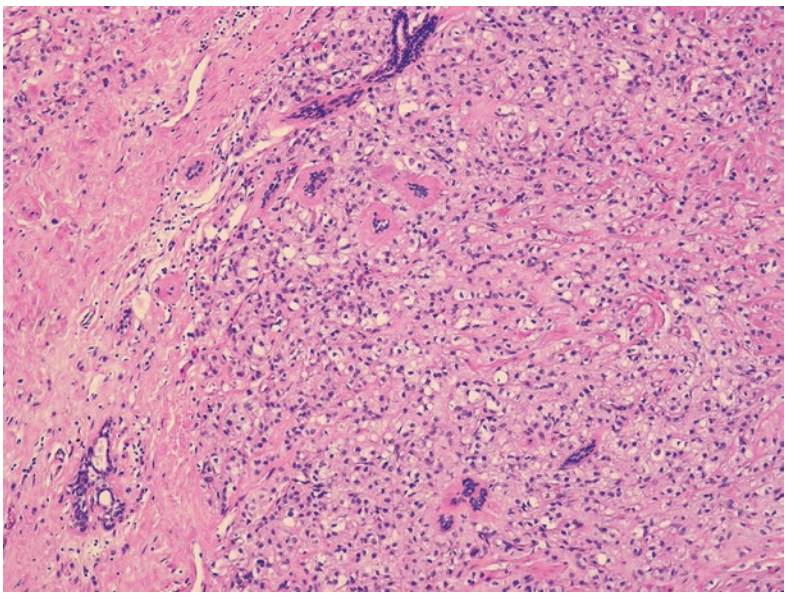

Fig. 2.18 Histiocytoid invasive lobular carcinoma. Sheets of pale histiocyte-like tumour cells surround resident ducts and lobules

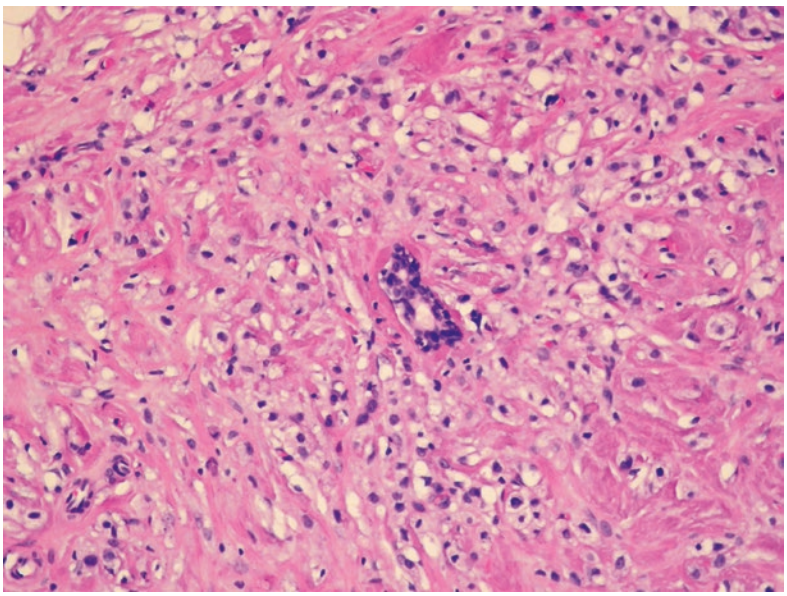

Fig. 2.19 Histiocytoid invasive lobular carcinoma. Higher magnification shows pale histiocyte-like cells surrounding a benign duct, extending among pink collagen fibres. The tumour cells possess ill-defined cytoplasmic membranes

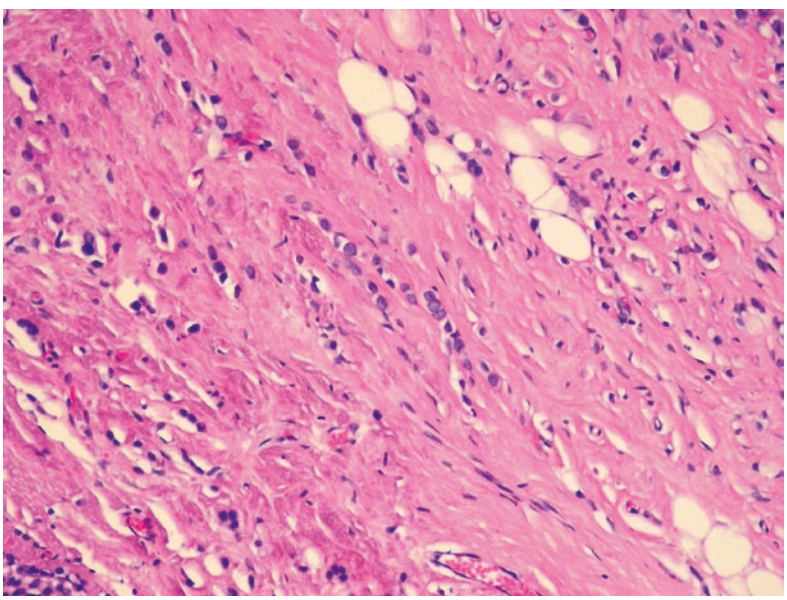

Fig. 2.20 Histiocytoid invasive lobular carcinoma. Focally, the tumour usually features more conventional invasive lobular carcinoma patterns of linear cords and pearl-like strands of bland tumour cells

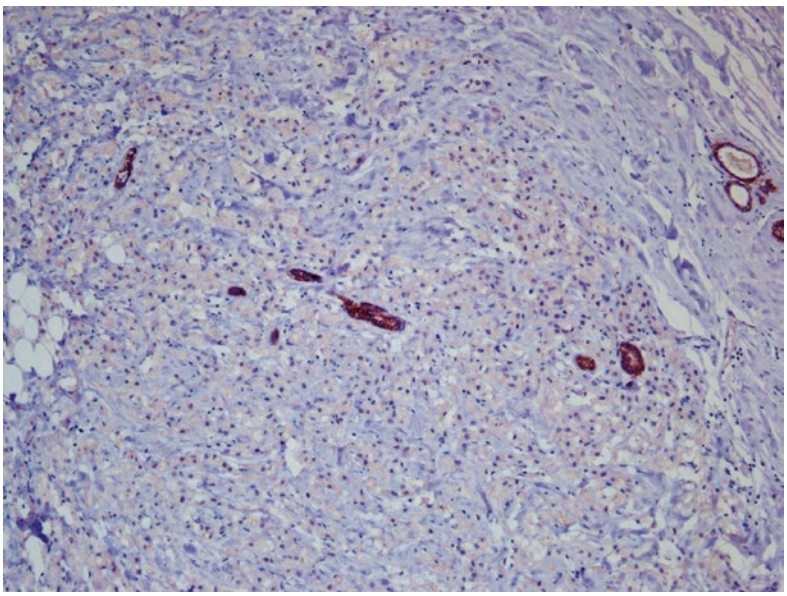

Fig. 2.21 Histiocytoid invasive lobular carcinoma. Immunohistochemistry for E-cadherin shows negative staining of the tumour cells, while the residual benign ducts are positively decorated

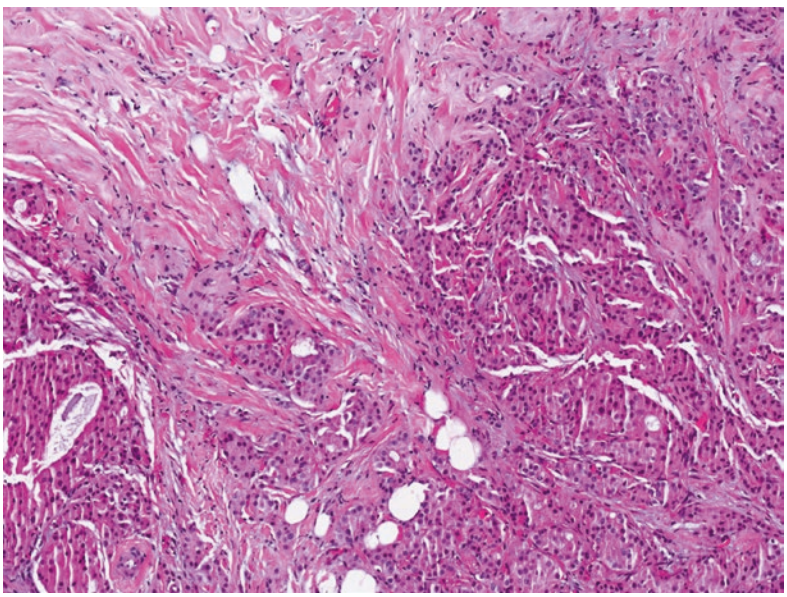

Fig. 2.22 Invasive apocrine carcinoma. Invading nests and trabeculae of tumour cells show ample pink cytoplasm with hyperchromatic nuclei

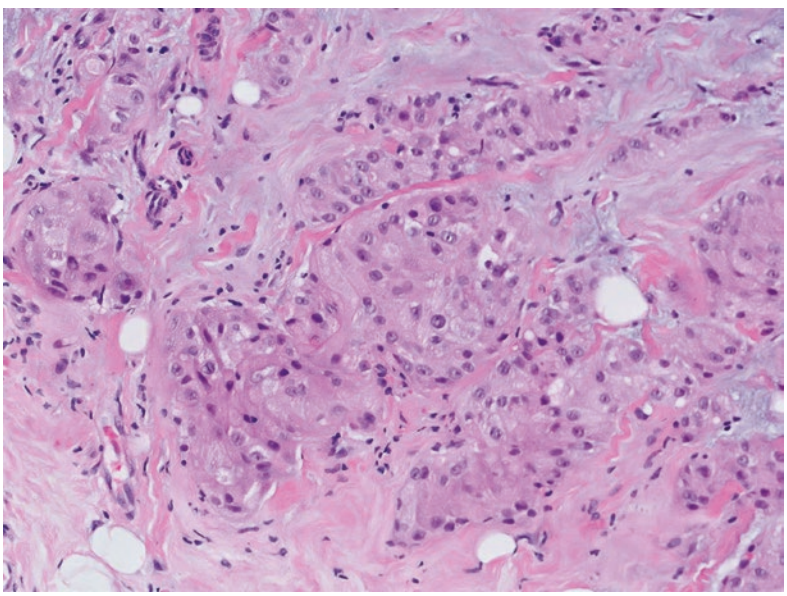

Fig. 2.23 Invasive apocrine carcinoma. High magnification of irregular islands of invading apocrine cells shows ample pink-to-pale, slightly vacuolated cytoplasm. The nuclei are vesicular and contain visible nucleoli

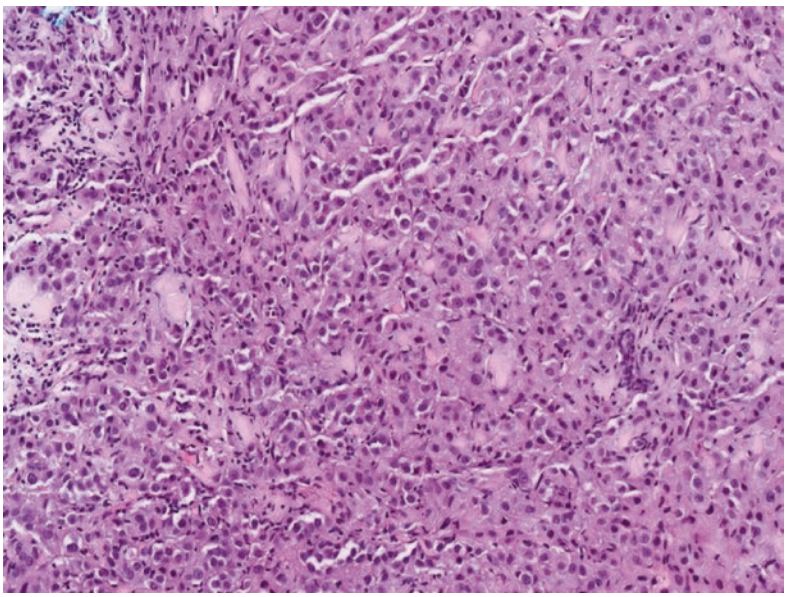

Fig. 2.24 Invasive apocrine carcinoma. Sheets of polygonal cells with pink cytoplasm are present

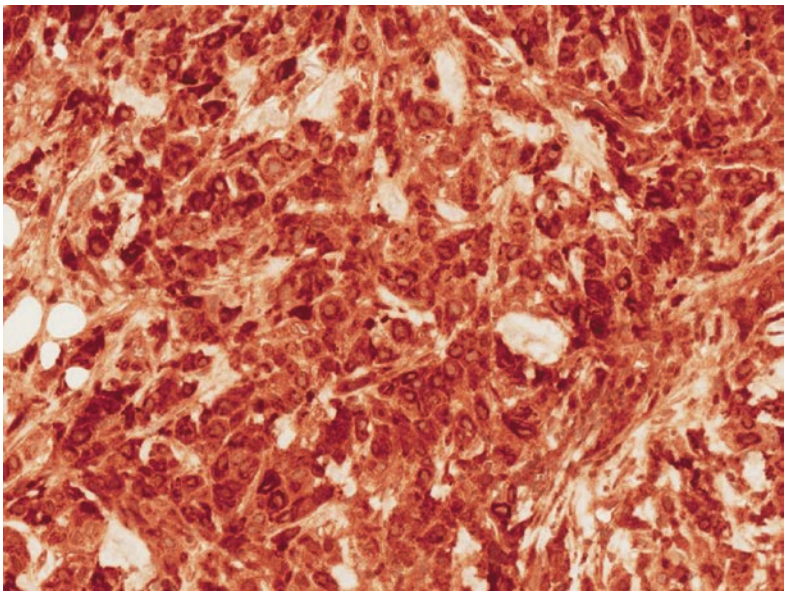

Fig. 2.25 Invasive apocrine carcinoma. GCDFP-15 immunohistochemistry shows diffuse cytoplasmic reactivity of tumour cells

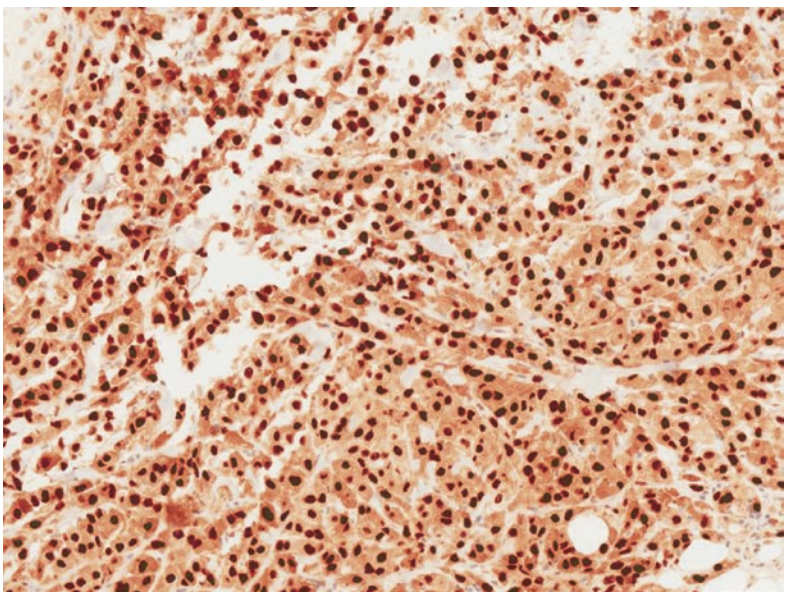

Fig. 2.26 Invasive apocrine carcinoma shows positive nuclear staining for androgen receptor. There is a light cytoplasmic blush, regarded as non-specific

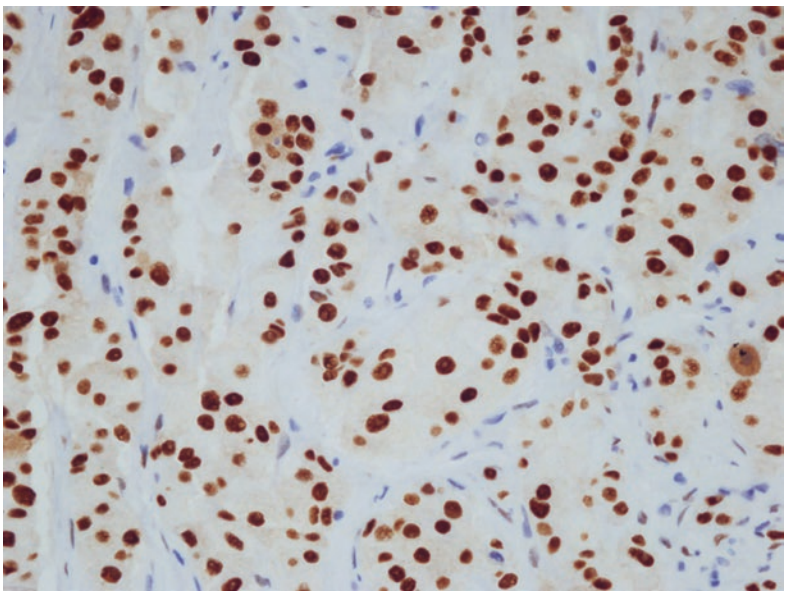

Fig. 2.27 Higher magnification of androgen receptor immunohistochemistry shows positive nuclear staining in tumour cells

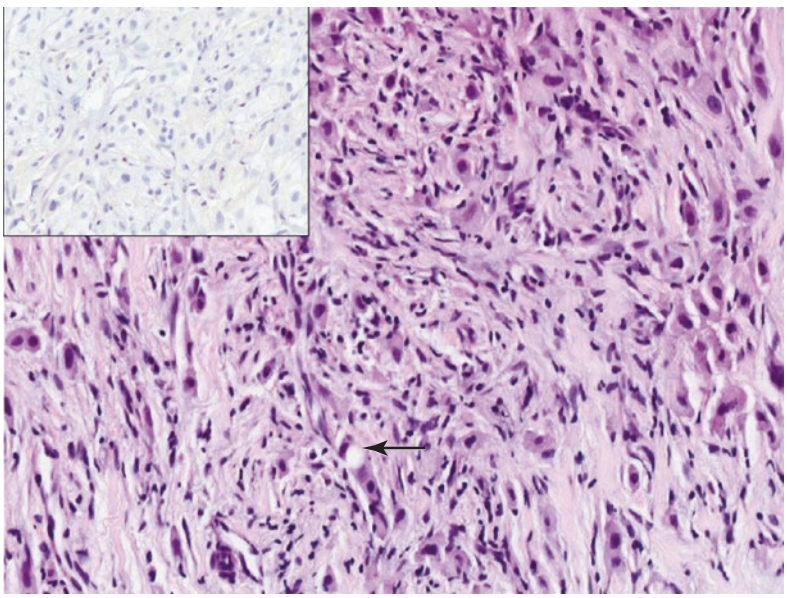

Fig. 2.28 Invasive lobular carcinoma with pleomorphic apocrine features. In this tumour, malignant cells with slightly discohesive appearances are seen within a fibrous stroma. One tumour cell also shows a cytoplasmic vacuole (*arrow*). Inset shows negative staining for E-cadherin on immunohistochemistry

Prognosis and Therapy Considerations

Duct ectasia is a benign self-limiting condition and no treatment is necessary in most cases. An excisional biopsy performed to establish the diagnosis can also help to alleviate any symptomatic discharge. Recurrence is not common. Duct ectasia is not associated with an increased risk for development of subsequent breast cancer.

Fat Necrosis

Definition

Fat necrosis can be defined as injury to adipose tissue of the breast that may be due to trauma, surgery, radiation, or other insults.

Clinical and Epidemiological Features

Traumatic fat necrosis tends to occur in pendulous breasts, with involvement of the superficial subcutaneous tissue as well. History of a traumatic episode may or may not be available. Clinical presentation can be with a painless breast lump, skin retraction, or dimpling. Thickening of the skin may be seen.

Imaging Features

Fat necrosis may manifest radiologically as a mass (Fig. 2.29), calcifications, or both. The mass is usually poorly defined, round to oval, and measures less than 2 cm. Less frequently, fat necrosis presents as a cystic, circumscribed, and radiolucent mass. Mammogram shows a lucent mass

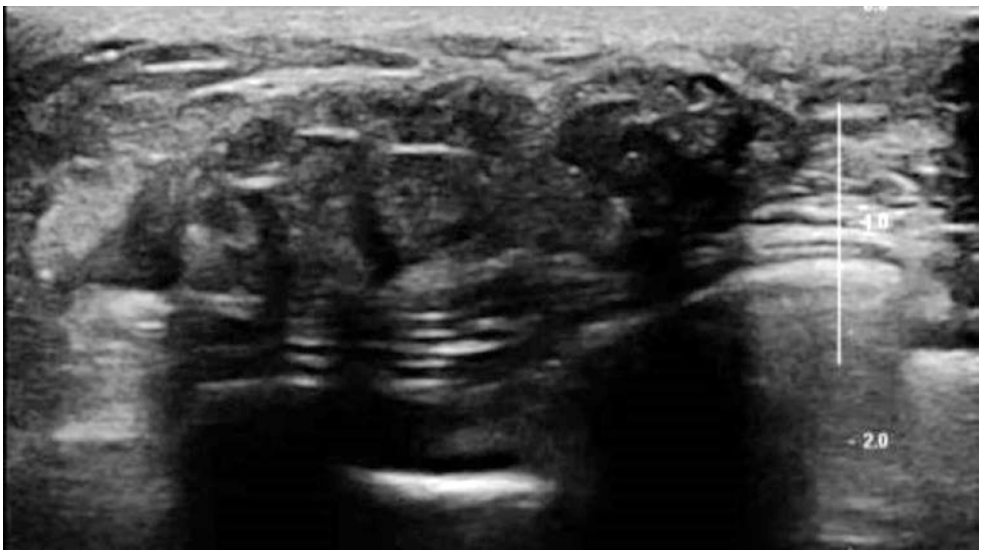

Fig. 2.29 Fat necrosis presenting as a lump in the chest wall, in a patient who previously underwent mastectomy and axillary clearance with a flap reconstruction for breast carcinoma. Ultrasound shows a lobulated heterogeneous mass within the flap that accounts for the palpable lump, radiologically mimicking breast carcinoma recurrence (Courtesy of Dr. Lester Leong)

with a diagnostic rim of eggshell calcifications. It may also be associated with coarse heterogeneous calcifications. If there is significant fibrosis, the lesion can appear spiculated and irregular. Fat necrosis has a spectrum of sonographic appearances that can evolve over time, appearing anechoic, complex solid–cystic, solid hypoechoic, and spiculated. MRI shows an enhancing mass with internal fat signal which is characteristically of low intensity on fat-suppression sequences.

Pathologic Features

Macroscopic Pathology

The gross appearance of fat necrosis depends on the duration of the lesion. Early lesions may appear haemorrhagic and indurated. After several weeks the breast parenchyma may appear yellow-grey. Cystic degeneration can occur with formation of large cystic lesions that sometimes contain oily or necrotic fluid.

Microscopic Pathology

Necrotic adipocytes show vacuolated cytoplasm with degenerate nuclei, often accompanied by foamy histiocytes and inflammatory cells in the intervening septa (Fig. 2.30). Foreign-body-type multinucleated giant cells, haemorrhage, and calcifications can be present. Coalescence of necrotic adipocytes may lead to an acellular cystic zone (Figs. 2.31 and 2.32). Breast ducts and lobules in proximity may demonstrate reactive atypia and squamous metaplasia (Figs. 2.33 and 2.34). If radiation therapy is the aetiology of the fat necrosis, cytological atypia and vascular changes secondary to radiation can occur.

Differential Diagnosis

Invasive Breast Carcinoma

Fat necrosis may be accompanied by nuclear atypia of degenerating adipocytes as well as reactive histiocytes and can be mistaken for invasive carcinoma, including the histiocytoid invasive lobular carcinoma. This is exacerbated in frozen sections especially in situations when intraoperative assessment of margins of wide excisions is practised. Fat necrosis of tissue around the prior biopsy cavity may be sampled as a margin and may thus be erroneously interpreted as positive (Fig. 2.35).

Metaplastic Carcinoma

Squamous metaplasia of ducts and acini in the immediate vicinity of fat necrosis may resemble invasive carcinoma with squamous (metaplastic) features (Fig. 2.36). Reactive nuclear atypia may aggravate this appearance. Caution should be exercised when interpreting epithelial islands at the edge of fat necrosis or granulation.

Prognosis and Therapy Considerations

Fat necrosis is self-limiting and will resolve, but concern for cancer on clinicoradiological findings often leads to excision for histologic evaluation.

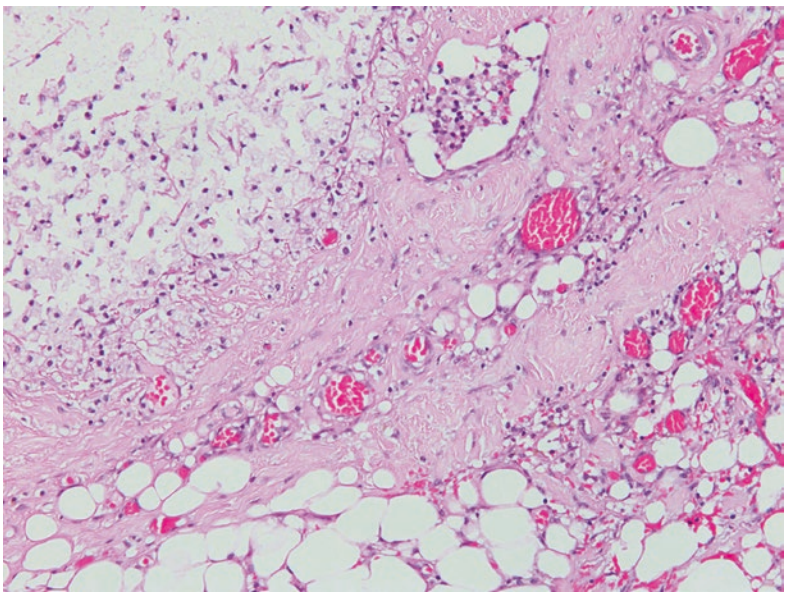

Fig. 2.30 Fat necrosis with foamy histiocytes in the wall of a previous biopsy cavity. Congestion and necrotic adipocytes are seen in the right lower field, while a collection of histiocytes is observed in the left upper field. A dilated lymphovascular channel shows several lymphocytes and histiocytes

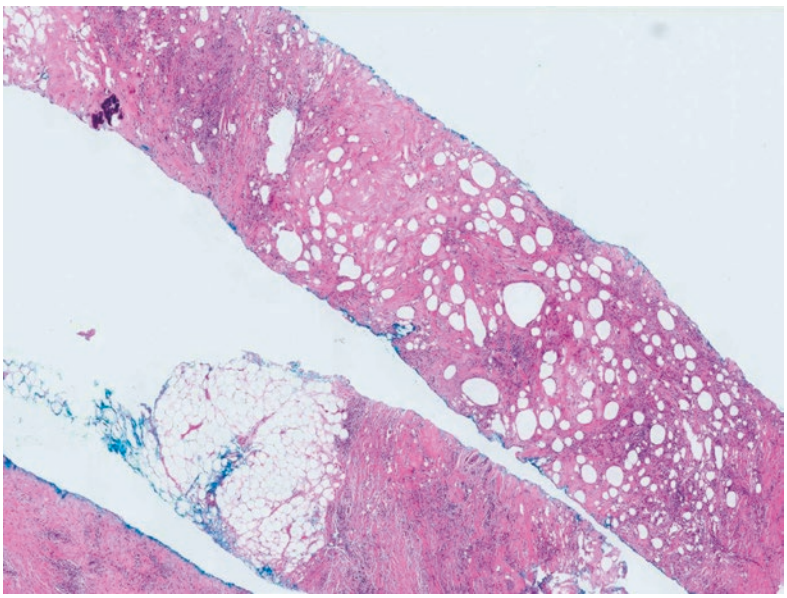

Fig. 2.31 Fat necrosis. Core biopsies of a radiologically worrisome lesion at the site of previous surgery. Low magnification shows fibrosis, chronic inflammation, and fat necrosis, with degenerate adipocytes and some cystic spaces. Coarse calcifications are present in one core

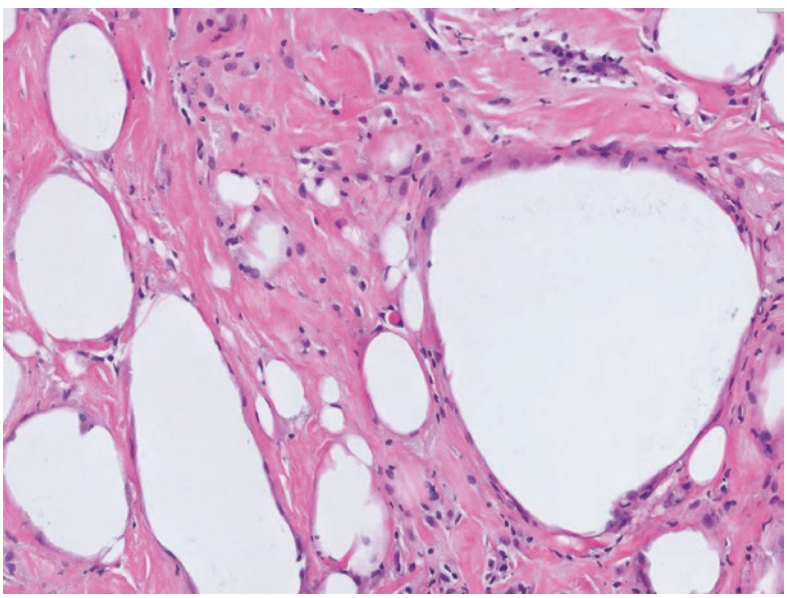

Fig. 2.32 Fat necrosis. Coalescence of degenerate adipocytes leads to acellular microcysts that are lined by histiocytes and fibrosis

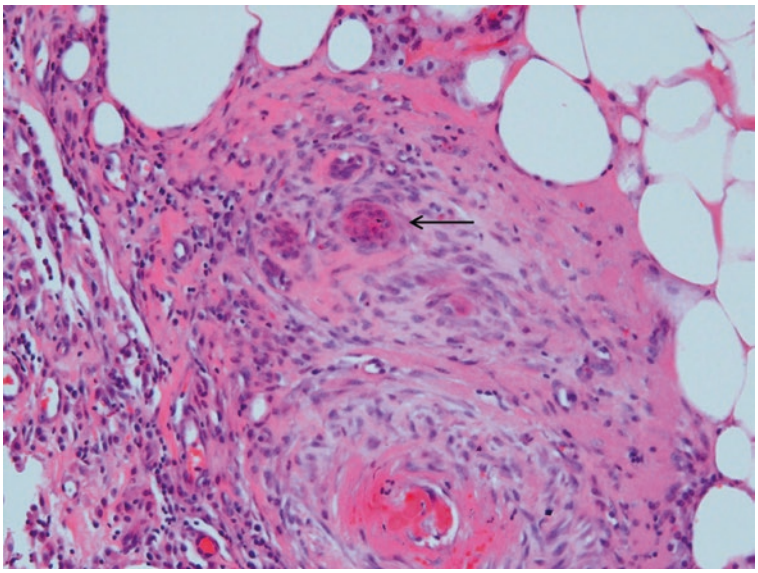

Fig. 2.33 Fat necrosis with squamous metaplasia in ductules of an adjacent lobule. One of the ductules (*arrow*) shows a whorl-like appearance with effacement of the lumen, composed of cells with pink cytoplasm

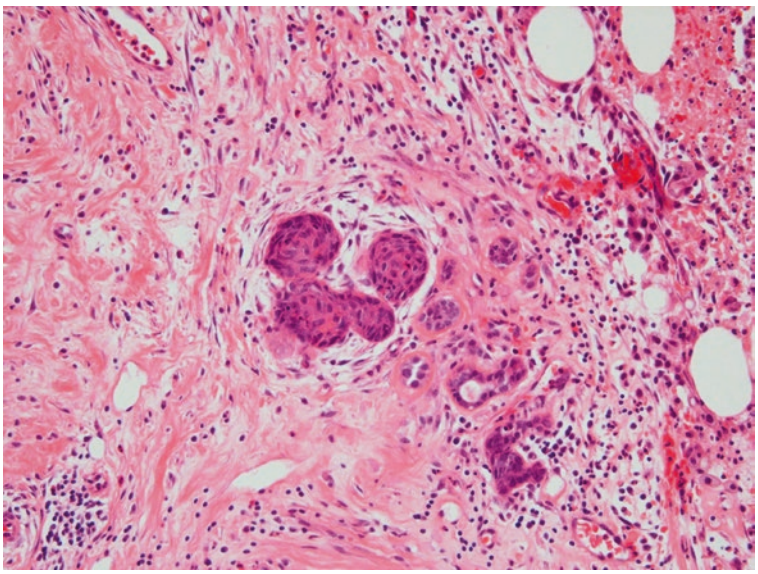

Fig. 2.34 The lobule lying adjacent to chronic inflammation and fibrinous material of the prior biopsy cavity shows a few ductules with squamous metaplasia, while the remaining ductules of the same lobule are not affected

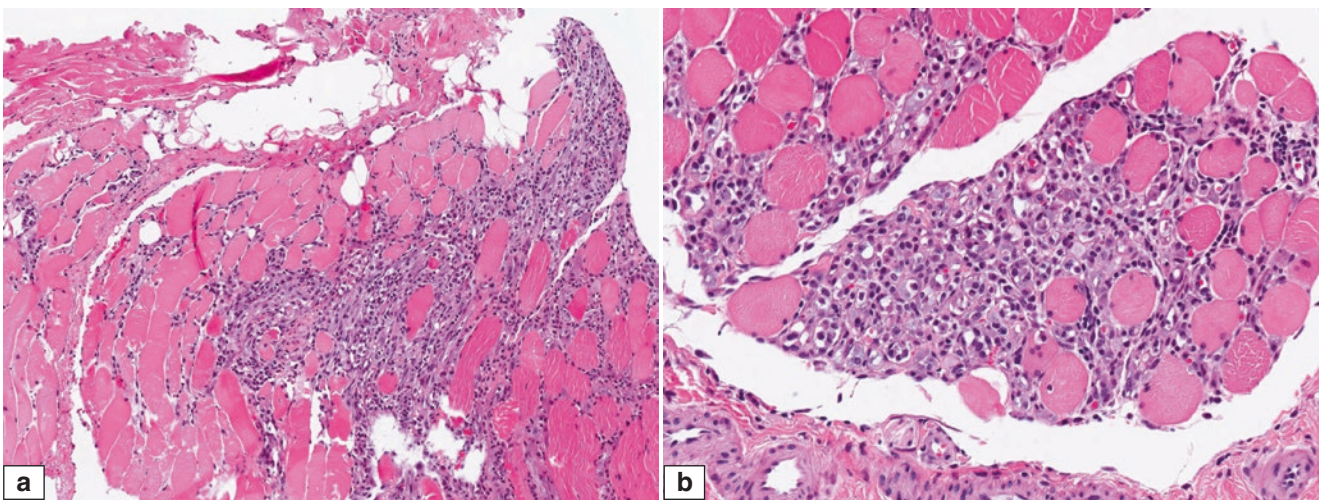

Fig. 2.35 (**a**) Histiocytes among skeletal muscle fibres, occurring in sheets and effacing muscle fibres. The irregular involvement may resemble the permeative nature of an invasive carcinoma. (**b**) Histiocytes among skeletal muscle fibres at the base of a breast resection mimicking carcinoma. The presence of granulation and fat necrosis in the vicinity, as well as accompanying inflammatory cells, are clues to the reactive and inflammatory origin of the cells

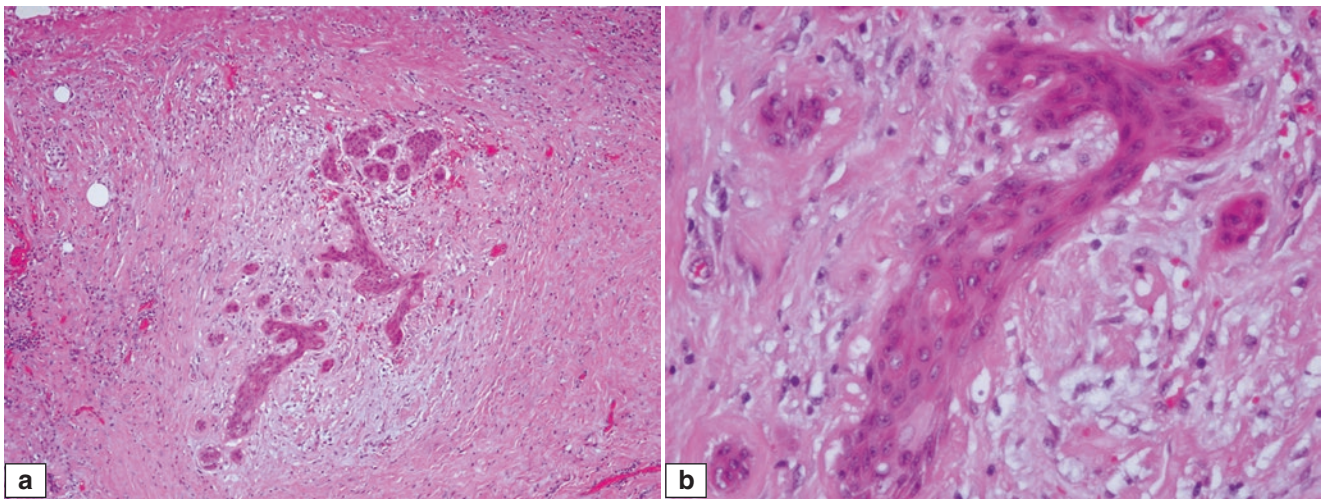

Fig. 2.36 (**a**) Squamous metaplasia of a lobule in the fibrous vicinity of fat necrosis. Note the retained lobular architecture at low magnification, with the solidified terminal ducts and ductules replaced by metaplastic squamous cells with pink cytoplasm. This may be mistaken for residual metaplastic carcinoma in a cavity wall. (**b**) Squamous metaplasia adjacent to fat necrosis. High magnification of ducts with squamous metaplasia shows a pavemented appearance of the polygonal cells with pink cytoplasm, intercellular windows and a semblance of intercellular bridges. The mild reactive nuclear atypia may raise concern for a neoplastic process, especially with the small epithelial nests in the stroma. Clues to the benign nature are the lobulocentricity, adjacent fat necrosis and inflammation, reactive nature of the atypia evidenced by the smooth nuclear contours and small nucleoli, and lack of high-grade atypia

Mastitis

Definition

Mastitis is a broad term that refers to inflammation in the breast. It can be further specified to define different forms of mastitis, such as puerperal and granulomatous lobular mastitis. The term 'plasma cell mastitis' has been used to refer to duct ectasia. The aetiology of granulomatous lobular mastitis is unknown, and it is a diagnosis of exclusion after other specific causes of granulomatous inflammation in the breast have been ruled out.

Clinical and Epidemiological Features

Puerperal mastitis occurs in the post-partum period, usually a few weeks after the onset of lactation and breast-feeding, with *Staphylococcus aureus* from the skin being the most frequent aetiological organism. Both plasma cell mastitis and granulomatous lobular mastitis are also described to occur post-pregnancy, though overlapping terminologies may account for these reports. There can be redness and warmth of the skin over the breast that mimic inflammatory breast carcinoma.

Imaging Features

Signs of soft tissue oedema and hyperaemia, as well as thickening of the overlying skin, can be observed. There may also be dilated ducts with internal echoes and wall thickening.

Pathologic Features

Macroscopic Pathology

Gross appearances are variable with soft-to-firm areas depending on the proportion of inflammatory cells to fibrous stroma, the latter seen in more chronic lesions (Fig. 2.37).

Microscopic Pathology

Histologically, puerperal mastitis shows acute and chronic inflammation, sometimes with abscess formation (Figs. 2.38 and 2.39). Plasma cell mastitis shows a predominance of plasma cells, while in granulomatous lobular mastitis, the granulomas are lobulocentric, often contain neutrophils, and are non-necrotising (Figs. 2.40 and 2.41). Coalescence of granulomas may obscure the appearance of lobulocentricity. Multinucleated giant cells of Langhans type, epithelioid histiocytes, and lymphocytes contribute to the granulomas.

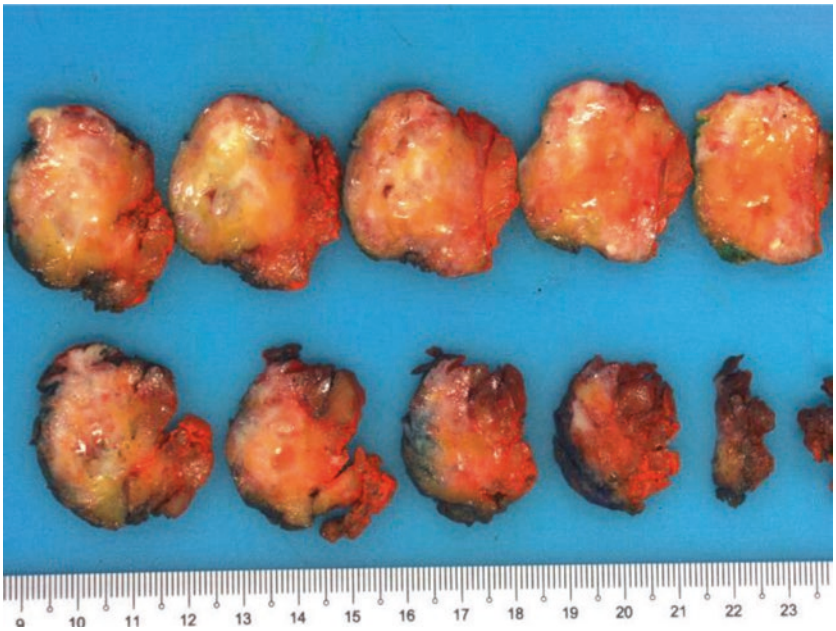

Fig. 2.37 Mastitis. Gross sections of a breast excision which showed mastitis on histology. Macroscopically, there are whitish fibrous areas interspersed with yellowish tan zones, with a few scattered small cystic foci

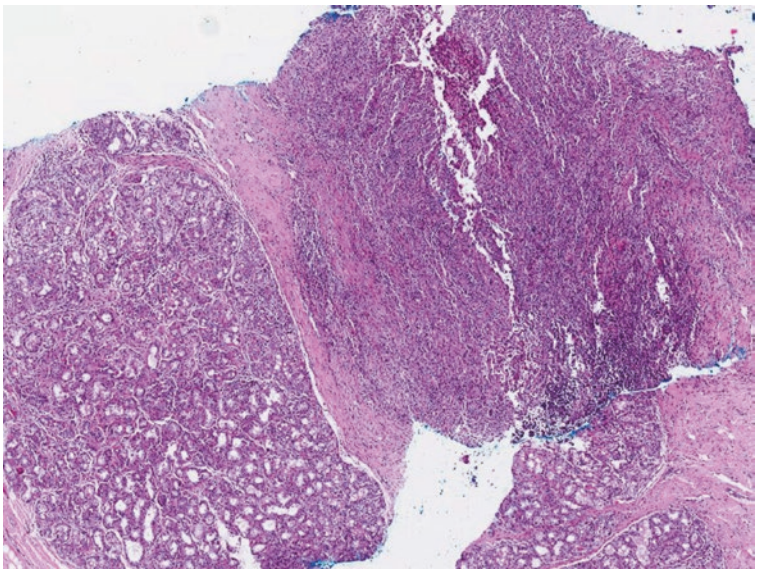

Fig. 2.38 Puerperal mastitis. Lactational hyperplasia with enlarged lobules demonstrating secretory activity is seen adjacent to a collection of inflammatory cells in this core biopsy

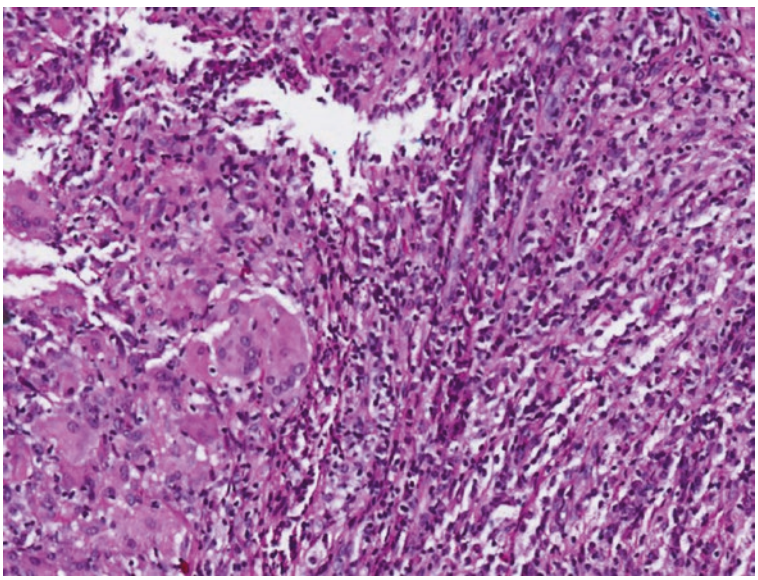

Fig. 2.39 Puerperal mastitis with granulomatous inflammation. Closer scrutiny shows foreign-body-type multinucleated giant cells as well as epithelioid histiocytes among chronic inflammatory cells of lymphocytes and plasma cells, admixed with some polymorphs. The giant-cell reaction is likely related to disrupted ducts with their contents evoking a foreign-body tissue response

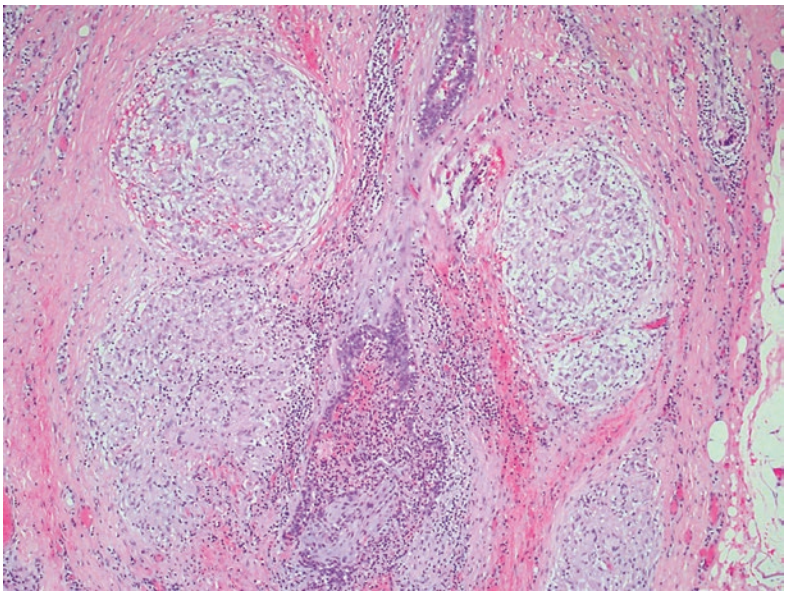

Fig. 2.40 Granulomatous lobular mastitis. Epithelioid granulomas are seen flanking a terminal ductal lobular unit

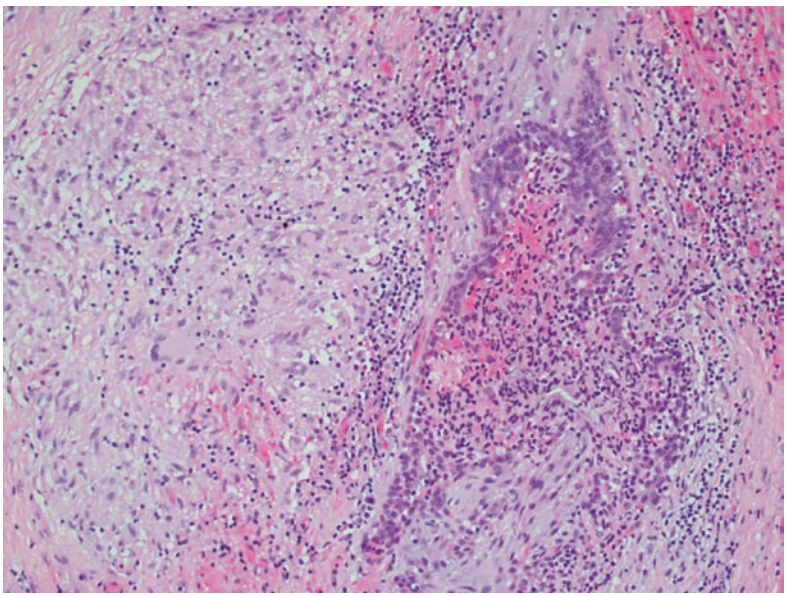

Fig. 2.41 Granulomatous lobular mastitis. Higher magnification shows a non-necrotising granuloma in the breast tissue adjacent to a duct which is partially effaced by inflammatory cells. Several Langhans type multinucleated giant cells are seen among the epithelioid histiocytes

Differential Diagnosis

Periductal Mastitis with Granulomas

In contrast to granulomatous lobular mastitis, the granulomas in periductal mastitis are consequent to disrupted duct contents and hence represent a foreign-body-type reaction (Figs. 2.42, 2.43, and 2.44). Periductal mastitis has been used synonymously with duct ectasia.

Infective Granulomatous Inflammation

Infections from tuberculous, fungal, and parasitic organisms can cause granulomatous inflammation in the breast. Both tuberculous- and fungal-related granulomas are often associated with necrosis. The organisms may be identified through Ziehl–Neelsen and fungal stains, as well as through cultures or molecular studies (Figs. 2.45 and 2.46).

Necrotising Granulomatous Vasculitis

Vasculitis may rarely involve the breast, usually as part of systemic manifestations of diseases such as Wegener's granulomatosis and polyarteritis nodosa. In Wegener's granulomatosis, necrotising granulomas may be seen in conjunction with vascular inflammation. In contrast, the granulomas in granulomatous lobular mastitis are non-necrotising and are not associated with vasculitis (Fig. 2.47).

Sarcoidosis

This is a rare lesion in the breast and is recognised in the context of an established diagnosis of sarcoidosis. Sarcoidal granulomas are non-necrotising and usually tight and well formed, with epithelioid histiocytes accompanied by lymphocytes. Asteroid and Schaumann bodies may be present.

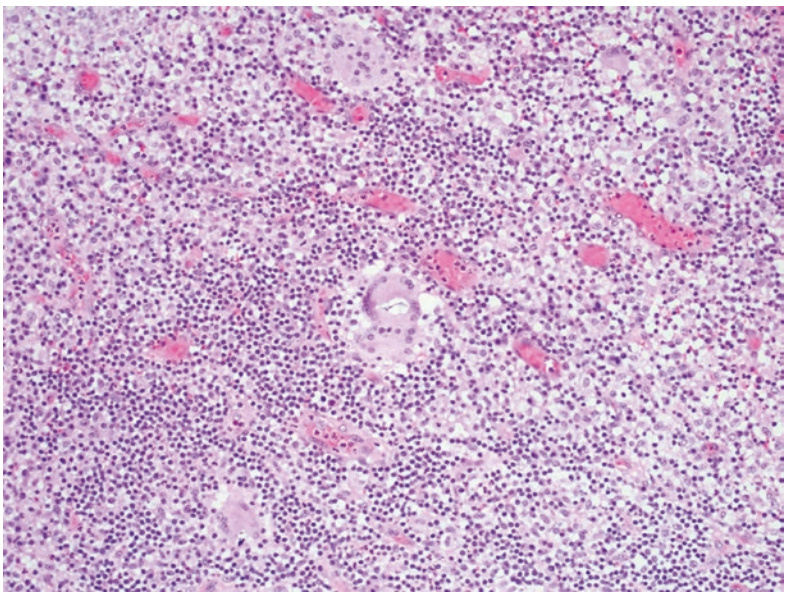

Fig. 2.42 Granulomatous mastitis. Foreign-body-type multinucleated giant cells enclose foreign material within the cytoplasm, surrounded by lymphocytes, plasma cells, and histiocytes. Many cases of granulomatous mastitis are secondary to inflammation of ducts with the giant-cell response due to a reaction to disrupted duct contents. A diagnosis of idiopathic granulomatous lobular mastitis is one of exclusion, after more common causes of granulomatous mastitis have been ruled out

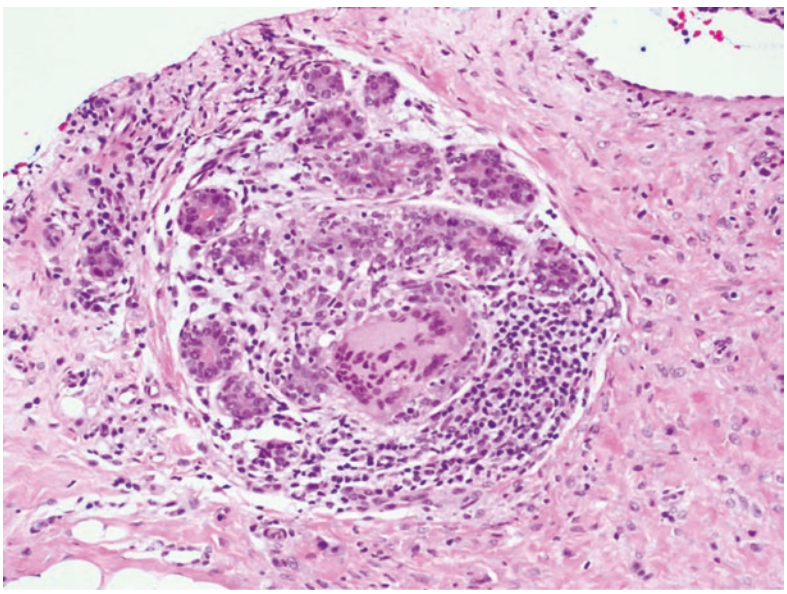

Fig. 2.43 Granuloma within a lobule, with a multinucleated giant cell among lymphocytes and plasma cells

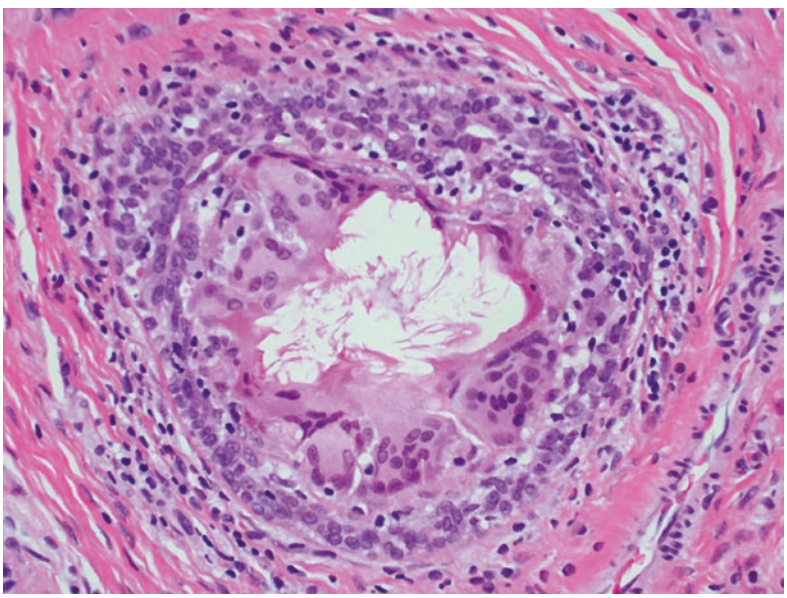

Fig. 2.44 Foreign-body-type multinucleated giant cells enclosing wispy foreign material, effacing a duct where the epithelial cells appear to surround and frame the foreign-body giant cells

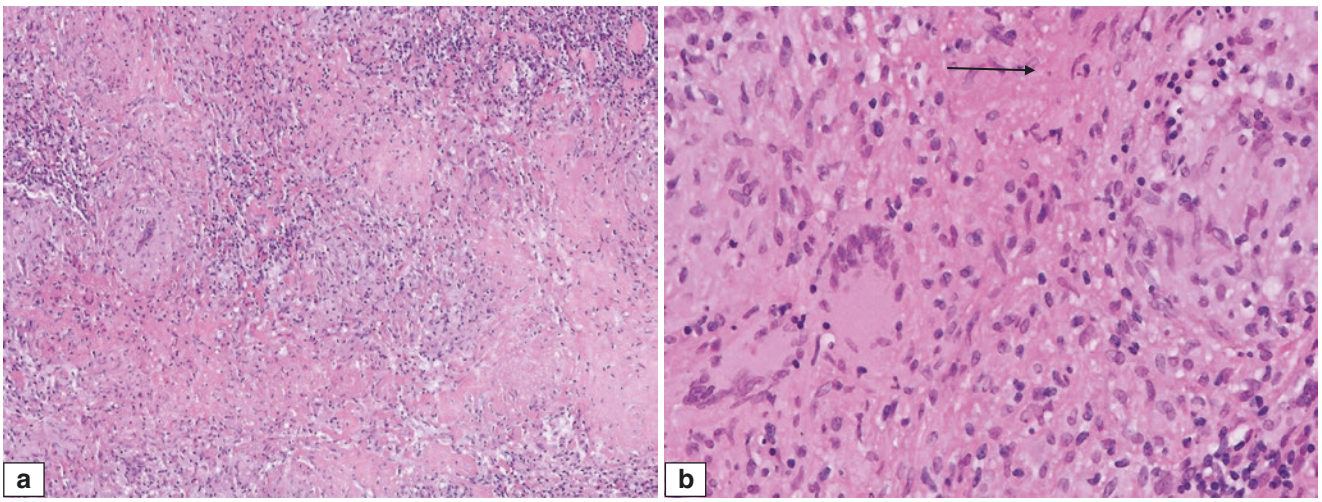

Fig. 2.45 (**a**) Necrotising granulomatous inflammation in the breast from mycobacterial infection, with epithelioid histiocytes and Langhans-type multinucleated giant cells accompanied by lymphocytes and zones of necrosis. (**b**) High magnification shows Langhans-type multinucleated giant cells, slipper shaped epithelioid histiocytes and scattered lymphocytes. Pink amorphous material with karyorrhexis (*arrow*) representing necrosis is present

Fig. 2.46 An acid-fast bacillus is seen on the Ziehl–Neelsen stain confirming mycobacterial infection

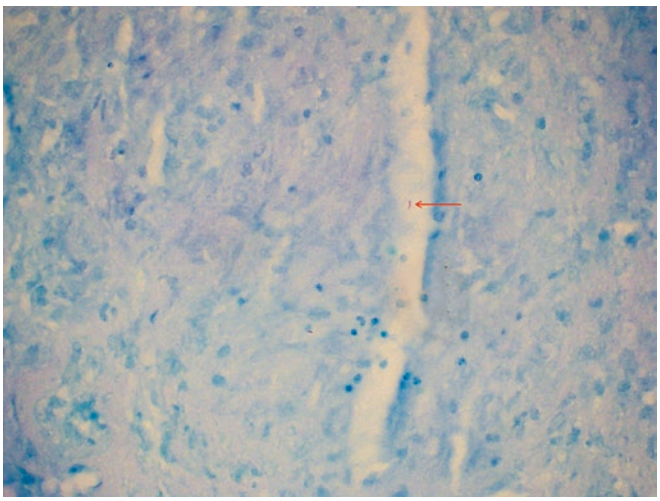

Carcinoma-Related Granulomas

Granulomas may be seen adjacent to in situ and invasive breast carcinoma (Fig. 2.48). They are usually small and composed of small clusters of histiocytes with occasional foreign-body-type multinucleated giant cells.

Silicone Granuloma

A foreign-body-type multinucleated giant-cell reaction can be seen around either injected free silicone or silicone leaked from implants (Figs. 2.49 and 2.50). Around intact implants, a synovial-type lining can be present (Figs. 2.51 and 2.52).

Prognosis and Therapy Considerations

Granulomatous lobular mastitis is usually cured through excision, though steroids have been used to treat this condition [6].

Diabetic Mastopathy (Sclerosing Lymphocytic Lobulitis)

Definition

Diabetic mastopathy or sclerosing lymphocytic lobulitis refers to a constellation of pathological changes in the breast possibly resulting from abnormalities in glycosylation and collagen degradation in patients with diabetes. Other synonymous terms are diabetic fibrous breast disease, fibrous mastopathy, lymphocytic mastitis and fibrosis, and lymphocytic lobulitis. Originally described in patients with insulin-dependent type 1 diabetes mellitus, particularly in patients with microvascular complications, similar histological alterations have been documented in other conditions such as Hashimoto's thyroiditis, hypothyroidism, and autoimmune diseases such as systemic lupus erythematosus and Sjogren's disease. Isolated cases of sclerosing lymphocytic lobulitis without diabetes or autoimmune disease have rarely been reported.

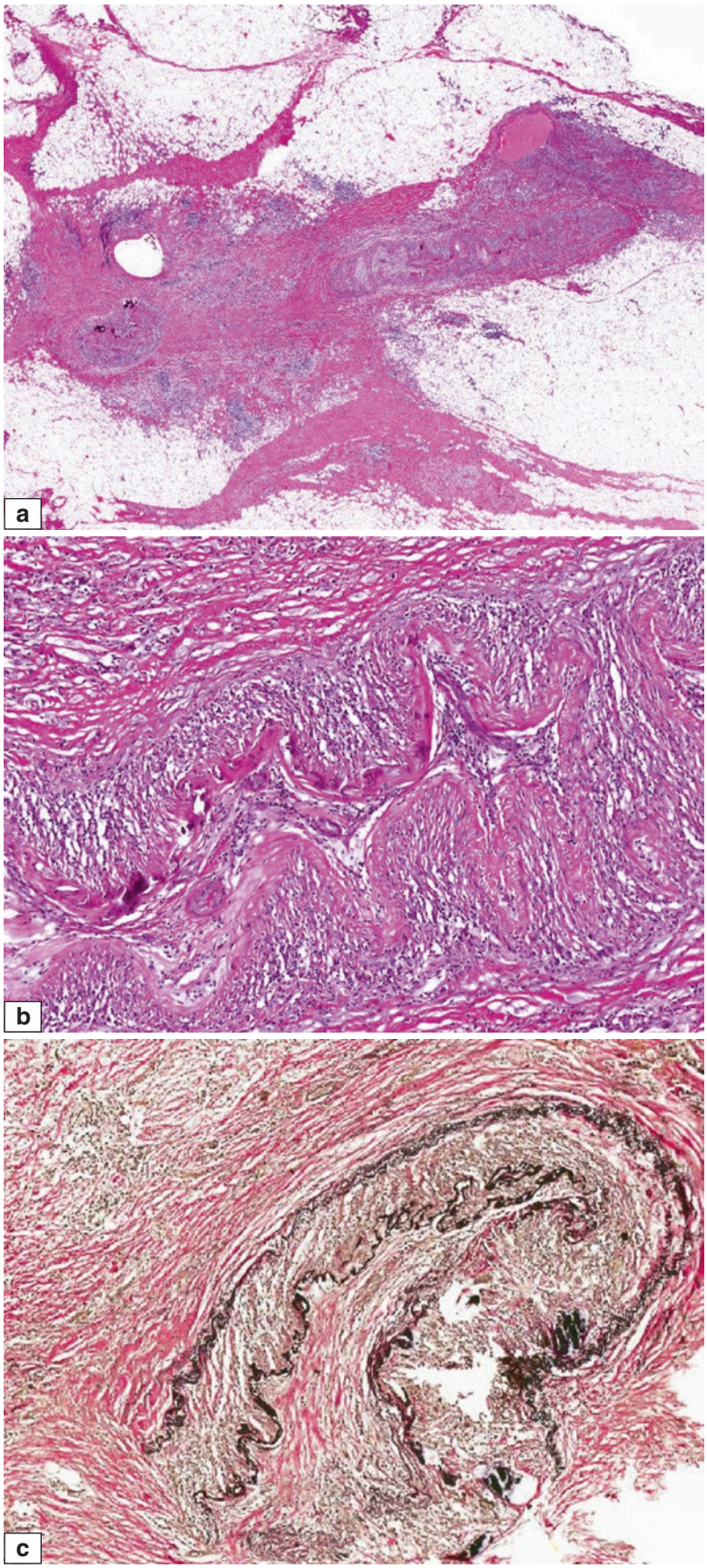

Fig. 2.47 Vasculitis in the breast. (**a**) This was an excision for a radiologically detected nodule in the breast post wide excision and radiation treatment for prior breast carcinoma. At low magnification, part of the wall of a blood vessel cut longitudinally is present in a fibrotic stroma, accompanied by patchy chronic inflammation. (**b**) Higher magnification shows calcifications with intimal fibrosis and inflammatory cells in the vascular wall. (**c**) Elastic van Gieson stain shows fragmentation and reduplication of the internal elastic lamina of the partially destroyed vessel

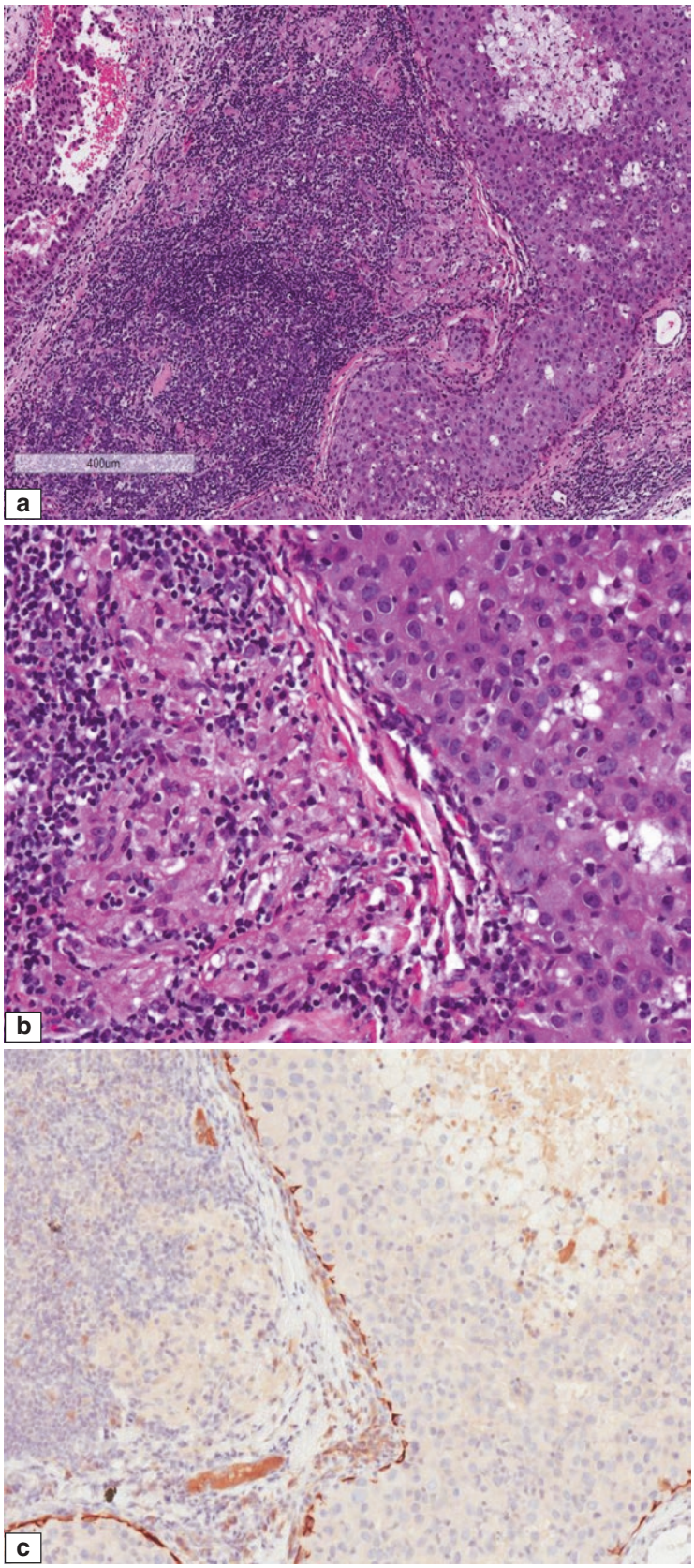

Fig. 2.48 Epithelioid granuloma adjacent to DCIS. (**a**) Low magnification shows a fairly dense lymphocytic infiltrate in the stroma in between two ducts affected by DCIS. (**b**) At high magnification, a collection of epithelioid histiocytes admixed with lymphocytes and plasma cells is observed just adjacent to the wall of an affected duct containing intermediate nuclear grade DCIS. Several scattered lymphocytes are also seen among the DCIS cells. (**c**) Immunohistochemistry for CK5/6 shows positive staining of the peripheral rim of myoepithelial cells around the duct with DCIS, while the epithelioid histiocytes are negative. Sometimes, epithelioid histiocytes may mimic epithelial cells raising suspicion of microinvasion; however their folded gentle nuclei, delicate cytoplasm with ill-defined borders, admixed lymphocytes and lack of keratin immunostaining are helpful features to make the distinction

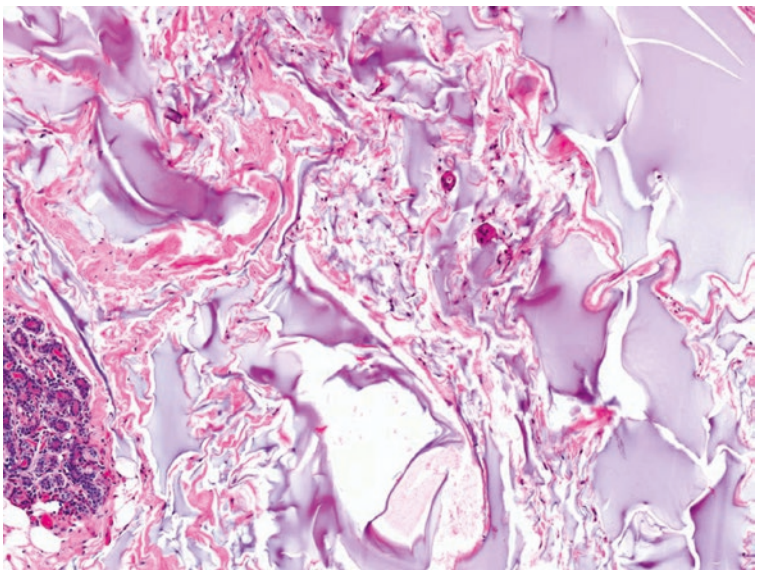

Fig. 2.49 Foreign-body giant-cell reaction to polyacrylamide gel injection for breast augmentation. Note the bluish-tinged acellular material that may mimic mucin of mucinous breast lesions

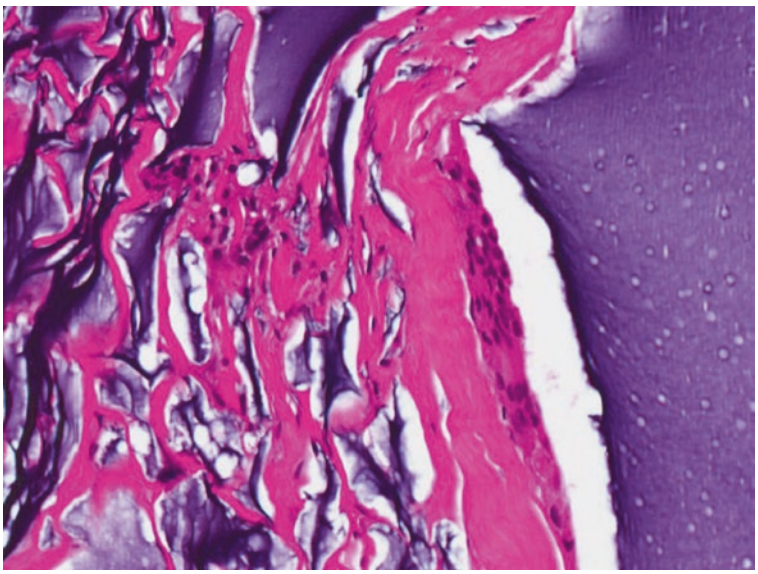

Fig. 2.50 Foreign-body giant-cell reaction to polyacrylamide gel injection. High magnification of extracellular foreign material, partially rimmed by foreign-body-type multinucleated giant cells

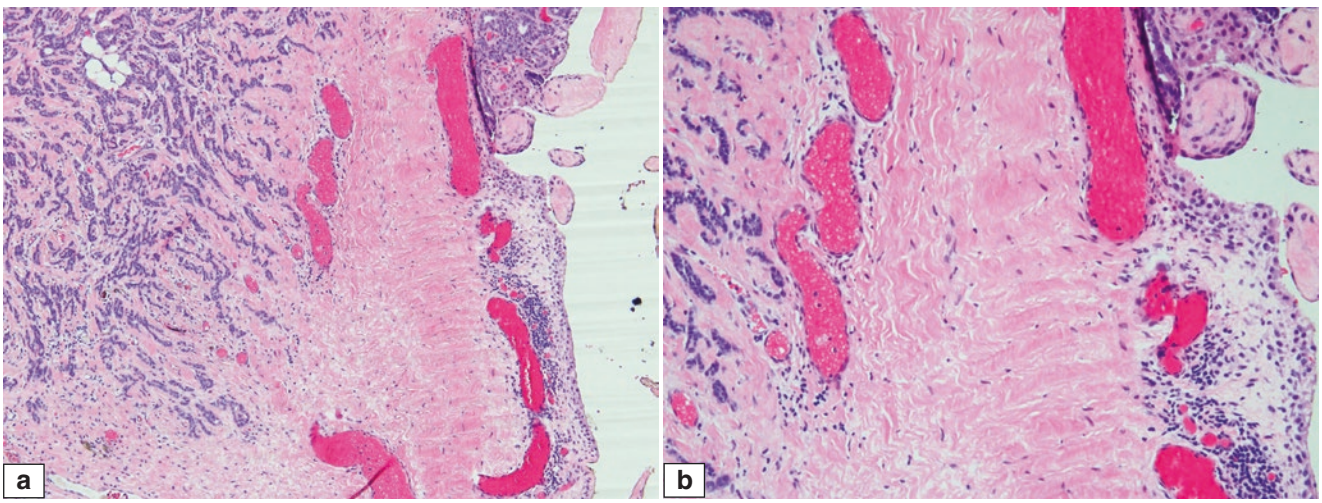

Fig. 2.51 Silicone implant wall (*right*) with a synovial-type lining. (**a**) There is an invasive ductal carcinoma in the tissue adjacent to the implant wall. (**b**) Higher magnification shows the synovial-type cells resembling histiocytes rimming the wall of the implant. A few cords and nests of invasive carcinoma cells are seen in the adjacent stroma

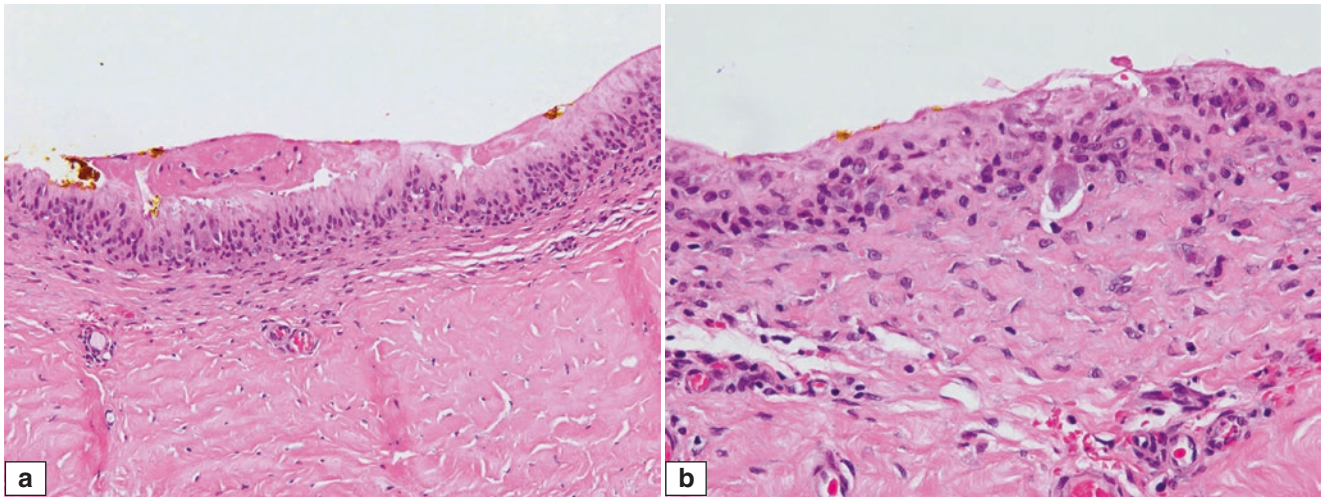

Fig. 2.52 Silicone implant wall. (**a**) Synovial metaplasia is seen, comprising synoviocyte-like cells resembling histiocytes, that line the wall of the implant. (**b**) Higher magnification shows histiocyte-like synovial-type lining cells, interspersed with occasional lymphocytes. Some of the synovial-type cells may appear multinucleated

Clinical and Epidemiological Features

Diabetic mastopathy most often occurs in young premenopausal women, with rare cases reported in men. It can be seen in both type 1 and type 2 diabetics, although it is more frequently associated with type 1 insulin-dependent cases. Patients may present clinically with a painless breast lump that is often single and unilateral. Multiple and bilateral lesions may occur.

Imaging Features

Imaging shows dense parenchyma with indistinct borders that may be diffuse or focal. It especially mimics malignancy on ultrasound examination because of its ill-defined hypoechoic mass-like appearance with posterior acoustic shadowing. Biopsy is frequently required to exclude malignancy.

Pathologic Features

Macroscopic Pathology

The gross appearance is of firm-to-hard fibrous tissue with a greyish-white cut surface and ill-defined borders. A distinct nodule is not seen.

Microscopic Pathology

Diabetic mastopathy shows marked fibrosis and collagenous stroma that can appear keloidal. Interspersed acellular pale collagen is seen. Lymphocytic lobulitis with lymphocytes within the lobules, around ducts and ductules, is a key histologic feature. Lymphocytes may also be observed around vessels and nerves (Fig. 2.53).

Immunohistochemical characterisation reveals predominantly mature B-lymphocytes with a small population of T cells and, rarely, plasma cells. Germinal centres are not typically present. Involved lobules may be atrophic or unremarkable. Plump myofibroblasts referred to as epithelioid myofibroblasts are seen (Fig. 2.54), initially thought to be specific for diabetes. These cells have abundant cytoplasm and oval vesicular nuclei resembling histiocytes. In contrast to histiocytes, which are typically found in small groups, epithelioid myofibroblasts tend to be individual cells isolated from one another by dense collagen. Later, these epithelioid myofibroblasts were reported in nondiabetic patients and are noted to be absent in a quarter of cases with diabetes. They need to be distinguished from multinucleated stromal giant cells that have multiple hyperchromatic nuclei and scant cytoplasm, which are incidentally found in benign breast tissue.

Differential Diagnosis

Fibrous Scar

Reparative fibrosis from a variety of causes may lead to an appearance reminiscent of the collagenous bundles in diabetic mastopathy. Accompanying chronic inflammation secondary to scarring may also mimic lymphocytic lobulitis, though this tends to be more patchy, dispersed, and not lobulocentric. The presence of haemosiderin and absence of epithelioid myofibroblasts in fibrous scarring may be helpful distinguishing features. Postsurgical scarring may demonstrate a foreign-body giant-cell response (Fig. 2.55).

Fibromatosis

Fibromatosis, a locally infiltrative lesion, shows sweeping fascicles of fibroblasts and myofibroblasts with accompanying collagen that at low magnification may resemble the

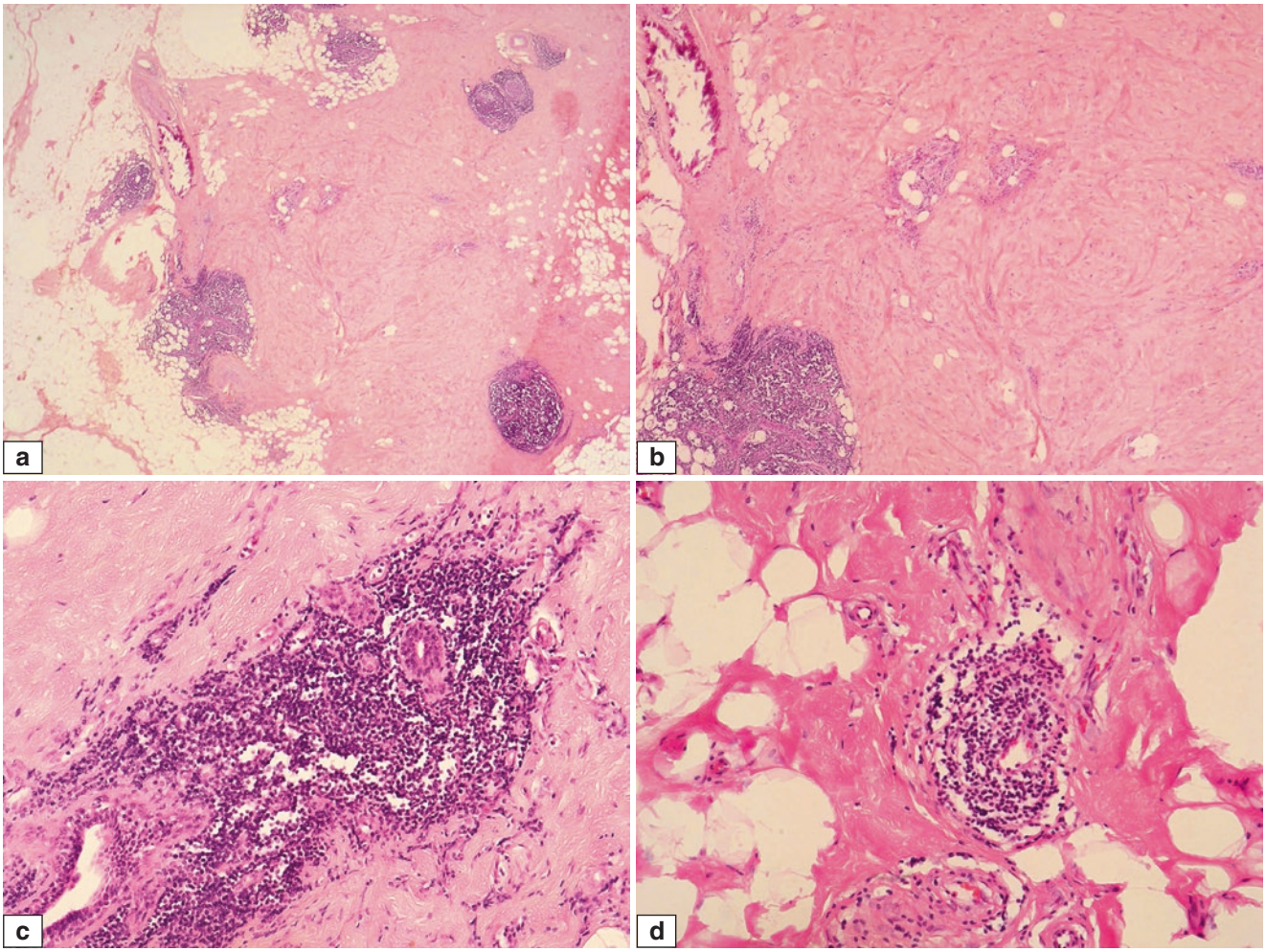

Fig. 2.53 Diabetic mastopathy. (**a**) Low magnification shows broad expanses of fibrous parenchyma with scattered collections of chronic inflammatory cells. Calcifications are also present. (**b**) Medium magnification shows pink keloidal-type collagen in narrow bundles among paler pink zones. The lymphocytic collections are centred within a lobule, although the lobule is not readily appreciated at low magnification, being obscured by the lymphocytic infiltrate. (**c**) Lymphocytic lobulitis shows relatively dense aggregates of lymphocytes within a lobule, surrounding the terminal duct and ductules. (**d**) Lymphocytes are seen around a small blood vessel as well

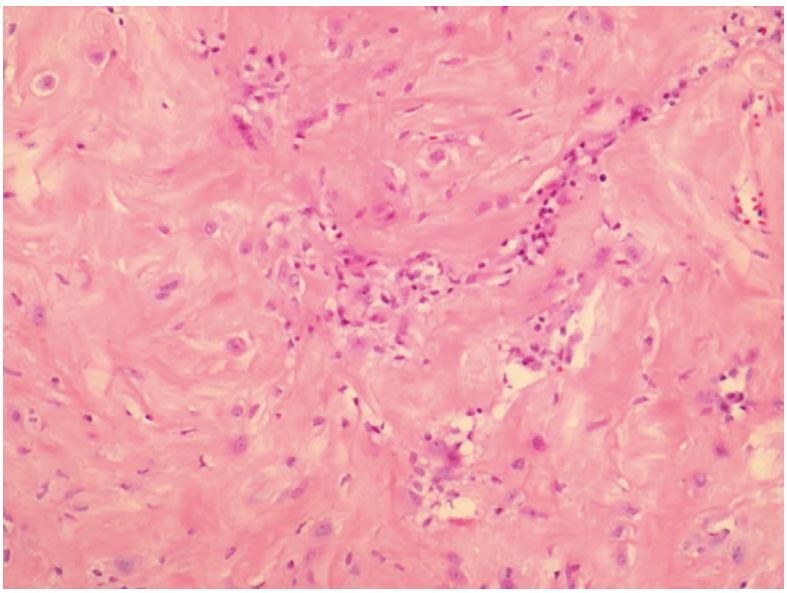

Fig. 2.54 Diabetic mastopathy. Plump epithelioid myofibroblasts are individually dispersed in the stroma, together with several lymphocytes

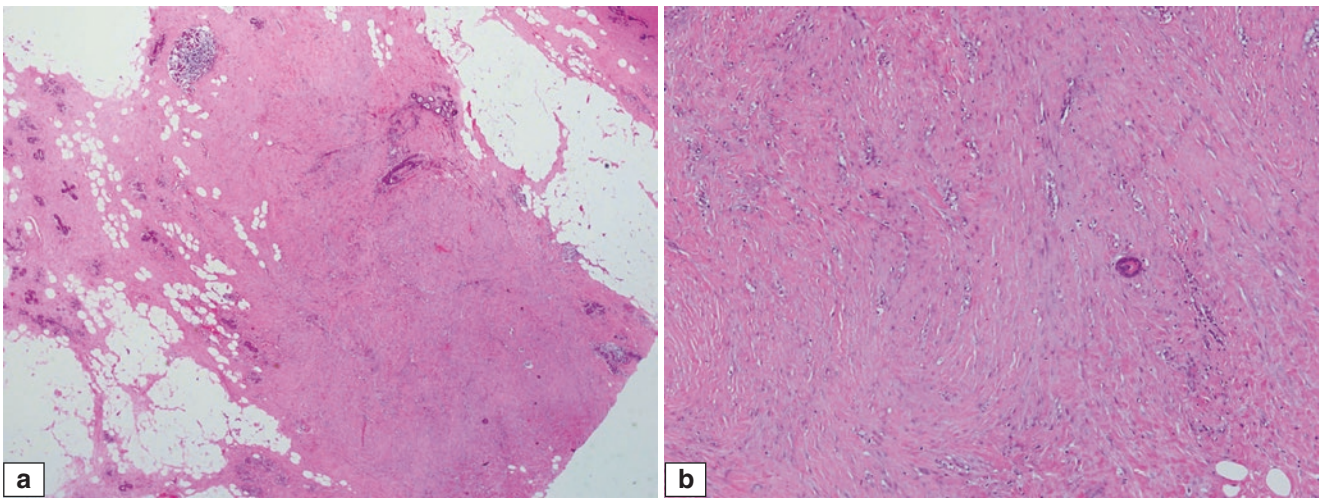

Fig. 2.55 Postoperative fibrosis (nine weeks after surgical biopsy). (**a**) Low magnification shows a zone of fibrosis with loss of breast lobules. Together with a few scattered lymphocytes, which are seen in lobules as well, there is a resemblance to diabetic mastopathy. Clinical information of prior biopsy, presence of haemosiderin deposits, granulation, fat necrosis, and foreign-body giant-cell reaction, assist in making the distinction. (**b**) Slightly wavy collagen fibres are seen as part of the reparative fibrosis from previous biopsy. A small epithelial nest is entrapped within the fibrosis. When the prior instrumentation or surgery is remote, granulation or fat necrosis may not be present. In such cases, the clinical history is key. The waviness and pallor of the collagen occurring in a broad band-like manner with haemosiderin deposits may be helpful

collagenous fibrosis of diabetic mastopathy. In fibromatosis, however, there is usually a waviness to the nuclei, and the spindle cell proliferation has a permeative front with extension in between lobules (Fig. 2.56). Lymphocytic lobulitis is usually absent in fibromatosis. If needed, immunohistochemistry for nuclear beta-catenin staining may be helpful in corroborating a diagnosis of fibromatosis, although it is not specific (Fig. 2.57).

Amyloid

Pale amorphous amyloid may superficially resemble the collagenous stroma of diabetic mastopathy. Amyloid, however, is clumpy with a pale colouration as compared to diabetic mastopathy, which shows pink, smooth, and sometimes hyalinised keloidal collagen. Foreign-body-type giant cells may be seen around amyloid, which also accumulates in lobules and perivascular locations (Figs. 2.58 and 2.59). Amyloid can extend into adipose septa forming amyloid rings (Fig. 2.60). Congo red staining with apple-green birefringence on polarised optics confirms amyloidosis.

IgG4-Related Sclerosing Mastitis

IgG4-related disease is a recently recognised disorder characterised by the formation of inflammatory pseudotumours in various organs due to dense sclerosis and lymphoplasmacytic infiltrates associated with increased serum IgG4 levels. The disease characteristically affects exocrine glands (pancreas, salivary, and lacrimal glands). However, it has been described in nearly every organ, and, although rare, mammary involvement has been reported as part of IgG4-related disease. Patients, mostly women, present with ill-defined non-tender masses which may be radiologically detected (Fig. 2.61). Key histologic features are dense fibrosis with prominent lymphoplasmacytic infiltrates without specific lobulocentricity or periductal localisation, prominent storiform stromal sclerosis, effacement of lobules, and phlebitis (Fig. 2.62) [7]. IgG4-positive plasma cells predominate on immunohistochemistry, usually in excess of 50 per high-power field (Fig. 2.63). Serum IgG4 is often raised. In contrast, diabetic mastopathy shows relatively few plasma cells which are without IgG4 dominance.

Malignant Lymphoma

Lymphoma in the breast tends to diffusely infiltrate the stroma, a pattern that is distinct from the lymphocytic lobulitis seen in diabetic mastopathy. Additionally, immunostaining and molecular analysis will reveal a clonal proliferation of lymphoid cells in lymphoma, but not in diabetic mastopathy.

Prognosis and Therapy Considerations

Diabetic mastopathy may be subjected to excision due to the clinicoradiological mimicry of cancer. Excision is curative, though occasional recurrences are described. Some lesions can be self-limited and spontaneously regress.

Infections

Definition

Infections in the breast result from a variety of organisms ranging from bacterial, mycobacterial, fungal, and parasitic.

Clinical and Epidemiological Features

Bacterial infections usually occur in the setting of lactation-associated mastitis secondary to obstruction of lactiferous ducts, leading to abscesses that require antibiotic treatment and

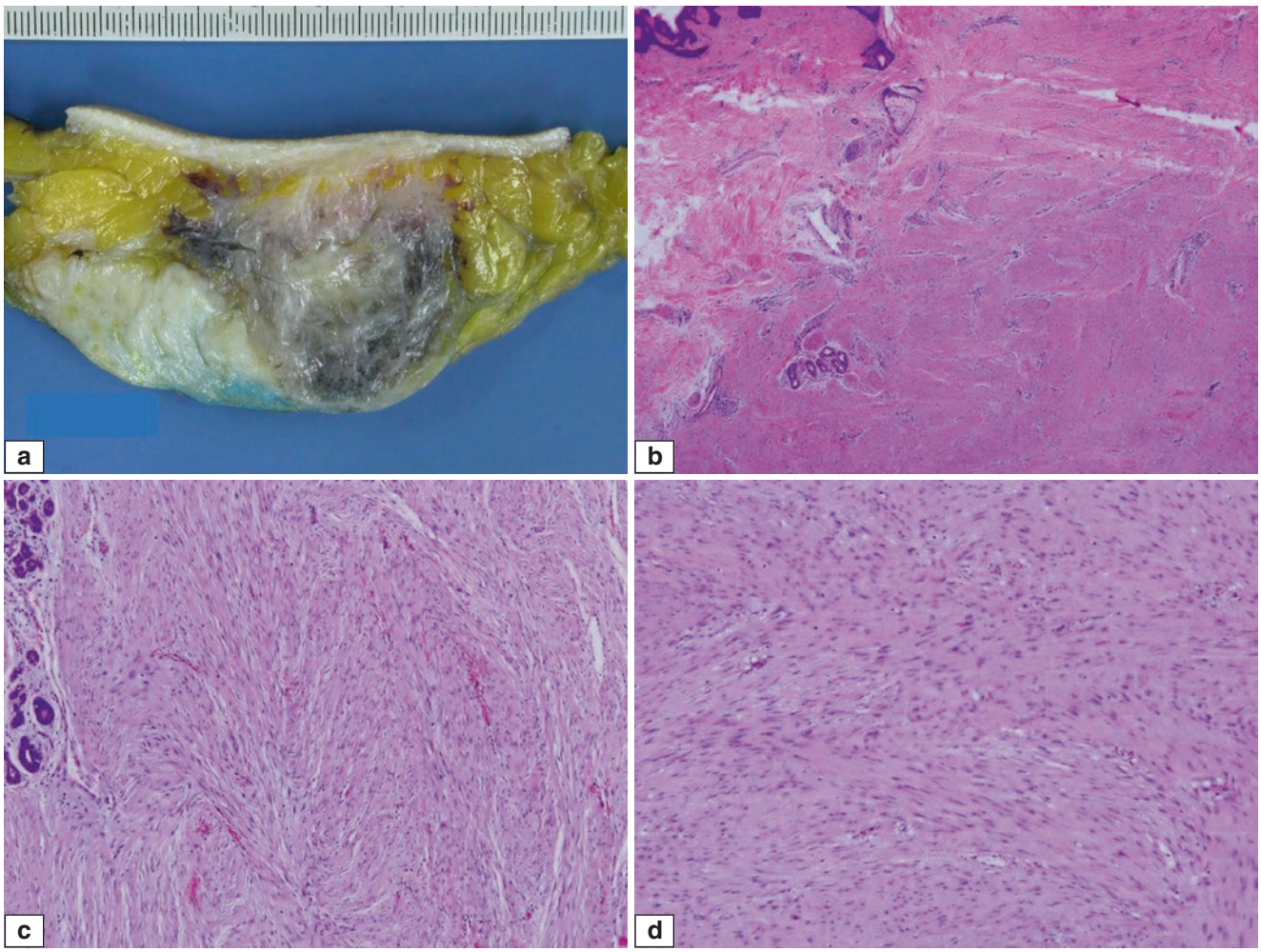

Fig. 2.56 Fibromatosis. (**a**) Mastectomy shows a whorled greyish-white tumour with ill-defined contours, merging with a whitish fibrous area of the breast. (**b**) Low magnification shows the intersecting fascicles of spindle cells extending around breast lobules and adnexal structures of the skin. (**c**) Higher magnification shows the spindle cells with elongated flattened nuclei with a slight waviness, set in long intersecting fascicles. The spindle cells encase a lobule at the edge. There is no lymphocytic lobulitis. (**d**) The spindle cells show bland nuclear features, without significant atypia or increased mitoses

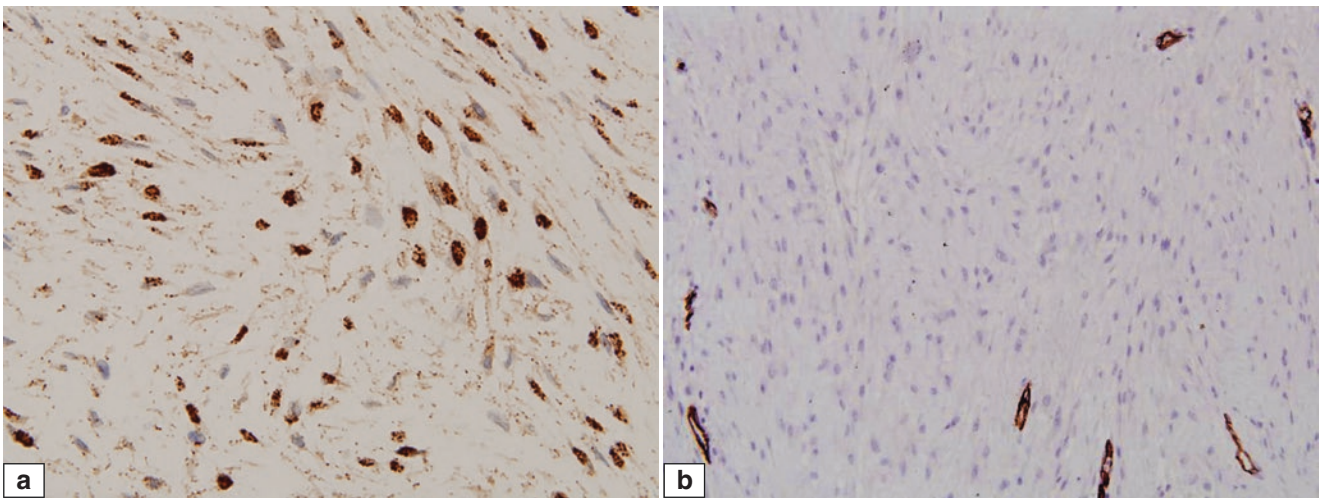

Fig. 2.57 Fibromatosis. (**a**) Beta-catenin immunohistochemistry shows nuclear staining of the spindle cells. (**b**) CD34 is absent in the spindle cells, highlighting only interspersed small vessels

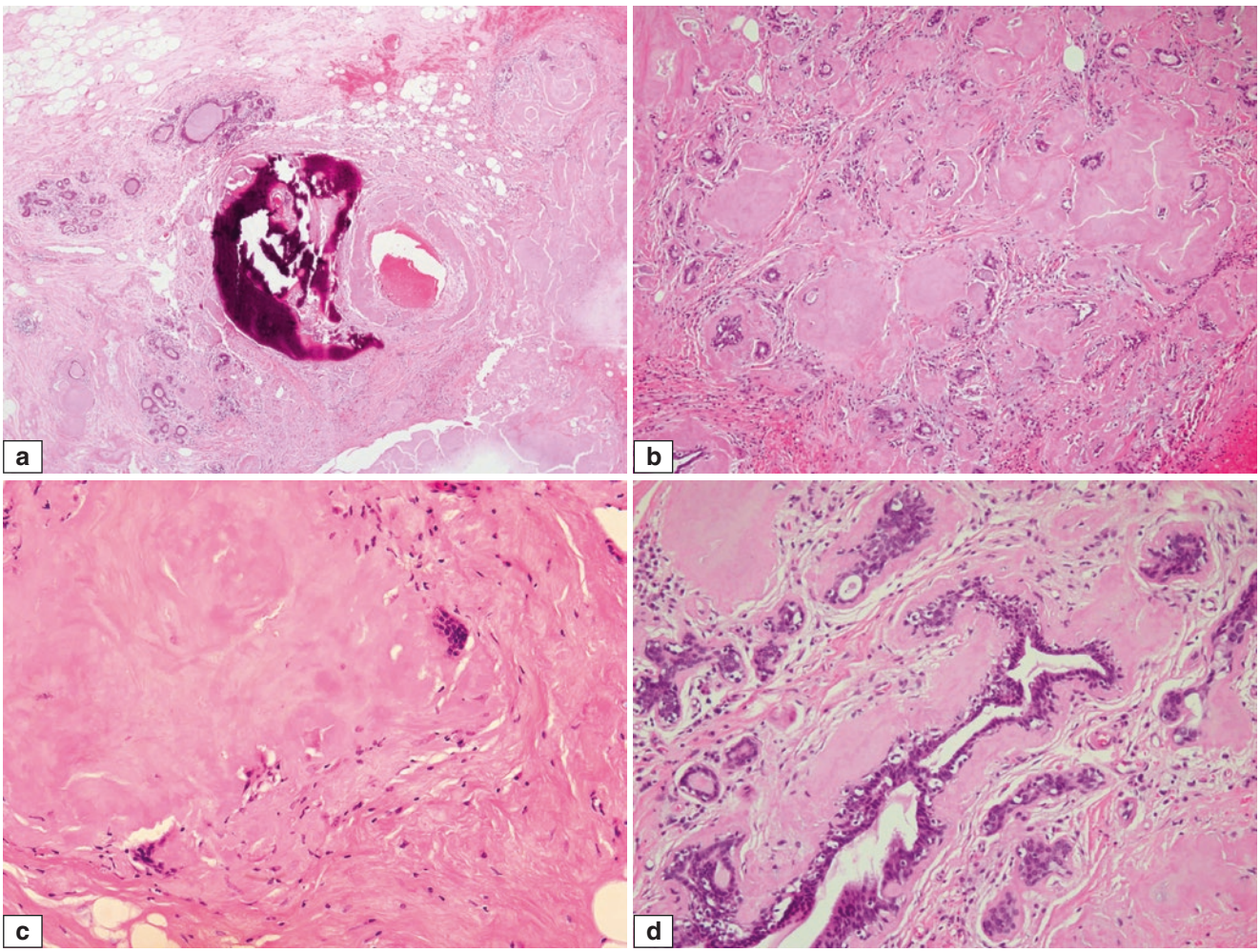

Fig. 2.58 Amyloidosis. (**a**) Clumps of amorphous acellular pale pink material are seen in the breast parenchyma, accompanied by coarse fractured calcifications. (**b**) Clumpy amorphous pale pink material extends into lobules and surrounds ductules. Effacement of ductules is seen. (**c**) Foreign-body-type multinucleated giant cells are seen around amyloid deposits. (**d**) The acellular material surrounds terminal ducts and ductules, which may on cursory view resemble thickening of the basement membranes and stromal hyalinisation seen in lobular atrophy

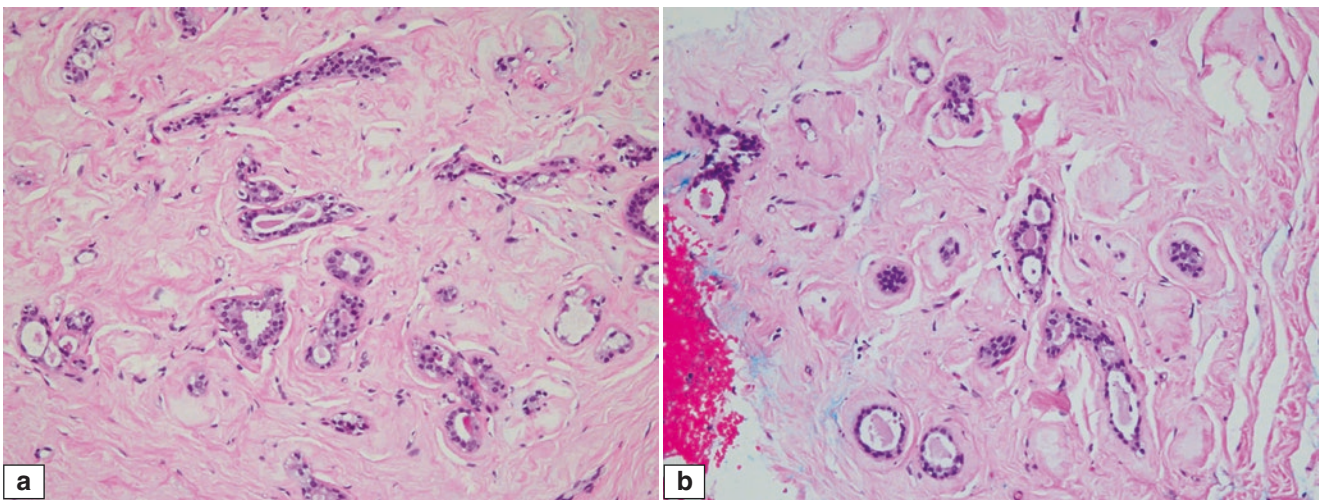

Fig. 2.59 Lobular atrophy. (**a**) In contrast to the clumpy material in amyloidosis, stromal hyalinisation in lobular atrophy has a glassy hyaline quality, associated with variable thickening of the basement membranes. (**b**) Hyalinisation around diminutive ductules may resemble amyloid but does not have the clumpy amorphous quality of amyloid deposits. Foreign body type multinucleated giant cells which may be found around amyloid deposits are absent

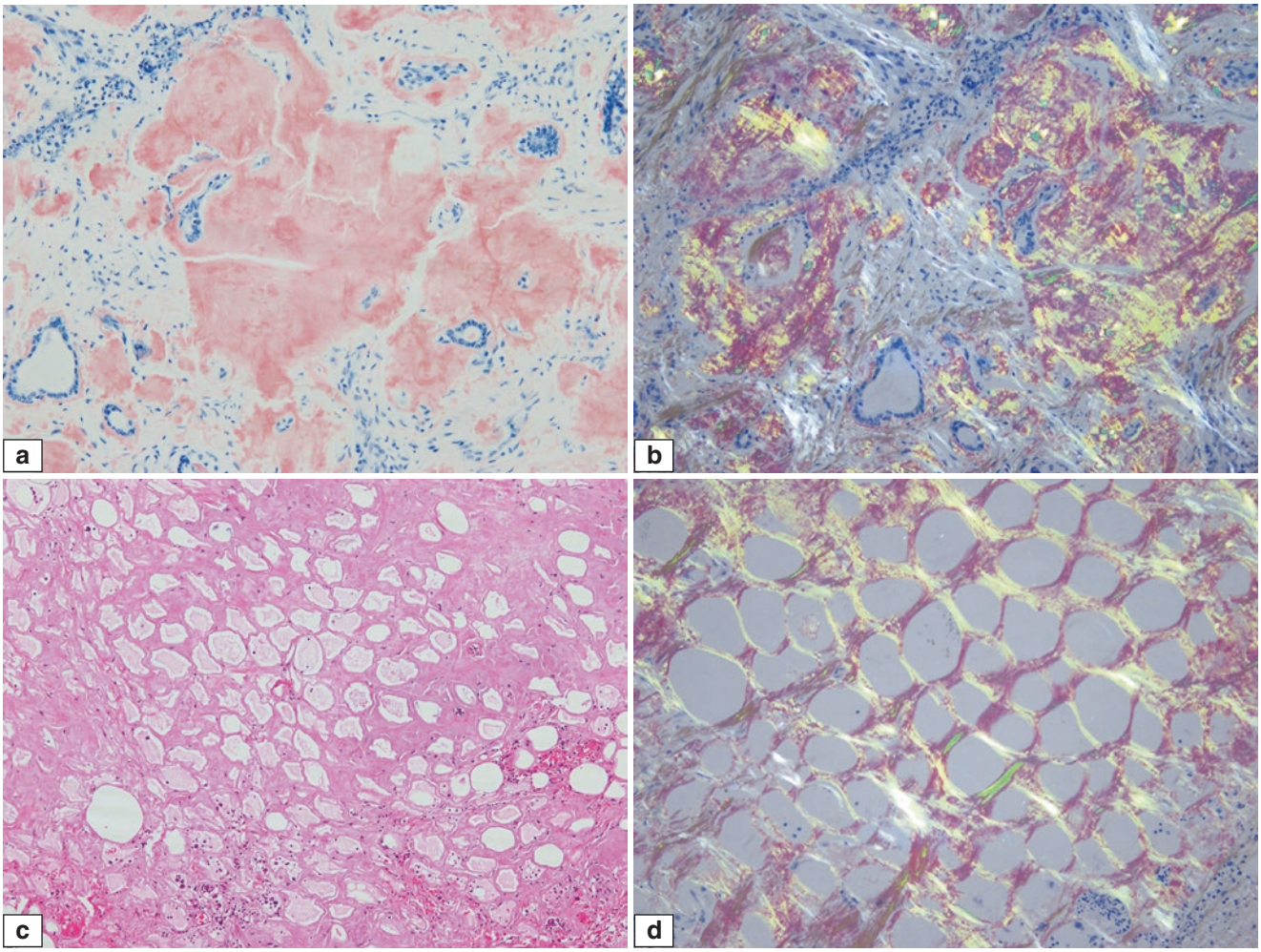

Fig. 2.60 Amyloidosis. (**a**) Congophilia of amyloid deposits in the breast (congo red stain). (**b**) Apple-green birefringence confirms amyloid deposits on polarised optics. (**c**) The amyloid material may also extend along the septa of the adipose tissue, expanding the spaces in between degenerate adipocytes and forming amyloid rings. Haemorrhage and a few scattered inflammatory cells are present. (**d**) Polarised optics show apple-green birefringence of congophilic material in the adipose septa of the breast

Fig. 2.61 IgG4-related sclerosing mastitis. A nodular hypoechoic lesion is observed on ultrasound of the right breast

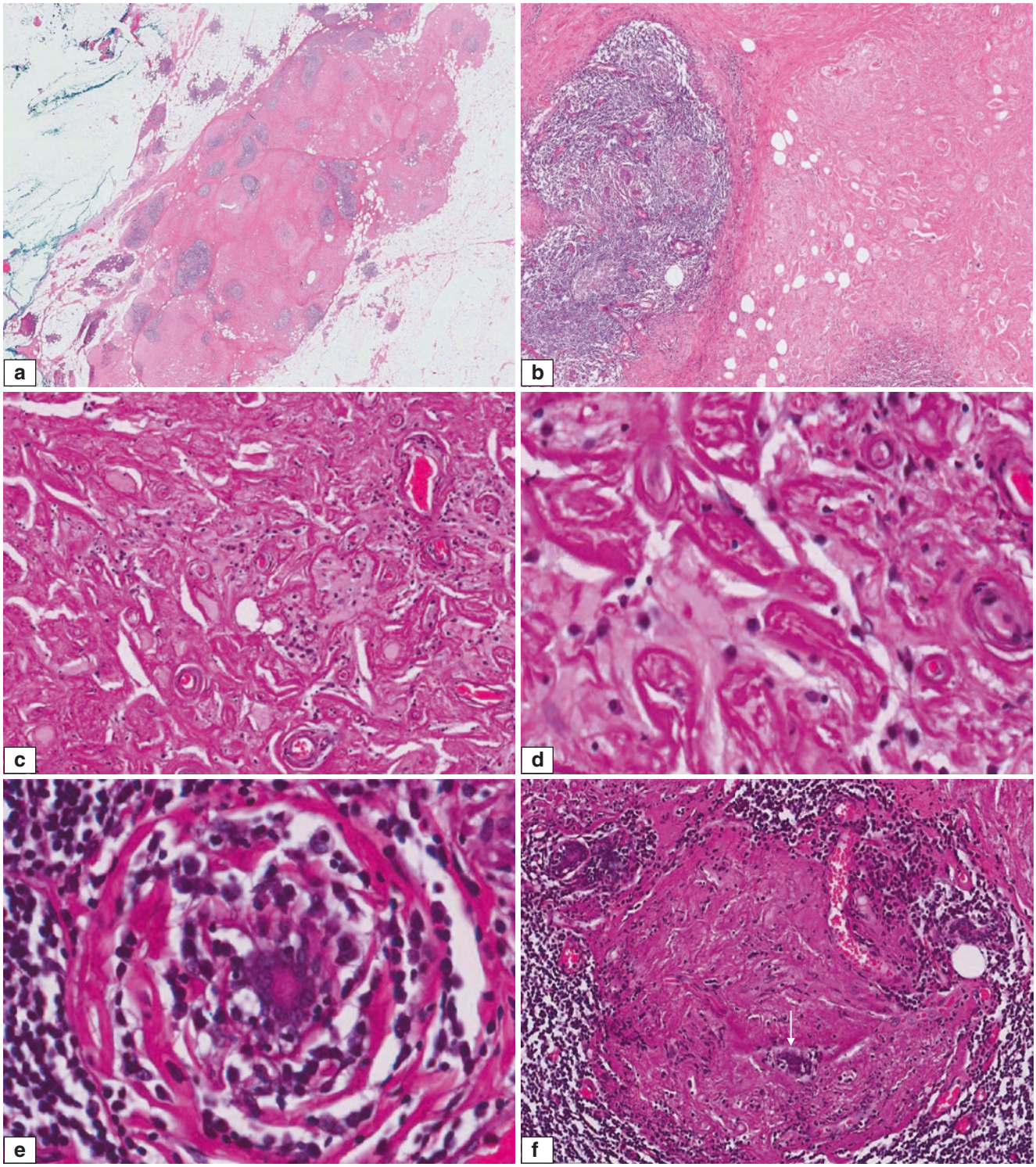

Fig. 2.62 IgG4-related sclerosing mastitis. (**a**) This nodular lesion of the breast shows extensive sclerosis with patchy lymphoid aggregates. (**b**) In the sclerosed part of the breast, ghost outlines of ducts can be seen. Lymphocytic aggregates with germinal centres are observed around preserved breast lobules. (**c**) The sclerosing process effaces ducts and lobules and involves blood vessels, with accompanying lymphocytes and plasma cells. (**d**) High magnification of the sclerosing process that leads to the formation of hyalinised tombstones of effaced tubules. Small vessels also demonstrate hyalinisation of their walls. (**e**) The duct in the centre is partially obscured by chronic inflammation with lymphocytes and plasma cells. There is whorl-like fibrosis around the duct. (**f**) Sclerosis and lobular atrophy, with lymphocytic infiltrates, are present. A residual small ductule is observed in the midst of a zone of sclerosis (*arrow*)

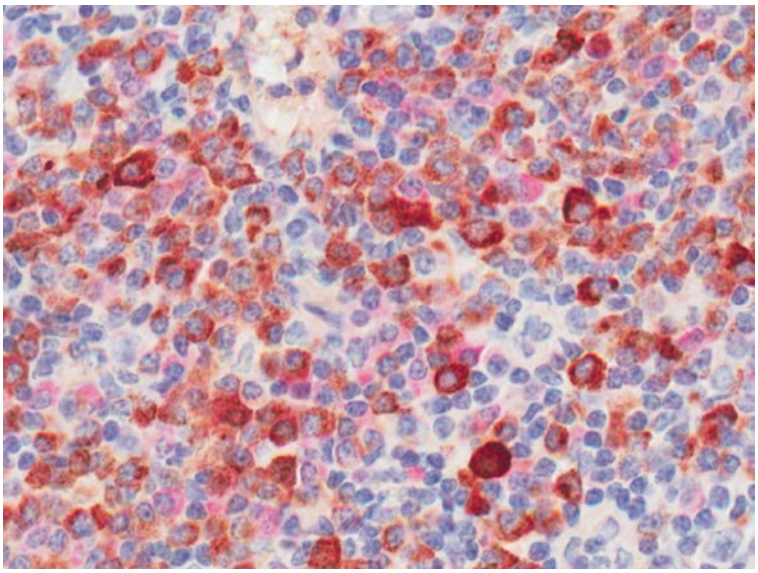

Fig. 2.63 IgG4-related sclerosing mastitis. Immunohistochemistry with dual IgG4 (*brown*) and IgG (*red*) antibodies shows a predominance of the IgG4 subtype in the plasma cells, corroborating the diagnosis (Courtesy of Dr. Leonard Tan)

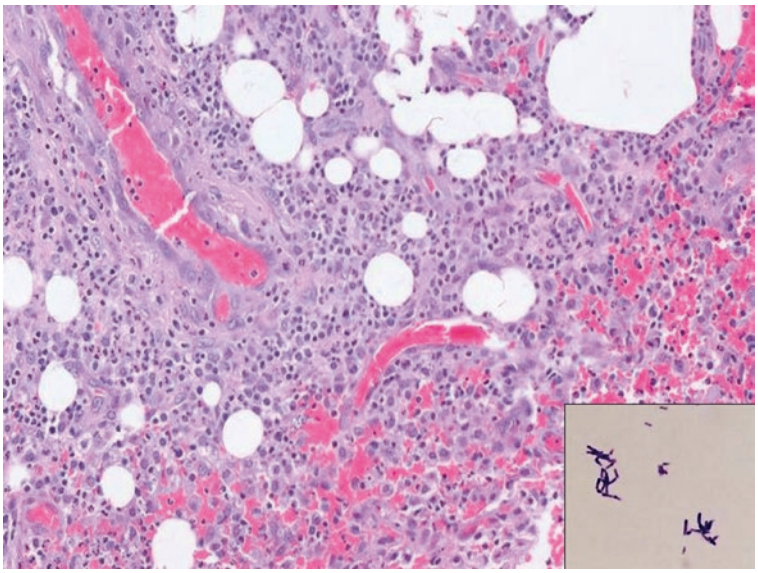

Fig. 2.64 Cystic neutrophilic granulomatous mastitis. Inflamed haemorrhagic granulation tissue in the abscess wall shows empty spaces, within which bacterial organisms may be identified with gram stains. Inset shows Corynebacterium kroppenstedtii which are gram-positive organisms that can be cultured from the abscess tissue (inset courtesy of Dr Ai Ling Tan)

sometimes excision. In particular, cystic neutrophilic granulomatous mastitis associated with gram-positive bacteria such as corynebacteria should be considered (Fig. 2.64) [8–10]. Fungal infections are seen in immunocompromised individuals, and while mycobacterial infections may be encountered in less well-developed countries, they can also be seen in patients with the acquired immunodeficiency syndrome.

Imaging Features

Mammography may show densities that can mimic malignancy.

Pathologic Features

Macroscopic Pathology

Nodular greyish-yellow lesions with soft-to-firm consistency may be observed.

Microscopic Pathology

Histological appearances depend on the type of organisms. Bacterial infections show acute inflammation and abscess formation. Specifically, the following are present in cystic neutrophilic granulomatous mastitis: collections of polymorphs with granulation tissue, granulomas, and cystic spaces containing gram-positive bacteria, which are often corynebacteria. Occasionally, these bacteria may not be identified [10]. Mycobacterial infections exhibit necrotising granulomatous inflammation with caseation. Fungal infections are also accompanied by necrotising granulomas, which may sometimes involve blood vessels. Parasites such as filariasis and cysticercosis can be recognised from their structures (Figs. 2.65 and 2.66). Cultures are useful in confirming the infective aetiologic agent.

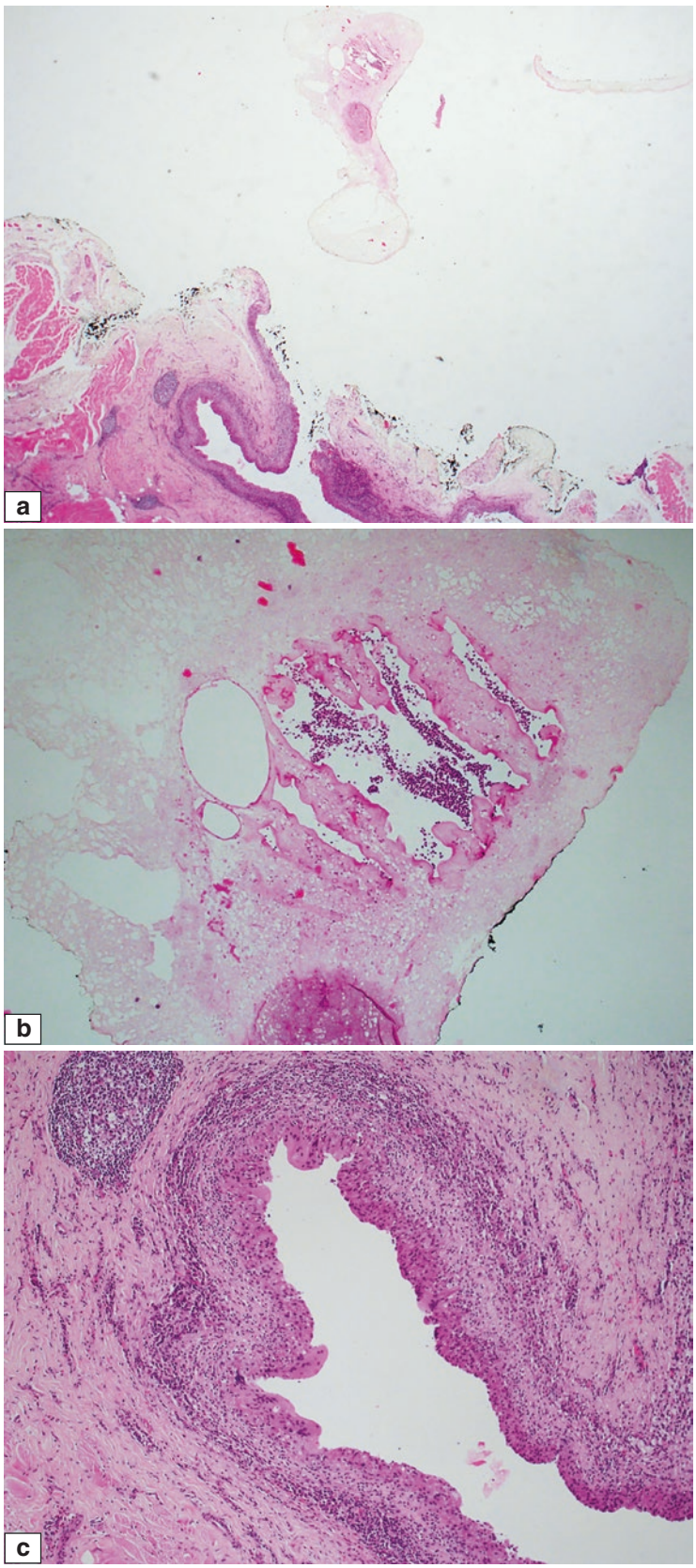

Fig. 2.65 An unusual infection presenting as a breast lump—cysticercosis. (**a**) The parasite is seen lying loose while the histiocytic wall of the collapsed cavity within which it was previously enclosed is present in the lower field, adjacent to skeletal muscle of the chest wall. No normal breast tissue is present. The cysticercus is a larval tapeworm that can be found within muscle tissue of an infected individual. (**b**) Higher magnification of the parasite showing its internal structure. (**c**) The cystic cavity which contained the parasite is lined by a layer of histiocytes with a chronic inflammatory cell cuff. The finding of an empty cavity rimmed by histiocytes should prompt a search for an underlying cause including parasitic organisms

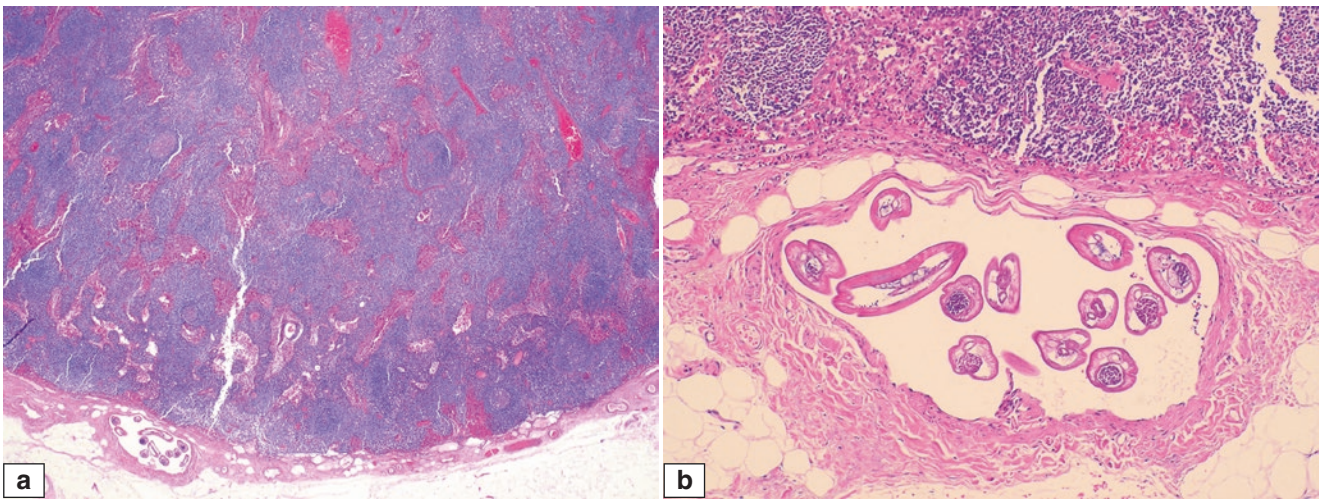

Fig. 2.66 (**a**) An axillary lymph node containing a parasite with features of filariae in the perinodal lymphovascular space (Courtesy of Dr. Leonard Tan). (**b**) Higher magnification of parts of the roundworm of Filarioidea type residing within the lymphatic space just adjacent to the axillary nodal capsule

Differential Diagnosis

Necrotising Granulomatous Vasculitis

In this condition, vessels are affected and no organisms are found on special stains or molecular studies. While necrotising granulomas with vasculitis may be the initial presenting features of Wegener's granulomatosis, more frequently there are already systemic signs and symptoms that point to the disease.

Granulomatous Lobular Mastitis

In granulomatous lobular mastitis, there is lobulocentricity of granulomas without necrosis.

Prognosis and Therapy Considerations

Prognosis and therapy depend on the underlying disease.

References

1. Kadowaki M, Nagashima T, Sakata H, Sakakibara M, Sangai T, Nakamura R, et al. Ectopic breast tissue in axillary lymph node. Breast Cancer. 2007;14(4):425–8.
2. Maiorano E, Mazzarol GM, Pruneri G, Mastropasqua MG, Zurrida S, Orvieto E, et al. Ectopic breast tissue as a possible cause of false-positive axillary sentinel lymph node biopsies. Am J Surg Pathol. 2003;27(4):513–8.
3. Sweeney DJ, Wylie EJ. Mammographic appearances of mammary duct ectasia that mimic carcinoma in a screening programme. Australas Radiol. 1995;39(1):18–23.
4. Fox SB, Lee A. Granular cell tumour. In: Lakhani SR, Ellis IO, Schnitt SJ, Tan PH, van de Vijver MJ, editors. WHO classification of tumours of the breast. Lyon: WHO Press; 2012. p. 134.
5. Tan PH, Harada O, Thike AA, Tse GM. Histiocytoid breast carcinoma: an enigmatic lobular entity. J Clin Pathol. 2011;64(8):654–9.
6. Wilson JP, Massoll N, Marshall J, Foss RM, Copeland EM, Grobmyer SR. Idiopathic granulomatous mastitis: in search of a therapeutic paradigm. Am Surg. 2007;73(8):798–802.
7. Cheuk W, Chan AC, Lam WL, Chow SM, Crowley P, Lloydd R, et al. IgG4-related sclerosing mastitis: description of a new member of the IgG4-related sclerosing diseases. Am J Surg Pathol. 2009;33(7):1058–64.
8. Taylor GB, Paviour SD, Musaad S, Jones WO, Holland DJ. A clinicopathological review of 34 cases of inflammatory breast disease showing an association between corynebacteria infection and granulomatous mastitis. Pathology. 2003;35(2):109–19.
9. Renshaw AA, Derhagopian RP, Gould EW. Cystic neutrophilic granulomatous mastitis: an underappreciated pattern strongly associated with gram-positive bacilli. Am J Clin Pathol. 2011;136(3):424–7.
10. D'Alfonso TM, Moo TA, Arleo EK, Cheng E, Antonio LB, Hoda SA. Cystic neutrophilic granulomatous mastitis: further characterization of a distinctive histopathologic entity not always demonstrably attributable to corynebacterium Infection. Am J Surg Pathol. 2015;39(10):1440–7.

Fibroepithelial Lesions

3

Fibroepithelial neoplasms of the breast are characterised by proliferation of both epithelial and stromal components and include the common fibroadenoma and the less frequently occurring phyllodes tumour.

Fibroadenoma

Definition

The fibroadenoma is a common benign fibroepithelial tumour of females in the reproductive age group, although it may be diagnosed at any age.

Clinical and Epidemiological Features

Fibroadenomas present clinically as single or multiple lumps or nodules which are mobile, smooth contoured, and untethered to the skin on palpation.

Imaging Features

Mammographic screening has led to detection of fibroadenomas in mature women, often observed radiologically as typically well-defined, wider-than-tall nodules that may have gentle lobulations. Characteristic coarse "popcorn" calcifications are common (Fig. 3.1). There may be internal septations, which appear echogenic on sonography and as non-enhancing thin lines on magnetic resonance imaging.

Pathologic Features

Macroscopic Pathology

Macroscopically, the fibroadenoma is usually encapsulated and shows circumscribed borders with a whitish-grey, bulging cut surface in which slit-like spaces are often evident (Figs. 3.2, 3.3, 3.4, 3.5, and 3.6). It is often rubbery in consistency and may have lobulated outlines. They can achieve large sizes, with fibroadenomas exceeding 5 cm in dimension being referred to as giant fibroadenomas.

Microscopic Pathology

Histologically, the fibroadenoma shows two patterns: "intracanalicular", with stroma compressing epithelial elements, and "pericanalicular", with stroma growing around open ductules (Figs. 3.7, 3.8, and 3.9). These microscopic patterns do not have clinical significance and often occur together in the same tumour. The epithelial compartment may show any alterations that can be observed in the breast, from usual ductal hyperplasia (Fig. 3.10), columnar cell change, atypical hyperplasia (Fig. 3.11), and in situ (Fig. 3.12) and invasive carcinomas (Fig. 3.13). It is reported that atypical hyperplasia confined within the fibroadenoma does not incur an increased risk of subsequent breast cancer development [1].

P.H. Tan, A.A. Sahin, *Atlas of Differential Diagnosis in Breast Pathology*, Atlas of Anatomic Pathology,
DOI 10.1007/978-1-4939-6697-4_3

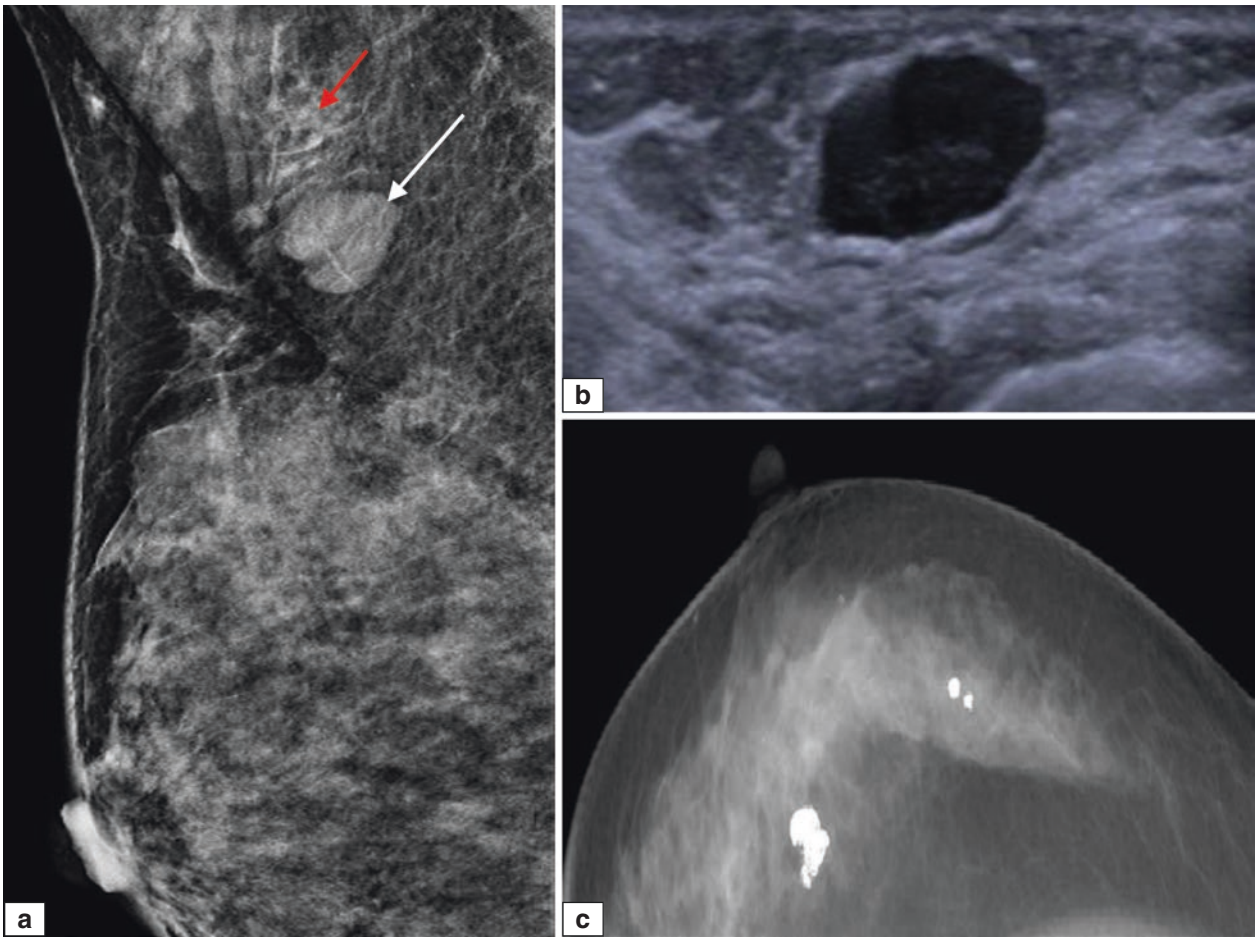

Fig. 3.1 Radiology of fibroadenoma. (**a**) In a 42 year old woman with a right axillary palpable lump, the mammogram shows a well-defined, gently lobulated, oval nodule in the right axilla (*white arrow*). Accessory breast tissue is also seen (*red arrow*). (**b**) Ultrasound shows a well-defined oval nodule in the right axilla which was confirmed to be a fibroadenoma on core biopsy. The hyperechoic tissue surrounding the nodule is related to accessory breast tissue. (**c**) In this craniocaudal (CC) mammogram view of a right breast, there are two lobulated 'popcorn' calcifications that are classical for involuting calcified fibroadenomas (Courtesy of Dr. Lester Leong)

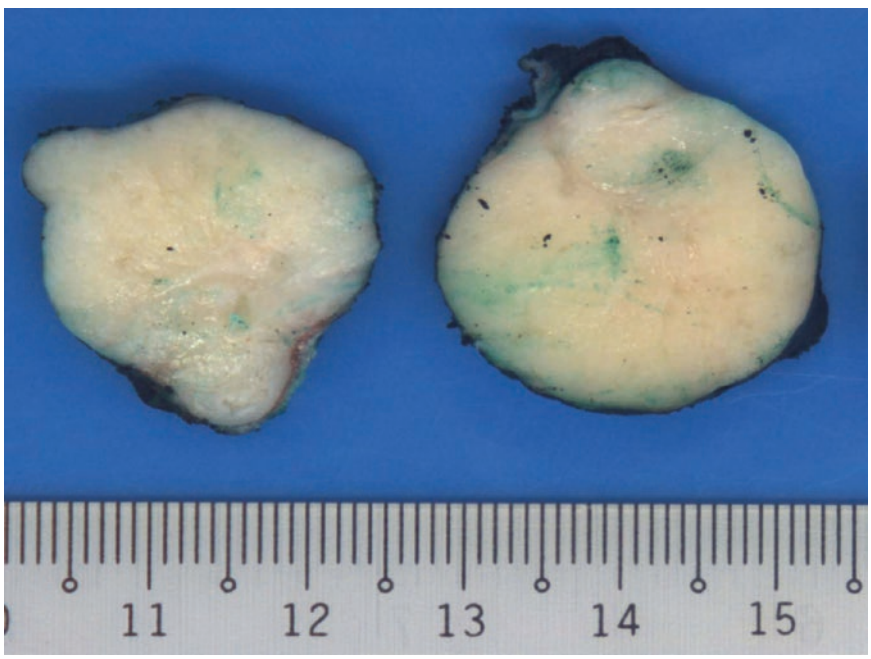

Fig. 3.2 Gross appearance of a fibroadenoma with a whitish whorled cut surface. The lobulated contours are seen as broad-based, bulging protrusions

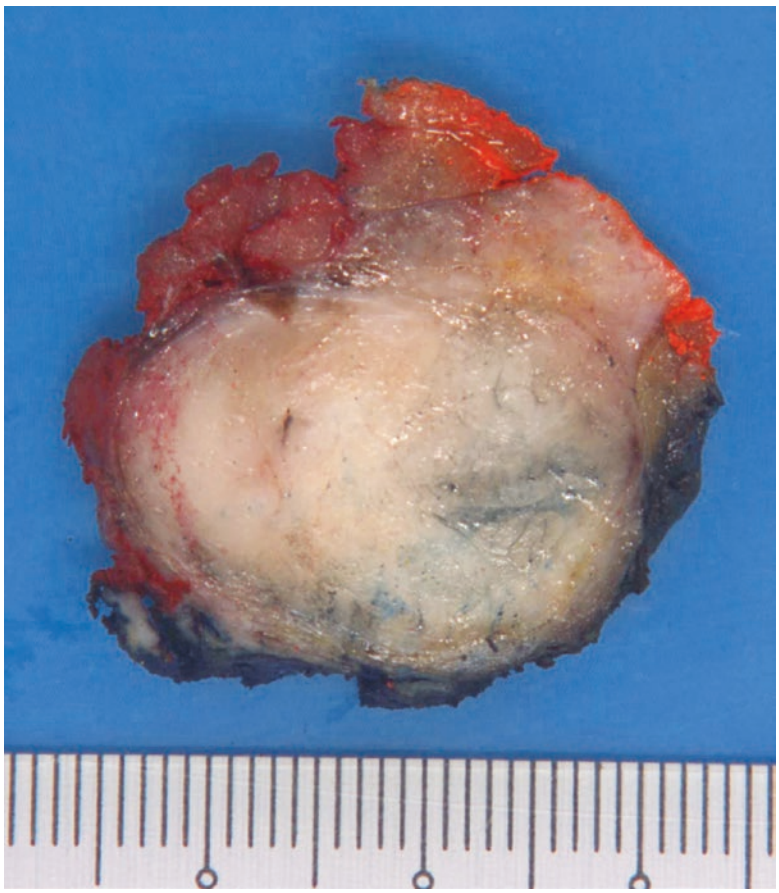

Fig. 3.3 Macroscopy of a fibroadenoma with myxoid areas, seen towards the periphery of the lesion

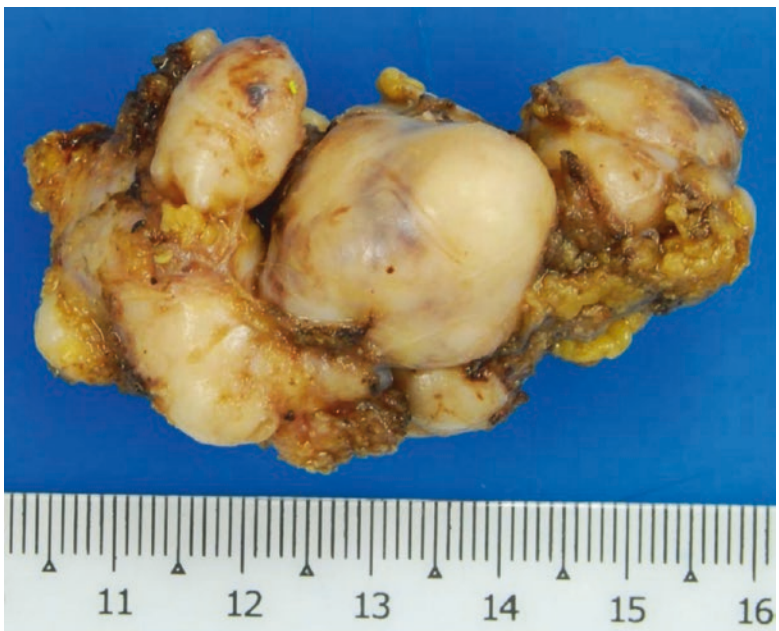

Fig. 3.4 Giant fibroadenoma measures 5.5 cm in maximum dimension, showing multiple lobulations with smooth external surfaces

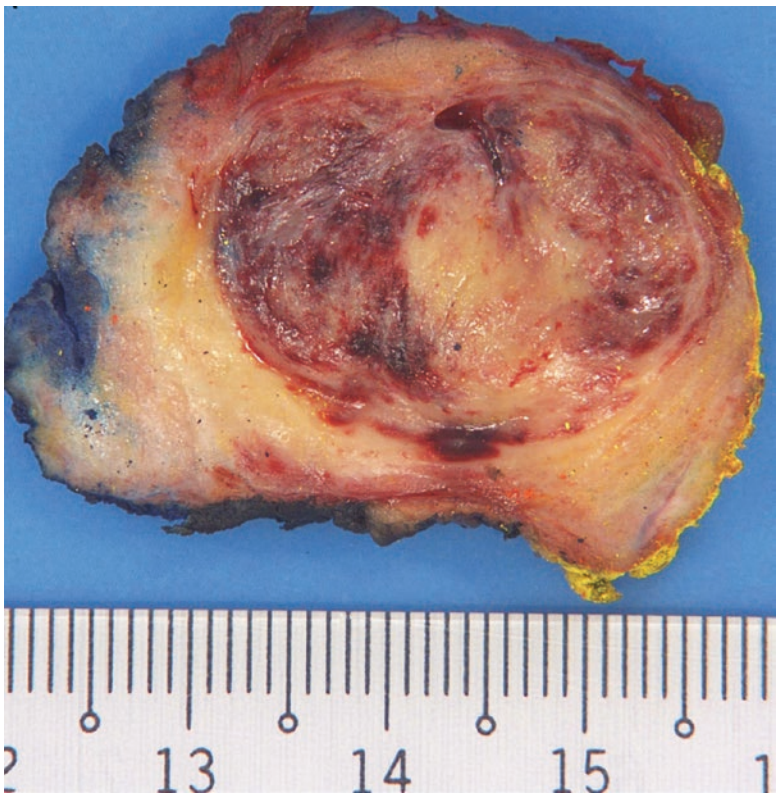

Fig. 3.5 Infarcted fibroadenoma shows extensive areas of haemorrhage. Its circumscribed outline delineates it from the surrounding fibrous breast tissue

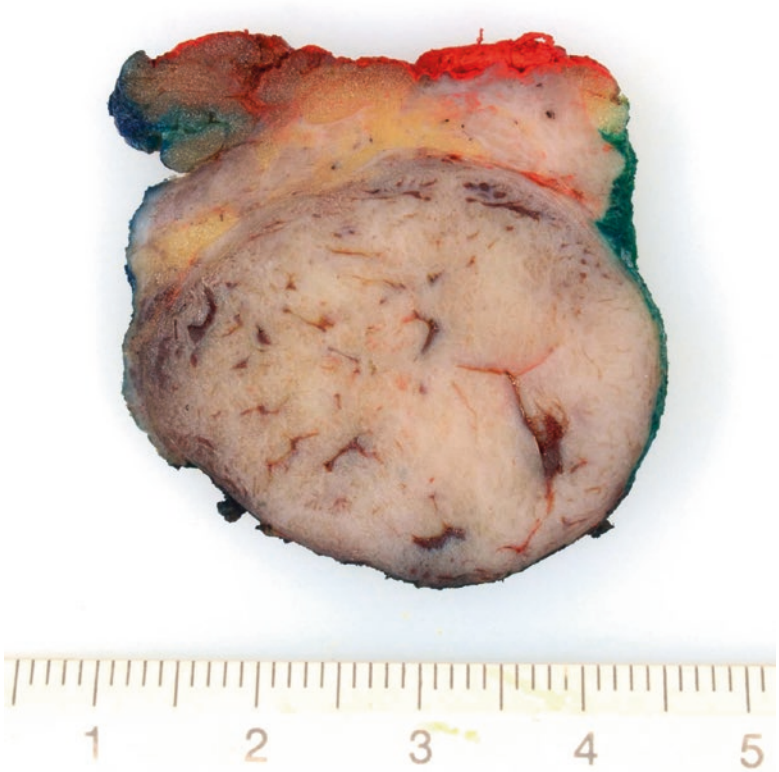

Fig. 3.6 A juvenile fibroadenoma shows a circumscribed border with a whitish fibrous cut surface containing slit-like spaces (Courtesy of Dr. Kenneth Chang)

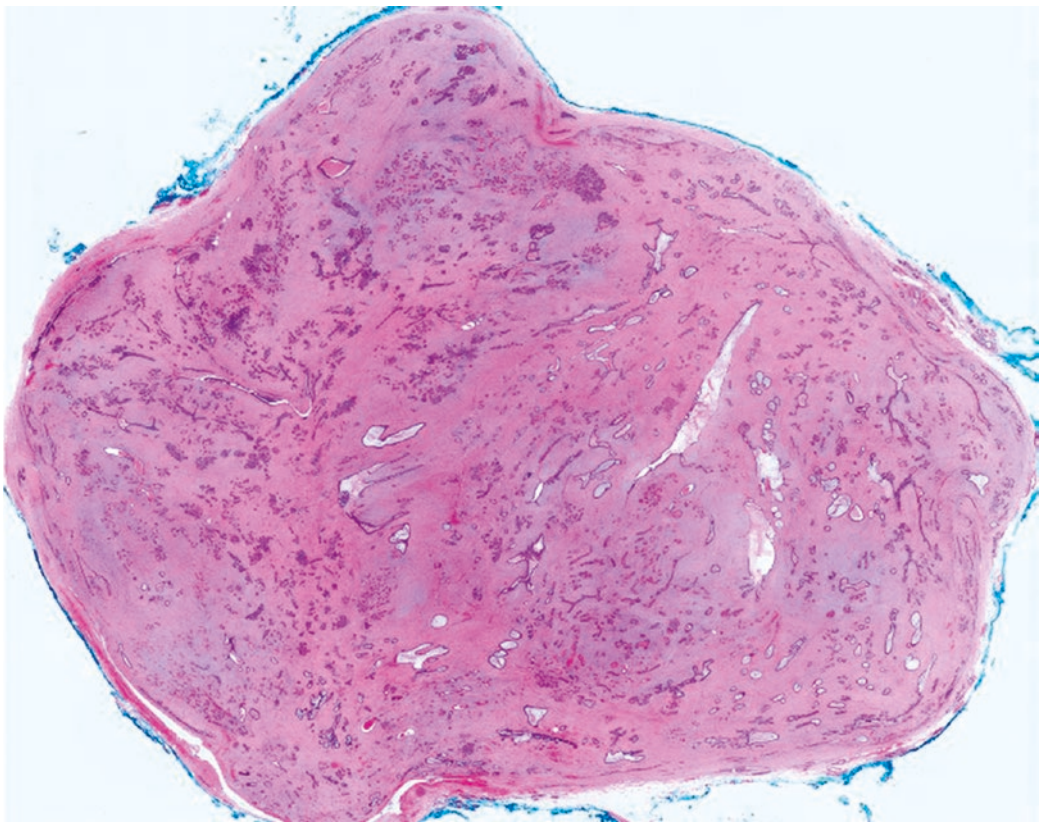

Fig. 3.7 Fibroadenoma. At scanning magnification, the lesion shows circumscribed and partly encapsulated margins, with proliferation of both epithelial and stromal components

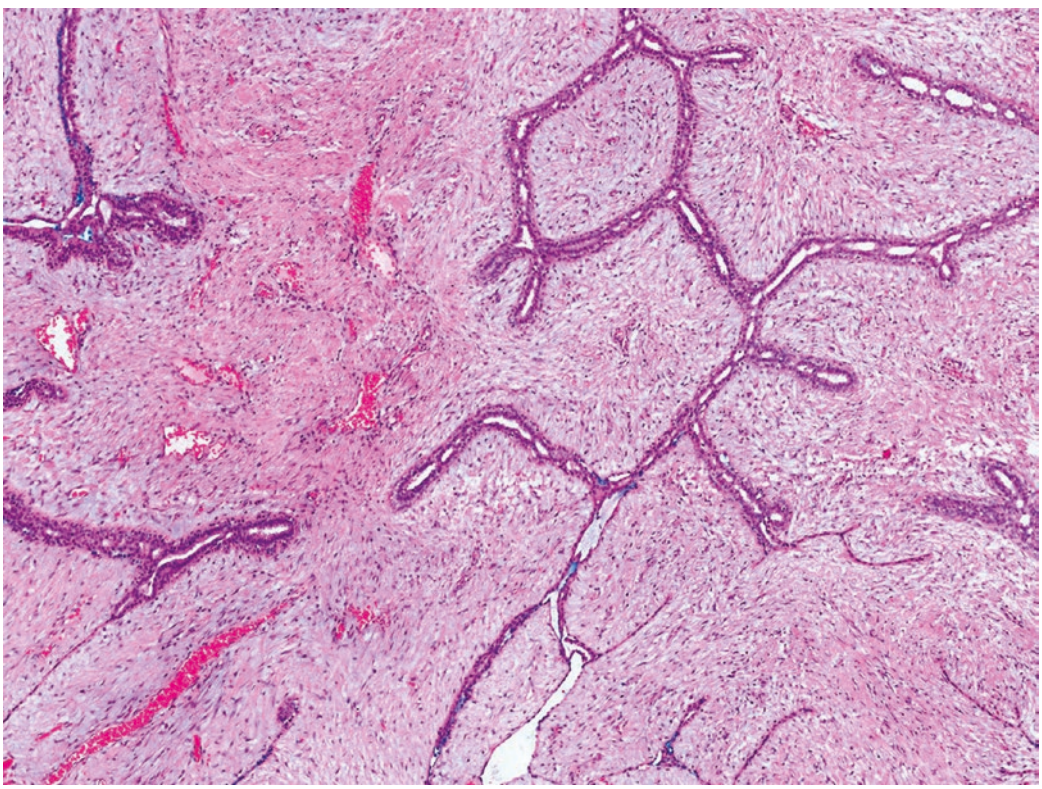

Fig. 3.8 Intracanalicular growth pattern of a fibroadenoma shows stroma growing into the epithelial compartment, compressing the epithelium, and stretching the ducts into elongated arc-like formations. The epithelium is bilayered, with luminal and myoepithelial layers

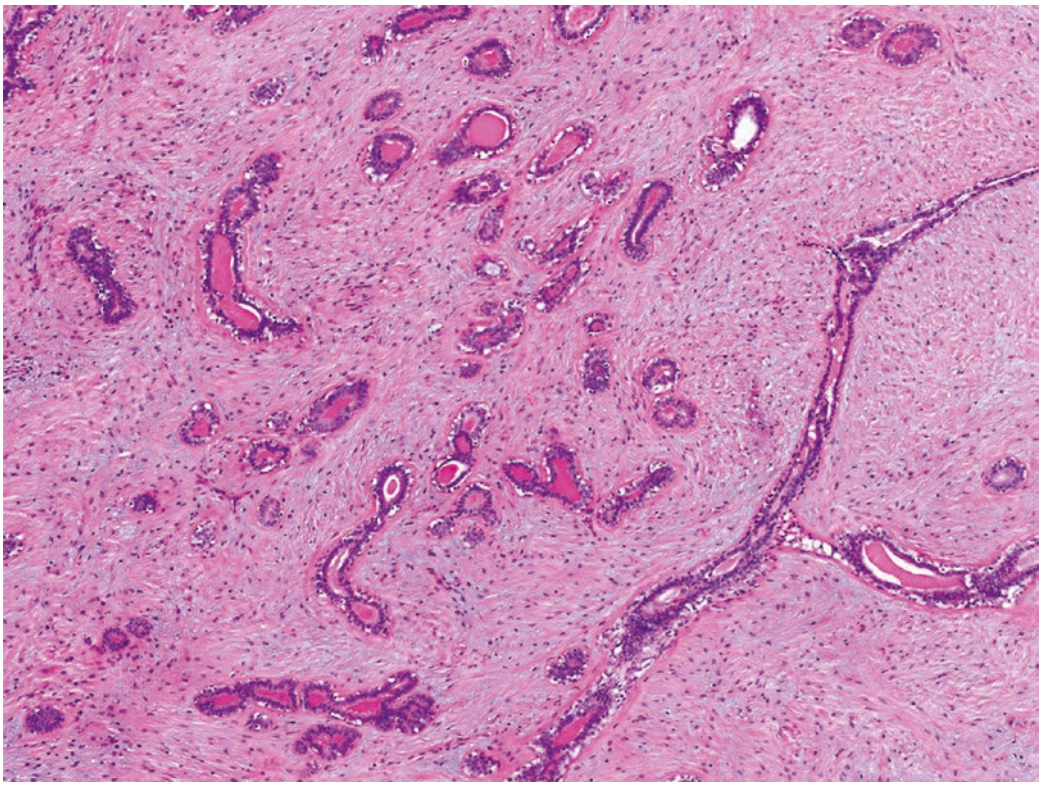

Fig. 3.9 Fibroadenoma with a predominantly pericanalicular growth pattern with the stroma growing around patent tubules

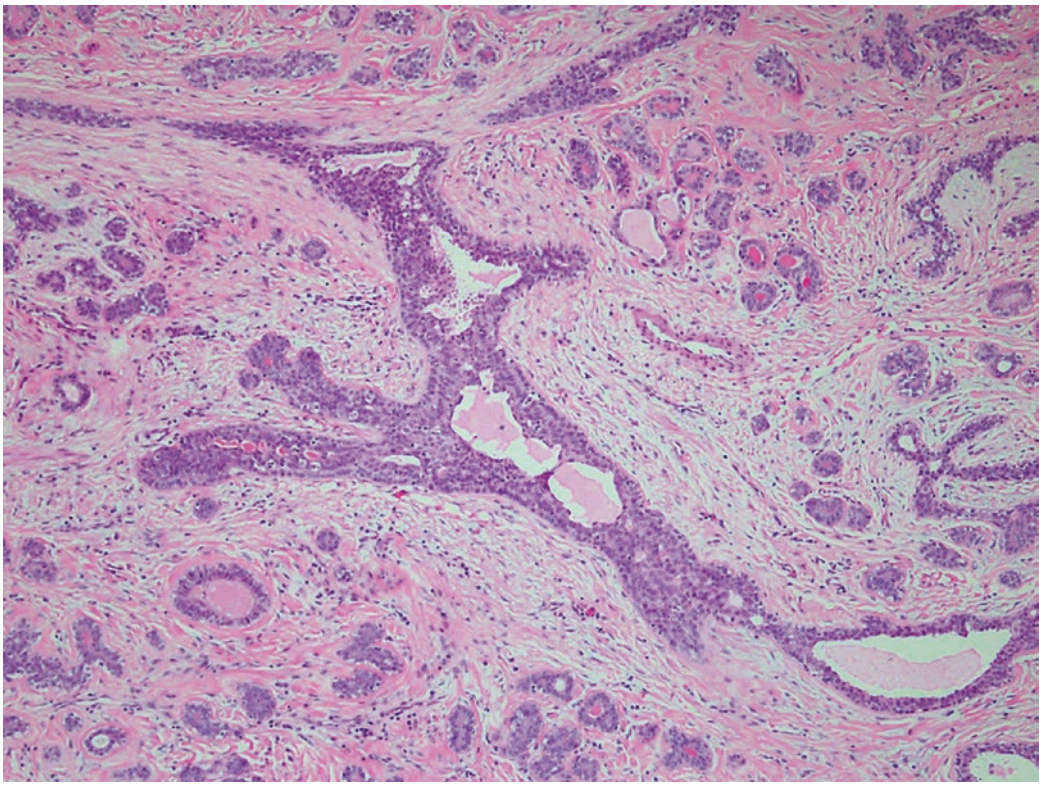

Fig. 3.10 Fibroadenoma with usual ductal hyperplasia. In this fibroadenoma, there is moderate usual ductal hyperplasia, with proliferation of epithelial cells forming protrusions into the lumen as well as displaying slit-like spaces among the epithelial cells

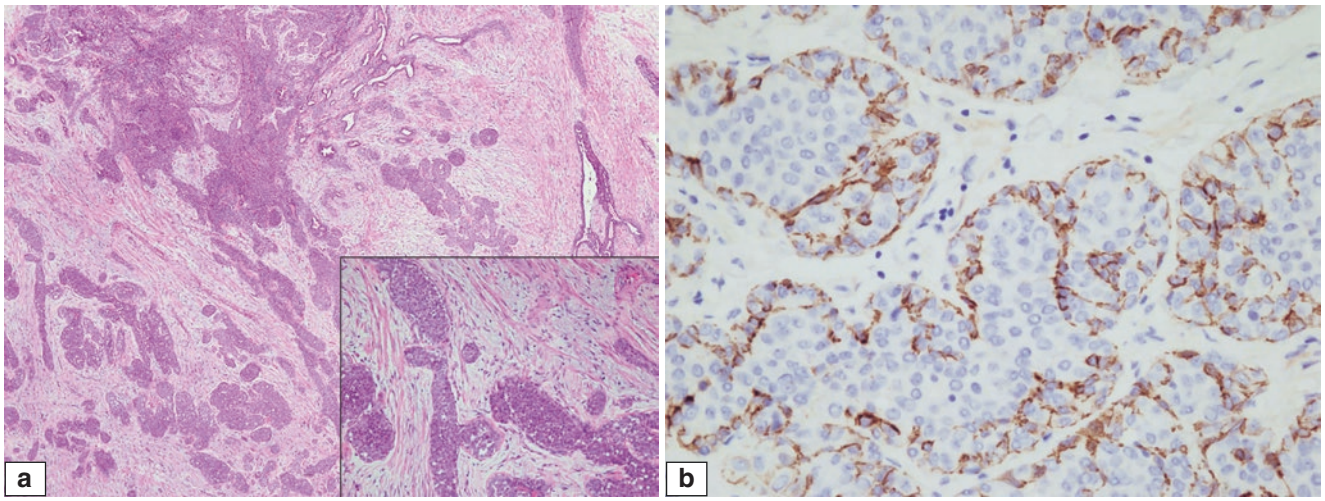

Fig. 3.11 Fibroadenoma with lobular neoplasia. (**a**) The epithelial compartment of this fibroadenoma shows distension of the acinar spaces by a proliferation of epithelial cells. Higher magnification shows the epithelial elements being filled by a discohesive population of rounded uniform epithelial cells with open vesicular nuclei, indistinct nucleoli, and thin cytoplasmic rims (*inset*) (**b**) Immunohistochemistry for E-cadherin shows absent staining in the lobular neoplastic cells. Cells that show positive reactivity are myoepithelial (seen as a peripheral rim) as well as residual luminal epithelial cells that are largely obscured by the lobular neoplastic cells

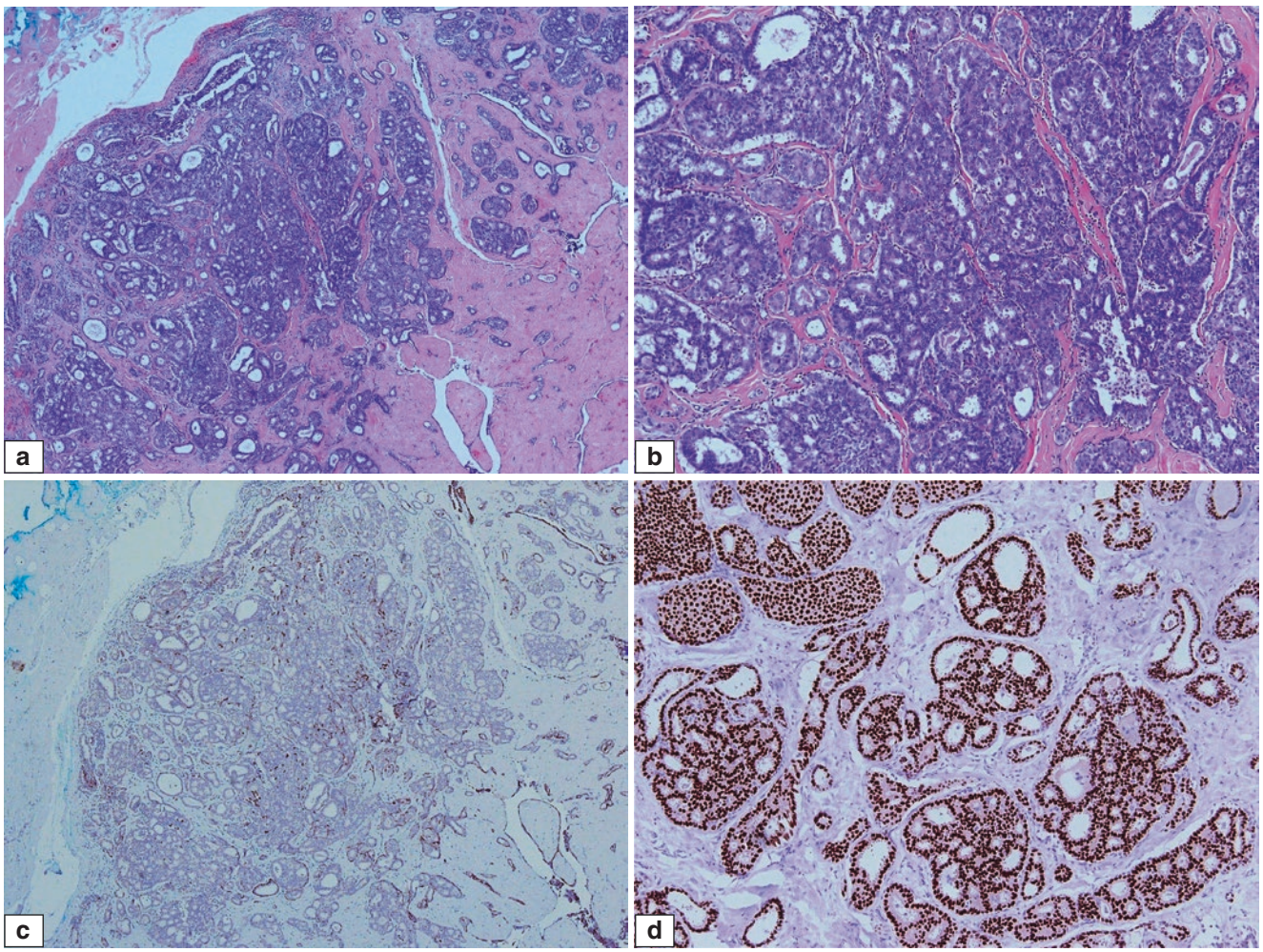

Fig. 3.12 Fibroadenoma with ductal carcinoma in situ (DCIS), low nuclear grade, cribriform pattern, without necrosis. (**a**) The circumscribed border of the fibroadenoma separates DCIS occurring within the lesion from the surrounding breast tissue. The predominantly intracanalicular growth pattern of the fibroadenoma with hyalinised stroma is seen in the lower right field. (**b**) Cribriform structures formed by uniform epithelial cells occupying the epithelial compartment of the fibroadenoma. (**c**) Immunohistochemistry for CK14 shows diminished staining within the cribriform epithelial population, with patchy albeit attenuated staining of myoepithelial cells at the periphery of ducts affected by DCIS. (**d**) Immunohistochemistry with ER shows diffuse nuclear staining of epithelial cells forming the cribriform structures

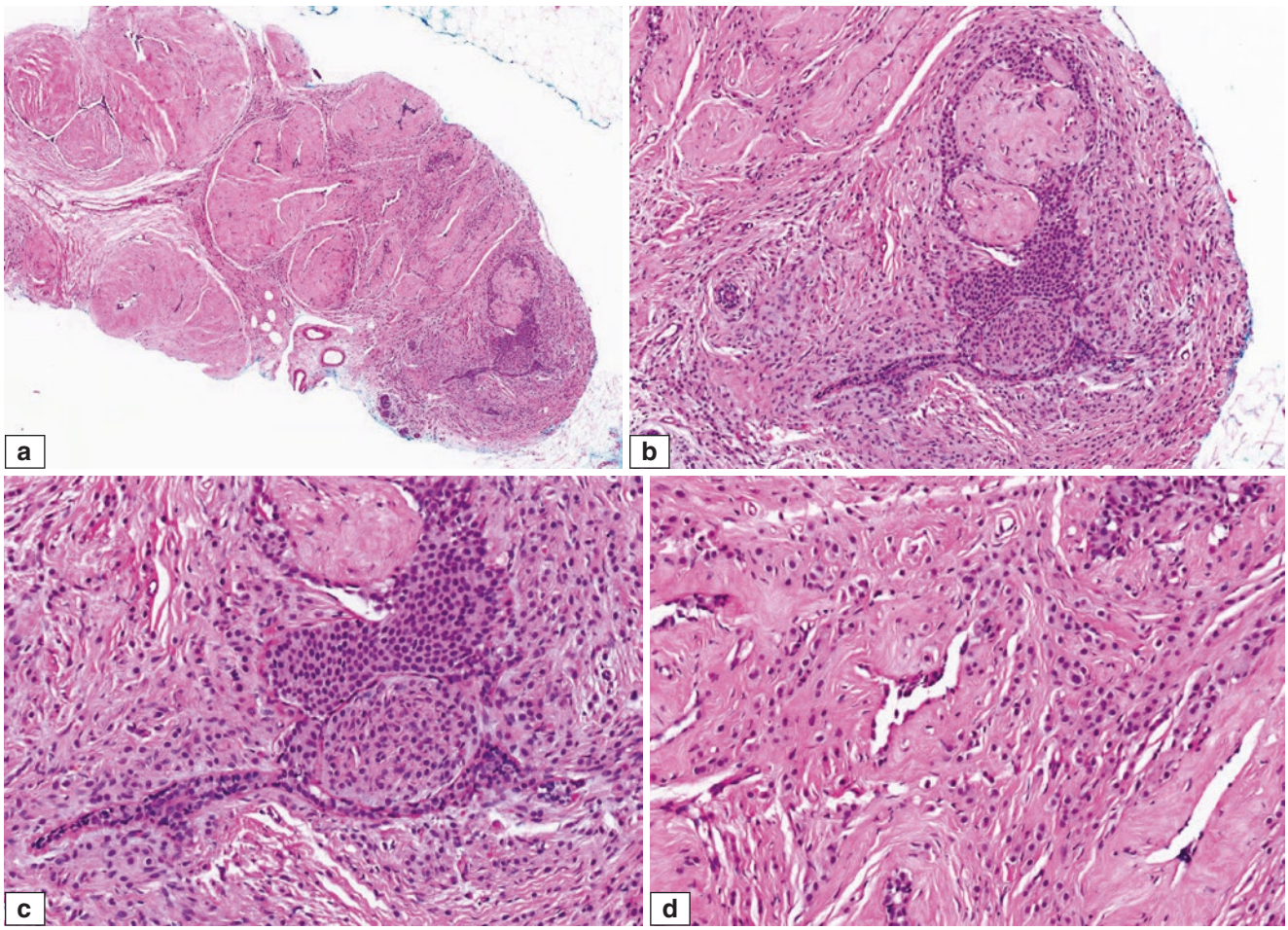

Fig. 3.13 Invasive lobular carcinoma (classic) in a fibroadenoma. (**a**) Core biopsy of a radiologic density in a 49-year-old woman. The architecture of a fibroadenoma is present at low magnification, showing an intracanalicular growth pattern. Part of the core shows a more cellular infiltrate occupying the stroma. (**b**) Higher magnification shows streams of cells with small nuclei encircling the epithelial compartment of the fibroadenoma, which is similarly involved by a monotonous cell population. (**c**) The epithelial compartment of the fibroadenoma is slightly distended by a similar population of monotonous cells of lobular carcinoma in situ, with nuclear features resembling those of the invasive component. (**d**) The invasive lobular carcinoma cells permeate in linear cords and as dispersed neoplastic cells within the hyalinised stroma of the fibroadenoma

The stroma can exhibit multinucleated giant cells (Fig. 3.14), which do not indicate stromal atypia. Fibroadenomas with cellular stroma are referred to as *cellular fibroadenomas* (Fig. 3.15), though the level of stromal cellularity needed for this diagnosis is subjective and may differ among pathologists. Fibroadenomas in children and young females under 20 years of age tend to have increased stromal cellularity and need to be distinguished from phyllodes tumours [2]. The presence of extensive myxoid stroma is seen in the *myxoid fibroadenoma* (Fig. 3.16). While myxoid fibroadenomas are described in the Carney's complex (myxoid neoplasms and pigmented skin lesions), most observed in the breast are unassociated with this clinical condition. In older women, the stroma can become hyalinised and sclerotic. Calcifications within the stroma can lead to radiological detection (Fig. 3.17). Lipomatous, smooth muscle (Fig. 3.18), and osteochondroid metaplasia may be seen (Fig. 3.19). Pseudoangiomatous stromal hyperplasia can be present (Fig. 3.20). Stromal mitotic activity is usually scarce, though small numbers of stromal cell mitoses may be seen in fibroadenomas in young or pregnant patients. In paediatric patients, mitotic activity can range up to seven mitoses per ten high-power fields [3]. Infarction may occur during pregnancy (Figs. 3.21).

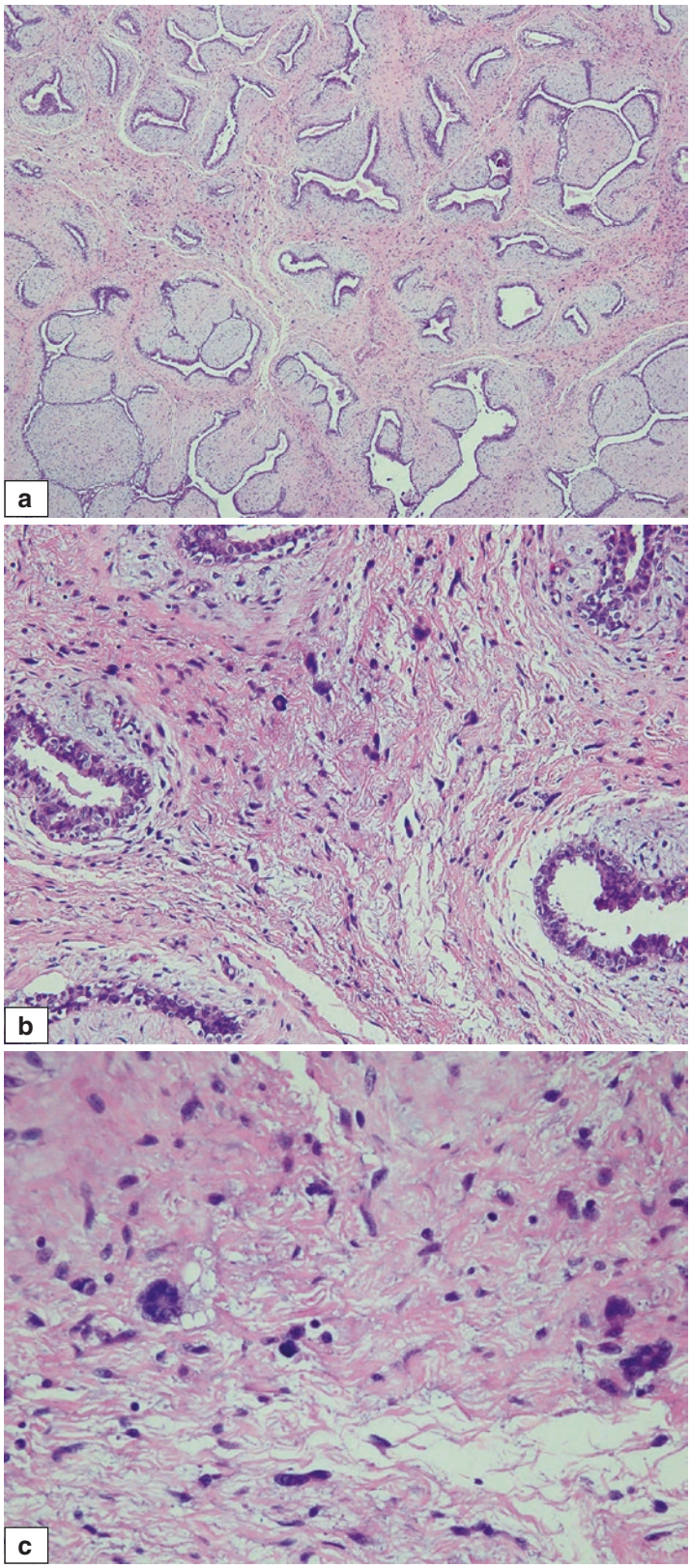

Fig. 3.14 Fibroadenoma with stromal multinucleated giant cells. (**a**) At low magnification, the stroma shows scattered cells with hyperchromatic nuclei. (**b**) The stromal multinucleated cells show smudged multilobated nuclei without discernible nucleoli or mitoses. These stromal cells do not contribute to assessment of stromal atypia in fibroepithelial lesions. (**c**) The stromal multinucleated cells can demonstrate a wreath-like arrangement of nuclei with inconspicuous pale cytoplasm. Adjacent stromal cells do not disclose significant nuclear atypia nor mitotic activity

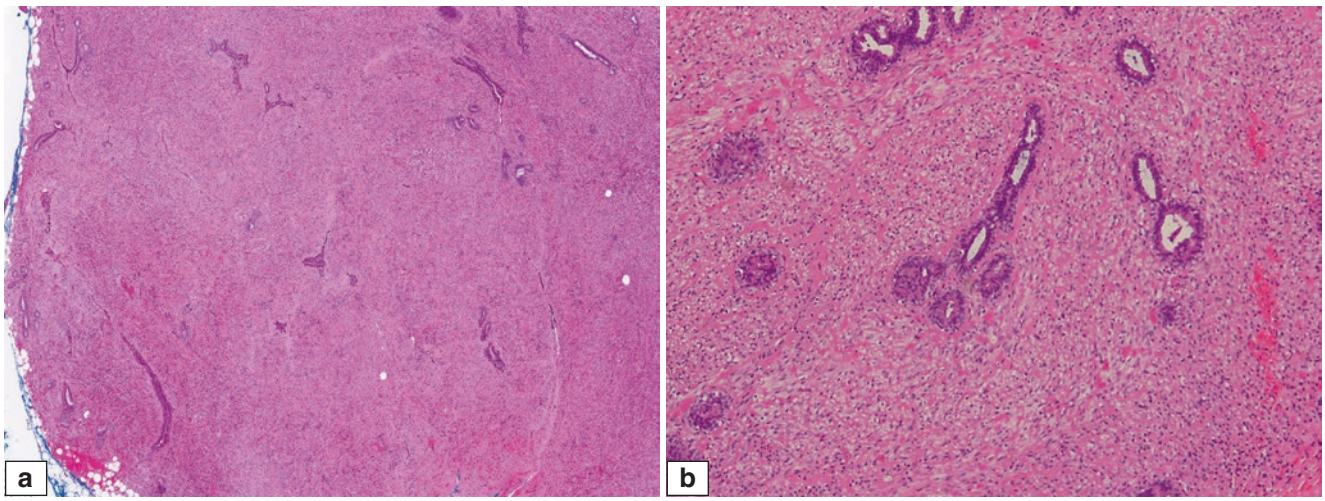

Fig. 3.15 (**a**) Low magnification view of a cellular fibroadenoma, with relatively uniform stromal cellularity punctuated by benign epithelial elements. (**b**) Cellular fibroadenoma shows increased stromal cellularity, with plump stromal cells surrounding tubules in a pericanalicular growth pattern

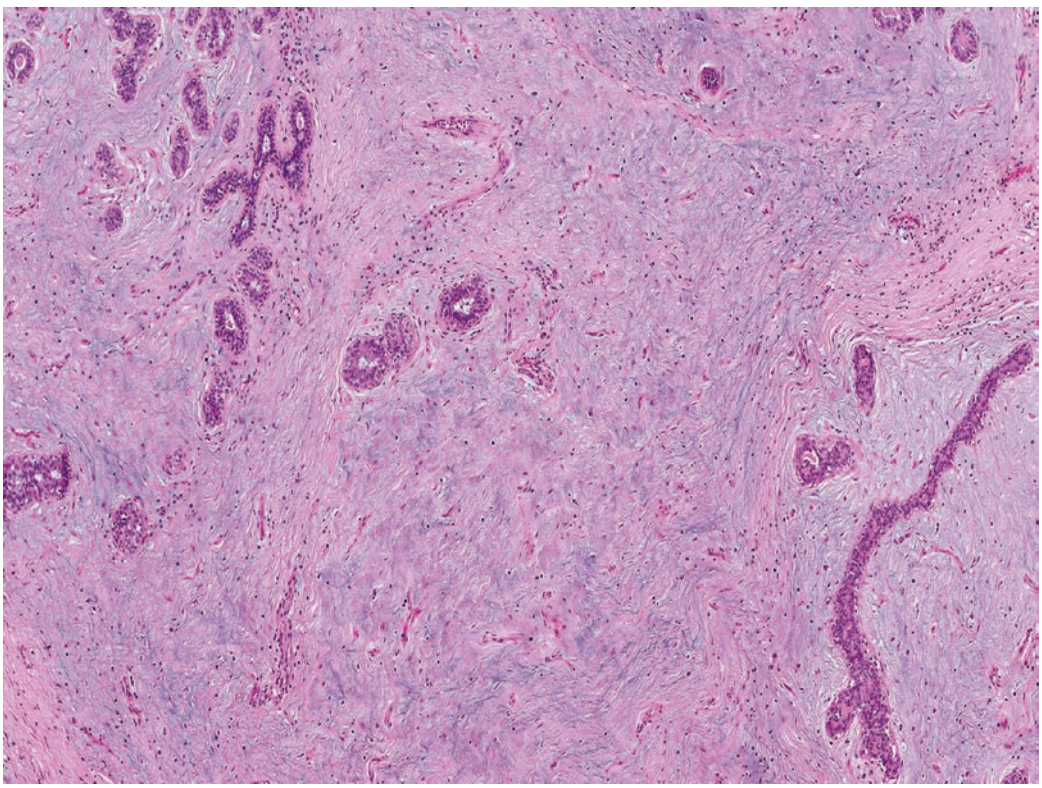

Fig. 3.16 Myxoid fibroadenoma. Epithelial elements are seen within a myxoid stroma containing greyish-blue ground substance

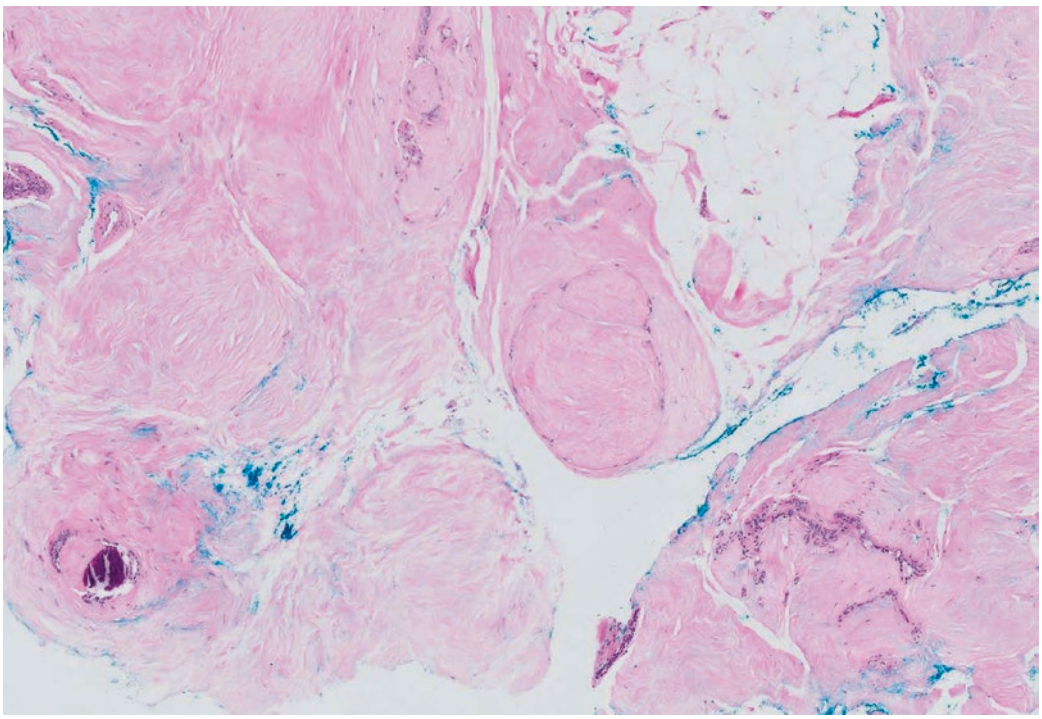

Fig. 3.17 Hyalinised calcified fibroadenoma. These lesions are detected on screening mammography and may be radiologically indeterminate leading to core biopsy for evaluation. This core biopsy shows scant epithelial elements among a hyalinised stroma. A fractured calcification is present in the lower left field

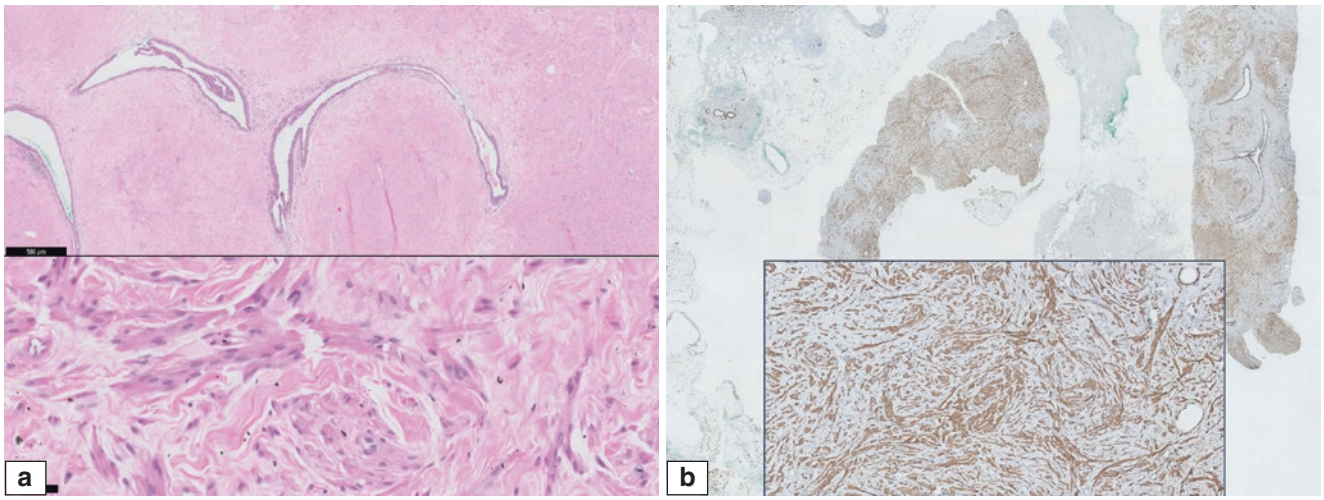

Fig. 3.18 Fibroadenoma with smooth muscle metaplasia in the stroma. (**a**) Upper field shows a low magnification view of the fibroadenoma with an intracanalicular growth pattern. The stroma discloses vague bundles of plump spindle cells with pink cytoplasm. The lower field shows high magnification of the spindle cells with elongated nuclei and tapered cytoplasm. (**b**) Immunohistochemistry for smooth muscle actin shows positive staining bundles in the stroma, with high magnification delineating the spindle cells confirming their smooth muscle nature

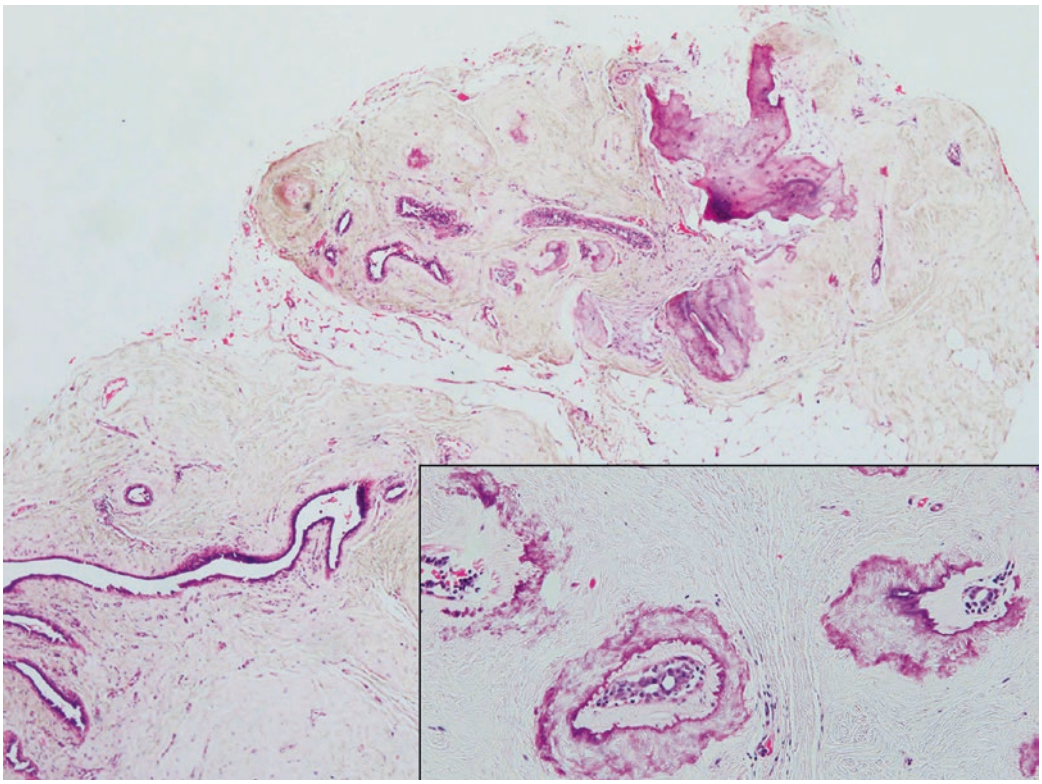

Fig. 3.19 Ossified fibroadenoma. Metaplastic bone formation is seen in the stroma of the core biopsy of this fibroadenoma. *Inset* shows bone deposition around the epithelial elements of this hyalinised fibroadenoma

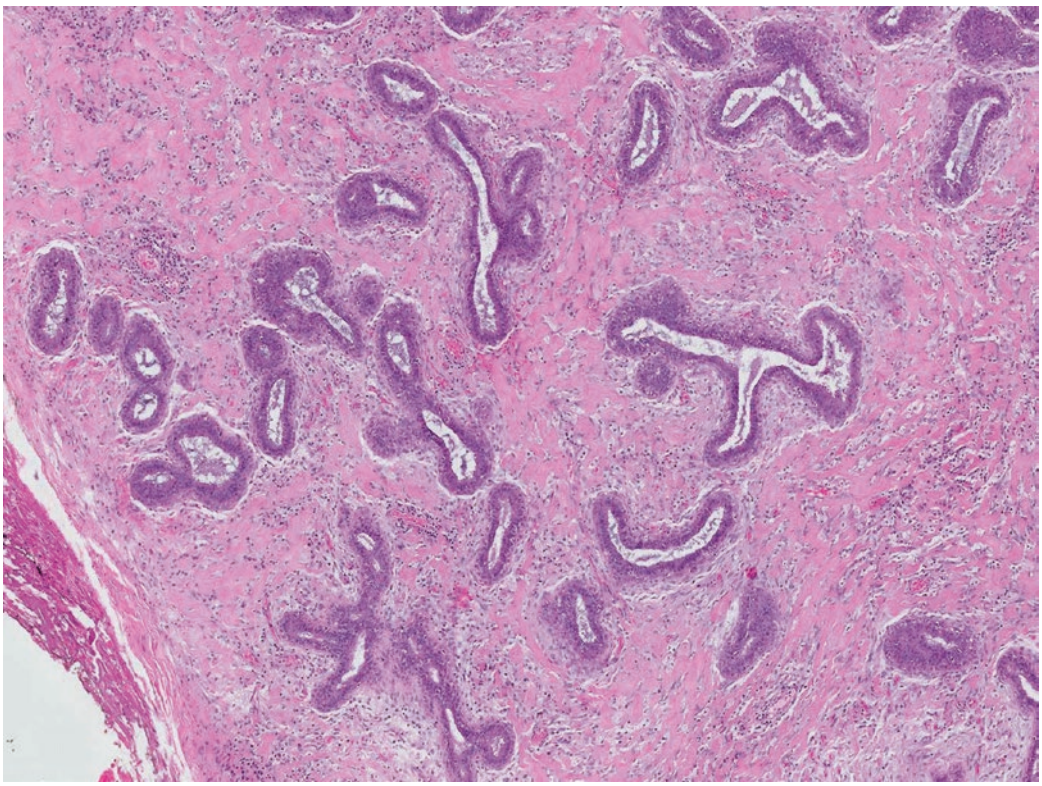

Fig. 3.20 Fibroadenoma with pseudoangiomatous stromal hyperplasia. The stroma of the fibroadenoma shows slit-like spaces lined by spindle nuclei. This may give the impression of increased stromal cellularity especially when there are scattered chronic inflammatory cells as well

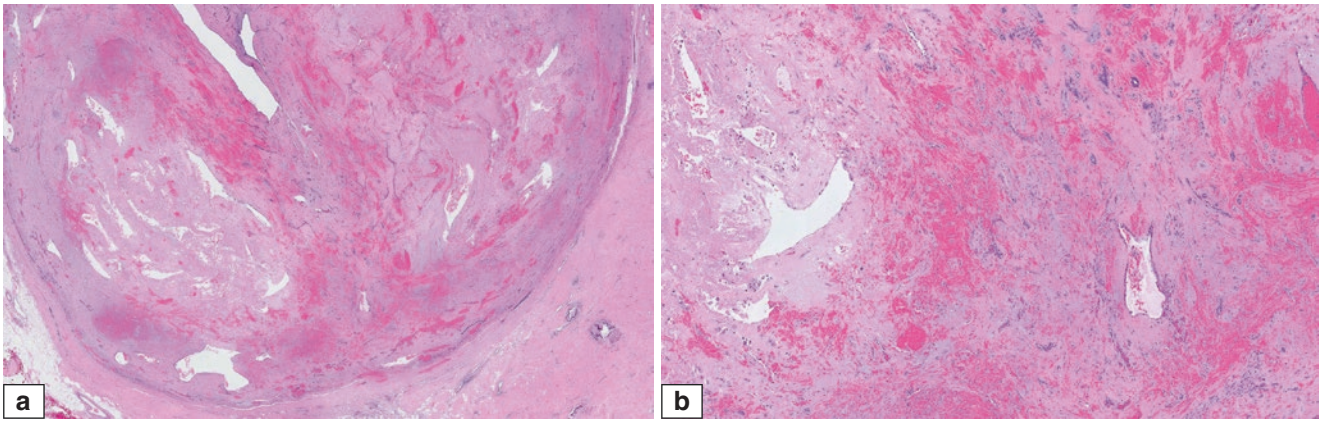

Fig. 3.21 Infarcted fibroadenoma. (**a**) At low magnification, the infarcted fibroadenoma shows areas of haemorrhage. (**b**) Areas of haemorrhage are seen in the stroma, with ghost outlines of necrotic epithelial and stromal cells

The juvenile fibroadenoma is encountered in younger patients, though it has been documented in older adults as well (Figs. 3.22 and 3.23). Often demonstrating a cellular stroma, the term juvenile fibroadenoma has sometimes been used synonymously with cellular fibroadenoma. We prefer to diagnose a juvenile fibroadenoma when there is a predominant pericanalicular growth pattern accompanied by usual ductal hyperplasia that may resemble epithelial changes of gynaecomastia (gynaecomastoid hyperplasia), in addition to cellular stroma featuring intersecting fibroblastic and myofibroblastic fascicles. Sometimes the epithelial changes mimic atypical ductal hyperplasia.

The complex fibroadenoma is diagnosed when there is sclerosing adenosis, epithelial calcifications, papillary apocrine metaplasia, and cysts measuring 3 mm or more in size [4]. The presence of any of these features can designate a fibroadenoma as "complex", though in our practice, we often reserve this diagnosis for fibroadenomas that either display a marked degree of these alterations or combination of alterations (Figs. 3.24 and 3.25). According to one study, complex fibroadenomas are associated with an increased relative risk of subsequent breast cancer (threefold), but the available data are insufficient to justify a different management approach for these lesions.

Differential Diagnosis

The rare **myxoma**, and the even rarer **low-grade fibromyxoid sarcoma**, may mimic the myxoid fibroadenoma, especially when the epithelial component is scant (Fig. 3.26).

The **tubular adenoma** consists of closely packed, rounded bilayered tubules resembling those in resting lobules. It is often encapsulated. Intervening stroma is usually scant and may appear cellular with accompanying lymphocytes. Grossly circumscribed, it can resemble the fibroadenoma, although it tends to be yellowish to tan brown with a softer consistency (Fig. 3.27). Histologically, it differs from the fibroadenoma by the dense arrangement of rounded tubules and the relative paucity of stroma. Luminal pink colloid-like secretions may be observed within the tubular lumens (Fig. 3.28).

Adenosis is defined by the presence of an increased number of acinar/ductular units, with retention of the overall lobular architecture on low-power histological assessment (Fig. 3.29). It may resemble the fibroadenoma and tubular adenoma when it forms an expansile nodular lesion, but is more often a microscopic process that lacks encapsulation. **Nodular sclerosing adenosis** is a closely related entity that comprises compressed tubules with a pseudoinvasive pattern, mimicking invasive lesions like tubular carcinoma.

The **lactating adenoma** occurs during pregnancy and lactation. While fibroadenomas and tubular adenomas with superimposed lactational changes may be referred to as lactating adenomas, most lactating adenomas tend to reflect lactational alterations in hyperplastic lobules. Grossly, it is circumscribed with brownish colouration and soft consistency (Fig. 3.30). Haemorrhage and infarction may be present (Fig. 3.31).

Fibroadenomas may contain sclerosing adenosis, which can mimic an invasive process, especially invasive lobular carcinoma or invasive tubular carcinoma occurring within the fibroadenoma (Fig. 3.32). Identification of preserved myoepithelial cells and intact basement membranes assists in confirming a non-invasive process. The absence of accompanying in situ and invasive disease in surrounding breast tissue is also a useful clue pointing away from an invasive process in the fibroadenoma. Table 3.1 shows a comparison of histologic features of these conditions.

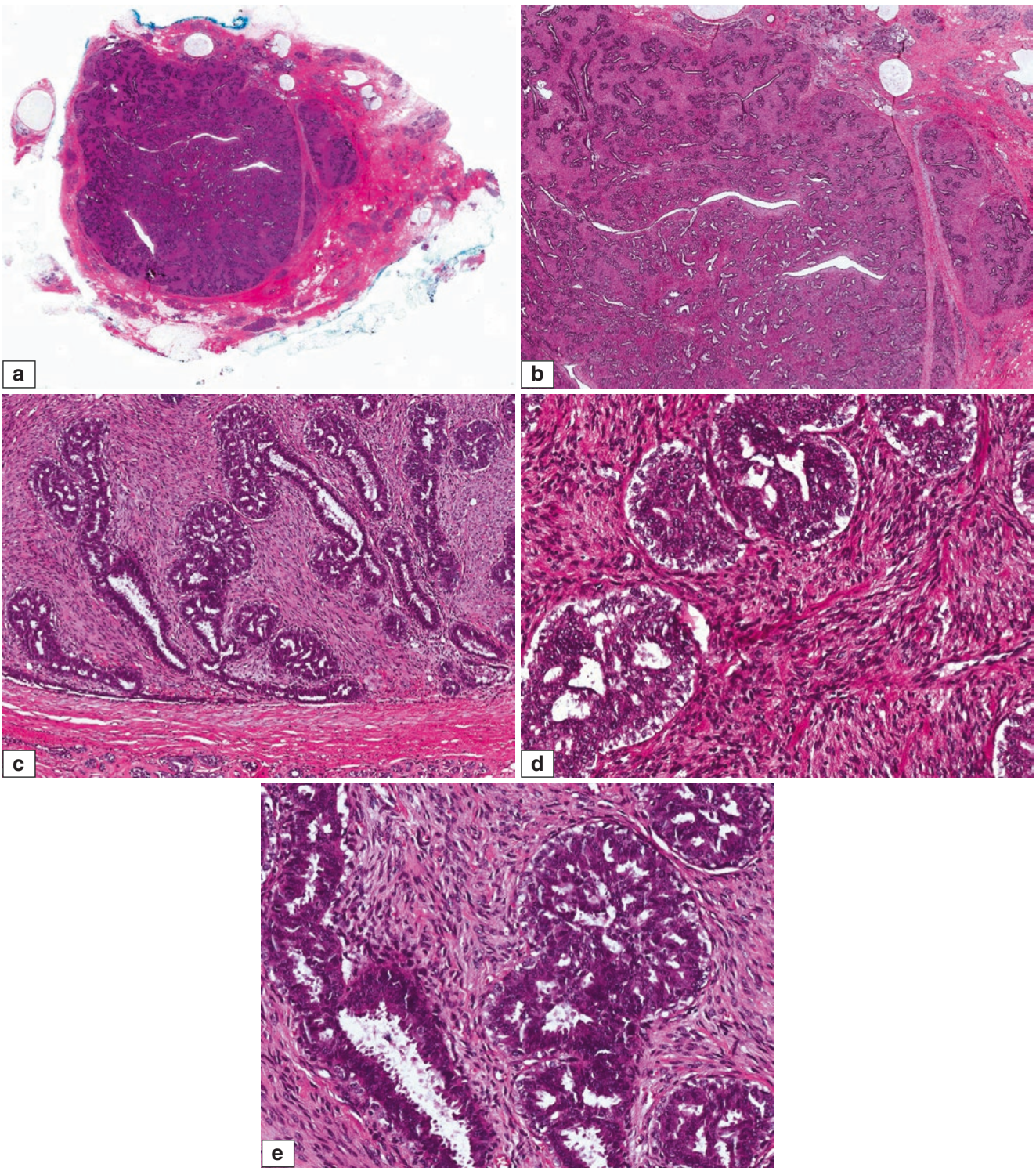

Fig. 3.22 Juvenile fibroadenoma in a 26-year-old woman. (**a**) Circumscribed contours are seen at low magnification. (**b**) The juvenile fibroadenoma shows well-delineated borders and a high density of epithelial elements. A few adjacent rounded nubbins of lesional tissue are present. (**c**) The epithelial component of the juvenile fibroadenoma shows a pericanalicular pattern with moderate usual ductal hyperplasia giving rise to sieve-like formations, embedded within a fairly cellular spindled stroma. The pattern of usual ductal hyperplasia with micropapillary and cribriform appearances may mimic atypical ductal hyperplasia. (**d**) The spindled stromal cells comprising both fibroblasts and myofibroblasts are disposed in sweeping fascicles, swirling around the epithelial structures. Stromal spindle cell nuclei are bland, elongated, and occasionally compressed. (**e**) The epithelial cells show columnar change with apical snouts, with a few short tufts peeping into the lumen, linking up to form bridges encircling irregular spaces

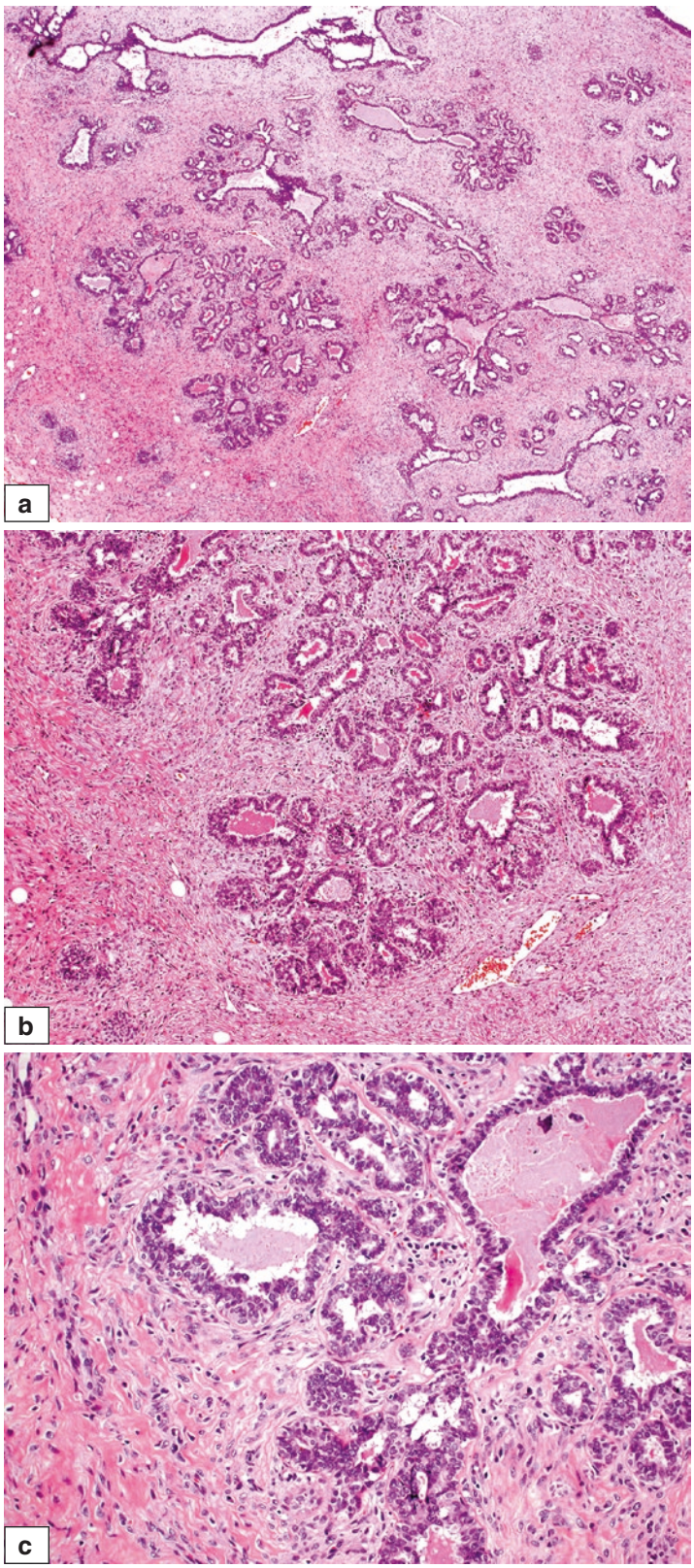

Fig. 3.23 Juvenile fibroadenoma in a paediatric patient. (**a**) Low magnification shows epithelial elements recapitulating the terminal ductal lobular unit dispersed within a slightly cellular stroma. (**b**) Medium magnification shows usual ductal hyperplasia with occasional pink viscid secretions within the duct lumens. The stroma shows relatively even and diffusely increased cellularity. (**c**) Ductal epithelial hyperplasia here is mostly mild, with short micropapillary and snoutlike protrusions into the luminal spaces. Surrounding stromal cells show ovoid-to-elongated plump vesicular nuclei (Courtesy of Dr. Kenneth Chang)

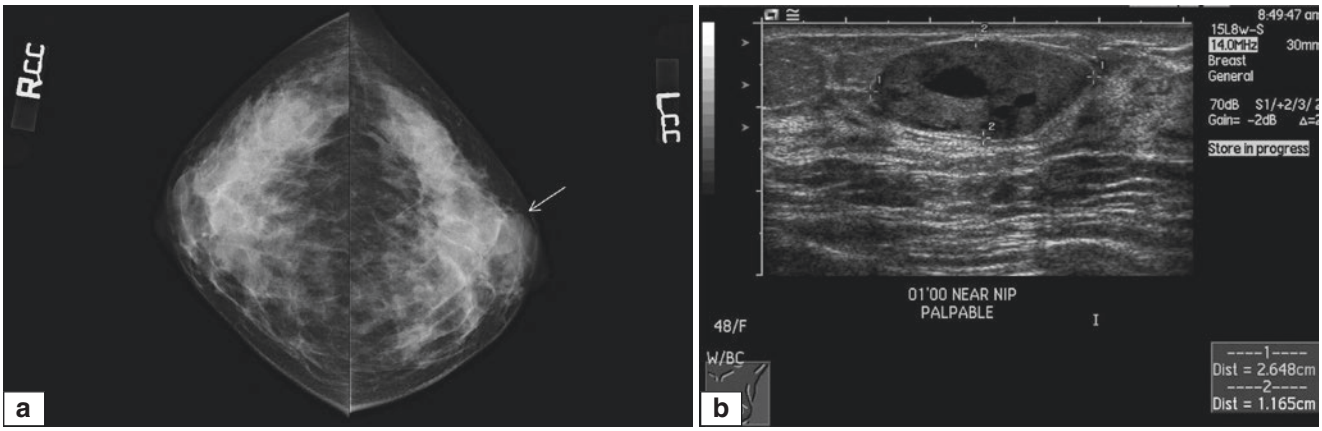

Fig. 3.24 Complex fibroadenoma. (**a**) Mammograms show a rounded opacity (*arrow*) in the left breast near the nipple (craniocaudal view). (**b**) Ultrasound shows a well-defined mass with internal echoes and cysts, measuring up to 2.6 cm

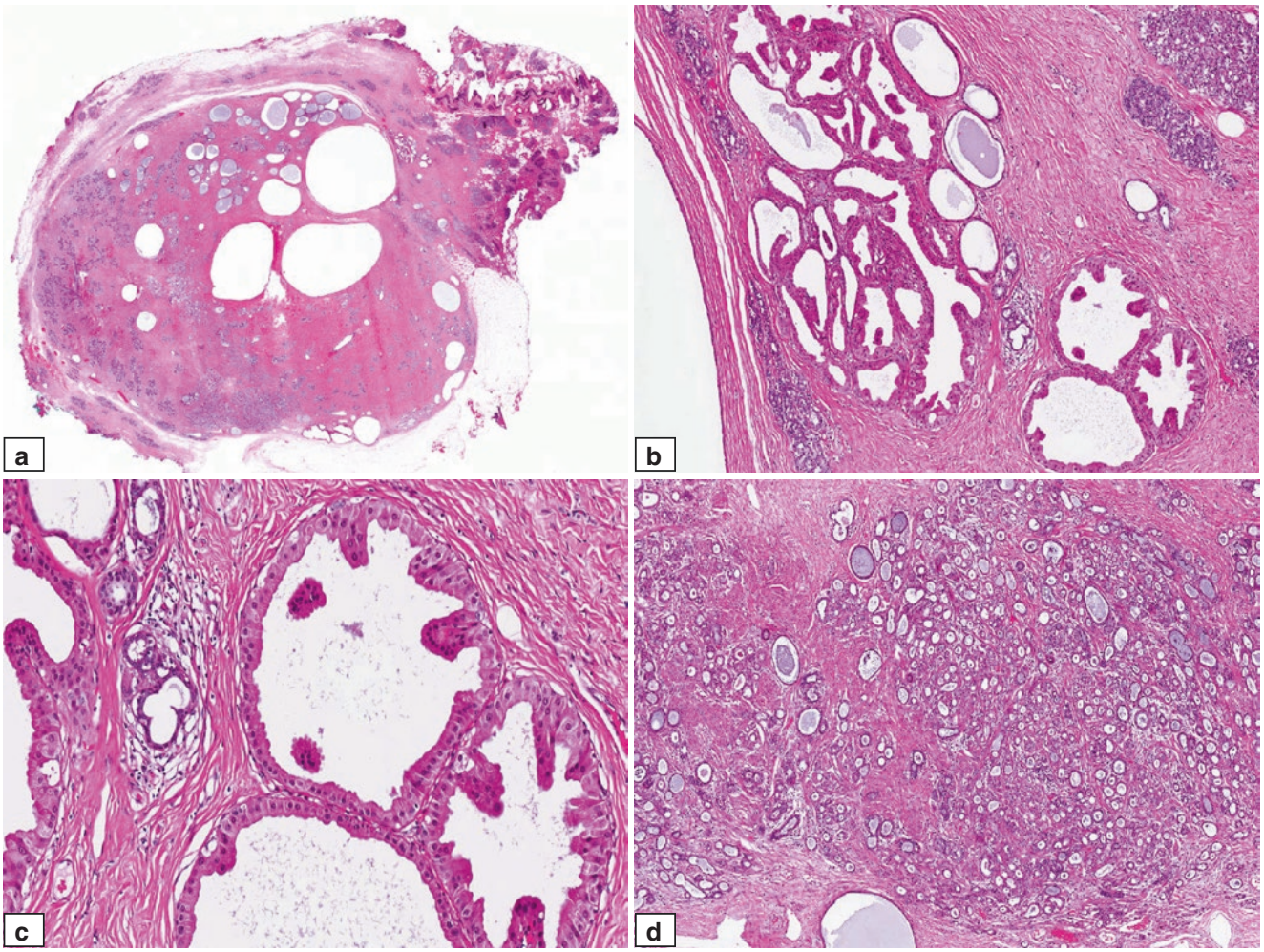

Fig. 3.25 Complex fibroadenoma. (**a**) Scanning view shows a well-circumscribed nodule punctuated by multiple cysts, expanding against the surrounding rim of breast tissue. (**b**) Cysts are lined by apocrine epithelium with papillary hyperplasia. (**c**) Higher magnification of the cysts lined by apocrine cells with luminal protrusions. (**d**) Sclerosing adenosis within a complex fibroadenoma, demonstrating closely packed tubules, some of which are compressed by myoepithelial cuffs. At low magnification, sclerosing adenosis appears to have a vaguely rounded contour. (**e**) Higher magnification of sclerosing adenosis shows both compressed as well as patent bilayered tubules. (**f**) Several patent lumens show pink secretions, with some appearing condensed and hardened into calcifications. (**g**) High magnification of the tubules containing luminal pink secretions, some appearing thick, hardened and almost calcific

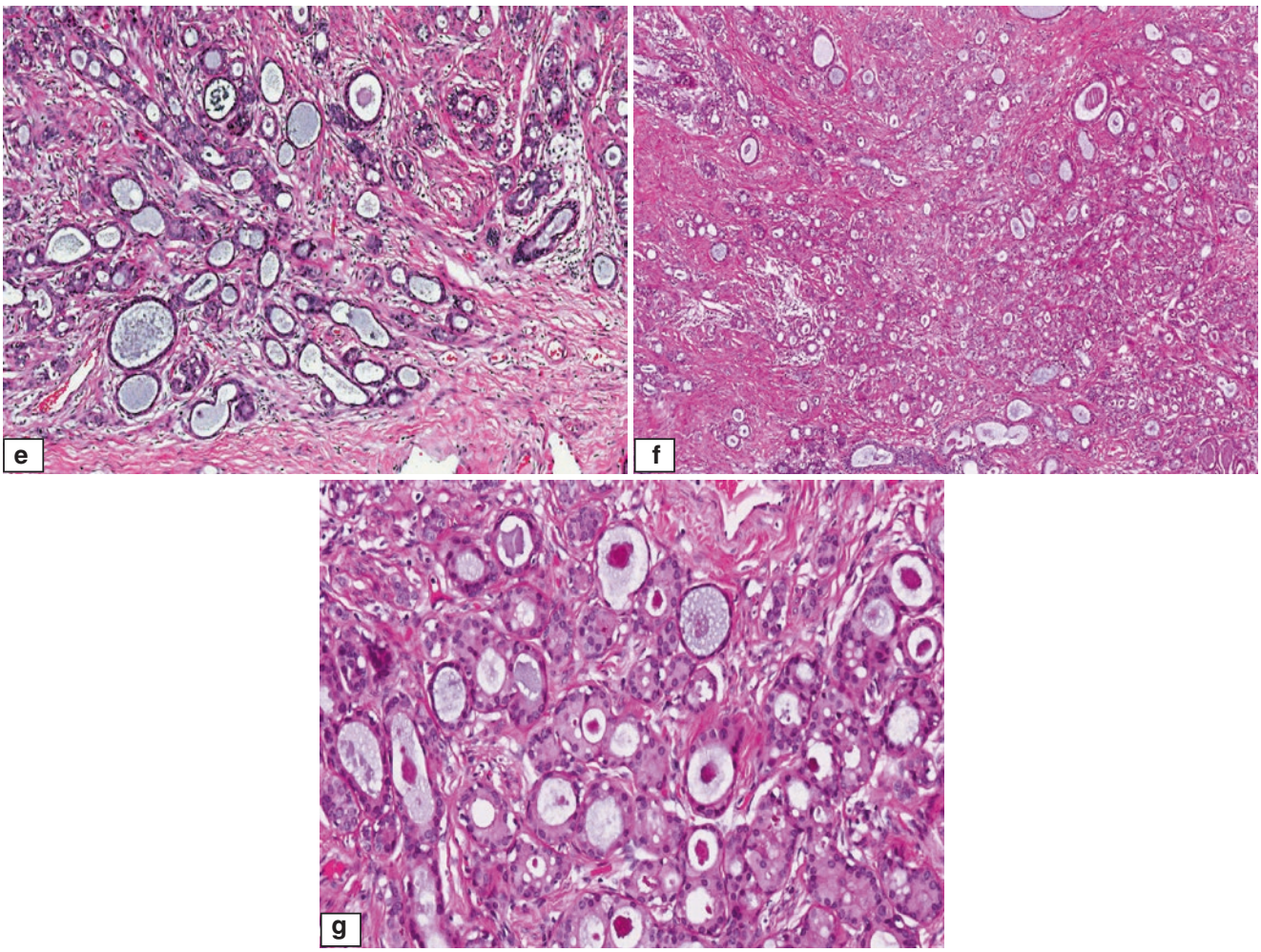

Fig. 3.25 (continued)

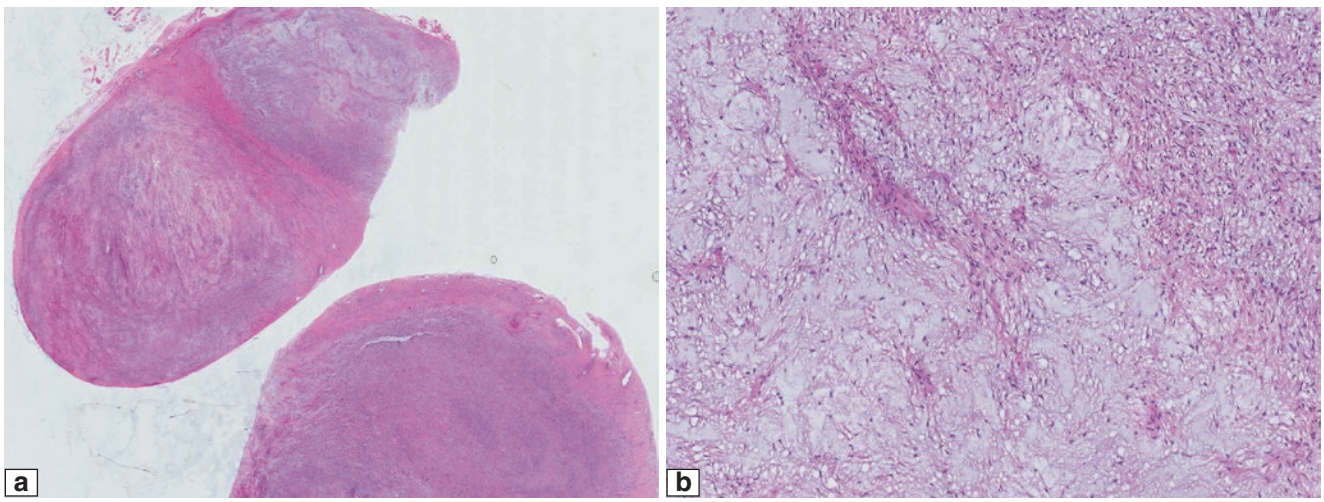

Fig. 3.26 (**a**) Low-grade fibromyxoid sarcoma, presenting as an axillary mass on screening mammography. At scanning magnification, the tumour has circumscribed boundaries with a spindle cell proliferation amid oedematous myxoid background. A cursory view may raise the differential of a myxoid fibroadenoma, except that this tumour is completely devoid of participating epithelial elements. (**b**) Higher magnification shows relatively bland spindle cells with variably myxoid and more cellular zones. The diagnosis was confirmed on fluorescence in situ hybridisation with the presence of FUS break-apart

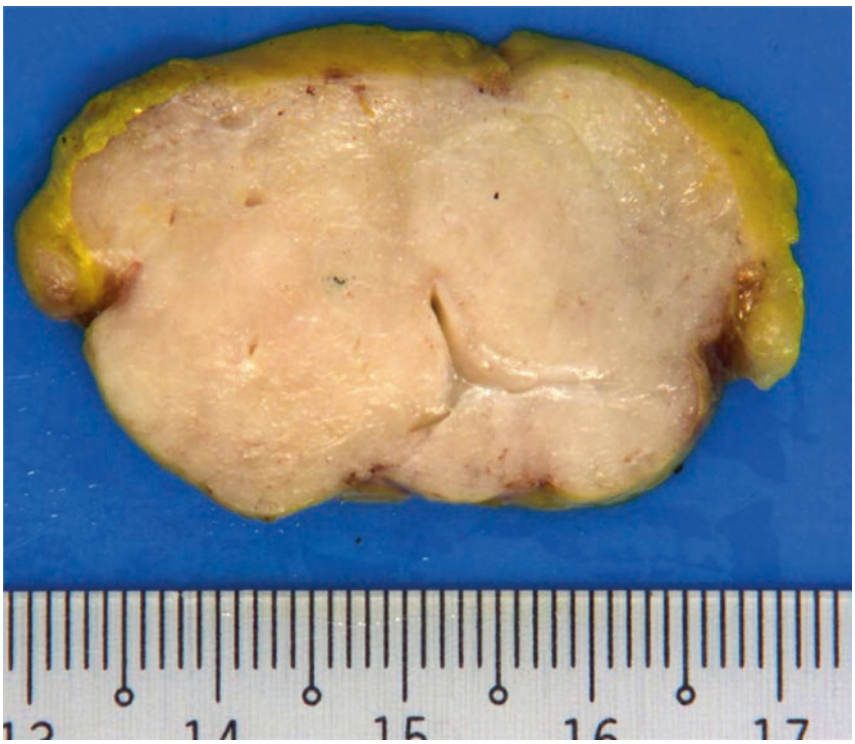

Fig. 3.27 Tubular adenoma. On gross inspection, the tubular adenoma appears greyish brown and is of softer consistency. Occasional curvaceous slit-like spaces are seen. A rim of adjacent adipose breast tissue is noted around the upper contour of the lesion

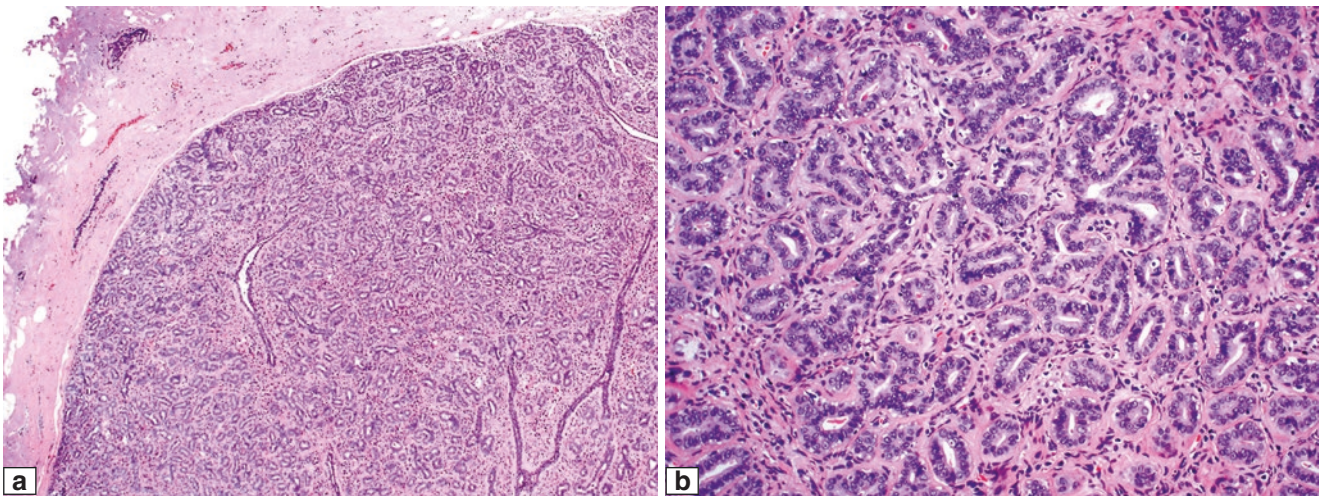

Fig. 3.28 Tubular adenoma. (**a**) At low magnification, the tubular adenoma shows a densely packed collection of rounded tubules with scant intervening stroma, contrasting with the fibroadenoma in which there is accompanying stromal proliferation separating the epithelial elements. Note the circumscribed boundary with adjacent breast tissue, with a semblance of a thin capsule in parts. (**b**) At higher magnification, the tubules show bilayering with cuboidal to columnar luminal epithelium rimmed by a variably conspicuous myoepithelial layer that may demonstrate clear-to-pale cytoplasm. Luminal epithelial cells may disclose vesicular nuclei with visible nucleoli that can sometimes be potentially worrying when scrutinized at high magnification. The absence of significant nuclear pleomorphism or mitoses, together with the well-preserved myoepithelial layer, are reassuring features. Note the scant stroma in between the tubules, with some tubules almost touching one another. In the pericanalicular fibroadenoma, the tubules are more dispersed and widely separated by stroma

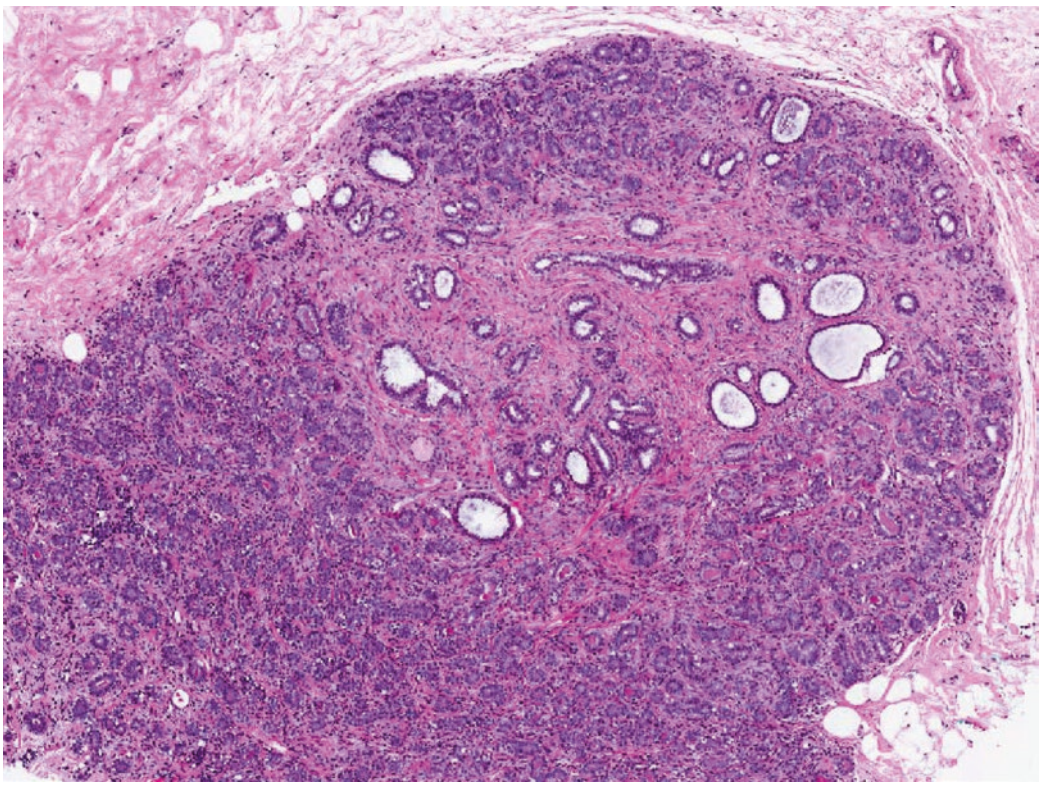

Fig. 3.29 Nodular adenosis. There is a nodular expansion of the lobule by an increased number of acini/ductules, some of which show mild dilatation. The periphery of this adenotic focus is rounded and pushing. There can be overlapping features with the tubular adenoma when the acini become closely packed, though nodular adenosis tends to be a microscopic alteration that generally does not lead to symptomatic presentation

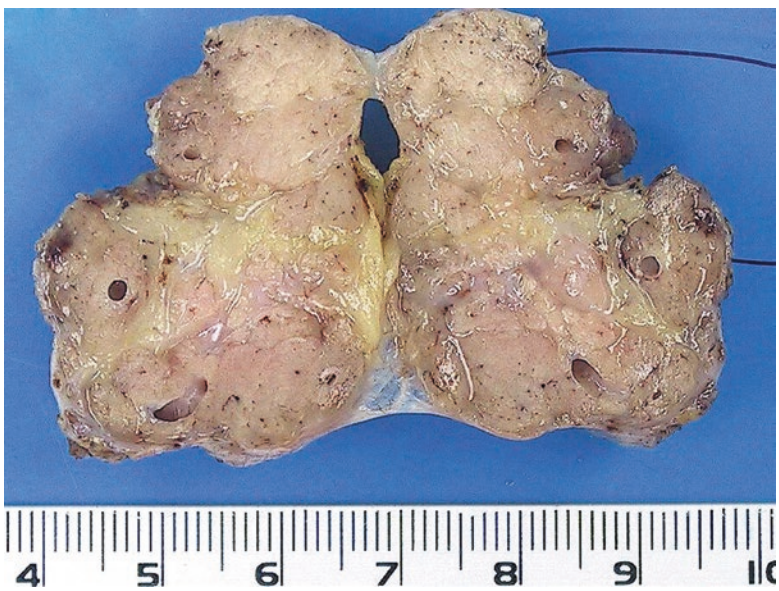

Fig. 3.30 Lactating adenoma. Macroscopic appearance of a lactating adenoma, sliced through to demonstrate its solid lobulated greyish-brown cut surface, disclosing intervening yellowish fatty areas as well as a few cysts

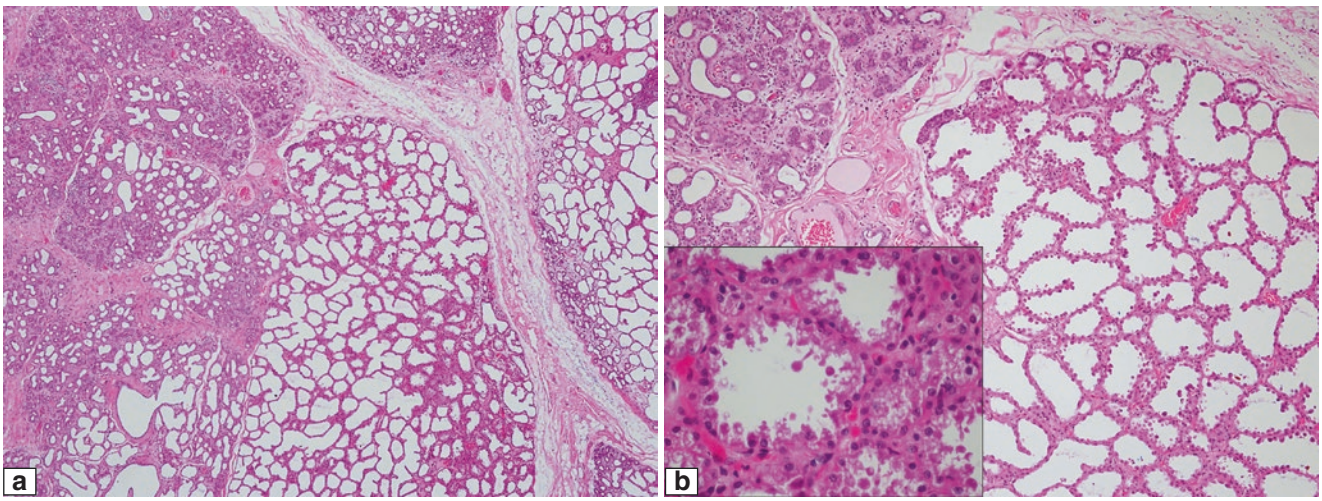

Fig. 3.31 Lactating adenoma. (**a**) At low magnification, the lactating adenoma shows enlarged lobules with increased numbers of closely packed acini. Some lobules disclose a greater degree of lactational change with dilated lumens, pink lining epithelium, and a few luminal epithelial projections. (**b**) Medium magnification shows juxtapositioning of a lobule with established lactational changes with one where secretory alterations are less well developed. Inset shows lining epithelial cells with pink bubbly cytoplasm with apical blebs and snouts

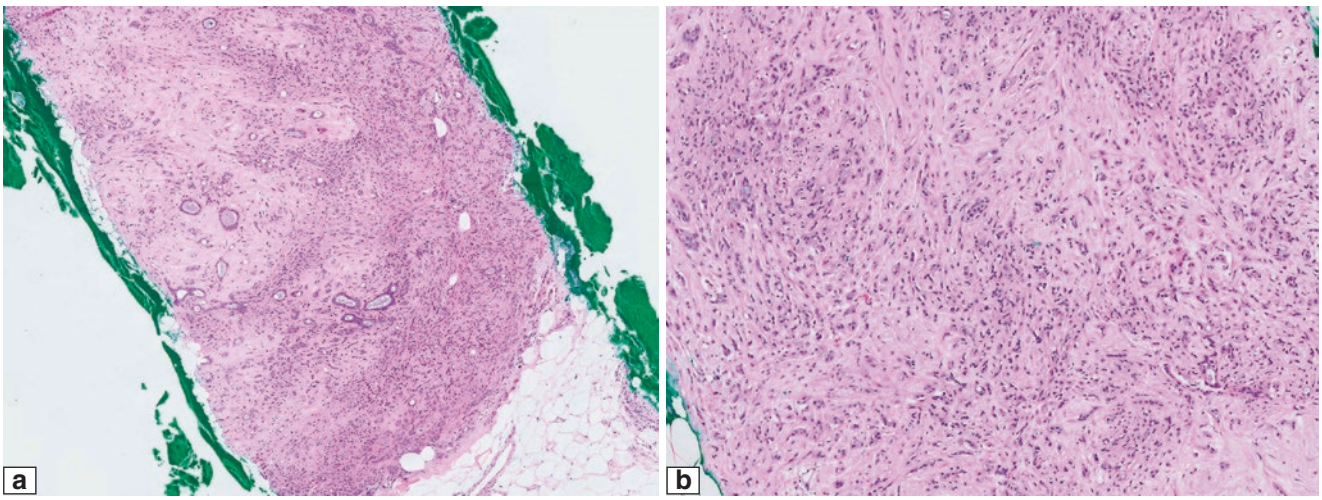

Fig. 3.32 Fibroadenoma with sclerosing adenosis. (**a**) Core biopsy of a radiologically detected nodule shows a fibroadenoma with sclerosing adenosis, which can mimic a fibroadenoma containing an invasive carcinoma. At low magnification, there are numerous compressed epithelial elements extending between and around ducts, giving a pseudoinvasive pattern. The edge of the fibroadenoma is seen as a relatively sharp interface with adjacent adipose tissue. (**b**) Medium magnification shows the small epithelial nests to be rimmed by a pink basement membrane sheath, with intervening collagenous stroma that is unadulterated by any desmoplastic or stromal response. The lobular architecture of sclerosing adenosis may be difficult to appreciate within a fibroadenoma. (**c**) Another area of the fibroadenoma with small compressed tubules. Bilayering may be appreciated at high magnification (*inset*). (**d**) Immunohistochemistry for p63 shows intact myoepithelial cells. (*left*) Low magnification discloses many myoepithelial cells among the epithelial elements. (*right*) High magnification shows positive p63 nuclear staining of myoepithelial cells interspersed among luminal epithelial cells which are negative for p63. (**e**) Immunohistochemistry for SMMS shows delineation of myoepithelial cells. Inset shows cytoplasmic reactivity of myoepithelial cells surrounding the luminal epithelial cells

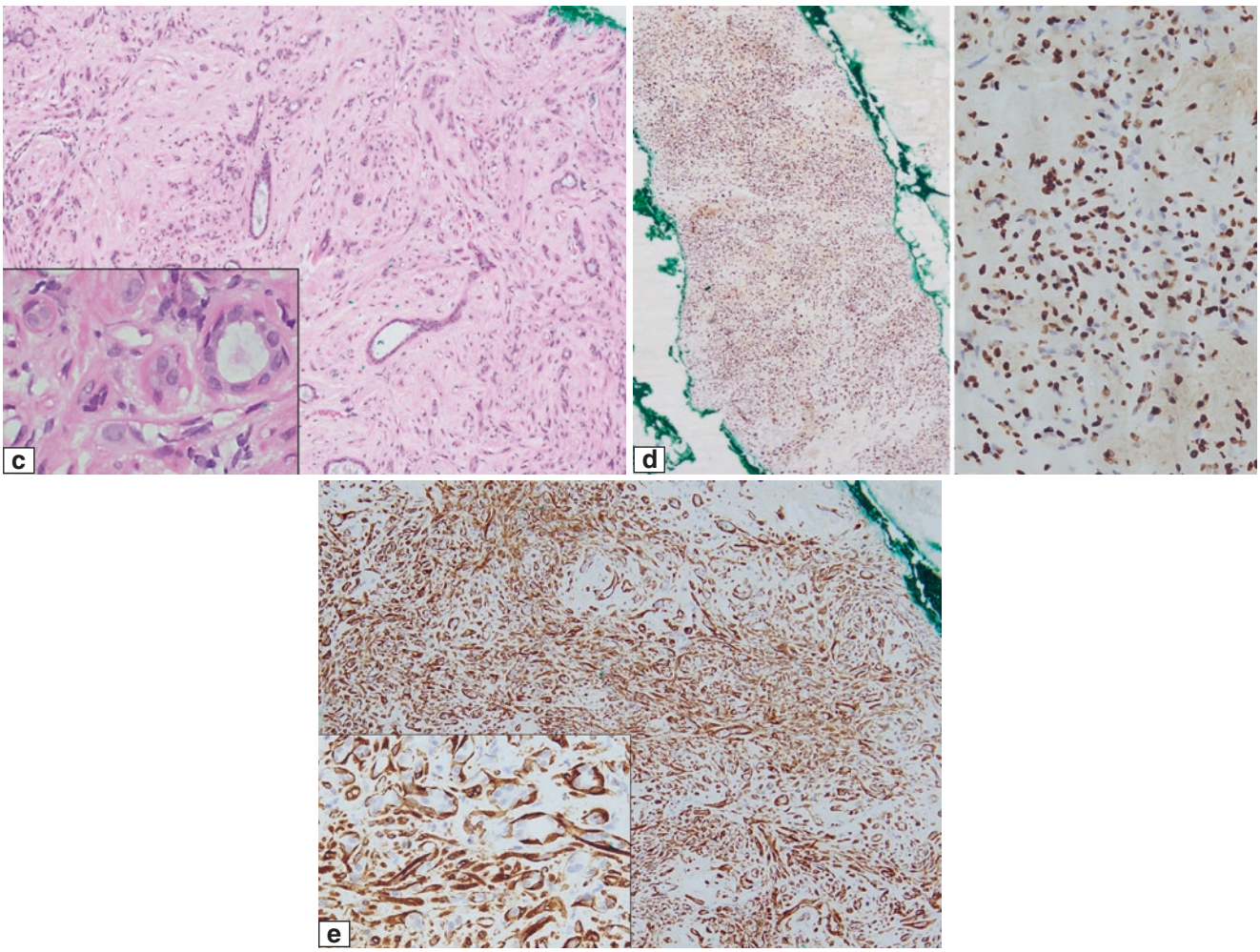

Fig. 3.32 (continued)

Table 3.1 Histological comparison of fibroadenomas containing sclerosing adenosis versus fibroadenomas with invasive lobular and tubular carcinomas

Histological feature	Fibroadenoma with sclerosing adenosis	Fibroadenoma with invasive lobular carcinoma	Fibroadenoma with invasive tubular carcinoma
Low magnification	Preserved rounded architecture of sclerosing adenosis	Invasive pattern of linear cords	Invasive pattern of haphazardly placed angulated tubules
Myoepithelial cells	Present (immunohistochemistry is a useful adjunct)	Absent	Absent
Basement membrane	Intact (PAS stain or immunohistochemistry is a useful adjunct)	Absent	Absent
Accompanying epithelial changes	Absence of atypical hyperplasia or in situ disease	Presence of lobular neoplasia	Presence of flat epithelial atypia, atypical ductal hyperplasia, or low-grade DCIS
Surrounding breast tissue	Other areas of sclerosing adenosis may be present	Invasive lobular carcinoma can be seen	Invasive tubular carcinoma can be seen

PAS periodic acid Schiff, *DCIS* ductal carcinoma in situ

Prognosis and Therapy Considerations

Fibroadenomas are benign tumours. When diagnosed on fine needle aspiration or core biopsy, they may be left alone without excision. Many institutions, however, adopt protocols that recommend excision, via either open or mammotome techniques, of lesions beyond a certain size, or if symptomatic.

Phyllodes Tumour

Definition

The phyllodes tumour is a fibroepithelial neoplasm which resembles the intracanalicular fibroadenoma. It differs from the latter by an exaggerated intracanalicular growth pattern that gives it a fronded leaf-like architecture, accompanied by stromal cellularity that may sometimes demonstrate peri-epithelial accentuation.

Clinical and Epidemiological Features

Phyllodes tumours affect women over a wide age range, though the mean and median age at diagnosis is in the fifth decade, in contrast to the fibroadenoma, which tends to occur in younger women. Phyllodes tumours constitute 0.3–1 % of all breast tumours, and 2.5 % of all fibroepithelial tumours [5]. They are seen more frequently in women of Asian and Hispanic descent [5, 6]. Malignant phyllodes tumours account for 2.1 % of all breast malignancies [7].

Phyllodes tumours can grow to enormous sizes. Clinically, these are symptomatic masses that may distort the breast when large, with skin ulceration occurring in extreme enlargement.

Imaging Features

Phyllodes tumours are radiologically rounded and bosselated masses. They can be indistinguishable from fibroadenomas on imaging, but unlike fibroadenomas they rarely calcify, and the presence of internal cystic spaces favours phyllodes (Fig. 3.33).

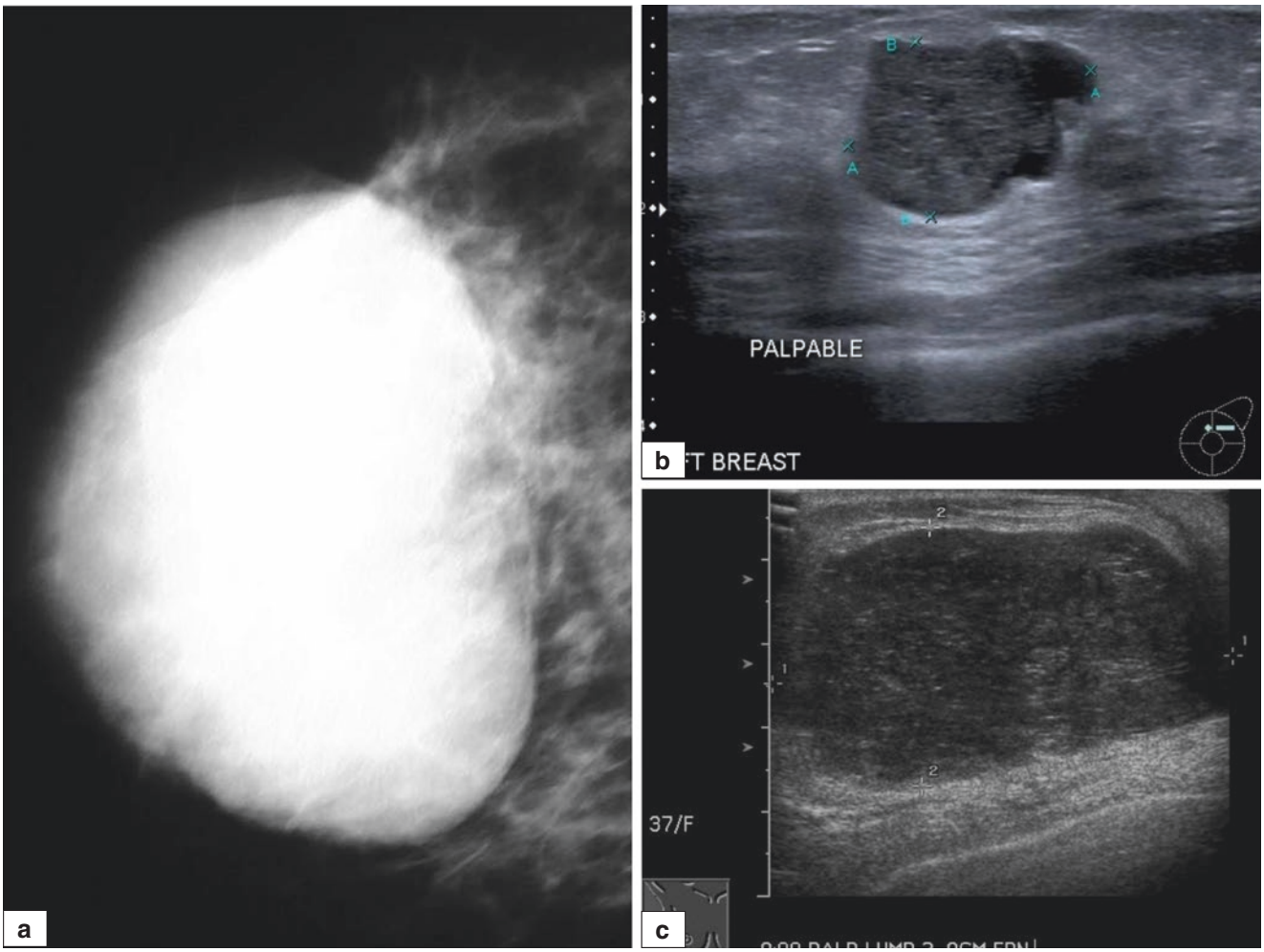

Fig. 3.33 Radiology of phyllodes tumour. (**a**) Mammographic image of a phyllodes tumour shows a large opaque rounded mass in the breast. (**b**) Ultrasonography of a phyllodes tumour demonstrates a lobulated, well-defined heterogeneous hypoechoic nodule with some cystic changes. The nodule measures up to 2.34 cm. (**c**) Another ultrasound image shows a relatively circumscribed hypoechoic heterogeneous mass measuring 5.14 cm maximally

Pathologic Features

Macroscopic Pathology

Grossly, phyllodes tumours have lobulated circumscribed borders, although microscopic unencapsulation and permeative borders may be seen despite apparent gross circumscription. Papillary stromal fronds projecting into cystic spaces may be visualised. Depending on the stromal quality, the consistency can be firm and fibrous, myxoid and watery, and soft and fleshy, with haemorrhage and necrosis seen in larger and malignant tumours. Cystic degeneration may occur (Figs. 3.34, 3.35, 3.36, 3.37, 3.38, 3.39, 3.40, 3.41, 3.42, 3.43, 3.44, and 3.45).

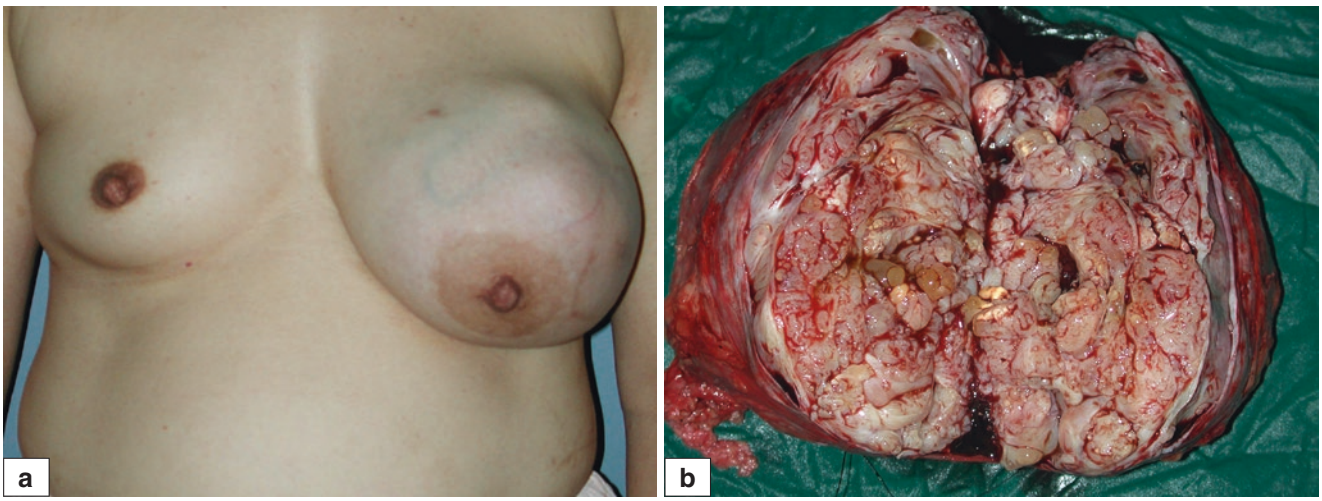

Fig. 3.34 (**a**) Large phyllodes tumour stretches the skin over the left breast with distension of superficial veins (Courtesy of Dr. Gay Hui Ho). (**b**) Resected left breast tumour, with the fresh unfixed specimen cut open to show fleshy whorled appearances with cystic, mucoid, and necrotic areas

Fig. 3.35 Mastectomy specimen containing a large phyllodes tumour in its formalin-fixed state, showing a greyish-brown appearance with lobulated contours, leafy architecture, whorled areas, and visible clefts. Histologically, the tumour showed borderline features

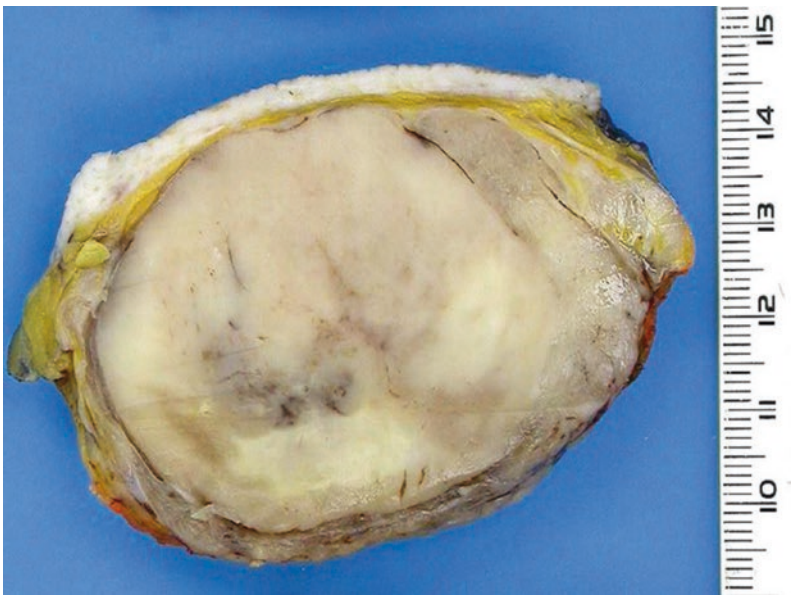

Fig. 3.36 Macroscopy of a malignant phyllodes tumour in the formalin-fixed state, disclosing a greyish-white solid fleshy appearance with haemorrhage and pale yellow necrotic zones. There is a grossly circumscribed and gently lobulated outline

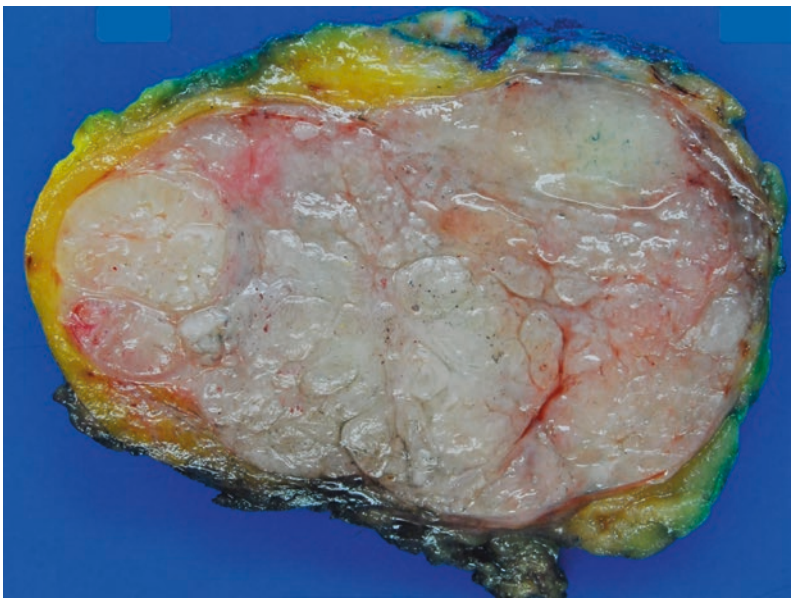

Fig. 3.37 Benign phyllodes tumour. Macroscopically, the tumour shows relatively circumscribed borders, with a whitish-grey lobulated appearance and some arc-like slits

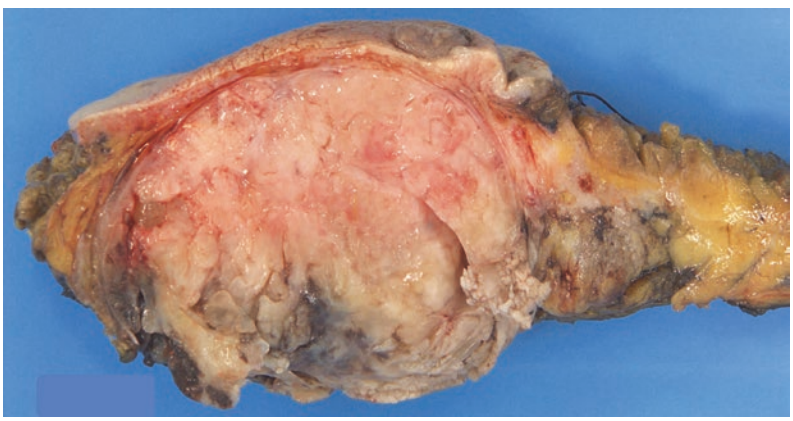

Fig. 3.38 Large benign phyllodes tumour that was surgically treated with mastectomy. Fronds are readily seen on macroscopic inspection

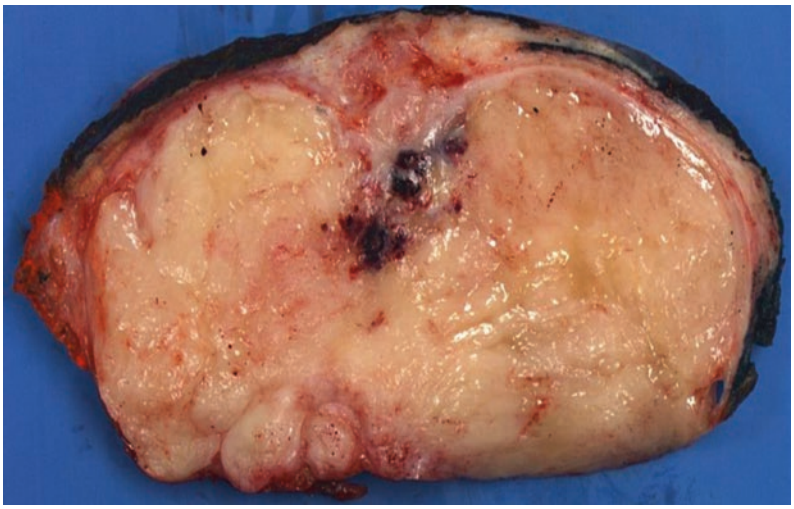

Fig. 3.39 Benign phyllodes tumour with circumscribed and lobulated outlines shows areas of haemorrhage

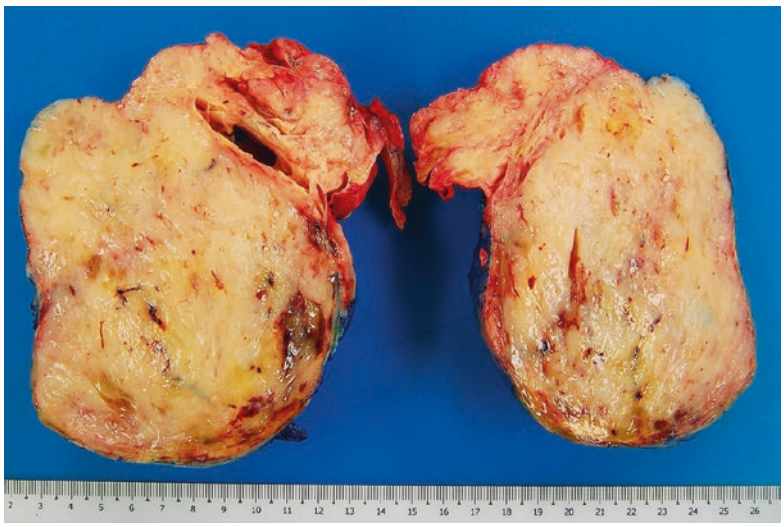

Fig. 3.40 Borderline phyllodes tumour. Bisected tumour shows areas of haemorrhage and scattered slit-like spaces within a fibrous whorled, yellowish grey-white parenchyma. Grade of phyllodes tumour is difficult to predict on the macroscopic appearances though necrosis and haemorrhage tend to be observed more frequently in malignant forms

Microscopic Pathology

Phyllodes tumours are divided into benign, borderline, and malignant grades. Histologically, appearances vary depending on the grade, which should be established in the most cellular zones with worst microscopic alterations (Fig. 3.46). Grading of phyllodes tumours is based on a constellation of histologic features: stromal parameters of atypia (Fig. 3.47), cellularity, mitotic activity (Fig. 3.48), overgrowth (Fig. 3.49) (defined as a low-power field comprising only stroma without epithelial elements), and nature of the tumour contours (pushing or permeative) (Fig. 3.50). Benign phyllodes tumours show mild stromal atypia and hypercellularity with few mitoses (four or fewer mitoses per ten high-power fields), pushing borders, and absence of stromal overgrowth (Figs. 3.51 and 3.52). Malignant phyllodes tumours show marked stromal atypia and hypercellularity, ten or more stromal mitoses per ten high-power fields, and presence of stromal overgrowth and permeative borders. Tumours with intermediate features are classified as borderline (Figs. 3.53 and 3.54). When malignant heterologous elements are seen, the tumour is considered malignant regardless of the status of other histological parameters (Figs. 3.55, 3.56, 3.57, 3.58, 3.59, 3.60, 3.61, 3.62, and 3.63).

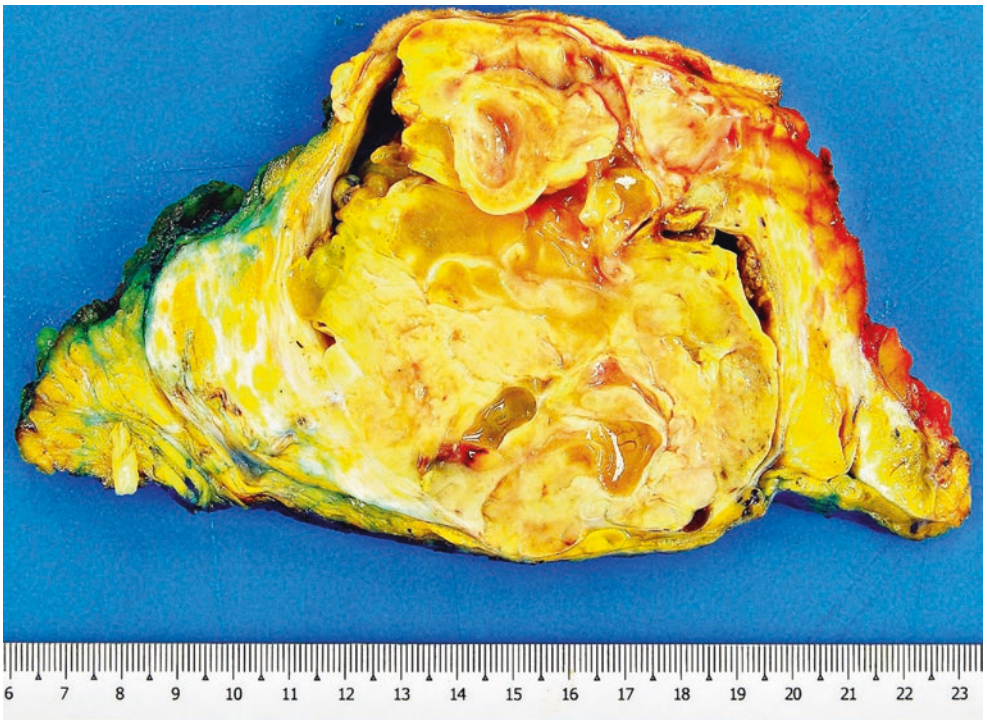

Fig. 3.41 Borderline phyllodes tumour. Cystic spaces are seen on cut section of the tumour which has a yellowish appearance

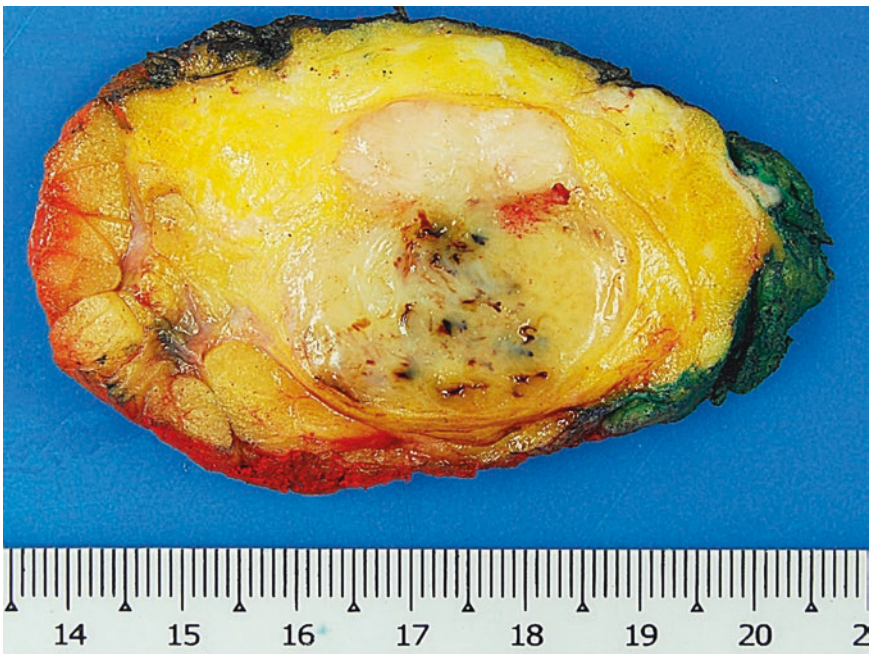

Fig. 3.42 Borderline phyllodes tumour. The tumour has a heterogeneous cut appearance, with one portion that is whitish and firm, while the other part with areas of haemorrhage discloses a softer, more ill-defined, and myxoid quality

Fig. 3.43 Borderline phyllodes tumour. The tumour has a large cystic component with fronds projecting into the collapsed cystic space

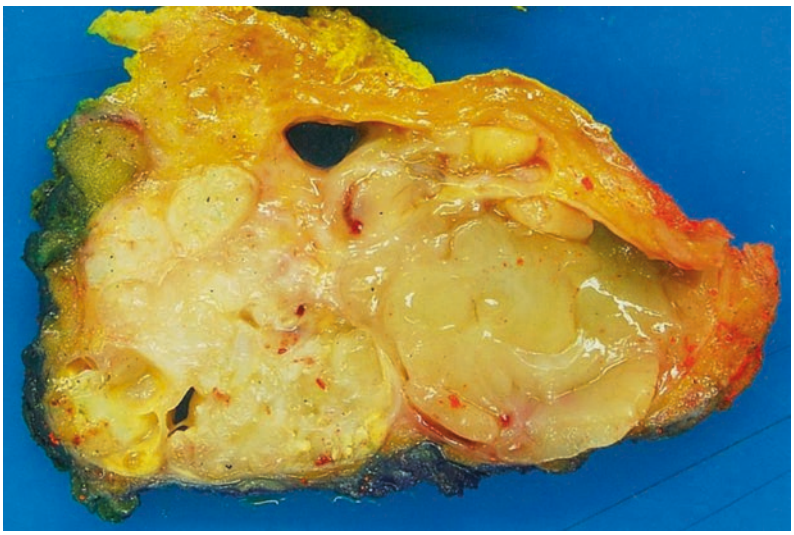

Fig. 3.44 Borderline phyllodes tumour. Cystic spaces, and whitish yellow and myxoid zones are present

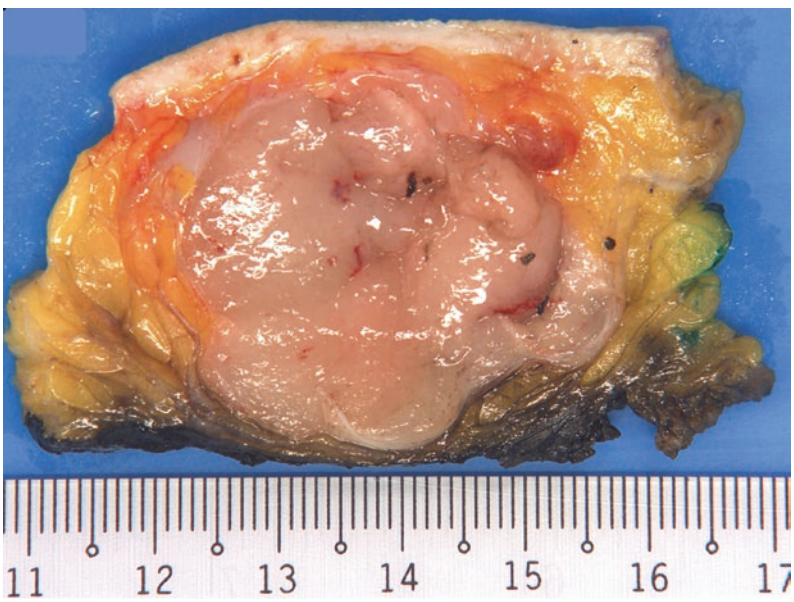

Fig. 3.45 Malignant phyllodes tumour. This is a recurrent tumour which shows a fleshy grey soft appearance, with a few nodular protrusions into the surrounding adipose tissue

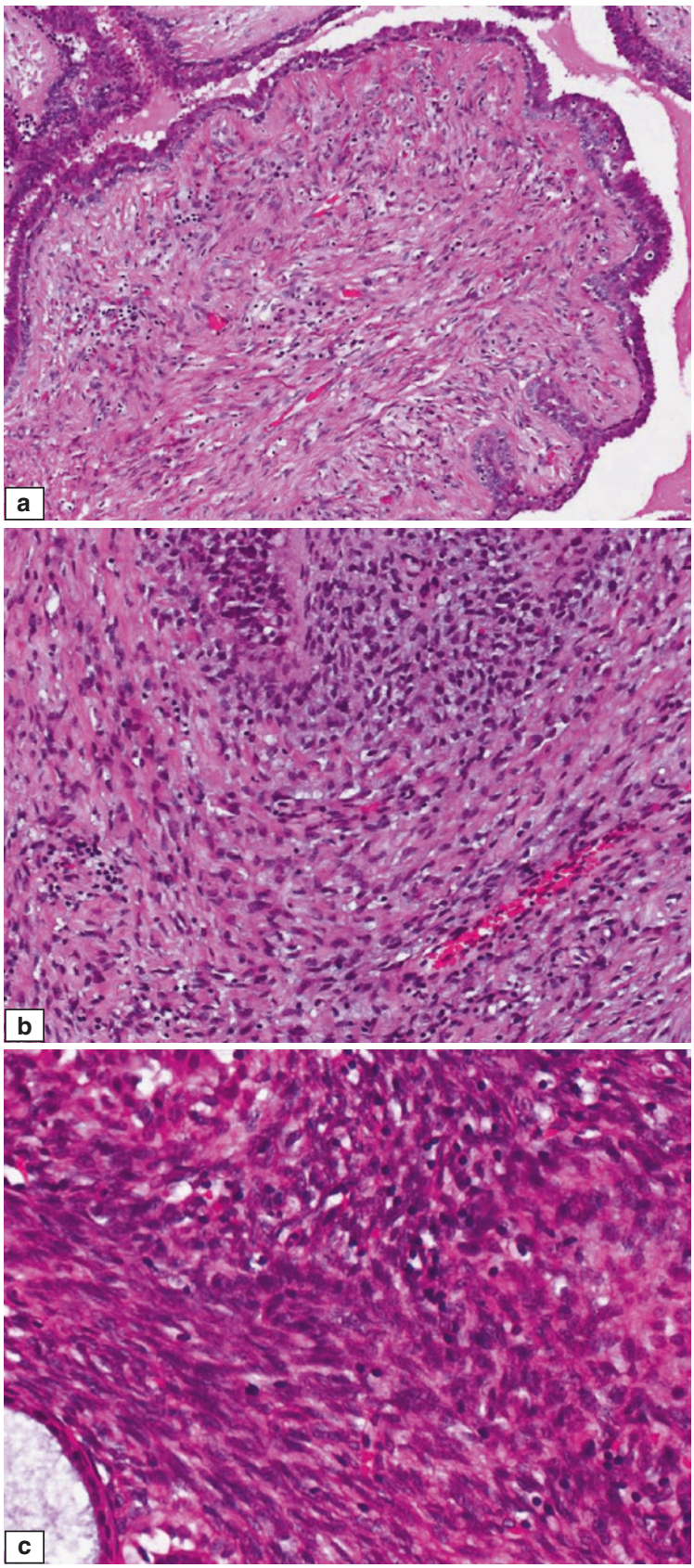

Fig. 3.46 Assessment of stromal cellularity in phyllodes tumours. (**a**) Mild stromal cellularity with some physical proximity of stromal nuclei but without significant touching. (**b**) Moderate stromal cellularity with greater crowding and occasional kissing of nuclei. (**c**) Marked stromal cellularity with densely aggregated nuclei with overlapping. Stromal cellularity is assessed in the areas of maximal nuclear crowding. It is important that sections are not thick, which may give an erroneous impression of increased cellularity (Reprinted from Tan et al. [3]; with permission)

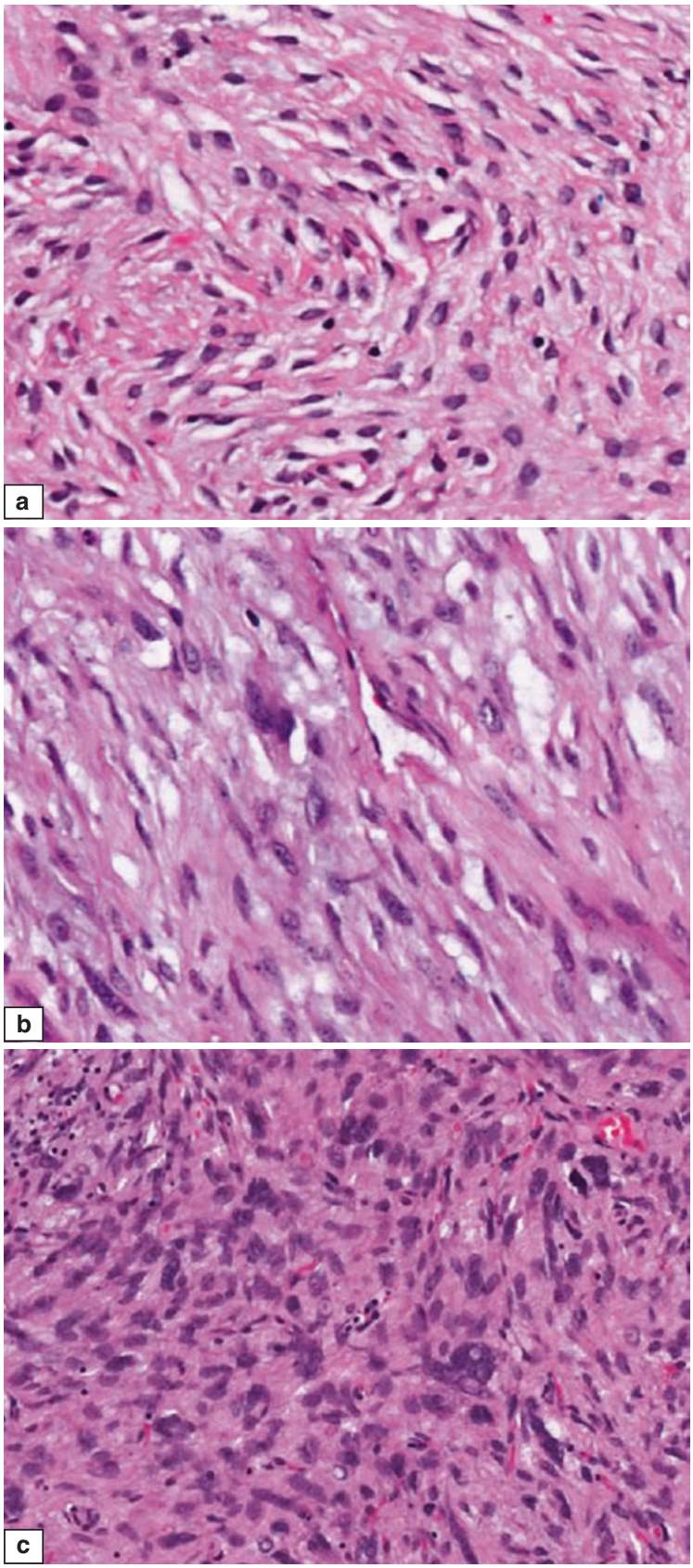

Fig. 3.47 Assessment of stromal atypia in phyllodes tumours. (**a**) Minimal nuclear atypia with banal features. (**b**) Moderate nuclear atypia with variation in nuclear size accompanied by hyperchromasia. (**c**) Marked nuclear atypia with pleomorphic, hyperchromatic nuclei. Some nuclei show giant forms with lobated nuclear contours. As with stromal cellularity, stromal atypia is evaluated in the worst areas of the tumour (Reprinted from Tan et al. [3]; with permission)

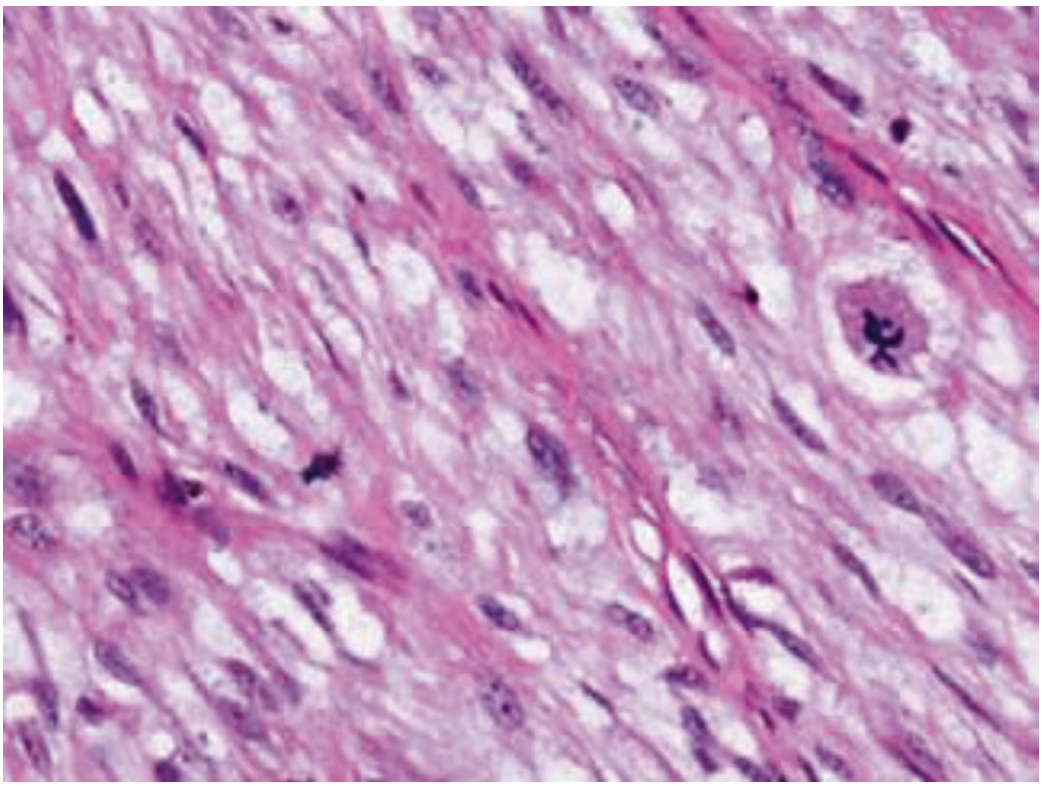

Fig. 3.48 Assessment of mitotic activity in phyllodes tumours. A benign tumour usually shows less than five mitoses per ten high power fields, a borderline lesion demonstrates between five and nine mitoses per ten high power fields, and a malignant tumour harbours ten or more mitoses per ten high power fields

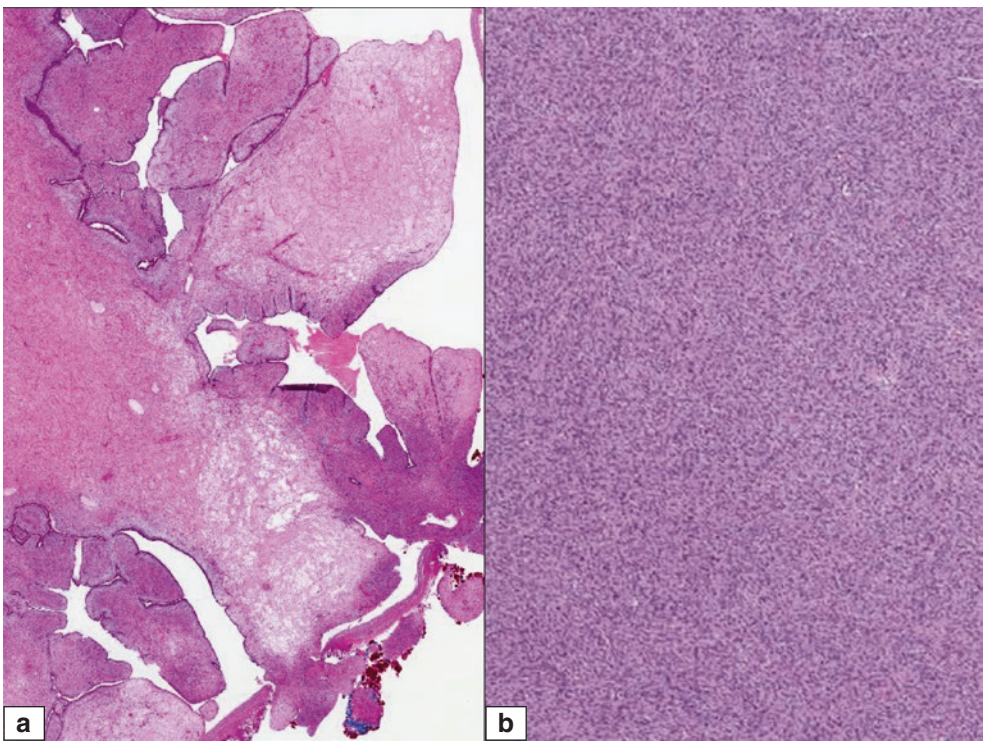

Fig. 3.49 Assessment of stromal overgrowth in phyllodes tumours. Stromal overgrowth is absent (**a**), when there is no expanse of stroma devoid of epithelial elements seen on a low-power field at 40× magnification (4× objective, 10× eyepiece). Conversely, stromal overgrowth is present (**b**) when there are only stromal elements without epithelium on a single low-power field. While the size of the low-power field may vary between microscopes, stromal overgrowth when present is usually obvious

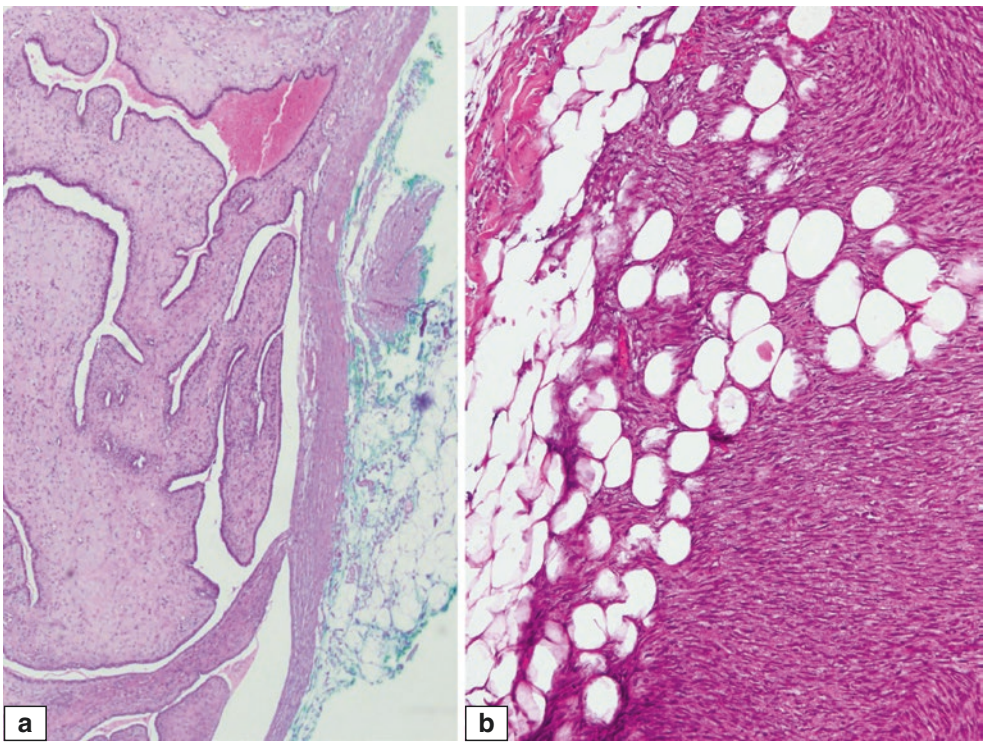

Fig. 3.50 Assessment of borders of phyllodes tumours. Circumscribed, smooth, and pushing borders with a fibrous rim (**a**), compared with permeative borders with tongue-like extensions of spindled stroma into surrounding fat (**b**). As the nature of the margins is an important histological parameter in the grading of phyllodes tumours, it is critical that tumour borders are appropriately sampled

Fig. 3.51 Cellular fibroepithelial lesion, interpreted as a benign phyllodes tumour shows a circumscribed pushing margin and mild stromal cellularity. The distinction of benign phyllodes tumour from a cellular fibroadenoma can be challenging, as there are many overlapping histologic features. Adequate sampling is important as the typical fronding and stromal hypercellularity may be focal. In cases where there is uncertainty despite representative sampling, it may be appropriate to adopt the term of benign fibroepithelial neoplasm, as such tumours have a low likelihood of recurrence (Reprinted from Tan et al. [3]; with permission)

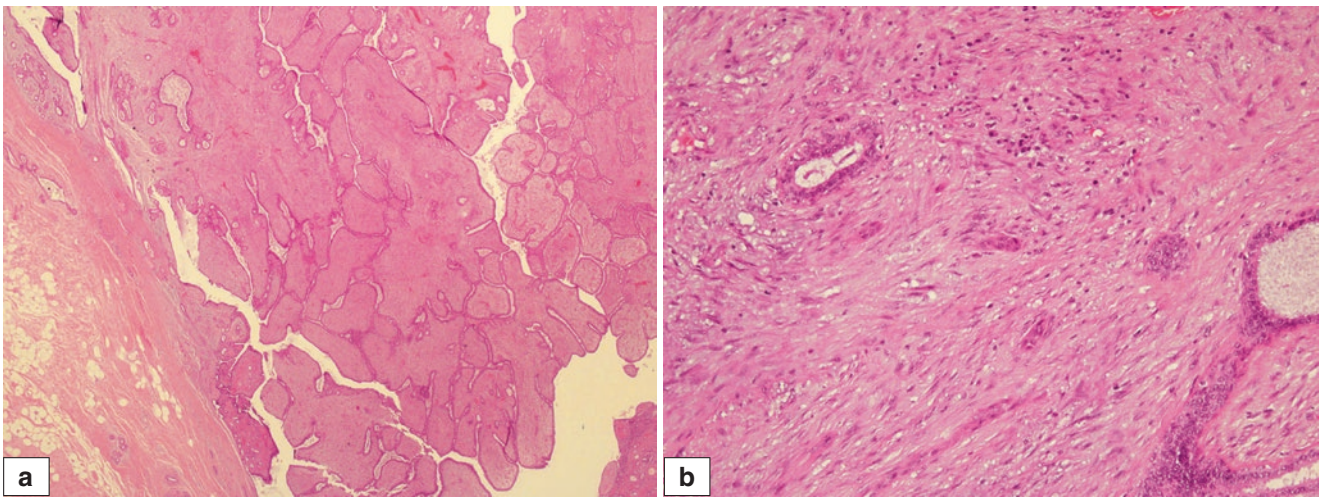

Fig. 3.52 (**a**) Benign phyllodes tumour composed of many broad stromal fronds covered by epithelium lining clefts and projecting into cystic spaces. There is a neat demarcation from the surrounding breast tissue by compressed fibrous stroma. (**b**) Scattered chronic inflammatory cells can be observed in the stroma, which may be mistaken for increased stromal cellularity. Occasional squamoid nests with epithelial cells assuming pink cytoplasm can be sometimes incidentally observed within the stroma without any significance

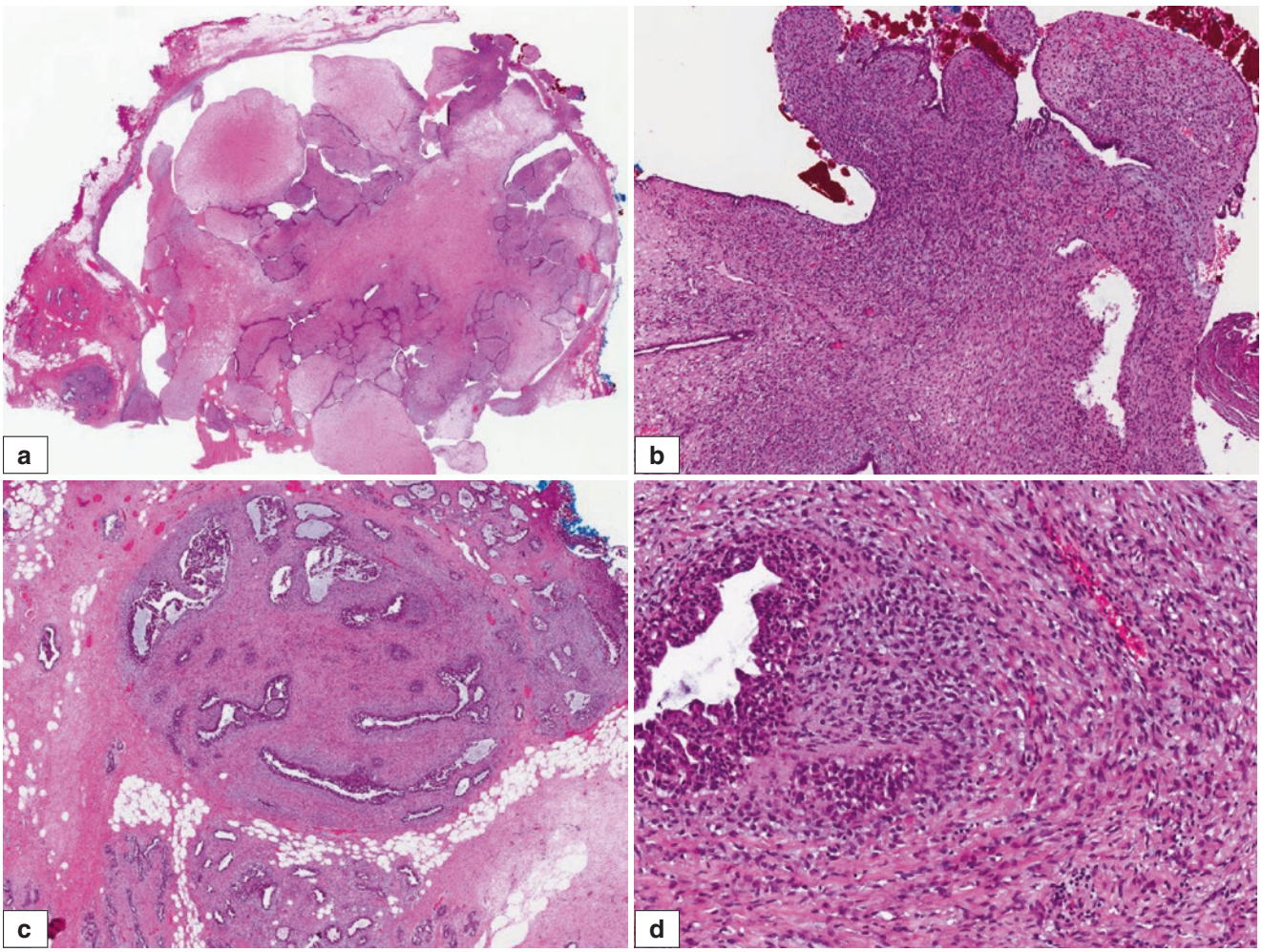

Fig. 3.53 Borderline phyllodes tumour. (**a**) Scanning magnification shows broad patulous fronds with deep clefts. Dilatation of the clefts gives rise to cystic spaces. This tumour possessed areas of moderate to marked stromal cellularity as well as permeative borders. (**b**) The stromal fronds show moderate to focally marked stromal hypercellularity. (**c**) Hypercellular stroma and permeative borders are present. (**d**) Stromal hypercellularity is variable, with accentuation of cellularity seen around ducts, referred to as peri-epithelial or subepithelial stromal hypercellularity. (**e**) Mitotic activity (*arrowed*). Mitoses numbered up to seven per ten high-power fields. Borderline features in this tumour are the moderate stromal hypercellularity, increased mitotic activity, and the permeative borders

Fig. 3.53 (continued)

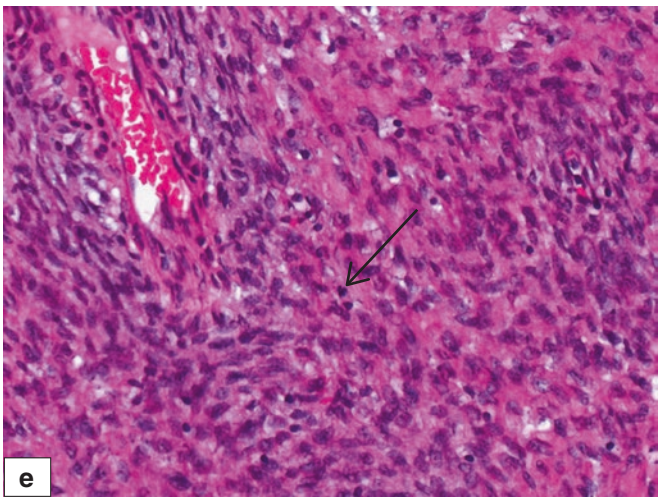

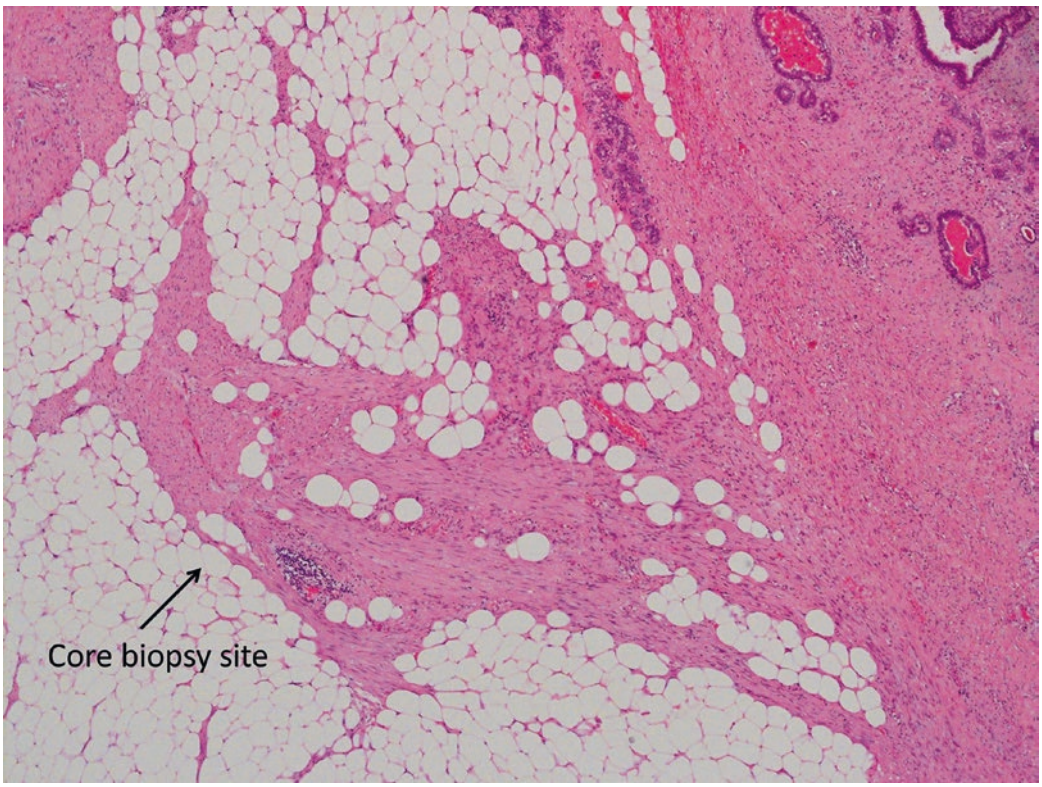

Fig. 3.54 Changes from previous core biopsy may mimic the permeative border of a phyllodes tumour. A history of previous biopsy together with histological presence of haemorrhage, inflammation, granulation, and haemosiderin deposits should allow the distinction

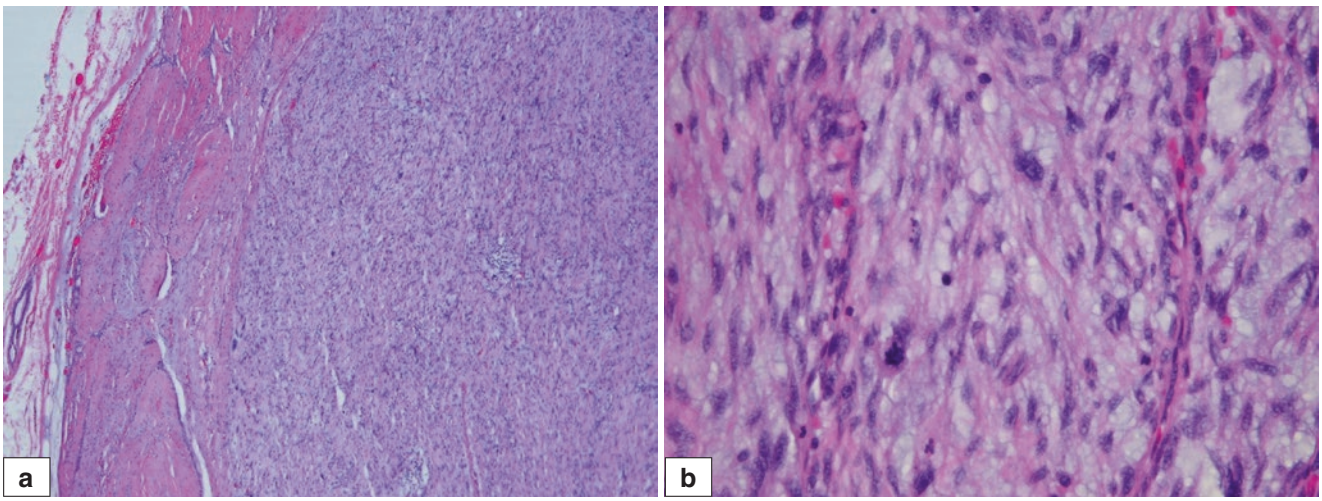

Fig. 3.55 Malignant phyllodes tumour. (**a**) Stromal overgrowth is seen adjacent to a benign-appearing fibroepithelial area. Phyllodes tumours have heterogeneous histology, and a core biopsy through the fibroadenomatous area can result in a diagnosis of fibroadenoma. It is important to correlate with clinical and radiological findings, with recommendation for excision if the lesion exceeds a certain size threshold or if there is a history of recent rapid growth in size. (**b**) Stromal nuclear atypia and mitoses are present

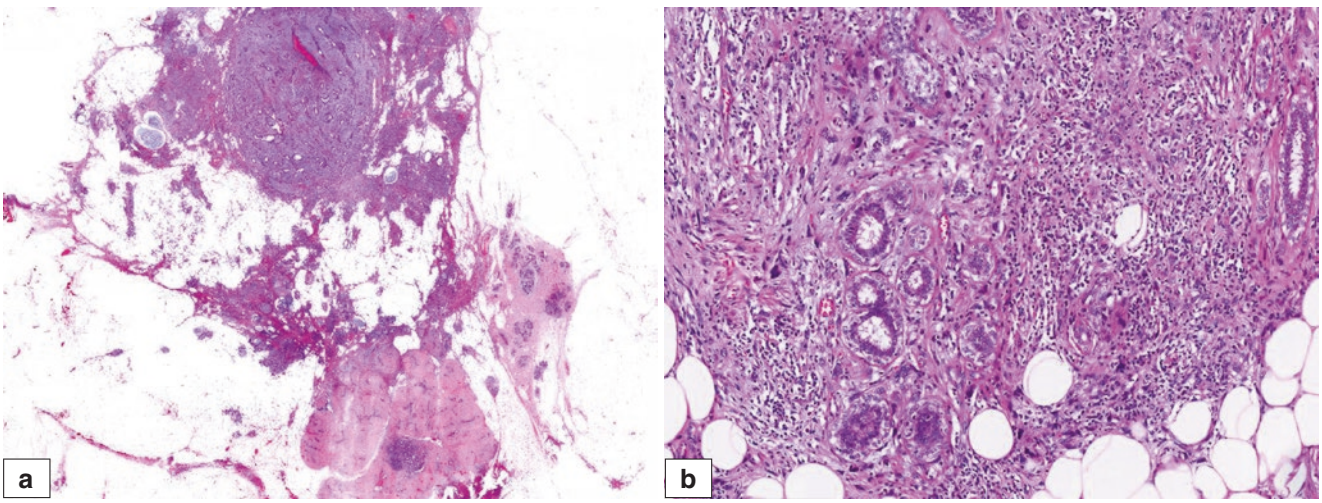

Fig. 3.56 (**a**) Malignant phyllodes tumour shows a hyalinised fibroadenomatoid zone juxtaposed with a cellular fibroepithelial lesion with irregular borders. (**b**) Marked nuclear pleomorphism and hyperchromasia are observed in the stromal cells. There is permeation of the stromal cells in between adjacent adipocytes

As with fibroadenomas, the epithelial component of phyllodes tumours may display a variety of changes, from usual ductal and atypical hyperplasia to in situ and invasive carcinoma (Fig. 3.64). Stromal multinucleated cells similar to those observed in fibroadenomas, that do not contribute to grading assessment, may also be encountered in phyllodes tumours [8]. These however, need to be distinguished from abnormal stromal cells with multilobated and bizarre nuclei that reflect stromal atypia (Fig. 3.65). Uncommonly, stromal cytoplasmic inclusions may be found, which are thought to be related to cytoplasmic microfilaments, and do not have a specific significance (Fig. 3.66).

Differential Diagnosis

Fibroadenoma, Cellular Fibroadenoma, Juvenile Fibroadenoma, and Benign Phyllodes Tumour

Fibroadenomas, especially those with areas of increased stromal cellularity, can be difficult to distinguish from the benign phyllodes tumour. The juvenile fibroadenoma, which often has increased stromal cellularity, may also pose difficulty in delineation from benign phyllodes tumour. Table 3.2 shows the key diagnostic characteristics of these tumours.

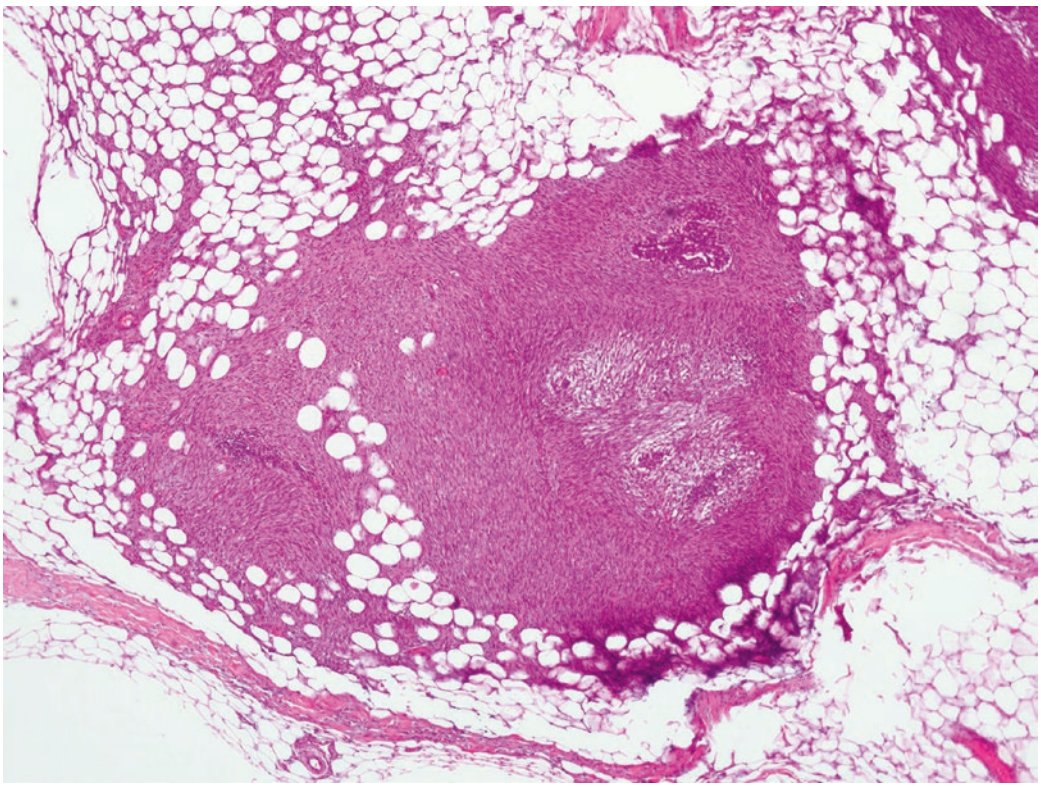

Fig. 3.57 Extensively permeative margins with hypercellular spindled stromal cells extending in a lattice-like manner into the surrounding fat of a malignant phyllodes tumour

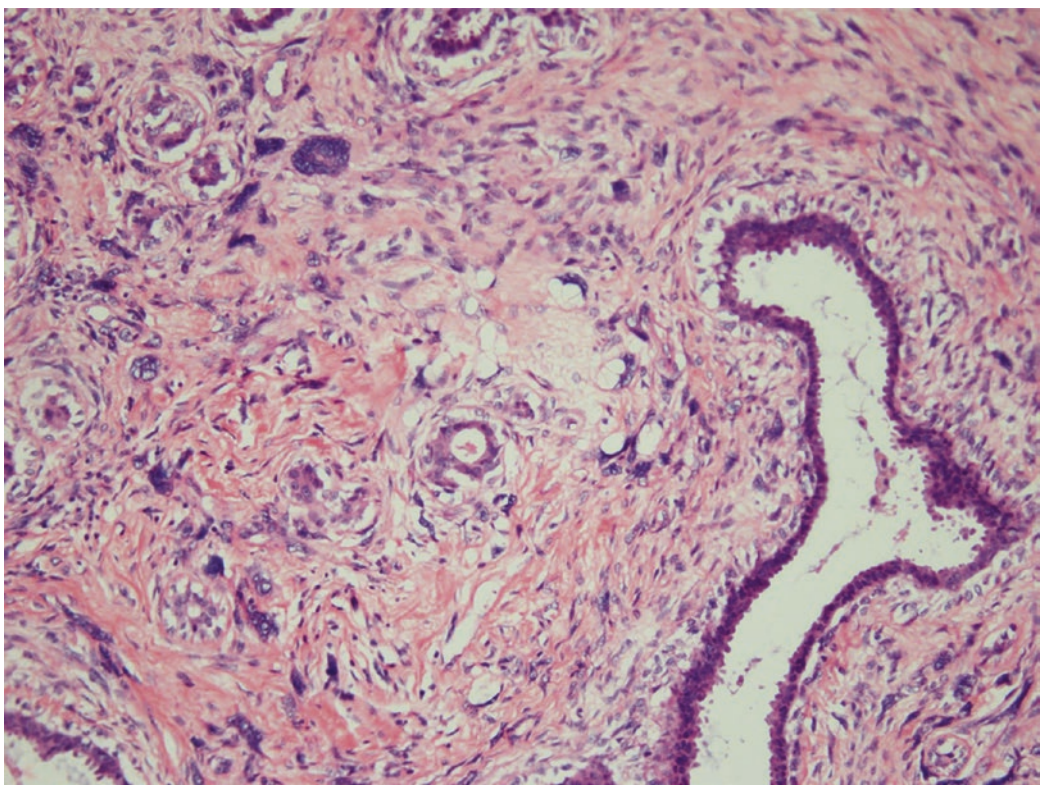

Fig. 3.58 Lipoblasts with hyperchromatic enlarged nuclei and scalloped nuclear contours are seen in the malignant stromal component, liposarcoma, of a malignant phyllodes tumour

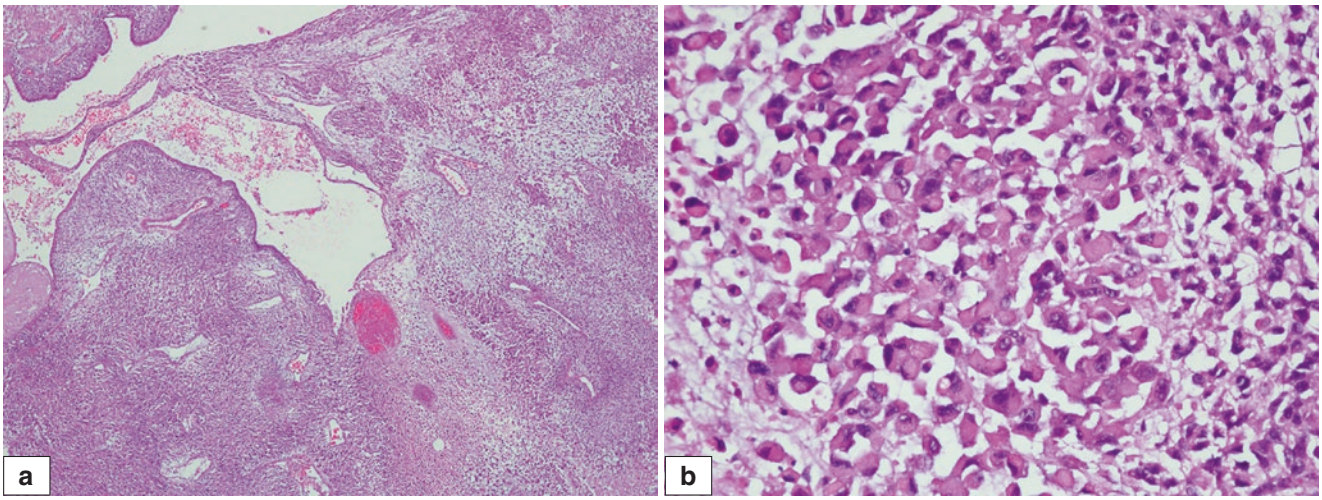

Fig. 3.59 (**a**) Low magnification of a malignant phyllodes tumour with epithelioid stromal cells and clusters of rhabdoid cells. (**b**) High magnification of rhabdoid cells with peripherally compressed hyperchromatic nuclei and ample pink cytoplasm

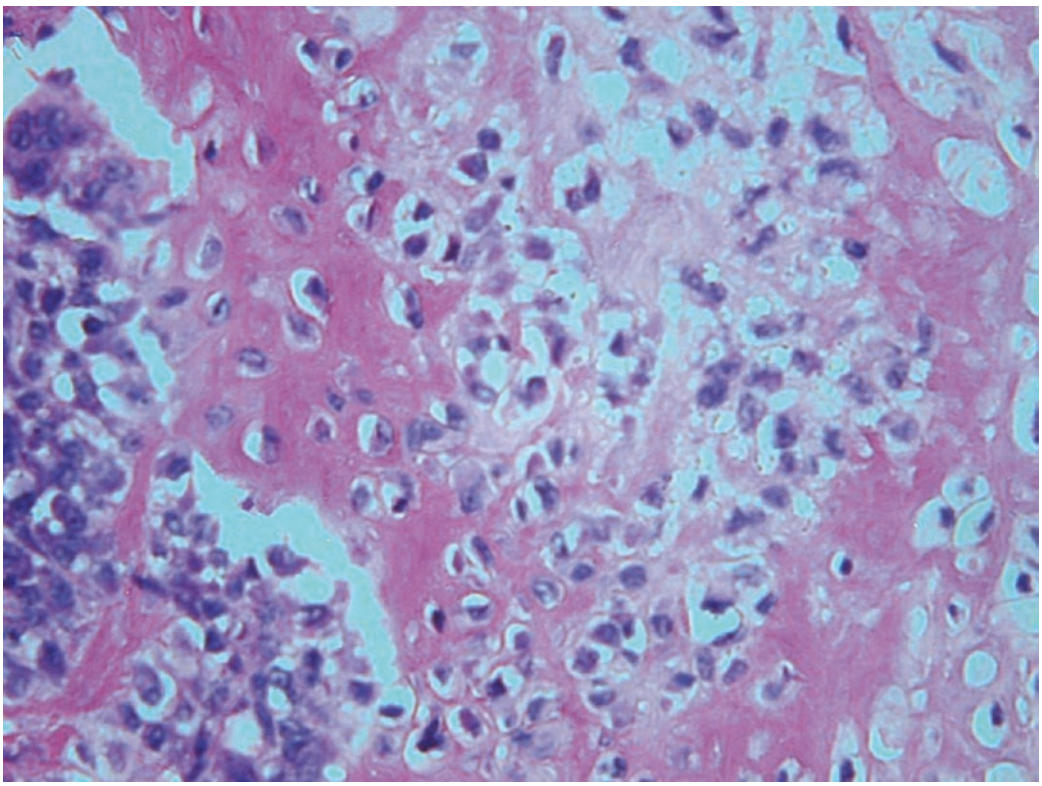

Fig. 3.60 Malignant osteoid (osteosarcoma) is seen indicating the presence of a heterologous osteosarcoma component. The microscopic finding of a malignant heterologous element in a phyllodes tumour places it into the malignant category, regardless of other histological parameters

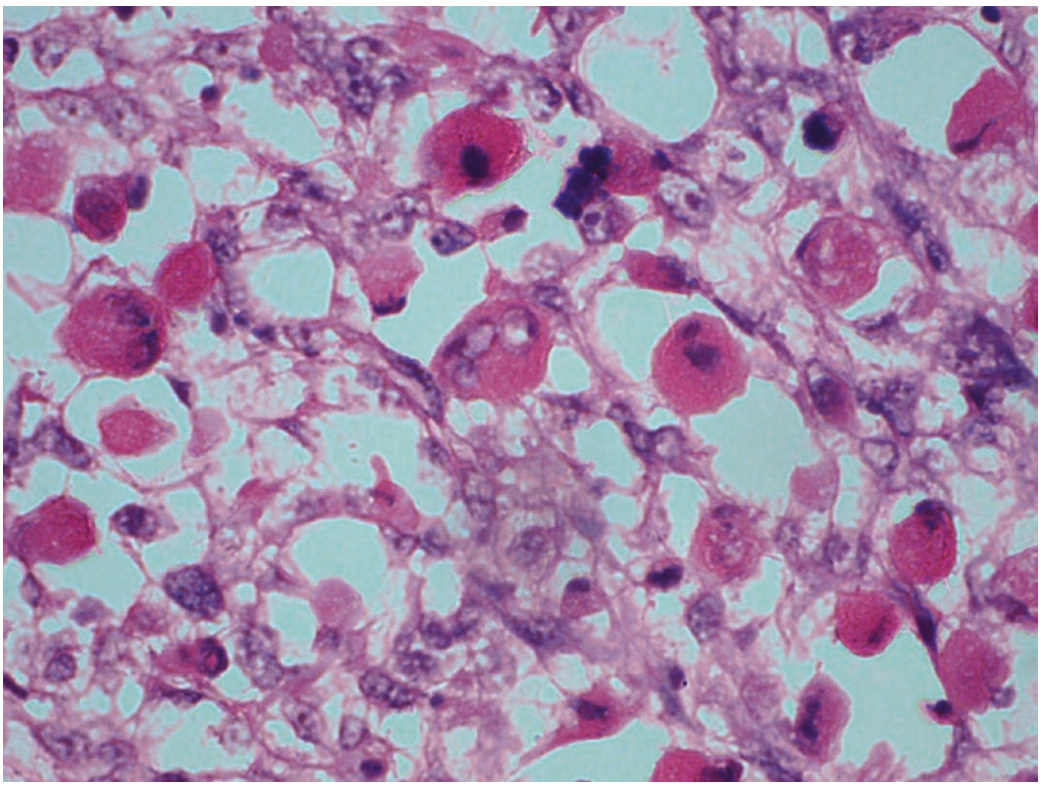

Fig. 3.61 Rhabdomyoblasts are seen in a malignant phyllodes tumour with heterologous differentiation

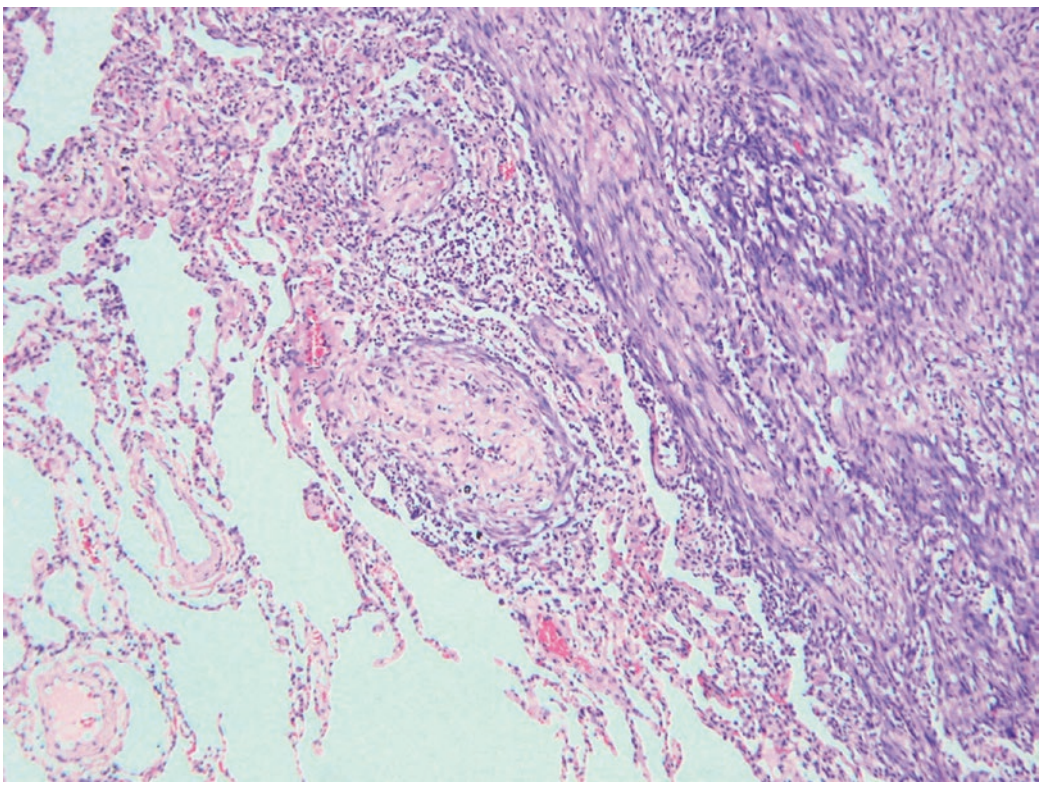

Fig. 3.62 Metastatic phyllodes tumour to the lung, composed only of the malignant stromal spindle component (right field)

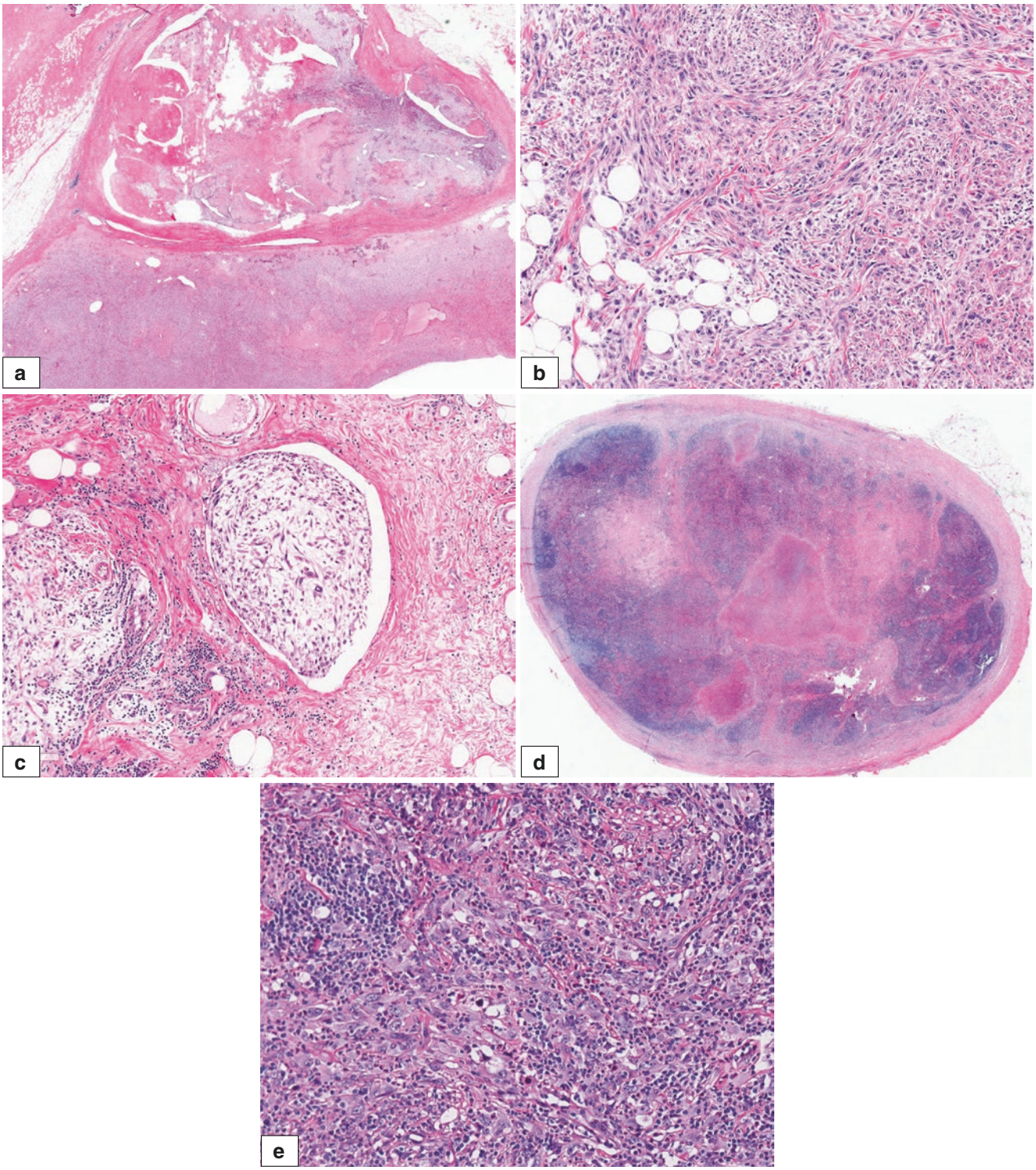

Fig. 3.63 Malignant phyllodes tumour with recurrence. (**a**) Original tumour showed stromal overgrowth in the lower field. (**b**) Recurrent tumour a year later showed increased stromal pleomorphism with brisk mitoses. (**c**) The recurrent tumour also demonstrated a lymphovascular embolus. (**d**) Metastasis of the malignant stromal component of the phyllodes tumour to a lymph node. Although nodal metastases from phyllodes tumours are rare, they can occur. In this particular case, a comprehensive histological review of the original malignant phyllodes tumour, recurrence and subsequent nodal metastasis, was conducted, in conjunction with application of adjunctive immunohistochemical studies. (**e**) Higher magnification of the metastasis to the lymph node, with pleomorphic plump epithelioid and spindle cells effacing the nodal architecture. Metastatic tumour cells bore histological resemblance to the recurrent tumour

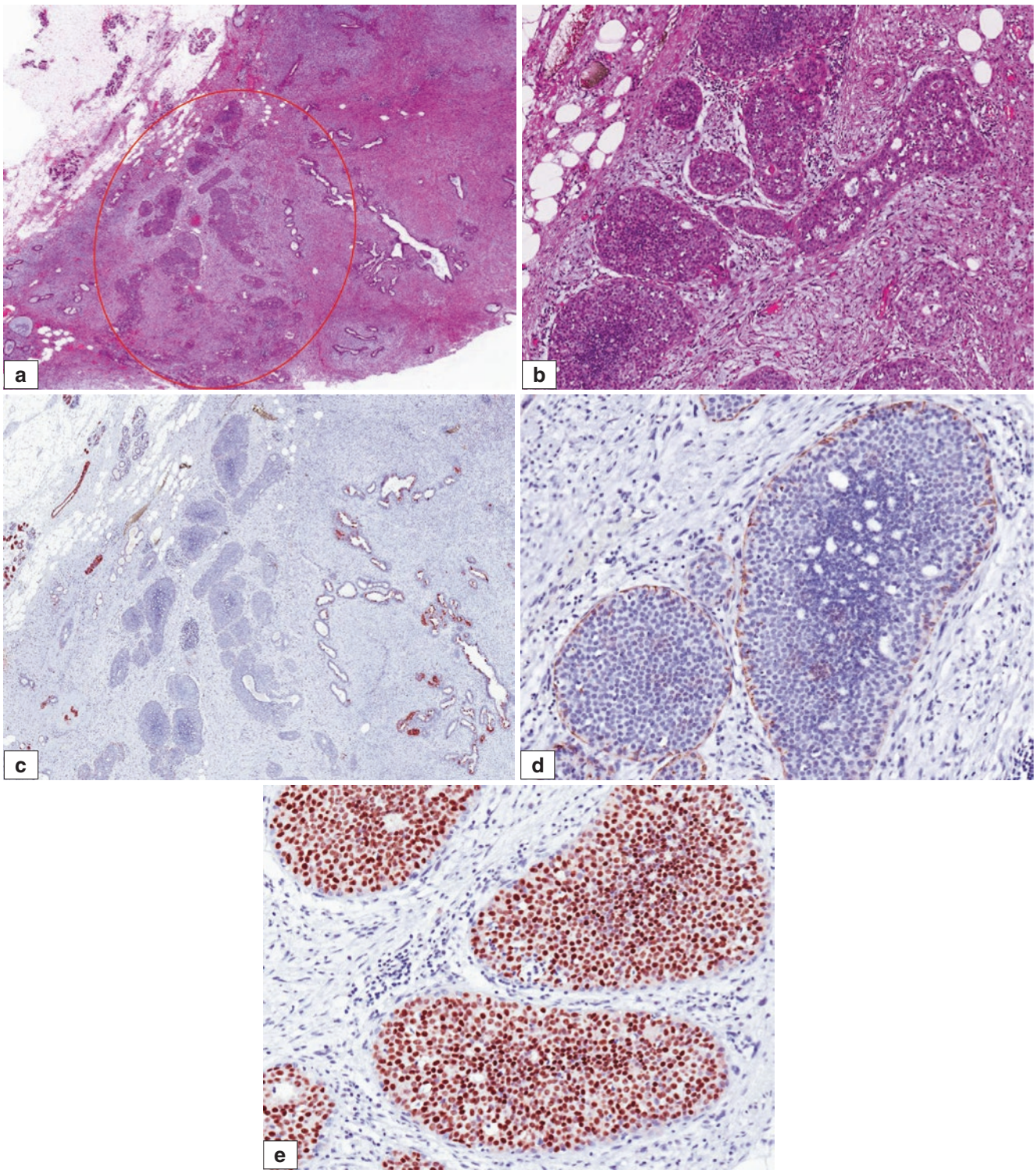

Fig. 3.64 (**a**) Borderline phyllodes tumour with a 5-mm focus of low nuclear grade ductal carcinoma in situ, DCIS (*circled*). (**b**) Borderline phyllodes tumour with ductal carcinoma in situ, low nuclear grade, solid, and cribriform patterns, without necrosis. The stromal cells show moderate atypia. (**c**) Immunohistochemistry with CK5/6 shows lack of staining in the abnormal expanded ducts. (**d**) Immunohistochemistry with CK14 shows lack of staining in the abnormal expanded ducts, with a positively highlighted rim of intact myoepithelial cells around the affected ducts. (**e**) Immunohistochemistry with ER shows diffuse positive staining of nuclei of lesional cells in the abnormal expanded ducts

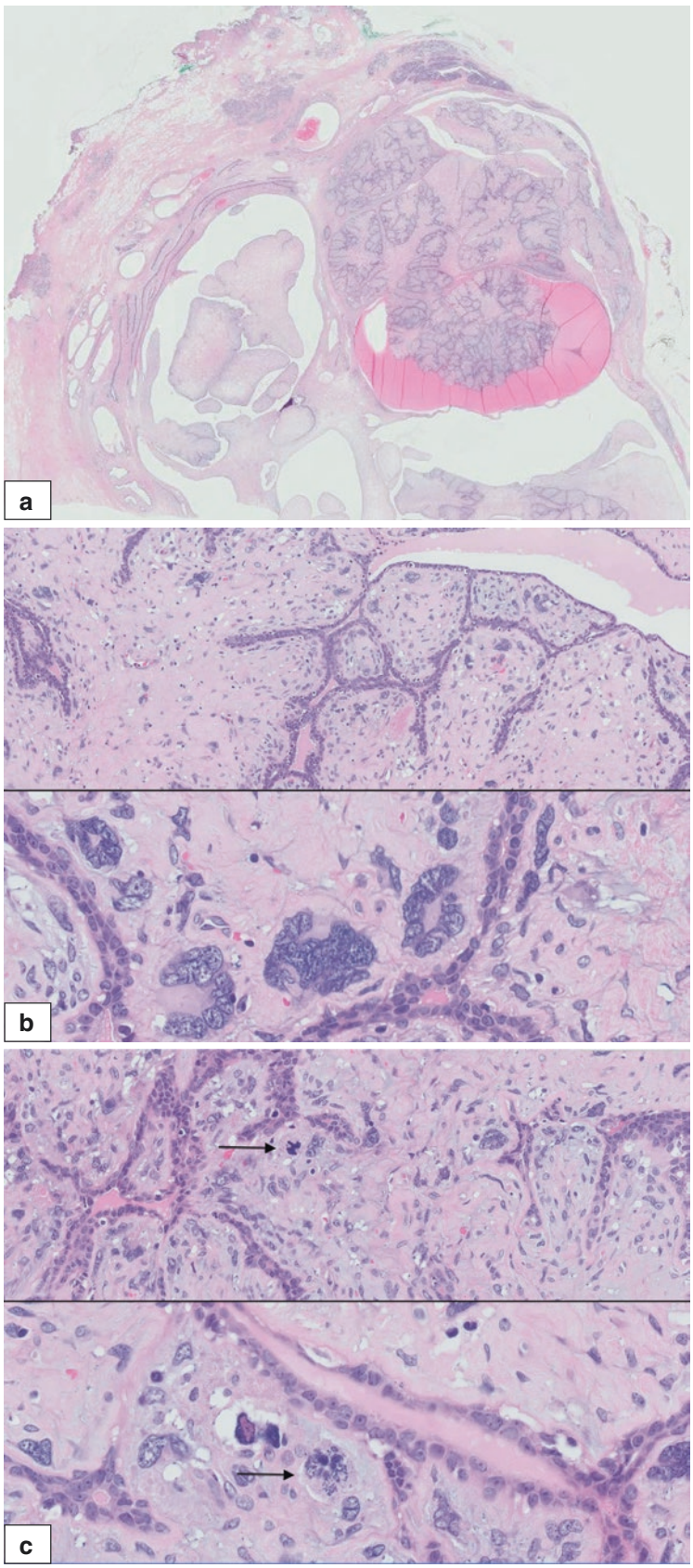

Fig. 3.65 Phyllodes tumour with stromal atypia and bizarre multinucleated giant cells. (**a**) Low magnification, broad stromal fronds project into cystic spaces. (**b**) Medium and high magnification shows bizarre multinucleated giants cells with polylobated nuclei. Moderate nuclear atypia is present in surrounding stromal cells. (**c**) Mitoses are present (*arrows*) including a tripolar mitosis (*upper field*). The tumour was initially classified as a benign phyllodes tumour, but due to the stromal atypia and mitotic activity, the tumour would be better classified as borderline. No stromal overgrowth or permeative border was seen.

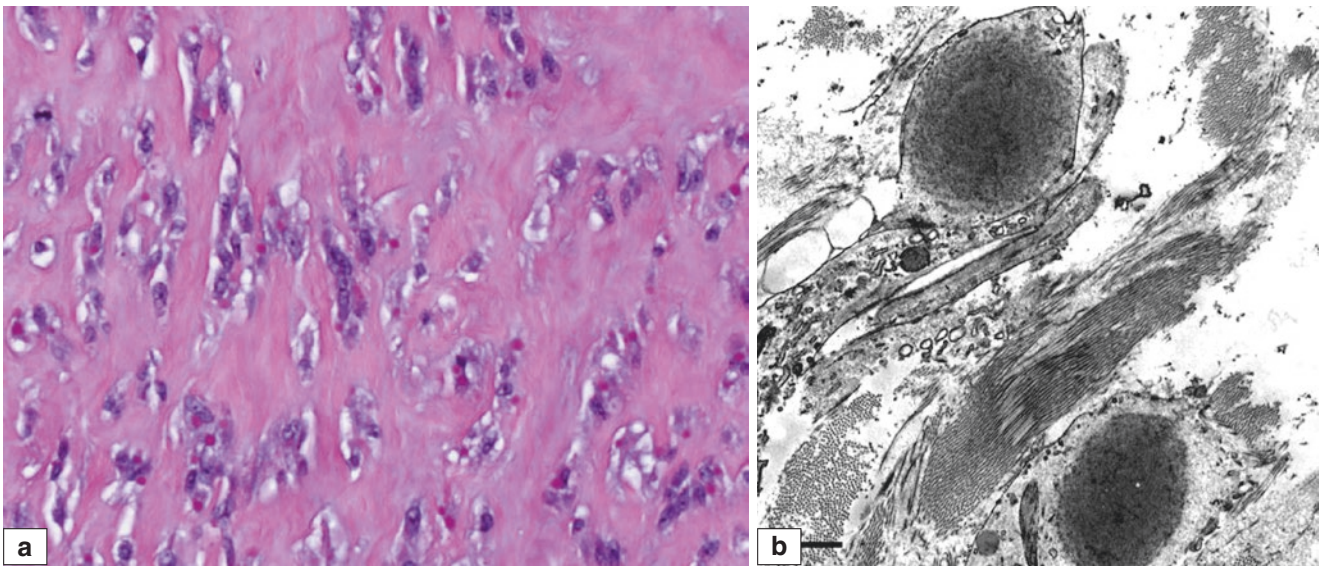

Fig. 3.66 Phyllodes tumour with cytoplasmic inclusions in stromal cells. (**a**) Stromal cells show hyaline pink globules within the cytoplasm, resembling inclusion bodies of infantile digital fibromatosis. These inclusions are likely related to cytoplasmic microfilaments. (**b**) Ultrastructural examination shows electron dense material within the stromal cells, likely composed of aggregated intermediate filaments

Table 3.2 Differentiating features of fibroadenoma, cellular fibroadenoma, juvenile fibroadenoma, and benign phyllodes tumour

Feature	Fibroadenoma (conventional)	Cellular fibroadenoma	Juvenile fibroadenoma	Benign phyllodes tumour
Age	Young women (reproductive age group)	Young women (less than 20 years)	Paediatric patients and young women	Mature women (mean age in fifth decade)
Size	Up to 3 cm	Up to 3 cm	Can be large	Usually large
Macroscopy	Rounded, circumscribed, rubbery, or myxoid	Rounded, circumscribed, rubbery, or soft	Rounded, circumscribed, rubbery, or soft	Lobulated, circumscribed, slit-like spaces, may have haemorrhagic infarction and cysts
Histological pattern	Intra- or pericanalicular or mixed	Intra- or pericanalicular or mixed	Usually pericanalicular	Exaggerated intracanalicular
Stromal cellularity	Usually low	Increased	Increased	Increased, may have peri-epithelial accentuation
Mitoses[a]	Usually none to rare	Usually none to rare	Usually none to rare	Up to four mitoses per 10 high-power fields
Leaf-like fronds	Absent or poorly formed without hypercellular stroma	Absent or poorly formed	Absent	Well formed, prominent, accompanied by hypercellular stroma
Elongated slit-like/ cystic spaces lined by bilayered epithelium	Rare	Rare	Rare	Can be present, associated with stromal fronds Cystic degeneration can occur
Microscopic borders	Circumscribed or encapsulated Rarely irregular periphery	Circumscribed or encapsulated Rarely irregular periphery	Circumscribed or encapsulated Rarely irregular periphery	Pushing contours with sometimes irregular periphery
Epithelium	None to variable UDH	None to variable UDH	UDH with gynaecomastoid changes	None to variable UDH

UDH usual ductal hyperplasia

[a]Although mitotic activity is usually nil to low in fibroadenomas, increased mitoses may be seen in fibroadenomas in the paediatric age group

A conservative approach is recommended for young patients in cases with features that are intermediate between cellular fibroadenoma and benign phyllodes tumour. The WHO 2012 working group recommends categorising such cases as benign fibroepithelial neoplasms to avoid unnecessary overtreatment [5]. This approach is supported by a recent consensus review [3], although it was cautioned that the term should be used sparingly.

Benign, Borderline, and Malignant Phyllodes Tumours

Grade assignment in phyllodes tumours follows the assessment of stromal features of atypia, hypercellularity, overgrowth and mitoses, and the nature of the tumour borders. Table 3.3 shows a guide to phyllodes tumour grading. While the grading appears straightforward, with sharp dividing lines, it is in fact a continuum, and there is substantial overlap in histologic characteristics between grades.

Malignant Phyllodes Tumour with Sarcomatous Stromal Overgrowth, Spindle Cell Metaplastic Carcinoma, and Primary Breast Sarcoma

Stromal overgrowth of a malignant phyllodes tumour can resemble a spindle cell metaplastic carcinoma (Figs. 3.67 and 3.68) or primary breast sarcoma (Fig. 3.69), particularly when the typical phyllodal fronded architecture is effaced. Apart from diligent sampling of these tumours to locate the characteristic leaf-like pattern of phyllodes tumour or conventional carcinoma component of spindle cell carcinoma, firm diagnoses usually require immunohistochemistry. The presence of diffuse p63 and keratin staining of spindle cells indicates a metaplastic carcinoma. It is important to note, however, that phyllodes tumours may manifest focal keratin staining of stromal cells [9], and p63 reactivity has recently been described in stromal cells of malignant phyllodes tumours [10]. Conversely, some metaplastic carcinomas may disclose heterogeneity in keratin positivity. More than one

Table 3.3 Comparison of histologic features of benign, borderline, and malignant phyllodes tumours

Histologic feature	Benign phyllodes tumour	Borderline phyllodes tumour	Malignant phyllodes tumour
Stromal cellularity	Mild	Moderate	Marked
Distribution of stromal hypercellularity	Variable	Variable	Diffuse
Stromal atypia	None to mild	Mild to moderate	Marked
Stromal mitoses	0–4 mitoses/10 HPF	5–9 mitoses/10 HPF	≥10 mitoses/10 HPF
Stromal overgrowth	Absent	Absent, very focal if present	Often present
Tumour borders	Pushing and rounded	Pushing and rounded, may be permeative	Permeative
Malignant heterologous elements	Absent	Absent	May be present

HPF high-power fields

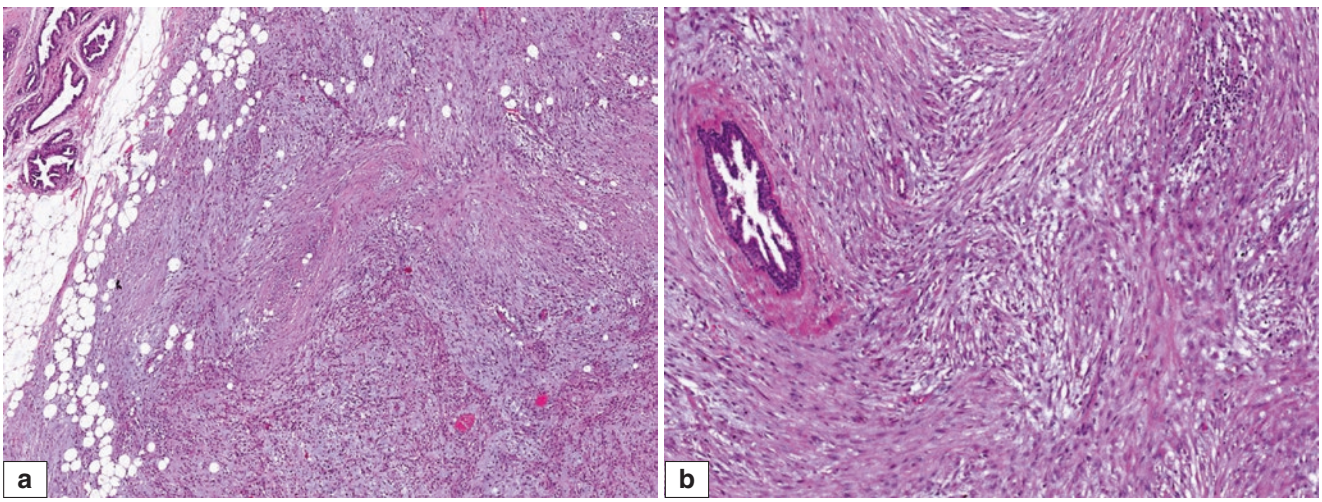

Fig. 3.67 Metaplastic spindle cell carcinoma. (**a**) At low magnification, the tumour shows spindle cells infiltrating the adipose stroma, mimicking stromal overgrowth and the permeative borders of a malignant phyllodes tumour. Loose oedematous zones are seen among the intersecting spindle cell sheaves. (**b**) A benign duct is seen in the midst of the spindle cell tumour. No epithelium lined fronds are present

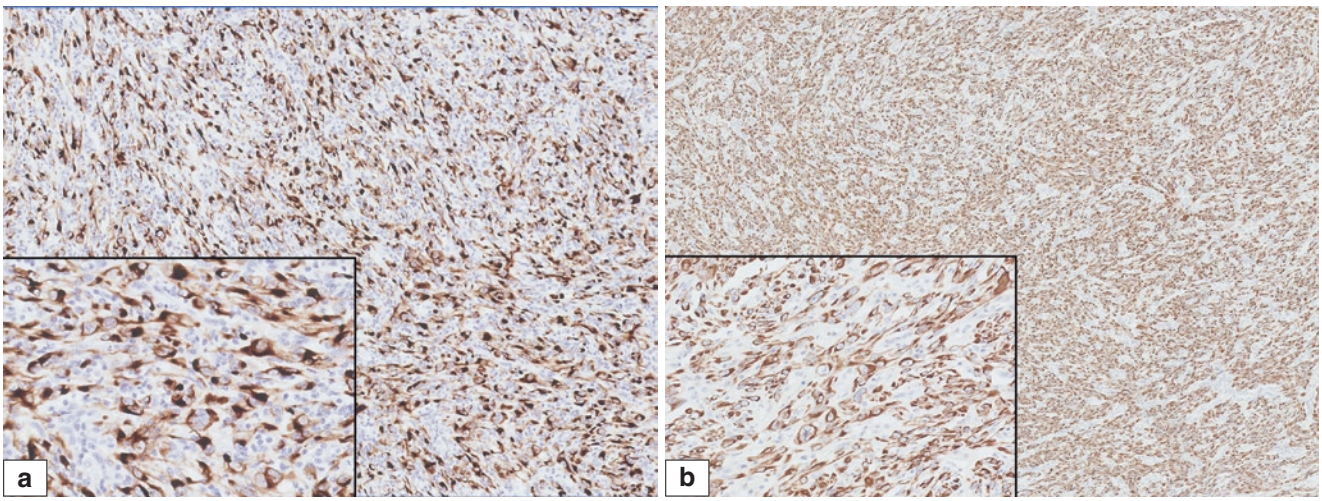

Fig. 3.68 Metaplastic spindle cell carcinoma. (**a**) Immunohistochemistry with Cam5.2 diffusely decorates the malignant spindle cells. Inset shows high magnification of the spindle cells displaying cytoplasmic reactivity. While a minority of phyllodes tumours may also disclose stromal reactivity for epithelial markers, positivity is limited to focal and few stromal cells. (**b**) High molecular weight keratin CK14 immunohistochemistry also shows diffuse staining of the malignant spindle cells. Inset shows high magnification of the spindle cells displaying cytoplasmic reactivity

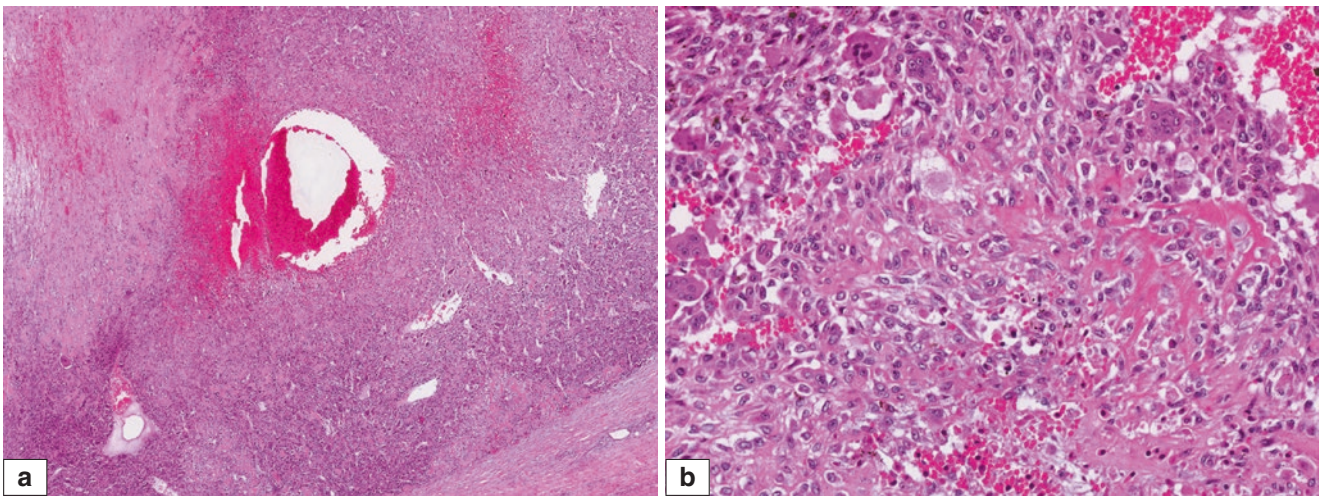

Fig. 3.69 Primary breast sarcoma. (**a**) The tumour shows sheets of malignant spindle cells with areas of haemorrhage. (**b**) Malignant osteoid is elaborated by the malignant spindle cells, indicating osteosarcoma. Scattered osteoclastic giant cells are seen. No epithelium-covered stromal fronds are seen. Immunohistochemistry for keratins is negative. The diagnosis of primary breast sarcoma is one of exclusion, with the need to rule out malignant phyllodes tumour and metaplastic carcinoma

block may sometimes need to be submitted for immunohistochemical interrogation. Selection of tumour blocks containing areas with more cohesive epithelioid-like cells may be more promising in yielding positive results on keratin immunohistochemistry. The diagnosis of primary breast sarcoma is one of exclusion, after phyllodes tumour and metaplastic carcinoma have been ruled out. Table 3.4 shows features that may help distinguish these tumours.

Phyllodes Tumour and Periductal Stromal Tumour

Previously referred to as periductal stromal sarcoma, the WHO classification of breast tumours in 2012 revised the terminology to a more "neutral" term, periductal stromal "tumour", avoiding the connotation of malignancy with "sarcoma", as the biological behaviour of this rarely diagnosed lesion remains uncertain. Instead of the presence of

well-formed stromal fronds capped by benign epithelium, the periductal stromal tumour consists of hypercellular collections of spindle cells present around pre-existing ducts and terminal ductal lobular units (Fig. 3.70). Some of these tumours progress to conventional phyllodes tumours, and they are therefore currently classified under the rubric of phyllodal neoplasms.

Prognosis and Therapy Considerations

Benign phyllodes tumours can recur locally, while malignant tumours are at higher risk of local recurrence and can metastasise. Borderline tumours tend to also locally recur and may rarely metastasise. Recurrence rates for benign, borderline, and malignant phyllodes tumours are 10 %–17 %, 20 %–25 %, and 23 %–27 %, respectively. Malignant tumours may metastasise and cause death in about 22 % of patients [10].

Prognostication based on grading has challenges. Each microscopic parameter has several tiers of assessment, resulting in a significant number of permutations that confound accuracy and precision. While grading at extreme ends of the spectrum of phyllodes tumours is reliable, tumours in between are subject to interobserver variability due to challenges in applying the specified histologic criteria.

Table 3.4 Distinguishing Features of Sarcomatous Stromal Overgrowth in Malignant Phyllodes Tumour, Spindle Cell Metaplastic Carcinoma, and Primary Breast Sarcoma

Feature	Malignant phyllodes tumour (stromal overgrowth)	Spindle cell metaplastic carcinoma	Primary breast sarcoma
Leaf-like fronds	Present (but may be hard to identify)	Absent	Absent
Peri-epithelial stromal accentuation	Present	Absent	Absent
Carcinoma (in situ and invasive)	Absent	May be present	Absent
Keratins (IHC)	Usually absent, may be focal reactivity	Present, but may be focal	Usually absent
High-molecular-weight keratins	Usually absent, may be focal reactivity	Present, but may be focal	Usually absent
p63, p40	Absent or present	Present, but may be focal	Usually absent

IHC immunohistochemistry

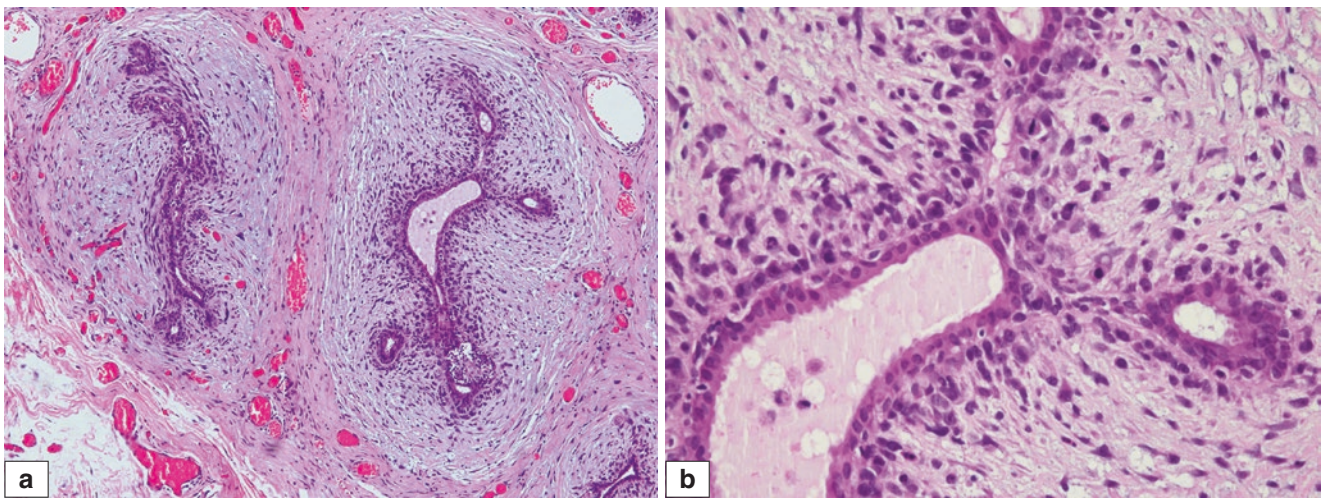

Fig. 3.70 (**a**) Periductal stromal tumour is an overlapping histological entity with phyllodes tumour, with the main difference being the absence of leaf-like processes. It is non-circumscribed, consisting of a spindle cell proliferation localised around open tubules. Progression to classic phyllodes tumour has been documented, suggesting that it may be part of the same spectrum of disease. (**b**) Periductal stromal tumour. Stromal cells in the peri-epithelial region display accentuation of cellularity with moderate nuclear pleomorphism and mitotic activity. Such tumours with cytologic anaplasia and increased mitoses may be referred to as periductal stromal sarcoma. It is recommended that the diagnoses of periductal stromal tumour, or periductal stromal sarcoma when malignant histologic features are present, be qualified as belonging to the spectrum of phyllodes tumours

A nomogram based on weighted parameters (AMOS criteria—stromal atypia, mitoses, overgrowth, surgical margins) attempts to circumvent the difficulties of conventional grading to allow individualised risk categorisation for patients diagnosed with phyllodes tumours (Fig. 3.71) [11–13].

The main therapy for phyllodes tumours is surgical excision. Although there is an approach for complete excision with negative margins for phyllodes tumours of all grades, there is some evidence to suggest that benign tumours that have been enucleated without ensuring negative margins may be expectantly followed, with complete excision if there is recurrence [14]. Borderline and malignant tumours should be resected completely. The role of adjuvant therapy is unclear [15, 16].

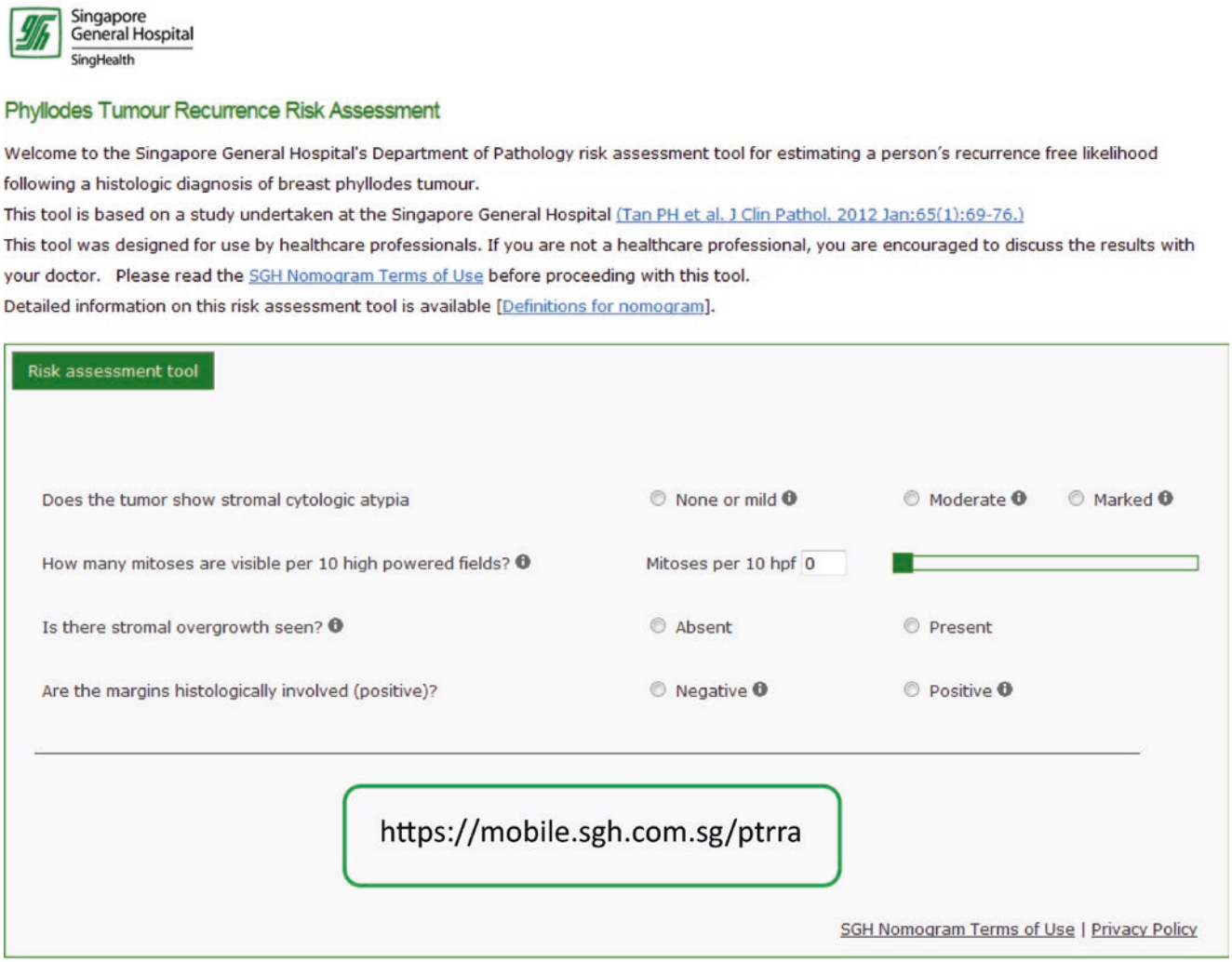

Fig. 3.71 Phyllodes tumour nomogram. Parameters used to generate a nomogram that can predict the risk of recurrence for the individual woman diagnosed with phyllodes tumour, based on the AMOS (atypia, mitoses, overgrowth, and surgical margins) criteria, which can be accessed at the website

References

1. Carter BA, Page DL, Schuyler P, Parl FF, Simpson JF, Jensen RA, et al. No elevation in long-term breast carcinoma risk for women with fibroadenomas that contain atypical hyperplasia. Cancer. 2001;92:30–6.
2. Tay TK, Chang KT, Thike AA, Tan PH. Paediatric fibroepithelial lesions revisited: pathological insights. J Clin Pathol. 2015;68(8): 633–41.
3. Tan BY, Acs G, Apple SK, Badve S, Bleiweiss IJ, Brogi E, et al. Phyllodes tumours of the breast: a consensus review. Histopathology. 2016;68(1):5–21.
4. Dupont WD, Page DL, Parl FF, Vnencak-Jones CL, Plummer Jr WD, Rados MS, et al. Long-term risk of breast cancer in women with fibroadenoma. N Engl J Med. 1994;331:10–5.
5. Tan PH, Tse G, Lee A, Simpson JF, Hanby AM. Fibroepithelial tumours. In: Lakhani SR, Ellis IO, Schnitt SJ, Tan PH, van de Vijver MJ, editors. WHO classification of tumours of the breast. Lyon: IARC; 2012. p. 142–7.
6. Tan PH, Jayabaskar T, Chuah KL, Lee HY, Tan Y, Hilmy M, et al. Phyllodes tumors of the breast: the role of pathologic parameters. Am J Clin Pathol. 2005;123:529–40.
7. Trends in cancer incidence in Singapore 1968–2007. Singapore Cancer Registry Report No. 7. National Registry of Diseases Office, Health Promotion Board 2008, Singapore.
8. Powell CM, Cranor ML, Rosen PP. Multinucleated stromal giant cells in mammary fibroepithelial neoplasms. A study of 11 patients. Arch Pathol Lab Med. 1994;118(9):912–6.
9. Chia Y, Thike AA, Cheok PY, Yong-Zheng Chong L, Man-Kit Tse G, Tan PH. Stromal keratin expression in phyllodes tumours of the breast: a comparison with other spindle cell breast lesions. J Clin Pathol. 2012;65:339–47.
10. Cimino-Mathews A, Sharma R, Illei PB, Vang R, Argani P. A subset of malignant phyllodes tumors express p63 and p40: a diagnostic pitfall in breast core needle biopsies. Am J Surg Pathol. 2014;38:1689–96.
11. Tan PH, Thike AA, Tan WJ, Thu MM, Busmanis I, Li H, Chay WY, Tan MH, Phyllodes Tumour Network Singapore. Predicting clinical behaviour of breast phyllodes tumours: a nomogram based on histological criteria and surgical margins. J Clin Pathol. 2012;65: 69–76.
12. Nishimura R, Tan PH, Thike AA, Tan MH, Taira N, Li HH, et al. Utility of the Singapore nomogram for predicting recurrence-free survival in Japanese women with breast phyllodes tumours. J Clin Pathol. 2014;67:748–50.
13. Chng TW, Lee JY, Lee CS, Li H, Tan MH, Tan PH. Validation of the Singapore nomogram for outcome prediction in breast phyllodes tumours: an Australian cohort. Journal of clinical pathology. 2016;69(12):1124–6
14. Tan EY, Tan PH, Yong WS, Wong HB, Ho GH, Yeo AW, et al. Recurrent phyllodes tumours of the breast: pathological features and clinical implications. ANZ J Surg. 2006;76:476–80.
15. Gnerlich JL, Williams RT, Yao K, Jaskowiak N, Kulkarni SA. Utilization of radiotherapy for malignant phyllodes tumors: analysis of the National Cancer Data Base, 1998-2009. Ann Surg Oncol. 2014;21:1222–30.
16. Guillot E, Couturaud B, Reyal F, Curnier A, Ravinet J, Laé M, et al. Management of phyllodes breast tumors. Breast J. 2011;17: 129–37.

Papillary Lesions

4

Papillary lesions of the breast demonstrate arborescent fronds or papillae composed of fibrovascular septa covered by epithelial cells.

Intraductal Papilloma

Definition

The intraductal papilloma is a benign lesion which shows bilayered epithelium composed of both luminal and myoepithelial cells surmounting well-developed fibrovascular cores. Solitary or central papillomas arise from large breast ducts occurring near the nipple-areolar region, while multiple or peripheral papillomas originate from the terminal ductal lobular units. Peripheral papillomas tend to be microscopic and are sometimes referred to as micropapillomas or papillomatosis. The term papillomatosis has also been used to refer to usual ductal hyperplasia, although it is preferably applied to lesions with papillary fronds and fibrovascular cores.

Clinical and Epidemiological Features

Patients with central papillomas may present with nipple discharge or a subareolar lump. Asymptomatic cases are detected on mammographic screening. Intraductal papillomas affect women over a wide age range and comprised 5.3 % of a series of benign breast biopsies [1].

Imaging Features

The intraductal papilloma can be mammographically occult or appear as well-defined or ill-defined soft tissue nodules on mammogram and ultrasound examination. The best imaging clue is an intraductal mass near the nipple. The ducts may or may not be dilated. The intraductal papilloma can appear as an intracystic mass when associated with a focally dilated duct (Fig. 4.1). Sometimes it can contain clustered microcalcifications or dense heterogeneous coarse calcifications. On galactography, it gives rise to an intraductal filling defect. Papillomas extending along the breast ductal system with ill-defined borders, as well as sclerosing papillomas presenting with distortion, are difficult to differentiate from malignancy.

Pathologic Features

Macroscopic Pathology

Intraductal papillomas form circumscribed rounded masses comprising fused papillary fronds attached to the wall of

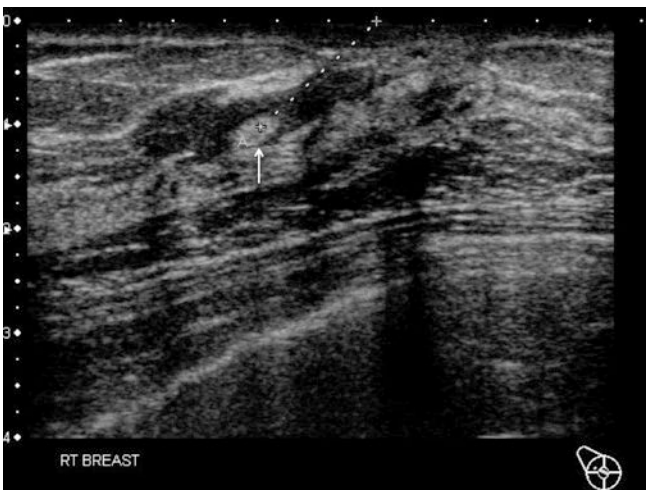

Fig. 4.1 Intraductal papilloma. Ultrasound shows a dilated duct with a mural nodule (*arrow*)

P.H. Tan, A.A. Sahin, *Atlas of Differential Diagnosis in Breast Pathology*, Atlas of Anatomic Pathology,
DOI 10.1007/978-1-4939-6697-4_4

the dilated duct into which the papilloma protrudes (Figs. 4.2, 4.3, 4.4, and 4.5). The lumen of the dilated duct can be seen as the cystic component of the whitish-grey tumour mass, while other times the mass can appear solidified with small spaces in between solid areas. Haemorrhage into the cyst may be present. Intraductal papillomas ramifying into ducts and their branches may appear less well defined.

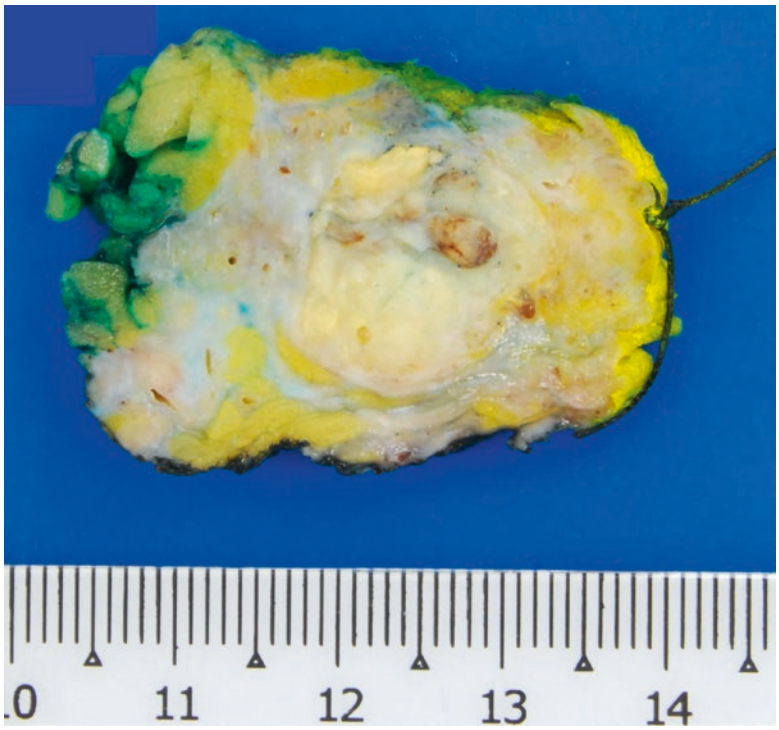

Fig. 4.2 Intraductal papilloma (central). Gross appearance shows a partially circumscribed yellowish-white lesion with a whitish fibrous wall. Occasional cystic spaces are seen. An area shows brownish discolouration that may be related to prior haemorrhage. Some whitish areas are also seen within the lesion, which correspond to fibrotic zones within the papilloma

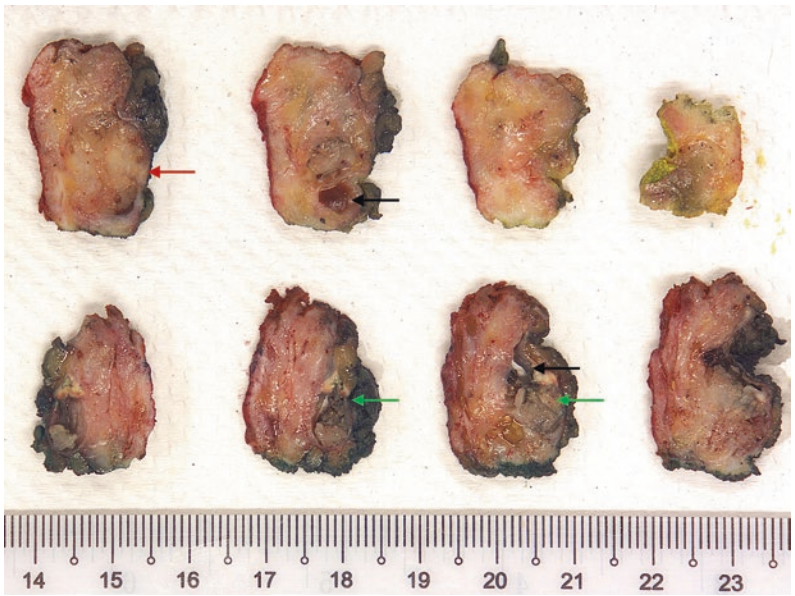

Fig. 4.3 Intraductal papilloma. Serial sections of a breast excision containing an intraductal papilloma which was confirmed histologically. In some of the breast slices, cystic areas are identified (*black arrows*). Solid portions are seen, which in some slices do not have a cystic component (*red arrow*), while in others they lie juxtaposed to the cystic areas with broad protrusions into the cystic cavity (*green arrows*)

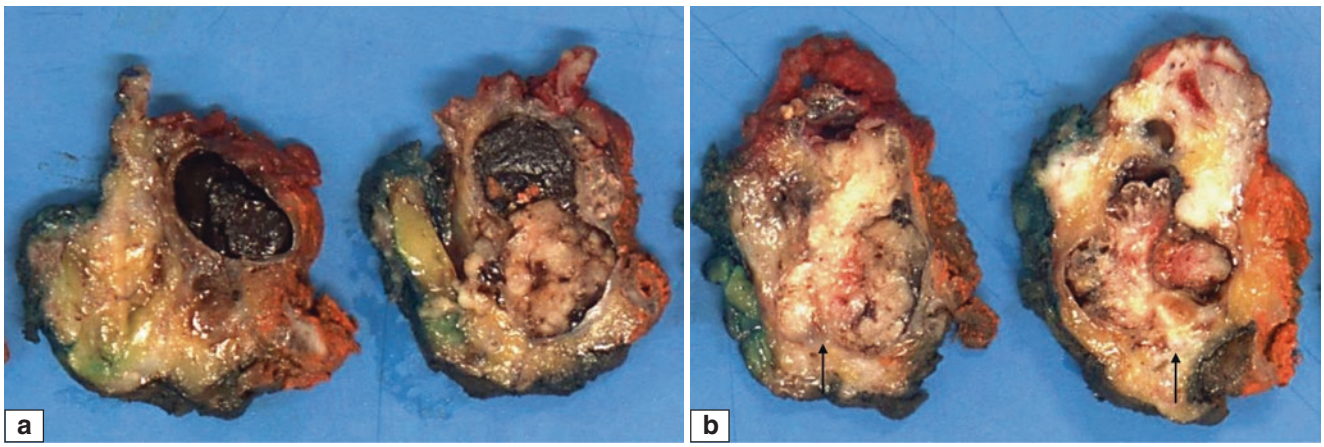

Fig. 4.4 Intraductal papilloma. (**a**) A solid-cystic tumour mass is seen. The cystic component is filled with altered blood which appears chocolate black in colour. The solid mass is adherent to the wall of the cavity which histologically corresponds to the cystically dilated duct from which the intraductal papilloma arises. The solid mass has a lobulated appearance. (**b**) A broad fronded appearance of the mass protruding into and filling up the cystic cavity is seen. The mass is connected to the wall of the cystic cavity by a broad base (*arrows*)

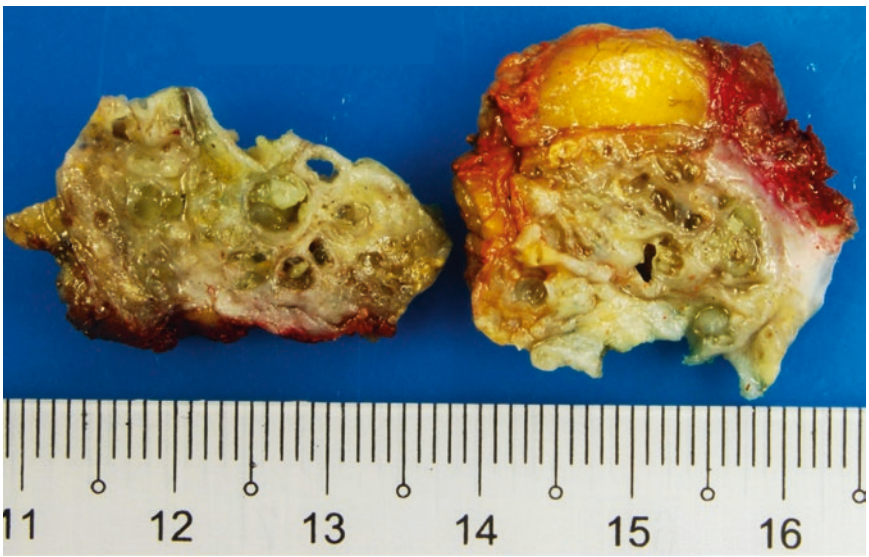

Fig. 4.5 Intraductal papilloma (peripheral). An excision specimen for multiple papillomas shows cysts of varying sizes within rubbery fibrous parenchyma. Within some cysts are mural nodules representing the micropapillomas

Microscopic Pathology

Distinct and anastomosing fronds with well-developed fibrovascular cores are covered by bilayered epithelial cells with myoepithelial preservation (Figs. 4.6 and 4.7). Usual ductal hyperplasia (UDH), apocrine metaplasia, and sclerotic hyalinised zones are often encountered (Figs. 4.8, 4.9, 4.10, and 4.11). Squamous metaplasia may be seen, especially adjacent to infarcted areas (Fig. 4.12). Myoepithelial cells may also be hyperplastic with spindled or epithelioid morphology (Figs. 4.13 and 4.14). Collagenous spherulosis can be seen (Fig. 4.15). Epithelial nests and tubules can be entrapped within sclerotic portions of the intraductal papilloma. These epithelial nests and tubules may be distorted, angulated, and squamoid, raising concern for invasion that may be refuted by confirming the presence of myoepithelial cells on immunohistochemistry (Figs. 4.16, 4.17, and 4.18).

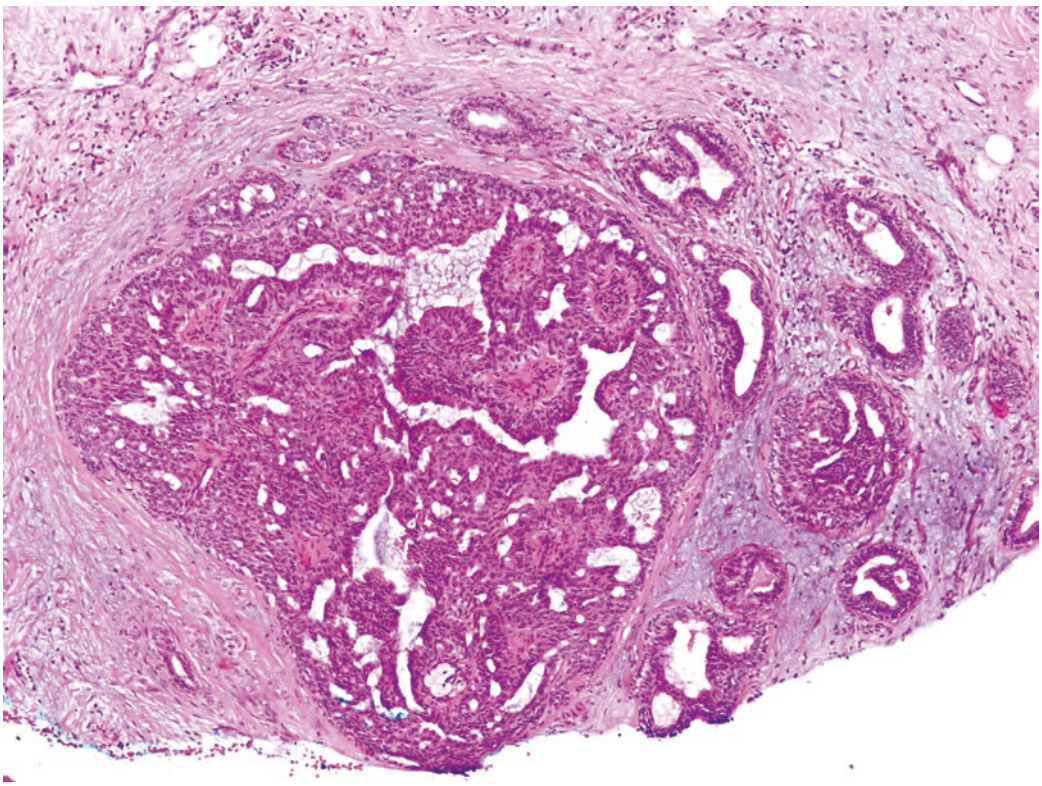

Fig. 4.6 Peripheral papilloma. This intraductal papilloma arises in the terminal ductal lobular unit and is also referred to as microscopic papilloma or micropapilloma

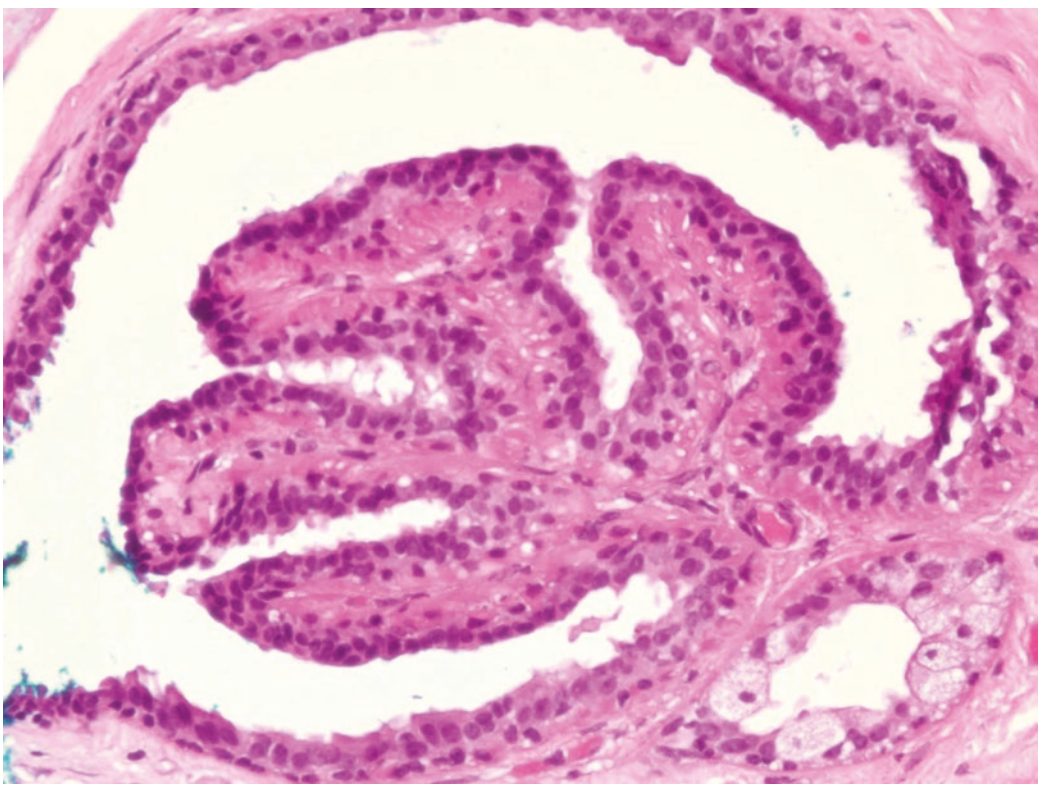

Fig. 4.7 Peripheral papilloma. A microscopic papilloma shows finger-like papillary fronds projecting into the dilated duct, resembling a glomerulus-like structure

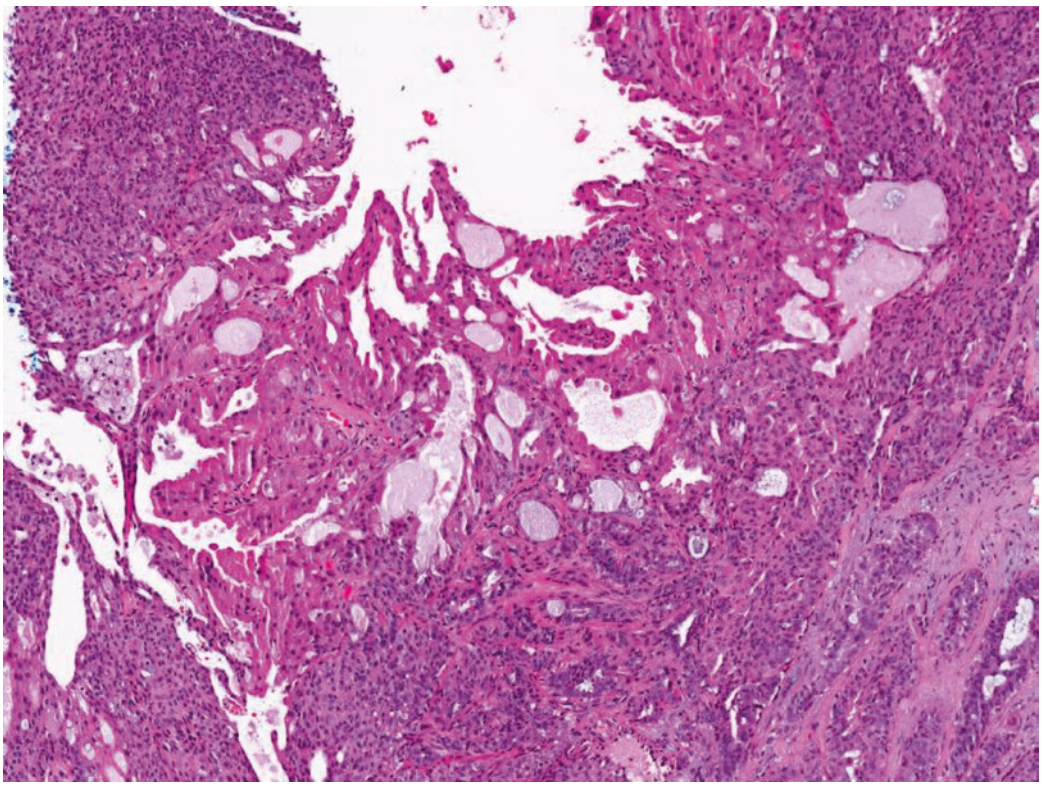

Fig. 4.8 Intraductal papilloma with apocrine metaplasia. The presence of apocrine metaplasia in a papilloma is often used as a feature supporting benignity. The apocrine cells contain ample pink cytoplasm, and nuclei are enlarged with discernible nucleoli. Apocrine metaplasia is usually observed in conjunction with usual ductal hyperplasia in the papilloma

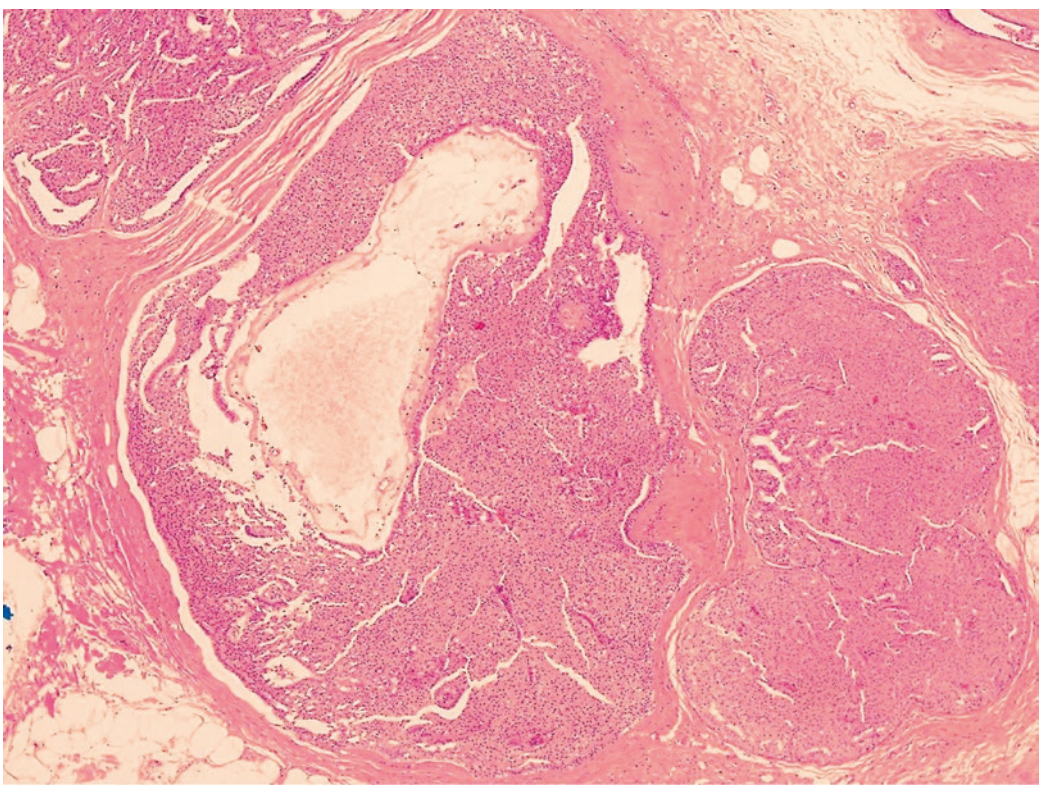

Fig. 4.9 Intraductal papilloma with florid (marked) usual ductal hyperplasia (UDH). Papillary fronds are obscured by the proliferation of epithelial cells, with the papillary architecture inferred from the congested fibrovascular septa coursing in between the epithelial cells

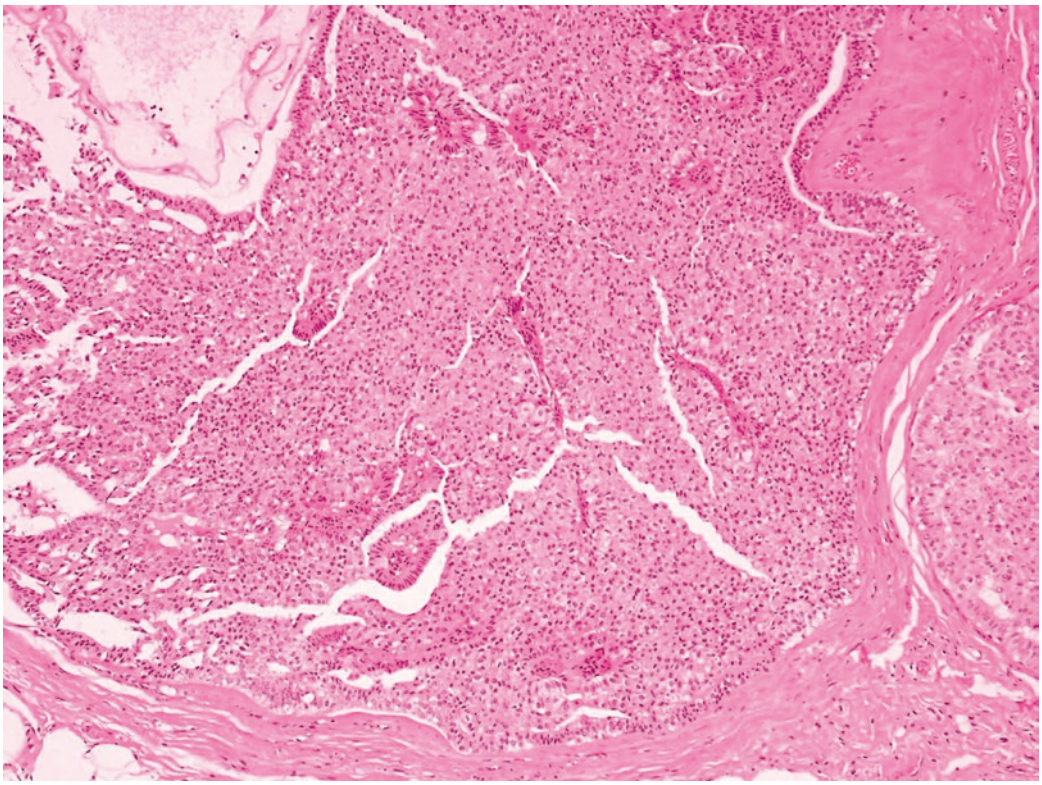

Fig. 4.10 Intraductal papilloma with florid UDH. Medium magnification shows the heterogeneous population of epithelial cells with areas of nuclear crowding and overlapping. Narrow fibrovascular septa are seen coursing among the epithelial cells

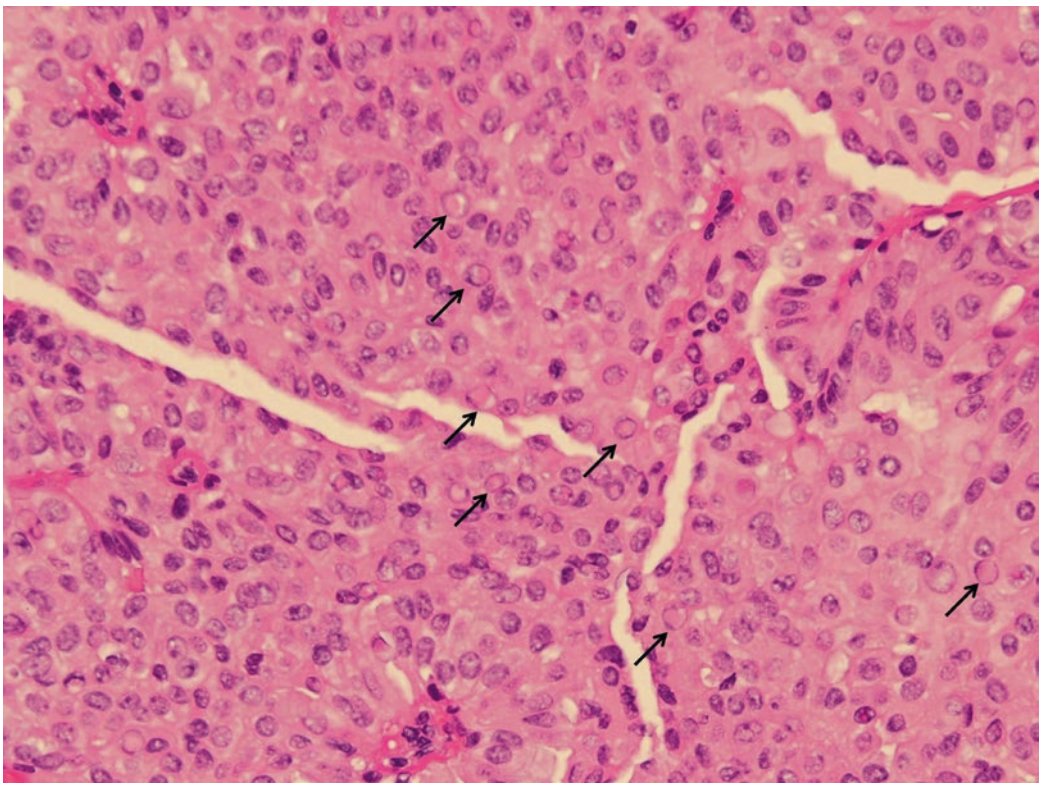

Fig. 4.11 Intraductal papilloma with florid UDH. Some ductal epithelial nuclei show pink intranuclear inclusions (*arrows* indicate some of these intranuclear inclusions), which have been described in florid UDH and ultrastructurally represent cytoplasmic invaginations into nuclei. Sometimes these intranuclear inclusions may have a more eosinophilic hue

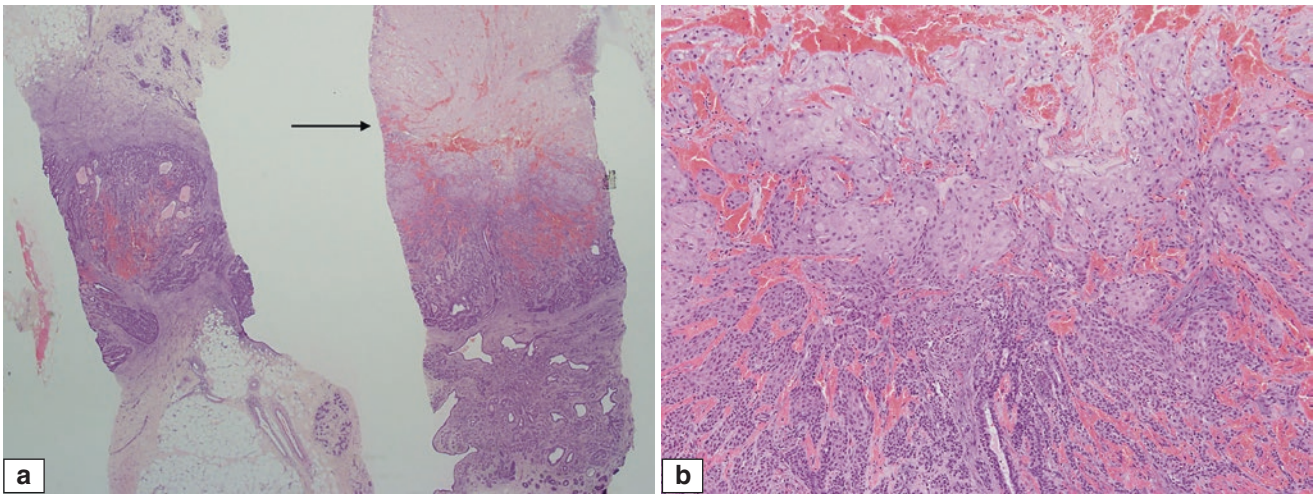

Fig. 4.12 Intraductal papilloma with infarction and squamous metaplasia. (**a**) Biopsy cores show portions of a benign intraductal papillary lesion with a solidified appearance composed of anastomosed papillary fronds. Infarction with haemorrhage is seen (*arrow*). (**b**) Higher magnification of the haemorrhagic edge of the infarcted zone shows squamous metaplasia composed of anastomosing pavemented trabeculae of polygonal cells with ample pink cytoplasm. Squamous metaplasia merges with epithelial nests and tubules in the non-metaplastic portions of the intraductal papilloma

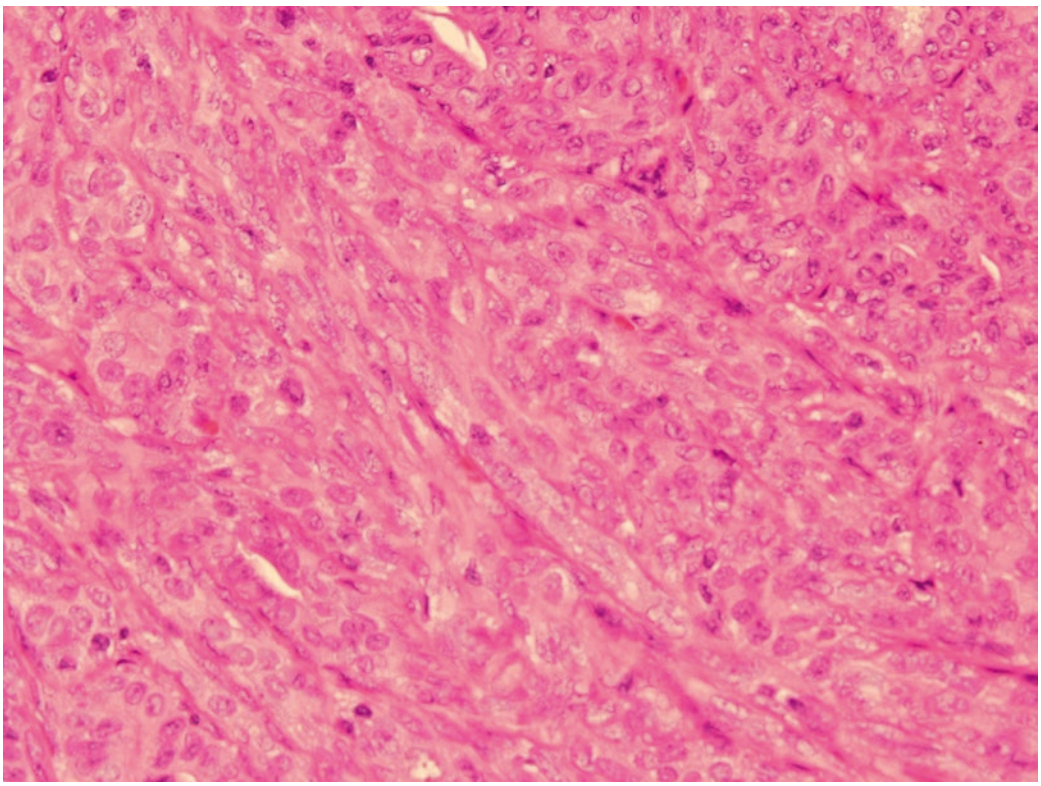

Fig. 4.13 Intraductal papilloma with florid UDH. Sometimes the epithelial proliferation may have a slightly spindled appearance with a sweeping sheet-like pattern. The spindle cells may be either of luminal epithelial or myoepithelial origin

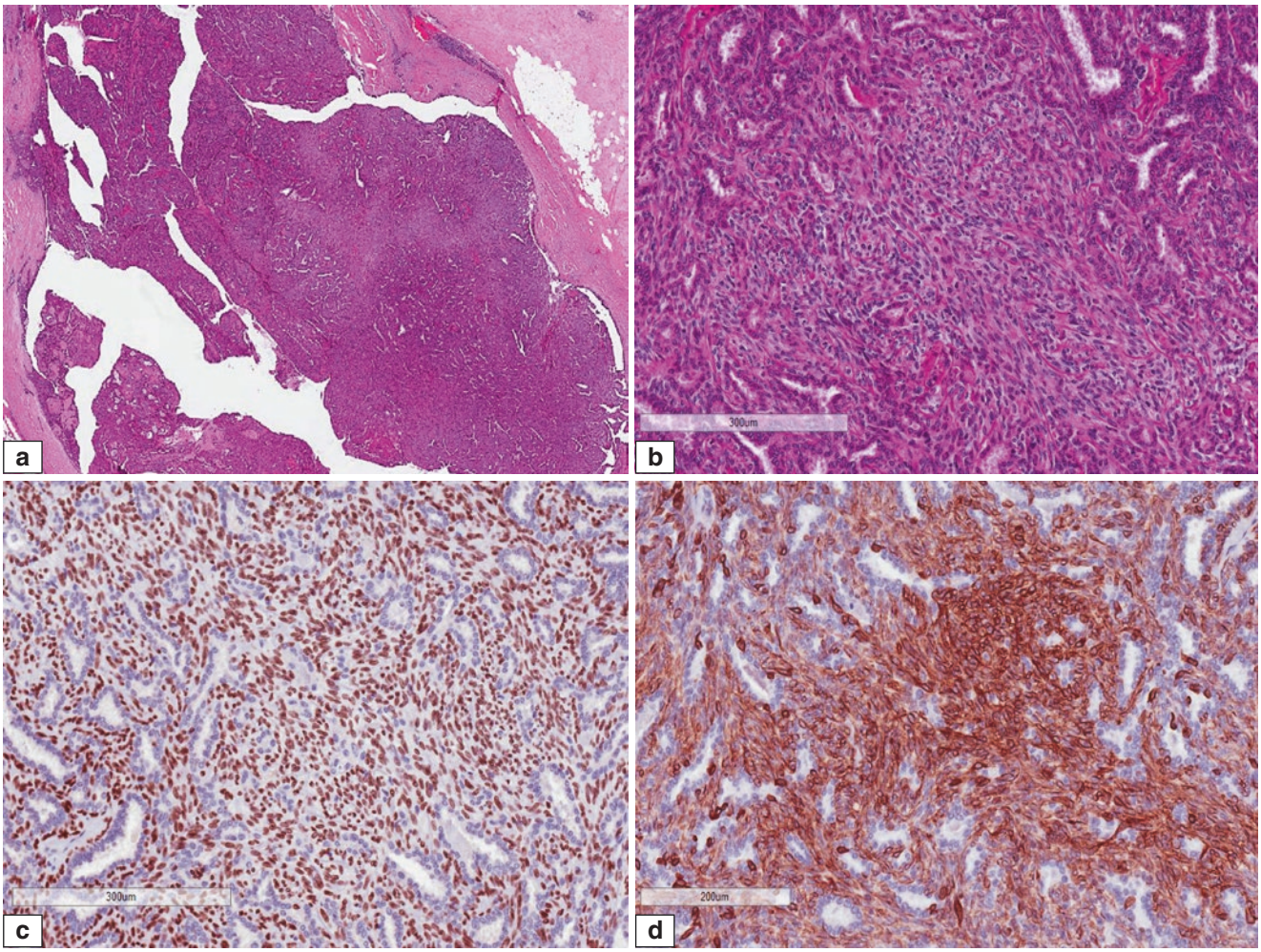

Fig. 4.14 Intraductal papilloma with myoepithelial hyperplasia. (**a**) Low magnification shows an intraductal papilloma distending the duct lumen. Several broad fronds are seen projecting into the cystically dilated duct lumen. (**b**) Higher magnification shows sheets of spindle cells in between tubules. Some of the spindle cells merge with myoepithelial cells of tubules. (**c**) Immunohistochemistry for p63 shows nuclear staining of the spindle cells, indicating a myoepithelial origin. Note the positive reactivity of myoepithelial cells rimming the tubules. (**d**) Immunohistochemistry for CK14 shows positive staining of the spindle cells corroborating a myoepithelial origin. These cells blend with the myoepithelial cells surrounding the luminal epithelial cells of tubules

The epithelial displacement phenomenon may be seen in surgical specimens of papillomas that have undergone prior instrumentation, and this may mimic invasive cancer [2]. These displaced epithelial nests are mostly limited to granulation tissue or fibrotic zones of the biopsy tract (Figs. 4.19 and 4.20). Immunohistochemistry may be helpful in confirming myoepithelial cuffing, but some displaced epithelial elements are devoid of a surrounding myoepithelial cell layer.

Differential Diagnosis

Intraductal Papilloma with Florid Usual Ductal Hyperplasia, Atypical Ductal Hyperplasia, and Low Nuclear Grade Ductal Carcinoma In Situ

Florid usual ductal hyperplasia (UDH) can make the papilloma seem solidified, with variable accompaniment by mitotic activity and even necrosis (Figs. 4.21, 4.22, 4.23, and 4.24). This can lead to overdiagnosis of malignancy. Hyperplastic ductal epithelial cells, however, show heterogeneity in size, shape, and placement, crowded and overlapping nuclei with intranuclear cytoplasmic inclusions [3], and irregular slit-like spaces, giving an appearance identical to UDH in background breast tissue. Lobular neoplasia (atypical lobular hyperplasia and lobular carcinoma in situ) may be seen within the intraductal papilloma (Fig. 4.25).

Atypical ductal hyperplasia (ADH) within an intraductal papilloma is diagnosed when a monotonous uniform epithelial population measuring less than 3 mm in extent is found within a recognisable benign intraductal papilloma (Fig. 4.26). When the abnormal epithelial population is 3 mm or more, low nuclear grade ductal carcinoma in situ (DCIS) within an intraductal papilloma is diagnosed [4]. Immunohistochemistry with high-molecular-weight keratins and oestrogen receptor (ER) can serve as an adjunct to diagnosing ADH/DCIS versus UDH within the intraductal papilloma (Figs. 4.27 and 4.28) [5].

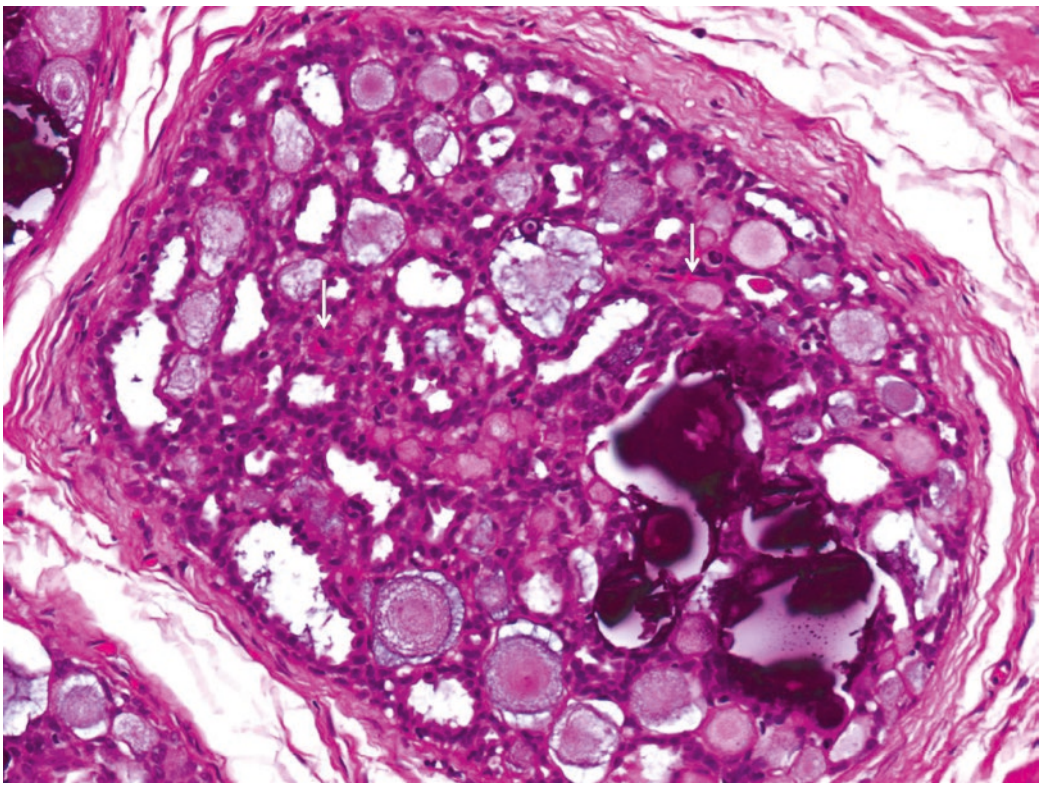

Fig. 4.15 Peripheral papilloma (micropapilloma) with collagenous spherulosis and calcifications. The papillary fronds are anastomosed. A clue to the underlying papillary architecture is the subtle presence of congested fibrovascular septa (*arrows*). Spaces containing basement membrane spherules may mimic the luminal spaces of cribriform ductal carcinoma in situ; however, the epithelial population in collagenous spherulosis is heterogeneous, which may be affirmed on immunohistochemistry with ER and high-molecular-weight keratins. Cells rimming the spherules are myoepithelial in nature

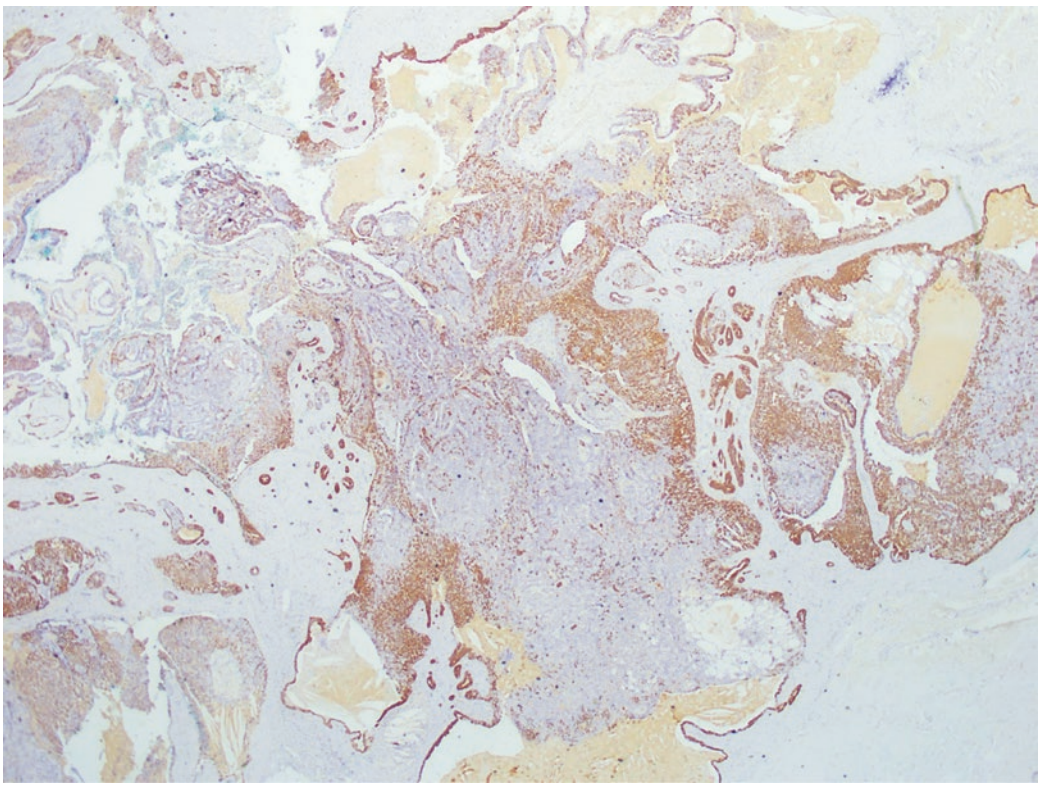

Fig. 4.16 Intraductal papilloma with florid UDH. Immunohistochemistry for CK14 (a high-molecular-weight cytokeratin) shows heterogeneous reactivity of the epithelial cells. This staining pattern is in contrast to papillary DCIS in which epithelial cells are usually uniformly nonreactive due to their clonal and luminal nature

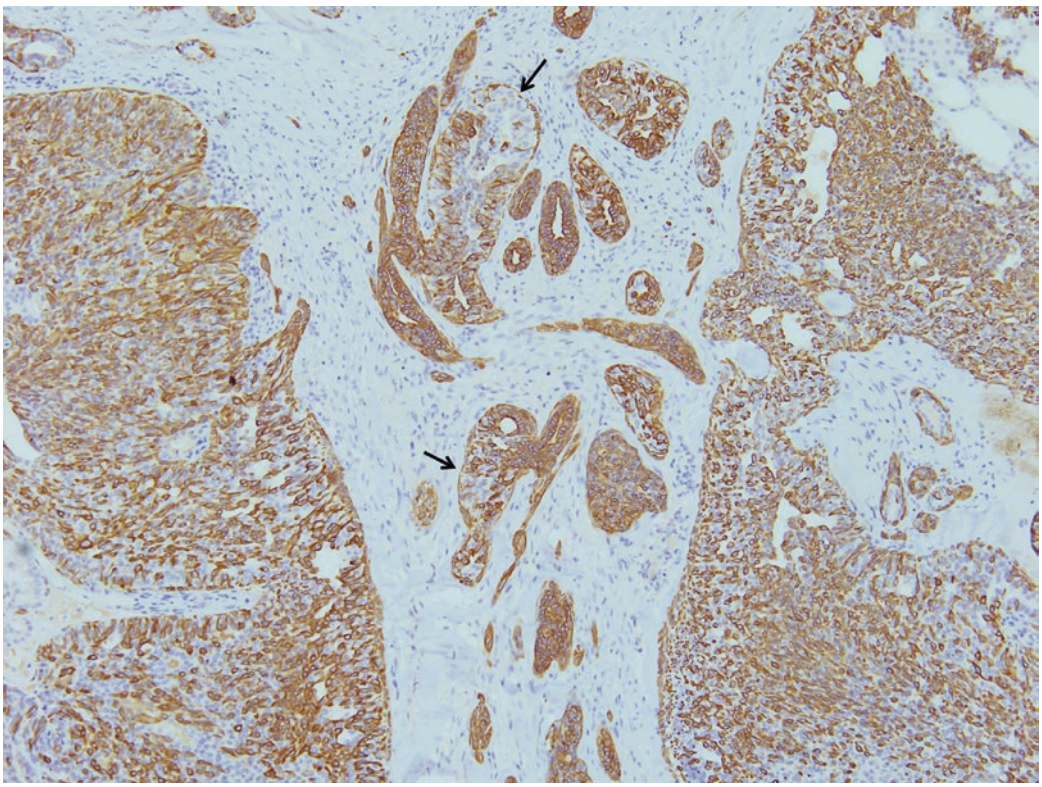

Fig. 4.17 Intraductal papilloma with florid UDH. Aside from demonstrating the mosaic-like heterogeneous staining in the epithelial population, immunohistochemistry for CK14 can also highlight preserved peripheral myoepithelial cells (*arrows*) in entrapped epithelial nests within sclerotic portions of the papilloma. These entrapped epithelial nests and tubules may mimic an invasive process due to their distorted outlines within fibrotic stroma

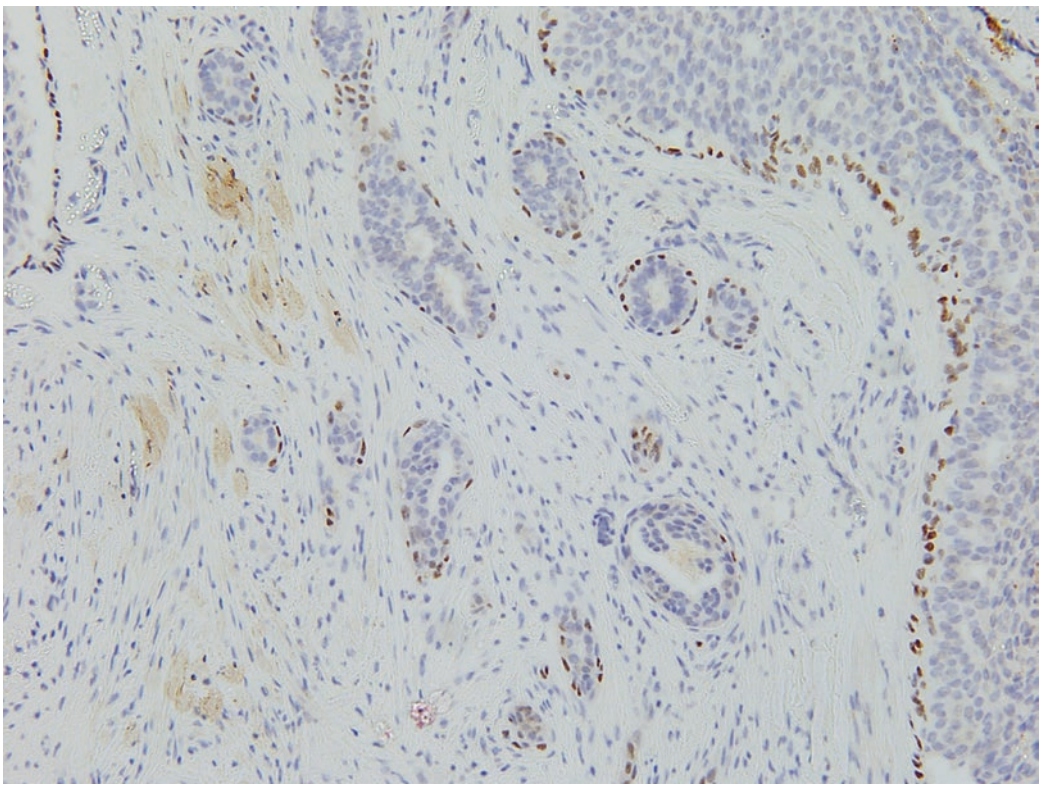

Fig. 4.18 Intraductal papilloma with epithelial nests within fibrotic stroma. Immunohistochemistry for p63 shows preserved peripheral myoepithelial cells around these epithelial nests and tubules, indicating a non-invasive nature. These slightly distorted epithelial nests and tubules can be found within sclerotic centres or fibrotic walls of the papilloma

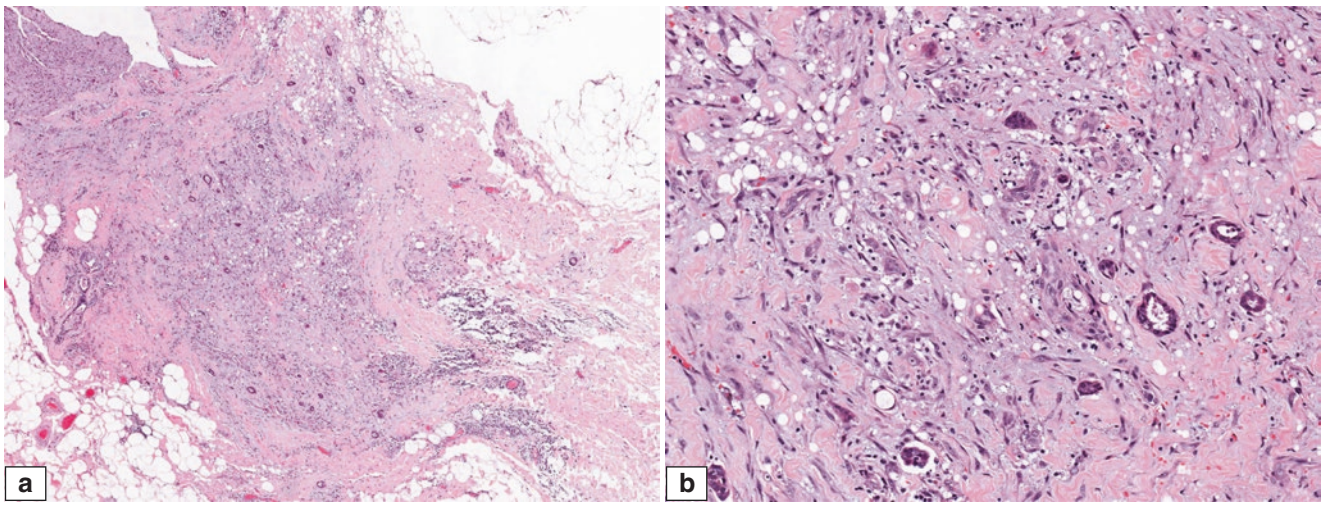

Fig. 4.19 Intraductal papilloma with epithelial displacement phenomenon. (**a**) Part of the intraductal papilloma is present in the upper field. In contiguity with the intraductal papilloma is an area of fibrosis with chronic inflammation and scattered small epithelial nests and tubules, related to prior instrumentation. (**b**) There are epithelial nests with a squamoid appearance within the loose, lightly inflamed reactive stroma. These should not be mistaken as invasive tumour nests. The epithelial displacement phenomenon is often seen after instrumentation, especially in papillary lesions

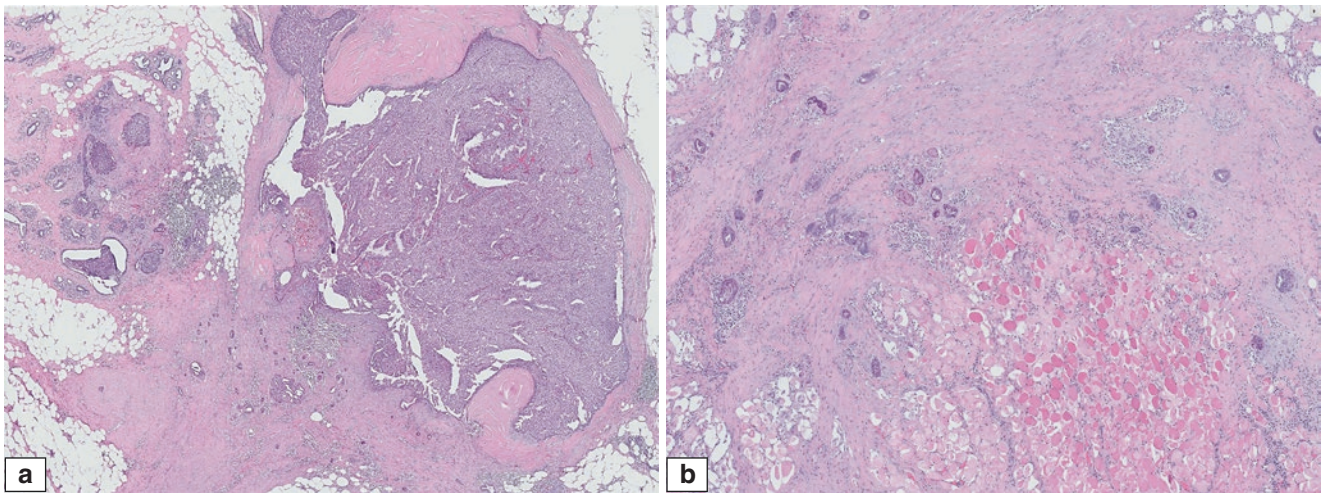

Fig. 4.20 Intraductal papilloma with epithelial displacement phenomenon. (**a**) At low magnification, the intraductal papilloma is surrounded by a fibrotic wall. A fibrotic zone in the left lower field is seen in contiguity with the wall of the intraductal papilloma, extending into the fat. Scattered small epithelial nests and tubules are seen in this fibrotic zone. (**b**) The fibrotic zone extends into the skeletal muscle, and epithelial nests and tubules are seen among the skeletal muscle fibres, which raised concern for invasion. (**c**) Review of the prior core biopsy shows portions of a benign intraductal papillary lesion with a fragment composed of skeletal muscle fibres, correlating with the organizing fibrosis extending into skeletal muscle in the subsequent excision specimen. (**d**) Immunohistochemistry for CK14 highlights many small epithelial nests and tubules within fibrosis, reflecting marked epithelial displacement. These epithelial elements are mostly confined to the reparative fibrotic areas and do not permeate into breast parenchyma elsewhere. Inset shows high magnification of a few epithelial nests and tubules. Some of the epithelial nests can possess a squamoid appearance on light microscopy, and together with their haphazard placement, may be erroneously interpreted as low grade adenosquamous carcinoma. (**e**) Immunohistochemistry for ER shows generally negative staining in the epithelial tubules and nests, with one tubule disclosing patchy epithelial nuclear reactivity (*arrow*). (**f**) Immunohistochemistry for p63 shows a patchily preserved rim of myoepithelial cells around epithelial nests and tubules (highlighted with nuclear p63 staining), which is helpful in affirming their displaced rather than invasive nature. Not always however, will p63 immunohistochemistry be able to detect a peripheral rim of myoepithelial cells, and in such instances, the diagnosis of displaced epithelium will rely on other histological features

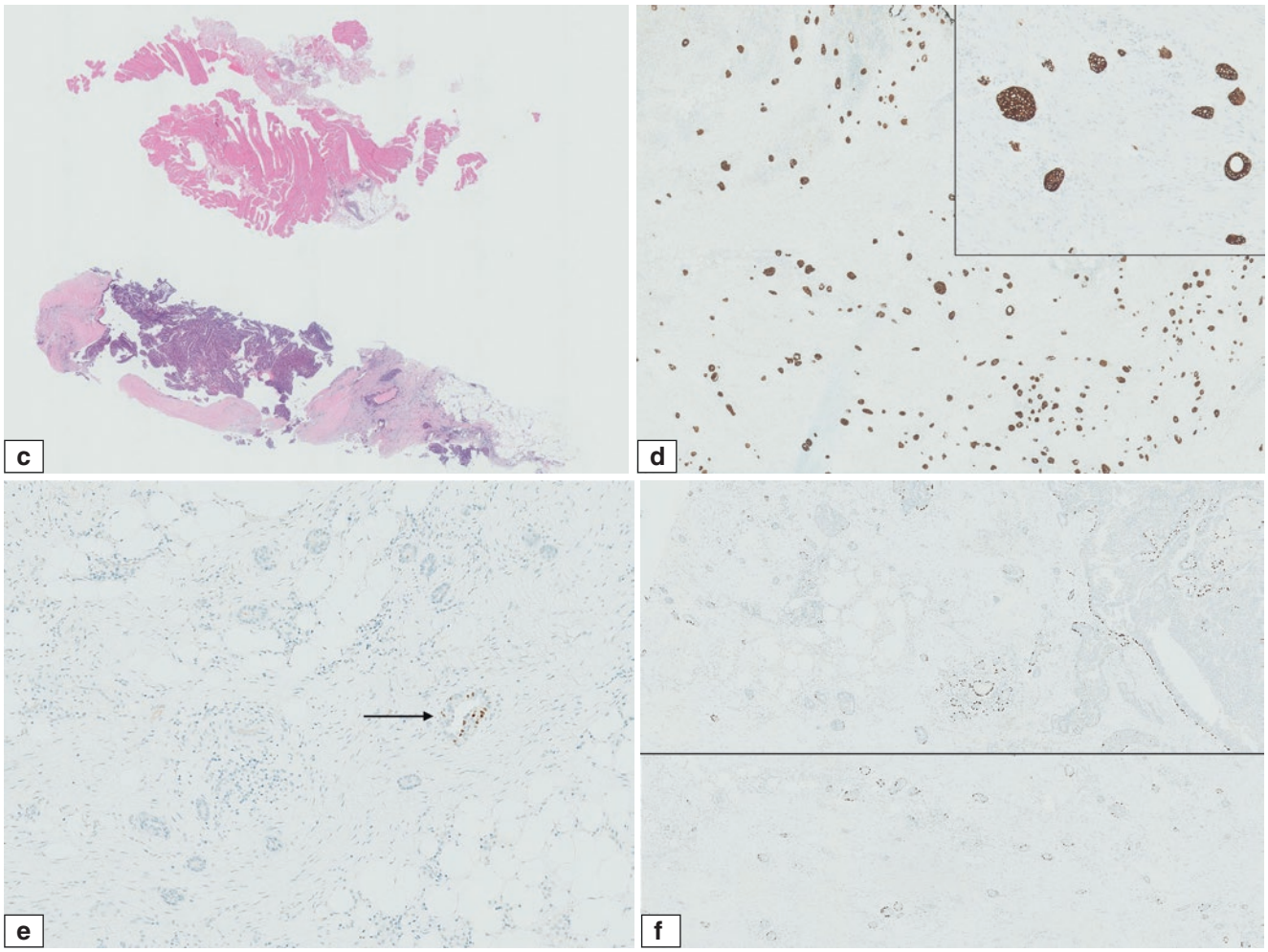

Fig. 4.20 (continued)

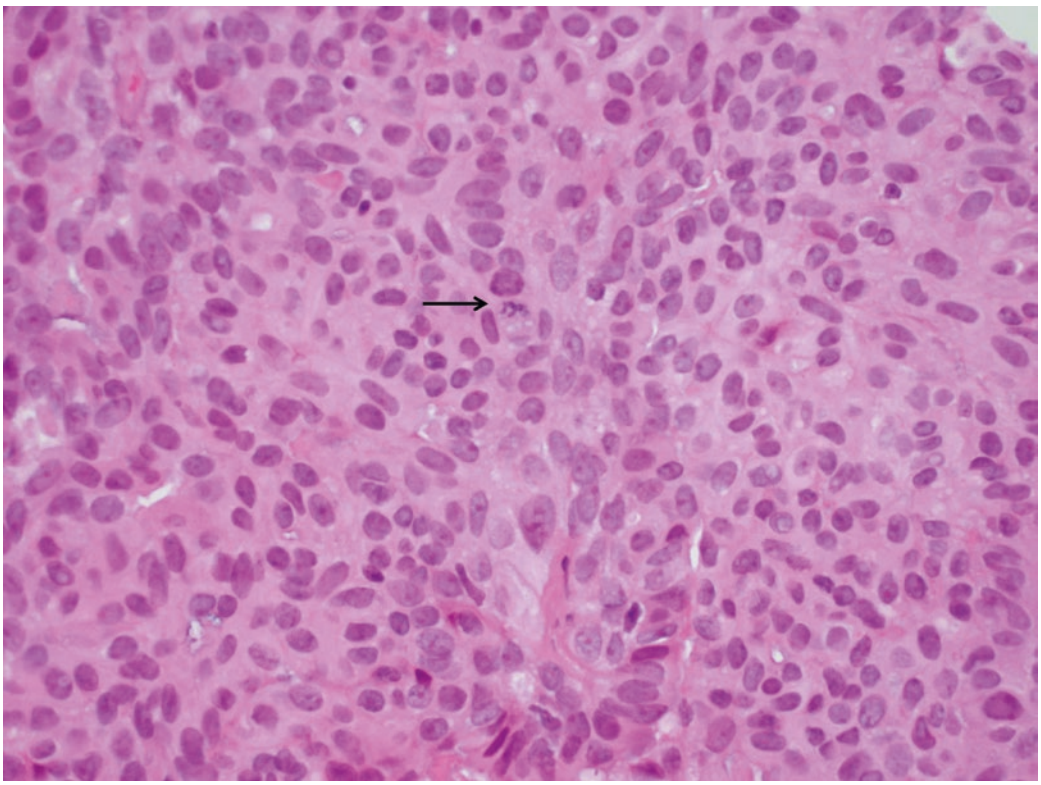

Fig. 4.21 Intraductal papilloma with florid UDH, showing a mitosis in an epithelial cell. Mitoses can be observed in UDH (*arrow*) and their presence does not connote malignancy. Epithelial nuclei may also vary in size with ovoid to more elongated forms. Nuclear crowding and overlapping are present in UDH in an intraductal papilloma

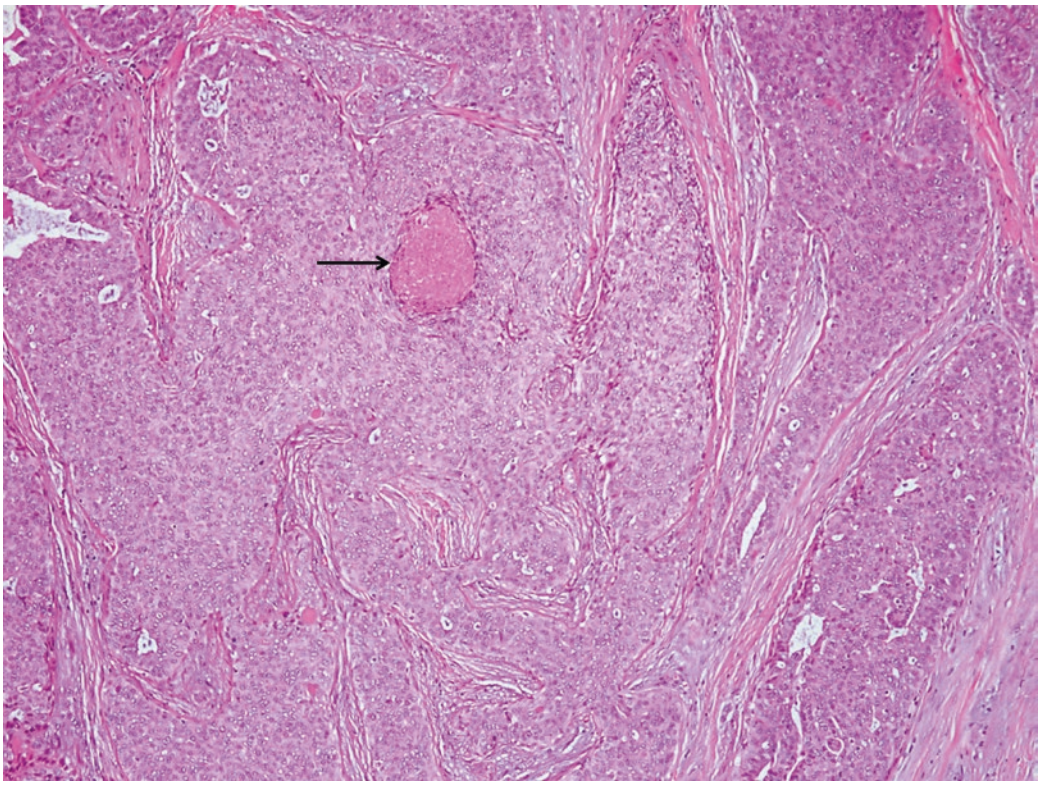

Fig. 4.22 Intraductal papilloma with florid UDH may show necrosis (*arrow*), seen here as a zone of pink amorphous material among hyperplastic ductal epithelial cells. The presence of necrosis should not necessarily lean towards a diagnosis of malignancy unless other characteristic features are present

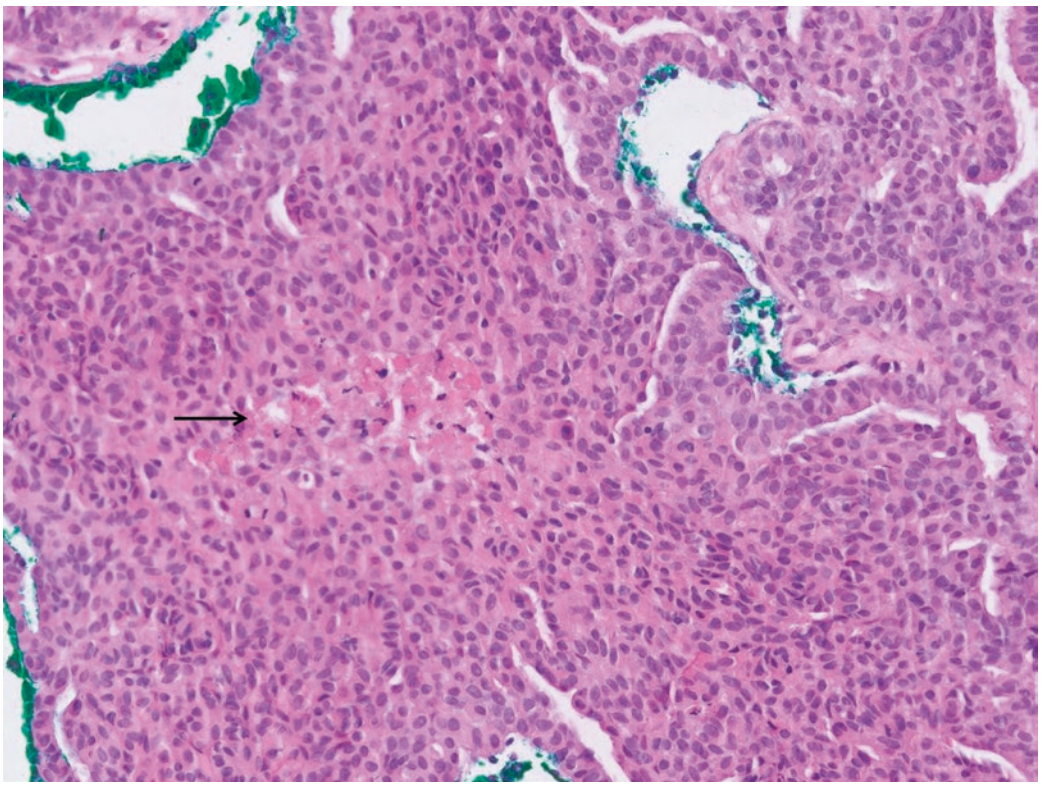

Fig. 4.23 Intraductal papilloma with florid UDH. Necrosis may also be focal and punctate, with scattered degenerate cells among some debris (*arrow*)

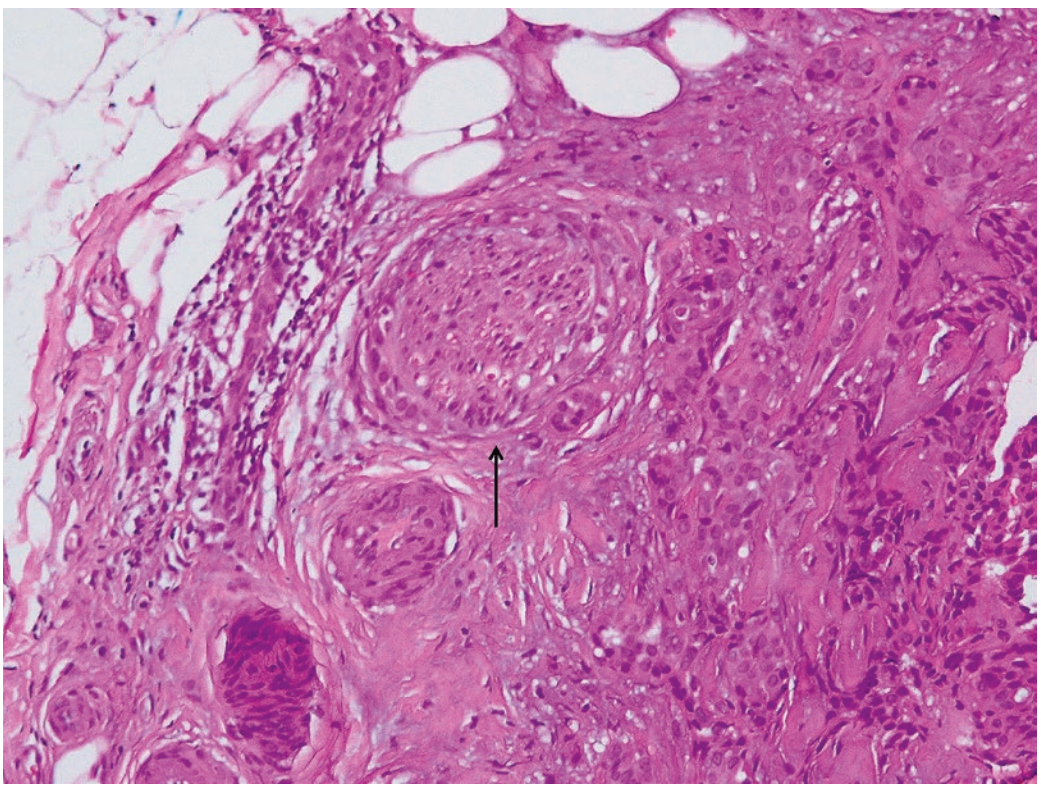

Fig. 4.24 Intraductal papilloma with perineural involvement in its fibrotic wall. The wall of an intraductal papilloma can be sclerotic, and apart from epithelial nests being entrapped in the fibrosclerotic stroma, perineural wrapping by epithelial cells (*arrow*) can also be rarely encountered

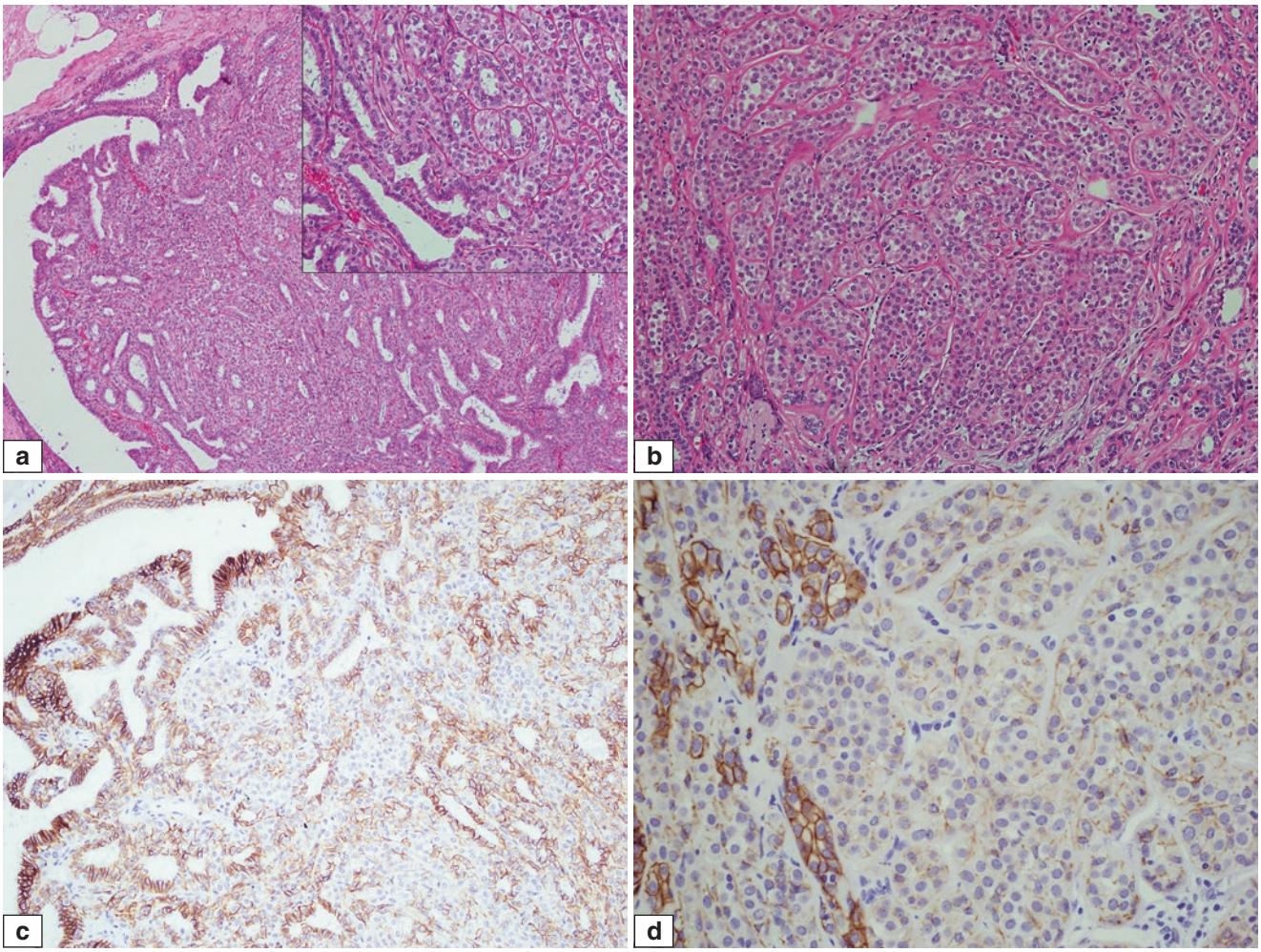

Fig. 4.25 Intraductal papilloma with atypical lobular hyperplasia. (**a**) Low magnification shows a population of rounded cells occupying the papillae. Inset shows cellular discohesion. (**b**) Discohesive rounded lobular neoplastic cells are seen within the intraductal papilloma. The distinction between atypical lobular hyperplasia and lobular carcinoma in situ may be challenging in the context of an intraductal papilloma, as the reference to the degree of lobular acinar distension and distortion which distinguishes them is not readily available. Comparison with lobular neoplastic changes in the surrounding breast tissue if present, and assessment of the degree of effacement of underlying papillary architecture by lobular neoplastic cells, are helpful. (**c**) Immunohistochemistry for E-cadherin shows negative staining of the lobular neoplastic cells. (**d**) Higher magnification of lobular neoplastic cells that display loss of E-cadherin immunohistochemical reactivity. Some lobular neoplastic cells show diminished and incomplete staining rather than complete absence of immunoreactivity.

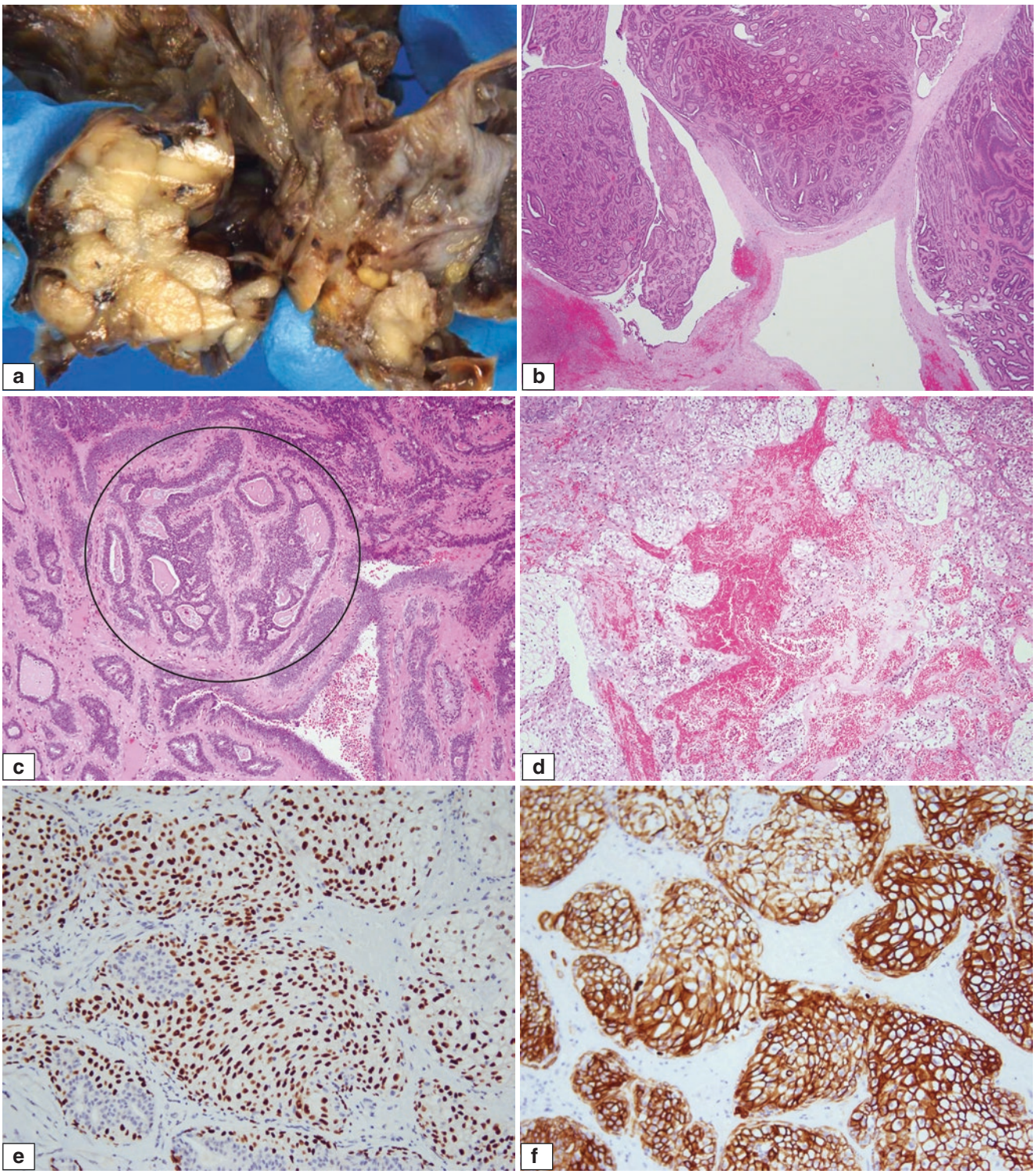

Fig. 4.26 Complex intraductal papilloma with atypical ductal hyperplasia and clear-cell squamous metaplasia. (**a**) Gross appearance shows a multilobulated lesion with partial cystic change. (**b**) At low magnification, the tumour shows predominantly rounded and nodular solidified papillary areas with fibrous enclosures. Areas of haemorrhage are present in the fibrous wall. The nodules project into the cystic spaces. (**c**) Atypical ductal hyperplasia (ADH) is observed as duct spaces containing a cribriform proliferation (*circled*). The cribriform spaces are well defined and are lined by relatively uniform epithelial cells. Rigid epithelial arches are also seen. Distinction of ADH from low nuclear grade ductal carcinoma in situ (DCIS) within an intraductal papilloma is based on size or extent of the cytoarchitecturally atypical alterations. The WHO working group recommends a threshold of 3 mm, with cytoarchitecturally atypical lesions measuring less than 3 mm being diagnosed as ADH, while those that are 3 mm and above are considered DCIS. The size criterion applies only to low nuclear grade lesions, as high nuclear grade alterations warrant a diagnosis of DCIS regardless of extent. (**d**) Haemorrhagic infarction is surrounded by epithelial nests with clear-cell change. Reactive nuclear atypia may be seen adjacent to infarction. (**e**) Immunohistochemistry for p63 shows positive nuclear staining in clear-cell areas, while adjacent ducts disclose peripheral myoepithelial nuclear reactivity. (**f**) Immunohistochemistry for CK5/6 shows positive staining of the clear cells supporting a squamous metaplastic origin

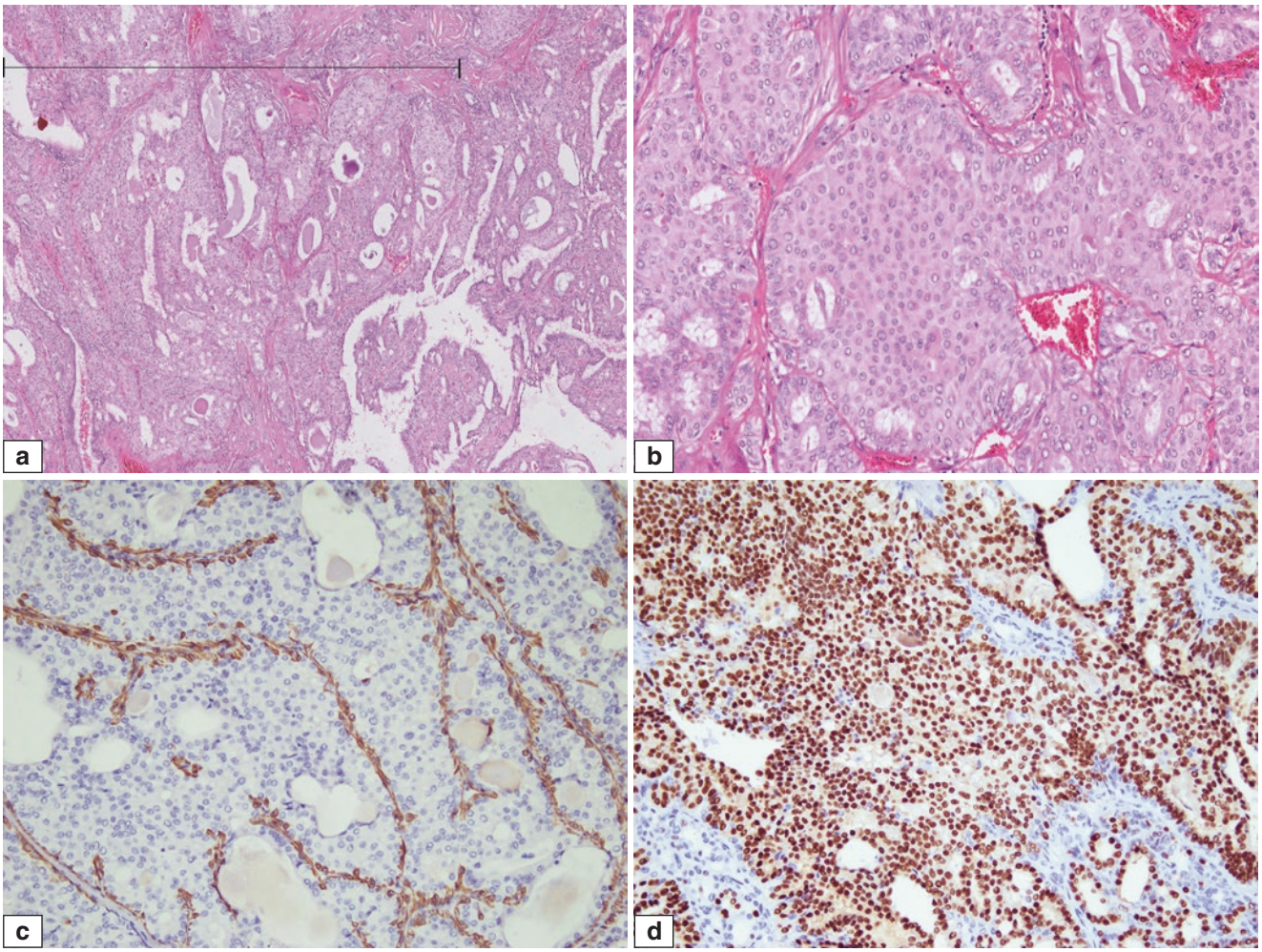

Fig. 4.27 Intraductal papilloma with ductal carcinoma in situ (DCIS). (**a**) This intraductal papilloma shows an area of relatively monotonous cribriform epithelial proliferation that exceeds 3 mm in extent (*horizontal line*). (**b**) Higher magnification of low nuclear grade DCIS composed of a uniform population of epithelial cells punctuated by well-defined cribriform spaces. (**c**) Immunohistochemistry for CK14 shows diminished staining of the epithelial cells. Only the peripheral myoepithelial cuff is decorated. (**d**) Immunohistochemistry for ER shows diffuse and intense nuclear staining of the epithelial cells, supporting a clonal neoplastic process

Sclerosing Intraductal Papilloma

This is an intraductal papilloma which has undergone extensive sclerosis with effacement of the underlying papillary architecture. Histologically, closely placed bilayered tubules are seen within a fibrotic wall (Fig. 4.29). The ductal adenoma is considered by some authors as representing one end of the spectrum of sclerosing papillomas, where there is complete effacement and solidification of papillary structures [6].

Adenomyoepithelioma

As adenomyoepithelioma may arise within the ducts and have a focally papillary architecture, it may be mistaken for an intraductal papilloma. An adenomyoepithelioma, however, usually comprises a balanced proliferation of both luminal epithelial and myoepithelial cells throughout the lesion, although there are lesions composed predominantly of myoepithelial cells in which the luminal epithelial component may be obscured (Fig. 4.30).

Juvenile Papillomatosis

Intraductal papillomas may be found in juvenile papillomatosis, a benign proliferative lesion that occurs in young women and children. Also described as 'Swiss cheese disease' due to the many cysts within dense fibrous stroma, juvenile papillomatosis features an admixture of histological alterations which include cysts, usual ductal hyperplasia, apocrine metaplasia, sclerosing adenosis, fibroadenomatoid hyperplasia, apart from intraductal papillomas. The finding of isolated papillomas and cysts in a young patient should not be diagnosed as juvenile papillomatosis, which comprises a wider spectrum and variety of proliferative changes (Fig. 4.31).

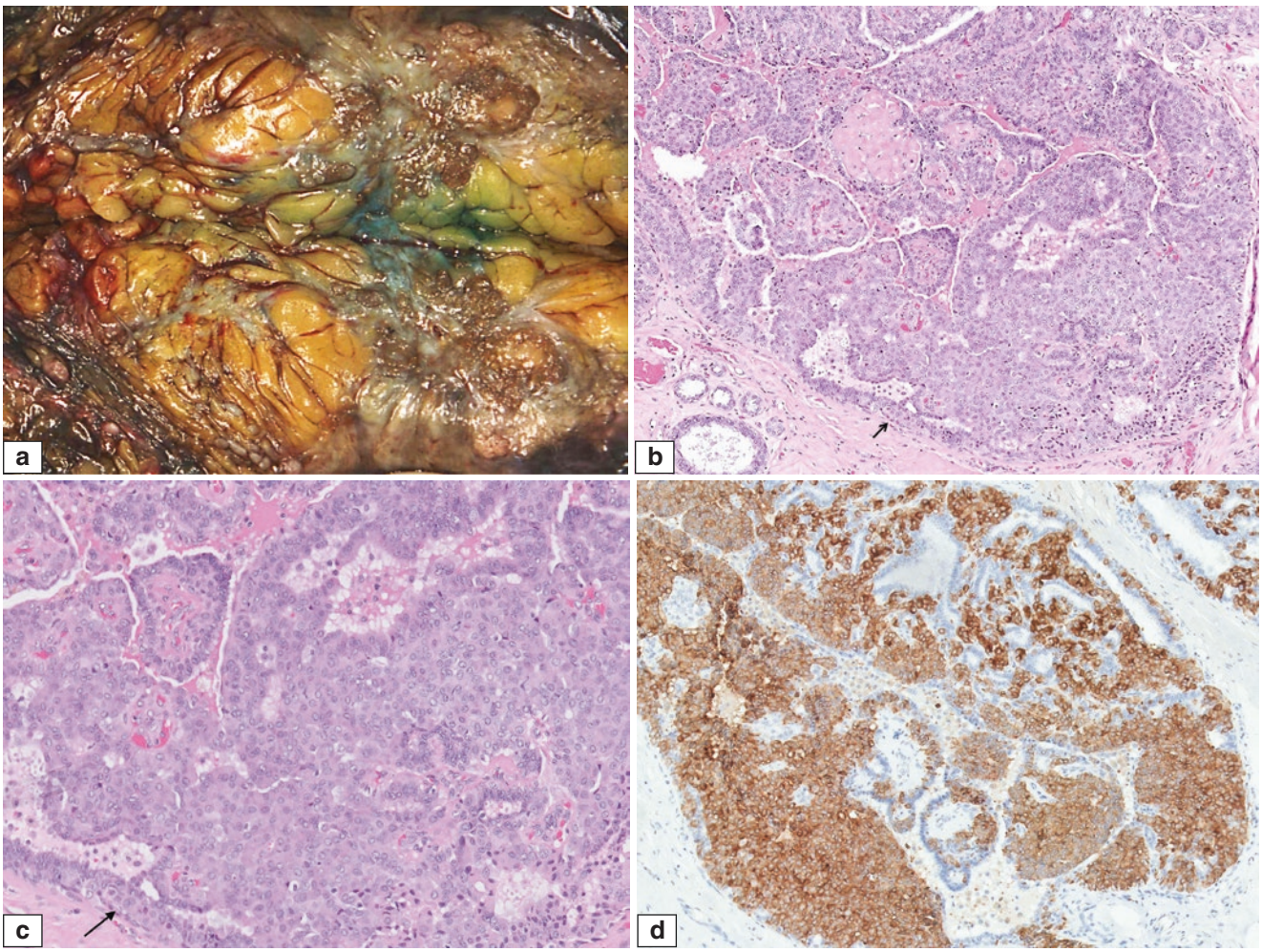

Fig. 4.28 Intraductal papilloma colonized by neuroendocrine DCIS. (**a**) In this sliced open mastectomy specimen, a lobulated brownish grey mass is seen, partially rimmed by whitish fibrous tissue. Histologically, this showed an intraductal papilloma with neuroendocrine DCIS. (**b**) In this intraductal papilloma in which the underlying papillary architecture is preserved, there is a population of relatively monotonous cells with amphophilic cytoplasm expanding papillary fronds and located deep to the luminal epithelium, focally giving a pagetoid appearance (arrow) of insinuation in between luminal and myoepithelial cells. (**c**) Higher magnification shows the monomorphic cells containing vesicular rounded nuclei with small inconspicuous nucleoli and pink to amphophilic cytoplasm. A focal pagetoid appearance is seen (*arrow*). (**d**) Immunohistochemistry for synaptophysin shows positive staining of the neuroendocrine cells within the intraductal papilloma

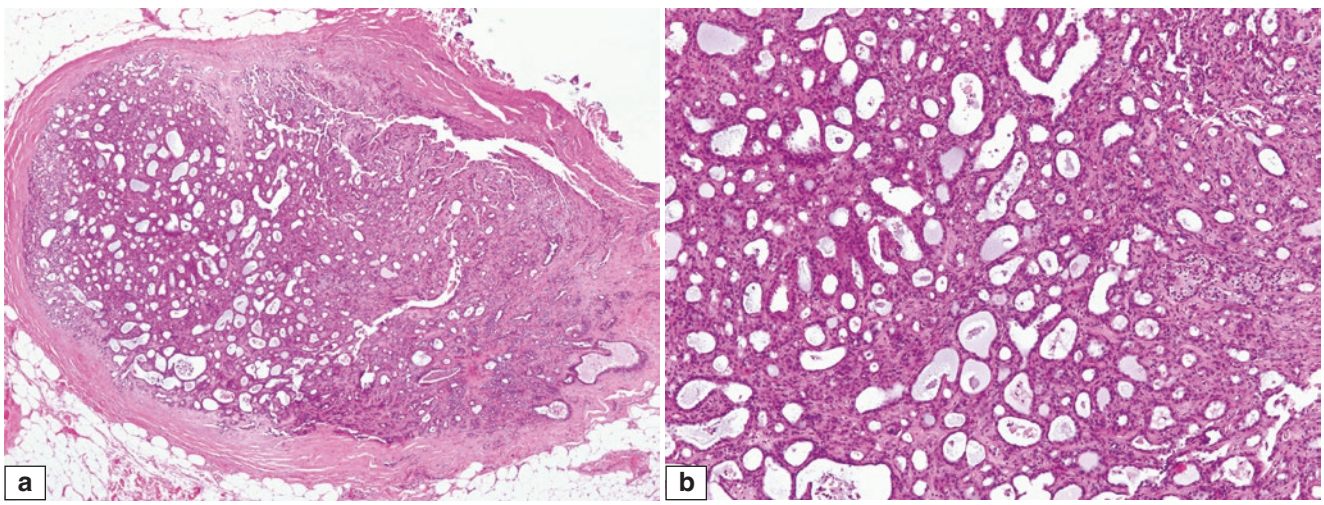

Fig. 4.29 (**a**) Sclerosing intraductal papilloma, also referred to as ductal adenoma when there is near complete-to-complete sclerosis leading to a predominant glandular lesion with hardly any fronds. Low magnification shows a solidified lesion with duct spaces, rimmed by a thick fibrous wall. A few papillary fronds are seen in the upper right field of the lesion. (**b**) Higher magnification shows a conglomeration of ducts with scant intervening stroma

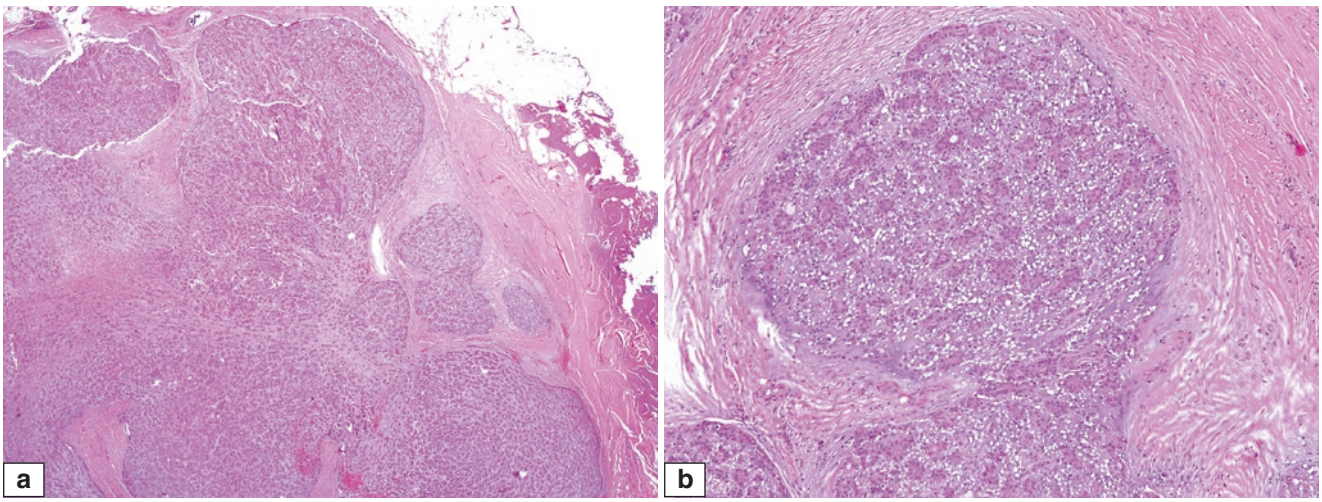

Fig. 4.30 (**a**) Adenomyoepithelioma may mimic an intraductal papilloma, as it can extend along ducts and have a papillary architecture. Here, the adenomyoepithelioma shows a lobulated appearance at low magnification, superficially reminiscent of an intraductal papilloma. (**b**) On higher magnification, there is a balanced proliferation of both luminal and myoepithelial cells, with the myoepithelial cells possessing clear cytoplasm

Invasive Low-Grade Carcinoma

Distorted epithelial nests and tubules within sclerotic portions of the intraductal papilloma may mimic a low-grade invasive carcinoma. Clues that they are benign and non-invasive in nature are the presence of myoepithelial cells and their focal occurrence within sclerotic zones without further extension beyond the confines of the papilloma. Squamoid changes or squamous metaplasia in some of these epithelial nests may raise consideration for low-grade adenosquamous carcinoma, but these changes are focal and limited without involvement of surrounding breast tissue away from the intraductal papilloma, negating a malignant invasive process (Fig. 4.32).

Similarly, displaced epithelial nests from previous core biopsy may result in the appearance of epithelial islands haphazardly placed within fibrous and inflamed granulation that can resemble invasion. These epithelial nests are usually limited to the biopsy tract.

Prognosis and Therapy Considerations

Intraductal papillomas are benign tumours that are associated with two- and threefold increased risk of subsequent breast cancer development for, respectively, central and peripheral varieties. When there is ADH or DCIS within the papilloma, the risk increases to between 5 and 7.5×, although this may be more related to atypical changes in the surrounding breast tissue than within the papilloma. When diagnosed on core biopsy, many institutions pursue complete excision via mammotome or open surgical techniques to avoid undersampling worse lesions, though follow-up without excision is increasingly being adopted for benign papillary lesions discovered on core biopsy (Fig. 4.33).

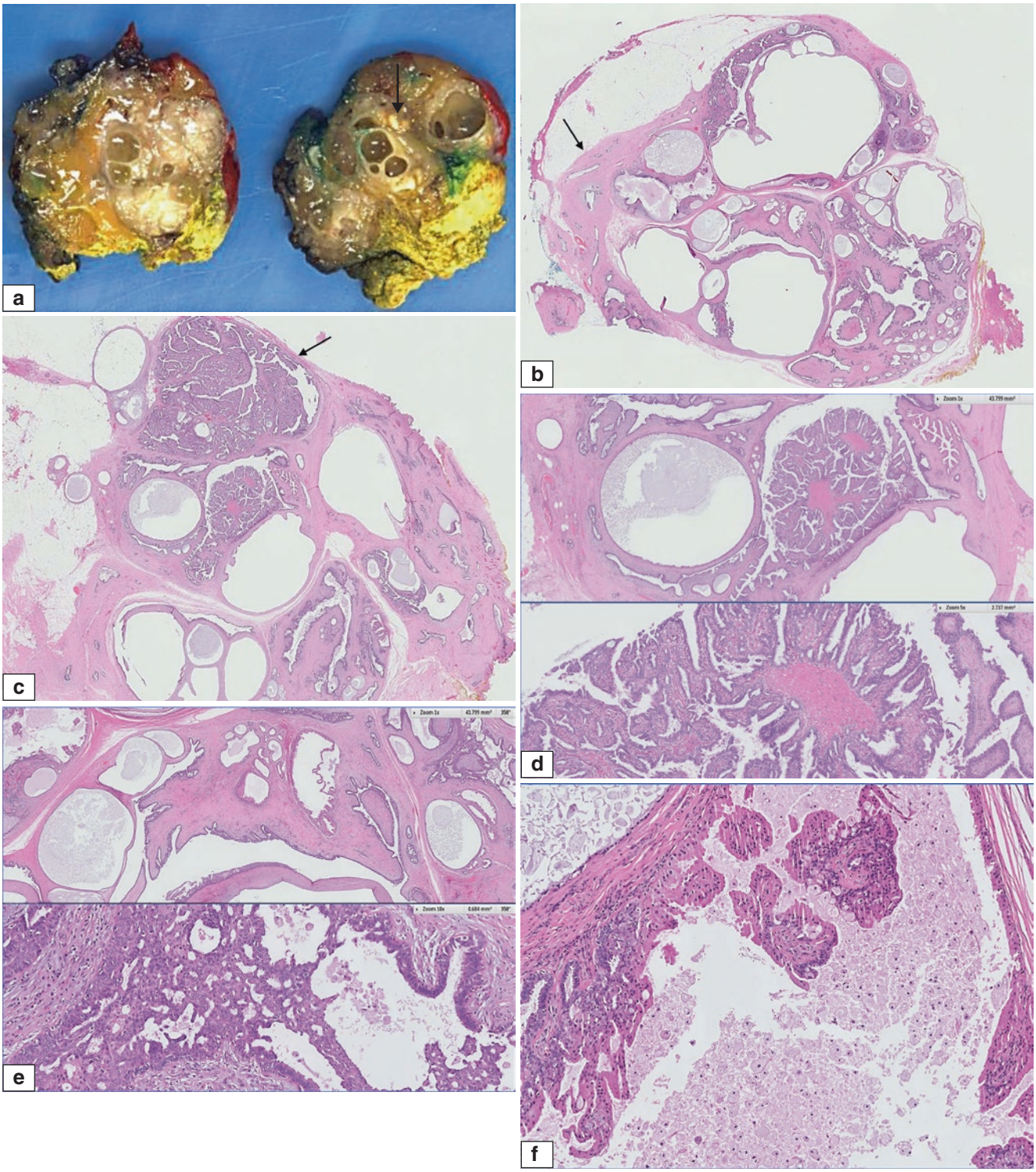

Fig. 4.31 Juvenile papillomatosis. (**a**) Multiple cysts of varying sizes are seen in a whitish fibrous background. There are a few yellowish areas (*arrow*) corresponding histologically to collections of foamy histiocytes. (**b**) Low magnification shows variably sized cysts with several luminal broad stromal folds and projections. A fibroadenomatoid appearance is noted (*arrow*). (**c**) An intraductal papilloma is seen, composed of arborescent papillary fronds with fibrovascular cores (*arrow*). (**d**) Higher magnification of the intraductal papilloma shows finger-like papillary fronds covered by benign bilayered epithelium, well supported by fibrovascular cores. (**e**) Apocrine metaplasia and broad stromal fronds (upper field), and usual ductal hyperplasia (lower field) are seen. (**f**) Apocrine metaplasia is noted along the cyst wall as well as covering the papillary fronds.

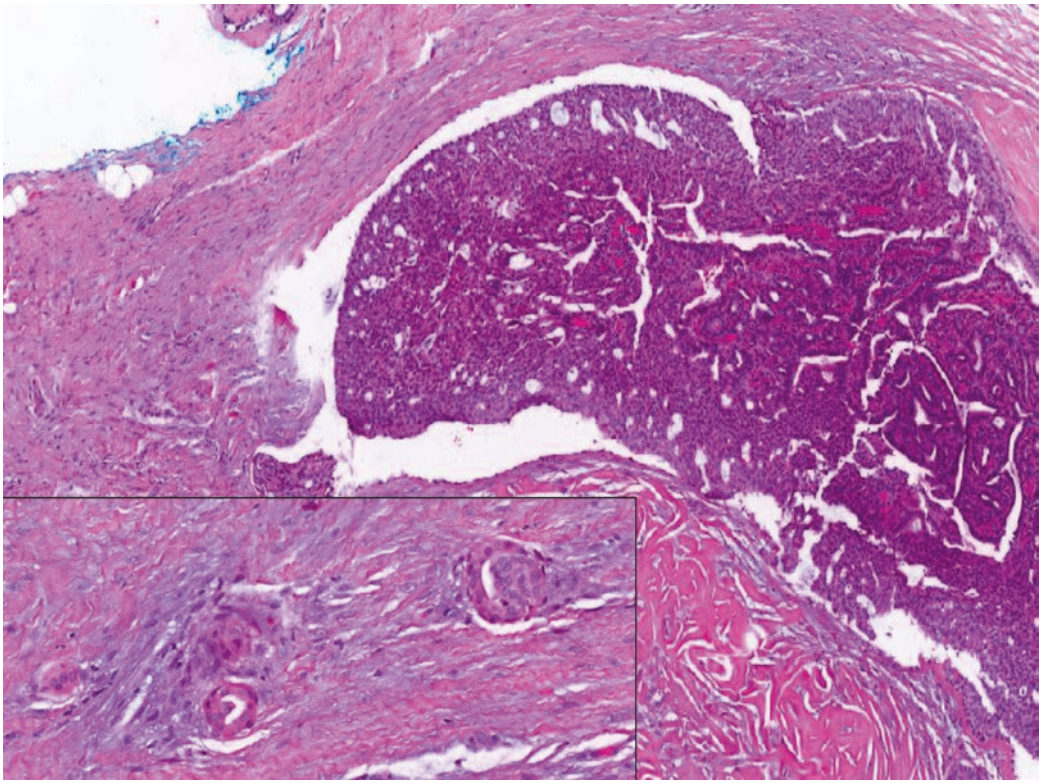

Fig. 4.32 Intraductal papilloma with sclerotic stroma. Within the sclerotic stroma are occasional small squamoid nests (*inset*) which should not be overinterpreted as low-grade adenosquamous carcinoma. Although low-grade adenosquamous carcinoma has been described arising from intraductal papillomas, they are more permeative and extend substantively into the surrounding tissue

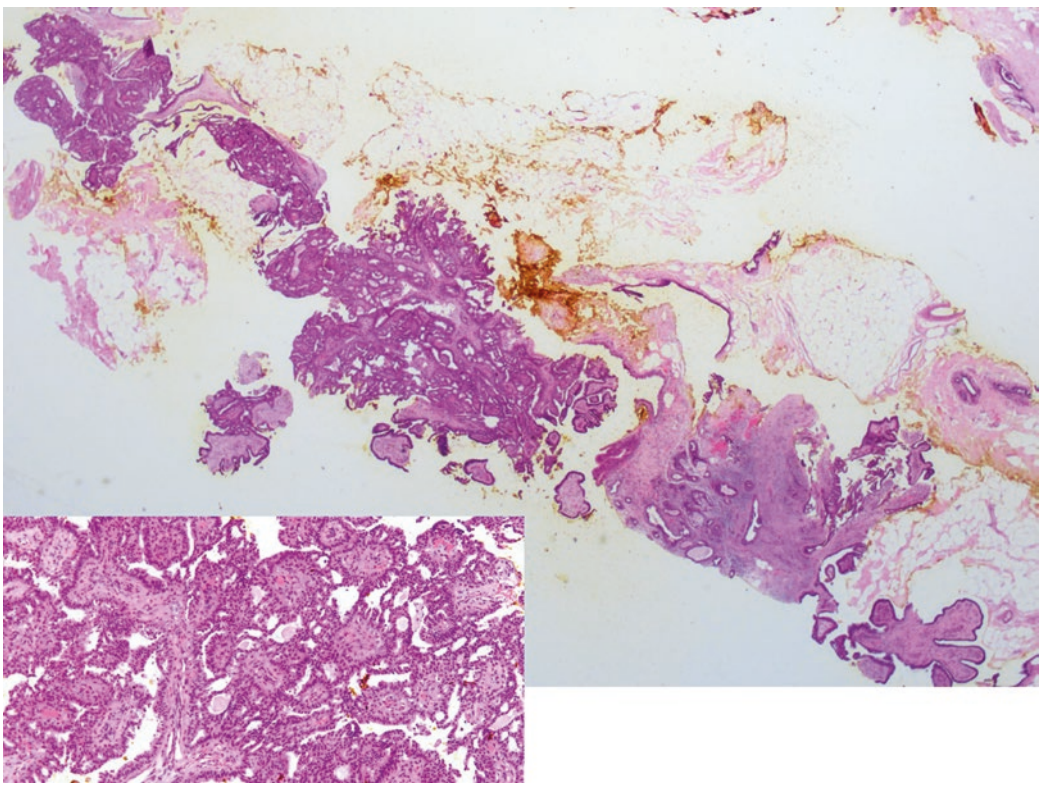

Fig. 4.33 Papillary lesion on core biopsy. The usual approach to the finding of a papillary lesion on core biopsy is to recommend complete excision, either via mammotome or open excision. Some centres opt to follow up such benign papillary lesions discovered on core biopsy. This core biopsy shows portions of a papillary lesion with anastomosed fronds, as well as a sclerotic portion within which are a few ducts. The *inset* shows the papillae supported by well-developed fibrovascular cores. While the findings are benign and may be in keeping with an intraductal papilloma, they may not be representative of unsampled portions of the lesion

Papillary Ductal Carcinoma In Situ (Intraductal Papillary Carcinoma)

Definition

Papillary DCIS is a non-invasive malignant lesion with papillary architecture arising within the ducts. In contrast to an intraductal papilloma with DCIS, papillary DCIS is regarded as a de novo in situ malignant papillary process without a morphologically recognisable benign papilloma in its background [4]. It is uncommon in its pure form and is often seen in conjunction with other morphological patterns of DCIS.

Clinical and Epidemiological Features

Patients may present with bloodstained nipple discharge or a breast lump.

Imaging Features

Radiological detection as a mass or clustered calcifications can be encountered. Ultrasound examination may detect an intraductal mass that can contain small cystic spaces or appear intracystic when associated with a dilated duct (Fig. 4.34).

Pathologic Features

Macroscopic Pathology

Papillary DCIS may appear as an area of induration of the breast or form ill-defined firm fibrotic areas. Small lesions may be difficult to identify grossly.

Microscopic Pathology

Histologically, slender papillae covered by a monotonous uniform population of epithelial cells are seen arising from the duct wall (Fig. 4.35). Myoepithelial cells between epithelium covering the papillae and the stromal cores are absent or diminished, while those surrounding the duct wall are generally preserved, although they may be attenuated and sparse. Columnar cells with variable stratification of hyperchromatic nuclei are commonly observed (Fig. 4.36, 4.37, 4.38, and 4.39). Nuclear grade is usually low to intermediate, with less frequent high-grade forms. Other morphological patterns of DCIS such as cribriform, micropapillary, and solid appearances may merge with papillary DCIS [4]. Occasionally, a dimorphic pattern of epithelial cells can be seen, with the second population mimicking myoepithelial cells, but which are in fact neoplastic epithelial cells with a different appearance (globoid cells) (Fig. 4.40).

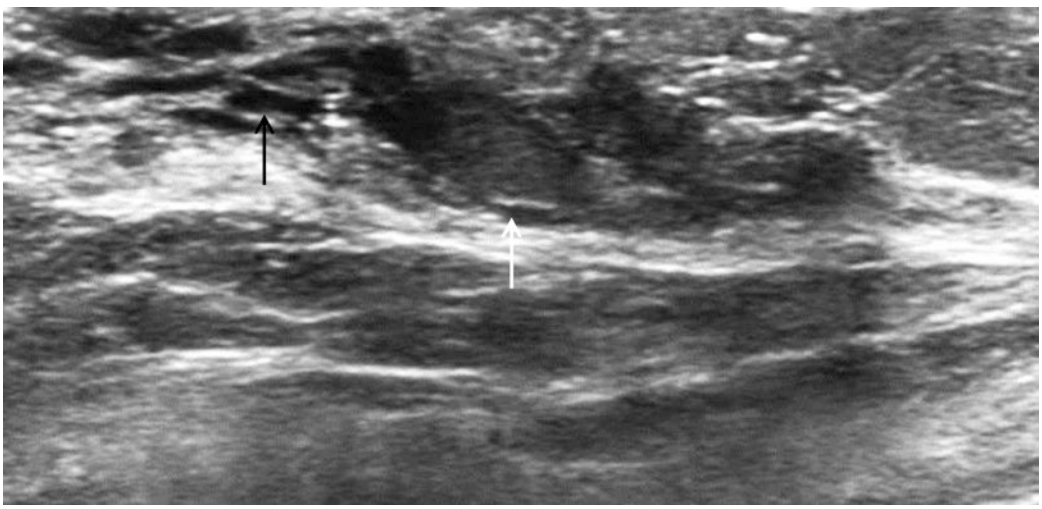

Fig. 4.34 Papillary DCIS. Ultrasound shows a tubular, lobulated solid mass (*white arrow*) that is filling and distending a prominent duct (*black arrow*) (Courtesy of Dr. Lester Leong)

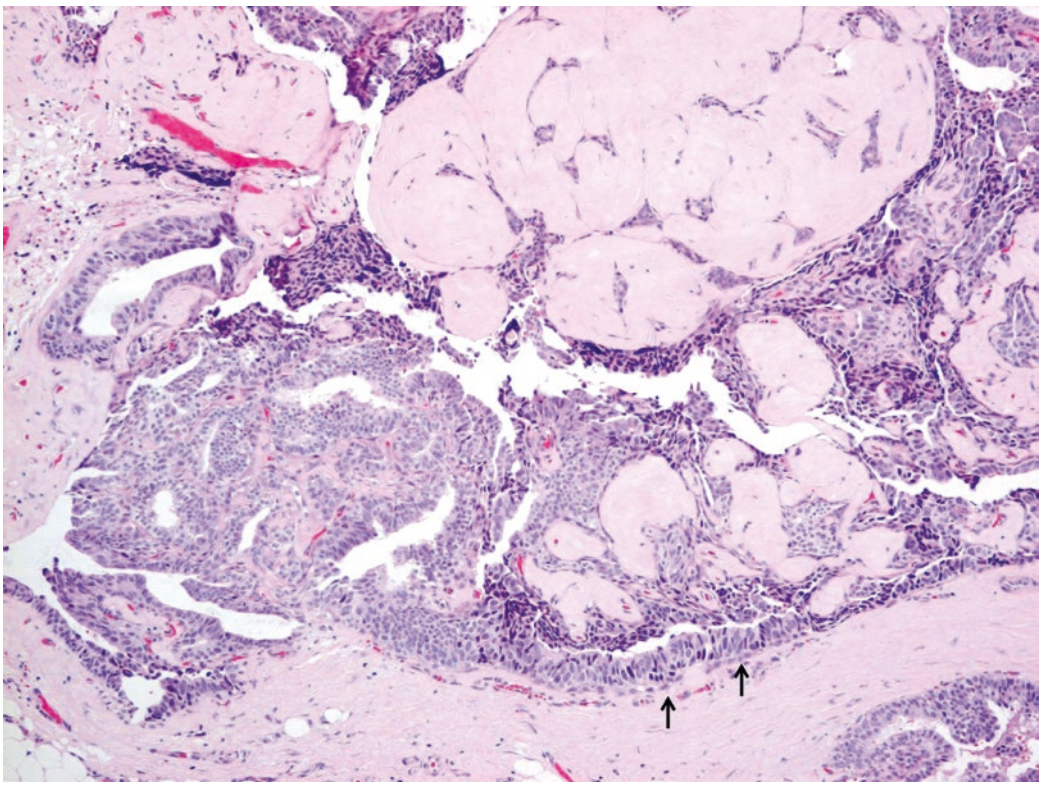

Fig. 4.35 Papillary DCIS. The duct is distended by a papillary lesion with anastomosed papillae covered by columnar cells with stratified nuclei. Hyalinised stroma is seen. Myoepithelial cells can be seen at the periphery of the duct wall (*arrows*)

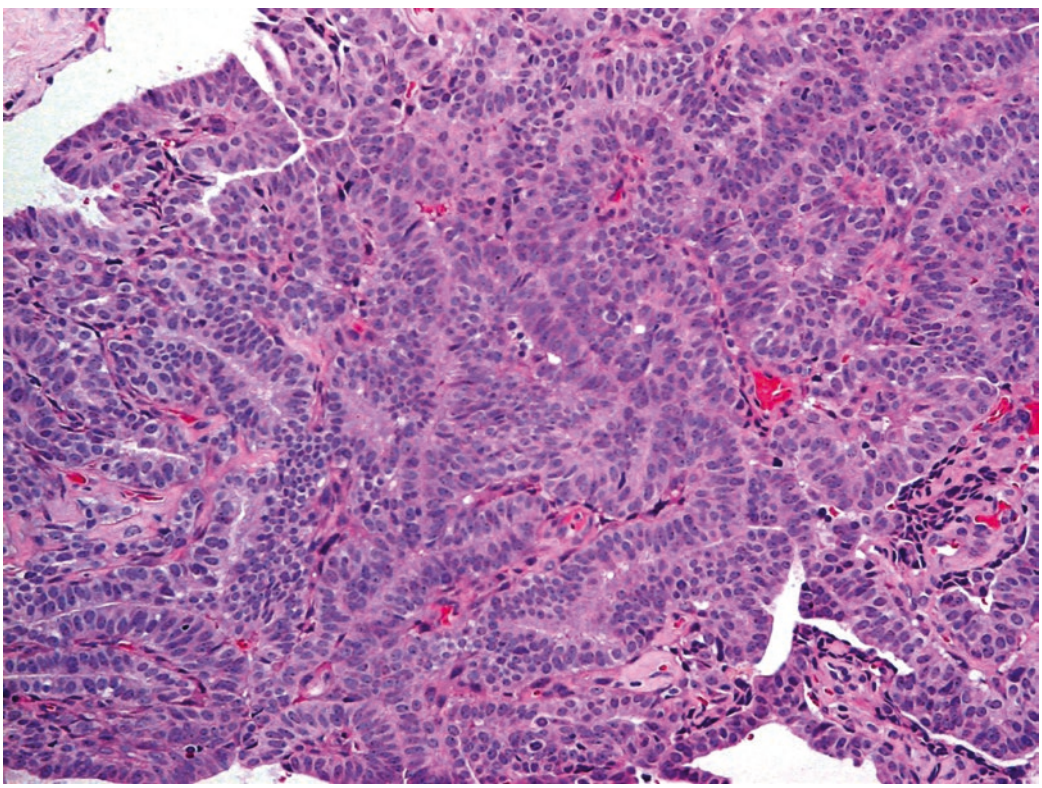

Fig. 4.36 Papillary DCIS. The slender congested septa are surmounted by a monotonous population of columnar cells with hyperchromatic stratified nuclei with small but discernible nucleoli

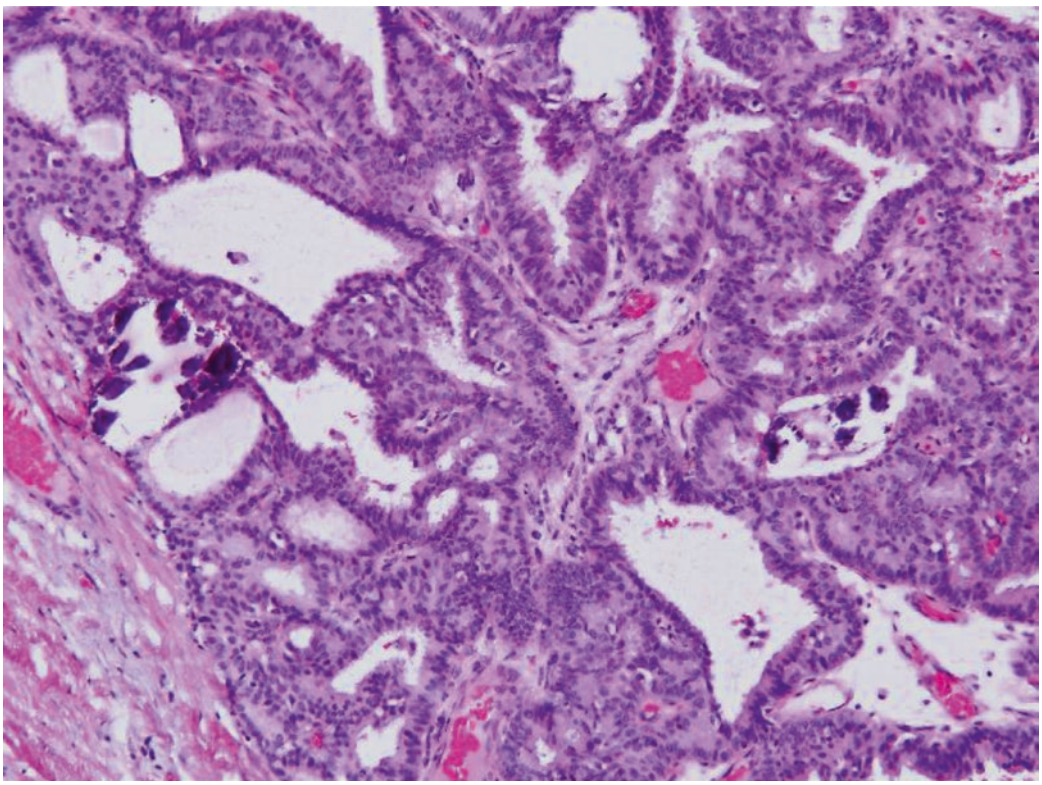

Fig. 4.37 Papillary DCIS. Occasional calcifications may be observed among the anastomosed papillary fronds. The spaces seen among the fused papillae show well-defined rigid outlines

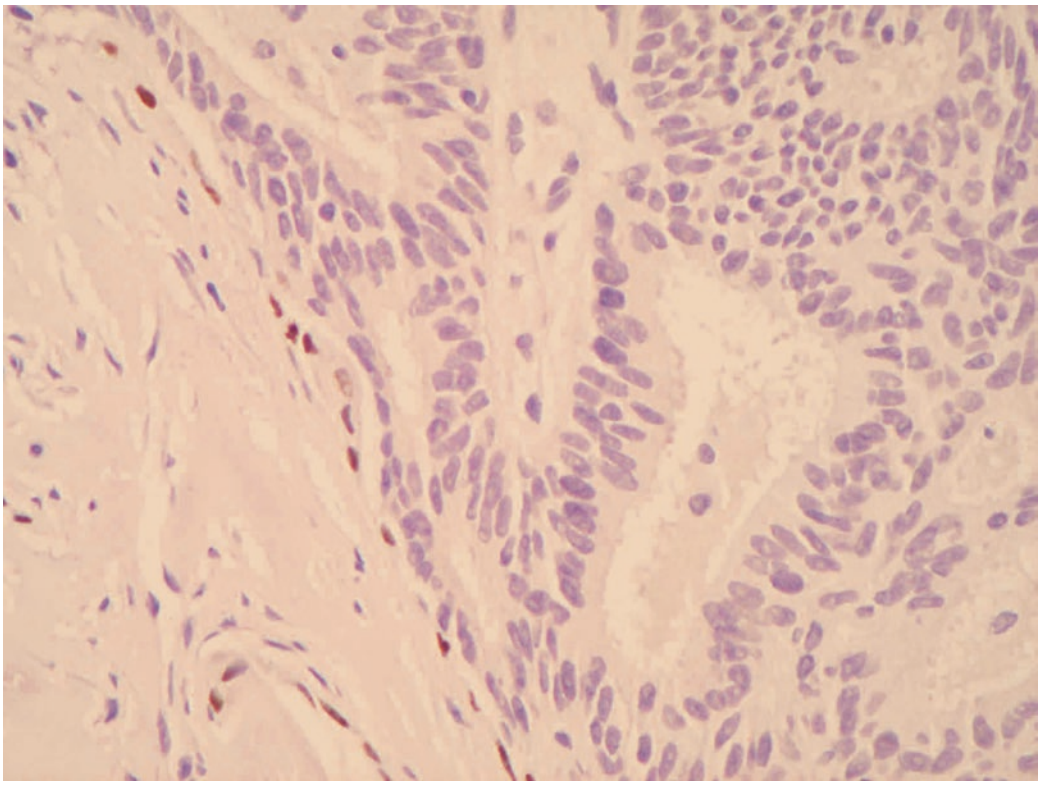

Fig. 4.38 Papillary DCIS. Immunohistochemistry for p63 shows attenuated positively stained myoepithelial nuclei along the periphery of the duct wall

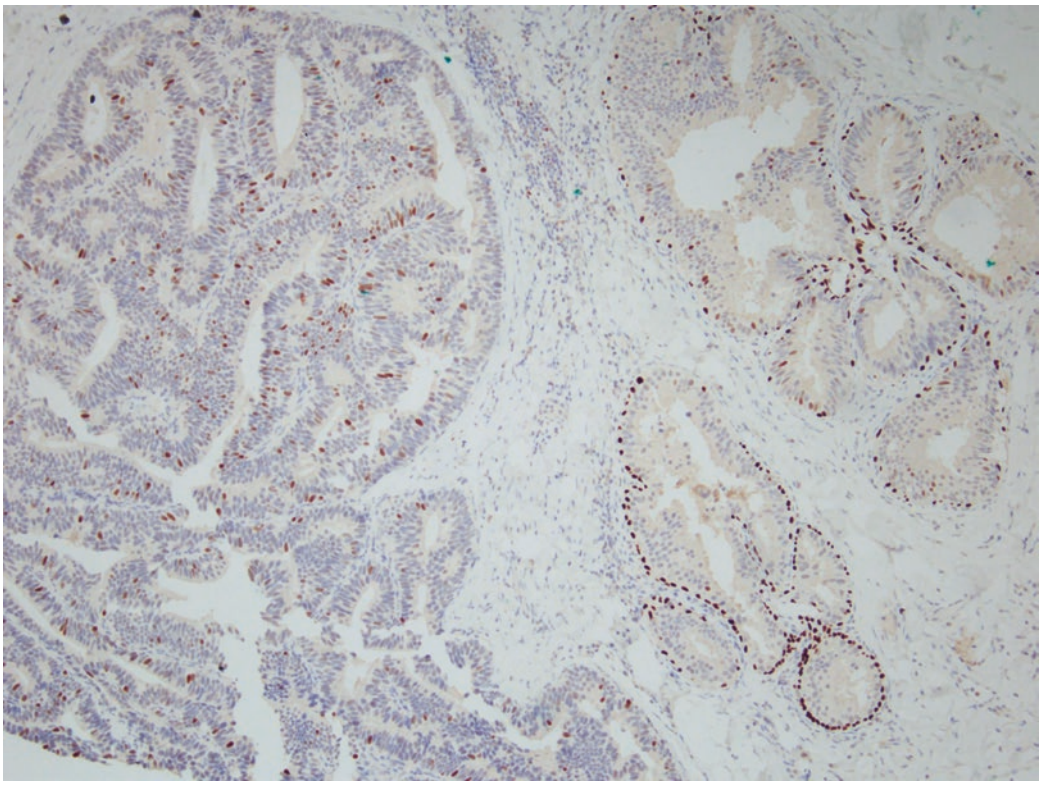

Fig. 4.39 Papillary DCIS. Aberrant nuclear staining for p63 can be observed in several neoplastic epithelial nuclei. However, there are no myoepithelial cells between the neoplastic epithelial cells and the fibrovascular stroma of the papillary fronds. Adjacent ducts show myoepithelial nuclei highlighted as a peripheral rim with p63 immunohistochemistry

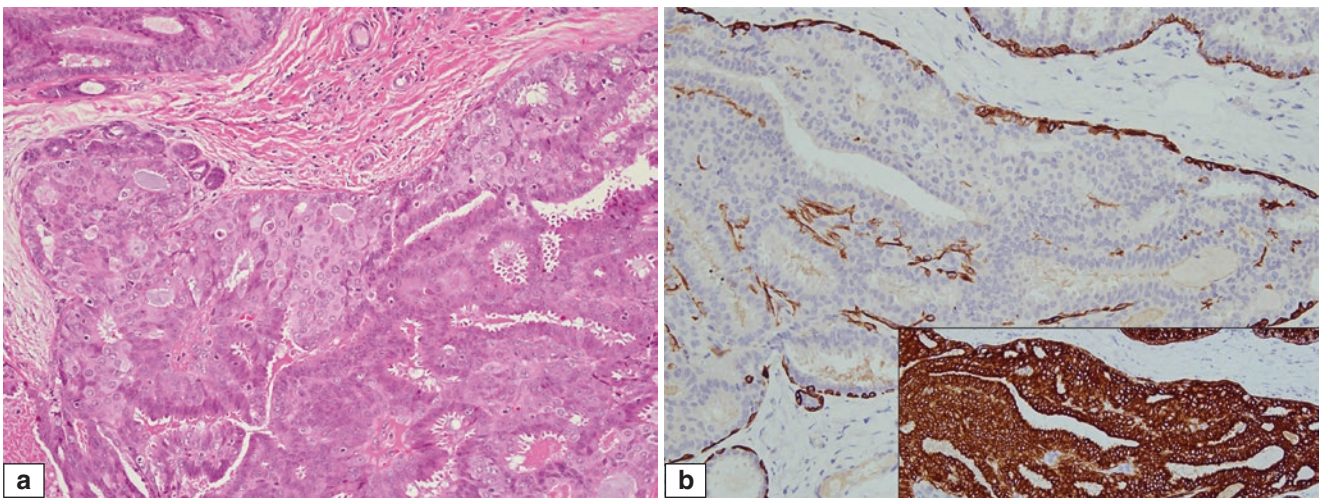

Fig. 4.40 Papillary DCIS with dimorphic pattern. (**a**) Malignant papillae are lined by a uniform population of columnar cells. There is a second population of rounded cells with more ample paler cytoplasm interdigitating among the columnar cells, giving a dual cell population. These rounded cells may mimic myoepithelial cells and potentially raise reservations regarding clonality of the epithelial population that is characteristic of papillary DCIS. (**b**) Immunohistochemistry for CK14 shows intact peripheral myoepithelial cells, with no staining observed for the second population of rounded cells insinuating among columnar cells. *Inset* shows diffuse CK7 positivity of epithelial cells of papillary DCIS

Differential Diagnosis

Intraductal Papilloma

Compared with papillary DCIS, the intraductal papilloma is composed of papillae covered by a heterogeneous epithelial cell population supported by well-developed fibrovascular stroma. Apocrine metaplasia is often encountered. A panel of immunohistochemical stains, including myoepithelial markers (Table 4.1), can be used when needed to help distinguish the two lesions.

Table 4.1 Histological comparison of papillary lesions

Feature	Intraductal papilloma	Intraductal papilloma with ADH/DCIS	Papillary DCIS	Encapsulated papillary carcinoma	Solid papillary carcinoma
Low magnification architecture	May be solitary or multiple	May be solitary or multiple	Papillary lesion extends along duct, usually associated with surrounding DCIS of other morphological patterns	Solitary expansile mass	Multinodular, lobulated mass
Papillae	Broad papillae with well-developed fibrovascular cores	Broad papillae with well-developed fibrovascular cores	Narrow papillae with slender fibrovascular cores	Narrow papillae with slender fibrovascular cores	Solid cellular nodules with fine vessels Papillae are inconspicuous
Myoepithelial cells	Present within papillae and at periphery	Present within papillae and at periphery Diminished in areas of ADH/DCIS	Absent or diminished within papillae Present at periphery	Absent or diminished within papillae Absent at periphery	Present or absent at periphery
Epithelial population	Heterogeneous population of luminal and myoepithelial cells, apocrine cells	Heterogeneous population of luminal and myoepithelial cells, apocrine cells Monotonous population in ADH/DCIS (low nuclear grade)	Monotonous single-cell population Usually low-to-intermediate nuclear grade, rarely high grade	Monotonous single-cell population Usually low-to-intermediate nuclear grade, rarely high grade	Monotonous single-cell population Usually low-to-intermediate nuclear grade Spindle cells may be present Neuroendocrine differentiation Mucin production
Surrounding breast tissue	Usual ductal hyperplasia Fibrocystic changes	ADH/DCIS may be present	DCIS usually present	DCIS may be present	DCIS may be present
IHC, p63	Positive within papillae and at periphery	Positive within papillae and at periphery Diminished in ADH/DCIS	Absent or diminished within papillae Present at periphery	Absent or diminished within papillae Absent at periphery	Present or absent at periphery
IHC, high-molecular-weight keratins	Positive within papillae and at periphery Heterogeneous staining in UDH	Positive within papillae and at periphery Diminished staining in ADH/DCIS	Absent or diminished within papillae Present at periphery	Absent or diminished within papillae Absent at periphery	Present or absent at periphery
IHC, ER	Heterogeneous positivity in UDH and luminal epithelium	Heterogeneous positivity in UDH and luminal epithelium Diffuse positivity in ADH/DCIS	Diffuse positivity	Diffuse positivity	Diffuse positivity

ADH atypical ductal hyperplasia, *DCIS* ductal carcinoma in situ, *ER* oestrogen receptor, *IHC* immunohistochemistry, *UDH* usual ductal hyperplasia

Intraductal Papilloma with ADH and DCIS

Papillary DCIS shows no discernible underlying benign intraductal papilloma, whereas ADH or DCIS arising within an intraductal papilloma shows recognisable architecture of the latter within which the abnormal epithelial process occurs. The underlying benign papilloma, however, may not always be readily apparent, and the use of myoepithelial markers may be required for its demonstration.

Encapsulated Papillary Carcinoma

The malignant papillae of both papillary DCIS and the encapsulated papillary carcinoma are similar. However, the encapsulated papillary carcinoma usually shows mass-like distension of the duct surrounded by a fibrous wall, while papillary DCIS extends along the duct without excessive distension. Apart from absent-to-diminished myoepithelial cells within the papillae, myoepithelial cells are also nearly always absent at the periphery of the encapsulated papillary carcinoma, but present in papillary DCIS.

Prognosis and Therapy Considerations

Prognosis is similar to other forms of DCIS, with surgical eradication being the management approach.

Encapsulated Papillary Carcinoma

Definition

An encapsulated papillary carcinoma is a malignant papillary tumour that forms a circumscribed mass with a fibrous capsule. Myoepithelial cells are invariably absent in the fibrous wall. It is also referred to as encysted papillary carcinoma [4].

Clinical and Epidemiological Features

Encapsulated papillary carcinoma forms a subset of papillary carcinomas. Patients may present with a breast lump with or without nipple discharge.

Imaging Features

Radiologically, the encapsulated papillary carcinoma is seen as a rounded mass which may reach a large size at presentation. On ultrasound examination, it presents as an irregular intracystic mass, sometimes with papillary projections. The cystic or dilated ductal component is commonly associated with echoes due to cellular debris and blood products (Fig. 4.41).

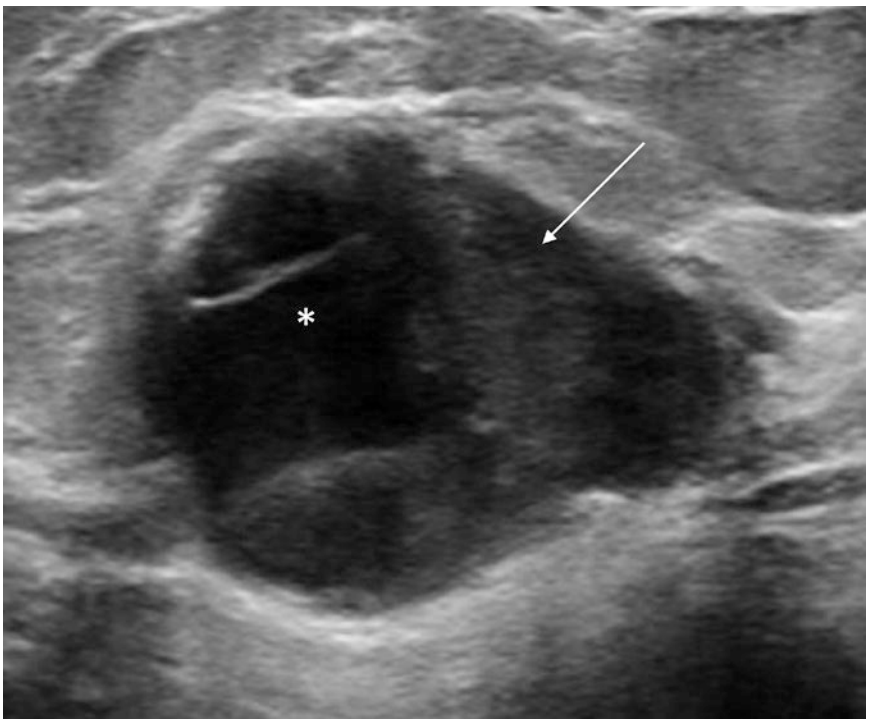

Fig. 4.41 Encapsulated papillary carcinoma presenting as a solid–cystic mass on sonography. The lobulated solid component (*arrow*) represents the papillary proliferation and shows some papillary projections. Mild internal echoes from haemorrhage are seen in the cystic space (*asterisk*) (Courtesy of Dr. Lester Leong)

Pathologic Features

Macroscopic Pathology

Encapsulated papillary carcinoma appears grossly as a circumscribed solid or solid–cystic mass. It may occur as a mural fleshy nodule within a dilated cystic space (Figs. 4.42, 4.43, 4.44, and 4.45).

Microscopic Pathology

Histologically, anastomosing slender papillae covered by a monotonous uniform population of low-to-intermediate nuclear grade epithelial cells project into a dilated space (Fig. 4.46). Rarely, the epithelial cells exhibit high nuclear grade [7], and necrosis may be seen. There is a fibrous wall of varying thickness surrounding the papillary mass (Fig. 4.47). Infarction can occur, which can hinder histological appraisal when extensive (Fig. 4.48). Myoepithelial cells are absent within the papillae and in the vast majority of cases are absent at the periphery of the lesion. Small protrusions or entrapment of neoplastic epithelium in the peripheral fibrous wall may be seen and do not warrant a diagnosis of invasion unless they breach the full thickness of the wall to extend into the surrounding breast tissue. Invasive disease, when present, is graded, subtyped, and staged separately. Size of the encapsulated papillary carcinoma is not added into the invasive tumour measurement (Figs. 4.49, 4.50, 4.51, and 4.52).

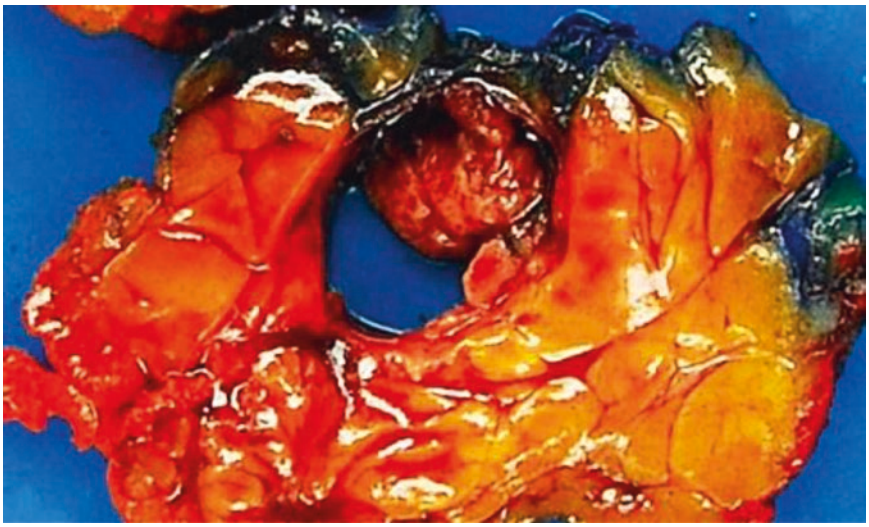

Fig. 4.42 Encapsulated papillary carcinoma. A soft haemorrhagic nodule protrudes into a cystic cavity

Fig. 4.43 Encapsulated papillary carcinoma. Mastectomy specimen which is sliced open from the base, shows an encapsulated cystic mass with a brownish-grey tumour enclosed within the cystic cavity

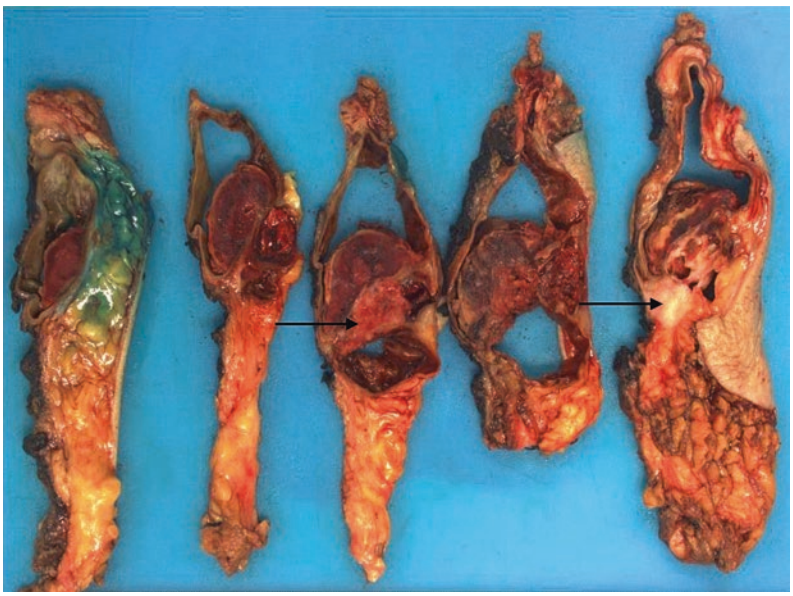

Fig. 4.44 Encapsulated papillary carcinoma. Serial slices through a mastectomy specimen show a solid-cystic tumour mass. There are more fleshy, brownish and whitish firm areas (*arrows*) in the cyst wall, which corresponded to invasive disease on histology. It is important when grossing such specimens, that close attention is paid to the presence of any solid and fleshy areas in the cyst wall, which should be sampled for histology to rule out accompanying invasive disease

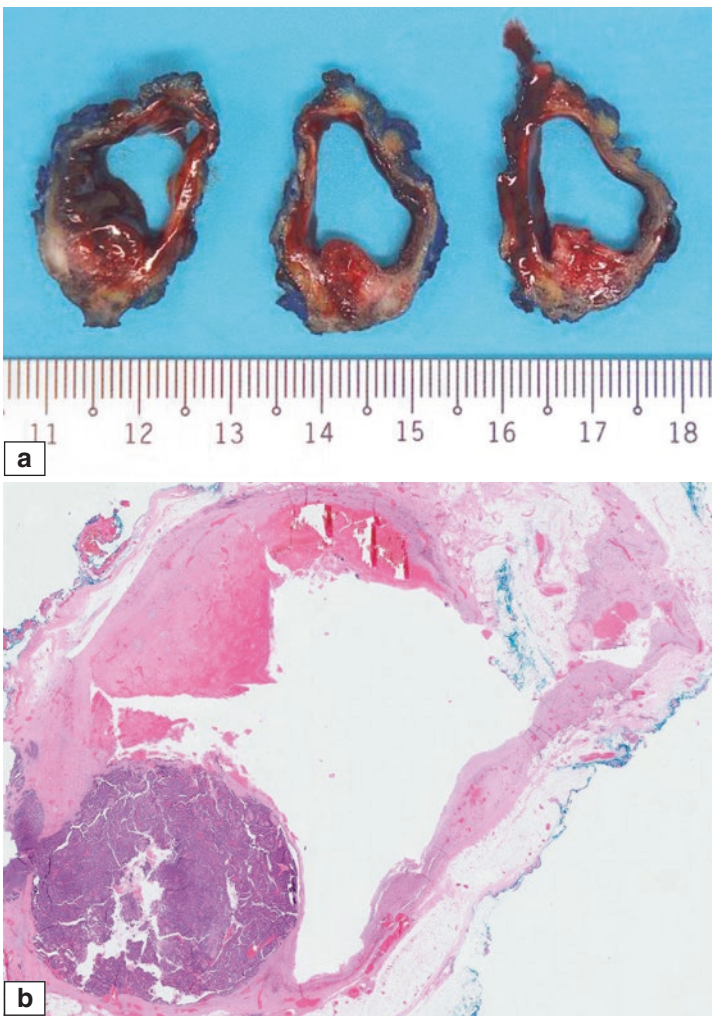

Fig. 4.45 Encapsulated papillary carcinoma. (**a**) Gross appearance of a cystic lesion with a solid mural nodule protruding into the cystic space. The cyst wall is coated with altered blood. (**b**) Low magnification shows the cystic space with haemorrhage and blood clots. In the wall of the cyst is a solid tumour nodule with papillary architecture

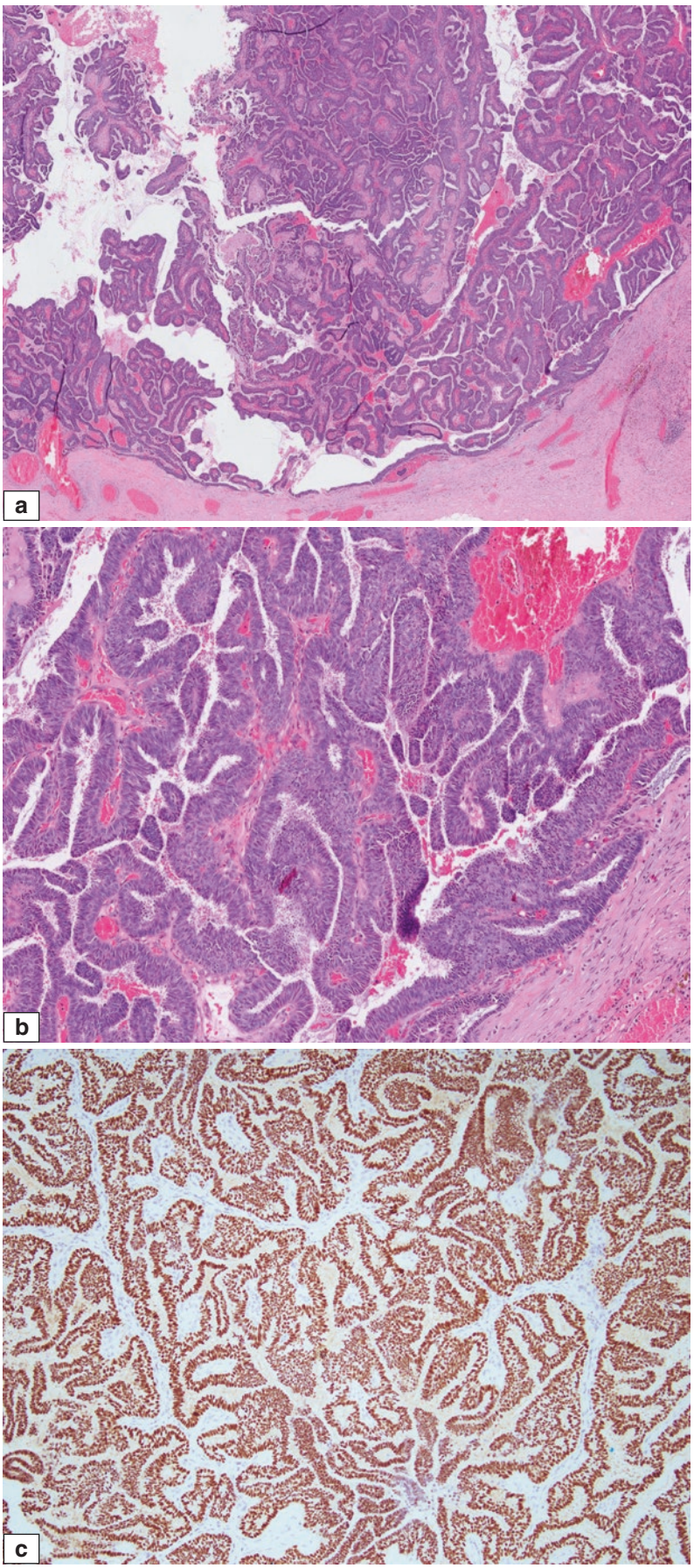

Fig. 4.46 Encapsulated papillary carcinoma. (**a**) Anastomosed papillae covered by hyperchromatic cells are present. (**b**) Higher magnification of the papillary fronds show covering by columnar epithelial cells with hyperchromatic stratified nuclei. (**c**) Encapsulated papillary carcinoma shows diffuse positive staining for oestrogen receptor (ER)

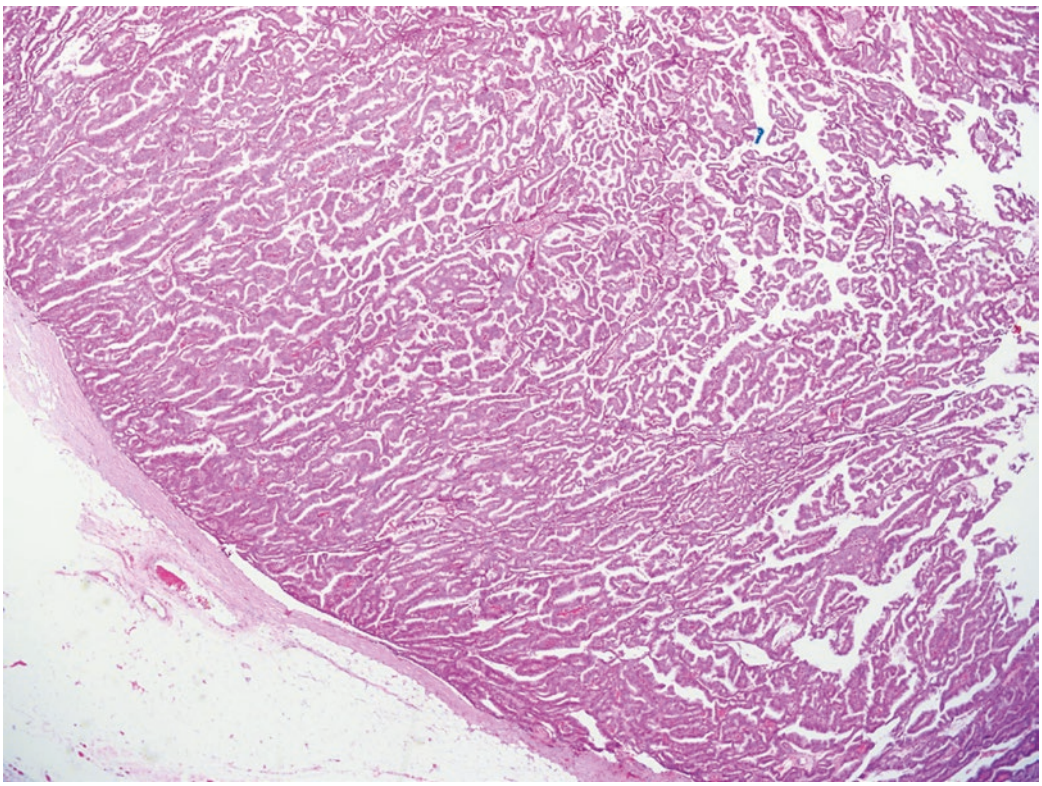

Fig. 4.47 Encapsulated papillary carcinoma. The encapsulated papillary carcinoma shows a fibrous capsule of variable thickness, surrounding anastomosed papillary fronds that are covered by a uniform population of epithelial cells. Fibrovascular septa are slender and narrow, and myoepithelial cells are diminished or absent. Myoepithelial cells are usually not identified along the outer wall of the encapsulated papillary carcinoma, leading to suggestions that this tumour represents an indolent form of invasive carcinoma with pushing contours or a carcinoma in transition from in situ to invasive malignancy. Nevertheless, the encapsulated papillary carcinoma is regarded as in situ (Tis) disease for staging purposes

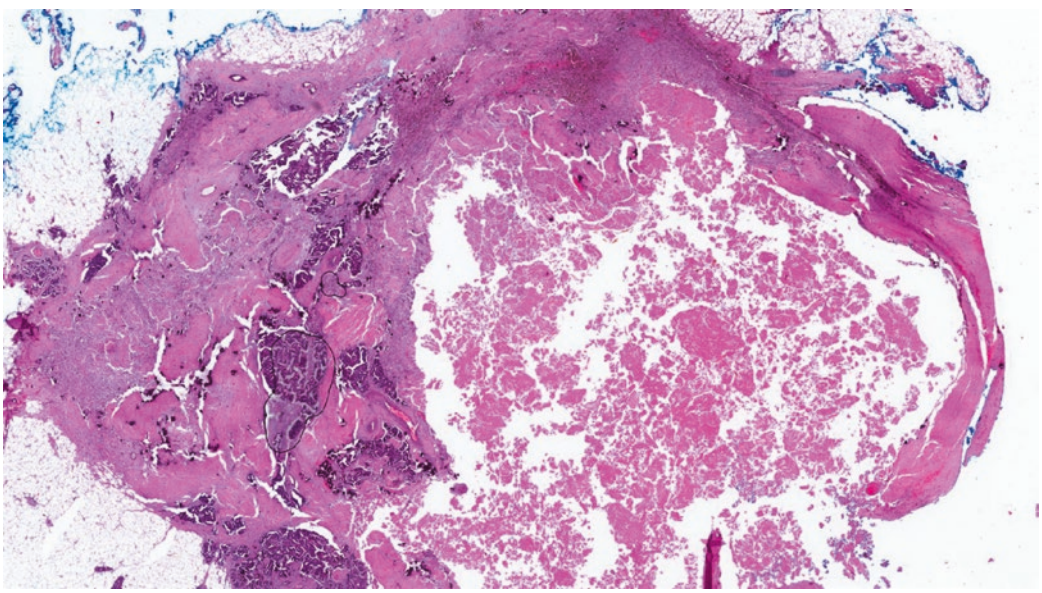

Fig. 4.48 Infarcted encapsulated papillary carcinoma with invasive cribriform carcinoma. At low magnification, necrotic pink material seen within the cystic cavity corresponds to the ghost papillary fronds of the encapsulated papillary carcinoma. A fibrous capsule of variable thickness is present. In the surrounding tissue is viable tumour with invasive cribriform histology and scattered calcifications

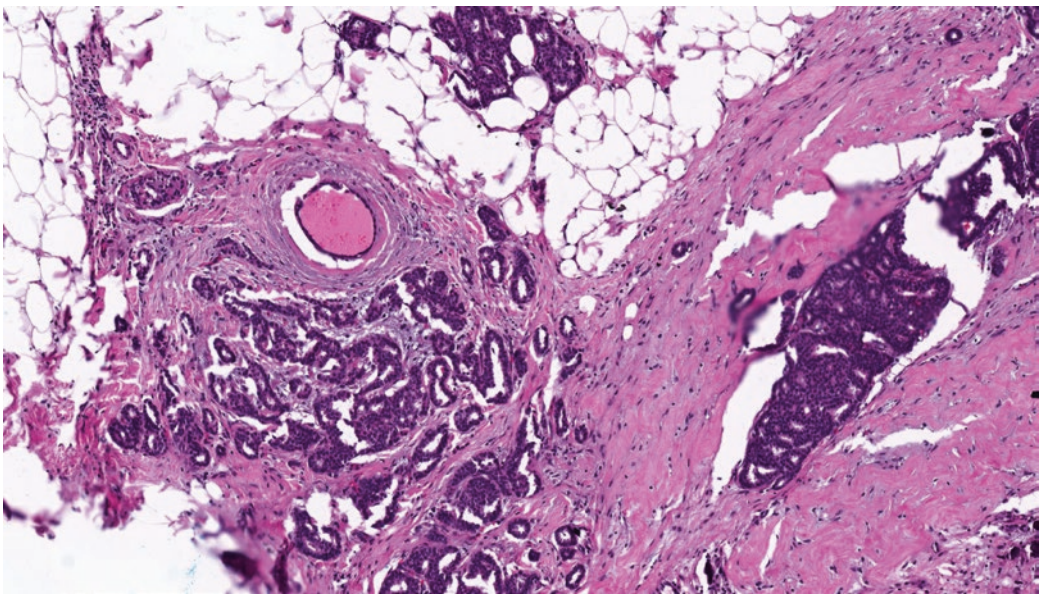

Fig. 4.49 Invasive cribriform carcinoma associated with encapsulated papillary carcinoma. Slightly crushed irregular islands of invasive cribriform carcinoma are seen extending beyond the wall of the encapsulated papillary carcinoma into the surrounding adipose tissue

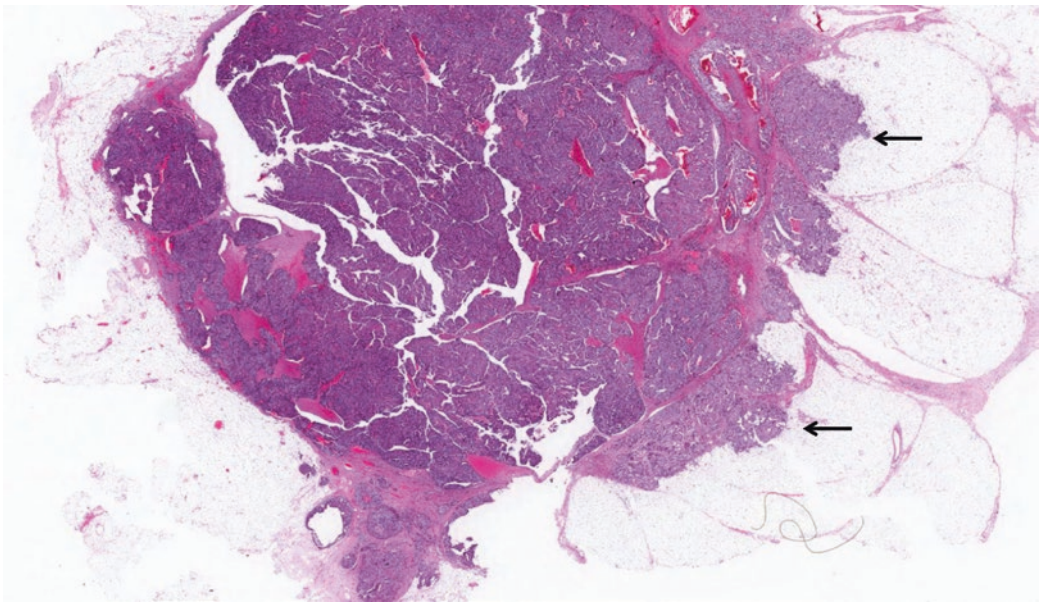

Fig. 4.50 Encapsulated papillary carcinoma with invasive ductal carcinoma. At scanning magnification, the tumour shows a partially circumscribed contour with a fibrous wall. Invasive carcinoma is seen in the right field, where irregular tumour nests extend beyond the tumour contours into the adipose tissue (*arrows*)

Differential Diagnosis

Intraductal Papilloma with ADH and DCIS

In contrast to the heterogeneity of intraductal papilloma, encapsulated papillary carcinoma comprises a single clonal population of malignant epithelial cells. Similarly, the underlying architecture of a benign intraductal papilloma is identifiable in those harbouring ADH and DCIS.

Solid Papillary Carcinoma

Like encapsulated papillary carcinoma, solid papillary carcinoma may form a nodular mass with more frequent

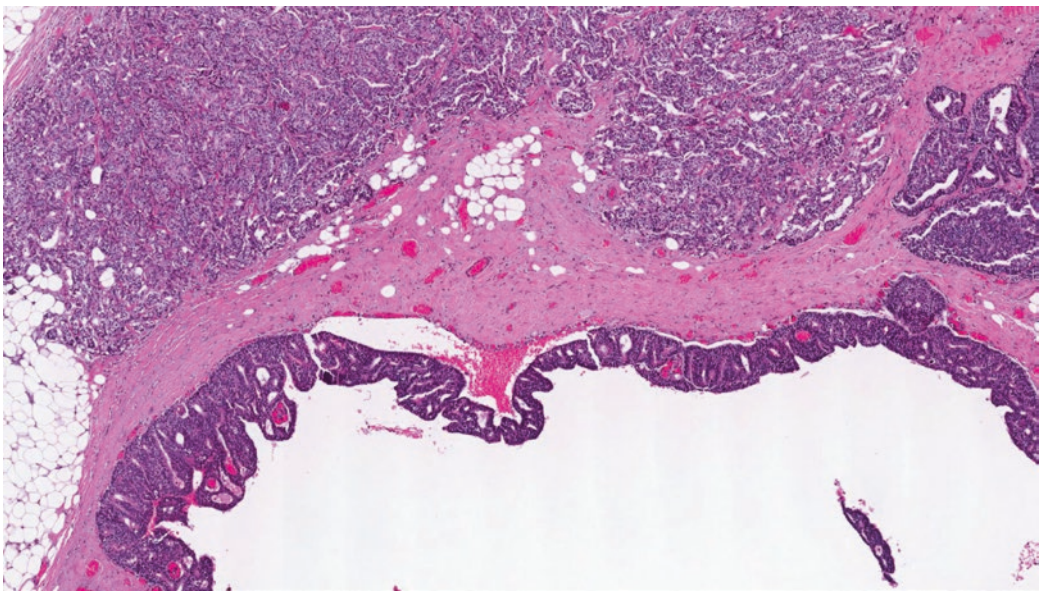

Fig. 4.51 Encapsulated papillary carcinoma (*lower field*) with invasive ductal carcinoma (*upper field*)

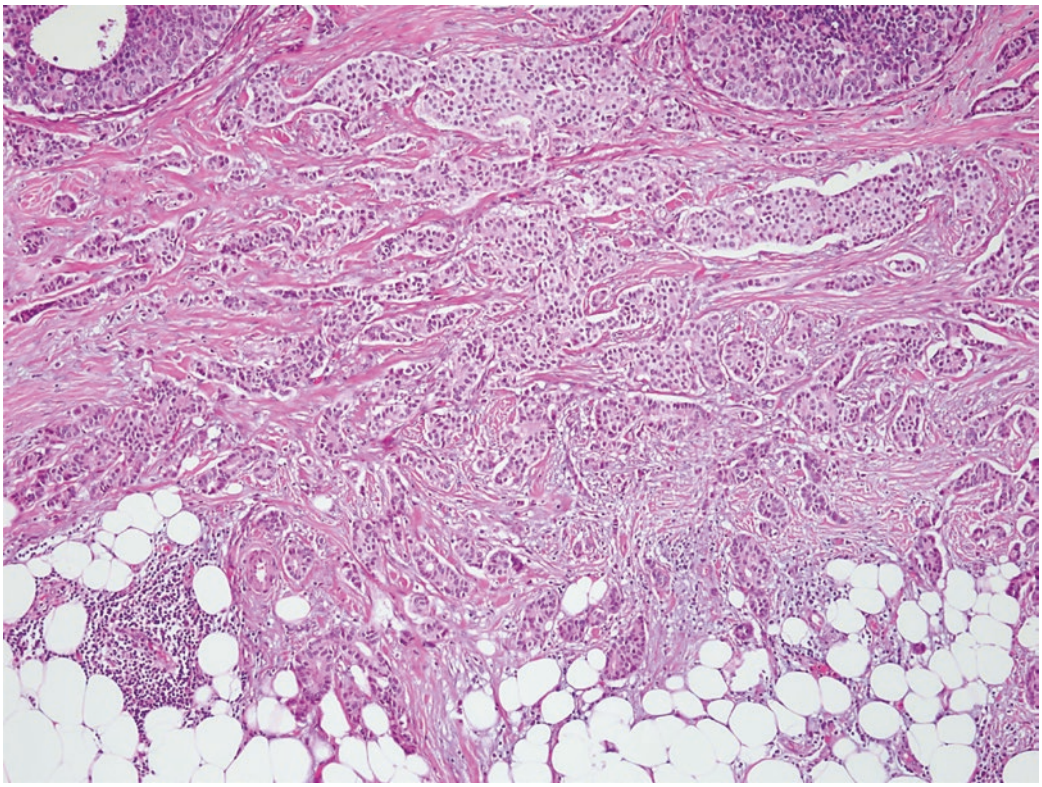

Fig. 4.52 Invasive ductal carcinoma (invasive carcinoma of no special type) adjacent to encapsulated papillary carcinoma. When an invasive carcinoma is seen in conjunction with an encapsulated papillary carcinoma, it is staged according to the size of the invasive component and does not include the size of the encapsulated papillary carcinoma

multinodular lobulated appearances. Histologically, the papillary architecture of solid papillary carcinoma is less obvious, with the tumour often being solidified with fine vessels coursing into the cellular epithelial nodules. Neuroendocrine differentiation and mucin are often observed, while myoepithelial cells can be present or absent around the epithelial nodules of solid papillary carcinoma.

Prognosis and Therapy Considerations

Encapsulated papillary carcinoma is currently staged and managed as non-invasive disease (Tis), despite notions of its being a low-grade form of invasive carcinoma due to absence of myoepithelial cells and rare occurrences of metastases to axillary lymph nodes [8]. Prognosis after excision is very favourable when there is no surrounding DCIS.

Solid Papillary Carcinoma

Definition

This is a malignant tumour consisting of multinodular, expansile solid epithelial masses whose underlying papillary architecture is subtly reflected by fine delicate vessels coursing through the cellular islands. Myoepithelial cells may be present, attenuated, or completely absent around the nodular masses. Neuroendocrine differentiation and mucin production are frequent. Solid papillary carcinoma should be qualified as either in situ (majority of cases) or invasive [9].

Clinical and Epidemiological Features

Solid papillary carcinoma usually occurs in women in the older age group. Patients may present with a breast lump, sometimes in the nipple-areolar region, with or without bloody nipple discharge.

Imaging Features

Solid papillary carcinoma may be observed as mammographic nodular masses or ultrasonographic hypoechoic lesions with lobulated contours (Fig. 4.53).

Pathologic Features

Macroscopic Pathology

Solid papillary carcinoma appears grossly as multinodular lobulated soft-to-firm masses. Tumours with mucin production may show a glistening cut surface (Figs. 4.54 and 4.55).

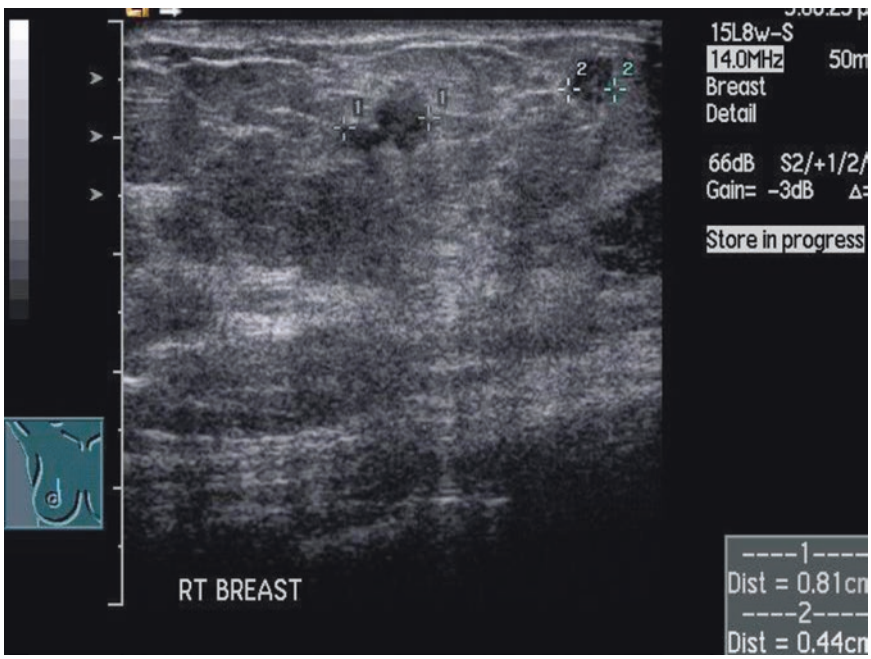

Fig. 4.53 Solid papillary carcinoma. Ultrasound shows hypoechoic lesions with lobulated margins

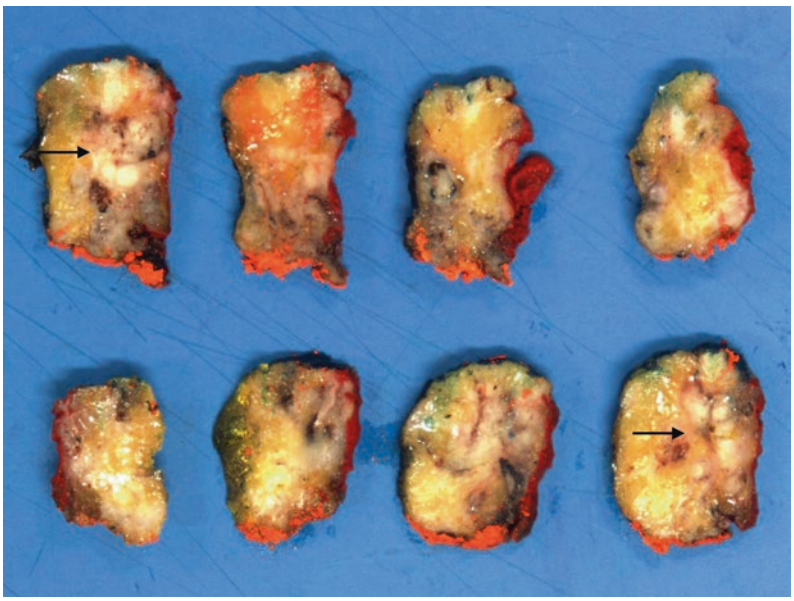

Fig. 4.54 Solid papillary carcinoma. Serial sections of a breast excision specimen containing a solid papillary carcinoma. The tumour is multinodular and lobulated (*arrows*). In some slices, the tumour is ill-defined and consists of firmer, fleshy nodular areas

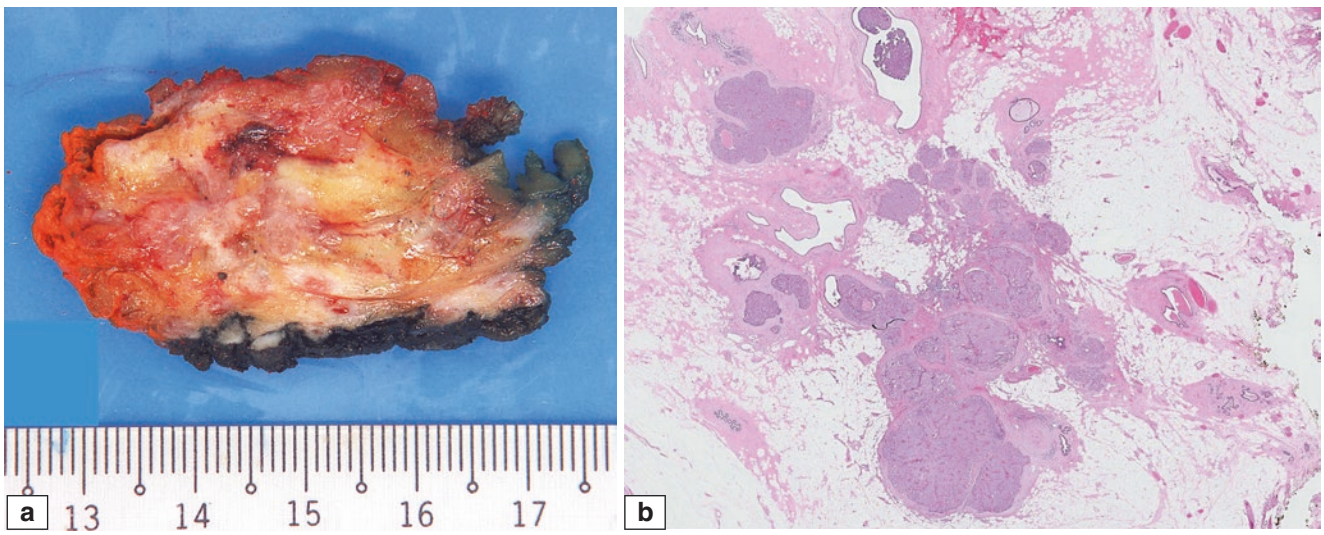

Fig. 4.55 Solid papillary carcinoma. (**a**) Gross appearance shows a vaguely lobulated soft-to-firm, greyish, slightly myxoid mass with whitish yellowish foci. A prominent haemorrhagic area is related to recent prior biopsy. (**b**) Low-magnification view of the mass with solidified ducts forming vague nodules corresponding to the gross appearance

Microscopic Pathology

Histologically, solid nodules of monotonous low or intermediate nuclear grade epithelial cells are punctuated by fine congested vessels (Figs. 4.56 and 4.57). Focal papillary formations may be seen. Epithelial nuclei possess fine chromatin with inconspicuous nucleoli, while cytoplasm can be eosinophilic to amphophilic when there is neuroendocrine differentiation. Sweeping spindle cell sheets, perivascular pseudorosettes, and mucin production may be observed (Figs. 4.58, 4.59, 4.60, 4.61, and 4.62). Myoepithelial cells are sometimes found around nodular tumour islands, but they may be attenuated or completely absent (Fig. 4.63). Despite the absence of myoepithelial cells, rounded islands of solid papillary carcinoma with pushing contours are regarded as non-invasive Tis disease. Apart from neuroendocrine differentiation, solid papillary carcinoma is usually diffusely oestrogen receptor positive (Figs. 4.64 and 4.65).

When the tumour islands are more irregular in outlines and occur as jigsaw puzzle-like pieces within desmoplastic stroma, a diagnosis of invasive solid papillary carcinoma is warranted (Figs. 4.66, 4.67, and 4.68). Invasive carcinoma of ductal, mucinous, neuroendocrine, and other subtypes may be associated with solid papillary carcinoma in situ. These are graded, subtyped, and staged separately. Size of solid papillary carcinoma in situ is not added into the invasive tumour measurement.

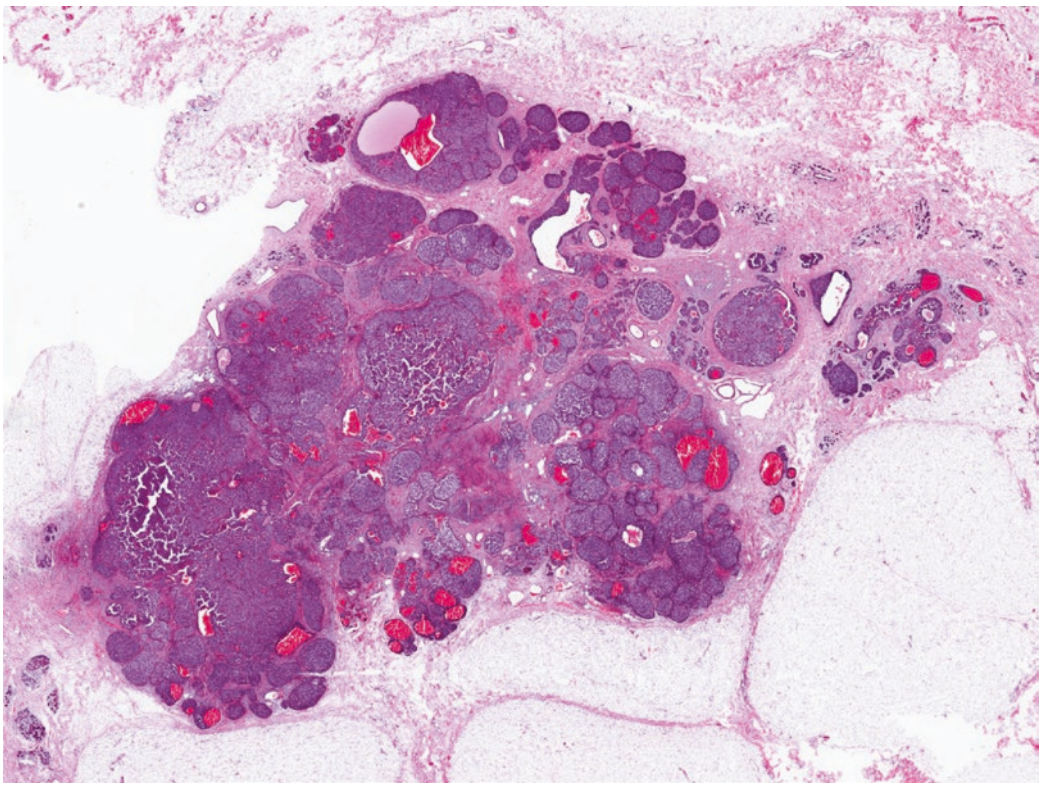

Fig. 4.56 Solid papillary carcinoma. Low magnification shows expanded ducts filled with epithelial cells, aggregated within fibrous stroma and giving a mass-like appearance. Some of the solidified expanded ducts are confluent. Cystic spaces with haemorrhage are seen

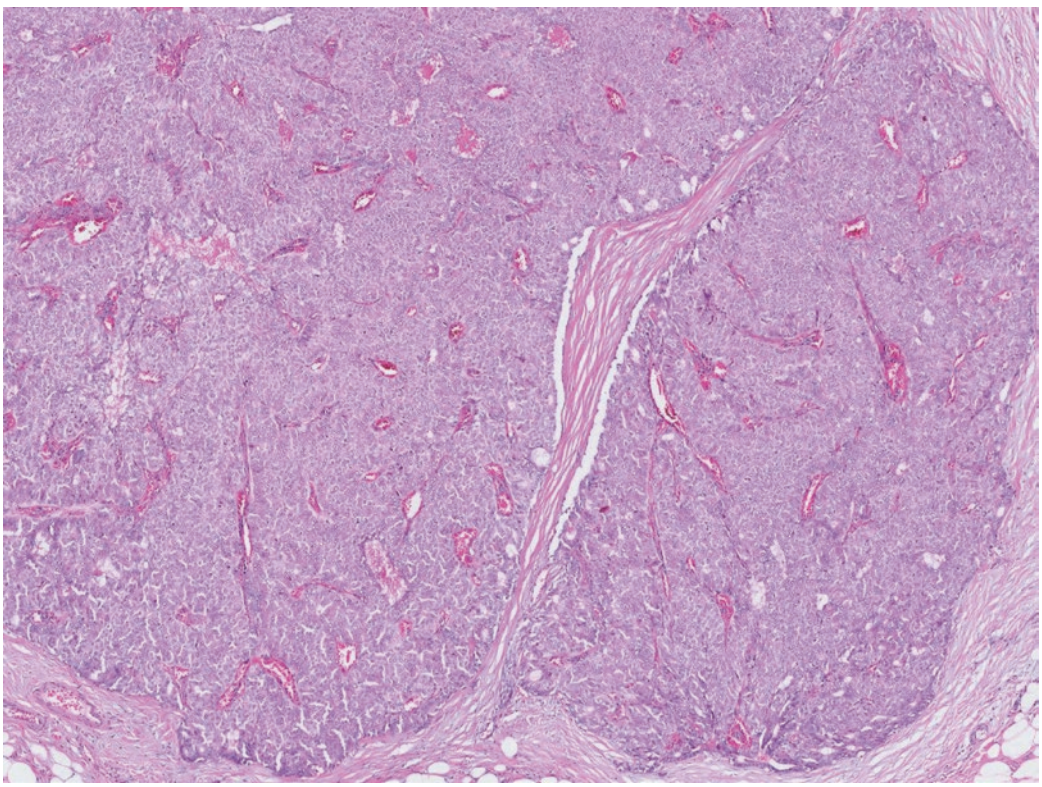

Fig. 4.57 Solid papillary carcinoma. Congested vessels course into the solid nodules of epithelial cells, giving a clue to the papillary architecture although well-developed papillary fronds are not seen

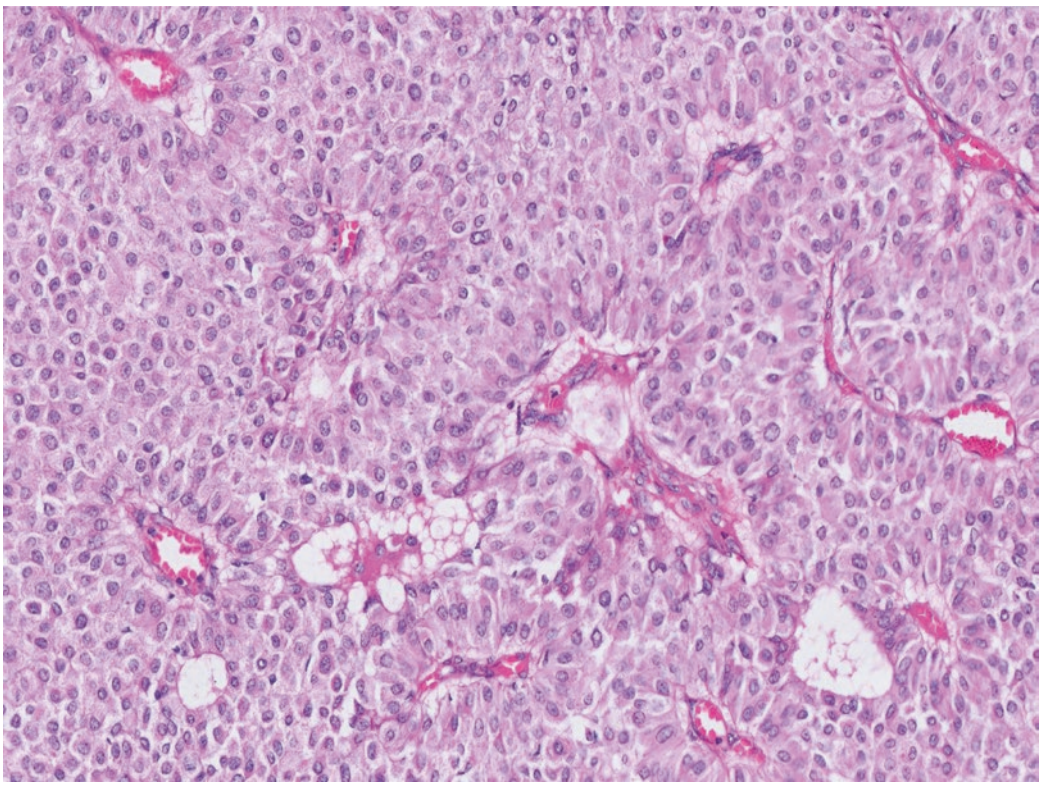

Fig. 4.58 Solid papillary carcinoma. Tumour cells show uniform vesicular nuclei with inconspicuous nucleoli. There is alignment of tumour cells around fibrovascular cores and septa, giving the appearance of perivascular rosettes. Cytoplasm of tumour cells shows amphophilic to pink hues

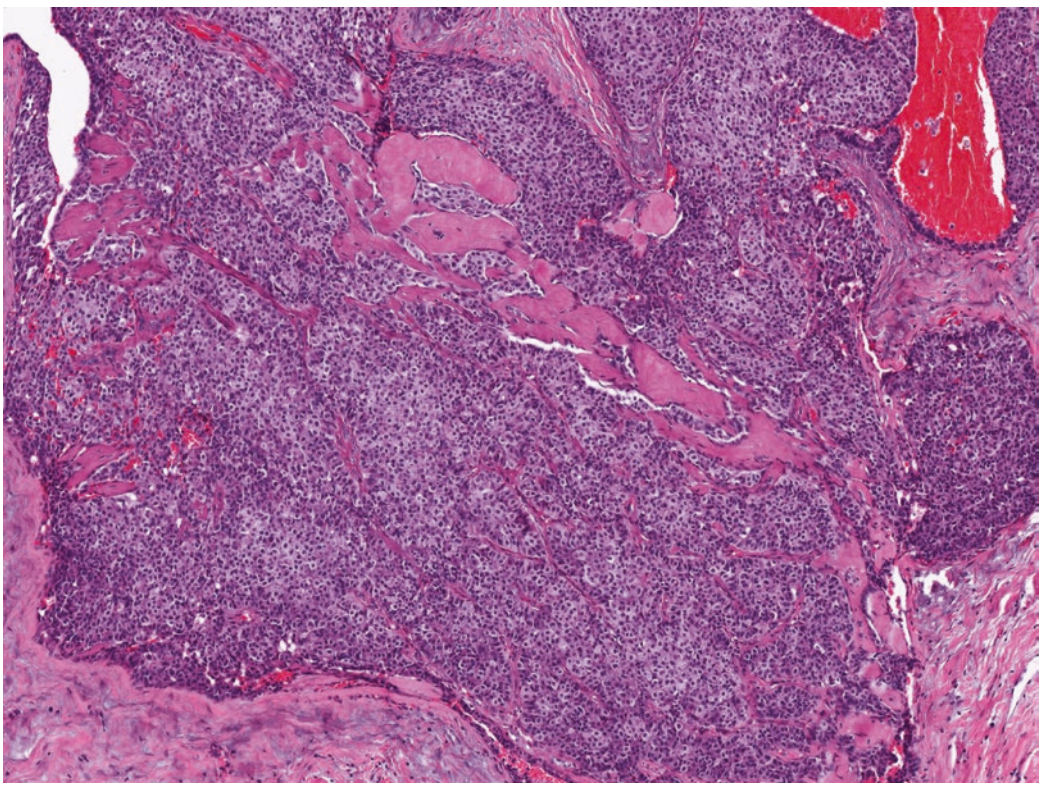

Fig. 4.59 Solid papillary carcinoma. Hyalinised stroma is seen among the solid sheets of tumour cells with amphophilic cytoplasm

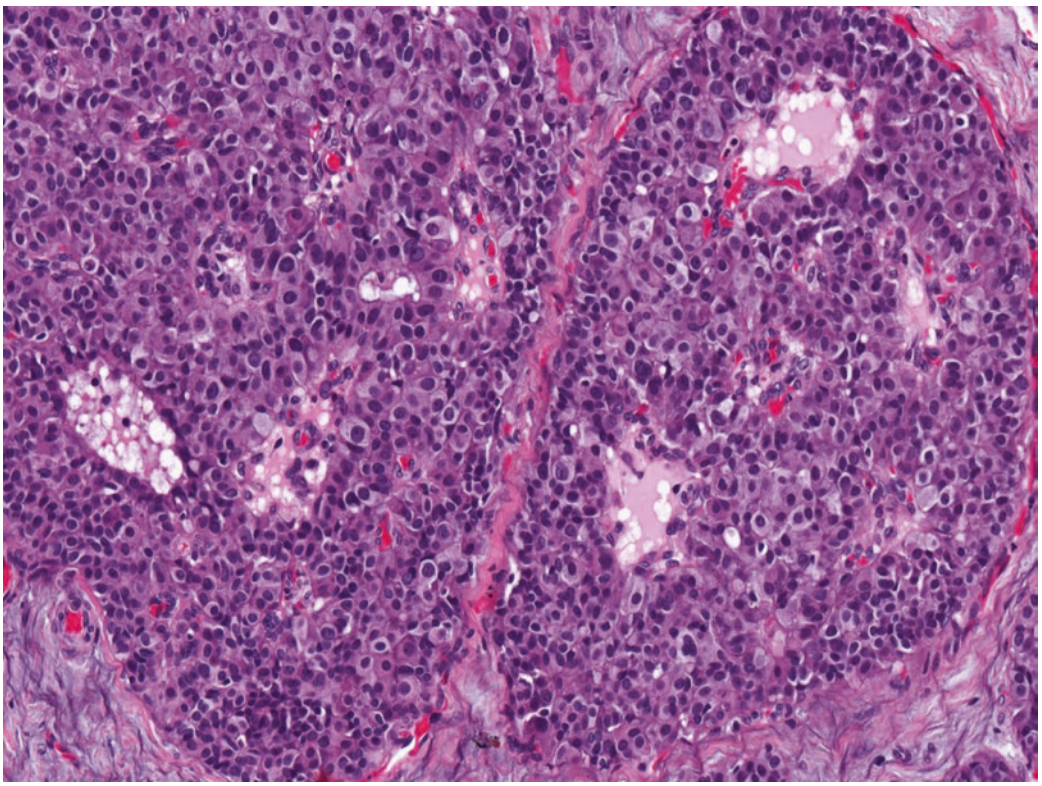

Fig. 4.60 Solid papillary carcinoma. A cribriform architecture is also seen, composed of uniform epithelial cells with amphophilic cytoplasm. Congested foci are clues to the presence of underlying fine vascularity

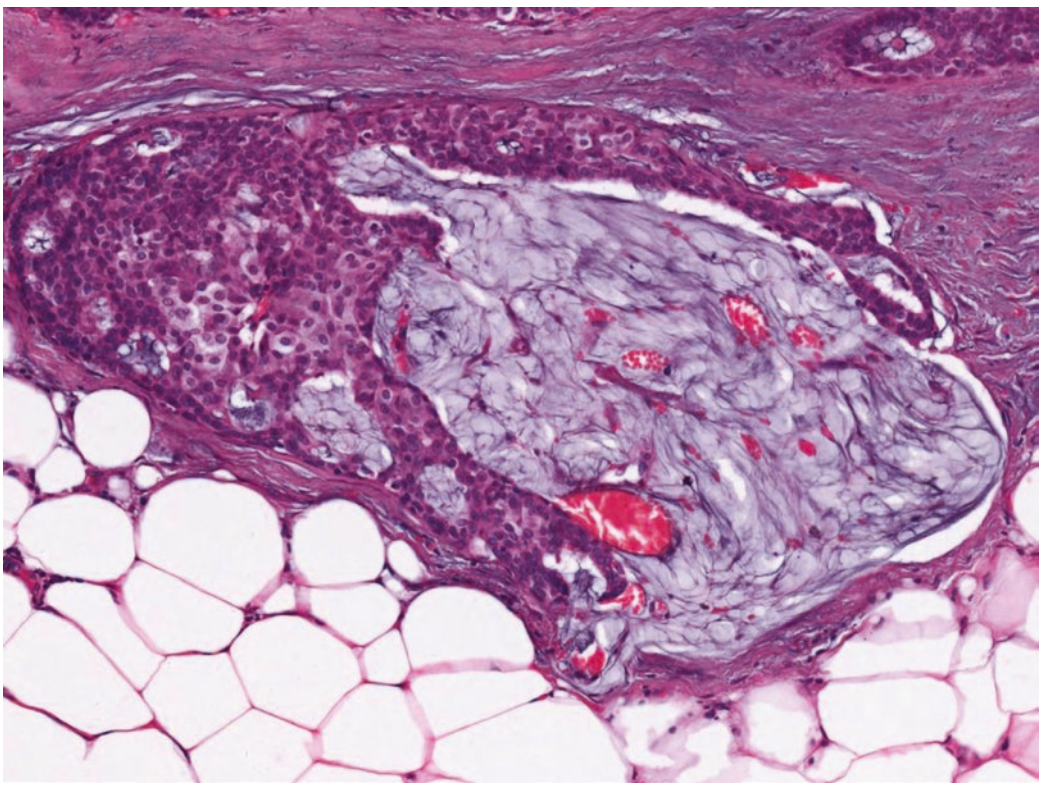

Fig. 4.61 Solid papillary carcinoma. Extracellular mucin may be present, which can be found as small puddles in between tumour cells or as mucin pools extruding into the stroma

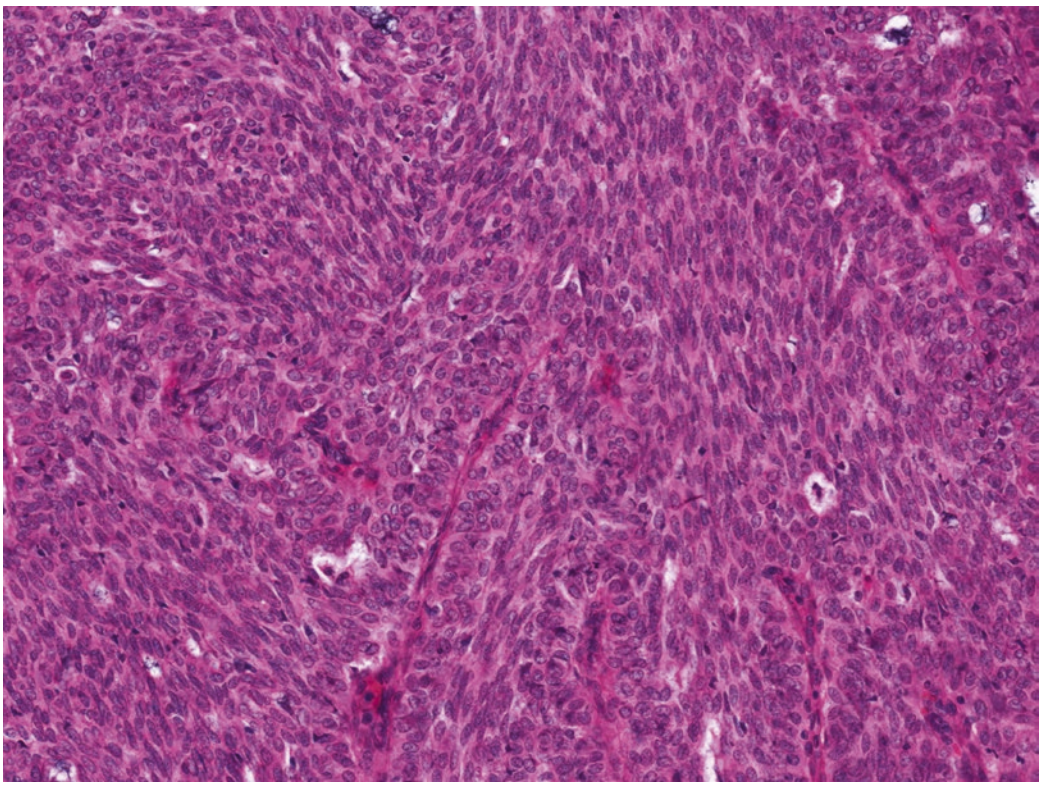

Fig. 4.62 Solid papillary carcinoma. Some tumours may disclose a spindled morphology that can mimic usual ductal hyperplasia. Spindle cells of solid papillary carcinoma tend to be monomorphic, with hardly any secondary luminal spaces, and are occasionally punctuated by slender narrow vessels

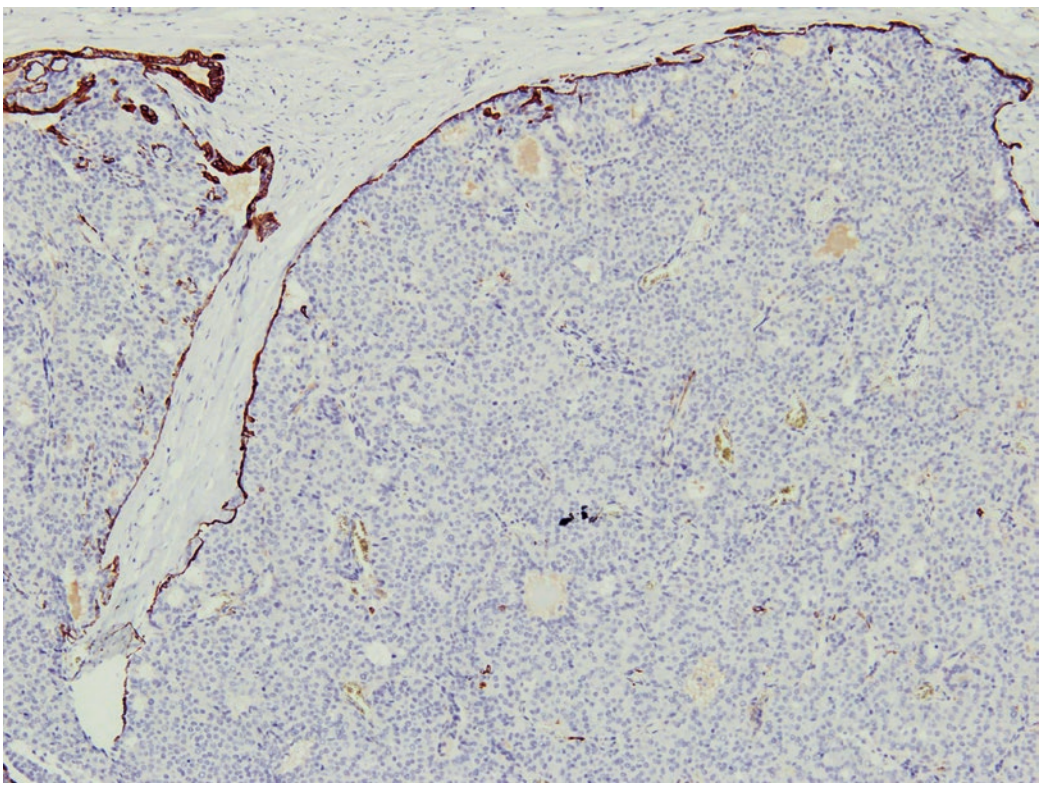

Fig. 4.63 Solid papillary carcinoma. Immunohistochemistry for CK14 shows positive staining of myoepithelial cells at the periphery of the large rounded islands, while there is absent staining within the epithelial population. Cases in which myoepithelial cells are preserved or which have rounded nodular contours represent in situ disease. It is important to specify if a case of solid papillary carcinoma represents in situ or invasive disease

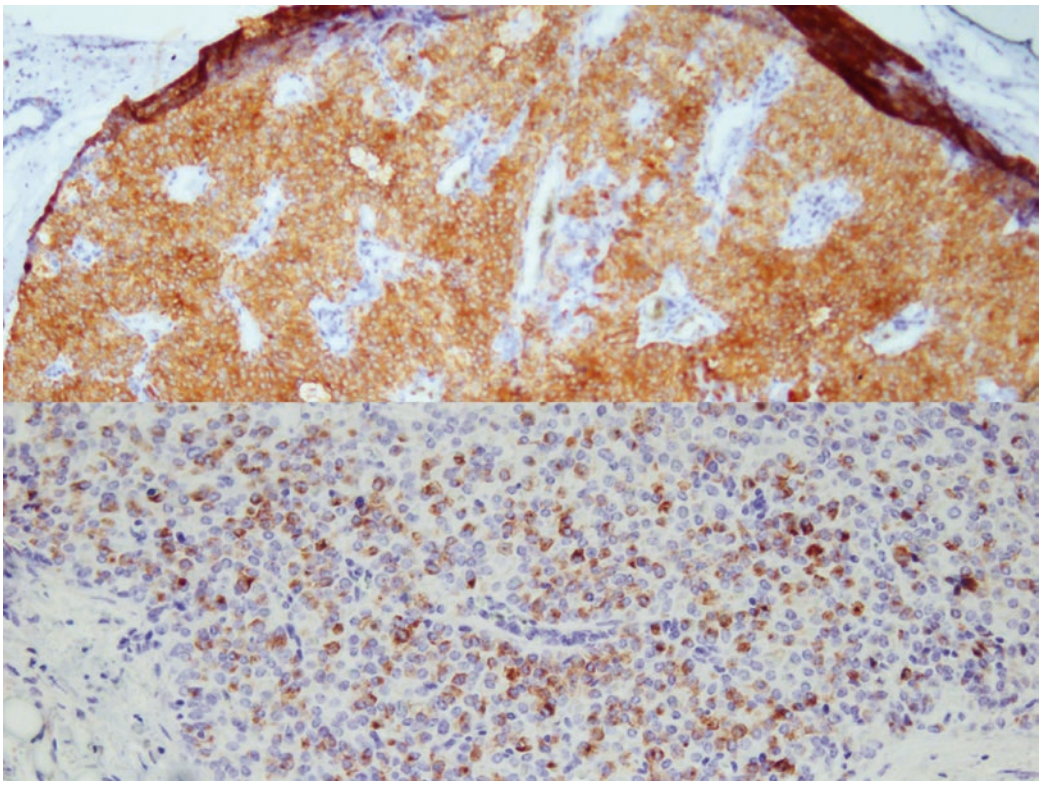

Fig. 4.64 Solid papillary carcinoma. Immunohistochemistry for neuroendocrine markers (synaptophysin, *upper panel*; chromogranin, *lower panel*) shows positive reactivity in tumour cells

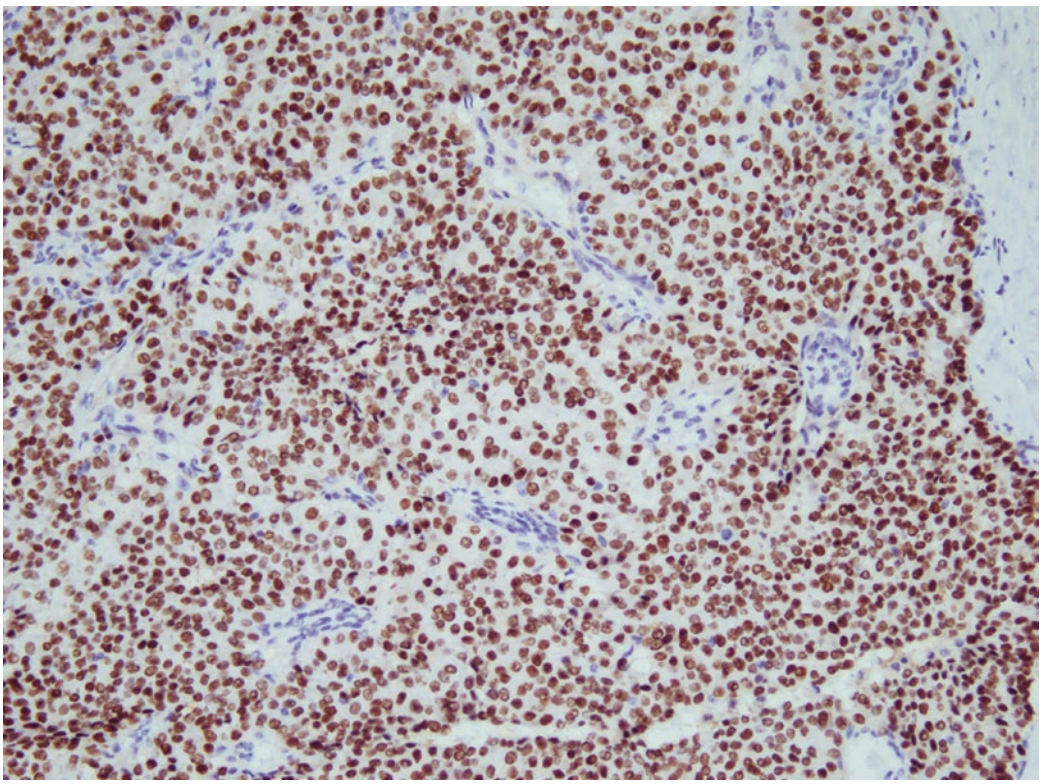

Fig. 4.65 Solid papillary carcinoma. ER is diffusely expressed in the tumour cell nuclei

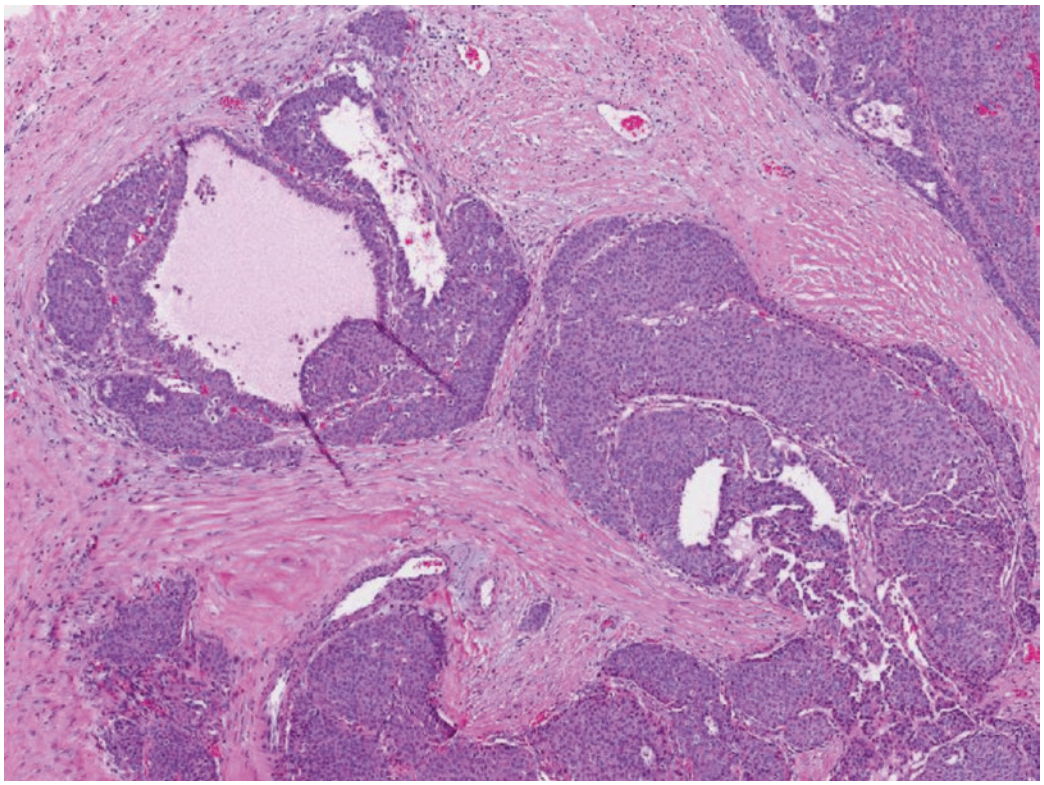

Fig. 4.66 Invasive solid papillary carcinoma. Tumour islands show irregular jagged contours within desmoplastic stroma. Invasion is further affirmed with the absence of myoepithelial cells on immunohistochemistry

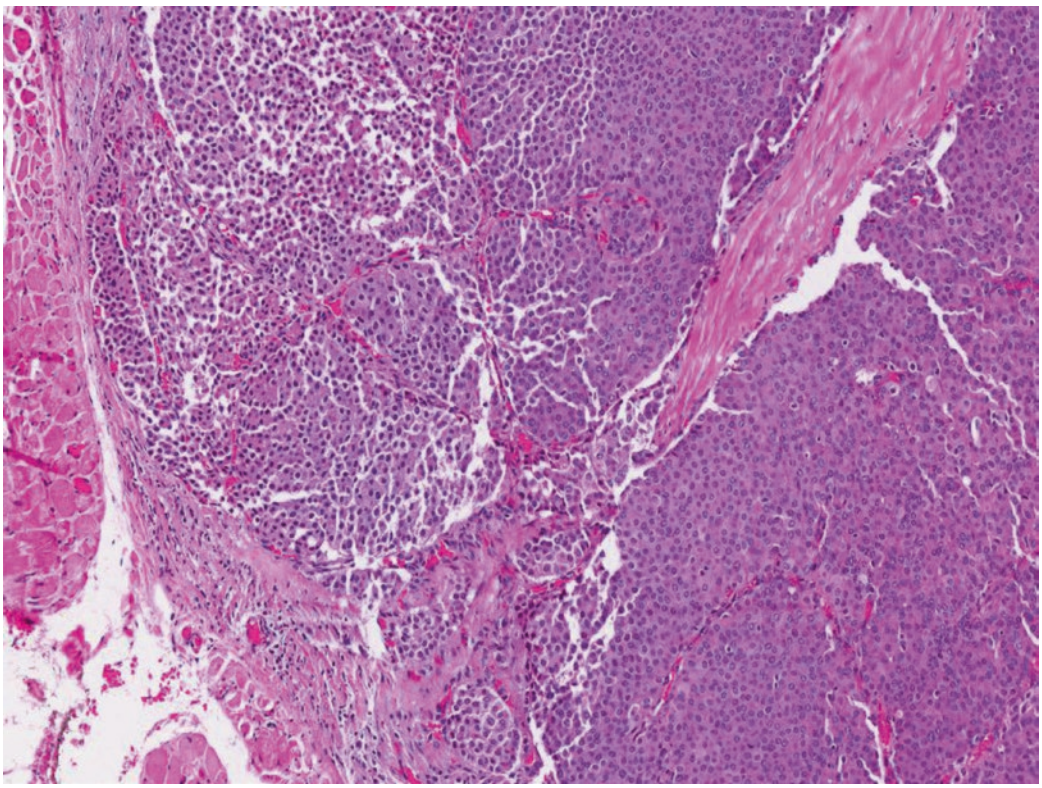

Fig. 4.67 Invasive solid papillary carcinoma. Solid tumour islands invested by fine congested vessels reside within fibrous stroma and focally extend into the skeletal muscle of the pectoralis major

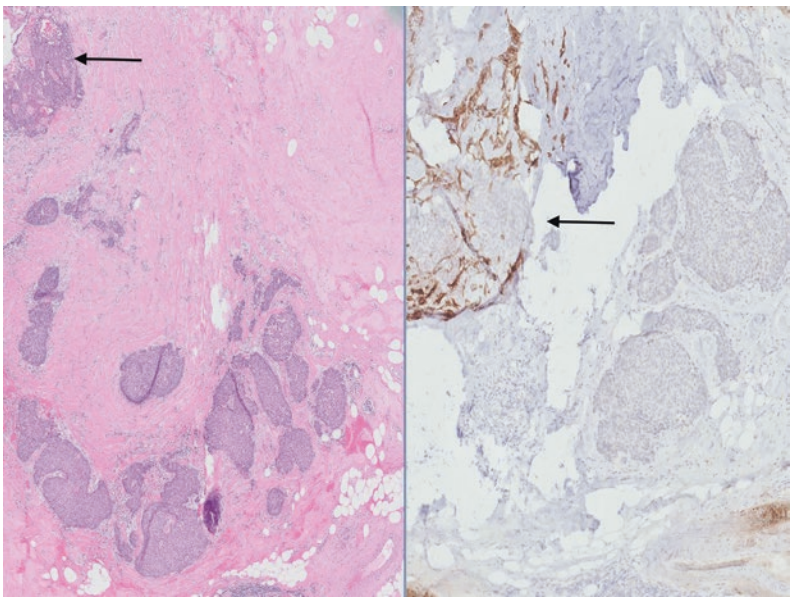

Fig. 4.68 Invasive solid papillary carcinoma. (**a**) Solid tumour islands with angulated and irregular outlines are seen within the fibrous stroma. The tumour nests have a jigsaw puzzle-like appearance. (**b**) Immunohistochemistry with CK5/6 shows no myoepithelial rimming of the tumour islands, confirming absence of myoepithelial cells, and corroborating the diagnosis of invasive disease. Absence of myoepithelial cells alone should not be regarded as diagnostic of invasion, as rounded islands of solid papillary carcinoma with smooth contours are considered in situ disease, even when myoepithelial cells are absent. An in situ solid papillary carcinoma component is present (*arrows*)

Differential Diagnosis

Intraductal Papilloma

The intraductal papilloma shows visible fronds and has a heterogeneous cell population. Intraductal papillomas may sometimes be seen juxtaposed to solid papillary carcinoma.

Encapsulated Papillary Carcinoma

Unlike solid papillary carcinoma which is usually multinodular, encapsulated papillary carcinoma shows a solitary expansile mass with a variably distinct fibrous capsule. Solidification of papillae, spindling of epithelial cells, perivascular pseudorosettes, neuroendocrine differentiation, are features of solid papillary carcinoma that are lacking in encapsulated papillary carcinoma.

Prognosis and Therapy Considerations

Solid papillary carcinoma without areas of conventional invasive carcinoma is currently staged and managed as non-invasive disease (Tis), despite occasional absence of myoepithelial cells and rare reports of metastases to axillary lymph nodes [10]. Prognosis after excision is generally favourable. The presence of a solid papillary carcinoma pattern is associated with favourable clinicopathological parameters when evaluated among breast cancers with neuroendocrine differentiation [11].

Invasive Papillary Carcinoma

Definition

Invasive papillary carcinoma is an invasive carcinoma with a papillary architecture in more than 90% of the tumour. Invasive carcinoma without papillarity that is associated with encapsulated papillary carcinoma or solid papillary carcinoma should not be referred to as invasive papillary carcinoma; it should be subtyped according to the morphological appearance of the invasive tumour [4, 9].

Clinical and Epidemiological Features

Invasive papillary carcinoma in its pure form is extremely rare, and there are no specific clinical or epidemiologic data.

Imaging Features

Invasive papillary carcinoma may present as a radiological or palpable mass. Associated spiculations are rare, and abnormal microcalcifications may be seen on mammography. On ultrasound examination, a complex solid–cystic mass with papillary projections and internal echoes from cellular debris and haemorrhage may be observed, with ill-defined margins reflecting invasion. The solid components are commonly hypervascular on colour Doppler.

Pathologic Features

Macroscopic Pathology

These tumours have solid fleshy appearances that may be friable due to papillary formation.

Microscopic Pathology

Histologically, papillary fronds are seen in the tumour as it invades into surrounding breast parenchyma (Figs. 4.69 and 4.70). Stromal desmoplasia and inflammation may be present at the advancing tumour front. The presence of invasive carcinoma with another morphological subtype in more than 10 % but less than 50 % of the tumour warrants designation as a tumour of mixed pattern.

Differential Diagnosis

Metastatic Papillary Adenocarcinoma

As invasive papillary carcinoma of the breast is very uncommon, possible metastasis from other organ sites such as the lung (Fig. 4.71) and ovary should be excluded. Uncommonly, thyroid papillary carcinoma may also metastasise to the breast but should be recognised by the presence of colloid production

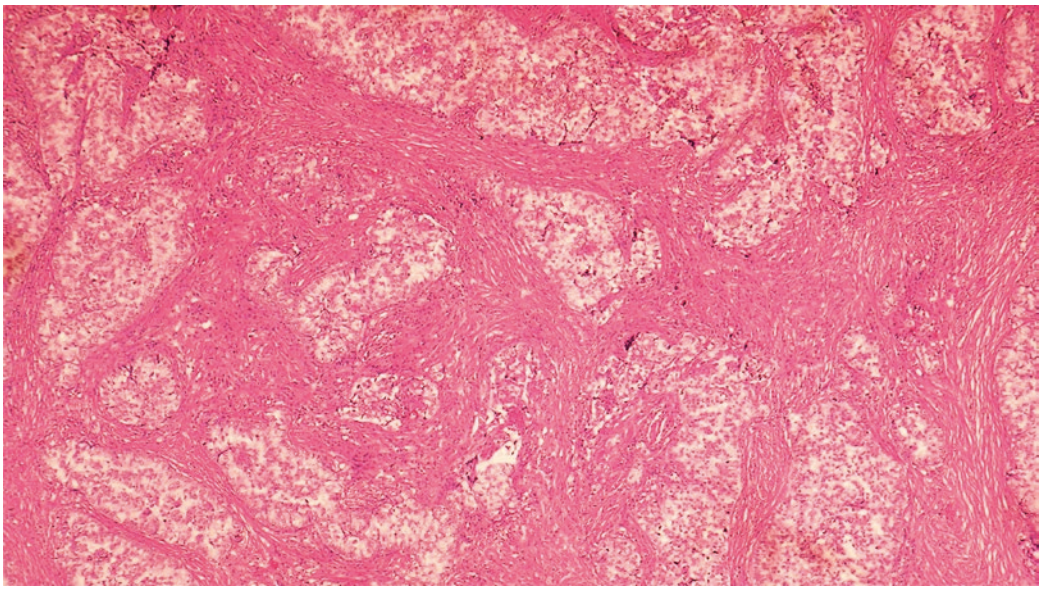

Fig. 4.69 Invasive papillary carcinoma shows islands of tumour recapitulating a papillary architecture within a desmoplastic stroma

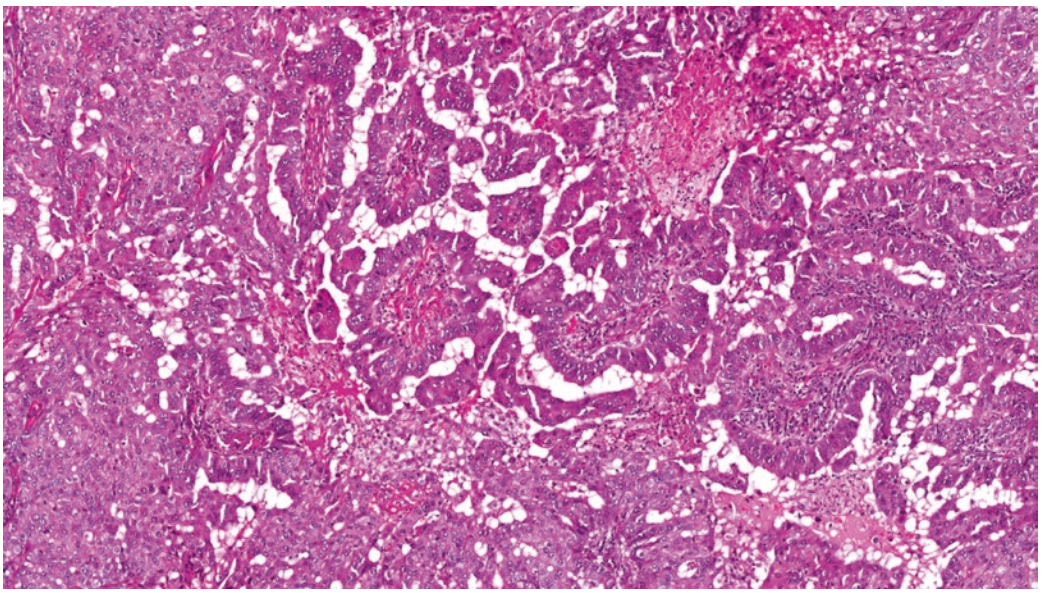

Fig. 4.70 Invasive papillary carcinoma. Papillary fronds are seen at the invasive tumour front

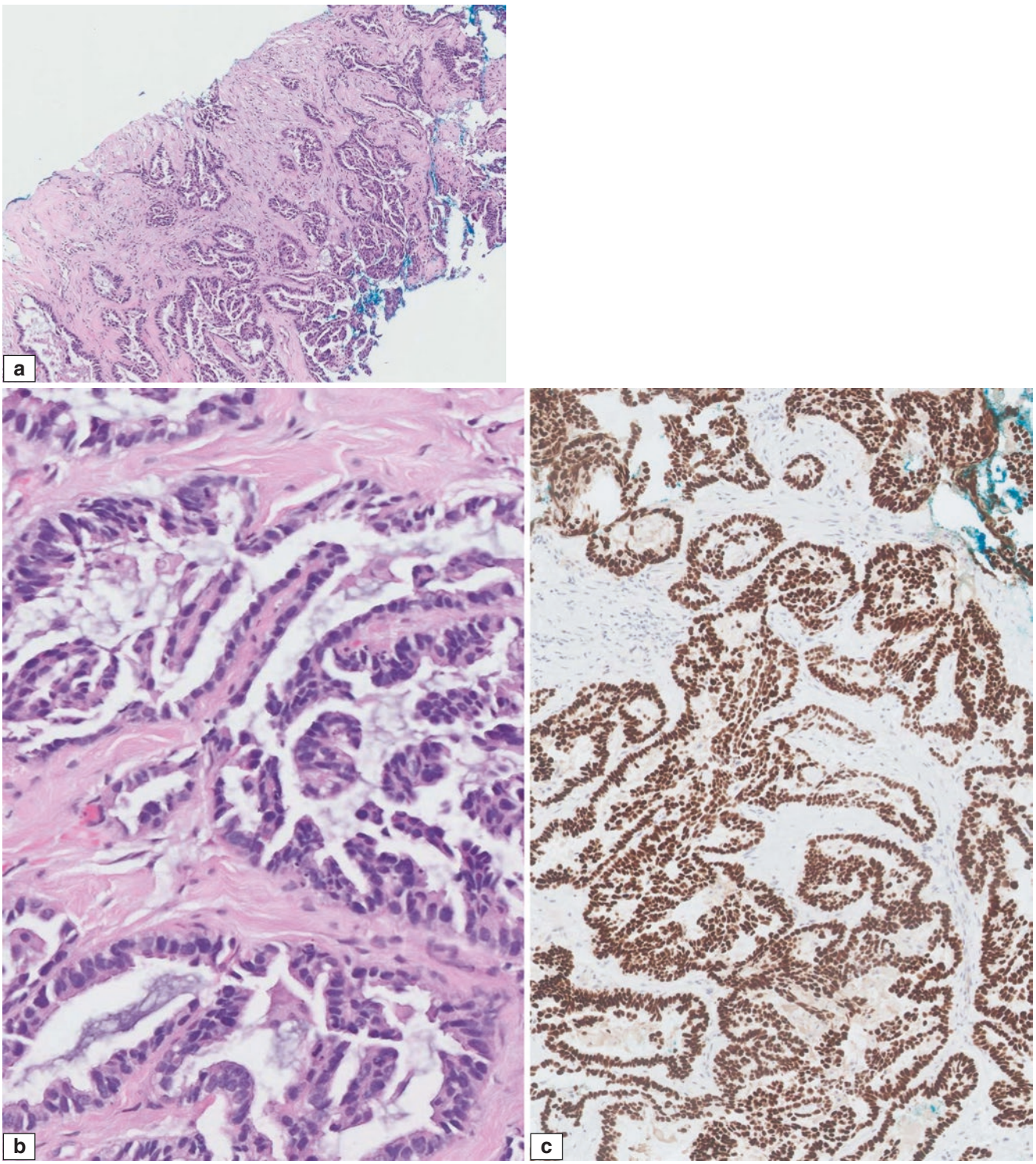

Fig. 4.71 Metastatic pulmonary adenocarcinoma to the breast shows glands with papillary luminal folds (**a**, **b**). Immunohistochemistry for TTF1 is diffusely positive in the nuclei of the tumour cells (**c**). As primary invasive papillary carcinoma is rare in the breast, the finding of an invasive tumour with papillary architecture occurring in the breast warrants exclusion of papillary metastases from other organ sites. Apart from comparison with the morphology of the non-mammary primary tumour, the use of immunohistochemistry can be diagnostically helpful. It is important to be aware of cross-reactivities of antibodies. For instance, TTF1 can be rarely positive in primary breast carcinomas, and ER can be expressed by lung adenocarcinomas. A panel of markers, including GATA3, which is expressed in breast carcinoma, is helpful

and typical nuclear morphology. Immunohistochemistry is a useful adjunct in distinguishing metastatic papillary carcinoma from primary breast disease. However, there is a need to be aware of antibody cross-reactivities. TTF1, which is usually used to determine a primary lung adenocarcinoma origin, may be expressed in 2.4 % of breast cancers [12]. A panel of markers, including GATA3, is recommended [13].

Encapsulated Papillary Carcinoma

Encapsulated papillary carcinoma shows a rounded contour with a fibrous capsule of varying thickness, contrasting with invasive papillary carcinoma where papillary tumour permeates the breast tissue in an irregular manner.

Invasive Micropapillary Carcinoma

This invasive cancer shows morular, often centrally hollow, clusters of tumour cells residing within empty spaces. There is an inside-out pattern where luminal surfaces of epithelial cells face outwards into the stromal spaces, indicating reverse polarity. These micropapillary collections of tumour cells are devoid of investment by fibrovascular septa, unlike the invasive papillary carcinoma where invading papillary processes are accompanied by fibrovascular cores (Figs. 4.72 and 4.73). Immunohistochemistry for epithelial membrane antigen (EMA) and MUC-1 shows staining of the outer surfaces of the cells forming the morules (Fig. 4.74).

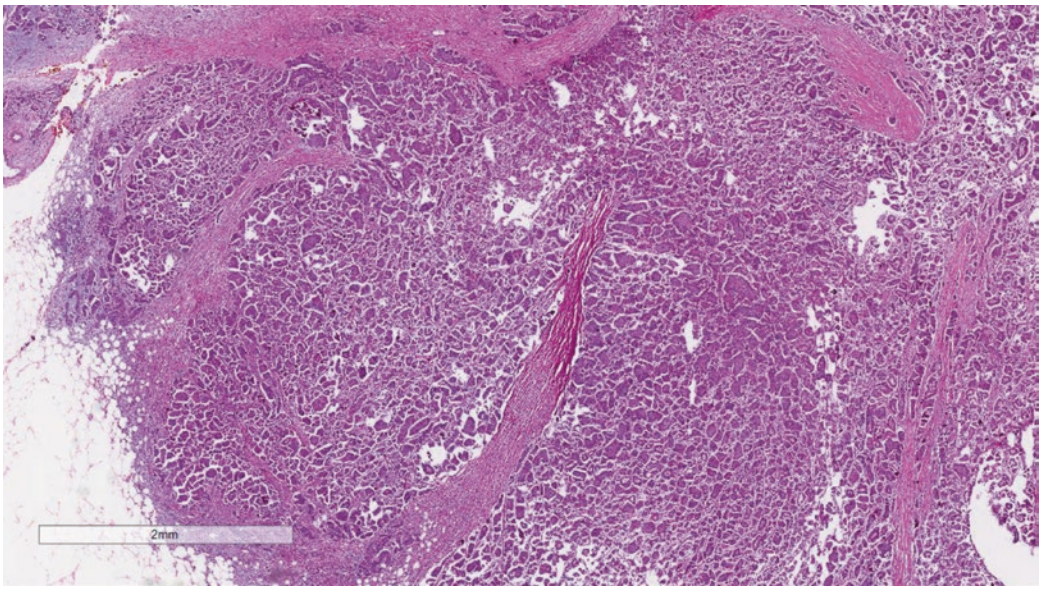

Fig. 4.72 Invasive micropapillary carcinoma shows morular nests of tumour cells surrounded by stromal spaces

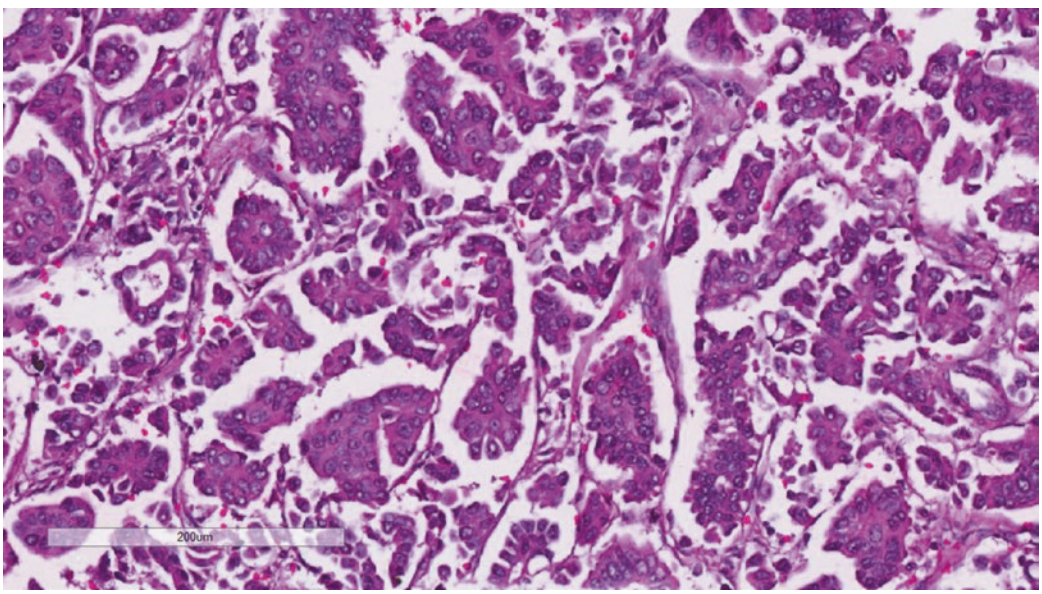

Fig. 4.73 Invasive micropapillary carcinoma. High magnification shows morular nests and micropapillary clusters of tumour cells with vesicular nuclei and discernible nucleoli. Several nests disclose central hollow spaces, while the micropapillary clusters are devoid of central fibrovascular cores. Empty spaces surround the tumour cells

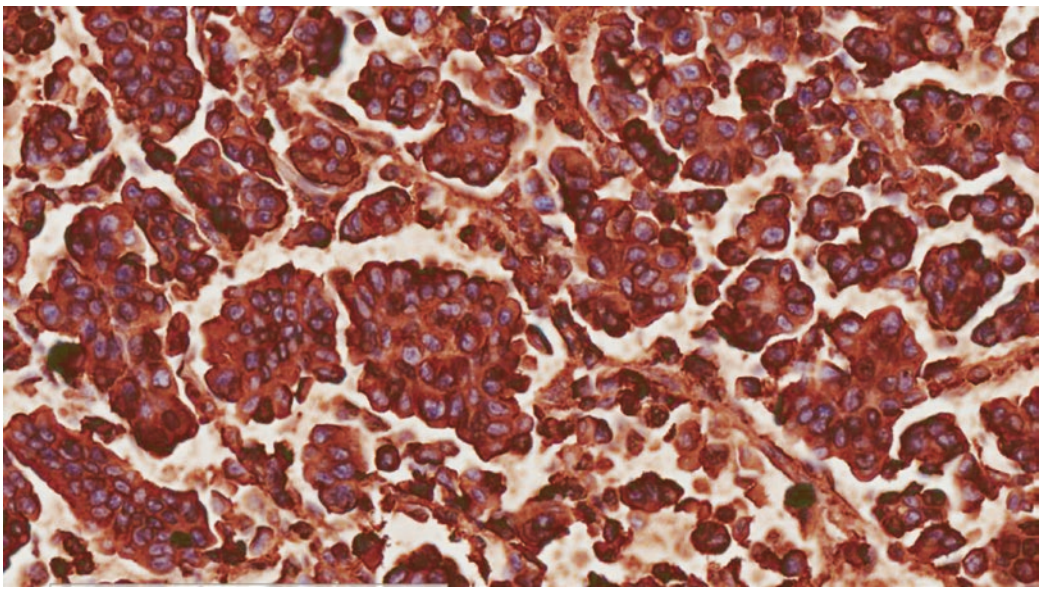

Fig. 4.74 Invasive micropapillary carcinoma. EMA immunohistochemistry shows accentuation of staining of the outer surfaces of epithelial cells forming the morular tumour clusters

Prognosis and Therapy Considerations

As invasive papillary carcinomas are rare, specific information regarding clinical behaviour is not known. Prognosis is related to grade and stage.

References

1. Lewis JT, Hartmann LC, Vierkant RA, Maloney SD, Shane Pankratz V, Allers TM, et al. An analysis of breast cancer risk in women with single, multiple, and atypical papilloma. Am J Surg Pathol. 2006;30:665–72.
2. Nagi C, Bleiweiss I, Jaffer S. Epithelial displacement in breast lesions: a papillary phenomenon. Arch Pathol Lab Med. 2005;129(11):1465–9.
3. Harada O, Hoe R, Lin J, Thike AA, Jara-Lazaro AR, Petersson F, et al. Intranuclear inclusions in epithelial cells of benign proliferative breast lesions. J Clin Pathol. 2011;64(9):776–80.
4. Lakhani SR, Ellis IO, Schnitt SJ, Tan PH, van de Vijver MJ. WHO classification of tumours of the breast. Lyon: IARC; 2012.
5. Tan PH, Aw MY, Yip G, Bay BH, Sii LH, Murugaya S, et al. Cytokeratins in papillary lesions of the breast: is there a role in distinguishing intraductal papilloma from papillary ductal carcinoma in situ? Am J Surg Pathol. 2005;29(5):625–32.
6. Lammie GA, Millis RR. Ductal adenoma of the breast—a review of fifteen cases. Hum Pathol. 1989;20(9):903–8.
7. Rakha EA, Varga Z, Elsheik S, Ellis IO. High-grade encapsulated papillary carcinoma of the breast: an under-recognized entity. Histopathology. 2015;66(5):740–6.
8. Mulligan AM, O'Malley FP. Metastatic potential of encapsulated (intracystic) papillary carcinoma of the breast: a report of 2 cases with axillary lymph node micrometastases. Int J Surg Pathol. 2007;15(2):143–7.
9. Tan PH, Schnitt SJ, van de Vijver MJ, Ellis IO, Lakhani SR. Papillary and neuroendocrine breast lesions: the WHO stance. Histopathology. 2015;66(6):761–70.
10. Nicolas MM, Wu Y, Middleton LP, Gilcrease MZ. Loss of myoepithelium is variable in solid papillary carcinoma of the breast. Histopathology. 2007;51:657–65.
11. Tan BY, Thike AA, Ellis IO, Tan PH. Clinicopathologic characteristics of solid papillary carcinoma of the breast. The American Journal of Surgical Pathology. 2016;40(10):1334–42.
12. Robens J, Goldstein L, Gown AM, Schnitt SJ. Thyroid transcription factor-1 expression in breast carcinomas. Am J Surg Pathol. 2010;34(12):1881–5.
13. Kawaguchi KR, Lu FI, Kaplan R, Liu YF, Chadwick P, Chen Z, et al. In search of the ideal immunopanel to distinguish metastatic mammary carcinoma from primary lung carcinoma: a tissue microarray study of 207 cases. Appl Immunohistochem Mol Morphol. 2014;22(4):266–74.

Benign Sclerosing Lesions

5

Many different types of both benign and malignant breast lesions can be associated with stromal fibrosis and collagen deposition and can be broadly classified as sclerosing lesions [1–3]. Recognising the aetiology of the fibrosis on excisional biopsy is usually not very difficult; however, extensive fibrosis and related histologic changes may create major diagnostic challenges on a limited sample such as a core needle biopsy. Sclerosing adenosis and radial scar/complex (radial) sclerosing lesion are two benign entities that will be described in this chapter. The main clinical significance of these lesions is that they may mimic invasive carcinoma clinically and radiographically as well as in gross and microscopic evaluations.

Sclerosing Adenosis

Definition

Adenosis is defined as a relative increase in the number of acinar units in a terminal ductal lobular unit. Sclerosing adenosis refers to adenosis with extensive fibrosis that includes compression and distortion of acinar units [4]. When proliferating glands expand lobular units significantly and form nodules or mass lesions, the terms nodular adenosis and adenosis tumour are used [5].

Clinical Features

Sclerosing adenosis is a frequent incidental microscopic finding in breast specimens removed for other indications. Sclerosing adenosis has been reported in 15–20% of breast biopsies without carcinoma. It occurs in a wide age group but is most frequent in perimenopausal women. Regression of sclerosing adenosis has been noted in postmenopausal women. Most lesions are less than 2 cm and can be unifocal or multiple. The majority are associated with microcalcifications and/or architectural distortion that leads to biopsy. Therefore, screen detection in an asymptomatic patient is the most common mode of discovery. Less commonly, the presenting symptom may be a mass lesion on palpation or on imaging. Rarely, sclerosing adenosis may be associated with breast pain.

Imaging Features

Sclerosing adenosis may present as microcalcifications, architectural distortion, or mass lesions (Fig. 5.1) [6]. Microcalcifications are typically described as amorphous and clustered; pleomorphic and punctate microcalcifications can also be associated with sclerosing adenosis. This latter pattern cannot be differentiated from that of carcinoma, and biopsy is required for definitive diagnosis. Increased density with irregular margins with or without microcalcifications can also be a radiographic finding of sclerosing adenosis. This pattern closely mimics invasive carcinoma, especially tubular carcinoma. Mass-forming lesions are typically well circumscribed or lobulated. There are usually no significant MR findings. Twenty percent of cases of sclerosing adenosis may show intermediate enhancement.

Pathologic Features

Macroscopic Pathology

The gross appearance of sclerosing adenosis depends on the size and microscopic composition of the lesion. Since the majority of sclerosing adenosis lesions are small and have a combination of stromal and glandular components, they are imperceptible on macroscopic evaluation. If a lesion has extensive fibrosis, it may appear as white and vaguely nodular (Fig. 5.2). Lesions composed predominantly of glandular components with epithelial proliferation may appear as circumscribed, rubbery, pale tan nodules.

P.H. Tan, A.A. Sahin, *Atlas of Differential Diagnosis in Breast Pathology*, Atlas of Anatomic Pathology,
DOI 10.1007/978-1-4939-6697-4_5

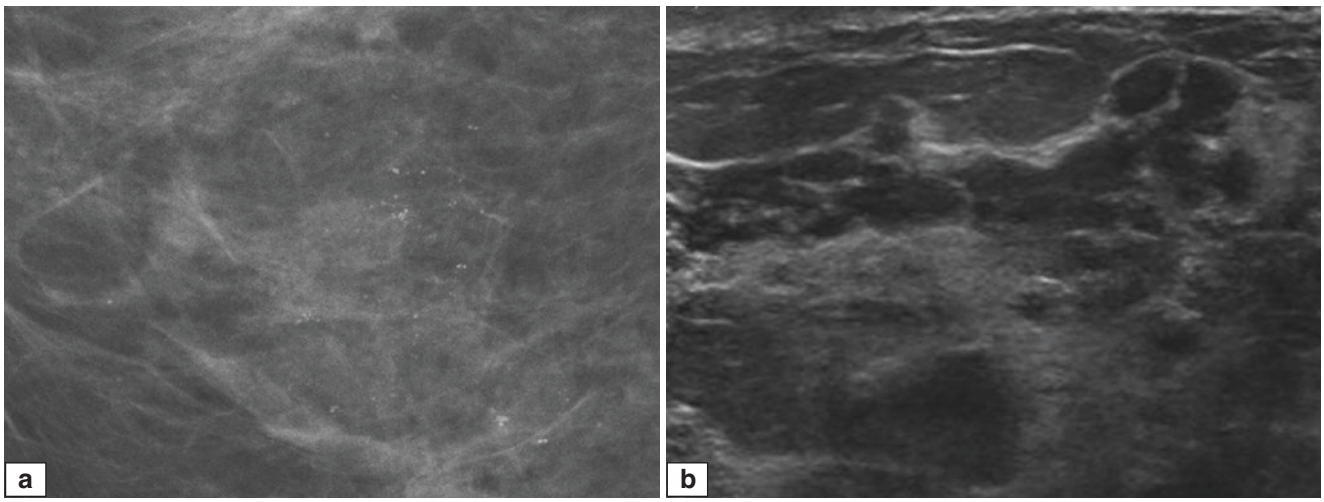

Fig. 5.1 Sclerosing adenosis. (**a**) Mammography shows a mix of powdery, punctate and rounded types of microcalcifications in this cluster. Stereotactic-guided percutaneous biopsy revealed that the calcifications were associated with sclerosing adenosis. (**b**) Ultrasound examination shows a group of lobulated and tubular-oriented nodules that can mimic ductal pathology on imaging. When sclerosing adenosis forms nodules or mass lesions, it is referred to as nodular sclerosing adenosis. (Courtesy of Dr. Lester Leong)

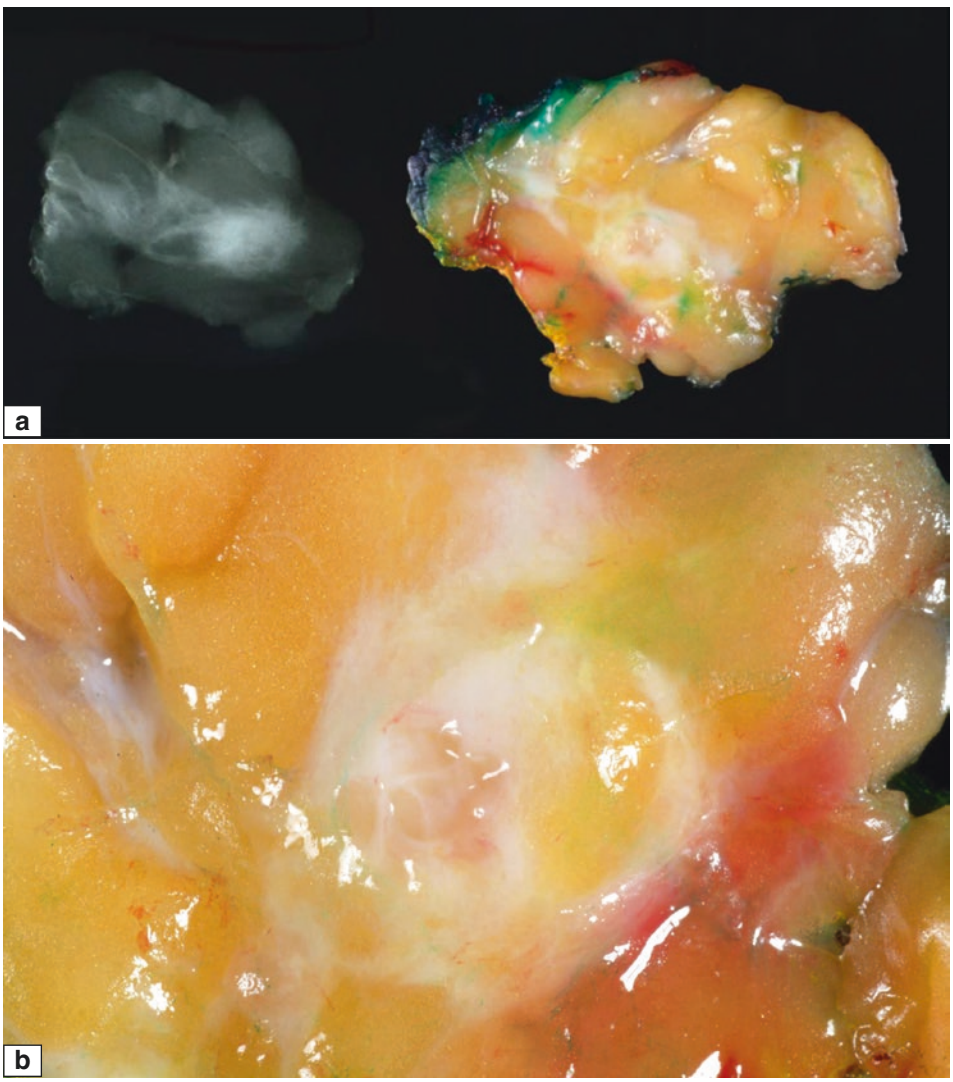

Fig. 5.2 Adenosis tumour. Gross and imaging features. (**a**) Imaging and specimen show a partially-circumscribed white nodule. (**b**) Higher magnification of specimen displays a mixture of grey-white and yellow tissue. Note that the grey-white tissue blends into adjacent fat

Microscopic Pathology

Sclerosing adenosis is characterised by enlarged lobular units due to nodular proliferation of ducts and acini that are compressed and distorted by stromal collagen (Figs. 5.3, 5.4, and 5.5) [4, 7]. The normal lobular appearance is distorted by fibrosis, particularly in the centre of the lesion, where distorted glands may have an angulated appearance and mimic invasive carcinoma (Fig. 5.6). However, the lobulocentric nature of the lesion, which is best appreciated on low magnification, is maintained and can be the most important histologic feature to differentiate it from invasive cancer (Fig. 5.6). The ducts have both luminal epithelial and peripheral myoepithelial cells. Although the presence of a dual cell population is easy to appreciate on haematoxylin and eosin (H&E) sections in most cases, confirmation by immunohistochemistry may be helpful in selective instances to illustrate the preservation of myoepithelial cells (Fig. 5.7). The ratio of epithelial and myoepithelial cells can vary significantly from case to case (Fig. 5.8).

In some cases, there is significant epithelial atrophy and preferential proliferation of myoepithelial cells. In others, both epithelial and myoepithelial components appear hyperplastic. The basement membrane around glands of sclerosing adenosis is usually thickened and prominent. Occasionally, both epithelial and myoepithelial cells undergo metaplastic changes. Apocrine metaplasia of epithelium, spindle cell morphology, and myoid differentiation of myoepithelium are commonly seen in sclerosing adenosis. The term apocrine adenosis is used when the entire lesion of sclerosing adenosis shows apocrine metaplasia (Fig. 5.9) [8–10]. Microcalcifications are a common microscopic feature of sclerosing adenosis and can be present either in fibrotic stroma or in ductal lumens. Atypical ductal and atypical lobular hyperplasia or in situ carcinoma may involve sclerosing adenosis. These may cause major diagnostic difficulties, especially on core needle biopsies. Involvement of sclerosing adenosis by ductal carcinoma in situ may mimic invasive carcinoma, and it is one of the commonly mistaken diagnoses on core needle biopsies. Ductal carcinoma in situ involving sclerosing adenosis can be high grade and arise within sclerosing adenosis. The integrity of the individual acini and preservation of myoepithelium may be difficult to appreciate on H&E sections alone (Figs. 5.10, 5.11, and 5.12). Lobulocentric architecture of sclerosing adenosis versus infiltrative growth pattern of invasive carcinoma, a background of dense fibrotic stroma of sclerosing adenosis versus the more cellular (desmoplastic) stroma of invasive carcinoma, should be useful in arriving at the correct diagnosis. Using immunohistochemical stains to highlight myoepithelial cells will be helpful [11–14].

Perineural pseudoinvasion has been reported in 2 % of sclerosing adenosis cases (Fig. 5.13) [15]. Sclerosing adenosis glands and ducts may be present around nerves, most commonly in the perineurium, but rarely in nerve fibres. The benign appearance of the glands and the preserved myoepithelial layer around the ducts will be helpful to differentiate these glands from invasive carcinoma.

Differential Diagnosis

Normal Breast Parenchyma

Breast lobules undergo involution with age and large involuting lobules may resemble sclerosing adenosis. Similarly, breast lobules enlarge during pregnancy and lactation, which usually is a diffuse process. During regression of pregnancy and lactational changes, the focal retention of involuting lobules can be confused with sclerosing adenosis. In contrast to normal breast parenchyma, ducts in sclerosing adenosis show prominent myoepithelial cells. In pregnancy- and lactation-related changes, the lining of ducts is composed predominantly of epithelial cells with plump hyperchromatic nuclei. In ducts of sclerosing adenosis, myoepithelial cells may predominate and basement membranes are thickened.

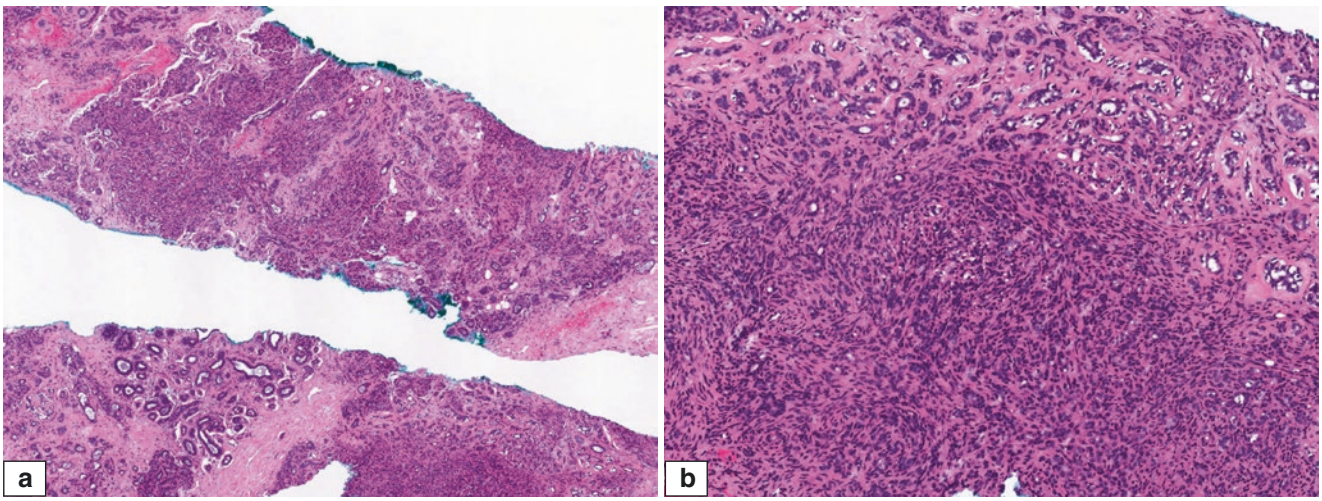

Fig. 5.3 Sclerosing adenosis. (**a**) Core biopsies show cellular areas at low magnification. (**b**) Medium magnification shows a dense population of cells with slightly spindled appearances, merging with small tubules with patent lumens. (**c**) Higher magnification shows small tubules among ovoid to spindle cells of myoepithelial origin. (**d**) CK14 immunohistochemistry shows prominent myoepithelial cells rimming the small tubules and compressed epithelial nests. (**e**) Immunohistochemistry for p63 also shows retention of myoepithelial cells. (**f**) Higher magnification shows p63 immunostaining of many myoepithelial nuclei among the luminal epithelial cells. Myoepithelial hyperplasia is often encountered in sclerosing adenosis

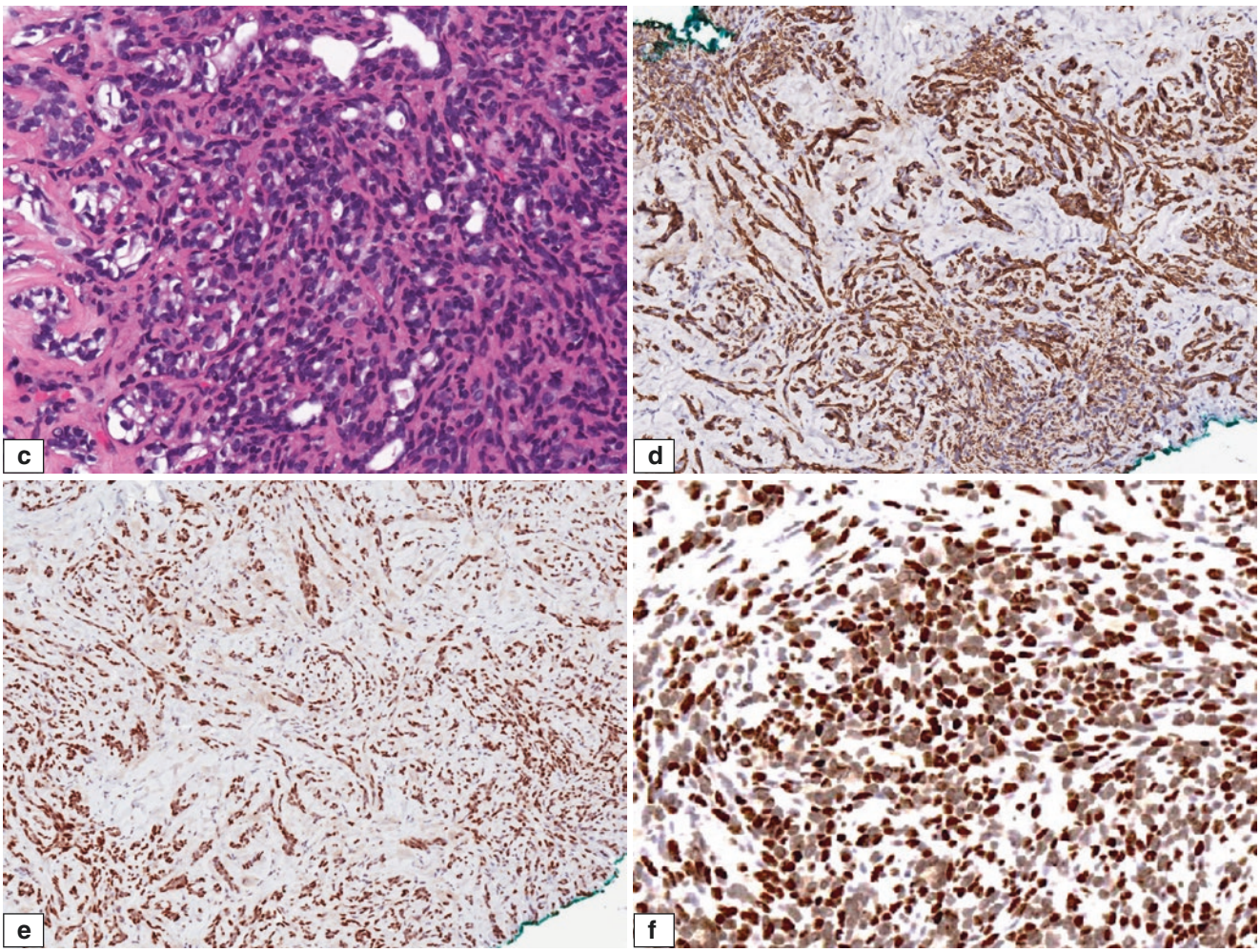

Fig. 5.3 (continued)

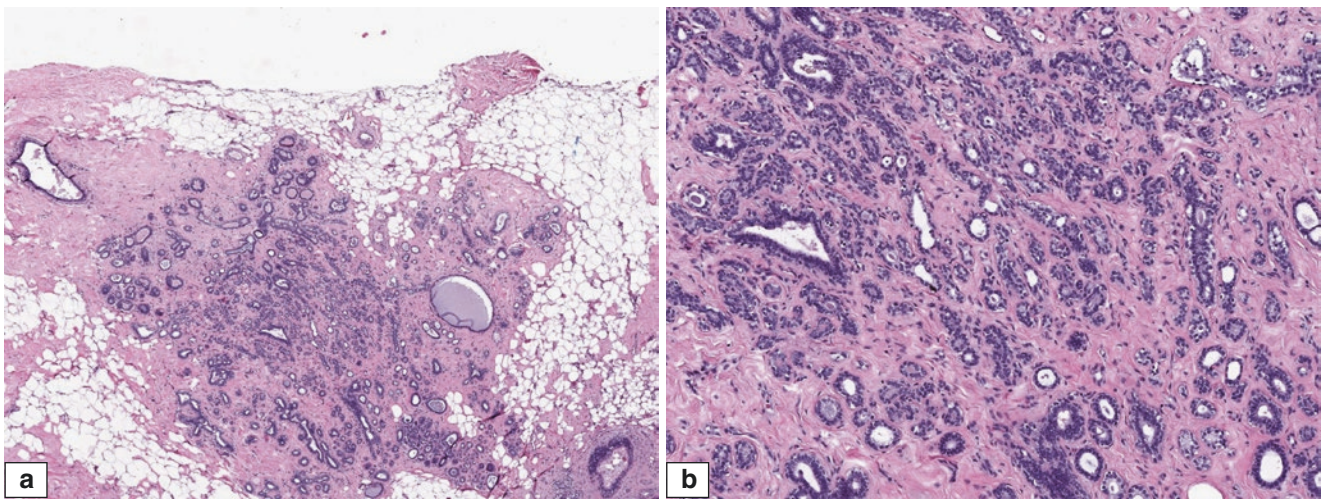

Fig. 5.4 Sclerosing adenosis. Microscopic features. (**a**) Low magnification of lobulocentric growth. (**b**) Medium magnification of (**a**) shows that some glands have collapsed closed lumens, while others have open tubular structures

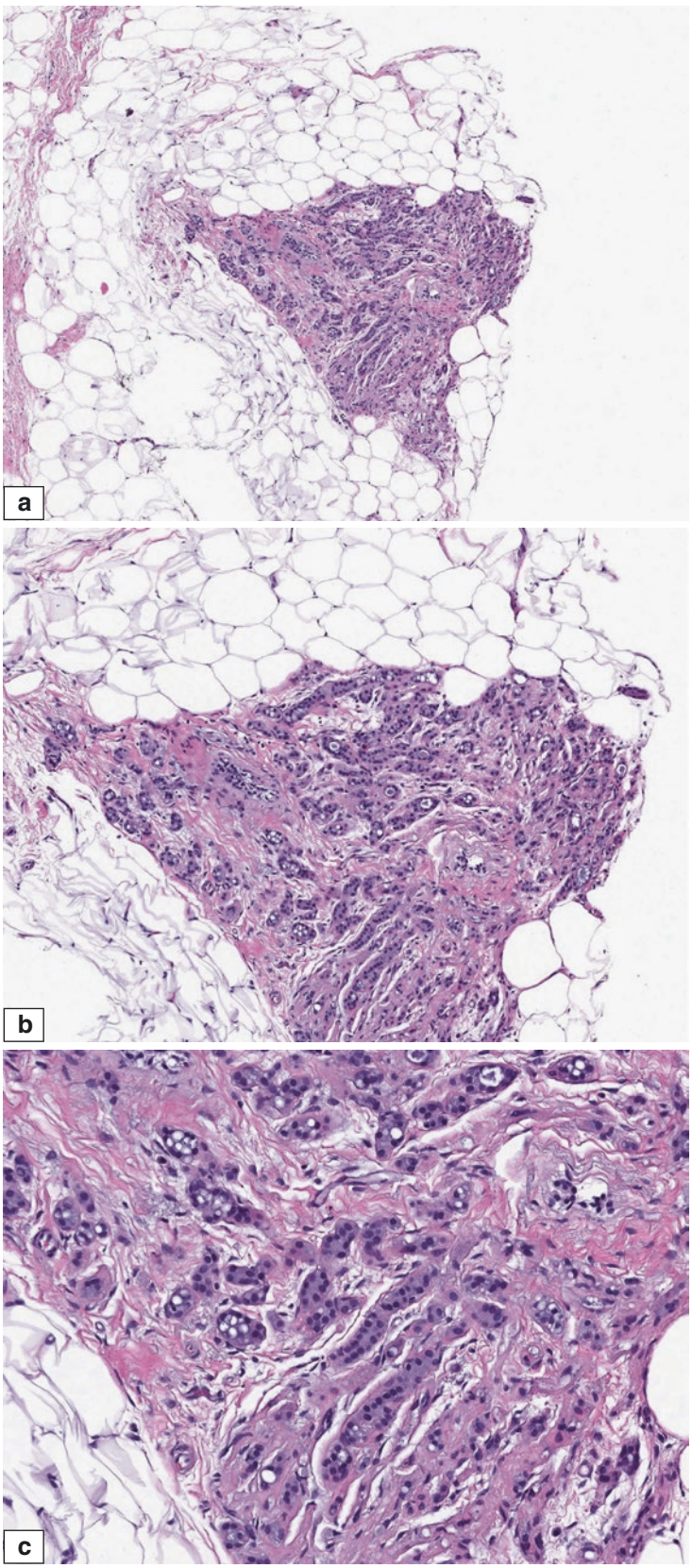

Fig. 5.5 Sclerosing adenosis. Microscopic features. (**a**) Low magnification shows a distinct nodule with sharp demarcation from adjacent breast parenchyma. (**b**) Medium magnification shows distorted small glands that have predominantly closed lumens. (**c**) High magnification of the same case shows a small glandular proliferation surrounded by dense collagenized stroma

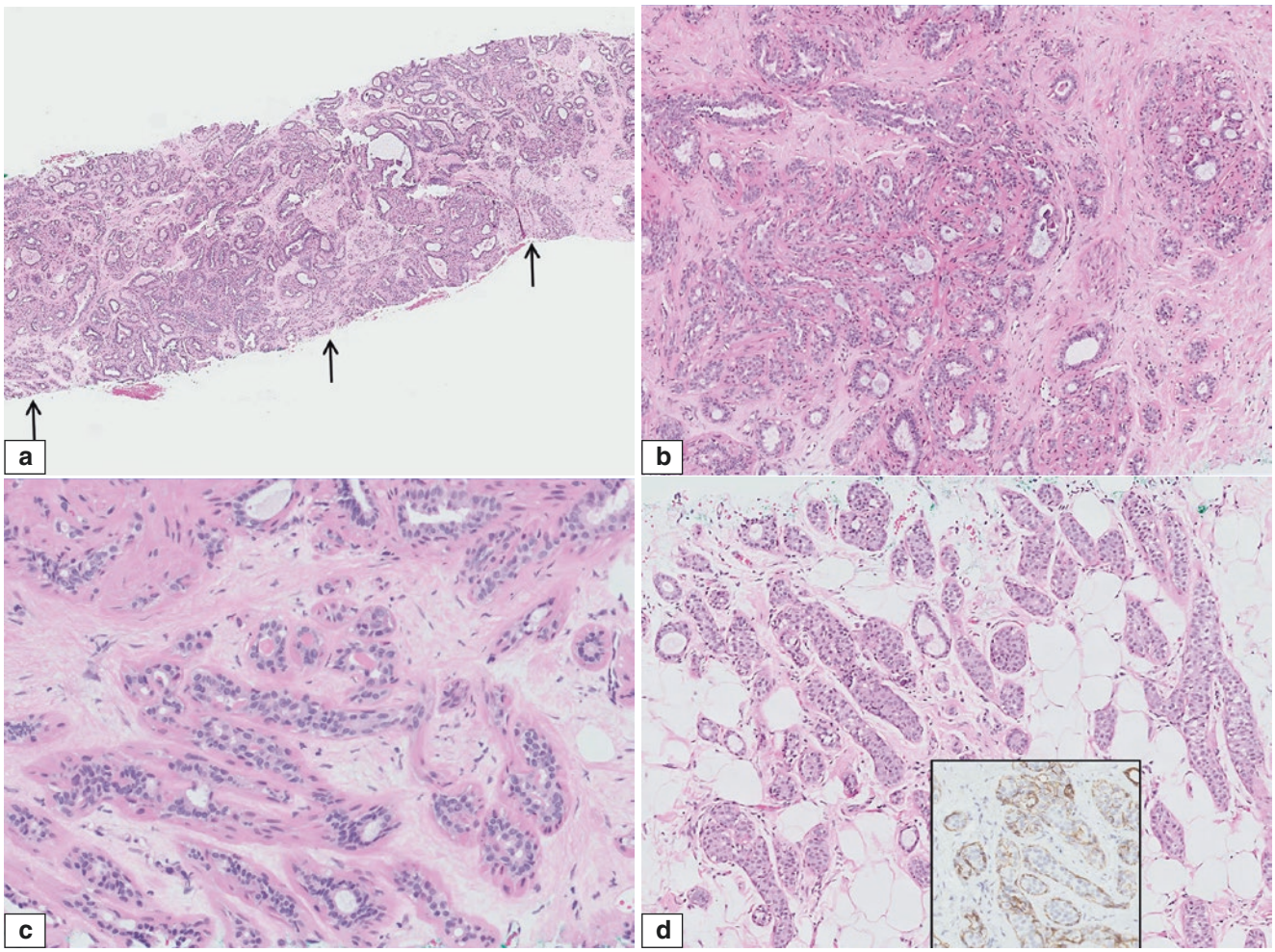

Fig. 5.6 Sclerosing adenosis. Microscopic features. (**a**) Low magnification of core needle biopsy shows a crowded glandular proliferation with fibrotic areas and a pseudo-infiltrative pattern (*arrows*). (**b**) Glands with open as well as compressed lumens are present, rimmed externally by spindled myoepithelial cells. Occasional luminal calcifications are seen. (**c**) High magnification shows the compressed ductules to be lined by bilayered epithelium – an inner luminal layer that is composed of cuboidal to flattened cells, and an outer layer of myoepithelial cells with spindled morphology and pink cytoplasm indicating myoid metaplasia. (**d**) Atypical lobular hyperplasia is seen superimposed on sclerosing adenosis. Inset shows negative immunohistochemical staining of lobular neoplastic cells for E-cadherin

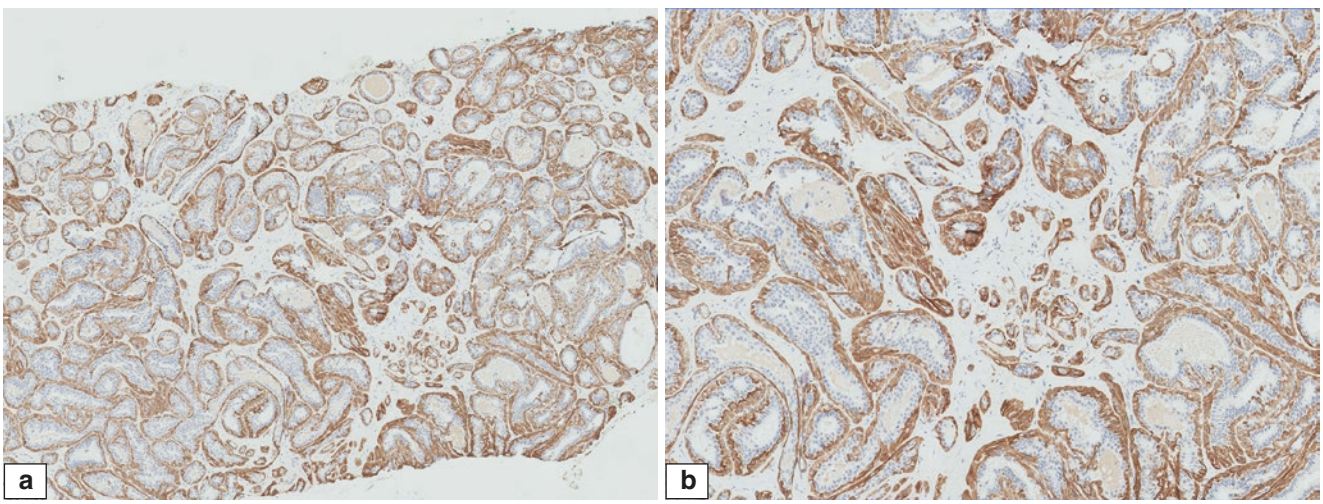

Fig. 5.7 Sclerosing adenosis. Immunohistochemical features. (**a**, **b**) Lower and higher magnification shows positive staining for smooth muscle myosin that highlights peripheral myoepithelial cells

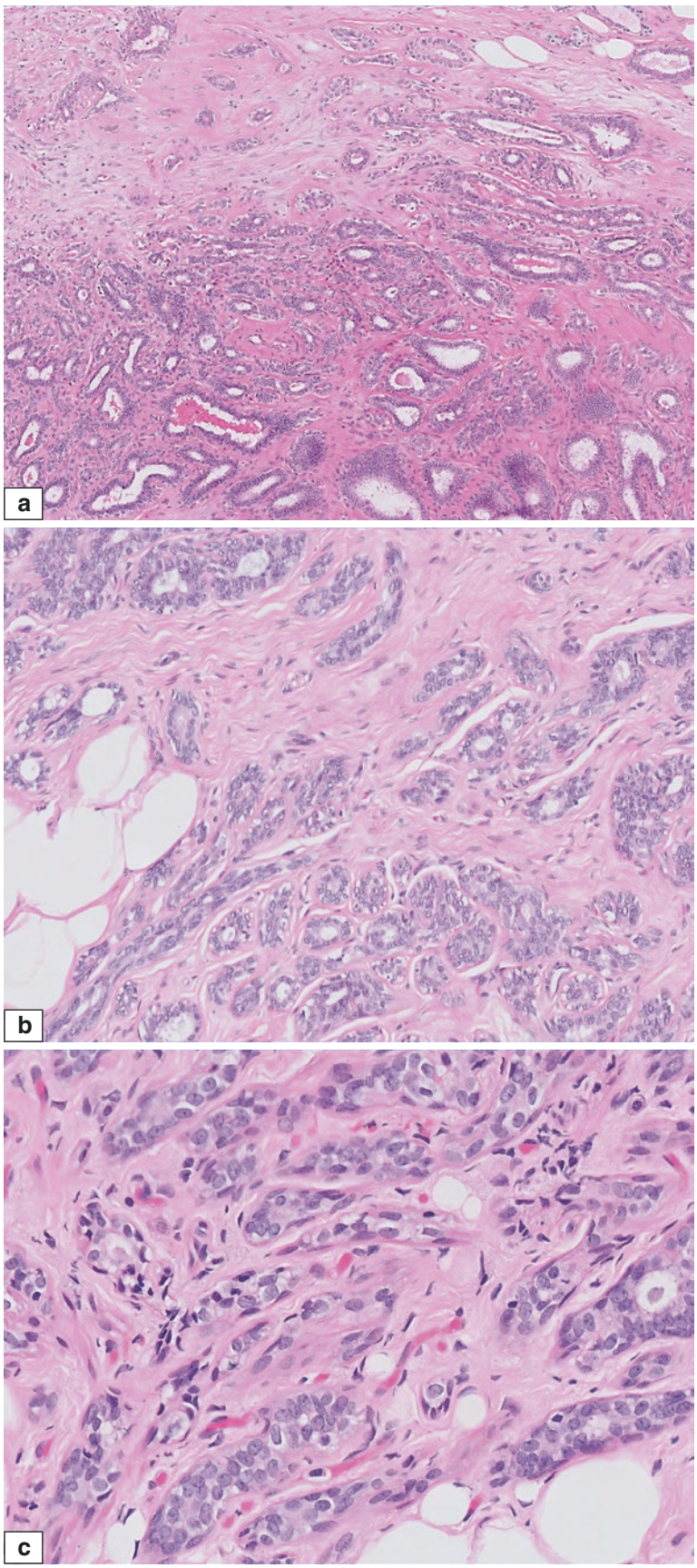

Fig. 5.8 Sclerosing adenosis. Microscopic features. (**a**) Low magnification shows sclerosis of several small atrophic glands associated with hypocellular stroma (*upper field*). (**b**) Closer view shows that the small glands are bilayered, with variably prominent myoepithelial cells. (**c**) High magnification shows compressed glands with myoepithelial cells in a linear distribution, which may mimic an invasive carcinoma growth pattern

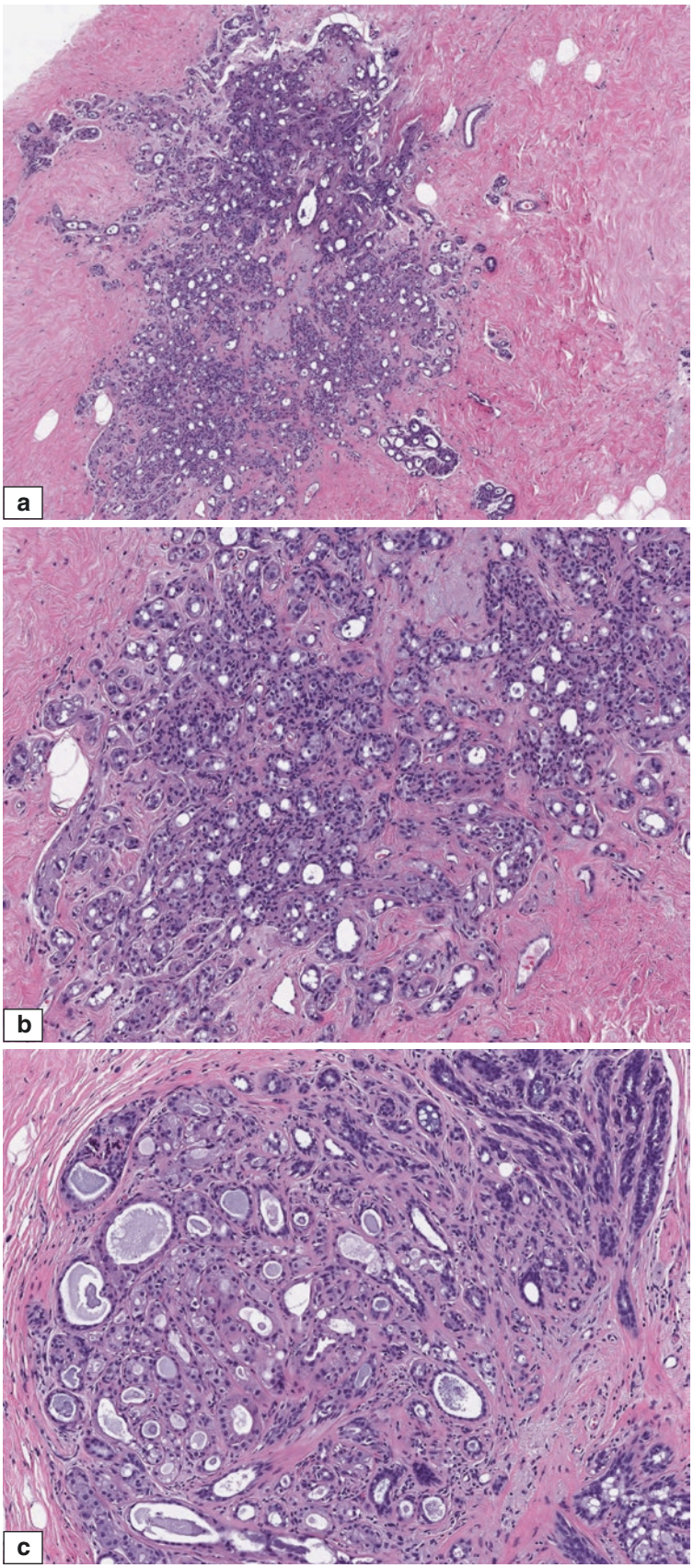

Fig. 5.9 Sclerosing adenosis with apocrine metaplasia (apocrine adenosis). Microscopic features. (**a**) Low magnification shows a lobulocentric proliferation of small glands in a fibrotic background. (**b**, **c**) Higher magnification shows apocrine metaplasia

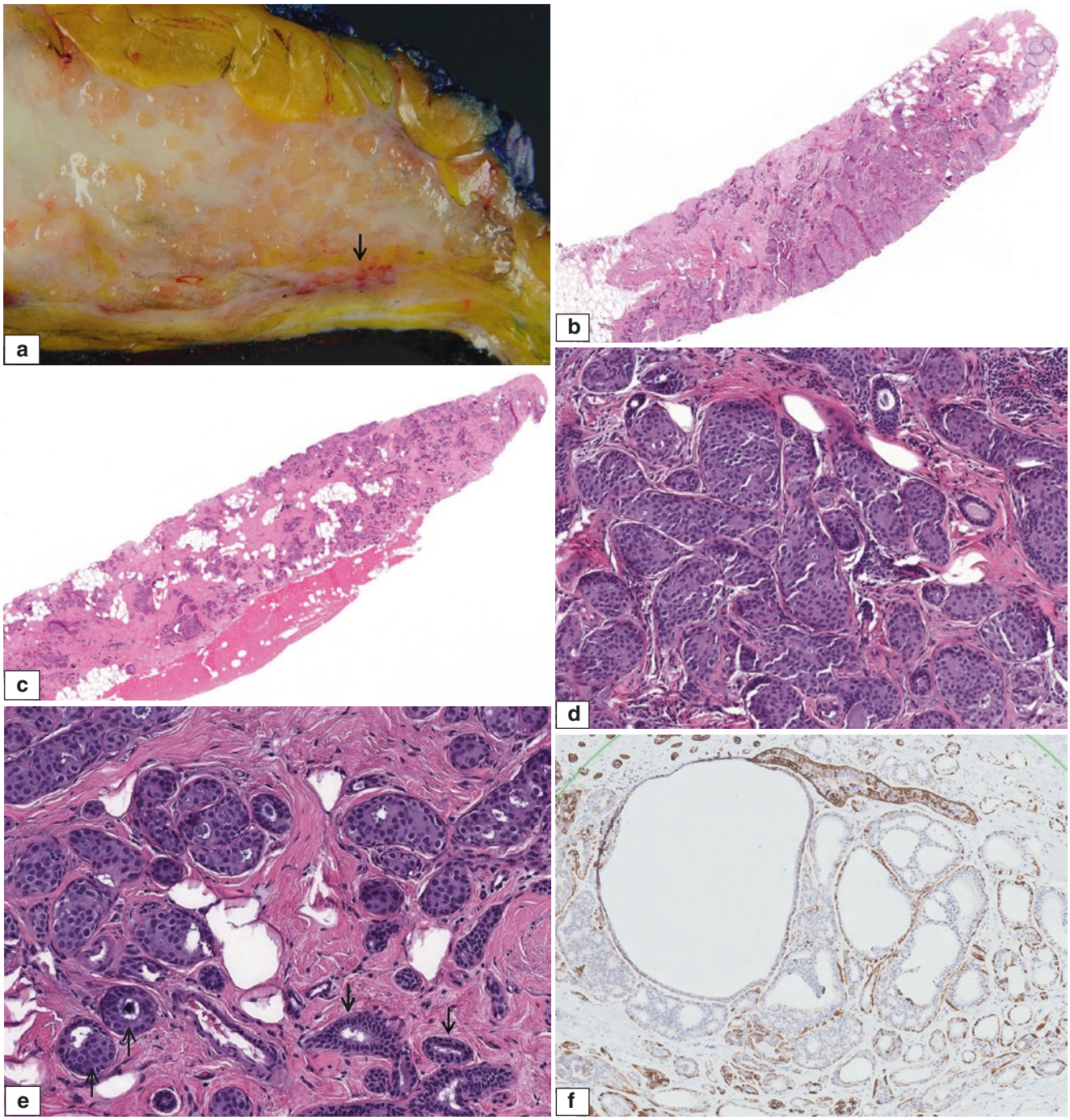

Fig. 5.10 Ductal carcinoma in situ (DCIS) involving sclerosing adenosis. Gross and microscopic features. (**a**) Specimen shows a haemorrhagic area (*arrow*) corresponding histologically to foci of glandular proliferation. (**b**, **c**) Low magnification of different areas of the prior core biopsy showing a glandular proliferation in a fibrous background. (**d**) Higher magnification indicates a proliferation of low-to-intermediate grade ductal carcinoma in situ cells expanding the glands. (**e**) A few scattered glands are not involved by DCIS (*arrows*). (**f**) Immunohistochemistry for CK14 decorates an intact outer layer of myoepithelial cells around DCIS

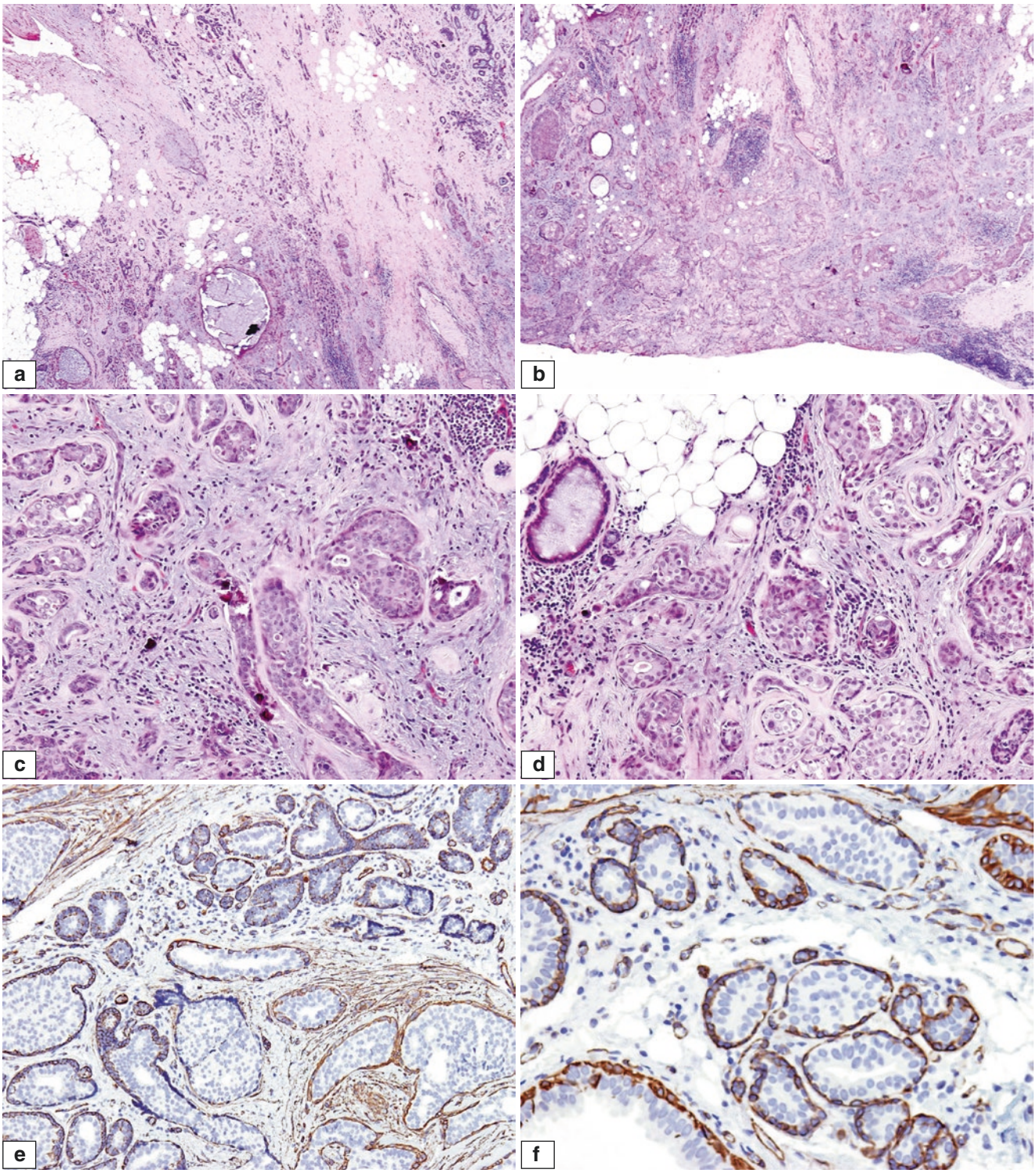

Fig. 5.11 DCIS involving sclerosing adenosis. Histologic and immunohistochemical features. (**a**) Low magnification shows a proliferation of varying sizes of glandular structures with focal infiltrative growth pattern. (**b**) Stroma is cellular. (**c**) Higher magnification shows that individual glandular structures contain pleomorphic-appearing cells. (**d**) Irregular contours of distorted glands appear infiltrative. (**e**, **f**) Staining for smooth muscle actin highlights myoepithelial cells wrapping around the tubules. No invasion is present. (**g**) Myoepithelial cells stain strongly positive for p63. (**h**) Myoepithelial cells, highlighted with p63 immunohistochemistry, are present around the irregular islands of DCIS, confirming non-invasion. On light microscopy and without the aid of myoepithelial immunohistochemical markers, histological appearances closely resemble invasive disease. Clues to the in situ nature are the hyalinised stroma and the presence of peripheral ovoid myoepithelial nuclei which are smaller than carcinoma cell nuclei. Convergence with recognizable sclerosing adenosis is another helpful microscopic cue

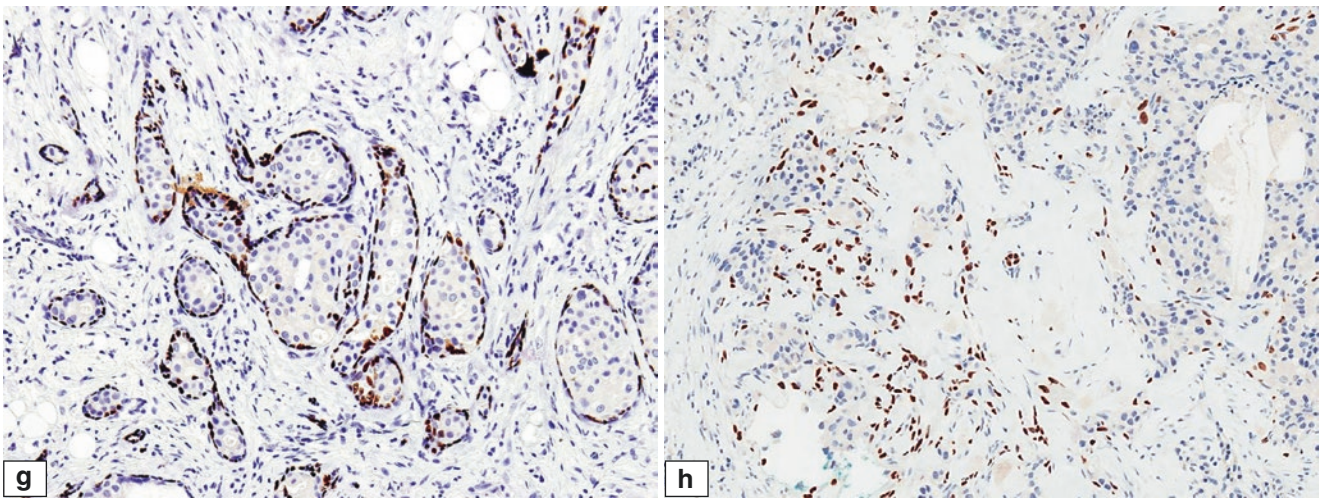

Fig. 5.11 (continued)

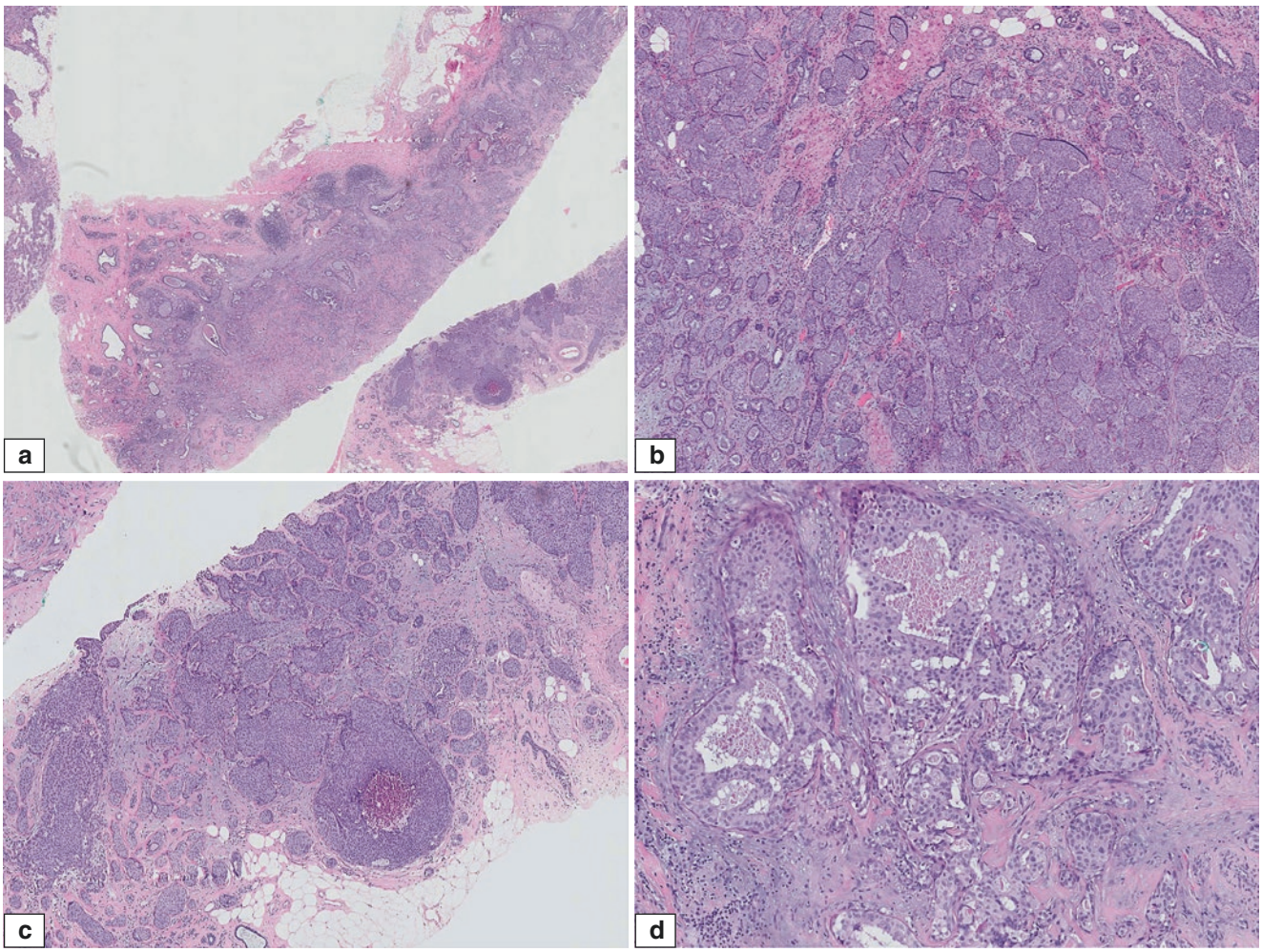

Fig. 5.12 Sclerosing adenosis with DCIS. (**a**) Core biopsies show a cellular proliferation at low magnification. (**b**) A solid tumour cell proliferation fills the ducts of sclerosing adenosis. A few unaffected tubules are seen. (**c**) The irregular pattern of the epithelial islands within the slightly oedematous stroma mimics invasive carcinoma. Comedonecrosis is seen in one expanded duct affected by DCIS. (**d**) Cribriform islands lined by in situ carcinoma cells with intermediate nuclear grade are noted. Debris is observed within several lumens

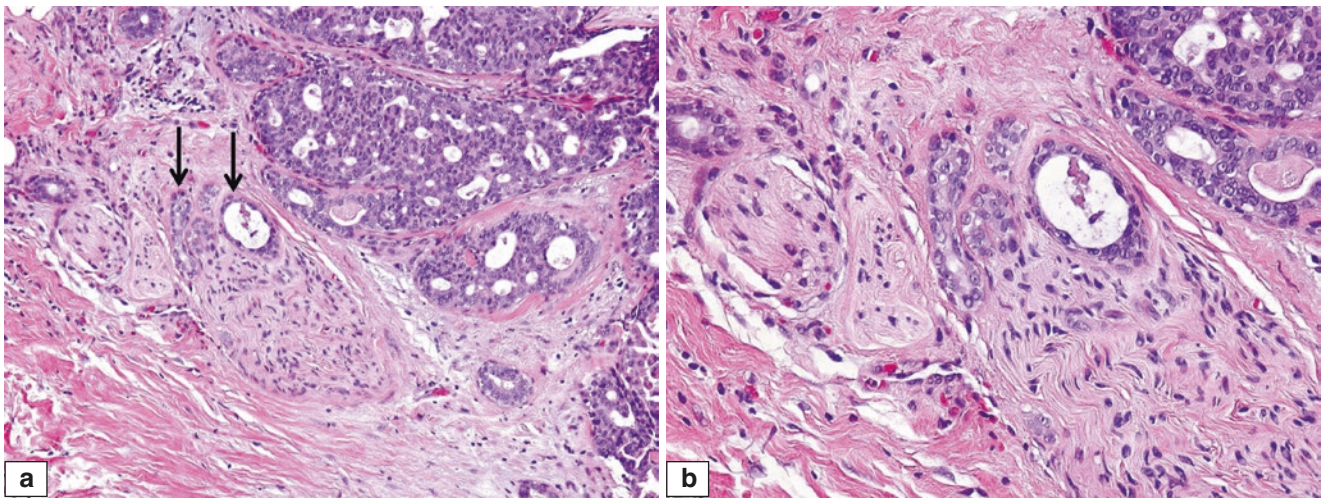

Fig. 5.13 Sclerosing adenosis with perineural invasion. Histologic features. (**a**, **b**) Small glands with identical morphologic features to adjacent sclerosing adenosis glands have infiltrated the perineural space (*arrows*). Note the lack of any stromal or inflammatory reaction

Microglandular Adenosis

A main differential diagnosis includes microglandular adenosis, which is characterised by a haphazard, non-lobulocentric proliferation of small round tubular structures that lack myoepithelial cells. Luminal spaces of microglandular adenosis are open and contain colloid-like secretions, in contrast to collapsed closed lumens of sclerosing adenosis.

Invasive Carcinoma

The haphazard infiltrative pattern of invasive carcinoma versus the lobulocentric growth pattern of sclerosing adenosis is the main histologic feature to differentiate them. Immunohistochemical staining for myoepithelial cells can be helpful to confirm the absence of a myoepithelial component in ducts of invasive carcinoma.

Prognosis and Therapy Considerations

Sclerosing adenosis reflects a generalised disturbance of the breast parenchyma including both stromal and epithelial components [4, 16]. It is not a direct precursor lesion of breast cancer but is associated with a doubling of the risk of breast cancer, which is the same risk as proliferative lesions without atypia such as florid hyperplasia. If the diagnosis of sclerosing adenosis is clearly established on a core needle biopsy, and there is no imaging or clinical discordance with this diagnosis, routine follow-up without excision is appropriate. Excision should be considered if there is an atypical epithelial proliferation involving sclerosing adenosis or an imaging or clinical discrepancy. Nassar et al. suggested that women with sclerosing adenosis showing increased Ki67 expression have increased risk of subsequent breast cancer [17–19].

Radial Scar/Complex Sclerosing Lesion

Definition

Radial scar and complex sclerosing lesion refer to proliferative breast lesions with typical stellate configuration on imaging and histologic evaluation. Radial scar and complex sclerosing lesion are considered to be the same process and are arbitrarily distinguished on the basis of size. Lesions up to 1 cm are designated as radial scars and larger ones as complex sclerosing lesions. The term “radial sclerosing lesion” encompasses both the radial scar and complex sclerosing lesion.

Clinical Features

A radial scar is usually found as an incidental microscopic finding in breast biopsies performed for other indications. The reported incidence varies from 5 to 28 % in the literature. Bilateral and multifocal lesions are frequent [20, 21].

Imaging Features

The typical mammographic finding is a stellate or spiculated lesion with a lucent centre mimicking invasive carcinoma (Fig. 5.14). Microcalcifications are uncommon in radial scars. When microcalcifications are present, they are usually identified in associated epithelial proliferations. On ultrasound evaluation, it appears as an ill-defined mass with surrounding distortion but it is commonly subtle or difficult to be visualised. It can be seen as an enhancing area with

spiculations and surrounding distortion on MRI which provides better visualisation and 3D localisation of subtle lesions [22, 23].

Pathologic Features

Macroscopic Pathology

Large radial scars/complex sclerosing lesions appear as stellate masses, which are indistinguishable from invasive carcinoma (Fig. 5.15).

Microscopic Features

Histologically, a radial scar or complex sclerosing lesion is composed of central elastotic stroma surrounded by numerous glands emanating from the centre (Fig. 5.16). The radiating ducts usually expand and show cystic dilatation around the periphery. Epithelial proliferation and metaplasia are commonly seen. Glands may be trapped at the central scar area and become angulated mimicking invasive carcinoma, especially tubular carcinoma (Figs. 5.17, 5.18, 5.19, 5.20, and 5.21). While lesional size is used to separate radial scar from the complex sclerosing lesion, there are some histological differences, with complex sclerosing lesions being usually more disorganized and may not always display a radial or radiating configuration. Just like other benign lesions, any type of atypical hyperplasia or in situ carcinoma can occur in a radial scar or complex sclerosing lesion. Invasive carcinomas may involve radial scars [24].

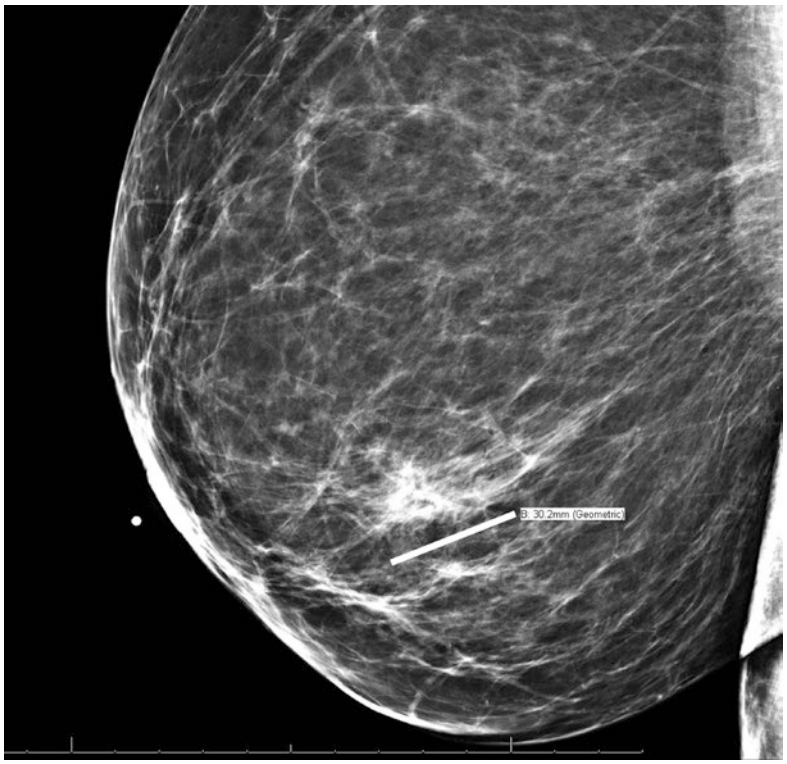

Fig. 5.14 Radial scar. Mammographic imaging. Imaging shows architectural distortion with fine spicules radiating from the central portion to the periphery

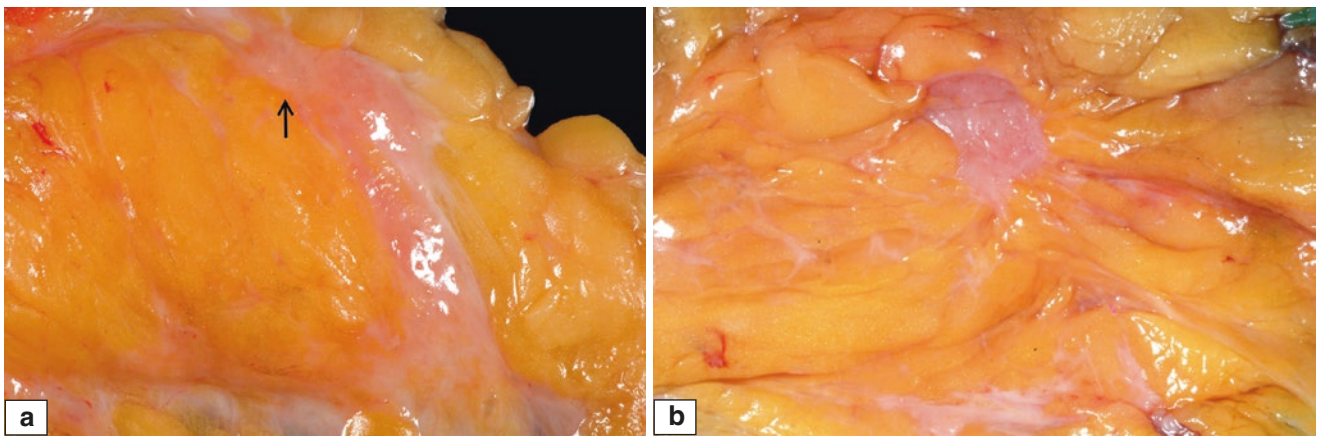

Fig. 5.15 Radial scar. Gross features. (**a**) Thin grey-white fibrous bands radiate into adipose tissue from the ill-defined whitish lesion (*arrow*). (**b**) A well-formed mass with radiating white streaks mimicking an invasive carcinoma

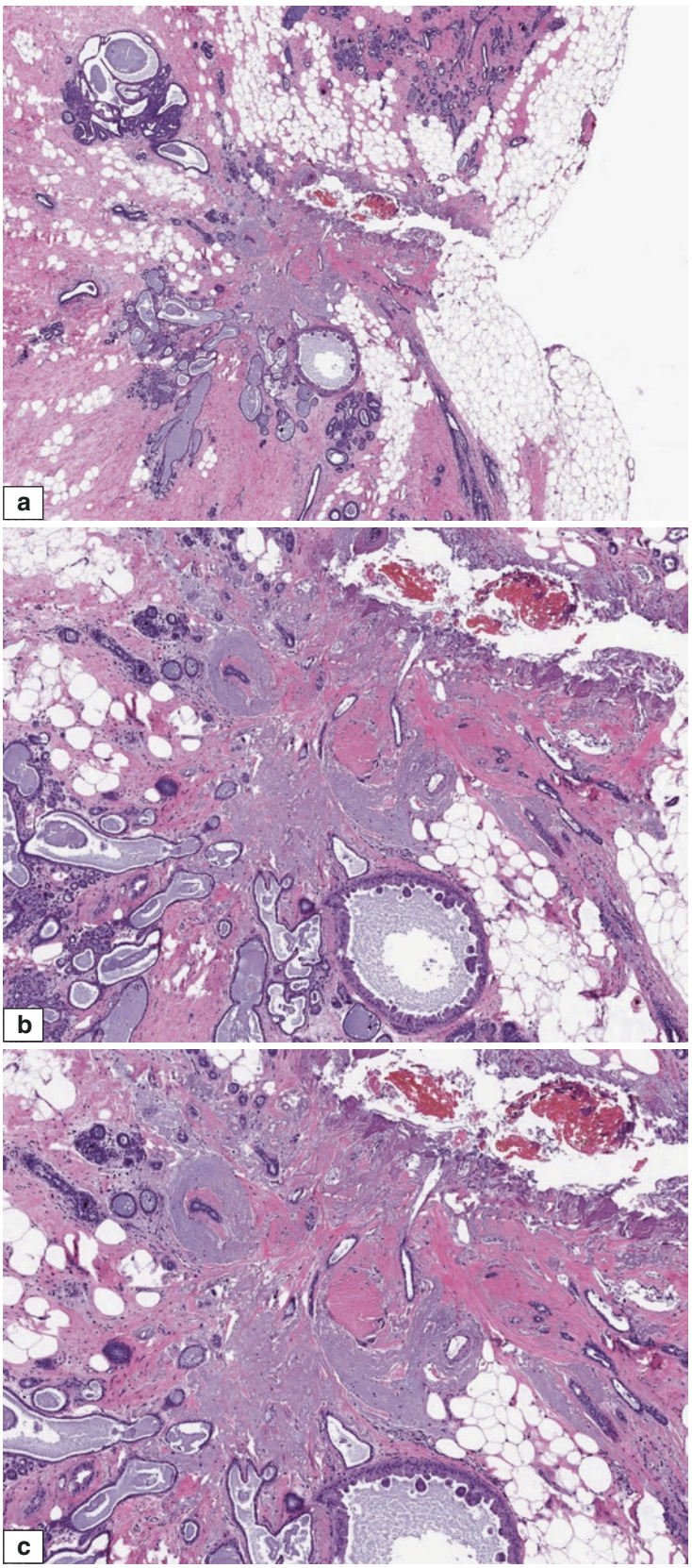

Fig. 5.16 Radial scar. Microscopic features. (**a**) Low magnification displays a central fibroelastotic core. Ducts are shown to be cystically dilated or collapsed around the periphery. (**b**, **c**) Medium and higher magnification of the same case showing a fibroelastotic centre as well as proliferation of ducts with a radiating pattern. Note the lumens are open and peripheral ducts have cystic change with apocrine metaplasia

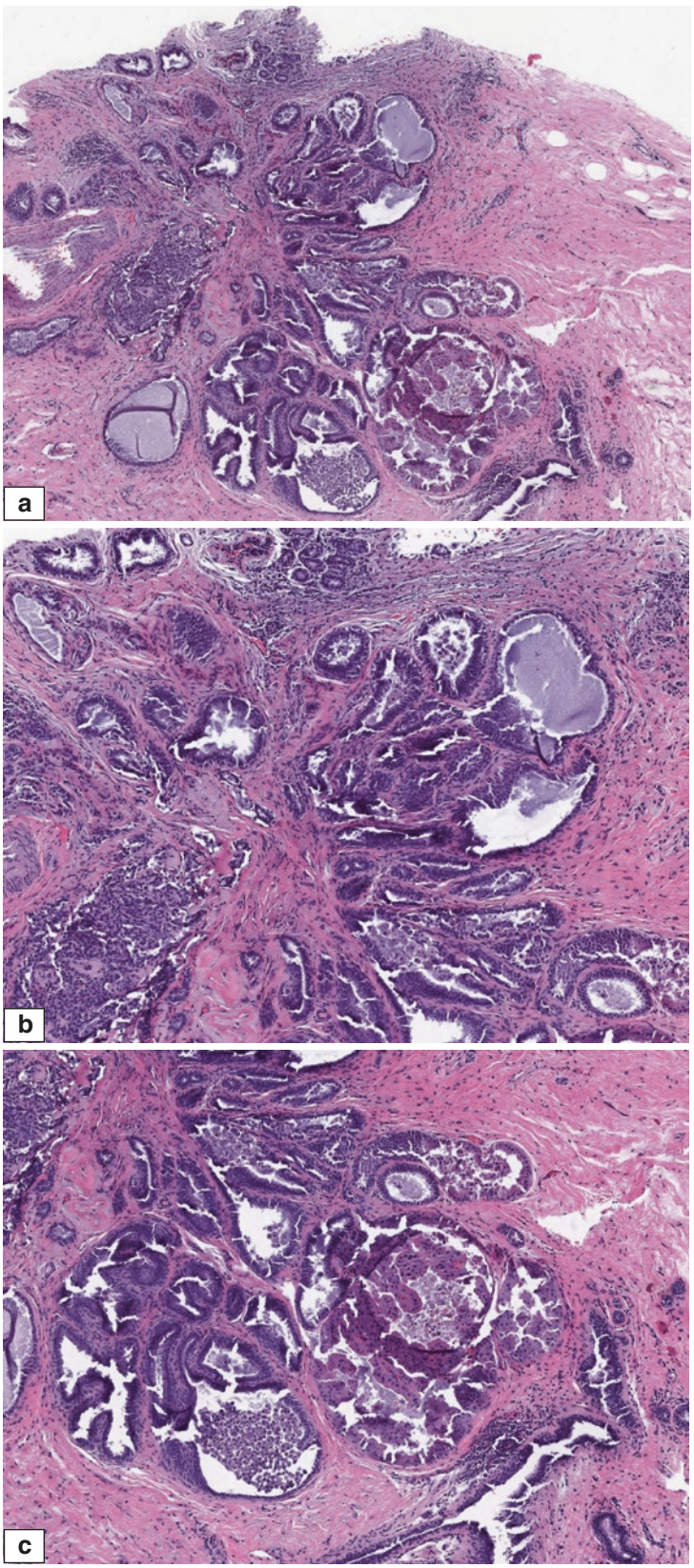

Fig. 5.17 Radial scar. Microscopic features. (**a**) Stellate ductal proliferation with central fibrosis. (**b**) Radiating ducts appear to be enlarged by epithelial hyperplasia with central ducts being smaller, angulated, and distorted by central fibrosis. (**c**) Higher magnification showing epithelial proliferation and apocrine metaplasia in peripheral ducts

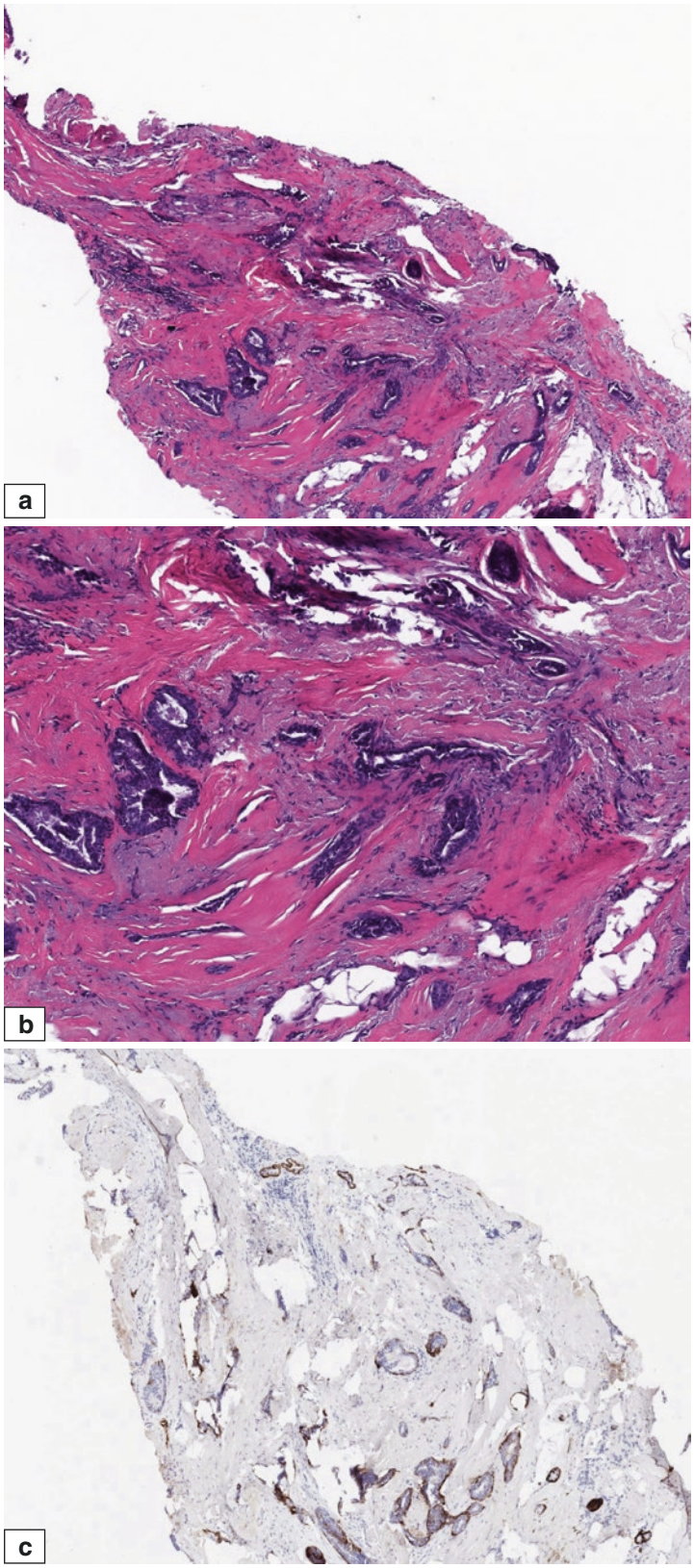

Fig. 5.18 Radial scar. Microscopic and immunohistochemical features. (**a**, **b**) Breast core needle biopsy showing irregular distribution of small ductules and tubular structures associated with hypocellular collagenized stroma. Due to marked stromal sclerosis, the tubules appear angulated and distorted, mimicking an invasive carcinoma. (**c**) Staining for smooth muscle actin highlights intact myoepithelial cells around these tubules, supporting a non-invasive nature

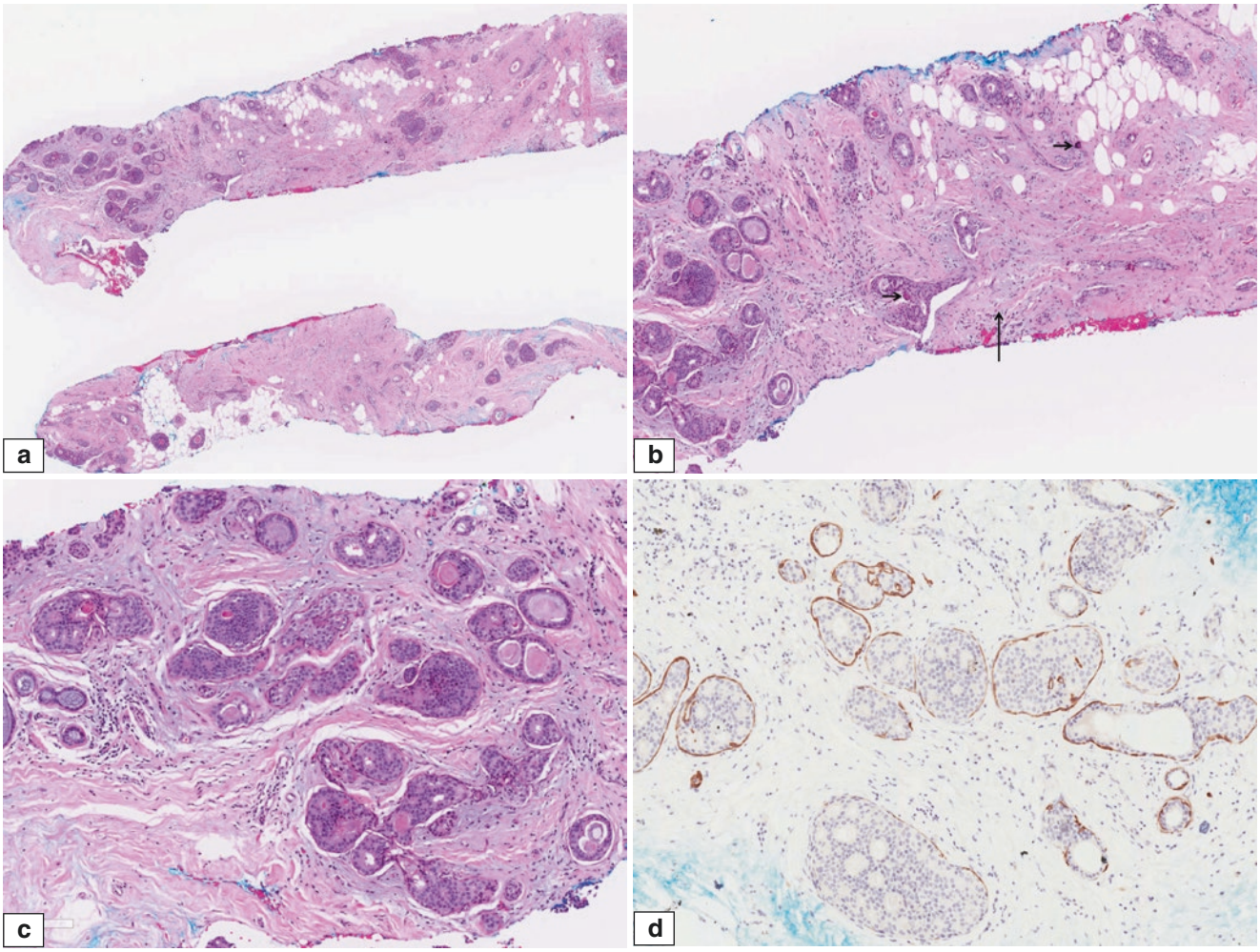

Fig. 5.19 Radial sclerosing lesion with DCIS. (**a**) Biopsy performed for a retroareolar breast distortion shows cores with fibrotic stroma and small areas of elastosis, in keeping with a radial sclerosing lesion. Several duct spaces are expanded and filled with a cribriform and solid epithelial population, observed in several cores. (**b**) Fibroelastotic stroma (*long vertical arrow*) is present. A few small calcifications are seen (*short horizontal arrows*). Ducts show a cribriform epithelial population. (**c**) Cribriform DCIS shows low nuclear grade features. (**d**) Immunohistochemistry for CK14 shows preservation of myoepithelial cells as an outer rim, while the in situ carcinoma cells are devoid of staining

Differential Diagnosis

Invasive Carcinoma

The haphazard infiltrative pattern of radial scar and complex sclerosing lesion simulates invasive carcinoma. The cytologic features of malignancy are lacking in a radial scar/complex sclerosing lesion (Table 5.1). Invasive carcinomas usually have more cytologic atypia. Immunohistochemical staining for myoepithelial cells can be helpful to confirm the absence of a myoepithelial component in invasive carcinoma, whereas radial scars show preservation of myoepithelial cells around glands (Fig. 5.17).

Prognosis and Therapy Considerations

Radial scars and complex sclerosing lesions are considered benign lesions associated with only a slightly increased risk of breast cancer, rather than being direct precursors. In most radial scar lesions, the increased risk of breast cancer is associated with the accompanying epithelial proliferation. Mammographic follow-up or complete surgical excision is the treatment of choice. If a radial scar is diagnosed on core needle biopsy and there are no atypical features, excision may not be required [25–27]. In particular, microscopic radial scars that are incidentally discovered on core needle biopsy do not require excision. Correlation with imaging and pathologic features is essential.

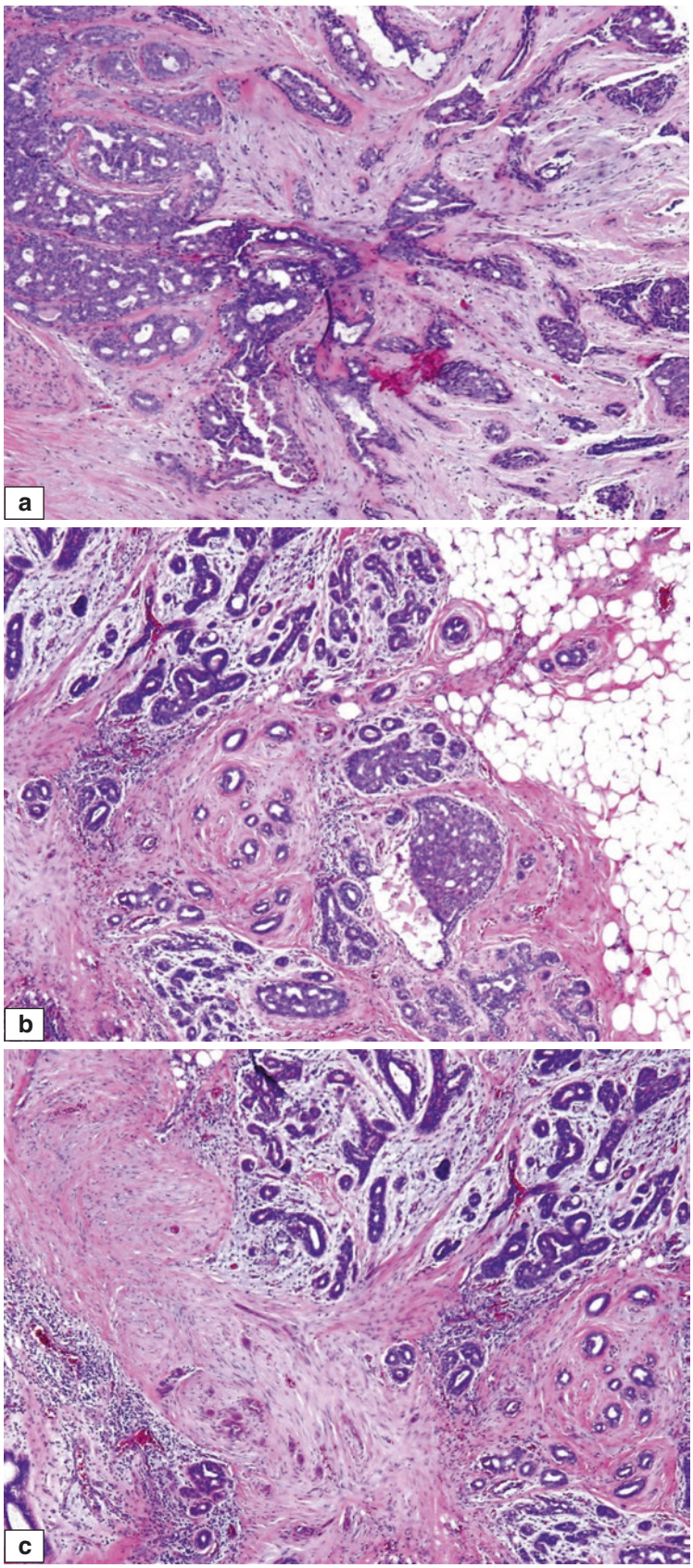

Fig. 5.20 Radial scar. Microscopic features. (**a**) Low magnification view shows a stellate arrangement of radially distributed small glands. (**b**, **c**), Medium and higher magnification showing tubular structures entrapped within the central zone mimicking invasive carcinoma

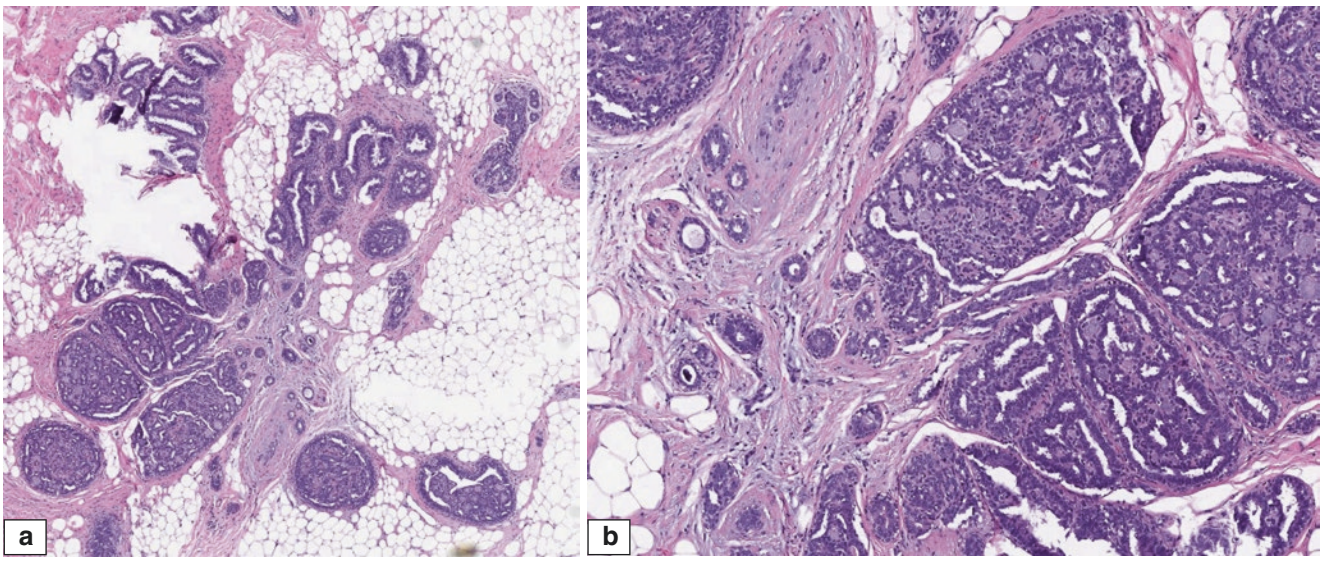

Fig. 5.21 Radial scar. Microscopic features. (**a**) The peripheral ductal spaces display epithelial proliferation. (**b**) The intraductal proliferation consists of both epithelial and myoepithelial cells, and there is collagenous spherulosis associated with the radial scar

Table 5.1 Differential diagnosis of sclerosing breast lesions

Histologic characteristics	Tubular carcinoma	Sclerosing adenosis	Radial scar/complex sclerosing lesion
Gland shape	Angulated	Round	Dilated
Gland size	Small	Small	Large
Lumen type	Open	Mostly closed	Open
Epithelial lining	Single layer	Two layers	Two layers
Gland distribution	Haphazard	Lobulocentric	Radial
Margins	Infiltrative	Circumscribed	Infiltrative
Collagen	Haphazard	Mostly prominent at periphery	Evenly distributed

References

1. Rabban JT, Sgroi DC. Sclerosing lesions of the breast. Semin Diagn Pathol. 2004;21(1):42–7.
2. D'Alfonso TM, Shin SJ. Small glandular proliferations of the breast. Surg Pathol Clin. 2012;5(3):591–643.
3. Spruill L. Benign mimickers of malignant breast lesions. Semin Diagn Pathol. 2016;33(1):2–12.
4. Brogi E. Adenosis and microglandular adenosis. In: Hoda SA, Brogi E, Koerner FC, Rosen PP, editors. Rosen's breast pathology. 4th ed. Philadelphia: Wolters Kluwer; 2014. p. 183–212.
5. Markopoulos C, Kouskos E, Phillipidis T, Floros D. Adenosis tumor of the breast. Breast J. 2003;9(3):255–6.
6. Taskin F, Köseoğlu K, Unsal A, Erkuş M, Ozbaş S, Karaman C. Sclerosing adenosis of the breast: radiologic appearance and efficiency of core needle biopsy. Diagn Interv Radiol. 2011;17(4):311–6.
7. Anderson JA, Carter D, Linell F. A symposium on sclerosing duct lesions of the breast. Pathol Annu. 1986;21(2):145–79.
8. Page DL, Simpson JF. What is apocrine adenosis, anyway? Histopathology. 2001;39(4):433–4.
9. Carter DJ, Rosen PP. Atypical apocrine metaplasia in sclerosing lesions of the breast: a study of 51 patients. Mod Pathol. 1991;4(1):1–5.
10. Seidman JD, Ashton M, Lefkowitz M. Atypical apocrine adenosis of the breast: a clinicopathologic study of 37 patients with 8.7-year follow-up. Cancer. 1996;12(12):2529–37.
11. Lee AH. Use of immunohistochemistry in the diagnosis of problematic breast lesions. J Clin Pathol. 2013;66(6):471–7.
12. de Moraes Schenka NG, Schenka AA, de Souza Queiroz L, de Almeida Matsura M, Alvarenga M, Vassallo J. p63 and CD10: reliable markers in discriminating benign sclerosing lesions from tubular carcinoma of the breast? Appl Immunohistochem Mol Morphol. 2006;14(1):71–7.
13. Werling RW, Hwang H, Yaziji H, Gown AM. Immunohistochemical distinction of invasive from noninvasive breast lesions: a comparative study of p63 versus calponin and smooth muscle myosin heavy chain. Am J Surg Pathol. 2003;27(1):82–90.
14. Pavlakis K, Zoubouli C, Liakakos T, Messini I, Keramopoullos A, Athanassiadou S, et al. Myoepithelial cell cocktail (p63 + SMA) for the evaluation of sclerosing breast lesions. Breast. 2006;15(6):705–12.
15. Taylor HB, Norris HJ. Epithelial invasion of nerves in benign diseases of the breast. Cancer. 1967;20(12):2245–9.
16. Visscher DW, Nassar A, Degnim AC, Frost MH, Vierkant RA, Frank RD, et al. Sclerosing adenosis and risk of breast cancer. Breast Cancer Res Treat. 2014;144(1):205–12.
17. Nassar A, Hoskin TL, Stallings-Mann ML, Degnim AC, Radisky DC, Frost MH, et al. Ki-67 expression in sclerosing ade-

nosis and adjacent normal breast terminal ductal lobular units: a nested case-control study from the Mayo Benign Breast Disease Cohort. Breast Cancer Res Treat. 2015;151(1):89–97.
18. Moritani S, Ichihara S, Hasegawa M, Endo T, Oiwa M, Shiraiwa M, et al. Topographical, morphological and immunohistochemical characteristics of carcinoma in situ of the breast involving sclerosing adenosis. Two distinct topographical patterns and histological types of carcinoma in situ. Histopathology. 2011;58(6):835–46.
19. Oiwa M, Endo T, Ichihara S, Moritani S, Hasegawa M, Iwakoshi A, et al. Sclerosing adenosis as a predictor of breast cancer bilaterality and multicentricity. Virchows Arch. 2015;467(1):71–8.
20. Koerner FC. Papilloma and related benign lesions. In: Hoda SA, Brogi E, Koerner FC, Rosen PP, editors. Rosen's breast pathology. 4th ed. Philadelphia: Wolters Kluwer; 2014. p. 183–212.
21. Nassar A, Conners AL, Celik B, Jenkins SM, Smith CY, Hieken TJ. Radial scar/complex sclerosing lesions: a clinicopathologic correlation study from a single institution. Ann Diagn Pathol. 2015;19(1):24–8.
22. Bianchi S, Giannotti E, Vanzi E, Marziali M, Abdulcadir D, Boeri C, et al. Radial scar without associated atypical epithelial proliferation on image-guided 14-gauge needle core biopsy: analysis of 49 cases from a single-centre and review of the literature. Breast. 2012;21(2):159–64.
23. Farshid G, Rush G. Assessment of 142 stellate lesions with imaging features suggestive of radial scar discovered during population-based screening for breast cancer. Am J Surg Pathol. 2004;28(12):1626–31.
24. Doyle EM, Banville N, Quinn CM, Flanagan F, O'Doherty A, Hill AD, et al. Radial scars/complex sclerosing lesions and malignancy in a screening programme: incidence and histological features revisited. Histopathology. 2007;50(5):607–14.
25. Resetkova E, Edelweiss M, Albarracin CT, Yang WT. Management of radial sclerosing lesions of the breast diagnosed using percutaneous vacuum-assisted core needle biopsy: recommendations for excision based on seven years of experience at a single institution. Breast Cancer Res Treat. 2011;127(2):335–43.
26. Lee KA, Zuley ML, Chivukula M, Choksi ND, Ganott MA, Sumkin JH. Risk of malignancy when microscopic radial scars and microscopic papillomas are found at percutaneous biopsy. AJR Am J Roentgenol. 2012;198(2):W141–5.
27. Berg JC, Visscher DW, Vierkant RA, Pankratz VS, Maloney SD, Lewis JT, et al. Breast cancer risk in women with radial scars in benign breast biopsies. Breast Cancer Res Treat. 2008;108(2):167–74.

Mucinous Lesions

6

Mucinous breast lesions represent a heterogeneous group of entities that are described together based on the presence of predominantly extracellular mucin as a common feature. Intracytoplasmic mucin may be seen rarely as part of benign metaplasia, but are more frequently observed in invasive and in situ carcinomas [1]. Mucinous breast lesions listed in the chapter range from benign conditions like cysts and dilated ducts with luminal mucin to mucocele-like lesions that can be associated with a range of epithelial proliferations, and to mucin-producing malignant neoplasms of mucinous carcinoma and solid papillary carcinoma with mucin production.

Cysts with Luminal Mucin and Mucinous Metaplasia

Definition

Cysts of varying sizes, commonly encountered in breast biopsies, comprise dilated ducts within fibrous parenchyma. While microscopic breast cysts are commonly encountered incidentally on histological assessment of breast tissue, duct dilatation can be minimal to significant, forming cysts that may be clinically symptomatic. These cysts often contain luminal secretions which are granular and eosinophilic. On occasion however luminal mucin which distends the ducts, may be observed.

Clinical and Epidemiological Features

Mild cystic changes of the breast are asymptomatic. The exact incidence of breast cysts is unknown; they are likely to be widely prevalent. When cystic dilatation is marked, patients may present with mastalgia, breast lumps, or lumpiness. Luminal mucin in ducts has been reported in 6 % of normal breasts, compared to its occurrence in benign ducts of 80 % of breasts containing mucinous carcinoma [2].

Imaging Features

Breast cysts can be seen on imaging. Scattered or loose groups of luminal microcalcifications are commonly observed on mammography. In particular, layering of calcium in microcysts giving rise to a teacup appearance on mammography is unique to cystic changes in the breast (Fig. 6.1).

Pathologic Features

Macroscopic Pathology

Breast cysts may be macroscopically occult. They are often associated with fibrous areas in the breast parenchyma within which are scattered small cysts (Fig. 6.2).

Microscopic Pathology

Breast lobules show variable dilatation of ducts and acini within fibrous stroma. Luminal mucin can occur as small amounts of wispy, acellular material within dilated ducts or as more abundant mucin that distends ducts (Fig. 6.3). Calcifications may be observed within the mucin (Fig. 6.4). When there is marked ductal distension with rupture and extrusion of mucin into surrounding stroma, the diagnosis of mucocele-like lesion is appropriate.

P.H. Tan, A.A. Sahin, *Atlas of Differential Diagnosis in Breast Pathology*, Atlas of Anatomic Pathology,
DOI 10.1007/978-1-4939-6697-4_6

Mucinous metaplasia is an uncommonly encountered microscopic alteration in the breast, in which lining epithelial cells show mucinous cytoplasm (Figs. 6.5 and 6.6).

Differential Diagnosis

Cystic Changes with Luminal Mucin Versus Mucocele-Like Lesion

The key difference between these lesions is the degree of distension of ducts by luminal mucin. Marked duct distension with mucin extravasation into surrounding stroma indicates a mucocele-like lesion. Calcifications superimposed on mucin may be observed in both conditions.

Mucinous Metaplasia Versus Mucoepidermoid Carcinoma

Mucoepidermoid carcinoma is a rare, salivary-gland type of breast cancer; in its low-grade variety, it may show a prevalence of mucous cells that can resemble mucinous metaplasia [3]. However, mucinous metaplasia does not show additional features of low-grade mucoepidermoid carcinoma such as the presence of intermediate and squamous cells, apart from the invasive nature of the latter (Fig. 6.7).

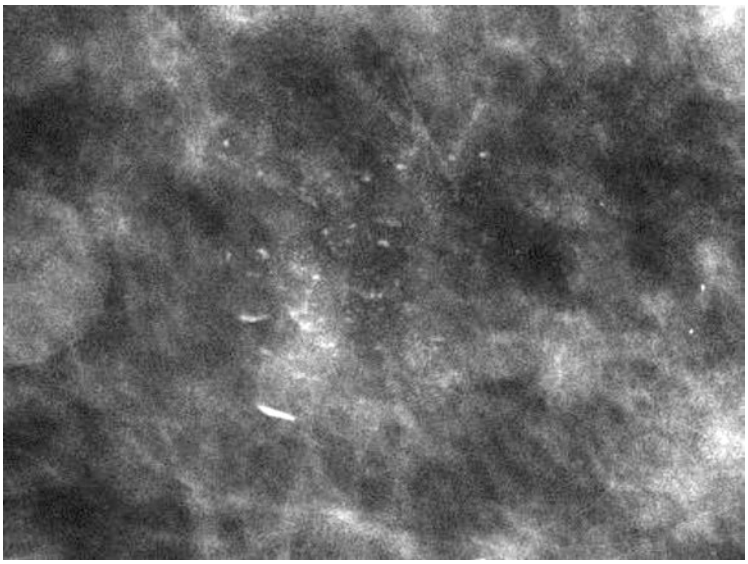

Fig. 6.1 Mammographic appearance of breast cysts. Magnification view in the true lateral projection shows teacups or layering of calcifications in the dependent aspect of microcysts (Courtesy of Dr. Lester Leong)

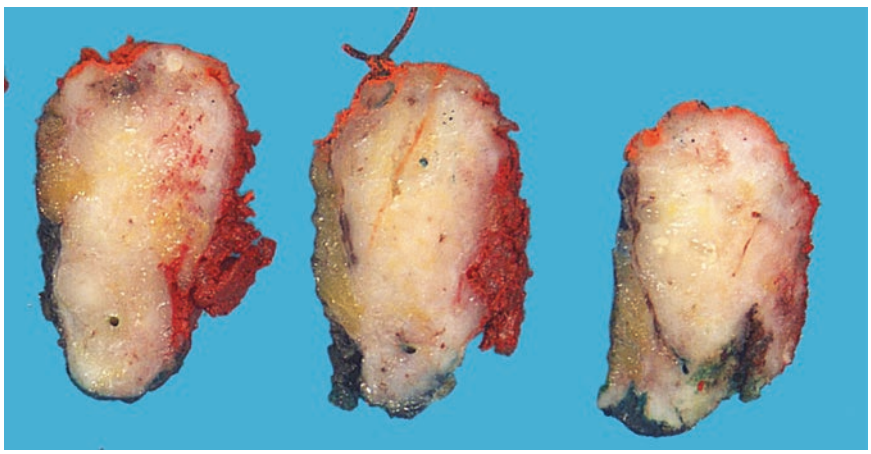

Fig. 6.2 Breast cystic change. Gross appearance shows ill-defined fibrous areas with scattered small cysts

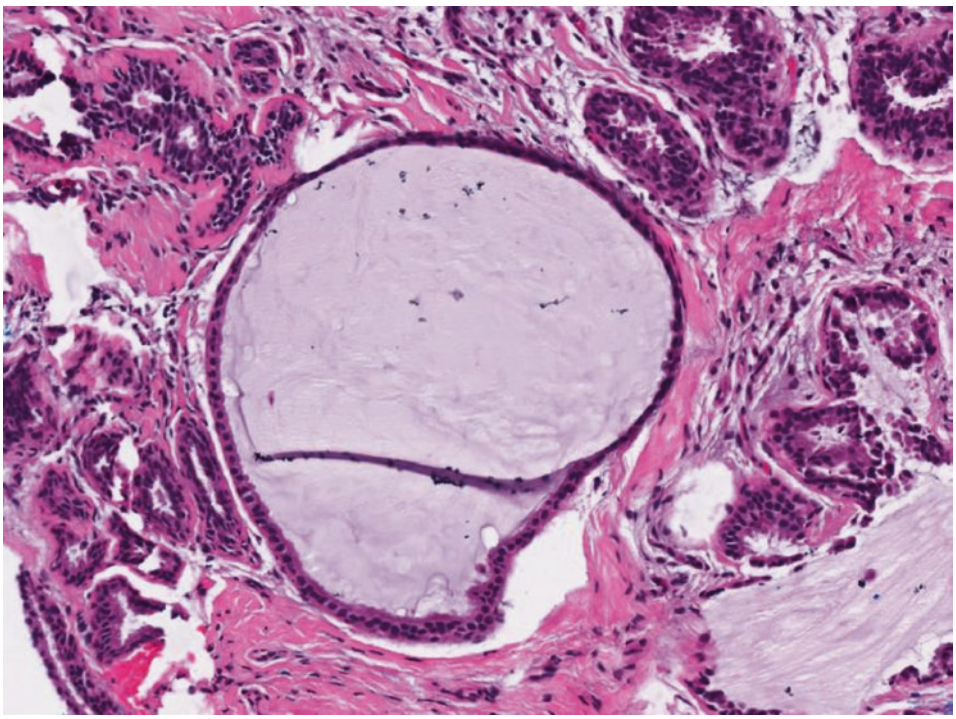

Fig. 6.3 Breast cyst with luminal mucin. Cystically dilated ducts contain luminal mucin. Although the lining of one of the affected ducts appears to be incomplete, no convincing extrusion of mucin into the surrounding stroma is seen. If there is mucin extravasation, the diagnosis of mucocele-like lesion is appropriate

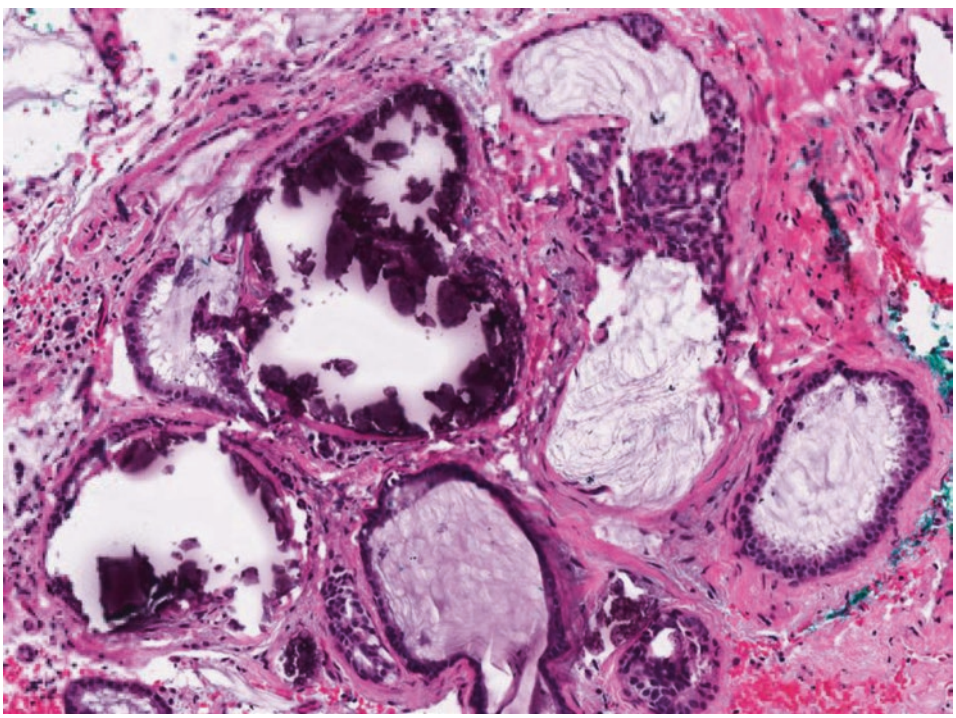

Fig. 6.4 Cystically dilated ducts contain luminal mucin and calcifications

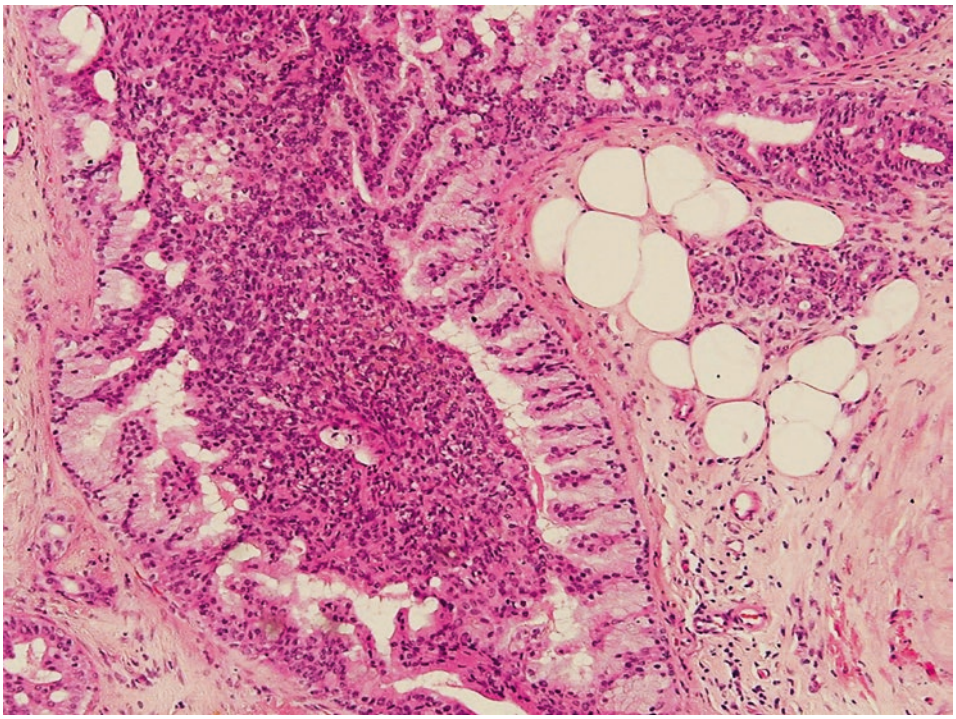

Fig. 6.5 A duct shows mucinous metaplasia of lining cells with basally oriented nuclei and mucinous cytoplasm. The duct architecture is preserved, with an outer rim of myoepithelial cells, with florid usual ductal hyperplasia filling the lumen

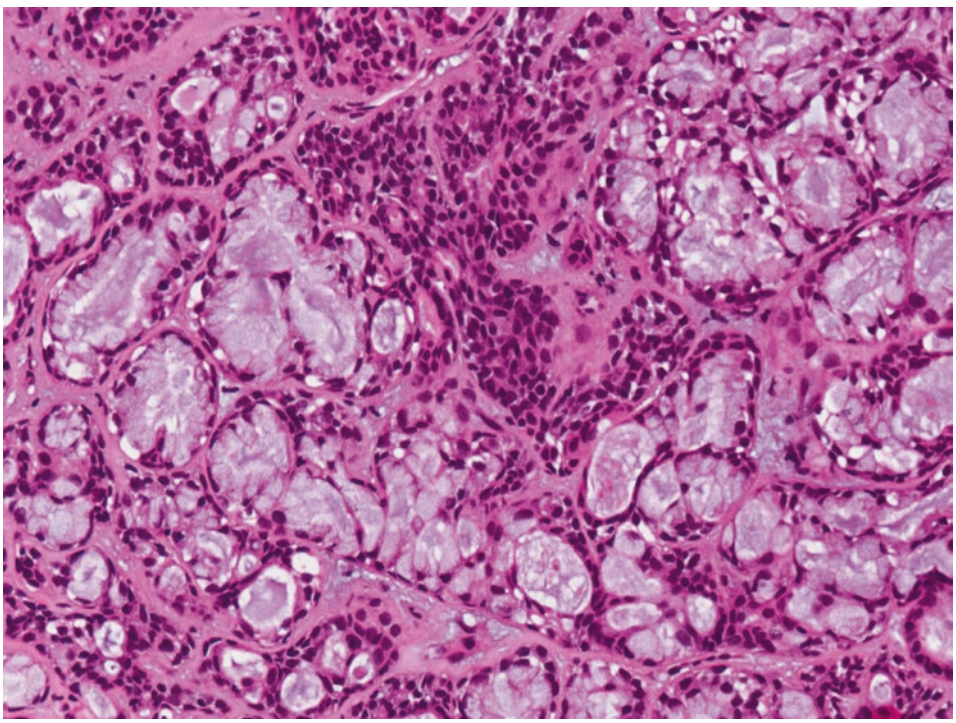

Fig. 6.6 Mucinous metaplasia observed within an intraductal papilloma. The underlying papillary architecture is not well appreciated at this high magnification. Here, mucinous cells replace the lining epithelium of tubules within the intraductal papilloma. Some luminal mucin is also found in the glands lined by mucinous cells

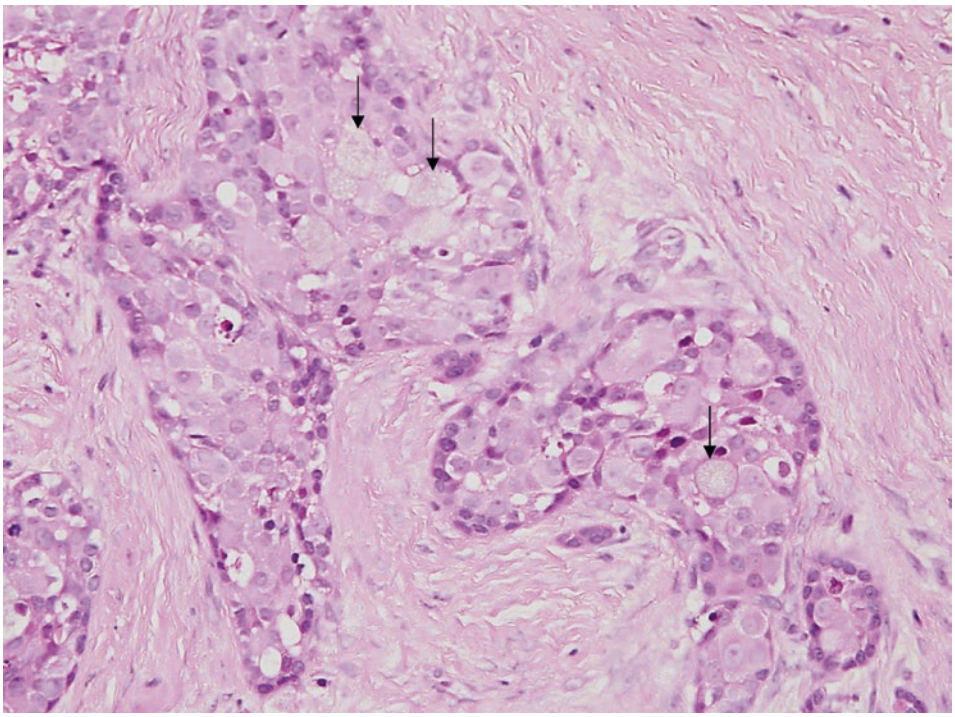

Fig. 6.7 Mucoepidermoid carcinoma. Invasive tumour islands incorporating mucinous cells (*arrows*) are seen within fibrotic stroma

Prognosis and Therapy Considerations

Breast cysts with luminal mucin and mucinous metaplasia have no clinical impact. Cysts can be accompanied by proliferative epithelial changes that may have corresponding risk implications for subsequent breast cancer development.

Mucocele-Like Lesions

Definition

Mucocele-like lesions (MLL) are defined by the presence of cysts and dilated ducts distended by mucin with associated rupture and mucin seepage into the surrounding breast stroma. The term "lesion" is preferred over "tumour", as the accompanying epithelial changes are often not neoplastic. Associated epithelial alterations are assessed separately.

Clinical and Epidemiological Features

The incidence of MLL is not known, though these lesions are increasingly detected in the mammographic era because of the occurrence of calcifications. Large MLL may present clinically as breast lumps.

Imaging Features

Clustered, coarse microcalcifications with or without a lobulated mass may be observed (Fig. 6.8).

Pathologic Features

Macroscopic Pathology

Mucin-containing cysts within fibrous stroma and grittiness related to calcifications can be present (Figs. 6.9 and 6.10).

Microscopic Pathology

Cysts distended by luminal mucin with mucin extravasation into the stroma are present. The lining of the mucin-filled cysts may be flattened, attenuated benign epithelium, or it may show a variety of alterations including usual ductal hyperplasia, columnar cell change, columnar cell hyperplasia, flat epithelial atypia, atypical ductal hyperplasia (ADH), and ductal carcinoma in situ (DCIS). Coarse calcifications may be seen in luminal and extruded mucin (Figs. 6.11, 6.12, and 6.13).

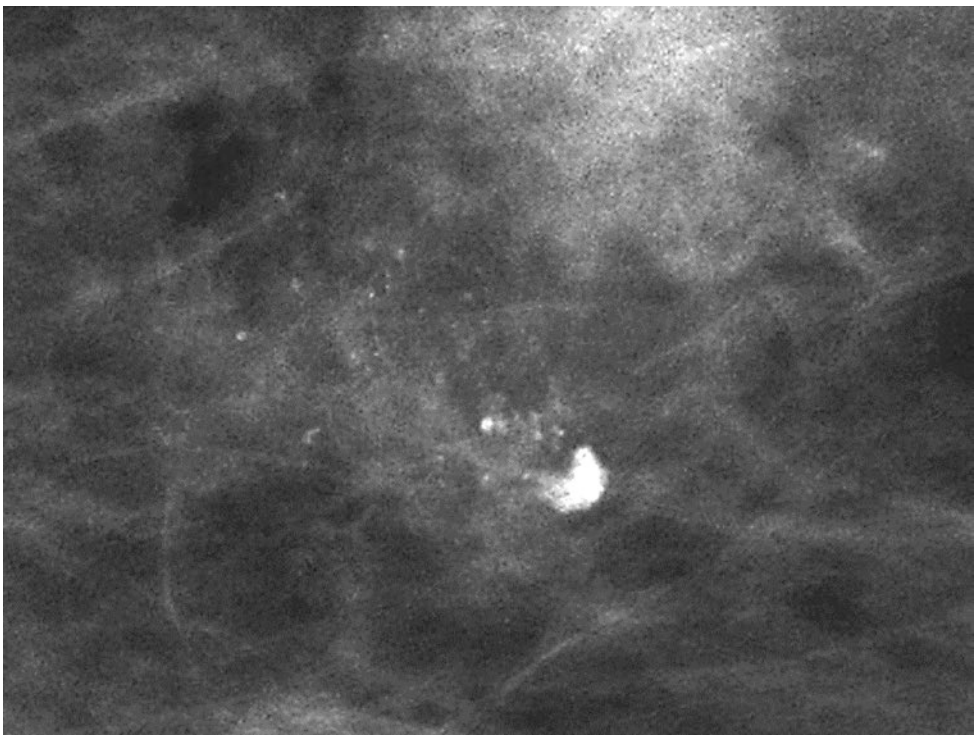

Fig. 6.8 Mucocele-like lesion. Magnification mammogram view shows a cluster of fine granular and amorphous microcalcifications together with a focus of coarse calcification (Courtesy of Dr. Lester Leong)

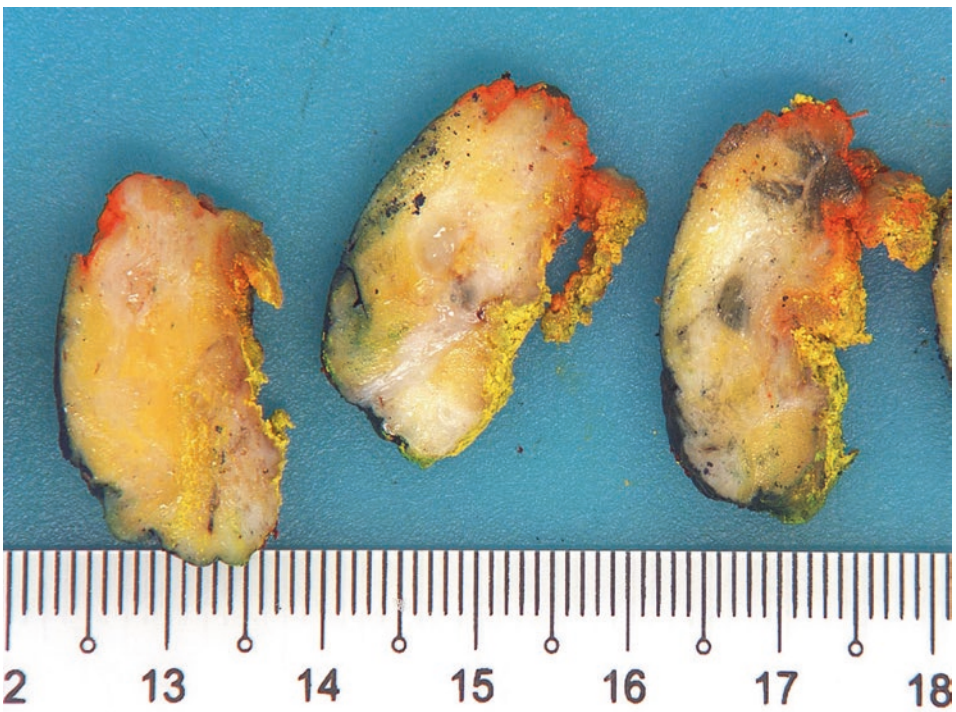

Fig. 6.9 Mucocele-like lesion with calcifications. Hookwire localisation excision specimen (hookwire has been removed) shows cysts with mucoid material on cut sections, within a fibrofatty parenchyma. Calcifications were identified histologically

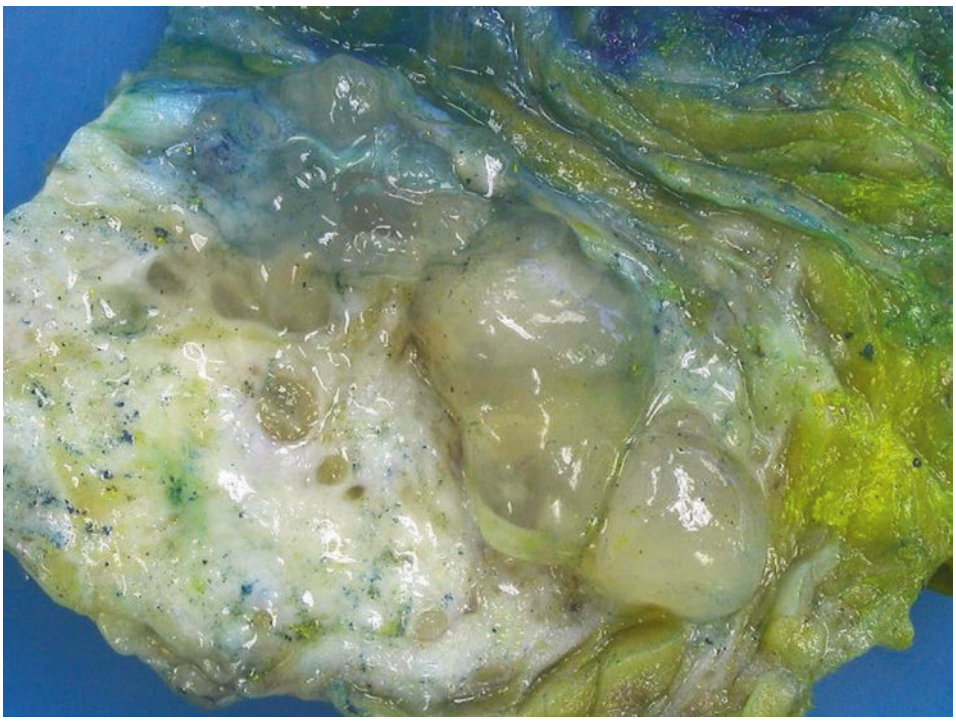

Fig. 6.10 Mucocele-like lesion with ductal carcinoma in situ (DCIS). Macroscopically, viscid mucin is seen extruding from the cut surface. DCIS was found on histological examination

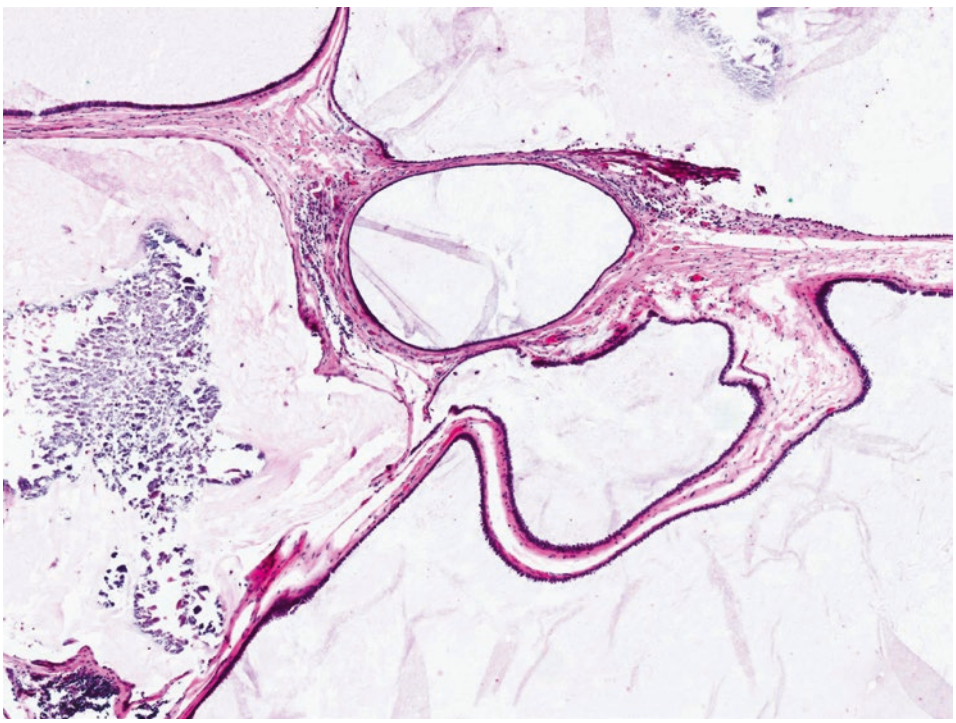

Fig. 6.11 Benign mucocele-like lesion with calcifications. Cystically dilated ducts are lined by attenuated epithelium without any cytoarchitectural atypia. Calcifications are observed within the mucin

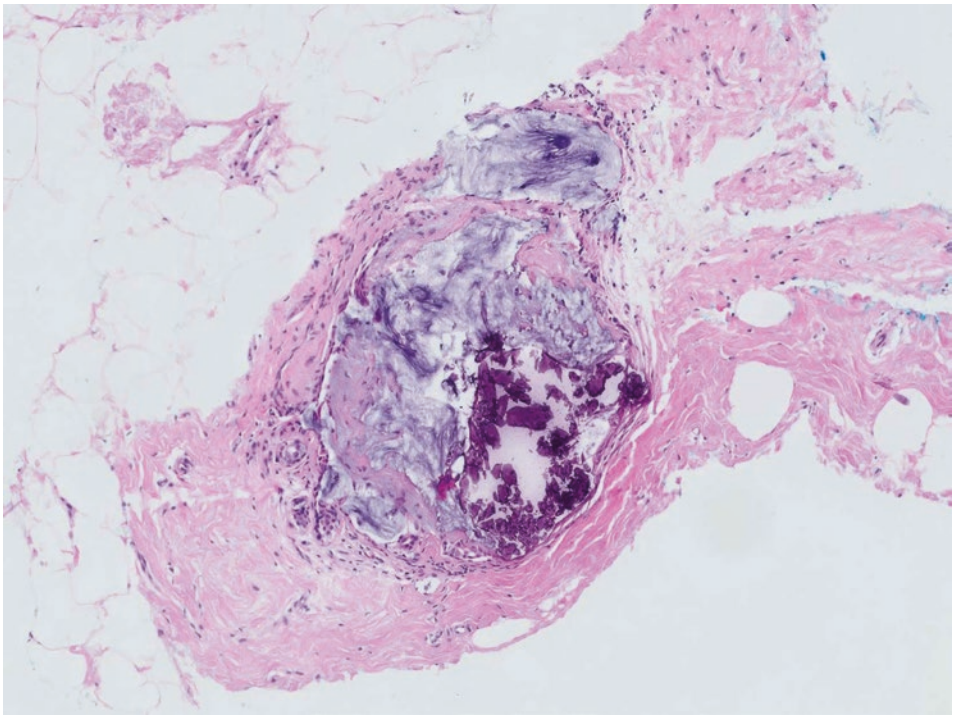

Fig. 6.12 Mucocele-like lesion with calcifications seen on core biopsy of mammographically detected calcifications

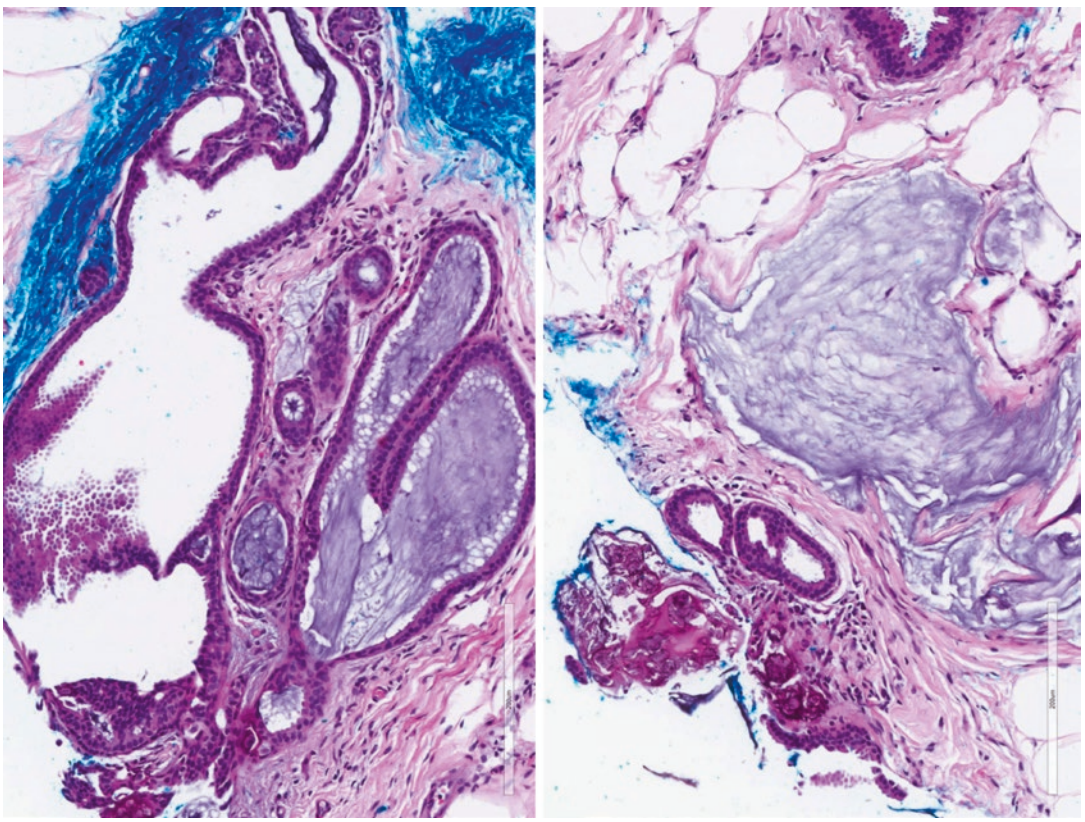

Fig. 6.13 Mucocele-like lesion on core biopsy. Cystically dilated ducts containing luminal mucin are present, with stromal mucin extravasation and scattered calcifications

Differential Diagnosis

MLL with ADH Versus MLL with Low Nuclear Grade DCIS

The distinction between MLL with ADH and MLL with low nuclear grade DCIS (Figs. 6.14 and 6.15) follows usual qualitative and quantitative criteria used to distinguish between these two lesions, with ADH diagnosed when duct spaces are only partially involved by the atypical epithelial population or when the lesional size does not exceed 2 mm. As MLL features dilated cysts, it may be difficult to apply the 2-mm size criterion. Using the involvement of two duct spaces as a diagnostic guide may be a practical alternative, although caution needs to be exercised in order not to overdiagnose small foci of atypical epithelial changes as DCIS. An appraisal of the entire lesion and a careful assessment of the extent of the atypical epithelial alterations are required.

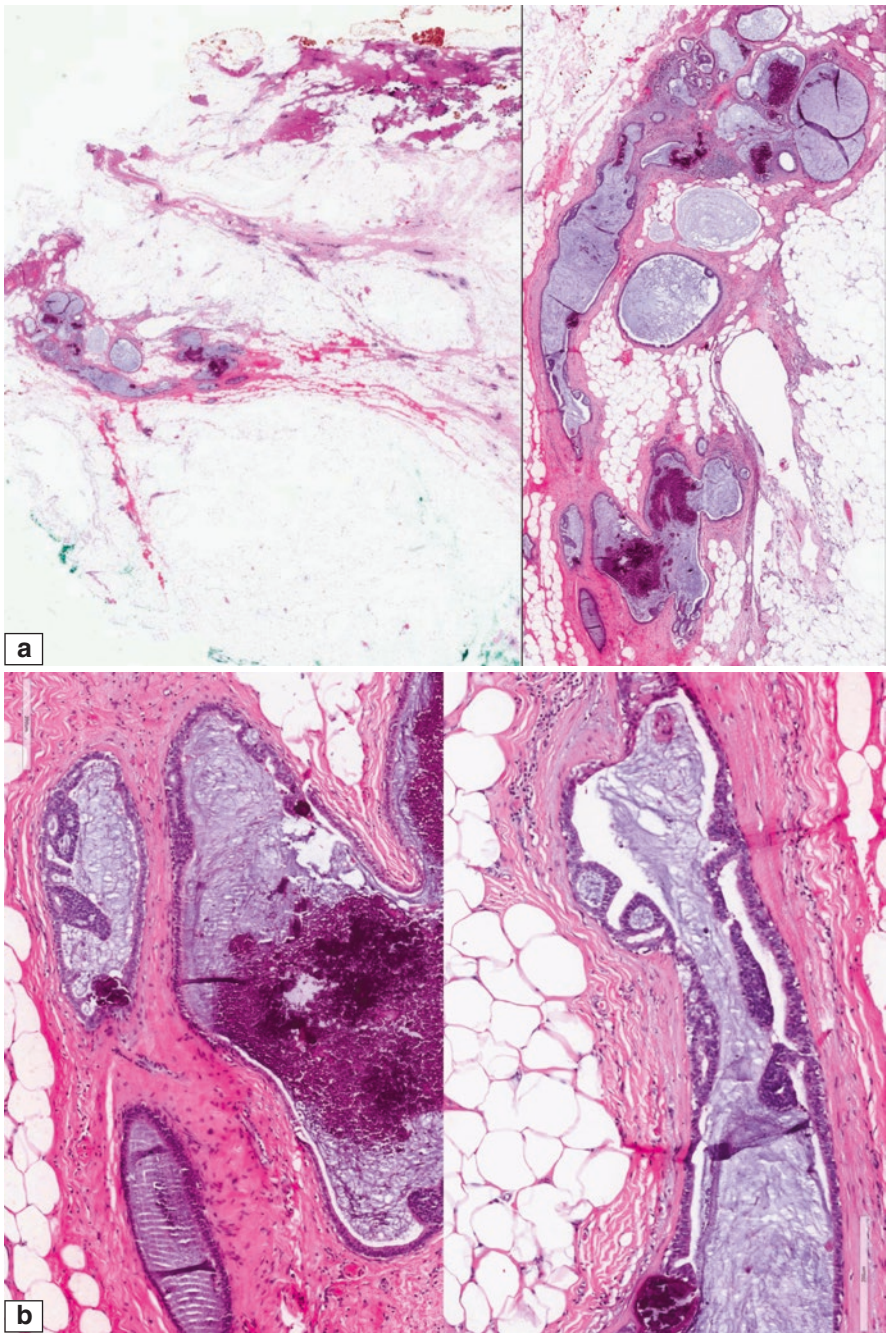

Fig. 6.14 (**a**) Mucocele-like lesion with a borderline lesion for which the differential diagnosis is between atypical ductal hyperplasia versus low nuclear grade ductal carcinoma in situ. Excision biopsy shows a cluster of cystically dilated ducts filled with mucin, accompanied by coarse calcifications. Several ducts show architectural atypia with arches and micropapillary projections which may be difficult to appreciate at this magnification. (**b**) On higher magnification, the ducts show rigid arches and cribriform spaces, with involvement of at least two duct spaces. Luminal mucin and calcifications are present. The lesional extent measured more than 2 mm, fulfilling the size criterion of DCIS, although size assessment may be challenging in these markedly distended ducts. Lesser degrees of involvement warrant a diagnosis of atypical ductal hyperplasia (ADH)

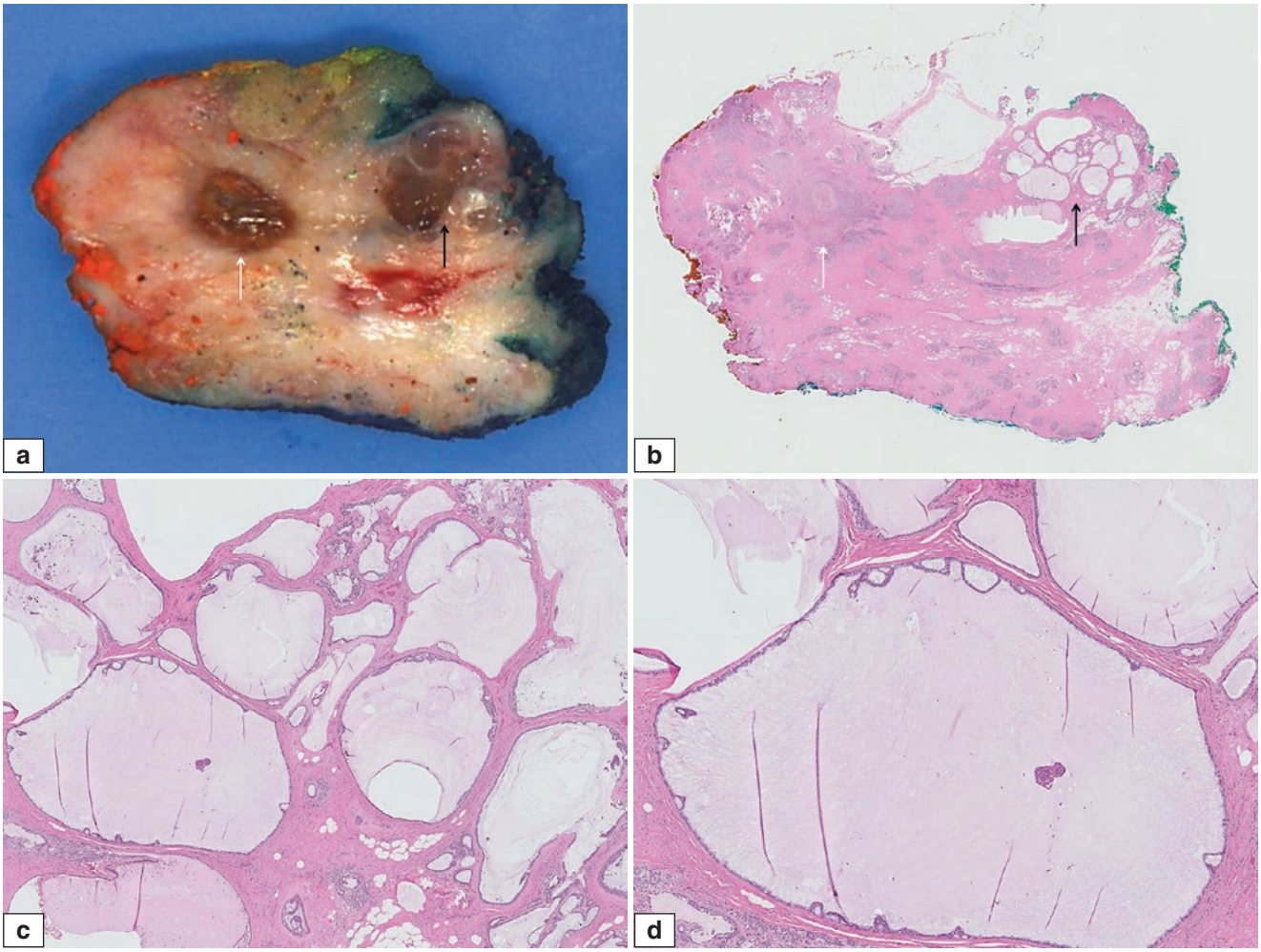

Fig. 6.15 Mucocele-like lesion with ductal carcinoma in situ. (**a**) Hookwire localisation excision biopsy of radiologically detected calcifications in the right breast shows a cluster of mucin-filled cysts near the tissue edge (*black arrow*). A yellowish-brown nodule (*white arrow*) is present, representing the previous mammotome biopsy site. Histological findings of the prior mammotome biopsy showed a mucocele-like lesion with atypical ductal hyperplasia accompanied by calcifications. (**b**) Corresponding histological section reveals distended cysts (*black arrow*) aggregated near the inked surgical edge of the tissue. The previous mammotome biopsy site is noted (*white arrow*). (**c**) The cystically dilated ducts are lined by flattened epithelium that is punctuated by rigid epithelial arches. Mucin distends the duct lumens, with spillage into the surrounding stroma. While the degree of epithelial architectural atypia depicted in this illustration may not qualify for a diagnosis of low grade ductal carcinoma in situ and may be considered atypical ductal hyperplasia in the absence of further ductal epithelial abnormalities, presence of a greater extent (> 2mm; or 2 or more affected ducts) of cytoarchitecturally abnormal epithelial changes could be regarded as ductal carcinoma in situ. Careful assessment of the extent of involvement is important to avoid overdiagnosing small foci of atypical epithelial alterations as ductal carcinoma in situ. (**d**) Higher magnification shows cytoarchitecturally abnormal epithelial changes in the wall of this distended duct. Stiff epithelial arches with secondary rigid lumens are seen. These abnormal alterations were found in several contiguous sections of the breast tissue, indicating a significant disease extent fulfilling the size criterion of low nuclear grade ductal carcinoma in situ

MLL Versus Cystic Hypersecretory Breast Lesions

MLL may resemble cystic hypersecretory hyperplasia and cystic hypersecretory carcinoma with similar cystically dilated ducts. However, the luminal contents differ, with mucin in MLL and colloid-like eosinophilic material in cystic hypersecretory lesions (Fig. 6.16).

MLL Versus Mucinous Cystadenocarcinoma

Mucinous cystadenocarcinoma is a vanishingly rare lesion resembling that reported in the pancreas and ovary [4]. It resembles MLL because of the presence of cystically dilated, mucin-filled ducts, but it differs from MLL because of its tall, columnar mucinous cells with basally oriented nuclei, and hormone receptor negativity (Fig. 6.17).

MLL with Detached Epithelium Versus Mucinous Carcinoma

Disruption of cyst walls in MLL can dislodge epithelium into the extruded mucin pools, raising concern for a mucinous carcinoma histologically (Fig. 6.18). This diagnosis is especially problematic when the MLL is accompanied by DCIS, making the detached epithelium similarly neoplastic and suspicious for mucinous carcinoma when found suspended within mucin (Figs. 6.19 and 6.20).

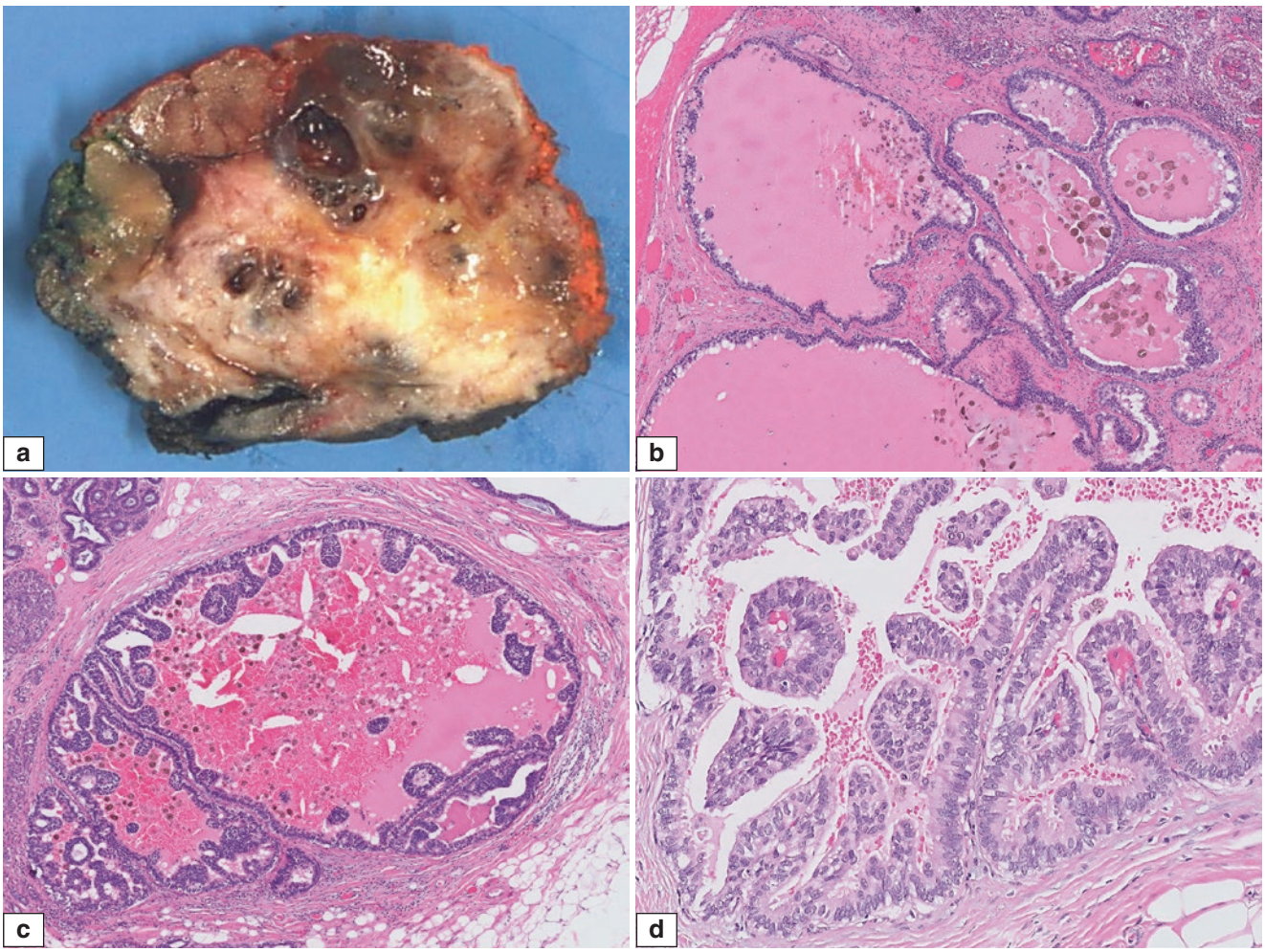

Fig. 6.16 Cystic hypersecretory carcinoma (in situ). (**a**) Macroscopic specimen shows clusters of cysts of varying sizes within a fibrous parenchyma. (**b**) Histologically, dilated ducts are filled with luminal pink proteinaceous secretions resembling colloid. Haemosiderophages are also present. The ducts are lined by columnar epithelium with micropapillary protrusions into the lumens. At this magnification and in this focus, cytoarchitectural abnormalities are not well appreciated. (**c**) Here, ducts are lined by uniform epithelial cells forming stiff arcades and rigid lumens, with micropapillary tufts projecting into distended lumens containing pink secretions admixed with blood and haemosiderophages. (**d**) High magnification shows columnar cells with stratified vesicular nuclei and occasionally discernible nucleoli lining the cystic duct wall as well as the papillary projections. Small amounts of pink secretions with red blood cells and haemosiderophages are seen in the lumen.

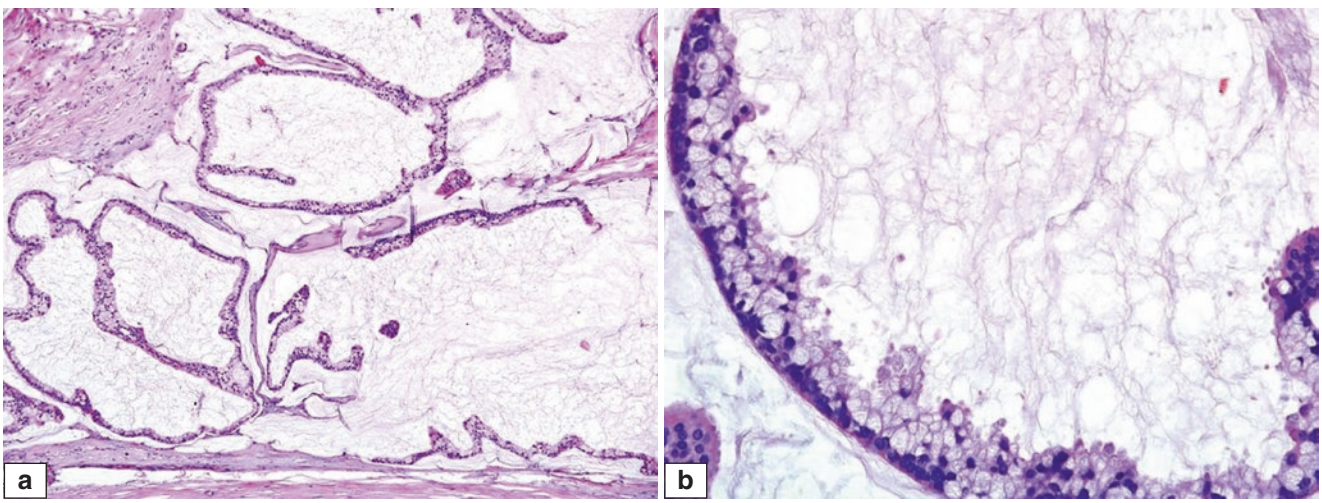

Fig. 6.17 Mucinous cystadenocarcinoma. (a) Low magnification shows cystically dilated ducts filled with luminal mucin, resembling the mucocele-like lesion. (b) High magnification shows neoplastic cells containing cytoplasmic mucin with basally oriented nuclei lining the dilated duct. Wispy luminal mucin is present (Courtesy of Dr Thomas Putti)

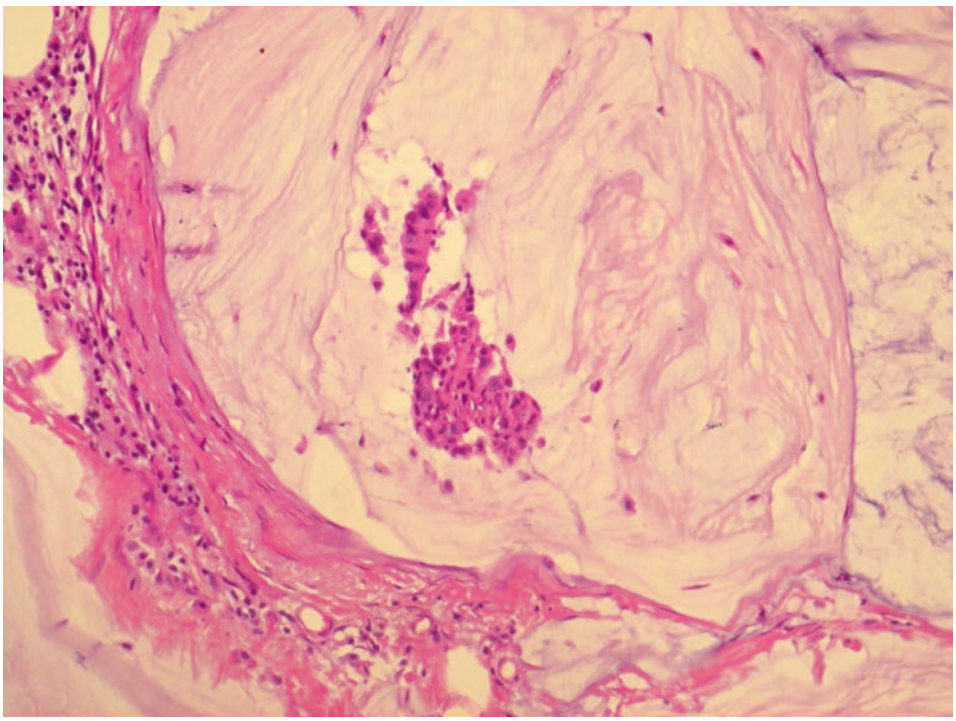

Fig. 6.18 Mucocele-like lesion with detached epithelium. Sometimes, detached clusters of epithelium may be observed within extravasated mucin pools of MLL. Distinguishing this finding from mucinous carcinoma may be challenging. Clues are the focal nature and heterogeneous appearance of the epithelial cells, including the presence of myoepithelial cells, which may sometimes be demonstrated with immunohistochemistry. On deeper levels, the focus is often diminished. Additionally, if the rest of the lesion shows no atypical epithelial changes, it is unlikely that the detached epithelium would reflect a neoplastic process

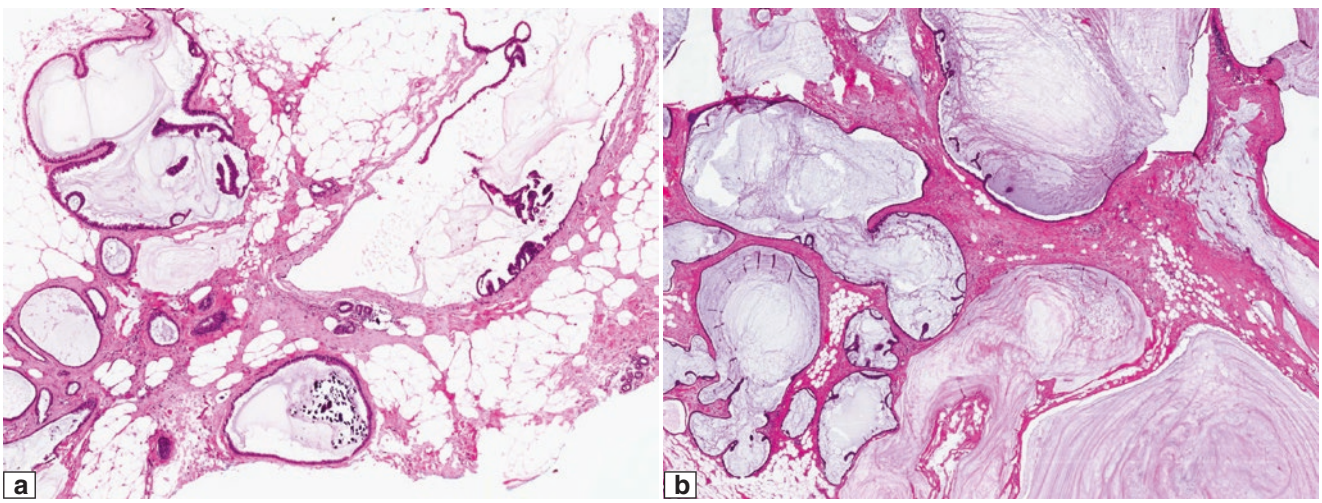

Fig. 6.19 Mucocele-like lesion with DCIS and detached epithelium. (**a**) Here, epithelial detachment is confined to the lumens of affected ducts. Consideration for mucinous carcinoma does not arise. (**b**) Several mucin-distended ducts show abnormal epithelial lining. Acellular mucin lakes are seen in the surrounding stroma. No floating neoplastic epithelium is present to suggest a mucinous carcinoma. Deeper levels are useful to exclude the possibility of an accompanying early invasive mucinous carcinoma

A practical approach is to review the epithelial changes in the MLL. If they are entirely benign, benignity for the detached epithelium is likely [5]. The diagnosis may be more challenging if ADH and/or DCIS accompanies the MLL. If the detached epithelial nests are few, focal, and observed in the vicinity of previous instrumentation tracts, they are unlikely to represent invasive carcinoma. Immunohistochemistry for the presence of myoepithelial cells may be helpful in indicating a non-invasive process, but only if positive. It is acknowledged, however, that sometimes it may be difficult to be entirely sure, and the possibility of microinvasion cannot be ruled out.

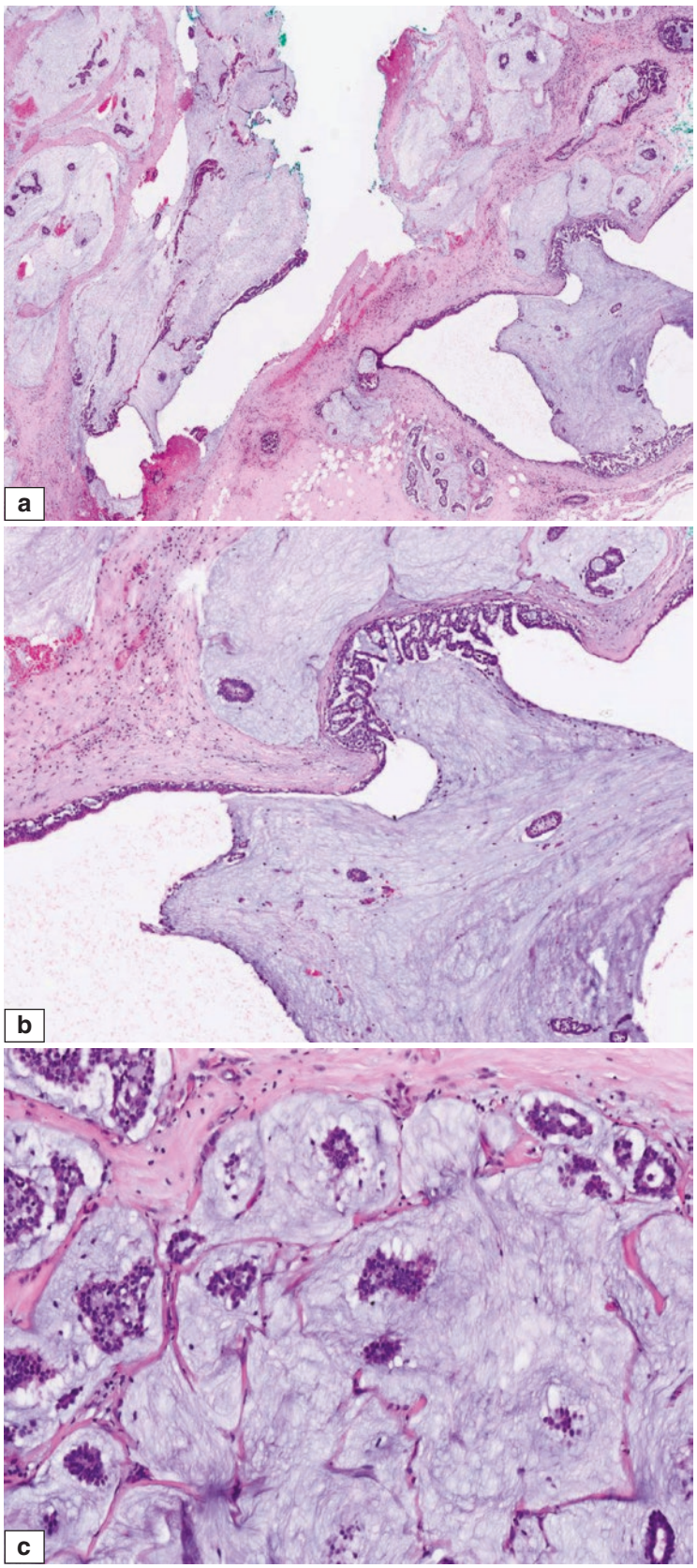

Fig. 6.20 Mucocele-like lesion with DCIS and adjacent mucinous carcinoma. (**a**) Many epithelial clusters are seen floating within extracellular mucin, adjacent to mucin-distended ducts with DCIS. (**b**) This duct, which is distended by mucin, shows features of low nuclear grade DCIS. In the adjacent stroma are pools of mucin with floating neoplastic epithelium, features of mucinous carcinoma. (**c**) Mucinous carcinoma adjacent to mucocele-like lesion with DCIS. The mucinous carcinoma comprises epithelial clusters that are completely surrounded by mucin pools

Some authors have described neovascularisation in mucinous DCIS, postulating that neoplastic mucin promotes formation of vessels and subsequent invasion of tumour cells into mucinous stroma [6]. This finding may be a subtle but helpful clue in favouring the presence of a malignant neoplastic process (Fig. 6.21).

Prognosis and Therapy Considerations

MLL with benign epithelial changes found on excision specimens do not require follow-up. Whether MLL with benign epithelial alterations on core biopsy require surgical excision is debatable [7]. It has been advocated that observation may be appropriate when there is no epithelial atypia or when all radiological calcifications associated with MLL have been removed through biopsy [8–10]. MLL with atypia or DCIS on core biopsy needs to be excised. MLL with ADH in excisions is managed with high-risk screening; MLL with DCIS in excisions is managed with complete resection.

Mucinous Carcinoma

Definition

Mucinous carcinoma, also known as mucoid, colloid or gelatinous carcinoma, consists of malignant epithelial nests floating within extracellular mucin.

Clinical and Epidemiological Features

Mucinous carcinoma is reported to account for about 2 % of all breast cancers, occurring in older women usually above 55 years of age.

Imaging Features

Mammographically, it presents as a dense mass (Fig. 6.22). The borders are slightly ill-defined, but there can be partially circumscribed margins. The mucinous contents give rise to posterior enhancement on sonography and high T2W signal on MRI, mimicking a benign mass.

Pathologic Features

Macroscopic Pathology

Mucinous carcinoma consists of a mucinous or gelatinous mass. It is grossly circumscribed and may demonstrate haemorrhage and lobulated contours (Figs. 6.23, 6.24, 6.25, and 6.26).

Microscopic Pathology

Malignant epithelial nests, usually with low or intermediate nuclear grade, are seen within mucin pools (Fig. 6.27). Both paucicellular (Capella type A) (Fig. 6.28) and hypercellular (Capella type B) (Fig. 6.29) tumours are described. Mucinous carcinoma is usually hormone receptor positive and human epidermal growth factor receptor 2 (HER2) negative (Fig. 6.30). Hypercellular mucinous carcinoma often demonstrates neuroendocrine differentiation (Figs. 6.31 and 6.32).

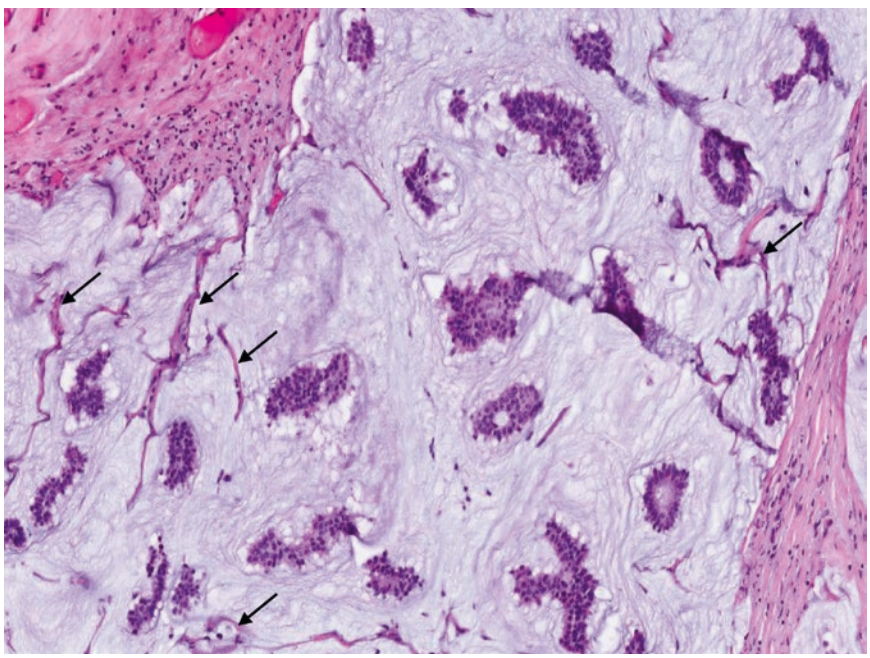

Fig. 6.21 Mucinous carcinoma. Malignant epithelial nests are floating within mucin pools. Narrow, delicate connective tissue septa with fine, subtle thin-walled vessels are present within the mucin (*arrows*), indicating neovascularization

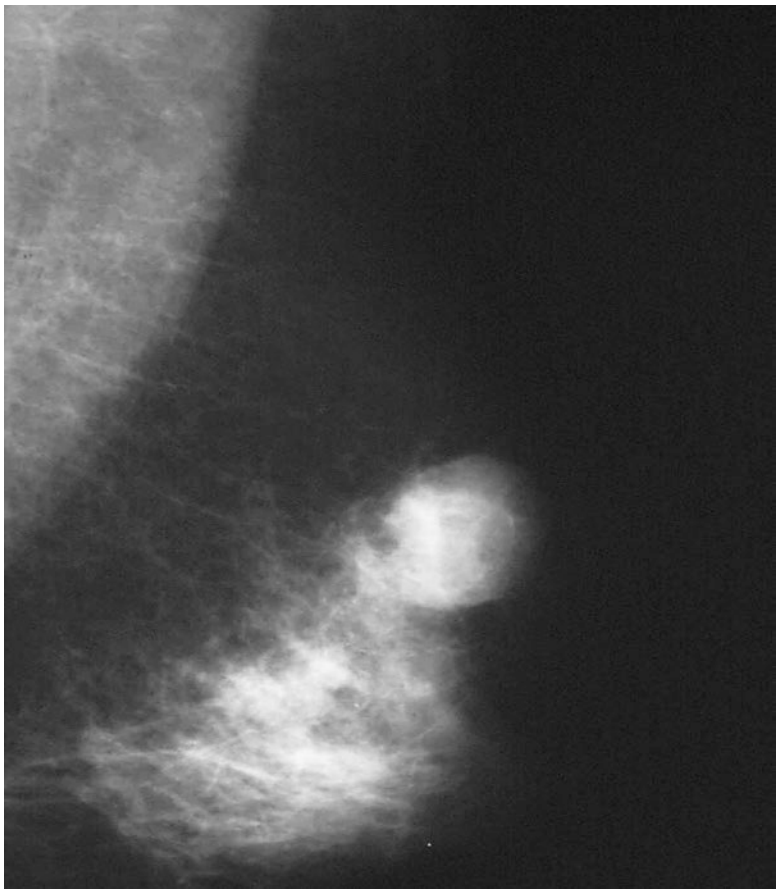

Fig. 6.22 Radiology of mucinous carcinoma. On mammography, a rounded mass is present, which may mimic a benign lesion

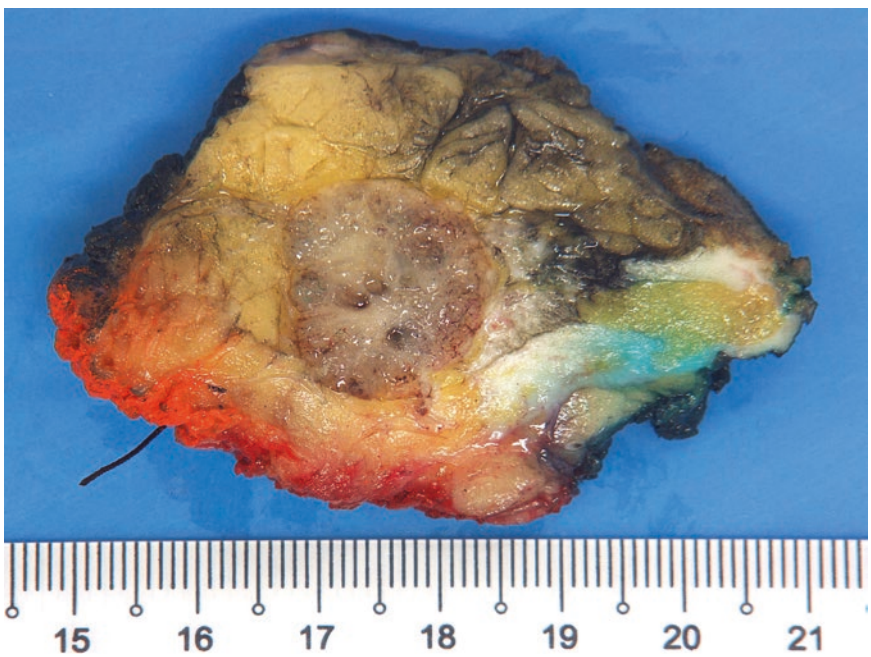

Fig. 6.23 Invasive mucinous carcinoma. Macroscopically, mucinous carcinoma shows a rounded appearance with relatively circumscribed contours with a gelatinous, glistening cut surface. Several cyst-like spaces are present

Fig. 6.24 Invasive mucinous carcinoma. A large, circumscribed, gelatinous, and haemorrhagic tumour with lobulated contours is present within the breast

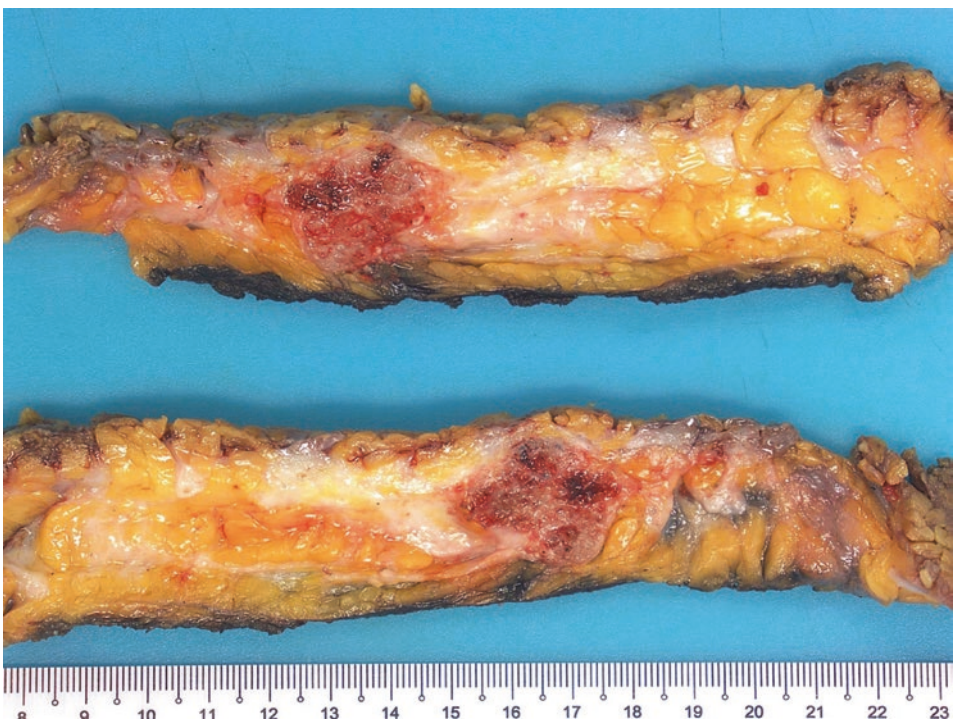

Fig. 6.25 Invasive mucinous carcinoma. Haemorrhagic tumour with a mucinous cut surface contains several cyst-like spaces

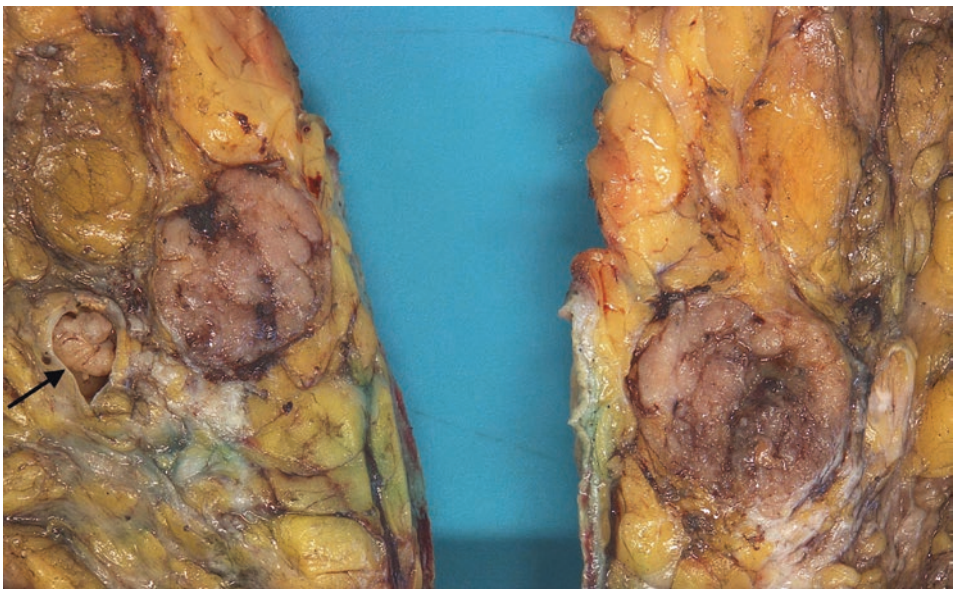

Fig. 6.26 Mixed ductal–mucinous carcinoma. More solid, fleshy, grey-white areas are present, admixed with gelatinous foci, the former representing the non-mucinous ductal component. Adjacent to the mixed ductal–mucinous carcinoma is an intraductal papilloma (*arrow*), confirmed histologically

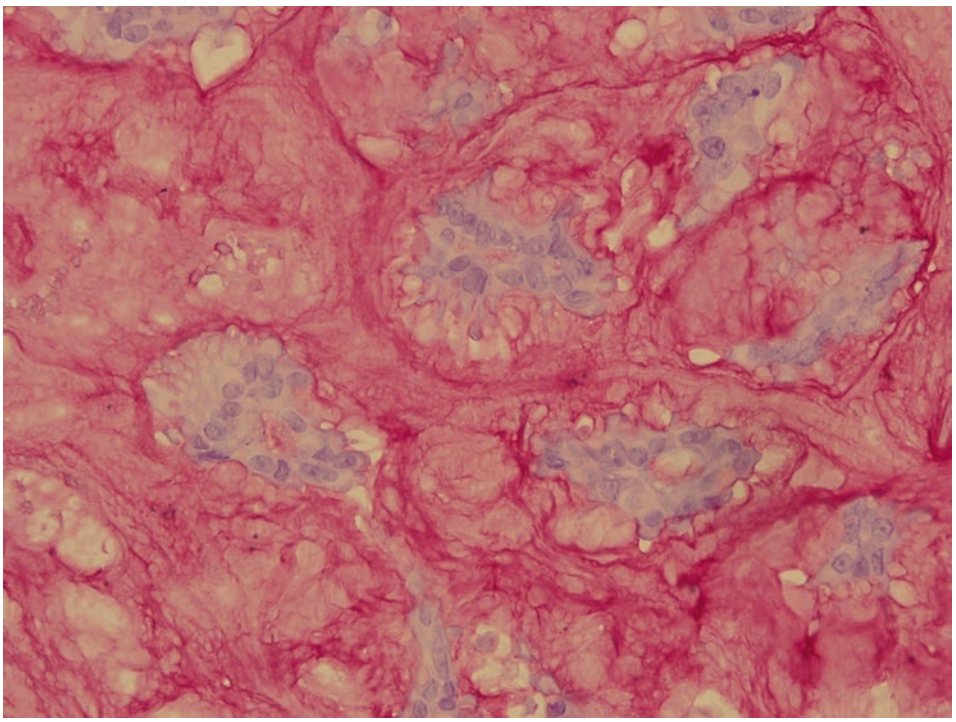

Fig. 6.27 Mucinous carcinoma. Mucicarmine stain highlights mucin with a rosy magenta hue. Tumour cells are suspended within the mucin pool

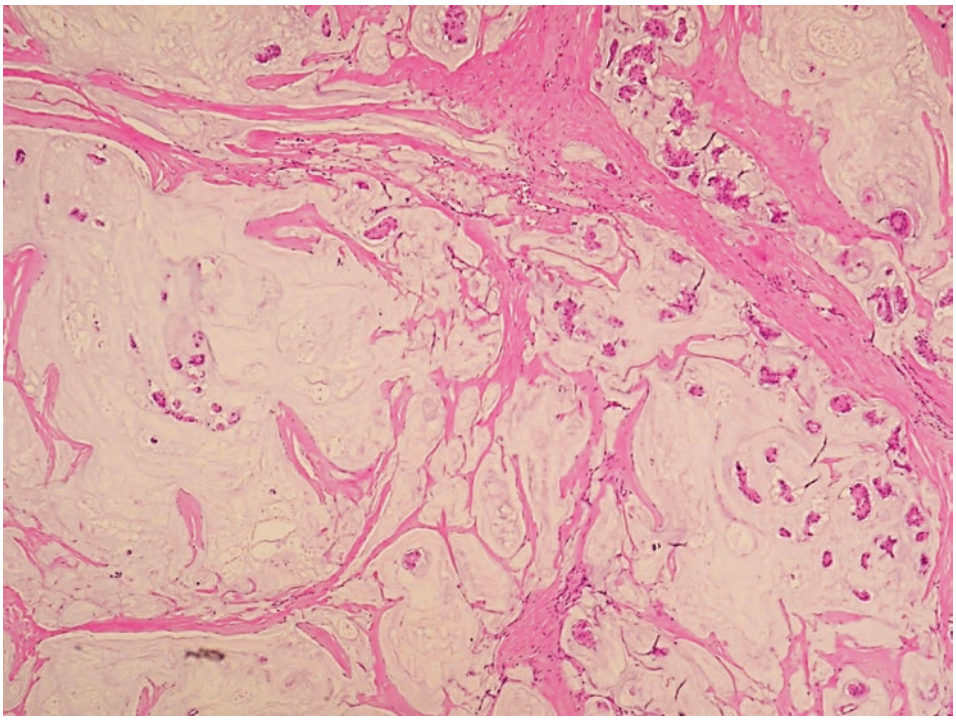

Fig. 6.28 Mucinous carcinoma, paucicellular variant (Capella type A), shows mucin lakes with a few scattered malignant epithelial nests

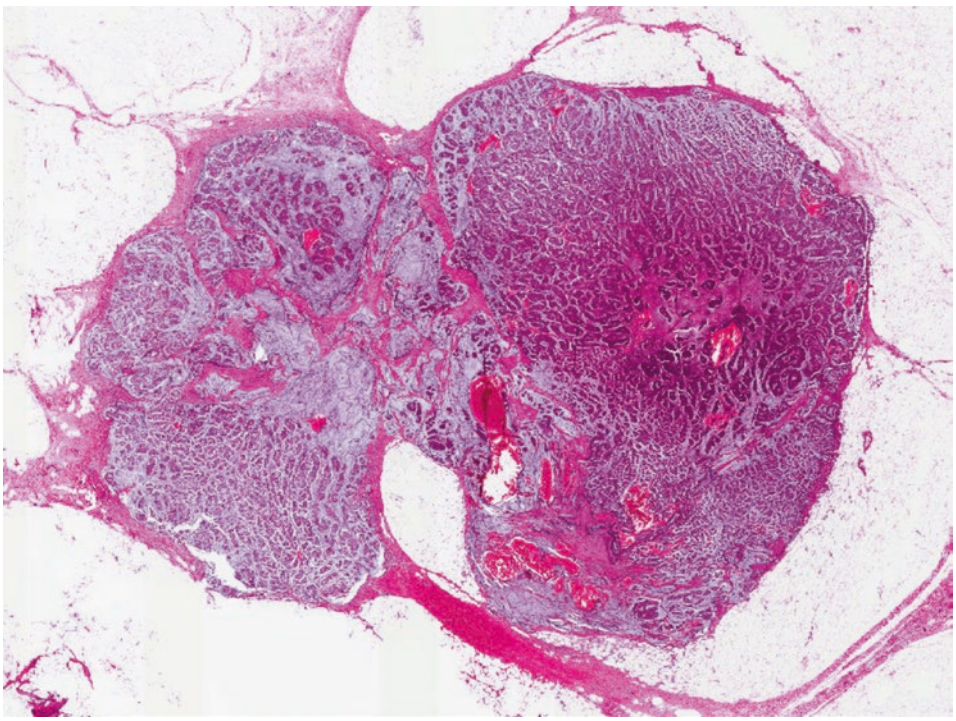

Fig. 6.29 Mucinous carcinoma, hypercellular variant (Capella type B), shows relatively circumscribed contours. Tumour islands are densely arranged and suspended within extracellular mucin

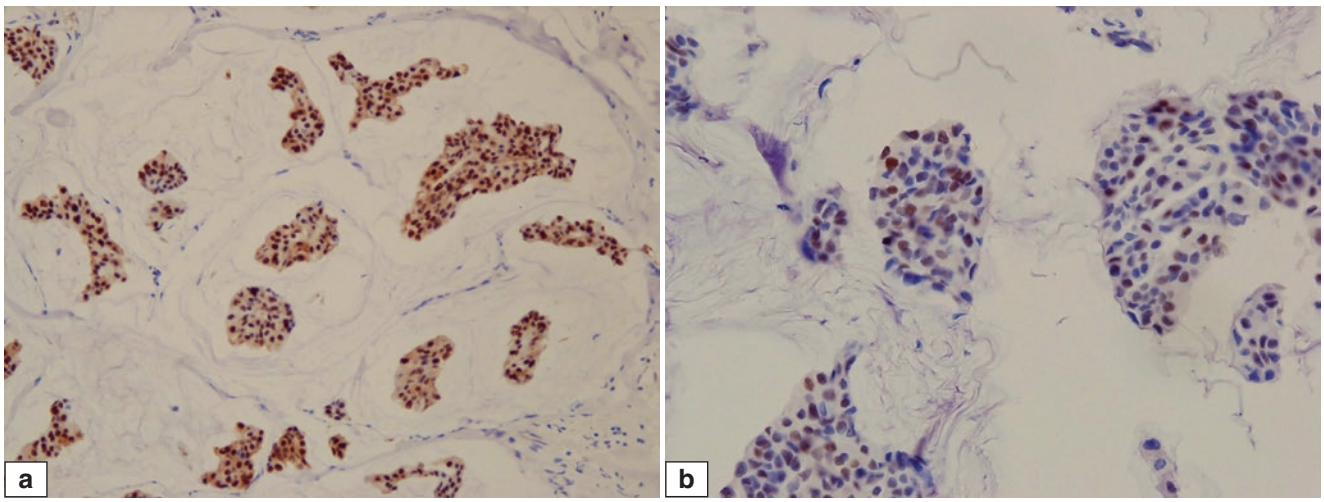

Fig. 6.30 (**a**) Mucinous carcinoma shows oestrogen receptor nuclear positivity. The majority of mucinous carcinomas are hormone receptor positive. (**b**) Immunohistochemistry for progesterone receptor shows patchy nuclear positivity in mucinous carcinoma cells

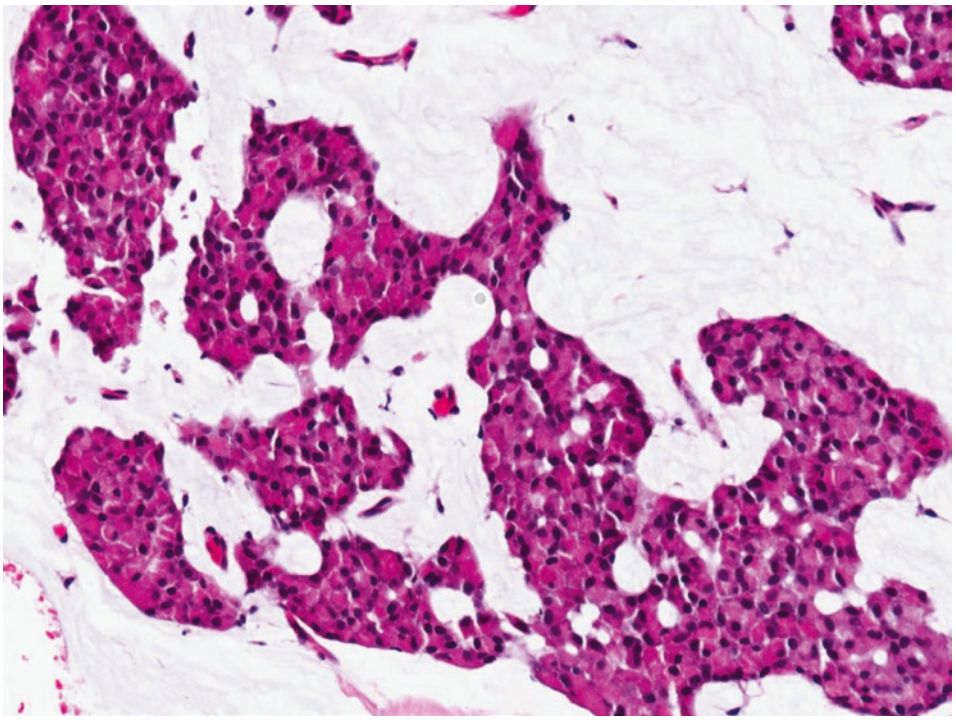

Fig. 6.31 Mucinous carcinoma. Tumour cells show eosinophilic cytoplasm, suggesting neuroendocrine differentiation, which can be confirmed on immunohistochemistry. Several tumour cells also disclose nuclear eccentricity

Differential Diagnosis

Mucinous Carcinoma Versus Mixed Ductal–Mucinous Carcinoma

Mucinous carcinoma is diagnosed when more than 90 % of the tumour shows characteristic appearances of tumour cells floating within mucin. When mucinous differentiation is seen in more than 50 % but less than 90 % of the tumour, with ductal features in the remainder, a diagnosis of mixed mucinous–ductal carcinoma is made (Figs. 6.33, 6.34 and 6.35).

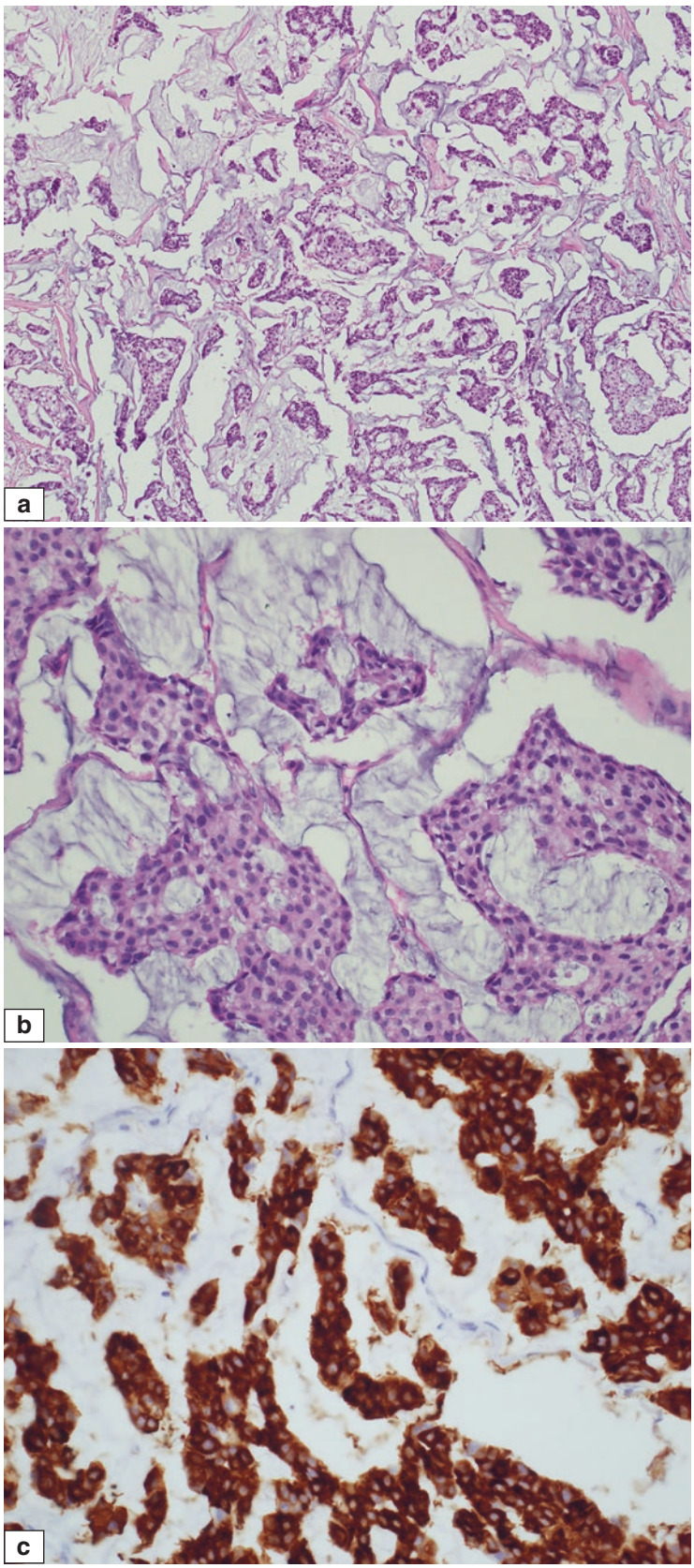

Fig. 6.32 (**a**) Hypercellular (type B) mucinous carcinoma shows neoplastic epithelium densely aggregated amid mucin pools. (**b**) High magnification shows islands of neoplastic epithelium with low nuclear grade features, suspended within mucin. (**c**) Immunohistochemistry for the neuroendocrine marker synaptophysin shows diffuse cytoplasmic reactivity in mucinous carcinoma cells

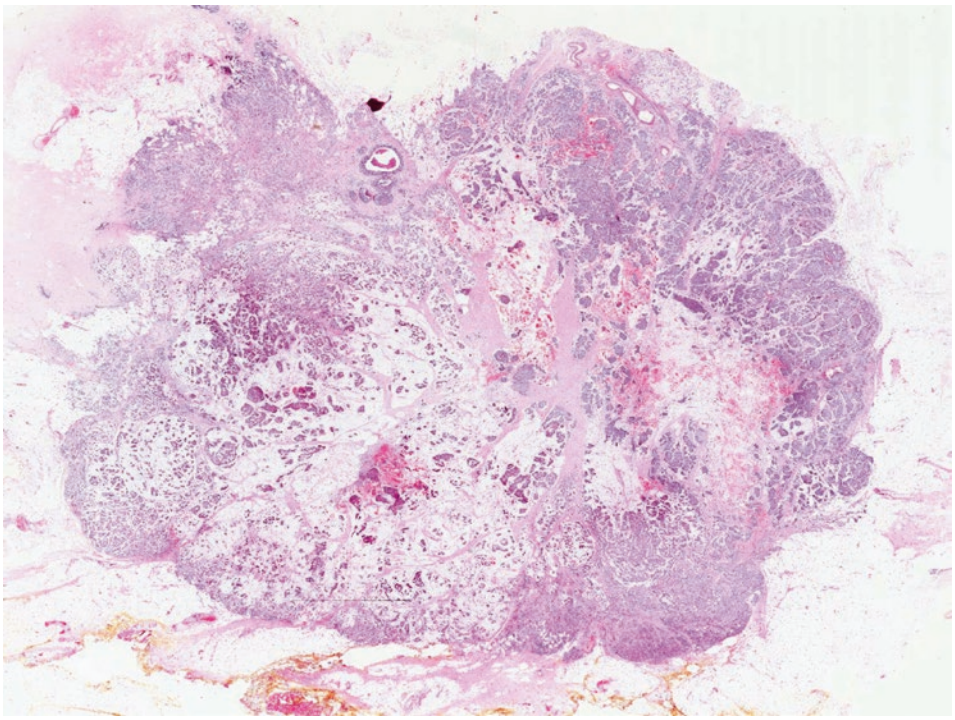

Fig. 6.33 Mucinous carcinoma. The tumour shows lobulated, relatively circumscribed contours. The mucin present contributes to the glistening gross appearance. Parts of the peripheral portions of the tumour do not show extracellular mucin and represent a focal non-mucinous component

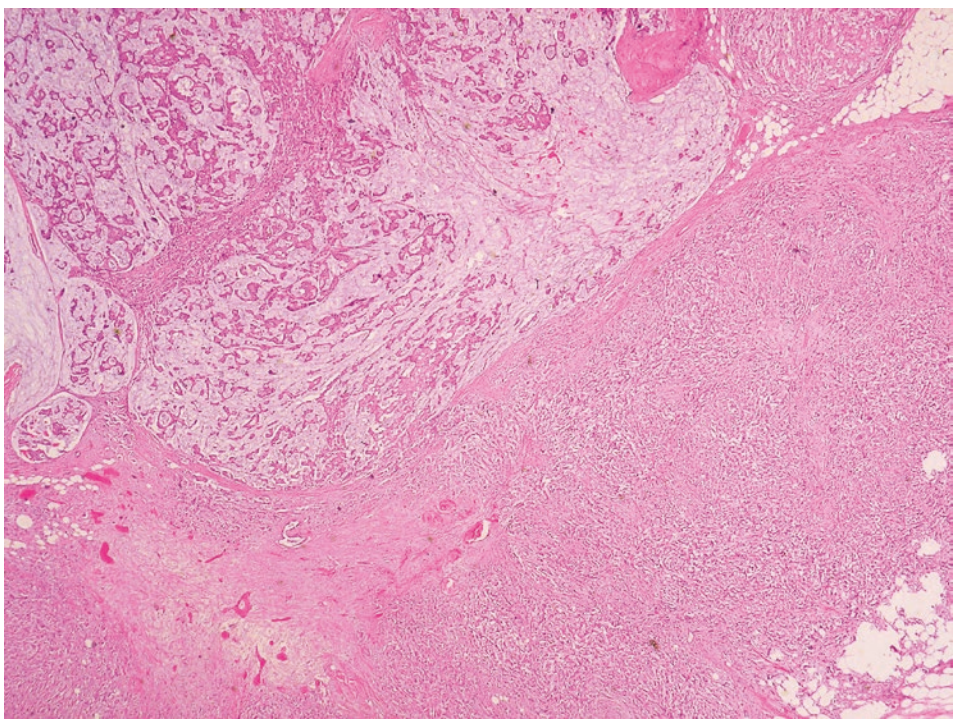

Fig. 6.34 Mixed mucinous–ductal carcinoma. Tumour nests floating within mucin are juxtaposed to invasive carcinoma of no special type (invasive ductal carcinoma), where no extracellular mucin is seen

Mucinous Micropapillary Carcinoma Versus Invasive Micropapillary Carcinoma

A recently characterised form of mucinous carcinoma shows a distinctive micropapillary arrangement of tumour cells. This form is reported to be a clinically aggressive subset of mucinous carcinoma, with cells of intermediate to high nuclear grade that are often hobnailed, accompanied by psammomatous calcifications (Fig. 6.36) [11]. The micropapillary pattern of neoplastic epithelial cells resembles invasive micropapillary carcinoma, but the difference lies in the mucinous background within which tumour nests reside in mucinous micropapillary carcinoma; malignant nests of invasive micropapillary carcinoma lie within retraction spaces (Figs. 6.37 and 6.38).

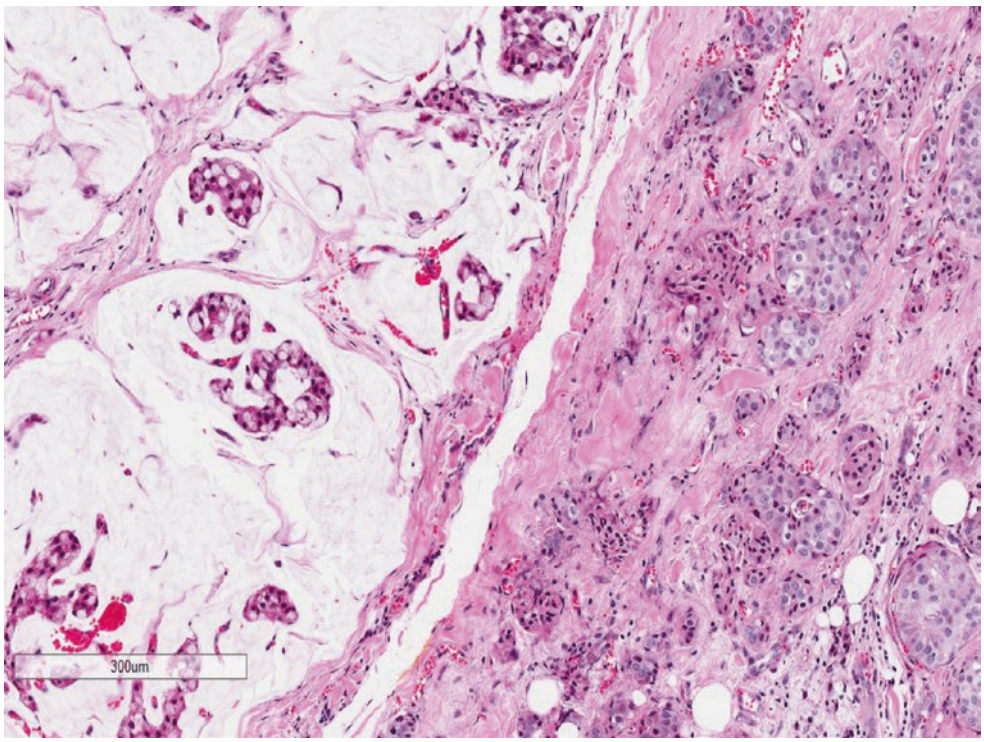

Fig. 6.35 Mixed mucinous-ductal carcinoma shows mucinous carcinoma with tumour nests suspended in mucin lakes (*left field*) while invasive ductal carcinoma comprising irregular solid islands of malignant cells are observed within fibrous stroma (*right field*)

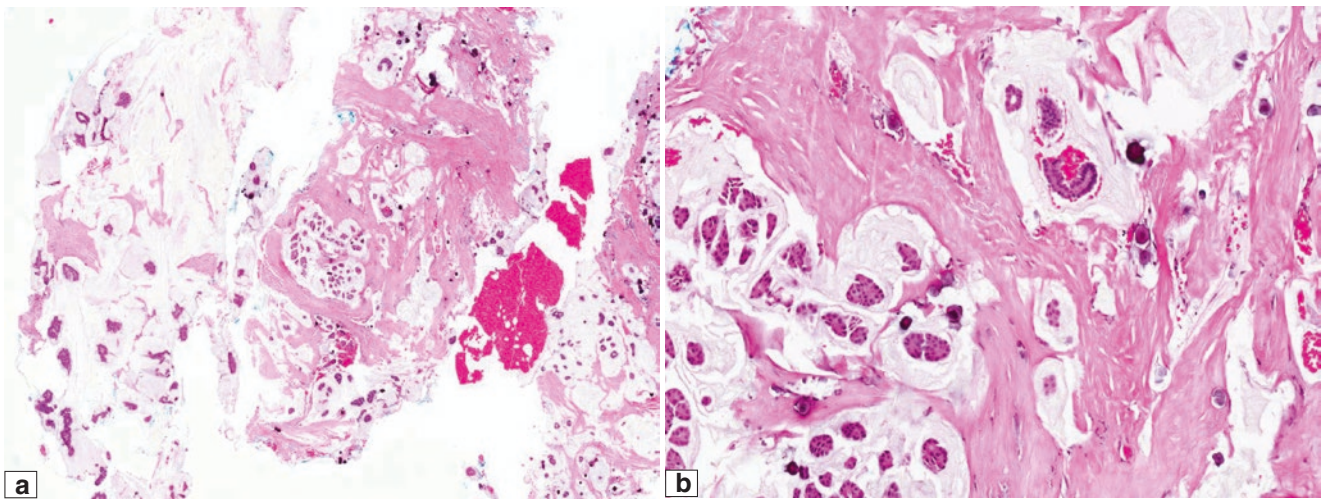

Fig. 6.36 (**a**) Mucinous micropapillary carcinoma on core biopsy. Micropapillary tumour nests float within abundant extracellular mucin, with accompanying calcifications. (**b**) Mucinous micropapillary carcinoma with calcifications. Morular tumour nests are completely enclosed by extracellular mucin, with accompanying calcifications

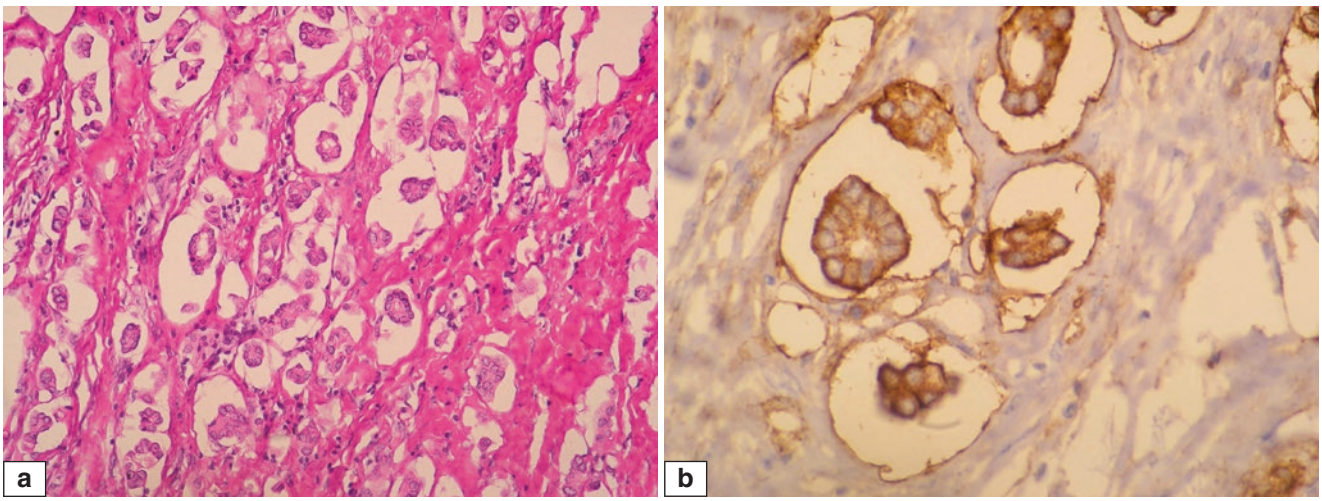

Fig. 6.37 Invasive micropapillary carcinoma. (**a**) The tumour nests morphologically resemble those in mucinous micropapillary carcinoma, but the spaces surrounding the tumour nests in invasive micropapillary carcinoma are empty, without any mucinous material. (**b**) Epithelial membrane antigen (EMA) immunohistochemistry shows accentuation of staining on the outer surfaces of tumour cells that face the retraction spaces

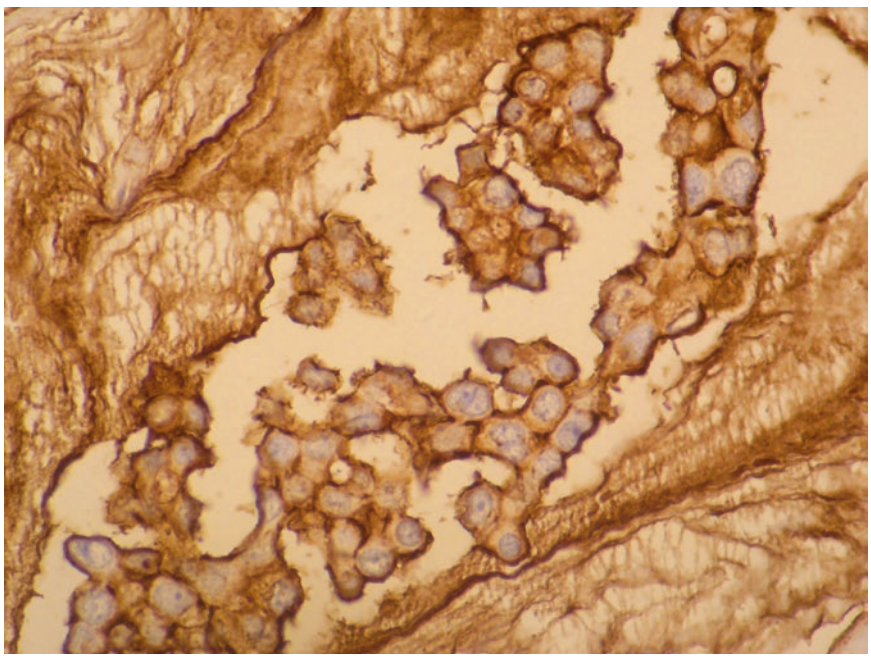

Fig. 6.38 Mucinous carcinoma. EMA immunohistochemistry also demonstrates accentuated staining of the outer surfaces of tumour cells in contact with extracellular mucin

Mucinous Carcinoma Versus Secretory Carcinoma

In secretory carcinoma, secretions that are pink and sometimes scalloped are observed within the lumens of neoplastic glands as well as within cytoplasmic lumens. In contrast, mucin in mucinous carcinoma is extracellular and envelopes tumour islands (Fig. 6.39).

Mucinous Carcinoma, Hypercellular Variant, with Neuroendocrine Differentiation Versus Solid Papillary Carcinoma with Mucin Production

These two lesions may coexist. However, categorisation as mucinous carcinoma requires suspension of tumour within mucin pools. In solid papillary carcinoma (in situ or inva-

sive), on the other hand, fine vessels extend into the midst of the tumour, with mucin within tumour cell cytoplasm or among tumour cells, rather than tumour cells being suspended within mucin lakes (Fig. 6.40).

Mucinous Carcinoma Versus Polyacrylamide Gel

Injections of polyacrylamide gel for breast augmentation may show histologic features slightly reminiscent of the mucin pools of mucinous carcinoma. However, polyacrylamide gel is acellular with a violaceous hue and is rimmed by foreign-body-type multinucleated giant cells (Fig. 6.41).

Prognosis and Therapy Considerations

Pure mucinous carcinoma has an excellent prognosis, with 10-year survivals exceeding 80 %. Mixed mucinous carcinomas have less excellent outcomes [12].

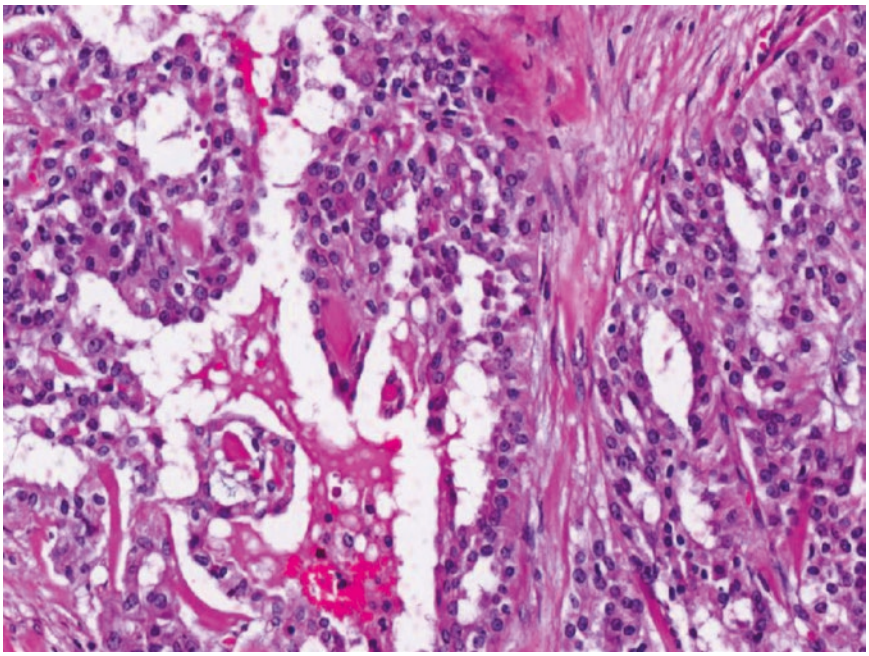

Fig. 6.39 Secretory carcinoma shows luminal pink, viscid, colloid-like secretions. The secretions are confined to glandular lumens or sometimes are observed within the cytoplasm of malignant cells. No stromal mucin pools are present

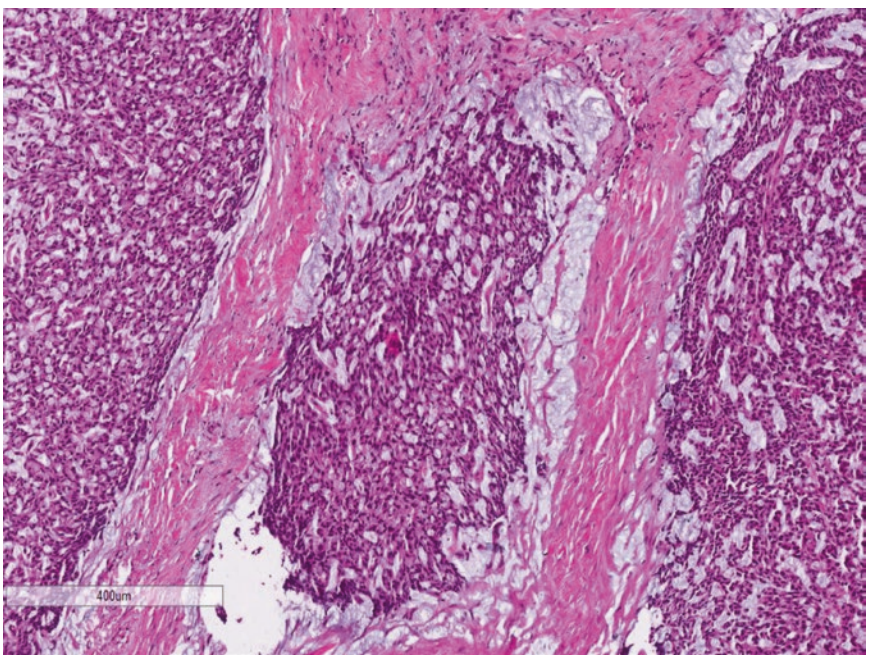

Fig. 6.40 Mucinous carcinoma, hypercellular variant, seen adjacent to solid papillary carcinoma with mucin production

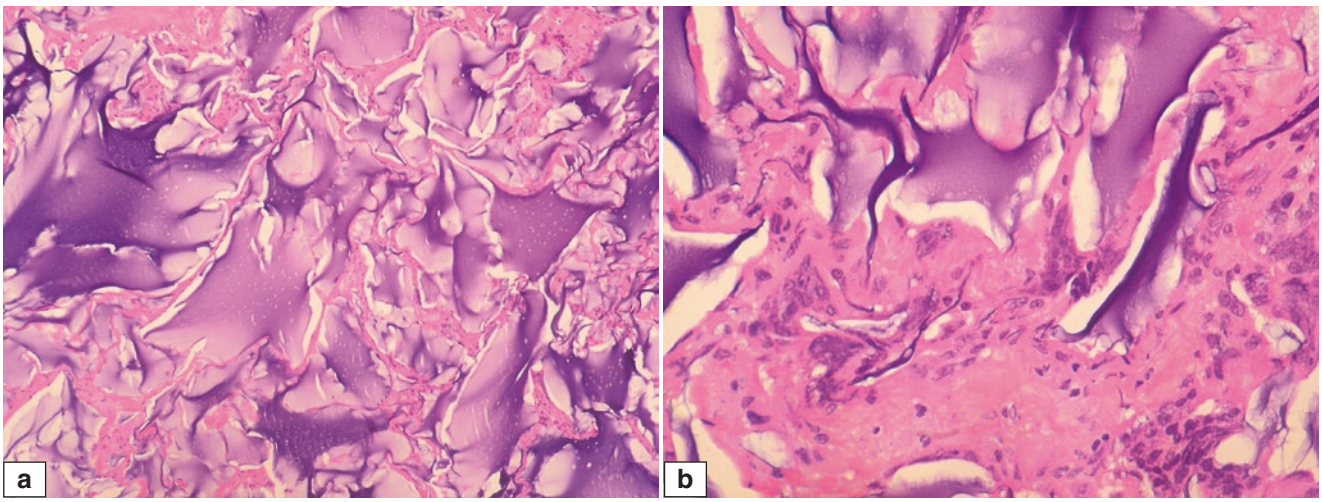

Fig. 6.41 Polyacrylamide gel injection. (**a**) Acellular pools of polyacrylamide gel within the breast parenchyma can mimic mucin pools, but these pools are acellular with a lilac hue and are rimmed by foreign-body giant cells. (**b**) High magnification shows foreign-body multinucleated giant cells surrounding the foreign substance

Solid Papillary Carcinoma with Mucin Production

Definition

Solid papillary carcinoma is a distinctive form of papillary carcinoma composed of expansile cellular nodules within which are relatively inconspicuous, delicate fibrovascular cores [13]. A solid growth pattern can be seen at low magnification. Neuroendocrine differentiation, spindle cell morphology, and mucin production are frequent (Fig. 6.42). Both in situ and invasive forms of solid papillary carcinoma exist, and it is necessary to specify whether a particular case represents the in situ or invasive counterpart or both (*see* section "Solid Papillary Carcinoma", in Chap. 4).

Clinical and Epidemiological Features

Solid papillary carcinoma usually occurs in women in the older age group. Those with mucin production form a subset of this tumour. Patients may present with a breast lump, sometimes in the nipple-areolar region, with or without bloody nipple discharge.

Imaging Features

Solid papillary carcinoma may be observed as mammographic nodular masses or ultrasonographic hypoechoic lesions with lobulated contours.

Pathologic Features

Macroscopic Pathology

Solid papillary carcinoma with mucin production can show a glistening appearance.

Microscopic Pathology

Solid nodules of monotonous low or intermediate nuclear grade epithelial cells are punctuated by fine, congested vessels, accompanied by variable amounts of mucin, which can be spotted between cells within the solid islands or seeping between tumour cells and stroma. When mucin becomes more abundant, enclosing tumour nests, it becomes difficult to distinguish solid papillary carcinoma with mucin production from the hypercellular variant of mucinous carcinoma.

Differential Diagnosis

Solid Papillary Carcinoma with Mucin Production Versus Intraductal Papilloma with Mucin

In solid papillary carcinoma, the epithelial population is uniformly composed of cells harbouring nuclei with fine chromatin, amphophilic to eosinophilic cytoplasm, and inconspicuous nucleoli. Fibrovascular septa are fine and imperceptible. Pseudorosettes and spindle cells can be seen (Fig. 6.43). In contrast, the intraductal papilloma with mucin shows a heterogeneous cell population with fronds supported by well-developed fibrovascular cores. Myoepithelial cells are present. Mucin is found within the cystic lumen of the papilloma (Fig. 6.44).

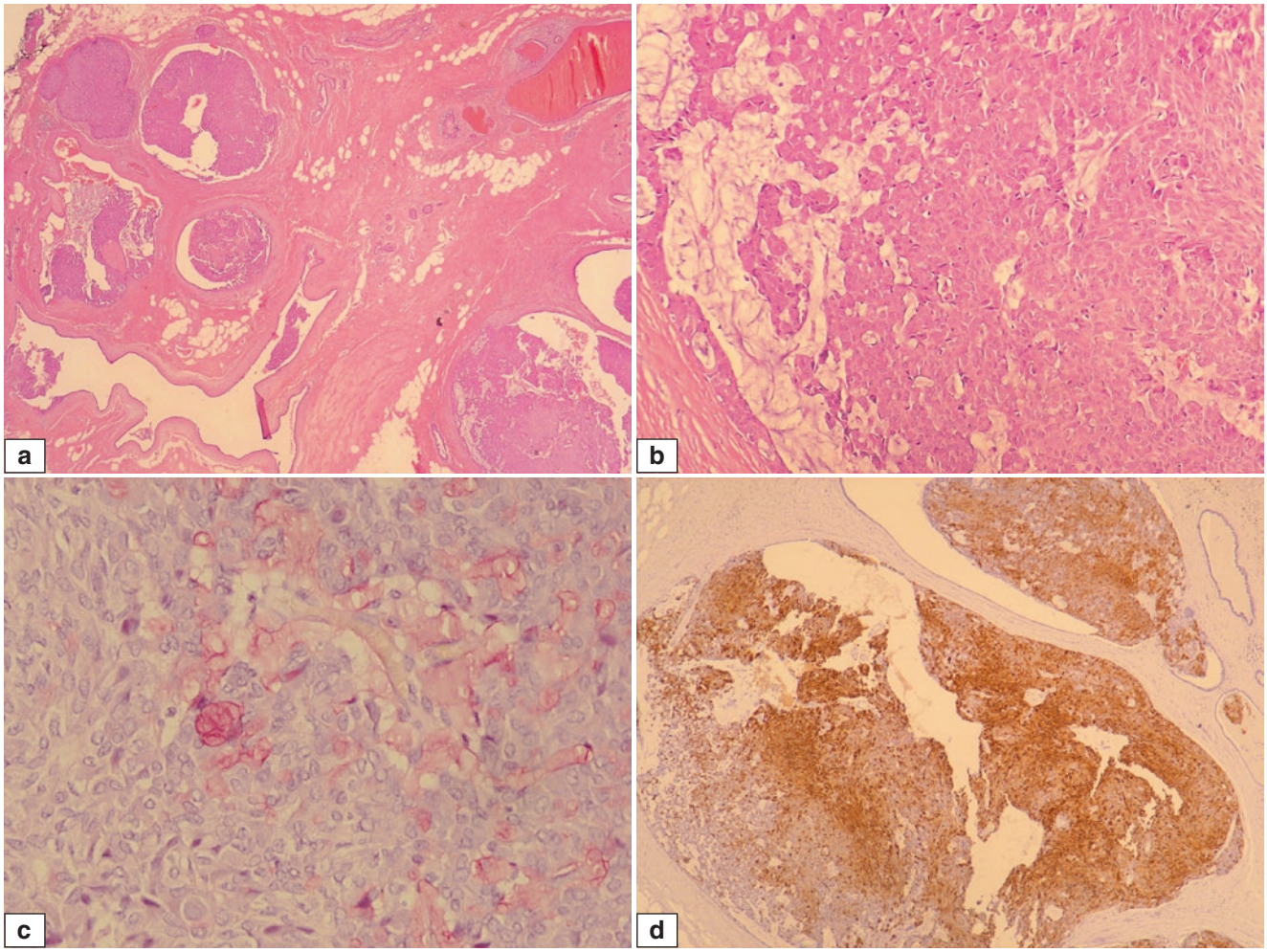

Fig. 6.42 Solid papillary carcinoma (in situ) with mucin production. (**a**) Parts of the tumour show an intraductal papillary appearance. Mucin is seen within the dilated ducts into which the papillary structures protrude. (**b**) Mucin is seen among tumour cells. There is a well-defined interphase of the tumour edge with the surrounding stroma. (**c**) Mucicarmine stain shows mucin accumulation between cells. (**d**) Immunohistochemistry for synaptophysin shows positive reactivity in the tumour cells, indicating neuroendocrine differentiation

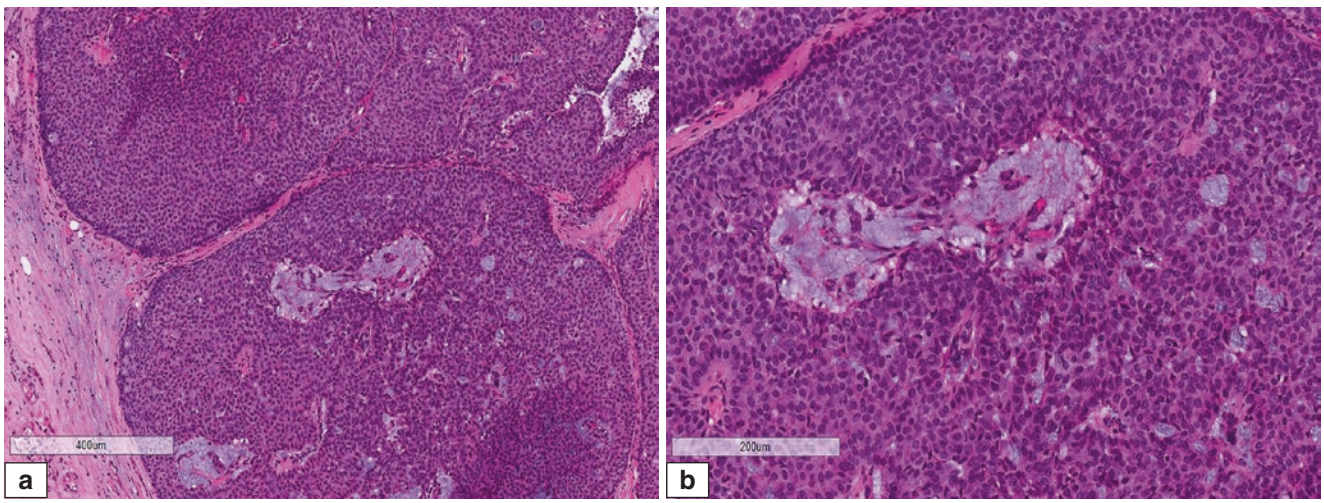

Fig. 6.43 Solid papillary carcinoma (in situ) with mucin production. (**a**) Large, rounded solid islands of uniform epithelial cells are punctuated by delicate fibrovascular septa. Mucin puddles are observed among the epithelial cells. (**b**) High magnification shows mucin among monotonous epithelial cells. Perivascular rosettes are seen. The epithelial cells show uniform nuclei with fine chromatin and amphophilic cytoplasm.

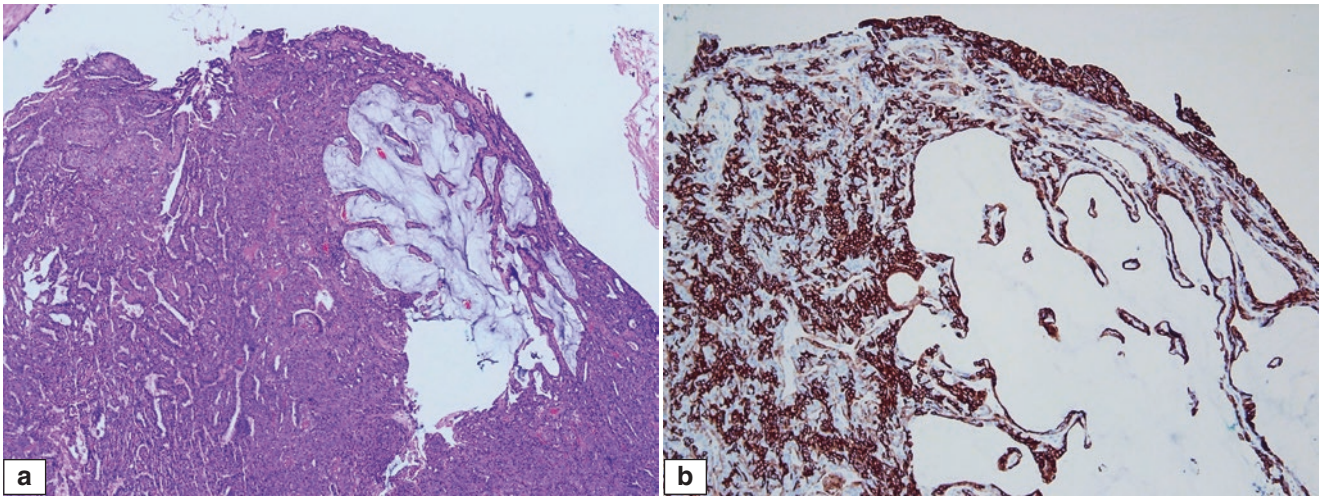

Fig. 6.44 Intraductal papilloma with mucin. (**a**) Extracellular mucin is seen within the intraductal papilloma. (**b**) Immunohistochemistry for CK14 shows a mosaic pattern of positivity among epithelial cells within the intraductal papilloma, supporting a benign process

Solid Papillary Carcinoma with Mucin Production Versus Hypercellular-Variant Mucinous Carcinoma

When mucin of solid papillary carcinoma tracks between the tumour and stroma, it becomes difficult to distinguish it from established mucinous carcinoma of the hypercellular variety. Mucinous carcinoma is diagnosed when mucin pools are extensive and completely surround the nests and islands of tumour. Solid papillary carcinoma may be associated with invasive mucinous carcinoma as well.

Prognosis and Therapy Considerations

Solid papillary carcinoma has a generally good prognosis [14], which also applies to those with mucin production.

References

1. Shim JY, Sahin AA. Mucinous lesions of the breast. Surgical Pathology 2, 2009;413–40.
2. O'Connell JT, Shao ZM, Drori E, Basbaum CB, Barsky SH. Altered mucin expression is a field change that accompanies mucinouc (colloid) breast carcinoma histogenesis. Hum Pathol 1998;29:1517–23.
3. Sapino A, Sneige N, Eusebi V. Mucoepidermoid carcinoma. In: Lakhani SR, Ellis IO, Schnitt SJ, Tan PH, van de Vijver MJ, editors. WHO classification of tumours of the breast. Lyon: IARC; 2012. p. 58.
4. Honma N, Sakamoto G, Ikenaga M, Kuroiwa K, Younes M, Takubo K. Mucinous cystadenocarcinoma of the breast. A case report and review of the literature. Arch Pathol Lab Med. 2003;127:1031–3.
5. Tan PH, Tse GM, Bay BH. Mucinous breast lesions: diagnostic challenges. J Clin Pathol. 2008;61:11–9.
6. Gadre SA, Perkins GH, Sahin AA, Sneige N, Deavers MT, Middleton LP. Neovascularization in mucinous ductal carcinoma in situ suggests an alternative pathway for invasion. Histopathology. 2008;53:545–53.
7. Jaffer S, Bleiweiss IJ, Nagi CS. Benign mucocele-like lesions of the breast: revisited. Mod Pathol. 2011;24:683–7.
8. Rakha EA, Shaaban AM, Haider SA, Jenkins J, Menon S, Johnson C, Yamaguchi R, Murphy A, Liston J, Cornford E, Hamilton L, James J, Ellis IO, Lee AH. Outcome of pure mucocele-like lesions diagnosed on breast core biopsy. Histopathology. 2013;62:894–8.
9. Sutton B, Davion S, Feldman M, Siziopikou K, Mendelson E, Sullivan M. Mucocele-like lesions diagnosed on breast core biopsy: assessment of upgrade rate and need for surgical excision. Am J Clin Pathol. 2012;138:783–8.
10. Begum SM, Jara-Lazaro AR, Thike AA, Tse GM, Wong JS, Ho JT, Tan PH. Mucin extravasation in breast core biopsies—clinical significance and outcome correlation. Histopathology. 2009;55:609-17.
11. Barbashina V, Corben AD, Akram M, Vallejo C, Tan LK. Mucinous micropapillary carcinoma of the breast: an aggressive counterpart to conventional pure mucinous tumors. Hum Pathol. 2013;44:1577–85.
12. Bussolati G, Sapino A. Mucinous carcinomas and carcinoma with signet-ring-cell differentiation. In: Lakhani SR, Ellis IO, Schnitt SJ, Tan PH, van de Vijver MJ, editors. WHO classification of tumours of the breast. Lyon: IARC; 2012. p. 60.
13. Tan PH, Schnitt SJ, van de Vijver MJ, Ellis IO, Lakhani SR. Papillary and neuroendocrine breast lesions: the WHO stance. Histopathology. 2015;66:761–70.
14. Tan BY, Thike AA, Ellis IO, Tan PH. Clinicopathologic characteristics of solid papillary carcinoma of the breast. Am J Surg Pathol. 2016;40:1334–42.

Apocrine Lesions

7

Apocrine morphology is characterised by abundant eosinophilic cytoplasm containing finely granular, periodic acid–Schiff (PAS)-positive, diastase-resistant granules and moderate to large, centrally or eccentrically located nuclei with prominent nucleoli and distinctive cell borders. It is commonly observed in a wide variety of breast lesions [1–4] (Fig. 7.1), ranging from simple cysts to intraductal proliferative lesions with and without atypia and to invasive carcinoma (Fig. 7.2). The majority of apocrine breast lesions are benign and have no major clinical consequences. They are often considered normal features of the female breast after the age of 25–30 years [5]. Some apocrine proliferations may cause diagnostic problems, however, especially when they involve pre-existing lesions such as adenosis or papilloma [3, 6]. Accurate diagnosis and classification of these lesions are important. The biologic and clinical significance of breast carcinomas with apocrine morphology remains controversial, mainly because of the subjectivity of histopathological criteria and the lack of specific biomarkers for reliable classification of this histological subtype of breast carcinoma. Identification of novel molecular markers that can define apocrine carcinoma and determine the true clinical significance of apocrine differentiation in breast cancer is an area of active research.

Gross cystic disease fluid protein 15 (GCDFP-15), originally isolated from the contents of a breast cyst, is a sensitive immunohistochemical marker of apocrine differentiation.

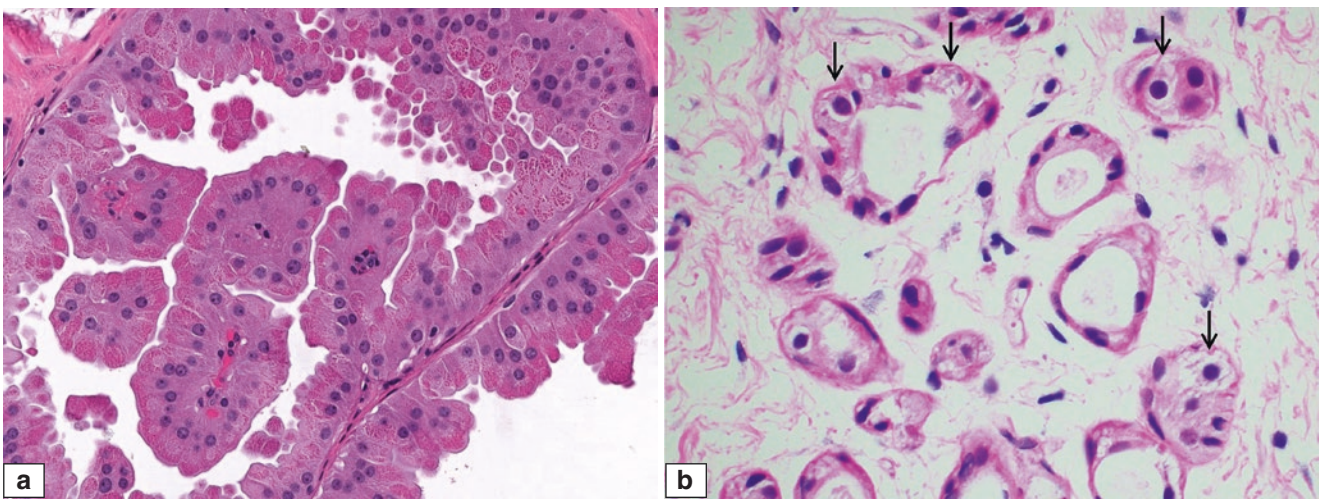

Fig. 7.1 Apocrine metaplasia. (**a**) On H&E staining, apocrine cells are characterised by abundant pink, granular cytoplasm and centrally located hyperchromatic nuclei, which may have one or two prominent nucleoli. The nuclear to cytoplasmic ratio is very low. The apical portions of the cells contain coarse eosinophilic granules. These type A apocrine cells are more commonly observed than type B apocrine cells which feature abundant foamy cytoplasm. (**b**) Type B apocrine cells (*arrows*) with abundant pale to foamy cytoplasm

P.H. Tan, A.A. Sahin, *Atlas of Differential Diagnosis in Breast Pathology*, Atlas of Anatomic Pathology,
DOI 10.1007/978-1-4939-6697-4_7

It can be used to confirm apocrine differentiation in both benign and malignant conditions (Fig. 7.3) [7, 8]. Some non-apocrine breast lesions can also be positive for GCDFP-15. Similarly, androgen receptor is a sensitive but not a specific marker of apocrine differentiation (Fig. 7.4). Today, apocrine differentiation is determined primarily on morphologic features.

This chapter reviews histopathologic features of apocrine lesions of the breast, with an emphasis on the differential diagnosis of benign, borderline, and malignant apocrine lesions.

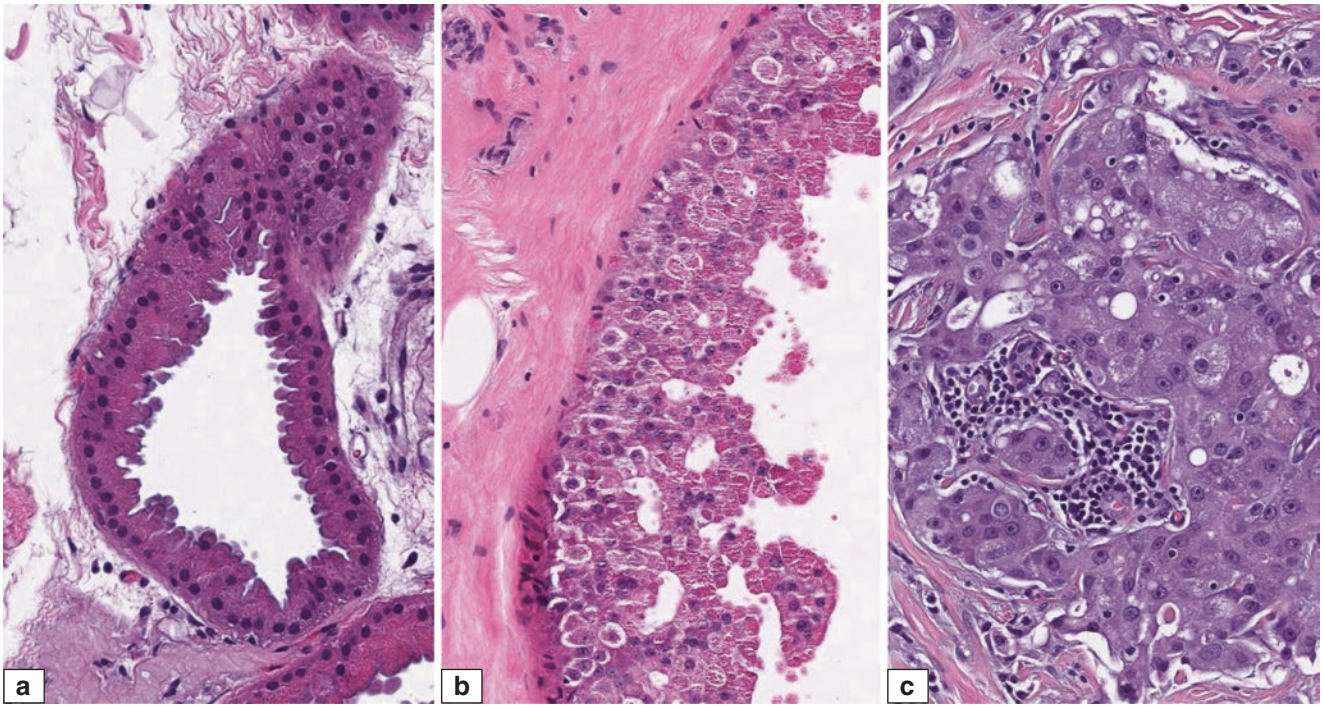

Fig. 7.2 Apocrine change in the breast is seen in a broad range of lesions. (**a**) Benign microcyst with apocrine metaplasia. (**b**) Usual ductal hyperplasia with apocrine change. (**c**) Invasive apocrine carcinoma

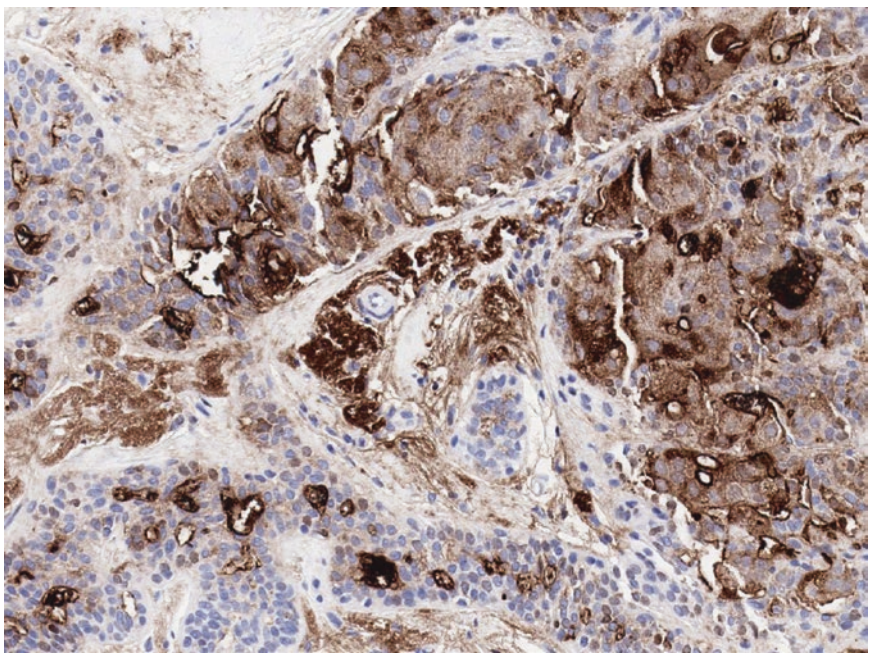

Fig. 7.3 Immunohistochemical staining for gross cystic disease fluid protein 15 (GCDFP-15). Almost all benign apocrine lesions and a great majority of malignant apocrine lesions show strong positivity for this marker

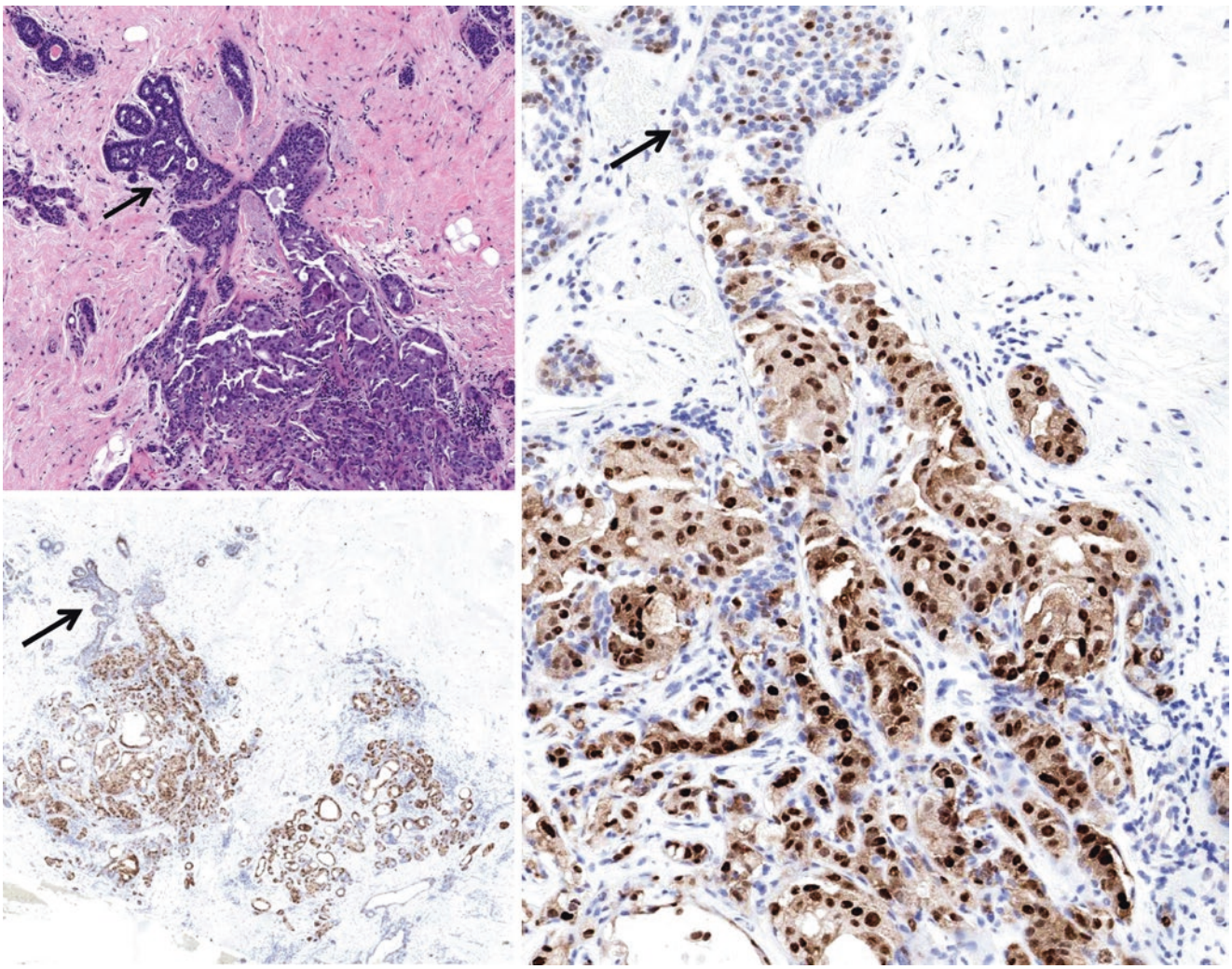

Fig. 7.4 Immunohistochemical staining for androgen receptor in adenosis with apocrine differentiation. Though apocrine cells show strong diffuse expression of androgen receptor, only scattered non-apocrine cells are positive (*arrow*)

Benign Lesions: Apocrine Metaplasia

Definition

Apocrine metaplasia, defined as the change of the breast epithelium into an epithelium similar to that found in apocrine glands of cutaneous origin, is quite common and is observed in a variety of benign breast lesions (cystic changes, fibroadenoma, papilloma, and sclerosing adenosis) (Figs. 7.5 and 7.6). Embryologically, the breasts develop from the anlage that gives rise to apocrine glands, but apocrine glands are not basic histologic components of the breast. There are several hypotheses regarding the origin of apocrine cells in breast tissue. The presence of apocrine epithelium is generally regarded as a metaplastic or degenerative process, but some suggest that apocrine cells may be a normal constituent of glandular structures of the breast and may represent apocrine glands of cutaneous origin entrapped in breast tissue [9]. Apocrine cells in the breast are histologically indistinguishable from apocrine cells in cutaneous apocrine glands.

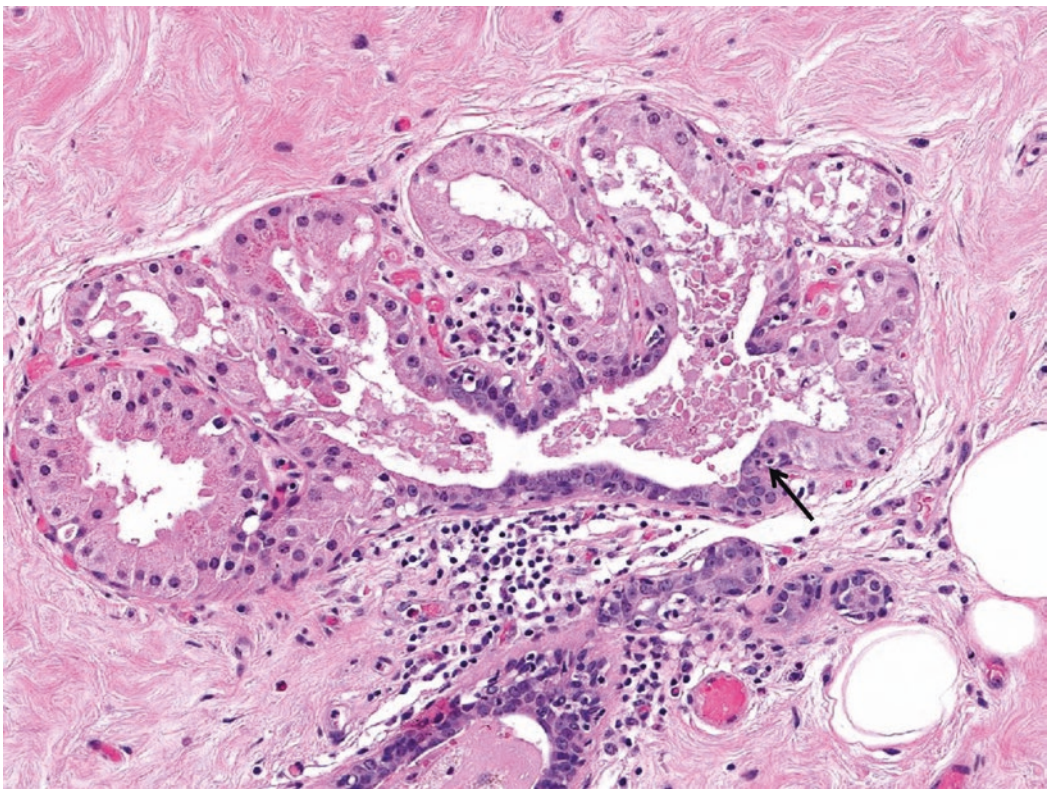

Fig. 7.5 Cystic duct with apocrine metaplasia. Transition from normal ductal epithelium to apocrine metaplasia is shown (*arrow*)

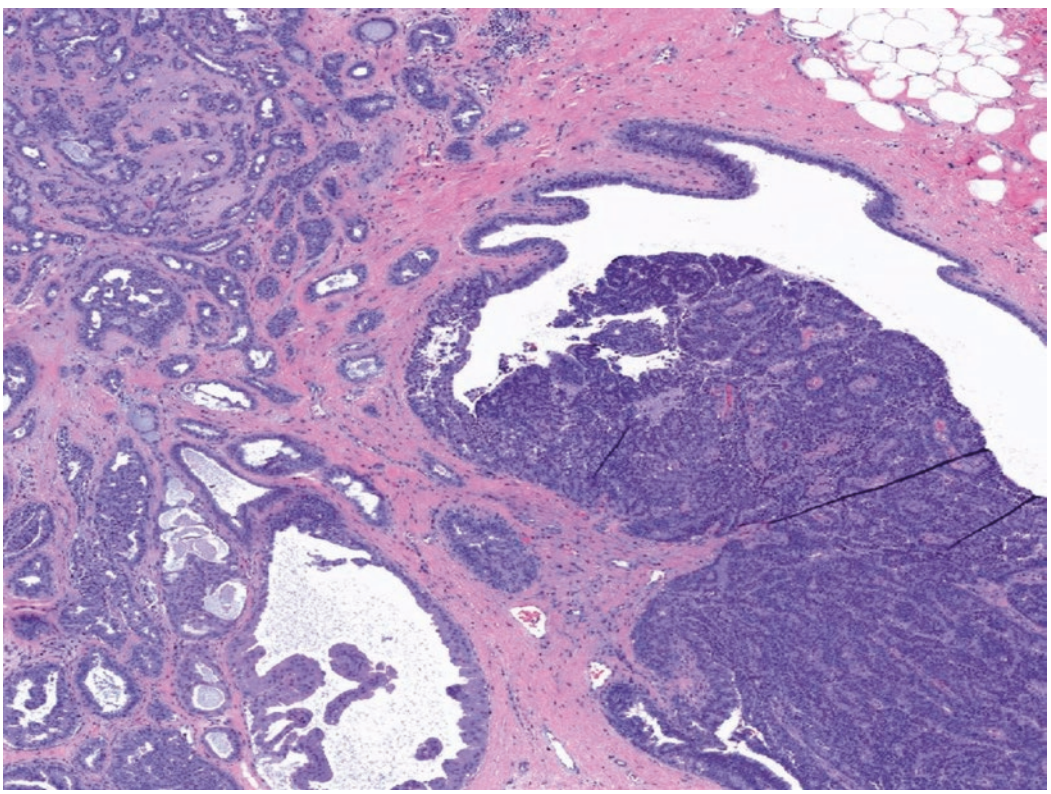

Fig. 7.6 Apocrine metaplasia is a common component of breast cystic changes (*left lower field*) and is frequently associated with adenosis and a broad range of benign proliferative changes. An intraductal papilloma is present (*right field*)

Clinical and Epidemiological Features

Apocrine metaplasia is frequently found along the epithelial lining of cysts (Fig. 7.7), which can be part of breast cystic changes that may present as a palpable mass (Fig. 7.8) or be associated with microcalcifications [3–5]. There is no specific clinical feature that can be attributed to apocrine metaplasia. Apocrine metaplasia is a common histologic finding in the female breast after 25–30 years of age [3–6, 10]. It is rarely seen in women younger than 20 years, and the frequency increases with age, being highest in the fifth decade.

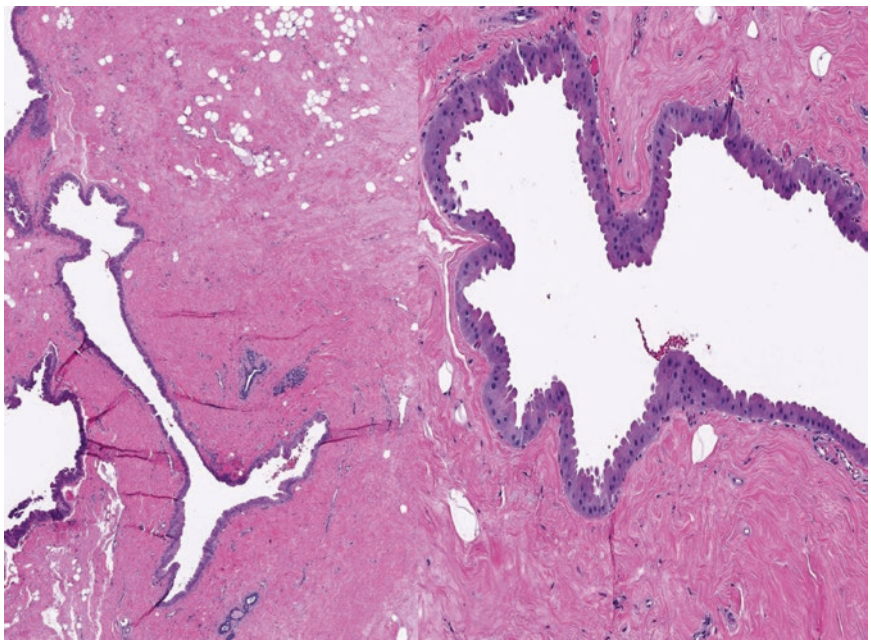

Fig. 7.7 Cystic apocrine metaplasia. Dilated cysts are lined by apocrine cells

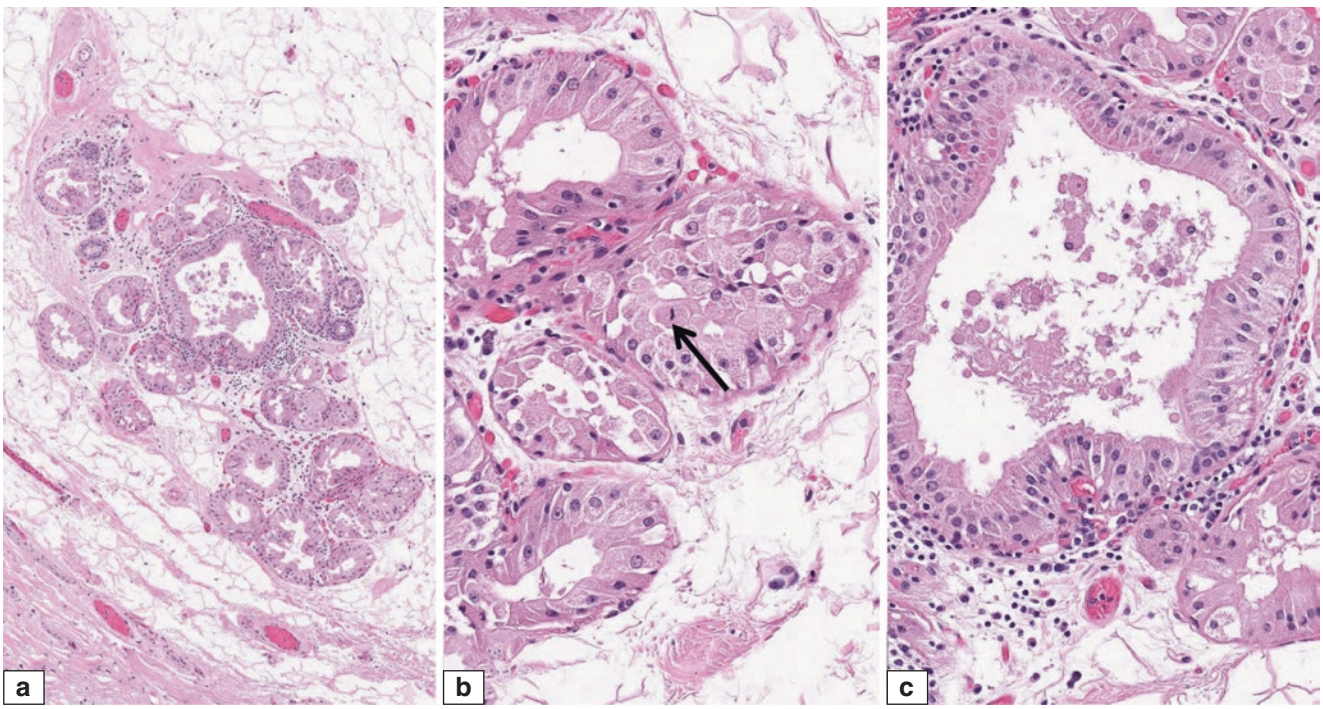

Fig. 7.8 Cystic apocrine metaplasia. (**a**, **b**) Cystically dilated glands lined by benign apocrine epithelium. (**c**) Higher magnification shows that the nuclei are centrally and basally located and there is no cytologic atypia. The lumen contains eosinophilic secretory material mixed with a few degenerative cells. Rare mitoses can be identified even in benign apocrine proliferations (**b**, *arrow*)

Imaging Features

Clusters of ducts with apocrine metaplasia may form a mass that can be identified on imaging. They may be associated with microcalcifications, which can be calcium phosphate or calcium oxalate (Fig. 7.9).

Pathologic Features

Macroscopic Pathology

There are no specific macroscopic findings associated with apocrine metaplasia. Large cystic lesions may be grossly visible and contain dark-coloured fluid.

Microscopic Pathology

Cystic apocrine metaplasia is composed of flat and cuboidal cells with abundant eosinophilic granular cytoplasm and round nuclei located in either the basal or central positions. The nuclei often have prominent nucleoli. The cells are typically evenly spaced and have distinct borders (Fig. 7.10).

Apocrine cells lining glands usually show apical snouts projecting into the lumen (Fig. 7.11). A myoepithelial layer is easily distinguishable, but diminished or focally absent myoepithelium has been reported in benign apocrine cysts.

Differential Diagnosis

Apocrine metaplasia has a distinct histological appearance that usually does not pose diagnostic difficulty. Other benign lesions such as duct ectasia with abundant histiocytes may mimic apocrine metaplasia (Fig. 7.12).

Prognosis and Therapy Considerations

Apocrine metaplasia is a benign lesion, and it is not considered to be associated with risk for developing breast cancer [3–6, 11].

Malignant Apocrine Lesions

Apocrine Ductal Carcinoma In Situ

Definition

Apocrine-like changes are common findings in ductal carcinoma in situ (DCIS) (Figs. 7.13 and 7.14). The incidence of pure apocrine DCIS is difficult to establish in the literature because of the variable diagnostic criteria used to define apocrine differentiation [12–17]. The presence of abundant eosinophilic cytoplasm and centrally located enlarged nuclei, which are the defining histologic features of apocrine differentiation, are common findings in high-grade DCIS. High-grade apocrine DCIS, characterised by proliferation of pure apocrine cells with marked nuclear pleomorphism, high mitotic rate, and comedonecrosis, presents the least diagnostic difficulty (Fig. 7.15). Comedonecrosis is a common finding in apocrine DCIS, and some experts require the presence of necrosis to establish the diagnosis of DCIS in apocrine proliferations [14, 16]. They consider that all apocrine DCIS should be at least intermediate grade based on nuclear features. Others support classification of apocrine DCIS into categories of low grade, intermediate grade, and high grade, similar to non-apocrine DCIS (Figs. 7.16, 7.17, 7.18, and 7.19) [16, 17].

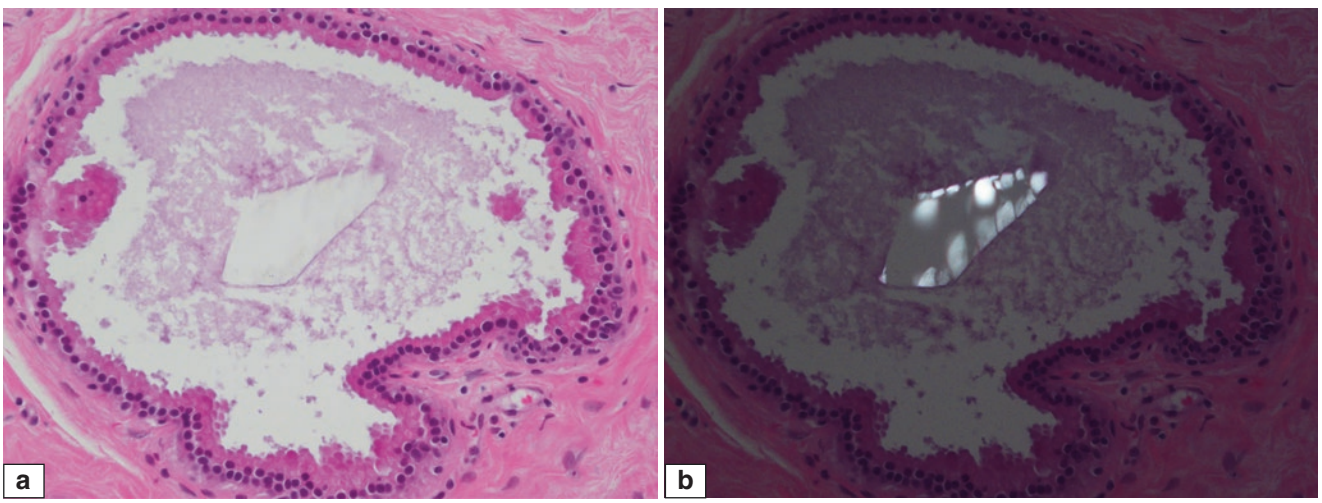

Fig. 7.9 (**a**) Apocrine cyst. A cystically dilated gland lined by apocrine cells shows luminal pale secretions and transparent calcium oxalate. (**b**) Polarised microscopy shows refractility of the calcium oxalate within the lumen

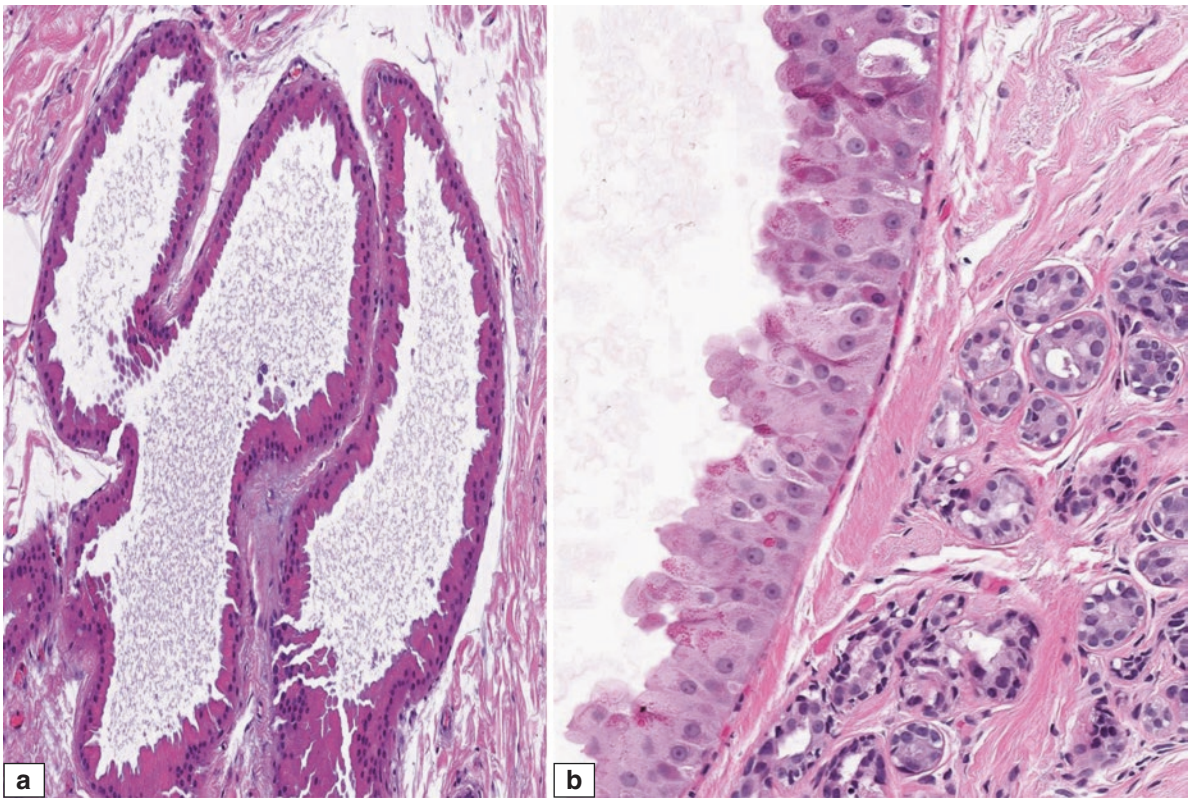

Fig. 7.10 Benign cystic apocrine metaplasia. The apocrine cyst lining may be a single layer (**a**) or multiple layers of apocrine cells (**b**). The cells are typically evenly spaced and have distinct borders

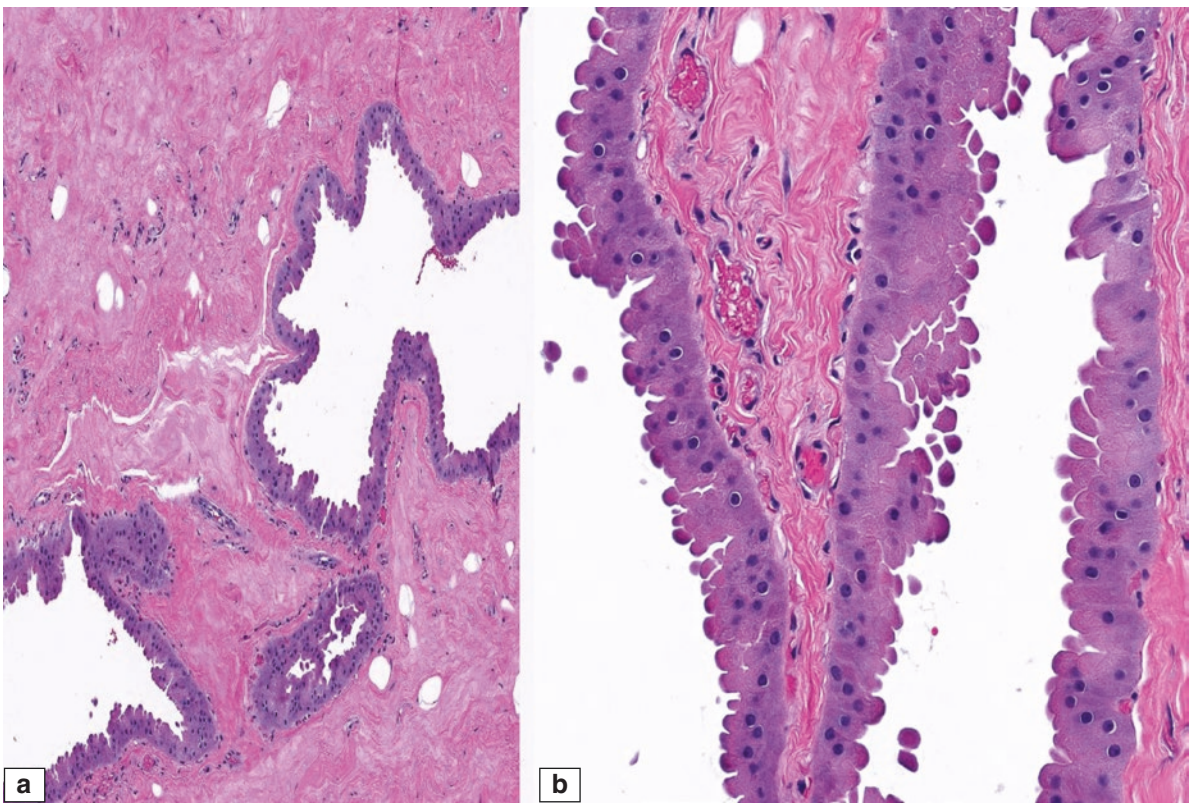

Fig. 7.11 Benign cystic apocrine metaplasia with typical apical snouts, low (**a**) and higher (**b**) magnification

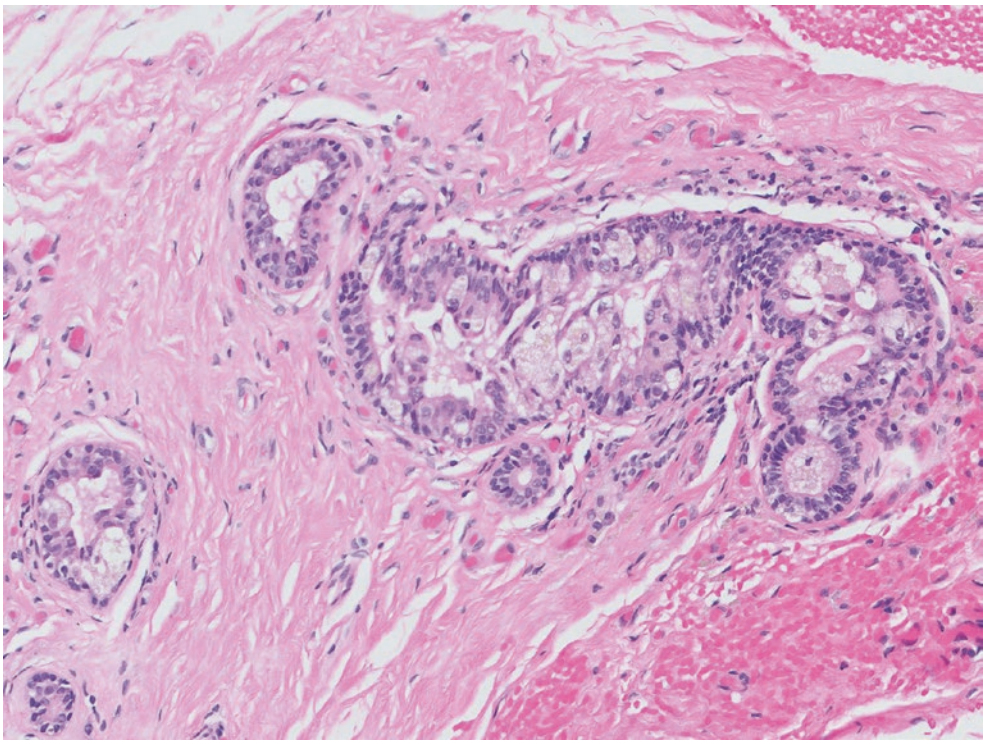

Fig. 7.12 Foamy histiocytes within the duct wall and lumen may mimic apocrine metaplasia. Here, the foamy histiocytes have ample pale brown cytoplasm reflecting intracytoplasmic ceroid or lipofuscin, whereas apocrine cells have pink cytoplasm. Presence of intraluminal foam cells with identical histological appearances as those along the duct wall, together with accompanying chronic inflammation, favour a histiocytic origin

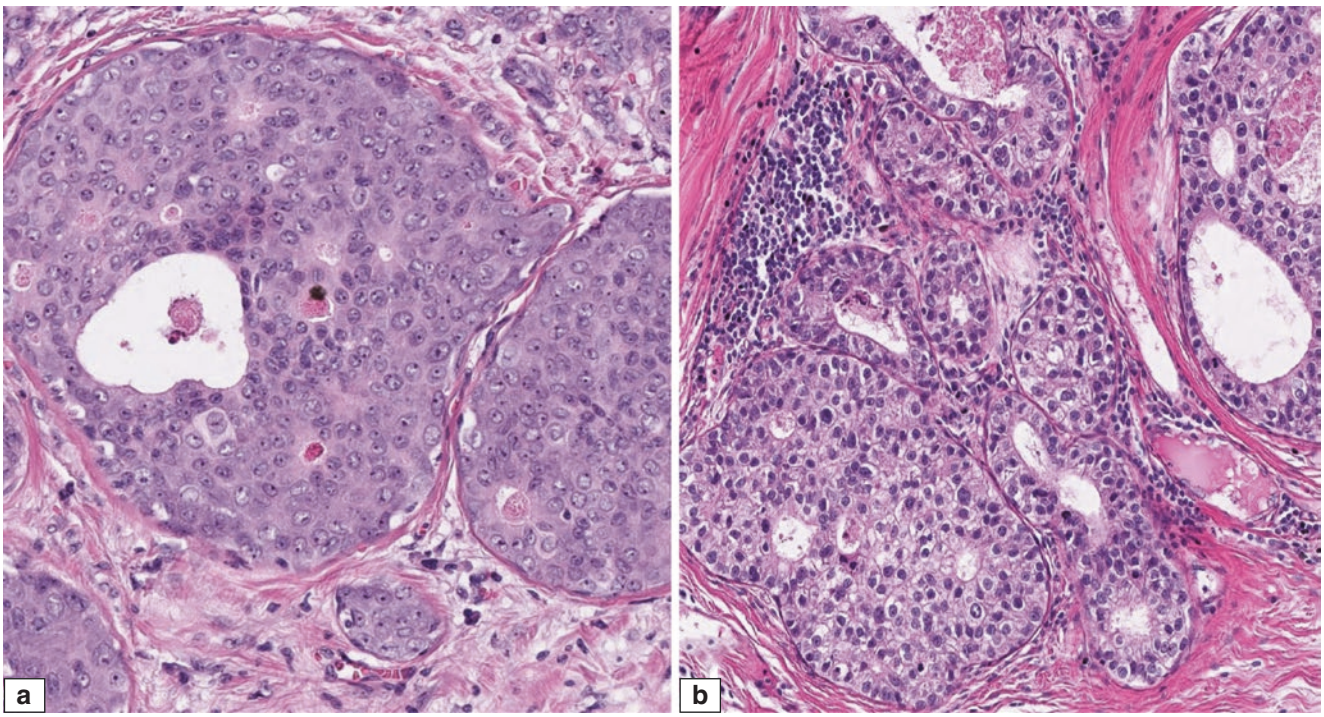

Fig. 7.13 Non-apocrine ductal carcinoma in situ (DCIS) mimicking apocrine differentiation. (**a**) Although the cells have eosinophilic cytoplasm, this proliferation is not classified as apocrine because of the lack of other characteristics of apocrine differentiation, such as cytoplasmic granularity and ample pink cytoplasm. (**b**) Similarly, this in situ ductal malignant proliferation is classified as non-apocrine

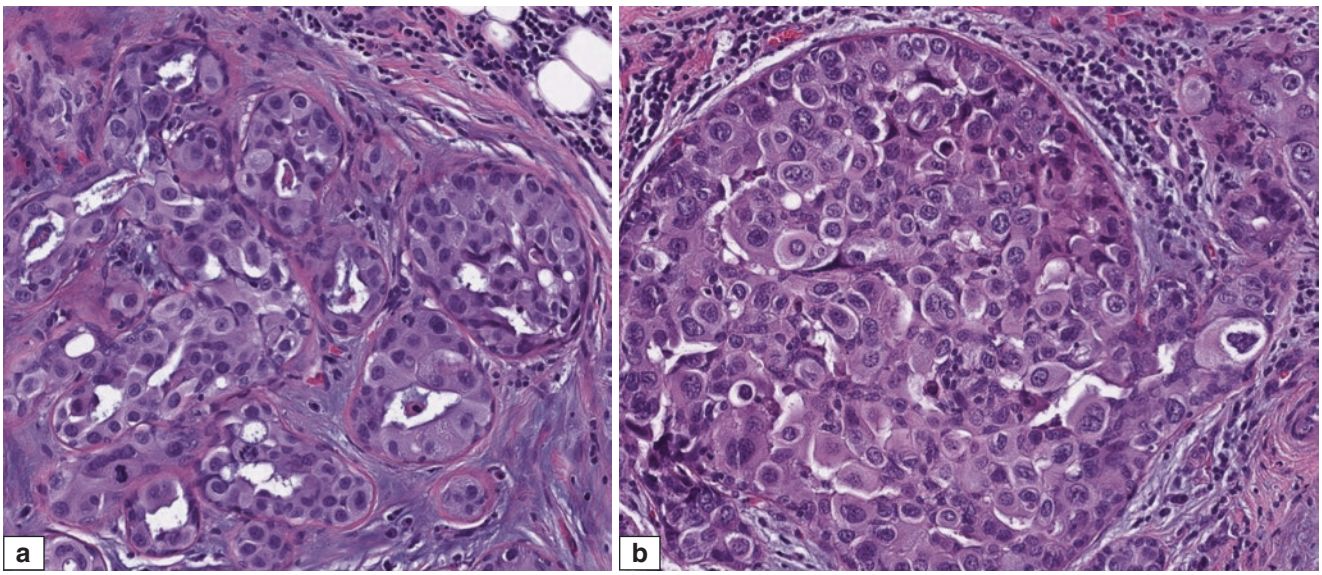

Fig. 7.14 High-grade ductal carcinoma in situ. (**a**, **b**) Although they have some features such as eosinophilic cytoplasm and prominent nucleoli, these cases are not classified as apocrine DCIS

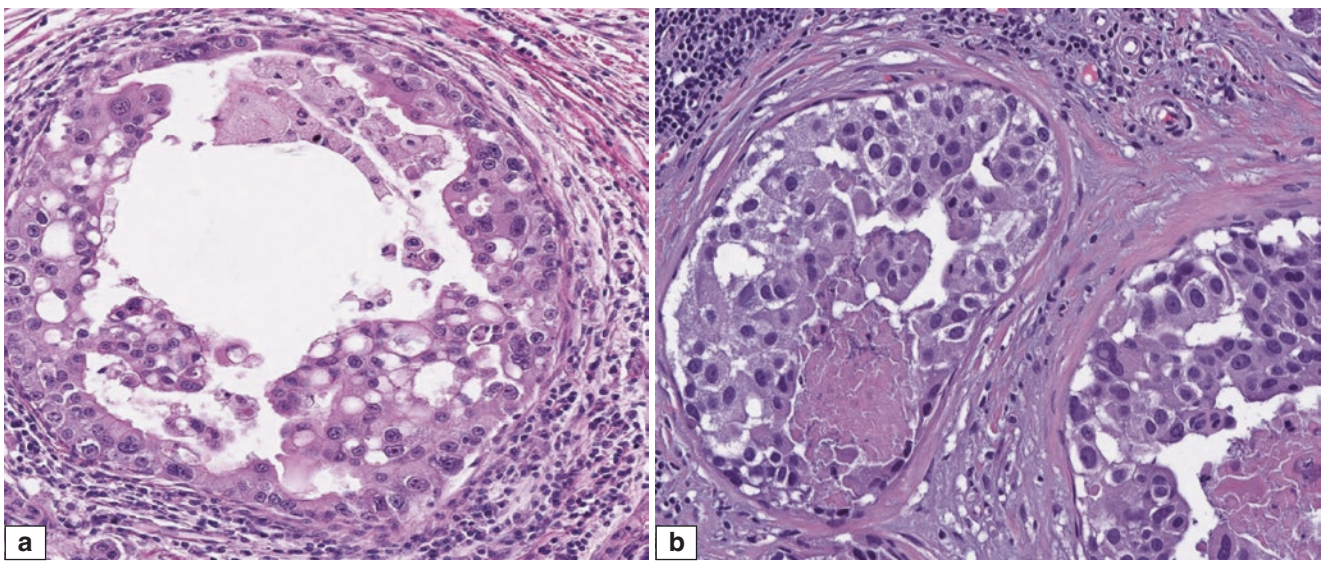

Fig. 7.15 Apocrine ductal carcinoma in situ. (**a**, **b**) Tumour cells show marked nuclear pleomorphism, granular eosinophilic cytoplasm, and prominent nucleoli. Necrosis is seen in (**b**)

Clinical and Epidemiological Features

Clinical and epidemiological features are similar to those of non-apocrine DCIS.

Imaging Features

There are no identifying imaging features specific to apocrine morphology. Similar to non-apocrine DCIS, apocrine DCIS may be associated with microcalcifications or may present as densities or masses.

Pathologic Features

Similar to non-apocrine DCIS, apocrine DCIS shows marked heterogeneity in terms of grading. In most cases, the diagnosis is not difficult because intermediate-grade or high-grade areas can be identified adjacent to low-grade apocrine lesions [18, 19]. The main diagnostic challenge is accurate categorisation of low-grade intraductal apocrine proliferations when they are identified on small biopsy specimens or when the low-grade apocrine proliferation is focal. Differentiating these lesions

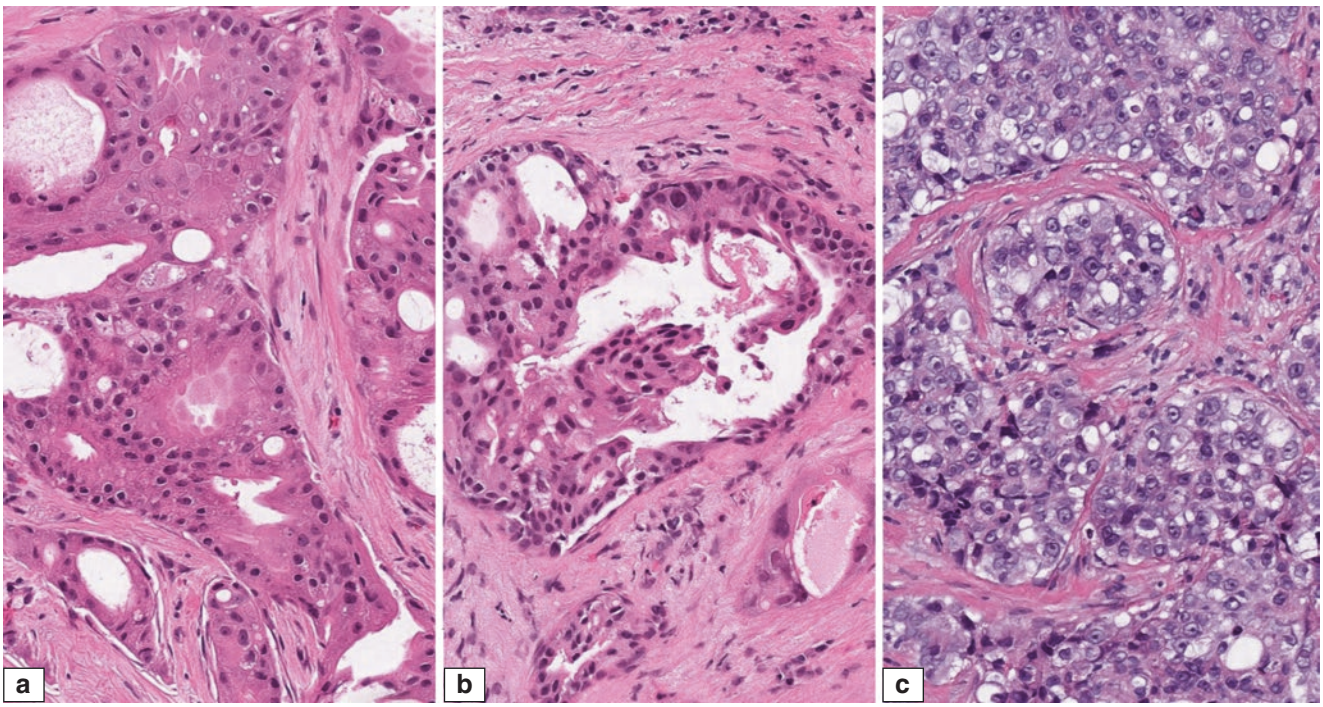

Fig. 7.16 Apocrine ductal carcinoma in situ. (**a**) Low grade. (**b**) Intermediate grade. (**c**) High grade

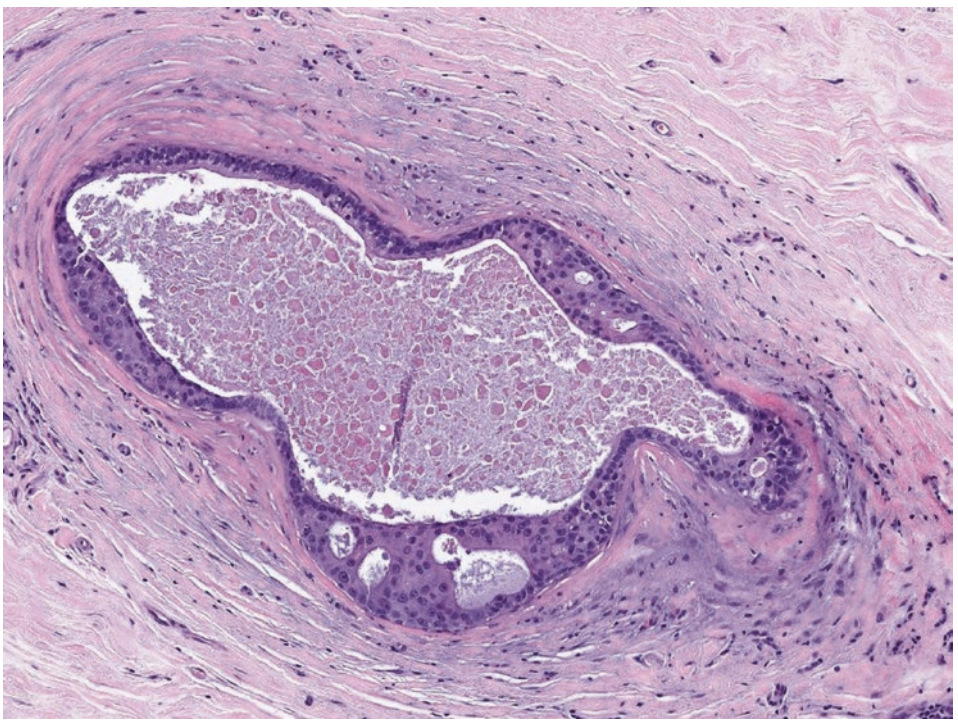

Fig. 7.17 Low-grade apocrine proliferation with focal cribriform architecture. Depending on its extent, this lesion can be classified as either a borderline lesion (atypical apocrine proliferation) or in situ ductal carcinoma

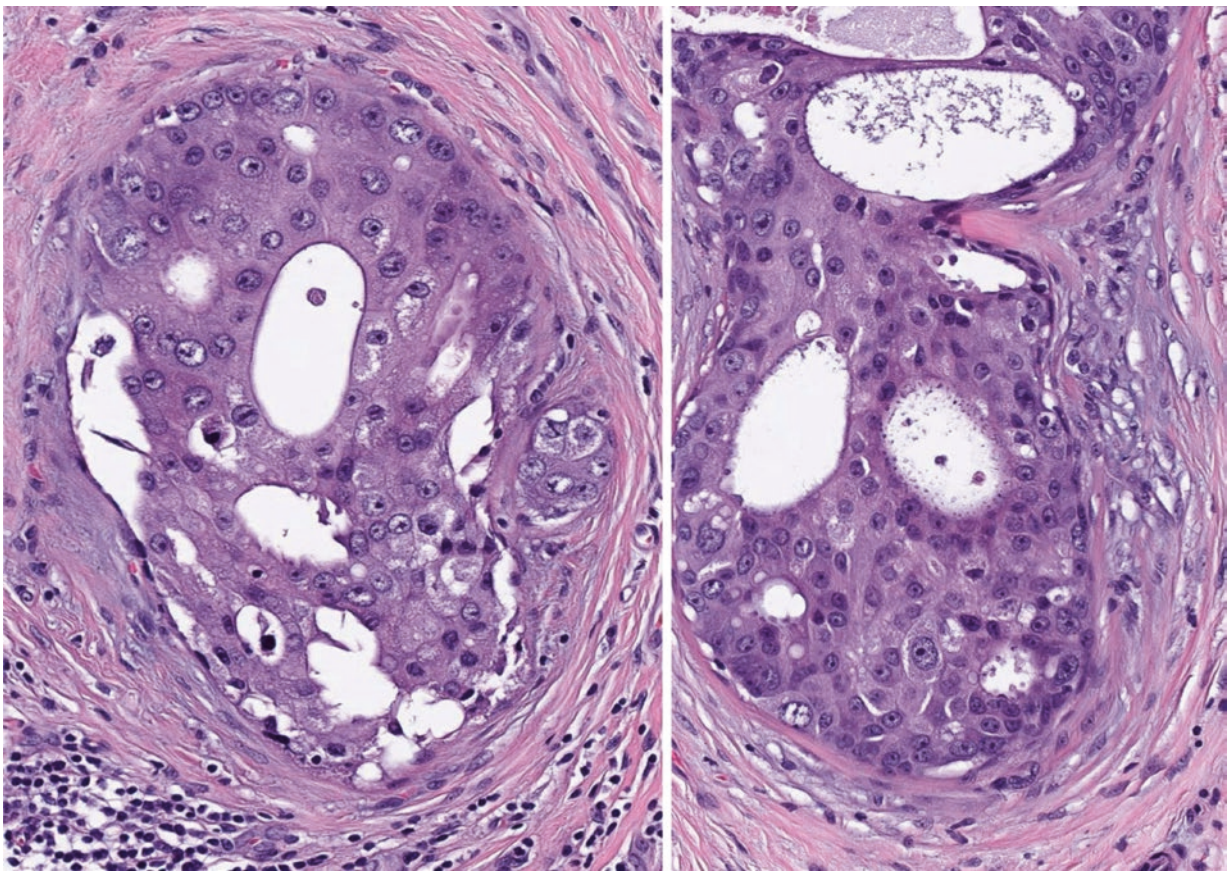

Fig. 7.18 Apocrine ductal carcinoma in situ shows a cribriform architecture with several well-defined spaces and high nuclear grade features

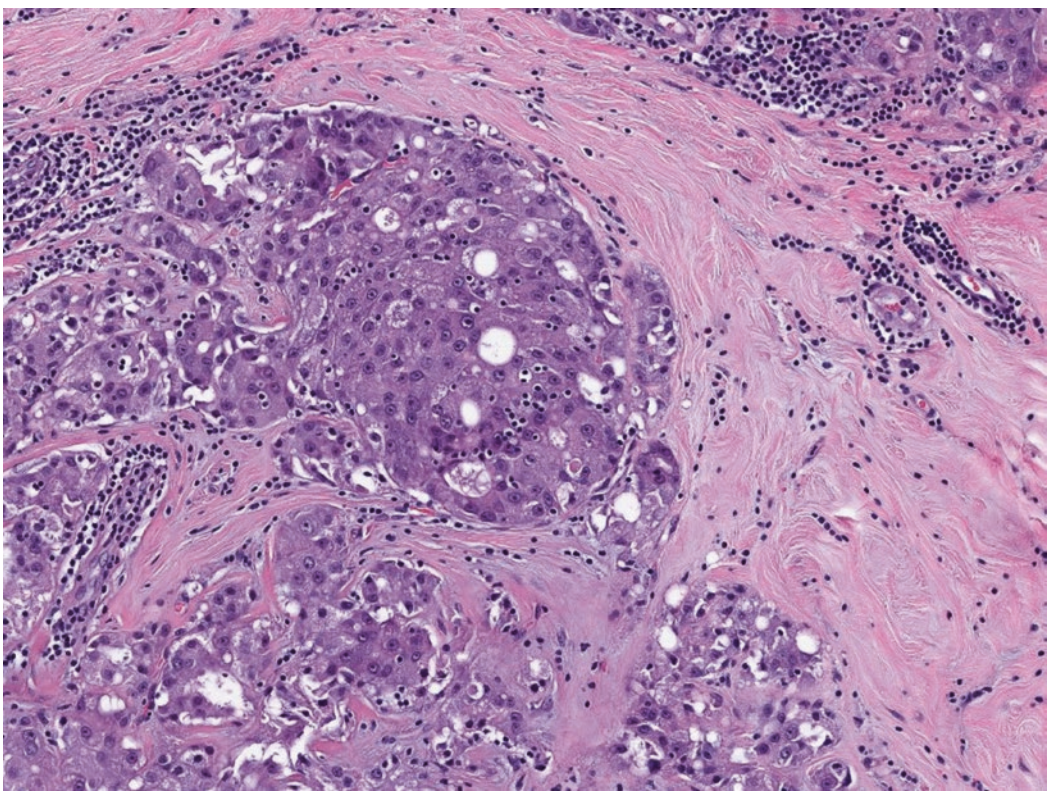

Fig. 7.19 Apocrine ductal carcinoma extending into adenosis and lobular units, distorting involved ducts and acini, making it difficult to separate in situ from invasive disease. Immunohistochemistry for myoepitheilial cells is helpful in distinguishing in situ from invasive components, with preserved myoepithelial cells in non-invasive elements

from complex benign proliferations can be challenging. Architectural complexity such as cribriforming, rigid arches, and bridges may serve as criteria to separate benign versus malignant intraductal proliferations of the breast in general, but benign intraductal apocrine proliferations can show similar complex architecture. Cytologic monotony is another feature that supports the atypical nature of an intraductal breast lesion, but cytologic monotony is a common finding in apocrine proliferations, even in benign apocrine metaplasia. In general, several features are used to distinguish apocrine DCIS from other intraductal apocrine proliferations: threefold variation in nuclear size, markedly enlarged nucleoli, necrosis, and mitotic activity (Fig. 7.20).

Differential Diagnosis

Apocrine Adenosis

The term "apocrine adenosis" has been used to describe a range of apocrine proliferations, including adenosis, sclerosing adenosis, radial scars, and complex sclerosing lesions with apocrine cytologic features (Fig. 7.21). Apocrine adenosis is typically a lobulocentric proliferation of small ducts and acini associated with architectural distortion secondary to stromal fibrosis (Fig. 7.22). The ducts and acini are lined by apocrine cells [20–25]. The term "atypical apocrine adenosis" is used to define cytologic atypia in these lesions. However, there is significant diagnostic difficulty in assessing cytologic atypia because even non-atypical apocrine cells have enlarged nuclei and prominent nucleoli, which may be regarded as morphologic evidence of "atypia". Although there are clinically validated studies to categorise non-apocrine lesions as non-atypical versus atypical hyperplasia, these criteria are not directly applicable to apocrine lesions. An intraductal lesion with cytologic atypia characterised by a significant increase in nuclear size (three-time difference compared with the nuclei of non-neoplastic apocrine cells), enlarged nucleolus or multiple nucleoli, and necrosis is highly suggestive of DCIS (Figs. 7.23 and 7.24). Caution should be exercised when these features are present singularly or are focal. In general, atypical apocrine lesions with cytologic atypia are small (2–3 mm) and involve only single ductal lobular units, whereas DCIS is usually more extensive (>8 mm) [25, 26].

Papillary Apocrine Change

Apocrine cells lining breast cysts may be arranged in papillary projections (Figs. 7.25 and 7.26). These changes may be associated with other ductal proliferative lesions of the breast such as florid usual ductal hyperplasia or atypical ductal hyperplasia. Additionally, papillary apocrine changes frequently coexist with columnar cell changes. When cystically dilated ducts are lined by multiple layers of apocrine epithelium with luminal infoldings, the term "papillary apocrine change" is used (Figs. 7.27 and 7.28) [27]. This term should not be confused with papillary lesions (chapter 4) and some authors prefer to regard papillary apocrine change as part of the broader category of apocrine metaplasia. According to the architectural complexity of these papillary structures, these lesions are subclassified as complex or highly complex papillary apocrine change in a review by Page et al. [27] (Figs. 7.29 and 7.30). Complex lesions are characterised as papillary structures forming cribriform spaces and arches (Figs. 7.31 and 7.32). Highly complex papillary apocrine lesions are described as papillary lesions with arches extending into the central portion of the ductal lumen and crossing or touching each other. The authors indicated that papillary apocrine change was associated with a mild increase in breast cancer risk. However, biopsy specimens with highly

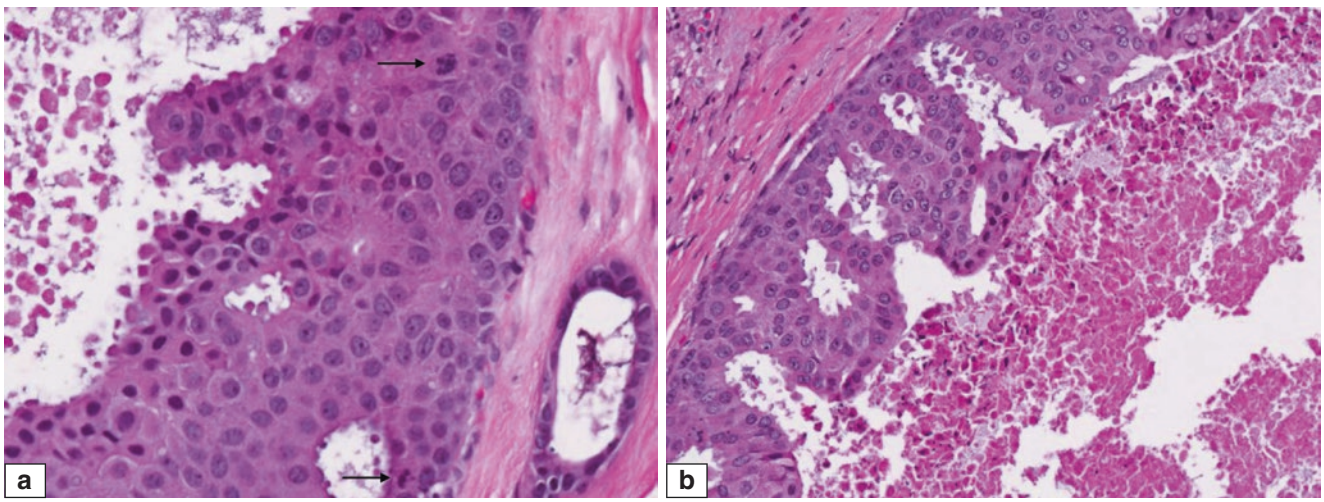

Fig. 7.20 Apocrine DCIS. (**a**) Marked variation in nuclear size of apocrine DCIS cells (threefold increase in size as compared with nuclei of an adjacent, relatively unaffected duct, *right field*) is present, as well as mitoses (*arrows*) and distinct nucleoli. (**b**) Amorphous necrosis is present

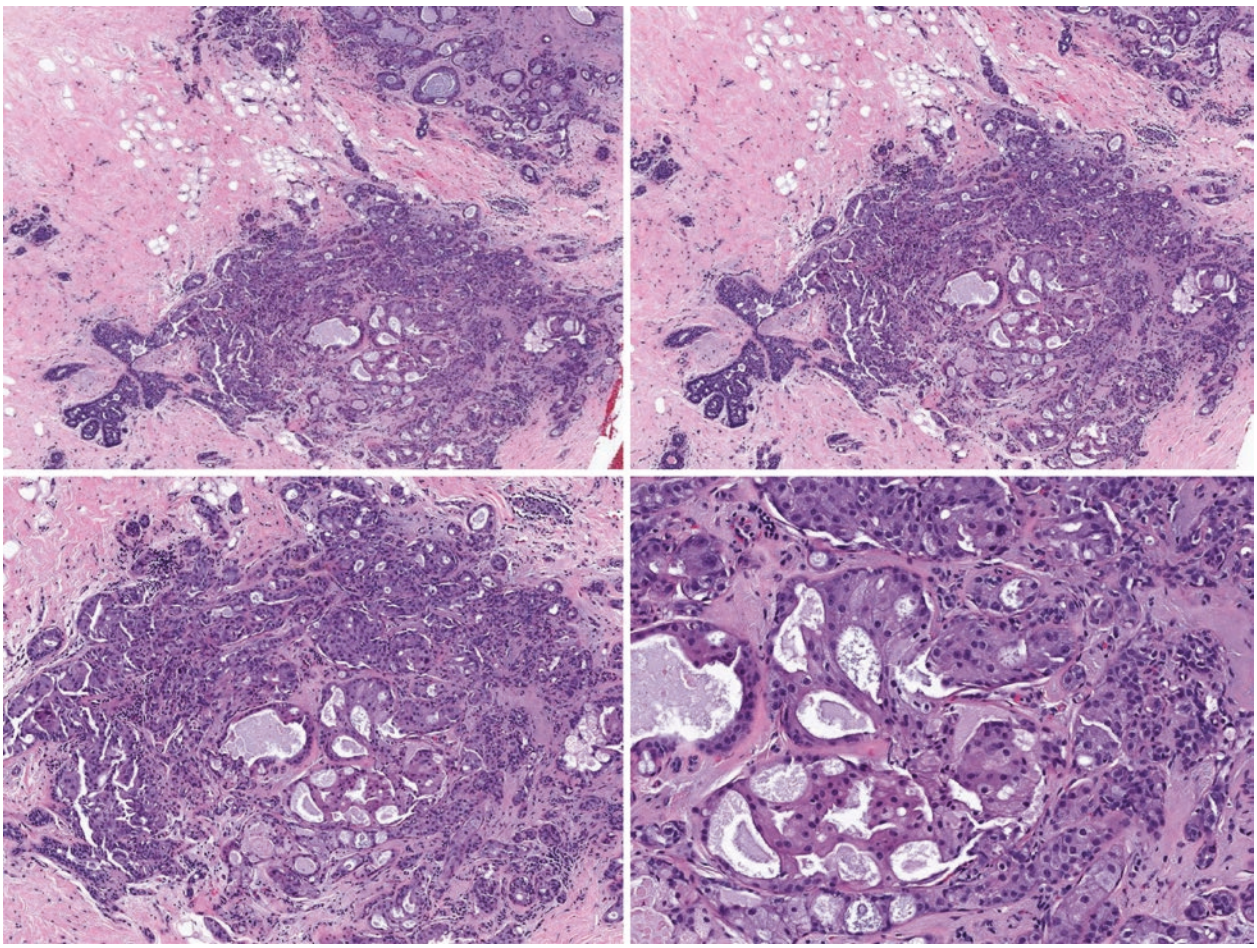

Fig. 7.21 Sclerosing adenosis focally involved by apocrine proliferation with cribriform architecture (apocrine adenosis). Although the complex cribriform architecture is suggestive of low-grade apocrine DCIS, the lesion is classified as atypical apocrine adenosis because of its limited extent. Note the lobulocentric configuration on low magnification

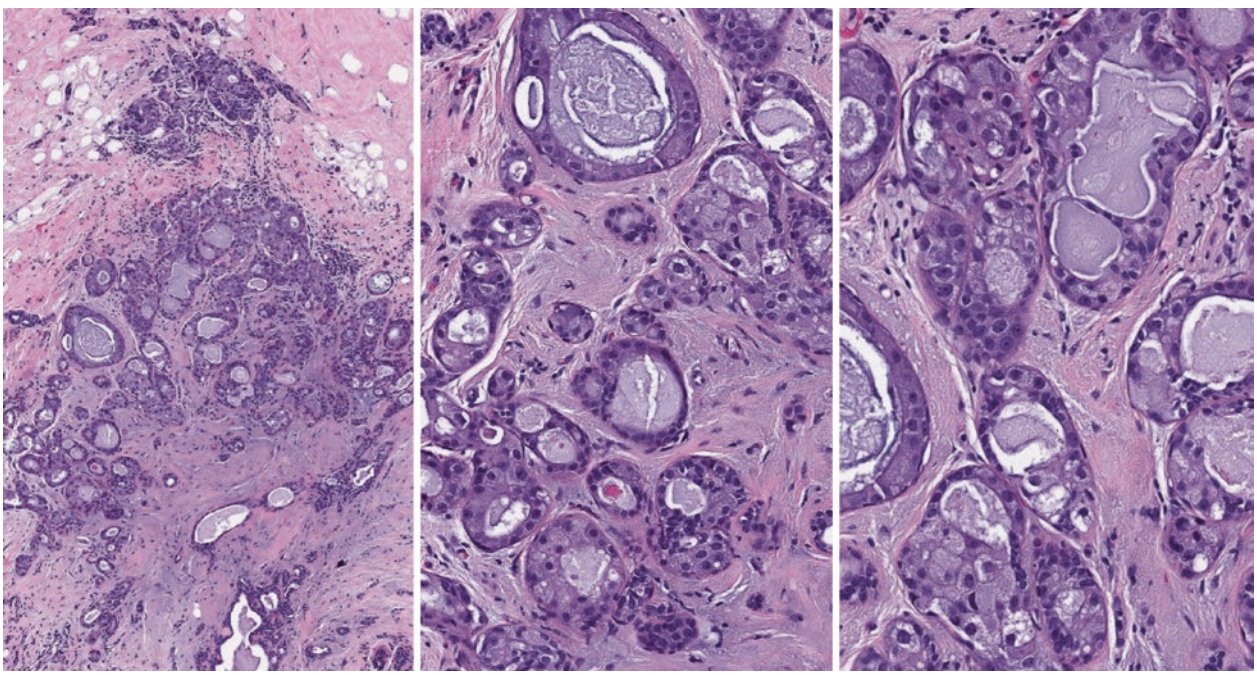

Fig. 7.22 Atypical apocrine adenosis. Apocrine change with focal cribriform architecture in a sclerosing lesion is shown

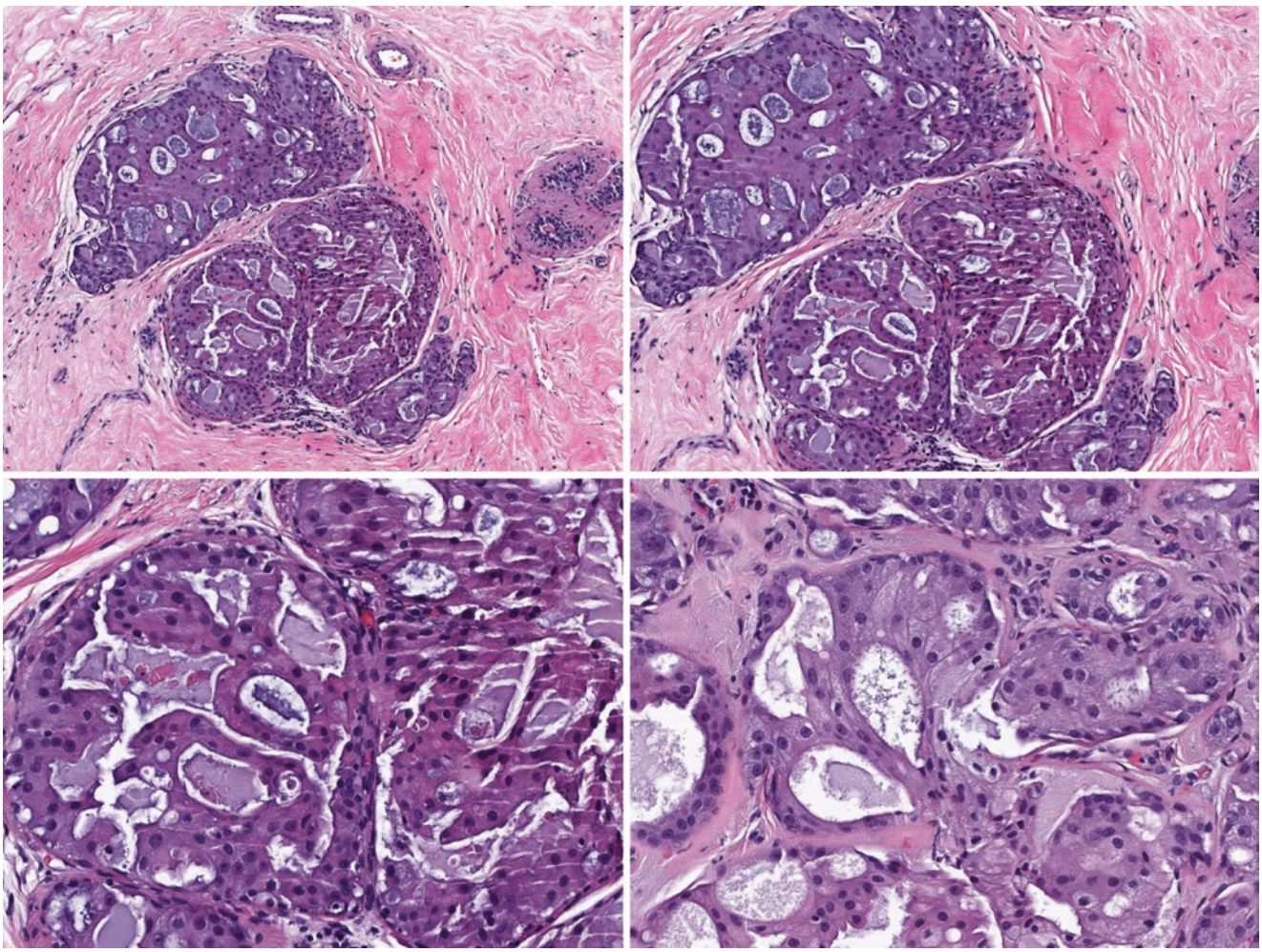

Fig. 7.23 Apocrine DCIS, low nuclear grade. The nuclei vary slightly in size and shape and they are larger than those found in normal apocrine metaplasia. The lesion measured more than 1 cm on the slide

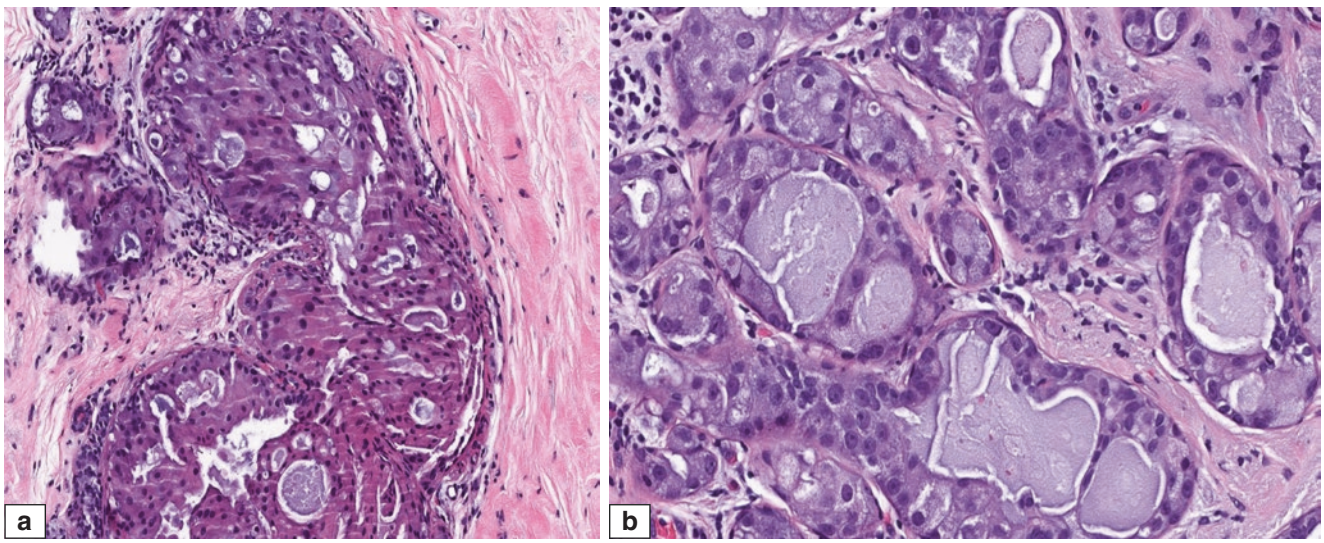

Fig. 7.24 (**a**, **b**) Apocrine DCIS is composed of cells with large, hyperchromatic nuclei and prominent nucleoli. These abnormal cytoarchitectural changes were extensive

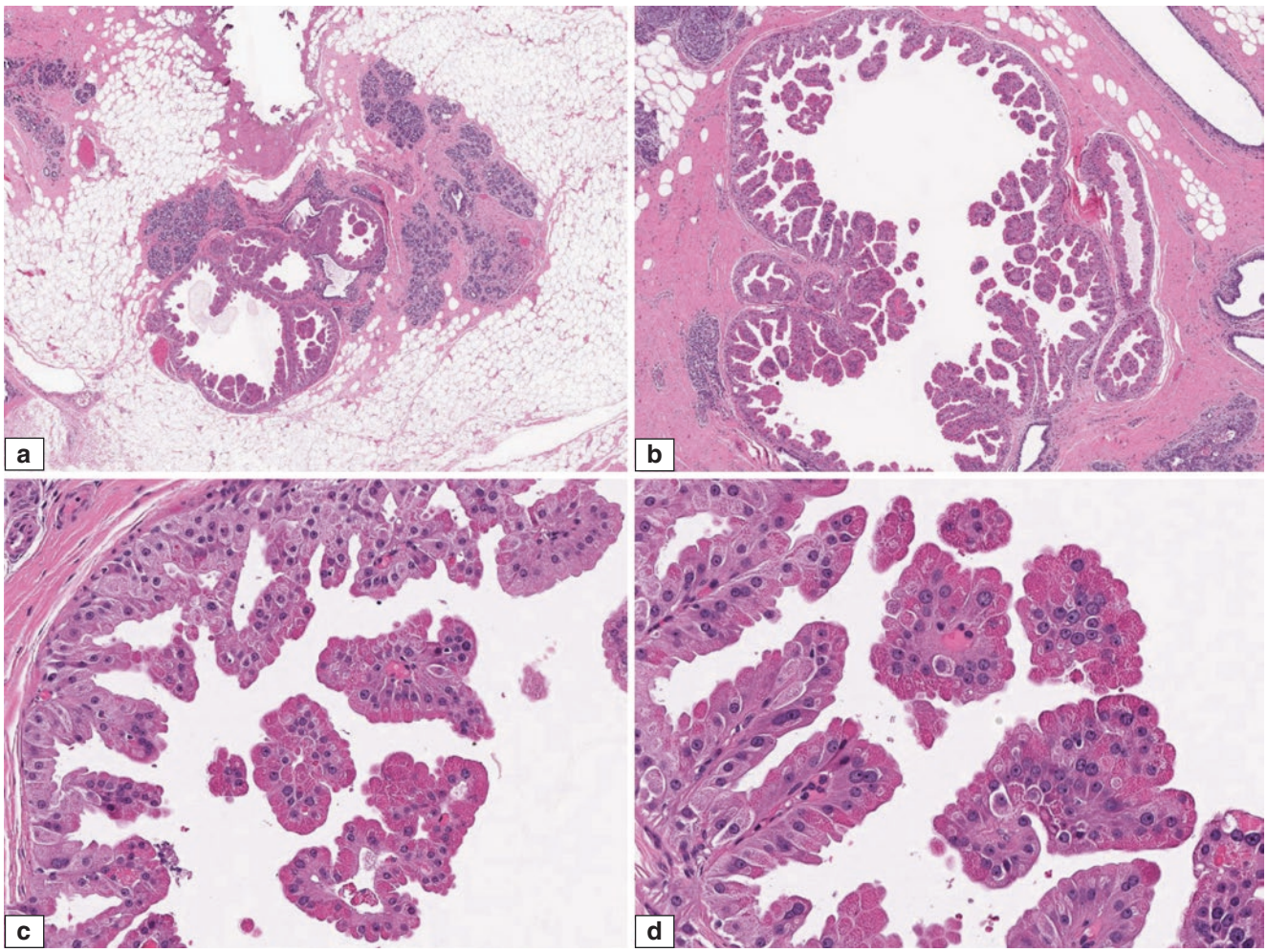

Fig. 7.25 Papillary apocrine metaplasia. (**a**–**d**) Micropapillary growth can be seen. The nuclei are uniform and regular, and there is no pleomorphism

complex papillary apocrine change had concurrent ductal epithelial proliferations, 20 % of which were atypical ductal hyperplasia and 80 % were other proliferative lesions such as usual ductal hyperplasia. They concluded that the increased risk of breast cancer was more related to ductal hyperplasia than to papillary apocrine change. Therefore, the presence of complex papillary apocrine lesions in a biopsy specimen may be considered a surrogate marker for significant proliferative change in the rest of the breast parenchyma. Pathologists should be alerted to search for high-risk lesions elsewhere in the specimen. When papillary apocrine change is complex, it may mimic apocrine DCIS. O'Malley and Bane [2] proposed the combination of cytologic and size criteria for distinguishing atypical apocrine lesions from apocrine DCIS. Apocrine DCIS should have nuclear enlargement in addition to cytologic atypia (defined as irregular nuclear membranes). Importantly, nuclear atypia should be extensive and not confined to only a few scattered cells. A few cytologically atypical cells may be observed even in benign apocrine metaplasia. Most experts use a minimum size of 4–8 mm, in conjunction with architectural atypia, as a requirement for establishing the diagnosis of low-grade apocrine DCIS. A borderline category has been proposed, consisting of proliferations with cytologic atypia that measure from 4 to 8 mm. Unfortunately, the clinical significance of such cases is unclear. Unless both cytologic and size criteria for in situ carcinoma are fully met, the lesion should not be classified as DCIS based on complex papillary architecture or cytologic atypia alone [26].

The coexistence of papillary apocrine change with columnar cell change and low-grade invasive carcinoma has been observed, and some authors postulate a common molecular pathway for the development of these lesions [28, 29]. Molecular apocrine lesions however, segregate with the ER-negative group of breast cancers, and may play a role in their pathogenesis [30].

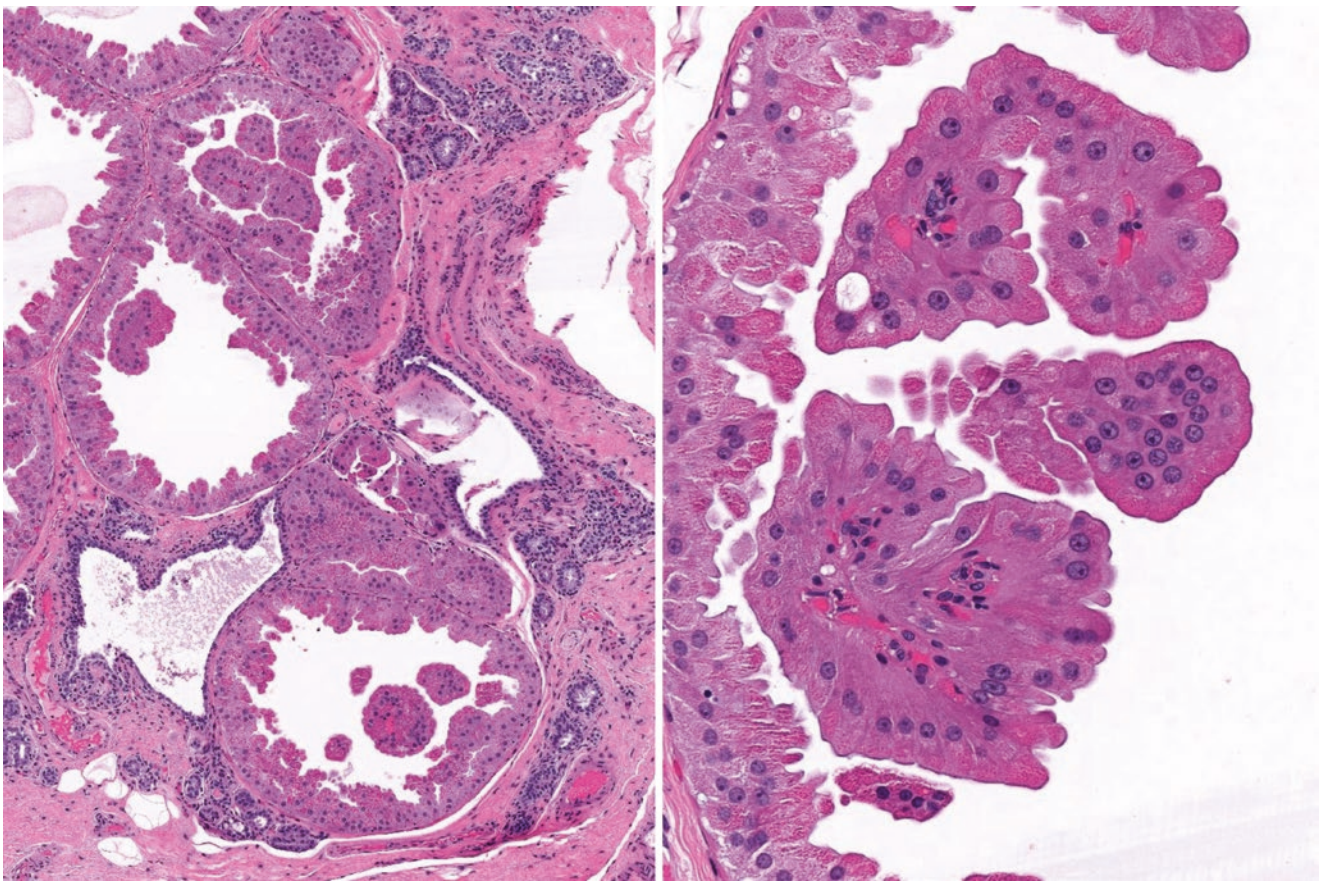

Fig. 7.26 Papillary apocrine metaplasia. Papillary tufts of apocrine cells with snouts protrude into glandular lumens

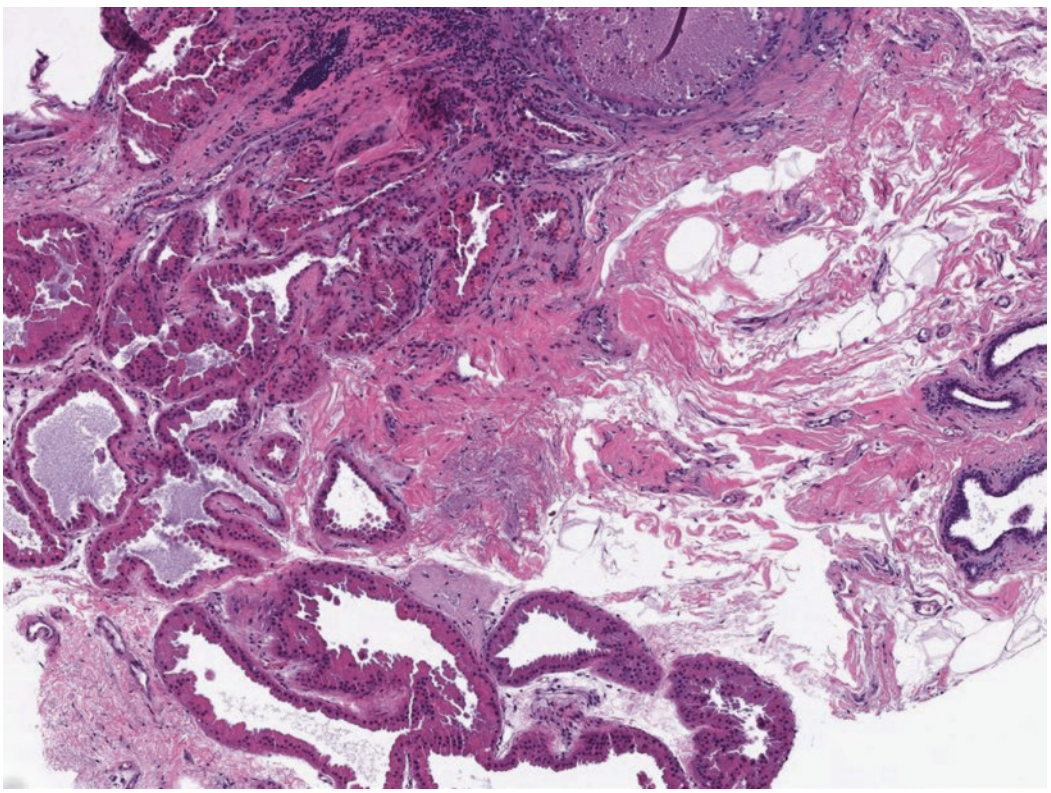

Fig. 7.27 Papillary apocrine metaplasia. Dilated terminal ductal lobular units show papillary fronds with architectural complexity

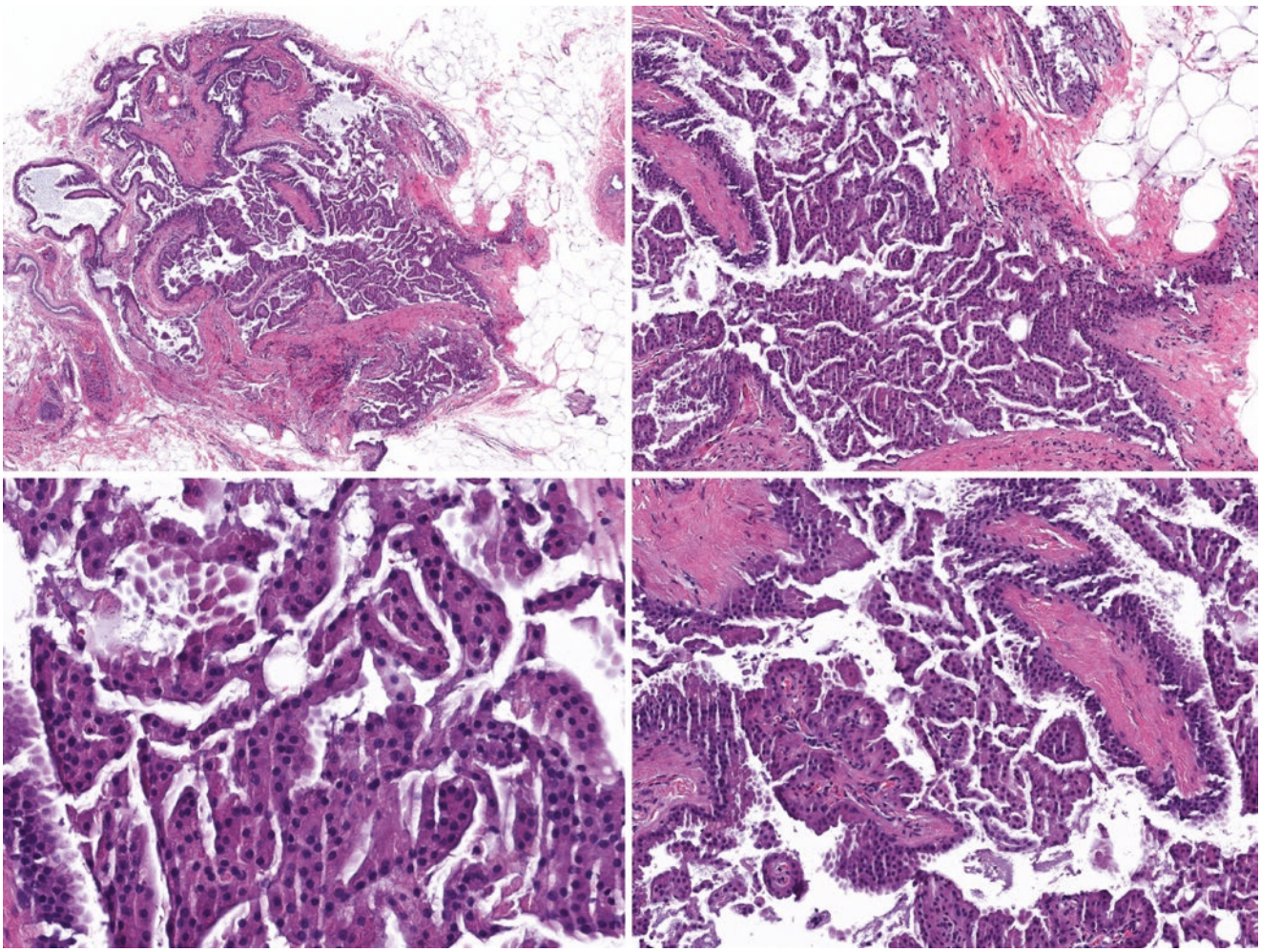

Fig. 7.28 Papillary apocrine metaplasia. Intraluminal papillary projections formed by apocrine cells are seen, giving a complex architectural appearance

Apocrine Adenoma

Apocrine adenoma is a rare, benign, neoplastic proliferation of the breast, characterised by a nodular proliferation of papillary and/or cystic apocrine breast ductal epithelium, surrounded by myoepithelial cells (Fig. 7.33). It is usually a well-demarcated mass lesion, and some may represent nodular sclerosing adenosis with extensive apocrine metaplasia. Based on the circumscription and the monotonous apocrine features of proliferating cells, this is usually a straightforward diagnosis [3, 31].

Prognosis and Therapy Considerations

In general, many apocrine DCIS cases show a mixture of histologic patterns and cytologic types. These do not appear to have a major biologic significance, so recognition of DCIS is more important than subcategorisation as apocrine DCIS. Treatment and prognosis depend mainly on other factors such as size, extent, margin status, and biomarker expression.

Invasive Apocrine Carcinoma

Definition

Invasive apocrine carcinoma has generally been regarded as a morphologic variant of invasive breast carcinoma not otherwise specified, rather than a special type of invasive cancer [32–36].

Clinical and Epidemiological Features

Invasive apocrine carcinomas of the breast are not clinically distinct from invasive carcinoma not otherwise specified. The reported incidence of apocrine carcinoma varies from <0.5 to 4 % in the literature [6, 16, 17, 32–37]. This variability in incidence is most likely due to the lack of well-defined diagnostic criteria to define apocrine carcinoma. In general, it is recommended that the term should be reserved for neoplasms in which almost all tumour cells show apocrine cytological features. In contrast, focal apocrine differentiation is

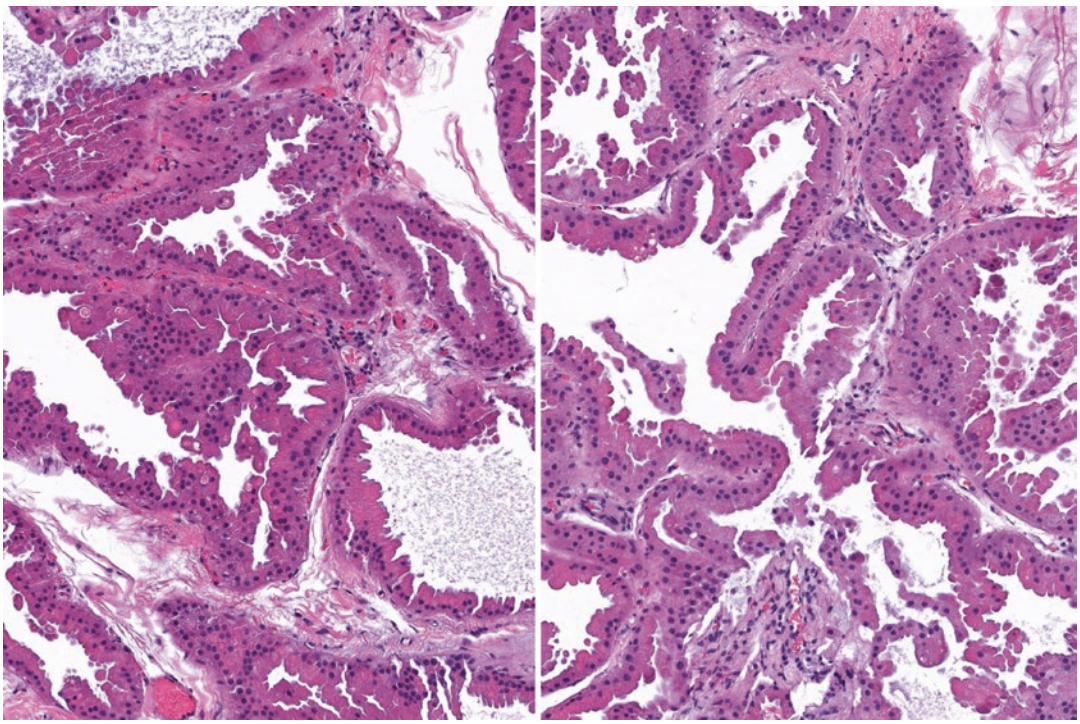

Fig. 7.29 Proliferative papillary apocrine metaplasia. Cystically dilated ducts are lined by multiple layers of apocrine epithelium

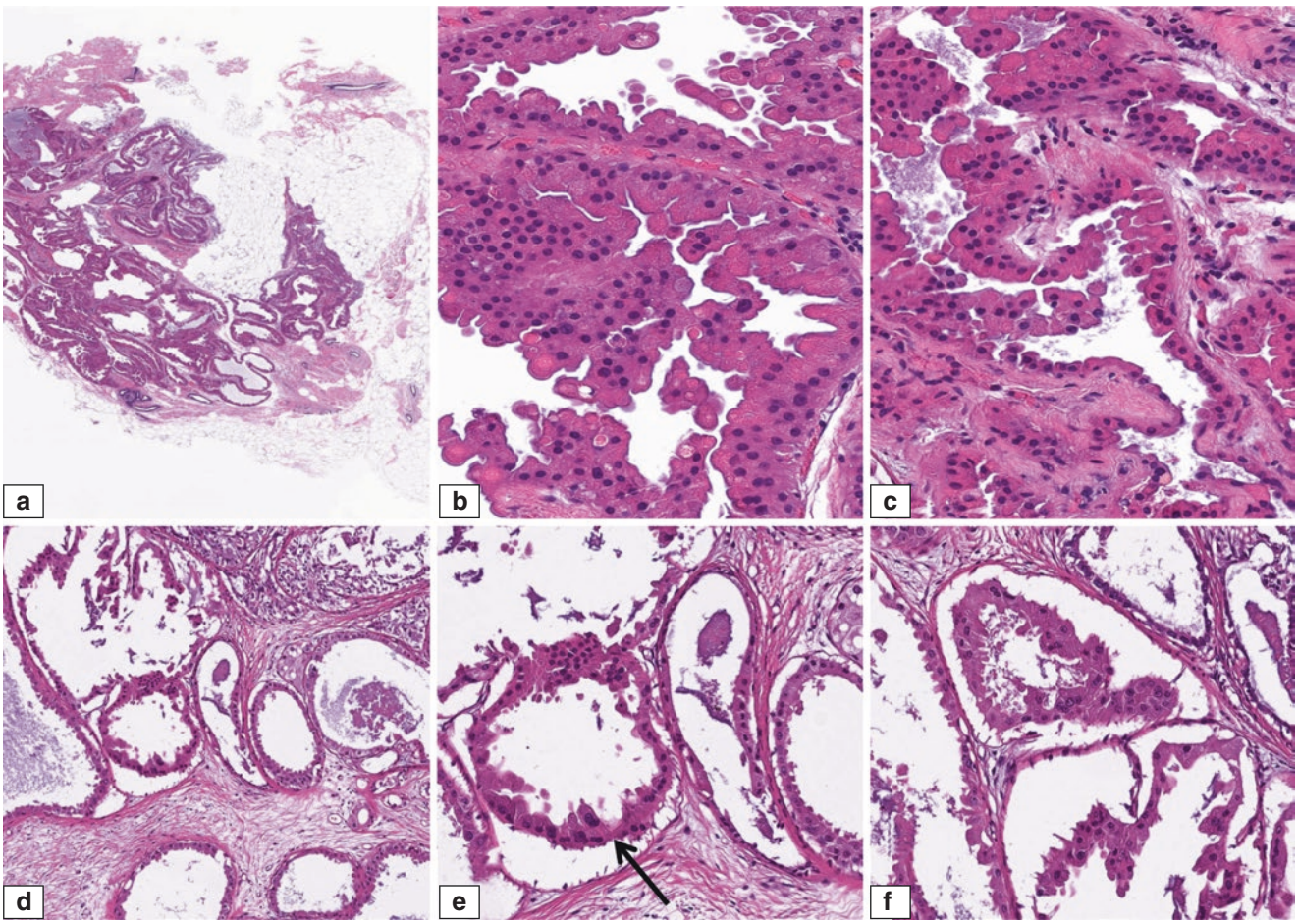

Fig. 7.30 Complex papillary apocrine metaplasia. (**a**–**c**) Architecturally complex papillary apocrine change shows arches extending into the central luminal space while crossing or touching each other. (**d**–**f**) Cytologic atypia (hyperchromasia and three-time size variation) can be focally present (*arrow*)

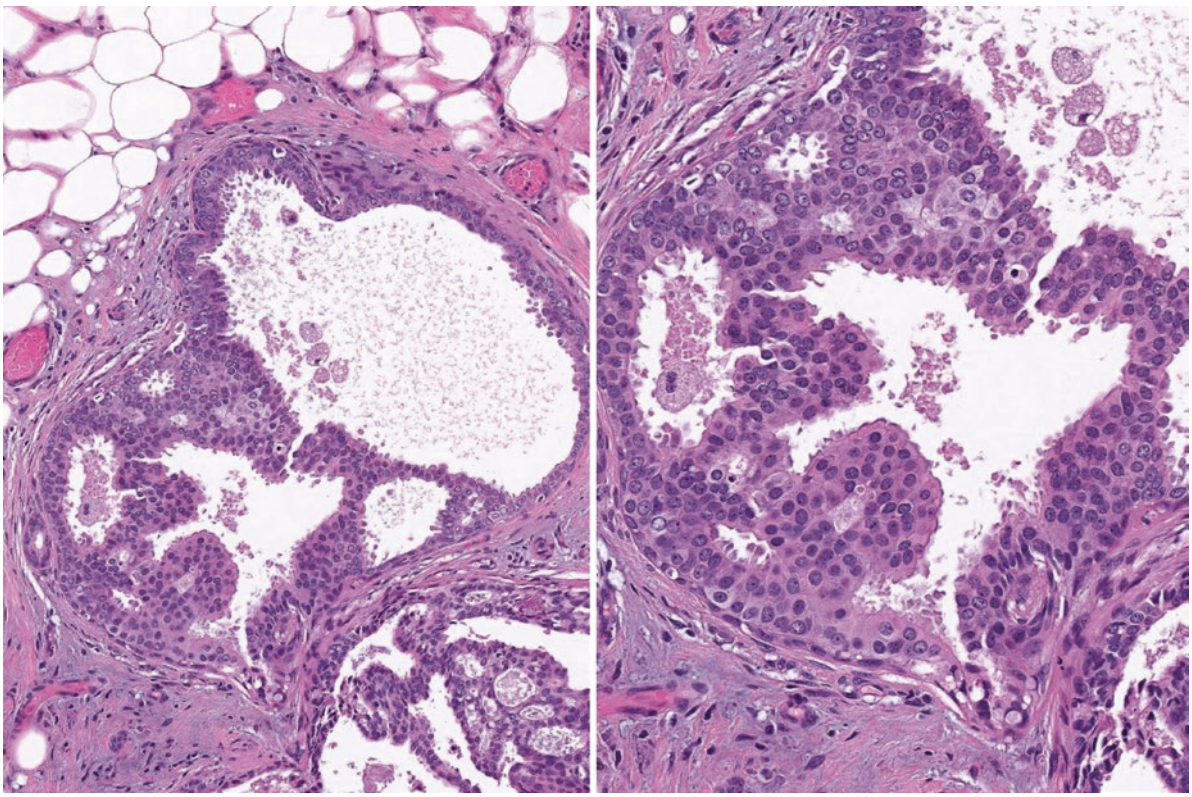

Fig. 7.31 Atypical ductal hyperplasia/low-grade DCIS in a background of apocrine change. A true cribriform architecture is more characteristic of low-grade apocrine DCIS. The conclusion of whether this represents atypical ductal hyperplasia or DCIS depends on the lesional extent of the cytoarchitectural atypia

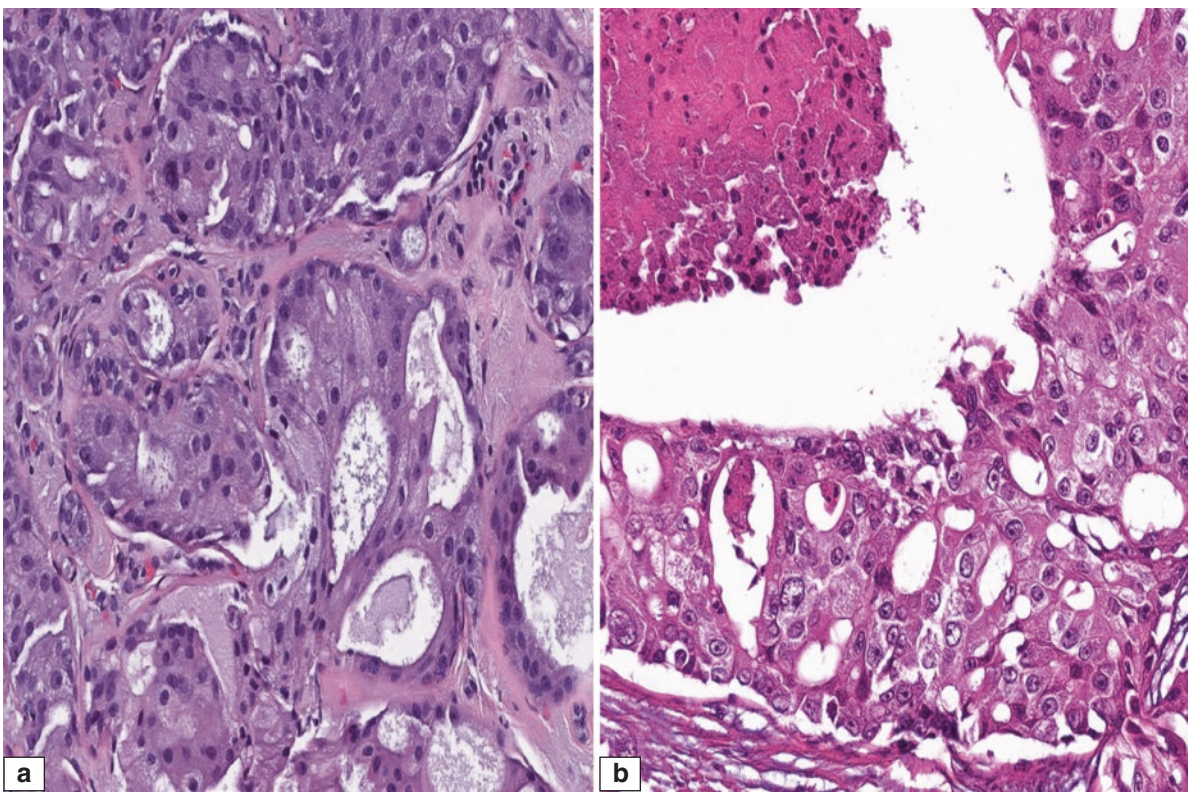

Fig. 7.32 Apocrine ductal carcinoma in situ. (**a**) Low-grade DCIS is characterised by cribriform architecture and a solid proliferation of apocrine cells with angular and hyperchromatic nuclei. Some authors require the size of this proliferation to be at least 8 mm in order to establish the diagnosis. Lesions measuring 4–8 mm may be classified as "borderline" lesions. (**b**) High-grade apocrine DCIS is characterised by marked nuclear pleomorphism, central comedonecrosis, and individual cell necrosis

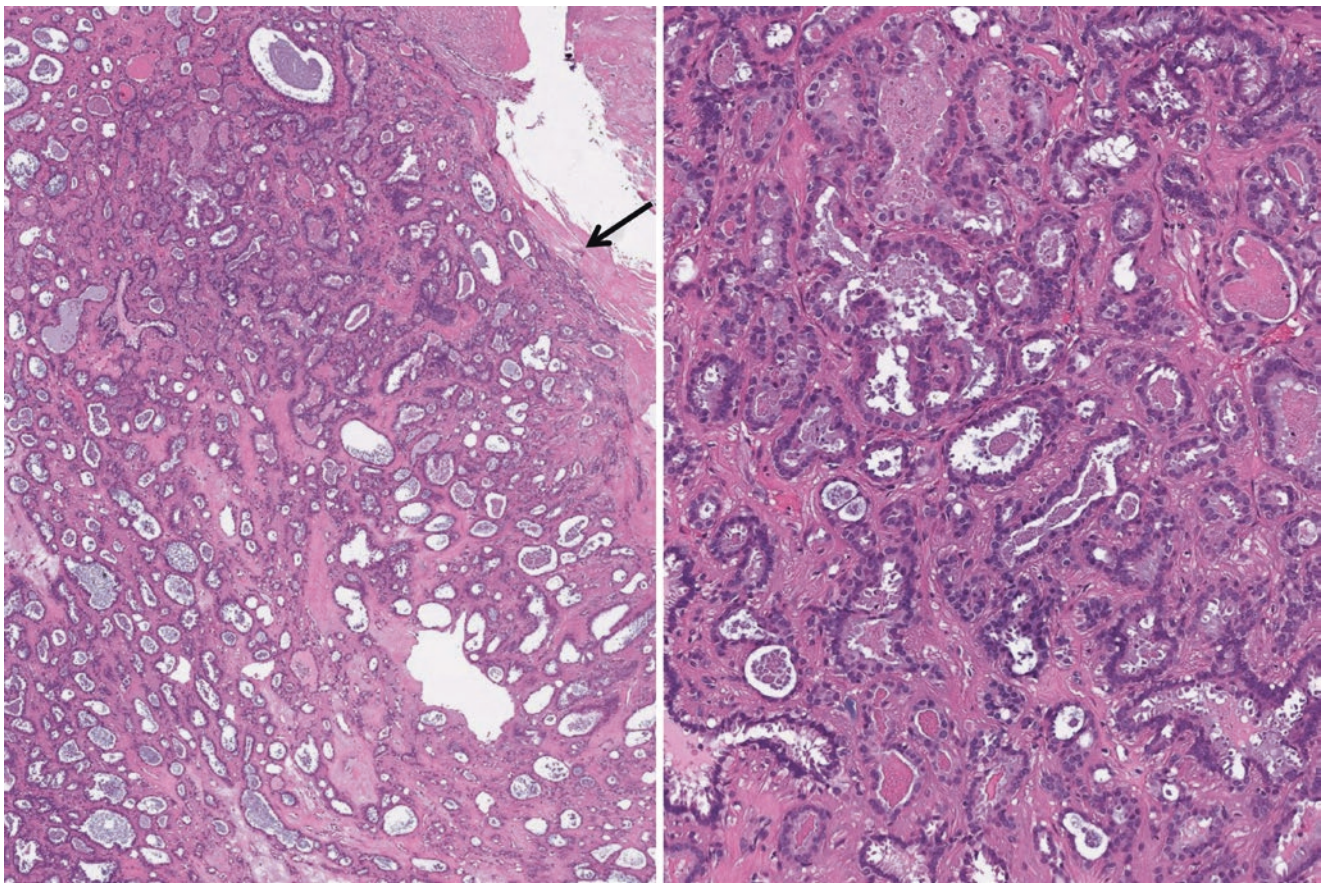

Fig. 7.33 Apocrine adenoma, composed of a proliferation of small glands lined by apocrine cells. Note the circumscription of the border of the lesion (*arrow*)

quite common and has been reported in up to 60 % of invasive carcinomas of no special type.

When the diagnosis of apocrine carcinoma is based on the immunohistochemical expression of GCDFP-15, the incidence of apocrine carcinoma has been as high as 70 % [16, 17]. Areas of apocrine differentiation have also been reported in other special types of invasive breast cancers, such as invasive papillary and lobular carcinomas [16, 17].

Imaging Features

Tumour size, presentation, incidence of lymph node positivity, and imaging findings of apocrine carcinomas do not differ significantly from invasive carcinomas of no specific type [38, 39].

Pathologic Features

Macroscopic Pathology

There are no distinct findings associated with apocrine carcinoma. Invasive apocrine carcinomas are grossly indistinguishable from other invasive breast carcinomas [34–37].

Microscopic Pathology

Microscopically, apocrine carcinomas show growth patterns similar to invasive carcinomas not otherwise specified. The only distinct feature is the cytological appearance. The cells typically have apocrine morphology with abundant granular cytoplasm and enlarged nuclei with prominent, often multiple, nucleoli (Figs. 7.34, 7.35, 7.36, and 7.37). The grade of the lesion can be low (grade 1), intermediate (grade 2), or high (grade 3). Necrosis and abundant mitoses are common in high-grade lesions (Figs. 7.38 and 7.39) [32–37]. Most apocrine carcinomas are of the ductal type, but lobular carcinomas (especially pleomorphic lobular carcinomas) may show apocrine cytologic features. At the ultrastructural level, apocrine carcinomas have abundant intracytoplasmic organelles including secretory granules, mitochondria, and incomplete cristae [16, 17].

Immunohistochemical Profile

Apocrine lesions have a distinct immunohistochemical profile [16, 17, 40]. A high percentage of invasive and in

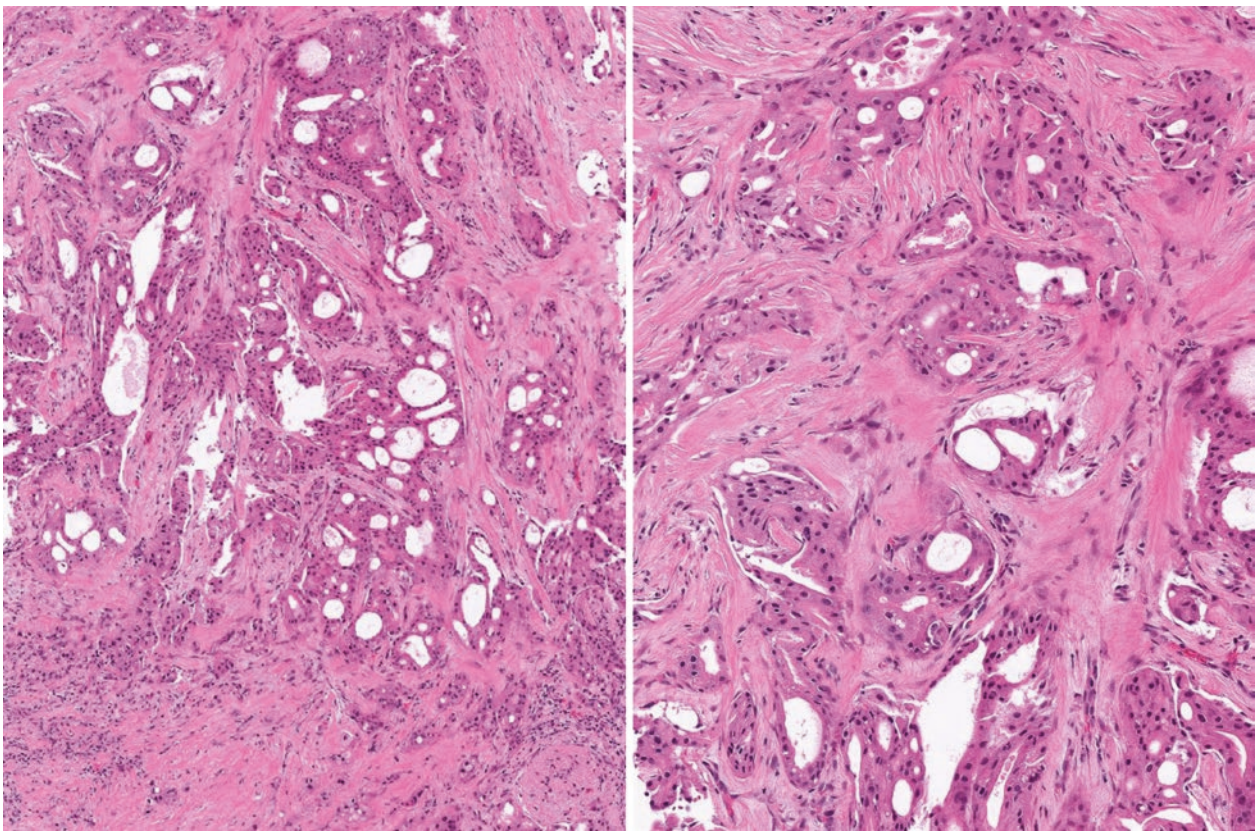

Fig. 7.34 Invasive apocrine carcinoma. Apocrine differentiation can be identified based on abundant granular cytoplasm and round, centrally located nuclei. A significant portion of the tumour must show this morphology in order to be classified as apocrine carcinoma

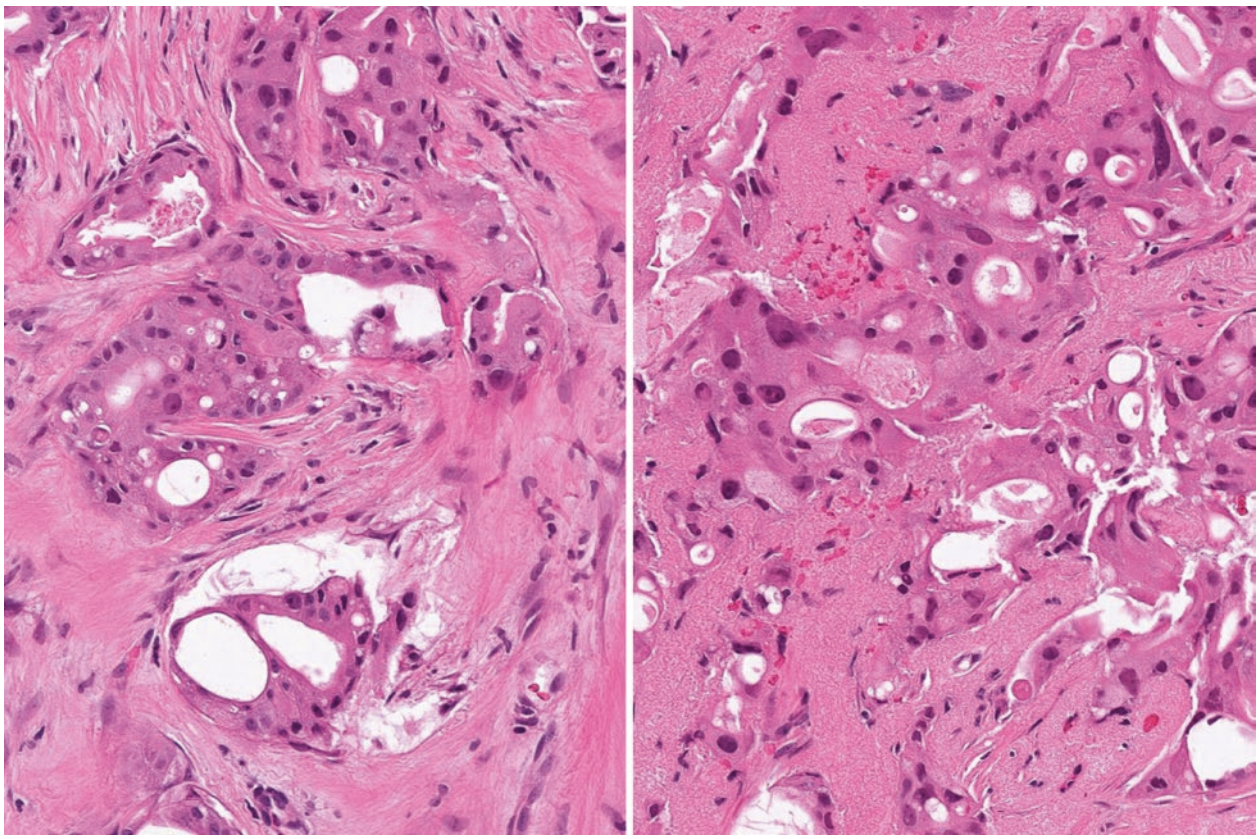

Fig. 7.35 Invasive apocrine carcinoma. Large tumour cells have abundant, granular, eosinophilic cytoplasm and large, round nuclei. Invasive apocrine carcinoma almost always shows moderate to marked nuclear pleomorphism

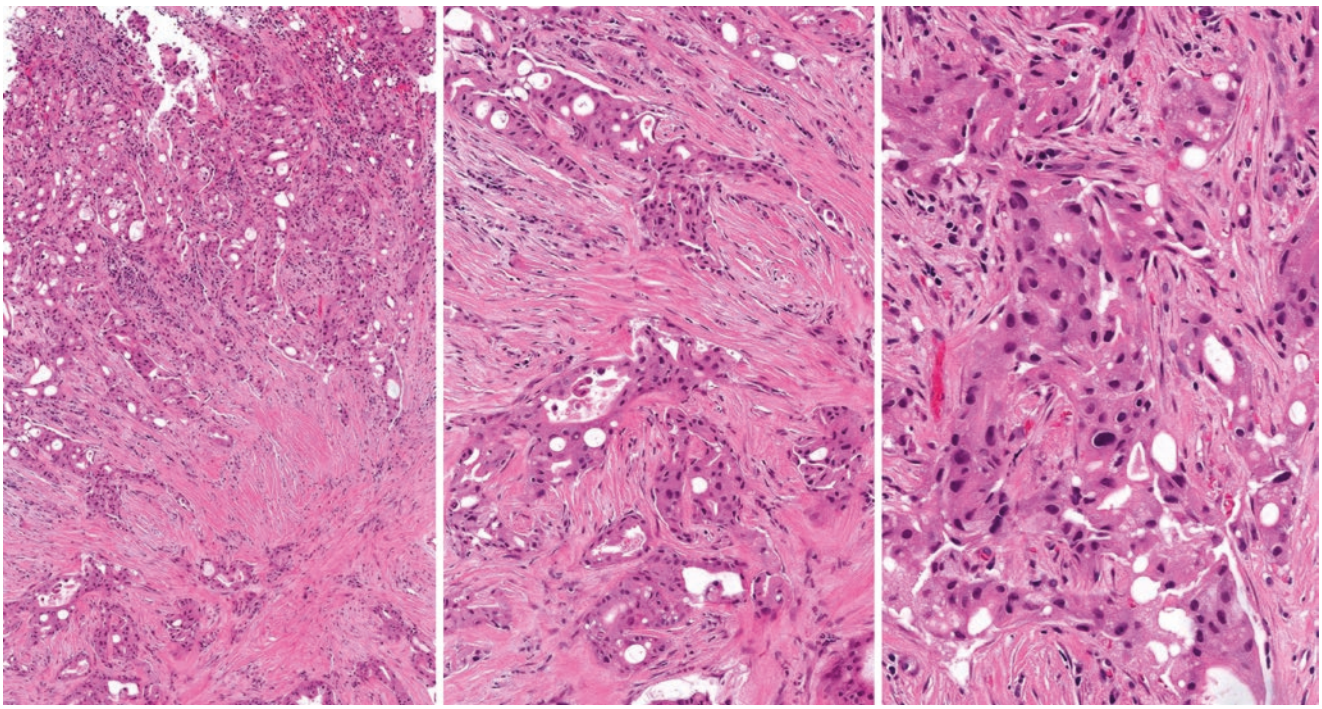

Fig. 7.36 Invasive apocrine carcinoma, intermediate grade (grade 2). Irregular clusters and nests of malignant apocrine cells infiltrate the stroma. The infiltrating tumour clusters have cribriform architecture. Tumour cells have pleomorphic nuclei

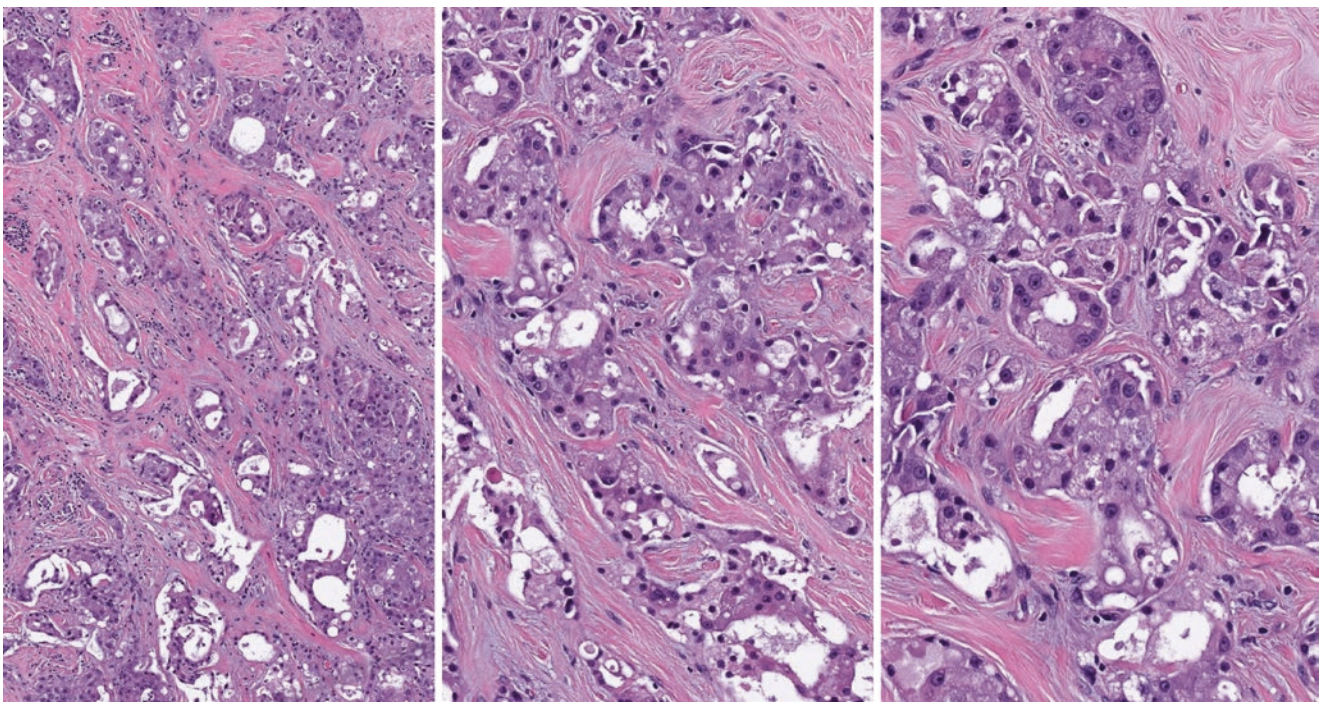

Fig. 7.37 Invasive apocrine carcinoma, intermediate grade (grade 2). Tumour cells have abundant eosinophilic and granular cytoplasm and large nuclei with prominent nucleoli. In apocrine carcinomas, tubule formation is rarely greater than 75 %

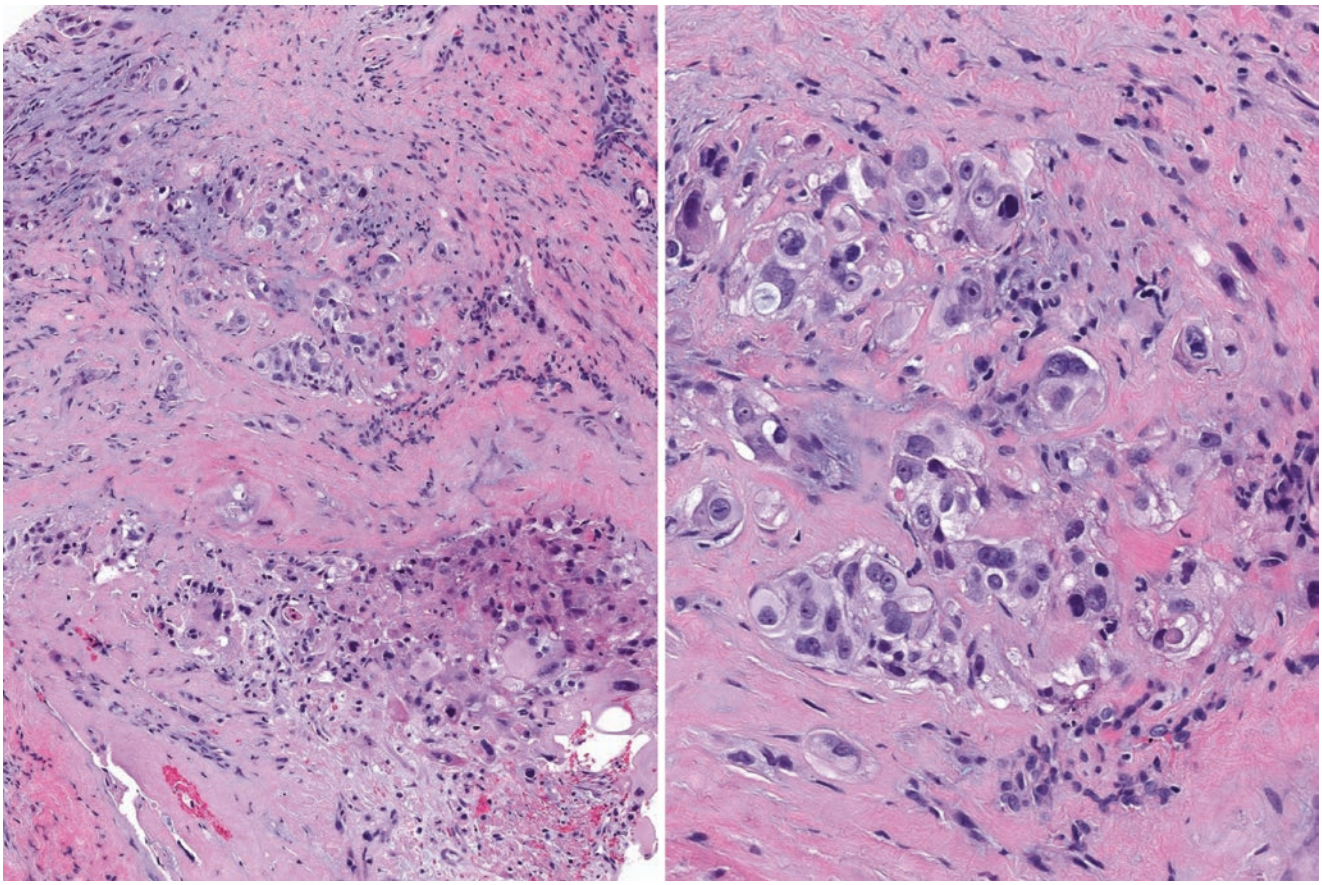

Fig. 7.38 Invasive apocrine carcinoma, high grade (grade 3). Markedly abnormal tumour cells infiltrate the surrounding fibrous tissue. The tumour cells have round to oval nuclei with distinct cell borders. Extensive individual cell necrosis is evident

situ carcinomas with apocrine morphology are positive for GCDFP-15 (Fig. 7.40), whereas fewer than 40 % of non-apocrine breast carcinomas show positivity. Similarly, a higher percentage of apocrine carcinomas show immunoreactivity for carcinoembryonic antigen, compared with non-apocrine carcinomas. Apocrine carcinomas, similar to invasive carcinomas not otherwise specified, have been reported to express CK7, CK8, and CK18. In general, CK20 is not commonly positive in breast carcinomas, but 50 % of invasive apocrine carcinomas have been reported to express CK20. Usually, there is no positivity for basal cytokeratins (CK5/6 and CK14) in apocrine carcinomas [40].

Both benign apocrine lesions and most malignant apocrine tumours are positive for androgen receptor expression (Figs. 7.41 and 7.42) [41–44]. Some experts require androgen receptor positivity for defining apocrine carcinoma. The majority of apocrine carcinomas are negative for oestrogen and progesterone receptors. Positivity for androgen receptor and negativity for oestrogen and progesterone receptor have been recognised as the "typical" apocrine phenotype [41–46]. Recently, Gromov et al. [47] have identified HMGCS2 and FABP7 as two novel markers to recognise apocrine differentiation in breast lesions.

Approximately half of apocrine carcinomas have been reported to show c-erbB-2 overexpression and gene amplification (Fig. 7.43). High levels of bcl-2, which is an anti-apoptotic protein, usually correlate with oestrogen receptor positivity in breast cancer [37, 44, 48, 49]. Routine evaluation of androgen receptor is not recommended in all breast carcinomas, but in certain subsets, such as triple-negative and c-erbB-2-positive tumours, such an evaluation can help in identifying a therapy target [50]. Almost 50 % of apocrine carcinomas have been reported to overexpress bcl-2 despite being oestrogen receptor negative. The clinical significance of this finding remains unknown (Table 7.1).

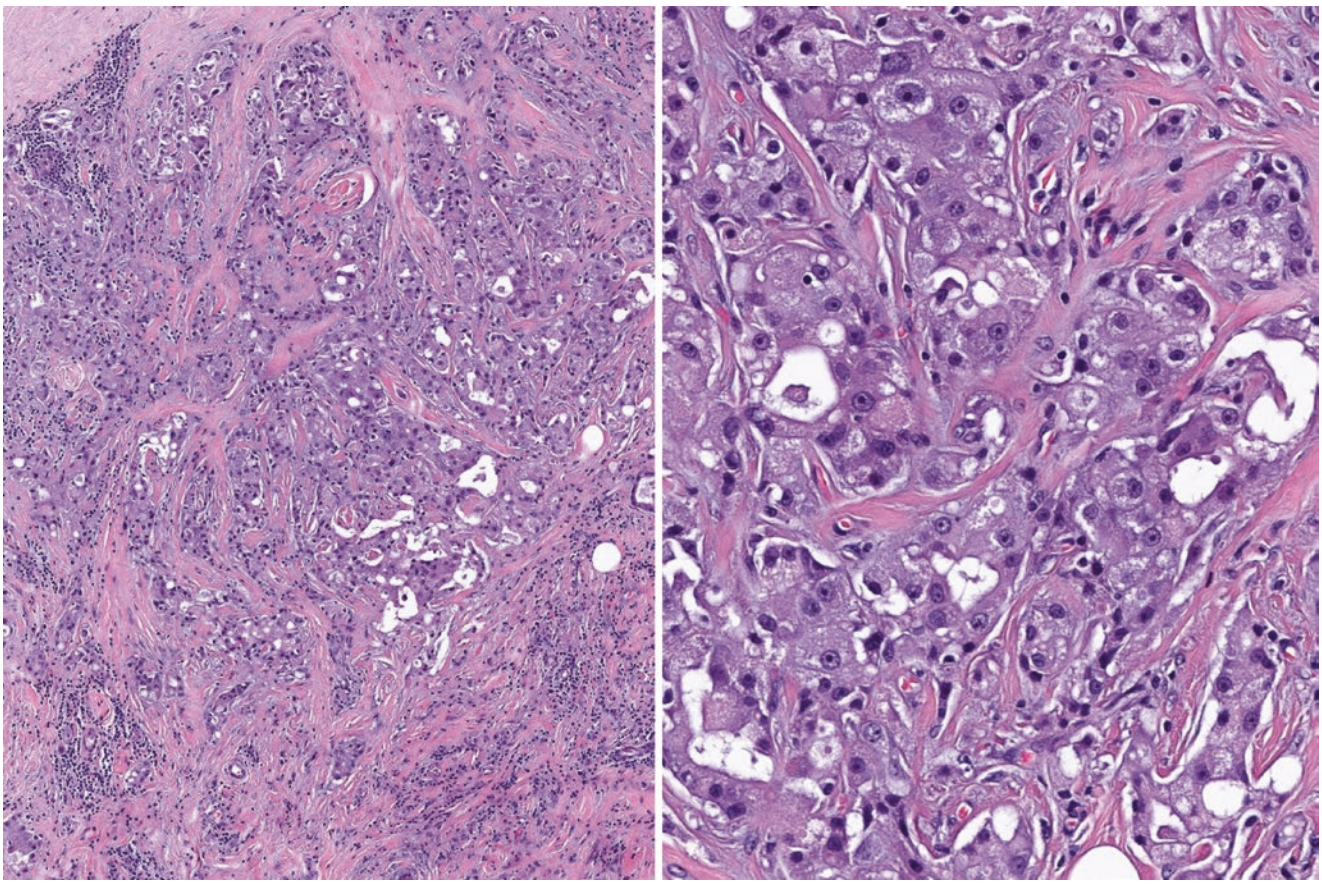

Fig. 7.39 Invasive apocrine carcinoma, high grade (grade 3). Nests, sheets, and cords of tumour cells with abundant, granular, eosinophilic cytoplasm are seen, as well as numerous mitotic figures

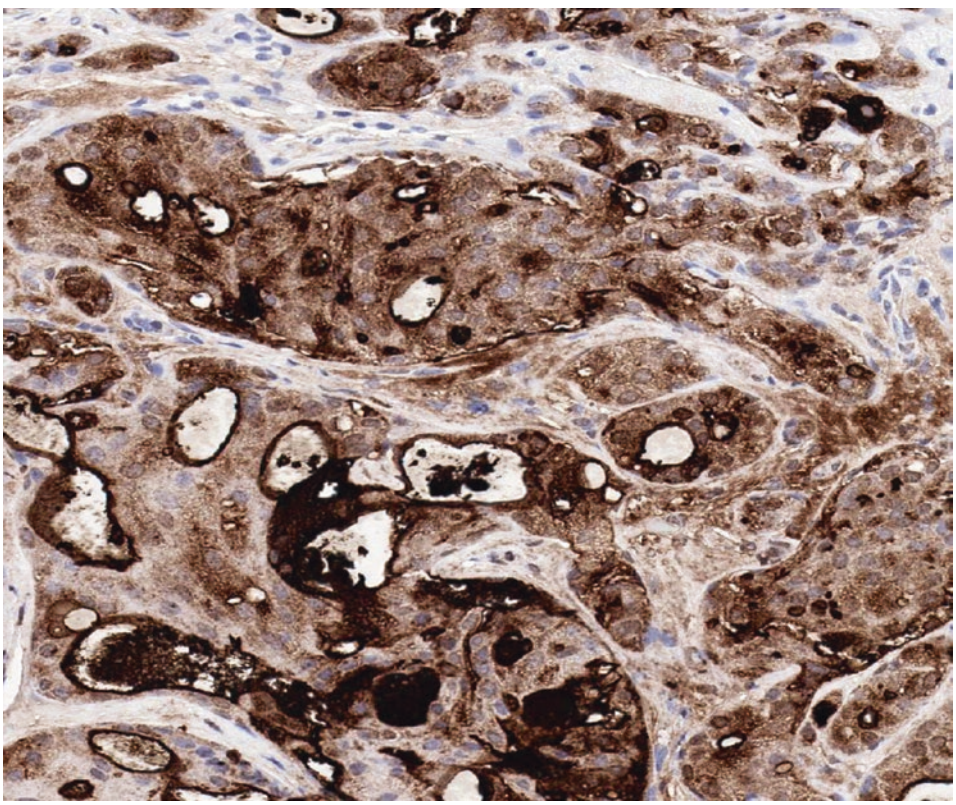

Fig. 7.40 Immunohistochemical staining for GCDFP-15 in invasive apocrine carcinoma shows diffuse and strong cytoplasmic positivity in the tumour cells

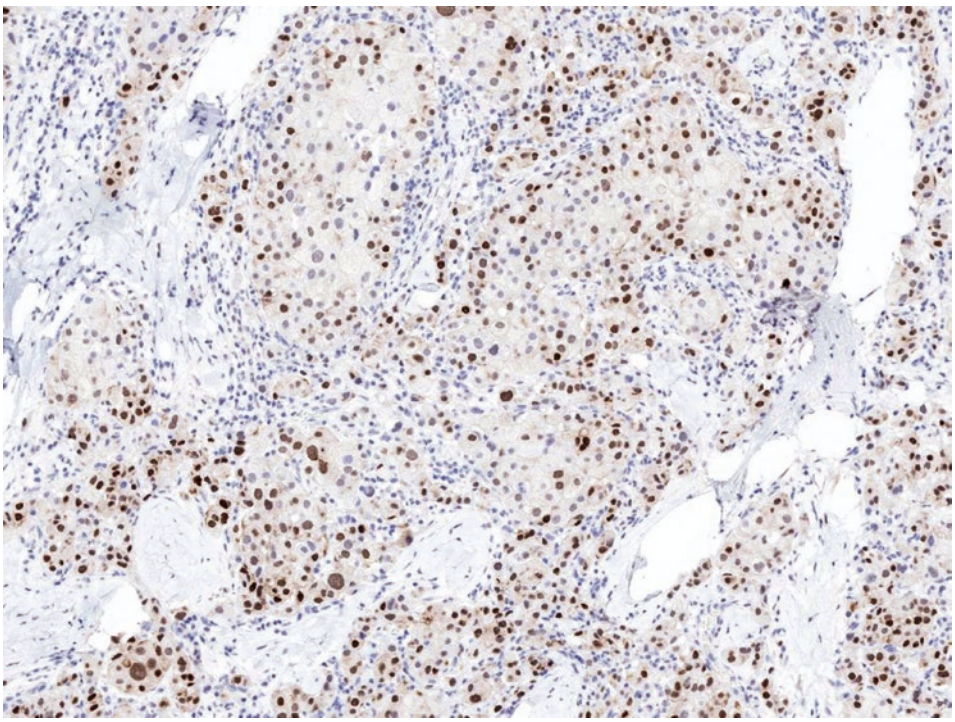

Fig. 7.41 Immunohistochemical staining for androgen receptor in invasive apocrine carcinoma shows positive nuclear reactivity

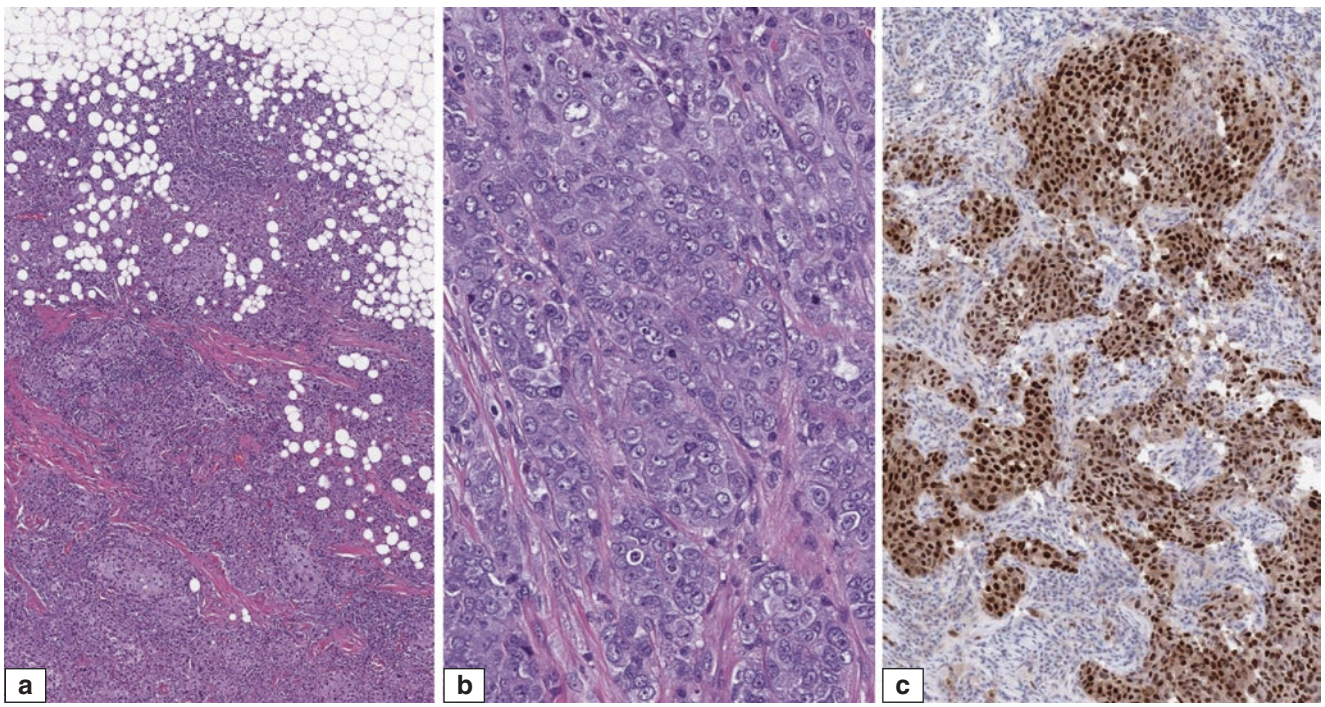

Fig. 7.42 High-grade invasive ductal carcinoma. (**a**) Tumour shows solid growth pattern. (**b**) Although the tumour cells have round nuclei, other characteristic features of apocrine differentiation are not seen. This lesion is classified as invasive carcinoma not otherwise specified. (**c**) Immunohistochemical staining for androgen receptor shows diffuse positivity. Androgen receptor is a commonly expressed receptor in all types of breast cancer, with reported positivity rates of 70–80 %, but by itself, it is not adequate for defining apocrine differentiation

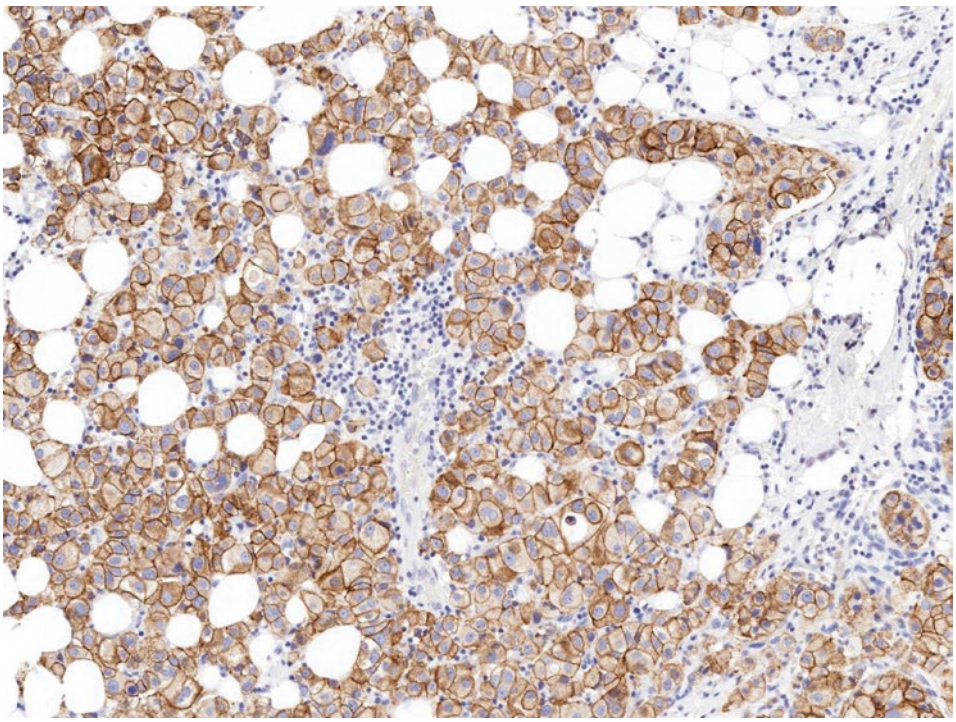

Fig. 7.43 Immunohistochemical staining for c-erbB-2, showing strong membrane immunoreactivity

Table 7.1 Immunohistochemical profile of apocrine lesions of the breast

Marker	Benign Lesions, %	Carcinomas, %
Androgen receptor	>90	>80
Oestrogen receptor	0	<10
Progesterone receptor	0	<10
c-erbB-2	10[a]	50
EGFR	0	50
p53	10	50
Bcl-2	0	50
E-cadherin	>90	80
GCDFP-15	>90	85

[a]Immunohistochemistry positive, gene amplification negative
EGFR epidermal growth factor receptor, *GCDFP* gross cystic disease fluid protein

Differential Diagnosis

Breast Neoplasms with Abundant Cytoplasm

Abundant eosinophilic, granular cytoplasm is a hallmark of cells of apocrine lesions. Many other epithelial and mesenchymal lesions of the breast may have abundant cytoplasm owing to accumulation of mitochondria, lysosomes, secretory granules, glycogen, or fat and thus may mimic apocrine carcinoma. These lesions include granular cell tumour and histiocytoid, lipid-rich, and secretory carcinomas [51]. Breast carcinomas with squamous differentiation or metastatic carcinomas also may have similar features mimicking apocrine breast cancer.

Granular cell tumours are characterised by a proliferation of cells with abundant, coarsely granular cytoplasm. In appearance, the cytoplasm and granules can be basophilic, in contrast to the eosinophilia of apocrine carcinoma (Fig. 7.44). Granular cell tumour nuclei are small and typically do not have prominent nucleoli, which are commonly seen in apocrine carcinomas. Immunohistochemical staining for cytokeratins (negative) and S100 (positive) is helpful in this diagnosis.

Histiocytoid breast cancer is characterised by abundant, pale to eosinophilic cytoplasm. The nuclei usually are not as large as in typical apocrine carcinoma, and they lack prominent nucleoli, which are a typical feature of apocrine carcinoma. The distinction may not be very easy in all cases,

and some experts regard this tumour as a subtype of apocrine carcinoma [52, 53], though it is usually categorised as a lobular subtype (Fig. 7.45) [53].

Lipid-rich breast cancer characteristically has abundant cytoplasm due to fat accumulation. In contrast to apocrine carcinoma, the cytoplasm of lipid-rich carcinoma appears clear on H&E sections. Special stains can demonstrate cytoplasmic fat accumulation (Fig. 7.46) [54].

Secretory carcinoma may have areas that mimic apocrine carcinoma, but secretory carcinoma has more luminal secretions and glandular differentiation. Nuclear enlargement and prominent nucleoli usually are not seen (Fig. 7.47).

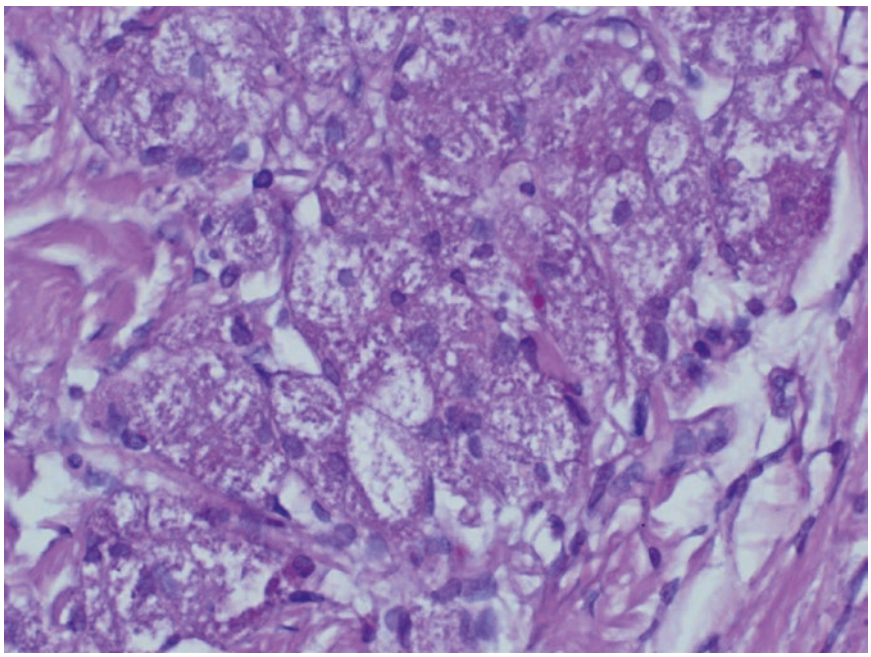

Fig. 7.44 Granular cell tumour. Tumour cells have copious amounts of granular cytoplasm, which can appear slightly basophilic. Nuclei are small without distinct nucleoli

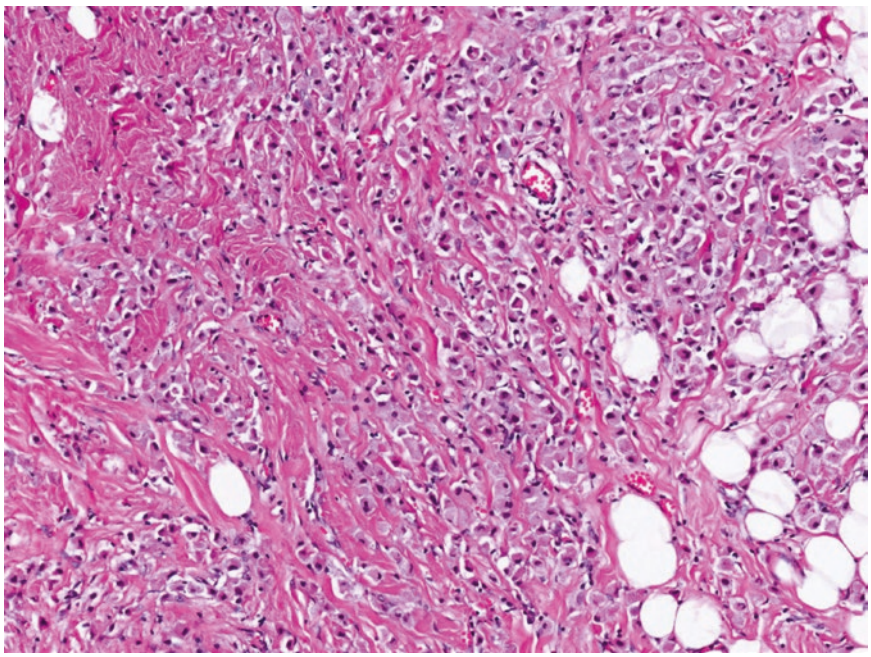

Fig. 7.45 Histiocytoid invasive breast carcinoma. Sheets of histiocyte-like cells invade the stroma, with hyperchromatic, eccentric nuclei and ample pale cytoplasm. Immunohistochemistry shows positive staining for MNF116 and negative reactivity for E-cadherin, supporting a lobular subtype

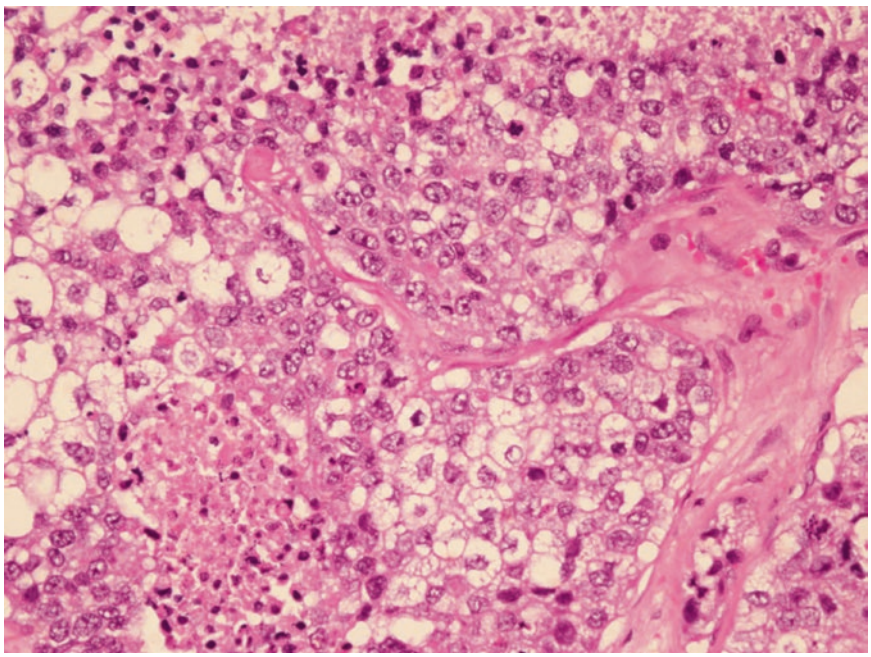

Fig. 7.46 Lipid-rich invasive breast carcinoma shows tumour cells with clear to vacuolated cytoplasm. The presence of cytoplasmic lipid may be confirmed with Oil Red O or Sudan black staining

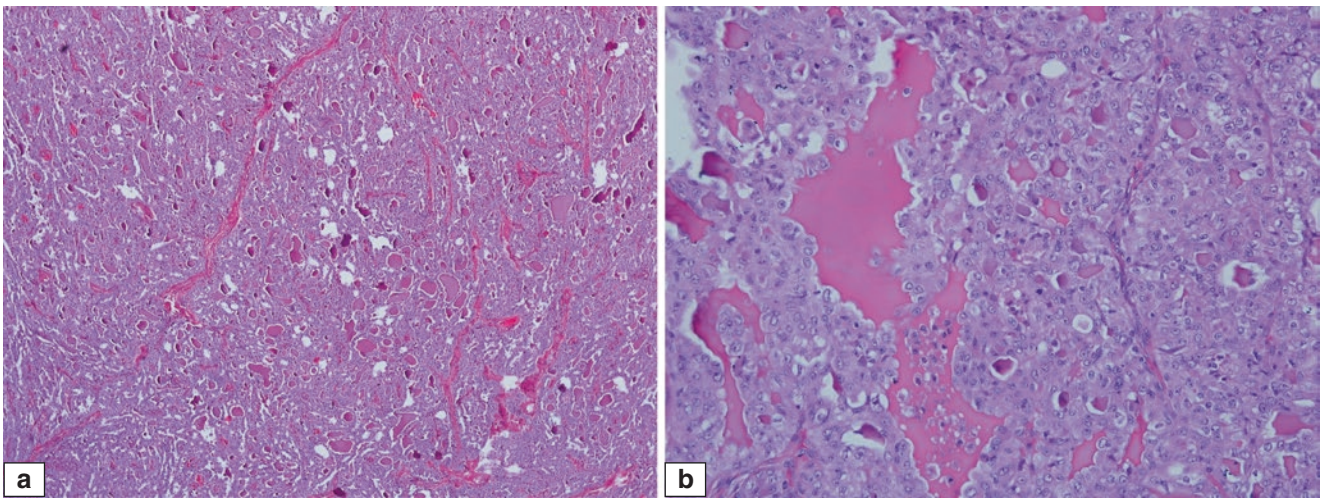

Fig. 7.47 Secretory carcinoma. (**a**) At low magnification, large sheets of pink tumour cells with glands that contain luminal dense secretions are present. (**b**) Scalloped, pink, colloid-like secretions are found among tumour cells, which demonstrate nuclear vesicularity with a few discernible nucleoli in this case, though most secretory carcinomas show bland nuclear features

GCDFP-15 staining can be helpful in differentiating this tumour from apocrine carcinoma, as secretory carcinomas are typically negative for GCDFP-15. Secretory carcinoma has a characteristic gene fusion transcript (*ETV6-NTRK3*), which can be detected by FISH analysis.

Focal or extensive squamous differentiation can be seen in breast carcinomas. Pink cytoplasm of squamous cells may mimic apocrine differentiation. The presence of keratinisation and intercellular bridges is helpful in identifying squamous differentiation (Fig. 7.48). Squamous cells are typically p63 positive, which is helpful in the differential diagnosis.

Metastatic Carcinomas

Any metastatic tumour with eosinophilic cytoplasm may mimic apocrine carcinoma. Melanoma, renal cell carcinoma, and oncocytic carcinomas may have cytologic features similar to those of apocrine carcinoma. In addition to clinical and

imaging findings, immunohistochemical stains are helpful. In general, the use of a panel of immunohistochemical markers instead of a single marker is recommended (Fig. 7.49). Aberrant expression of some markers may occur. Recently, napsin A expression, a sensitive marker for pulmonary adenocarcinoma, has been reported in about 40 % of breast apocrine carcinomas [55].

Apocrine Ductal Carcinoma In Situ (DCIS)

Just like non-apocrine-type DCIS, apocrine DCIS may mimic invasive carcinoma in small biopsy samples or when it involves pre-existing lesions, especially sclerosing lesions. As with non-apocrine lesions, immunohistochemical markers can be utilised to demonstrate intact myoepithelium in establishing a diagnosis of DCIS (Fig. 7.50). One caution is that myoepithelial staining may be discontinuous in both DCIS and benign apocrine lesions [56, 57].

Prognosis and Therapy Considerations

The concept that apocrine morphology may be associated with significant biological differences in both DCIS and invasive carcinoma is highlighted by recent molecular studies

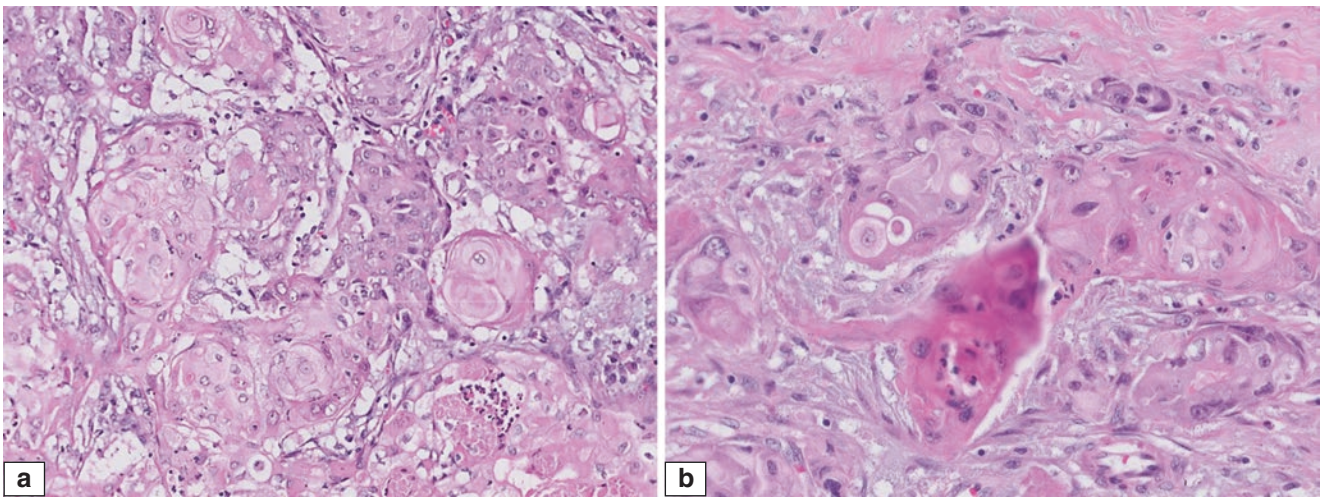

Fig. 7.48 Invasive carcinoma with squamous differentiation. (**a**) Anastomosing nests of tumour cells have a pavemented appearance with squamous whorls. (**b**) Tumour cells are polygonal and show ample pink cytoplasm with intercellular windows and bridges

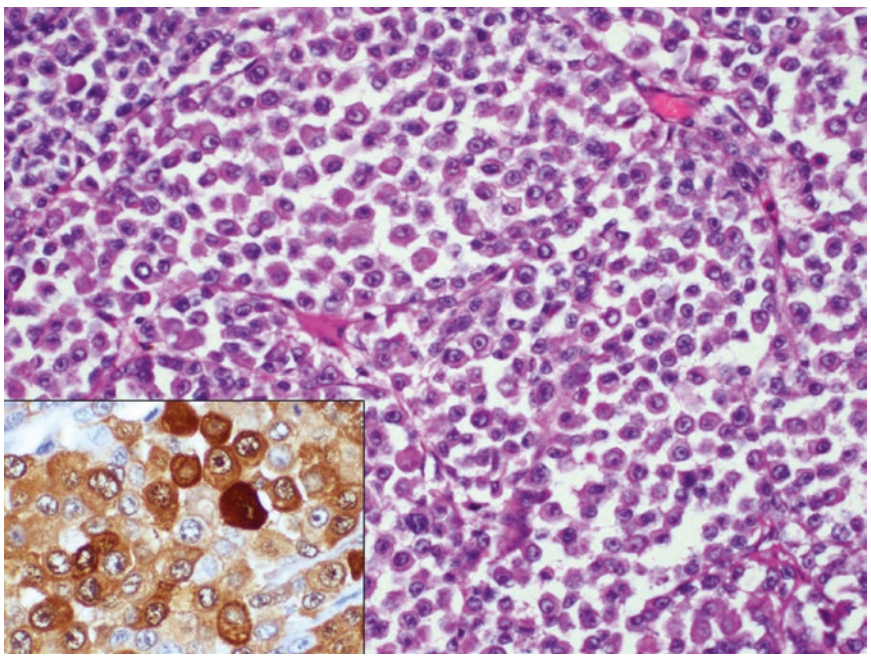

Fig. 7.49 Metastatic melanoma to the breast shows plump, rounded cells with pink cytoplasm. Nuclei are enlarged, with prominent nucleoli. Immunohistochemistry shows positive staining for S100 (*inset*) and HMB45

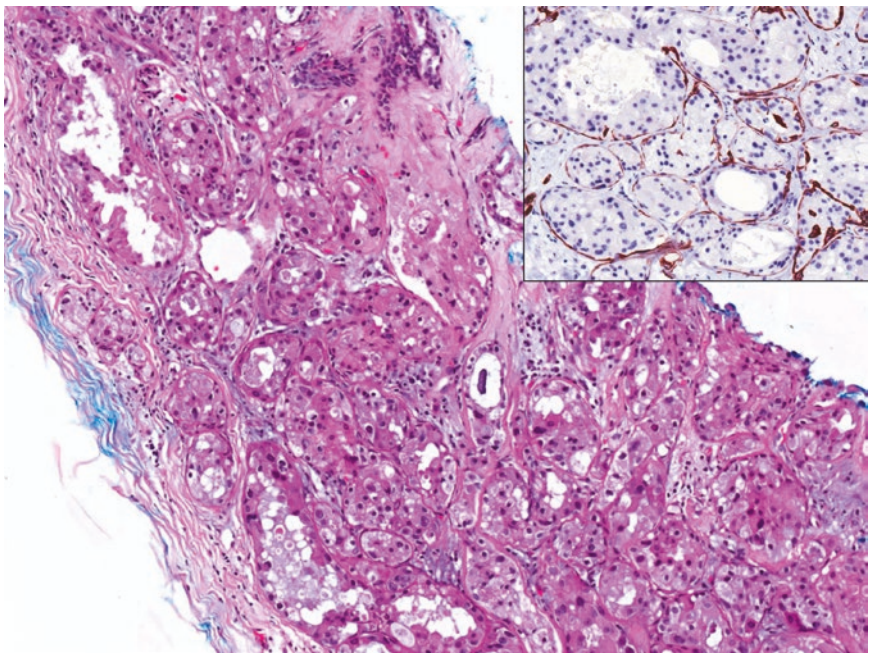

Fig. 7.50 Apocrine DCIS superimposed on sclerosing adenosis in a core biopsy specimen, mimicking invasive carcinoma. Immunohistochemistry shows an intact rim of myoepithelial cells with positive staining for CK14 (*inset*)

[58–60]. Apocrine carcinomas have been shown to have chromosomal abnormalities including losses and gains commonly seen in invasive carcinomas of no special type, but they are also found to harbour alterations not previously reported. These include losses at 2p and 9q and gains at 2q, 3p, and 13q. Using gene expression microarrays, Farmer et al. [61] reported a subset of breast tumours characterised by high androgen signalling, absence of oestrogen receptor, high rate of c-erbB-2 amplification, and enrichment of genes involved in lipid and amino acid metabolism. These tumours were reported to have predominantly apocrine features on histological examination and were referred to as the "molecular apocrine group". However, not all cases with gene expression patterns of this category meet histopathological criteria for apocrine carcinoma. The existence of a molecular apocrine signature to define a distinct type of breast carcinoma has been generally accepted, and 8–14 % of breast carcinomas are categorised as "molecular apocrine" by microarray analysis [59, 62]. Nevertheless, the association between molecular apocrine breast tumours and histologically defined apocrine carcinomas remains controversial. It has been suggested that the "molecular apocrine" group might be much broader than initially reported by microarray analysis. The clinical significance of these findings remains to be seen in future studies.

Based on the high frequency of androgen receptor expression, androgen receptor antagonist therapy has been suggested for apocrine breast cancer. However, early trials of androgen receptor-directed therapies did not yield encouraging results. With the development of next-generation androgen receptor antagonists, there is renewed interest in this approach [63, 64].

References

1. Bussolati G, Cattani MG, Gugliotta P, Patriarca E, Eusebi V. Morphologic and functional aspects of apocrine metaplasia in dysplastic and neoplastic breast tissue. Ann NY Acad Sci. 1986;464:262–74.
2. O'Malley FP, Bane A. An update on apocrine lesions of the breast. Histopathology. 2008;52:3–10.
3. Wells CA, El-Ayat GA. Non-operative breast pathology: apocrine lesions. J Clin Pathol. 2007;60:1313–20.
4. Zagorianakou P, Zagorianakou N, Stefanou D, Makrydimas G, Agnantis NJ. The enigmatic nature of apocrine breast lesions. Virchows Arch. 2006;448:525–31.
5. Gromov P, Espinoza JA, Gromova I. Molecular and diagnostic features of apocrine breast lesions. Expert Rev Mol Diagn. 2015;15:1011–22.
6. Masood S, Rosa M. The challenge of apocrine proliferations of the breast: a morphologic approach. Pathol Res Pract. 2009;205:155–64.
7. Celis JE, Gromov P, Moreira JM, Cabezón T, Friis E, Vejborg IM, et al. Apocrine cysts of the breast biomarkers, origin, enlargement, and relation with cancer phenotype. Mol Cell Proteomics. 2006;5:462–83.
8. Darb-Esfahani S, von Minckwitz G, Denkert C, Ataseven B, Högel B, Mehta K, et al. Gross cystic disease fluid protein 15 (GCDFP-15) expression in breast cancer subtypes. BMC Cancer. 2014;14:546–56.

9. Viacava P, Naccarato AG, Bevilacqua G. Apocrine epithelium of the breast: does it result from metaplasia? Virchows Arch. 1997;431:205–9.
10. Devitt JE. Clinical benign disorders of the breast and carcinoma of the breast. Surg Gynecol Obstet. 1981;152:437–40.
11. Celis JE, Moreira JM, Gromova I, Cabezón T, Gromov P, Shen T, et al. Characterization of breast precancerous lesions and myoepithelial hyperplasia in sclerosing adenosis with apocrine metaplasia. Mol Oncol. 2007;1:97–119.
12. O'Malley FP, Page DL, Nelson EH, Dupont WD. Ductal carcinoma in situ of the breast with apocrine cytology: definition of a borderline category. Hum Pathol. 1994;25:164–8.
13. Tavassoli FA, Norris HJ. Intraductal apocrine carcinoma: a clinicopathologic study of 37 cases. Mod Pathol. 1994;7:813–8.
14. Gerhard R, Costa JL, Schmitt F. Benign and malignant apocrine lesions of the breast. Exp Rev Anticancer Ther. 2012;12:215–21.
15. Lagios MD, Silverstein MJ. Outcomes and factors impacting local recurrence of ductal carcinoma in situ. Cancer. 2000;89:2323–5.
16. Broji E. Apocrine carcinoma. In: Hoda SA, Broji E, Koerner F, Rosen PP, editors. Rosen's breast pathology. 4th ed. Philadelphia: Wolters Kluwer; 2014. p. 645–66.
17. Bhargava R. Apocrine carcinoma of the breast. In: Dabbs DJ, editor. Breast pathology. Philadelphia: Elsevier Saunders; 2012. p. 502–11.
18. Consensus Conference on the classification of ductal carcinoma in situ. The Consensus Conference Committee. Cancer. 1997;80:1798–802.
19. Mardekian SK, Bombonati A, Palazzo JP. Ductal carcinoma in situ of the breast: the importance of morphologic and molecular interactions. Hum Pathol. 2016;49:114–23.
20. Page DL, Simpson JF. What is apocrine adenosis, anyway? Histopathology. 2001;39:433–4.
21. Endoh Y, Tamura G, Kato N, Motoyama T. Apocrine adenosis of the breast: clonal evidence of neoplasia. Histopathology. 2001;38:221–4.
22. Carter DJ, Rosen PP. Atypical apocrine metaplasia in sclerosing lesions of the breast: a study of 51 patients. Mod Pathol. 1991;4:1–5.
23. Fuehrer N, Hartmann L, Degnim A, Allers T, Vierkant R, Frost M, Visscher D. Atypical apocrine adenosis of the breast: long-term follow-up in 37 patients. Arch Pathol Lab Med. 2012;136:179–82.
24. Seidman JD, Ashton M, Lefkowitz M. Atypical apocrine adenosis of the breast. Cancer. 1996;77:2529–37.
25. Calhoun BC, Booth CN. Atypical apocrine adenosis diagnosed on breast core biopsy: implications for management. Hum Pathol. 2014;45:2130–5.
26. Visscher DW. Apocrine ductal carcinoma in situ involving a sclerosing lesion with adenosis: report of a case. Arch Pathol Lab Med. 2009;133:1817–21.
27. Page DL, Dupont WD, Jensen RA. Papillary apocrine change of the breast: associations with atypical hyperplasia and risk of breast cancer. Cancer Epidemiol Biomarkers Prev. 1996;5:29–32.
28. Elayat G, Selim AGA, Wells CA. Cell cycle alterations and their relationship to proliferation in apocrine adenosis of the breast. Histopathology. 2009;54:348–54.
29. Kosemehmetoglu K, Guler G. Papillary apocrine metaplasia and columnar cell lesion with atypia: is there a shared common pathway? Ann Diagn Pathol. 2010;14:425–31.
30. Lopez-Garcia MA, Geyer FC, Lacroix-Triki M, Marchió C, Reis-Filho JS. Breast cancer precursors revisited: molecular features and progression pathways. Histopathology. 2010;57(2):171–92.
31. Lui JE, Dahlstrom SB, James DT. Apocrine adenoma of the breast: diagnosis on large core needle biopsy. Pathology. 2001;33:149–52.
32. Vranić S, Schmitt F, Sapino A, Costa JL, Reddy S, Castro M, Gatalica Z. Apocrine carcinoma of the breast: a comprehensive review. Histol Histopathol. 2013;28:1393–409.
33. Abati AD, Kimmel M, Rosen PP. Apocrine mammary carcinoma. A clinicopathologic study of 72 cases. Am J Clin Pathol. 1990;94:371–7.
34. Wright L, Ng CE, Fasih T. Atypical breasts cancers. Int J Surg Case Rep. 2016;20:41–5.
35. Mossler JA, Barton TK, Brinkhous AD, McCarty KS, Moylan JA. Apocrine differentiation in human mammary carcinoma. Cancer. 1980;46:2463–71.
36. Eusebi V, Millis RR, Cattani MG, Bussolati G, Azzopardi JG. Apocrine carcinoma of the breast. A morphologic and immunocytochemical study. Am J Pathol. 1986;123:532–41.
37. Vranic S, Tawfik O, Palazzo J, Bilalovic N, Eyzaguirre E, Lee LM, et al. EGFR and HER-2/neu expression in invasive apocrine carcinoma of the breast. Mod Pathol. 2010;23:644–53.
38. Gilles R, Lesnik A, Guinebretiere JM, Tardivon A, Masselot J, Contesso G, Vanel D. Apocrine carcinoma: clinical and mammographic features. Radiology. 1994;190:495–7.
39. Seo KJ, An YY, Whang IY, Chang ED, Kang BJ, Kim SH, et al. Sonography of invasive apocrine carcinoma of the breast in five cases. Korean J Radiol. 2015;16:1006–11.
40. Vranic S, Marchiò C, Castellano I, Botta C, Scalzo MS, Bender RP, et al. Immunohistochemical and molecular profiling of histologically defined apocrine carcinomas of the breast. Hum Pathol. 2015;46:1350–9.
41. Selim AG, Wells CA. Immunohistochemical localisation of androgen receptor in apocrine metaplasia and apocrine adenosis of the breast: relation to oestrogen and progesterone receptors. J Clin Pathol. 1999;52:838–41.
42. Collins L, Cole KS, Marotti JD, Hu R, Schnitt SJ, Tamimi RM. Androgen receptor expression in breast cancer in relation to molecular phenotype: results from the Nurses' Health Study. Mod Pathol. 2011;24:924–31.
43. Gatalica Z. Immunohistochemical analysis of apocrine breast lesions: consistent over-expression of androgen receptor accompanied by the loss of estrogen and progesterone receptors in apocrine metaplasia and apocrine carcinoma in situ. Pathol Res Pract. 1997;193:753–8.
44. Vera-Badillo FE, Templeton AJ, de Gouveia P, Diaz-Padilla I, Bedard PL, Al-Mubarak M, et al. Androgen receptor expression and outcomes in early breast cancer: a systematic review and meta-analysis. J Natl Cancer Inst. 2014;106:djt319.
45. Robinson JL, MacArthur S, Ross-Innes CS, Tilley WD, Neal DE, Mills IG, Carroll JS. Androgen receptor driven transcription in molecular apocrine breast cancer is mediated by FoxA1. EMBO J. 2011;30:3019–27.
46. Iggo RD. New insights into the role of androgen and oestrogen receptors in molecular apocrine breast tumours. Breast Cancer Res. 2011;13:318.
47. Gromov P, Espinoza JA, Talman ML, Honma N, Kroman N, Timmermans Wielenga V, et al. FABP7 and HMGCS2 are novel protein markers for apocrine differentiation categorizing apocrine carcinoma of the breast. PLoS One. 2014;9, e112024.
48. Sapp M, Malik A, Hanna W. Hormone receptor profile of apocrine lesions of the breast. Breast J. 2003;9:335–6.
49. Moriya T, Sakamoto K, Sasano H, Kawanaka M, Sonoo H, Manabe T, Ito J. Immunohistochemical analysis of Ki-67, p53, p21, and p27 in benign and malignant apocrine lesions of the breast: its correlation to histologic findings in 43 cases. Mod Pathol. 2000;13:13–8.
50. Niemeier LA, Dabbs DJ, Beriwal S, Striebel JM, Bhargava R. Androgen receptor in breast cancer: expression in estrogen receptor-positive tumors and in estrogen receptor-negative tumors with apocrine differentiation. Mod Pathol. 2010;23:205–12.
51. Damiani S, Dina R, Eusebi V. Eosinophilic and granular cell tumors of the breast. Semin Diagn Pathol. 1999;16:117–25.

52. Eusebi V, Foschini MP, Bussolati G, Rosen PP. Myoblastomatoid (histiocytoid) carcinoma of the breast: a type of apocrine carcinoma. Am J Surg Pathol. 1995;19:553–62.
53. Tan PH, Harada O, Thike AA, Tse GMK. Histiocytoid breast carcinoma: an enigmatic lobular entity. J Clin Pathol. 2011; 64:654–9.
54. Lakhani SR, Ellis IO, Schnitt SJ, Tan PH, van de Vijver MJ. WHO classification of tumours of the breast. Lyon: IARC; 2012.
55. Vitkovski T, Chaudhary S, Sison C, Nasim M, Esposito MJ, Bhuiya T. Aberrant expression of napsin A in breast carcinoma with apocrine features. Int J Surg Pathol. 2016;24:377–81.
56. Cserni G. Benign apocrine papillary lesions of the breast lacking or virtually lacking myoepithelial cells—potential pitfalls in diagnosing malignancy. APMIS. 2012;120:249–52.
57. Tramm T, Kim JY, Tavassoli FA. Diminished number or complete loss of myoepithelial cells associated with metaplastic and neoplastic apocrine lesions of the breast. Am J Surg Pathol. 2011;35: 202–11.
58. Jones C, Damiani S, Wells D, Chaggar R, Lakhani SR, Eusebi V. Molecular cytogenetic comparison of apocrine hyperplasia and apocrine carcinoma of the breast. Am J Pathol. 2001;158:207–14.
59. Lehmann BD, Bauer JA, Chen X, Sanders ME, Chakravarthy AB, Shyr Y, Pietenpol JA. Identification of human triple-negative breast cancer subtypes and preclinical models for selection of targeted therapies. J Clin Invest. 2011;121:2750–67.
60. Celis JE, Cabezón T, Moreira JM, Gromov P, Gromova I, Timmermans-Wielenga V, et al. Molecular characterization of apocrine carcinoma of the breast: validation of an apocrine protein signature in a well-defined cohort. Mol Oncol. 2009;3:220–37.
61. Farmer P, Bonnefoi H, Becette V, Tubiana-Hulin M, Fumoleau P, Larsimont D, et al. Identification of molecular apocrine breast tumours by microarray analysis. Oncogene. 2005;24:4660–71.
62. Weisman PS, Ng CK, Brogi E, Eisenberg RE, Won HH, Piscuoglio S, et al. Genetic alterations of triple negative breast cancer by targeted next-generation sequencing and correlation with tumor morphology. Mod Pathol. 2016;29:476–88.
63. Coss CC, Jones A, Dalton JT. Selective androgen receptor modulators as improved androgen therapy for advanced breast cancer. Steroids. 2014;90:94–100.
64. Anestis A, Karamouzis MV, Dalagiorgou G, Papavassiliou AG. Is androgen receptor targeting an emerging treatment strategy for triple negative breast cancer? Cancer Treat Rev. 2015;41:547–53.

Vascular Lesions

8

A variety of vascular proliferations, both benign and malignant, can occur in the breast. Overall, they represent only a minority of tumours originating in the breast. Benign vascular lesions other than incidental perilobular haemangiomas are extremely rare in the breast. Malignant vascular lesions (angiosarcomas) are also rare, constituting less than 1 % of all breast neoplasms; they may be primary, or they may be secondary tumours occurring after radiation treatment. Also seen in association with radiation therapy are "atypical vascular lesions" affecting the skin of the breast. The relationship between atypical vascular lesions and radiation-associated angiosarcoma is still being debated and remains to be clarified. This chapter reviews the common vascular lesions in the breast, focusing on their diagnostic features and potential interpretive pitfalls.

Benign Vascular Lesions

Haemangioma

Definition

Haemangiomas are benign vascular proliferations that can arise in breast parenchyma. Most of these lesions, called perilobular haemangiomas, are smaller than 0.5 cm and are identified incidentally on microscopic evaluation. Perilobular haemangiomas are not confined histologically to a perilobular distribution; they can occur in intralobular or extralobular stroma and may not have any relationship with ducts or lobular units. When a benign vascular proliferation is large enough to form a clinically palpable mass or is detectable by imaging (usually larger than 0.5 cm), it is diagnosed as haemangioma.

Clinical and Epidemiological Features

Haemangiomas occur in both female and male breasts and have been reported in a wide age range (infants to 85 years old). Haemangiomas may also occur as part of rare genetic syndromes, including Kasabach–Merritt and Poland syndromes. Rare congenital cases have been reported. Some lesions resolve spontaneously.

Imaging Features

Most haemangiomas are incidental findings on biopsies performed for other reasons. Larger lesions may present as palpable masses or may be detected on imaging as superficial, well-demarcated, circumscribed, lobulated masses with an average size of 0.5–2 cm. Phleboliths or calcified venous thromboses may be present. They are commonly hyperechoic on ultrasound examination.

Pathologic Features

Macroscopic Features

In general, haemangiomas are lobulated, well-circumscribed, soft, or spongy lesions with a dark red, brown, or haemorrhagic appearance.

Microscopic Features

Just like haemangiomas arising anywhere else in the body, haemangiomas arising in the breast can be of a capillary, cavernous, or venous type (Figs. 8.1, 8.2, 8.3, 8.4, and 8.5). The histologic subclassification has no biologic or clinical significance (Table 8.1).

Cavernous Haemangioma

Cavernous haemangiomas, the most common histologic type, consist of a mesh of dilated vessels congested with red cells. The vascular channels usually do not anastomose and are lined by flat endothelial cells with inconspicuous nuclei.

Capillary Haemangioma

Capillary haemangiomas consist of densely packed proliferations of capillary-sized small vessels lined by flat endothelial cells. Frequently, a feeder vessel with a muscular wall can be identified.

P.H. Tan, A.A. Sahin, *Atlas of Differential Diagnosis in Breast Pathology*, Atlas of Anatomic Pathology,
DOI 10.1007/978-1-4939-6697-4_8

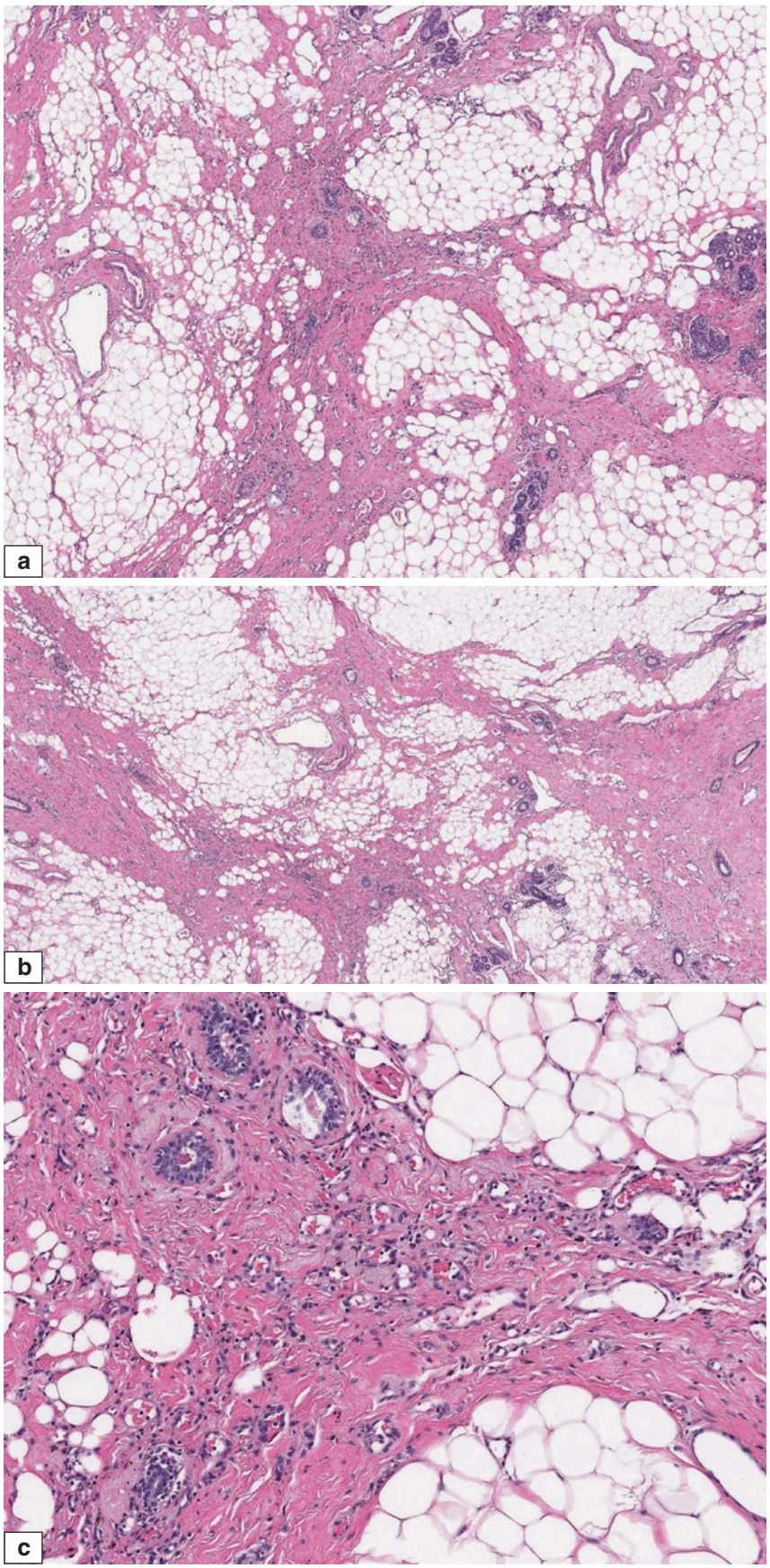

Fig. 8.1 Haemangioma. Microscopic features. (**a**, **b**) Proliferation of small capillaries in breast parenchyma. The vascular proliferation is supported by fibrous stroma. (**c**) Endothelial nuclei are flat and inconspicuous. No cytologic atypia is evident

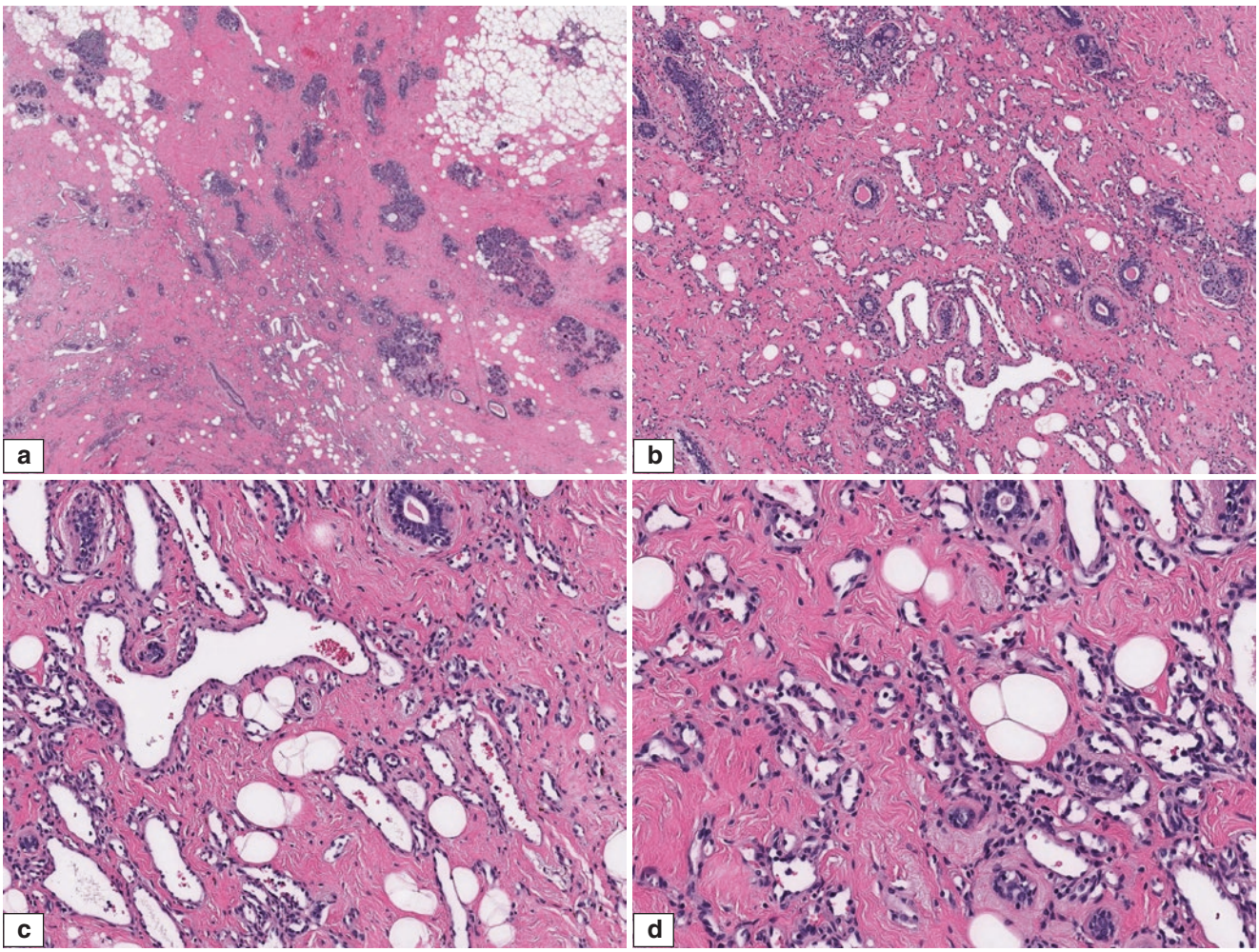

Fig. 8.2 Haemangioma. Microscopic features. (**a**–**d**) Proliferation of both small and large dilated vascular channels containing red blood cells

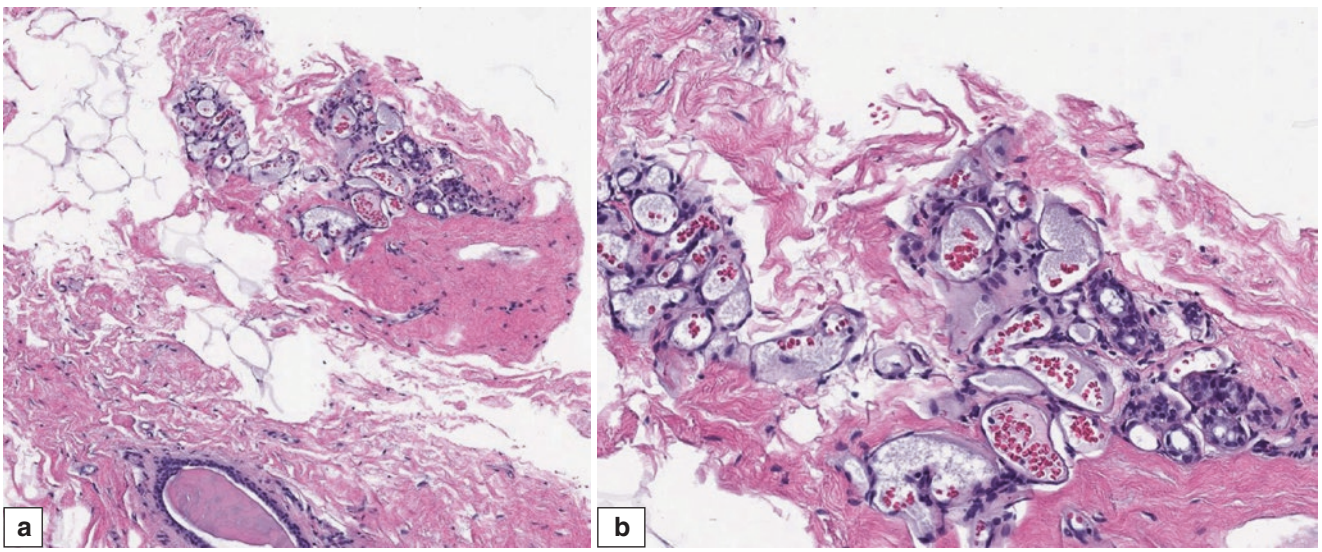

Fig. 8.3 Perilobular haemangioma. Microscopic features. (**a**) An aggregate of histologically benign capillaries in the periductal stroma. (**b**) Higher magnification of the same case shows that the lesion consists of thin-walled vessels that contain red blood cells

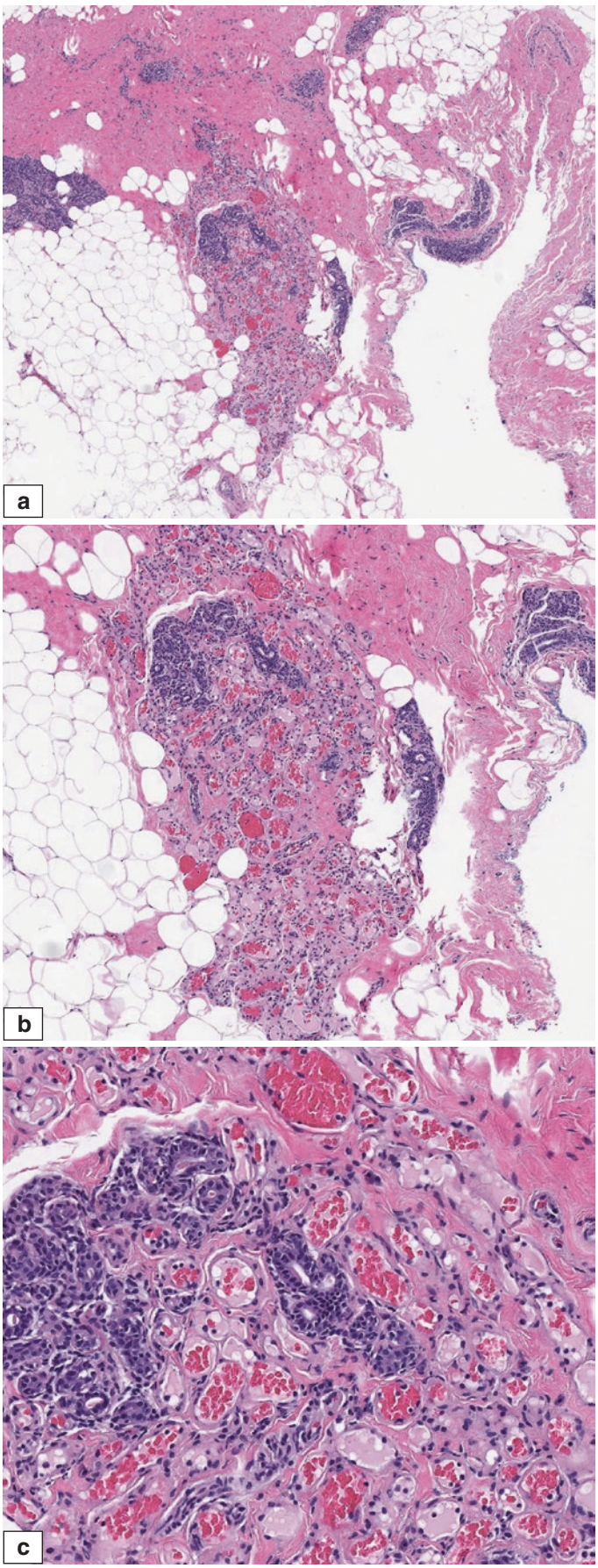

Fig. 8.4 Perilobular haemangioma. Microscopic features. (**a**, **b**) A collection of small vessels in periductal and perilobular stroma. (**c**) Vascular channels extend into intralobular stroma. Vascular channels are lined by small, flat endothelial cells

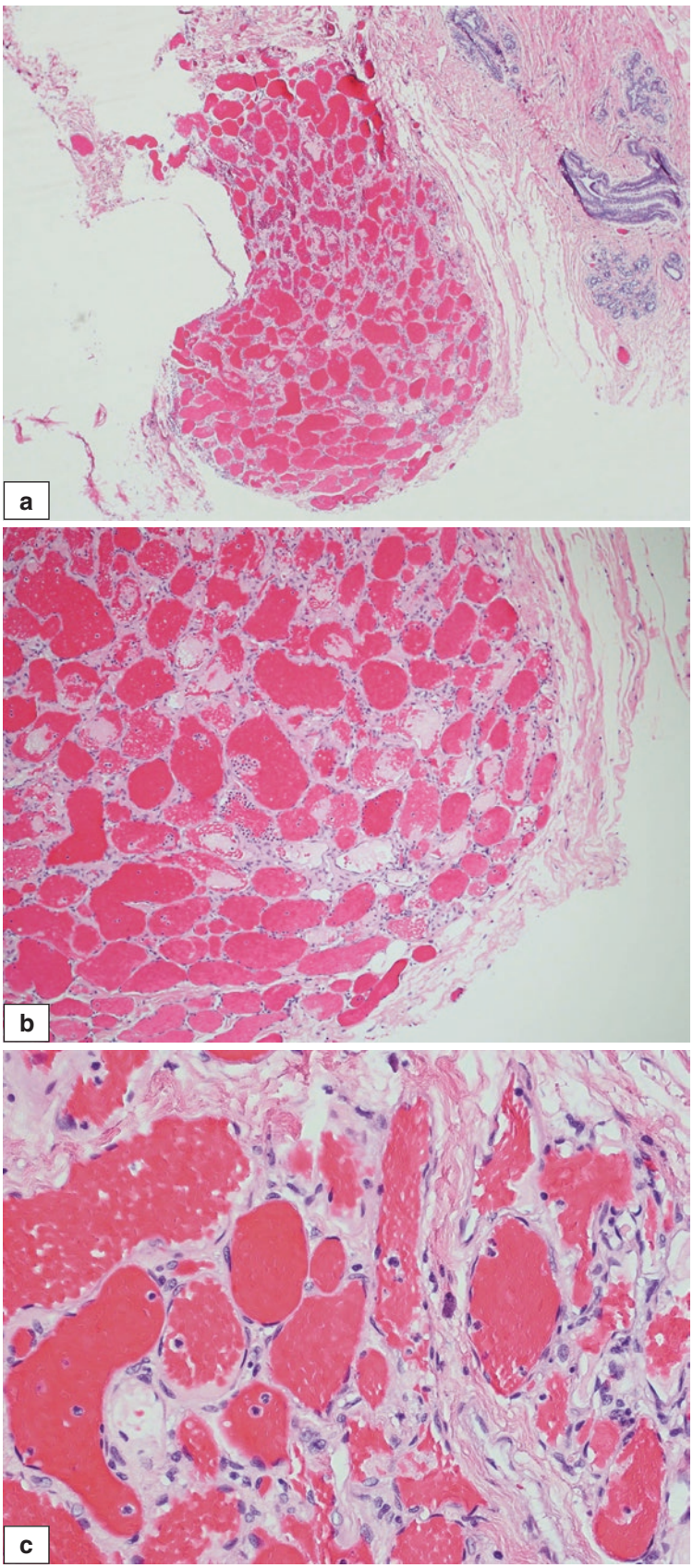

Fig. 8.5 Breast haemangioma. (**a**) Circumscribed collection of congested vessels of varying sizes is seen within the breast, with benign breast lobules in the adjacent breast parenchyma. (**b**) The blood vessels are intensely congested with red blood cells. The border shows a smooth circumscription. (**c**) High magnification shows flattened endothelial cells with no atypia. Thin, fibrous stroma is seen among the congested vessels

Table 8.1 Haemangiomas of the breast: key histologic features

Histologic type	Features
Cavernous	Large, dilated vascular spaces separated by fibrous septa
Capillary	Compact proliferation of small vessels Feeding vessel often present at the periphery of the lesion
Venous	Irregularly dilated vascular spaces with variable muscular walls
Complex	Mixture of large, dilated vessels and dense areas of small capillaries

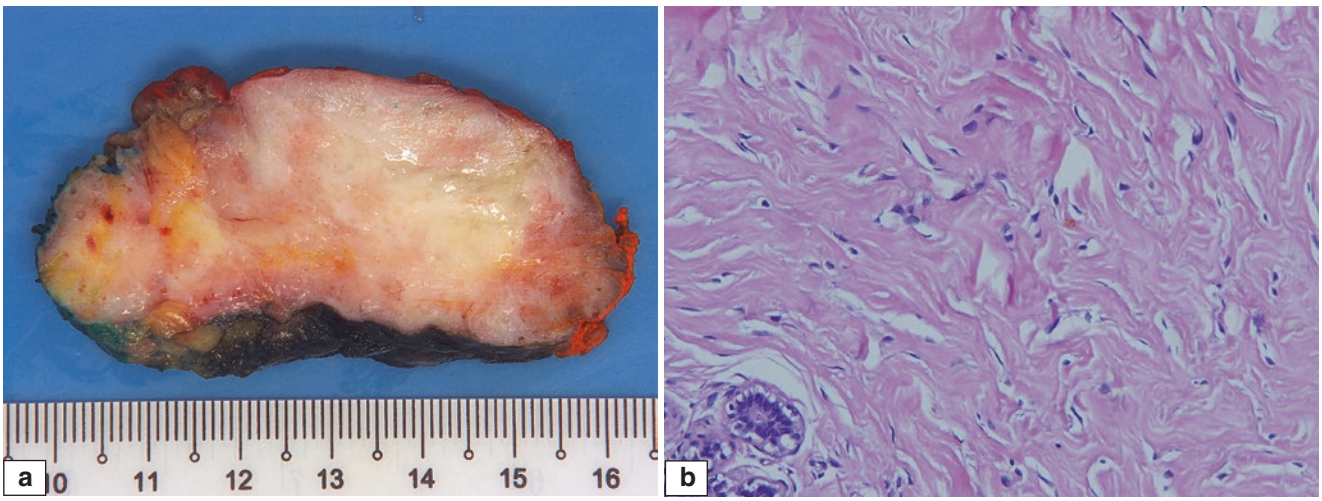

Fig. 8.6 Pseudoangiomatous stromal hyperplasia. (**a**) Macroscopy shows a diffuse, whitish, rubbery appearance. Several small cysts are seen, representing cystic changes in the breast. (**b**) Pseudoangiomatous stromal hyperplasia is often an incidental histological finding. (**b**) Note that the spaces are empty. The lining cells show flattened nuclei of fibroblasts and myofibroblasts

Venous Haemangioma

Venous haemangiomas consist of irregularly dilated vascular channels with vascular walls of varying thickness. A smooth muscle layer can be evident in the vascular walls. Vessels may contain homogeneous pink fluid (presumably lymph) in addition to red blood cells.

Complex Haemangioma

"Complex haemangioma" is a term used to describe haemangiomas that have variable patterns, with dilated vascular spaces admixed with dense areas of small capillary proliferation. A complex capillary network with focal anastomoses may be seen.

Differential Diagnosis

Angiosarcoma

The diagnosis of haemangioma is often straightforward. As most vascular lesions arising in the breast are malignant, angiosarcoma is the main differential diagnosis. There is a major difference in the growth pattern of these two lesions. Haemangiomas show lobular, well-circumscribed margins, whereas angiosarcomas typically have an infiltrative growth pattern with dissection into the breast parenchyma. Based on this difference, when the edges of the lesion can be assessed on excision, it is easy to establish whether the nature of the vascular lesion is benign or malignant. It may be difficult to establish the diagnosis if only a small biopsy specimen is obtained which does not include the entire tumour edge. In such a situation, it may be necessary to further evaluate the lesion. Additional histologic features that help to differentiate the two lesions include the lack of anastomosing channels and endothelial atypia in haemangiomas and the presence of large blood lakes in angiosarcomas.

Degenerative changes, including infarct and thrombosis, may occur in any type of haemangioma.

Thrombosis with recanalisation or endothelial proliferations, which may have a papillary configuration, can rarely occur. Papillary endothelial proliferation may mimic an angiosarcoma, especially on a small biopsy sample. The lack of cytologic atypia, a non-anastomosing growth pattern, and circumscription of haemangiomas should be helpful in establishing the diagnosis.

Pseudoangiomatous Stromal Hyperplasia

Pseudoangiomatous stromal hyperplasia (PASH) may morphologically mimic haemangioma. In contrast to haemangioma, the cells lining the spaces in PASH are stromal cells (myofibroblasts) and do not express vascular markers. The spaces of PASH are empty; the spaces in haemangiomas typically contain red cells. PASH tends to be a diffuse process, whereas haemangiomas are characteristically lobulated and well circumscribed (Fig. 8.6).

Lymphangioma

A lymphangioma is also a differential and can be distinguished by the relative absence of red blood cells within the

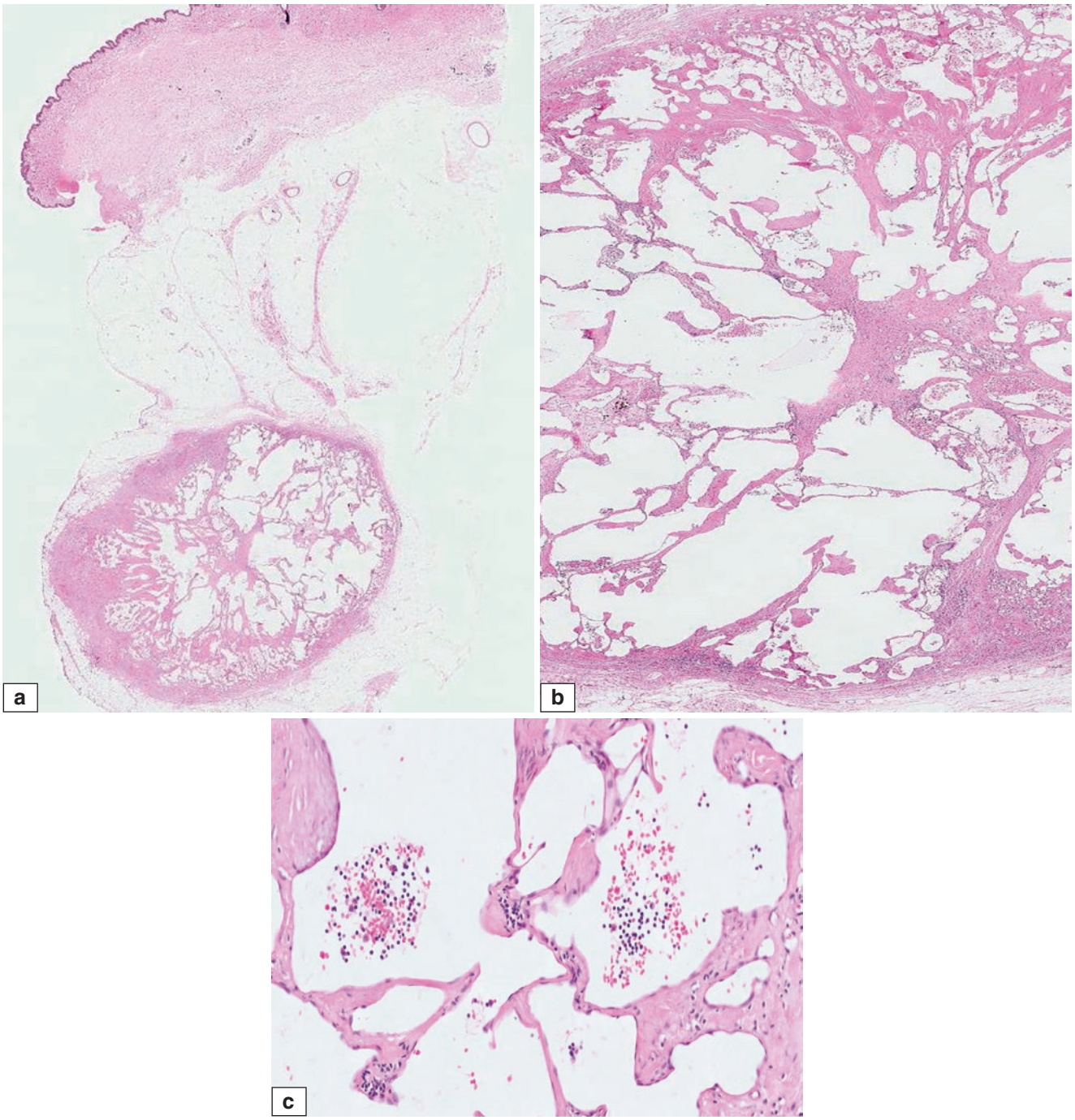

Fig. 8.7 Breast lymphangioma. (**a**) A circumscribed, nodular lesion is seen in the adipose tissue of the breast. The overlying dermis shows oedema. (**b**) Medium magnification shows empty spaces, which are interconnected among thin fibrous septa. (**c**) Lymphocytes are seen within the spaces, with some admixed red blood cells

spaces, which instead tend to contain lymphocytes (Fig. 8.7). D2-40 immunostaining decorates the lymphatic endothelium (Fig. 8.8).

Prognosis and Therapy Considerations

Haemangiomas are benign neoplasms, and simple excision is curative. If the diagnosis is established on a core biopsy, usually an excision is recommended to exclude an angiosarcoma because some angiosarcomas may have areas of overlapping histologic features with haemangiomas. Histologic evaluation of the entire lesion may be necessary to establish the diagnosis. Local recurrence or metastasis of completely excised haemangioma has not been reported. Although some angiosarcomas may have very benign-appearing areas mimicking haemangiomas, transition from haemangioma to angiosarcoma in the breast has not been documented.

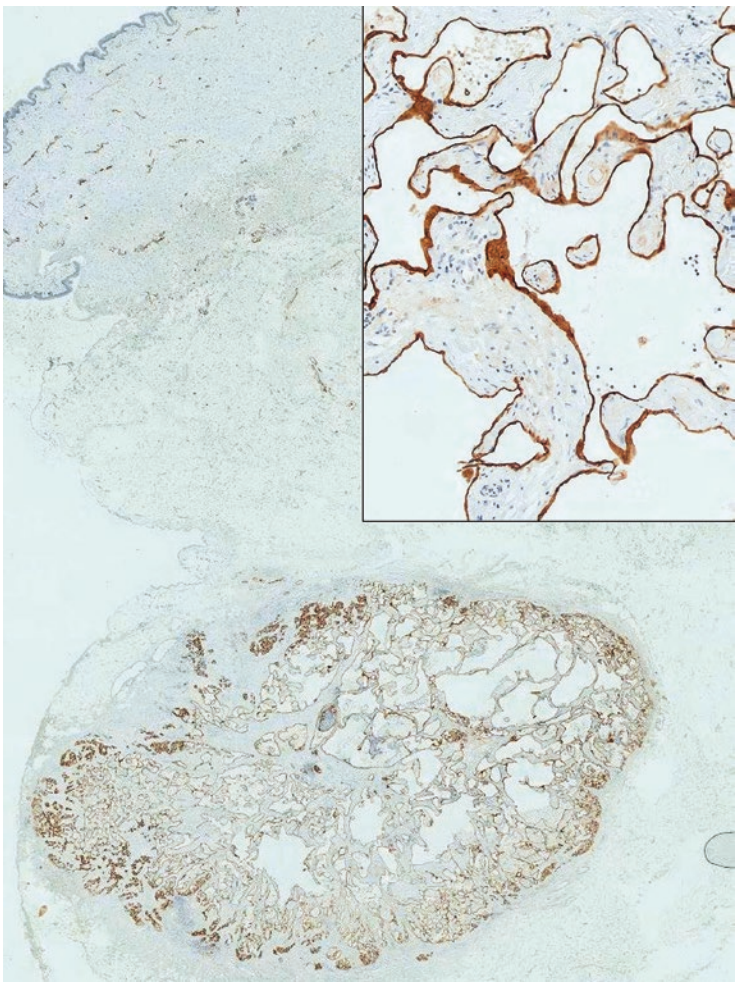

Fig. 8.8 Breast lymphangioma. Immunohistochemistry for D2-40 shows positive staining of the lining lymphatic endothelial cells. The *inset* shows higher magnification of the lymphatic endothelium

Angiolipoma

Definition

Angiolipoma is a benign neoplasm that may occur in the subcutis or in breast parenchyma. Angiolipomas are considered variants of lipomas. When the angiolipoma develops in the subcutaneous tissue overlying the breast, it presents as a well circumscribed and painful nodule. Angiolipoma arising within the breast parenchyma usually occurs as a small and painless nodule.

Clinical and Epidemiological Features

An angiolipoma manifests as a mass, which is either identified on imaging or palpated on physical examination.

Imaging Features

Mammographic and ultrasonographic features are very similar to those of haemangiomas. These lesions also present as superficial small masses, usually less than 2 cm They are often well-demarcated but can sometimes appear ill-defined. They are hyperechoic on ultrasound examination.

Pathologic Features

Macroscopic Features

Angiolipomas usually appear as well-circumscribed and often encapsulated masses. The cut surface is typically yellow and somewhat lobulated, indistinguishable from a conventional lipoma. As the vascular component increases, angiolipomas may appear more firm and red/brown.

Microscopic Features

Angiolipoma is characterised by a dispersed proliferation of small-calibre capillary vessels showing prominent intravascular fibrin microthrombi in a lipomatous background (Figs. 8.9 and 8.10). The lipomatous component has a benign appearance, with no nuclear atypia or pleomorphism. The small, round, usually thick-walled blood vessels tend to congregate at the periphery of the lesion. Fibrin thrombi may be the most conspicuous feature in some cases. In cellular angiolipoma, a prominent vascular component is seen with little to no admixed lipomatous elements.

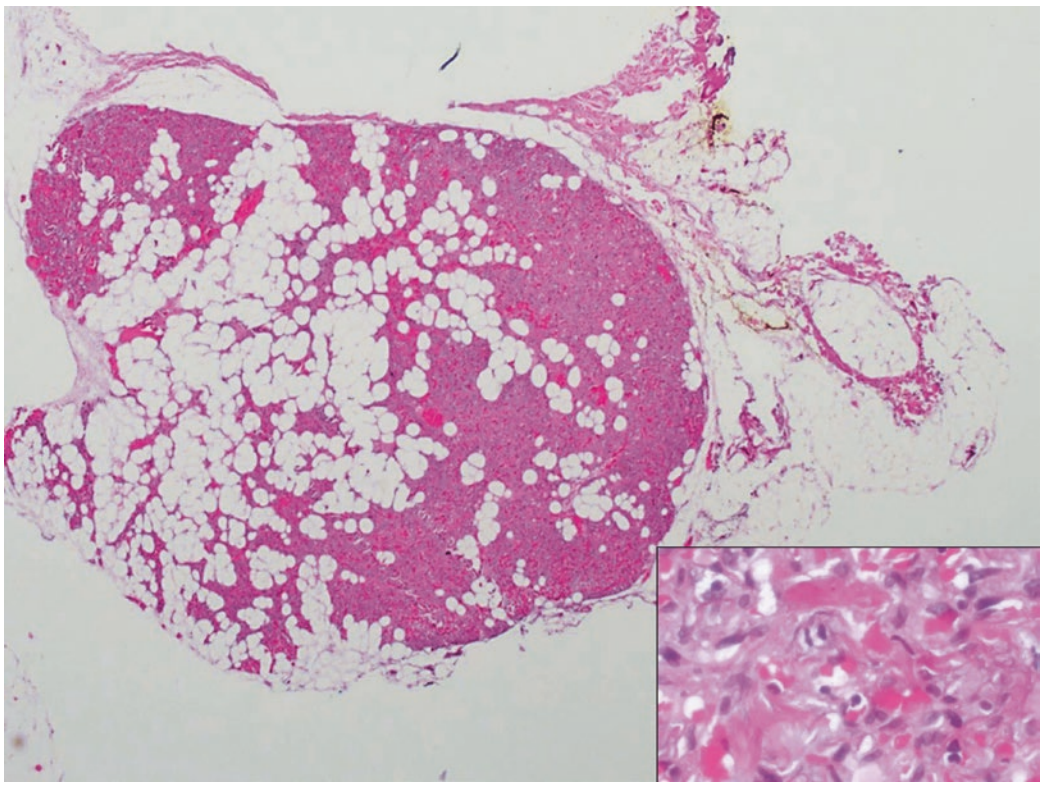

Fig. 8.9 Angiolipoma. Excision shows a circumscribed lipovascular lesion with congeries of congested capillaries interspersed with mature adipocytes (Reproduced with permission from Goh et al. [4]) *Inset* shows congested capillaries with occasional fibrin thrombi

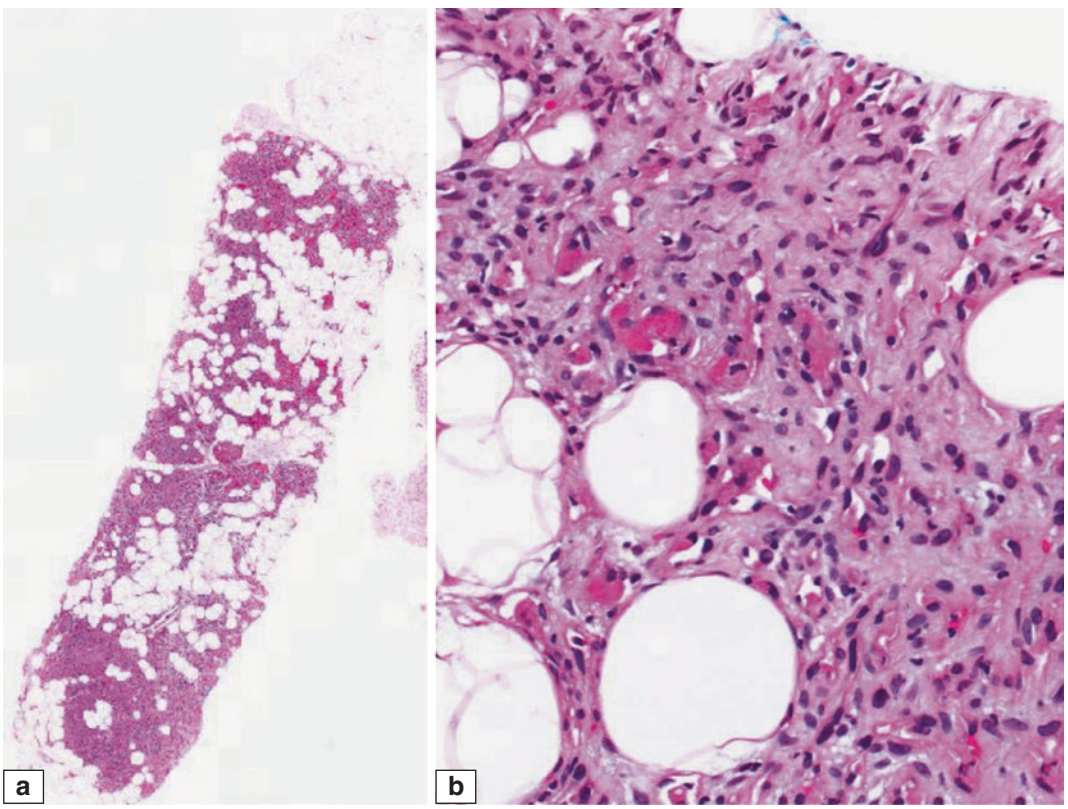

Fig. 8.10 Angiolipoma. (**a**) On core biopsy, the circumscribed border of the lesion is not readily appreciated histologically, though there is a clue from the upper end of the tissue core where a relatively distinct interphase of the lesion from the adjacent adipose is seen. (**b**) Higher magnification of the core biopsy material shows capillaries with fibrin thrombi. Although the subcutaneous location and radiological circumscription may point to the correct diagnosis, a benign conclusion of this lipovascular lesion on core biopsy is often not definitive, and excision may be required to confirm the diagnosis

Differential Diagnosis

Angiolipoma is usually a straightforward diagnosis. However, it may be difficult to recognise in some cases especially in small core biopsies. An excision may be required to exclude an angiosarcoma. Lipomatous–predominant angiolipoma may be confused with lipoma and atypical lipomatous tumour (ALT). Although both lipomas and angiolipomas are well circumscribed, often with thin fibrous capsules, lipomas usually have scant vascularity and do not possess fibrin microthrombi. ALTs show variation in nuclear size and shape in adipocytes of the lipomatous component, with occasional lipoblasts. Immunohistochemical stains for MDM2 and CDK4 demonstrate nuclear positivity in most ALTs. Cellular angiolipomas may be misdiagnosed as a haemangioma or angiosarcoma due to its high cellularity and inconspicuous adipose component. In contrast to angiolipoma, haemangiomas comprise vessels of different calibres without displaying any fibrin microthrombi. Angiosarcoma shows an infiltrative growth pattern with dissection into the breast parenchyma and nuclear atypia. Vascular channels in angiolipoma and angiosarcoma are positive for endothelial markers such as factor VIII, CD31, and CD34. Angiosarcoma however, lacks smooth muscle actin-positive pericytes surrounding its vasoformative channels.

Prognosis and Therapy Considerations

Angiolipomas are benign lesions and simple excision is curative.

Atypical Vascular Lesions of the Breast Skin

Definition

Atypical vascular lesions of the breast skin are radiation-associated lesions, which were first documented by Fineberg and Rosen. These lesions arise in patients who had received radiation therapy to the breast.

Clinical and Epidemiological Features

Initially thought to be precursors of angiosarcomas, follow-up studies have demonstrated that atypical vascular lesions of the breast skin have benign clinical behaviour in most patients. The mean patient age at presentation is 55–60 years. Skin lesions occur in the radiation field, typically 3–5 years after the completion of radiation therapy.

Pathologic Features

Macroscopic Features

Clinically, atypical vascular lesions of the breast skin present as flesh-coloured, erythematous or brownish, painless papules or patches on the irradiated skin, usually less than 1 cm in greatest dimension though they can reach larger sizes.

Microscopic Features

Atypical vascular lesions of the breast skin feature thin-walled, dilated, anastomosing small vascular channels that may disclose complex branching patterns (Fig. 8.11). The lesions may be well circumscribed, and wedge-shaped without extension into subcutaneous fat or breast parenchyma. A single layer of hyperchromatic endothelial cells without overt nuclear pleomorphism or atypia lines the vascular channels.

Differential Diagnosis

The main differential diagnoses for atypical vascular lesions of the breast skin are cutaneous haemangioma and radiation-associated angiosarcoma. Cutaneous haemangioma is usually well circumscribed and does not demonstrate any vasoformative dissection of dermal collagen; nuclear atypia is absent. As compared with atypical vascular lesions of the breast skin, cutaneous angiosarcomas are infiltrative, with invasion into the deep dermis and subcutaneous tissue. Extension of the lesion into subcutaneous tissue warrants the exclusion of angiosarcoma. Angiosarcomas are also characterised by cytologic pleomorphism. Amplification of *MYC* and *FLT4* genes is described in radiation-associated angiosarcoma, but is not encountered in atypical vascular lesions of the breast skin [1].

Prognosis and Therapy Considerations

Atypical vascular lesions follow a benign clinical course in most cases. Although new lesions can develop, progression to angiosarcoma is exceedingly rare. Surgical excision is the recommended treatment, and long-term follow-up is needed for detection of any recurrences.

Angiosarcoma

Definition

Angiosarcoma is a malignant vasoformative neoplasm that demonstrates endothelial differentiation.

Clinical and Epidemiological Features

Angiosarcoma of the breast may be primary, arising de novo within breast parenchyma, or it may be secondary, developing in the skin, chest wall, or breast parenchyma after surgical and radiation treatment for breast cancer. Primary angiosarcoma is the second-commonest sarcoma of the breast after malignant phyllodes tumour, accounting for 0.05 % of all primary breast malignancies [2]. The median age of patients with primary angiosarcoma is 40 years, versus 60–80 years for those with secondary disease. Affected women present with a mass, diffuse breast enlargement, or skin discolouration (Fig. 8.12). A history of prior radiation therapy is present in patients with secondary angiosarcoma.

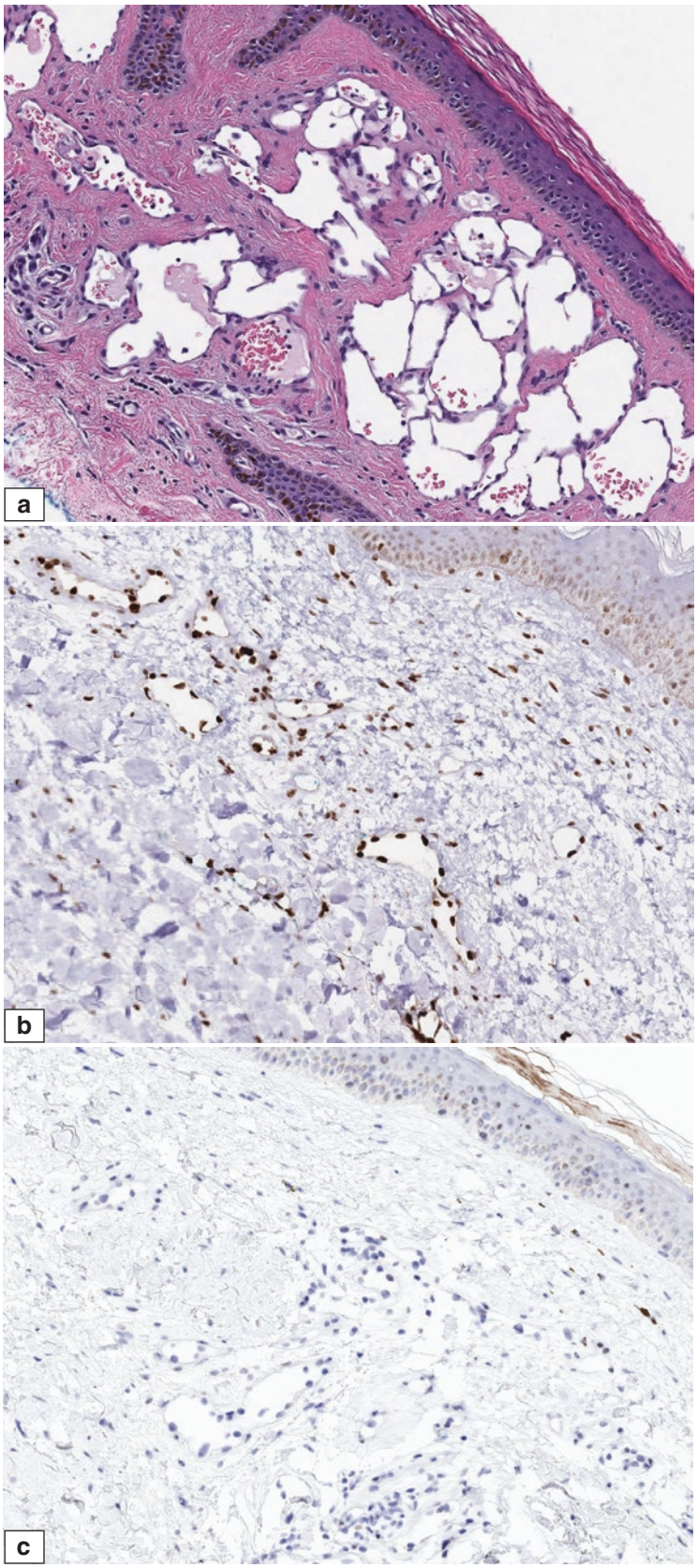

Fig. 8.11 Atypical vascular lesion. (**a**) Irregularly shaped ectatic vessels with occasionally plump nuclei are found within the dermis of the skin of the post-irradiated breast. (**b**) Fli1 immunohistochemistry shows positive reactivity in endothelial nuclei. (**c**) No c-Myc expression is present on immunohistochemistry

Imaging Features

Radiological findings may be normal or nonspecific [3]. When masses are visible, they may appear as oval, lobulated, or irregular lesions with ill-defined or circumscribed margins. The internal echogenicity on sonography is variable; lesions have been shown to appear heterogeneously hyperechoic, as opposed to the hypoechoic appearance of most breast cancers [4]. They can also present as ill-defined asymmetric densities on mammography and ill-defined, heterogeneously mixed hyper-hypoechoic breast tissue on sonography, without a discrete mass (Fig. 8.13) [5].

Fig. 8.12 Angiosarcoma of the breast. A large patch of purplish pink pigmentation of the skin over the breast is seen (Courtesy of Dr. Esther Chuwa)

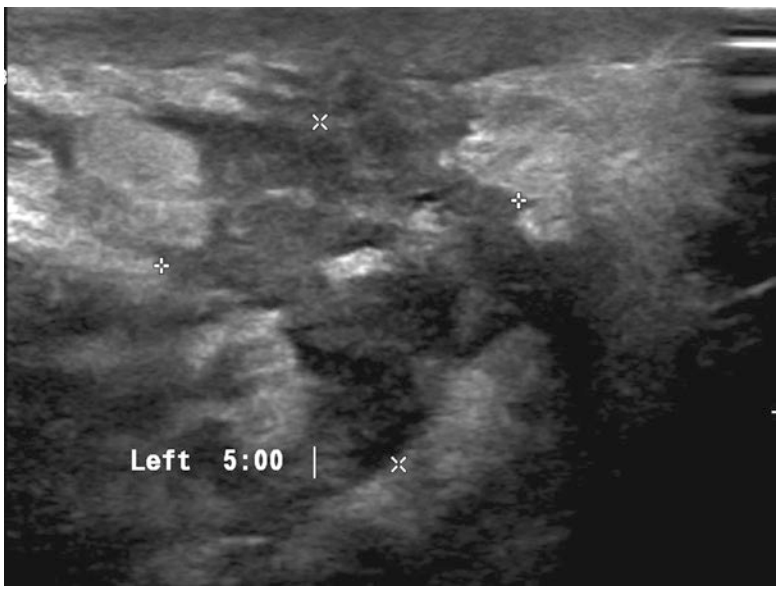

Fig. 8.13 Angiosarcoma. Ultrasonography shows an irregular, heterogeneous mass with internal acoustic shadows (Courtesy of Dr. Esther Chuwa)

Pathologic Features

Macroscopic Pathology

Angiosarcomas are typically haemorrhagic on gross appearance, and a deeply haemorrhagic lesion should raise suspicion of the diagnosis (Figs. 8.14 and 8.15). Borders are ill-defined, and there may be a spongy consistency, though poorly differentiated disease may be solid and firm.

Microscopic Pathology

Anastomosing vessels dissect through the breast parenchyma and lobules. In low-grade or well-differentiated lesions, vascular spaces are well-developed with minimal endothelial atypia (Figs. 8.16, 8.17, 8.18, 8.19, 8.20, 8.21, 8.22, 8.23, and 8.24).

Fig. 8.14 Angiosarcoma. Mastectomy specimen shows violaceous skin discolouration in the breast skin from involvement of the skin by angiosarcoma. This primary angiosarcoma developed in a woman without any history of prior radiation

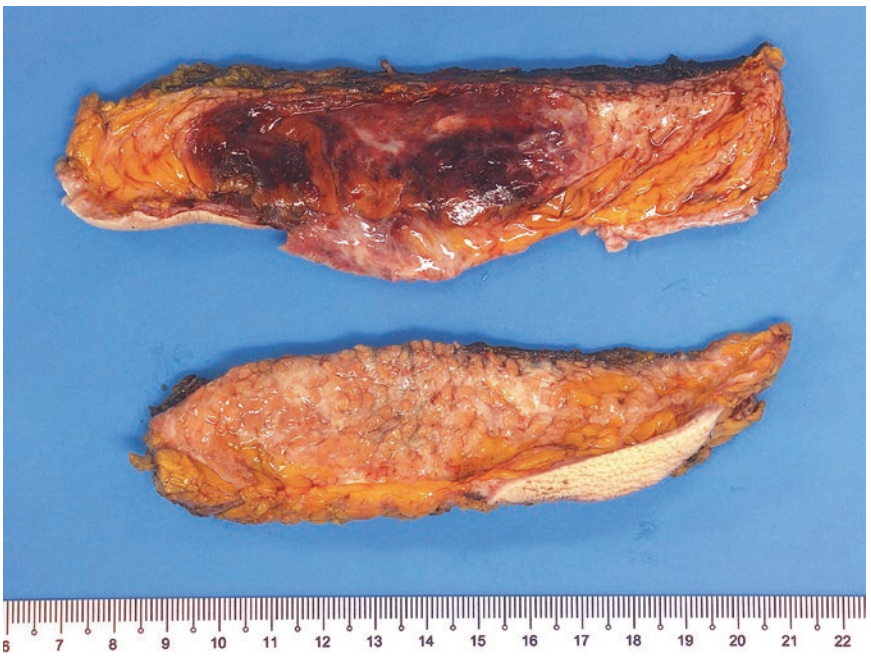

Fig. 8.15 Angiosarcoma. A large haemorrhagic lesion is observed on cut sections of the breast tissue (*upper field*). The borders are ill-defined. In other parts of the breast, a whitish-grey nodularity is observed due to lactational hyperplasia of the breast parenchyma (*lower field*)

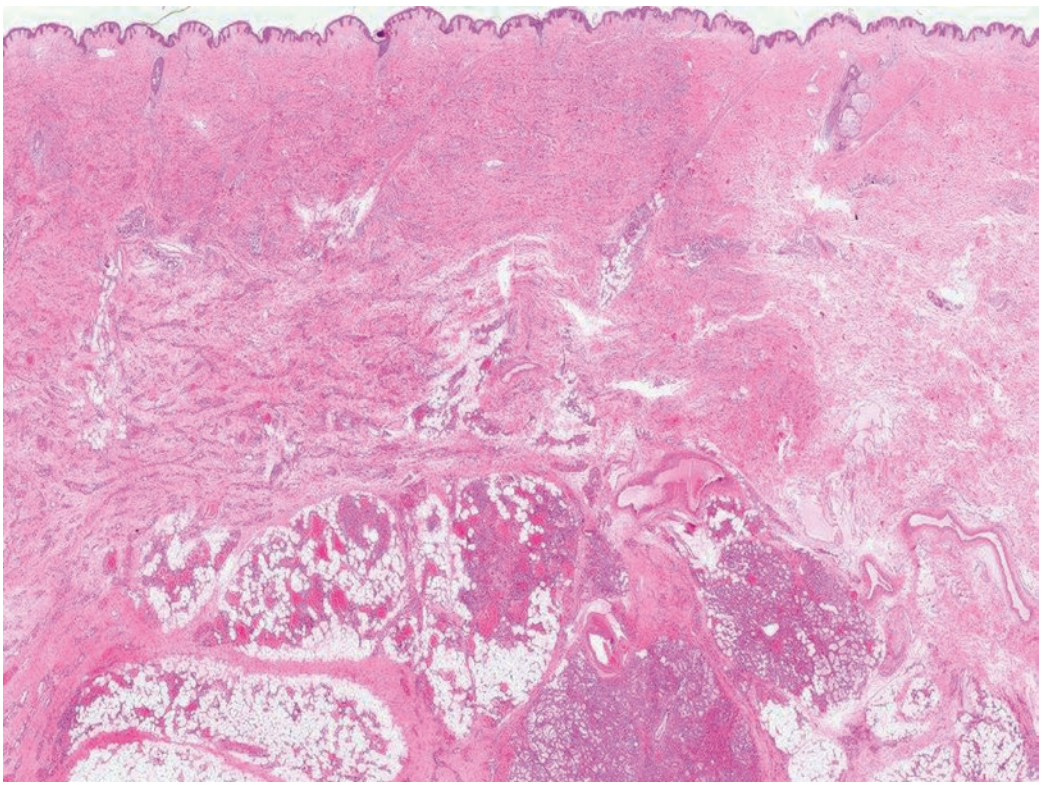

Fig. 8.16 Angiosarcoma. A vasoformative tumour is seen in the dermis, subcutaneous tissue, and breast parenchyma. Involvement by angiosarcoma of the dermis accounts for the pigmentation of the skin

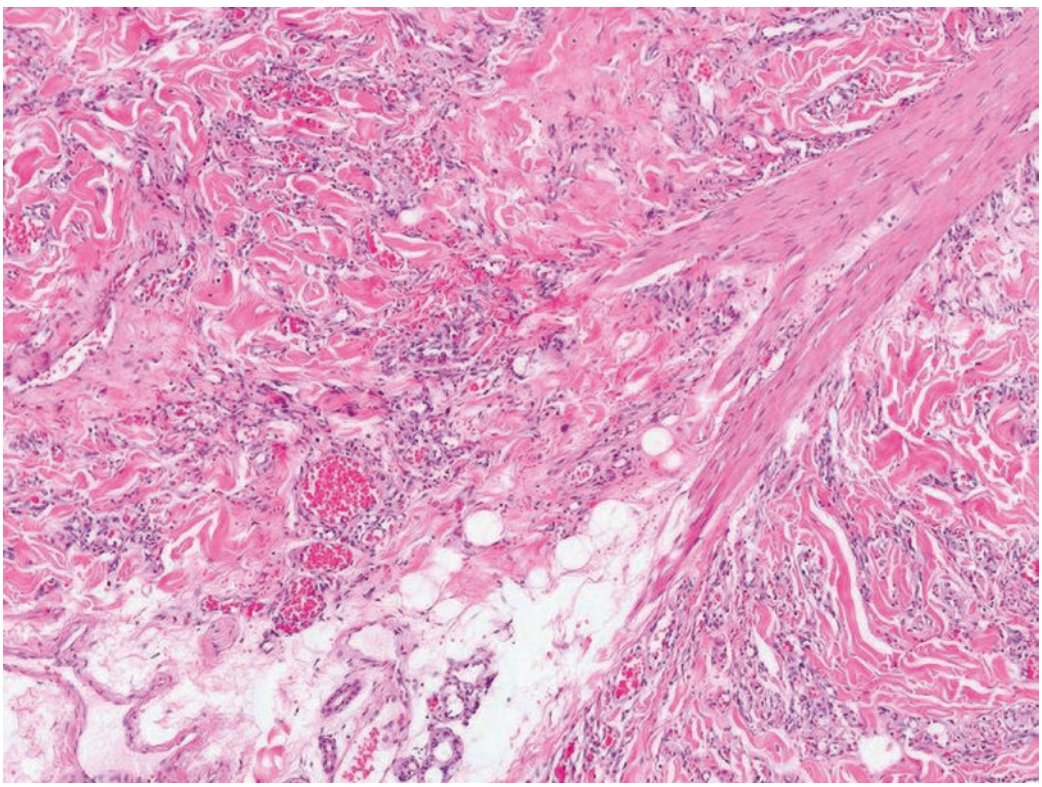

Fig. 8.17 Angiosarcoma. Small-calibre, congested vessels dissect through collagenous stroma of the dermis

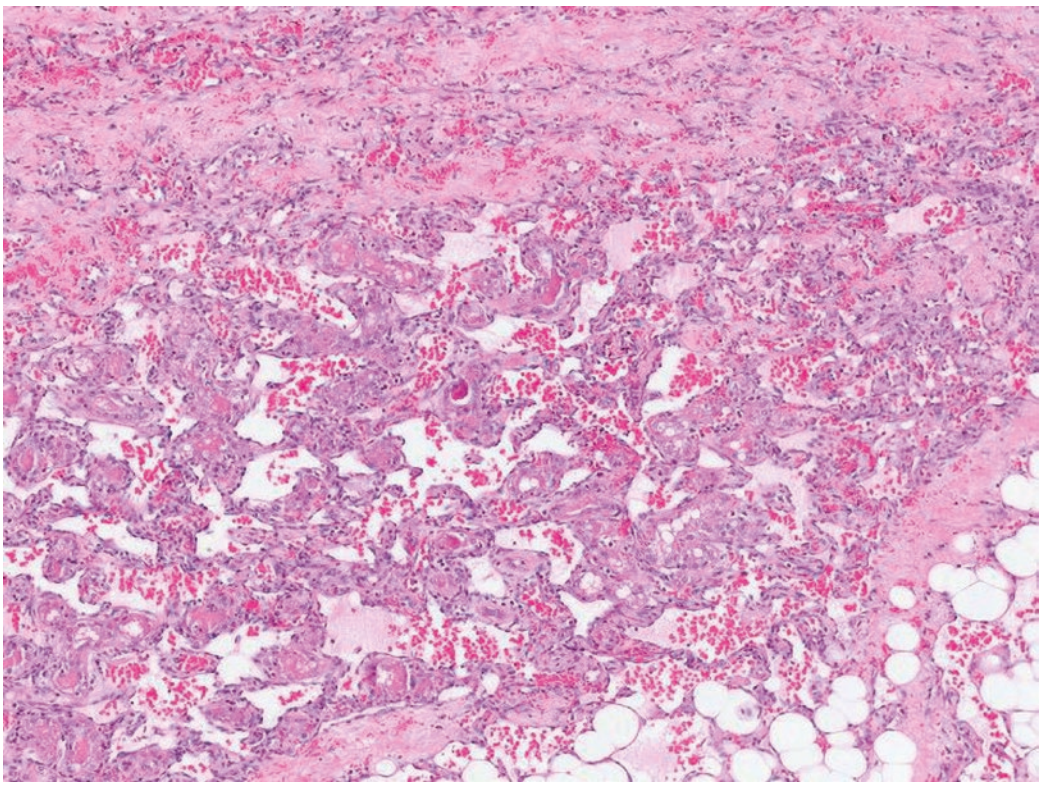

Fig. 8.18 Angiosarcoma. Anastomosing vessels show red blood cells in the vascular spaces. These vessels are in continuity with those of the dermis (*upper field*)

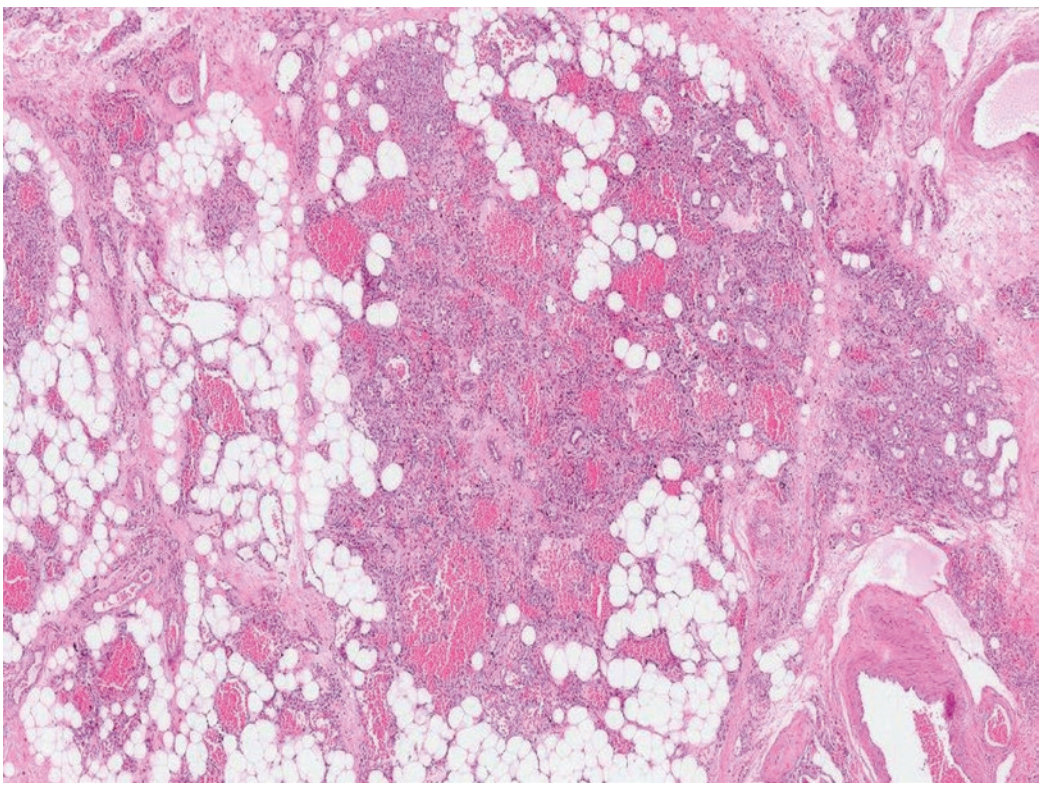

Fig. 8.19 Angiosarcoma. Collections of neoplastic vessels are interspersed among adipocyte lobules, reminiscent of angiolipoma. In contrast to angiolipoma, which usually occurs in the subcutaneous plane and has a circumscribed border, angiosarcoma of the breast is permeative, with anastomosing and destructive vasoformative growth, and it involves the parenchyma of the breast

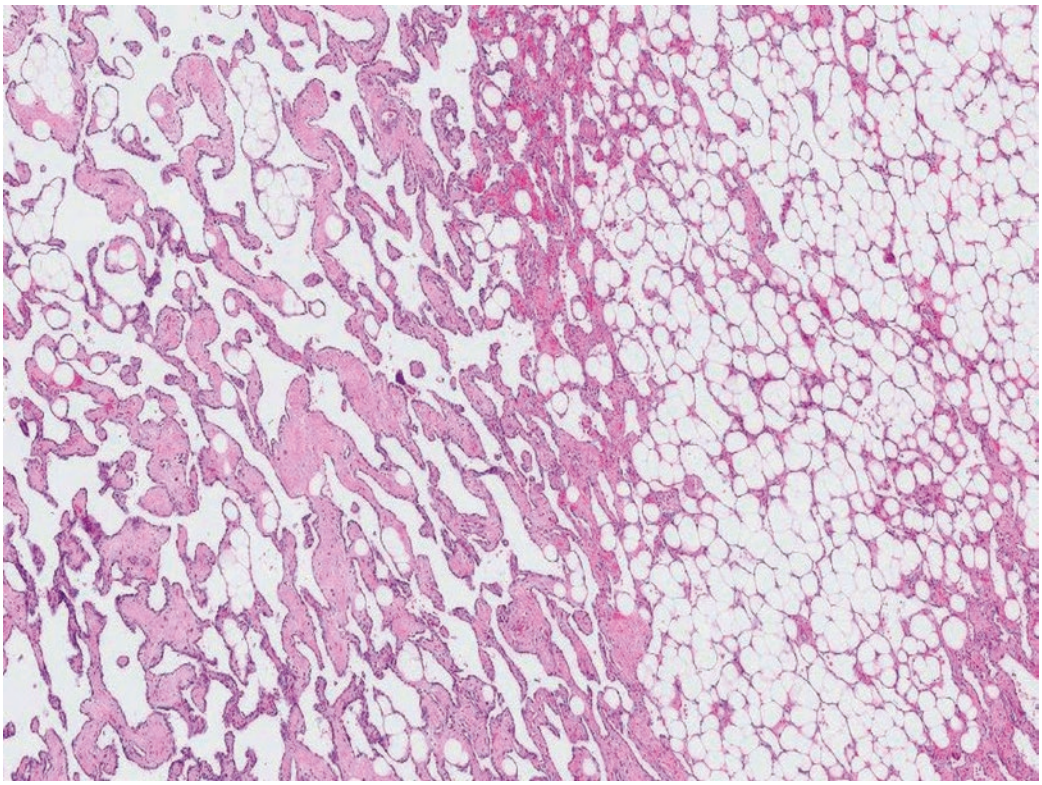

Fig. 8.20 Angiosarcoma. Complex anastomosing vasculature is seen, with a pseudoalveolar pattern (*left field*). Free-floating fibrous stroma covered by neoplastic endothelial cells is seen in some of the spaces. Small vessels percolate among adipocytes (*right field*). This is a well-differentiated or low-grade angiosarcoma, as the vascular spaces are relatively well formed, endothelial atypia is mild, and no solid spindle cell foci are present

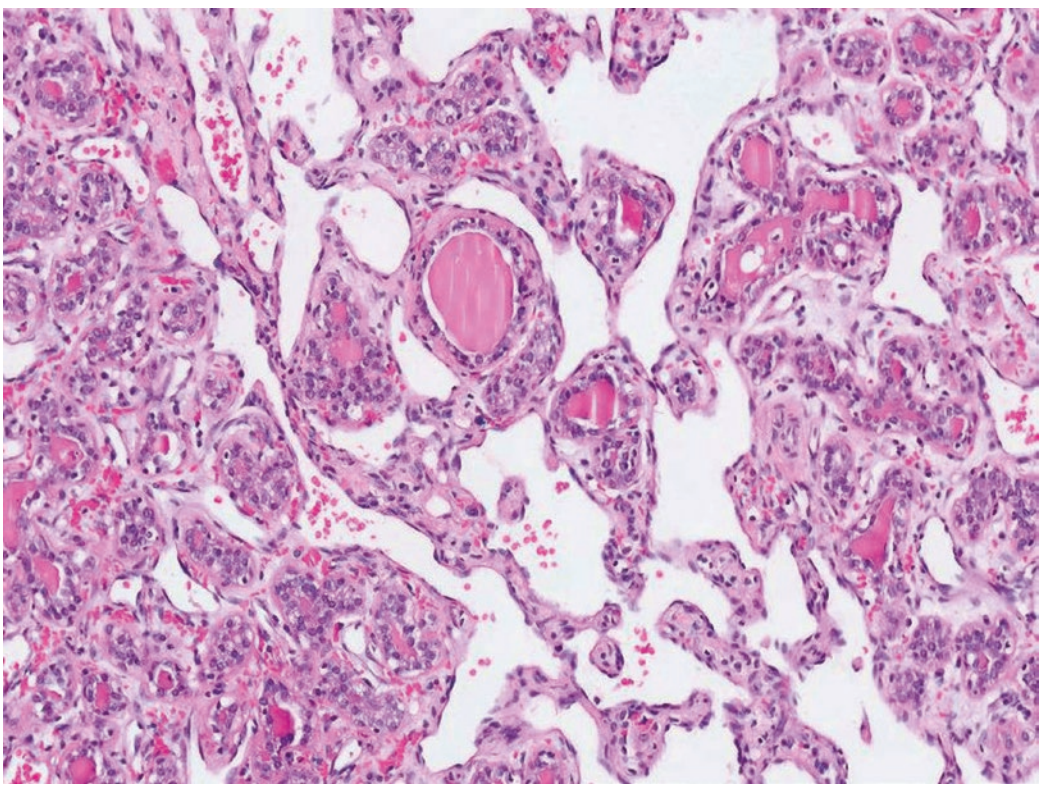

Fig. 8.21 Angiosarcoma. The neoplastic vessels invade the lobule and extend between the acini. The bilayered acini with luminal pink secretions are splayed apart by the abnormal vessels

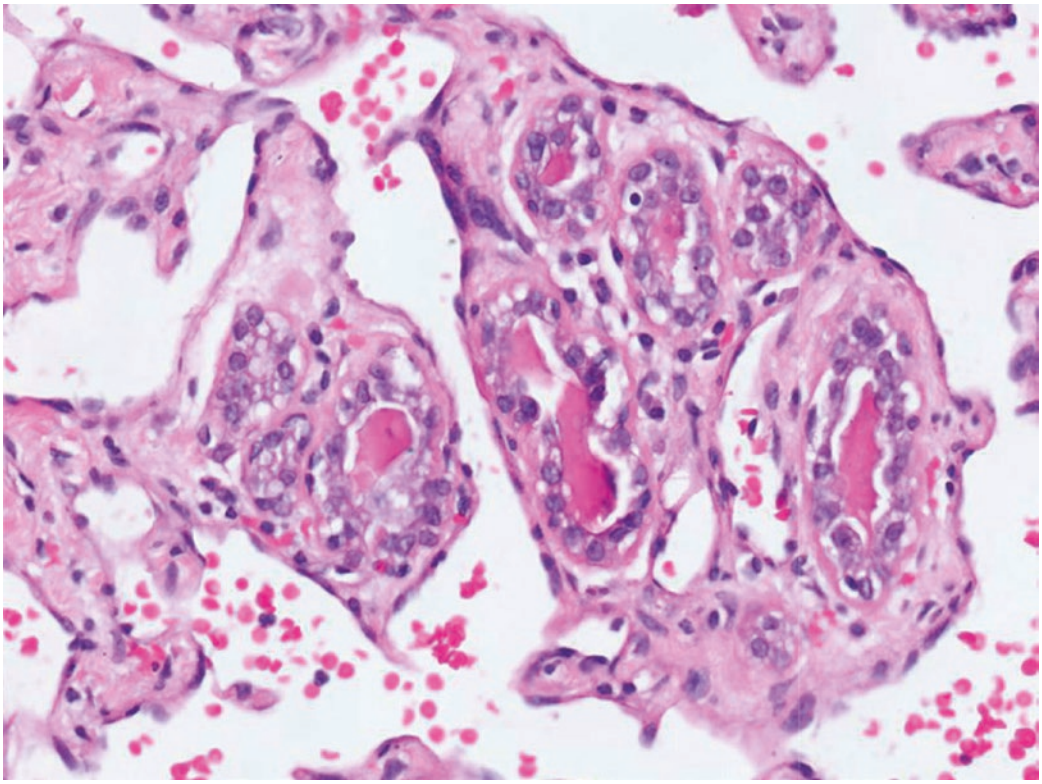

Fig. 8.22 Angiosarcoma. This low-grade, well-differentiated lesion shows anastomosing vessels dissecting through a breast lobule, separating groups of bilayered acini with luminal pink secretions. Neoplastic endothelial cells show flattened nuclei with minimal atypia. Red blood cells are seen within the vascular spaces. The diagnosis of angiosarcoma is based on the diffusely permeative pattern and anastomosing nature of the vessels, as endothelial atypia is mild in low-grade tumours

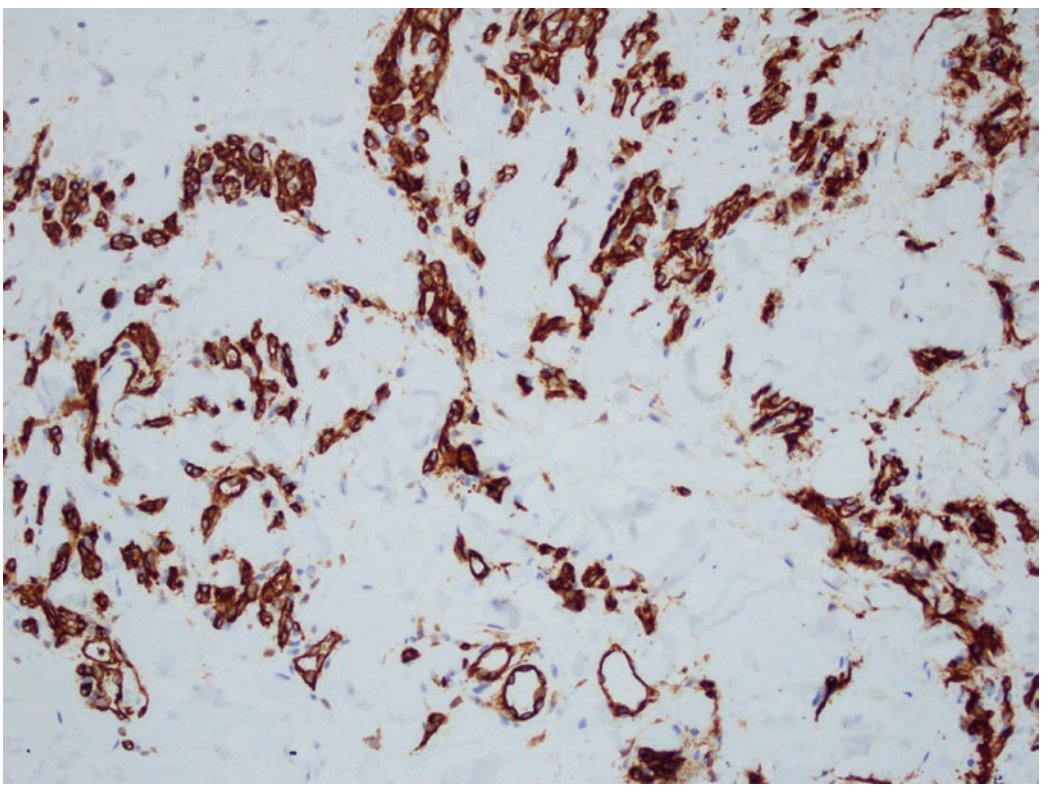

Fig. 8.23 Angiosarcoma. Immunohistochemistry for CD31 shows positive reactivity of the cells lining variably sized spaces

In high-grade or poorly differentiated tumours, vessels are inconspicuous with a predominantly solid, spindle cell appearance accompanied by brisk mitoses and necrosis, often requiring immunohistochemistry to confirm the endothelial origin of the spindle cells. Blood lakes may be seen (Figs. 8.25, 8.26, 8.27, 8.28, 8.29, and 8.30).

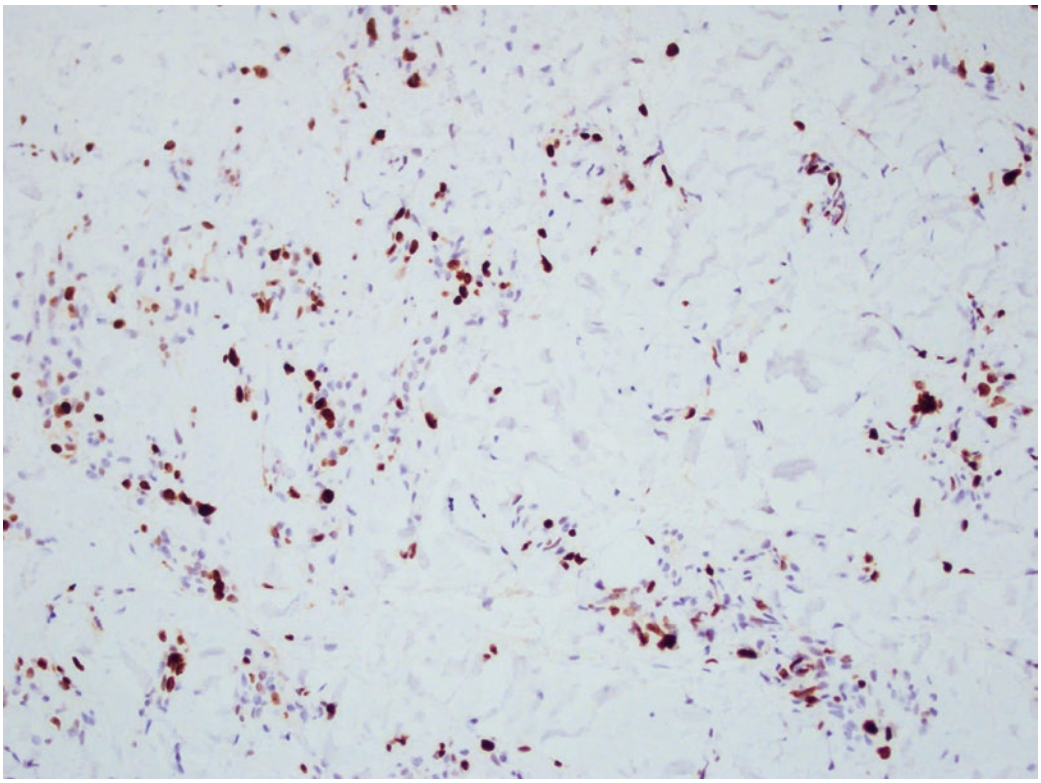

Fig. 8.24 Angiosarcoma. Ki67 immunohistochemistry shows increased proliferation fraction of the endothelial cells

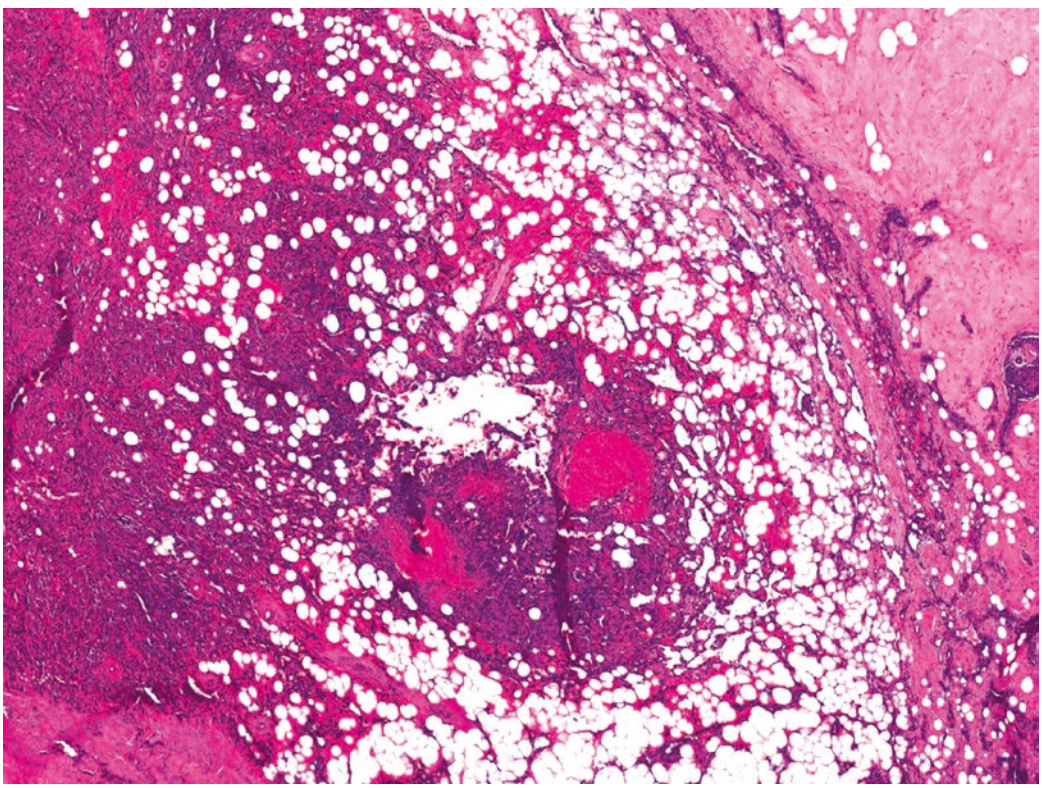

Fig. 8.25 Angiosarcoma, intermediate to poorly differentiated. More solid foci of spindle cells are seen permeating the breast parenchyma. Areas of haemorrhage are present among the spindle cells

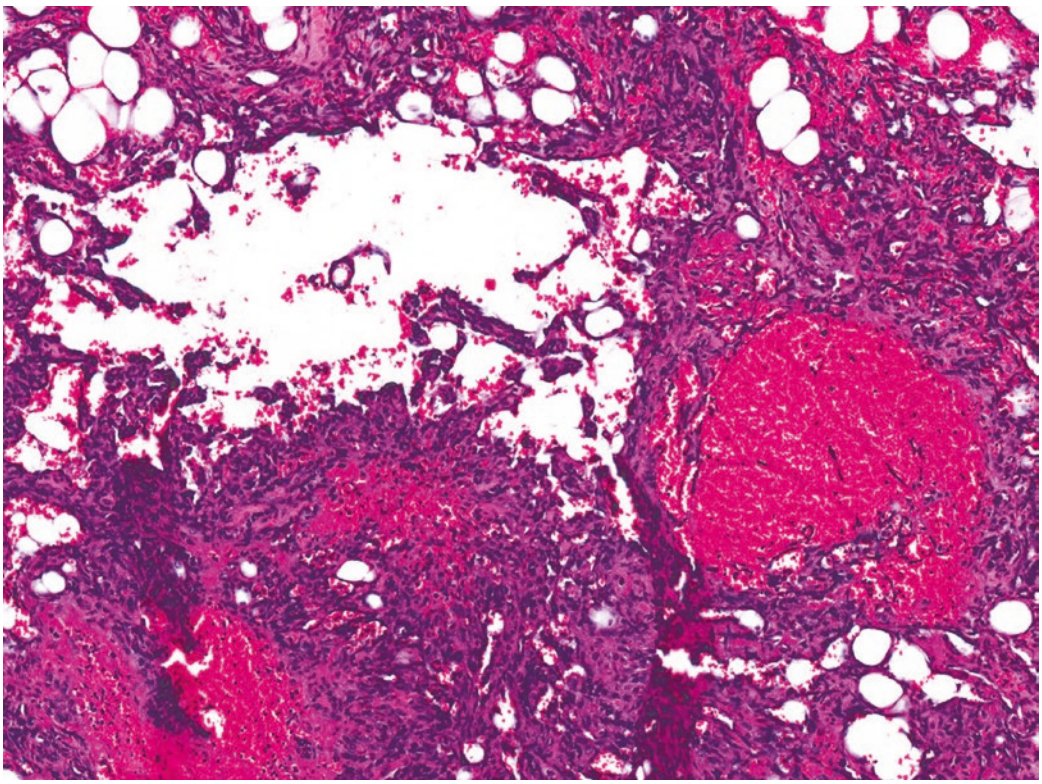

Fig. 8.26 Angiosarcoma, intermediate to poorly differentiated. Blood lakes or pools of red blood cells are seen. Coalescent vascular spaces are present, within which are free-floating scaffolds of malignant endothelial cells

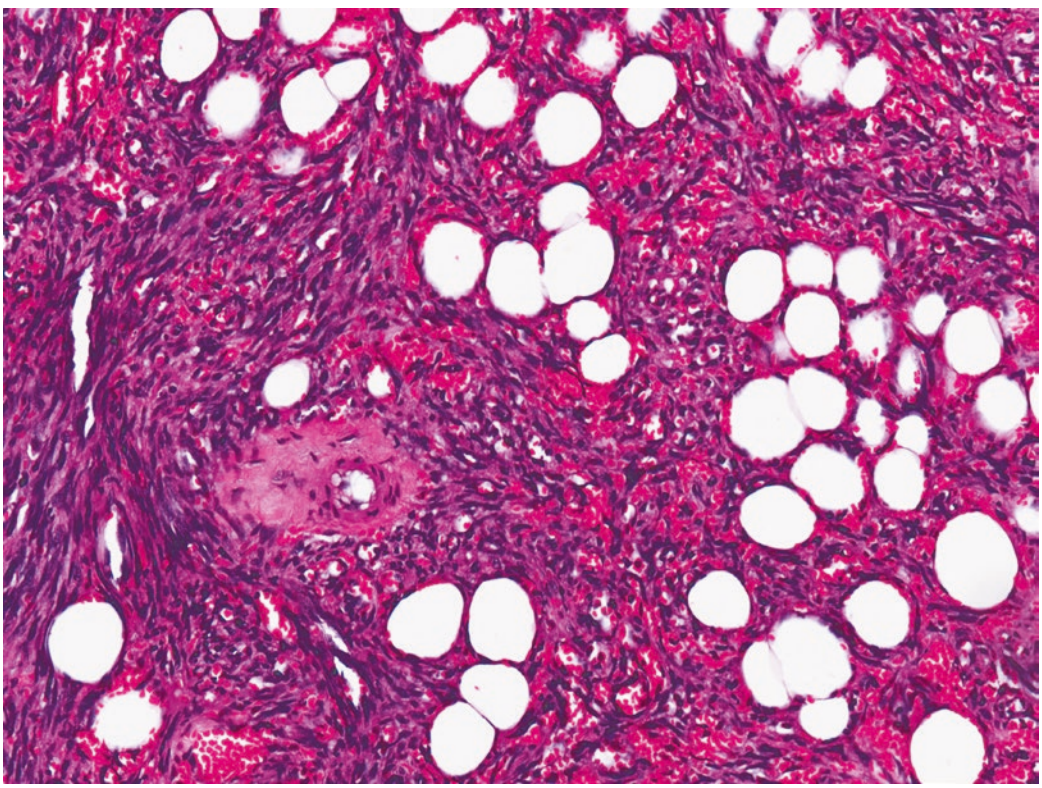

Fig. 8.27 Angiosarcoma, intermediate to poorly differentiated. Solid sheets of malignant spindle cells (*left field*) merge with areas in which spindle cells surround small spaces containing puddles of red blood cells, representing attempts at vessel formation by malignant endothelial cells

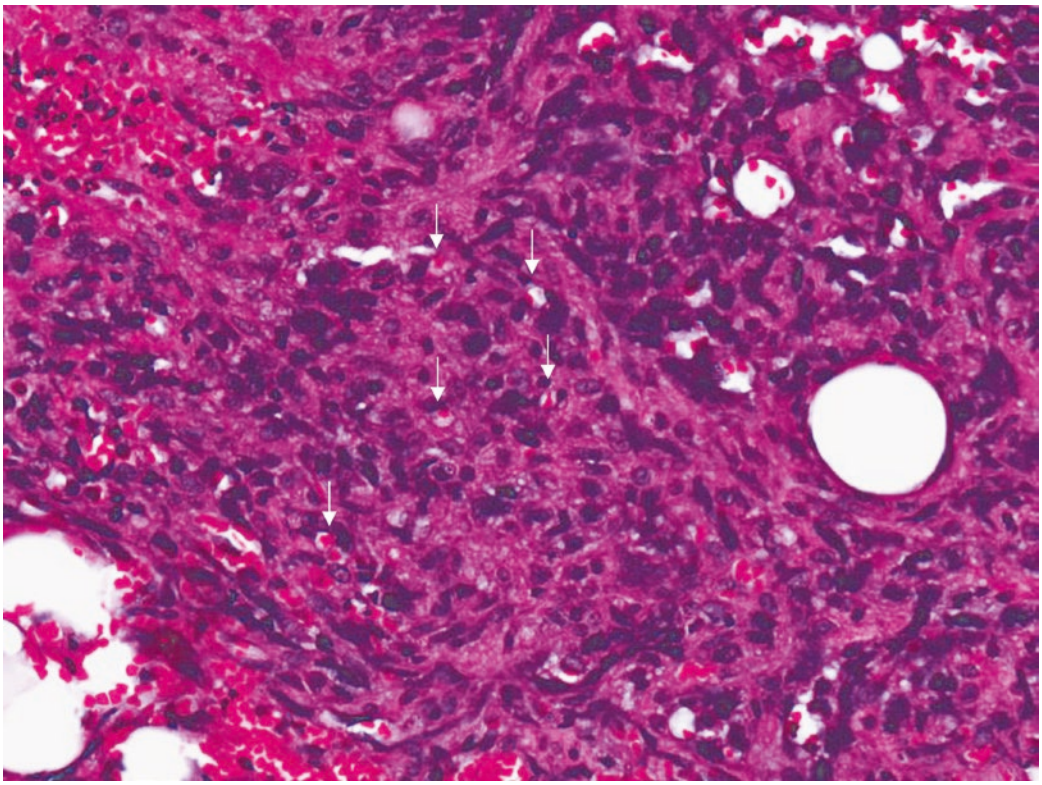

Fig. 8.28 Angiosarcoma, intermediate to poorly differentiated. Malignant endothelial cells show hyperchromatic nuclei with marked nuclear pleomorphism. There are individual cell lumens containing single red blood cells (*white arrows*), which are useful clues to a vasoformative origin

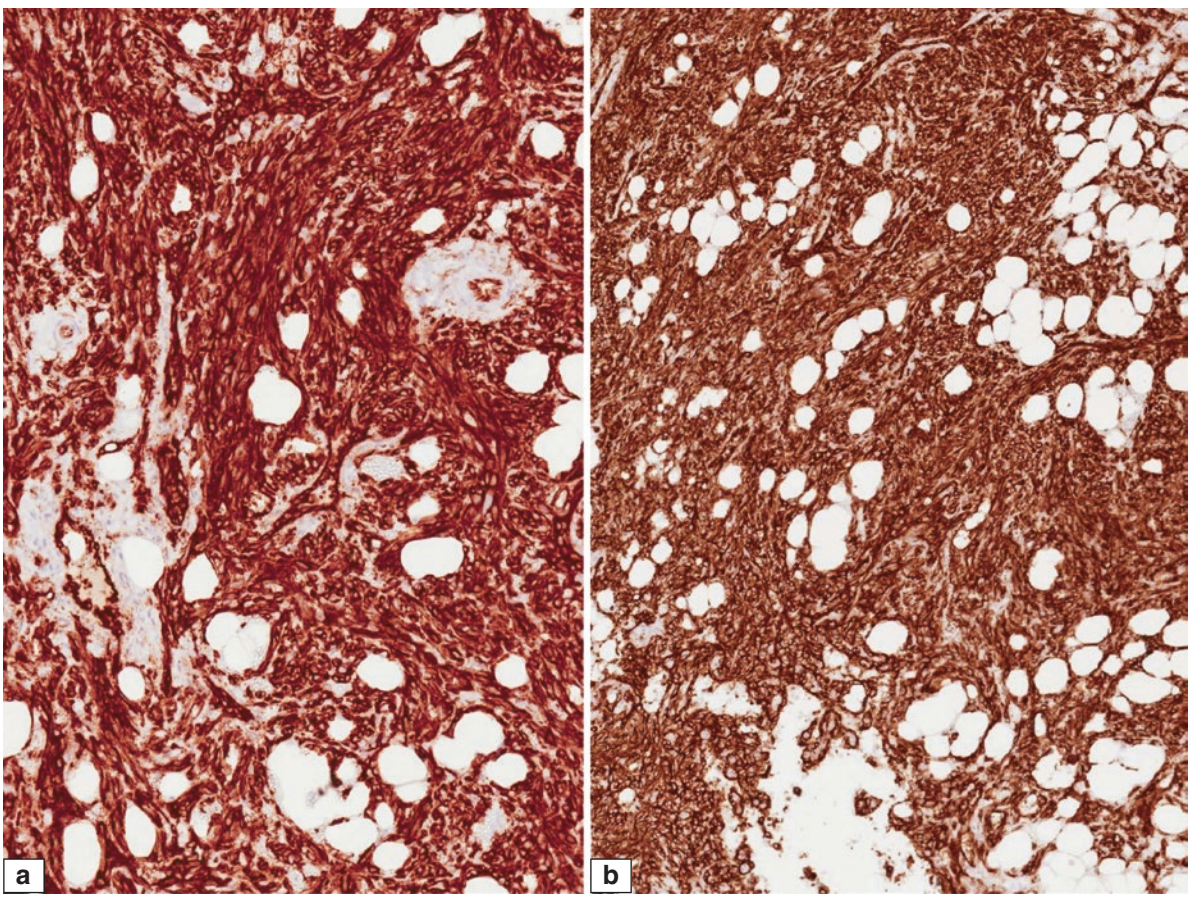

Fig. 8.29 Angiosarcoma, intermediate to poorly differentiated. CD31 (**a**) and CD 34 (**b**) immunohistochemistry shows diffuse and intense staining of the spindle cells

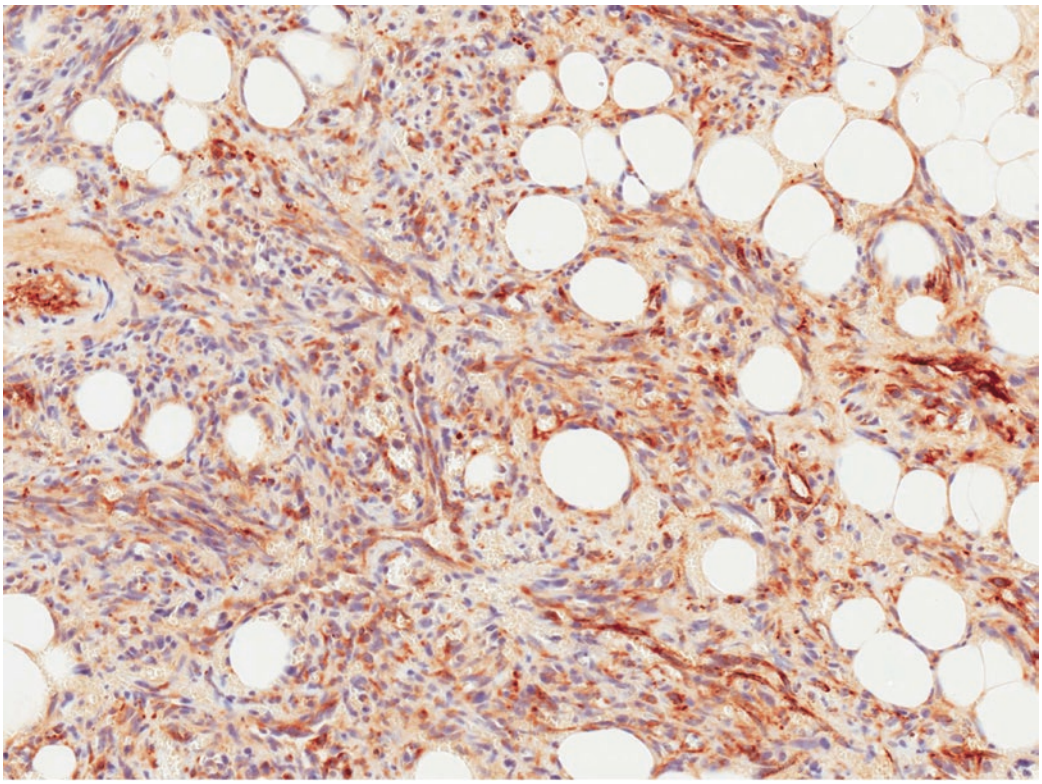

Fig. 8.30 Angiosarcoma, intermediate to poorly differentiated. Factor VIII immunohistochemistry shows positive staining of the spindle cells and decorates the neoplastic endothelial cells lining the slit-like vessels

The epithelioid variant of angiosarcoma particularly mimics carcinoma, and close examination is needed to identify its vasoformative nature, especially in limited core biopsy material. The presence of haemorrhage, slit-like spaces, individual cell lumens containing red blood cells, and negativity for hormone receptors and c-erbB-2 are useful clues to the correct diagnosis (Figs. 8.31, 8.32, 8.33, and 8.34).

Intermediate-grade angiosarcoma shows endothelial atypia, multilayering, and mitoses without the diffuse solid appearance of high-grade tumours. Immunohistochemistry for CD31, CD34, factor VIII, ERG and D2-40 helps verify the endothelial origin (Fig. 8.35). Proliferation index using Ki67 is variable depending on histologic grade, with high-grade angiosarcomas displaying markedly increased proliferative activity (Fig. 8.36). c-Myc positivity (overexpression and amplification) is reported in radiation-induced secondary angiosarcoma (Figs. 8.37 and 8.38).

Differential Diagnosis

Pseudoangiomatous Stromal Hyperplasia

Pseudoangiomatous stromal hyperplasia (PASH) comprises anastomosing slit-like spaces lined by myofibroblasts, mimicking vascular spaces of a well-differentiated angiosarcoma (Figs. 8.39 and 8.40). A hormonally related lesion, progesterone receptor expression is often seen in the myofibroblast nuclei. Actin, desmin, and calponin are also positive in PASH, in contrast to angiosarcoma, which is negative for these markers. Endothelial markers are negative in PASH, except for CD34, which is positive in both.

Angiolipoma

Similar to angiolipomas elsewhere, these can occur in the breast subcutis and often do not extend into breast parenchyma. Congeries of capillaries, which may contain fibrin thrombi, are admixed with mature adipocytes. Borders of the angiolipoma are circumscribed, differing from angiosarcoma, which demonstrates a permeative appearance.

Haemangioma

The haemangioma is a benign proliferation of mature vessels. It is histologically circumscribed and may show calcifications and thrombosis. The vessels are of variable calibres and are lined by endothelial cells without significant atypia. Capillary, cavernous, and venous haemangiomas can occur, and histologically similar areas may be encountered in well-differentiated angiosarcoma. Papillary endothelial hyperplasia associated with an organising thrombus may be mistaken for angiosarcoma. The perilobular haemangioma displays vessels within the lobule as well as in the interlobular stroma (Figs. 8.41 and 8.42).

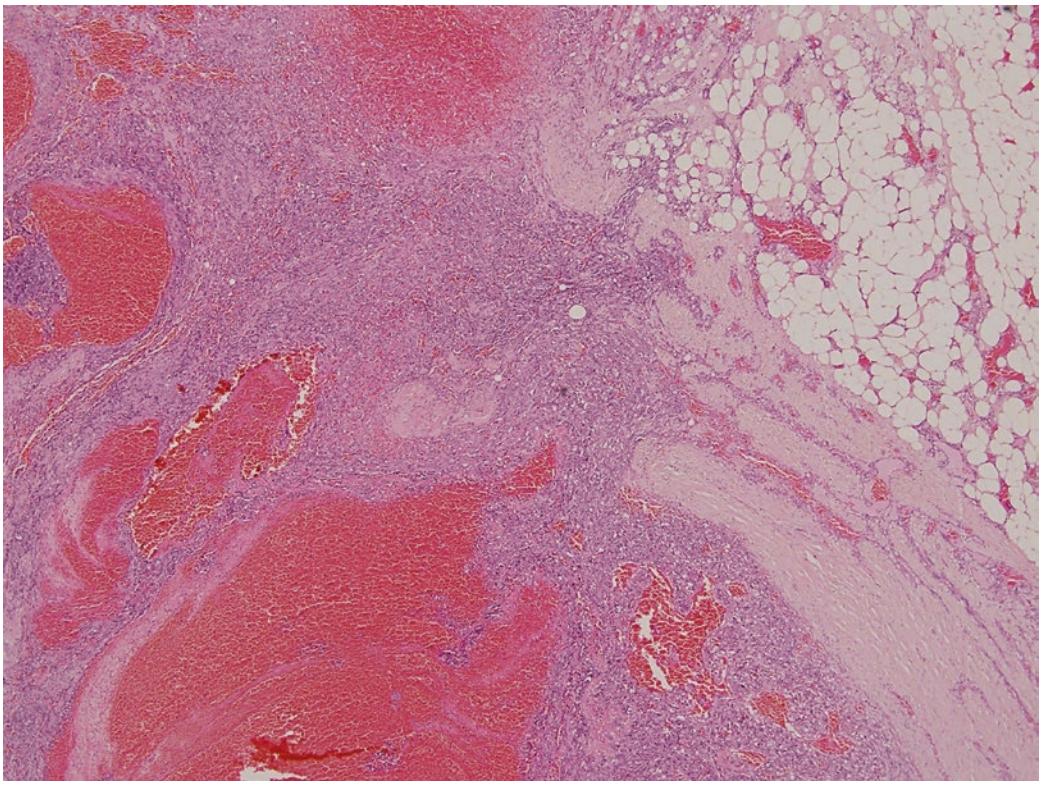

Fig. 8.31 Angiosarcoma, intermediate grade. Large pools of blood are present within the tumour, which shows infiltration into adipose tissue

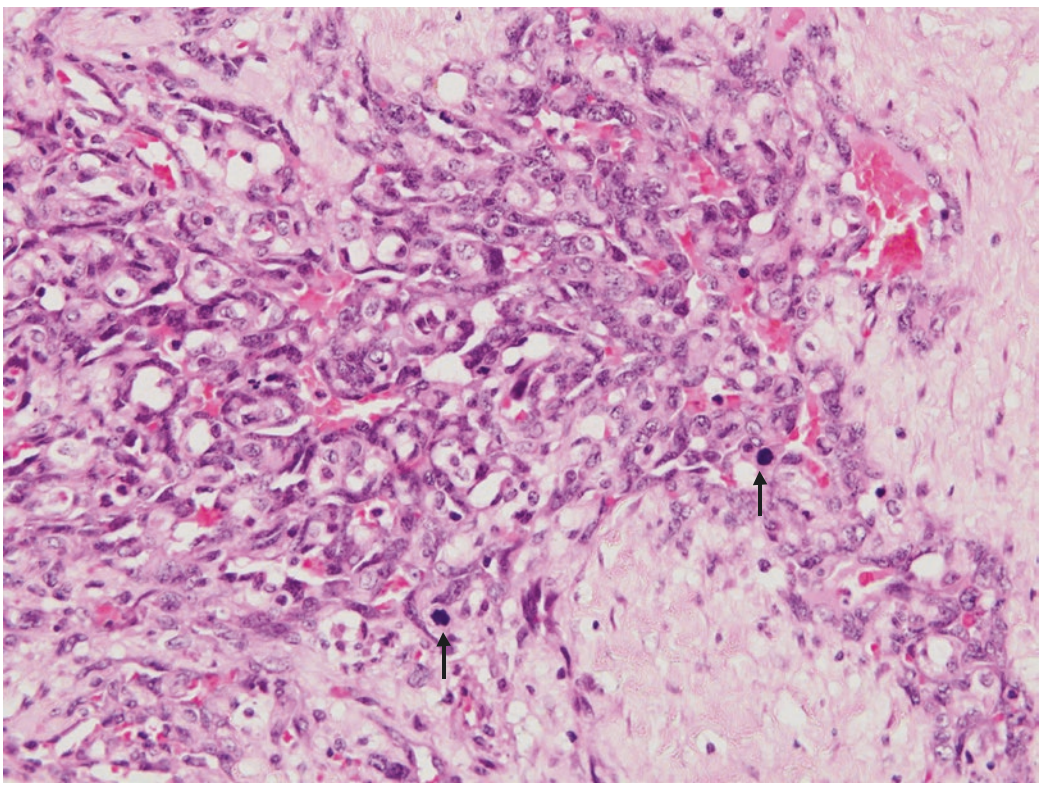

Fig. 8.32 Angiosarcoma, intermediate grade. Anastomosing vessels are lined by abnormal endothelial cells with scattered mitoses (*arrows*). Red blood cells are seen within the vascular spaces

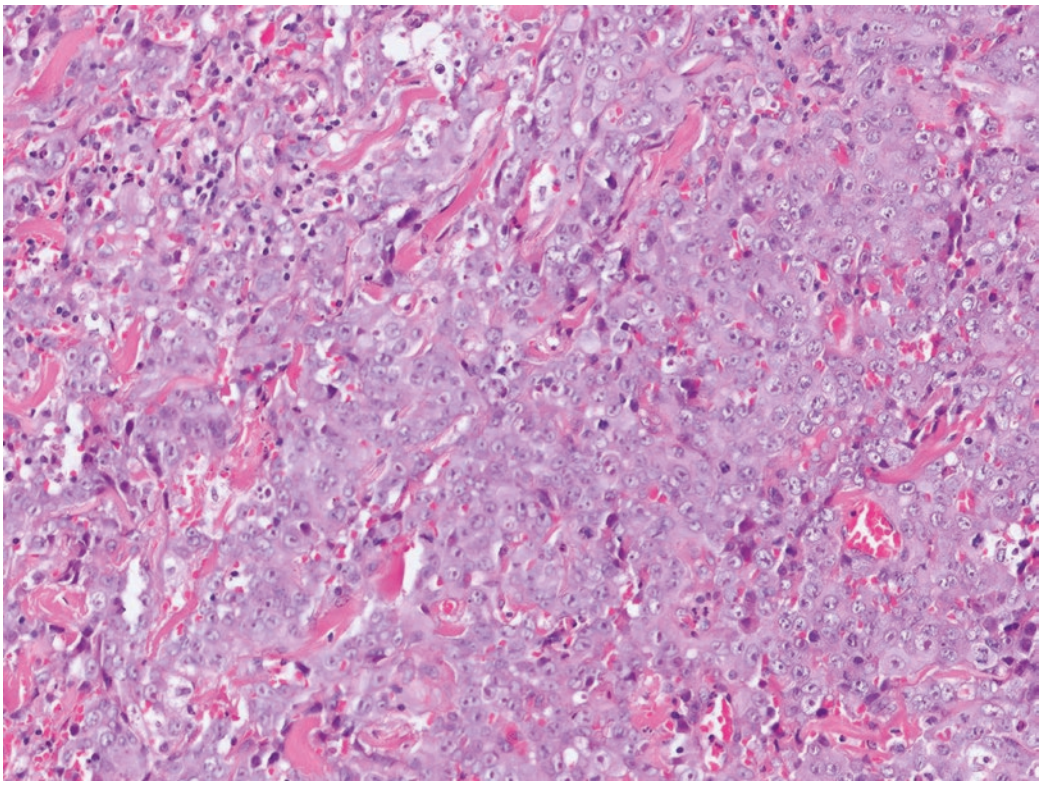

Fig. 8.33 Epithelioid angiosarcoma, occurring in an irradiated breast after wide excision for breast carcinoma. Sheets of malignant epithelioid cells with enlarged vesicular nuclei and prominent nucleoli are seen invading the breast tissue, closely resembling a high-grade carcinoma. Clues to the vasoformative nature are the presence of extravasated red cells within spaces and small lumens lined by the epithelioid cells, or red cells found within intracytoplasmic lumens of the epithelioid cells

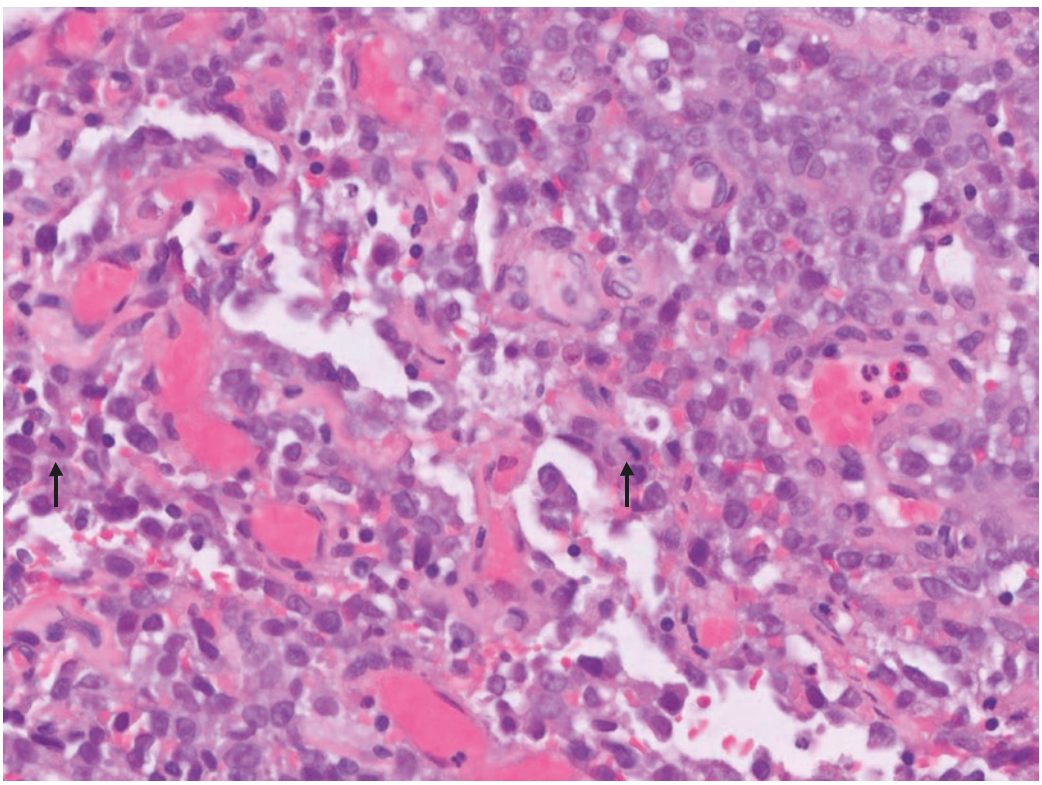

Fig. 8.34 Epithelioid angiosarcoma. Abortive vessels are noted among the malignant epithelioid cells. Scattered mitoses are present (*arrows*)

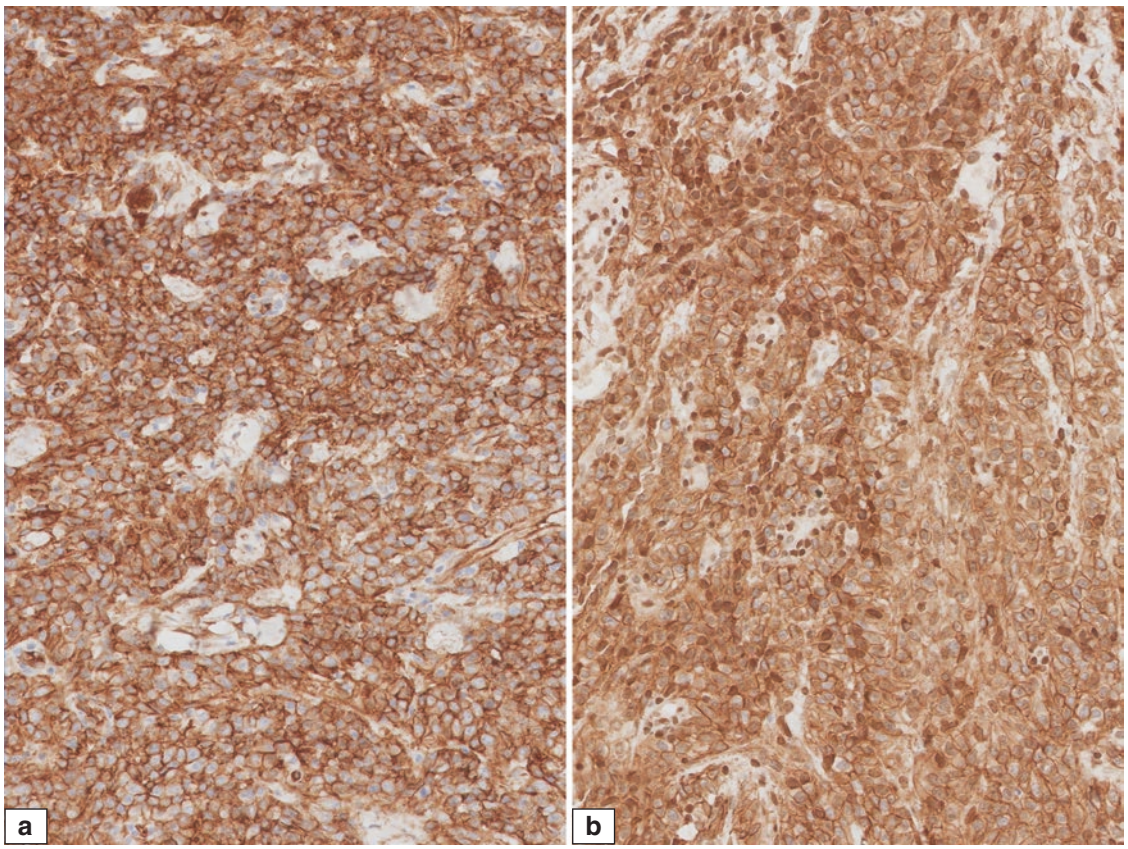

Fig. 8.35 Epithelioid angiosarcoma. Immunohistochemistry for CD31 (**a**) and D2-40 (**b**) shows positive reactivity in the epithelioid cells, confirming their endothelial origin. There should be a high index of suspicion for this diagnosis when there are the following features: history of breast irradiation, extensively haemorrhagic tumour, presence of abortive vessels within the tumour, absence of in situ carcinoma, and triple-negative status. Epithelioid angiosarcoma is a particular pitfall on core biopsy material

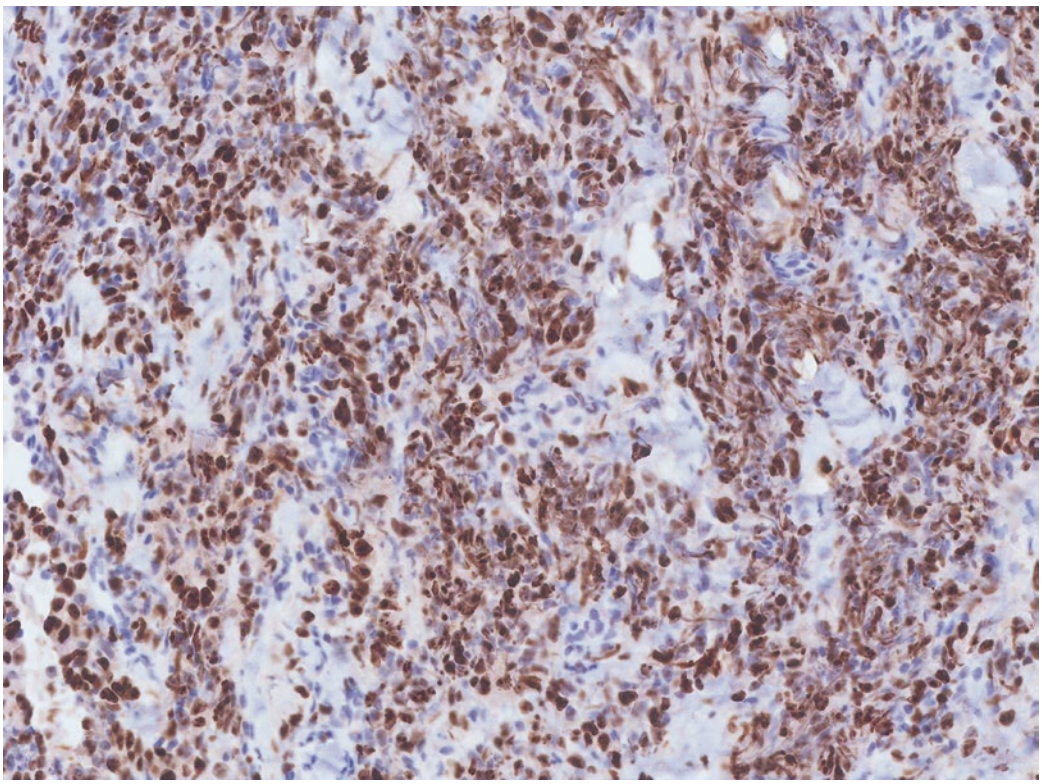

Fig. 8.36 Epithelioid angiosarcoma. Immunohistochemistry for Ki67 shows a high proliferation fraction with diffuse nuclear staining of tumour cells

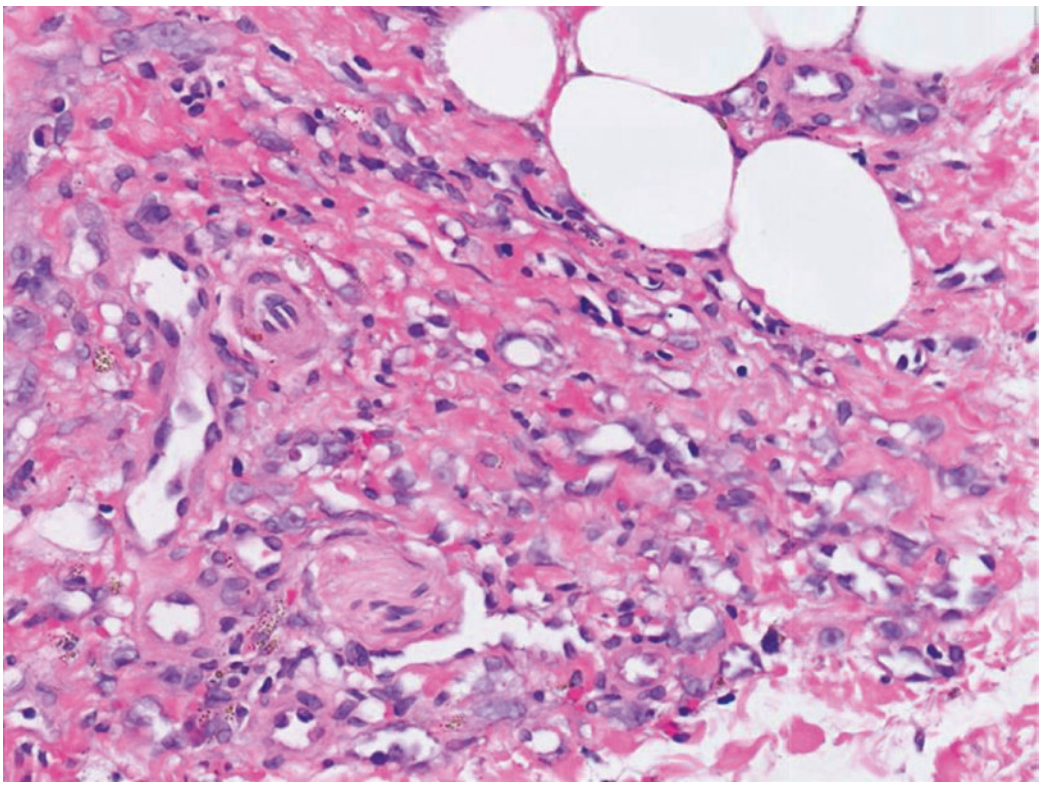

Fig. 8.37 Angiosarcoma, post-irradiation. Irregular vessels are lined by endothelial cells with moderate nuclear atypia and variably conspicuous nucleoli. A small nerve is trapped amid the anastomosing vessels

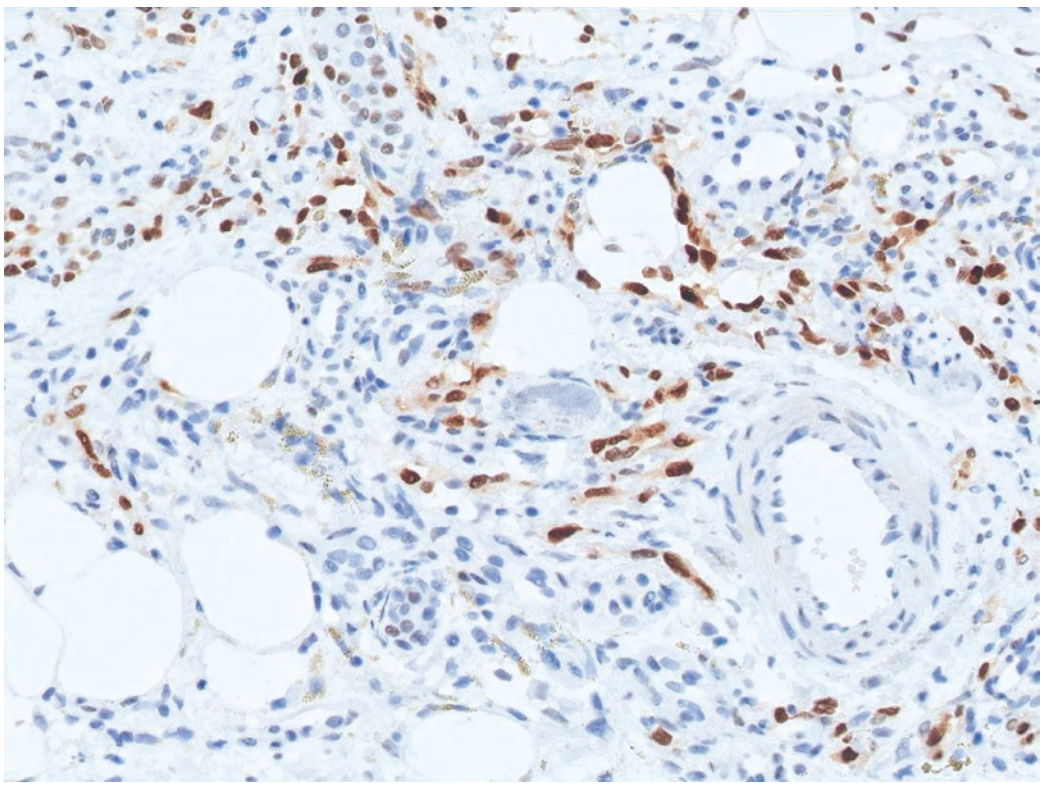

Fig. 8.38 Angiosarcoma, post-irradiation. Immunohistochemistry for c-Myc shows positive nuclear staining of the neoplastic endothelial cells. c-Myc overexpression or amplification is reported in angiosarcoma secondary to irradiation

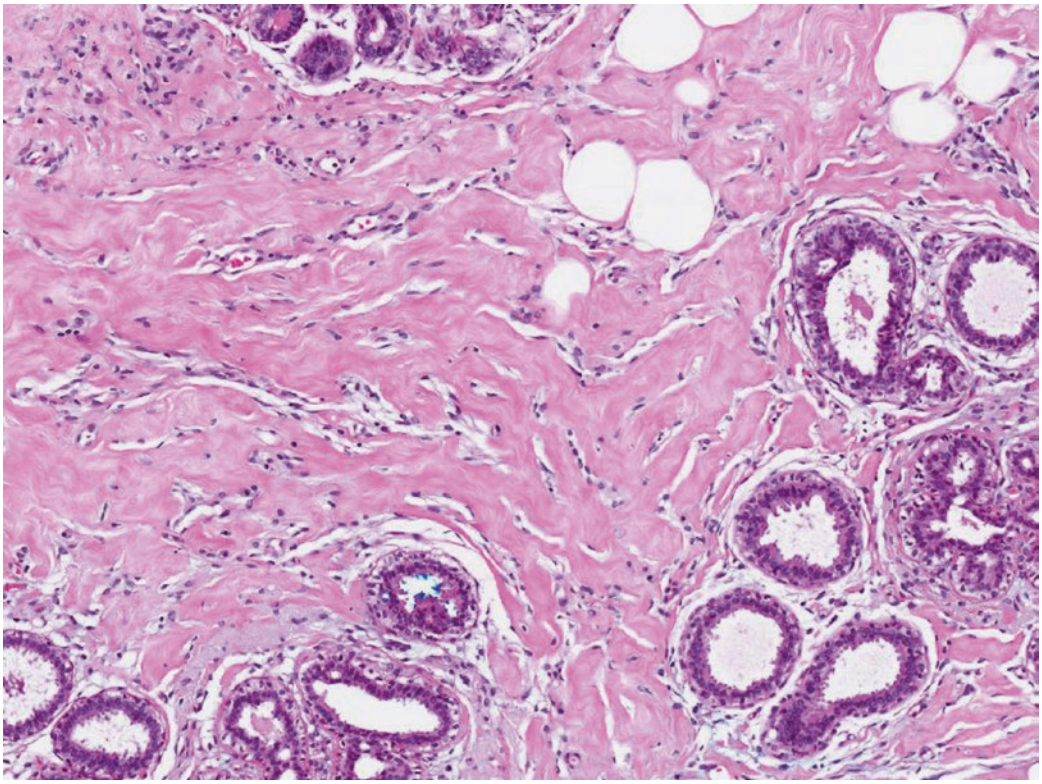

Fig. 8.39 Pseudoangiomatous stromal hyperplasia. Slit-like spaces lined by myofibroblasts with flattened nuclei are seen in the interlobular and intralobular stroma

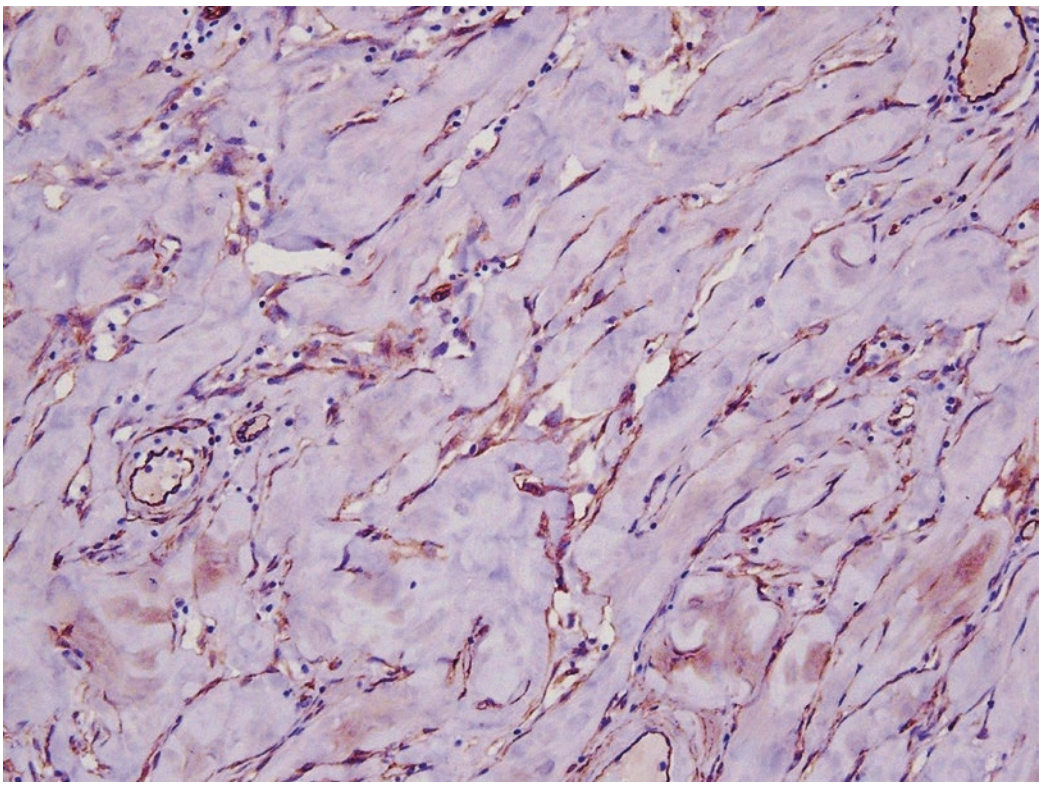

Fig. 8.40 Pseudoangiomatous stromal hyperplasia. Immunohistochemistry for CD34 shows positive reactivity of myofibroblasts that rim the slit-like spaces

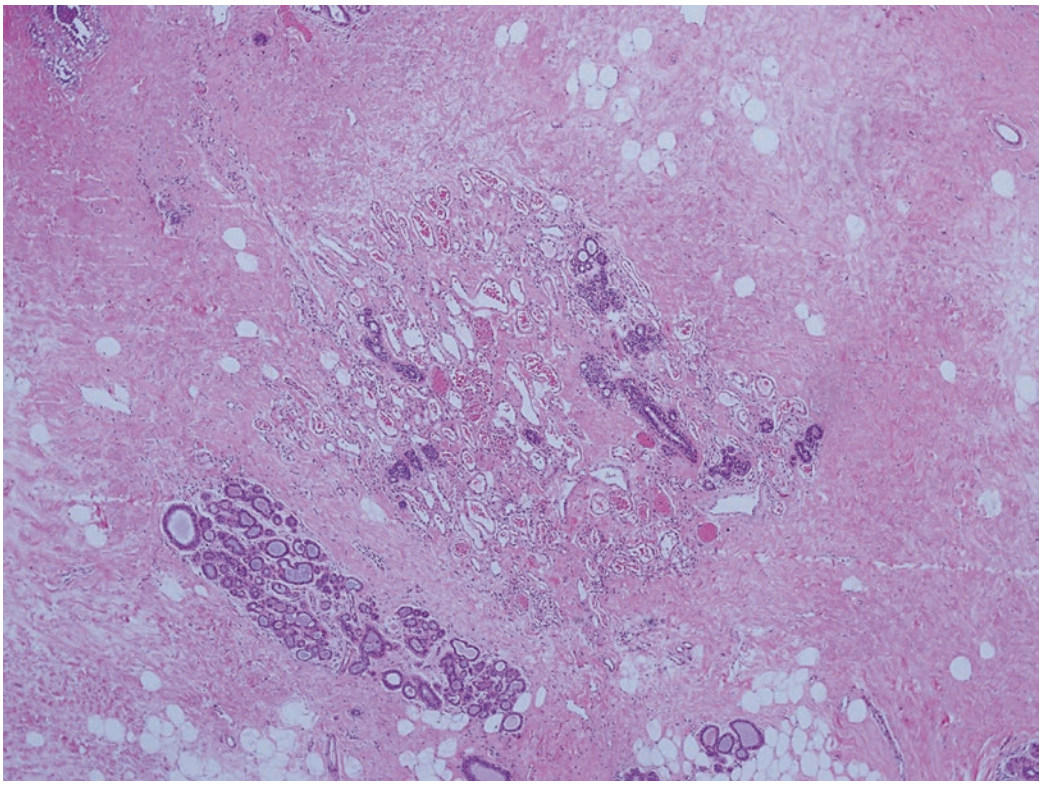

Fig. 8.41 Perilobular haemangioma. Ectatic capillaries are found within the lobular stroma. There is a relatively circumscribed outline with a few capillaries extending into the interlobular stroma. The lesion is usually microscopic and often incidental

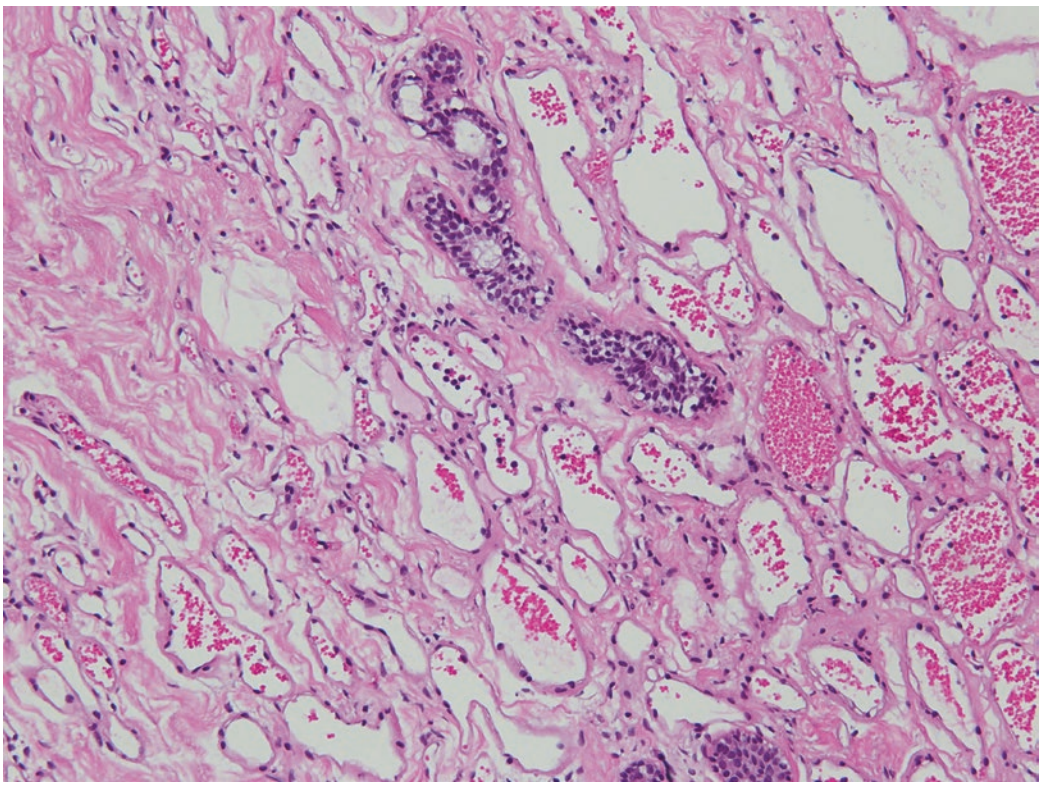

Fig. 8.42 Perilobular haemangioma. Ectatic capillaries are lined by flattened endothelial cells with luminal red blood cells. These capillaries are present between ductules within the lobule. In contrast to angiosarcoma, the perilobular haemangioma does not efface underlying structures

Angiomatosis

Also known as diffuse angioma, angiomatosis is a very uncommon lesion in the breast, comprising a proliferation of variably sized abnormal vessels in the interlobular breast stroma, without destroying or disrupting the lobules.

Atypical Vascular Lesion

This angioformative lesion develops in the skin of the breast after conservation surgery and radiotherapy for breast carcinoma. It may be a potential precursor to angiosarcoma though most are clinically indolent. The lesion occurs in the radiation field, forming geographically shaped vessels lined by plump endothelial cells. In contrast to secondary radiation-related angiosarcomas, atypical vascular lesions do not show c-Myc amplification or protein expression [6].

Kaposi Sarcoma

Kaposi sarcoma, a low-grade vascular neoplasm that expresses human herpes virus 8 (HHV8) [7], may rarely develop in the breast or skin overlying the breast. It can be limited to the breast or can occur as part of disseminated cutaneous disease [8]. Histologically, it has wide-ranging appearances, including vessels that dissect through dermal collagen accompanied by a mild inflammatory infiltrate and hyaline globules. The presence of human immunodeficiency virus (HIV), lesions elsewhere, and identification of HHV8 within the lesion support the diagnosis of Kaposi sarcoma (Fig. 8.43).

Metaplastic Carcinoma with Pseudoangiomatoid Features

The acantholytic variant of metaplastic squamous cell carcinoma with spaces between malignant cells (pseudoangiomatoid variant) may mimic angiosarcoma (Figs. 8.44, 8.45, and 8.46). In metaplastic carcinoma, the pseudoangiomatoid spaces merge with more recognisable metaplastic carcinoma areas. Immunohistochemistry for epithelial markers is helpful to confirm metaplastic carcinoma, though keratins may be expressed in epithelioid angiosarcomas [9]; p63 is reported to be observed (at least focally) in 24 % of malignant vascular lesions of the breast [10].

Prognosis and Therapy Considerations

Although grade was described as being non-prognostic in a large series of breast angiosarcomas, with low-grade lesions also capable of metastasising [11], recent studies indicate the utility of grade and histological parameters in prognostication [12, 13]. Metastases usually occur to the lungs, skin, bone, and liver; the lymph nodes are infrequently affected.

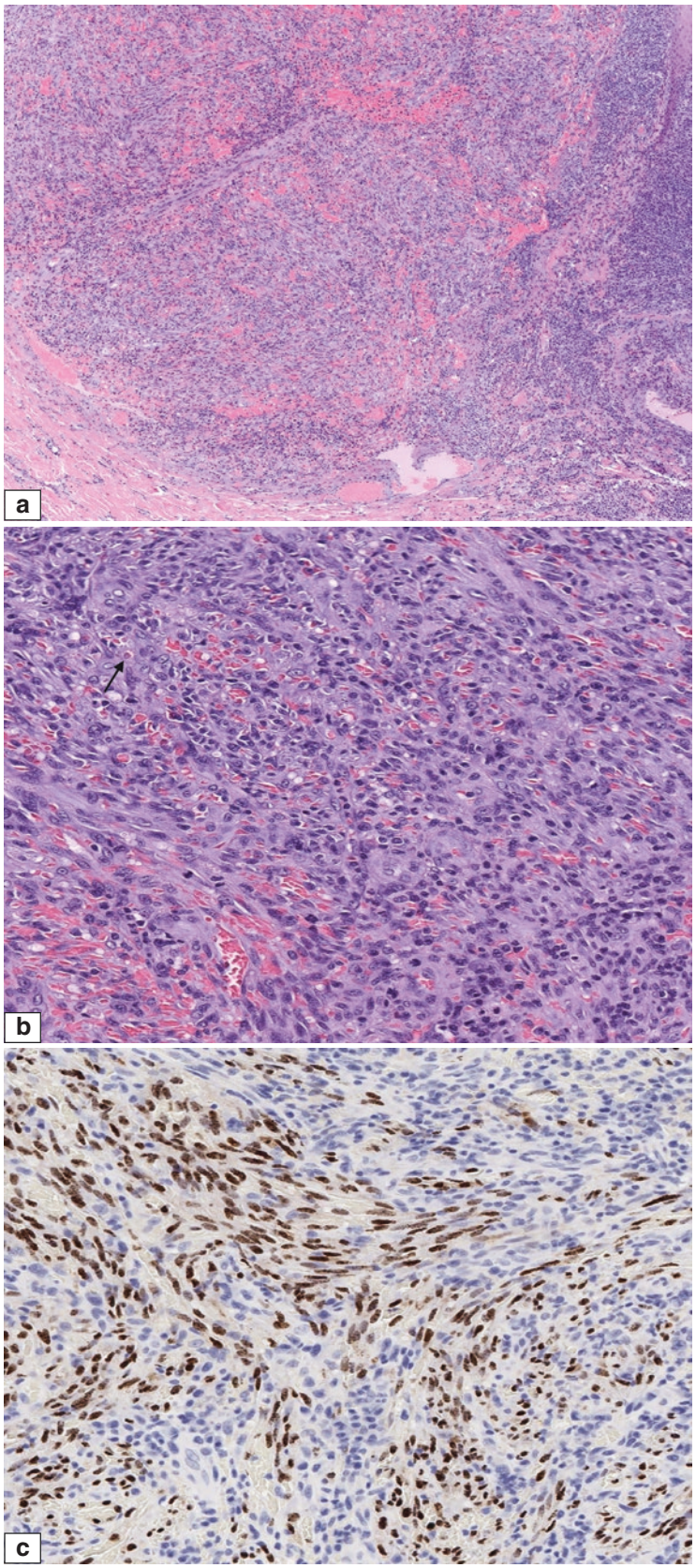

Fig. 8.43 Kaposi sarcoma. (**a**) A cellular spindle cell lesion is present on the chest wall. Small pools of blood are seen among the spindle cells. (**b**) Red blood cells are seen in the slit-like spaces among plump spindle cells that contain ovoid-to-elongated vesicular nuclei, with inconspicuous nucleoli and occasional mitoses. A rare hyaline globule is seen (*arrow*). (**c**) Immunohistochemistry shows positive nuclear staining for human herpesvirus 8 (HHV8), which is present in almost all Kaposi sarcoma lesions

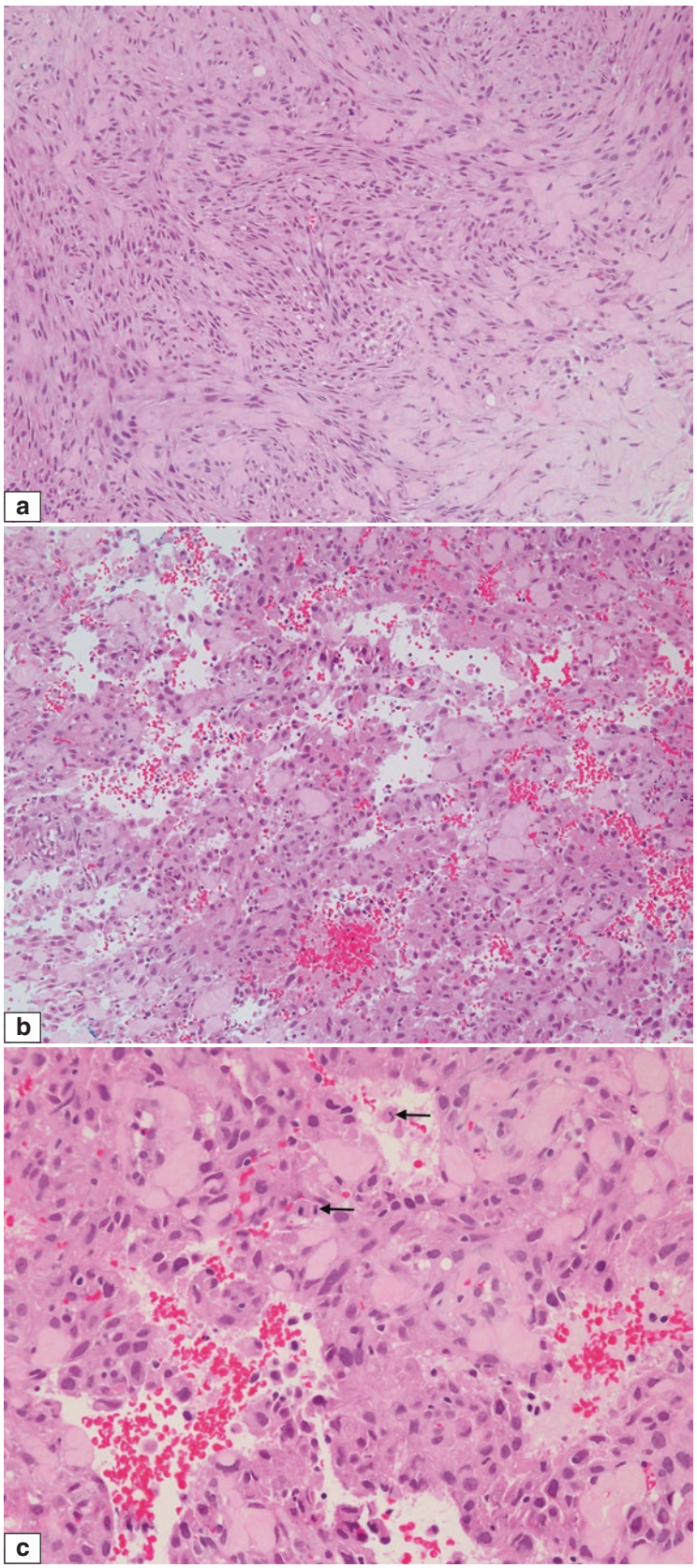

Fig. 8.44 Spindle cell metaplastic carcinoma with pseudoangiomatoid features. (**a**) Intersecting fascicles of spindle cells show pleomorphic, hyperchromatic nuclei. Pseudoangiomatoid features are not well appreciated here, although there are several small spaces among the spindle cells that contain occasional red blood cells. (**b**) In this section, the spaces are better visualised, with separation of more epithelioid tumour cells giving the appearance of pseudovascular spaces containing extravasated red blood cells. (**c**) Higher magnification shows blood-filled spaces among epithelioid tumour cells with pleomorphic nuclei and scattered mitoses (*arrows*)

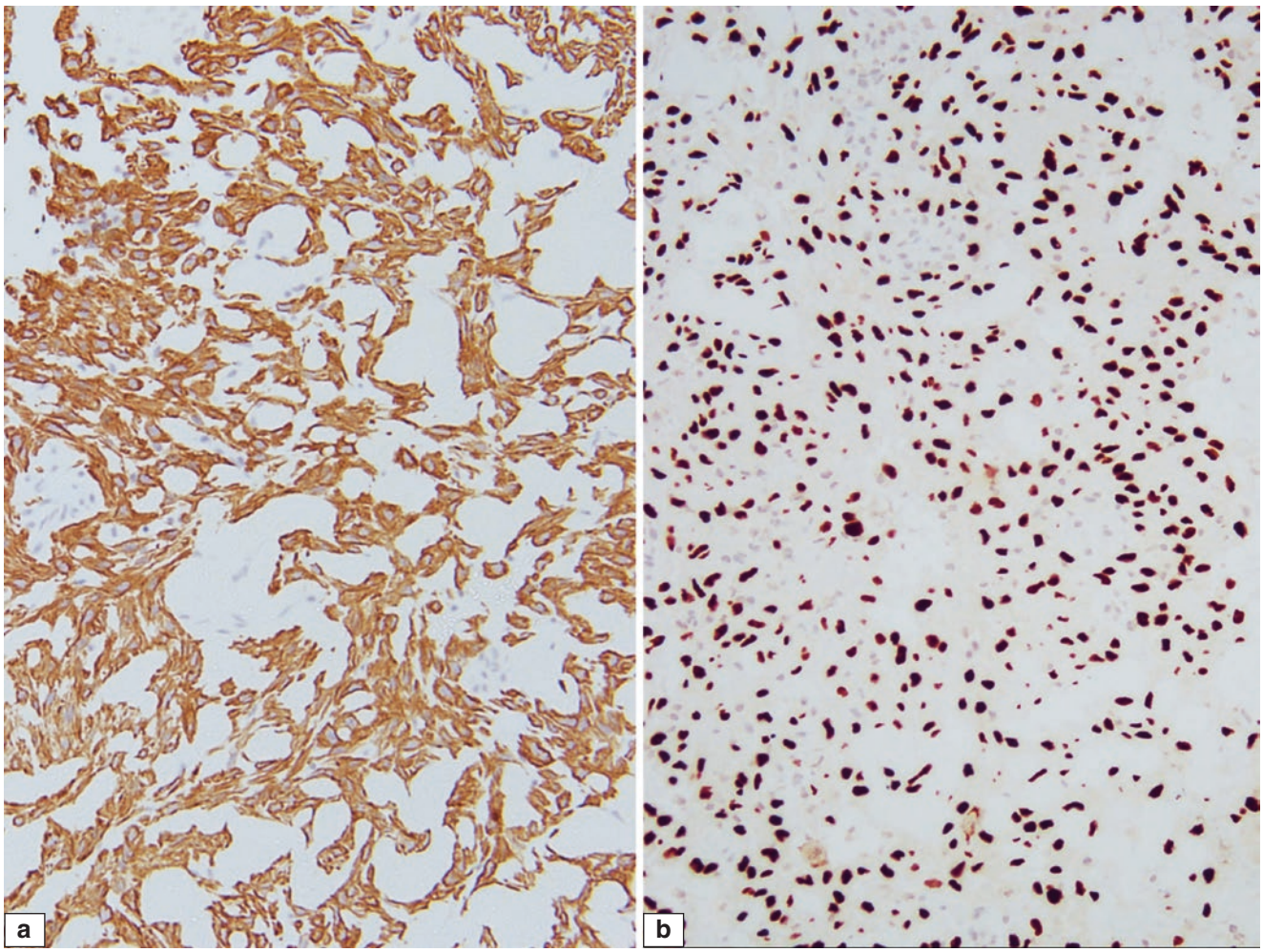

Fig. 8.45 Spindle cell metaplastic carcinoma with pseudoangiomatoid features. Immunohistochemistry shows diffuse positive staining of epithelioid and spindle tumour cells for CK14 (**a**) and p63 (**b**), indicating an epithelial origin. Endothelial cell markers were negative

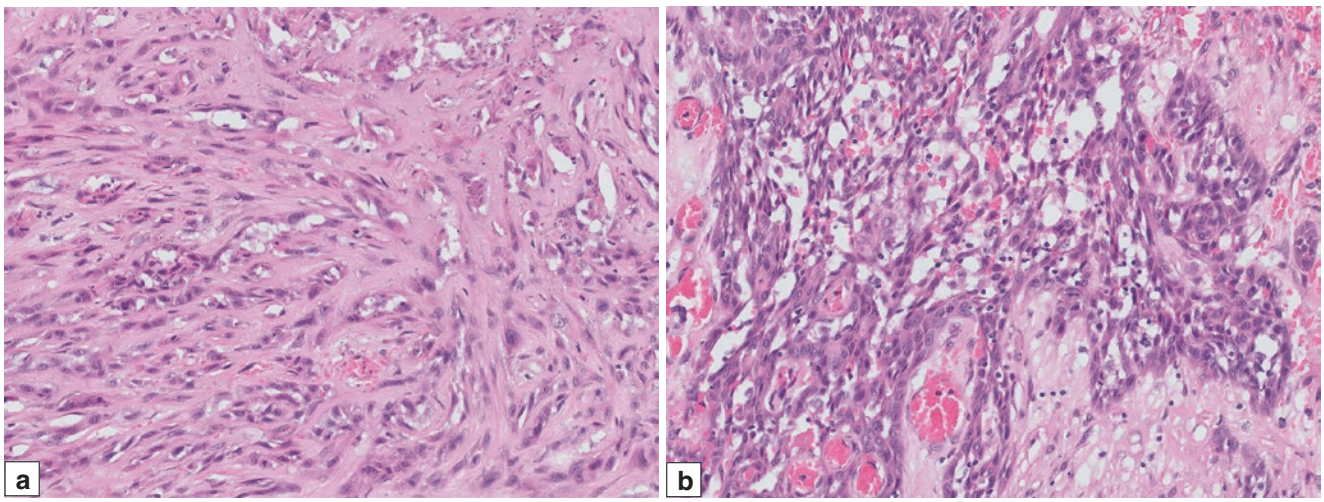

Fig. 8.46 Spindle cell metaplastic carcinoma with pseudoangiomatoid features. (**a**) Tumour shows spindle cells with variably sized nuclei and several spaces resembling vascular lumens. A few epithelioid as well as more nested groups of cells are noted. (**b**) Here, the tumour forms a cohesive aggregate of abnormal cells separated by an untidy meshwork of irregular spaces, some of which contain red blood cells. While the spaces give a pseudovascular appearance, the sharp and well defined interphase of the island of abnormal cells with the stroma suggests their epithelial nature. (**c**) Immunohistochemistry for CK14 confirms the epithelial nature of the invasive tumour, with permeative, anastomosing and tight aggregates of malignant cells. (d) At higher magnification, several spaces can be observed among the CK14 immunoreactive tumour cells that resembled vascular spaces on H&E microscopy

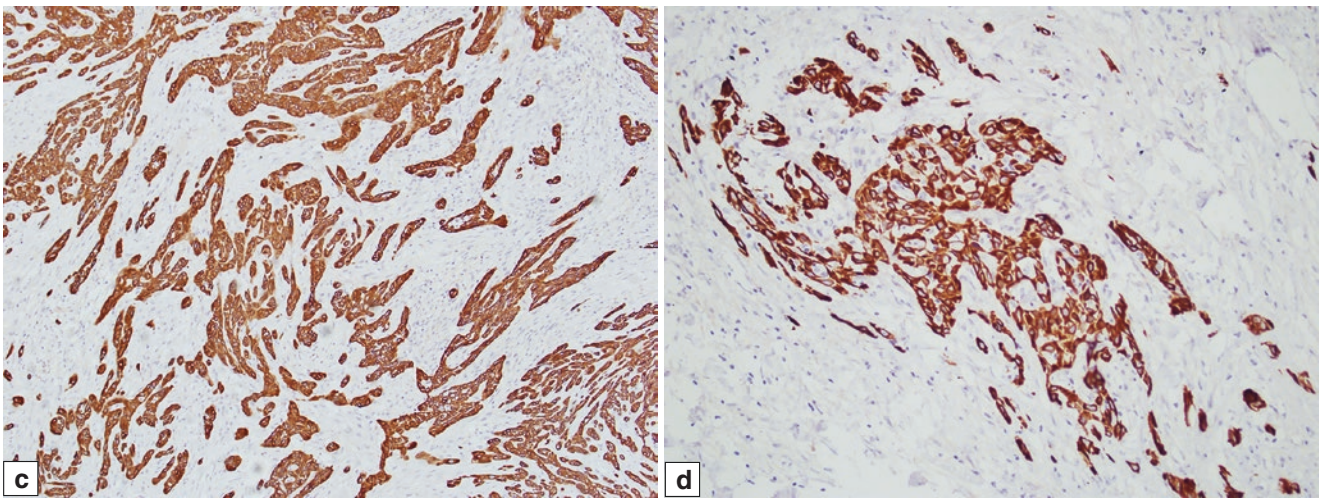

Fig. 8.46 (continued)

References

1. Guo T, Zhang L, Chang NE, Singer S, Maki RG, Antonescu CR. Consistent MYC and FLT4 gene amplification in radiation-induced angiosarcoma but not in other radiation-associated atypical vascular lesions. Genes Chromosomes Cancer. 2011;50:25–33.
2. Fletcher CDM, McGrogan G, Fox SB. Angiosarcoma. In: Lakhani SR, Ellis IO, Schnitt SJ, Tan PH, van de Vijver MJ, editors. WHO classification of tumours of the breast. Lyon: IARC Press; 2012. p. 135–46.
3. Liberman L, Dershaw DD, Kaufman RJ, Rosen PP. Angiosarcoma of the breast. Radiology. 1992;183:649–54.
4. Goh LW, Wong SL, Tan PH. Four cases of echogenic breast lesions: a case series and review. Singapore Med J. 2016;57:339–43.
5. Yang WT, Hennessy BT, Dryden MJ, Valero V, Hunt KK, Krishnamurthy S. Mammary angiosarcomas: imaging findings in 24 patients. Radiology. 2007;242:725–34.
6. Fraga-Guedes C, André S, Mastropasqua MG, Botteri E, Toesca A, Rocha RM, et al. Angiosarcoma and atypical vascular lesions of the breast: diagnostic and prognostic role of *MYC* gene amplification and protein expression. Breast Cancer Res Treat. 2015;151:131–40.
7. Patel RM, Goldblum JR, Hsi ED. Immunohistochemical detection of human herpes virus-8 latent nuclear antigen-1 is useful in the diagnosis of Kaposi sarcoma. Mod Pathol. 2004;17:456–60.
8. Pantanowitz L, Dezube BJ. Kaposi sarcoma in unusual locations. BMC Cancer. 2008;8:190.
9. Rao P, Lahat G, Arnold C, Gavino AC, Lahat S, Hornick JL, et al. Angiosarcoma: a tissue microarray study with diagnostic implications. Am J Dermatopathol. 2013;35:432–7.
10. Kallen ME, Nunes Rosado FG, Gonzalez AL, Sanders ME, Cates JM. Occasional staining for p63 in malignant vascular tumors: a potential diagnostic pitfall. Pathol Oncol Res. 2012;18:97–100.
11. Nascimento AF, Raut CP, Fletcher CD. Primary angiosarcoma of the breast: clinicopathologic analysis of 49 cases, suggesting that grade is not prognostic. Am J Surg Pathol. 2008;32:1896–904.
12. Ghareeb ER, Bhargava R, Vargo JA, Florea AV, Beriwal S. Primary and radiation-induced breast angiosarcoma: clinicopathologic predictors of outcomes and the impact of adjuvant radiation therapy. Am J Clin Oncol. 2016;39:463–7.
13. Pandey M, Sutton GR, Giri S, Martin MG. Grade and prognosis in localized primary angiosarcoma. Clin Breast Cancer. 2015;15:266–9.

Intraductal Proliferative Lesions

9

Intraductal proliferative epithelial lesions are a heterogeneous group that have in common an epithelial proliferation within the terminal ductal lobular unit of the breast. They affect women over a broad age range and are associated with varying risks of subsequent breast cancer. Some lesions, such as ductal carcinoma in situ (DCIS), may be direct but non-obligate precursors to invasive carcinoma.

Usual Ductal Hyperplasia

Definition

In usual ductal hyperplasia (UDH), epithelial cells proliferate to fill the duct space (Fig. 9.1). UDH is also referred to as usual epithelial hyperplasia, intraductal hyperplasia, epitheliosis, hyperplasia of usual type, and hyperplasia without atypia.

Fig. 9.1 Breast duct cut in a transverse section shows a bilayered epithelial lining, with luminal epithelial cells rimmed by an outer myoepithelial layer. The myoepithelial cells here have a slightly myoid appearance with plump pink cytoplasm

P.H. Tan, A.A. Sahin, *Atlas of Differential Diagnosis in Breast Pathology*, Atlas of Anatomic Pathology,
DOI 10.1007/978-1-4939-6697-4_9

Clinical and Epidemiological Features

UDH associated with cysts and fibrosis may present as breast lumpiness.

Imaging Features

UDH does not have a characteristic radiological picture. Clustered amorphous, punctate, or pleomorphic microcalcifications can occur on mammography and can be mixed with or indistinguishable from microcalcifications of low-grade DCIS, atypical ductal hyperplasia, and other benign processes. On sonography, the appearance is diverse, ranging from well-defined lesions to indeterminate, ill-defined masses depending on the associated lesions.

Pathologic Features

Macroscopic Pathology

As UDH is a microscopic finding, there is no specific macroscopic abnormality unless the UDH occurs within an underlying lesion such as a cyst, radial scar, or papilloma.

Microscopic Pathology

Mild UDH shows three to four layers of epithelial cells lining the walls of ducts. The epithelial cells project into the duct lumens without anastomosis, bridging, or fusion of the epithelial tufts. The inner lining of the duct has a ruffled appearance due to irregular protrusions of the hyperplastic epithelial cells (Fig. 9.2). In moderate UDH, epithelial cells exceed four layers and efface part of the duct lumen. Epithelial nuclei are crowded and overlapped, with ovoid-to-elongated shapes. Irregular, slit-like spaces may be observed, particularly at the periphery of the epithelial proliferation (Figs. 9.3, 9.4, and 9.5). Florid or marked UDH shows an exaggerated appearance of epithelial proliferation obscuring the duct lumen, sometimes filling the lumen completely. Nuclei are overlapped and have a streaming pattern. Nuclear grooves, pseudoinclusions, occasional mitoses, and even necrosis can be seen (Figs. 9.6, 9.7, and 9.8).

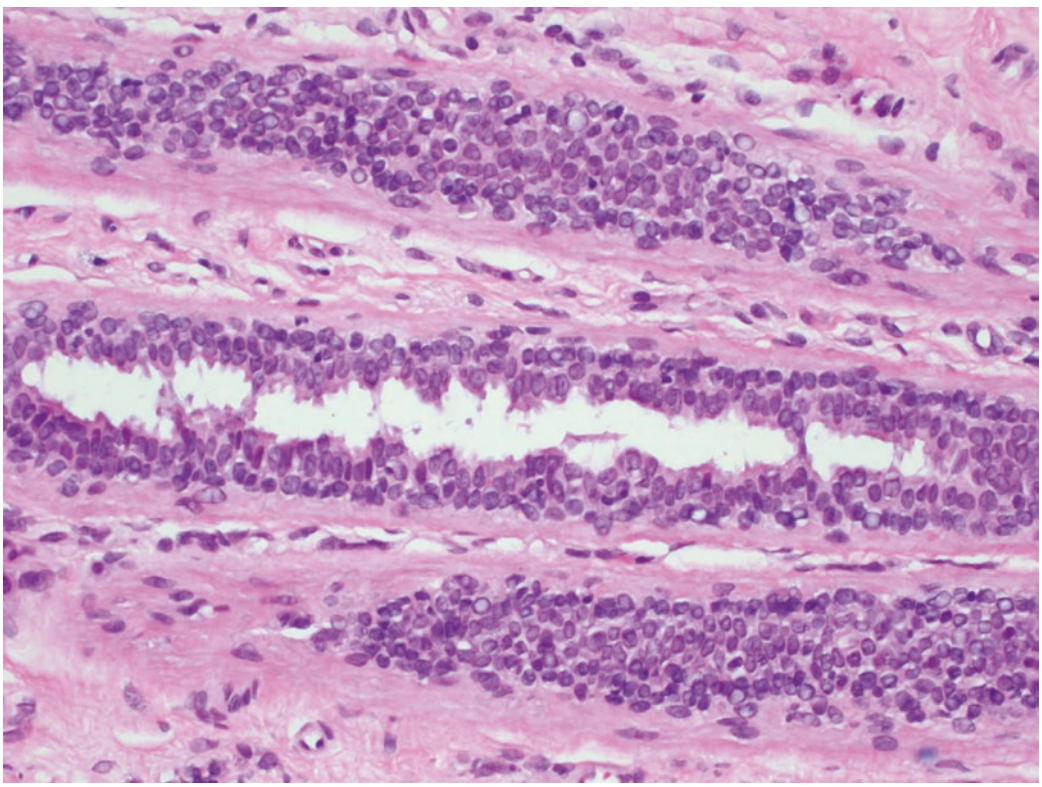

Fig. 9.2 Usual ductal hyperplasia (UDH) of a mild degree, showing three to four layers of epithelial cells lining the duct wall, with a ruffled luminal contour

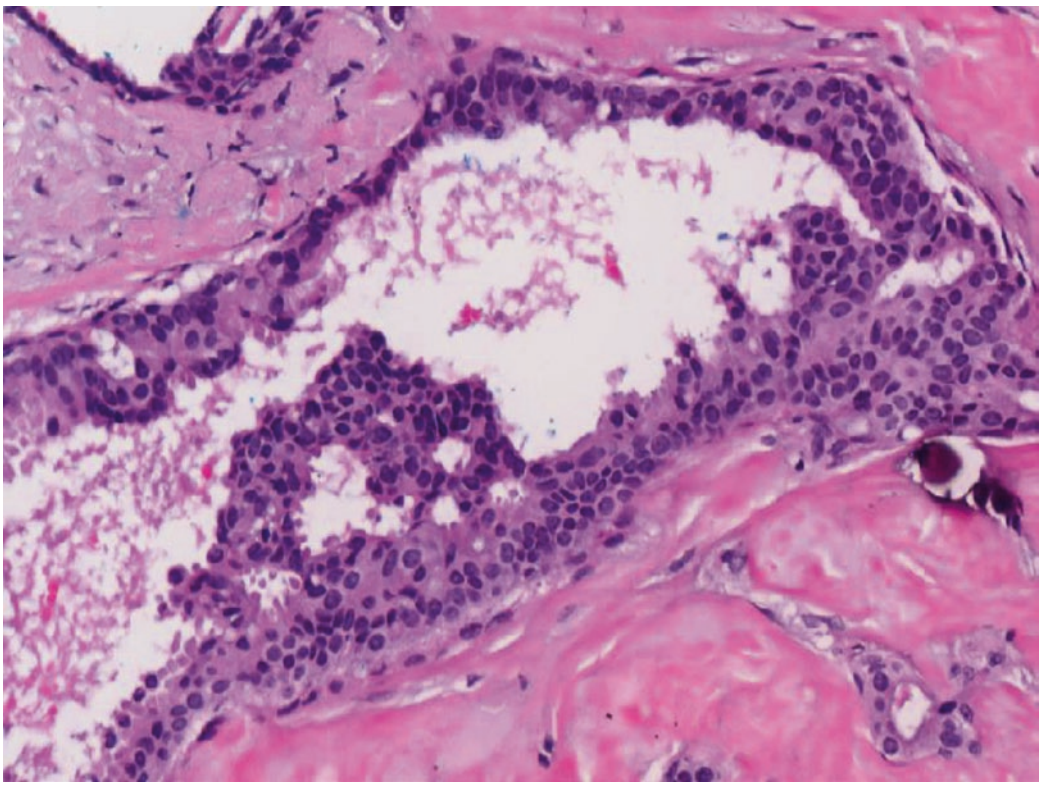

Fig. 9.3 Moderate UDH. Epithelial cells pile and anastomose, forming secondary luminal spaces that have ruffled borders. Epithelial nuclei are crowded and heterogeneous. A stromal calcification is seen adjacent to the duct

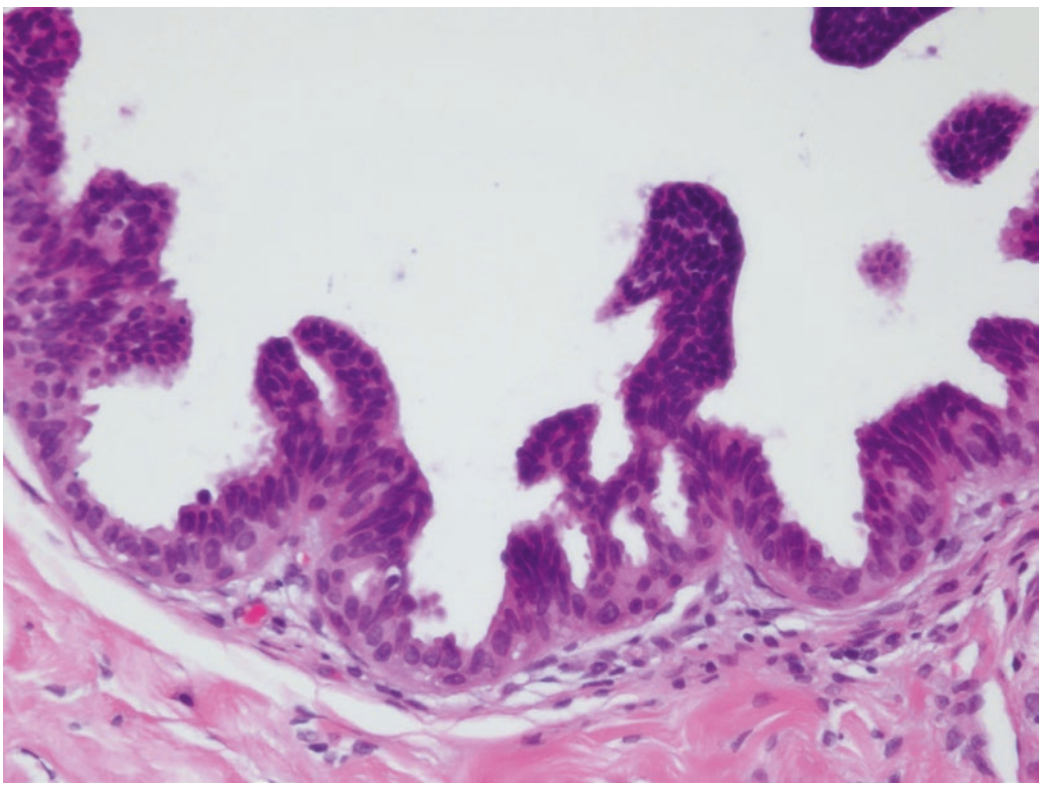

Fig. 9.4 Moderate UDH. The epithelial cells proliferate to form protrusions into the duct lumen, without traversing or effacing the lumen. A differential diagnosis is atypical ductal hyperplasia, but the epithelial tufts are non-rigid, with epithelial nuclei that appear heterogeneous and overlapping. Luminal spaces have gentle contours

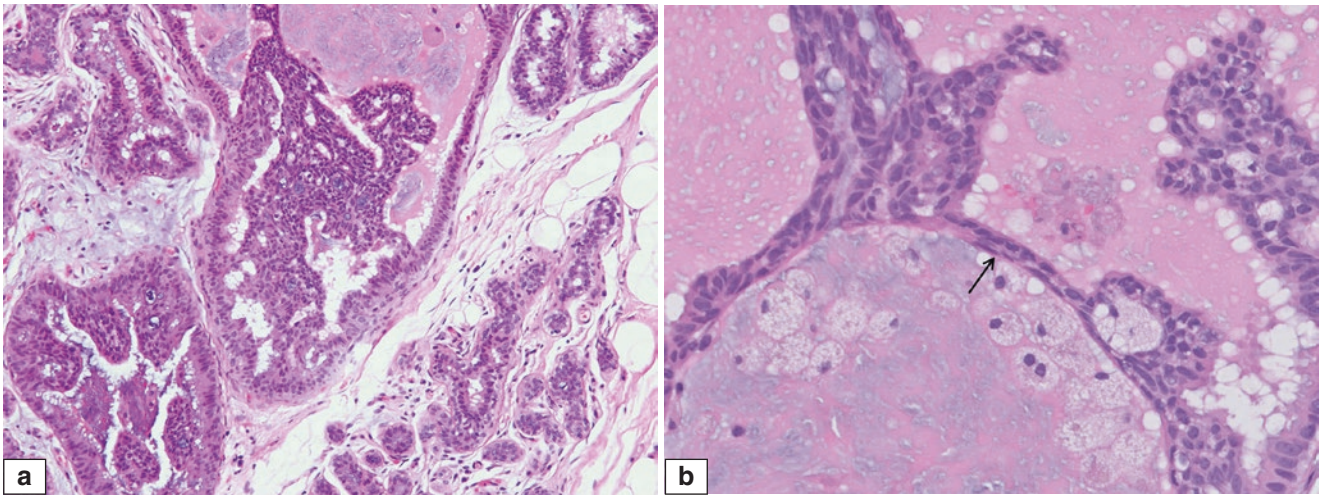

Fig. 9.5 Moderate UDH. (**a**) Proliferating epithelial cells protrude into duct lumens, forming soft arches that feature nuclei oriented in parallel to the direction of the arches. Secondary luminal spaces are variably sized and slit-like. (**b**) High magnification shows crowded and overlapped epithelial nuclei, with those along the arches being oriented parallel to the direction of the arch (*arrow*)

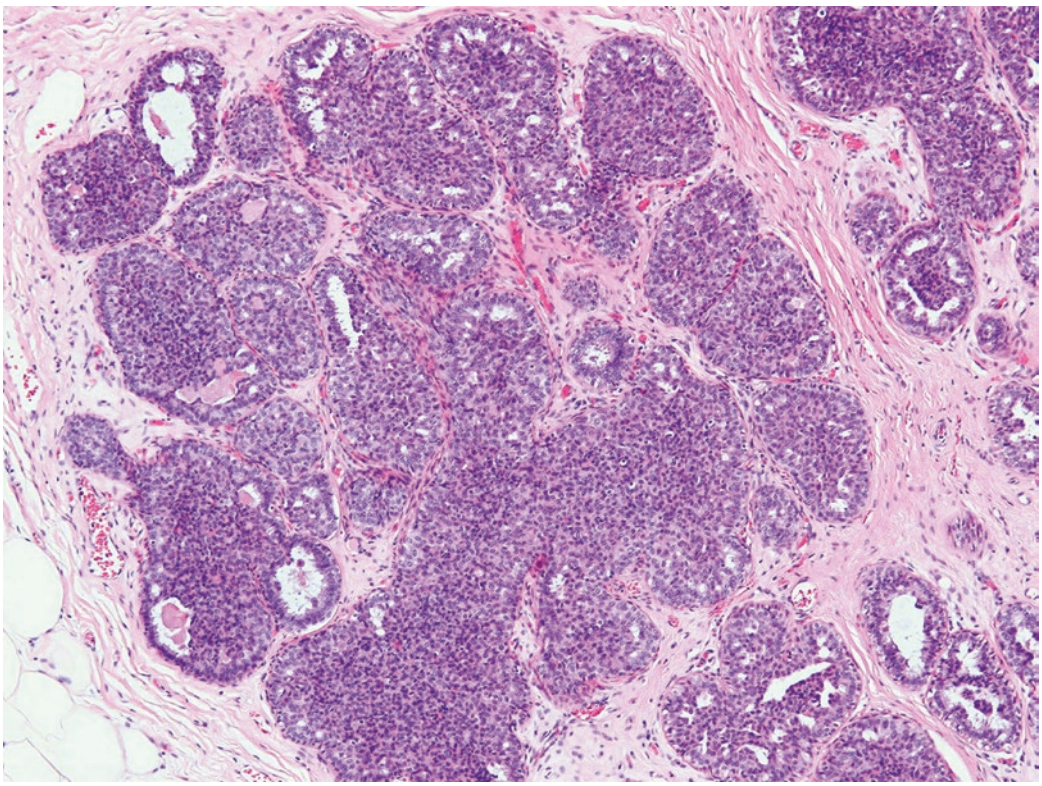

Fig. 9.6 Usual ductal hyperplasia. A lobule shows UDH of varying degrees, with a predominance of florid UDH, where crowded epithelial cells efface the ductular lumens

Differential Diagnosis

UDH Versus Atypical Ductal Hyperplasia/Low-Grade Ductal Carcinoma In Situ

UDH shows a heterogeneous epithelial population with uneven nuclear placement and overlapping. Spaces are irregular, rimmed by swirling epithelial nuclei with their longitudinal axes aligned around the spaces. Atypical ductal hyperplasia (ADH) and low nuclear grade DCIS, on the other hand, show areas of cytoarchitectural atypia, with clonality as evidenced by the uniform cell population within a rigid architectural framework, where well-defined cribriform spaces and rigid micropapillae are present. Immunohistochemistry for CK5/6, CK14, and oestrogen receptor (ER) can help

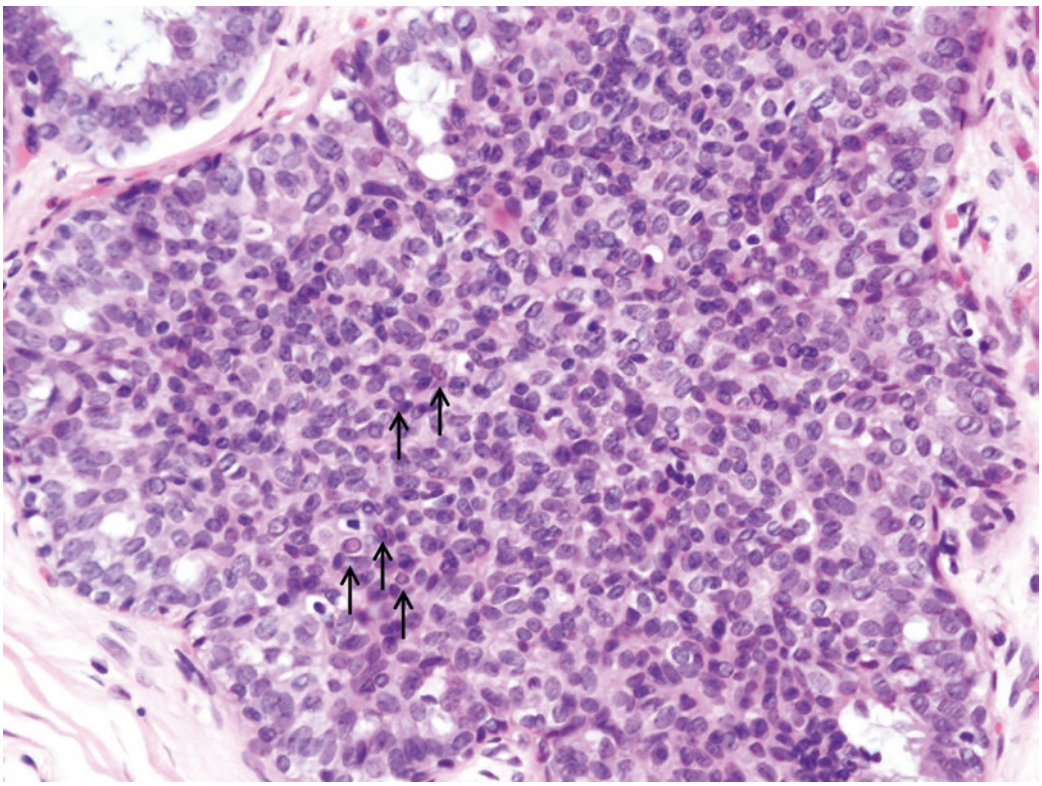

Fig. 9.7 Florid UDH with a heterogeneous population of epithelial cells filling the duct space, containing haphazardly placed nuclei that are overlapping. Irregular spaces are seen towards the periphery of the duct. Intranuclear inclusions (*arrows*) are present

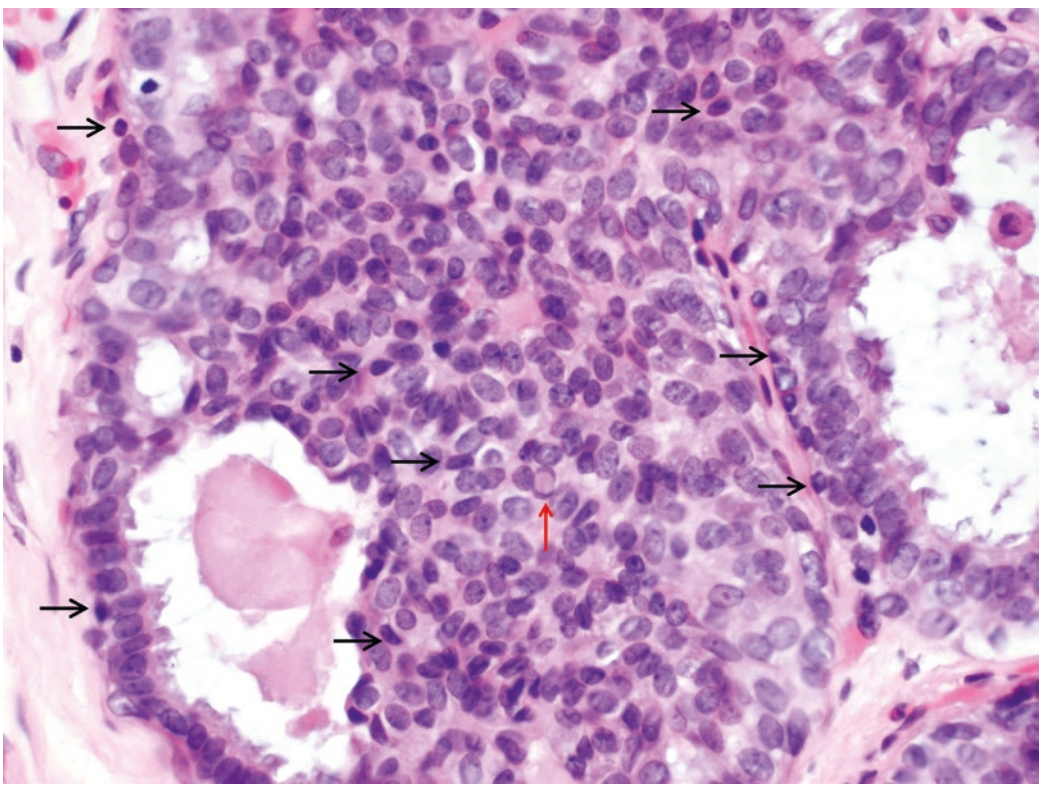

Fig. 9.8 Usual ductal hyperplasia. Darker, ovoid myoepithelial nuclei are seen at the periphery of the duct and are also occasionally discerned among the proliferative epithelial cells (*black arrows* indicate some representative myoepithelial nuclei). An intranuclear inclusion (*red arrow*) is seen

distinguish UDH from ADH and low nuclear grade DCIS, with CK5/6 and CK14 demonstrating a heterogeneous cell population with mosaic-like staining pattern for UDH, compared with diminished to absent reactivity in ADH and low nuclear grade DCIS. Similarly, ER is patchily reactive with variable nuclear immunostaining intensity in UDH, whereas it is diffusely and strongly positive in ADH and low nuclear grade DCIS (Figs. 9.9, 9.10, 9.11, 9.12, 9.13, 9.14, and 9.15).

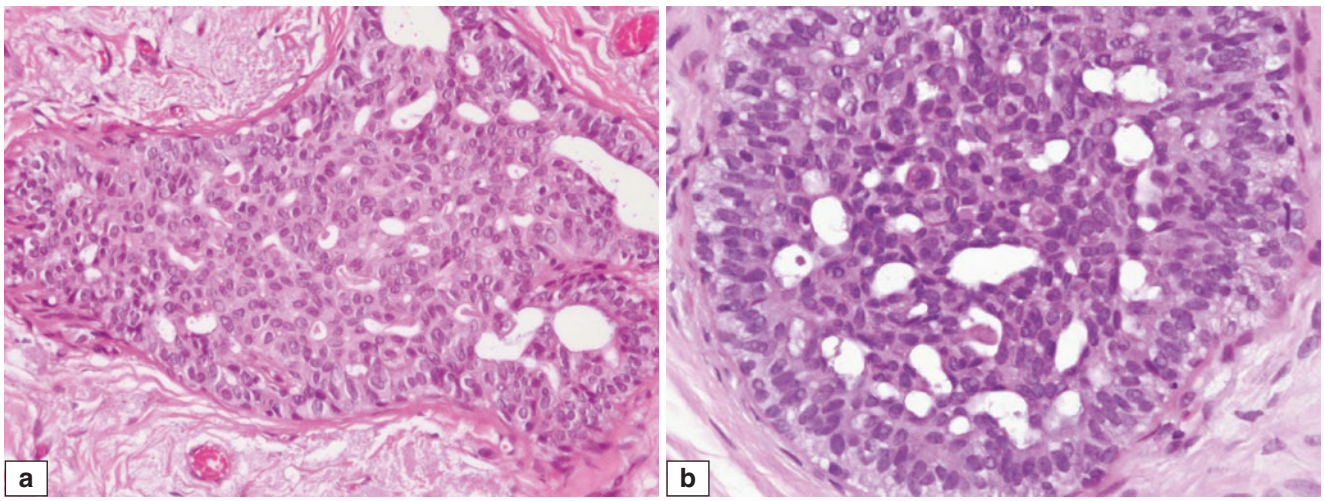

Fig. 9.9 Florid UDH. (**a**) The duct space is filled with epithelial cells featuring crowded, overlapping, vesicular, ovoid-to-elongated nuclei with occasional grooves, with interspersed irregular, slit-like spaces. Longitudinal axes of epithelial nuclei tend to align around and parallel to luminal spaces. (**b**) High magnification shows a heterogeneous epithelial population with crowded and overlapping nuclei. The irregular slit-like spaces are lined by epithelial cells with nuclei that have their longitudinal axes oriented in parallel to the spaces

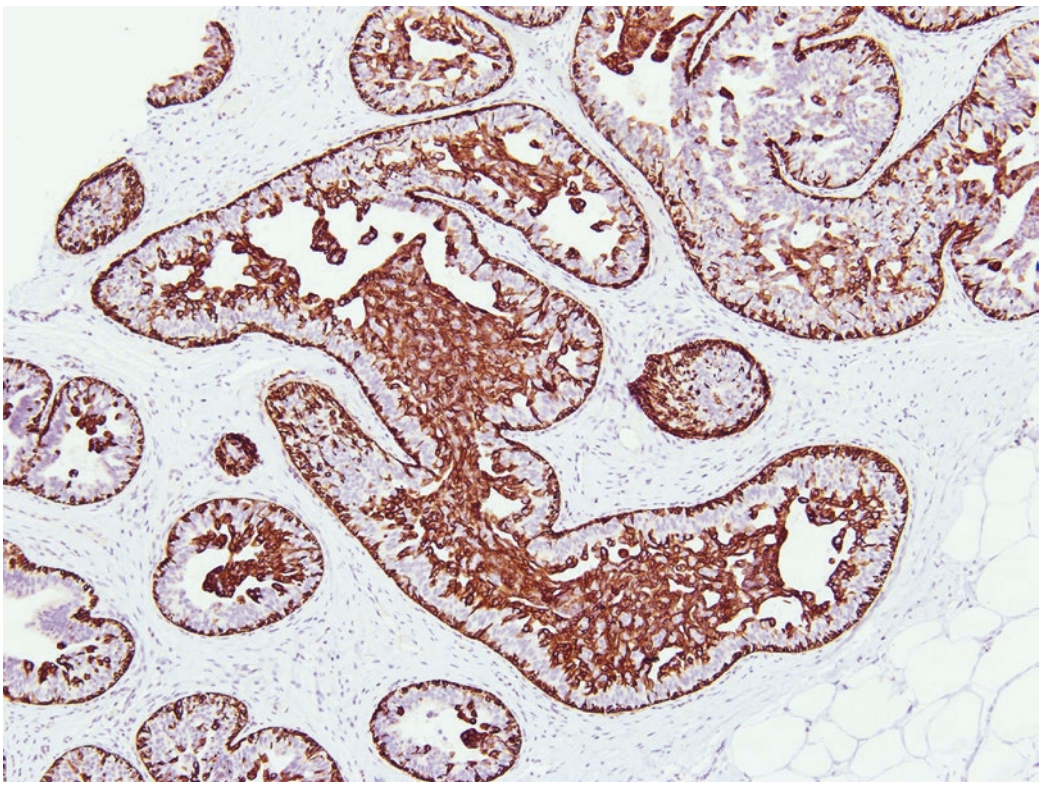

Fig. 9.10 Usual ductal hyperplasia. Immunohistochemistry for CK14 shows mosaic-like positivity of epithelial cells in UDH. Peripheral myoepithelial cells are also decorated

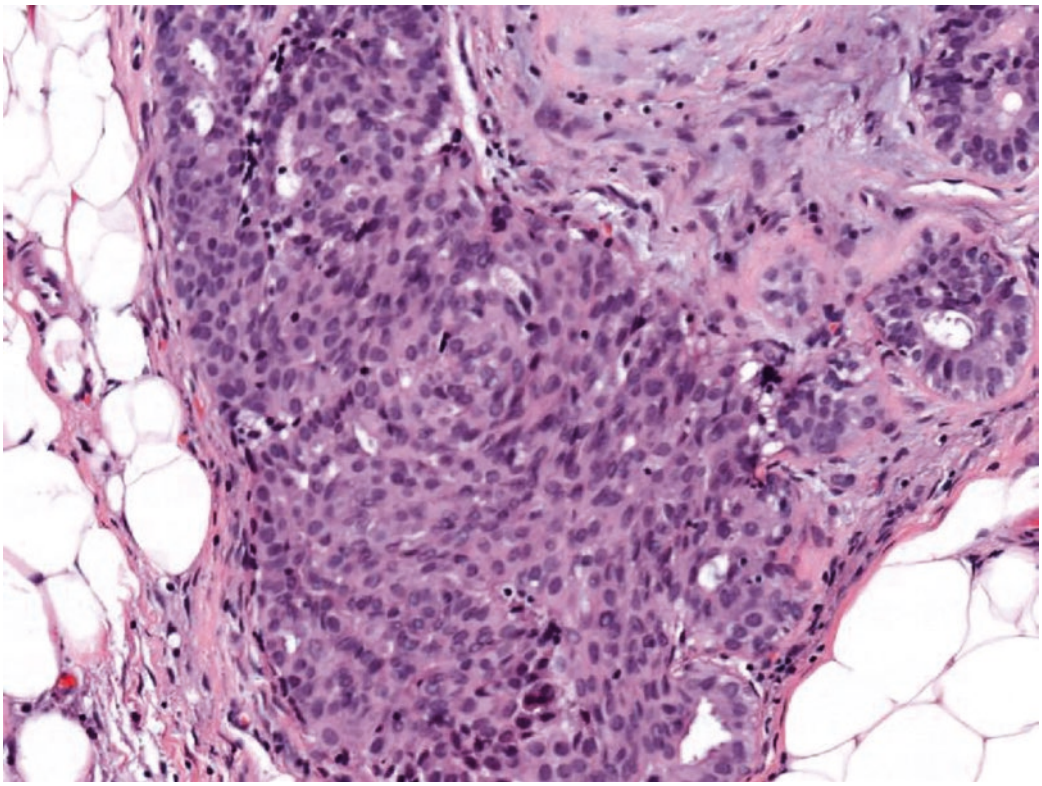

Fig. 9.11 Florid UDH. A duct is filled with a proliferation of epithelial cells with streaming nuclei, which show overlapping and crowding. A few slit-like spaces are present. The cell population is heterogeneous, with variable nuclear sizes

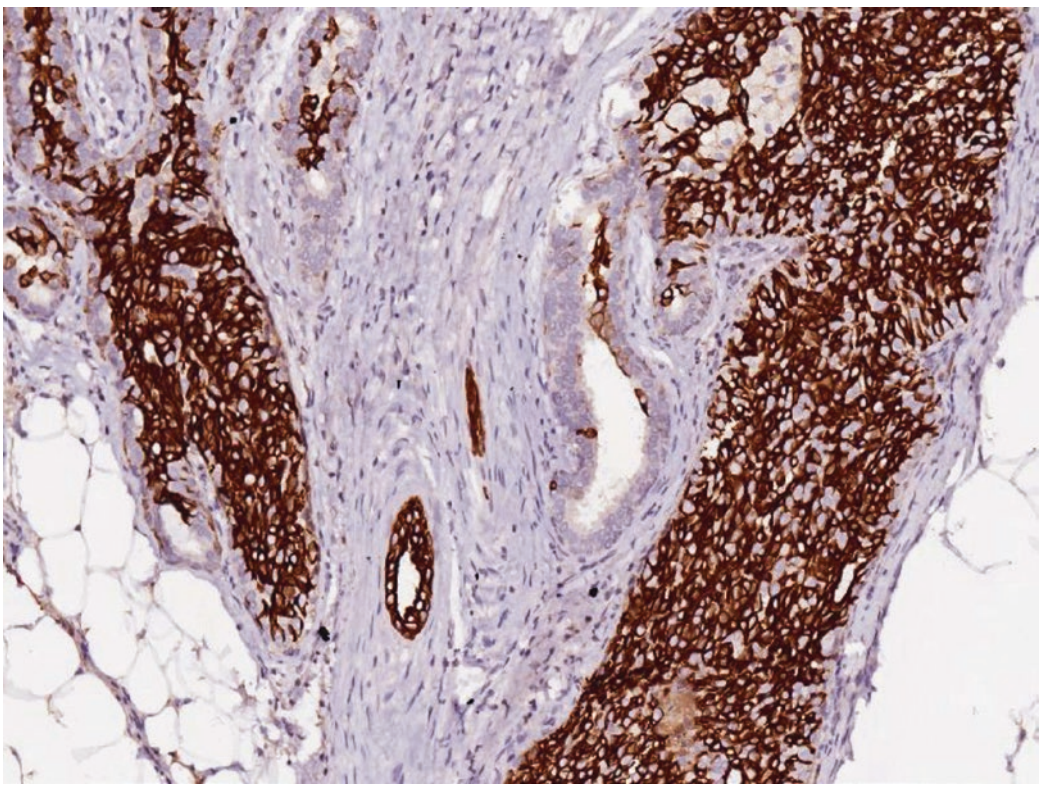

Fig. 9.12 Florid UDH. CK5/6 immunohistochemistry shows a mosaic pattern of epithelial cell staining in ducts with UDH

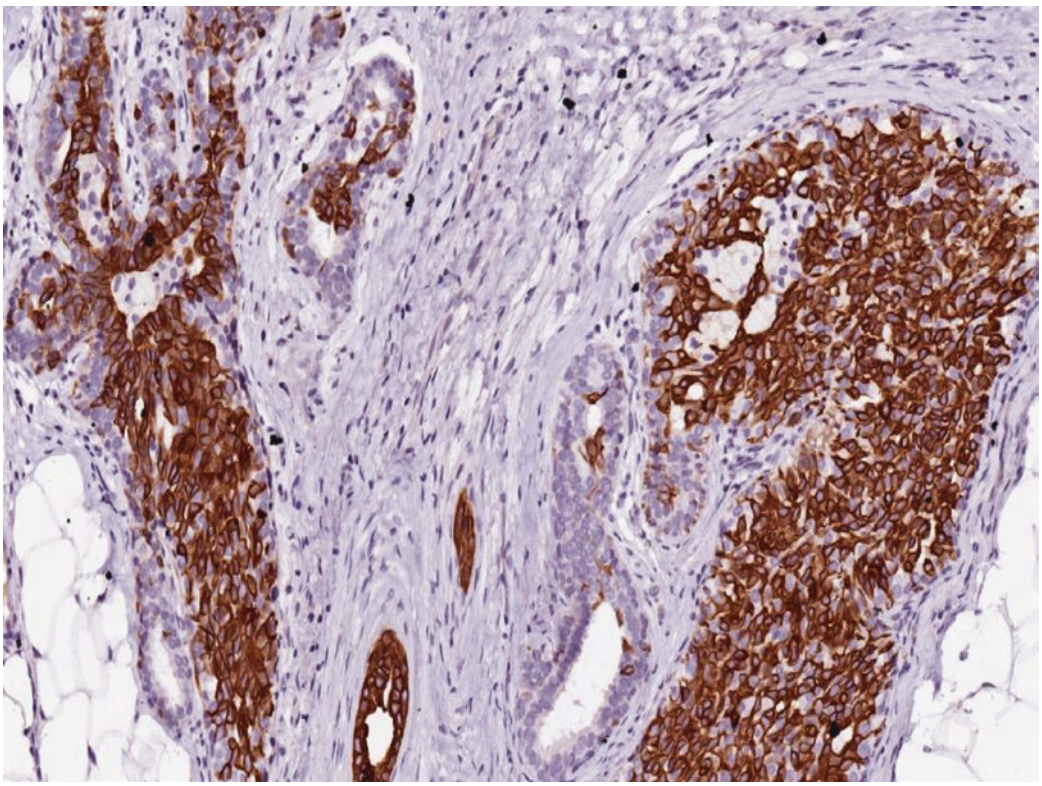

Fig. 9.13 Florid UDH. CK14 immunohistochemistry shows a mosaic pattern of epithelial cell staining in ducts with UDH. CK5/6 and CK14 staining patterns are usually similar, although sometimes antibody sensitivities may vary. A panel approach is recommended when immunohistochemistry is applied, using antibodies that the laboratory has validated and is familiar with

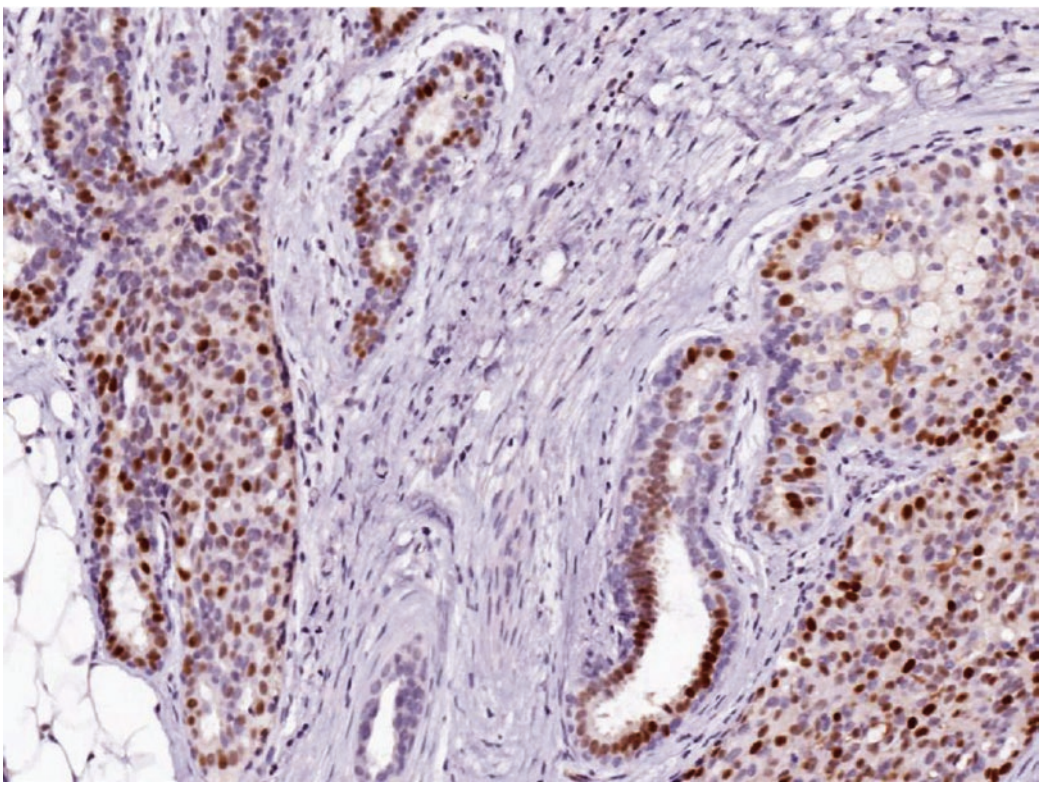

Fig. 9.14 Florid UDH. ER immunohistochemistry shows a non-diffuse, patchy pattern of epithelial nuclear staining in ducts with UDH. Note that the staining intensity also varies, with a range of intensities from weak to strong

UDH Versus Intermediate Nuclear Grade DCIS

Sometimes, the heterogeneous appearance of epithelial cells with reactive nuclear atypia in moderate and florid UDH may mimic intermediate nuclear grade DCIS (Figs. 9.16 and 9.17). The presence of mitoses and necrosis which may be encountered in UDH may exacerbate the differential diagnostic challenge. Clues to a benign diagnosis are the epithelial nuclear features of UDH, with vesicularity and smooth nuclear contours without clumpy chromatin or prominent nucleoli. These epithelial cells are often admixed with ovoid, darker myoepithelial cells. The haphazard overlapping placement with slit-like spaces and supportive immunohistochemistry allow a correct diagnosis.

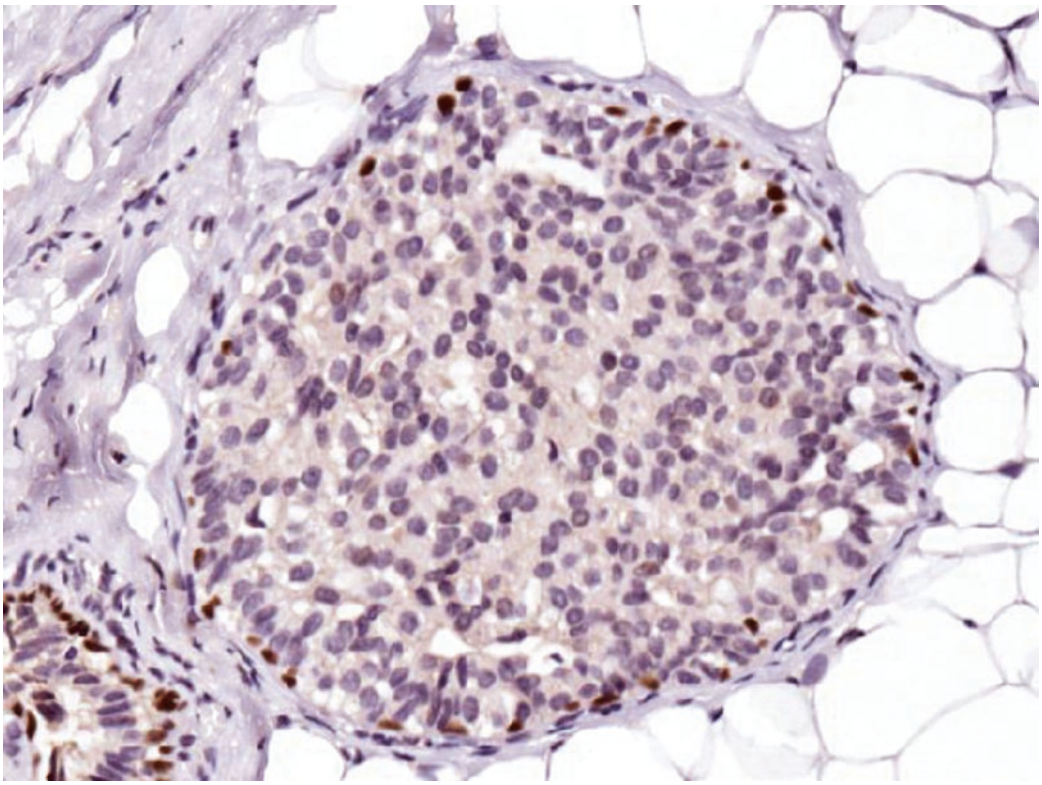

Fig. 9.15 Florid UDH. Immunohistochemistry for p63 highlights peripheral myoepithelial cells, but it does not demonstrate the mosaic pattern of staining depicted with antibodies to high-molecular-weight keratins (CK5/6 and CK14) observed in UDH. Hence, p63 is less useful in differentiating UDH from atypical ductal hyperplasia (ADH) and low-grade ductal carcinoma in situ (DCIS)

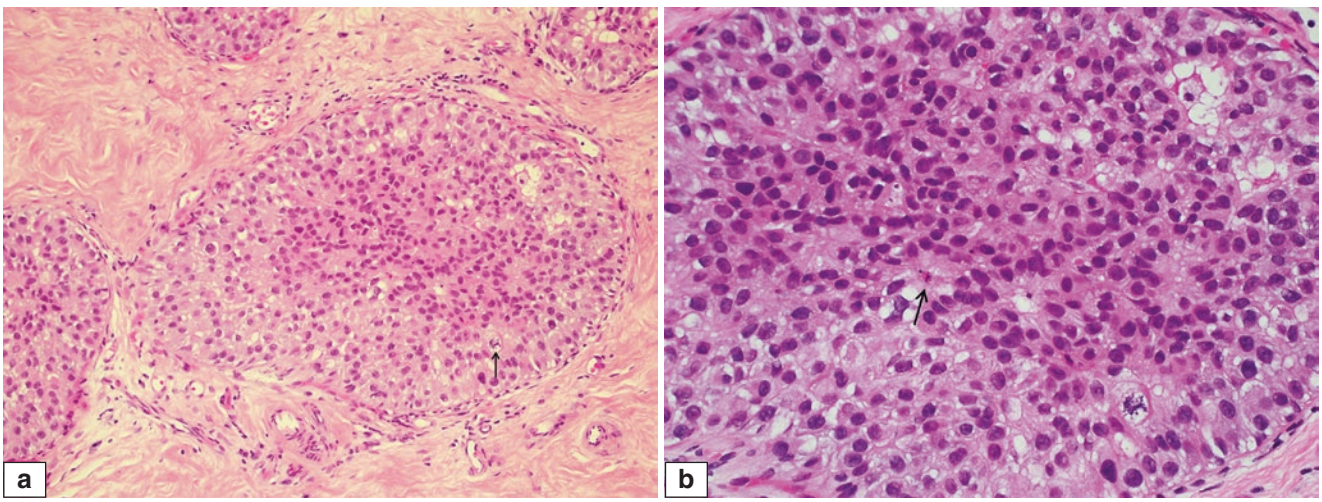

Fig. 9.16 DCIS, intermediate nuclear grade. (**a**) Complete filling of the duct space by DCIS cells with variability in nuclear size and small intervening spaces among the epithelial cells is reminiscent of florid UDH. Clues to a more sinister nature are the atypical mitosis (*arrow*), karyorrhexis, and more pronounced cytologic atypia. Additionally, surrounding ducts show features of DCIS. (**b**) Higher magnification of the malignant epithelial cells shows moderate nuclear pleomorphism. Individual cell necrosis (*arrow*), karyorrhexis and a mitosis are present

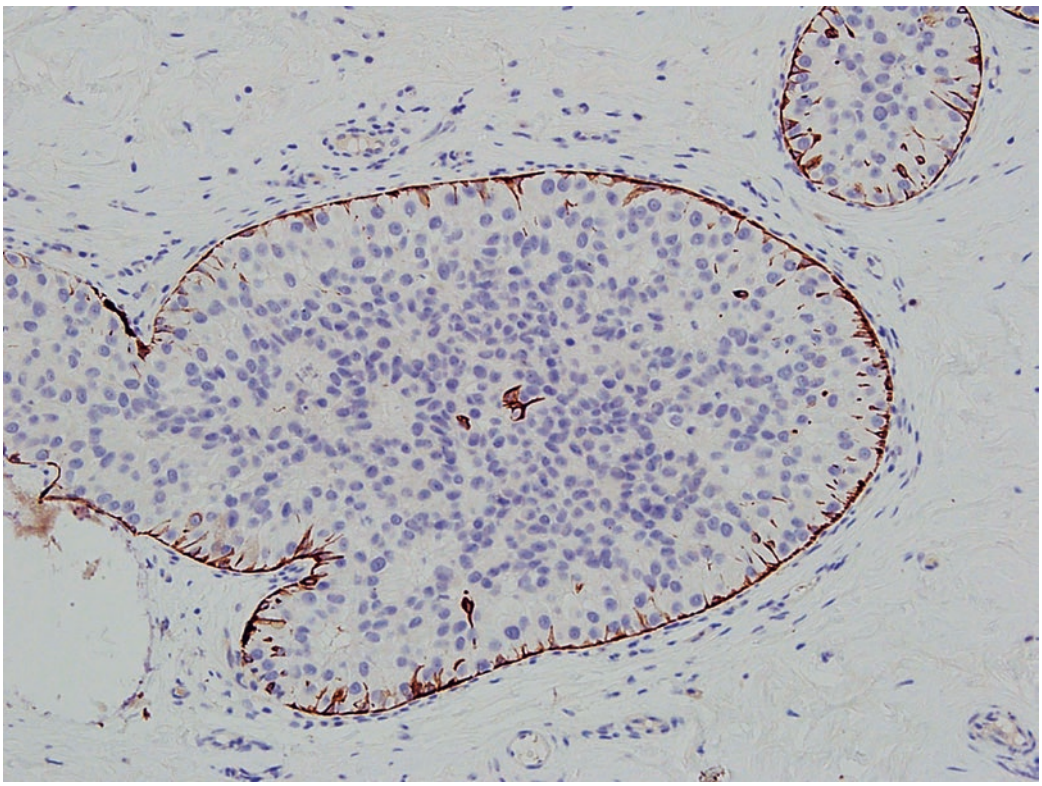

Fig. 9.17 DCIS, intermediate nuclear grade. Immunohistochemistry for CK14 shows a peripheral intact rim of positively staining myoepithelial cells, whereas the neoplastic DCIS population is largely nonreactive

Prognosis and Therapy Considerations

UDH is reported to be associated with a 1.5–2 times increased risk of subsequent breast cancer development, with the risk applicable to both breasts, but this estimate is based on long-term follow-up studies. Whether an individual woman with UDH will develop breast cancer is unknown, and currently UDH is not regarded as a significant risk factor that would alter clinical management.

Columnar Cell Change and Flat Epithelial Atypia

Definition

Columnar cell change is an alteration of the terminal ductal lobular unit featuring slightly dilated ducts and ductules lined by columnar cells that often possess apical snouts, accompanied by luminal secretions that not infrequently calcify (Figs. 9.18, 9.19, and 9.20). Columnar cell change is known by several other terms, including blunt duct adenosis, columnar alteration of lobules, columnar metaplasia, hyperplastic unfolded lobules, hyperplastic enlarged lobular units, and enlarged lobular units with columnar alteration.

The term *columnar cell hyperplasia* is used when there is more than one layer of columnar epithelial cells.

Flat epithelial atypia is diagnosed when there is mild nuclear atypia in columnar cell change/hyperplasia, with slightly enlarged, rounded nuclei with visible nucleoli, with cytologic appearances similar to those of low nuclear grade DCIS (Figs. 9.21 and 9.22). Synonymous terms are *columnar cell change with atypia* or *columnar cell hyperplasia with atypia*.

Clinical and Epidemiological Features

Columnar cell change and flat epithelial atypia are clinically asymptomatic lesions, which can be detected on mammographic screening because of the accompanying calcifications.

Imaging Features

Clustered, indistinct amorphous-type, or fine pleomorphic microcalcifications that are deposited within the terminal ductal lobular units can be observed on mammography (Fig. 9.23). Cysts may be encountered on sonography if the columnar cell change or flat epithelial atypia is associated with cystic changes.

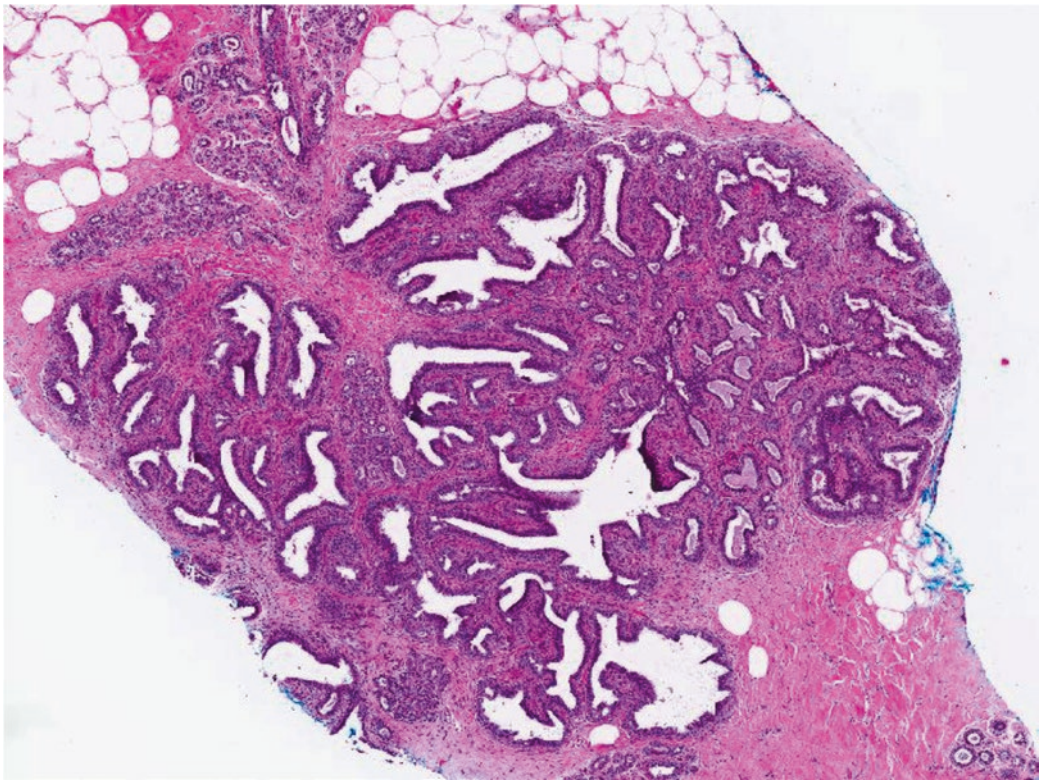

Fig. 9.18 Columnar cell change. At low magnification, several ductules within the enlarged lobule are slightly dilated

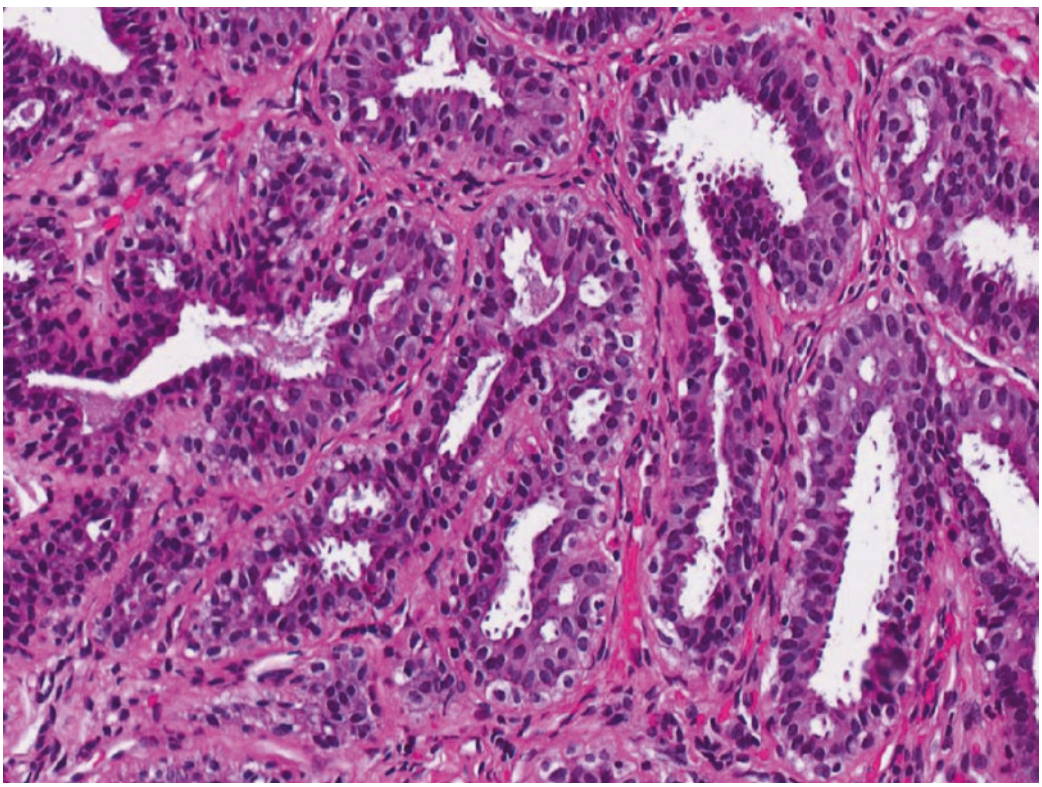

Fig. 9.19 Columnar cell change. Luminal pink secretions are seen

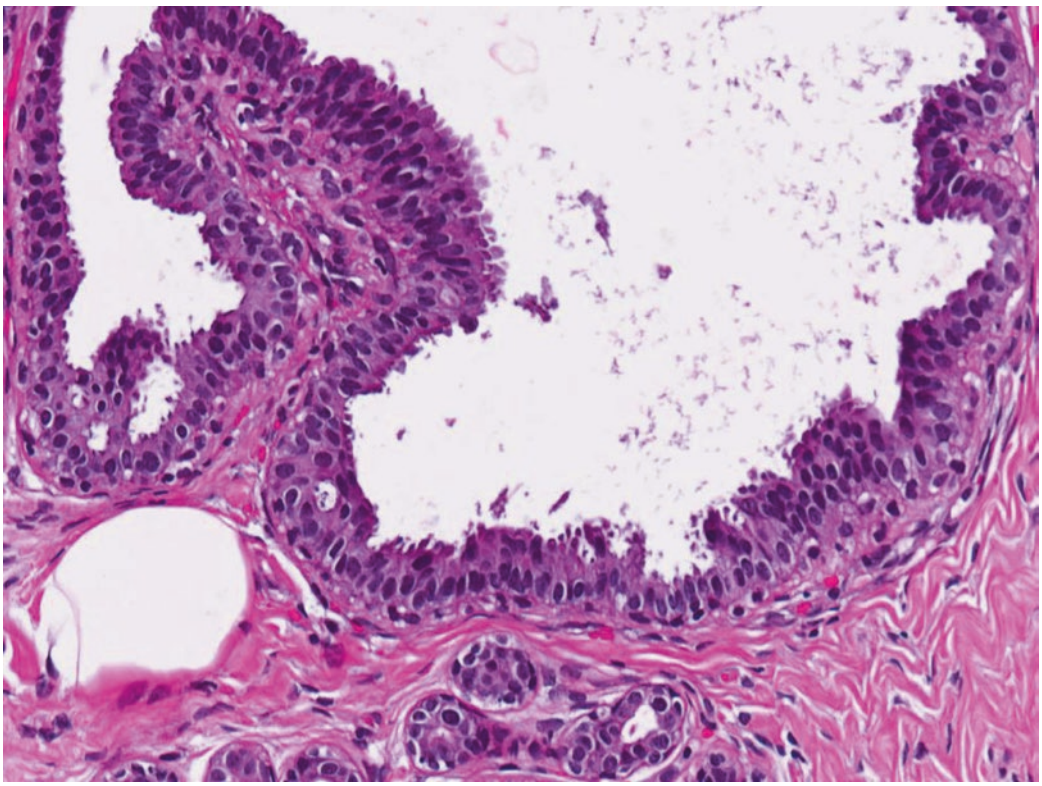

Fig. 9.20 Columnar cell change. In the duct, the lining epithelium is composed of columnar cells with the long axes of the nuclei oriented perpendicularly to the basement membrane. Where there is piling and stratification of nuclei, the term *columnar cell hyperplasia* is used. The apical portions of the columnar cells disclose apical snouts represented by cytoplasmic blebs

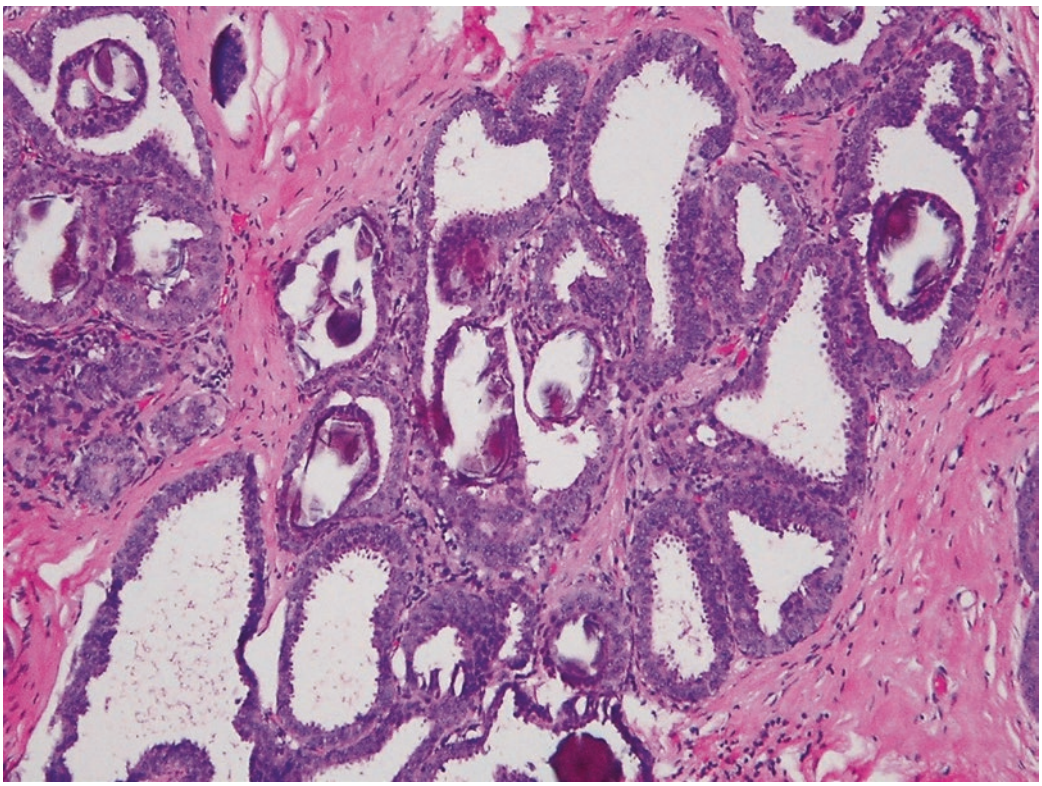

Fig. 9.21 Flat epithelial atypia (columnar cell change with nuclear atypia). The ducts are lined by a relatively flat layer of epithelial cells with apical snouts. There is a "dark" appearance of the epithelial cells at low magnification, contributed by the increased nuclear–cytoplasmic ratios. Psammomatous calcifications are observed

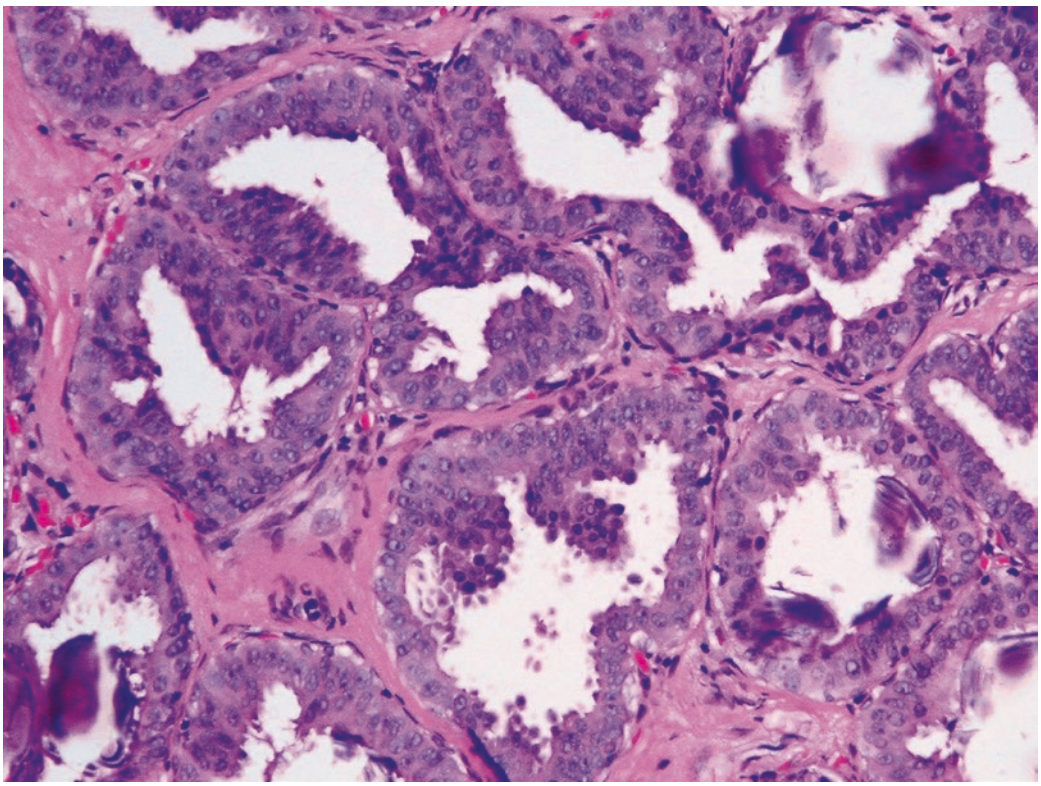

Fig. 9.22 Flat epithelial atypia. Short, mound-like protrusions of epithelial cells may be encountered in flat epithelial atypia, but the presence of clear-cut architectural atypia in the form of micropapillae, arches, or bridges warrants the diagnosis of ADH

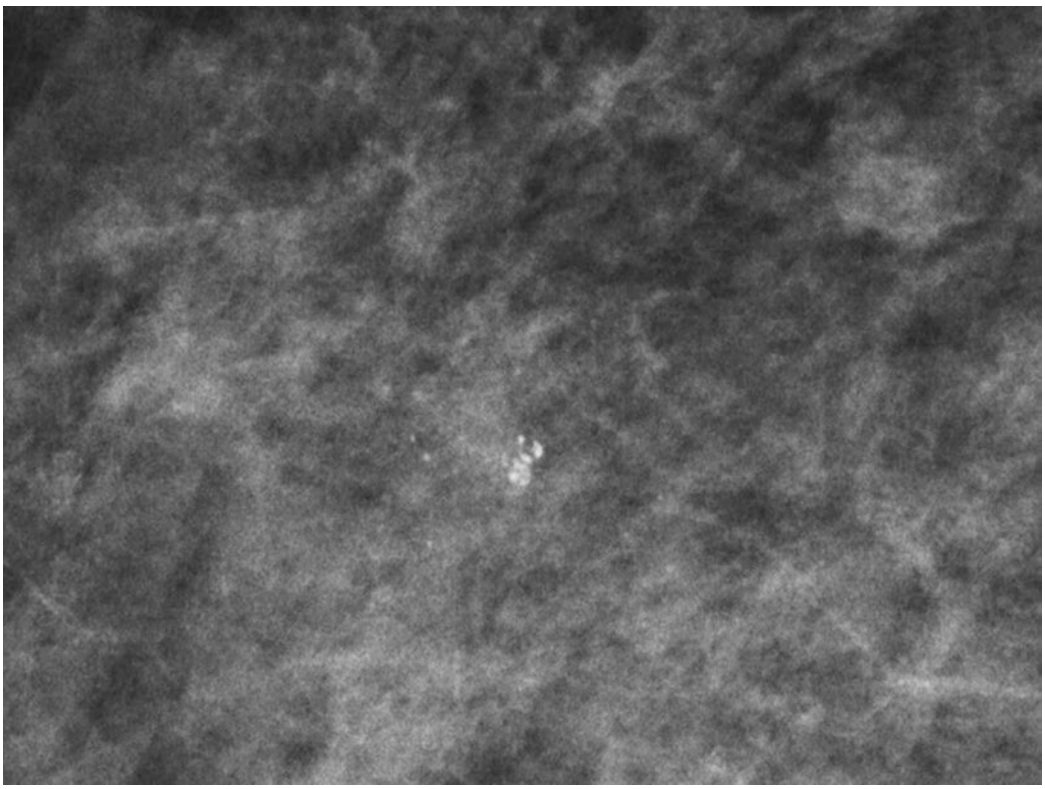

Fig. 9.23 Columnar cell change and flat epithelial atypia are often associated with calcifications that are detected on mammography. Here, the calcifications are clustered and resemble crushed stones

Pathologic Features

Macroscopic Pathology

There are no specific gross alterations. Cysts may be observed if there is accompanying cystic change of ducts and ductules. Grittiness related to calcifications can be present when the tissue is sliced.

Microscopic Pathology

Histologically, columnar cell change features mild dilatation of terminal ducts and ductules surrounded by a loose stroma, which may appear slightly cellular. Lining epithelial cells disclose columnar shapes with vertical axes exceeding their widths, set perpendicularly to the underlying basement membranes. Nuclei are ovoid or elongated and are also oriented along the vertical plane. Apical snouts, luminal secretions, and calcifications are often present. Columnar cell hyperplasia shows multiple layers of columnar epithelial cells, leading to an irregular, ruffled luminal contour, often with a micropapillary or mound-like appearance.

In flat epithelial atypia, epithelial cells become more cuboidal in shape, with slightly enlarged, rounded, vesicular nuclei that have discernible but usually small nucleoli. Because of cellular uniformity and monotony, the luminal surface appears relatively flat and rigid at low magnification. Additionally, there is a darker appearance that is due to increased nuclear–cytoplasmic ratios. As in columnar cell change, luminal secretions and calcifications are frequently present. By definition, if architectural atypia is observed in such a lesion, it should be classified as ADH. Lobular neoplasia, ADH, and low-grade in situ and invasive carcinomas can be found in proximity because of the similar genetic abnormalities [1] (Figs. 9.24 and 9.25).

Differential Diagnosis

UDH Versus Columnar Cell Change/Hyperplasia

In UDH, there is variability of the epithelial cell population without distinct columnarity, contrasting against columnar cell change or hyperplasia, in which the epithelial cells assume columnar shapes, with stratification in columnar cell hyperplasia. On immunohistochemistry, ER shows patchy nuclear reactivity in UDH, whereas columnar cell change or hyperplasia is usually diffusely ER positive (Fig. 9.26). Similarly, columnar cells are nonreactive with basal cytokeratins, whereas heterogeneous basal cytokeratin staining is observed in UDH.

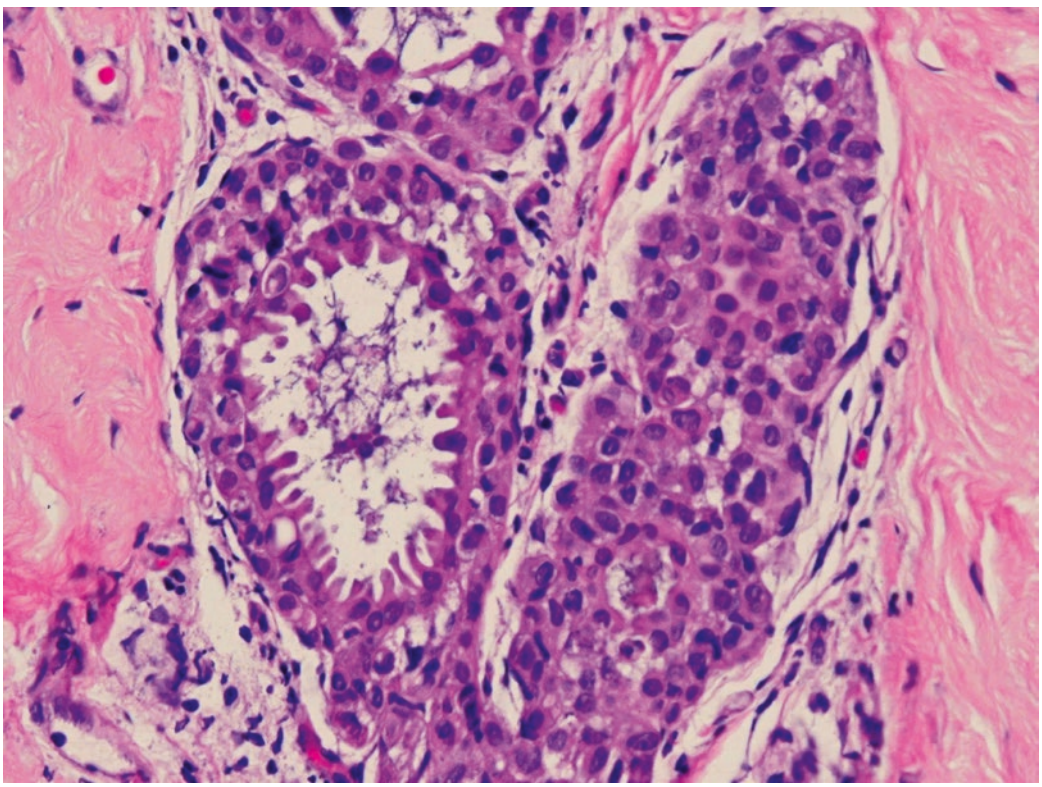

Fig. 9.24 Columnar cell change with atypical lobular hyperplasia. Columnar cell change with nuclear atypia (flat epithelial atypia), ADH, lobular neoplasia, low-grade DCIS, and low-grade invasive carcinoma share similar genetic abnormalities and have been referred to as belonging to the low-grade neoplasia family of breast lesions. Here, a duct with luminal cells demonstrating prominent apical snouts is surrounded by discohesive lobular neoplastic cells that have also involved adjacent ductules

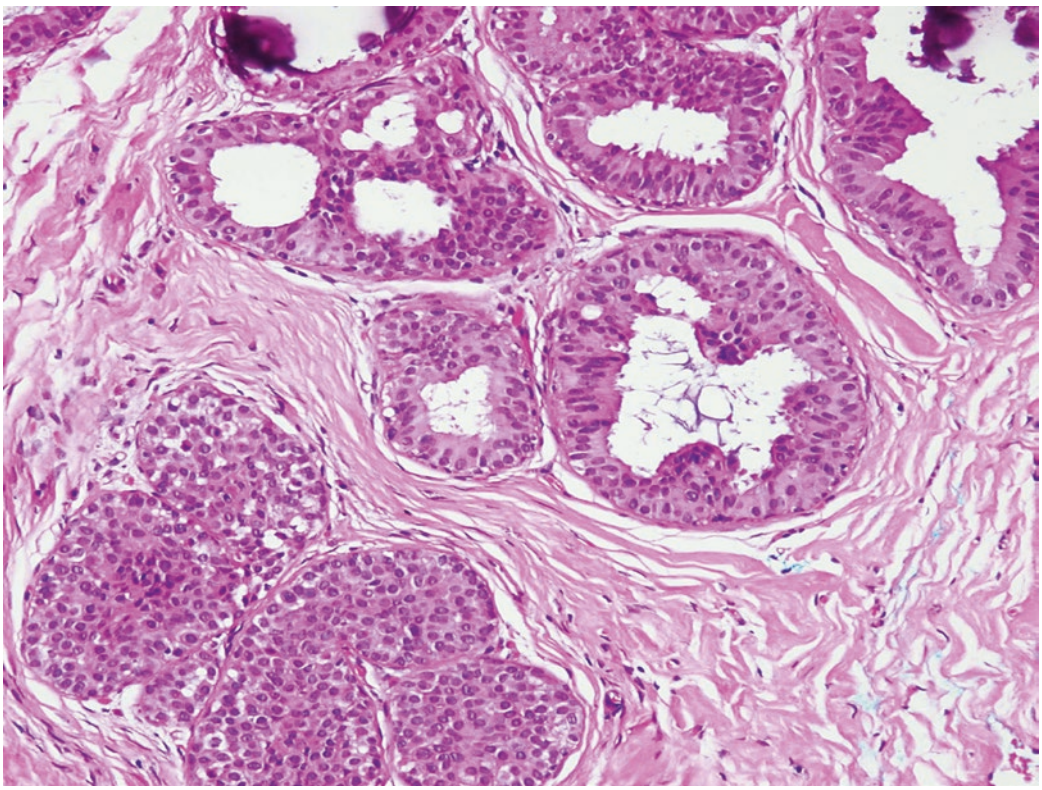

Fig. 9.25 Columnar cell hyperplasia with lobular neoplasia. Several ductules lined by columnar cells with stratified nuclei, associated with calcifications, are present. Lobular neoplasia, with features bordering on lobular carcinoma in situ, is observed in the same lobule where mildly distended acini filled with a population of uniform and slightly discohesive cells are seen

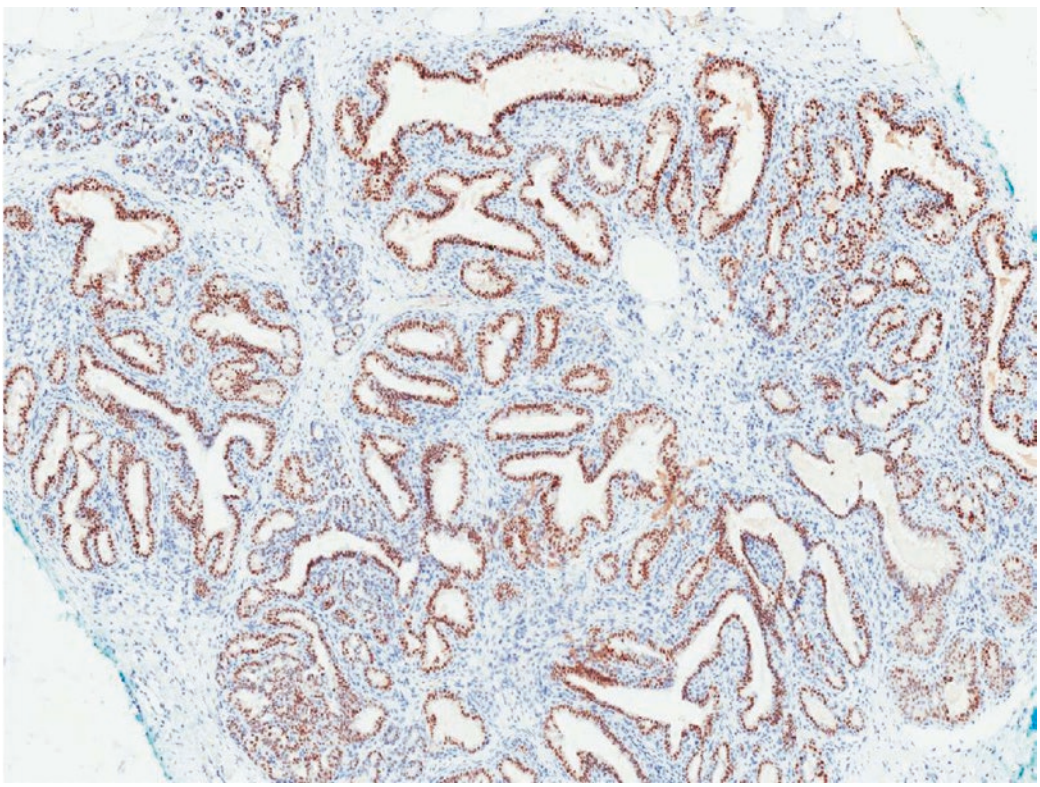

Fig. 9.26 Columnar cell change. Oestrogen receptor (ER) staining shows relatively diffuse nuclear positivity of columnar cells

Columnar Cell Change/Hyperplasia Versus Flat Epithelial Atypia

The distinction between columnar cell change or hyperplasia and flat epithelial atypia rests on the presence of nuclear atypia. This distinction may be rather subjective [2, 3], making consistent diagnosis of flat epithelial atypia challenging. It was reported that nuclear size is increased in flat epithelial atypia [4]. Clues to flat epithelial atypia include a relatively rigid luminal contour and darker-appearing cells (because of increased nuclear–cytoplasmic ratios) with more cuboidal shapes, rounded nuclei, and visible nucleoli.

Flat Epithelial Atypia Versus Atypical Ductal Hyperplasia or Low Nuclear Grade DCIS

The cells of flat epithelial atypia are similar to those of ADH or low nuclear grade DCIS. The key difference is the presence of architectural atypia in the latter, with patterns of micropapillary, cribriform, solid, and papillary morphology.

Flat Epithelial Atypia Versus High Nuclear Grade DCIS

High nuclear grade features of a single layer to a few layers of abnormal cells lining duct walls should be diagnosed as DCIS. High nuclear grade cytological atypia is incompatible with flat epithelial atypia (Figs. 9.27, 9.28, 9.29, and 9.30).

Prognosis and Therapy Considerations

Columnar cell change or hyperplasia has a very low risk (about 1.5×) for subsequent breast cancer development, which may be related to other concurrent lesions [5]. Though the risk for flat epithelial atypia is considered higher, it is believed to be significantly lower than the risk associated with ADH and atypical lobular hyperplasia. As such, its presence in excision specimens does not warrant specific clinical management if no worse lesions are seen. The approach to its finding on core biopsy is controversial, however, and requires close multidisciplinary discussion [6, 7]. A recent study

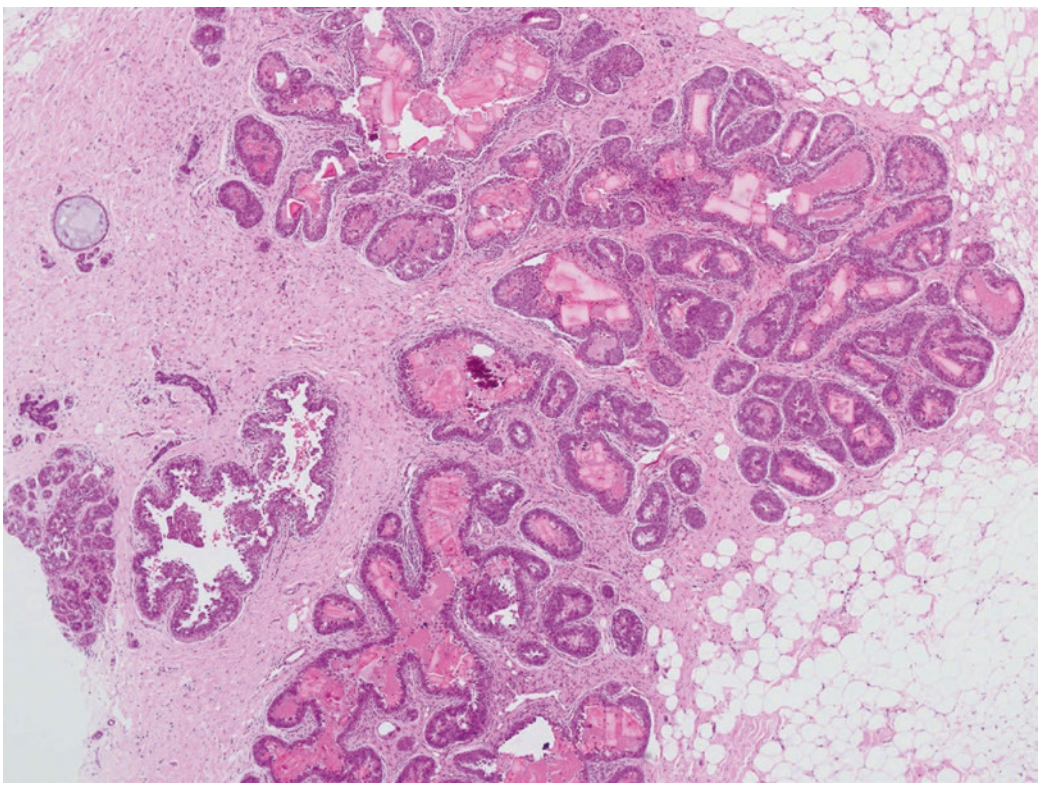

Fig. 9.27 DCIS, clinging subtype, resembling flat epithelial atypia at low magnification. Luminal pink secretions, rectangular crystals, and calcifications are present

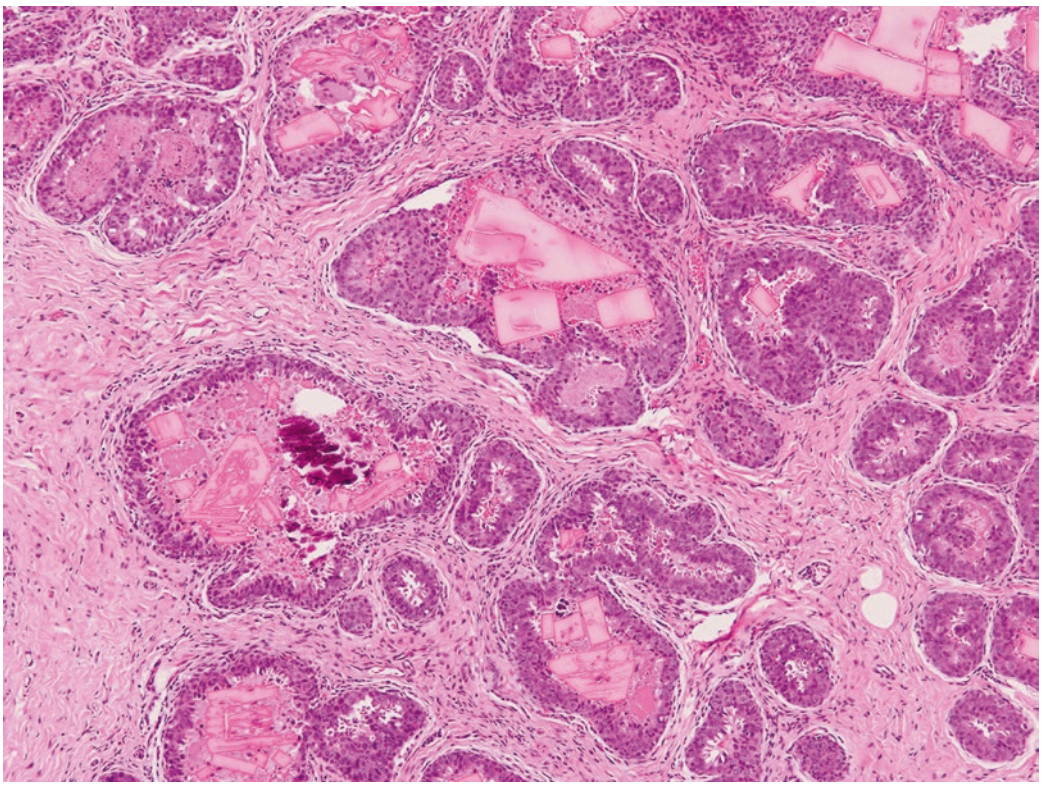

Fig. 9.28 DCIS, clinging subtype, at medium magnification, shows mostly single-layered epithelium with apical snouts

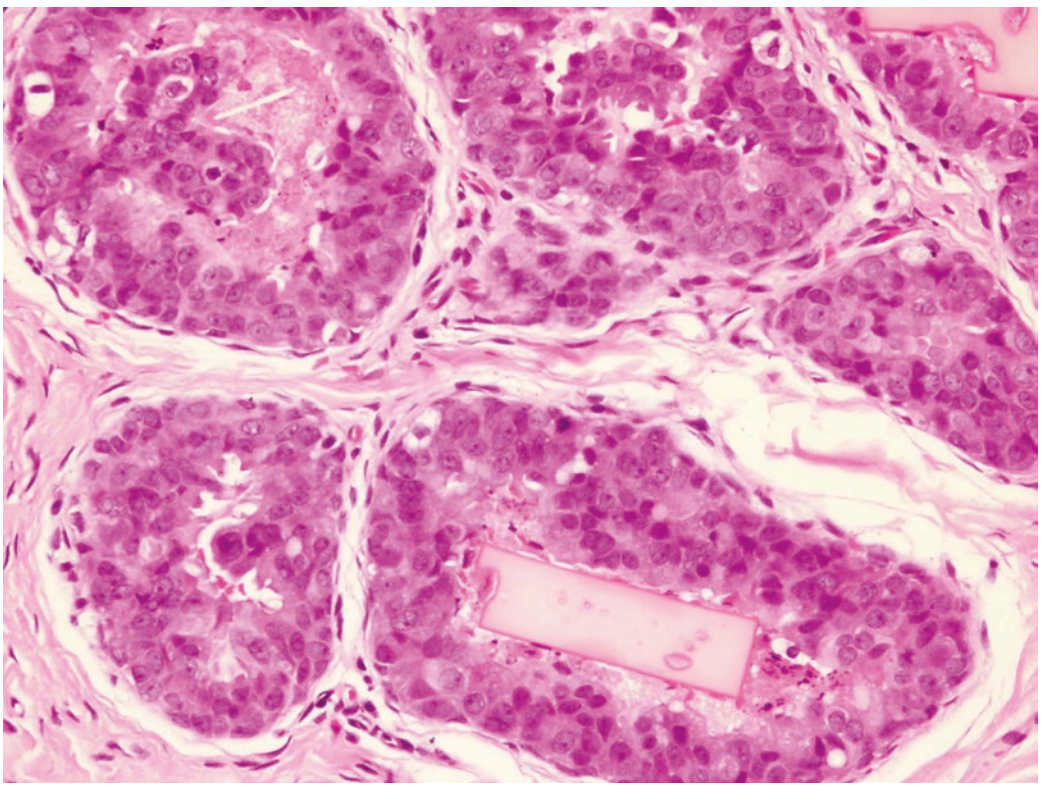

Fig. 9.29 DCIS, clinging subtype, with moderate to marked nuclear atypia at high magnification, and luminal debris with rectangular crystals

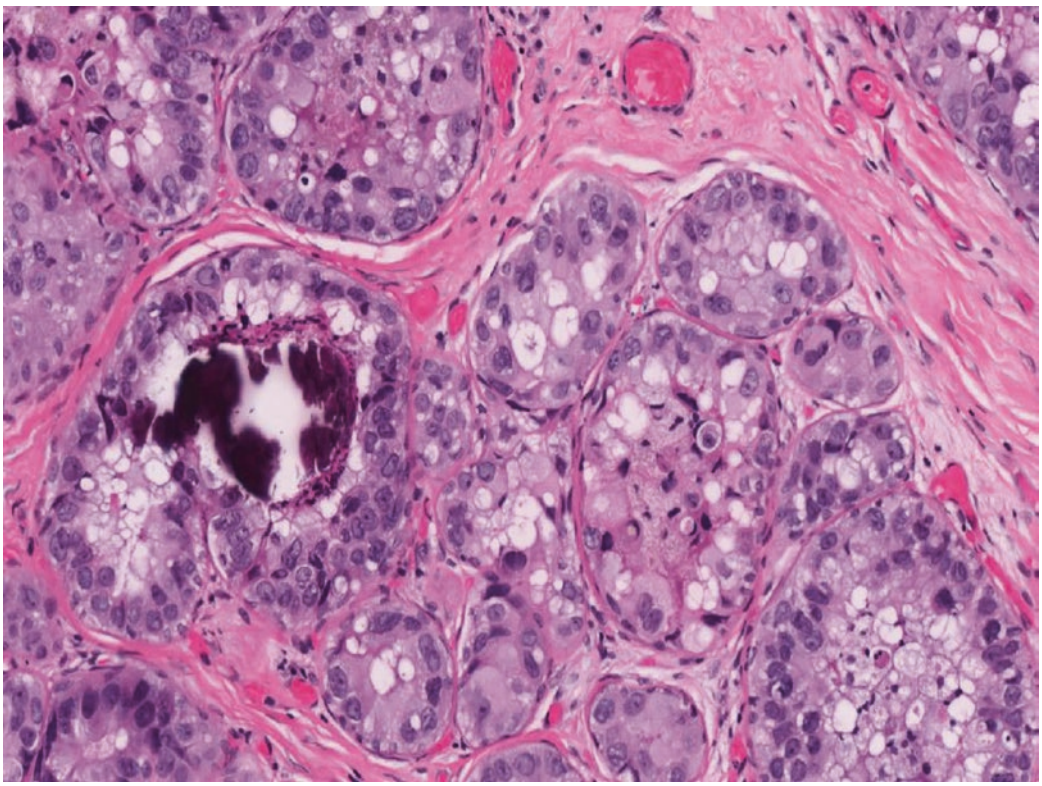

Fig. 9.30 DCIS, high nuclear grade, which may resemble flat epithelial atypia because of the single-layered lining of abnormal epithelial cells, associated with calcifications. However, the nuclear atypia here is of moderate to marked degree, with accompanying necrotic debris incompatible with flat epithelial atypia

found that flat epithelial atypia did not confer an independent risk of breast cancer beyond that associated with proliferative breast disease without atypia or atypical hyperplasia [5].

Atypical Ductal Hyperplasia

Definition

Atypical ductal hyperplasia (ADH) is a clonal proliferation of monomorphic epithelial cells involving the terminal ductal lobular unit, with architectural atypia constituted by cribriform, micropapillary, papillary, and solid morphologies. Patients with ADH harbour a risk of subsequent breast cancer development that is three to five times greater than in the general population.

Clinical and Epidemiological Features

As ADH is a microscopic lesion, it is almost always asymptomatic, but it can be associated with calcifications or accompany other lesions such as cystic changes, so the presentation may be through mammographic detection of, or symptoms from, associated lesions.

Imaging Features

Clustered microcalcifications that are often indistinct and amorphous in morphology can be seen on mammography. The microcalcifications may also appear pleomorphic and indistinguishable from those observed in DCIS. ADH does not have any characteristic features on sonography, but it may occasionally involve underlying conditions like intraductal papillomas or fibroadenomas. ADH is often an incidental finding from biopsy for other lesions. There is no specific MRI morphology for ADH. It can be found as enhancing masses or non-mass enhancing lesions (likely related to accompanying lesions) that are focal, linear, or regional in distribution, with no reliable MR imaging features to predict upgrade.

Pathologic Features

Macroscopic Pathology

No specific macroscopic changes are present, apart from accompanying cystic changes and grittiness due to associated calcifications.

Microscopic Pathology

ADH resembles low nuclear grade DCIS, but it is a more limited lesion, which measures 2 mm or less, or only partially involves ducts. A useful histological guide is that ADH is diagnosed only when low nuclear grade DCIS is being seriously considered. Cytologically, ADH shows monomorphic, low-grade nuclei in atypical architectural formations. Calcifications may be observed (Figs. 9.31, 9.32, 9.33, 9.34, 9.35, and 9.36).

Differential Diagnosis

UDH Versus ADH

Florid UDH should not be classified as ADH. In florid UDH, a heterogeneous population of epithelial cells fills and effaces the ductal lumen. Nuclear overlapping and variability, streaming, and slit-like spaces are present in florid UDH. In contrast, ADH shows a homogeneous epithelial population with rigid architectural patterns.

ADH Versus Low Nuclear Grade DCIS

Quantitative criteria are used to distinguish ADH from low nuclear grade DCIS, as the epithelial cells of these two lesions are qualitatively similar. ADH is a small, usually focal lesion, either partially involving ducts or completely involving ducts but measuring only up to 2 mm in maximal extent. A similar lesion measuring more than 2 mm may be diagnosed as low nuclear grade DCIS. Although the size criterion appears objective and is widely used, it is acknowledged that this cut-off is arbitrary, intended to avoid overtreatment of small, focal, low-grade lesions. The WHO working group also accepts the approach of using two or more membrane-bound spaces involved by a monotonous neoplastic population to define low-grade DCIS, with lesions below this threshold regarded as ADH [8]. As both ADH and low nuclear grade DCIS are composed of a similar clonal cell population, immunohistochemical panels are unable to distinguish these lesions.

ADH Versus Collagenous Spherulosis

ADH with a cribriform pattern may mimic collagenous spherulosis (Figs. 9.37 and 9.38). In collagenous spherulosis, however, the cribriform spaces are pseudolumens rimmed by myoepithelial cells, whereas the true lumens of ADH are surrounded by neoplastic epithelial cells. Also, ADH shows a uniform population of ER-positive epithelial cells, whereas collagenous spherulosis features a mixed population of both luminal and myoepithelial cells.

Fig. 9.31 Atypical ductal hyperplasia. Part of the wall of this cystically dilated duct shows abnormal architecture with bland epithelial cells forming rigid spaces. A stiff epithelial arch is seen in another part of the duct wall. A few fractured calcifications are observed within the cystic lumen

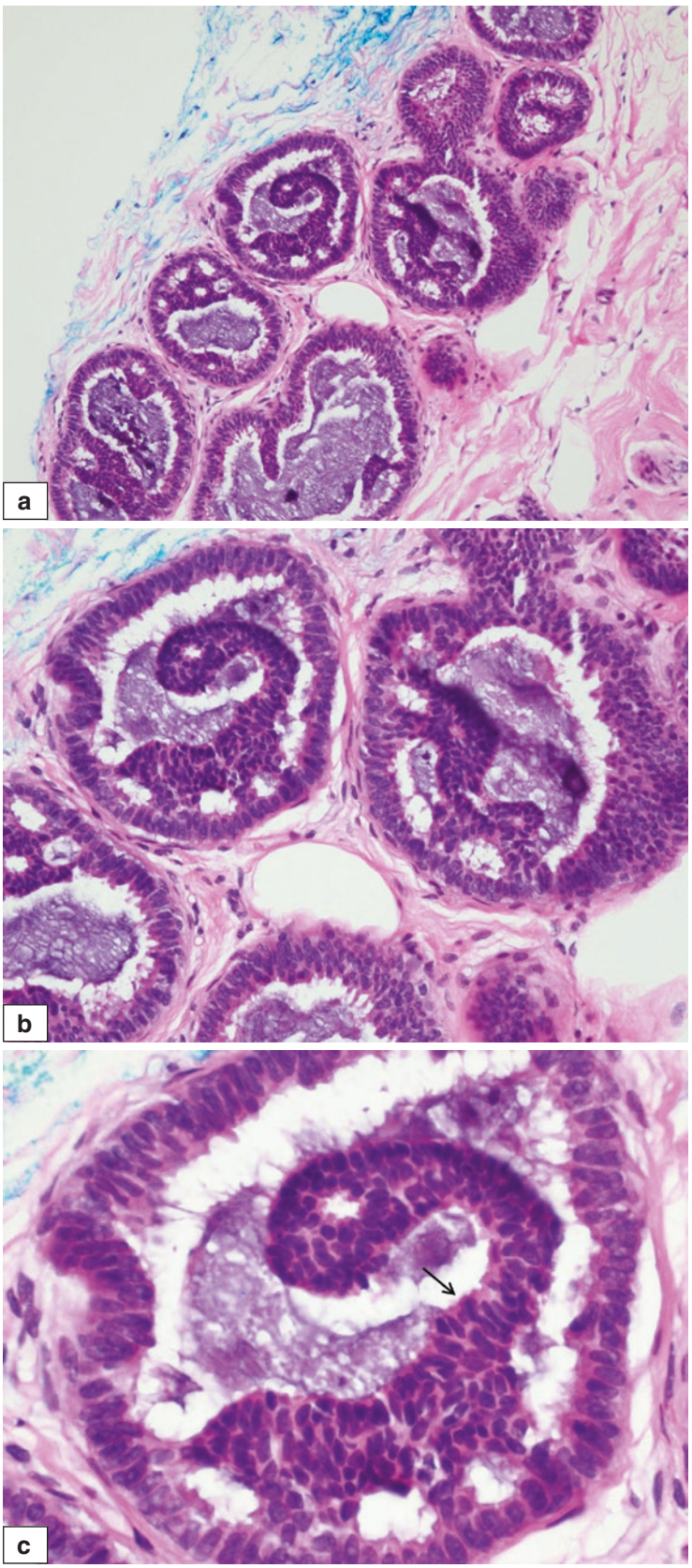

Fig. 9.32 Atypical ductal hyperplasia. (**a**) Several small ducts in this core biopsy show an atypical epithelial proliferation with partial involvement of the duct spaces. Calcifications and some mucinous material are seen within the lumens. (**b**) Higher magnification shows atypical architecture with epithelial structures containing nuclei that are partially overlapping, with some nuclei oriented perpendicularly to the directions of the bridges. (**c**) High magnification shows epithelial nuclei that are oriented perpendicularly to the direction of the epithelial bar (*arrow*)

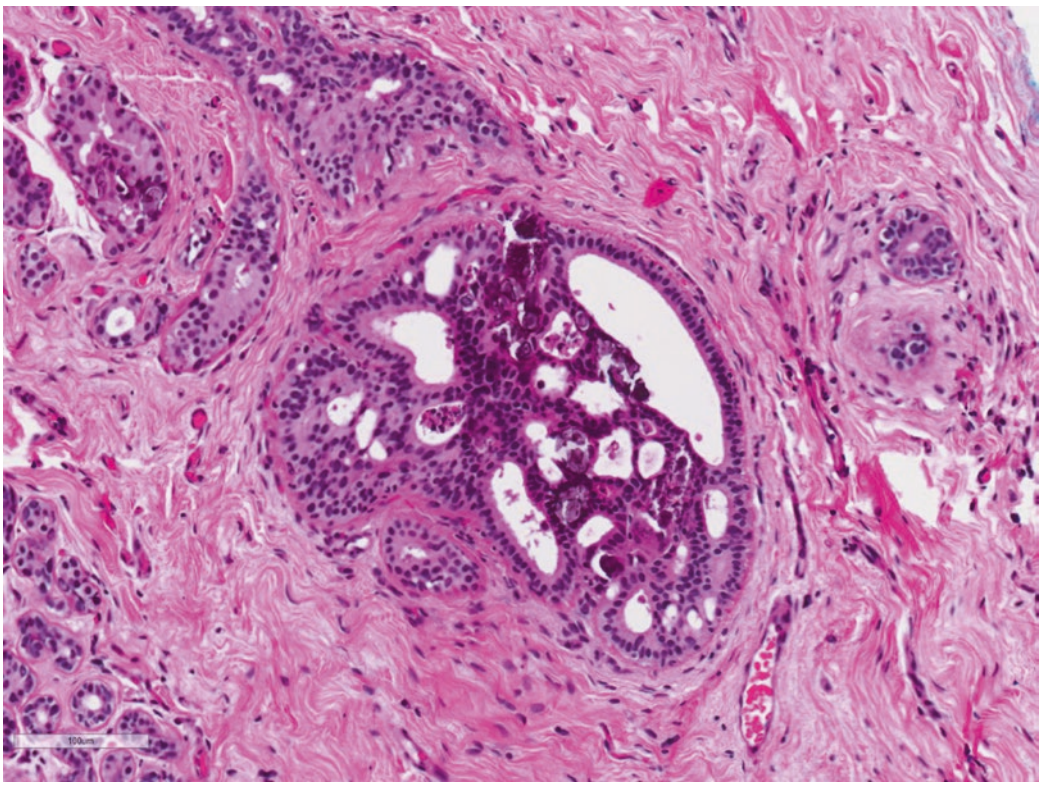

Fig. 9.33 Atypical ductal hyperplasia shows one duct space with a cribriform pattern and calcifications. Luminal spaces are crisp, but epithelial cells along the walls of these lumens are oriented in parallel. Though the morphological appearance resembles low-grade DCIS, both qualitative and quantitative criteria are not fulfilled, and the diagnosis is that of ADH

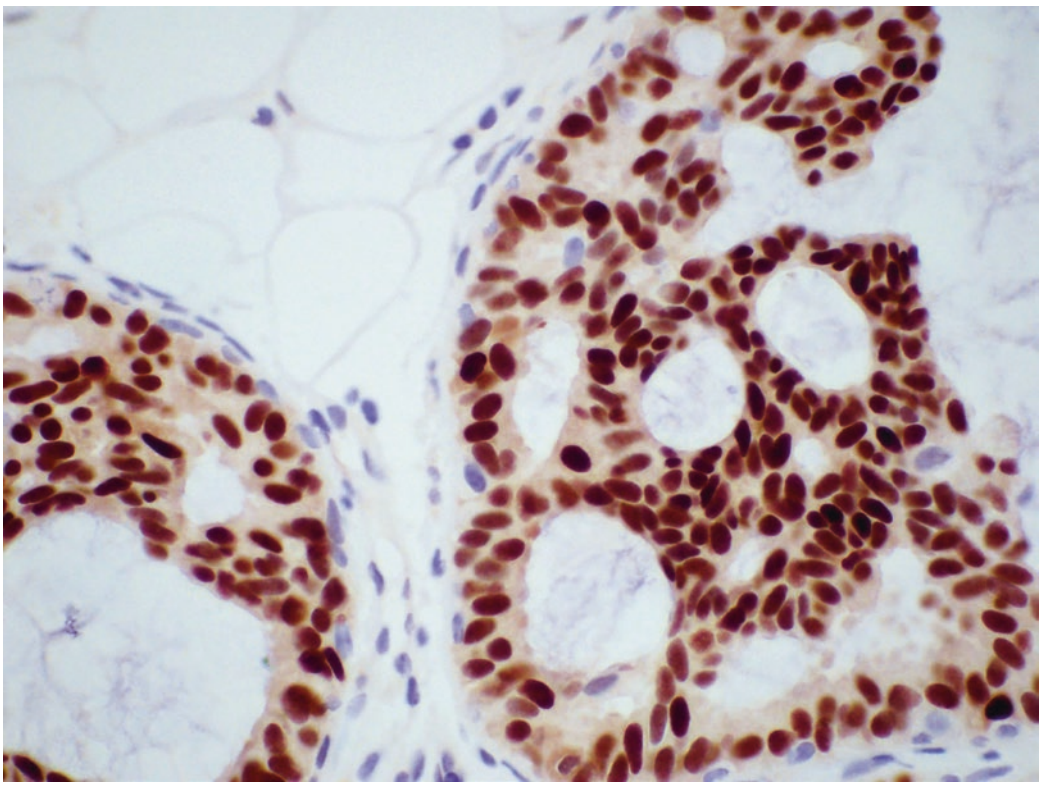

Fig. 9.34 Atypical ductal hyperplasia. ER immunohistochemistry shows diffuse and intense nuclear staining of epithelial cells. The staining pattern is similar to that of low-grade DCIS, differing from UDH, in which ER staining is patchy, non-diffuse, and variable in intensity

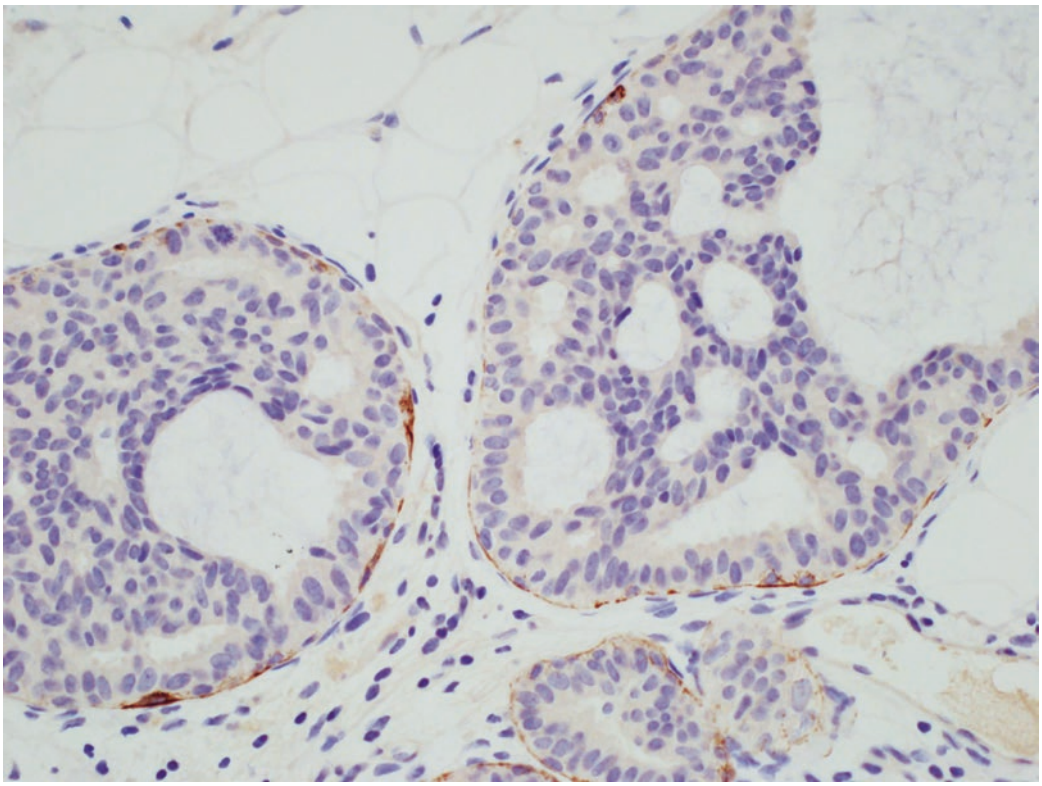

Fig. 9.35 Atypical ductal hyperplasia. CK14 immunohistochemistry highlights only the peripheral rim of myoepithelial cells. No staining is seen around secondary lumens, in contrast with collagenous spherulosis, which is a mimic of cribriform ADH/DCIS

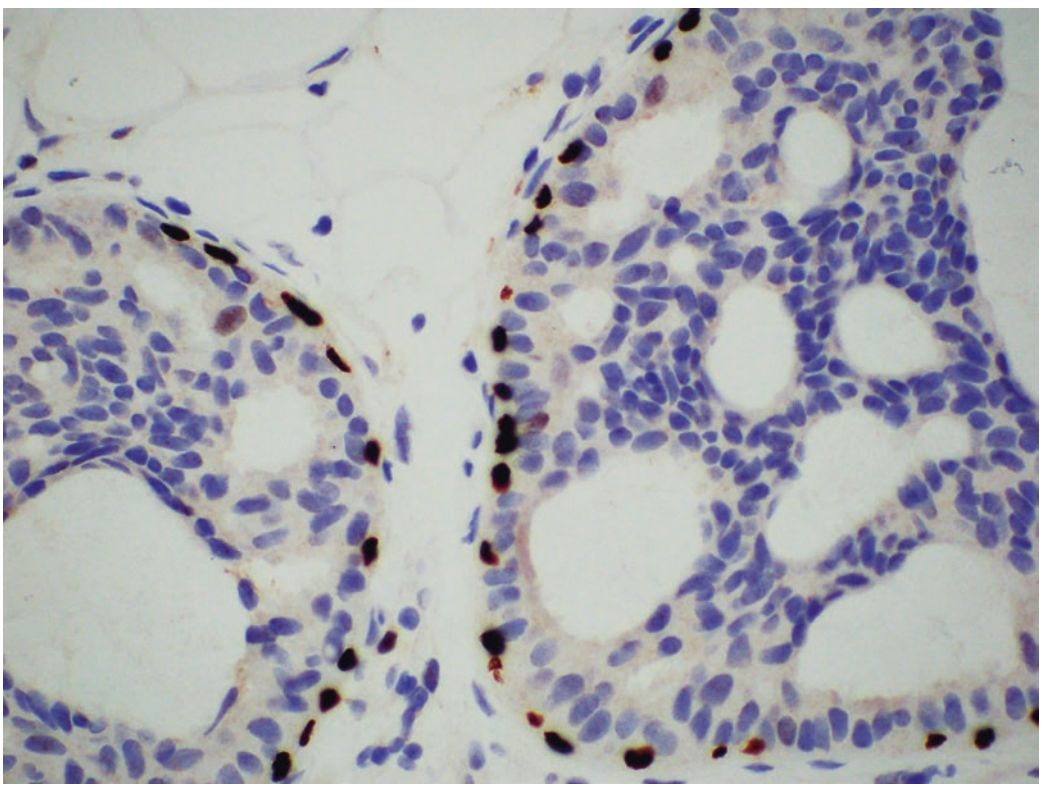

Fig. 9.36 Atypical ductal hyperplasia. Immunohistochemistry for p63 shows positive nuclear staining of myoepithelial cells around the duct wall. As with CK14, no staining of cells is seen around secondary lumens, unlike collagenous spherulosis

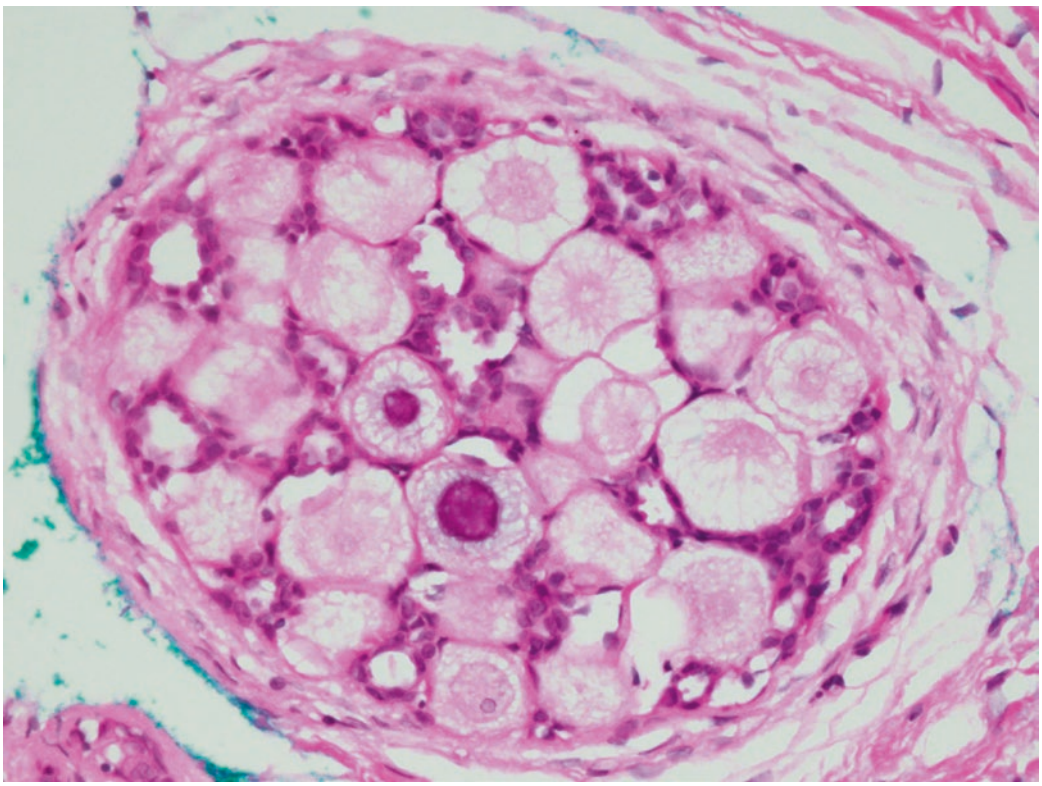

Fig. 9.37 Collagenous spherulosis. Its cribriform appearance and well-defined spaces can mimic ADH or low nuclear grade DCIS with cribriform morphology. Differences from the latter are the absence of a monotonous cell population, the presence of attenuated myoepithelial cells lining the spaces, and pink spherules with wispy, radiating extensions composed of basement membrane material elaborated by myoepithelial cells

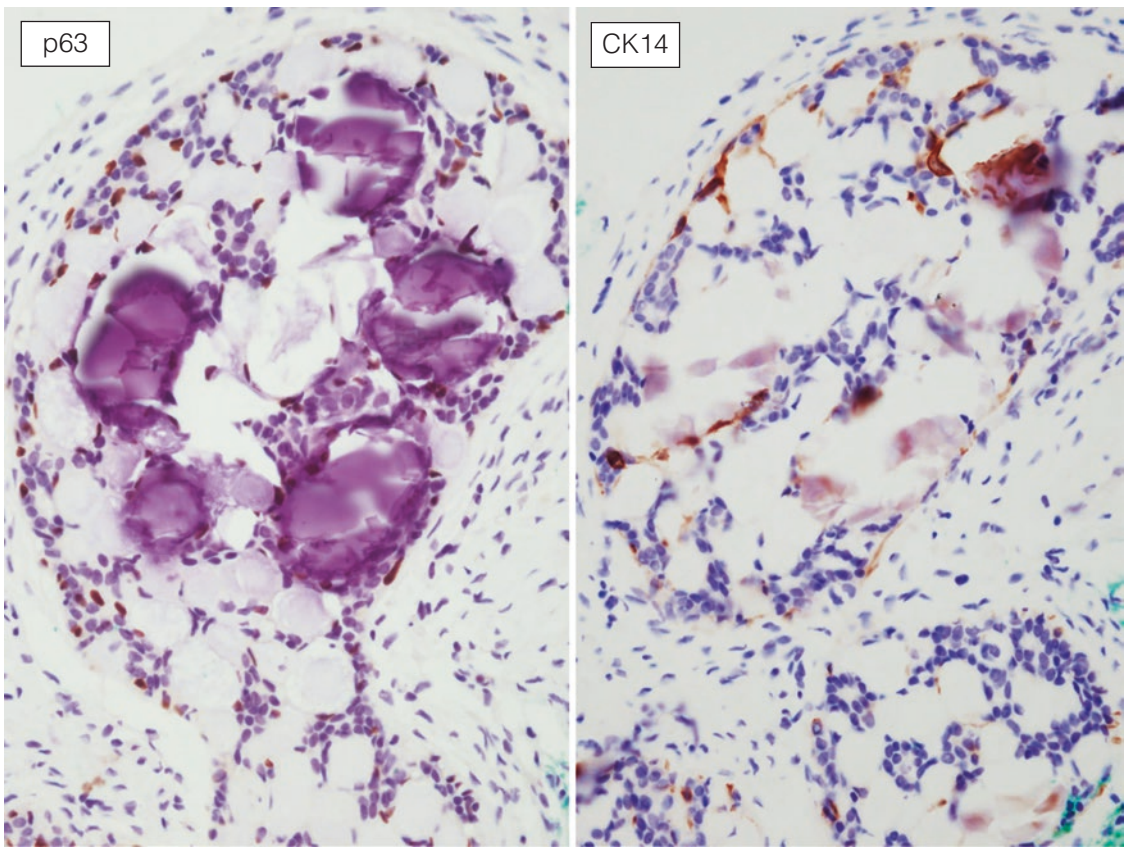

Fig. 9.38 Collagenous spherulosis. On immunohistochemistry, myoepithelial cells that are highlighted by p63 and CK14 are seen rimming the cribriform spaces. Fractured calcifications are noted

Prognosis and Therapy Considerations

With ADH, the risk of subsequent breast cancer is three to five times higher than the risk for the general population, and the risk applies to both breasts. Women with ADH are subjected to high-risk screening and in some cases risk reduction with anti-oestrogen therapy. If ADH is discovered on core biopsy, an excision is usually performed to exclude a larger lesion that would warrant a diagnosis of DCIS.

Ductal Carcinoma In Situ

Definition

Ductal carcinoma in situ (DCIS) is a non-invasive malignant epithelial cell proliferation that is confined within the basement membranes, arising in the terminal ductal lobular unit, with cytological atypia that ranges from mild to marked in severity. DCIS is a non-obligate precursor to most invasive breast carcinomas.

Clinical and Epidemiological Features

With the advent of mammographic screening, the incidence of DCIS has increased tremendously in recent decades, as many cases are associated with calcifications that are radiologically detected. Currently, DCIS accounts for 25–30 % of all newly detected breast cancers. Occasionally, DCIS may present symptomatically as a mass, nipple discharge, or nipple erosion (Paget disease) (Figs. 9.39 and 9.40).

Imaging Features

DCIS is often associated with microcalcifications visualised on mammography. The type of microcalcifications observed radiologically depends on the DCIS grade. Powdery, amorphous microcalcifications are associated with low-grade lesions. Linear, branching-type microcalcifications due to casting of necrotic cells within ducts are highly associated with high-grade DCIS [9]. Pleomorphic calcification morphology can be due to any grade of DCIS (Fig. 9.41). Occasionally, DCIS may present as radiological masses, particularly in cases with papillary architecture or when high-grade DCIS is accompanied by stromal fibrosis. Discrete masses with indistinct margins or intraductal masses with a tubular, ductal configuration may be seen on sonography. MRI is poor in the assessment of low-grade DCIS but has a very high sensitivity for DCIS overall. Lesions on MRI that demonstrate linear or clumped non-mass enhancement with ductal or segmental distribution are highly suspicious for DCIS.

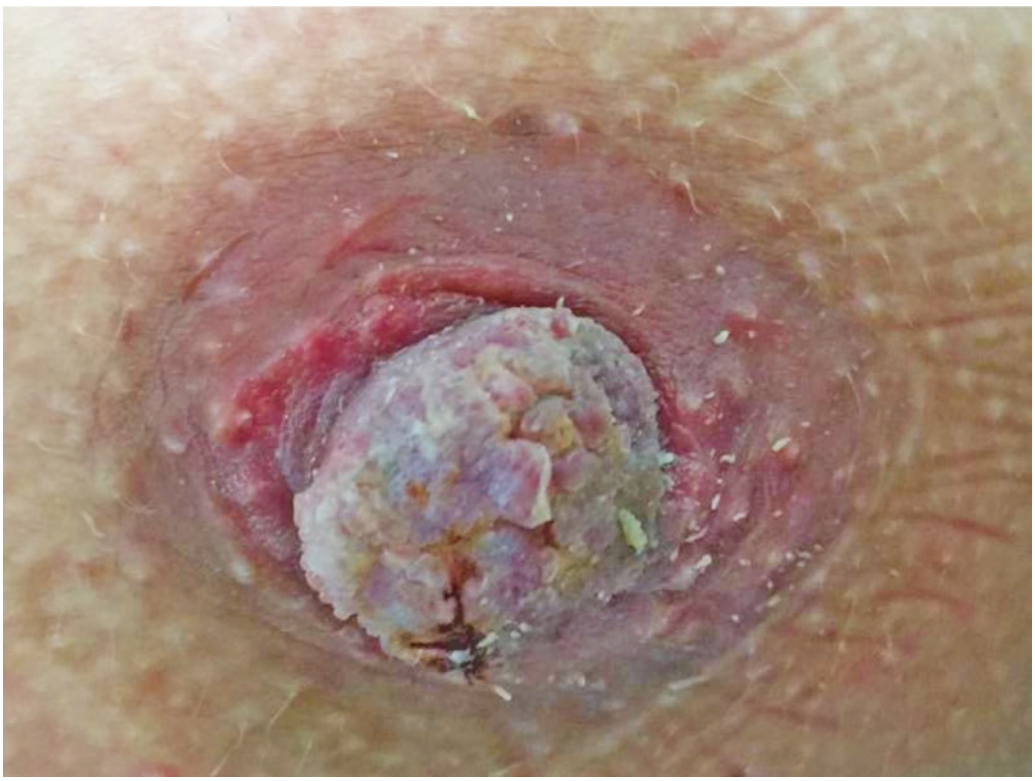

Fig. 9.39 Paget disease of the breast. The nipple is covered by a whitish coat of flaky material with irregular protuberances (Courtesy of Dr. Joy Lee)

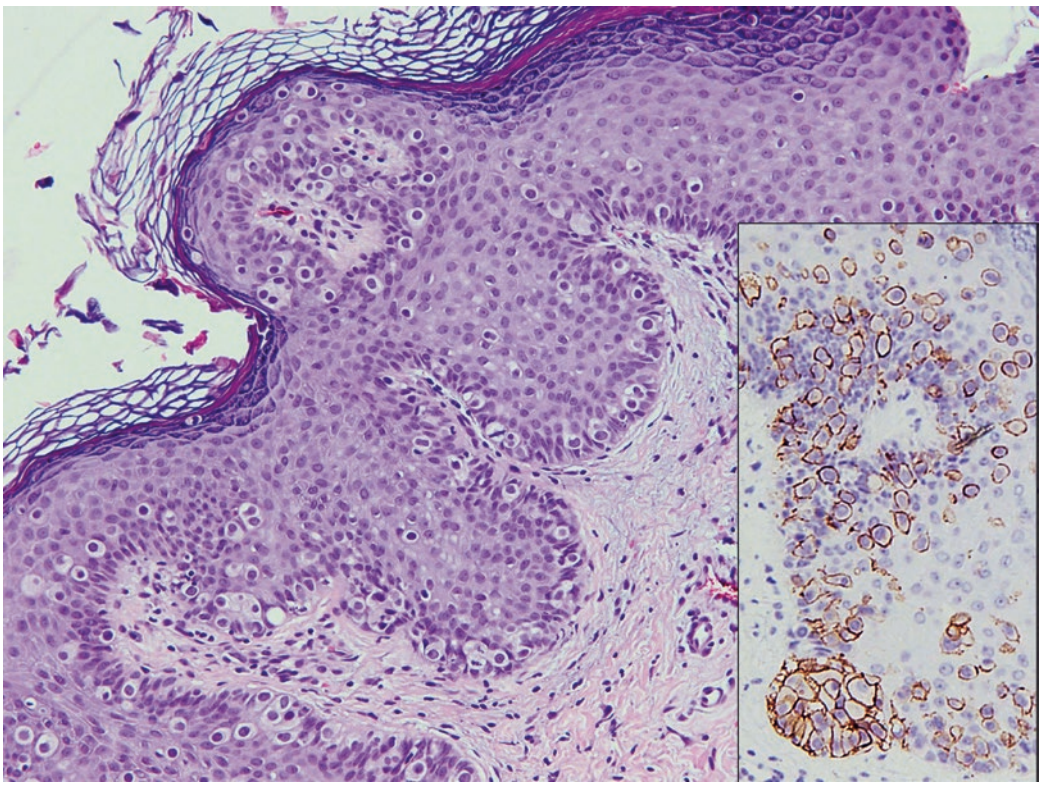

Fig. 9.40 Paget disease of the breast. Abnormal cells are scattered throughout the nipple epidermis, featuring enlarged vesicular nuclei with visible nucleoli and occasional mitoses. *Inset* shows positive membrane staining for c-erbB-2 in the tumour cells on immunohistochemistry, a characteristic of Paget disease that is almost always associated with underlying high nuclear grade DCIS and, in some cases, invasive carcinoma

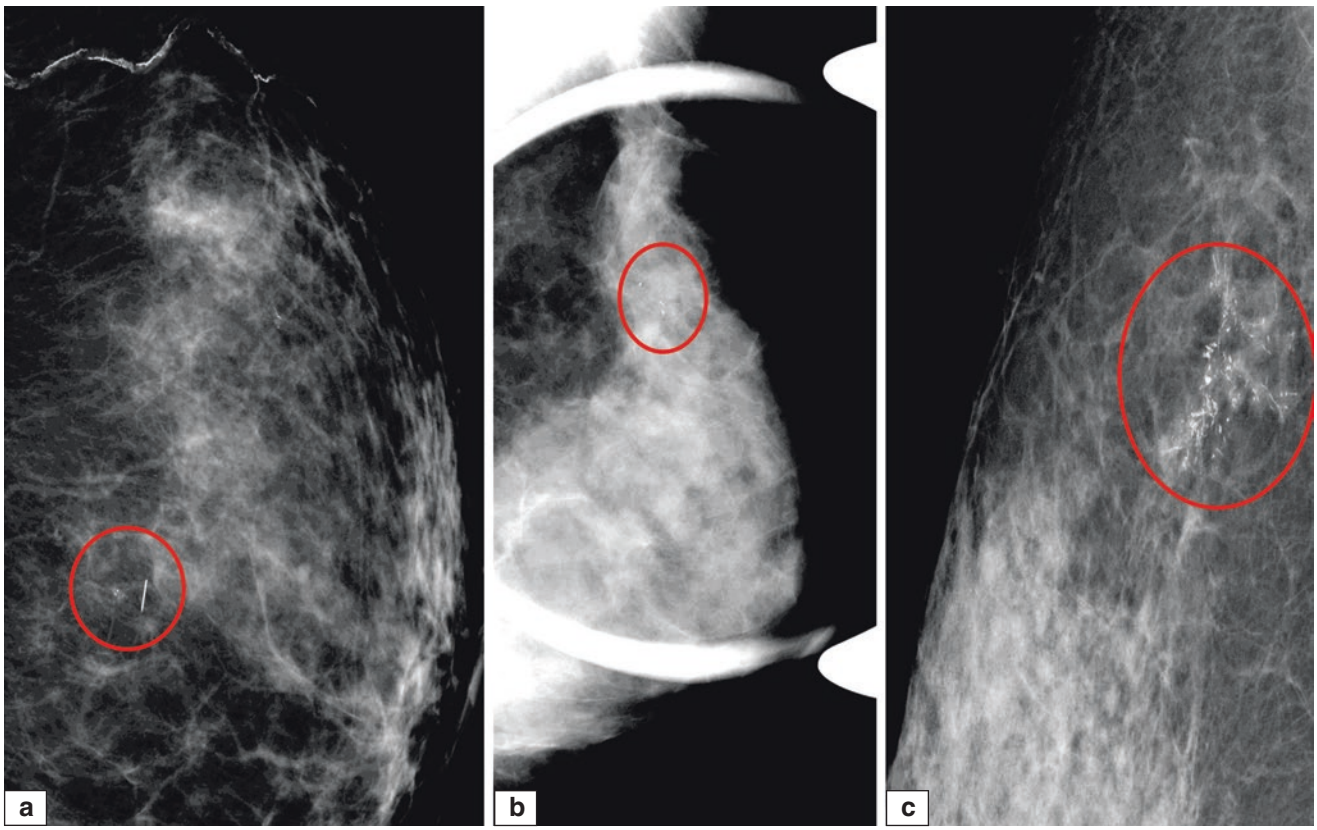

Fig. 9.41 Radiology of DCIS. (**a**) Tight cluster of slightly pleomorphic microcalcifications histologically corresponding to low nuclear grade DCIS (*circled*). (**b**) Loose cluster of pleomorphic microcalcifications associated with intermediate nuclear grade DCIS (*circled*). (**c**) Linear branching microcalcifications seen in high nuclear grade DCIS (*circled*)

Pathologic Features

Macroscopic Pathology

Small lesions of DCIS may not be visible macroscopically. When the lesions are associated with cysts or fibrosis, or when they harbour luminal necrosis, DCIS may appear as an indurated area with firmer consistency, punctuated by yellowish, necrotic foci that extrude debris when compressed (Figs. 9.42, 9.43, and 9.44).

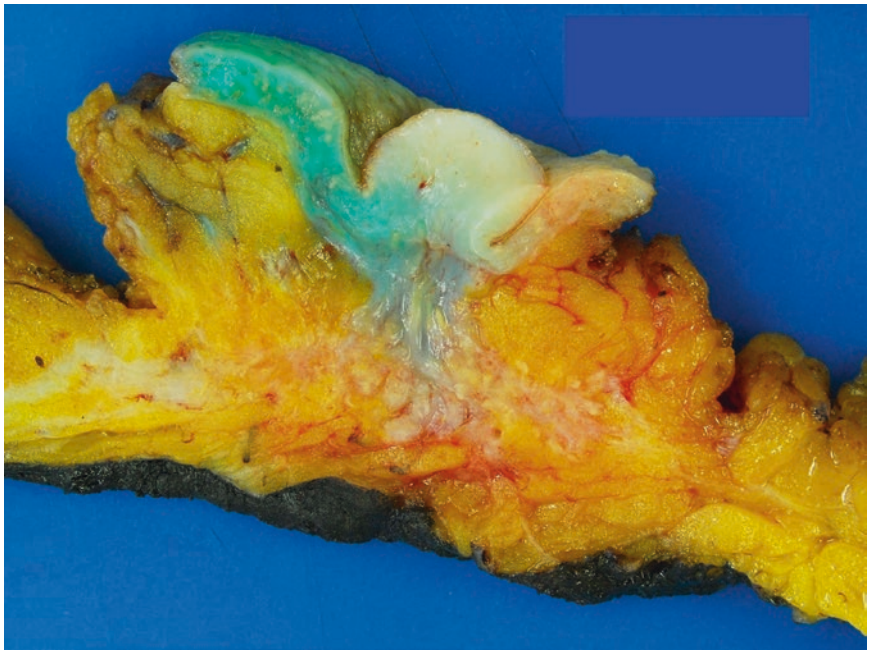

Fig. 9.42 DCIS, high nuclear grade. Mastectomy shows grey to yellow nodularities in the breast parenchyma deep to the nipple

Fig. 9.43 DCIS extensively involving the breast. Parenchymal fibrosis is interspersed with multiple cysts containing pale yellow, brown, and haemorrhagic contents. Some of the macroscopic cysts correspond histologically to cystically dilated ducts involved by DCIS, with the yellowish contents representing necrotic material

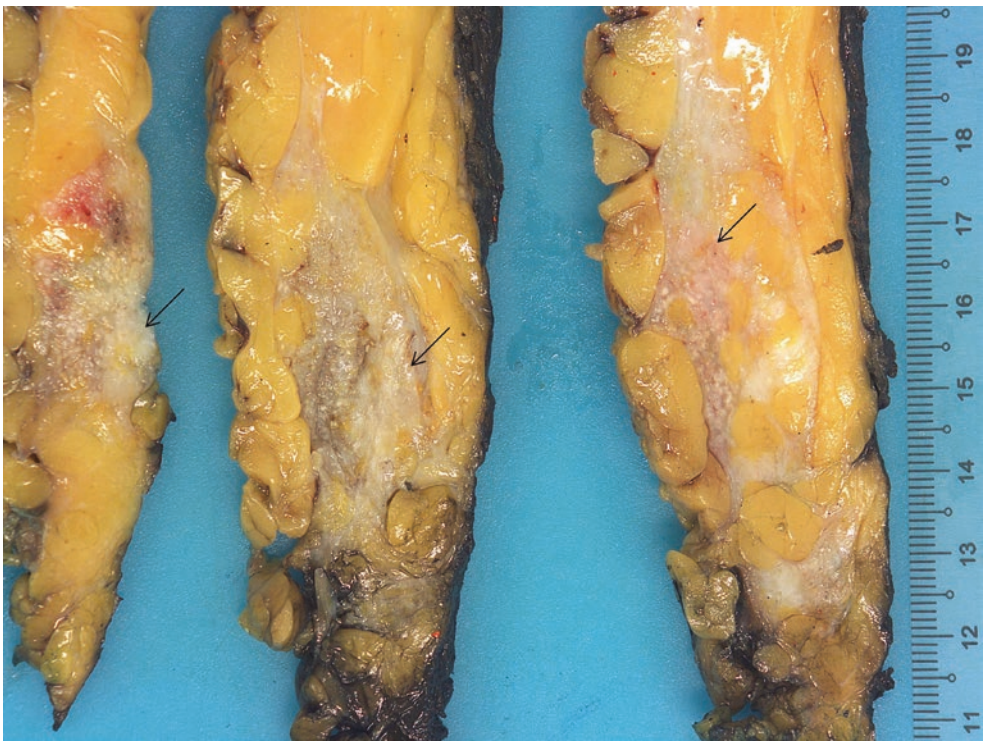

Fig. 9.44 DCIS shows multiple small nodularities within the fibrous breast parenchyma. More solid, fleshy areas correspond histologically to invasive carcinoma (*arrows*). It is important to detect and sample these solid areas during macroscopic evaluation of the specimen, in order not to miss associated invasive disease

Microscopic Pathology

DCIS shows a variety of histological patterns, with cribriform, comedo, micropapillary, solid, and papillary architectures being the most frequently observed (Figs. 9.45, 9.46, 9.47, 9.48, 9.49, 9.50, 9.51, 9.52, 9.53, and 9.54). Less commonly, clear-cell (Fig. 9.55) and spindle forms are seen, the latter classified with solid papillary carcinoma in situ. These patterns do not have predictive or prognostic impact, although the micropapillary variety has been reported to be more often multicentric (Figs. 9.56 and 9.57) [10]. DCIS is currently classified according to nuclear grade, with low-, intermediate-, and high-grade categories. The presence of necrosis is an important feature, and calcifications allow correlation with radiological findings. Larger cases of DCIS are more often associated with occult invasion. High nuclear grade DCIS may be accompanied by stromal fibrosis and chronic inflammation, with the distorted contours of the involved spaces sometimes mimicking invasion. Overexpression of the protein c-erbB-2 is observed more frequently in DCIS, especially the high-grade variety, than in invasive carcinoma (Fig. 9.58).

Differential Diagnosis

Low Nuclear Grade DCIS Versus Lobular Carcinoma In Situ (Classic)

The solid pattern of low nuclear grade DCIS may resemble classic lobular carcinoma in situ (LCIS). In contrast to the pavemented cell arrangement with well-defined cytoplasmic membranes of DCIS, the cells of LCIS are discohesive, with indistinct membranes and cells falling away from each other. Occasional intracytoplasmic lumens are seen. Adjacent atypical lobular hyperplasia with pagetoid involvement of ducts may support a lobular phenotype of the solid epithelial proliferation, whereas other patterns of DCIS may be seen in continuity with solid DCIS. Immunohistochemistry for E-cadherin can arbitrate. It is important to make the distinction on core biopsies, as the diagnosis of DCIS requires surgical excision, but classic LCIS may not always warrant excision, depending on radiologic–pathologic correlation (Figs. 9.59, 9.60, 9.61, 9.62, 9.63, and 9.64).

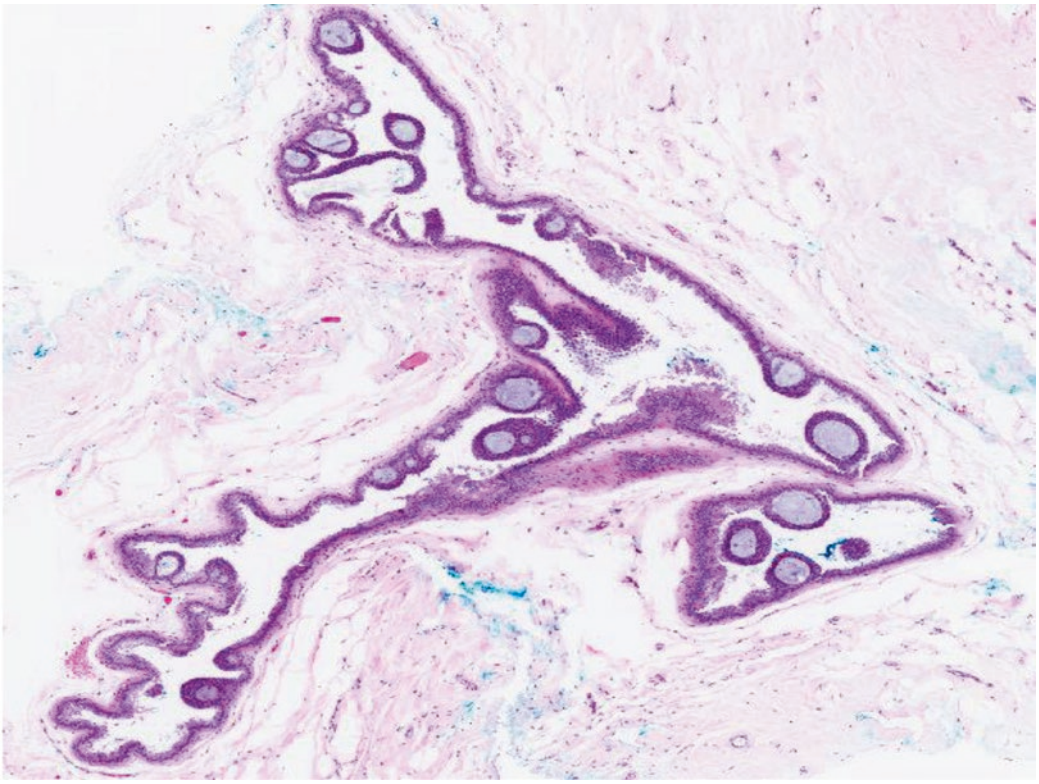

Fig. 9.45 DCIS, low nuclear grade, micropapillary and cribriform patterns with rigid arches. Two duct spaces are involved by the cytoarchitecturally atypical epithelial population. The maximal lesional extent exceeds 2 mm. The differential diagnosis is ADH, but the involvement of two duct spaces and the size of the lesion (exceeding 2 mm) favour low nuclear grade DCIS

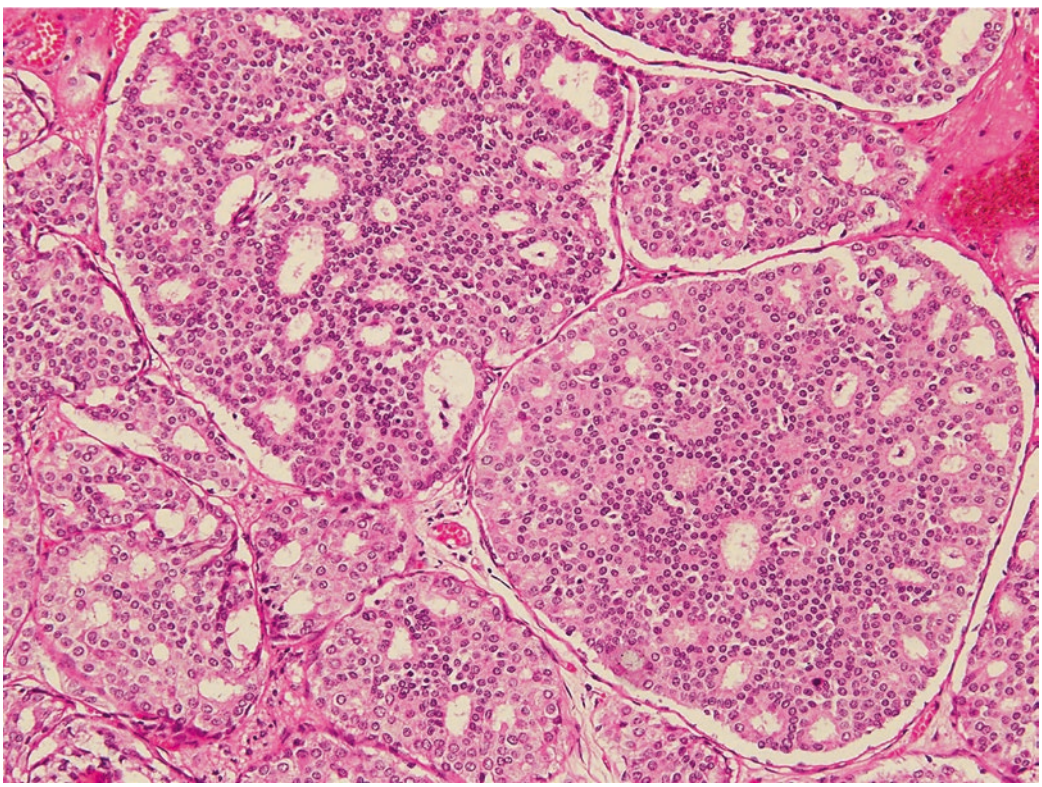

Fig. 9.46 DCIS, low nuclear grade, cribriform pattern, with punched-out, sieve-like luminal spaces among monotonous epithelial cells

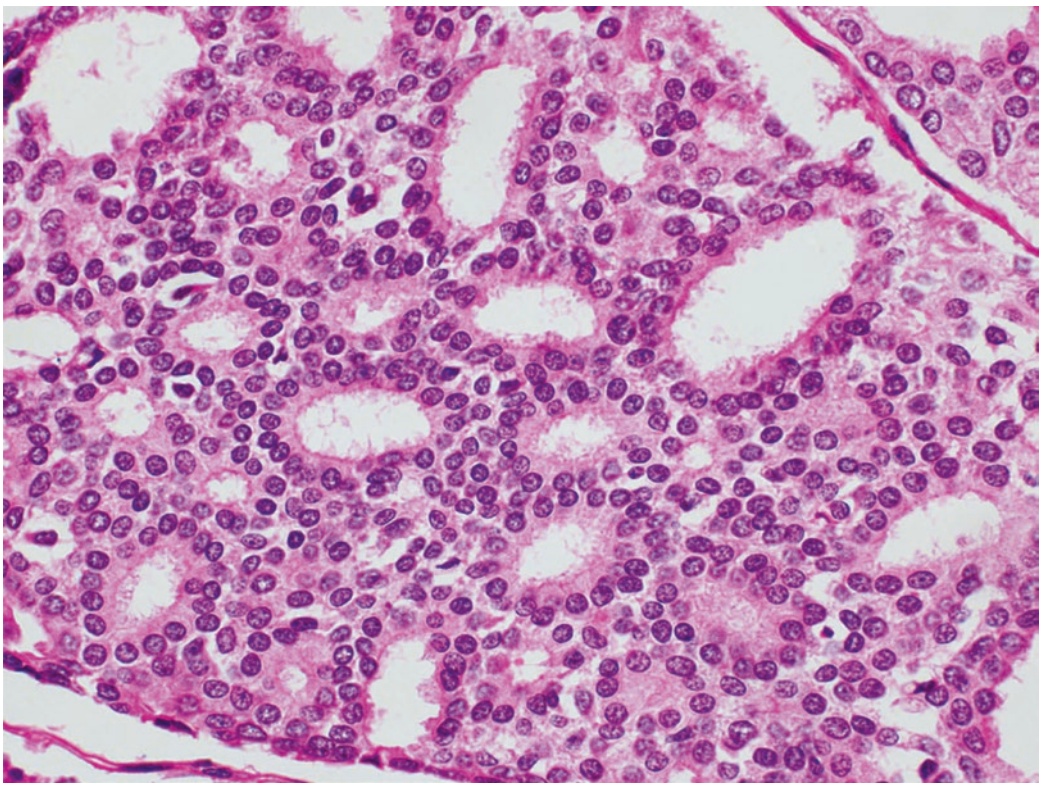

Fig. 9.47 DCIS, low nuclear grade, with cribriform spaces rimmed by epithelial cells that are polarised or oriented with their apical borders towards the cribriform lumens

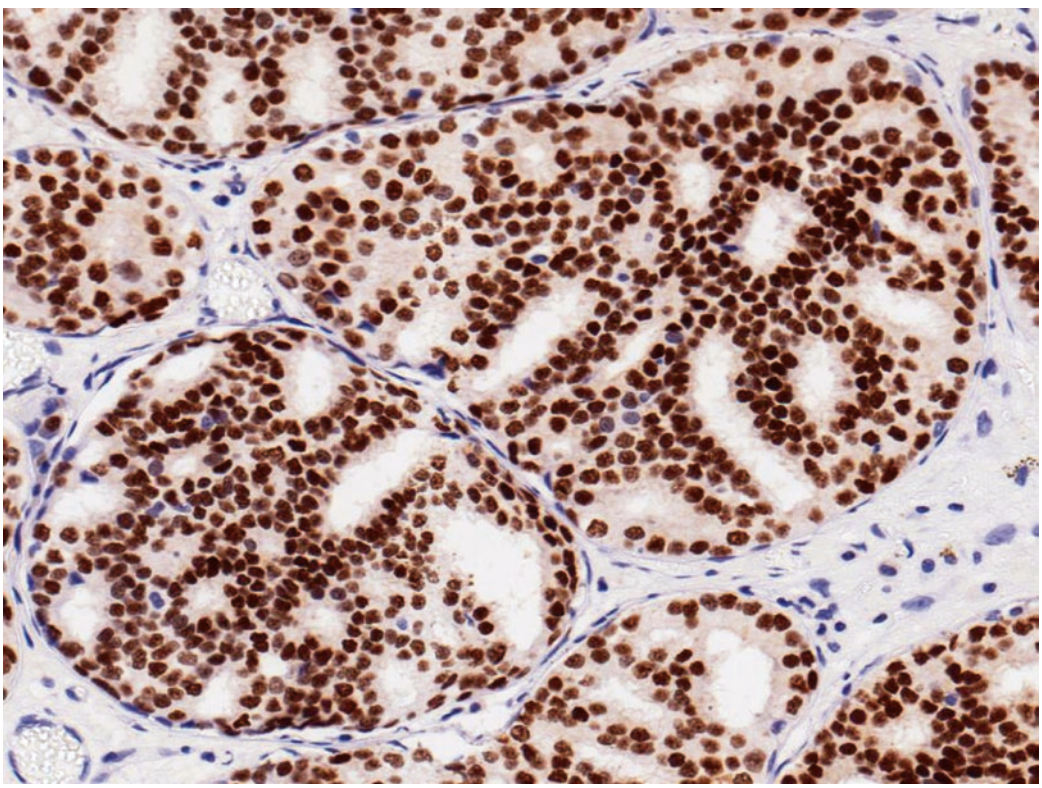

Fig. 9.48 ER immunohistochemistry in low nuclear grade DCIS, showing diffuse and uniform nuclear staining with relatively even intensity. In contrast, non-diffuse, patchy staining is seen in UDH, which demonstrates variable staining intensities

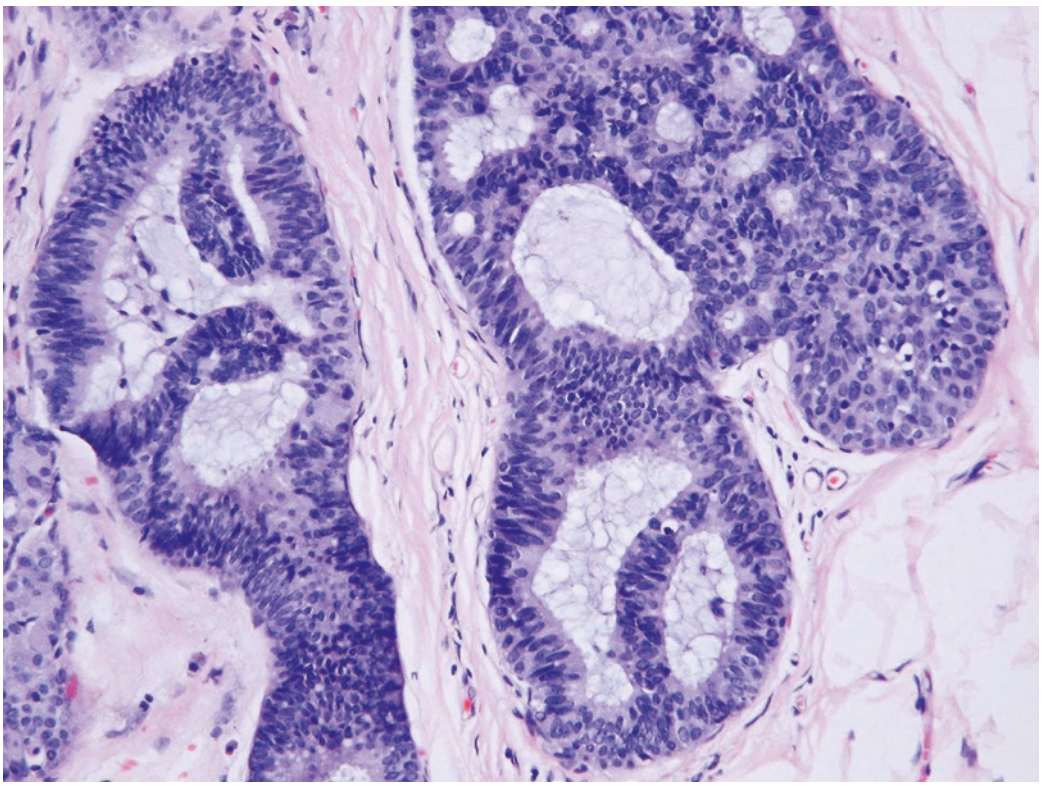

Fig. 9.49 DCIS, low nuclear grade, composed of well-defined luminal spaces and rigid epithelial bridges that show nuclei oriented perpendicularly to the direction of the bridge. Some wispy mucin is present in the luminal spaces

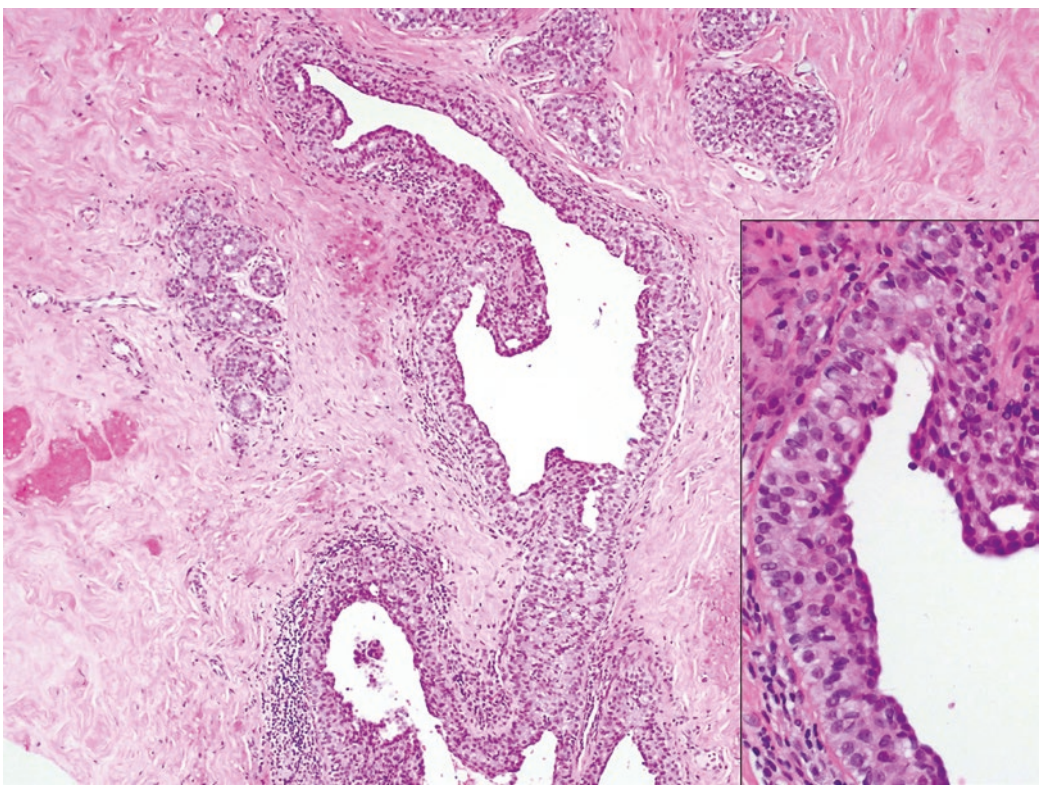

Fig. 9.50 DCIS with a pagetoid appearance, with neoplastic cells extending along a duct. *Inset* shows the attenuation of the luminal layer of epithelial cells, with DCIS cells containing enlarged vesicular nuclei with visible nucleoli insinuating between the luminal epithelial and myoepithelial cells. Pagetoid extension is usually described as a feature of lobular neoplasia, but infrequently it can also be encountered in DCIS

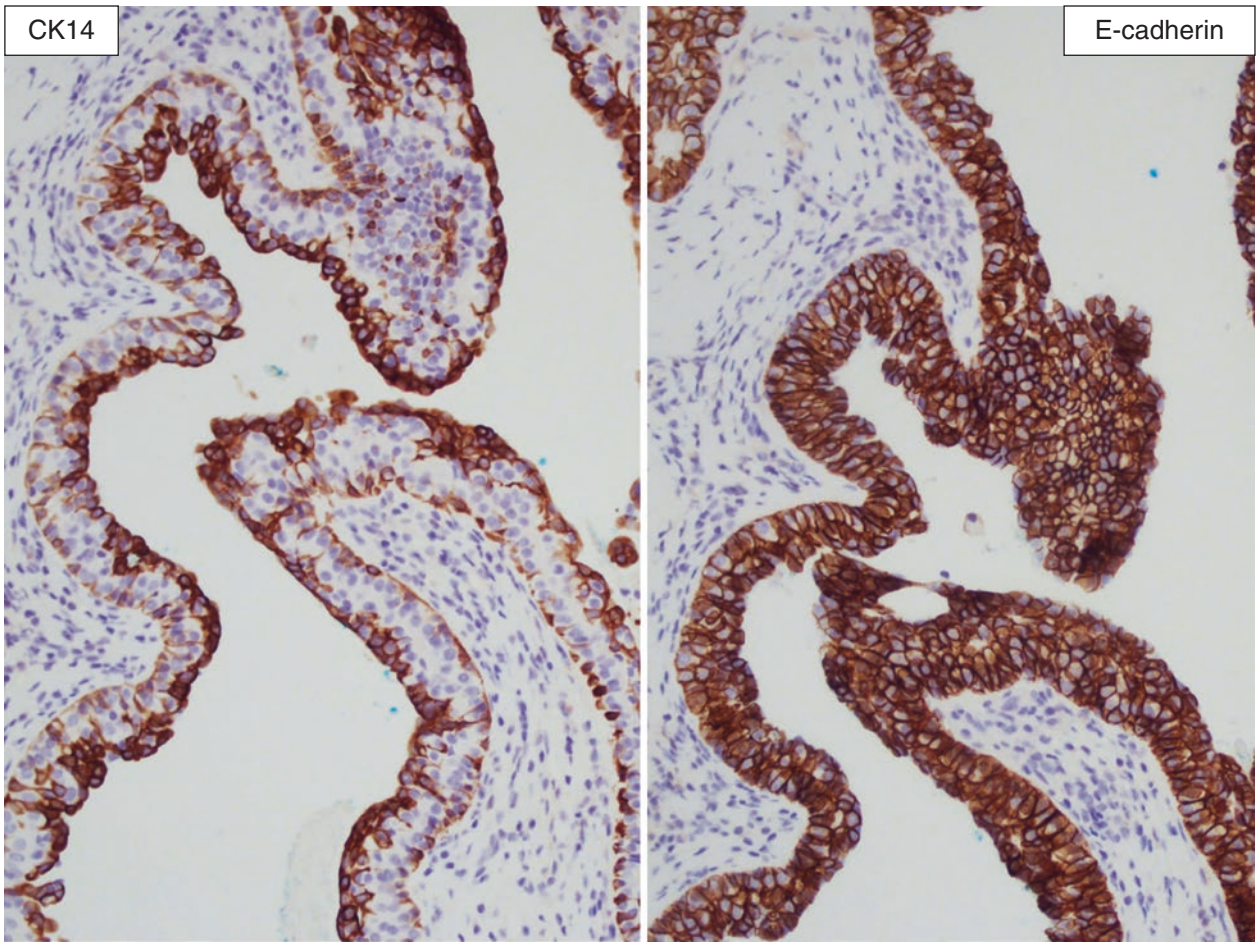

Fig. 9.51 DCIS with a pagetoid appearance. Immunohistochemistry for CK14 shows negative reactivity of the tumour cells; immunohistochemistry for E-cadherin shows complete membrane staining, supporting a ductal phenotype of the tumour cells

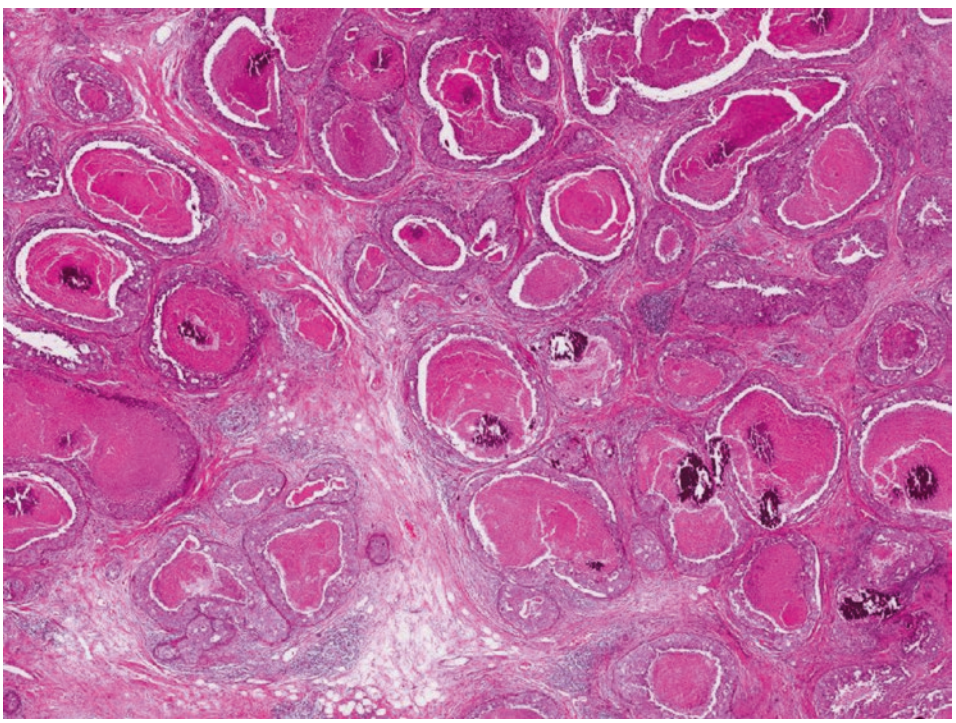

Fig. 9.52 DCIS, high nuclear grade with comedonecrosis and calcifications

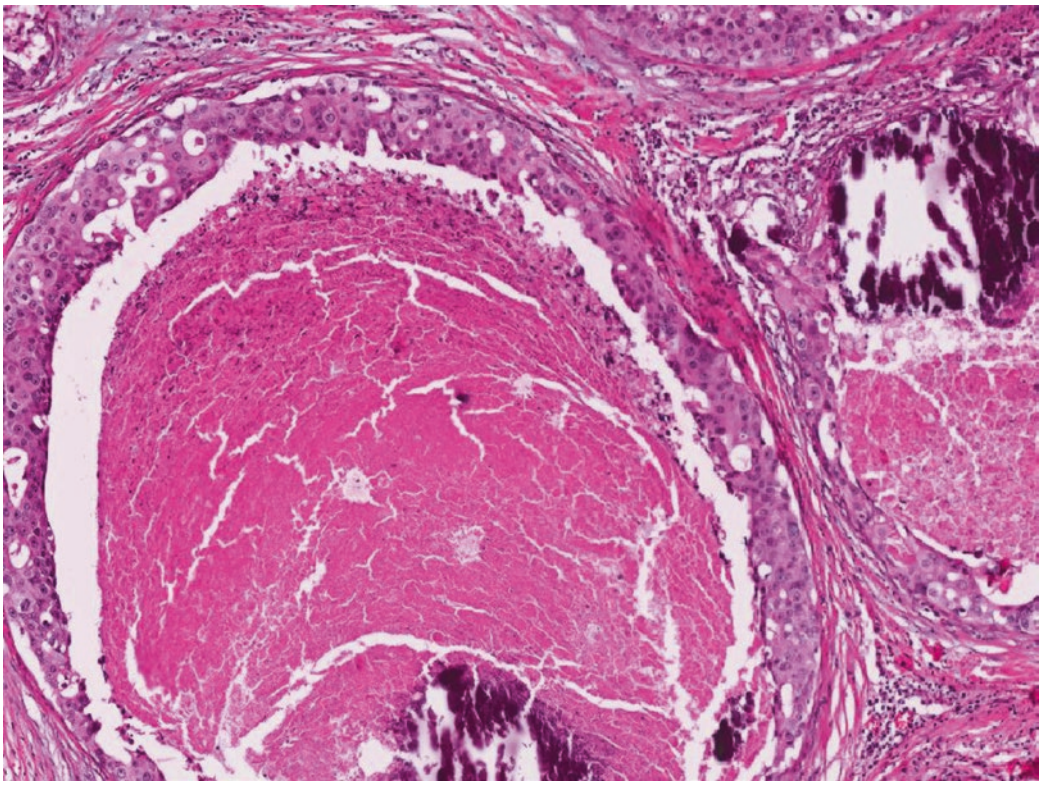

Fig. 9.53 High nuclear grade DCIS. Necrosis composed of amorphous debris with karyorrhexis is present within the ductal lumens. Fractured calcifications are observed within the necrosis

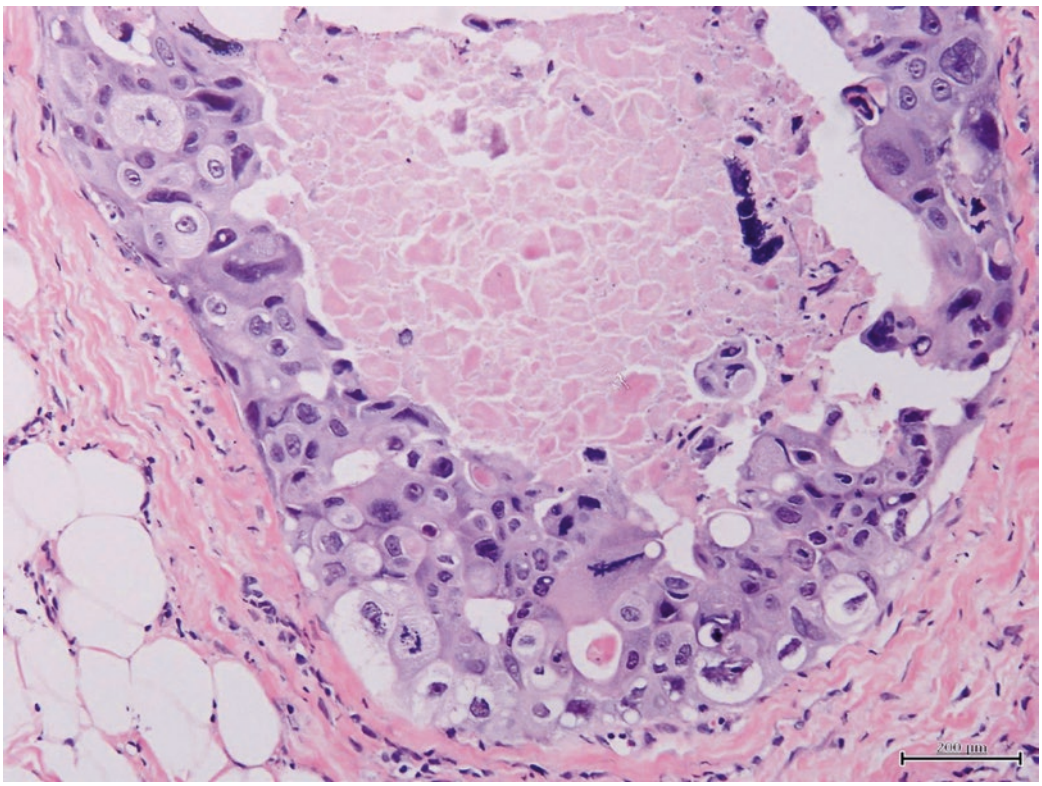

Fig. 9.54 High nuclear grade DCIS with comedonecrosis. Tumour cells show marked nuclear pleomorphism with abnormal mitoses. Degenerate epithelial cells and karyorrhectic debris are found within the lumen

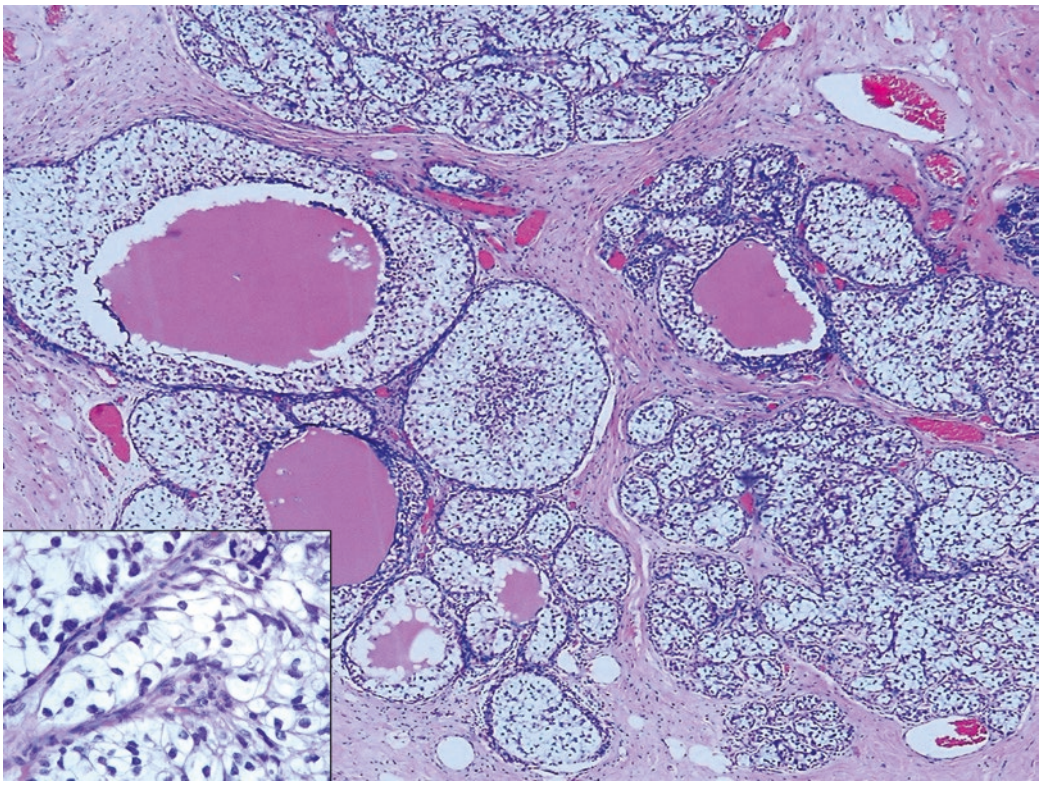

Fig. 9.55 DCIS with clear cells. Ducts with clear-cell DCIS are expanded by a population of cells with ample clear cytoplasm. A few ducts contain pink secretions. *Inset* shows high magnification of the clear cells, with ovoid, dense nuclei and abundant clear cytoplasm

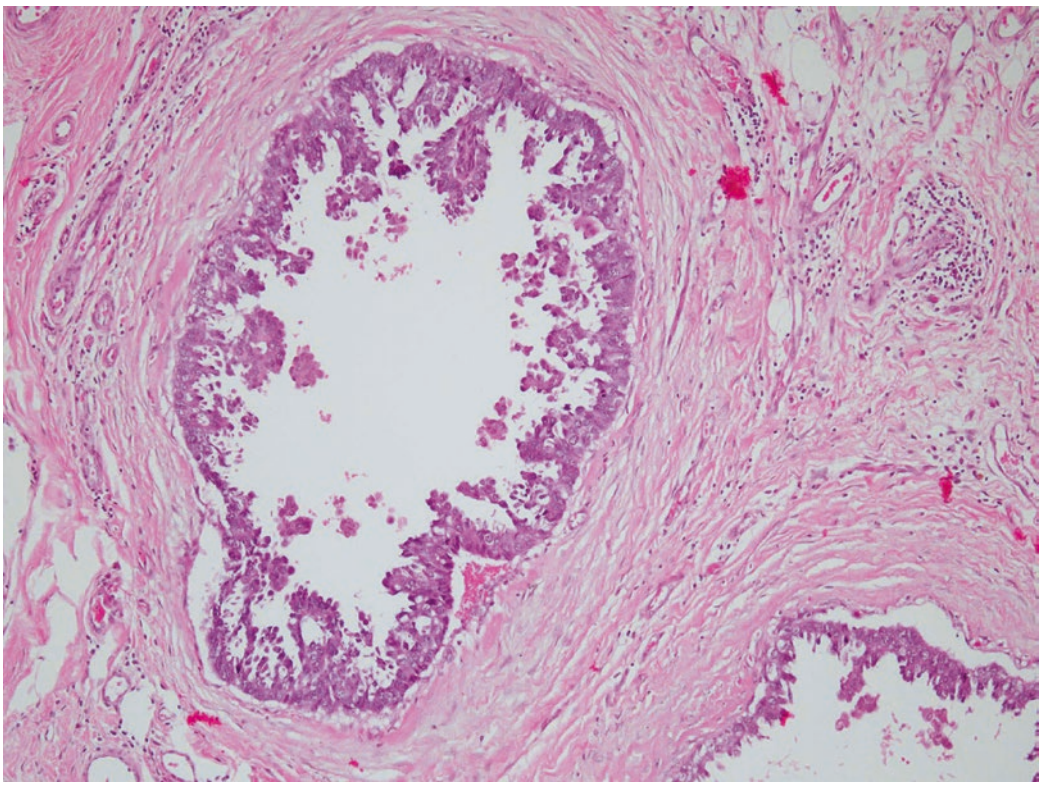

Fig. 9.56 DCIS, intermediate nuclear grade, micropapillary pattern. At low magnification, the affected ducts show micropapillary protrusions of neoplastic epithelial cells into the lumen. Some of the cells appear hobnailed. The surrounding stroma is fibrotic, with a few scattered chronic inflammatory cells

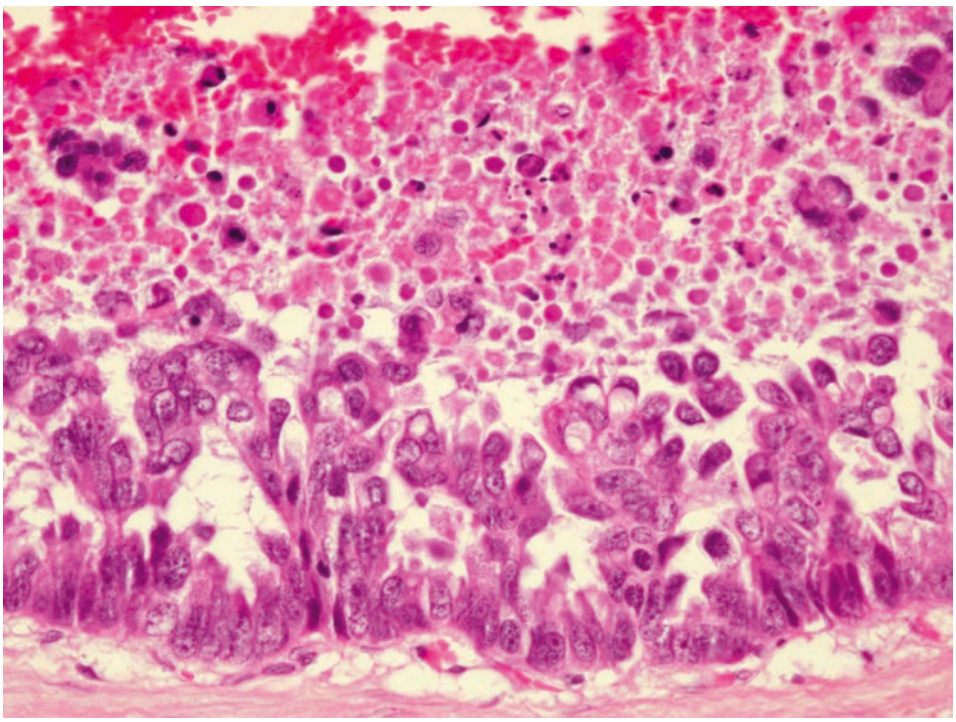

Fig. 9.57 DCIS, intermediate nuclear grade, micropapillary pattern. At high magnification, the nuclei are hobnailed and vesicular, containing small to more conspicuous nucleoli. Occasional cells with cytoplasmic vacuoles are noted. The lumen contains necrotic debris with degenerate tumour cells

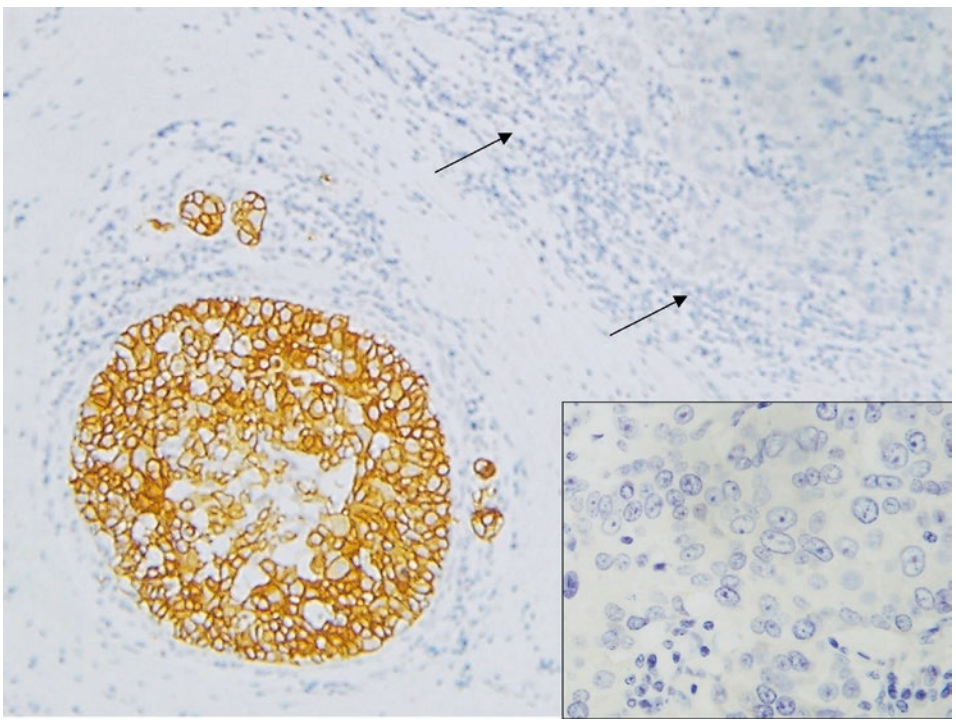

Fig. 9.58 DCIS with overexpression of c-erbB-2. In this case, the accompanying invasive ductal carcinoma is negative for c-erbB-2 (*arrows*, *inset*). Possible explanations for this discordance in c-erbB-2 expression between in situ and invasive disease may be that its expression is diminished during evolution from in situ to invasive breast carcinoma or that invasive disease occurs via mechanisms that do not involve the *c-erbB-2* gene. An alternative postulate is that a proportion of c-erbB-2-negative invasive breast cancers are preceded by a very transient in situ stage, hence diluting the overall numbers of c-erbB-2-positive invasive carcinomas as compared with DCIS. It is important to report the c-erbB-2 status for the invasive component rather than for the in situ element

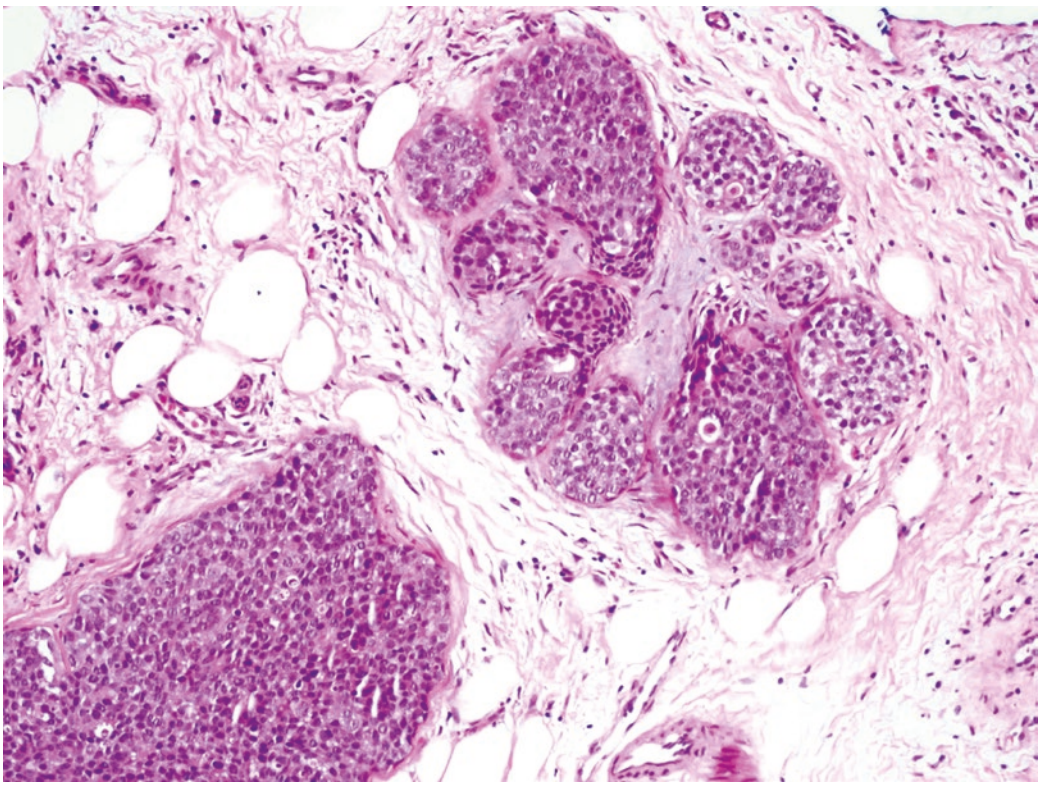

Fig. 9.59 DCIS, low nuclear grade with solid morphology. This pattern may mimic lobular carcinoma in situ, with duct and acinar spaces completely filled by the neoplastic population

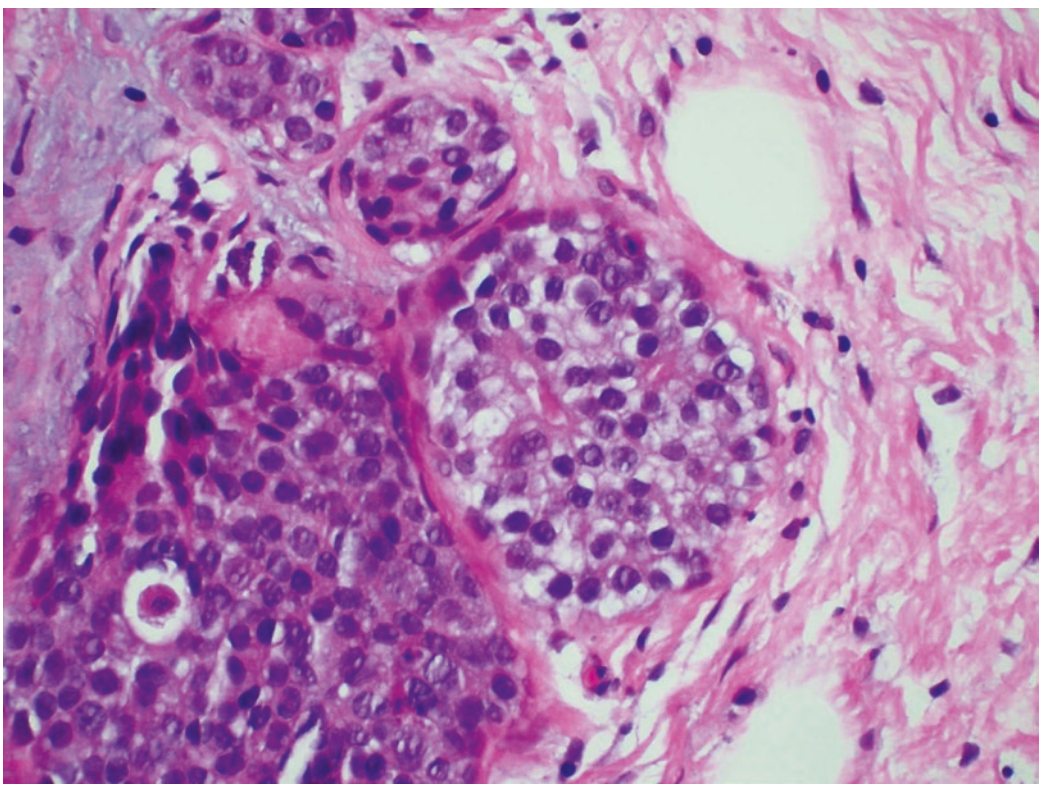

Fig. 9.60 DCIS, low nuclear grade with solid morphology. Closer scrutiny shows that the epithelial cells have relatively distinct cell boundaries, with the cell membranes tightly apposed between cells

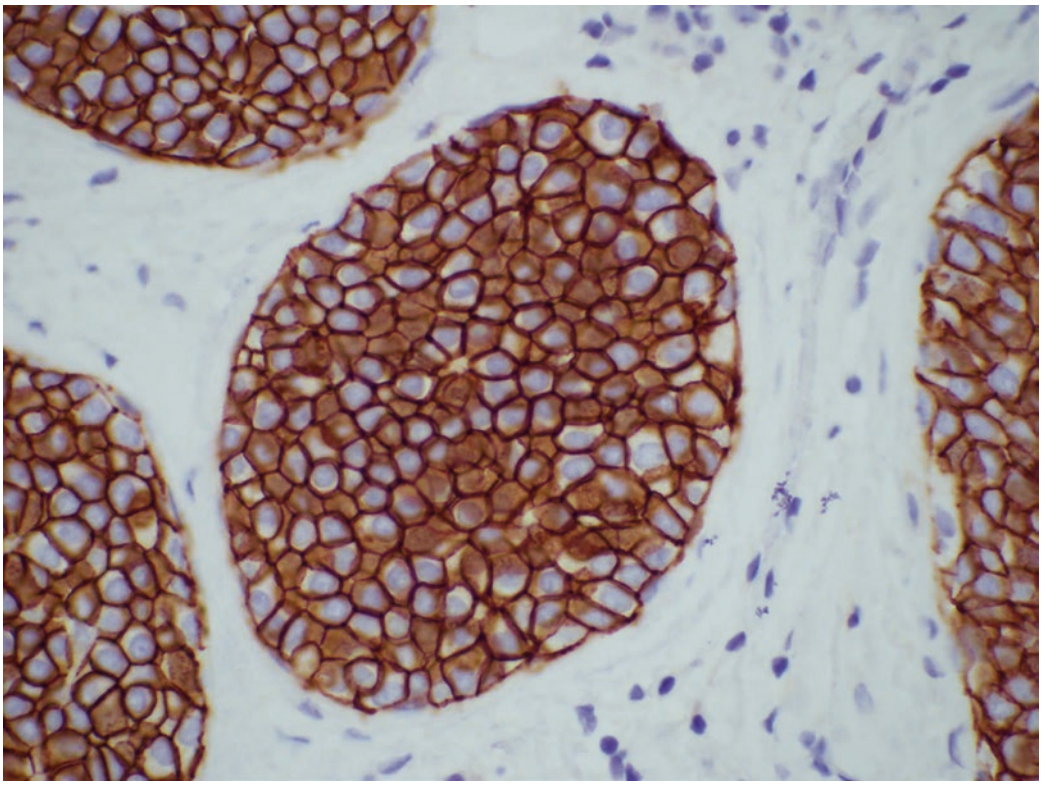

Fig. 9.61 DCIS, low nuclear grade with solid morphology. Immunohistochemistry for E-cadherin discloses complete membrane staining of the neoplastic cells, corroborating a ductal phenotype

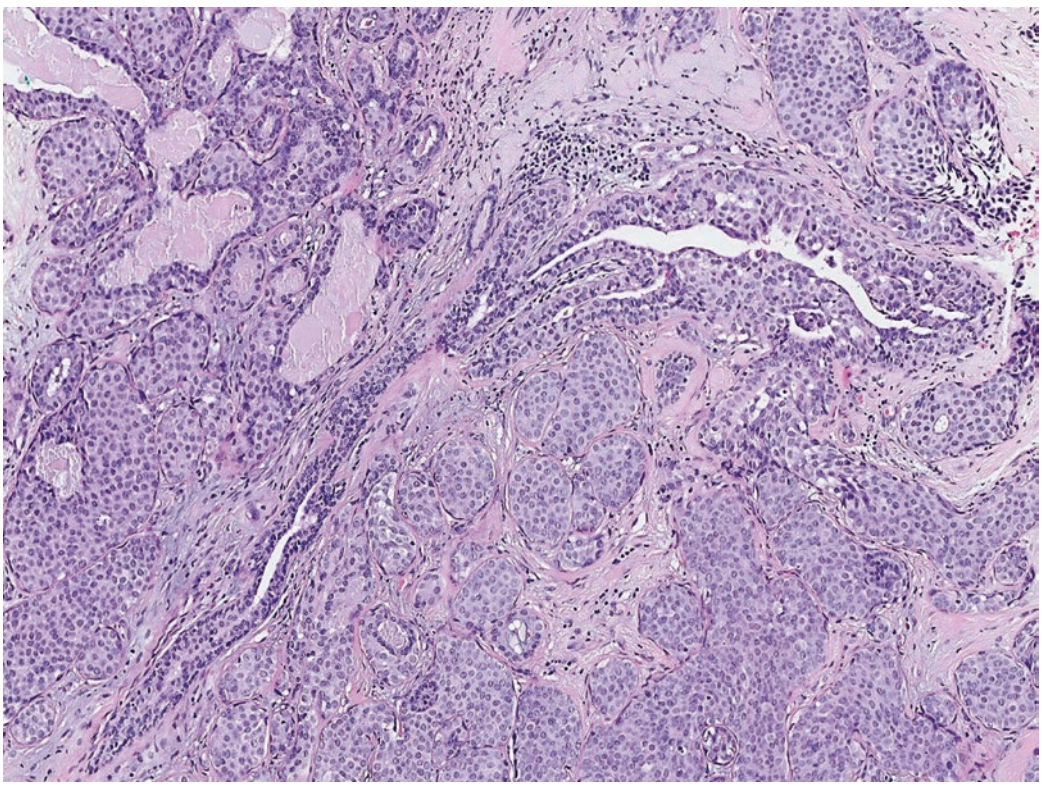

Fig. 9.62 Lobular carcinoma in situ (LCIS). Acini are distended and filled by a relatively uniform, monotonous cell population. The pagetoid extension along the terminal duct is a characteristic feature of lobular neoplasia (atypical lobular hyperplasia and LCIS)

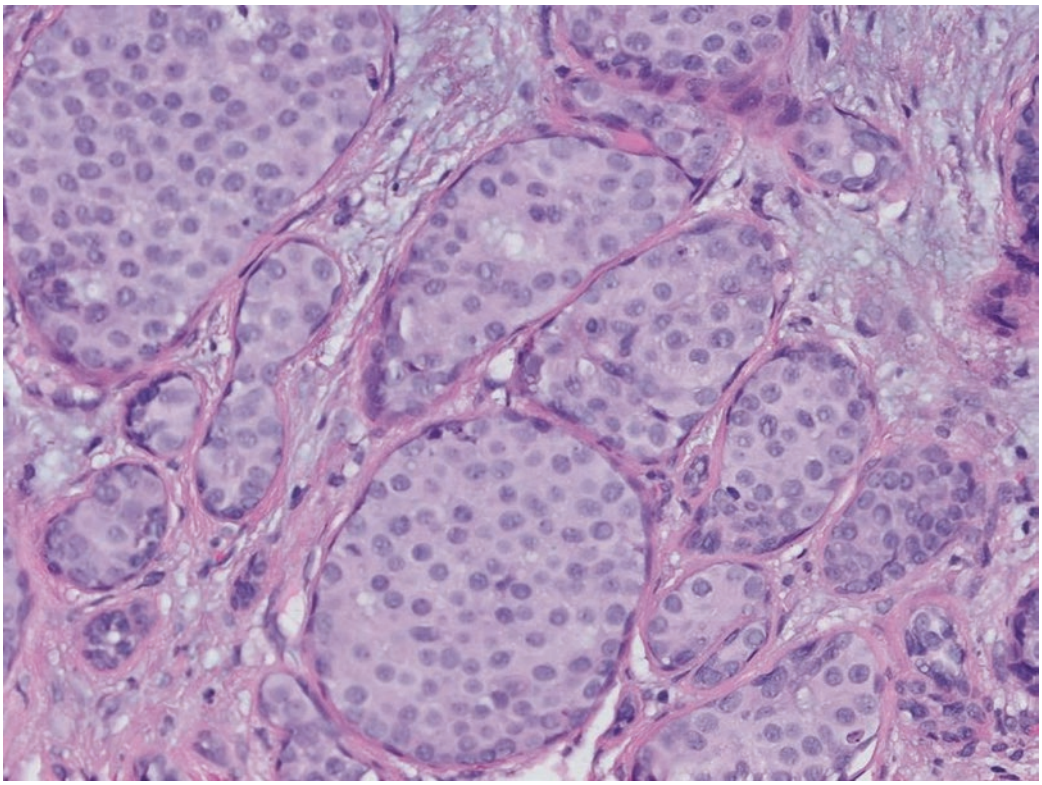

Fig. 9.63 LCIS closely mimics solid-type DCIS. Some discohesion is observed among the lobular neoplastic cells

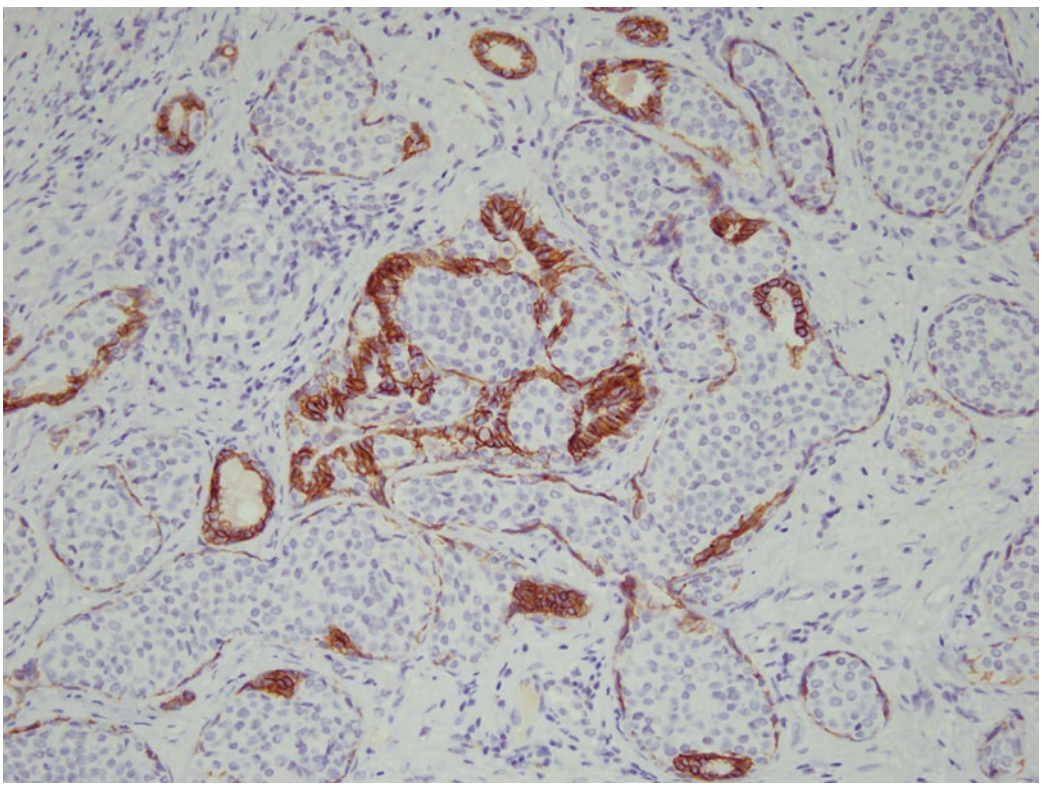

Fig. 9.64 LCIS. Immunohistochemistry for E-cadherin is negative in the lobular neoplastic cells, with positive staining observed in myoepithelial cells and residual luminal epithelial cells

Low Nuclear Grade DCIS with Spindle Cells Versus Florid UDH

Spindle cell DCIS, low nuclear grade, usually shows neuroendocrine differentiation and is part of the spectrum of solid papillary carcinomas in situ. As the spindle cells in this form of DCIS often show a streaming appearance, they mimic benign UDH. Spindle cell DCIS tends to occur in older women presenting with bloody nipple discharge. Histology shows uniform spindle cells with relative lack of nuclear overlapping, fine stippled nuclear chromatin, granular cytoplasm, and absence of slit-like secondary luminal spaces. Immunohistochemistry shows diminished or absent staining for CK5/6 and CK14, but ER is diffusely positive (Figs. 9.65, 9.66, 9.67, and 9.68) [11].

High Nuclear Grade DCIS Versus Pleomorphic Lobular Carcinoma In Situ

Pleomorphic LCIS is not infrequently mistaken for high nuclear grade DCIS with both lesions often showing comedonecrosis and calcifications. Clues to pleomorphic LCIS are cellular discohesion, presence of classic LCIS, as well as atypical lobular hyperplasia. An apocrine cytomorphology is commonly associated with pleomorphic LCIS although apocrine features can also be found in high nuclear grade DCIS. Immunohistochemistry for E-cadherin can help make the distinction, though in many institutions, pleomorphic LCIS is often managed in a similar manner to DCIS (Figs. 9.69 and 9.70).

DCIS Versus Microinvasive Carcinoma

Microinvasive carcinoma is defined as an invasive focus measuring not more than 1 mm in maximal extent. In high nuclear grade DCIS, the distortion of affected duct outlines, with resulting irregular protrusions of tumour cells within an inflamed background, may resemble microinvasion, but these protrusions retain contact with the duct involved by DCIS and may also sometimes manifest myoepithelial cells, which can be further confirmed with immunohistochemistry. Tangential sectioning and lobular involvement by DCIS may lead to small tumour nests emerging from a variably inflamed background, suggesting microinvasion. When further levelled, however, these foci disappear or show their contiguity with adjacent intact ducts (Figs. 9.71, 9.72, 9.73, and 9.74).

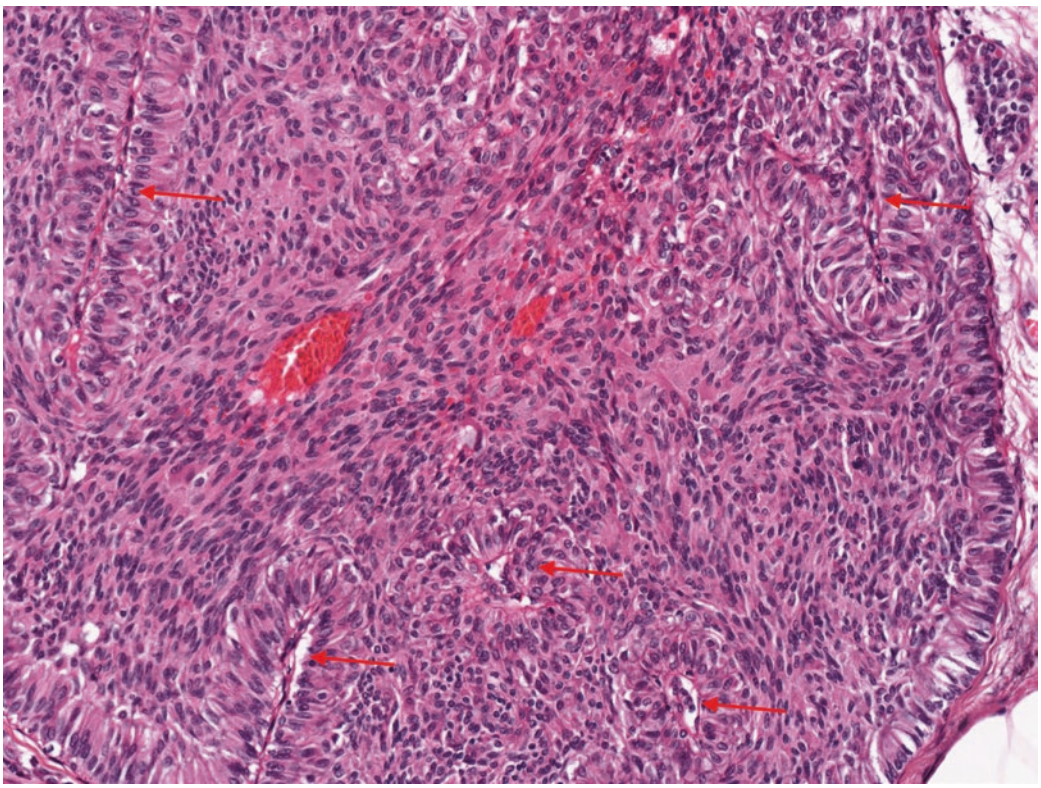

Fig. 9.65 Spindle cell DCIS with low nuclear grade mimics florid UDH. Clues are the relatively uniform spindle population and fine, narrow vessels coursing into the solid epithelial proliferation (*red arrows*), suggesting that this lesion belongs to the solid papillary carcinoma group. Occasionally, small intercellular mucin puddles may be discerned, not present in this case

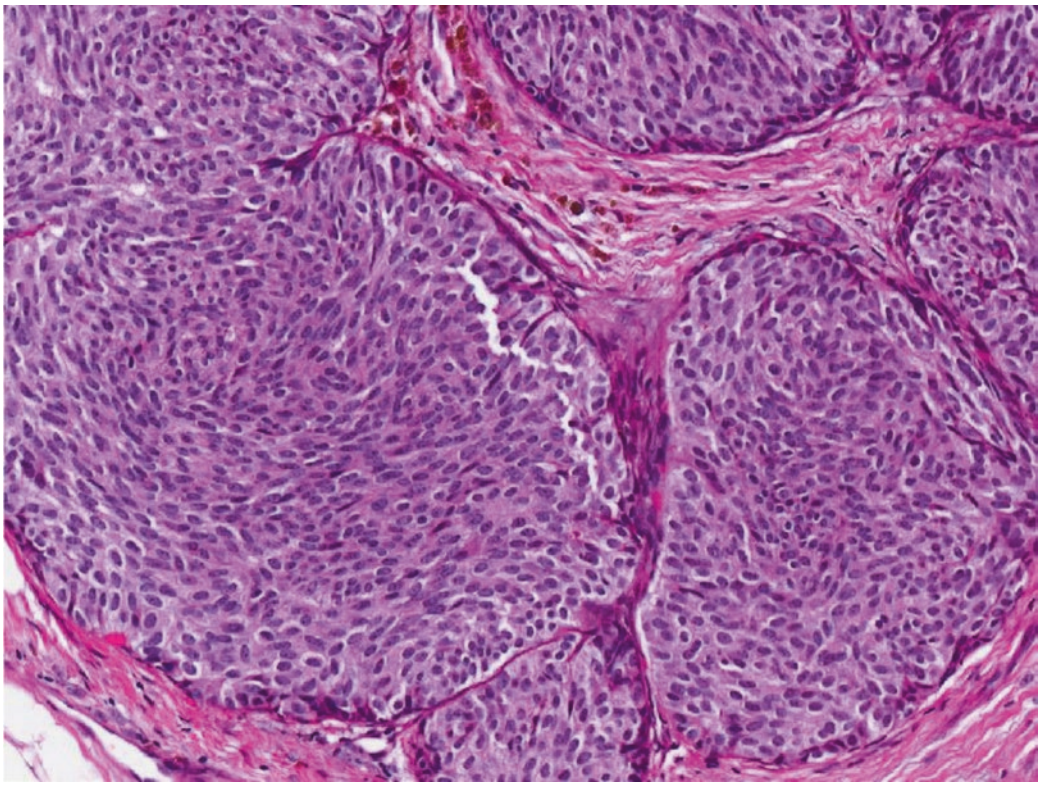

Fig. 9.66 Spindle cell DCIS with low nuclear grade. Ducts are expanded and filled with a uniform and monotonous epithelial population of spindle cells, which stream and swirl in a similar single direction without significant nuclear overlapping.

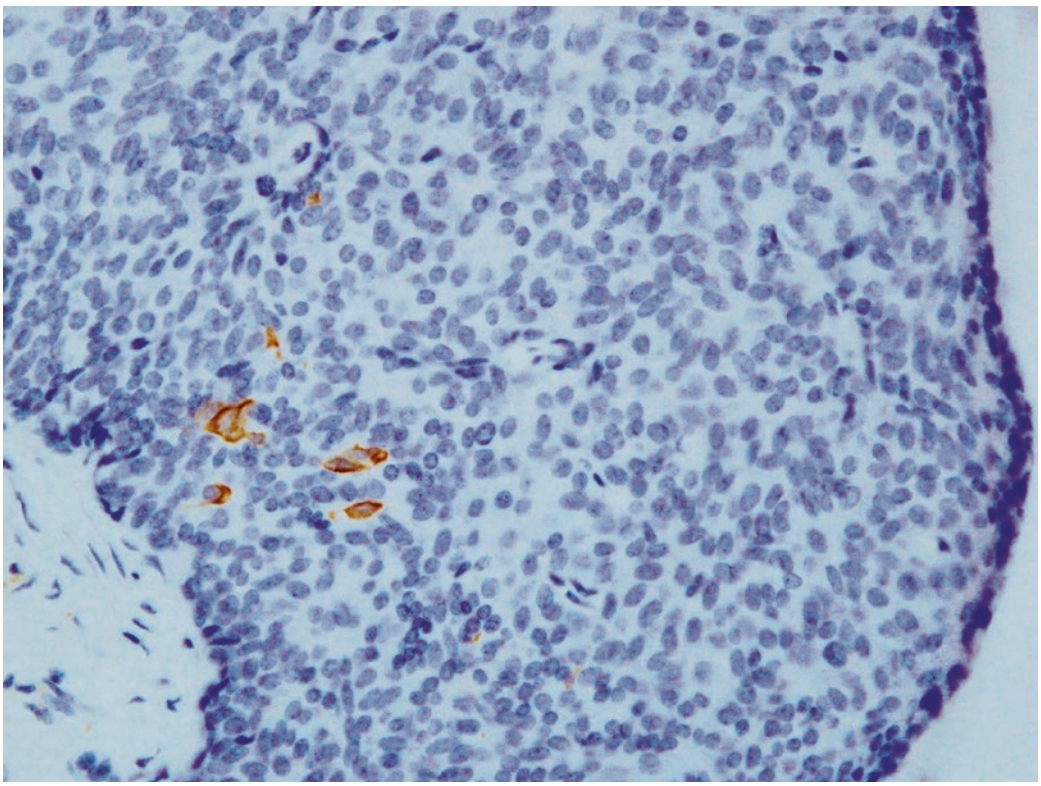

Fig. 9.67 Spindle cell DCIS. Immunohistochemistry for CK14 shows hardly any staining among the epithelial cells

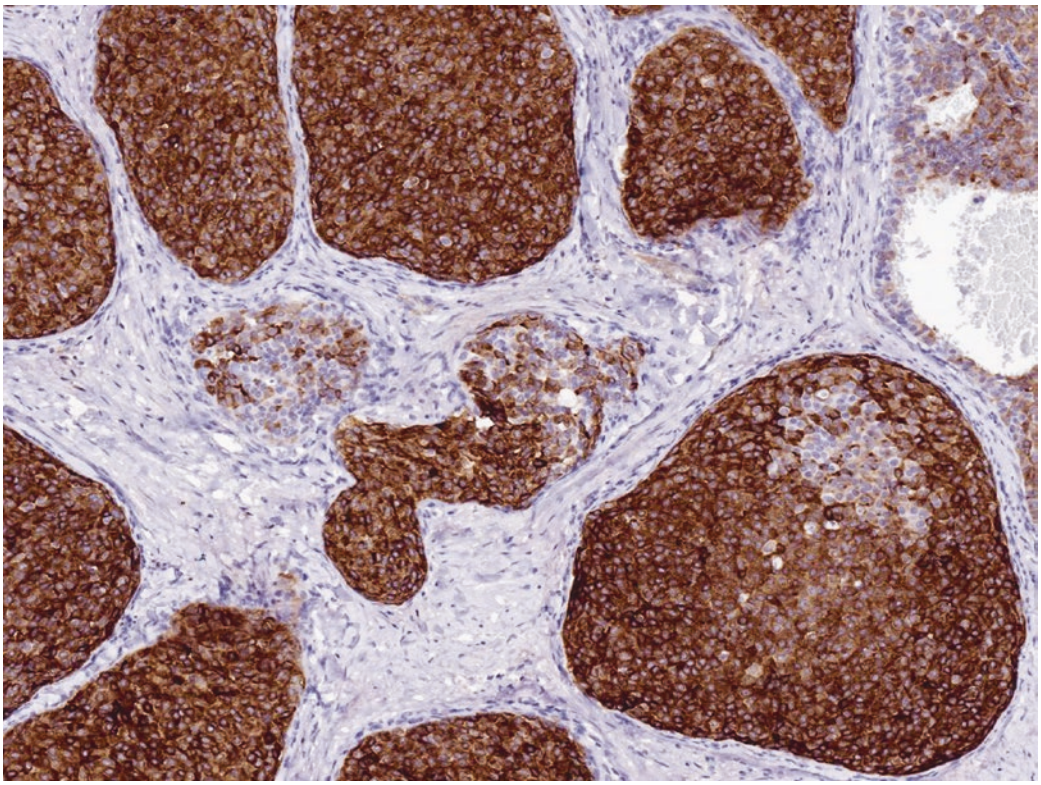

Fig. 9.68 Spindle cell DCIS. Synaptophysin immunohistochemistry shows diffuse positivity, indicating neuroendocrine differentiation, which is often encountered in solid papillary carcinoma

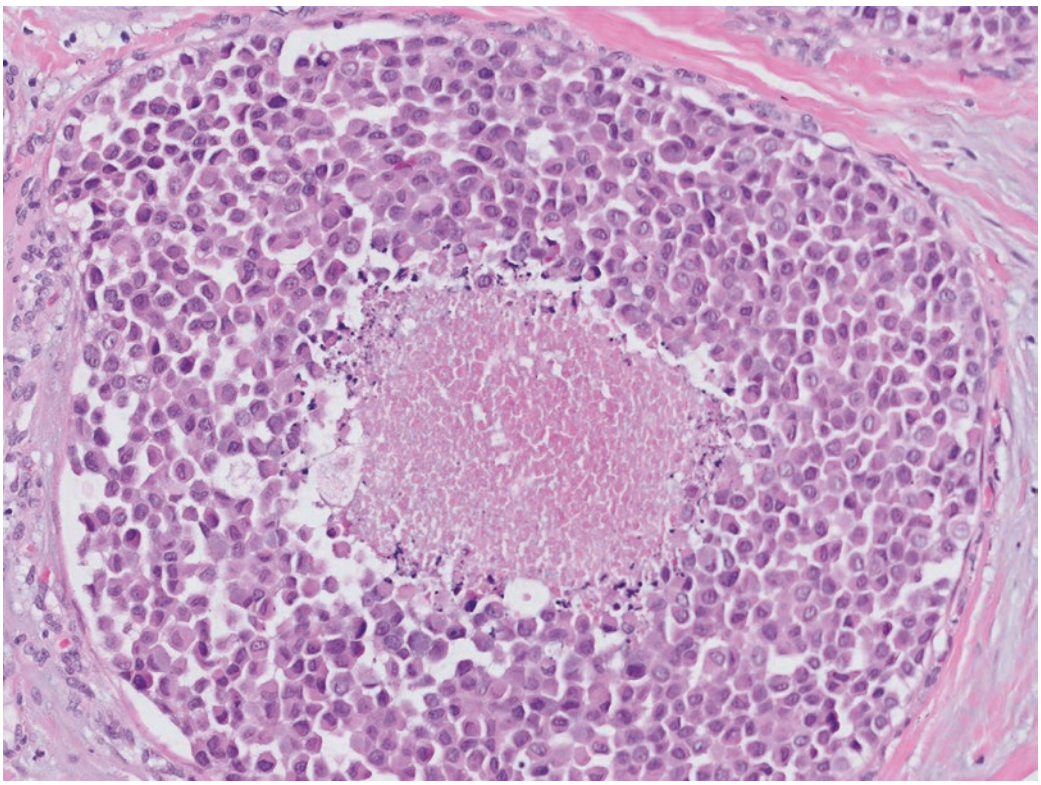

Fig. 9.69 LCIS with necrosis and pleomorphic features, mimicking high nuclear grade DCIS. The malignant cells are poorly cohesive and have pink cytoplasm reminiscent of an apocrine appearance

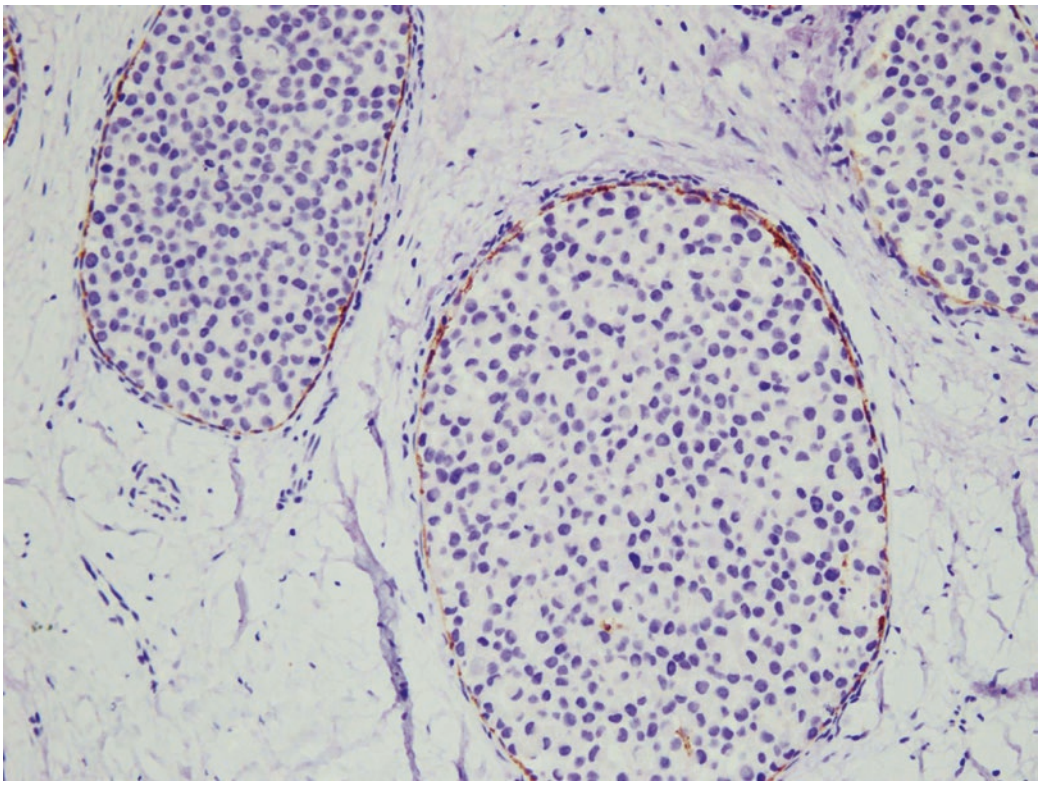

Fig. 9.70 LCIS with pleomorphic features. Immunohistochemistry for E-cadherin is negative in the tumour cells, confirming a lobular Phenotype. Necrosis is not observed here

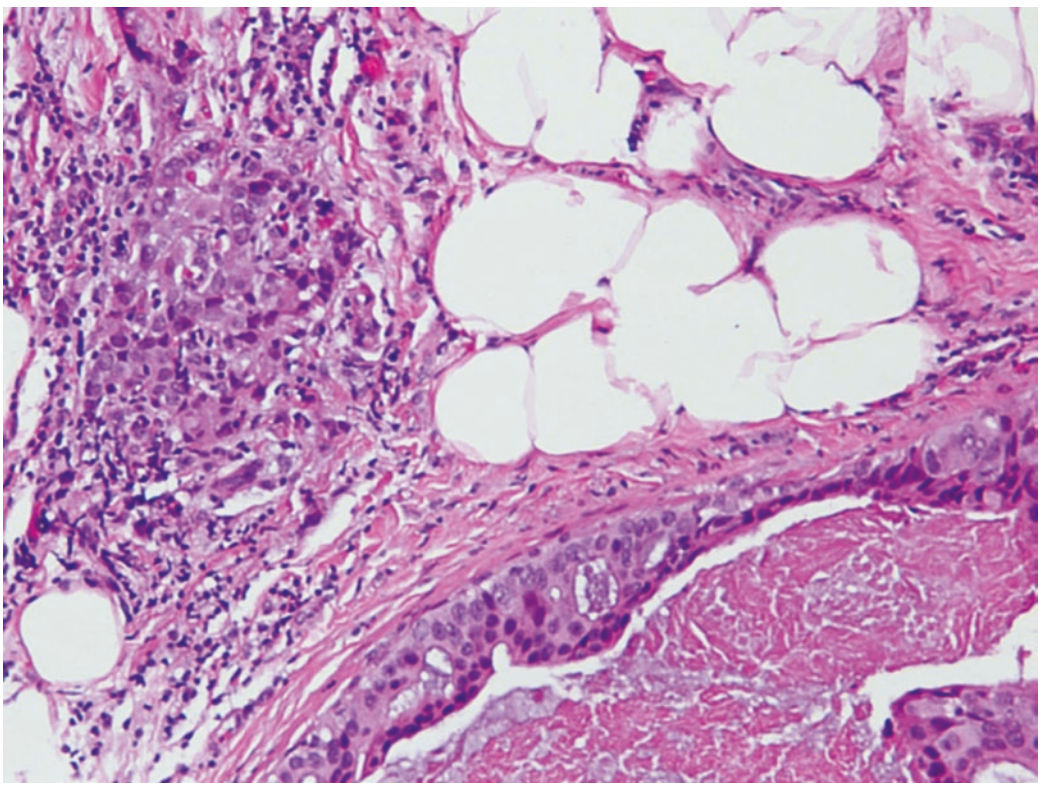

Fig. 9.71 DCIS with adjacent microinvasion. Microinvasion is defined as invasive carcinoma that measures up to 1 mm in maximal extent. In this case, a duct involved by DCIS is present in the right lower field. In the immediate vicinity are nests of tumour cells that have irregular contours, accompanied by chronic inflammation. These irregular nests measure less than 1 mm in maximal extent. The measurement is determined from the actual size of the invasive focus, and does not include the distance of the invasive focus from the basement membrane of the adjacent duct affected by DCIS

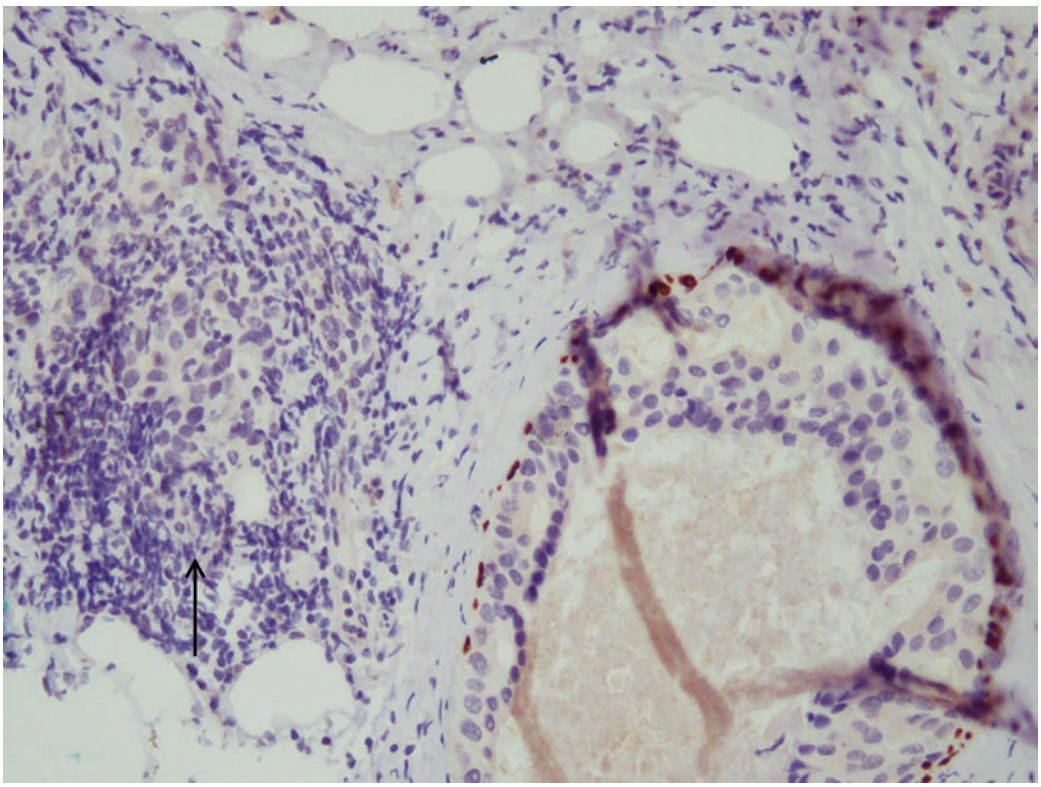

Fig. 9.72 DCIS with microinvasion. Immunohistochemistry for p63 shows intact myoepithelial cells around the island of DCIS. In contrast, they are absent from the nests of microinvasive carcinoma (*arrow*)

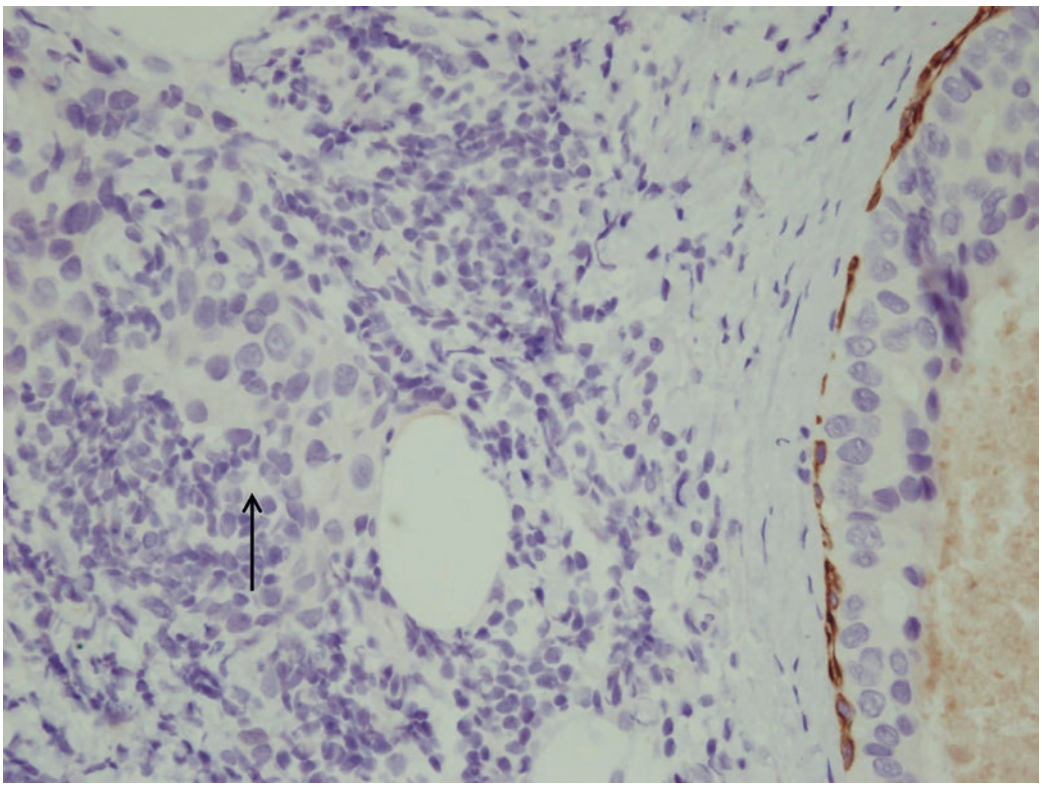

Fig. 9.73 DCIS with microinvasion. Immunohistochemistry for CK5/6 shows intact myoepithelial cells around the island of DCIS, in contrast to their absence from the nests of microinvasive carcinoma (*arrow*)

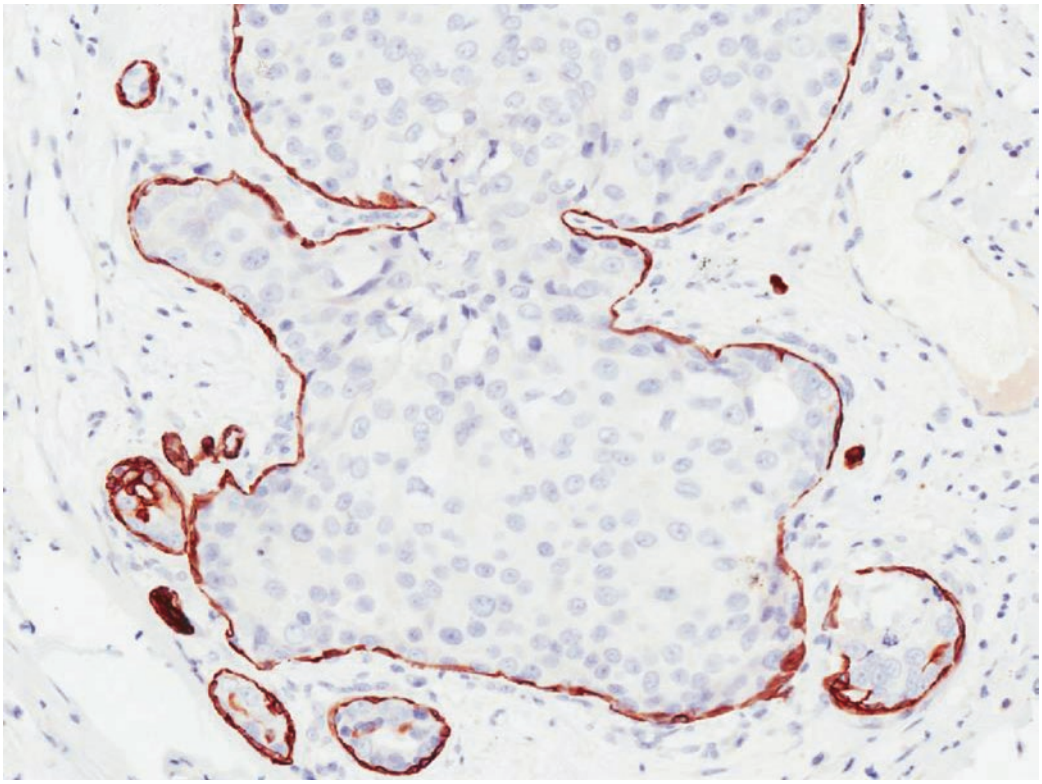

Fig. 9.74 DCIS with irregular protrusions mimicking microinvasion. In this duct affected by DCIS, there are bulges of tumour cells into the stroma, as well as smaller, rounded nests in close proximity. No stromal reaction is present, and the presence of CK14-positive myoepithelial cells around these nests indicates that they are non-invasive and are likely to be tangential sections of the outer, undulant contours of the DCIS-affected duct

DCIS Superimposed on Sclerosing Adenosis Versus Invasive Carcinoma

It can be particularly challenging to differentiate invasive carcinoma from DCIS superimposed on sclerosing adenosis. Not infrequently, invasive carcinoma has been erroneously diagnosed in such cases. It is useful to survey the lesion at low magnification, whereupon the lobular architecture of the underlying sclerosing adenosis may be appreciated. Often, benign ductules of sclerosing adenosis that are uninvolved by DCIS may be observed at the lesional periphery and merging with it. Another clue is the presence of an intact, hyaline basement membrane sheath around sclerosing adenotic ducts within unperturbed compact stroma, although it is noted that some invasive carcinomas may also elaborate basement membrane material. Immunohistochemistry can affirm the presence of myoepithelial cells around DCIS superimposed on sclerosing adenosis (Figs. 9.75, 9.76, 9.77, 9.78, 9.79, 9.80, 9.81, 9.82, 9.83, 9.84, 9.85, 9.86, and 9.87).

DCIS Versus Lymphovascular Emboli

Tumour emboli plugging lymphovascular spaces can resemble DCIS, with endothelial nuclei mimicking those of myoepithelial cells. D2-40, which decorates endothelial cells, is also reactive with myoepithelial cells and hence is not useful in this setting (Fig. 9.88). DCIS is either observed as an expanded lobule with several duct spaces involved by the malignant epithelial proliferation or seen adjacent to other unaffected lobules. In contrast, lymphovascular emboli are often noted at the advancing front of an invasive tumour and may be located together with other vessels, away from lobules. Myoepithelial immunohistochemistry is helpful, with antibodies to p63 and basal cytokeratins being potentially more suitable than smooth muscle ones, which may also decorate smooth muscle fibres around vascular spaces (Fig. 9.89).

Prognosis and Therapy Considerations

DCIS is a non-obligate precursor of invasive carcinoma. The duration to progression varies; high-grade forms transform to invasive disease more quickly than low-grade lesions, which can take many years before invasion occurs. Current management of DCIS is complete excision with negative margins. Adjuvant radiation is usually administered for conservatively excised cases. Hormonal therapy has a role in hormone receptor-positive DCIS. A trial of active surveillance in non-high grade DCIS diagnosed on core biopsy is underway in the United Kingdom [12].

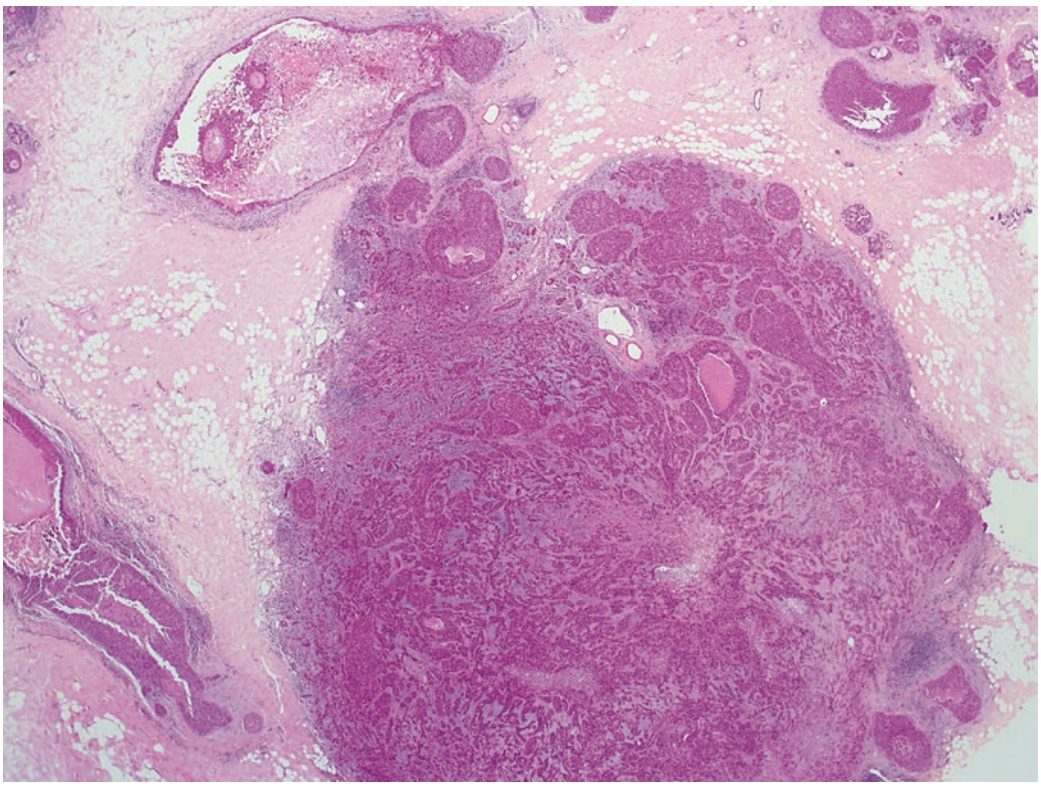

Fig. 9.75 DCIS superimposed on sclerosing adenosis closely mimicking invasive carcinoma. At low magnification, there is a cellular tumour nodule with relatively circumscribed boundaries within breast tissue that also displays DCIS in surrounding ducts and lobules. Chronic inflammation is present around the periphery of the tumour nodule

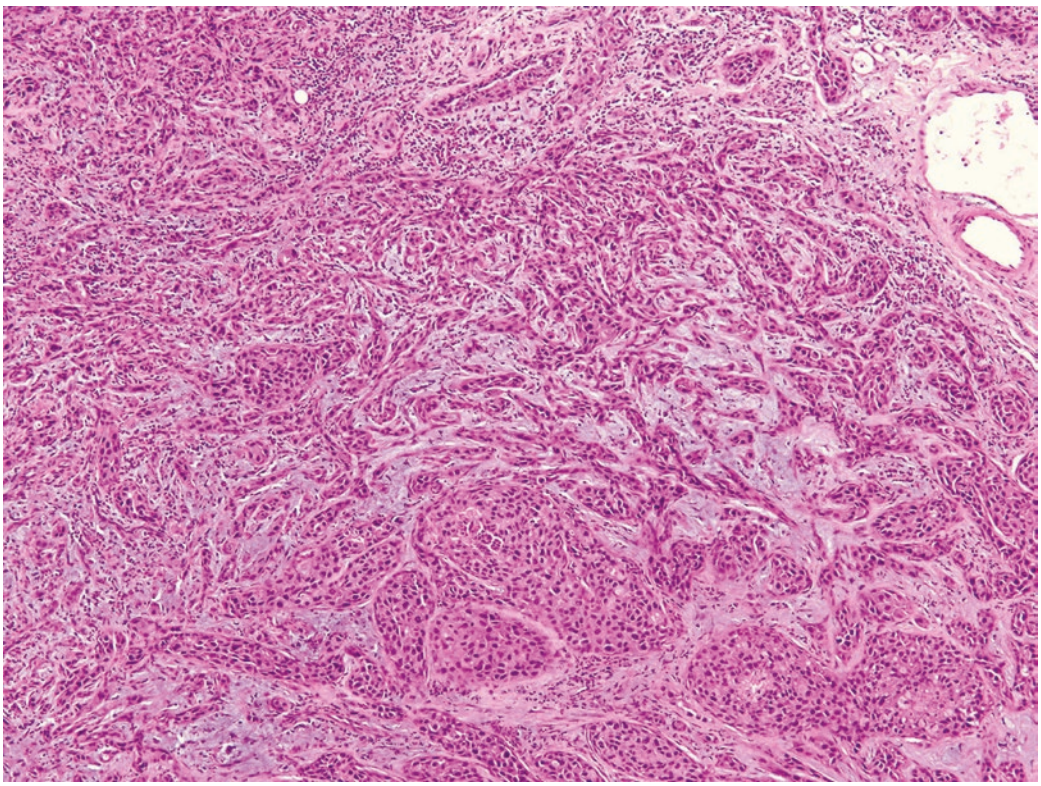

Fig. 9.76 DCIS superimposed on sclerosing adenosis. At higher magnification, epithelial nests and trabeculae anastomose within a slightly myxoid stroma with mild chronic inflammatory cell infiltrates

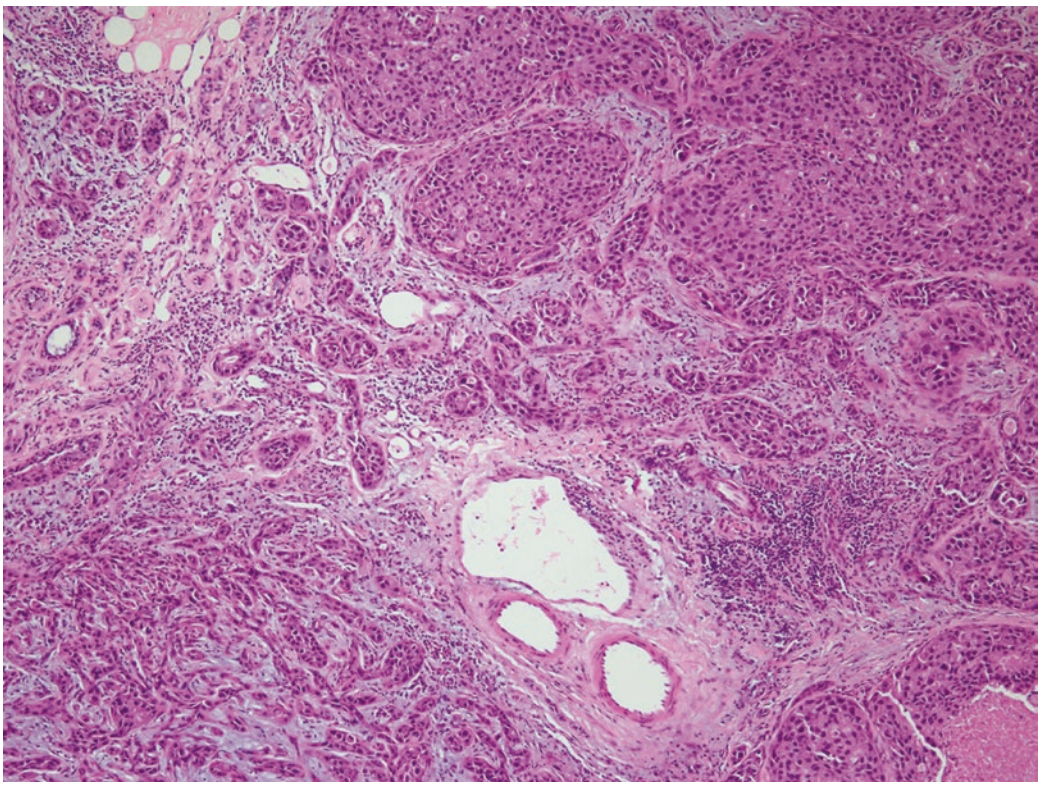

Fig. 9.77 DCIS superimposed on sclerosing adenosis. Many epithelial nests show rounded edges. There is a subtle appearance of the merging of these nests with adjacent lobules

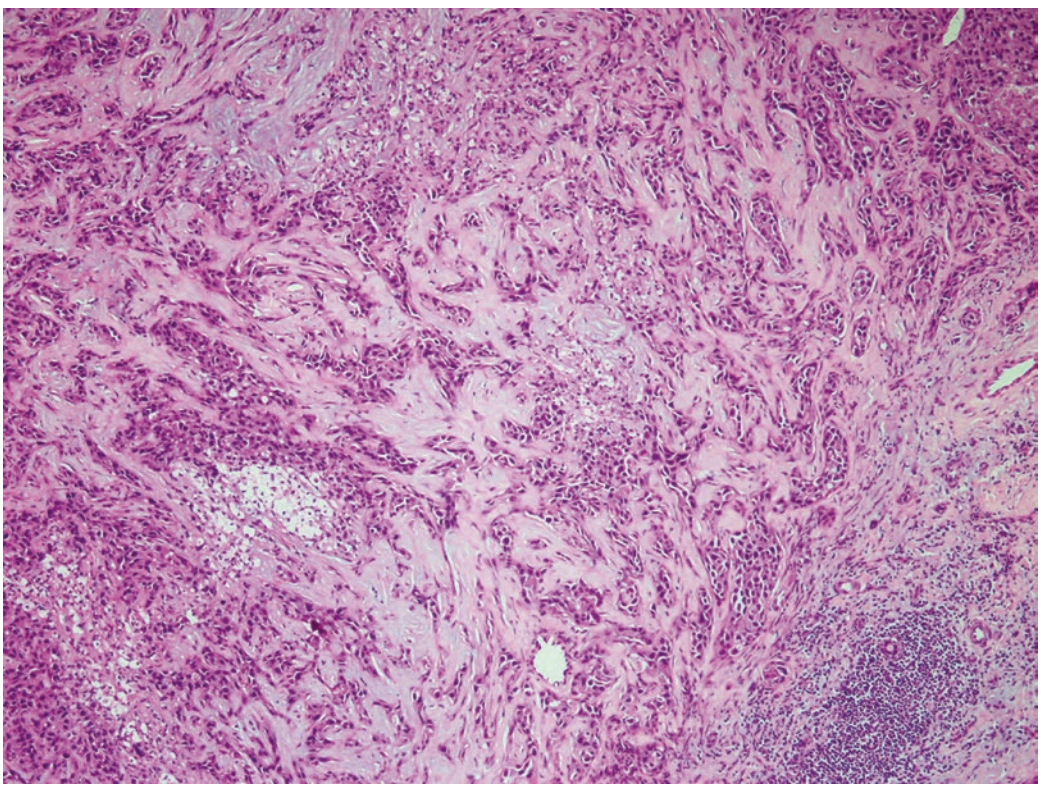

Fig. 9.78 DCIS superimposed on sclerosing adenosis. Hyalinisation is present around the anastomosing tumour nests

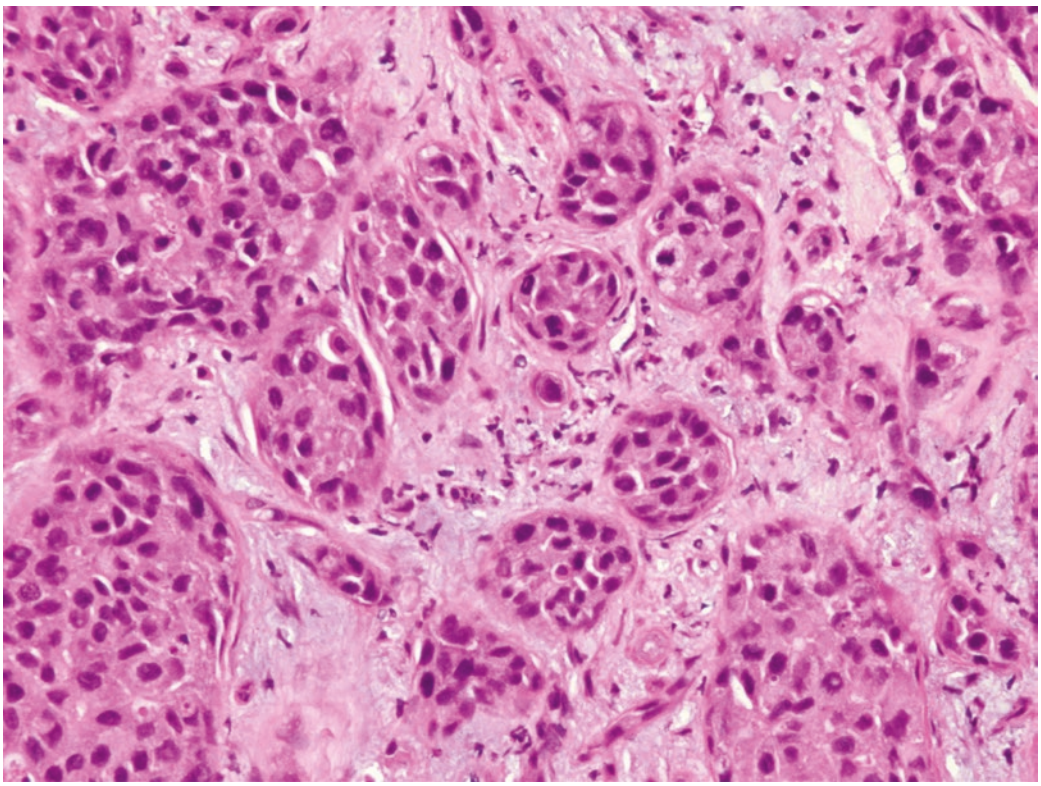

Fig. 9.79 DCIS superimposed on sclerosing adenosis. On high magnification, the epithelial nests are round and appear rimmed by a thin basement membrane layer

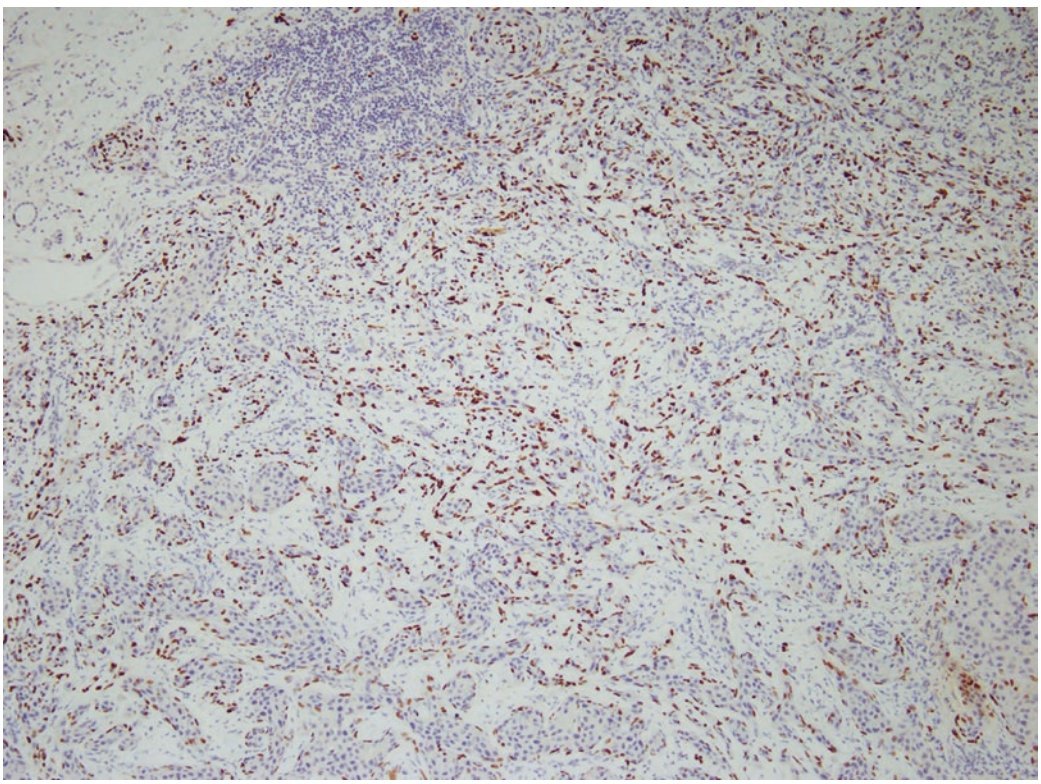

Fig. 9.80 DCIS superimposed on sclerosing adenosis. Immunohistochemistry with p63 shows myoepithelial nuclei that are preserved around the tumour nests

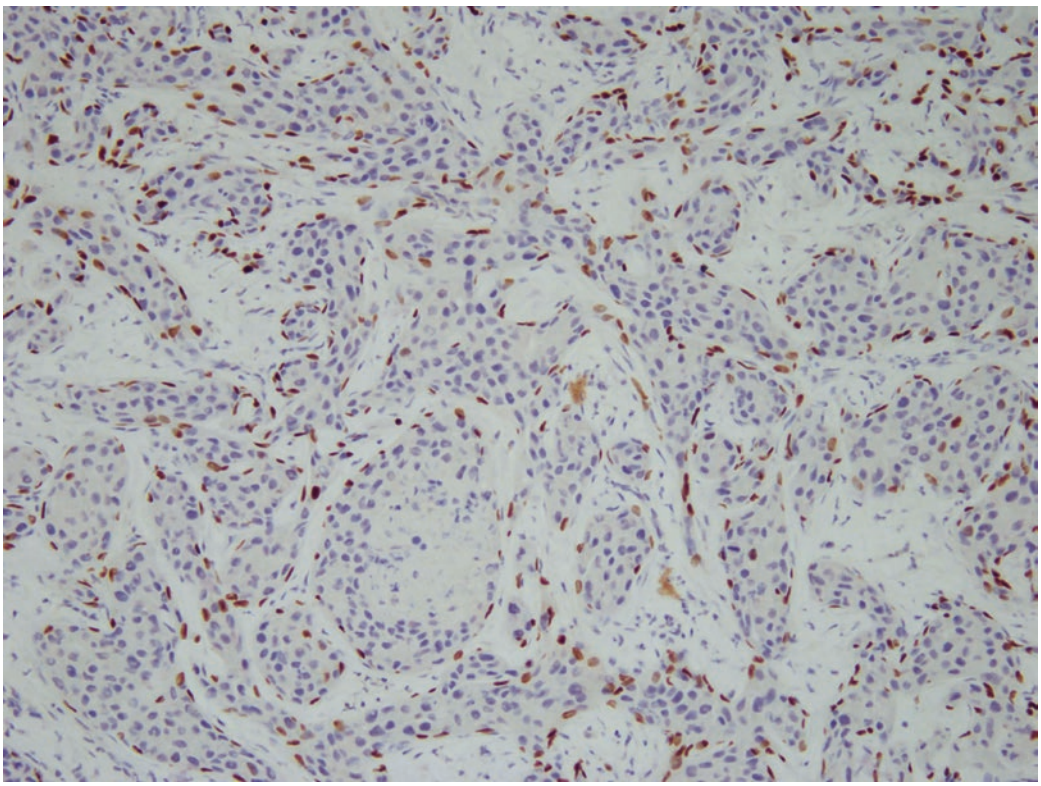

Fig. 9.81 DCIS superimposed on sclerosing adenosis. Higher magnification shows myoepithelial nuclei stained with p63 rimming the epithelial nests, indicating a non-invasive process

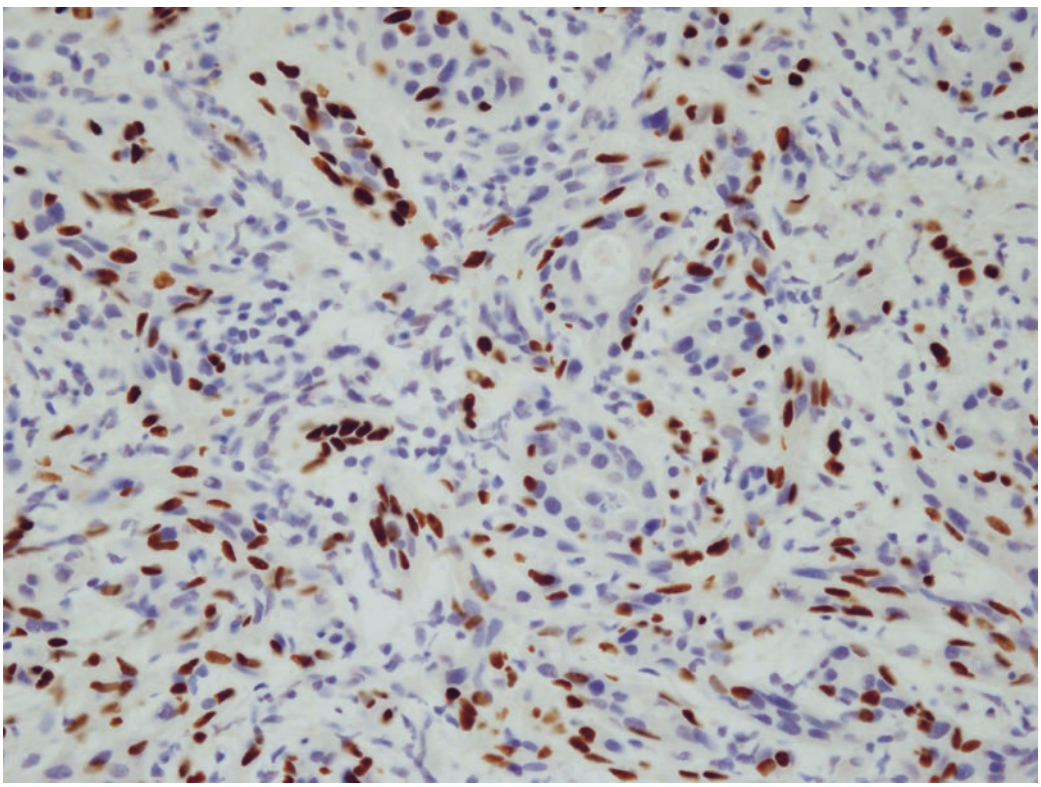

Fig. 9.82 DCIS superimposed on sclerosing adenosis. High magnification of myoepithelial nuclei that are positively highlighted by p63 immunohistochemistry

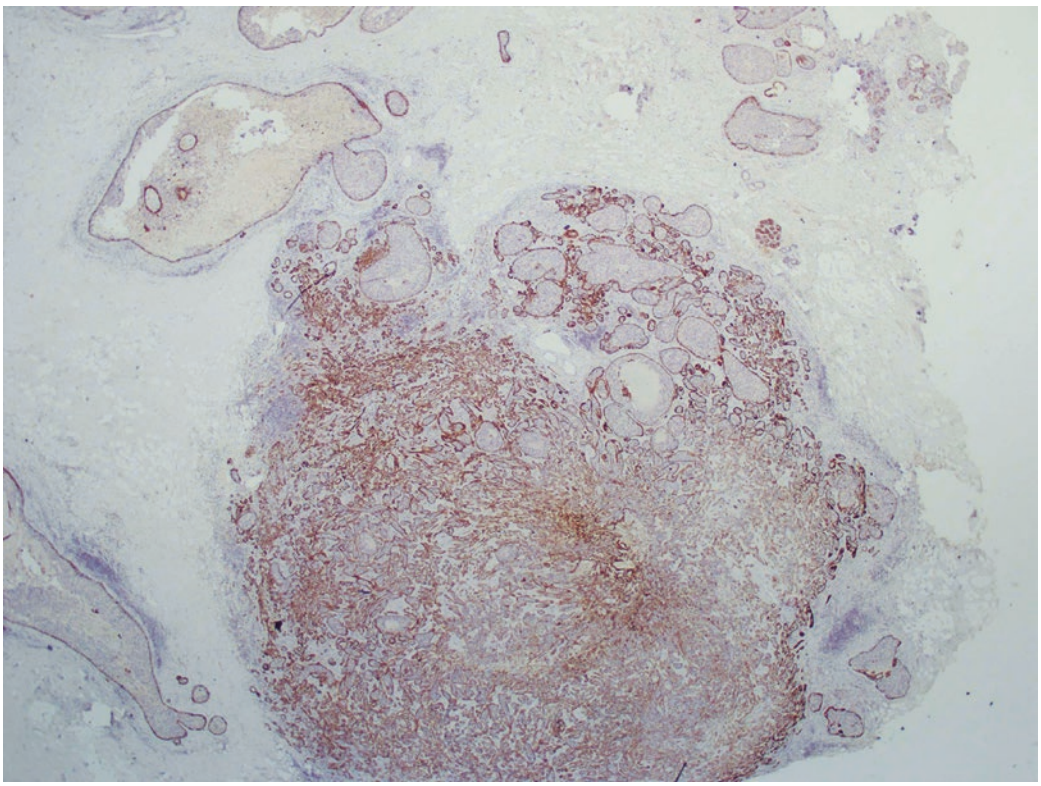

Fig. 9.83 DCIS superimposed on sclerosing adenosis. Low magnification of CK5/6 in the tumour nodule, demonstrating its presence in the lesion, with a clear peripheral rim of positivity in adjacent DCIS

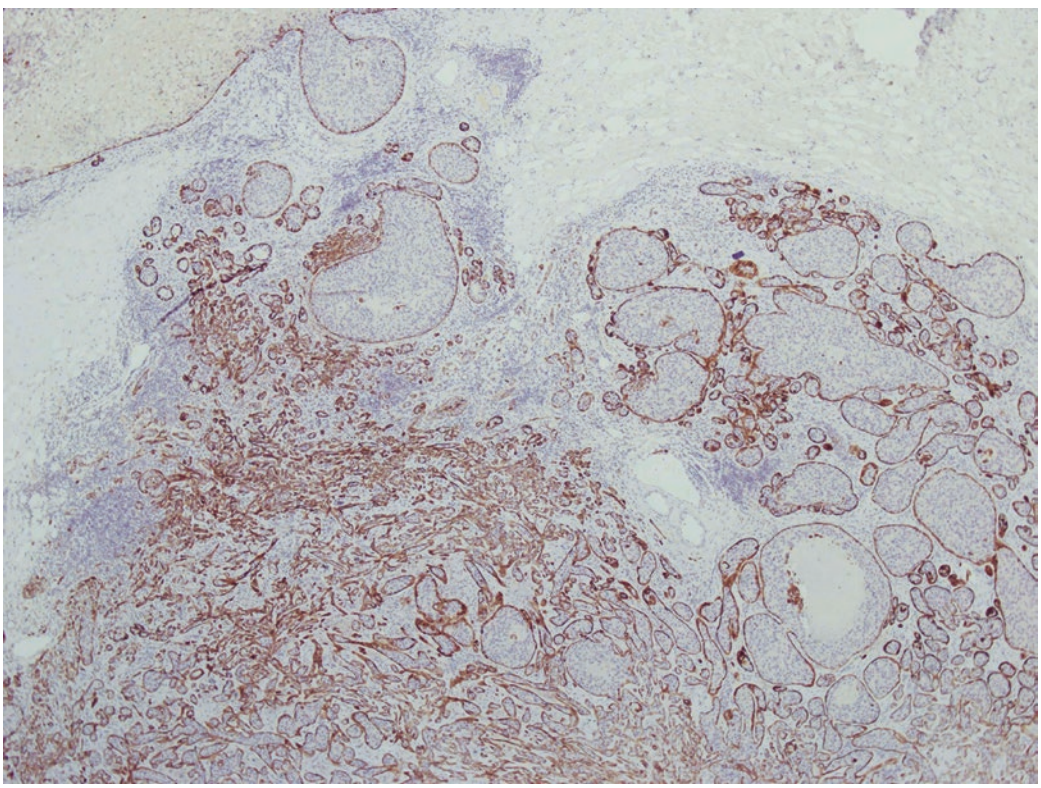

Fig. 9.84 DCIS superimposed on sclerosing adenosis. CK5/6 immunohistochemistry shows the preserved rims of myoepithelial cells in the larger DCIS islands, as well as in DCIS superimposed on sclerosing adenosis

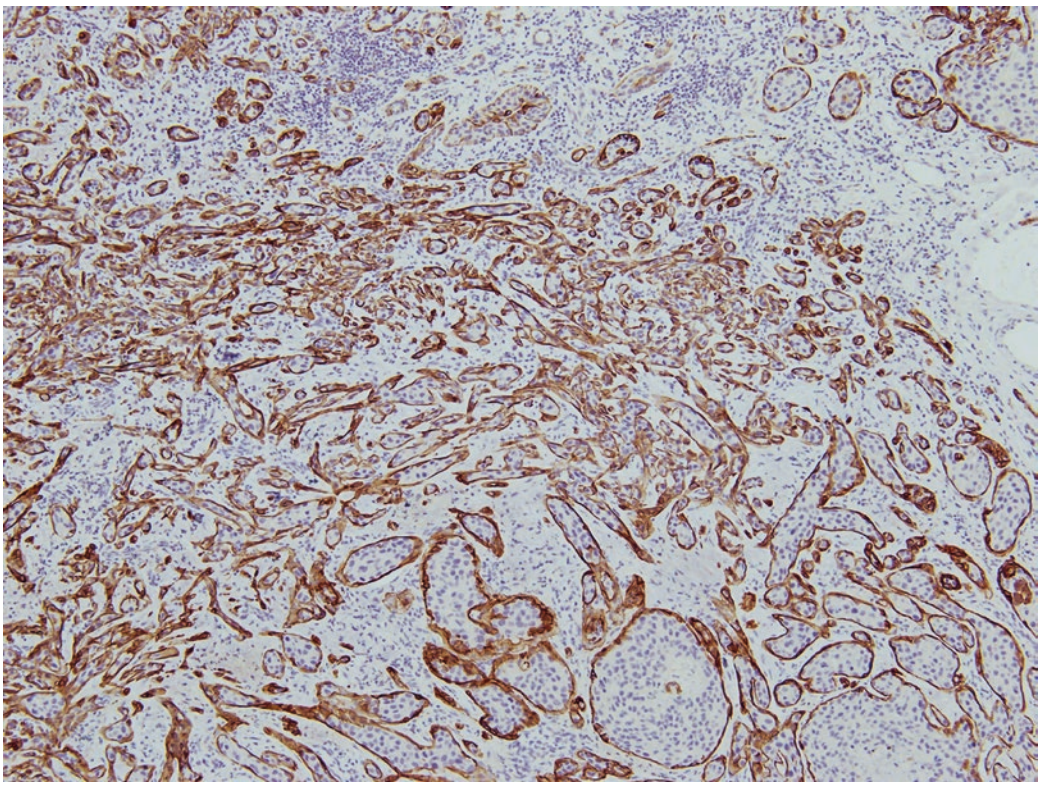

Fig. 9.85 DCIS superimposed on sclerosing adenosis. Medium magnification shows a peripheral CK5/6-positive myoepithelial rim around the tumour nests

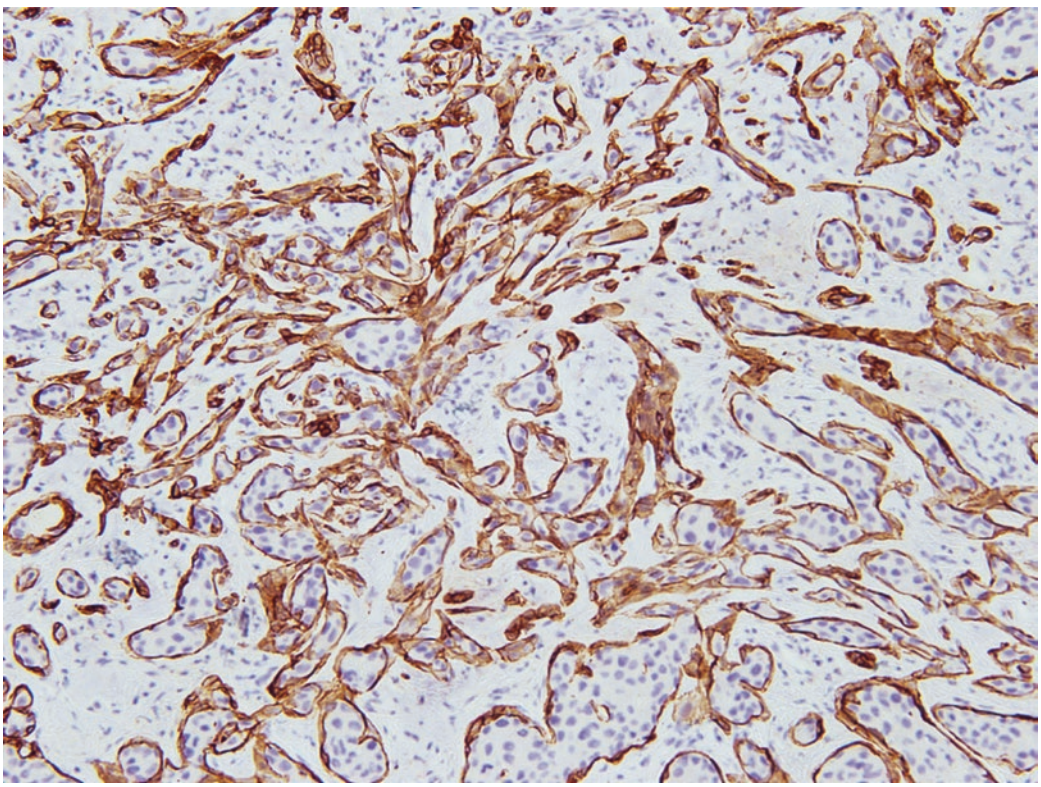

Fig. 9.86 DCIS superimposed on sclerosing adenosis. High magnification of CK5/6 immunohistochemistry with decoration of myoepithelial cells around tumour islands

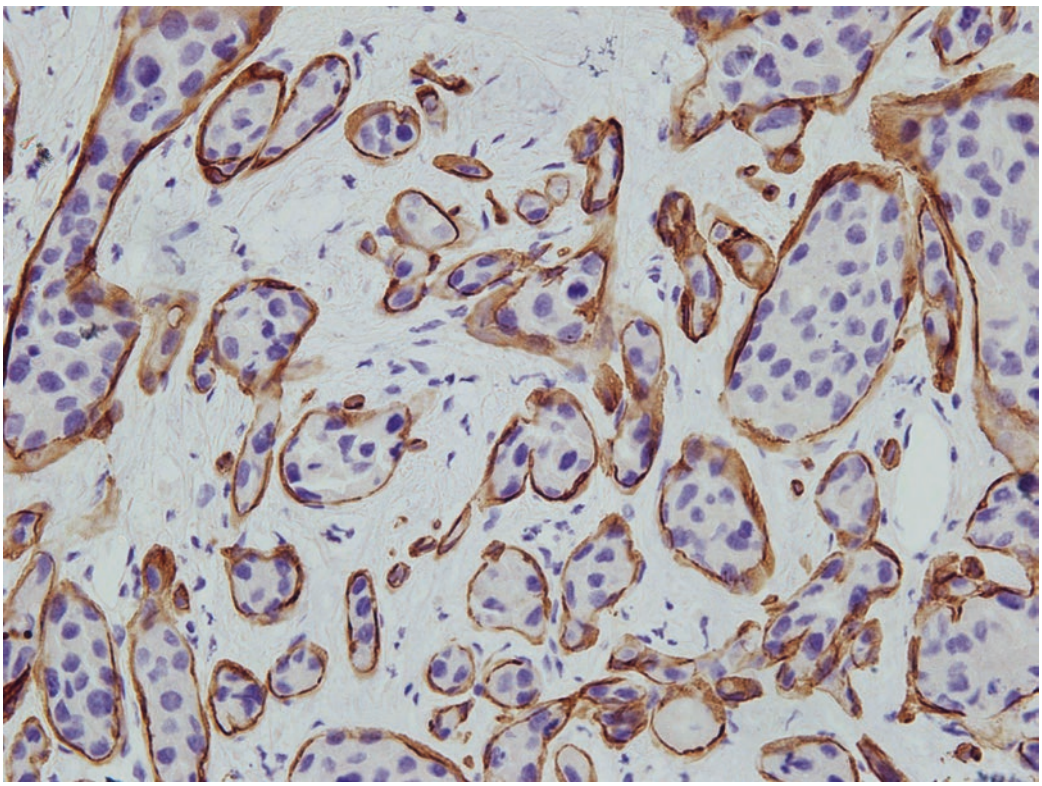

Fig. 9.87 DCIS superimposed on sclerosing adenosis. Intact myoepithelial cells unveiled by CK5/6 immunohistochemistry

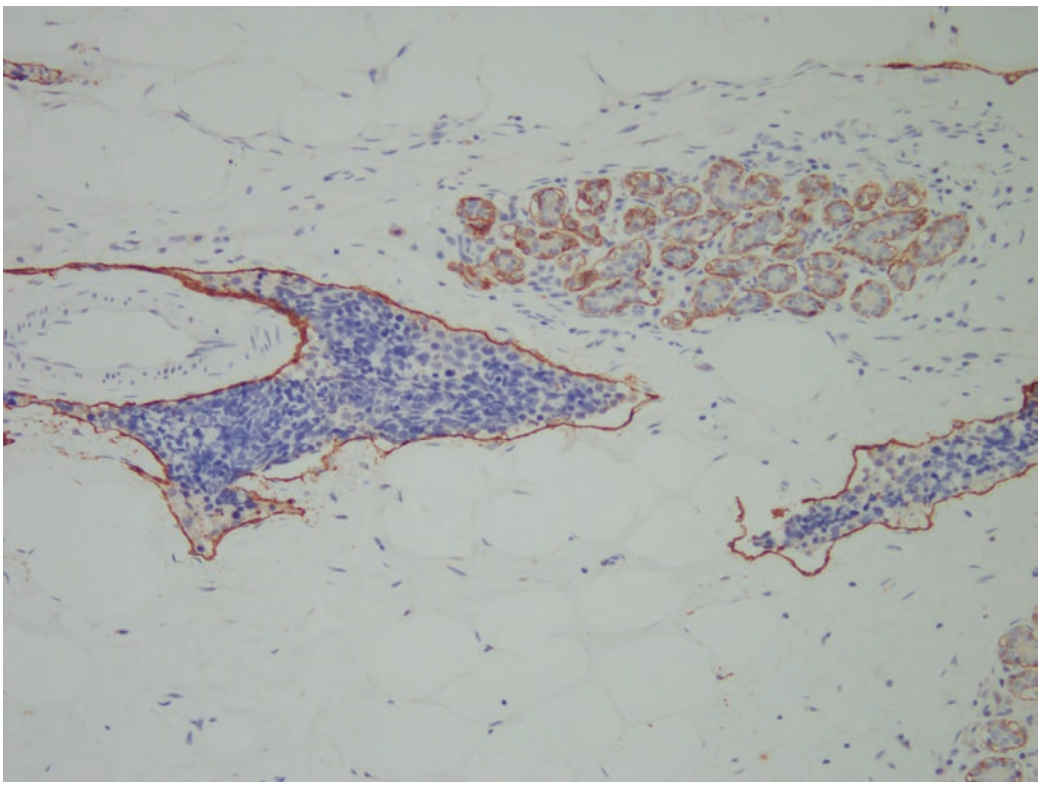

Fig. 9.88 Lymphovascular emboli mimicking DCIS. Lymphovascular spaces are filled with tumour cells, which can mimic a duct involved by DCIS, especially if D2-40 is used as a myoepithelial marker, as it also highlights endothelial cells. A benign lobule is present, with ductules rimmed by positively stained myoepithelial cells on D2-40 immunohistochemistry. In the interlobular stroma are lymphovascular spaces containing tumour cells. D2-40 immunohistochemistry decorates endothelial cells, which have a flattened continuous appearance, compared with the more polygonal positivity of myoepithelial cells

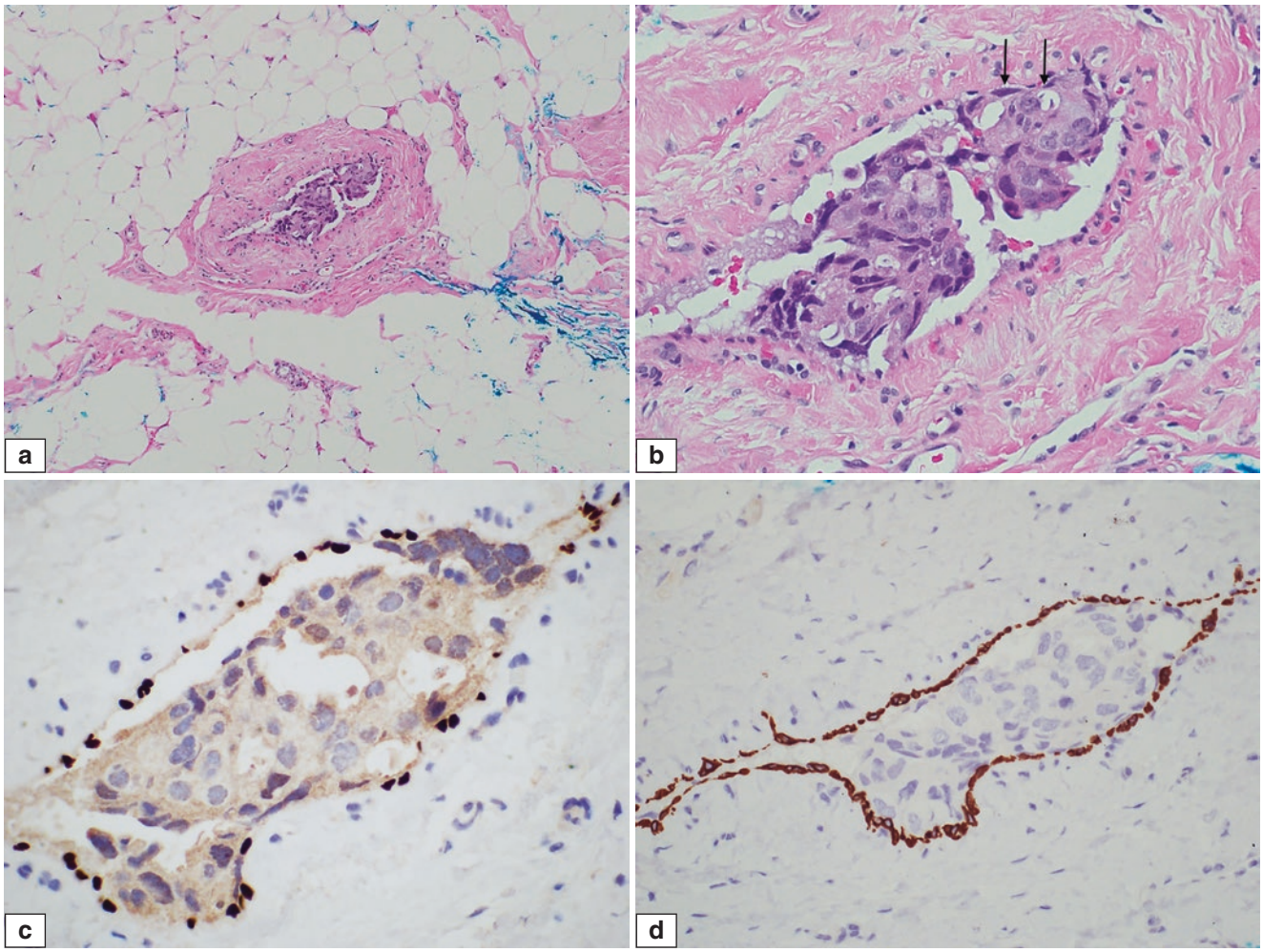

Fig. 9.89 DCIS mimicking a lymphovascular embolus. (**a**) At low magnification, malignant cells are partially attached to the wall of a space mimicking a lymphovascular tumour embolus. (**b**) High magnification shows high nuclear grade malignant tumour cells that are adherent to the wall of a space that appears to be lined by flattened cells which may be misinterpreted as endothelial cells. On closer scrutiny however, an outer layer of cells resembling myoepithelial cells (*arrows*) is seen cuffing the tumour cells. (**c**) Immunohistochemistry confirms that the cells lining the space are myoepithelial cells with positive nuclear staining for p63. The separation or retraction of malignant cells of DCIS from its duct wall can sometimes be observed, especially in specimens that may not be optimally fixed. (**d**) CK14 immunohistochemistry shows cytoplasmic reactivity of the myoepithelial cells rimming the affected duct wall. Endothelial markers are negative

References

1. Abdel-Fatah TM, Powe DG, Hodi Z, Reis-Filho JS, Lee AH, Ellis IO. Morphologic and molecular evolutionary pathways of low nuclear grade invasive breast cancers and their putative precursor lesions: further evidence to support the concept of low nuclear grade breast neoplasia family. Am J Surg Pathol. 2008;32:513–23.
2. Gomes DS, Porto SS, Balabram D, Gobbi H. Inter-observer variability between general pathologists and a specialist in breast pathology in the diagnosis of lobular neoplasia, columnar cell lesions, atypical ductal hyperplasia and ductal carcinoma in situ of the breast. Diagn Pathol. 2014;9:121.
3. Tan PH, Ho BC, Selvarajan S, Yap WM, Hanby A. Pathological diagnosis of columnar cell lesions of the breast: are there issues of reproducibility? J Clin Pathol. 2005;58:705–9.
4. Lim CN, Ho BC, Bay BH, Yip G, Tan PH. Nuclear morphometry in columnar cell lesions of the breast: is it useful? J Clin Pathol. 2006;59:1283–6.
5. Said SM, Visscher DW, Nassar A, Frank RD, Vierkant RA, Frost MH, et al. Flat epithelial atypia and risk of breast cancer: a Mayo cohort study. Cancer. 2015;121:1548–55.
6. Calhoun BC, Sobel A, White RL, Gromet M, Flippo T, Sarantou T, Livasy CA. Management of flat epithelial atypia on breast core biopsy may be individualized based on correlation with imaging studies. Mod Pathol. 2015;28:670–6.
7. Dialani V, Venkataraman S, Frieling G, Schnitt SJ, Mehta TS. Does isolated flat epithelial atypia on vacuum-assisted breast core biopsy require surgical excision? Breast J. 2014;20:606–14.
8. Schnitt SJ, Ellis IO, van de Vijver MJ, Sgroi D, Lakhani SR, Simpson J, et al. Intraductal proliferative lesions: introduction and overview. In: Lakhani SR, Ellis IO, Schnitt SJ, Tan PH, van de Vijver MJ, editors. WHO classification of tumours of the breast. Lyon: IARC; 2012. p. 82–94.
9. Tan PH, Ho JT, Ng EH, Chiang GS, Low SC, Ng FC, Bay BH. Pathologic-radiologic correlations in screen-detected ductal carcinoma in situ of the breast: findings of the Singapore breast screening project. Int J Cancer. 2000;90:231–6.

10. Schwartz GF, Patchefsky AS, Finklestein SD, Sohn SH, Prestipino A, Feig SA, Singer JS. Nonpalpable in situ ductal carcinoma of the breast. Predictors of multicentricity and microinvasion and implications for treatment. Arch Surg. 1989;124:29–32.
11. Tan PH, Lui GG, Chiang G, Yap WM, Poh WT, Bay BH. Ductal carcinoma in situ with spindle cells: a potential diagnostic pitfall in the evaluation of breast lesions. Histopathology. 2004;45:343–51.
12. Francis A, Thomas J, Fallowfield L, Wallis M, Bartlett JM, Brookes C, Roberts T, Pirrie S, Gaunt C, Young J, Billingham L, Dodwell D, Hanby A, Pinder SE, Evans A, Reed M, Jenkins V, Matthews L, Wilcox M, Fairbrother P, Bowden S, Rea D. Addressing overtreatment of screen detected DCIS; the LORIS trial. Eur J Cancer. 2015;51(16):2296–303.

Lobular Lesions (Lobular Neoplasia, Invasive Lobular Carcinoma)

10

Lobular breast lesions described in this chapter encompass a spectrum of conditions that share in common a proliferation of neoplastic lobular-type cells, which are morphologically rounded, mostly uniform cells with a tendency for discohesion.

Lobular neoplasia refers to the presence of these cells within the terminal ductal lobular unit, with or without pagetoid extension along terminal and segmental ducts. Lobular neoplasia includes atypical lobular hyperplasia and lobular carcinoma in situ (LCIS), which are distinguished by the degree and extent of lesional involvement of the terminal ductal lobular unit.

Invasive lobular carcinoma comprises invading tumour cells with lobular morphology and unique patterns of infiltration.

Lobular Neoplasia (Atypical Lobular Hyperplasia and Lobular Carcinoma In Situ)

Definition

Lobular neoplasia is a non-invasive, abnormal proliferation of discohesive cells within the lobule. Lobular neoplastic cells are characterised by aberration of the E-cadherin gene leading to a dysfunctional E-cadherin protein, an intercellular adhesion molecule. Lobular neoplasia usually features cells with uniform, rounded morphology referred to as type A cells, but it may also be composed of type B cells with moderate nuclear variation.

Clinical and Epidemiological Features

Lobular neoplasia may be encountered in up to 4 % of breast core biopsies, often in premenopausal women [1]. As it is usually an incidental lesion discovered during histologic evaluation of biopsy specimens and excisions performed for other clinicoradiological indications, there are no specific clinical or radiological characteristics of lobular neoplasia per se. Unusually, lobular neoplasia may be mass forming, resulting in clinical or radiological detection, and occasionally it can be associated with necrosis and calcifications leading to mammographic discovery [2].

Imaging Features

Most lobular neoplastic lesions do not have specific imaging features, apart from those variants that are mass forming or accompanied by calcifications. The majority are incidental findings on biopsy. Sampled microcalcifications are not commonly found within the lobular neoplasia itself, but are discovered more frequently in adjacent cystic alterations or atypical ductal hyperplasia. Lobular carcinoma in situ (LCIS) can occasionally form irregular masses and present as suspicious non-mass enhancement on MRI [3]. Pleomorphic LCIS may display clustered, punctate, or pleomorphic-type microcalcifications on mammography [4].

Pathologic Features

Macroscopic Pathology

Lobular neoplasia is usually a microscopic lesion that does not produce a macroscopic abnormality. Mass-forming examples can be associated with a grossly visible lesion (Fig. 10.1), and those harbouring calcifications can be gritty in consistency.

P.H. Tan, A.A. Sahin, *Atlas of Differential Diagnosis in Breast Pathology*, Atlas of Anatomic Pathology,
DOI 10.1007/978-1-4939-6697-4_10

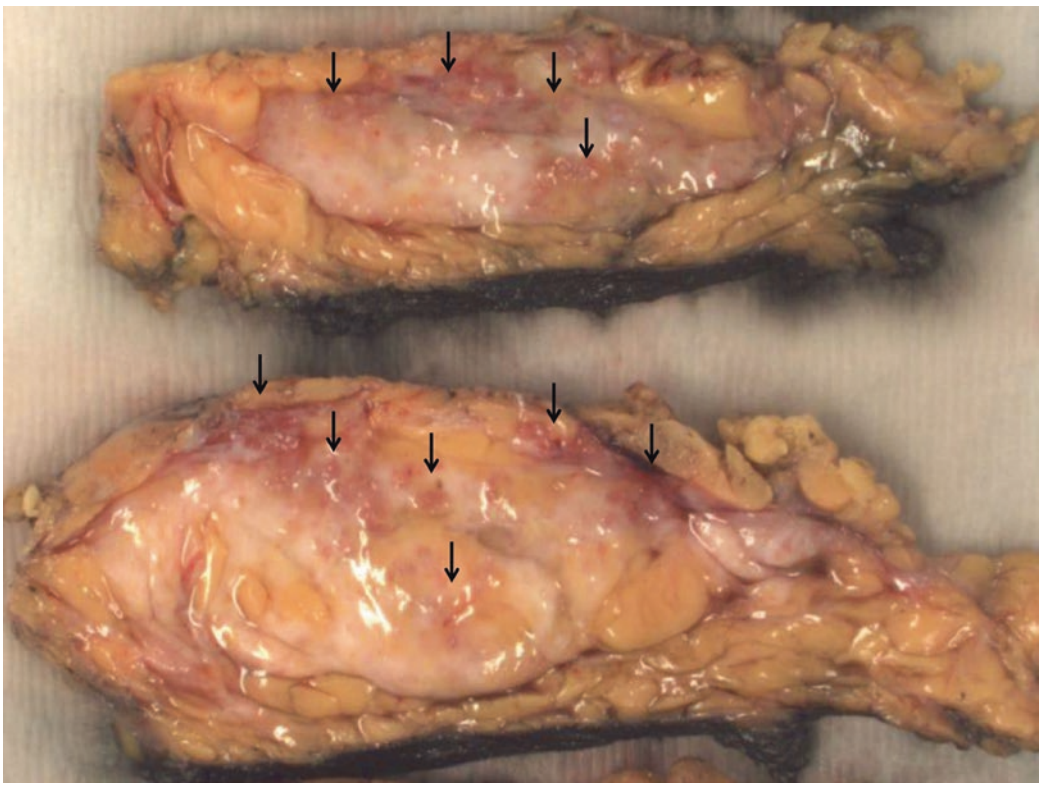

Fig. 10.1 Florid lobular carcinoma in situ (LCIS). This skin-sparing mastectomy specimen shows multiple fleshy nodules with a pinkish-grey appearance (*arrows*) amid fibrofatty breast parenchyma

Microscopic Pathology

Both atypical lobular hyperplasia and LCIS are composed of monomorphic, discohesive, round cells in the terminal ductal lobular unit, differing by the severity of involvement of lobules. In atypical lobular hyperplasia, the neoplastic cells variably fill the acini, leading to rounded acinar contours, but they do not significantly distend or distort the acinar shapes (Figs. 10.2, 10.3, 10.4, 10.5, 10.6, 10.7, 10.8, 10.9, and 10.10). In LCIS, there is filling of all acini in the affected lobule, accompanied by distention and/or distortion of at least half of the filled acini (Figs. 10.11, 10.12, 10.13, 10.14, 10.15, 10.16, 10.17, 10.18, and 10.19). Not infrequently, there is a gradation of changes, and it may be difficult to clearly separate atypical lobular hyperplasia from LCIS. There is also interobserver variability in the assessment of the degree of lobular neoplastic changes. It is useful to distinguish atypical lobular hyperplasia from LCIS because the risk implications for subsequent development of breast carcinoma differ, but to do so is admittedly challenging in some cases, whereupon *lobular neoplasia* may be applied as an encompassing term. Lobular neoplasia can coexist with columnar cell lesions, flat epithelial atypia, atypical ductal hyperplasia, and low-grade invasive carcinoma, referred to as the "low nuclear grade neoplasia family" of breast lesions (Figs. 10.20, 10.21, 10.22, and 10.23) [5].

Marked nuclear pleomorphism, often with apocrine cytomorphology, is sometimes seen in LCIS and is referred to as the *pleomorphic variant* (Figs. 10.24, 10.25, 10.26, 10.27, 10.28, 10.29, 10.30, 10.31, 10.32, 10.33, 10.34, and 10.35) [6]. Necrosis and calcifications may be found in pleomorphic LCIS, but they can also be observed in classic forms of the disease. Lobular neoplasia with type B cells should not be diagnosed as pleomorphic LCIS. When required, E-cadherin immunohistochemistry can be used to confirm a lobular phenotype, displaying negative staining of the lobular neoplastic cells [7]. It is important to be familiar with aberrant E-cadherin staining patterns (Figs. 10.36, 10.37, and 10.38) [7]. Other immunohistochemical markers include p120 catenin and β-catenin, which show cytoplasmic rather than membrane localisation of staining [8].

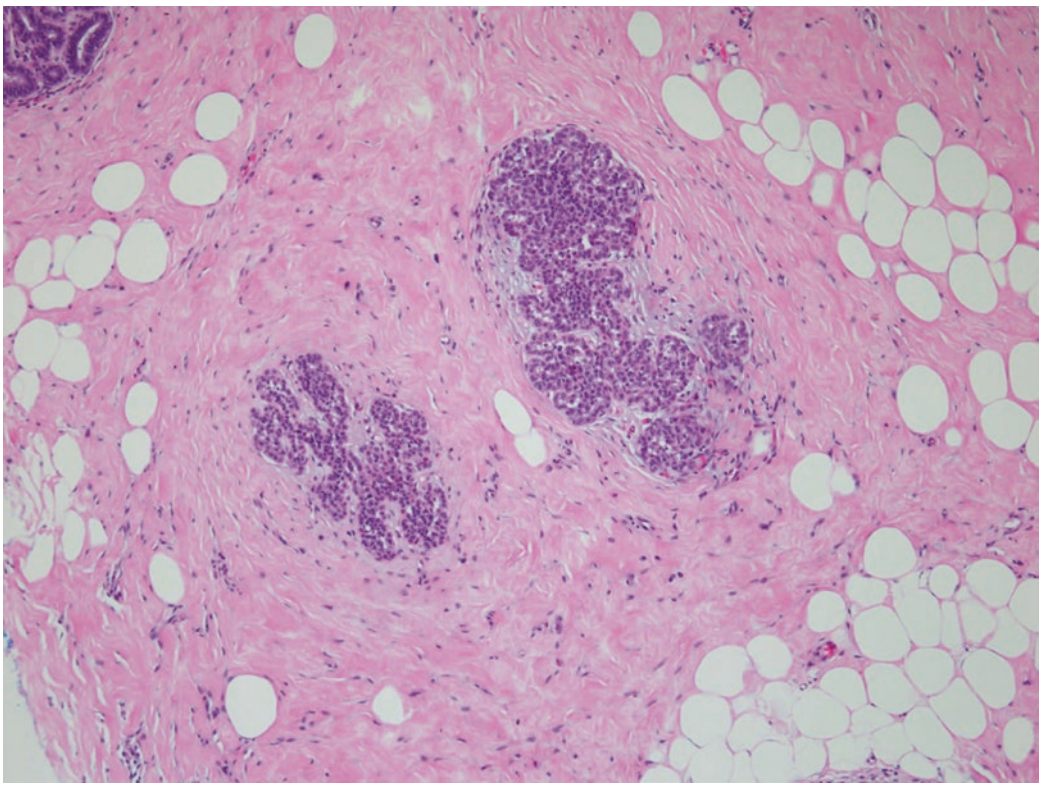

Fig. 10.2 Atypical lobular hyperplasia. At low magnification, the terminal ductal lobular units contain monomorphic, discohesive cells. The luminal spaces of terminal ducts and acini are obscured

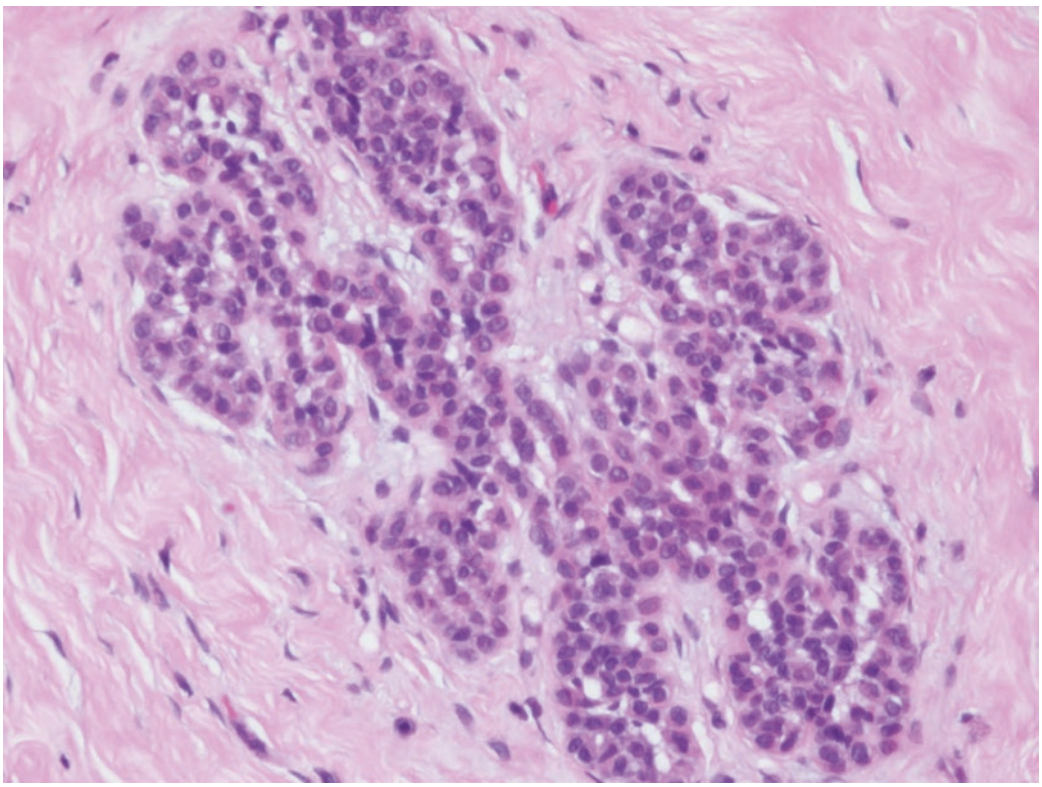

Fig. 10.3 Atypical lobular hyperplasia. High magnification shows the discohesive cells filling the acinar spaces. No distension or distortion of the acinar outlines is seen

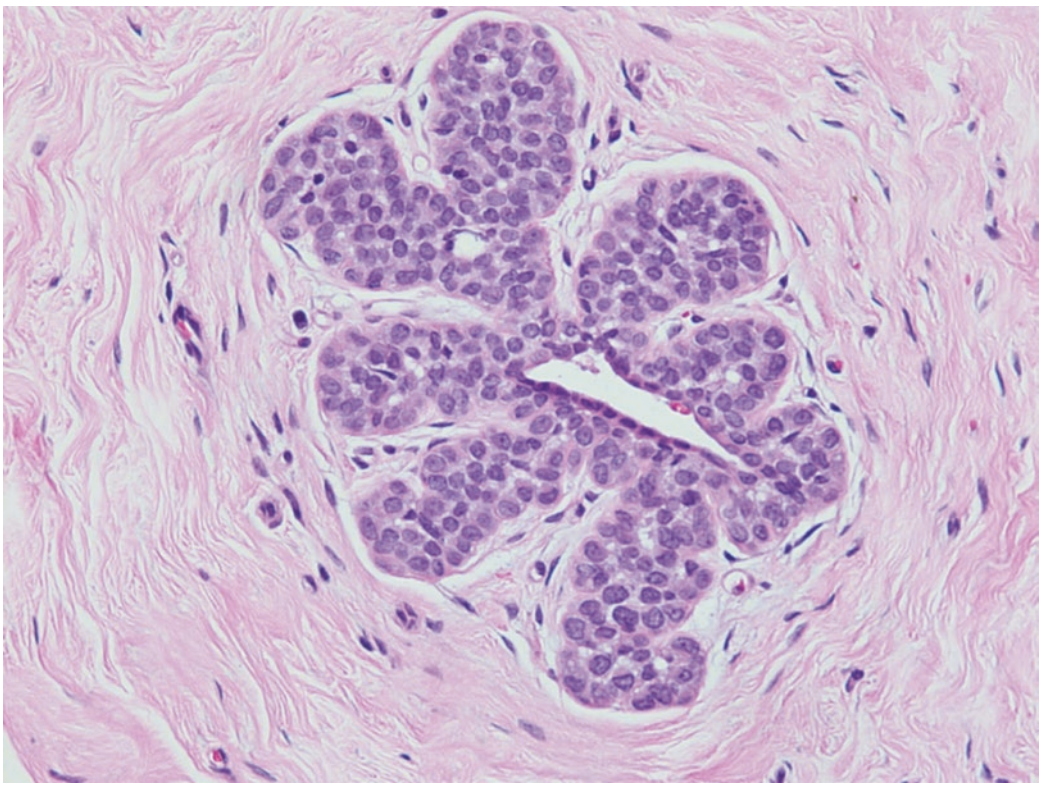

Fig. 10.4 Atypical lobular hyperplasia shows a monomorphic, discohesive epithelial population filling the acini. The cells display inconspicuous spaces in between them, with ill-defined cell contours and cytoplasmic membranes. The epithelial lining of the terminal duct is attenuated. These lobular neoplastic cells are of type A morphology

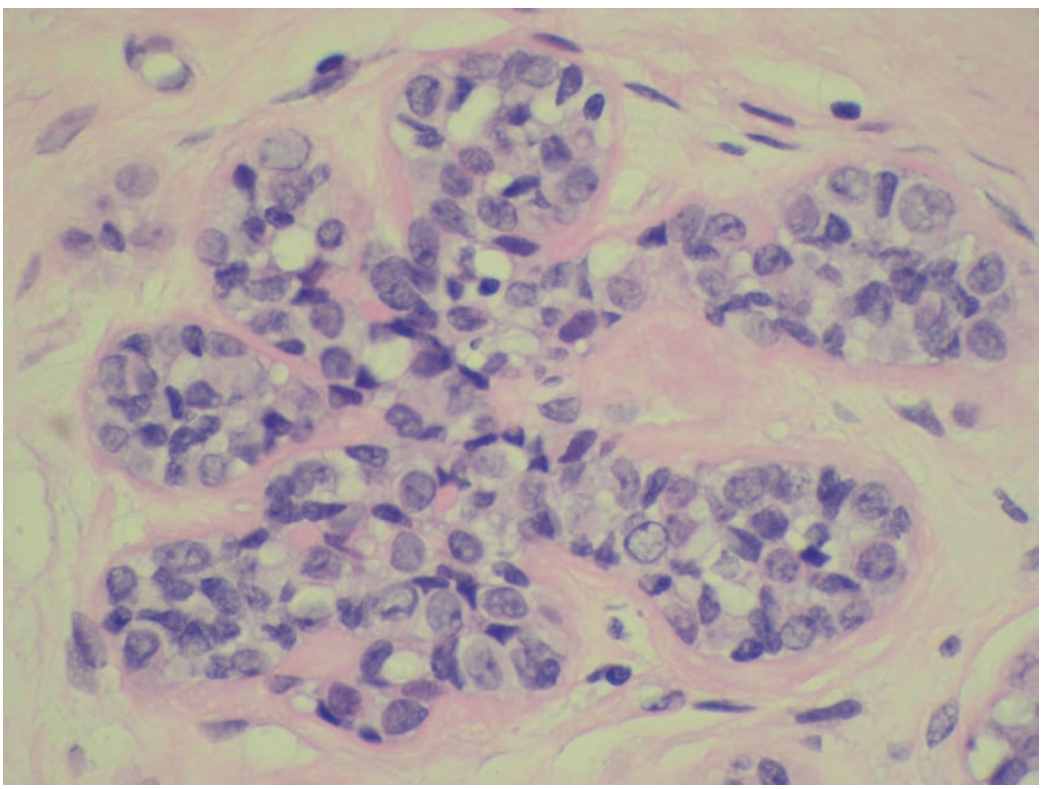

Fig. 10.5 Atypical lobular hyperplasia. Lobular neoplastic cells show a greater degree of nuclear variation, with several slightly enlarged, vesicular nuclei and discernible nucleoli; features are consistent with type B cells. Occasional cytoplasmic vacuoles are seen

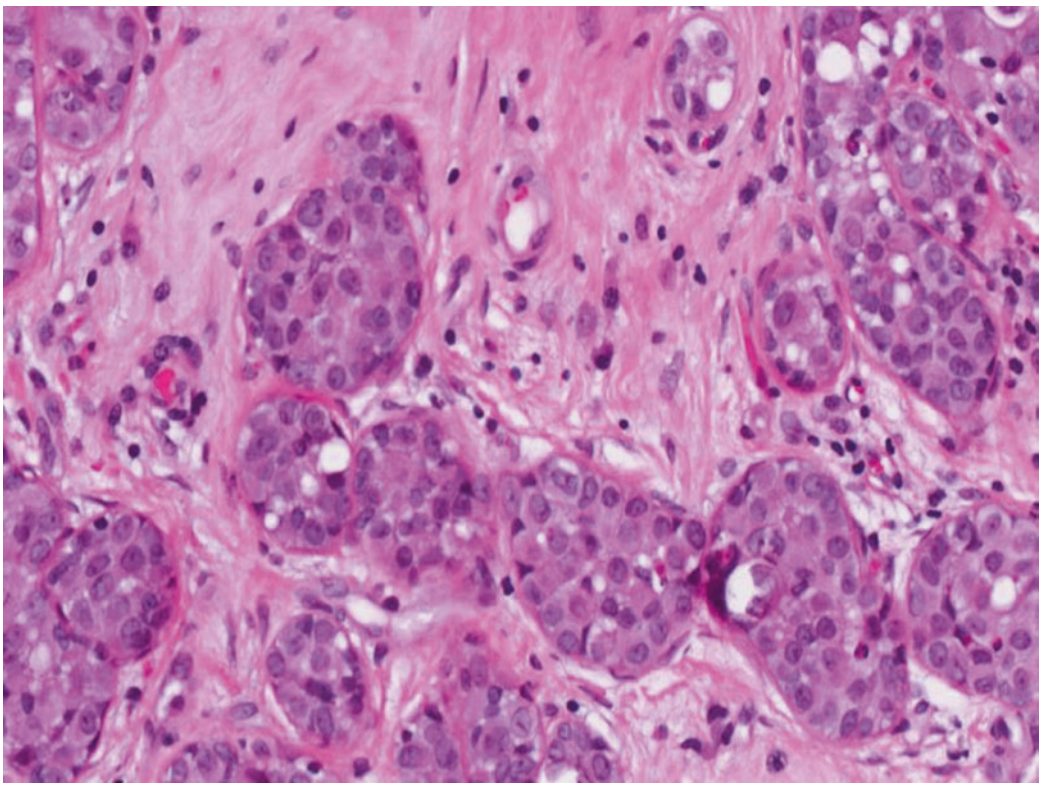

Fig. 10.6 Atypical lobular hyperplasia shows cells with cytoplasmic vacuoles and discohesion, filling but not distending acinar spaces of the lobule. Affected acini show rounded contours

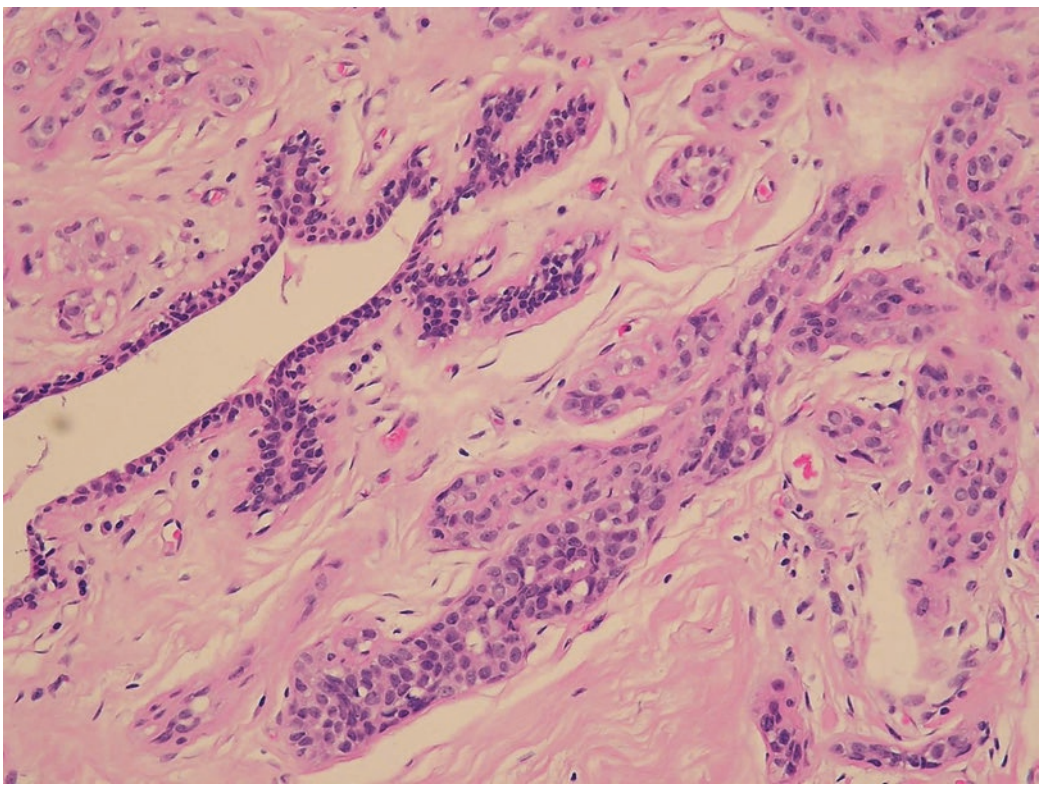

Fig. 10.7 Atypical lobular hyperplasia is seen adjacent to an unaffected terminal duct, with atypical lobular neoplastic cells filling the affected terminal duct and acini

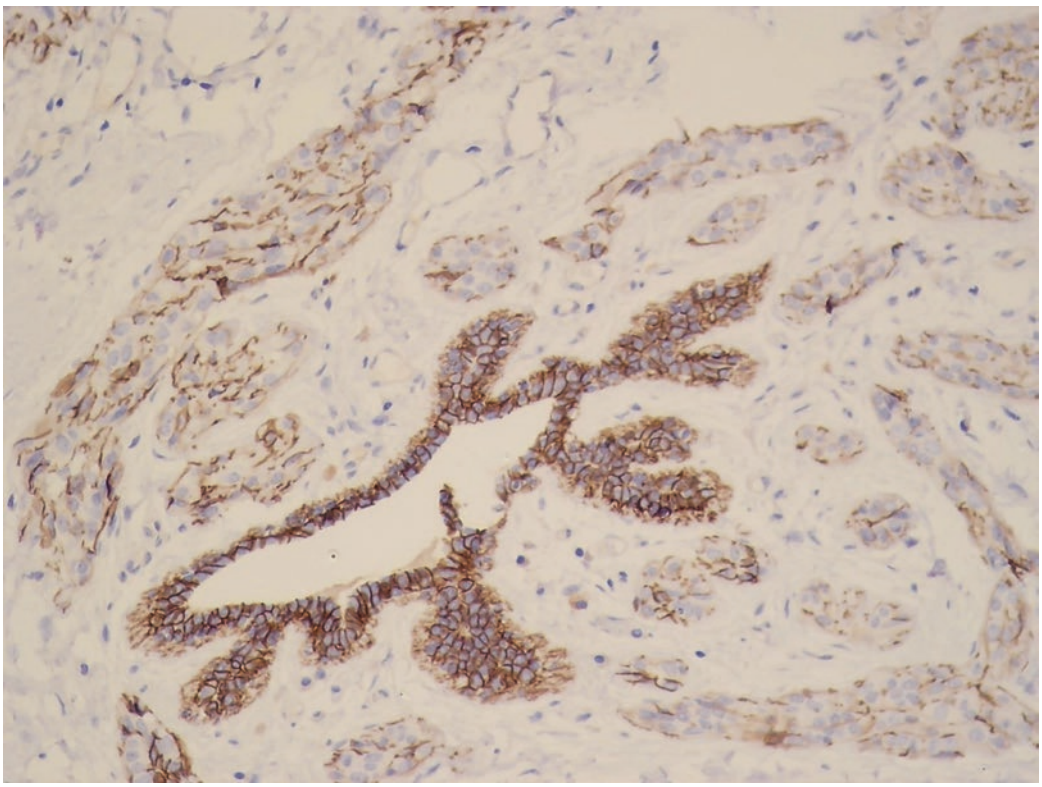

Fig. 10.8 Atypical lobular hyperplasia. E-cadherin immunohistochemistry shows diminished and absent staining in the lobular neoplastic cells. There appears to be some patchy E-cadherin staining in affected ducts and acini, which may reflect staining of intermingled myoepithelial cells. Some lobular neoplastic cells can also demonstrate diminished and incomplete E-cadherin staining of their cytoplasmic membranes

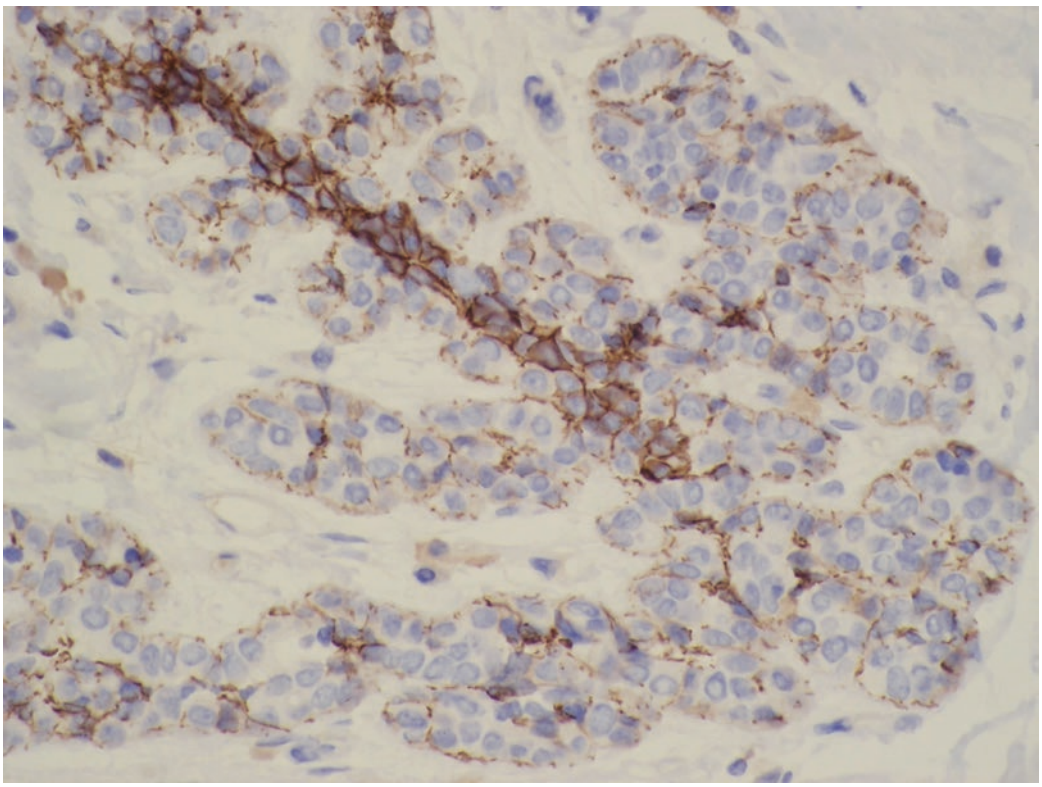

Fig. 10.9 Atypical lobular hyperplasia. E-cadherin immunostaining shows positive cytoplasmic membrane reactivity of the epithelial cells lining the terminal duct, whereas the lobular neoplastic cells are devoid of E-cadherin expression, apart from some staining likely originating from intermingled myoepithelial cells

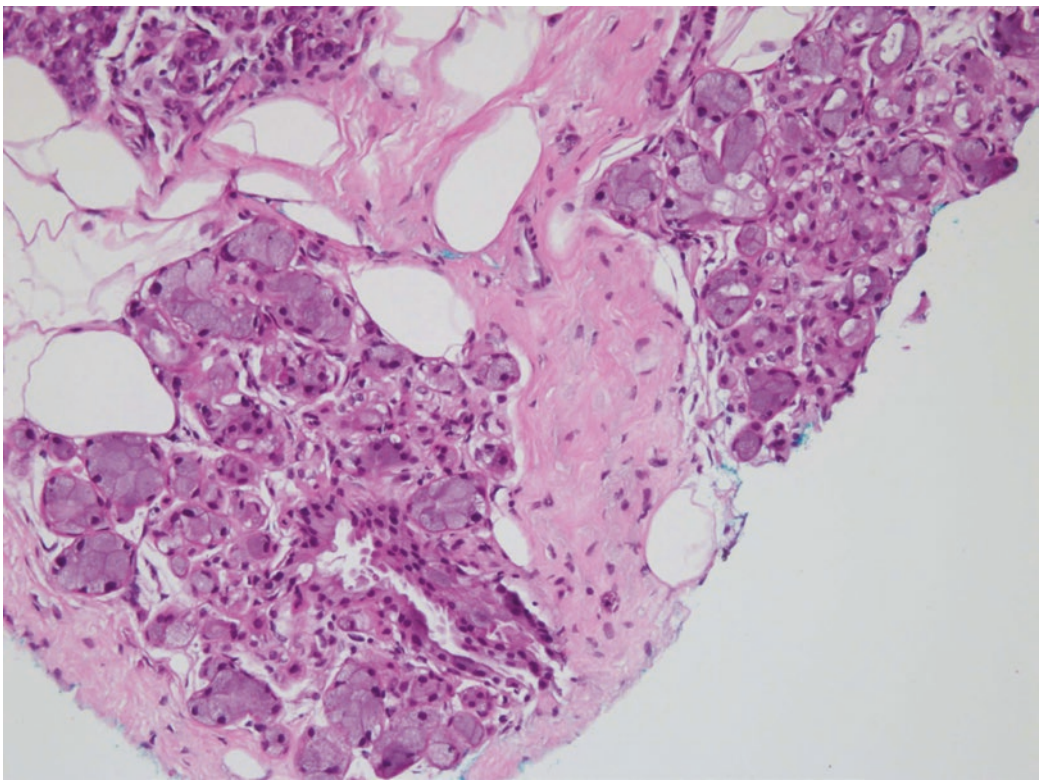

Fig. 10.10 Lobular neoplasia (atypical lobular hyperplasia) featuring a histiocytoid appearance

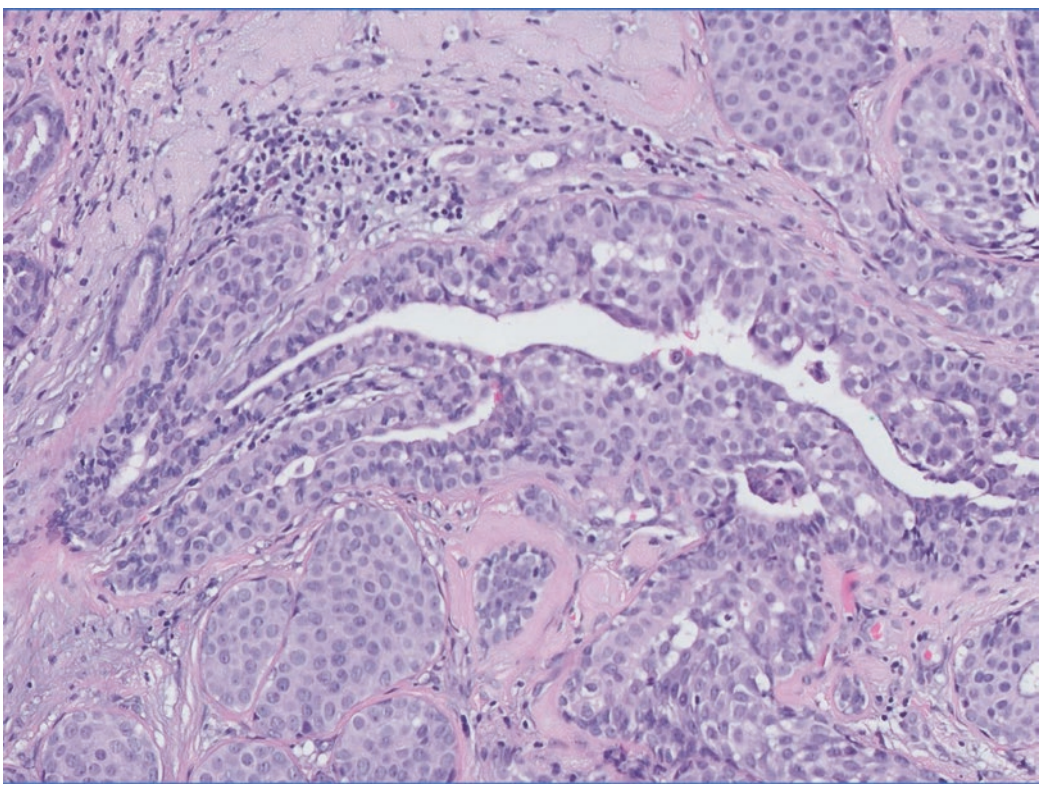

Fig. 10.11 Lobular carcinoma in situ (LCIS) with pagetoid extension along the terminal duct. Lobular neoplastic cells insinuate in between the luminal epithelium and the myoepithelial cells. Pagetoid extension may be encountered in both atypical lobular hyperplasia and LCIS. Adjacent acini are distended by lobular neoplastic cells with distortion of their outlines, features of LCIS

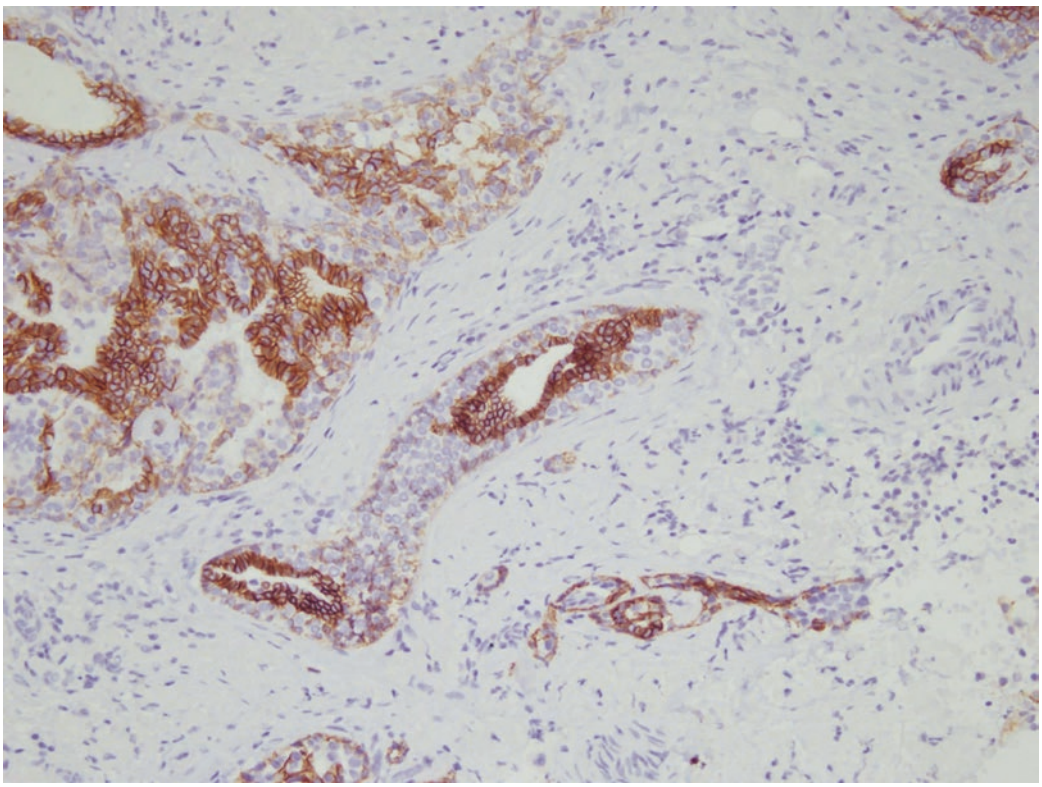

Fig. 10.12 Lobular neoplasia with pagetoid extension. E-cadherin immunohistochemistry shows preserved staining in luminal epithelial cells; the lobular neoplastic cells are negative. It is difficult to be certain from this illustration whether the lesion represents atypical lobular hyperplasia or LCIS; a final conclusion will depend on assessing the entire lesion especially the severity of changes in the acini

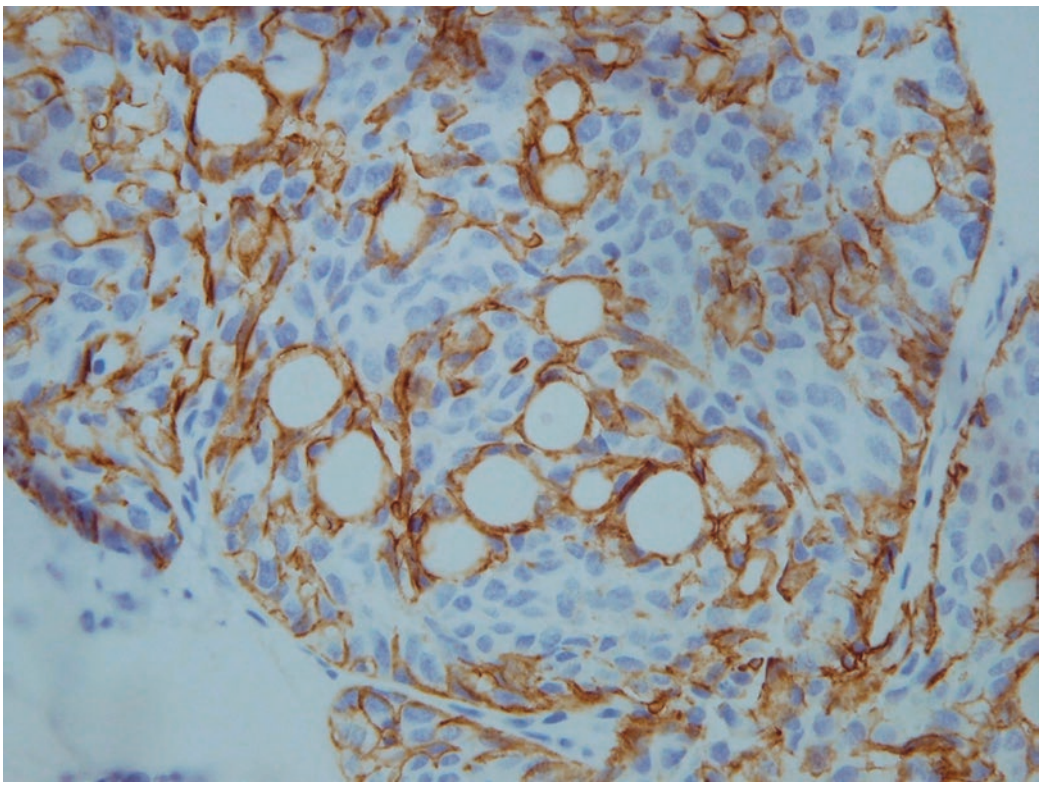

Fig. 10.13 E-cadherin immunohistochemistry shows negative staining of LCIS cells, whereas there is positive staining for attenuated luminal epithelial cells, as well as the peripheral myoepithelial cells

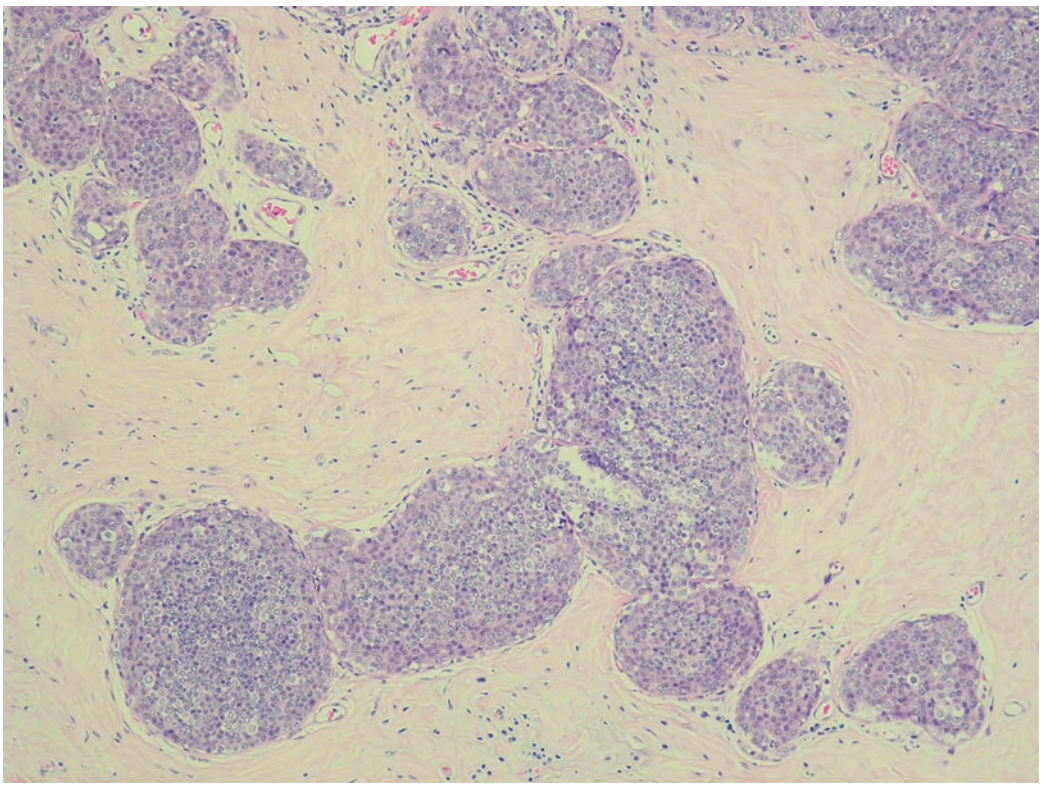

Fig. 10.14 Lobular carcinoma in situ. Duct and acinar spaces are completely filled and distended by lobular neoplastic cells. When assessing whether there is distension of acini, comparison with adjacent uninvolved lobules is useful

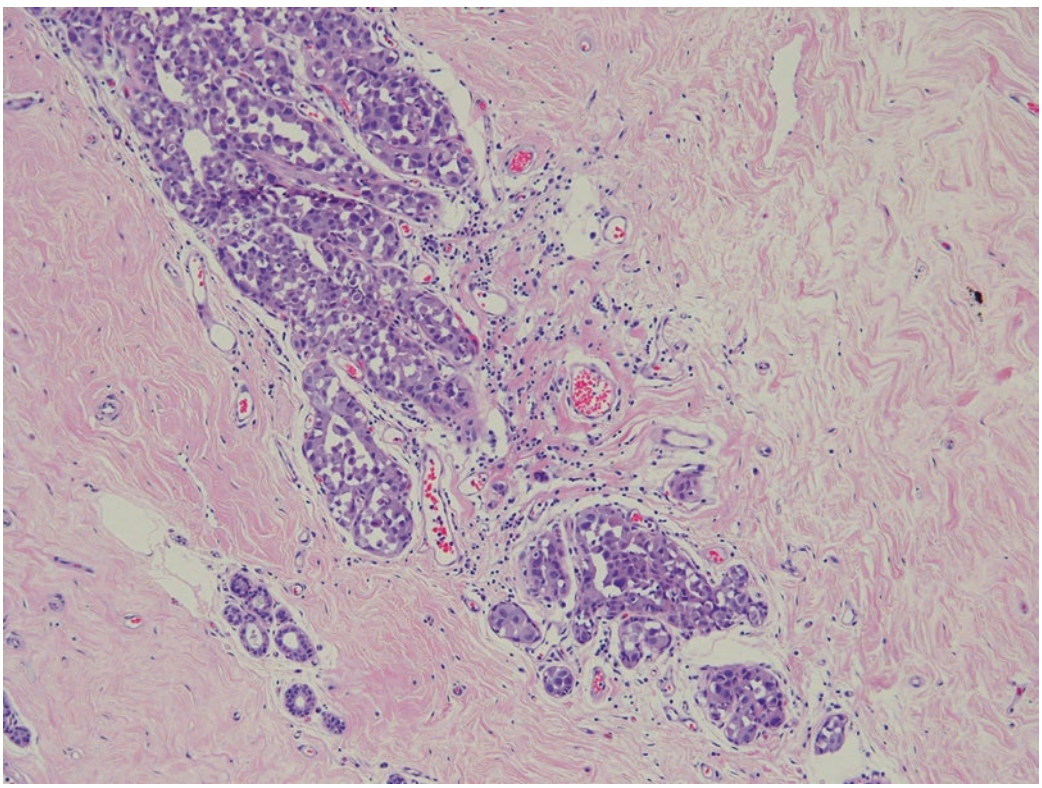

Fig. 10.15 Lobular carcinoma in situ. At low magnification, LCIS shows discohesive cells with pink cytoplasm suggesting an apocrine cytomorphology. Several unaffected acini are seen; when compared with acini involved by lobular neoplasia, there is confirmation of acinar distension by lobular neoplastic cells

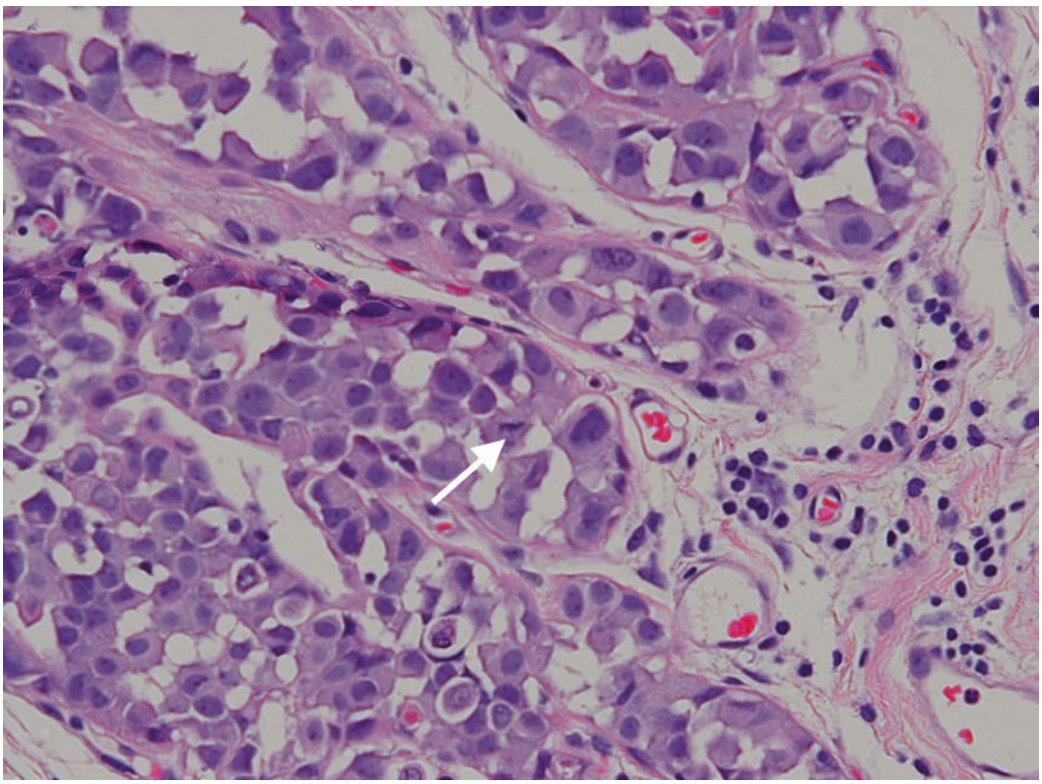

Fig. 10.16 Lobular carcinoma in situ with apocrine pleomorphic features. Here, the nuclei show moderate and marked pleomorphism, with pink cytoplasm indicating apocrine cytomorphology. A mitosis is seen (*white arrow*)

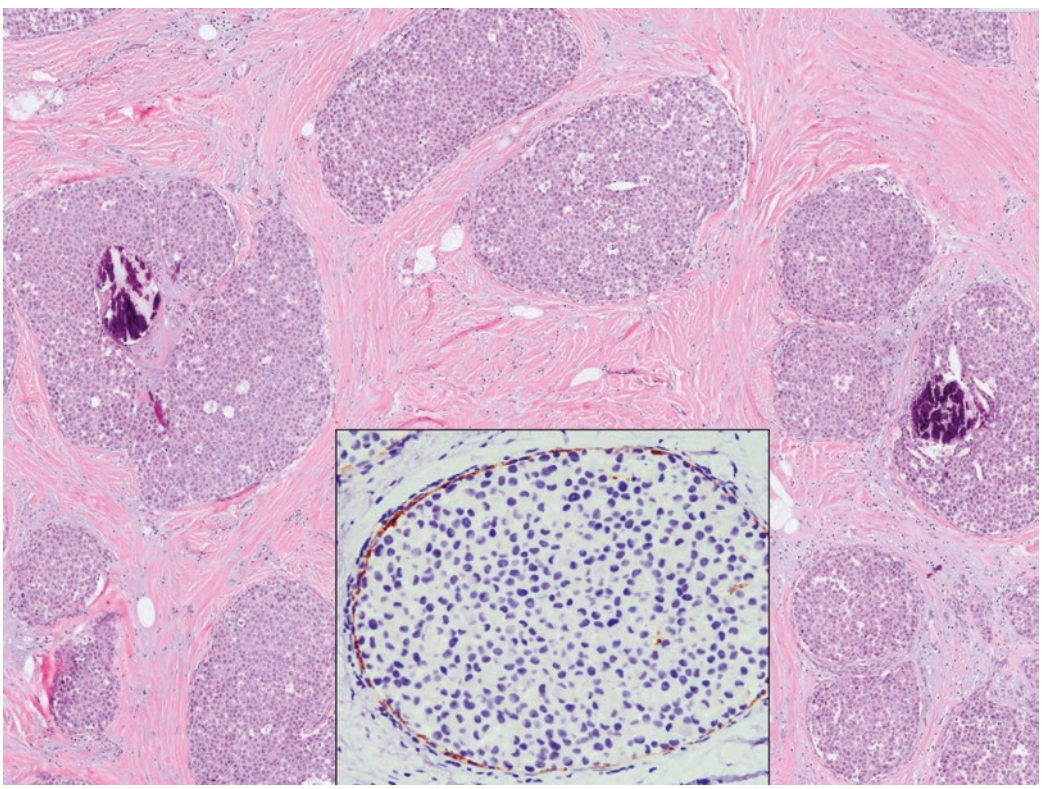

Fig. 10.17 Lobular carcinoma in situ. Fractured calcifications are observed in several distended islands of LCIS. *Inset* shows negative E-cadherin staining of LCIS cells

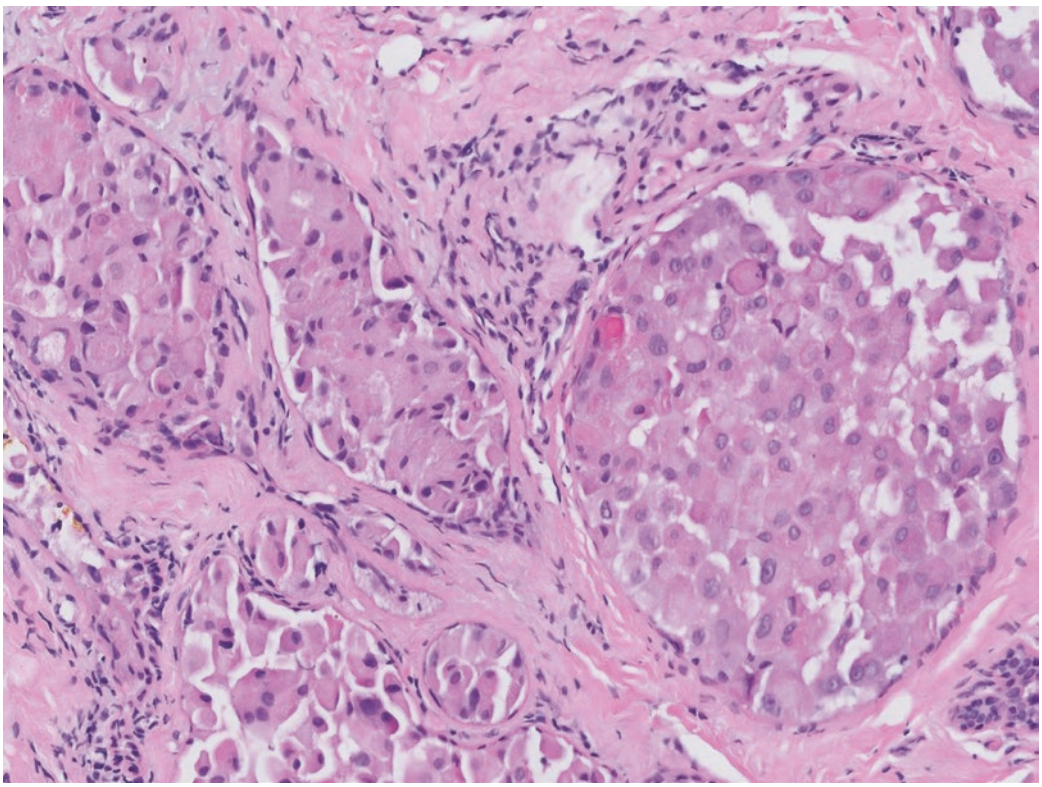

Fig. 10.18 Lobular carcinoma in situ with apocrine features. Apocrine cells with characteristic pink cytoplasm and enlarged vesicular nuclei with discernible nucleoli distend the duct spaces. The cells show discohesion

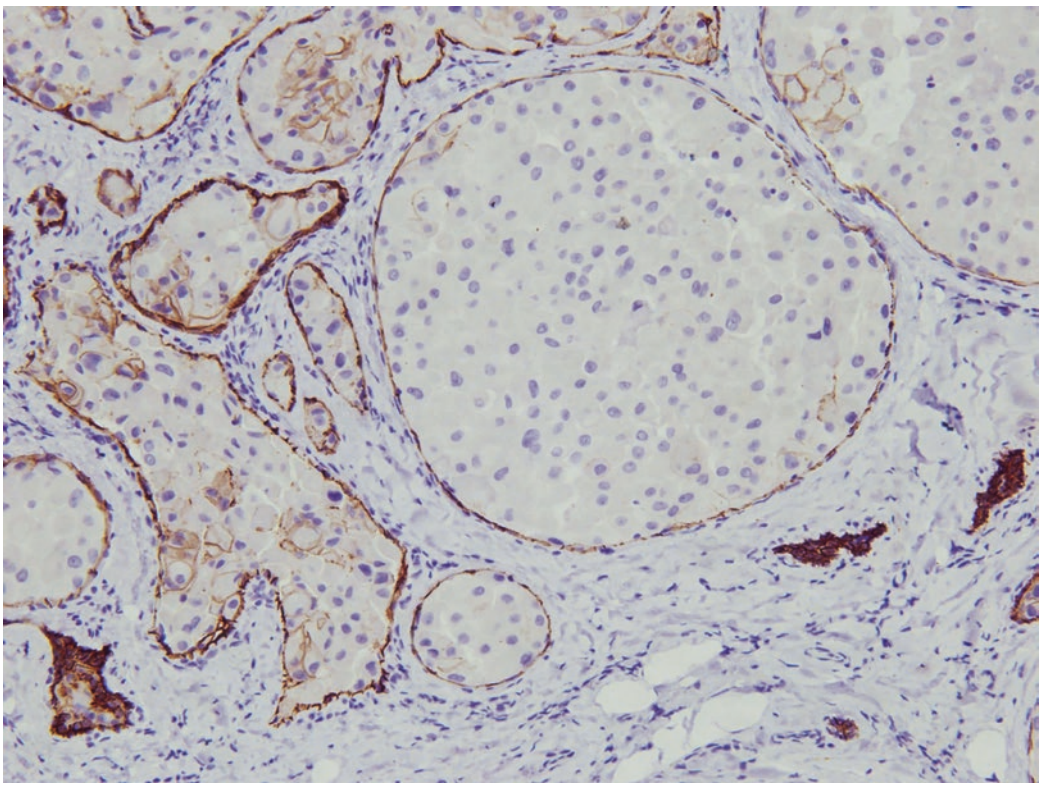

Fig. 10.19 Lobular carcinoma in situ with apocrine features. E-cadherin immunohistochemistry shows negative staining of the lobular neoplastic cells. A few individual cells in several affected spaces disclose incomplete cytoplasmic membrane staining

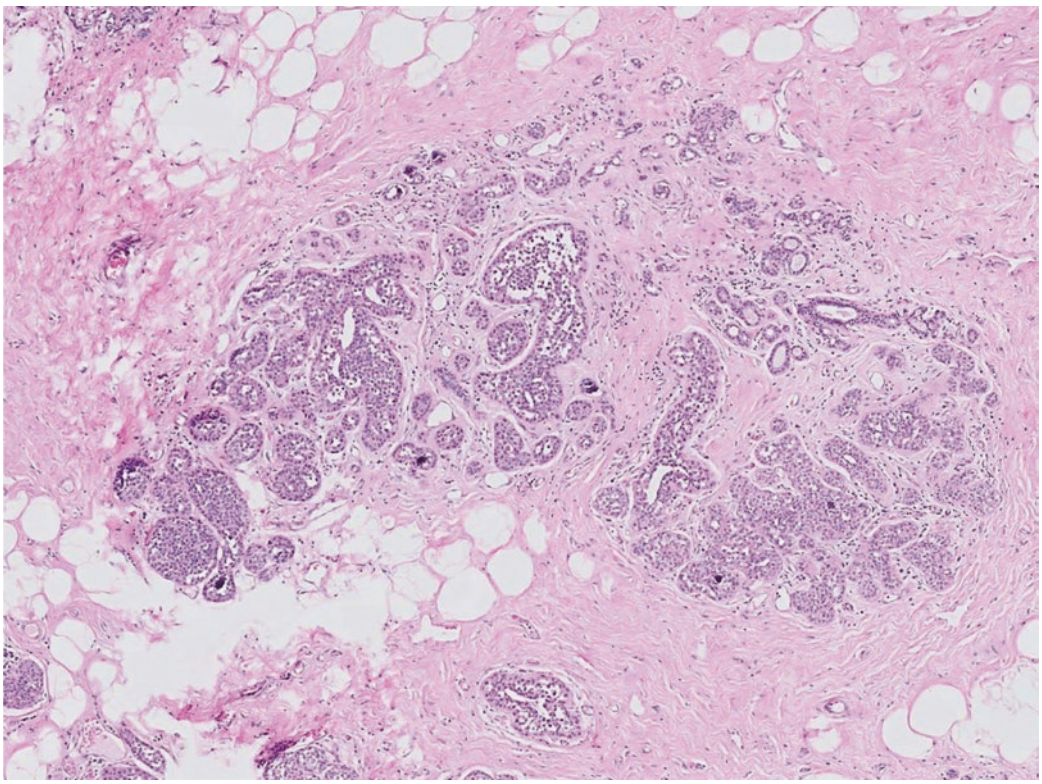

Fig. 10.20 Lobular neoplasia associated with calcifications. Infrequently, lobular neoplasia may be accompanied by calcifications, which can be detected mammographically. More often, lobular neoplasia is incidentally identified adjacent to columnar cell lesions that calcify, rather than being directly associated with calcifications

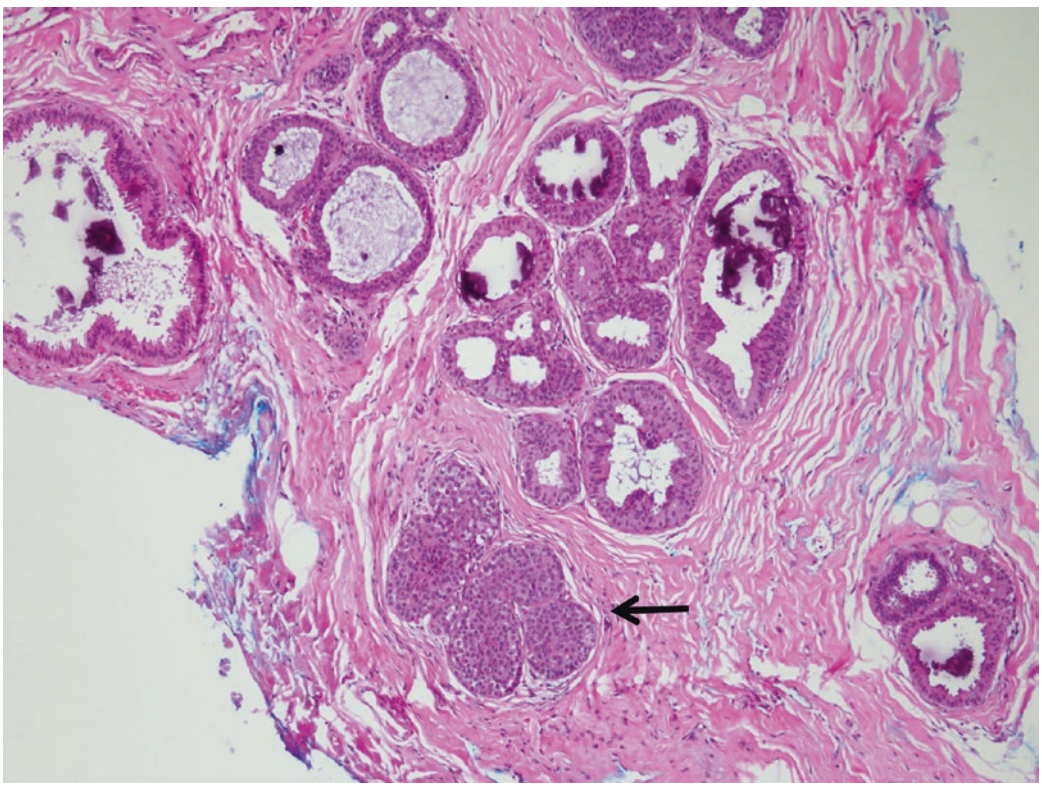

Fig. 10.21 Lobular carcinoma in situ (*arrow*) with adjacent columnar cell hyperplasia and calcifications

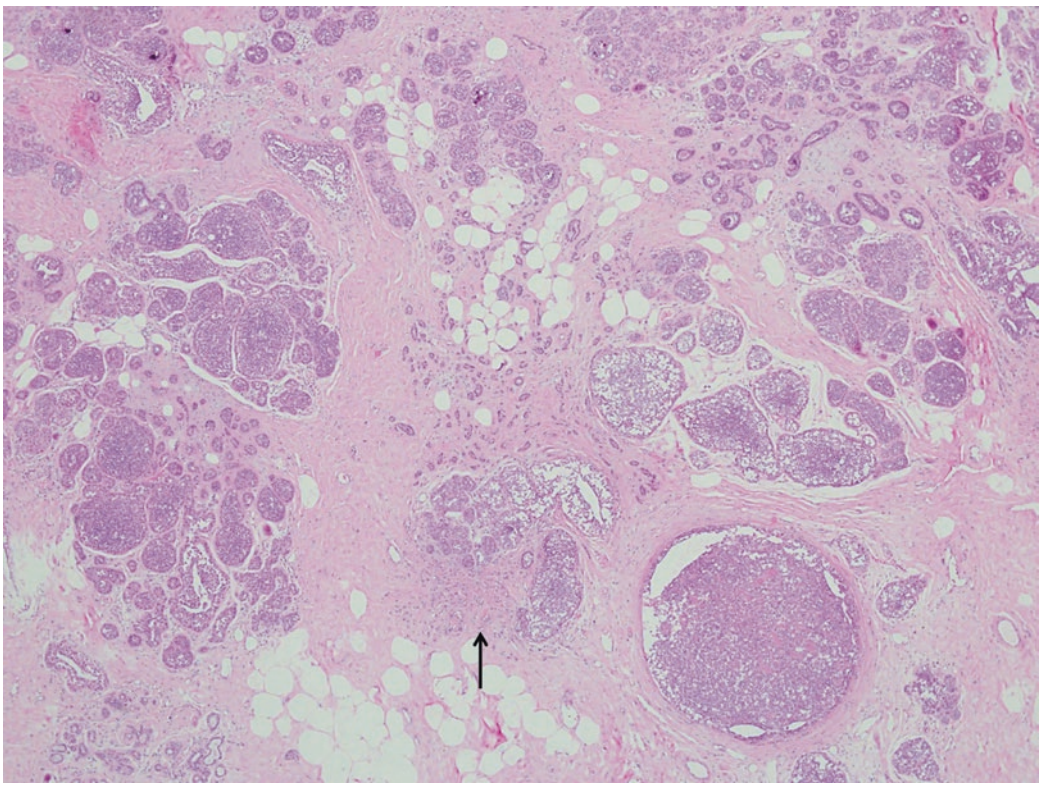

Fig. 10.22 Lobular carcinoma in situ with invasive tubular carcinoma. Low magnification of breast tissue shows LCIS affecting multiple terminal ductal lobular units. Centrally, there is an invasive tubular carcinoma composed of haphazardly placed tubules. Invasive lobular carcinoma is also present (*arrow*) but is difficult to appreciate at this low magnification

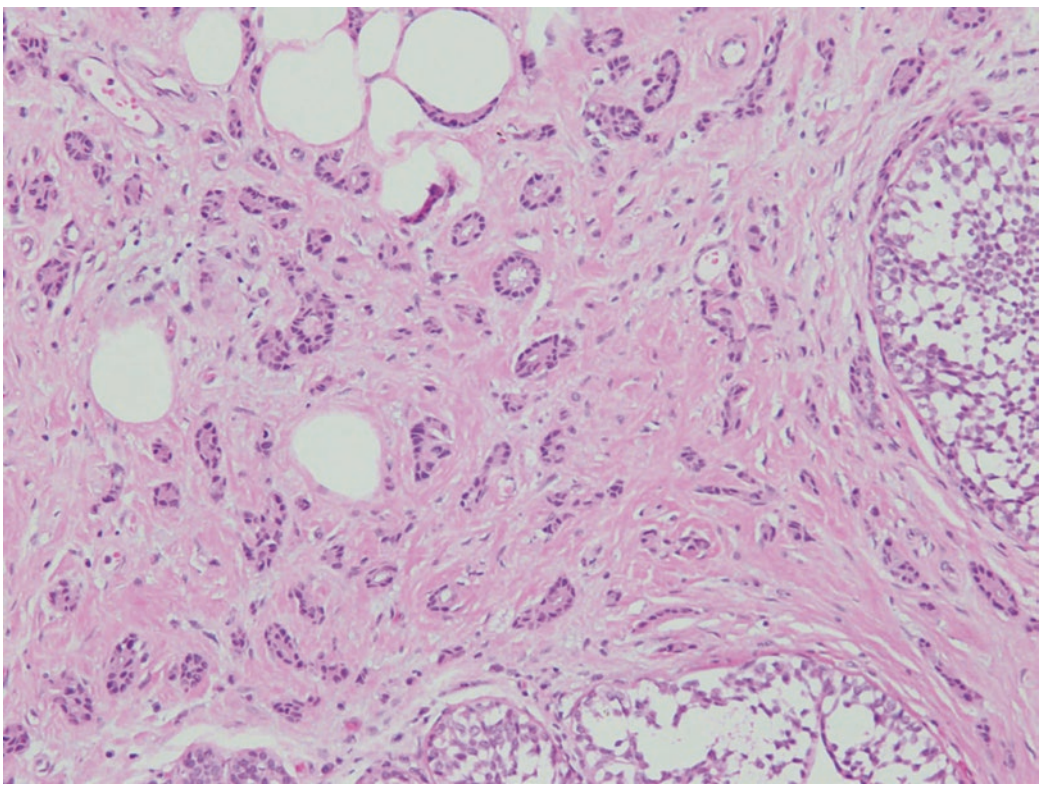

Fig. 10.23 Lobular carcinoma in situ with invasive tubular carcinoma. Patent, rounded, and angulated tubules of invasive tubular carcinoma are found adjacent to LCIS. Lobular neoplasia, flat epithelial atypia, atypical ductal hyperplasia, and low-grade invasive carcinomas form part of the spectrum of the low nuclear grade neoplasia family of breast lesions

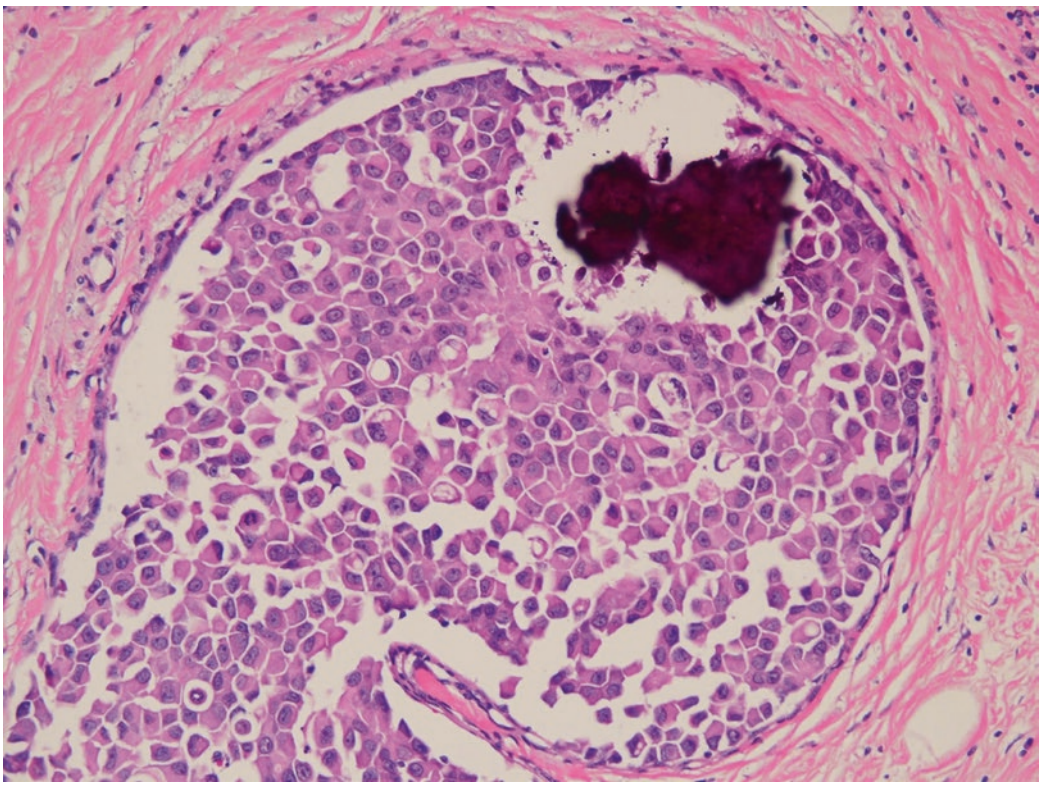

Fig. 10.24 Pleomorphic LCIS. This duct space is expanded by abnormal, discohesive cells with moderate to marked nuclear pleomorphism. Some cells show cytoplasmic vacuoles. Cytoplasm of many cells is pink, giving an apocrine appearance. A calcification is noted. The diagnosis of pleomorphic LCIS requires the presence of marked nuclear pleomorphism (grade 3 nuclei)

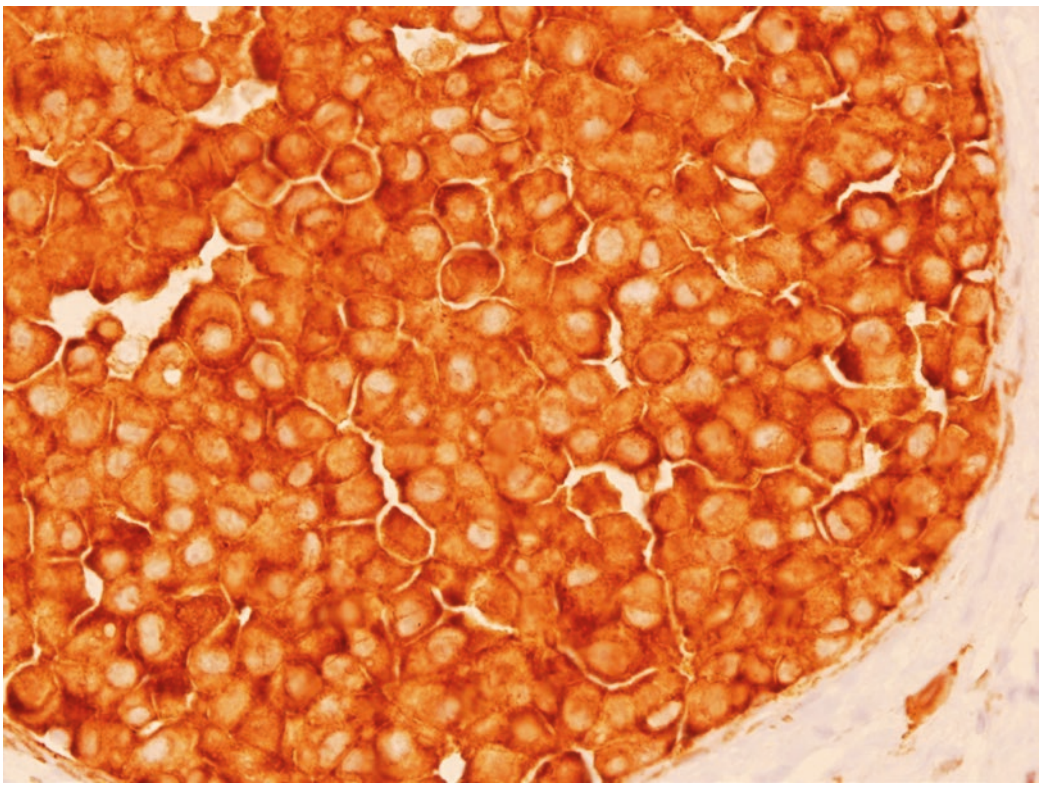

Fig. 10.25 Pleomorphic LCIS. Immunohistochemistry for p120 catenin shows cytoplasmic localisation of staining, without any membrane reactivity. In interpreting p120 catenin staining, it is important to compare with the internal positive controls of benign ducts and ductules, which display crisp membrane positivity, in contrast to the cytoplasmic reactivity of lobular neoplasia and invasive lobular carcinoma. Sometimes, apposition or overlapping of lobular neoplastic and lobular carcinoma cells can lead to an accentuation of staining near the cytoplasmic membrane, which may mimic membrane staining (Reprinted from Ho and Tan [6]; with permission)

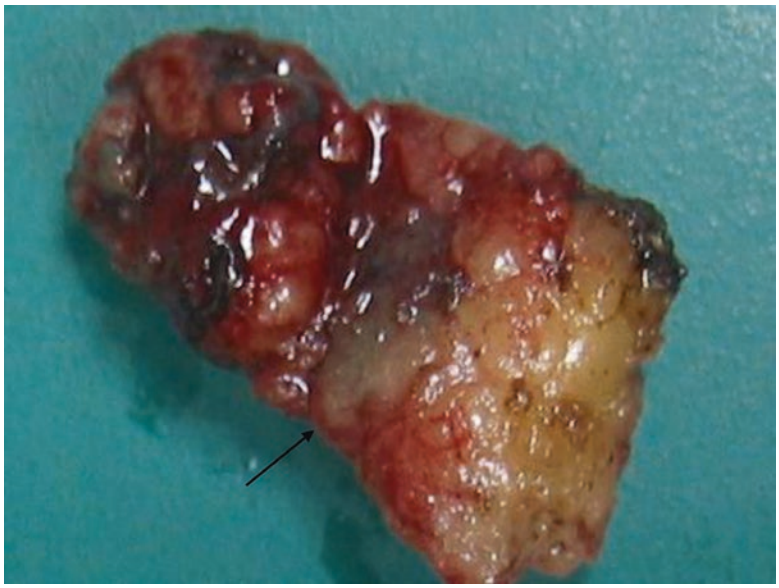

Fig. 10.26 Lobular carcinoma in situ within a radial sclerosing lesion. Excision of a radiologically stellate lesion shows an ill-defined, whitish, firm area in the breast tissue (*arrow*). Histological assessment disclosed a radial sclerosing lesion with superimposed LCIS

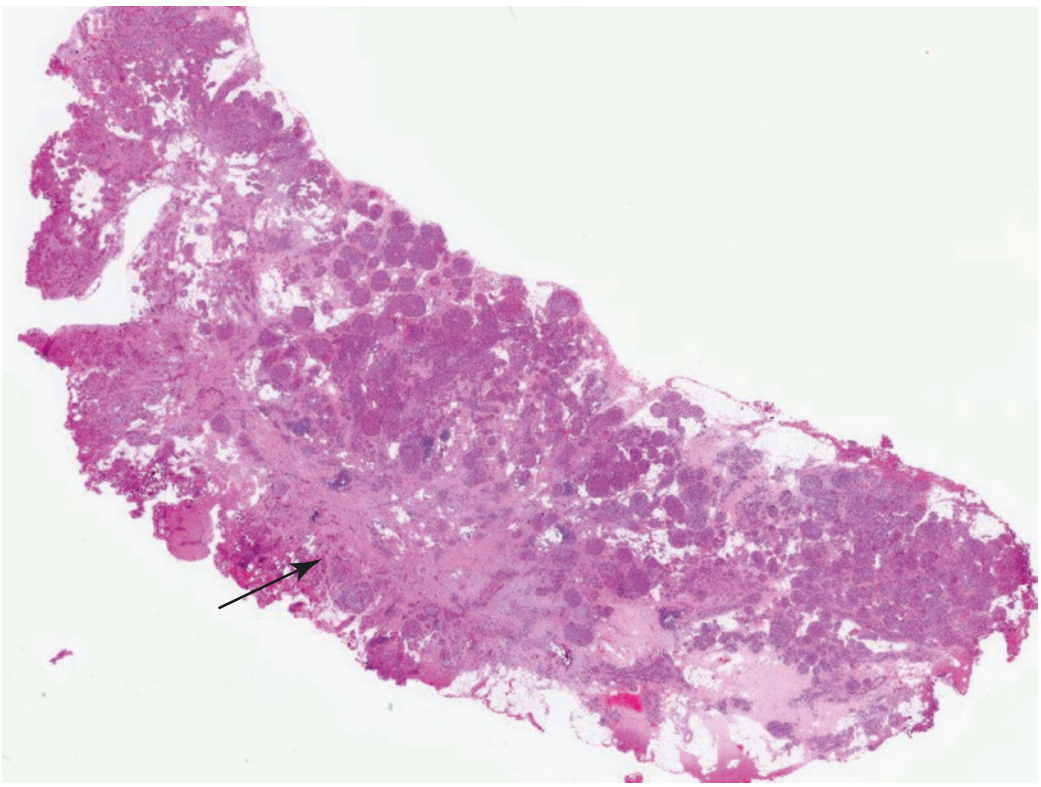

Fig. 10.27 Lobular carcinoma in situ within a radial sclerosing lesion. At scanning magnification, the fibrotic core of the radial sclerosing lesion is seen (*arrow*). Solidified epithelial islands radiate from the fibrotic centre

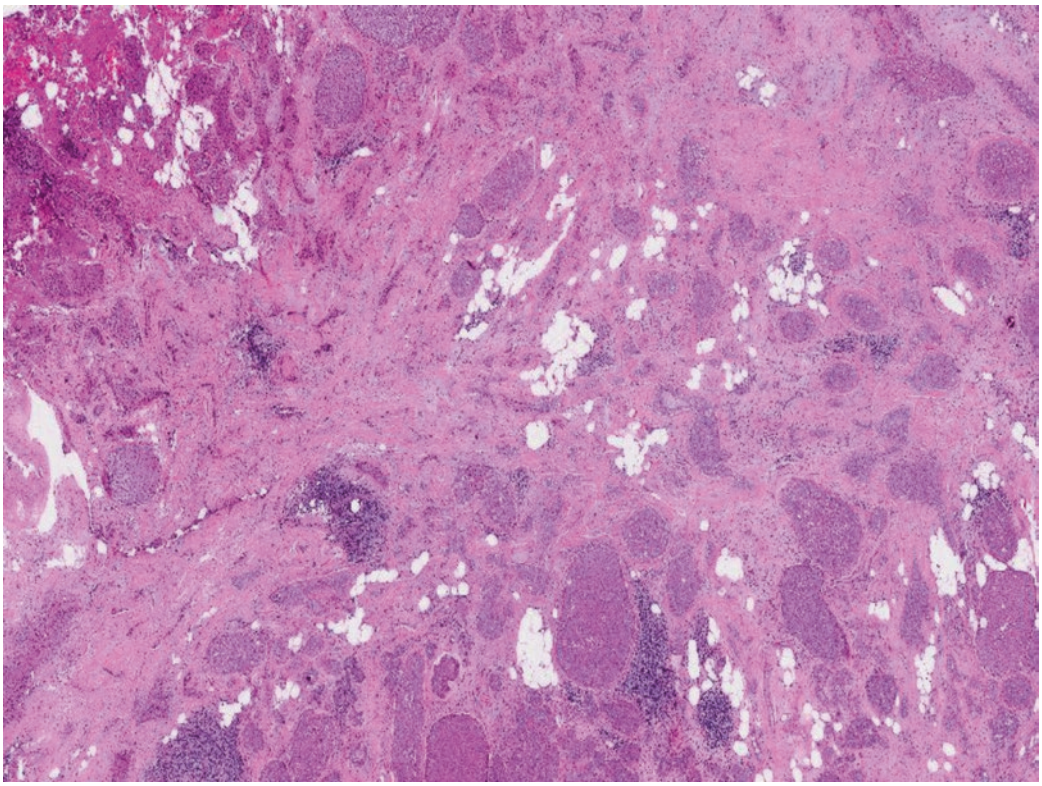

Fig. 10.28 Lobular carcinoma in situ within a radial sclerosing lesion. At low magnification, there is a central fibrotic nidus around which the solidified duct spaces emanate

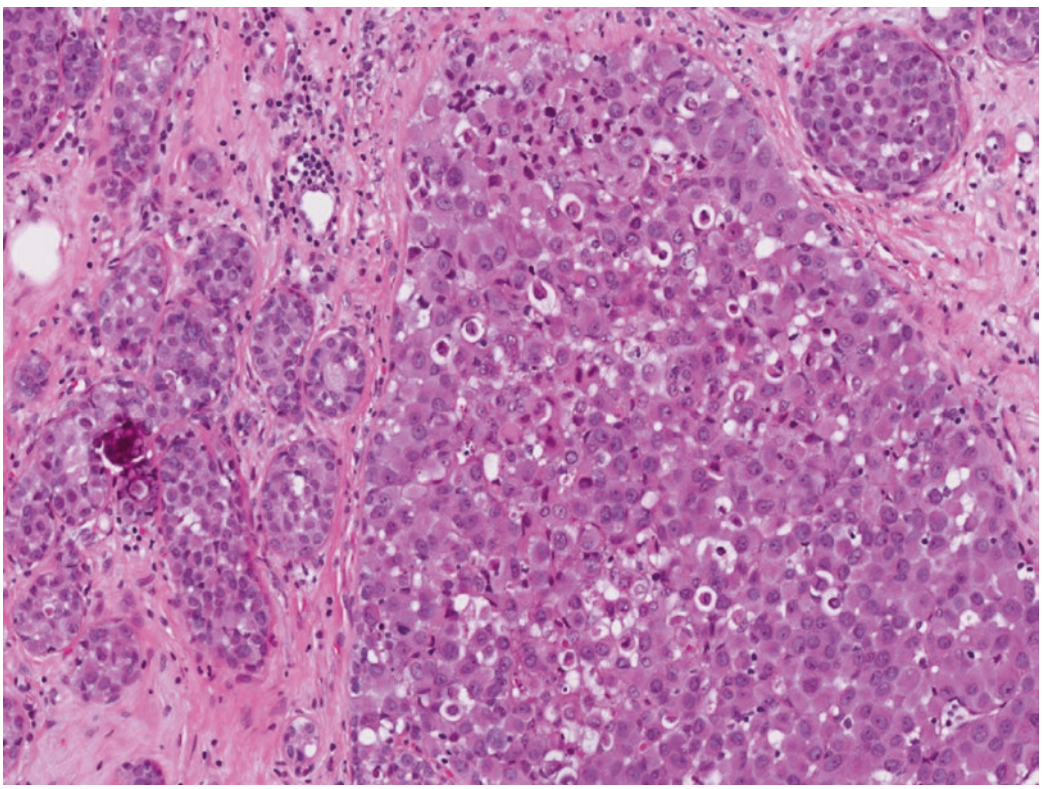

Fig. 10.29 Lobular carcinoma in situ within a radial sclerosing lesion. A discohesive cell population fills the duct and acinar spaces. The largest duct space is distended by pleomorphic apocrine cells with intercellular spaces and apoptosis, features of pleomorphic apocrine LCIS. Surrounding acini contain a more uniform population of classic LCIS, accompanied by a calcification (*left field*)

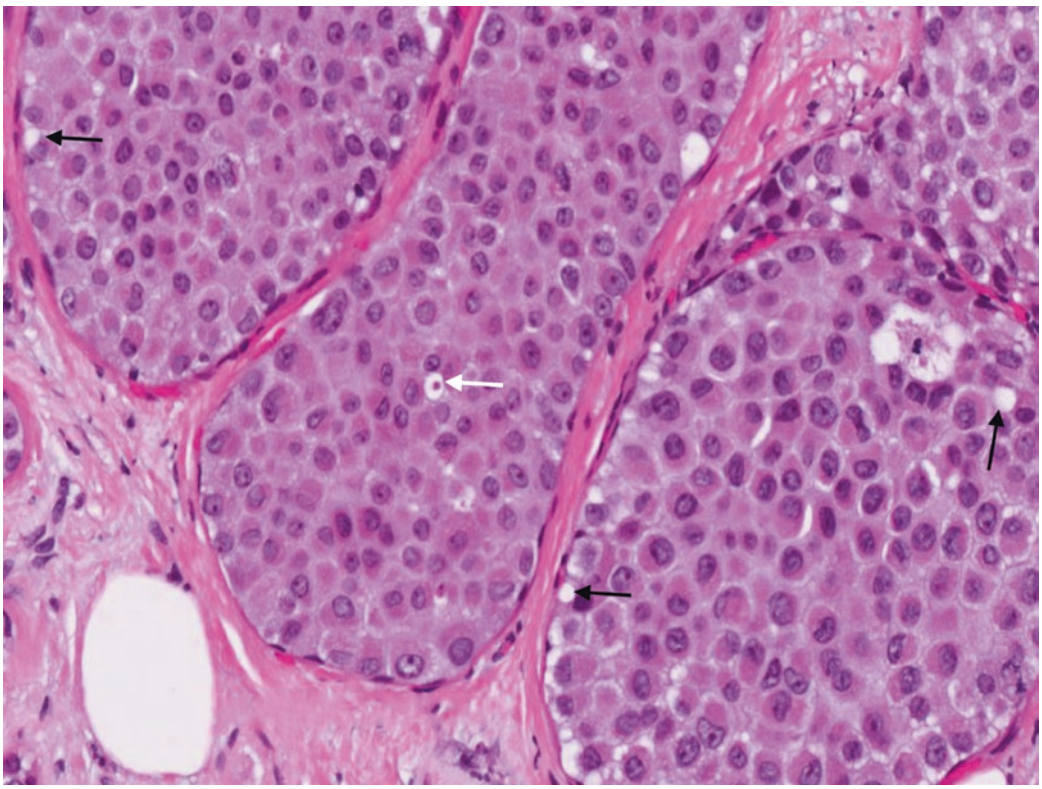

Fig. 10.30 Lobular carcinoma in situ with pleomorphic apocrine features. Occasional intracytoplasmic lumens are present (*black arrows*), with a targetoid secretory droplet observed in one lumen (*white arrow*)

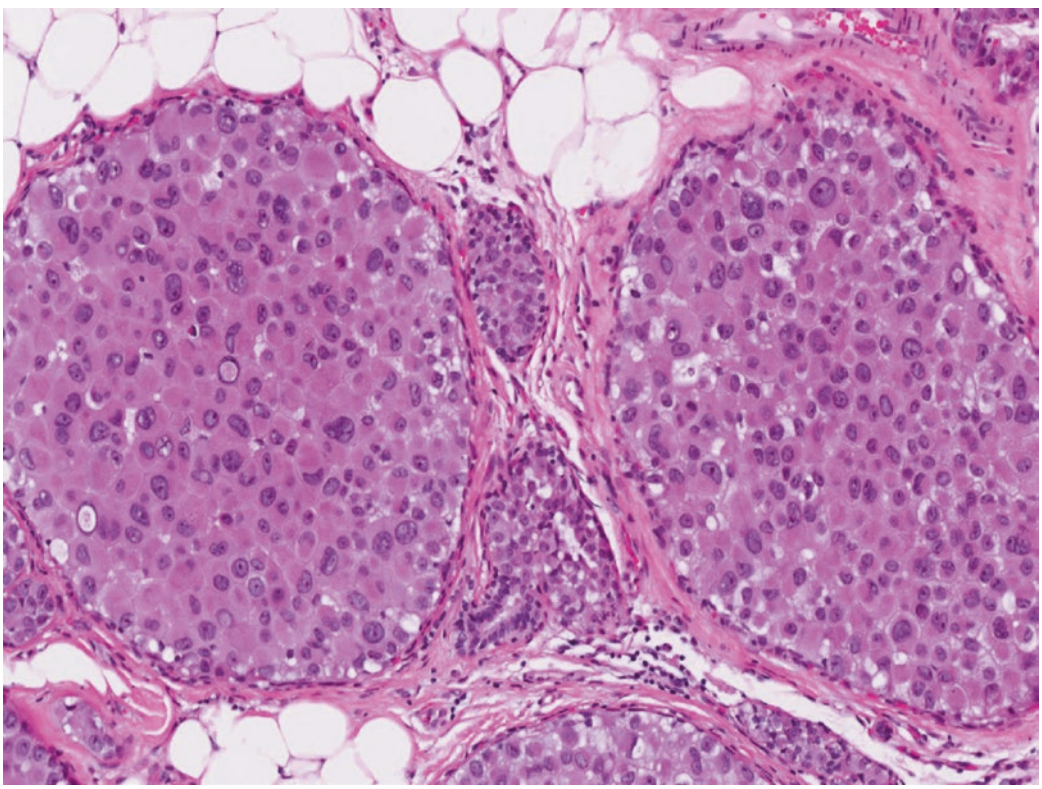

Fig. 10.31 Pleomorphic apocrine LCIS. Discohesive apocrine cells with moderate to marked nuclear pleomorphism and pink cytoplasm distend duct spaces

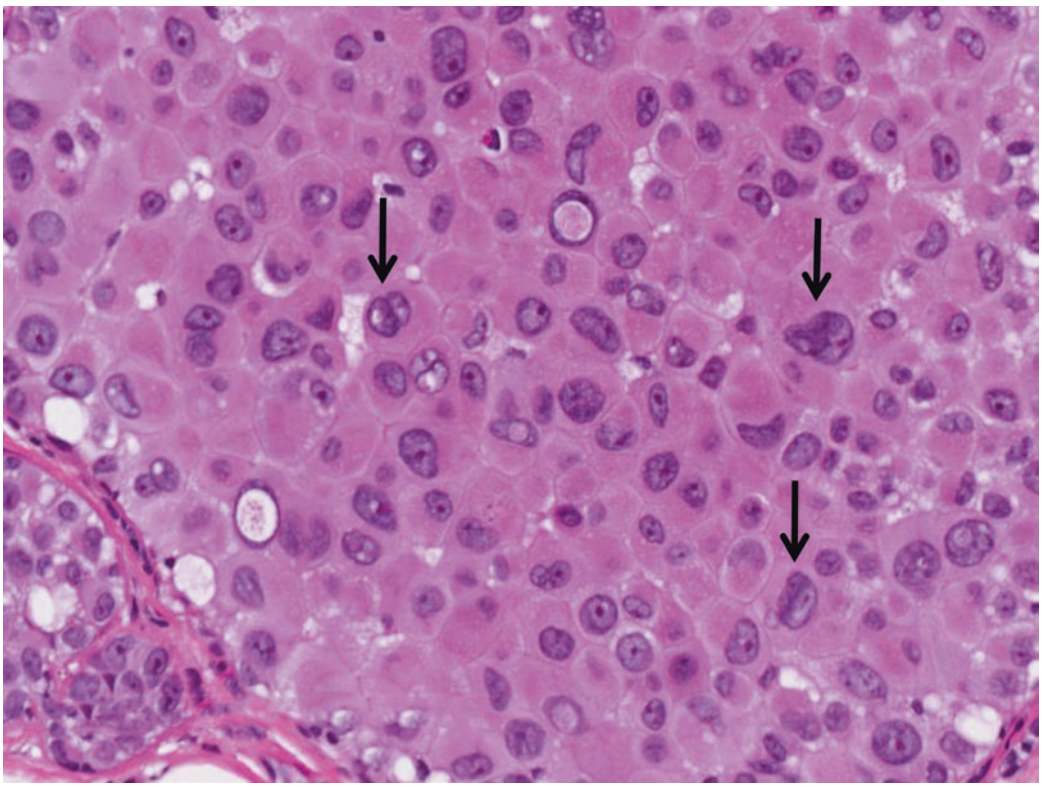

Fig. 10.32 Pleomorphic apocrine LCIS. Multinucleation (*arrows*) and intranuclear inclusions are present

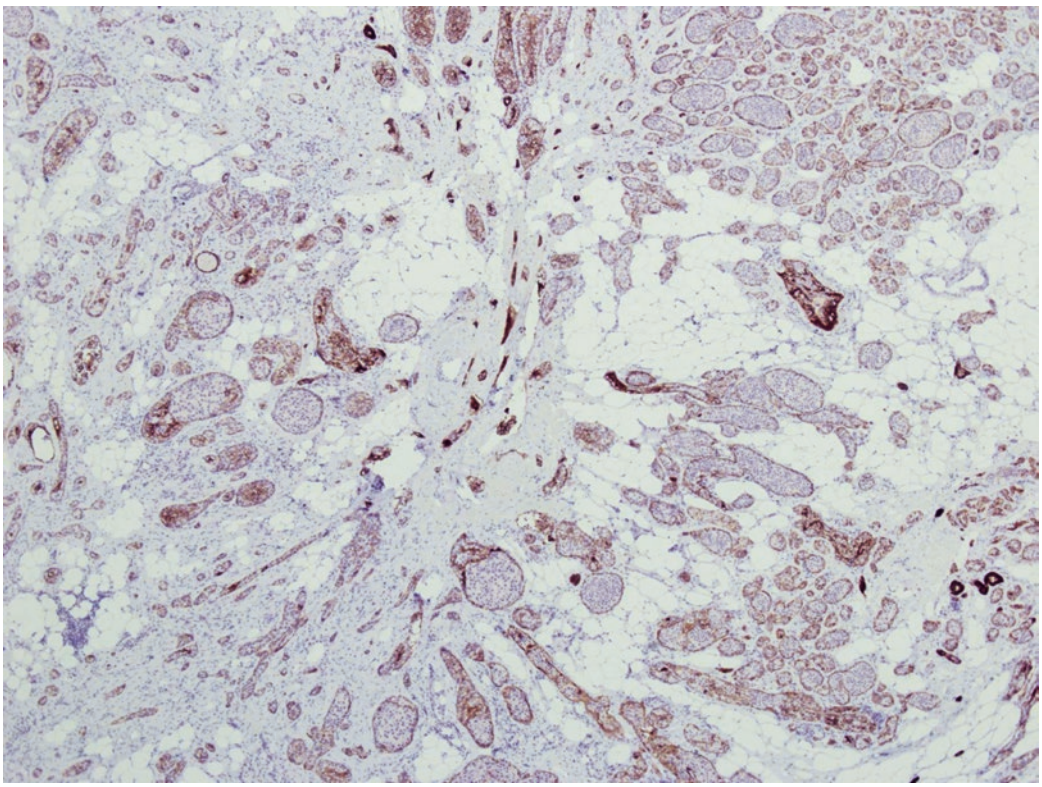

Fig. 10.33 Lobular carcinoma in situ within a radial sclerosing lesion. E-cadherin immunohistochemistry shows loss of staining in the lobular neoplastic cells

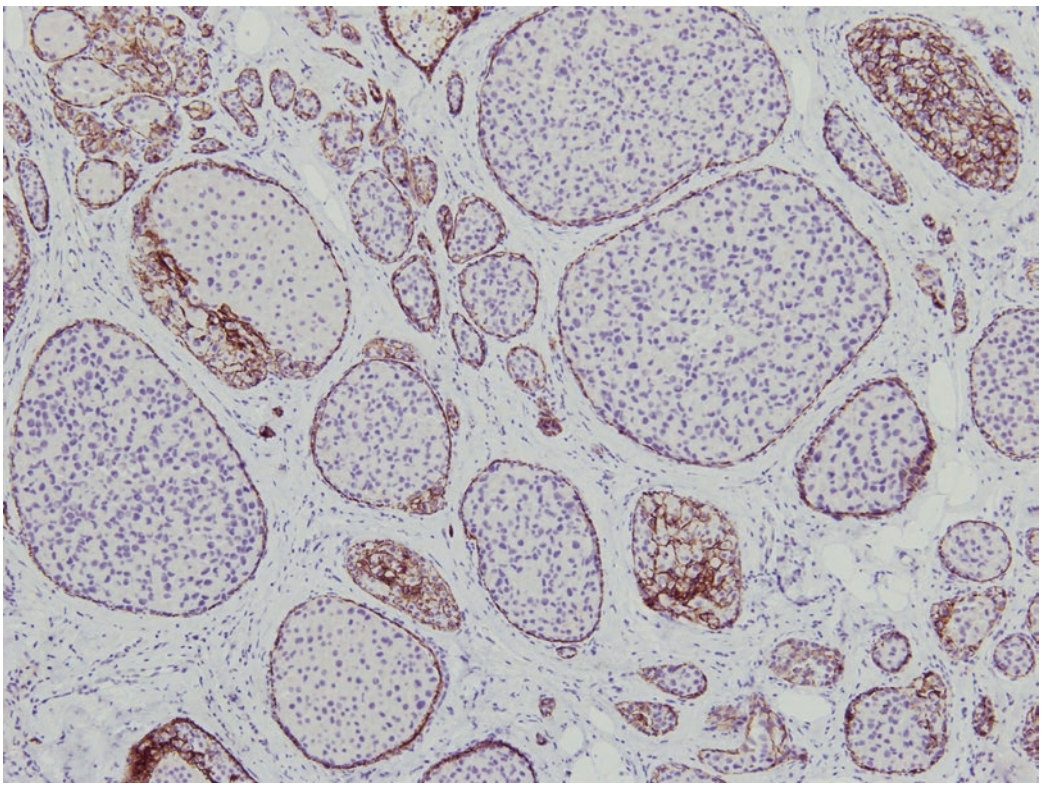

Fig. 10.34 Lobular carcinoma in situ within a radial sclerosing lesion. Higher magnification shows negative staining for E-cadherin in the lobular neoplastic cells, with a positively stained peripheral myoepithelial rim

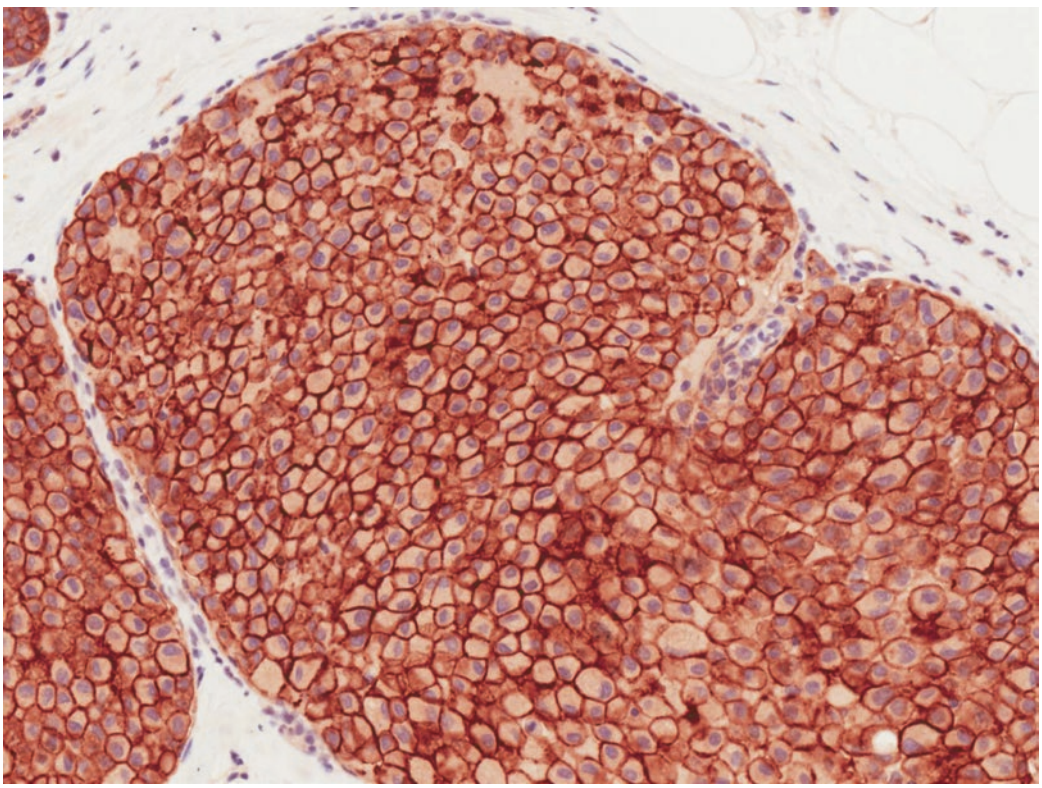

Fig. 10.35 Pleomorphic apocrine LCIS shows positive staining for c-erbB-2 (HER2). This type of staining is not performed for prognostic purposes, but it can be applied to support a pleomorphic morphology, as pleomorphic LCIS has a higher rate of c-erbB-2 overexpression

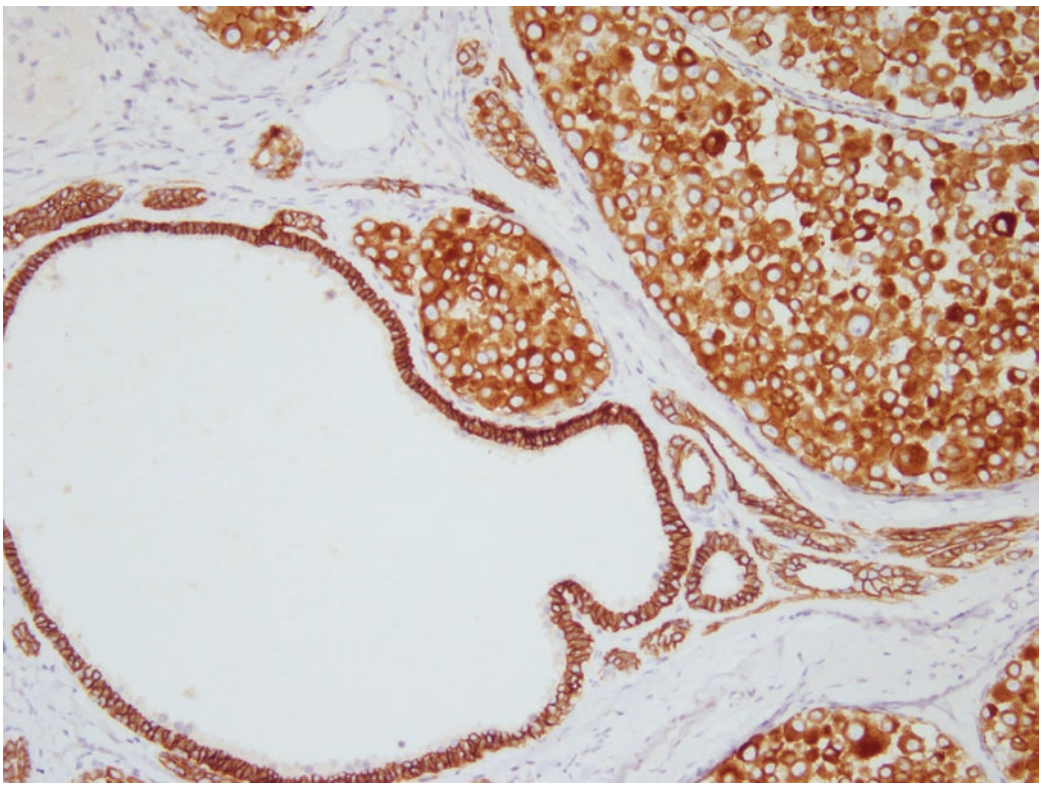

Fig. 10.36 Aberrant E-cadherin staining in LCIS shows cytoplasmic rather than membrane staining, contrasting against the membrane localisation of E-cadherin in the adjacent ducts

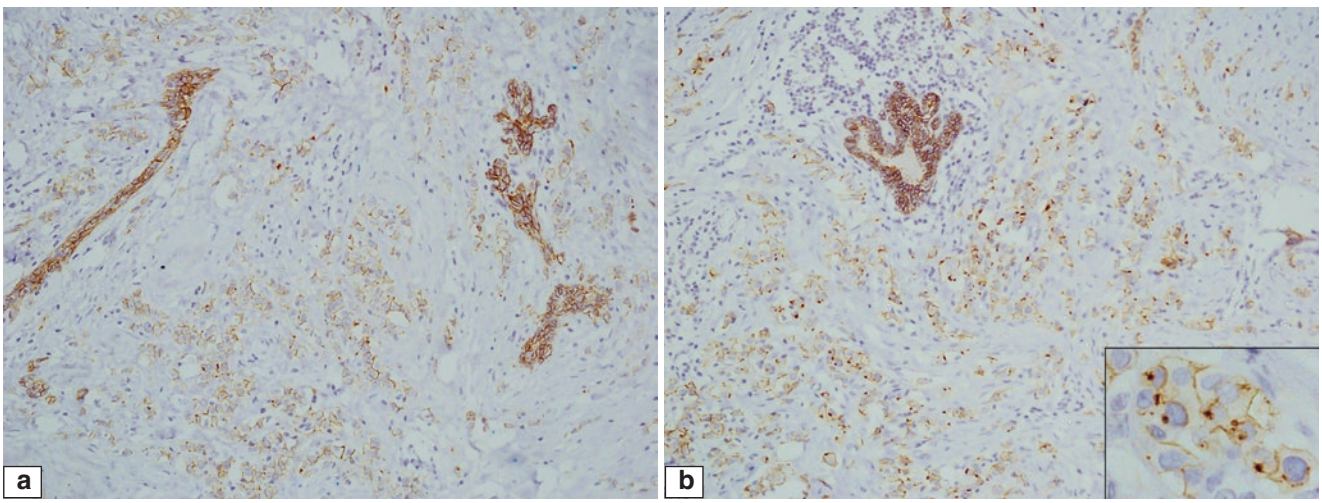

Fig. 10.37 Aberrant E-cadherin staining. (**a**) Invasive lobular carcinoma cells show diminished intensity and incomplete membrane staining for E-cadherin, contrasting against the benign ducts and acini, which disclose more intense membrane reactivity of epithelial cells. (**b**) A globular, dot-like staining is seen in the cytoplasm of invasive lobular carcinoma cells. Inset shows paranuclear globular staining for E-cadherin of lobular carcinoma cells

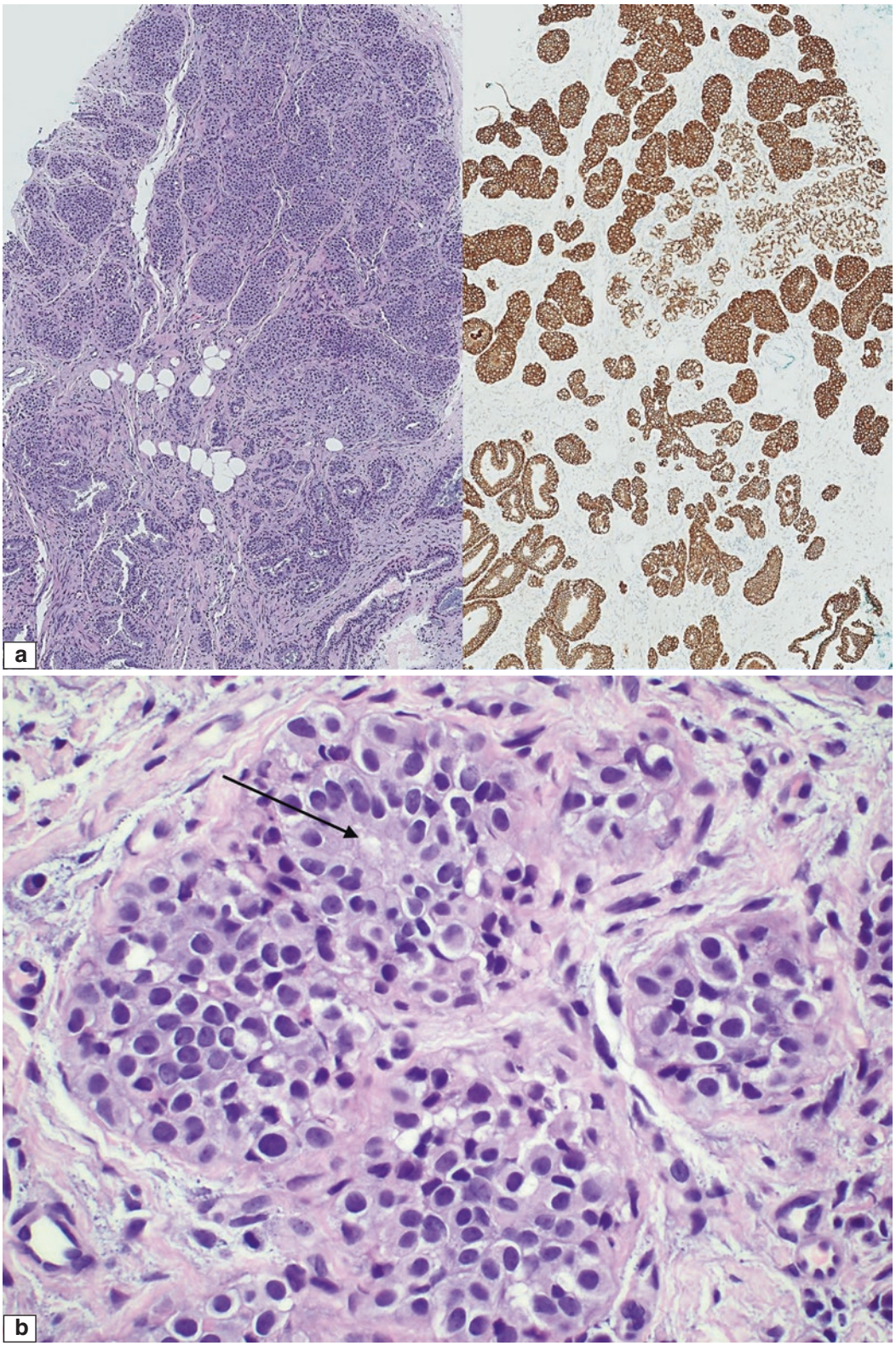

Fig. 10.38 (**a**) Lobular neoplasia comprising both atypical lobular hyperplasia and lobular carcinoma in situ is present in the breast tissue (*left*), confirmed with E-cadherin immunohistochemistry that reveals diminished staining in several of the affected acini. Some of the acini that are affected by lobular neoplasia however, appear to retain E-cadherin staining at this magnification. (**b**) Higher magnification of several acini affected by lobular neoplasia, with rounded discohesive cells with occasional intracytoplasmic lumens. A small acinar lumen is discerned (*arrow*). (**c**) Immunohistochemistry of apparently positive E-cadherin membrane staining in acini that on light microscopy showed involvement by lobular neoplasia. Close scrutiny shows epithelial cells lining the central lumens of the acini to disclose smooth continuous linear staining of their cytoplasmic membranes (*black arrows*), while the surrounding cells display thick clumpy membrane positivity (*red arrows*), which may be interpreted as aberrant staining. (**d**) Closer view of E-cadherin immunostaining shows thick, clumpy and smudgy cytoplasmic membrane staining of lobular neoplastic cells, compared against the smooth, uninterrupted and continuous cytoplasmic membrane staining of luminal epithelial cells

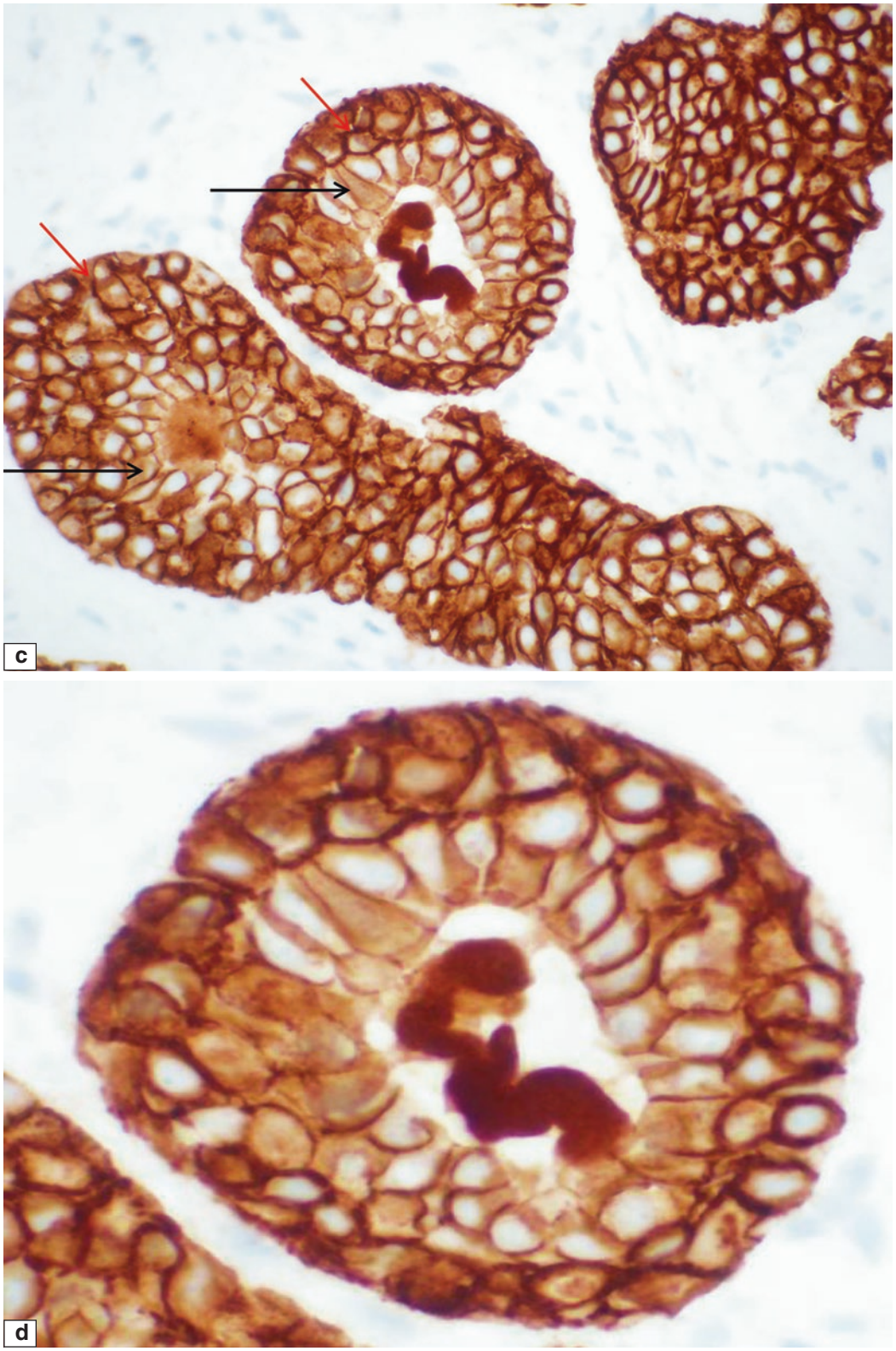

Fig. 10.38 (continued)

Differential Diagnosis

Myoepithelial Hyperplasia and Apocrine Cells

Myoepithelial hyperplasia may resemble lobular neoplasia when the hyperplastic myoepithelial cells encroach against and obscure luminal epithelial cells (Figs. 10.39 and 10.40). These myoepithelial cells may display pale to clear cytoplasm with round nuclei that mimic lobular neoplasia. Lobular neoplasia is often multifocal, whereas myoepithelial hyperplasia may be confined to specific acini within a lobule, and cellular discohesion is not a distinct feature. Immunohistochemistry for E-cadherin is helpful in verifying its membranous retention in myoepithelial hyperplasia, although the staining in myoepithelial cells may be slightly less intense than in the luminal epithelial cells. Occasionally, apocrine cells in acini can also mimic lobular neoplastic cells (Figs. 10.41, 10.42, 10.43, and 10.44).

Solid Ductal Carcinoma In Situ, Low Nuclear Grade

Lobular carcinoma in situ (classic type) may resemble solid ductal carcinoma in situ (DCIS) of low nuclear grade (Figs. 10.45, 10.46, 10.47, and 10.48). Distinguishing features are discussed in the section "Low Nuclear Grade DCIS Versus Lobular Carcinoma In Situ (Classic)", in Chapter 9.

Lobular Cancerisation

Lobular cancerisation refers to DCIS involvement of pre-existing lobules that retain the lobular architecture [9]. Usually, an invasive ductal carcinoma is present in the vicinity. In lobular cancerisation, acini are variably distended by in situ ductal carcinoma cells, giving a solid growth pattern that resembles LCIS. When lobular cancerisation shows high nuclear grade, it mimics pleomorphic LCIS (Figs. 10.49 and 10.50).

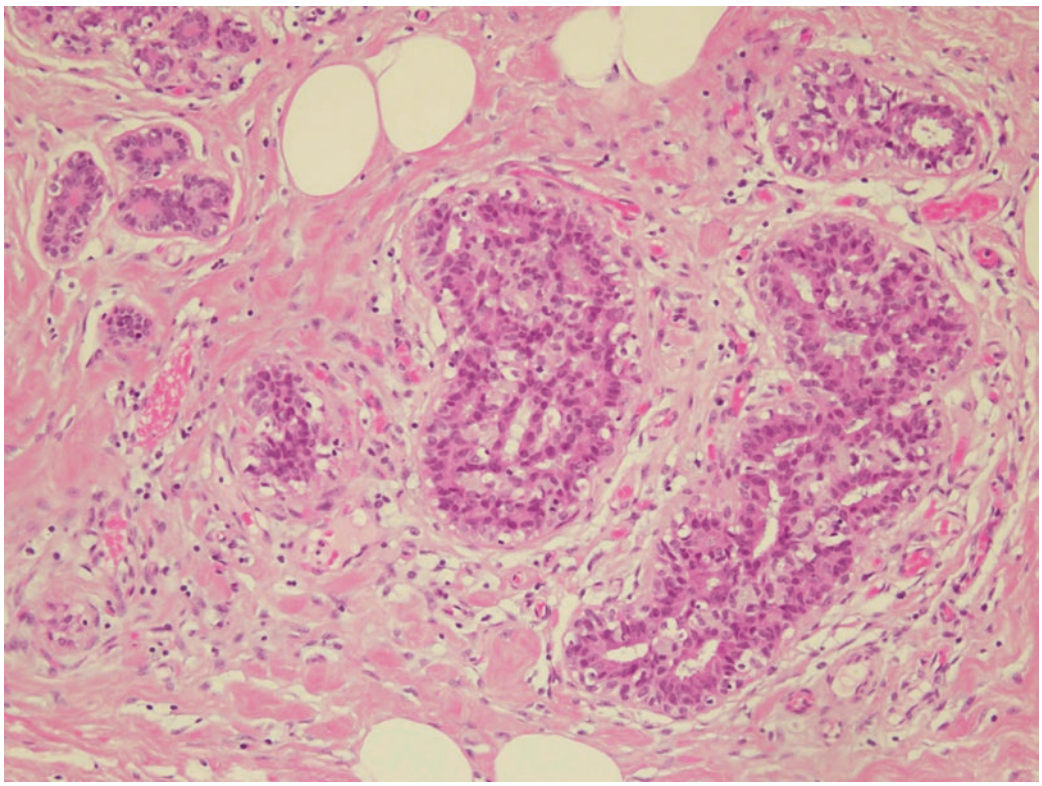

Fig. 10.39 Myoepithelial hyperplasia. Prominence of myoepithelial cells at the periphery of ducts and acini may resemble lobular neoplasia. In contrast to lobular neoplasia, myoepithelial hyperplasia is seen as a layer of cells at the periphery, without substantial effacement of the luminal epithelial population

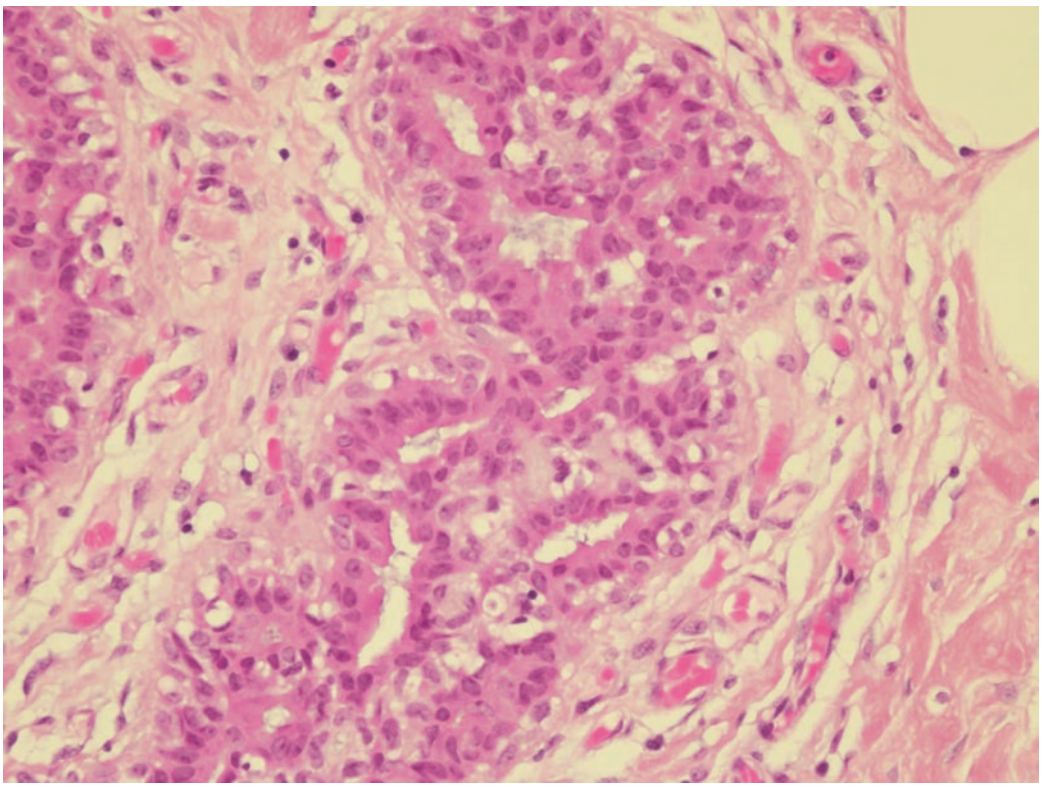

Fig. 10.40 Myoepithelial hyperplasia. Prominent myoepithelial cells are seen rimming the luminal epithelial cells. There is no effacement of the luminal spaces, nor rounded contouring of acini

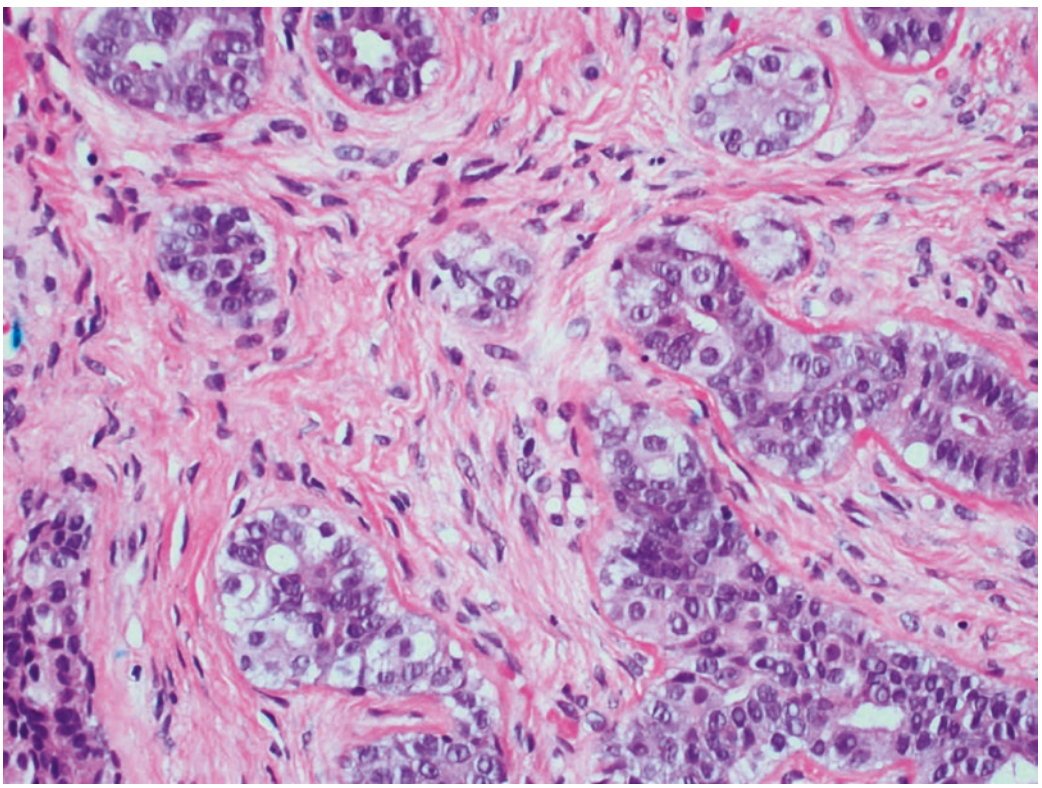

Fig. 10.41 Apocrine cells in acini resembling lobular neoplasia. In a few acini of this lobule, there are scattered rounded, plump cells with pale to light pink cytoplasm and central vesicular nuclei, interspersed among the luminal epithelial cells and myoepithelial cells, mimicking atypical lobular hyperplasia

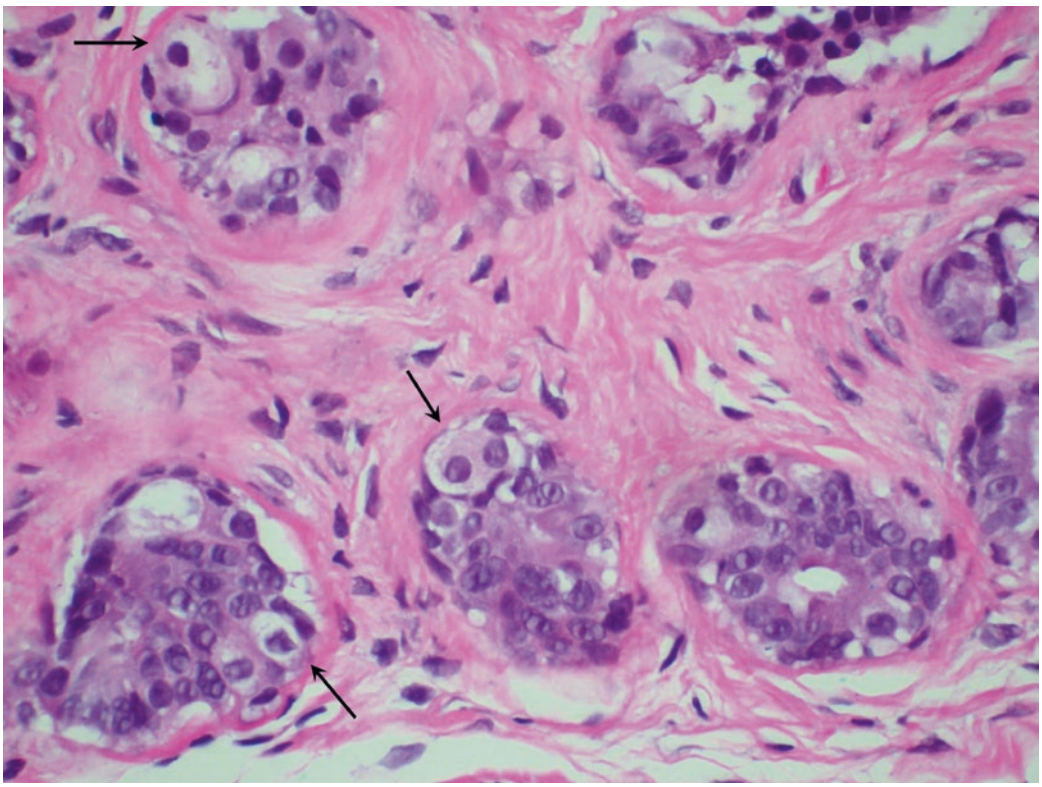

Fig. 10.42 Apocrine cells in acini mimicking lobular neoplasia. Plump, rounded apocrine cells are seen in the acini (*arrows*)

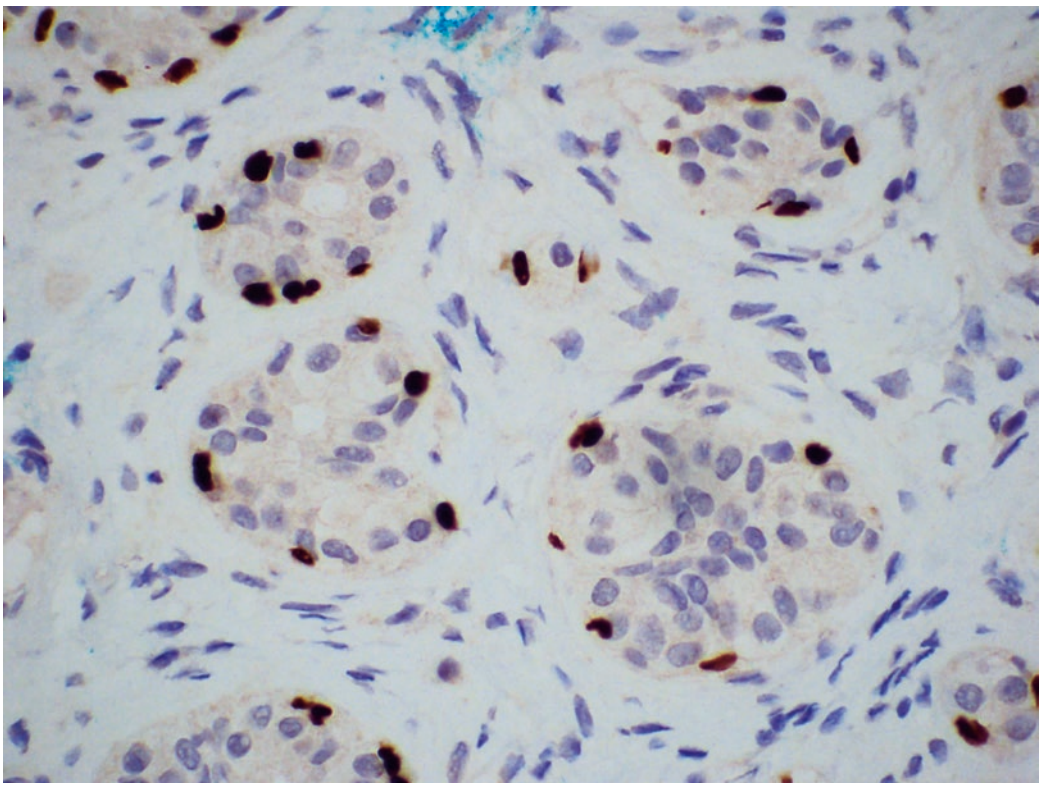

Fig. 10.43 Apocrine cells in acini mimicking lobular neoplasia. Immunohistochemistry for p63 shows positive nuclear staining of myoepithelial cells; the apocrine cells and luminal epithelial cells are negative

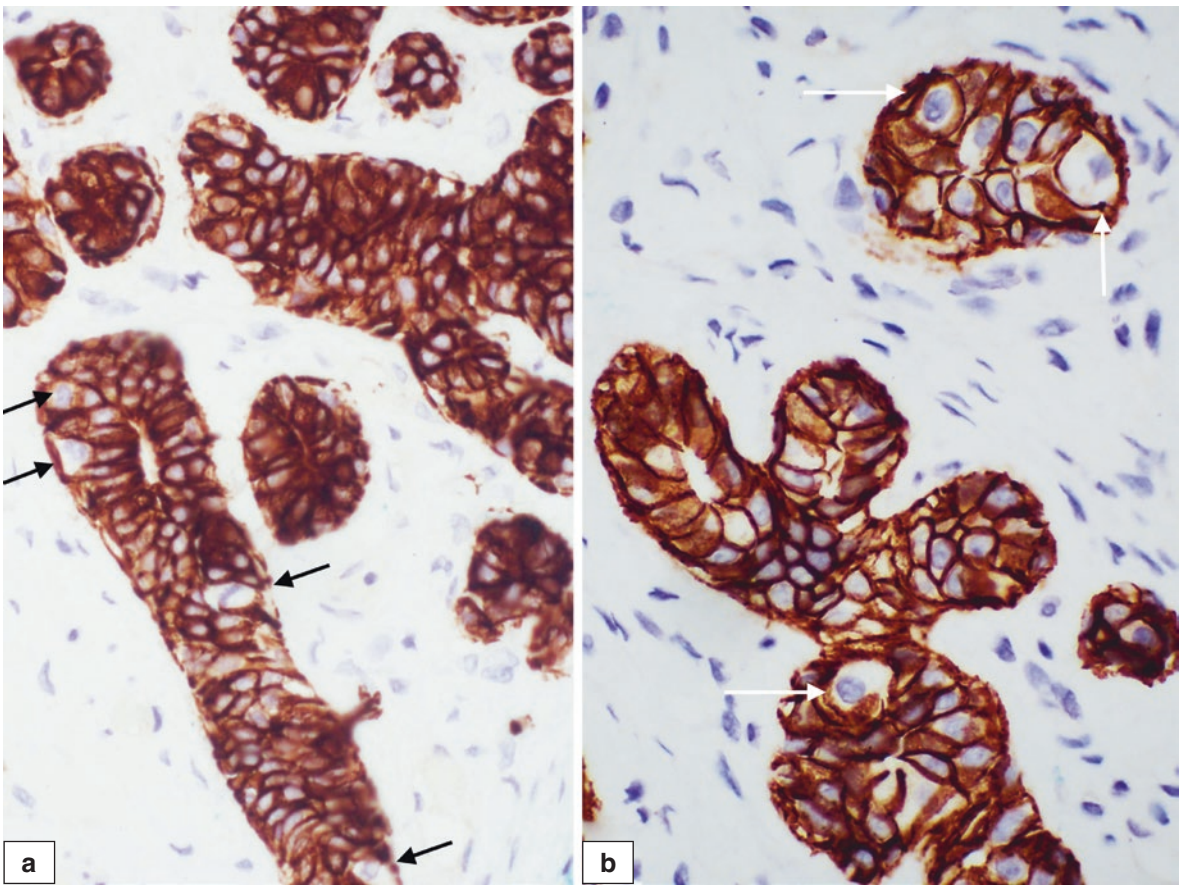

Fig. 10.44 Apocrine cells in acini mimicking lobular neoplasia. Immunohistochemistry for CK7 (**a**) shows positive membrane staining of the apocrine cells (*black arrows*). Similarly, E-cadherin also decorates the cytoplasmic membranes of the apocrine cells (*white arrows*, **b**)

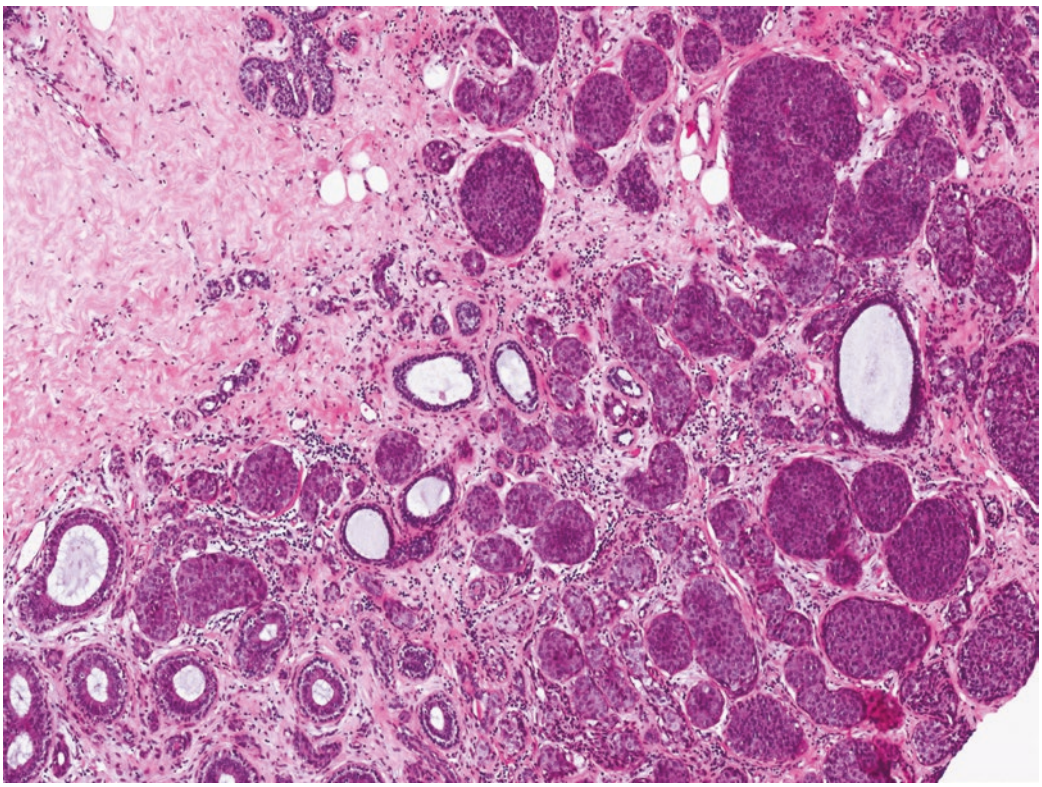

Fig. 10.45 Solid ductal carcinoma in situ (DCIS) in sclerosing adenosis. Several duct spaces are expanded and solidified by a monomorphic epithelial population, with rounded contours resembling LCIS

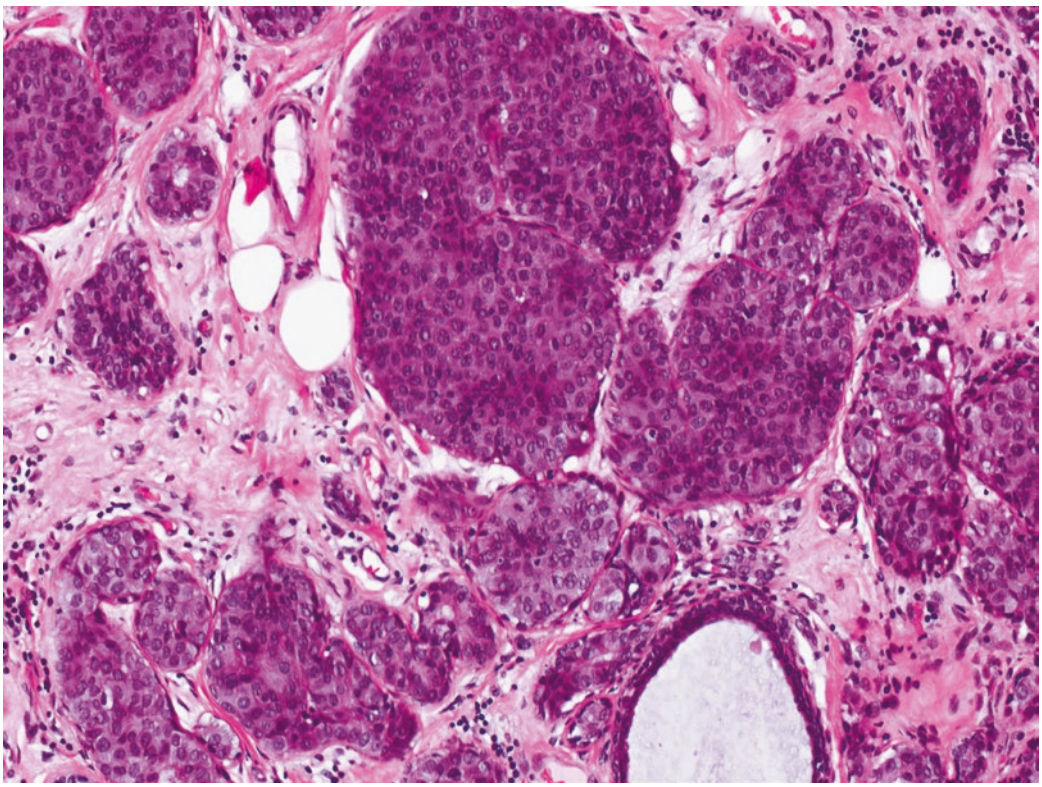

Fig. 10.46 Solid DCIS. Higher magnification shows solidified duct spaces filled with a monomorphic epithelial population of low nuclear grade. Clues to the ductal origin are the presence of true luminal spaces with polarisation of epithelial cells, which may be very subtle and difficult to identify. Here, no obvious luminal spaces are seen

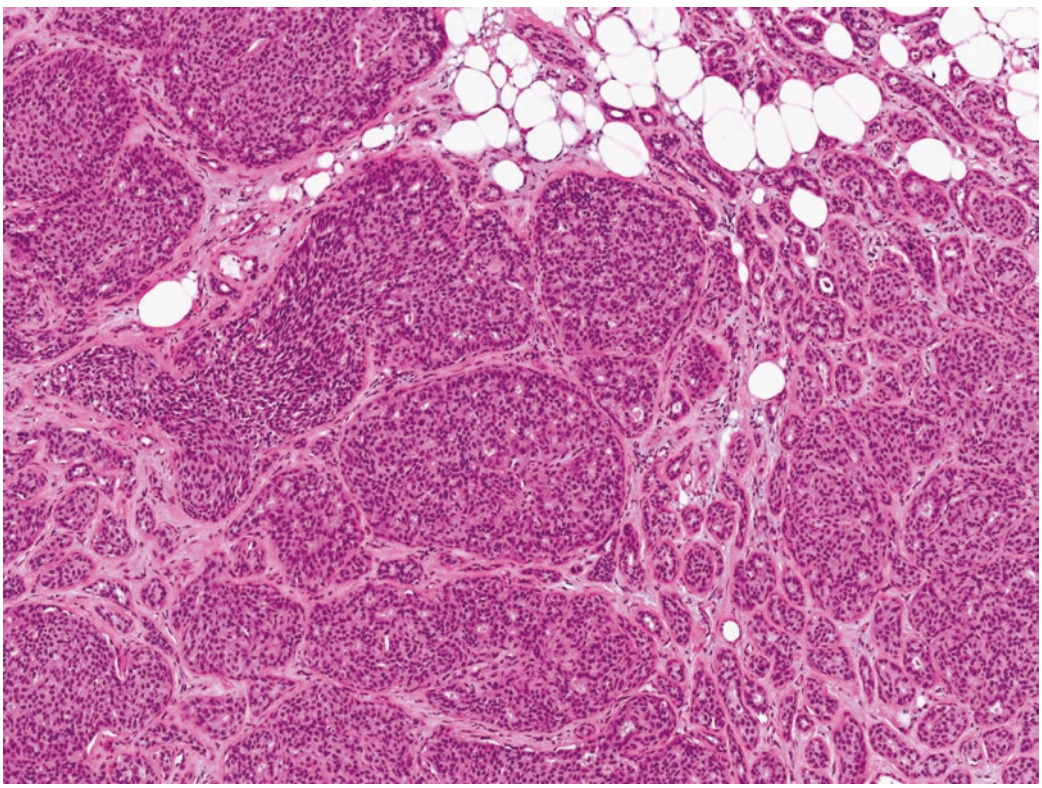

Fig. 10.47 Solid DCIS. Merging with the solidified islands are expanded ducts containing a morphologically similar epithelial population but with scattered luminal spaces around which polarisation of epithelial cells is noted. Here, some of the islands show a cribriform appearance

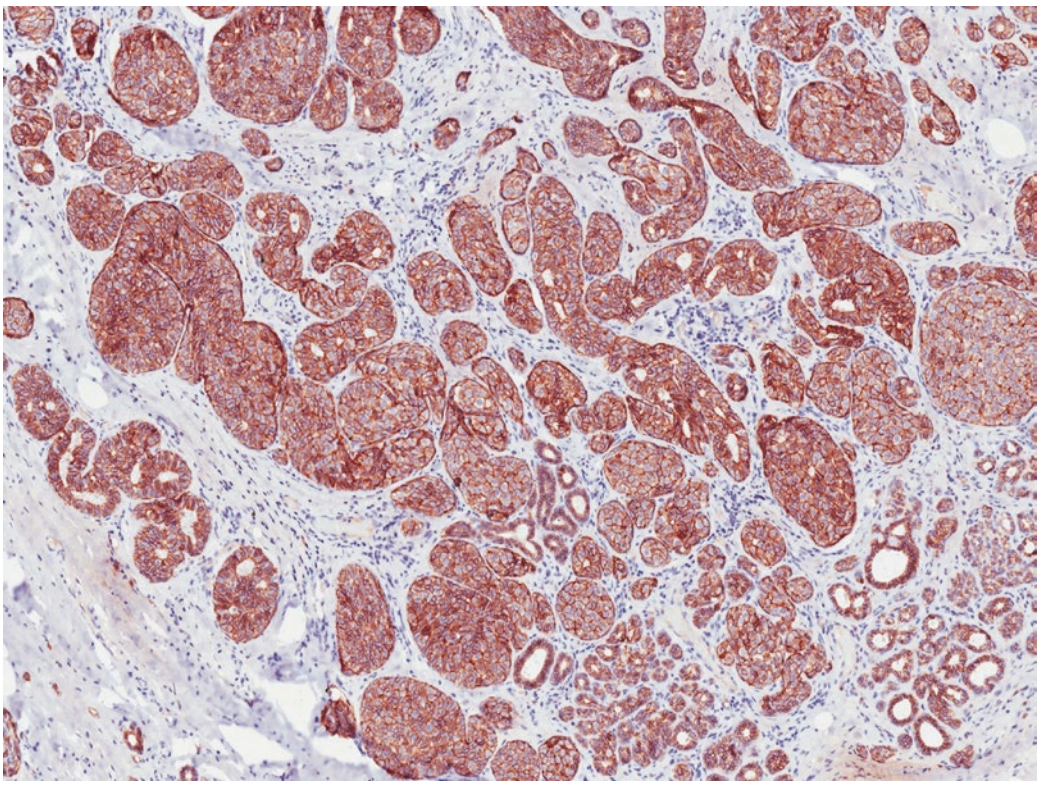

Fig. 10.48 Solid DCIS. E-cadherin immunohistochemistry shows cytoplasmic membrane reactivity of the in situ carcinoma cells, corroborating a ductal phenotype

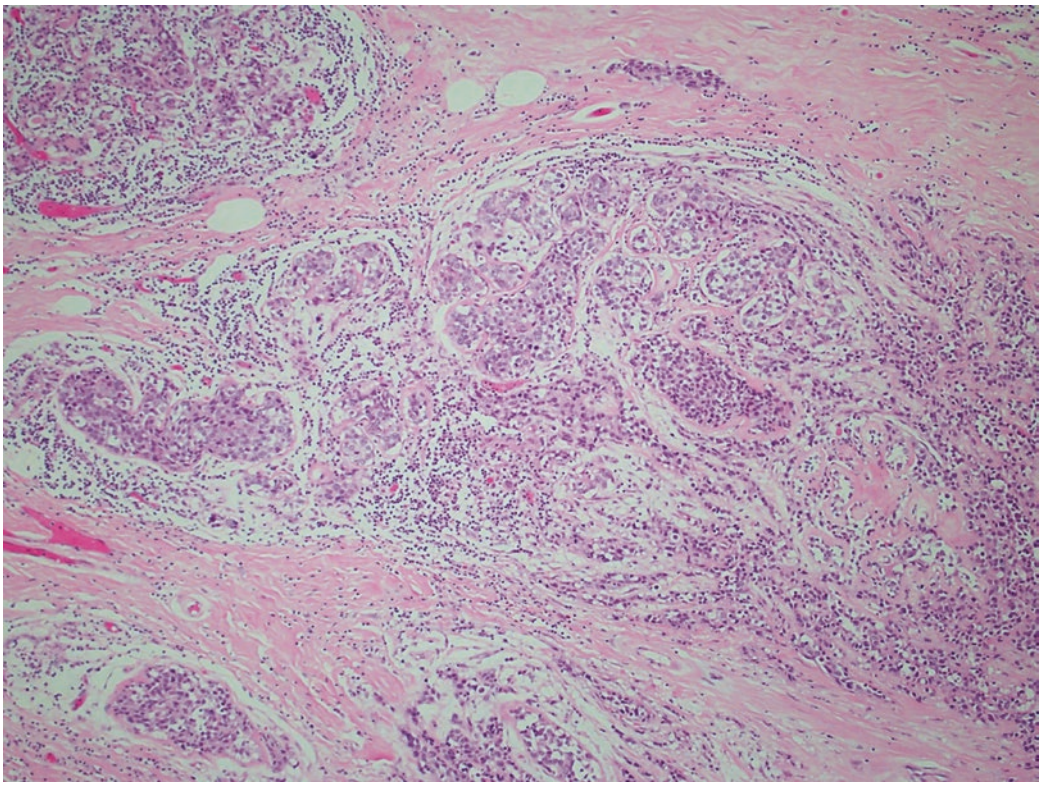

Fig. 10.49 Lobular cancerisation. In cancerisation of lobules, the underlying architecture of the lobule is preserved and identifiable, with tumour cells replacing the epithelium. The result is a solidified appearance of the affected acini resembling LCIS. More conventional DCIS can be seen. Invasive carcinoma (*right field*) can be seen extending into the stroma of the lobule, with malignant cells "cancerising" the terminal duct and acini

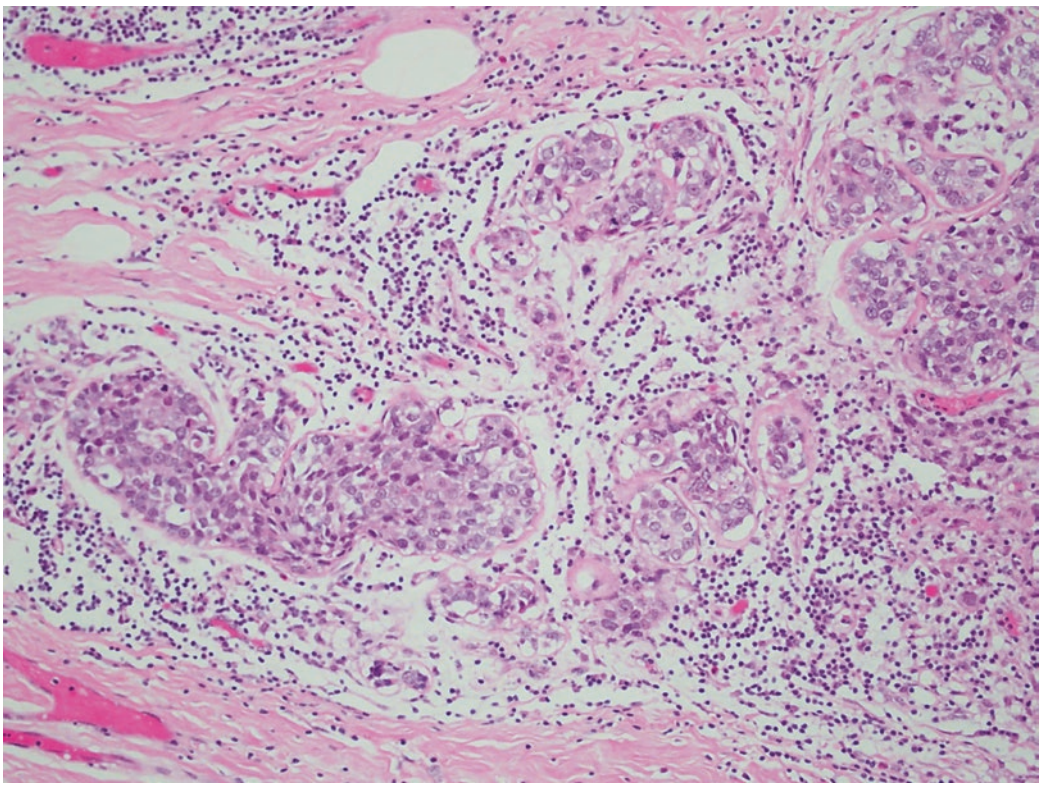

Fig. 10.50 Lobular cancerisation. Terminal duct and acini are filled with carcinoma cells. Stromal oedema and chronic inflammation are present

High Nuclear Grade Ductal Carcinoma In Situ

Pleomorphic LCIS is often mistaken for high nuclear grade DCIS (Figs. 10.51 and 10.52). Distinguishing features are discussed in the section "High Nuclear Grade DCIS Versus Pleomorphic Lobular Carcinoma In Situ" in Chapter 9.

Dimorphic Pattern of Ductal Carcinoma In Situ

Some forms of DCIS may have two cell populations, with the outer set of neoplastic cells potentially mimicking paget-oid lobular neoplasia (Figs. 10.53, 10.54, and 10.55).

Lobular Neoplasia in Collagenous Spherulosis

The occurrence of lobular neoplasia in collagenous spherulosis accentuates its resemblance to low nuclear grade cribriform DCIS, because of the monomorphic appearance of the lobular neoplastic cells replacing the epithelial cell population, punctuated by cribriform spaces containing basement membrane spherules. Cellular discohesion and E-cadherin immunohistochemistry will help in securing the correct diagnosis (Figs. 10.56, 10.57, 10.58, 10.59, 10.60, and 10.61).

Invasive Lobular Carcinoma

Lobular neoplasia involving sclerosing adenosis may mimic invasive lobular carcinoma (Figs. 10.62 and 10.63). On the other hand, early invasive lobular carcinoma associated with LCIS can be very subtle, observed as dispersed single cells or small groups of cells, which may potentially be dismissed on cursory examination as innocuous stromal nuclei or inflammatory cells. It is important to have a high index of suspicion for small or microinvasive foci in the presence of florid LCIS, especially when there is a sprinkling of cells within altered oedematous or fibrotic stroma (Figs. 10.64, 10.65, 10.66, 10.67, 10.68, and 10.69).

Prognosis and Therapy Considerations

Lobular neoplasia represents both a risk factor and non-obligate precursor for subsequent invasive breast cancer of lobular and ductal subtypes in both breasts, although about two thirds occur in the ipsilateral breast. The risk of invasive breast cancer development is four to five times that of the general population for atypical lobular hyperplasia and eight to ten times for LCIS. Negative surgical margins are not pursued for lobular neoplasia (atypical lobular hyperplasia and classic LCIS), but mass-forming (florid) and pleomorphic LCIS may be regarded as potentially biologically aggressive, with corresponding treatment strategies that include complete excision.

When lobular neoplasia is discovered on core biopsy, close clinicoradiological correlation is needed. Incidentally discovered lobular neoplasia does not warrant further excision if there is radiologic–pathologic concordance.

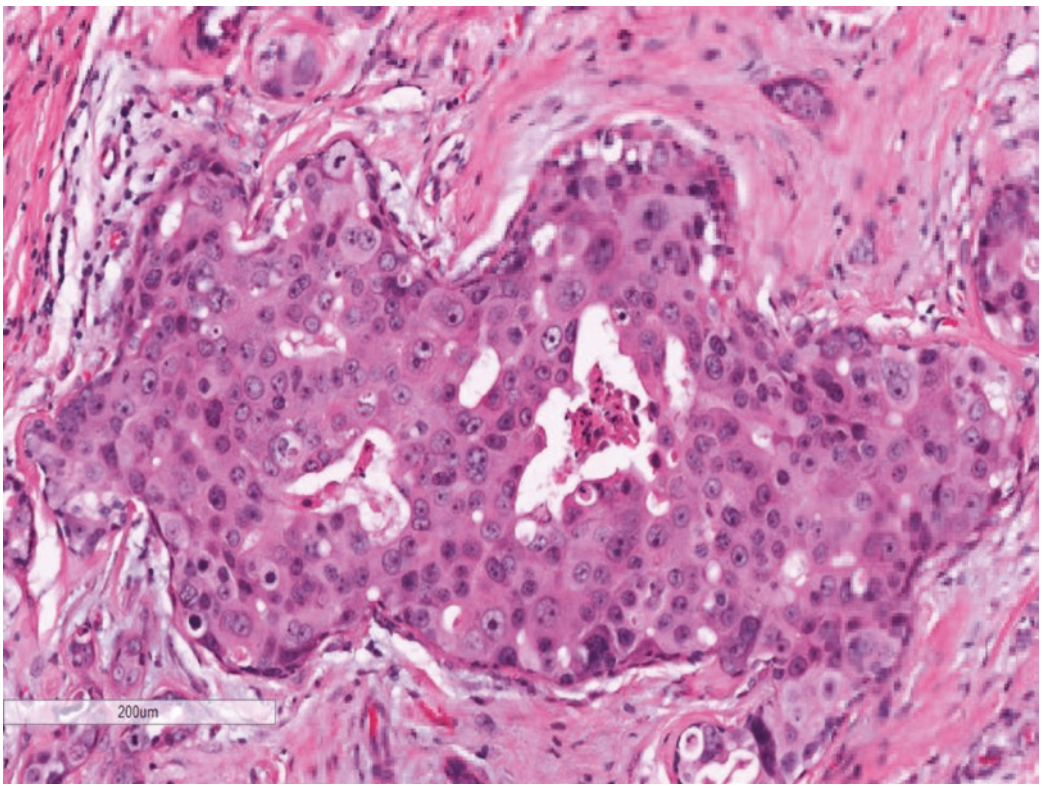

Fig. 10.51 High nuclear grade DCIS. The duct is expanded by high-grade malignant cells with enlarged vesicular nuclei, distinct nucleoli, and pink cytoplasm, which may resemble pleomorphic LCIS. Necrosis and scattered irregularly sized spaces are present

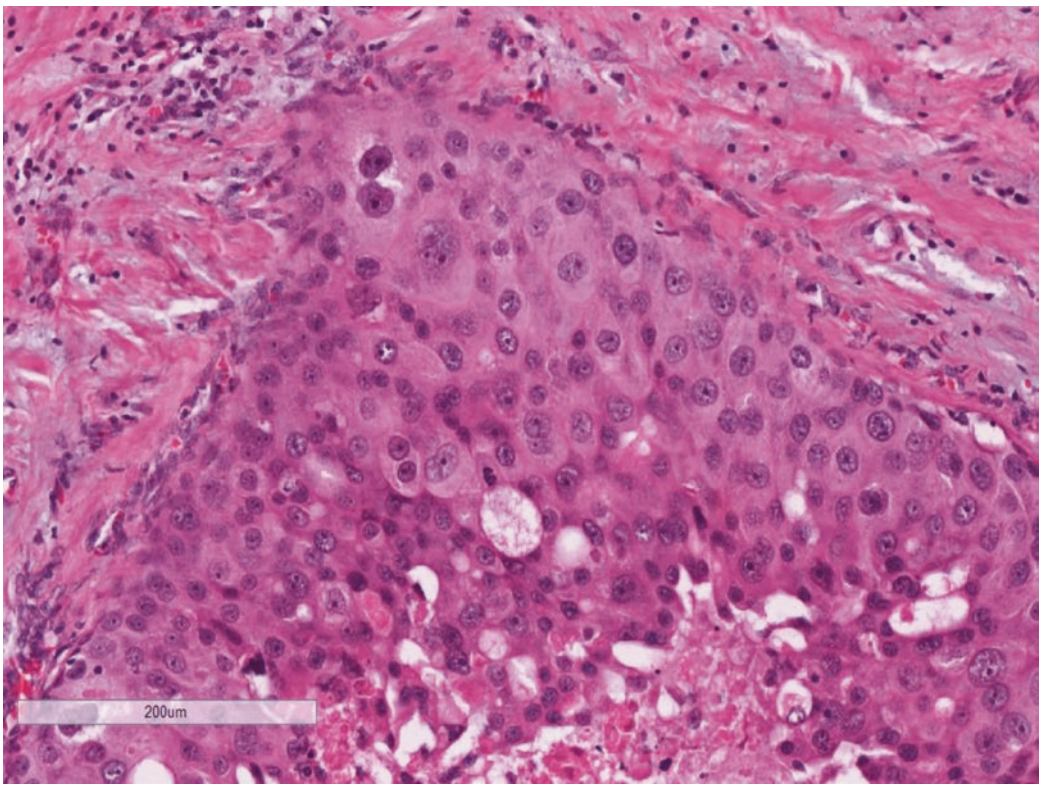

Fig. 10.52 High nuclear grade DCIS. Comedonecrosis is present (*lower field*). In situ ductal carcinoma cells do not display significant discohesion, apart from the few irregular spaces among the tumour cells. Usually, other patterns of DCIS, such as cribriform and micropapillary morphologies, may be seen and assist in making the correct diagnosis. In pleomorphic LCIS, accompanying classic lobular neoplasia may be observed

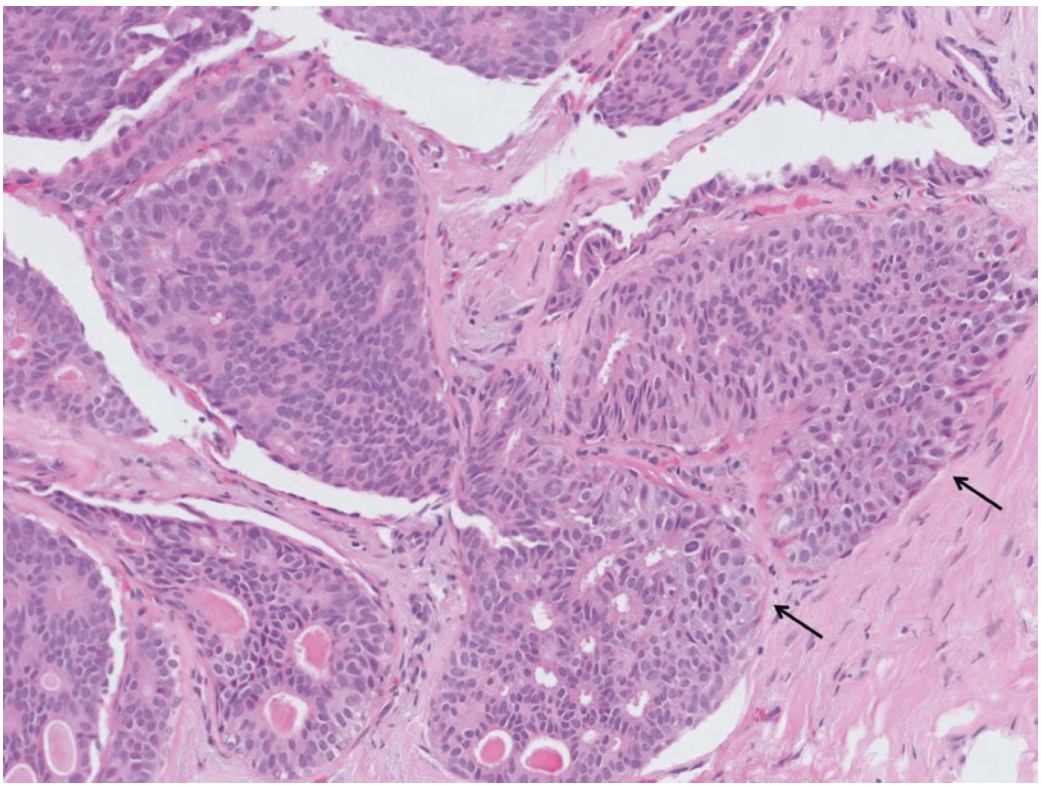

Fig. 10.53 Dimorphic pattern of DCIS. Cribriform DCIS with well-defined luminal spaces is present. Pink luminal secretions are seen. In two affected ducts, there is a second population of rounded cells at the periphery (*arrows*), which may mimic lobular neoplasia

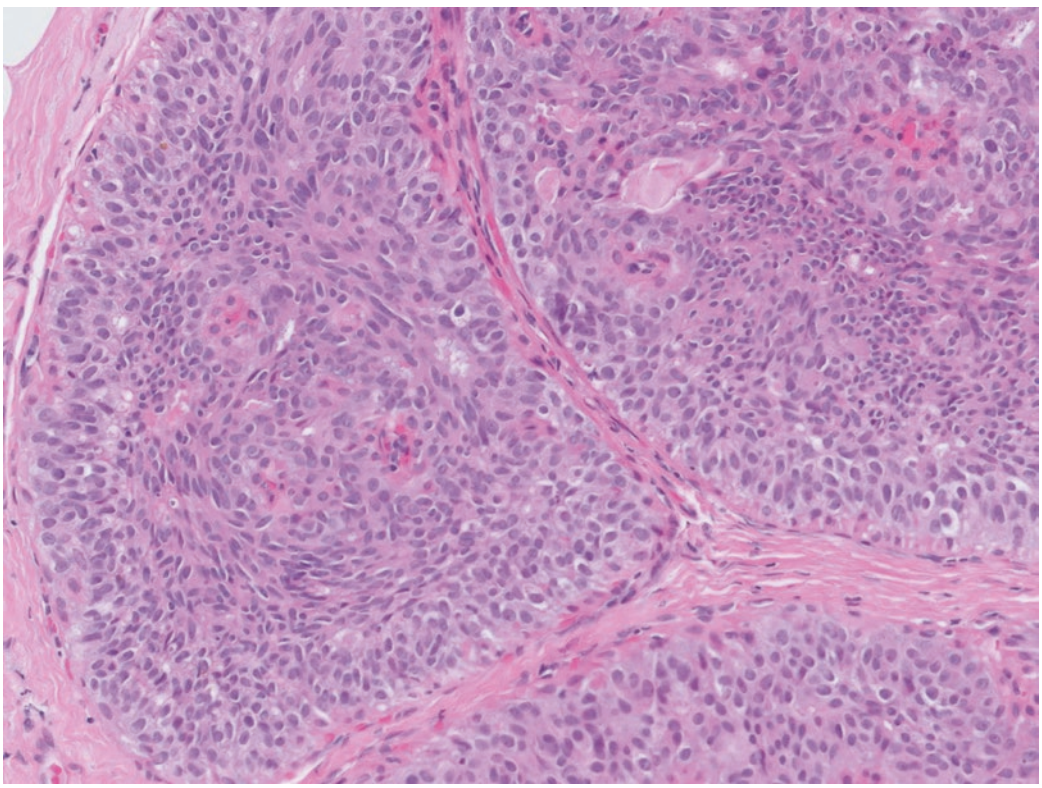

Fig. 10.54 Dimorphic pattern of DCIS. A peripheral rim of plumper, more rounded cells encircles a central population of cells with smaller, darker, and more elongated nuclei

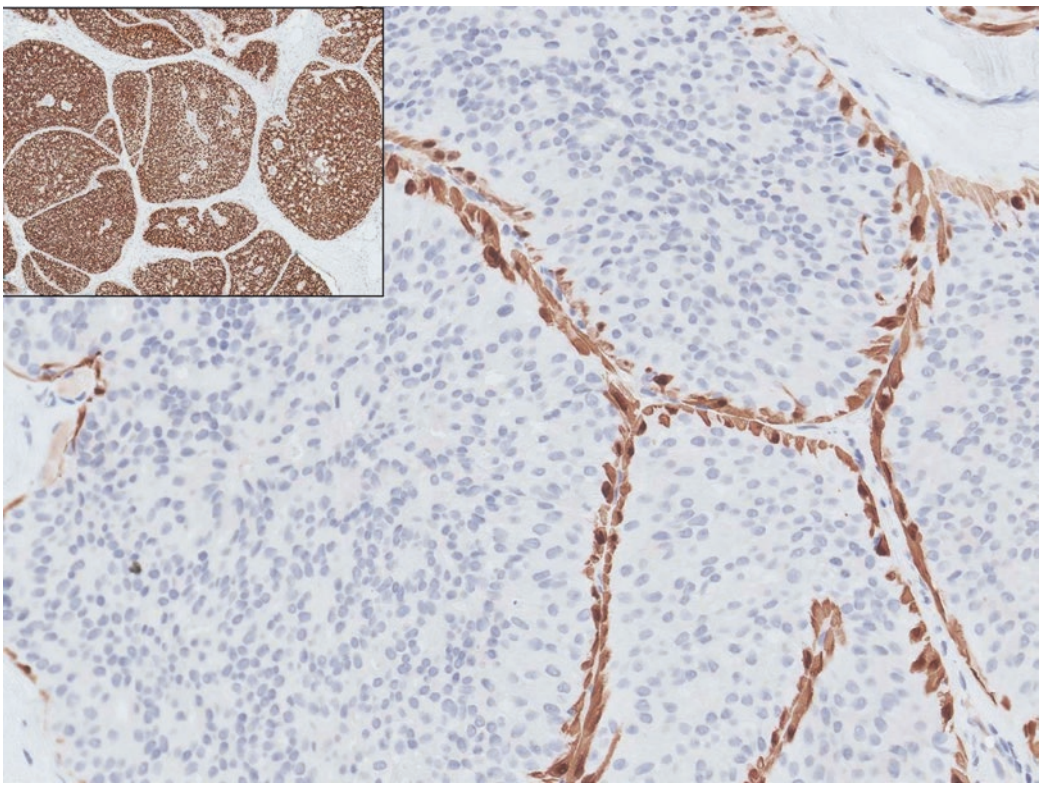

Fig. 10.55 Dimorphic pattern of DCIS. Immunohistochemistry for p63/CK14 shows a peripheral layer of myoepithelial cells. The epithelial population filling the duct spaces is completely negative, corroborating a clonal process. ER immunostaining (*inset*) shows diffuse, intense reactivity of the epithelial cells

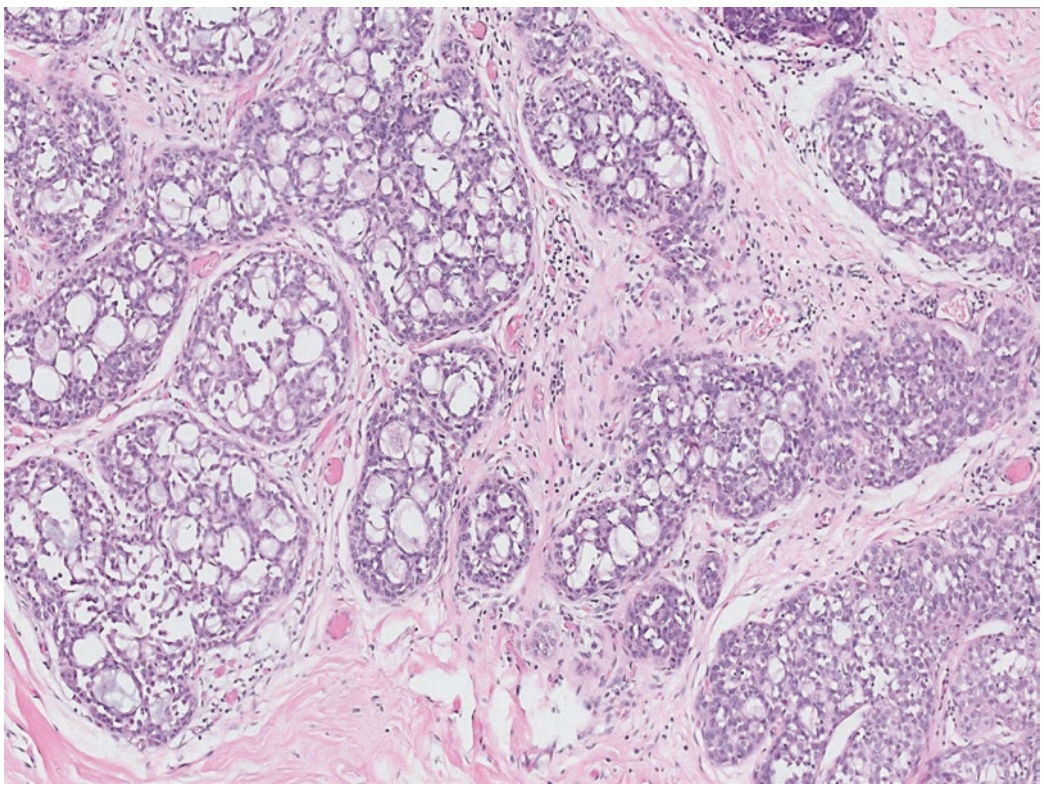

Fig. 10.56 Collagenous spherulosis with lobular neoplasia. Atypical lobular hyperplasia involves ducts with cribriform spaces containing basement membrane material, with the monomorphic appearance of the lobular neoplastic cells resulting in a close resemblance to cribriform DCIS

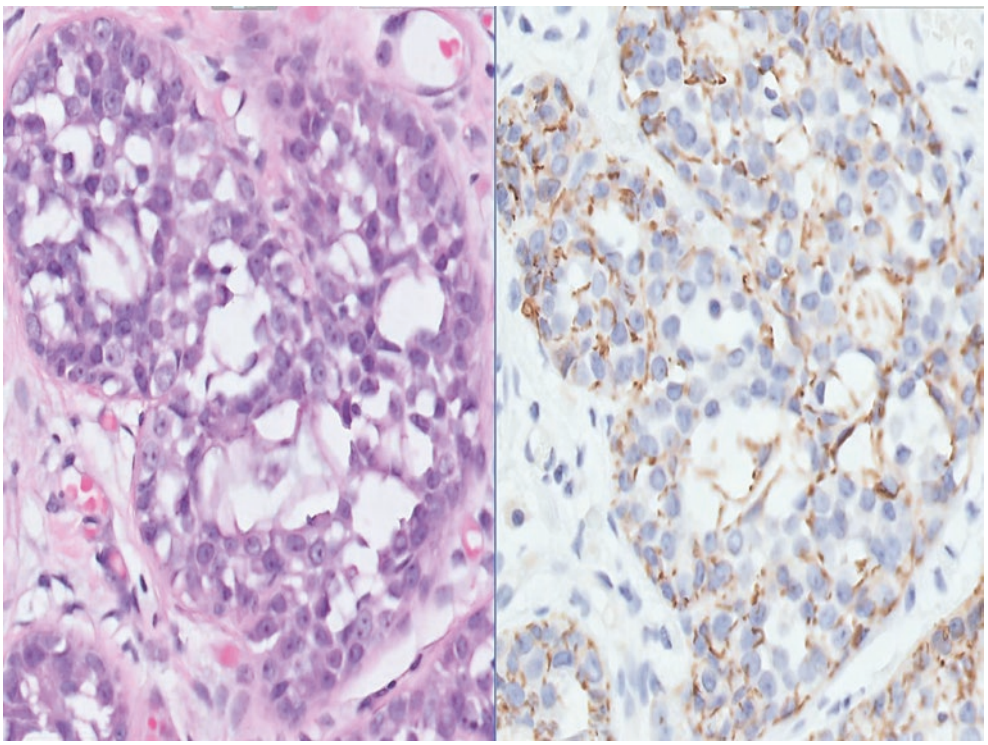

Fig. 10.57 Collagenous spherulosis with lobular neoplasia. E-cadherin immunohistochemistry shows negative reactivity of the lobular neoplastic cells, with faint, incomplete staining representing intermingled myoepithelial cells

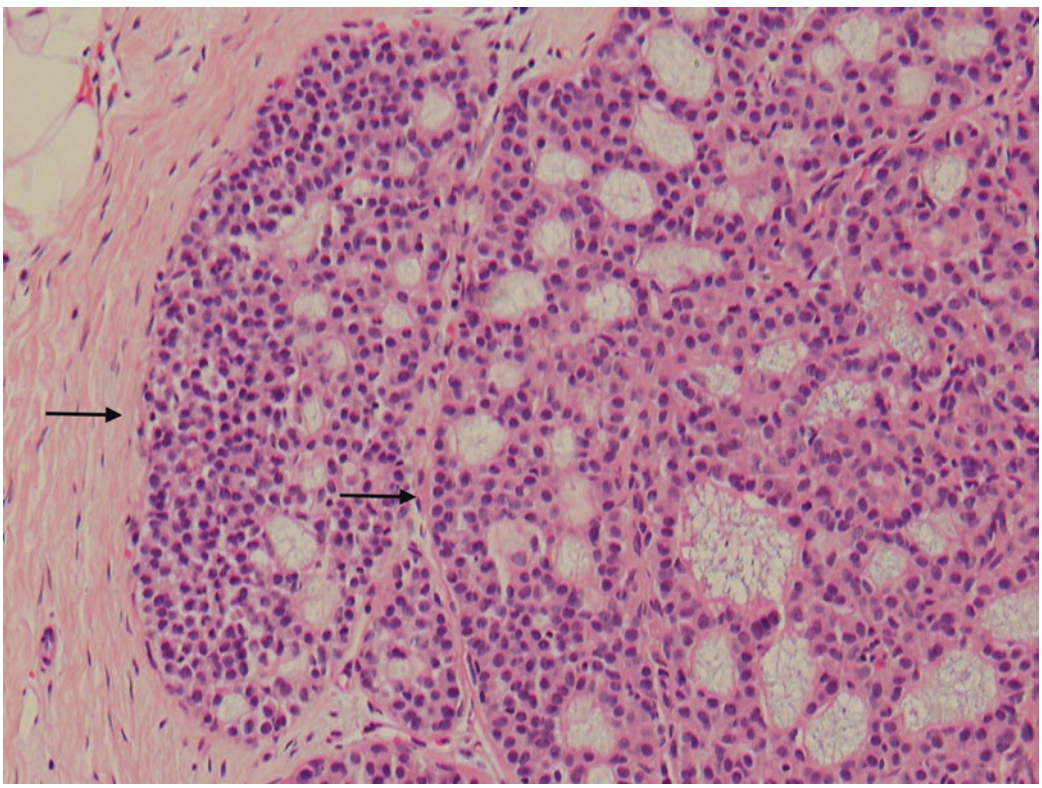

Fig. 10.58 Collagenous spherulosis with lobular neoplasia. The cribriform spaces contain wispy, delicate material. Lobular neoplastic cells colonise the ducts with collagenous spherulosis, with discohesive, monomorphic cells populating the left duct space and the peripheral portion of the larger duct space (*arrows*)

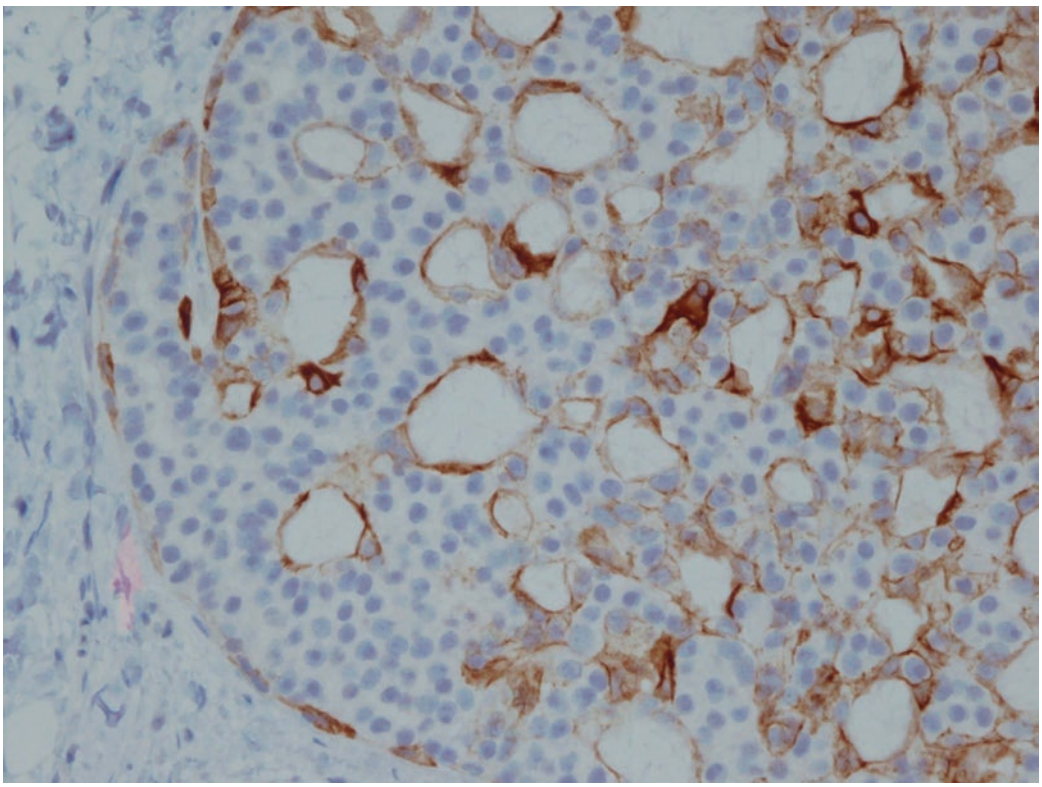

Fig. 10.59 Collagenous spherulosis with lobular neoplasia. Immunohistochemistry for CK14 shows positively stained myoepithelial cells at the periphery of the duct, as well as decorate attenuated myoepithelial cells lining the pseudoluminal spaces. Collagenous spherulosis is an epithelial–myoepithelial lesion, with myoepithelial cells elaborating the basement membrane material contained within the pseudoluminal spaces

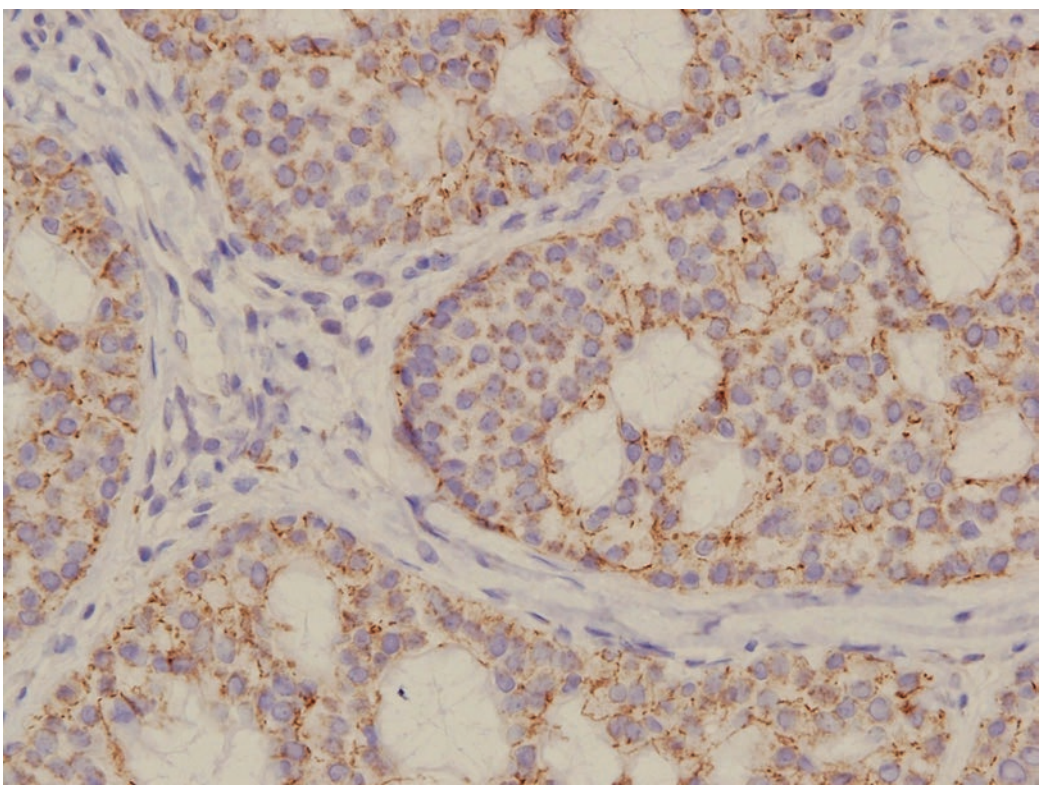

Fig. 10.60 Collagenous spherulosis with lobular neoplasia. E-cadherin immunohistochemistry shows negative reactivity in the lobular neoplastic cells. There is accentuation of staining at the periphery of the ducts and around the cribriform spaces, reflecting staining of myoepithelial cells, but the staining is diminished and not complete or crisp

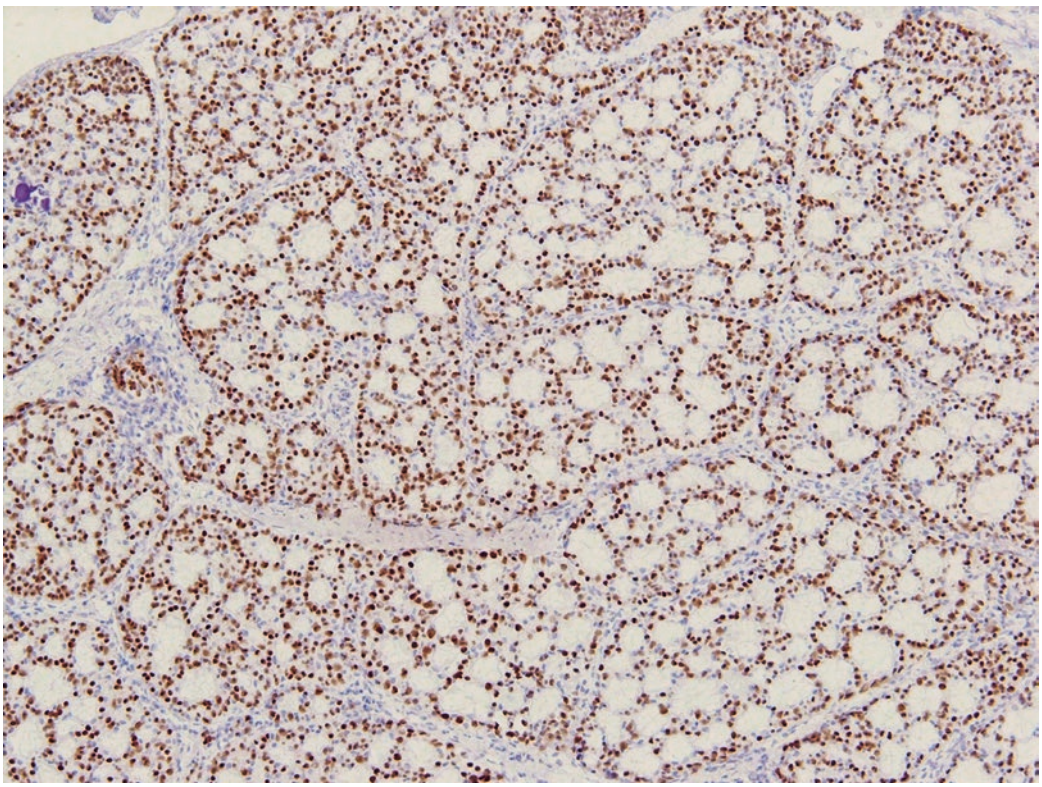

Fig. 10.61 Collagenous spherulosis with lobular neoplasia. Oestrogen receptor (ER) immunohistochemistry shows diffusely positive nuclear staining of lobular neoplastic cells, which exacerbates the resemblance to low nuclear grade cribriform DCIS

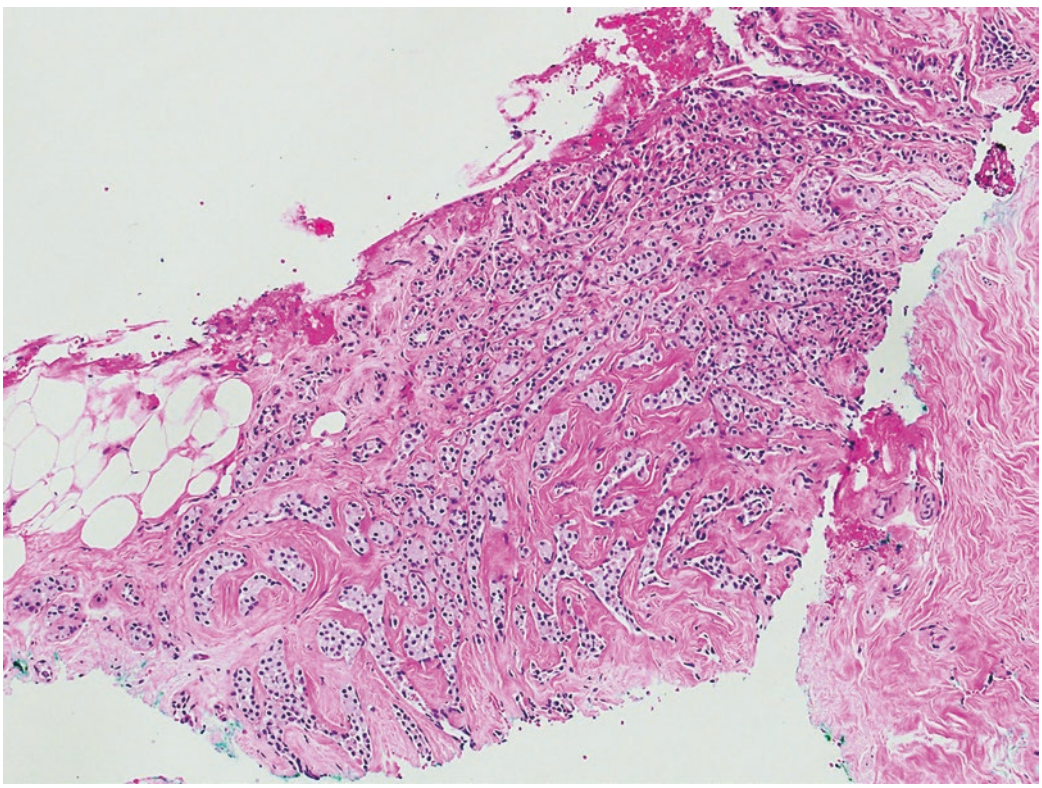

Fig. 10.62 Lobular neoplasia involving sclerosing adenosis, mimicking invasive carcinoma. In this core biopsy, lobular neoplasia is seen effacing the tubules of sclerosing adenosis, resembling invasive carcinoma. The overall intact architecture of the lobule can be observed at low magnification. The presence of myoepithelial cells can be confirmed using immunohistochemistry

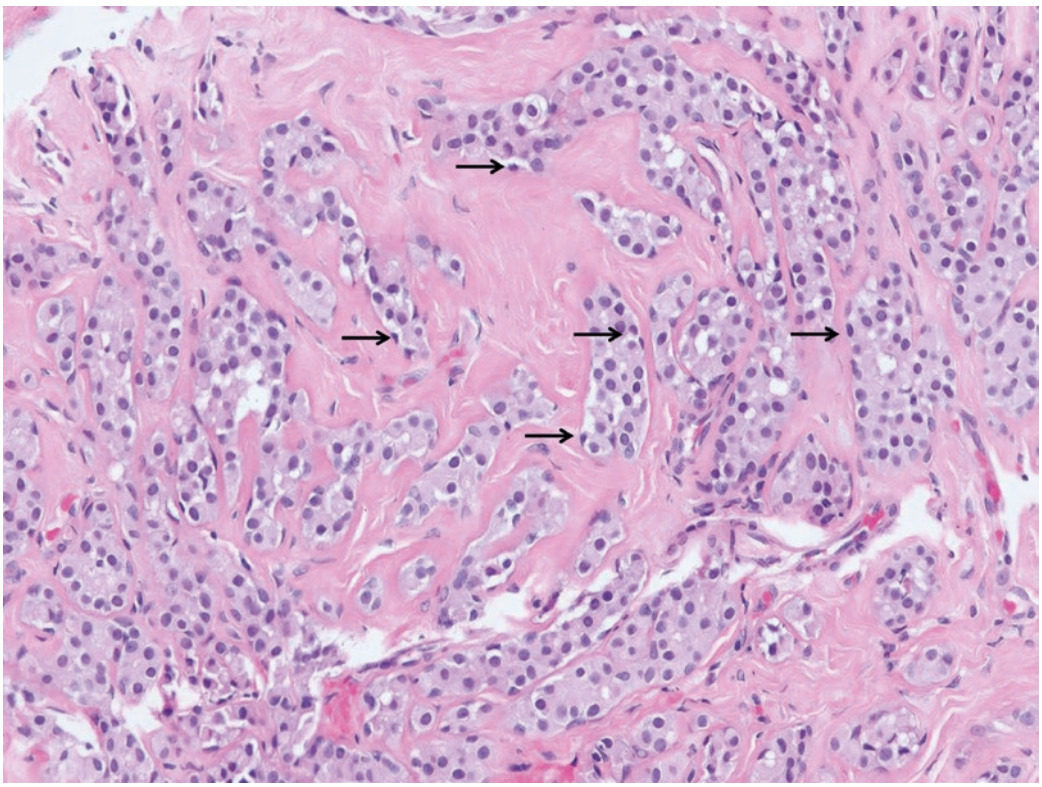

Fig. 10.63 Lobular neoplasia involving sclerosing adenosis, mimicking invasive carcinoma. At higher magnification, myoepithelial nuclei are observed in the epithelial nests (*arrows* point to a few myoepithelial nuclei). The stroma is collagenised

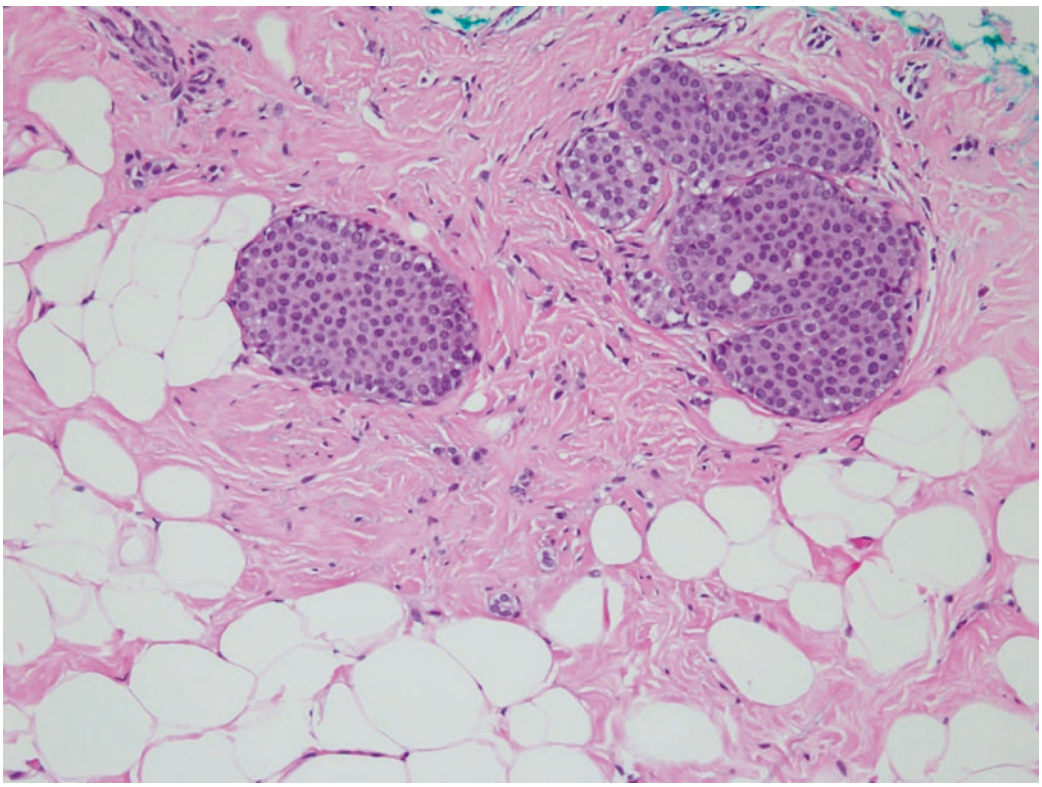

Fig. 10.64 Lobular carcinoma in situ with a small focus of invasive lobular carcinoma. A few scattered nuclei are seen in the stroma adjacent to the acini distended by LCIS. These nuclei, which appear bland, could very easily be overlooked as stromal nuclei or inflammatory cells

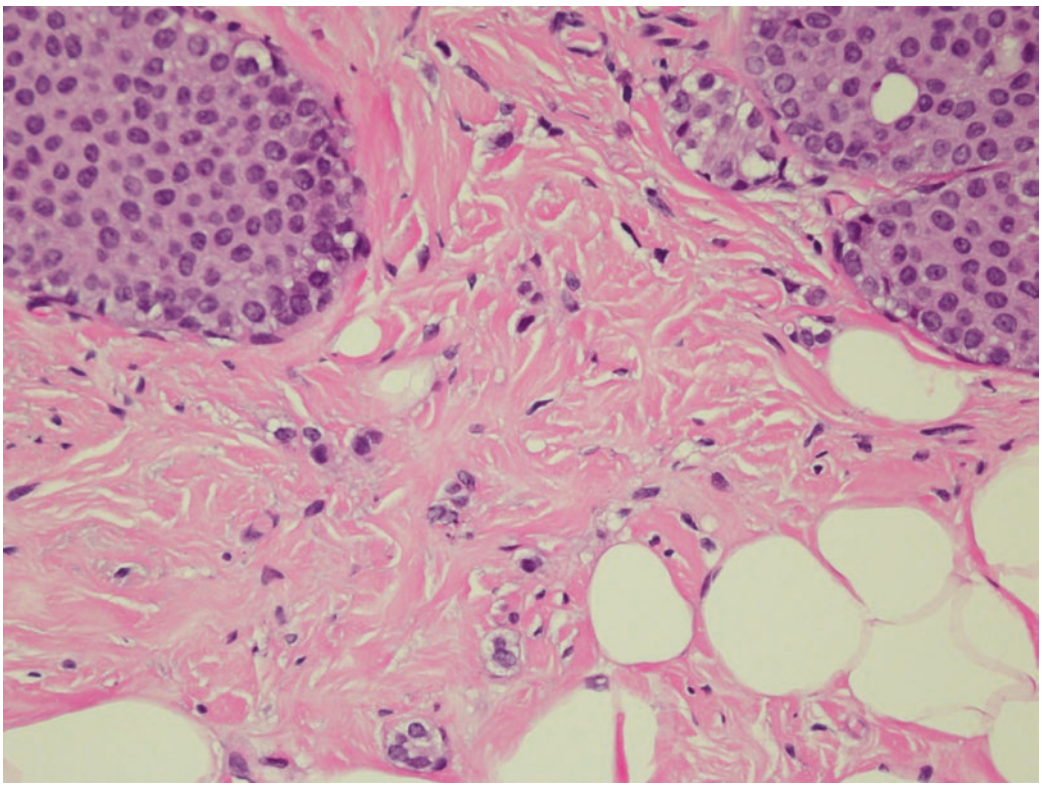

Fig. 10.65 Lobular carcinoma in situ with a small focus of invasive lobular carcinoma. On closer scrutiny, these dispersed cells are rounded and show vesicular to dense nuclei similar to those of the adjacent LCIS. In the *lower field*, occasional small clusters of cells are seen

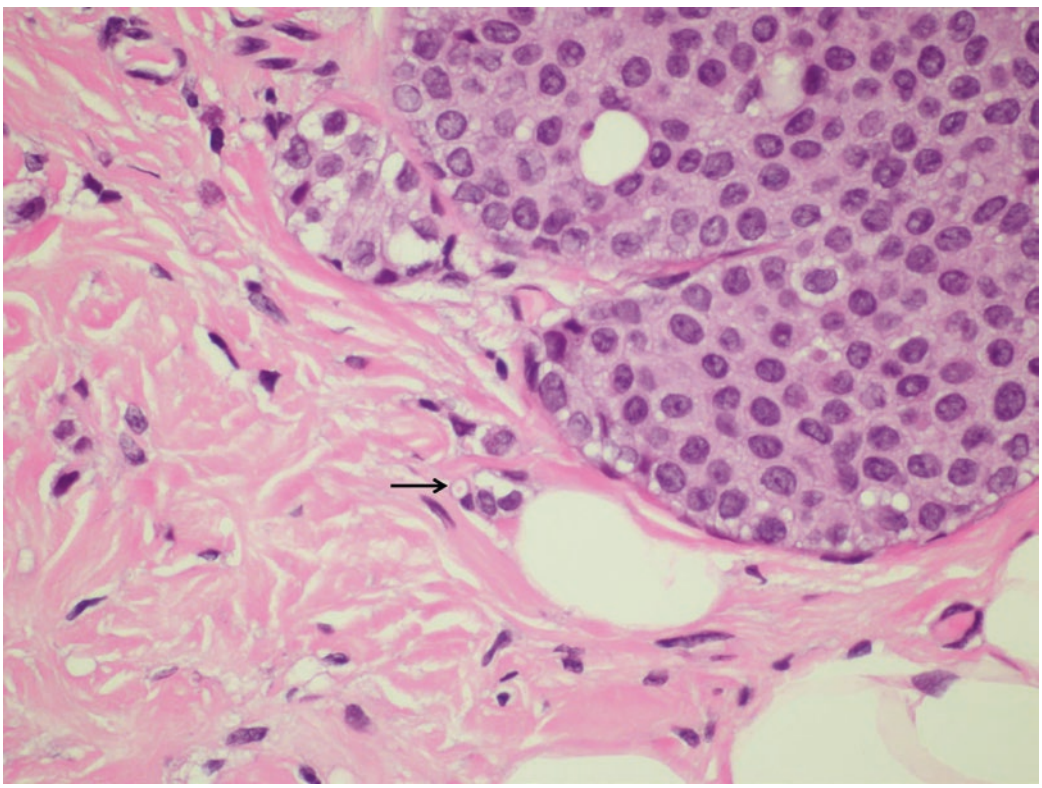

Fig. 10.66 Lobular carcinoma in situ with a small focus of invasive lobular carcinoma. An invasive carcinoma cell with an intracytoplasmic vacuole containing a targetoid secretion is noted (*arrow*)

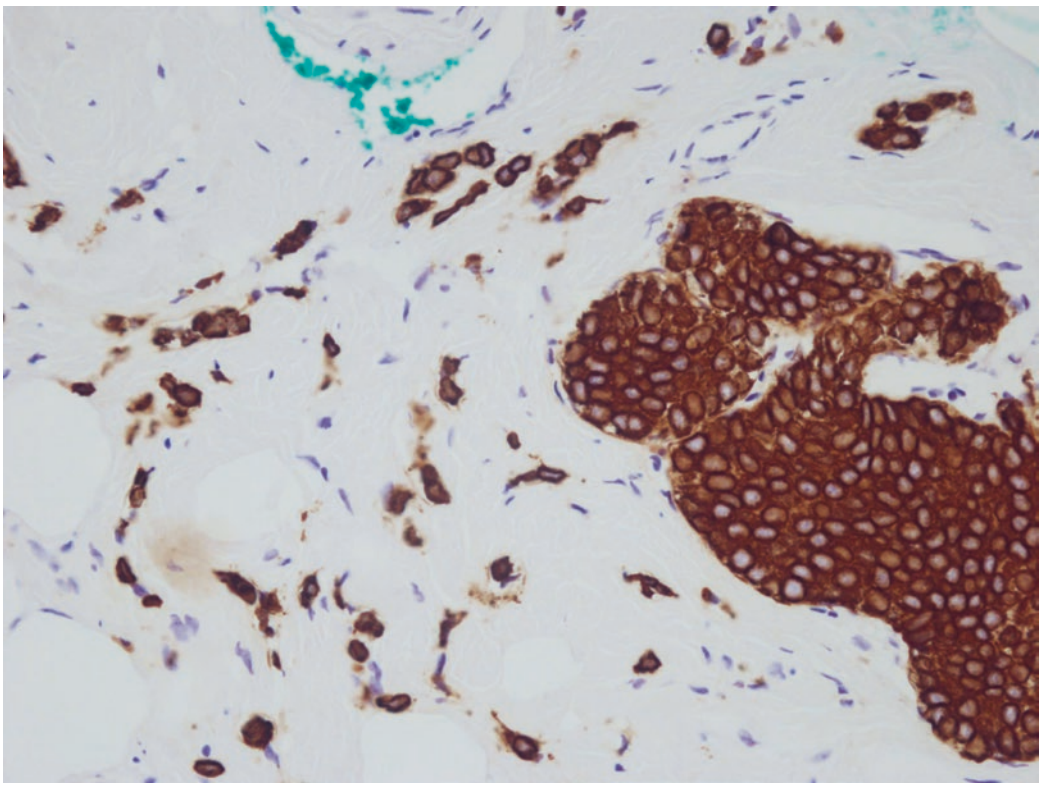

Fig. 10.67 Lobular carcinoma in situ with a small focus of invasive lobular carcinoma. MNF116 immunohistochemistry unveils a greater number of single and small aggregates of tumour cells in the stroma around LCIS

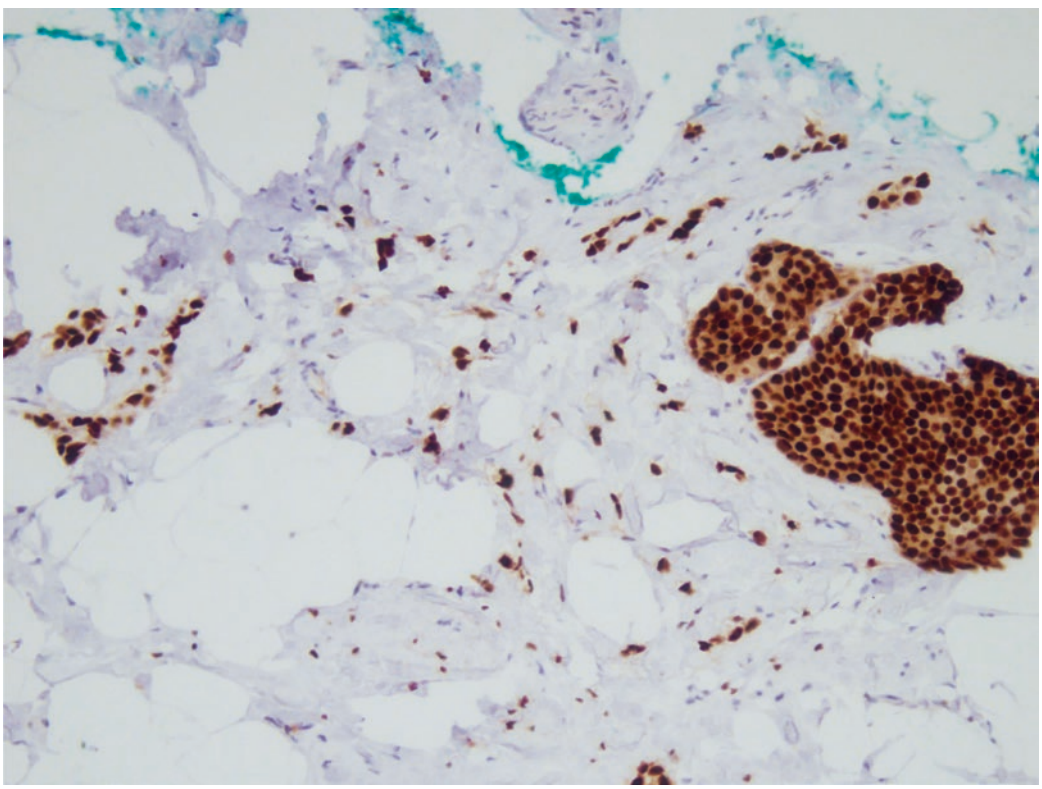

Fig. 10.68 Lobular carcinoma in situ with a small focus of invasive lobular carcinoma. ER immunohistochemistry shows strong nuclear staining of both in situ and invasive lobular carcinoma cells

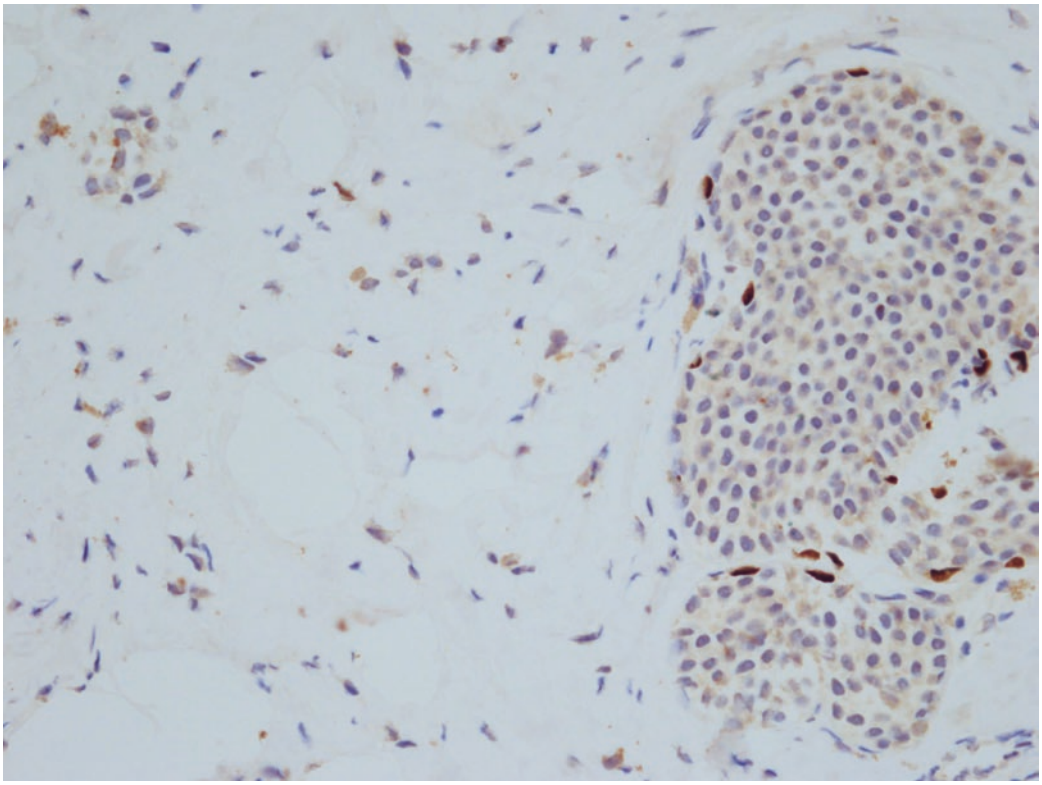

Fig. 10.69 Lobular carcinoma in situ with a small focus of invasive lobular carcinoma. Immunohistochemistry for p63 shows a few retained myoepithelial nuclei around LCIS, whereas the invasive carcinoma cells are negative

Invasive Lobular Carcinoma

Definition

Invasive lobular carcinoma comprises discohesive, monomorphic tumour cells with linear and targetoid patterns of infiltration, often accompanied by lobular neoplasia. Like lobular neoplasia, invasive lobular carcinoma harbours mutations in the E-cadherin gene resulting in a dysfunctional E-cadherin protein.

Clinical and Epidemiological Features

Invasive lobular carcinoma accounts for 5–15 % of all invasive breast cancers; it generally occurs in postmenopausal women. An increased incidence over the past few decades is believed to be related to hormone replacement therapy and greater alcohol consumption.

Imaging Features

Invasive lobular carcinoma can be difficult to detect on imaging. On mammography, it can present as a mass with ill-defined or spiculated margins, an ill-defined asymmetric density, or an area of architectural distortion (Fig. 10.70). Not infrequently, these carcinomas are radiologically occult because of the lack of desmoplastic reaction to invading tumour. On sonography, they commonly occur as ill-defined or spiculated masses, but they can also present as vague, ill-defined, mass-like, hypoechoic areas of echotexture change and posterior shadowing, with no visible discrete mass. Solid-type, signet-ring, and alveolar subtypes of invasive lobular carcinoma are more disposed to forming lobulated, circumscribed masses [10].

MRI is more sensitive for identifying invasive lobular carcinoma, but it is also known that it may not enhance or demonstrate the classic type of rapid wash-in and wash-out enhancement kinetics. Invasive lobular carcinoma is usually observed as an ill-defined or spiculated mass on MRI, and it may be associated with a conglomerate of closely grouped masses or enhancing foci. It can also present with architectural distortion and areas of heterogeneous, non-mass enhancement with no definite discrete mass. Contraction of the breast volume may occasionally be observed.

Invasive lobular carcinoma has a high predisposition for multicentric and contralateral disease. Hence, MRI and ultrasound screening of the rest of the ipsilateral breast and the contralateral breast are usually suggested. Radiologic–pathologic size discordance is common, with the pathologic size tending to be larger than radiologic size estimates.

Pathologic Features

Macroscopic Pathology

Invasive lobular carcinomas have a range of macroscopic appearances (Figs. 10.71, 10.72, and 10.73). Some may be grossly difficult to identify, as the breast parenchyma appears deceptively normal, with only more firm, fibrous areas; others comprise stellate lesions and irregular masses.

Microscopic Pathology

Invasive lobular carcinoma shows discohesive cells percolating the stroma in linear arrays or single cells. Tumour cells also surround benign ducts and acini in a circumferential manner, described as a targetoid arrangement of invasion. In the classic form, tumour cells are monomorphic with generally bland nuclei (Figs. 10.74, 10.75, 10.76, 10.77, and 10.78). Intracytoplasmic vacuoles may be pres-

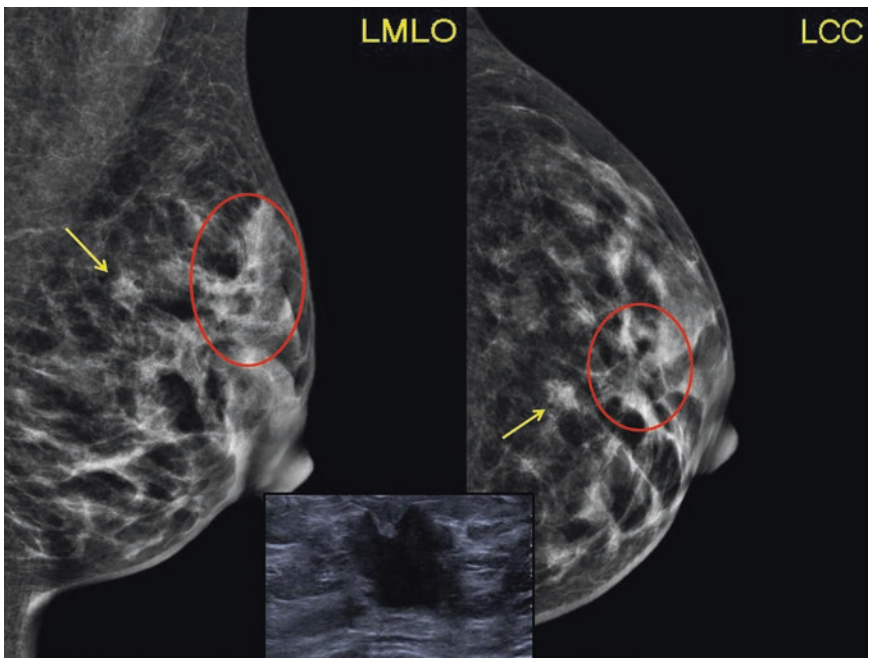

Fig. 10.70 Invasive lobular carcinoma. There is an area of mild distortion in the left upper outer periareolar region with straightening of the Cooper's ligaments owing to the primary tumour (*red circles*). The mass is not well appreciated in this mammographically dense breast. There is also a small satellite malignant mass noted more posteriorly (*yellow arrows*). Ultrasound (*inset*) shows an ill-defined, irregular mass associated with distortion in the surrounding breast tissue. (Courtesy of Dr. Lester Leong)

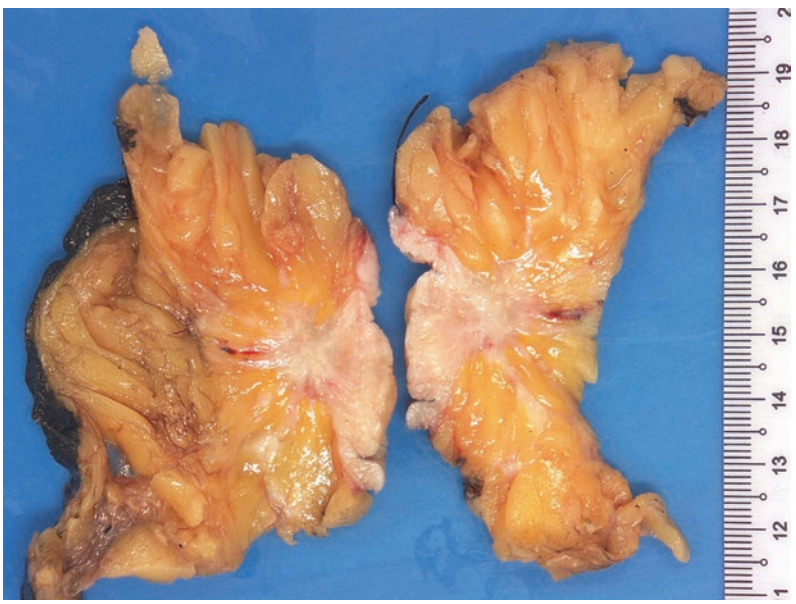

Fig. 10.71 Invasive lobular carcinoma. A stellate, irregular tumour is present deep to the nipple, which appears retracted in these mirror slices from a mastectomy specimen

ent, which are not specific to invasive lobular carcinoma (Figs. 10.79 and 10.80). Other patterns include alveolar, solid, tubulolobular, and pleomorphic (Fig. 10.81, 10.82, 10.83, 10.84, 10.85, 10.86, 10.87, and 10.88). The invasive tubulolobular subtype is described as demonstrating positive E-cadherin membrane staining [11, 12]. Invasive pleomorphic lobular carcinoma is characterised by grade 3 nuclei and may often show apocrine cytomorphology. Rare subtypes are histiocytoid and signet-ring forms (Figs. 10.89, 10.90, 10.91, 10.92, 10.93, and 10.94). Invasive lobular carcinoma is nearly always ER positive, variably progesterone receptor positive, and c-erbB-2 negative, although the pleomorphic variant may be hormone receptor negative and c-erbB-2 positive.

Fig. 10.72 Invasive lobular carcinoma. In this mastectomy specimen, serial slices show an ill-defined whitish lesion (*arrows*). Invasive lobular carcinoma occasionally may be difficult to identify grossly

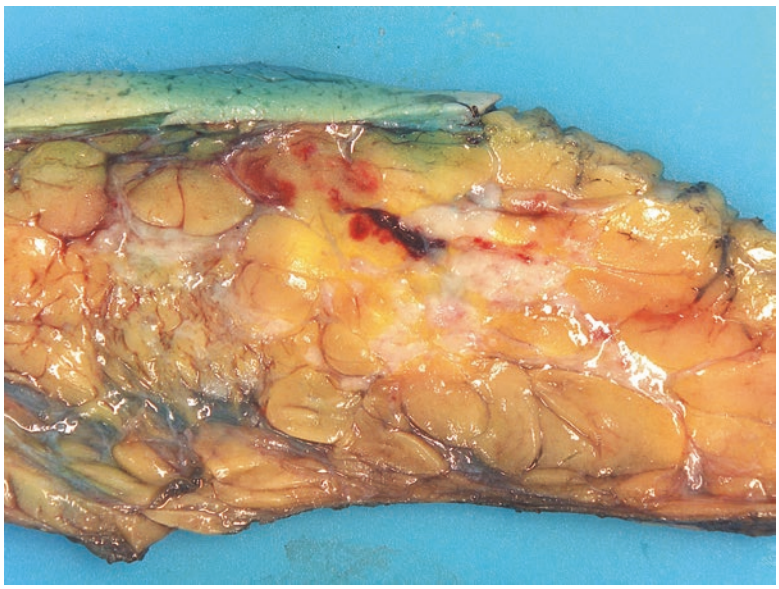

Fig. 10.73 Invasive lobular carcinoma. Irregular whitish areas are seen. Haemorrhage represents prior core biopsy

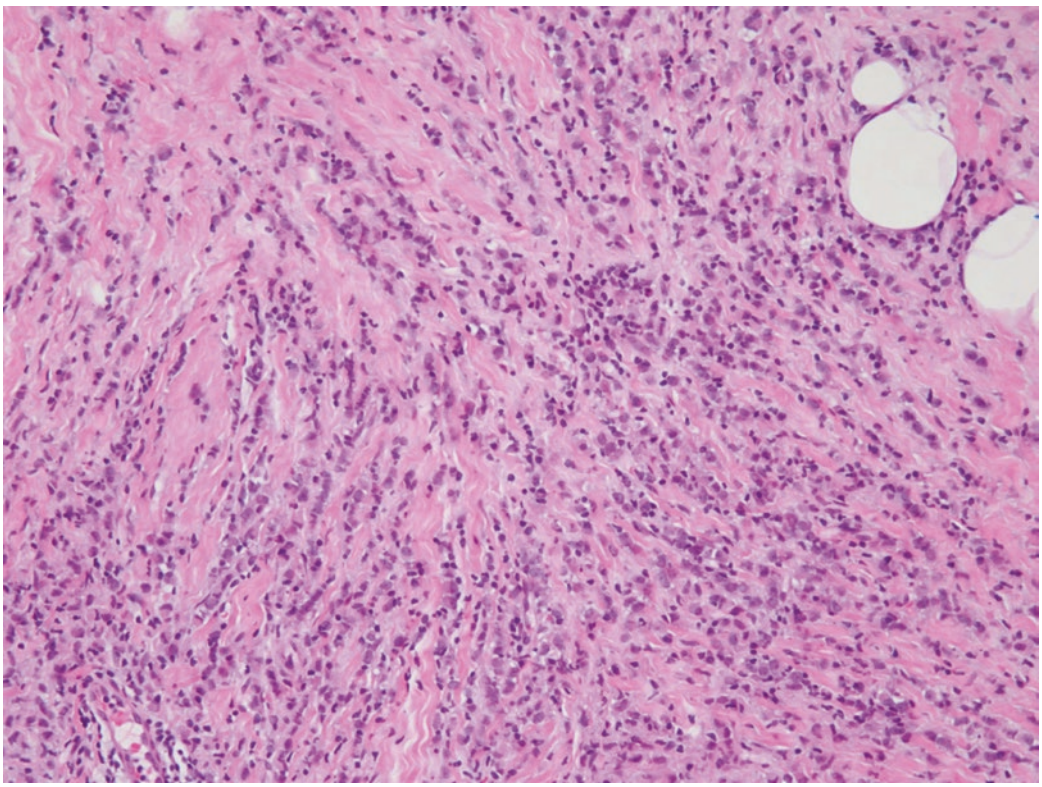

Fig. 10.74 Invasive lobular carcinoma, classic type. Linear streams and single cords of tumour cells with mostly uniform nuclei percolate through the stroma, without eliciting a significant desmoplastic reaction

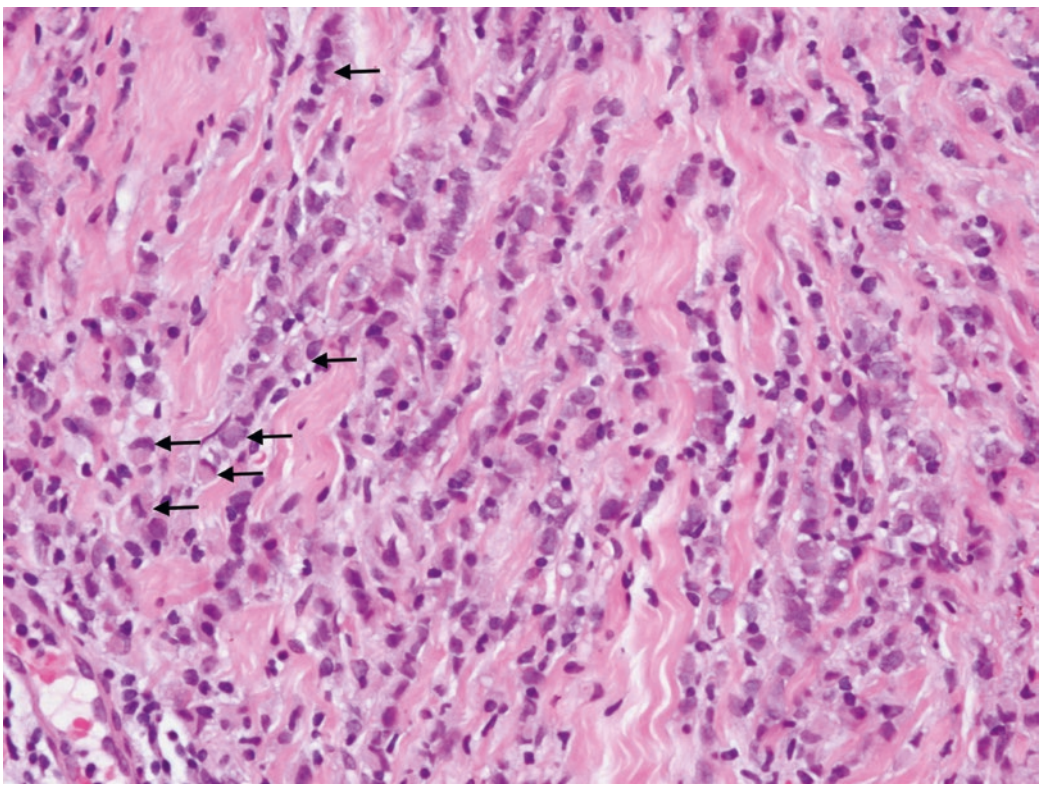

Fig. 10.75 Invasive lobular carcinoma, classic type. Higher magnification shows some of the tumour cells harbouring eccentric nuclei, giving a signet-ring cell appearance (*arrows*)

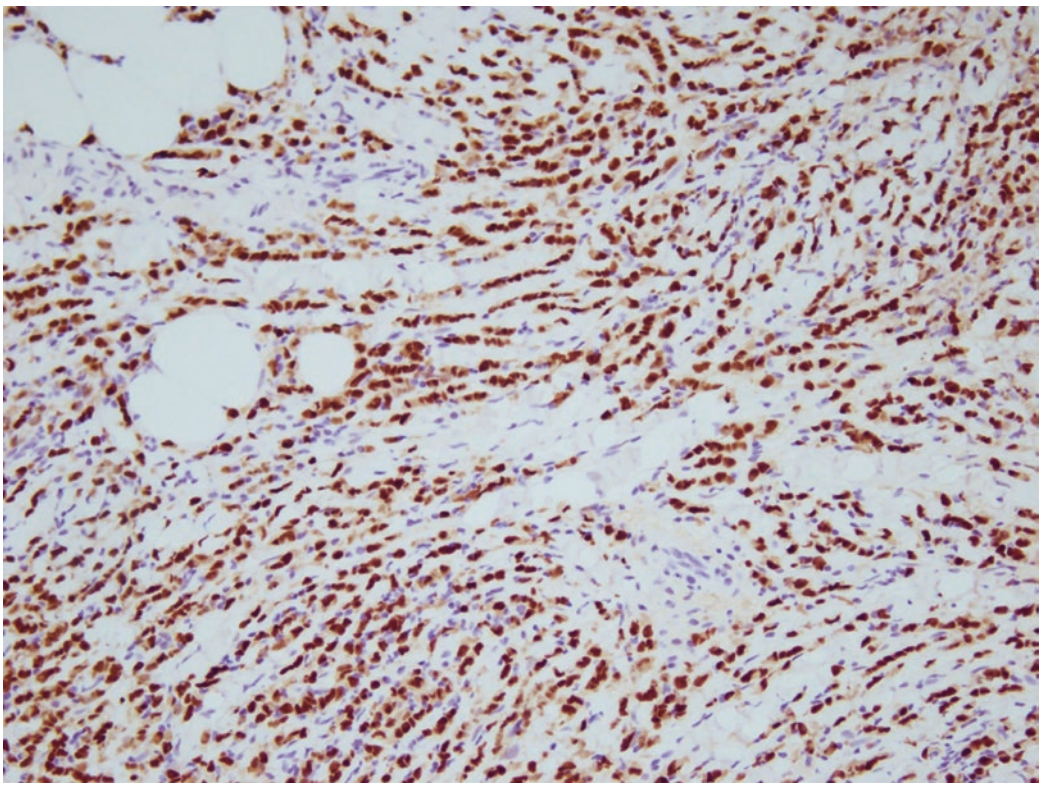

Fig. 10.76 Invasive lobular carcinoma, classic type. Immunohistochemistry shows diffuse nuclear positivity for ER

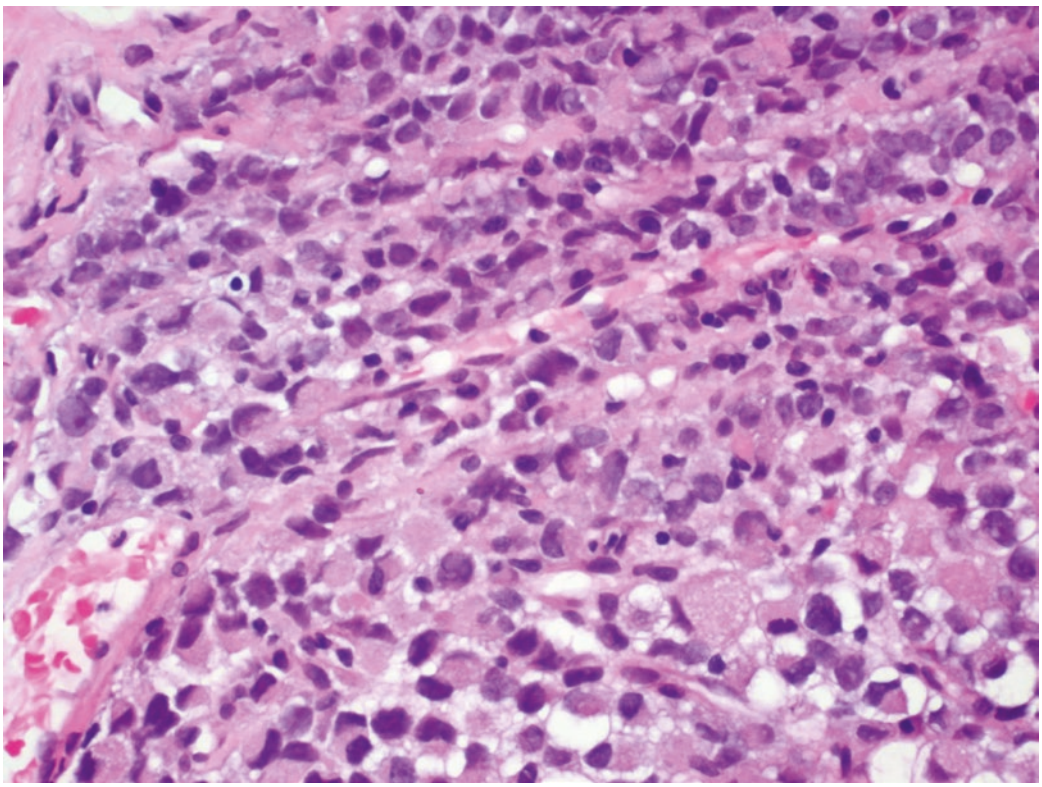

Fig. 10.77 Invasive lobular carcinoma, pleomorphic subtype. Tumour cells show moderate to marked nuclear pleomorphism and hyperchromasia. Several tumour cells show peripherally compressed nuclei with ample pale to pink cytoplasm, giving a signet-ring cell appearance

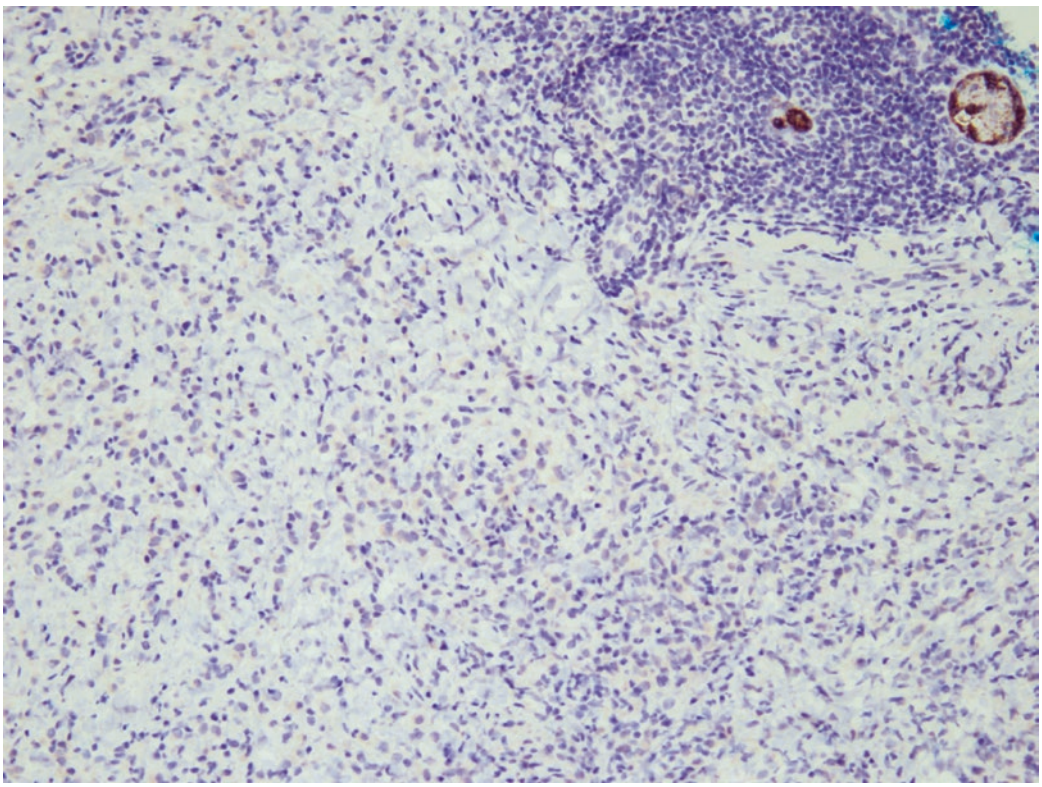

Fig. 10.78 Invasive lobular carcinoma. E-cadherin immunohistochemistry shows negative staining of tumour cells, with resident benign ducts displaying positive staining

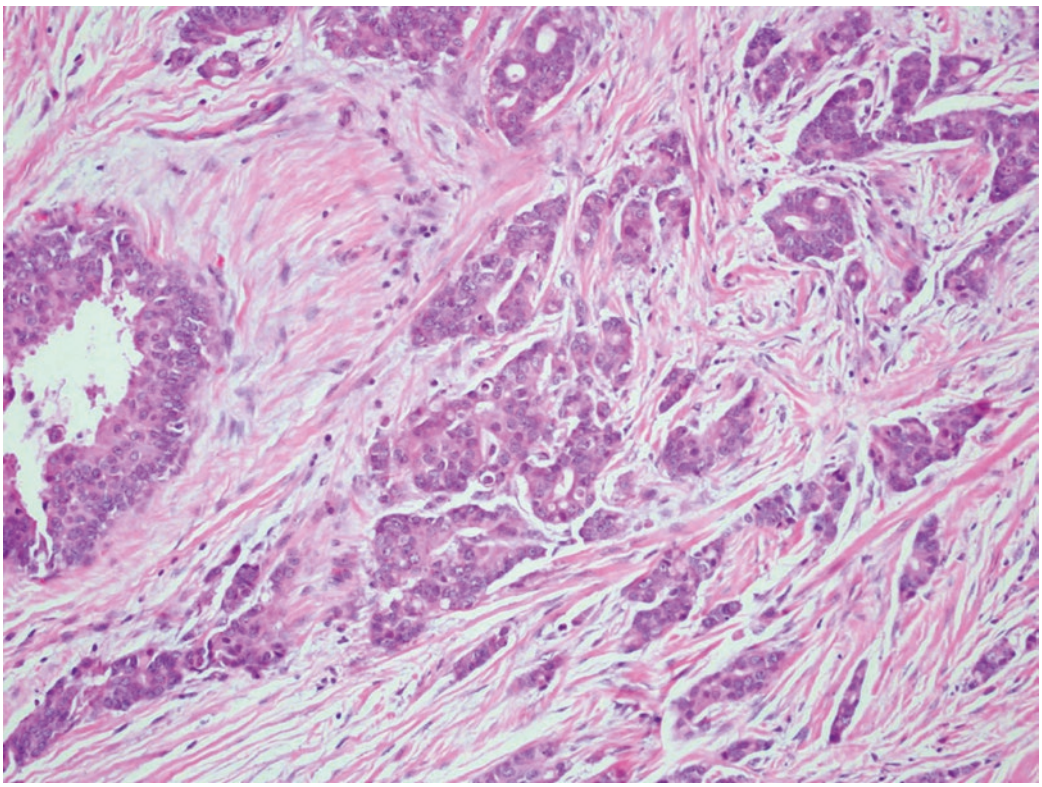

Fig. 10.79 Invasive ductal carcinoma with cytoplasmic vacuoles. Irregular, anastomosed tubules are seen within the desmoplastic stroma. Occasional cytoplasmic vacuoles are noted in a few tumour cells

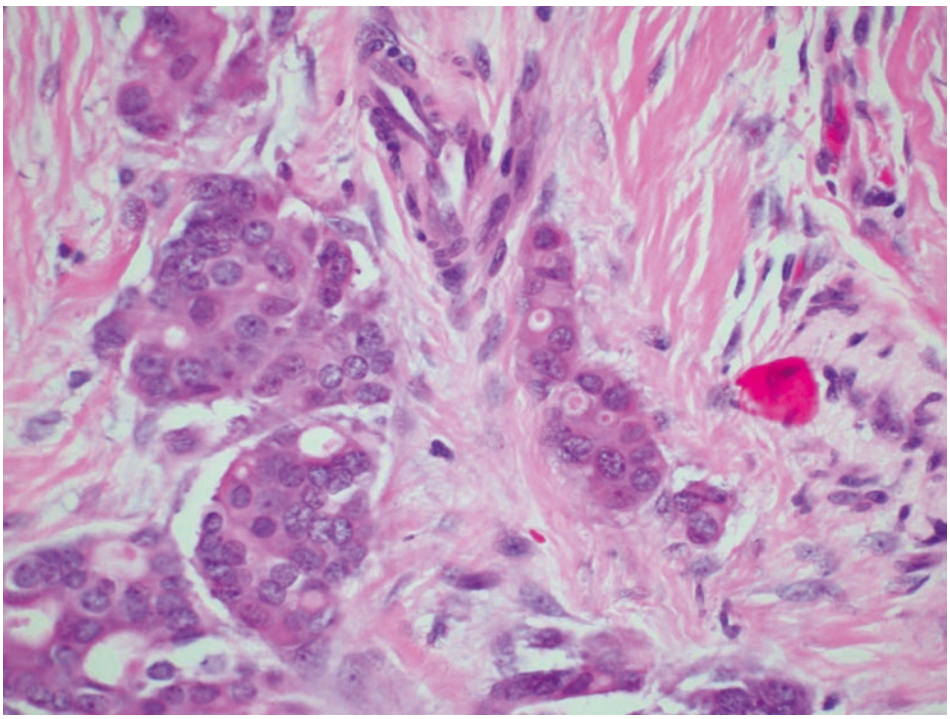

Fig. 10.80 Invasive ductal carcinoma with cytoplasmic vacuoles. At high magnification, several tumour cells show cytoplasmic vacuoles with targetoid secretions. Cytoplasmic vacuoles are not specific to invasive lobular carcinoma; they can be also found in other invasive carcinoma subtypes

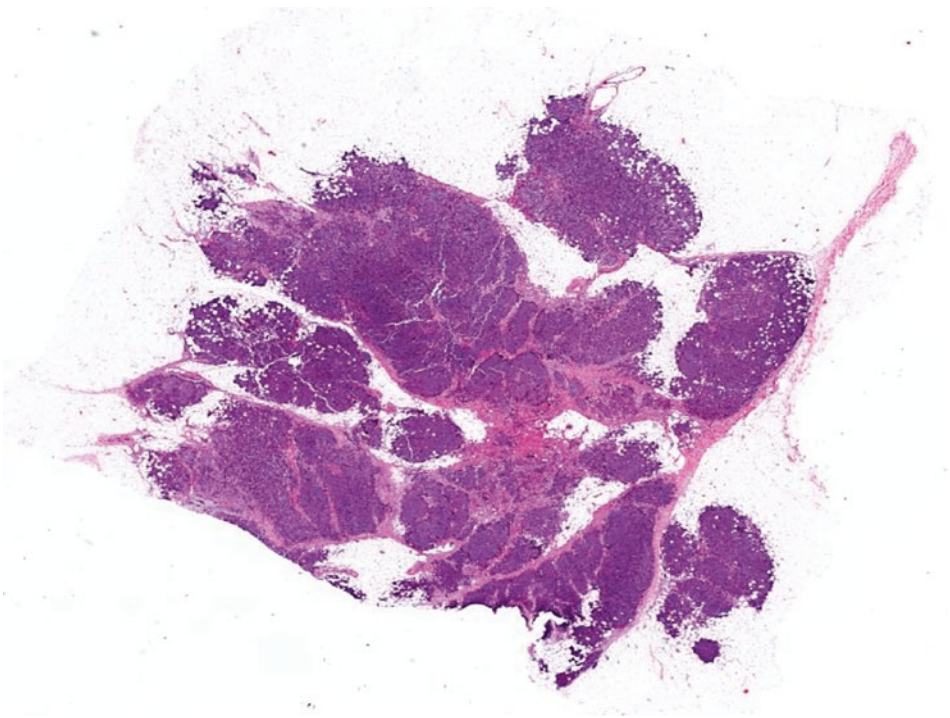

Fig. 10.81 Invasive lobular carcinoma, solid subtype. Scanning magnification shows solid nests of tumour cells with irregular outlines within the adipose

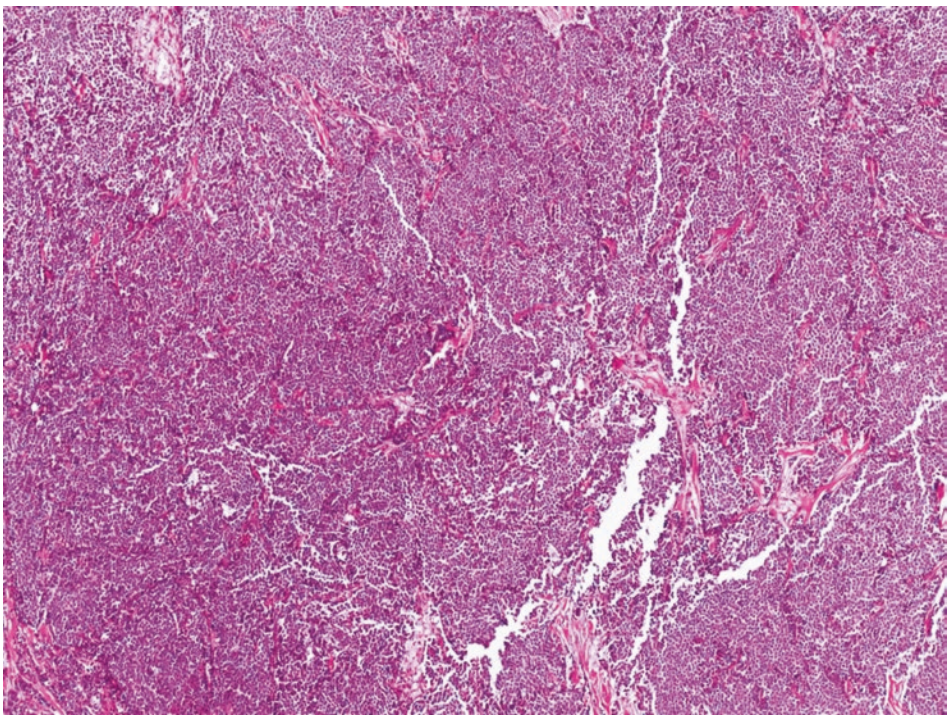

Fig. 10.82 Invasive lobular carcinoma, solid type. Solid confluent sheets of tumour cells permeate the breast parenchyma

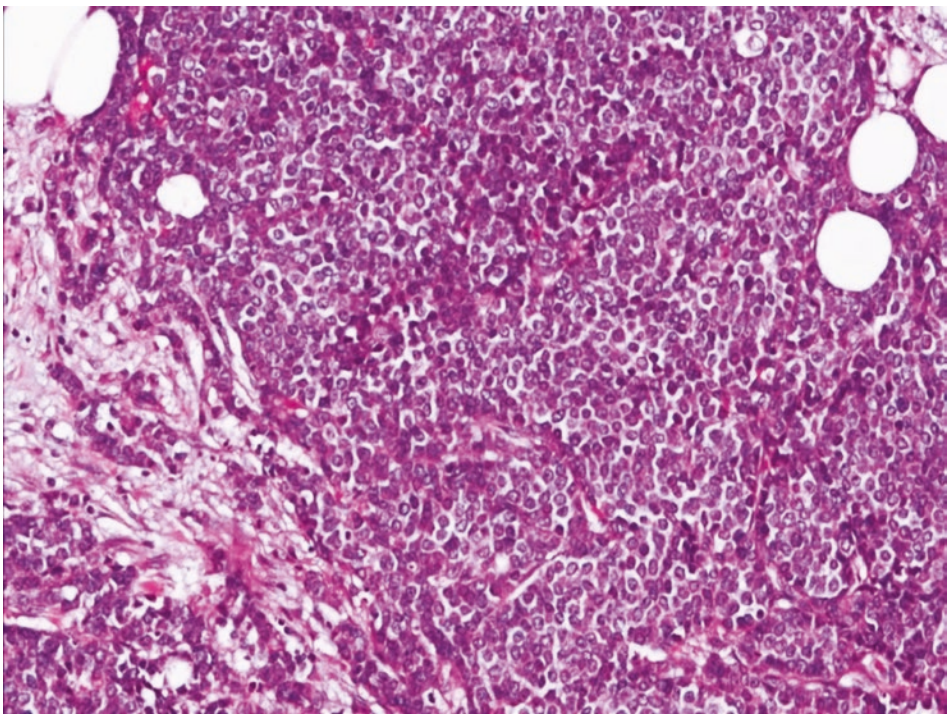

Fig. 10.83 Invasive lobular carcinoma, solid type. Monomorphic tumour cells show uniform nuclei with inconspicuous cytoplasmic membranes and discohesion

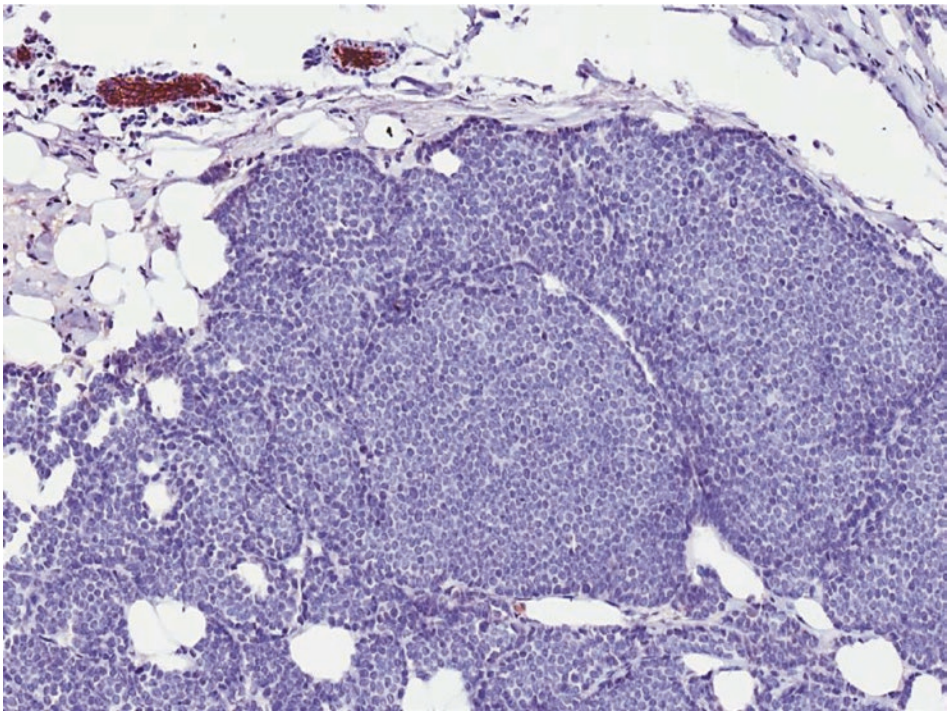

Fig. 10.84 Invasive lobular carcinoma, solid type. E-cadherin immunohistochemistry is negative in the tumour cells, with resident benign ducts in the *upper field* serving as the internal positive control

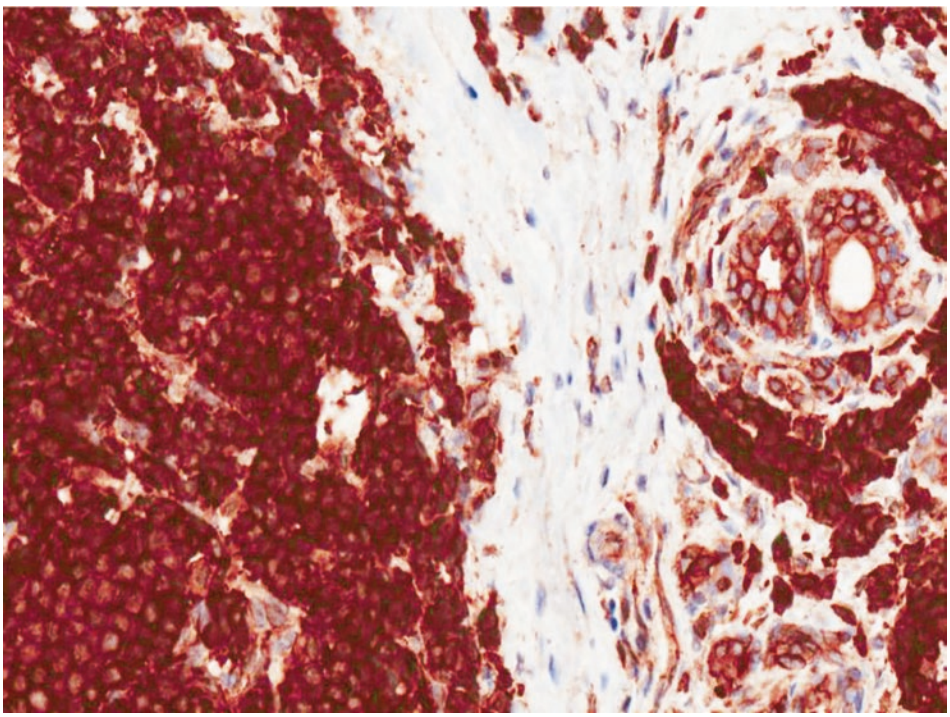

Fig. 10.85 Invasive lobular carcinoma, solid type. Immunohistochemistry for p120 catenin shows cytoplasmic staining; in comparison, benign ducts show cytoplasmic membrane staining

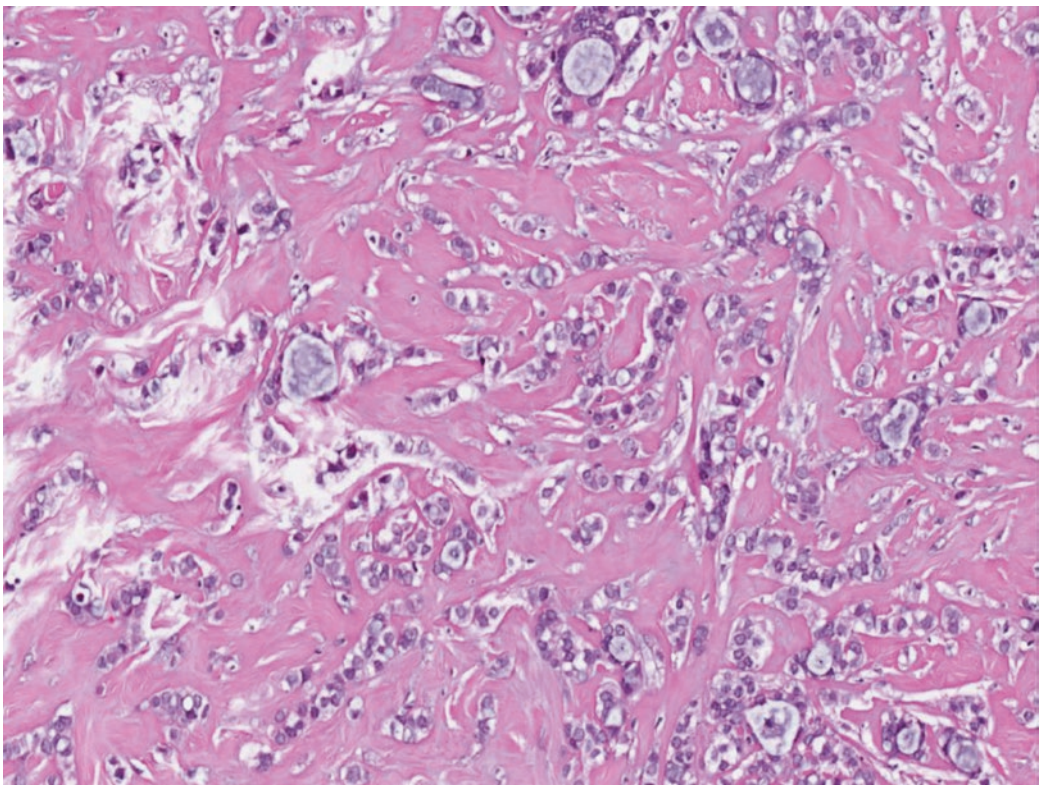

Fig. 10.86 Invasive tubulolobular carcinoma. Linear cords of tumour cells are punctuated by luminal spaces within a hyalinised stroma

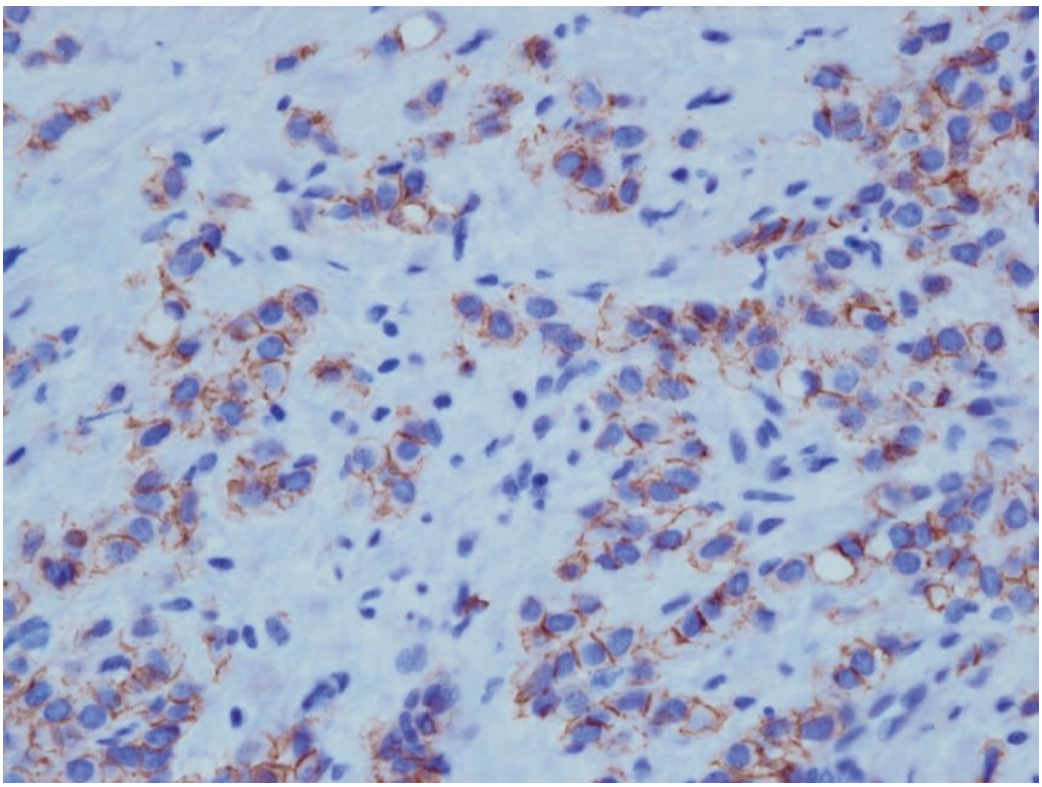

Fig. 10.87 Invasive tubulolobular carcinoma. E-cadherin immunohistochemistry shows diminished and incomplete membrane staining of the tumour cells. Some reports of tubulolobular carcinoma have documented retention of E-cadherin cytoplasmic membrane positivity, suggesting that this subtype may be of ductal rather than lobular phenotype, but the WHO classification of 2012 [1] classifies it within the spectrum of invasive lobular carcinomas

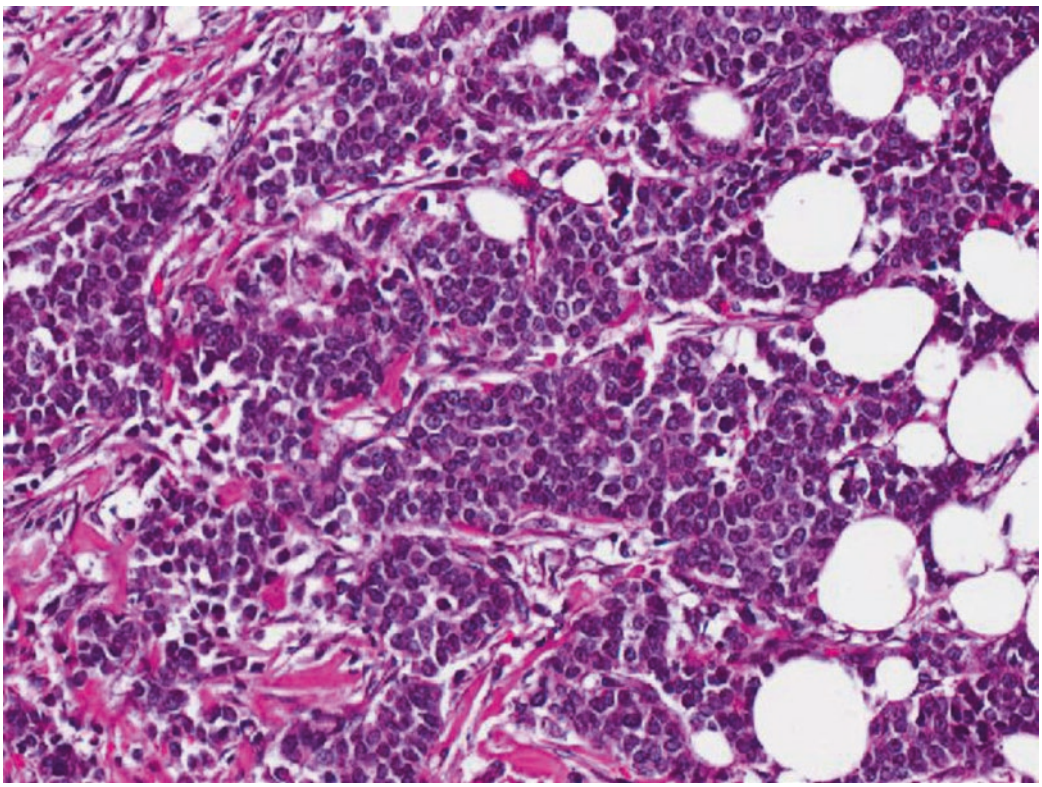

Fig. 10.88 Invasive lobular carcinoma, alveolar variant. Invasive lobular carcinoma cells form nests and groups of 20 or more tumour cells that infiltrate the breast parenchyma. An admixture of different patterns may be seen in the same tumour

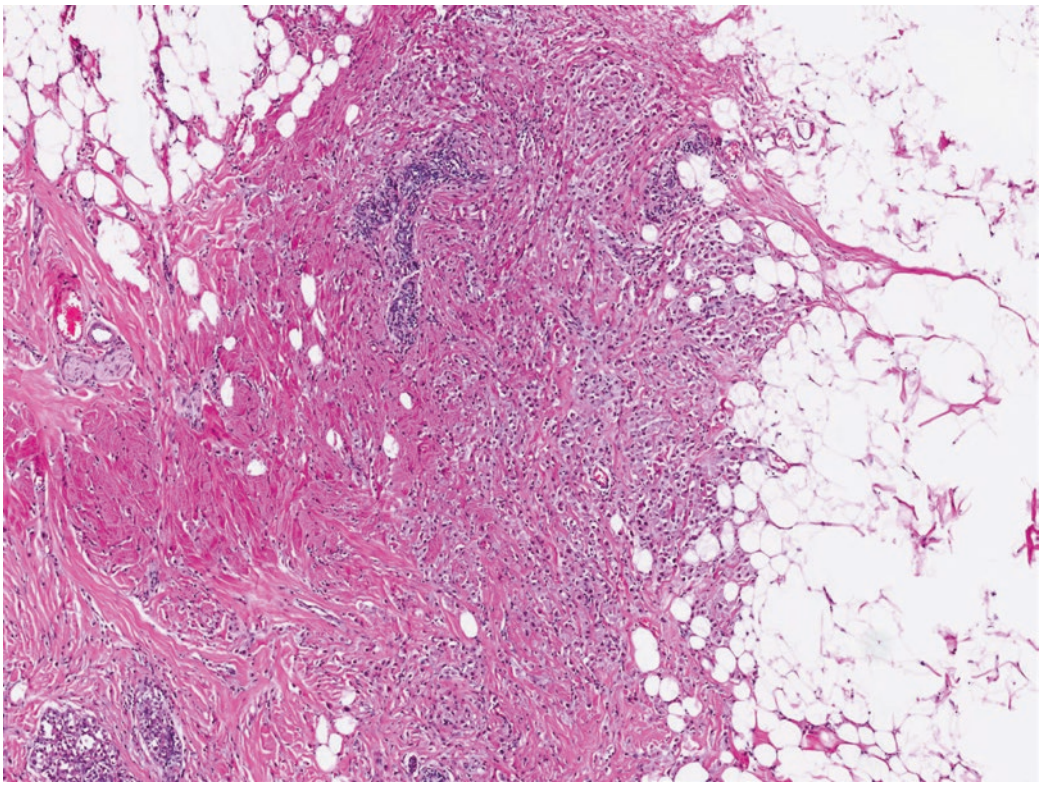

Fig. 10.89 Histiocytoid invasive lobular carcinoma. At low magnification, sheets of pale cells are present, resembling histiocytes

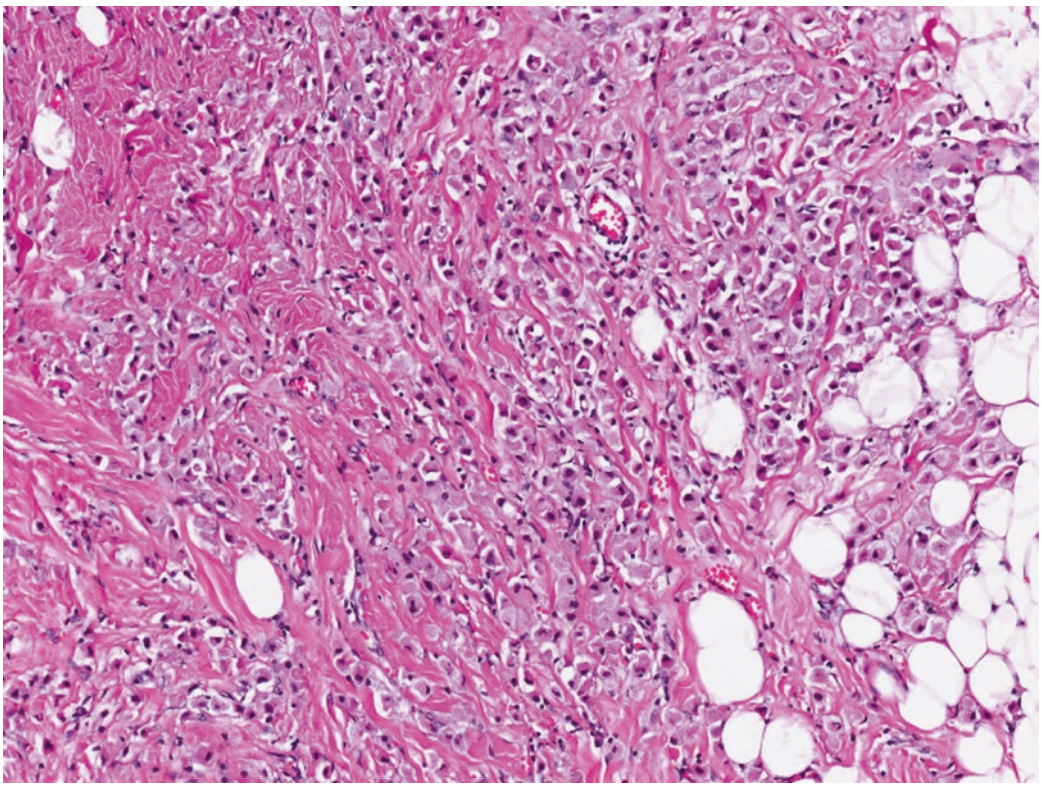

Fig. 10.90 Histiocytoid invasive lobular carcinoma. Sheets of pale cells resembling foamy histiocytes are seen percolating through the fibroadipose stroma. Many cells have eccentric, hyperchromatic nuclei. Accompanying inflammatory cells are scant

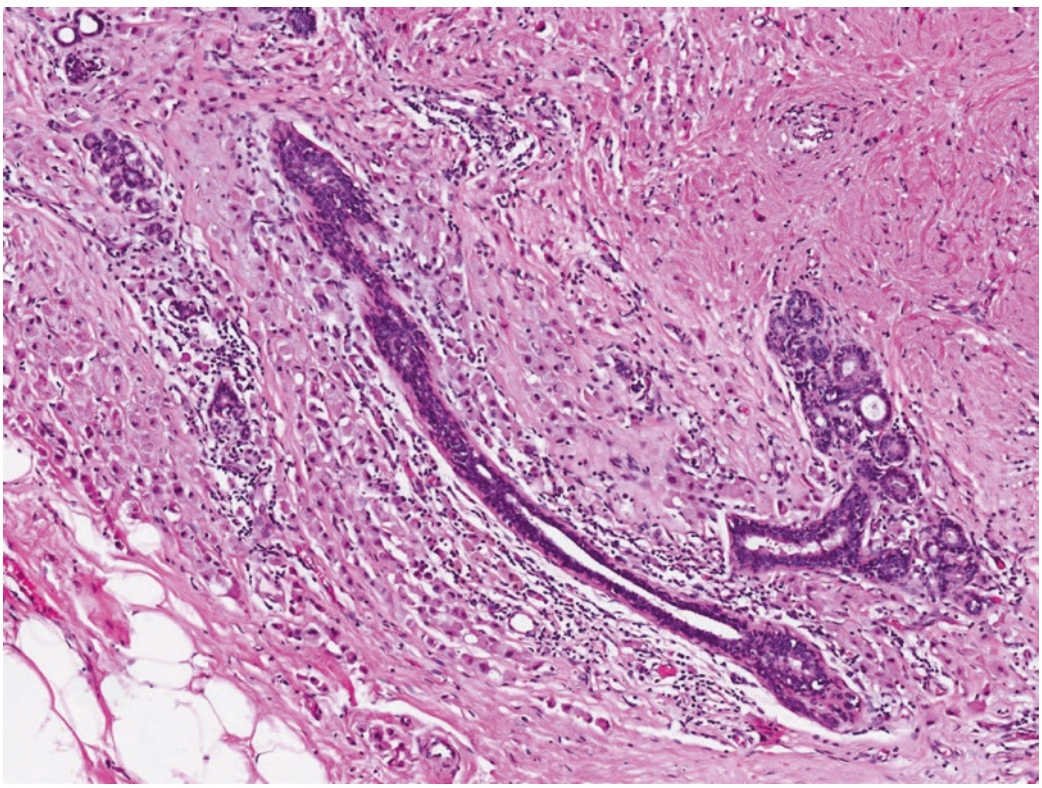

Fig. 10.91 Histiocytoid invasive lobular carcinoma. Tumour cells encircle the terminal duct, giving a targetoid pattern of infiltration

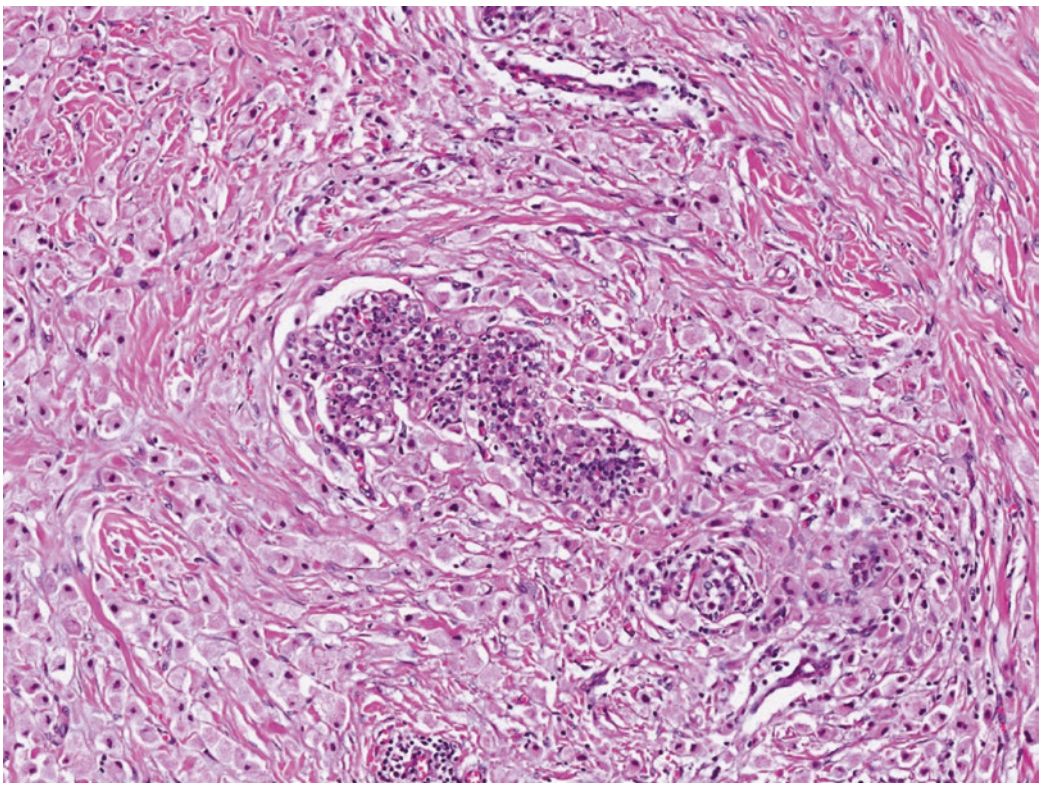

Fig. 10.92 Histiocytoid invasive lobular carcinoma. Lobular neoplasia is present amid the invading histiocytoid carcinoma cells

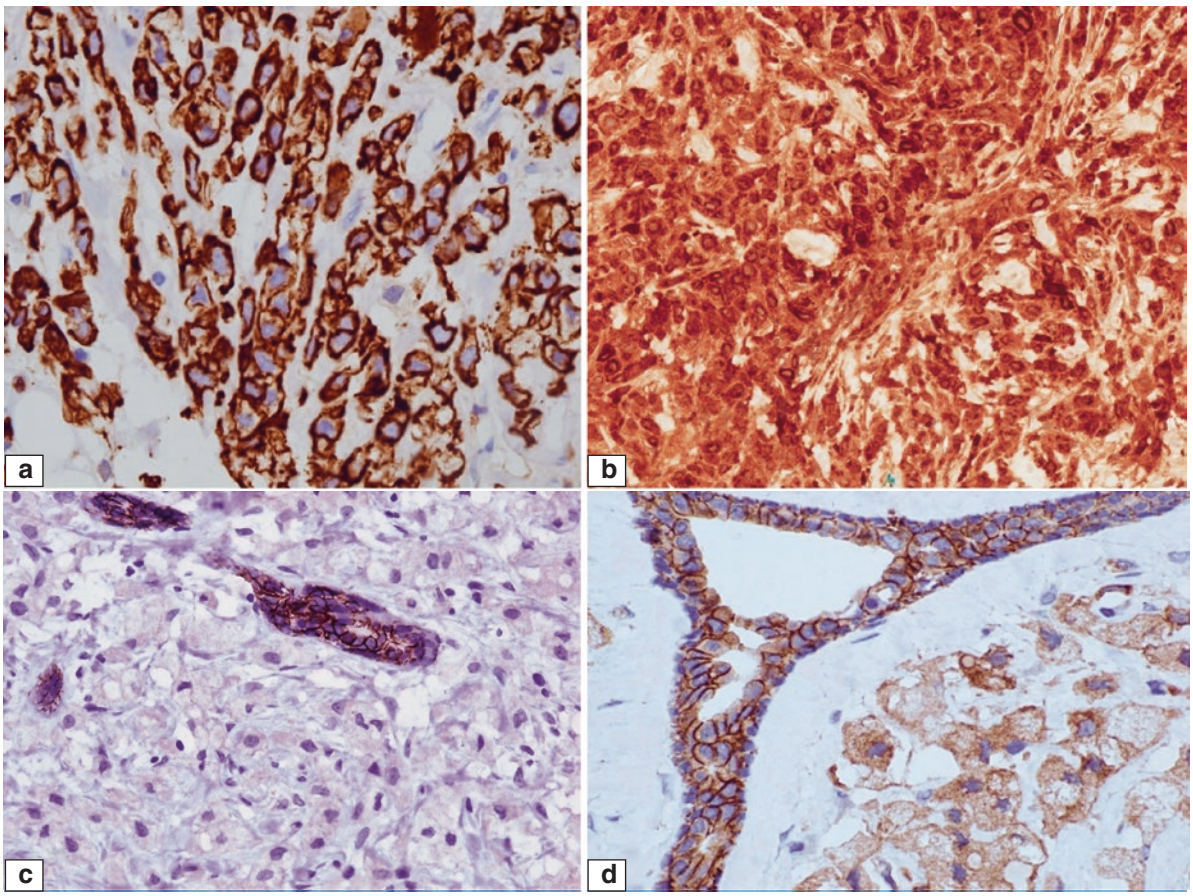

Fig. 10.93 Immunohistochemistry shows positive cytoplasmic reactivity of histiocytoid invasive lobular carcinoma cells for CK7 (**a**) and GCDFP-15 (**b**); E-cadherin is negative (**c**), and p120 catenin (**d**) shows cytoplasmic localisation of positive reactivity instead of cytoplasmic membrane staining

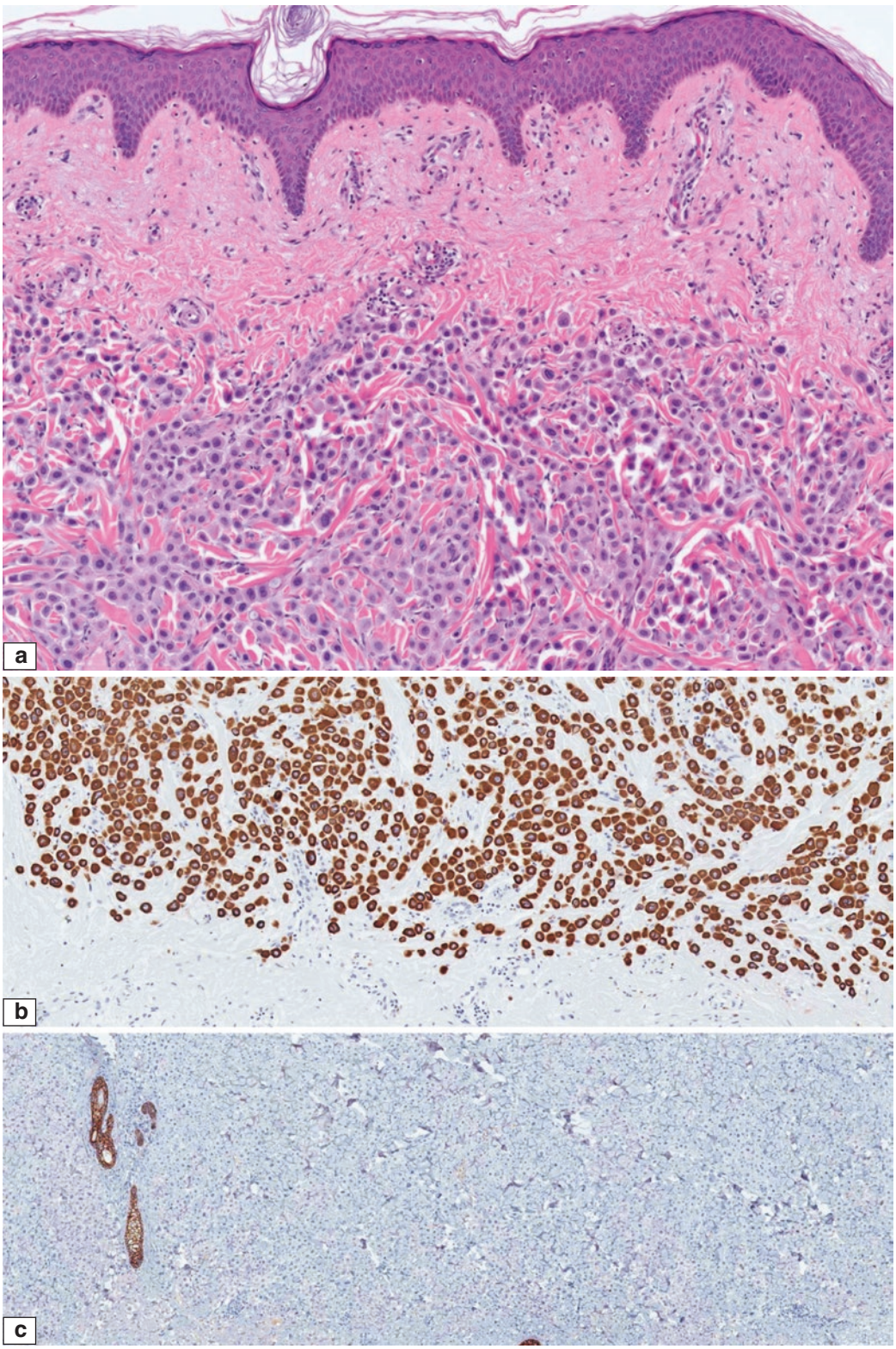

Fig. 10.94 (**a**) Recurrent histiocytoid invasive lobular carcinoma in the skin of the chest wall. Because of the often bland appearance of the histiocytoid carcinoma cells, such an infiltrate may be mistaken for benign histiocytes. Clues to the correct diagnosis are the nuclear atypia (readily evident in this case), coexistence with classic or pleomorphic invasive lobular carcinoma, and lack of accompanying inflammatory cells. A history of previous breast carcinoma should increase the index of suspicion in recurrent cases. (**b**, **c**) Immunohistochemistry shows positive reactivity of the tumour cells for CK7 (**b**), with absent staining for E-cadherin (**c**)

Differential Diagnosis

Sclerosing Adenosis

When sclerosing adenosis is severe and tubular lumens are obscured, the nuclei of both luminal and myoepithelial cells resemble those of classic invasive lobular carcinoma (Figs. 10.95, 10.96, and 10.97). Clues to the correct diagnosis are the occasional lumens and the presence of myoepithelial cells, which can be verified with immunohistochemistry for myoepithelial markers.

Histiocytic Inflammation

The histiocytoid variant of invasive lobular carcinoma can appear deceptively bland and resemble a histiocytic inflammation. The presence of lobular neoplasia and classic invasive lobular carcinoma is helpful in making the correct diagnosis. In contrast, histiocytic inflammation tends to be accompanied by other inflammatory cells and may be related to duct ectasia, fat necrosis, and other inflammatory processes (Fig. 10.98).

Myofibroblastoma

Myofibroblastoma, especially the epithelioid variant, may be mistaken for invasive lobular carcinoma, particularly on limited material such as core biopsy. Plump myofibroblasts can mimic invasive lobular carcinoma cells, further aggravated by their ER positivity. The circumscribed boundary of the myofibroblastoma (which may not be appreciated on core biopsy) is a helpful feature. Myofibroblastoma is positive for CD34 and negative with epithelial markers (Figs. 10.99, 10.100, 10.101, and 10.102).

Invasive Ductal Carcinoma with Low Nuclear Grade Features

Invasive ductal carcinoma with mild nuclear pleomorphism and a narrow trabecular or nested form of infiltration may resemble invasive lobular carcinoma (Fig. 10.103). Tubular differentiation and E-cadherin staining favour a ductal phenotype, though the tubulolobular variant of invasive lobular carcinoma may be difficult to separate from a low-grade invasive ductal carcinoma, especially since the tubulolobular variant also has been reported to be E-cadherin positive.

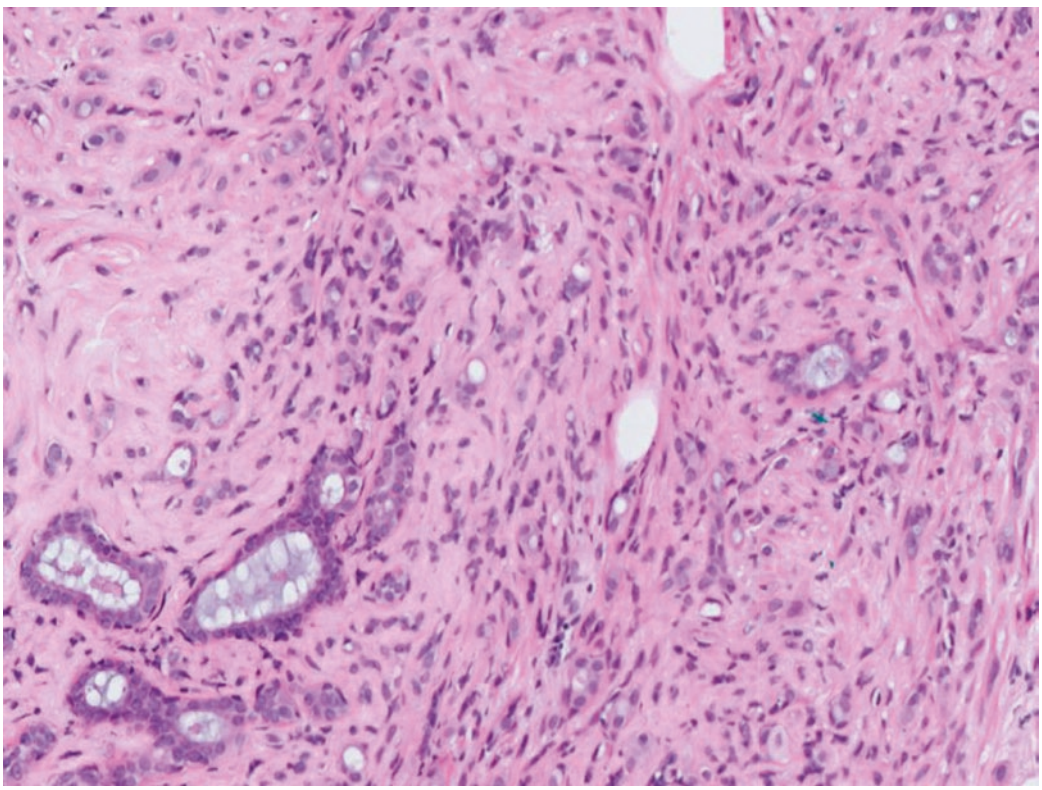

Fig. 10.95 Sclerosing adenosis. Compressed and elongated epithelial nests are present, featuring inconspicuous tubular lumens. There is merging with benign ducts and acini

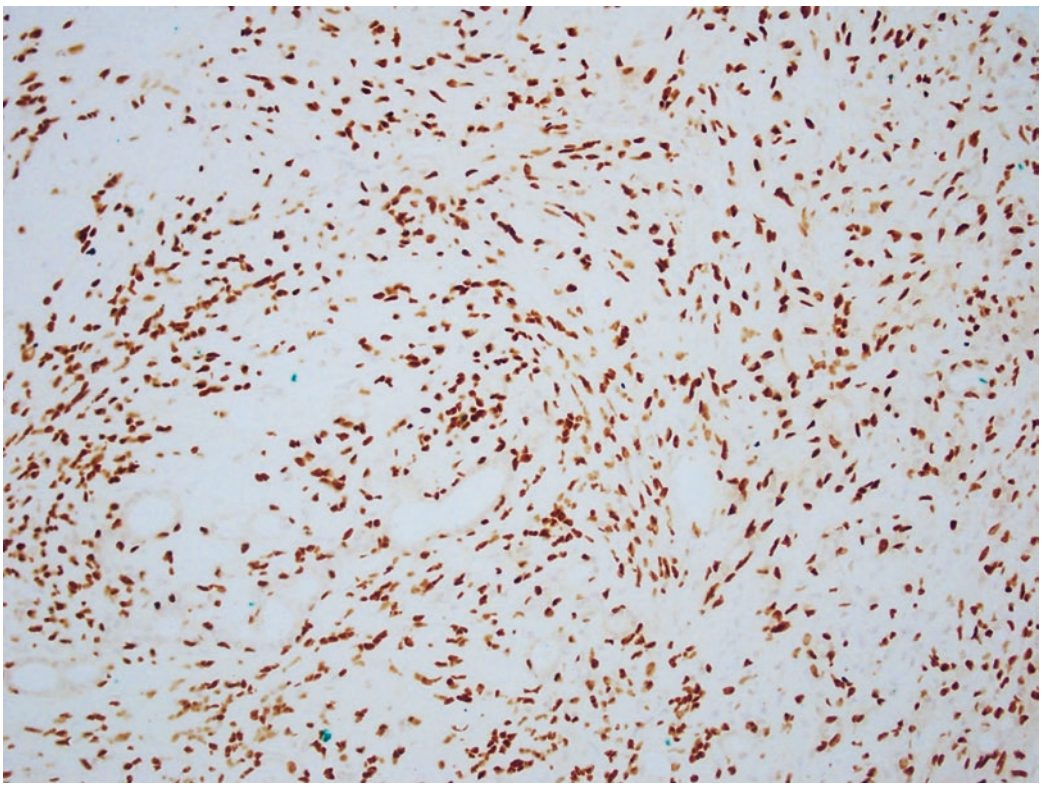

Fig. 10.96 Sclerosing adenosis. Immunohistochemistry for p63 shows many myoepithelial cell nuclei, indicating their preservation in a benign, non-invasive process

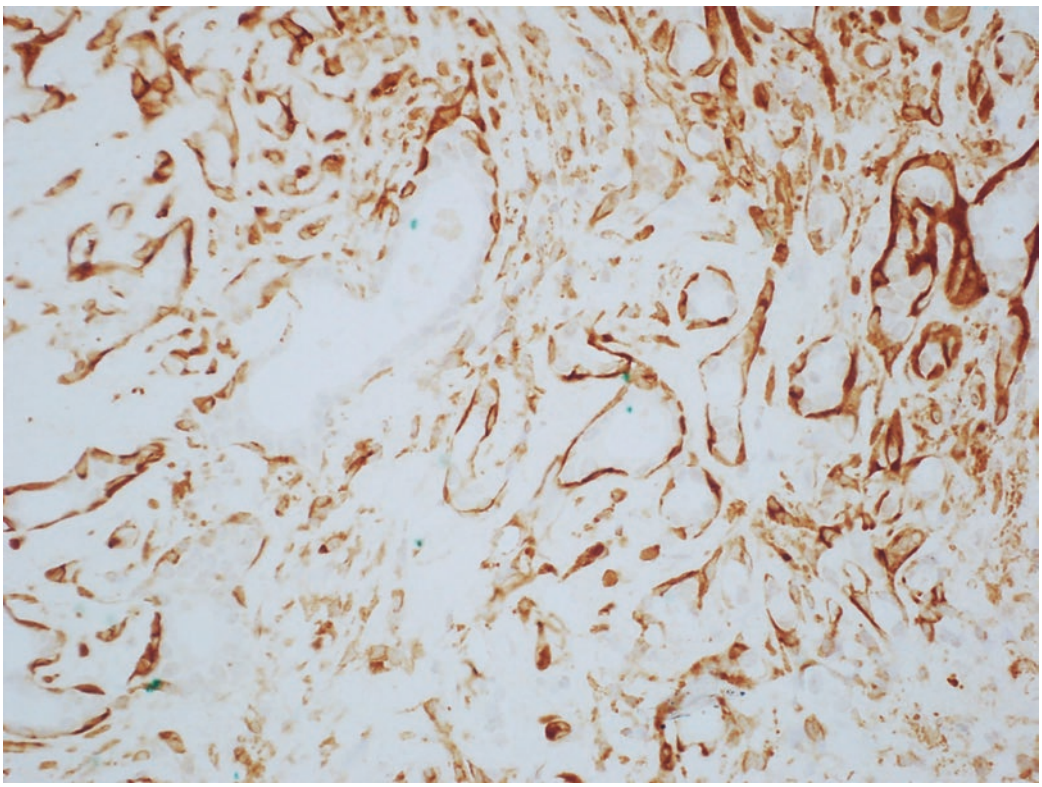

Fig. 10.97 Sclerosing adenosis. Immunohistochemistry for smooth muscle myosin heavy chain (SMMS) shows cytoplasmic decoration of intact myoepithelial cells

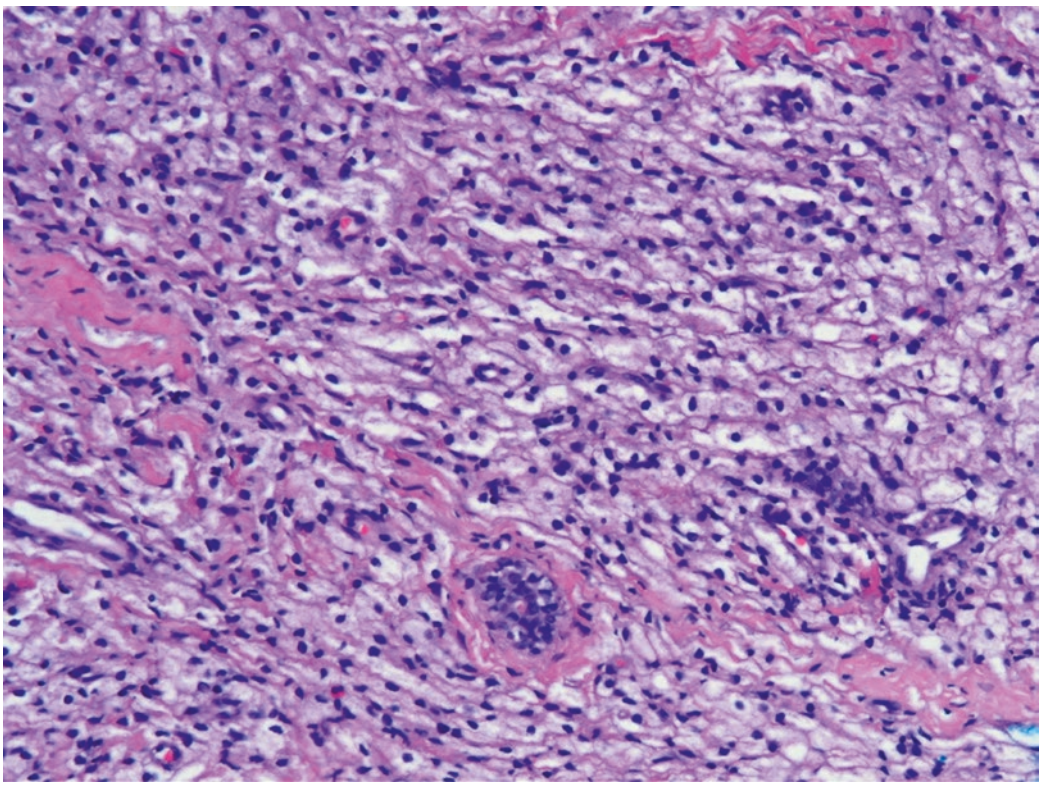

Fig. 10.98 Histiocytic inflammation. Sheets of pale histiocytes with small bland nuclei are present. A few lymphocytes are scattered among the histiocytes

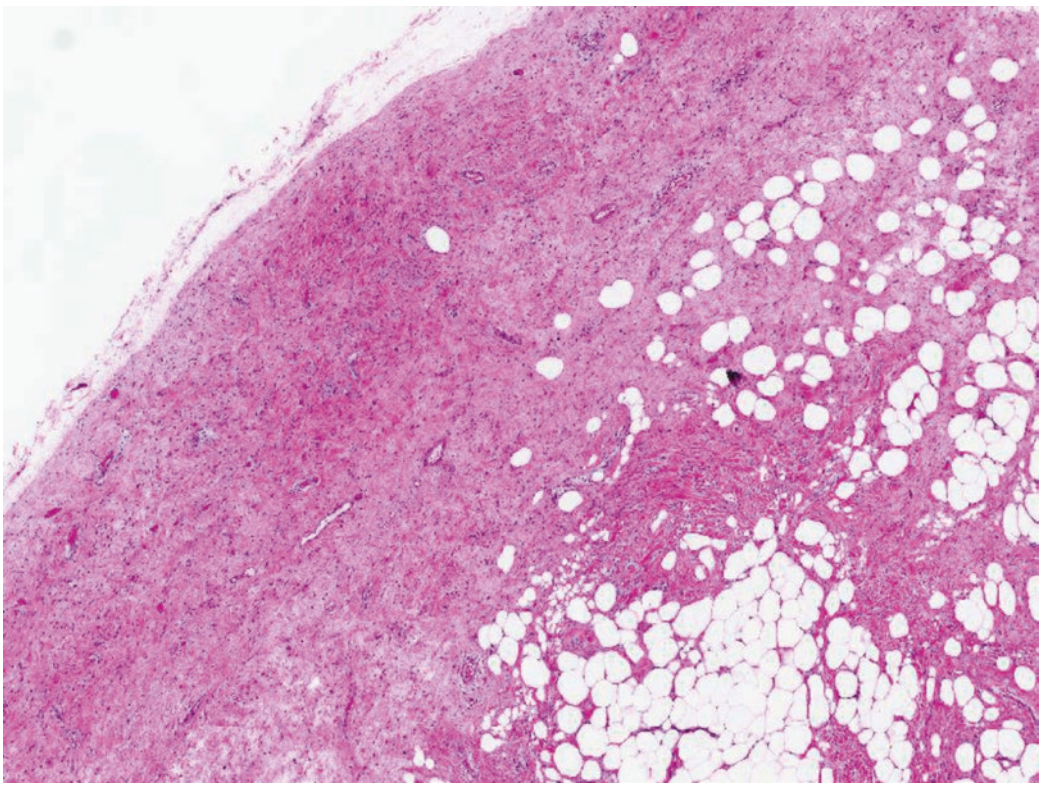

Fig. 10.99 Myofibroblastoma. This benign neoplasm is composed of stromal fibroblasts and myofibroblasts. It has a circumscribed border, which is a helpful feature in affirming its benign nature. Adipose tissue is often present, resembling a spindle cell lipoma which is regarded as closely related to the myofibroblastoma

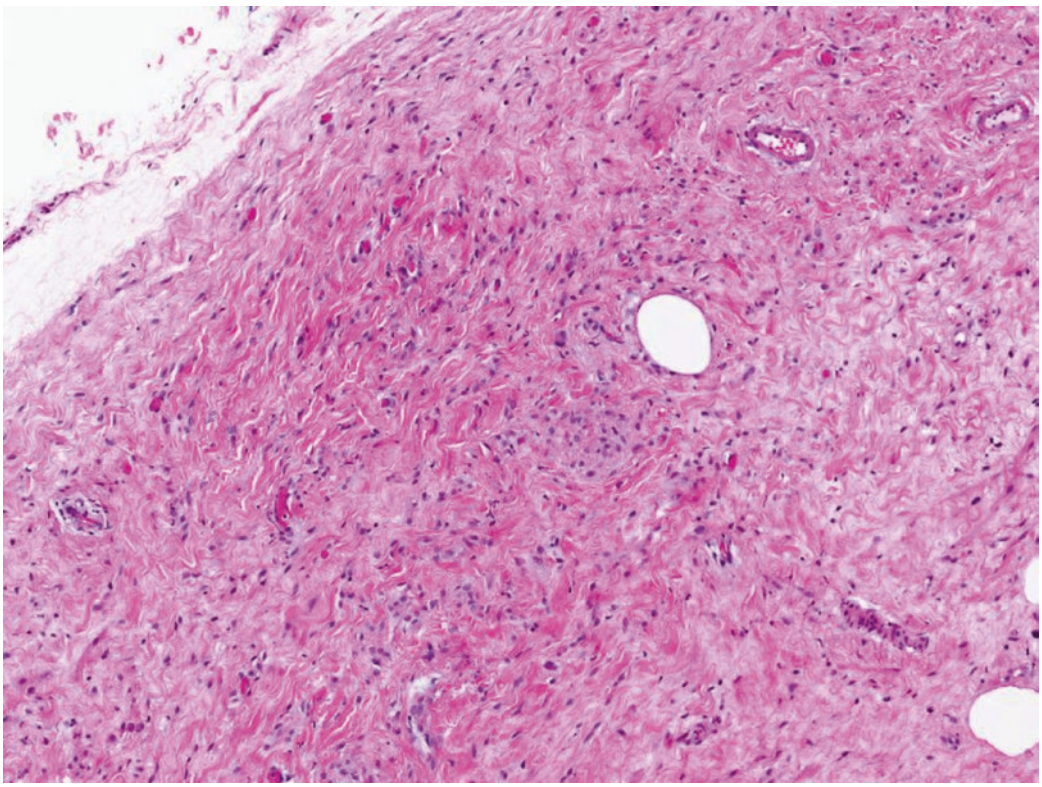

Fig. 10.100 Myofibroblastoma. Some of the stromal cells may contain rounded nuclei aligned in a linear pattern resembling invasive lobular carcinoma. The well-circumscribed border of the tumour, with no accompanying lobular neoplasia, should help point to the correct diagnosis

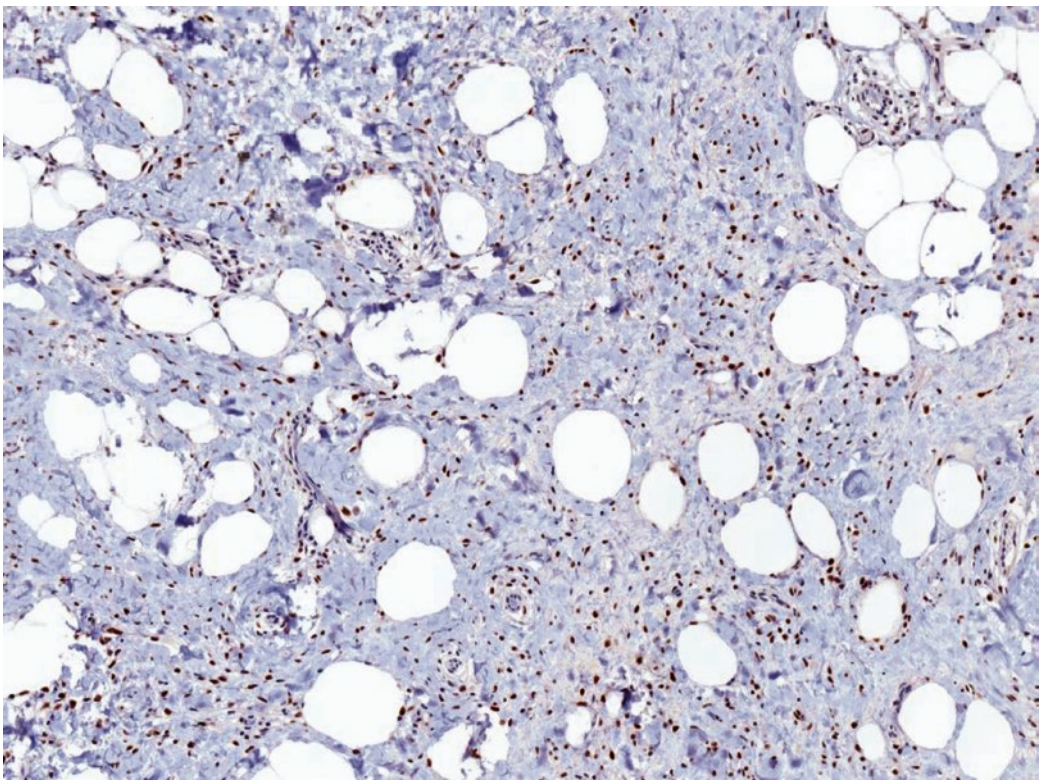

Fig. 10.101 Myofibroblastoma. Immunohistochemistry shows positive nuclear staining for ER, which may accentuate its resemblance to invasive lobular carcinoma. Keratin immunostaining is negative

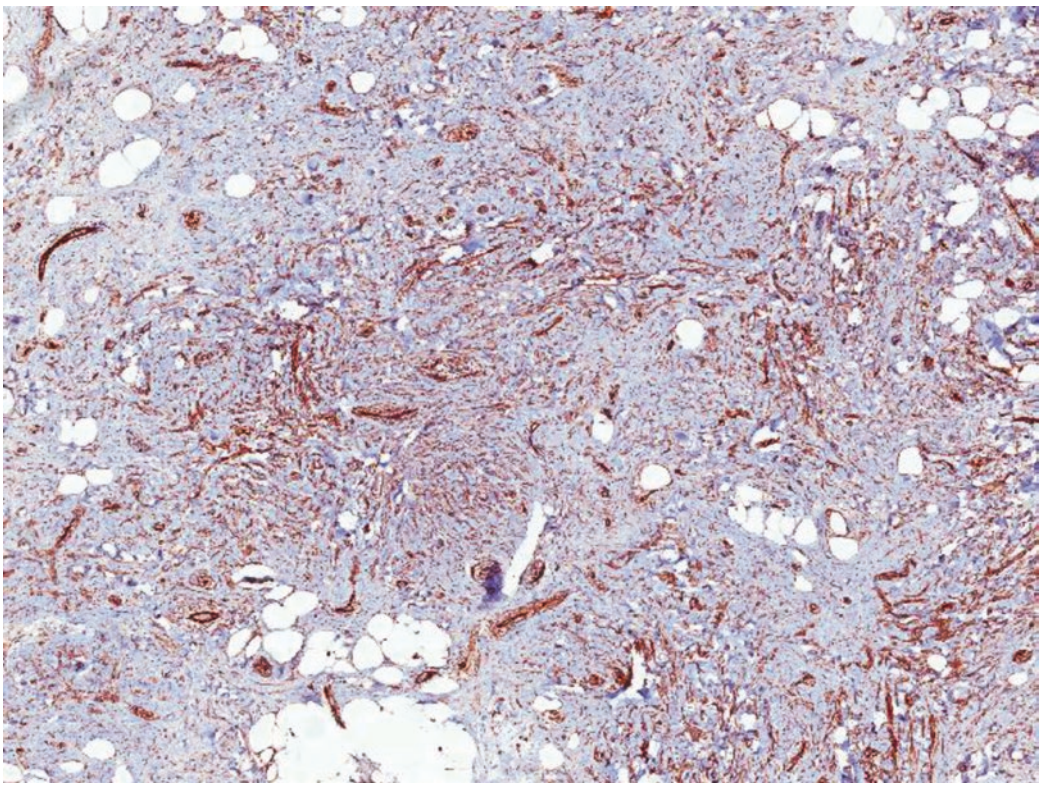

Fig. 10.102 Myofibroblastoma. CD34 decorates the spindle stromal cells. Fluorescence in situ hybridisation confirms deletion of chromosome 13q14 in most myofibroblastomas

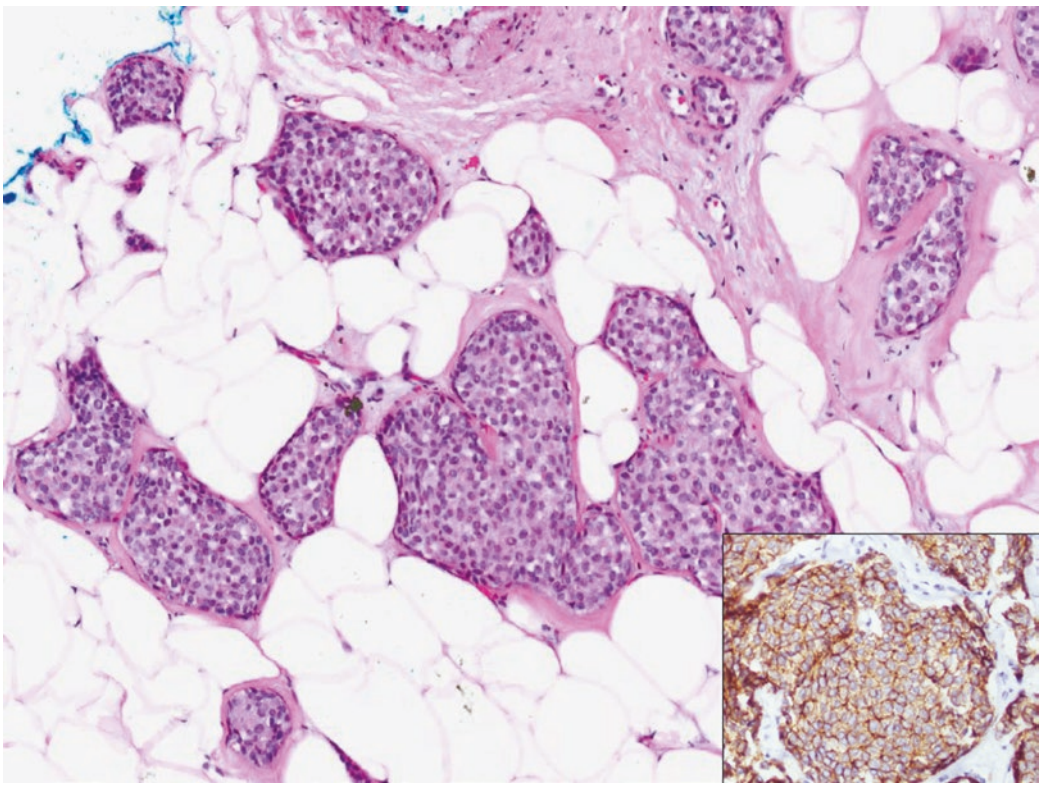

Fig. 10.103 Invasive ductal carcinoma with a nested pattern, resembling an alveolar variant of invasive lobular carcinoma. *Inset* shows positive E-cadherin staining of the cytoplasmic membranes of tumour cells

Invasive Carcinoma with Neuroendocrine Features

Carcinoma with neuroendocrine features comprising rounded tumour nests can be mistaken for the alveolar variant of invasive lobular carcinoma because of the uniform appearance of the tumour cells (Figs. 10.104 and 10.105). Fine, even nuclear chromatin, cytoplasmic amphophilia and granularity, spindling, pseudorosettes, and a plasmacytoid appearance are clues to a neuroendocrine nature. Immunohistochemistry for neuroendocrine markers is helpful.

Invasive Apocrine Carcinoma

As pleomorphic invasive lobular carcinoma may harbour apocrine cytomorphology, it can mimic invasive apocrine carcinoma (Figs. 10.106 and 10.107). Both feature GCDFP-15 positivity, but invasive apocrine carcinoma is also E-cadherin positive.

Malignant Lymphoma

Discohesion and uniformity of invasive lobular carcinoma cells can closely resemble a low-grade malignant lymphoma (Figs. 10.108, 10.109, 10.110, 10.111, 10.112, 10.113, 10.114, 10.115, 10.116, 10.117, and 10.118). Clues to the correct diagnosis are the presence of lobular neoplasia and classic invasive lobular carcinoma, with cytoplasmic vacuoles in lobular neoplastic and carcinoma cells. Accompanying lymphocytes are usually seen in malignant lymphoma.

Metastatic Signet-Ring Cell Carcinoma

When signet-ring cell features are extensive, possible metastasis from organs such as the stomach may need to be considered (Fig. 10.119).

Prognosis and Therapy Considerations

Whether the prognosis for invasive lobular carcinoma is better than for invasive ductal carcinoma is debatable; reports have suggested better, similar, and poorer prognostic outcomes. In terms of metastases, invasive lobular carcinoma has a greater tendency to metastasise to the bone, gastrointestinal tract, uterus, meninges, and serosal surfaces (Fig. 10.120).

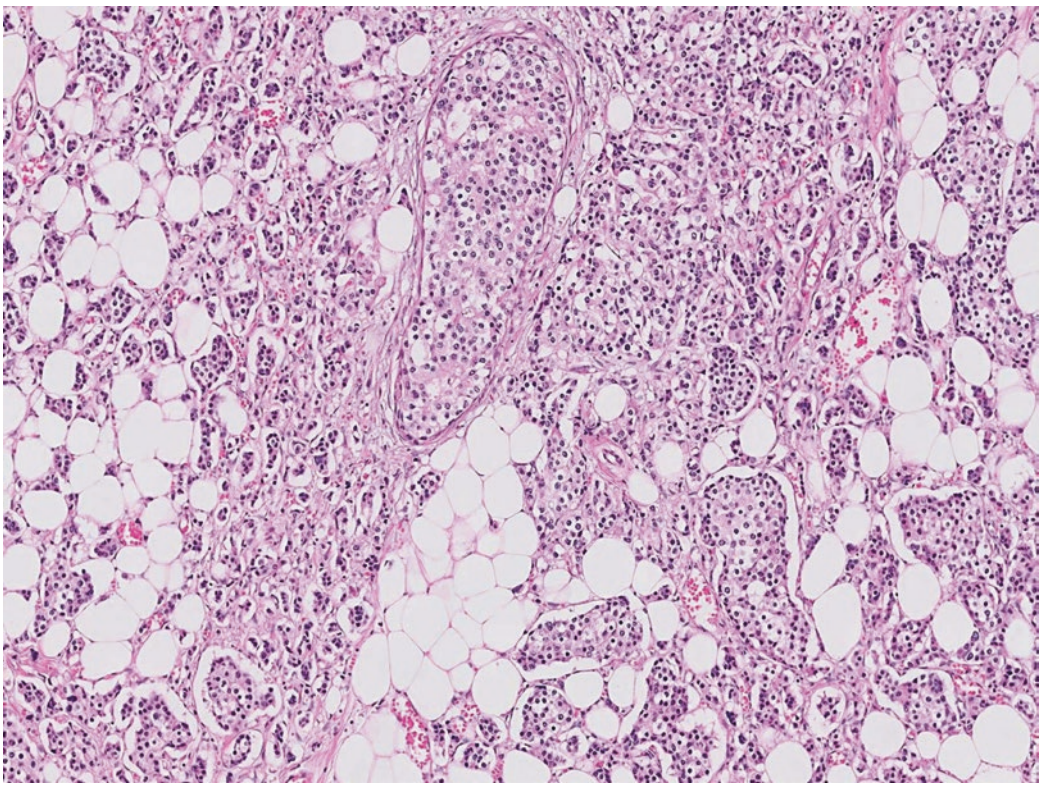

Fig. 10.104 Invasive carcinoma with neuroendocrine features. Some of the small, solid nests may resemble the alveolar variant of invasive lobular carcinoma

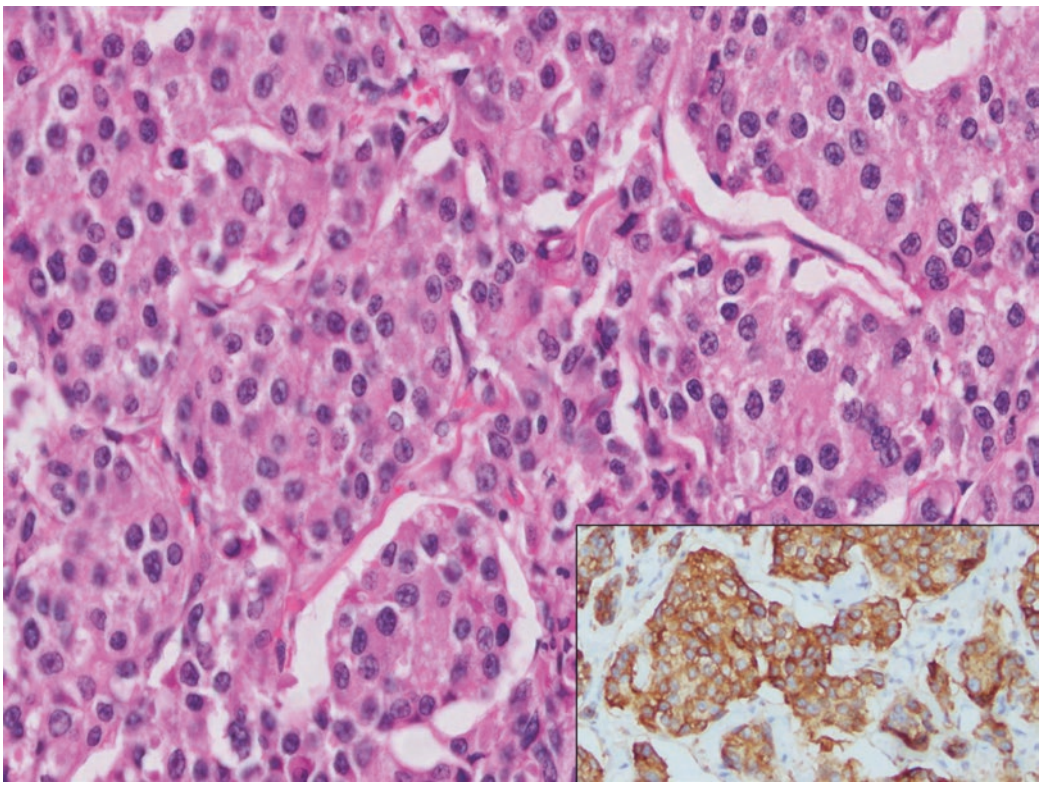

Fig. 10.105 Invasive carcinoma with neuroendocrine features. Rounded nests of tumour cells are present, with relatively uniform nuclei with fine chromatin and pink, granular cytoplasm. *Inset* shows positive staining of the tumour cells for synaptophysin

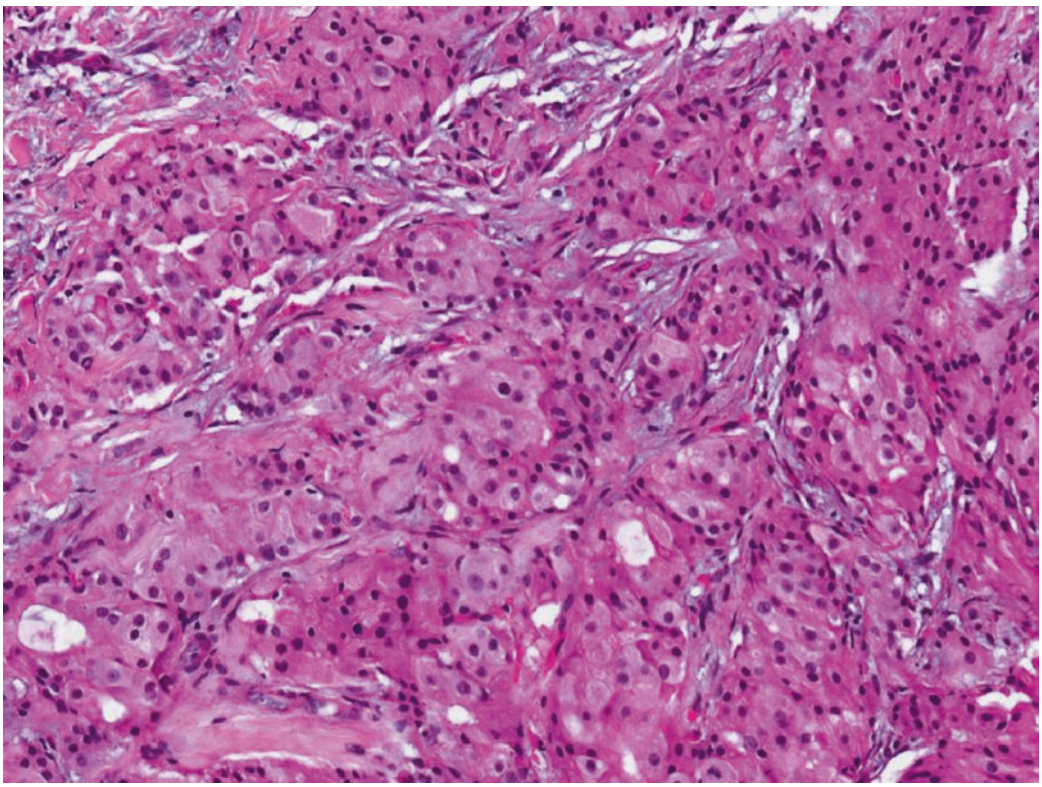

Fig. 10.106 Invasive carcinoma with apocrine features. Anastomosing trabeculae of tumour cells with ample pink cytoplasm and dense nuclei are seen extending through the stroma

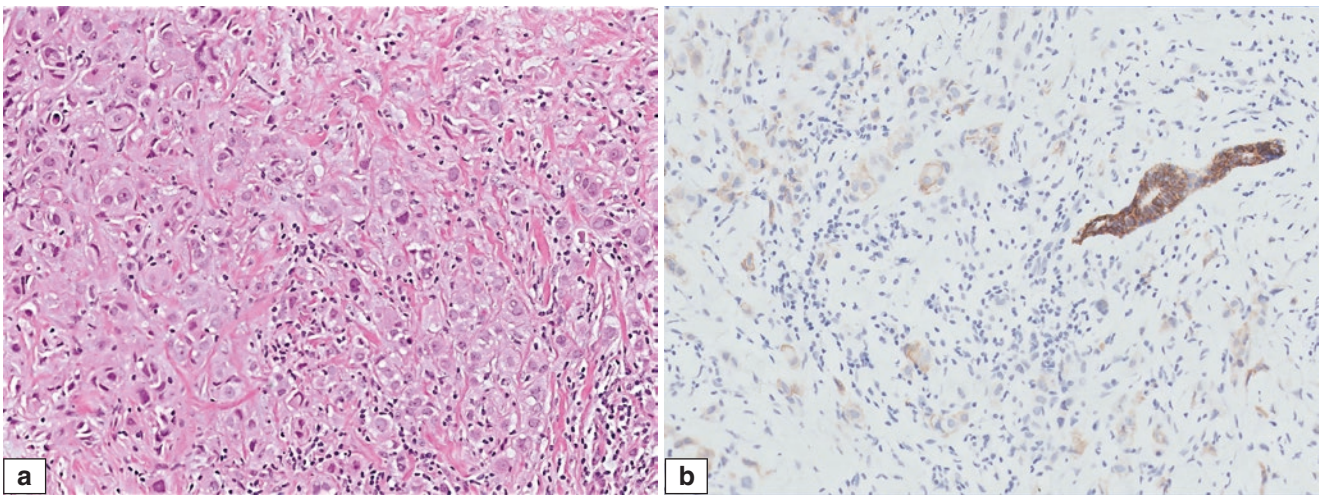

Fig. 10.107 Invasive lobular carcinoma with pleomorphic apocrine features. (**a**) Small nests and singly disposed discohesive cells show ample pale to pink cytoplasm with pleomorphic vesicular nuclei and distinct nucleoli. (**b**) Immunohistochemistry for E-cadherin shows diminished to absent staining in the invasive lobular carcinoma cells. A benign duct in the section serves as the internal positive control

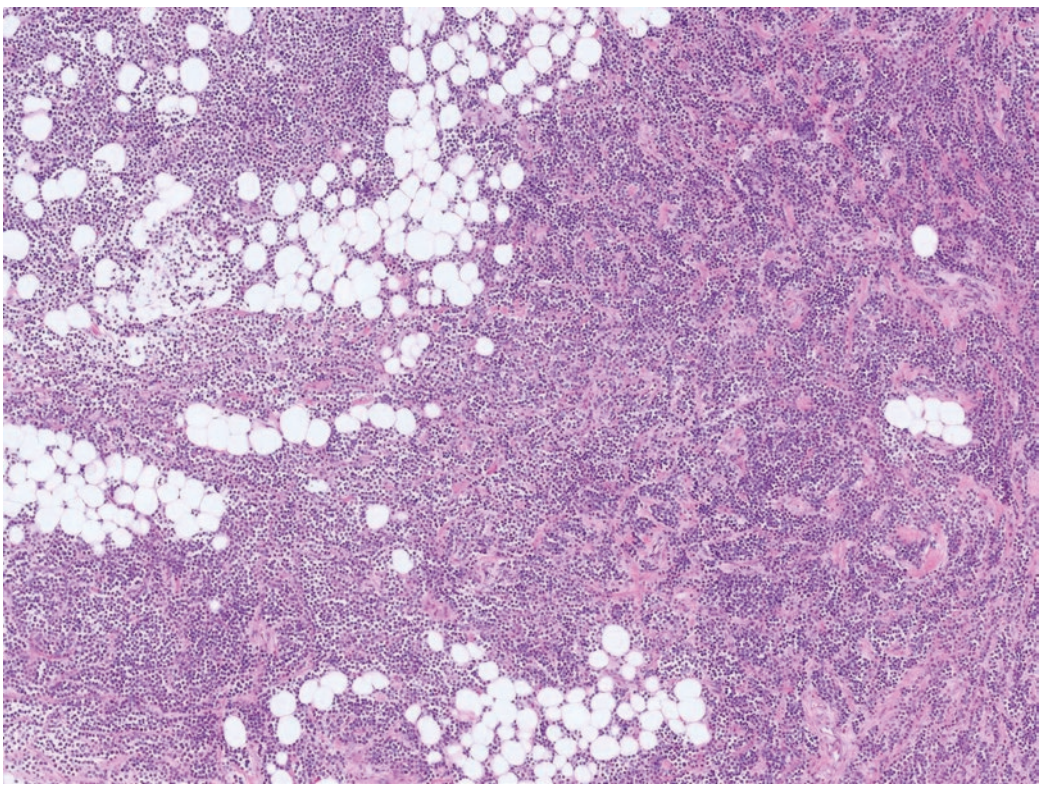

Fig. 10.108 Invasive lobular carcinoma mimicking lymphoma. At low magnification, sheets of cells with dark nuclei permeate the fibroadipose breast tissue, extending between the adipocytes

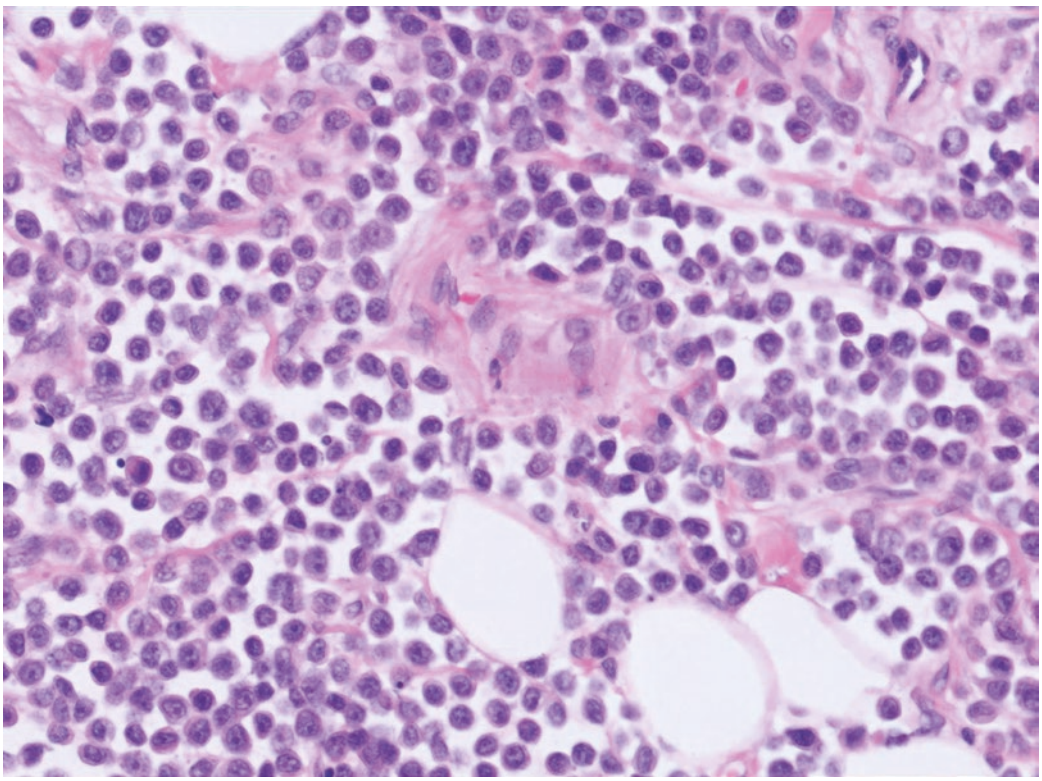

Fig. 10.109 Invasive lobular carcinoma mimicking lymphoma. Discohesive tumour cells show vesicular nuclei with discernible nucleoli and thin cytoplasmic rims that appear amphophilic, resembling malignant lymphoid cells

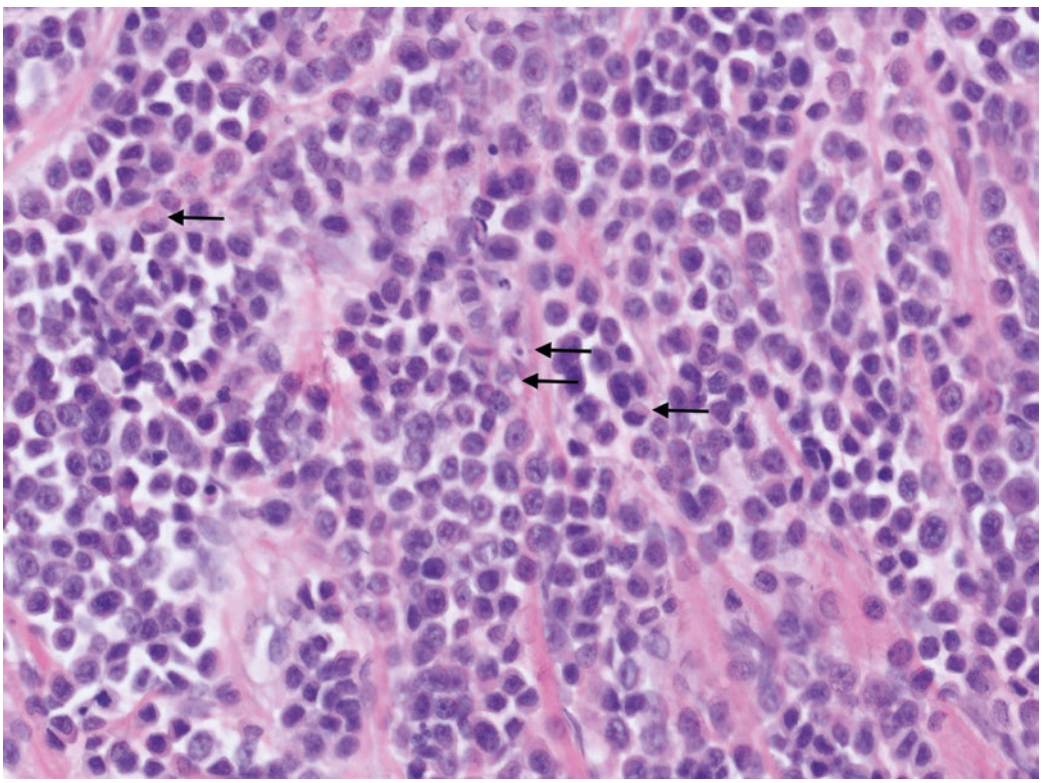

Fig. 10.110 Invasive lobular carcinoma mimicking lymphoma. Some of the discohesive tumour cells show nuclei with a semblance of nuclear folds. Occasional cytoplasmic vacuoles are present (*arrows*)

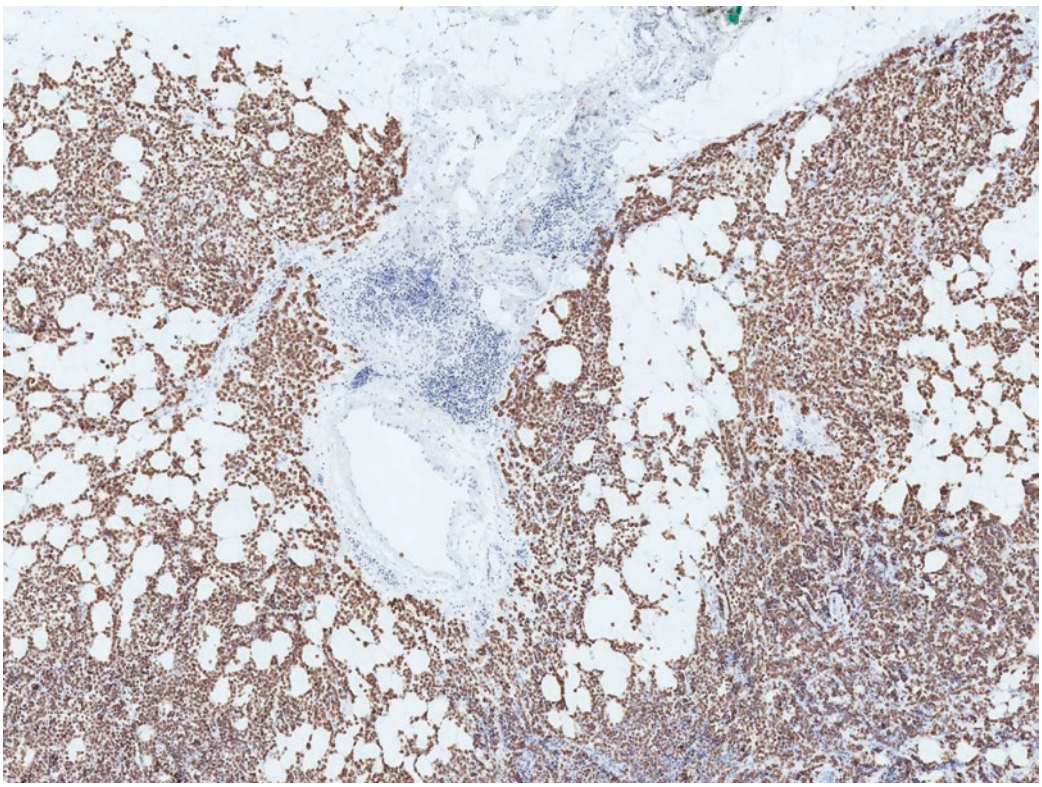

Fig. 10.111 Invasive lobular carcinoma mimicking lymphoma. Immunohistochemistry for MNF116 shows diffuse positive reactivity of the tumour cells

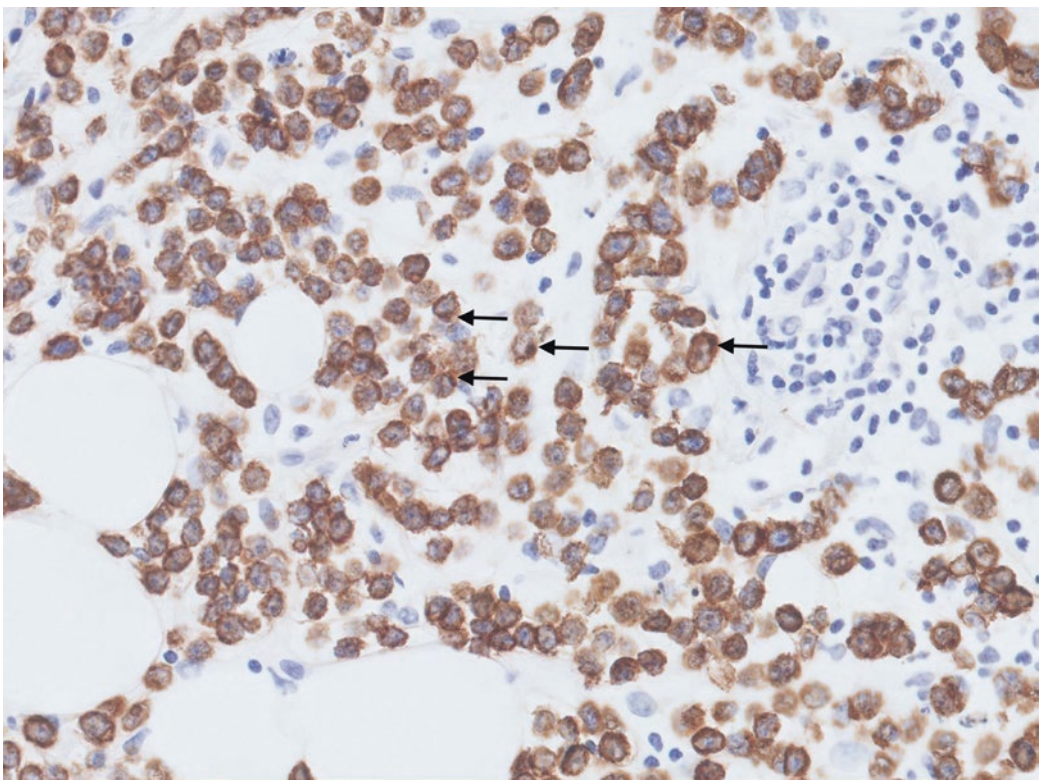

Fig. 10.112 Invasive lobular carcinoma mimicking lymphoma. Immunohistochemistry for MNF116 shows positive cytoplasmic reactivity of the tumour cells, with an accentuated, almost dot-like staining in some cells (*arrows*)

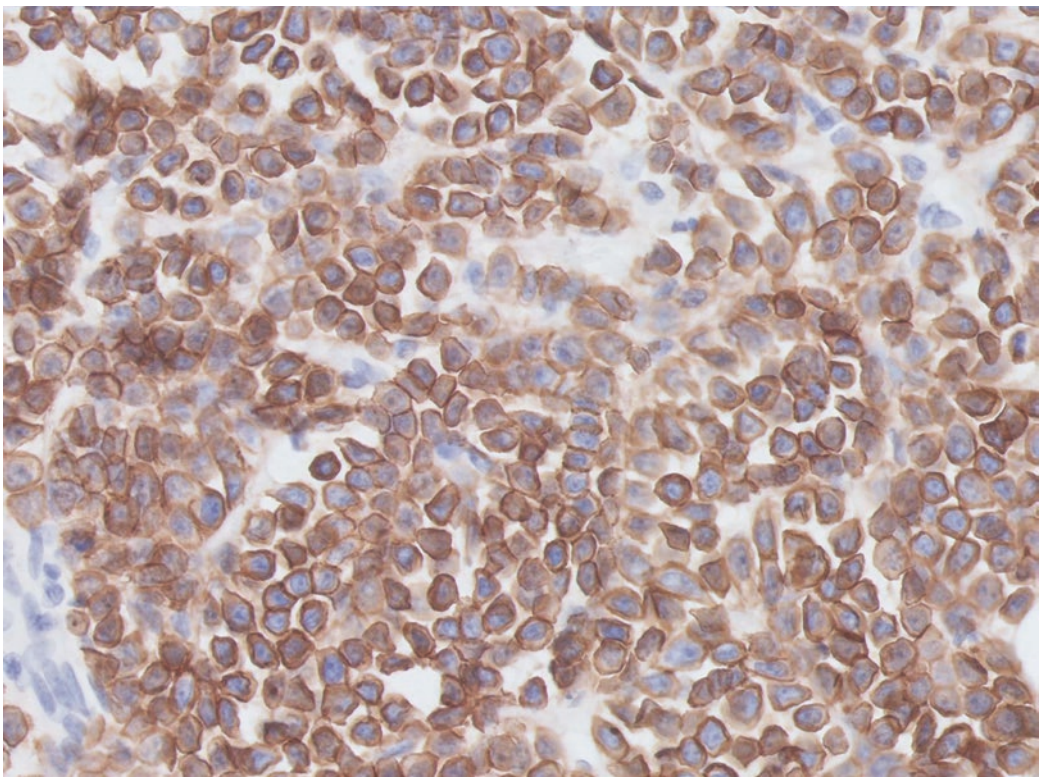

Fig. 10.113 Invasive lobular carcinoma mimicking lymphoma. E-cadherin immunohistochemistry shows apparent cytoplasmic membrane staining, which is unexpected for invasive lobular carcinoma cells, but some tumour cells show diminished reactivity. When E-cadherin does not corroborate the morphologic appearance, p120 catenin, which is part of the same complex, may be more informative

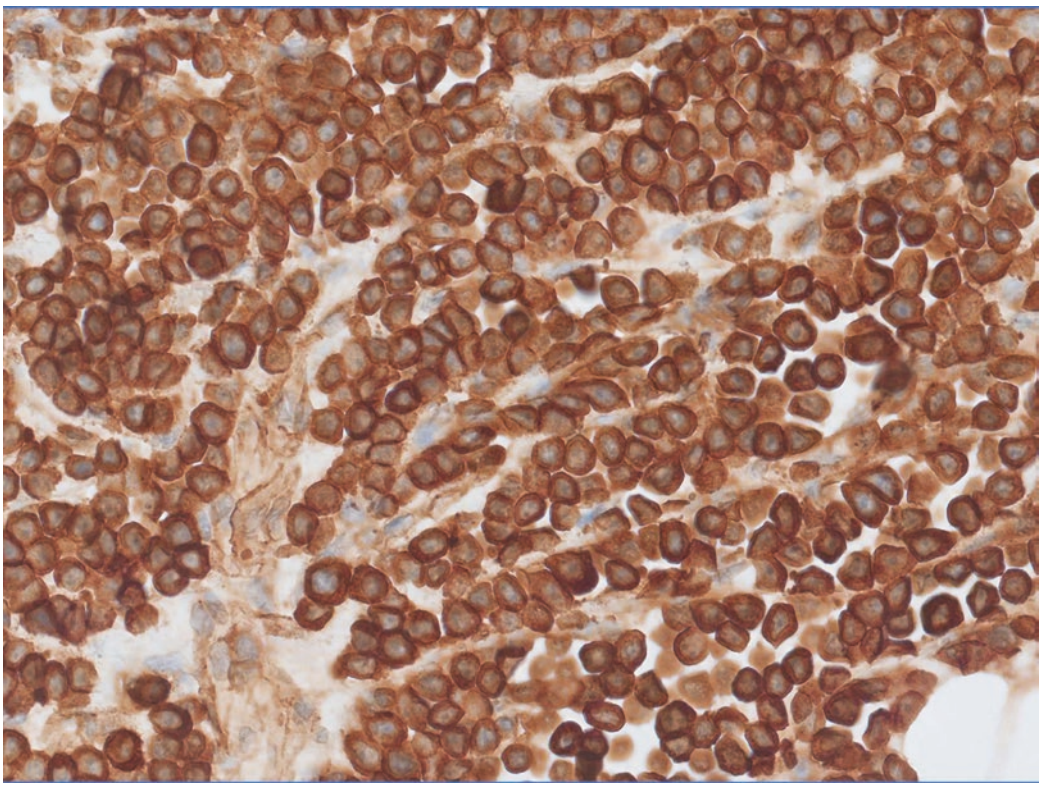

Fig. 10.114 Invasive lobular carcinoma mimicking lymphoma. Immunohistochemistry for p120 catenin shows cytoplasmic localisation of positive staining, rather than delineating the cytoplasmic membranes of tumour cells

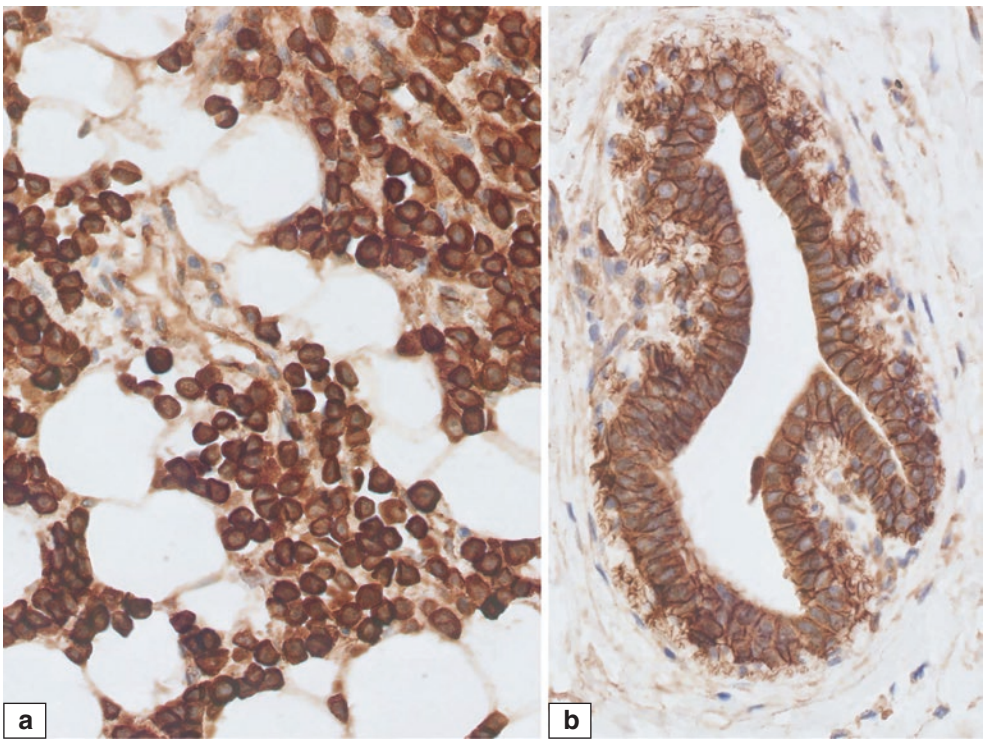

Fig. 10.115 Invasive lobular carcinoma mimicking lymphoma. (**a**) Immunohistochemistry for p120 catenin shows cytoplasmic staining of lobular carcinoma cells. (**b**) By comparison, positive cytoplasmic membrane staining of benign ductal epithelium is observed as a well-defined delineation of the cytoplasmic membranes. In lobular carcinoma cells, there is a smudgy cytoplasmic reactivity without precise decoration of the cytoplasmic membranes

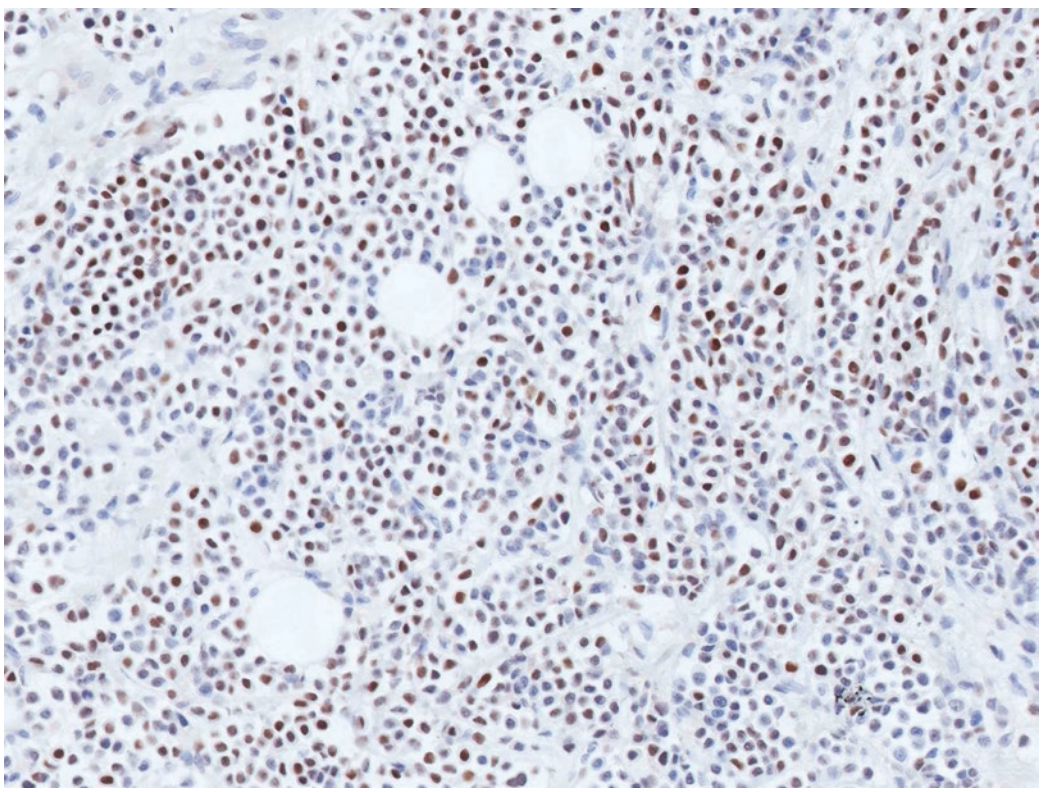

Fig. 10.116 Invasive lobular carcinoma mimicking lymphoma. Immunohistochemistry shows positive nuclear staining for ER. Lymphoid markers were negative

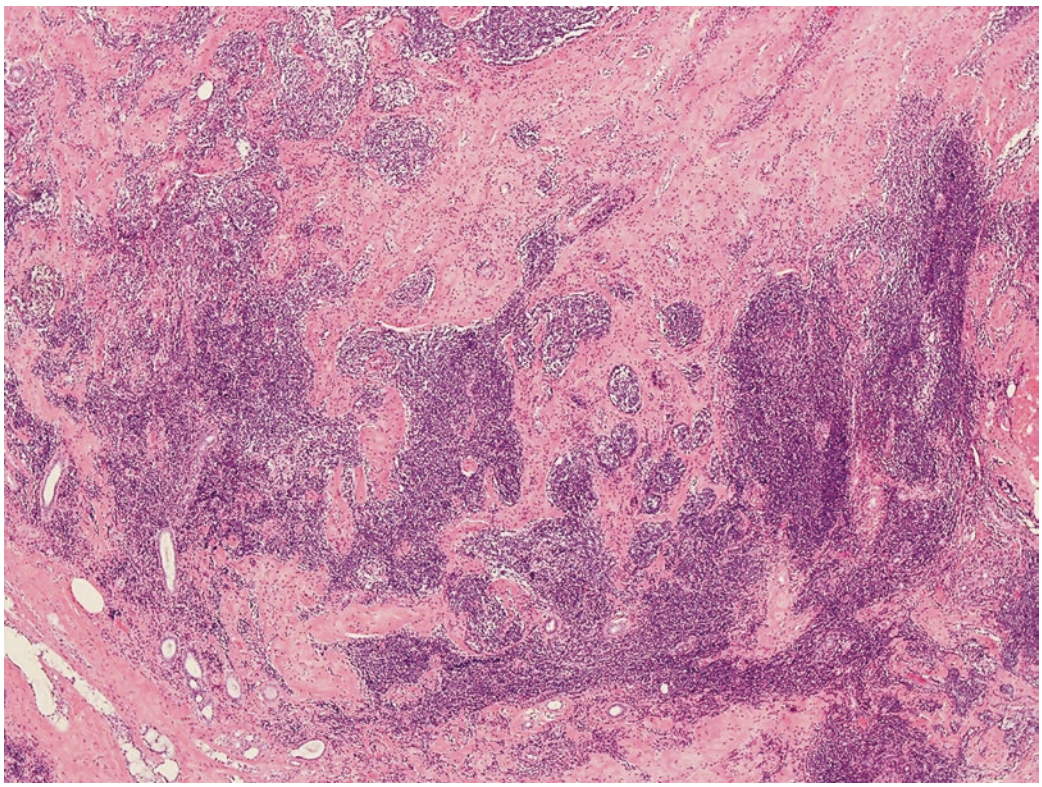

Fig. 10.117 Breast lymphoma (low grade, small lymphocytic). Dense collections of lymphoid cells are seen within the breast parenchyma

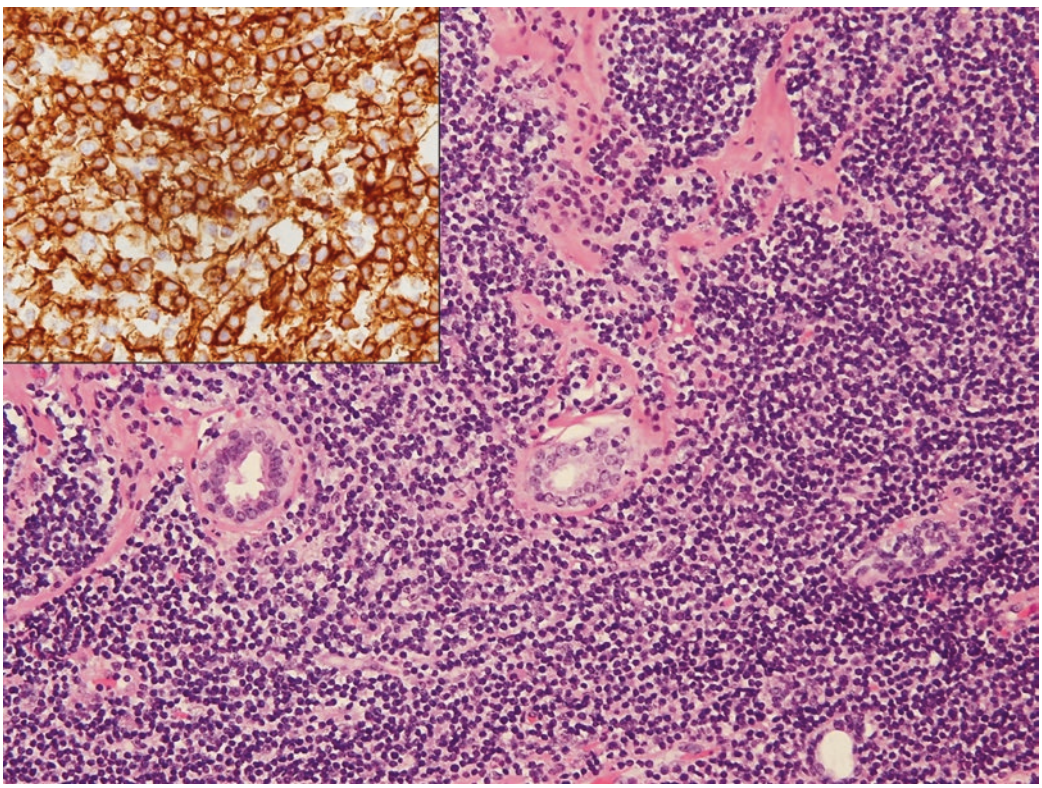

Fig. 10.118 Breast lymphoma (small lymphocytic, low grade, B cell). Sheets of small- to intermediate-sized lymphoid cells extend around benign ducts. *Inset* shows positive staining for CD20, a B-cell marker

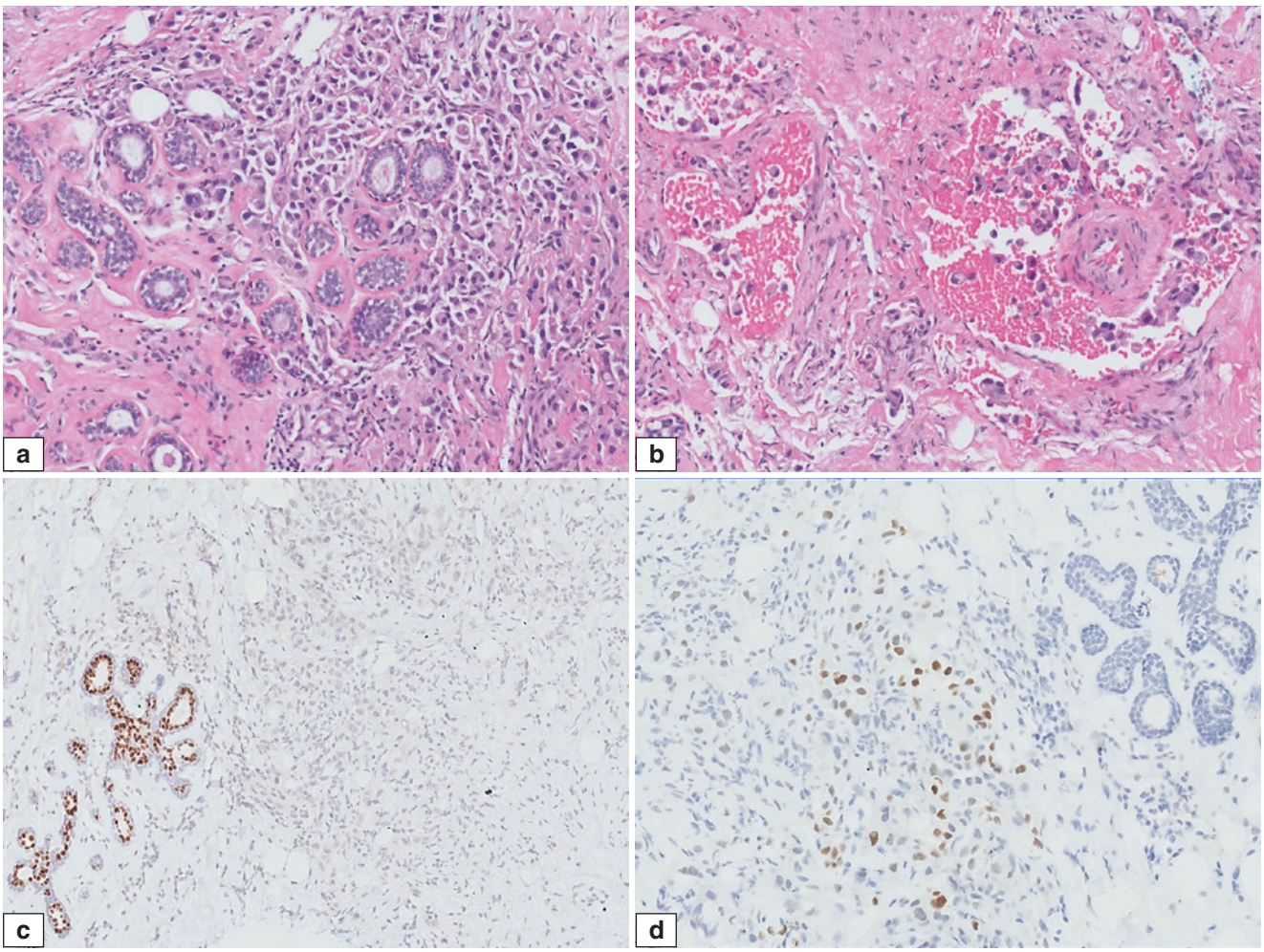

Fig. 10.119 Metastatic gastric signet ring adenocarcinoma to the breast. (**a**) Malignant cells with signet ring appearances infiltrate among benign breast ductules. (**b**) Many lymphovascular tumour emboli are present in the breast tissue. (**c**) Immunohistochemistry for ER is negative in the metastatic carcinoma cells. Note the positive internal control of benign breast ducts and ductules which show nuclear reactivity of luminal epithelial cells for ER. (**d**) CDX2 immunohistochemistry shows patchy nuclear staining of metastatic carcinoma cells. The diagnosis of a metastasis to the breast requires correlation of clinicoradiological information with histological findings, aided by relevant adjunctive immunohistochemical stains

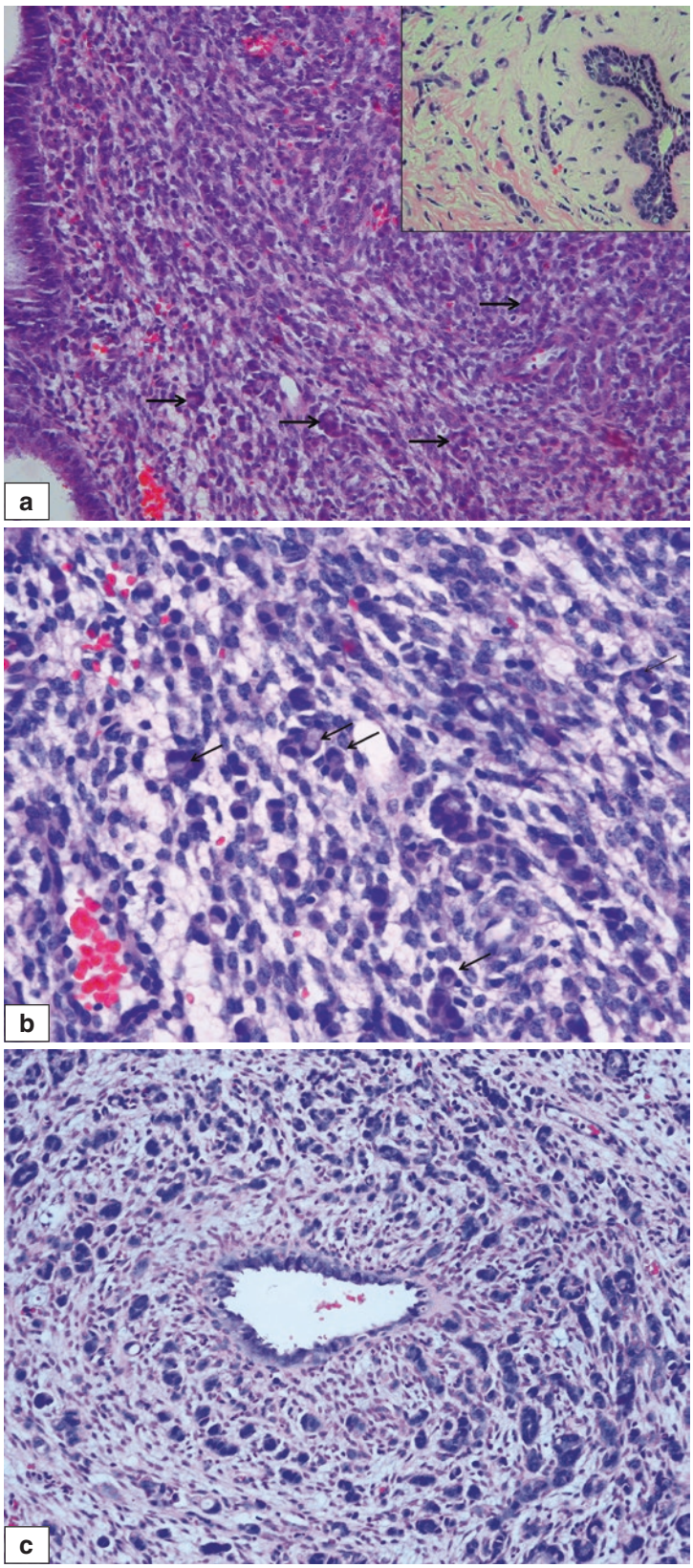

Fig. 10.120 Metastatic lobular carcinoma to the endometrium. (**a**) Invasive lobular carcinoma can metastasise to unusual sites. Here, metastatic lobular carcinoma cells are seen within the endometrial stroma. The malignant cells may be difficult to discern in the midst of the endometrial stromal cells. Close examination identifies the small clusters of cells with occasional cytoplasmic vacuoles (*arrows* indicate some of these clusters). Benign endometrial glandular epithelium is present in the left field. Inset shows invasive lobular carcinoma of the breast diagnosed previously. (**b**) At higher magnification, the malignant lobular cells are seen in small clusters with cytoplasmic vacuoles and occasional eccentric nuclei resembling signet-ring cells (*arrows*). (**c**) In this section of the endometrial currettings, malignant cells are more readily appreciated as groups and cords of tumour cells within the endometrial stroma surrounding an endometrial gland in the centre

References

1. Lakhani SR, Schnitt SJ, O'Malley F, van de Vijver MJ, Simpson P, Palacios J. Lobular neoplasia. In: Lakhani SR, Ellis IO, Schnitt SJ, Tan PH, van de Vijver MJ, editors. WHO classification of tumours of the breast. Lyon: IARC; 2012. p. 78–80.
2. Maxwell AJ, Clements K, Dodwell DJ, Evans AJ, Francis A, Hussain M, et al. The radiological features, diagnosis and management of screen-detected lobular neoplasia of the breast: findings from the Sloane Project. Breast. 2016;27:109–15.
3. Liberman L, Morris EA, Dershaw DD, Abramson AF, Tan LK. Ductal enhancement on MR imaging of the breast. AJR Am J Roentgenol. 2003;181:519–25.
4. Georgian-Smith D, Lawton TJ. Calcifications of lobular carcinoma in situ of the breast: radiologic-pathologic correlation. AJR Am J Roentgenol. 2001;176:1255–9.
5. Abdel-Fatah TM, Powe DG, Hodi Z, Reis-Filho JS, Lee AH, Ellis IO. Morphologic and molecular evolutionary pathways of low nuclear grade invasive breast cancers and their putative precursor lesions: further evidence to support the concept of low nuclear grade breast neoplasia family. Am J Surg Pathol. 2008;32:513–23.
6. Ho BC, Tan PH. Lobular neoplasia of the breast: 68 years on. Pathology. 2009;41:28–35.
7. Canas-Marques R, Schnitt SJ. E-cadherin immunohistochemistry in breast pathology: uses and pitfalls. Histopathology. 2016;68:57–69.
8. Dabbs DJ, Kaplai M, Chivukula M, Kanbour A, Kanbour-Shakir A, Carter GJ. The spectrum of morphomolecular abnormalities of the E-cadherin/catenin complex in pleomorphic lobular carcinoma of the breast. Appl Immunohistochem Mol Morphol. 2007;15(3):260–6.
9. Collins LC, Achacoso N, Nekhlyudov L, Fletcher SW, Haque R, Quesenberry Jr CP, et al. Relationship between clinical and pathologic features of ductal carcinoma in situ and patient age: an analysis of 657 patients. Am J Surg Pathol. 2009;33:1802–8.
10. Butler RS, Venta LA, Wiley EL, Ellis RL, Dempsey PJ, Rubin E. Sonographic evaluation of infiltrating lobular carcinoma. AJR Am J Roentgenol. 1999;172:325–30.
11. Kuroda H, Tamaru J, Takeuchi I, Ohnisi K, Sakamoto G, Adachi A, et al. Expression of E-cadherin, alpha-catenin, and beta-catenin in tubulolobular carcinoma of the breast. Virchows Arch. 2006;448:500–5.
12. Esposito NN, Chivukula M, Dabbs DJ. The ductal phenotypic expression of the E-cadherin/catenin complex in tubulolobular carcinoma of the breast: an immunohistochemical and clinicopathologic study. Mod Pathol. 2007;20:130–8.

Spindle Cell Lesions

11

A spindle cell is a fusiform cell that is tapered at both ends. Although both luminal epithelial and myoepithelial cells may assume spindle shapes, spindle cell lesions of the breast usually refer to conditions that are composed of mesenchymal or mesenchymal-like cells that harbour elongated and stretched cytoplasm. A variety of different lesions may comprise mesenchymal spindle cells, including nodular fasciitis, fibrous scarring, pseudoangiomatous stromal hyperplasia, myofibroblastoma, fibromatosis, stromal overgrowth in phyllodes tumour, and sarcoma. Mesenchymal-like malignant epithelial cells are encountered in fibromatosis-like and spindle cell metaplastic carcinomas.

Nodular Fasciitis

Definition

Nodular fasciitis is a self-limited clonal proliferation of fibroblasts and myofibroblasts.

Clinical and Epidemiological Features

Nodular fasciitis is rare in the breast parenchyma. It may occur in the subcutis and deeper in the chest wall, clinically masquerading as a breast mass. Rapid onset with pain and tenderness is typical, with spontaneous involution over a couple of months.

Imaging Features

Nodular fasciitis is a mimic of breast malignancy on imaging, usually presenting as ill-defined, spiculated nodular masses, although well-circumscribed, benign-appearing masses have also been described. It is commonly seen superficially in the subcutaneous fascia but can also be found deep to the muscle or intramuscularly. It is usually hypoechoic on sonography because of its fibrous content [1, 2].

Pathologic Features

Macroscopic Pathology

Nodular fasciitis has a greyish-white, myxoid appearance.

Microscopic Pathology

Histologically, plump, spindled fibroblasts and myofibroblasts are arranged in a fascicular pattern with oedema, microhaemorrhages with red cell extravasation, and scattered inflammatory cells, giving a "feathery" tissue culture-like appearance (Figs. 11.1 and 11.2). Reactive nuclear changes with vesicularity and rare mitoses may be observed (Fig. 11.3). Immunohistochemically, there is reactivity for smooth muscle actin, but desmin is usually negative (Fig. 11.4). No staining is seen for keratins, CD34, or S100. Proliferative myositis is a microscopically similar lesion, differing from nodular fasciitis by the presence of plump, ganglion-like cells (Figs. 11.5, 11.6, and 11.7).

P.H. Tan, A.A. Sahin, *Atlas of Differential Diagnosis in Breast Pathology*, Atlas of Anatomic Pathology,
DOI 10.1007/978-1-4939-6697-4_11

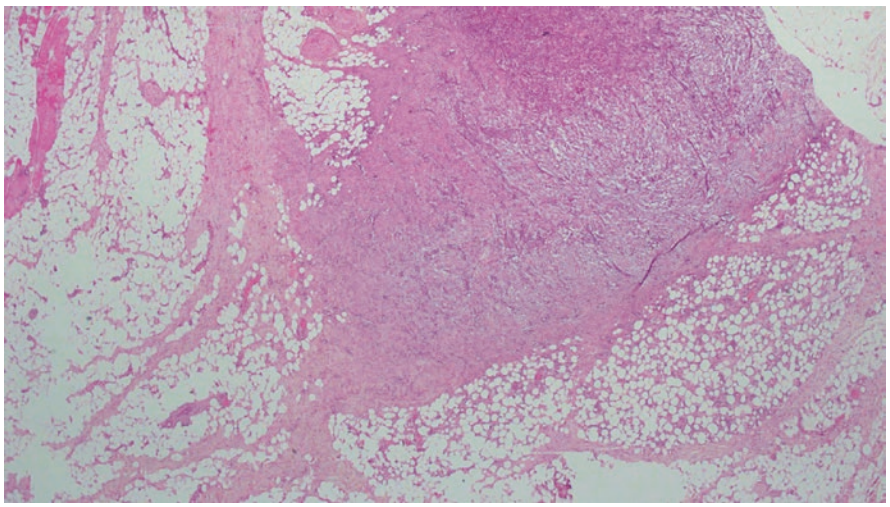

Fig. 11.1 Nodular fasciitis. Low-magnification view shows a spindle cell lesion with ill-defined boundaries. A few skeletal muscle fibres are seen in the vicinity (*left upper field*)

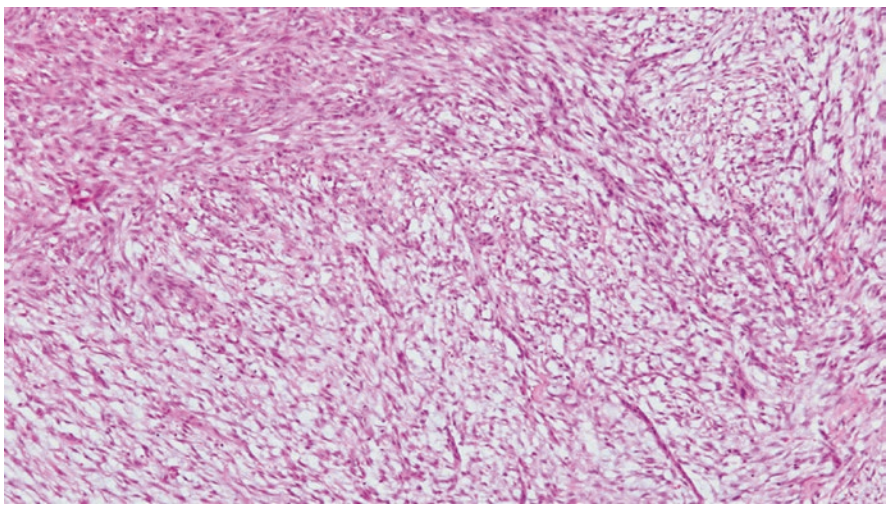

Fig. 11.2 Nodular fasciitis. A feathery tissue culture-like oedematous appearance is seen at medium magnification. Several dark nuclei of scattered lymphocytes are present

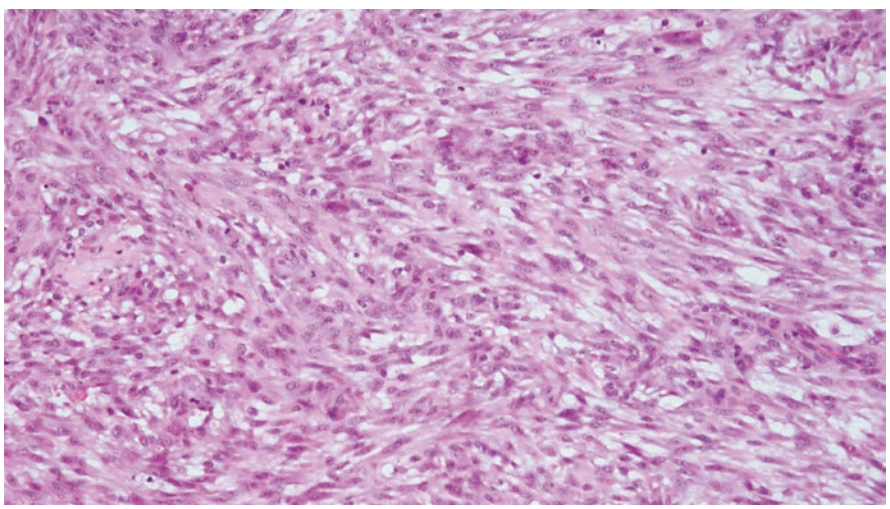

Fig. 11.3 Nodular fasciitis. High magnification shows elongated and ovoid vesicular nuclei with inconspicuous nucleoli. Cytoplasm is tapered, with ill-defined outlines. Rare mitoses may be seen. A light sprinkle of lymphocytes with dense nuclei is found among the spindle cells

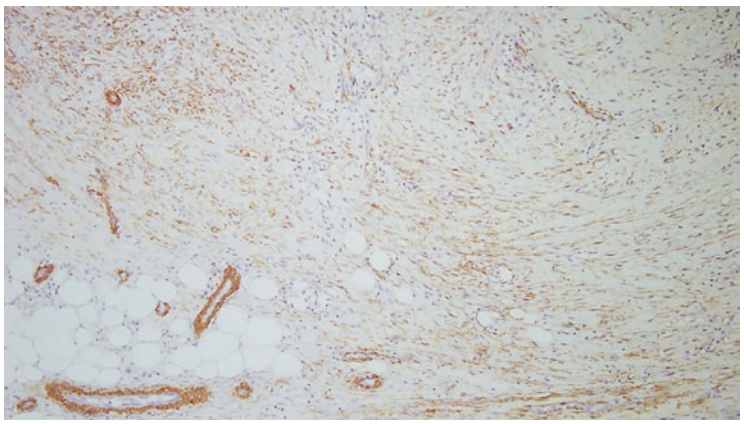

Fig. 11.4 Immunohistochemistry for smooth muscle actin shows positive reactivity of the spindle cells, which comprise both myofibroblasts and fibroblasts

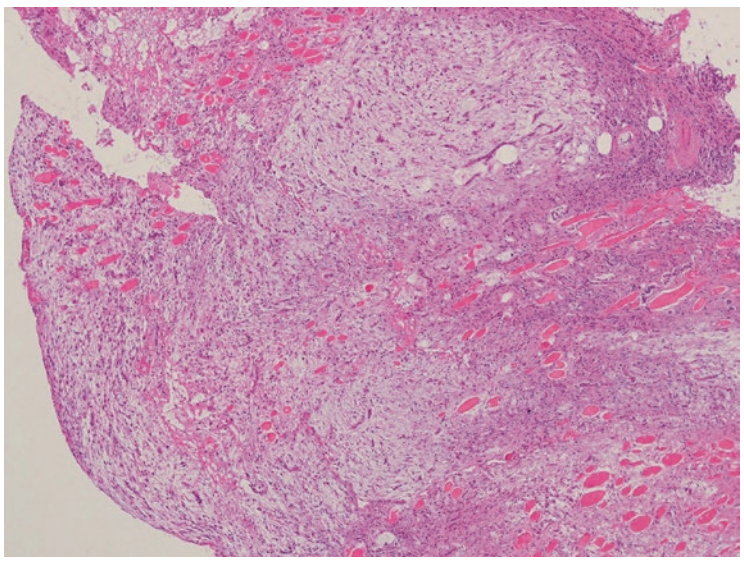

Fig. 11.5 Proliferative myositis. The patient presented clinically with a breast lump. Histologically, the excised specimen showed an oedematous spindle cell proliferation of fibroblasts and myofibroblasts with ill-defined margins, incorporating skeletal muscle fibres and scattered small vessels

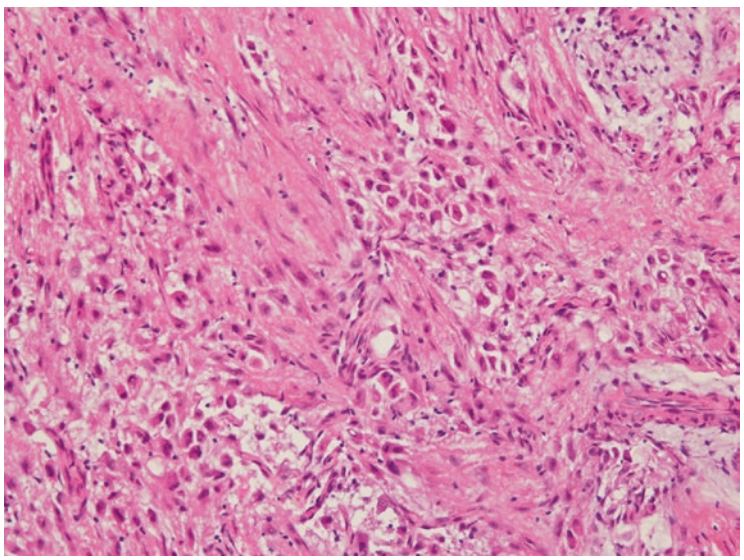

Fig. 11.6 Proliferative myositis. Plump, ganglion-like cells are seen among oedematous fibrous stroma

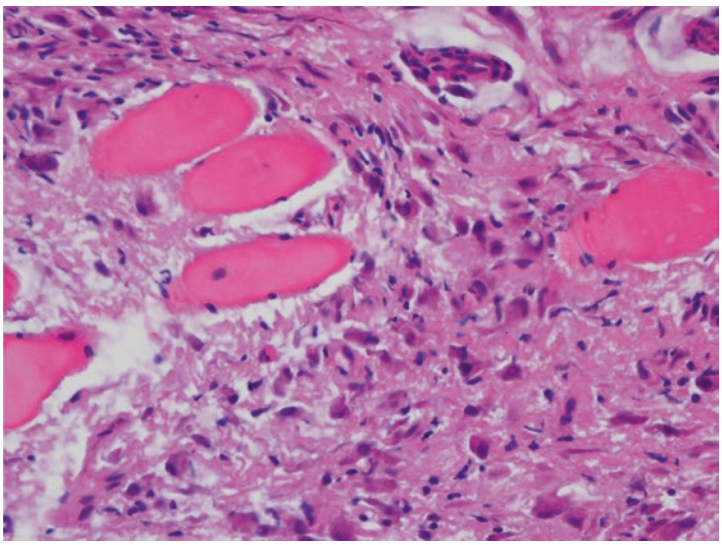

Fig. 11.7 Proliferative myositis. Ganglion-like cells are observed among skeletal muscle fibres

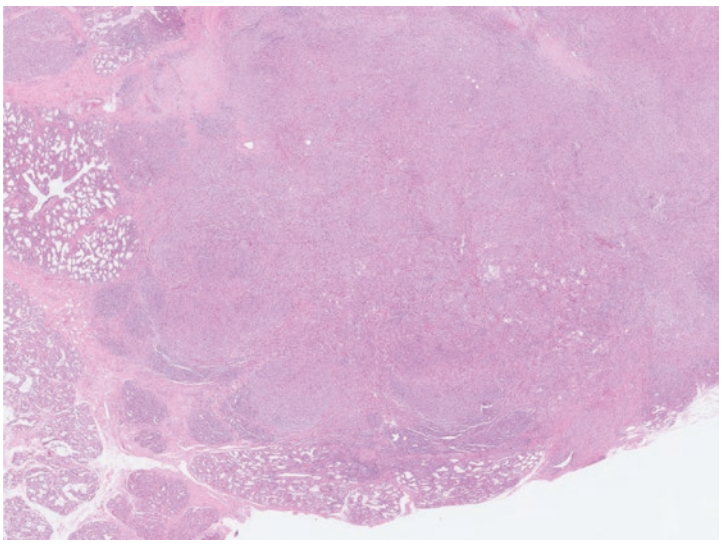

Fig. 11.8 Inflammatory myofibroblastic tumour. A lesion with a lobulated outline is seen at low magnification

Differential Diagnosis

Fibrous Scarring

Fibrous scarring occurs consequent to tissue injury, most commonly after instrumentation. In the immediate postoperative or post-biopsy period, granulation tissue may resemble nodular fasciitis. An exuberant tissue response can lead to a nodular spindle lesion referred to as a spindle cell nodule [3].

Fibromatosis

In fibromatosis, there are long, intersecting fascicles of spindle cells in a collagenous background. The spindle cells show elongated, wavy nuclei. Oedema and inflammation seen in nodular fasciitis are usually absent.

Fibromatosis-Like Metaplastic Carcinoma

Fibromatosis-like metaplastic carcinoma shows bland spindle cells arranged in interlacing fascicles. There is usually no tissue culture-like appearance. Transitioning to plumper epithelioid cells and occasional squamous foci are seen. Immunohistochemical positivity for keratins confirms its epithelial nature, with p63 often being expressed as well.

Inflammatory Myofibroblastic Tumour

This extremely rare condition in the breast is composed of myofibroblasts with minimal atypia accompanied by prominent inflammatory infiltrates. Ganglion-like cells may be observed. Immunohistochemistry shows positive reactivity for smooth muscle actin, and some lesions also demonstrate desmin and keratin staining. Anaplastic lymphoma kinase (*ALK*) rearrangements are seen in 50 % of cases, manifesting as positive immunohistochemical staining for the ALK protein (Figs. 11.8, 11.9, 11.10, and 11.11).

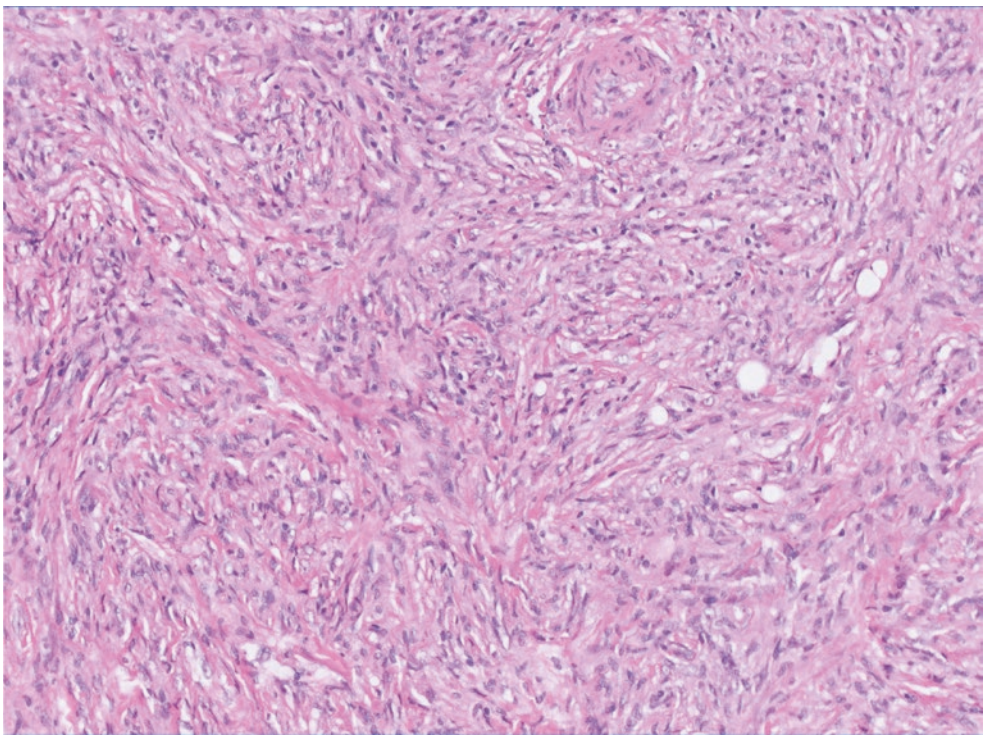

Fig. 11.9 Inflammatory myofibroblastic tumour. Scattered dense nuclei of lymphocytes are interspersed among spindle cells with bland nuclear features

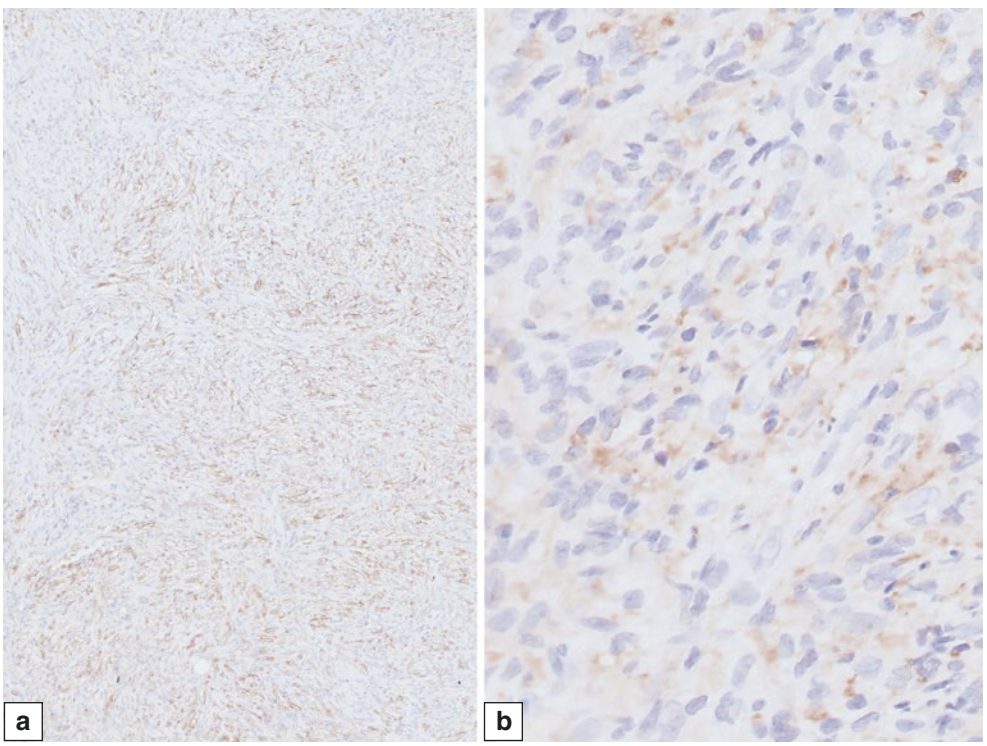

Fig. 11.10 Inflammatory myofibroblastic tumour. (**a**) Immunohistochemistry shows smooth muscle actin (SMA) positivity of the spindle cells, supporting a myofibroblastic origin. (**b**) Anaplastic lymphoma kinase (ALK) shows patchy cytoplasmic reactivity

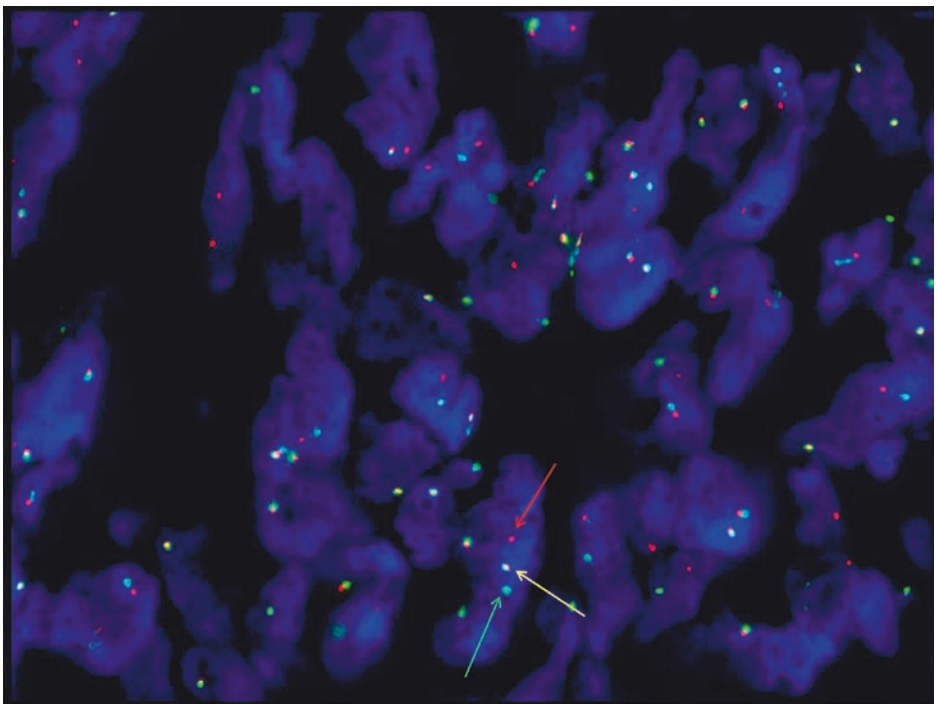

Fig. 11.11 Inflammatory myofibroblastic tumour. Interphase nuclei show rearrangement of the ALK break-apart probe using fluorescence in situ hybridisation. The signal pattern consists of one yellow fusion signal (*yellow arrow*), one red signal (3′ *ALK* gene, *red arrow*), and one green signal (5′ *ALK* gene, *green arrow*), indicating disruption of the *ALK* gene at 2p23 (Courtesy of Cytogenetics Laboratory, SGH Pathology)

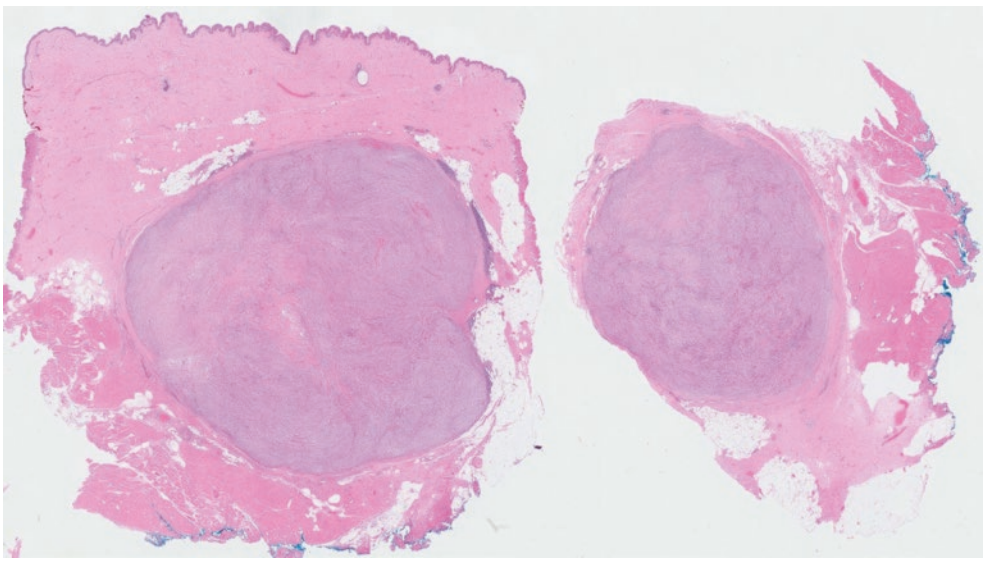

Fig. 11.12 Myofibroblastic sarcoma. Chest wall lesion occurring after mastectomy for recurrent ductal carcinoma in situ with prior wide excision and radiation treatment for invasive ductal carcinoma

Sarcoma

Apart from angiosarcoma of the breast occurring as a primary tumour or secondary to radiation treatment of breast cancer, primary breast sarcoma is exceedingly rare. There have been anecdotal reports of sarcomas of myofibroblastic origin (Figs. 11.12, 11.13, 11.14, 11.15, and 11.16) [4, 5]. The possibility that the sarcoma originates from an underlying malignant phyllodes tumour must be ruled out.

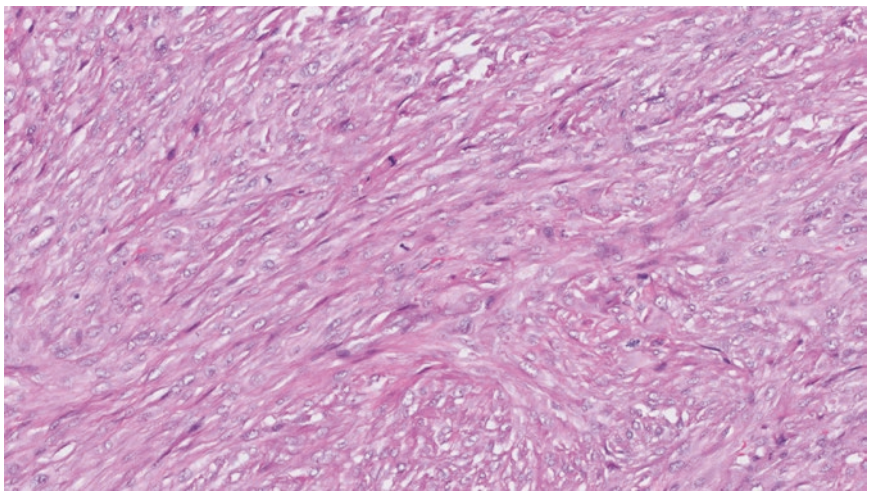

Fig. 11.13 Myofibroblastic sarcoma. Sheets of plump spindle cells with vesicular nuclei and mitotic activity

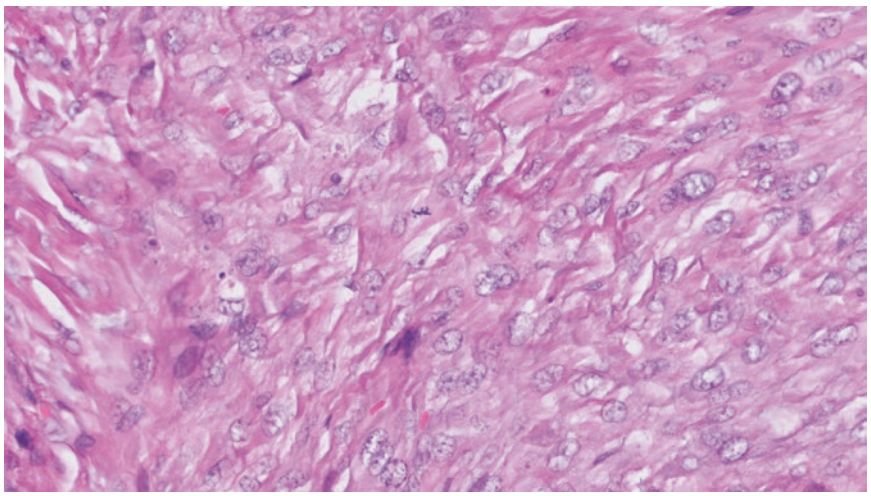

Fig. 11.14 Myofibroblastic sarcoma. High magnification shows spindle cells with enlarged, variably sized vesicular nuclei with occasionally discernible nucleoli and ill-defined cytoplasmic borders

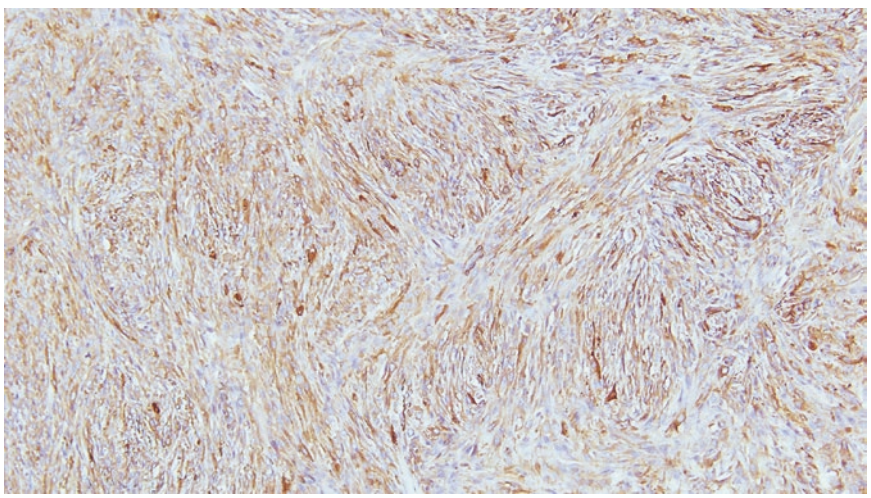

Fig. 11.15 Myofibroblastic sarcoma. SMA immunohistochemistry shows diffuse cytoplasmic reactivity of the spindle cells. Immunohistochemistry showed focal reactivity for low molecular weight keratins, but high molecular weight keratins and p63 were negative

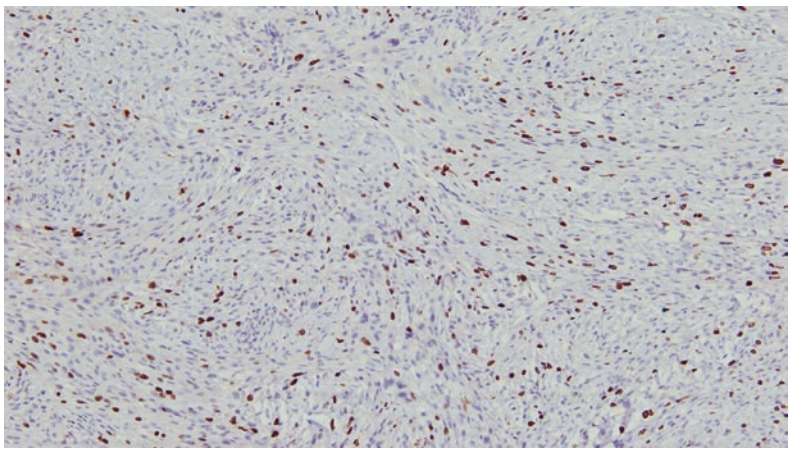

Fig. 11.16 Myofibroblastic sarcoma. MIB1 (Ki67) immunohistochemistry shows positively stained nuclei of spindle cells

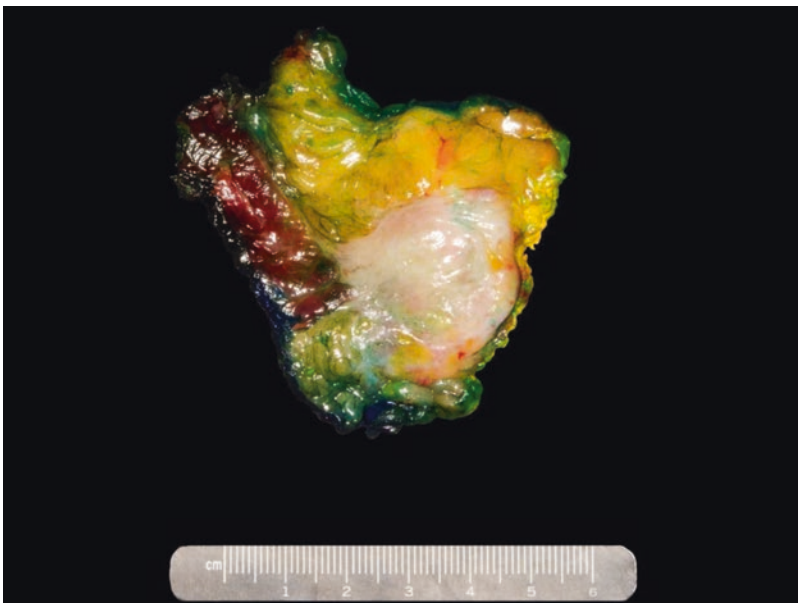

Fig. 11.17 Fibromatosis. Gross specimen shows a whitish whorled lesion with both circumscribed and ill-defined margins within the breast parenchyma and involving the chest wall muscle

Prognosis and Therapy Considerations

Nodular fasciitis is a spontaneously resolving lesion.

Fibromatosis

Definition

Fibromatosis is a locally aggressive but non-metastasising lesion composed of fibroblasts and myofibroblasts.

Clinical and Epidemiological Features

Fibromatosis presents as a breast mass or may arise in the interpectoral region with extension into the breast parenchyma. Skin retraction may be observed. There can be an association with trauma or breast implants.

Imaging Features

Fibromatosis can mimic breast malignancy, presenting as an ill-defined mass with spiculations, typically adjacent to or arising from the pectoralis muscle.

Pathologic Features

Macroscopic Pathology

A fibrous, whorled appearance with ill-defined borders may be observed on cut sections (Fig. 11.17). Size can range from a few millimetres detected radiologically to clinical presentation as a mass.

Microscopic Pathology

Fibromatosis consists of long, intersecting fascicles of spindle cells with flattened wavy nuclei without atypia (Figs. 11.18, 11.19, and 11.20). Mitoses are usually absent; if present, they are few. Extension around benign breast lobules and a few chronic inflammatory infiltrates may be observed at the periphery. Immunohistochemically, there is reactivity for nuclear beta-catenin (Fig. 11.21), but this is not specific, as beta-catenin staining has been found in metaplastic spindle cell carcinoma, phyllodes tumours, and fibrosarcoma. SMA and desmin may be expressed. No staining is seen for keratins, CD34, or S100 (Fig. 11.22). The diagnosis of fibromatosis is particularly challenging on core biopsy (Figs. 11.23, 11.24, 11.25, 11.26, 11.27, and 11.28).

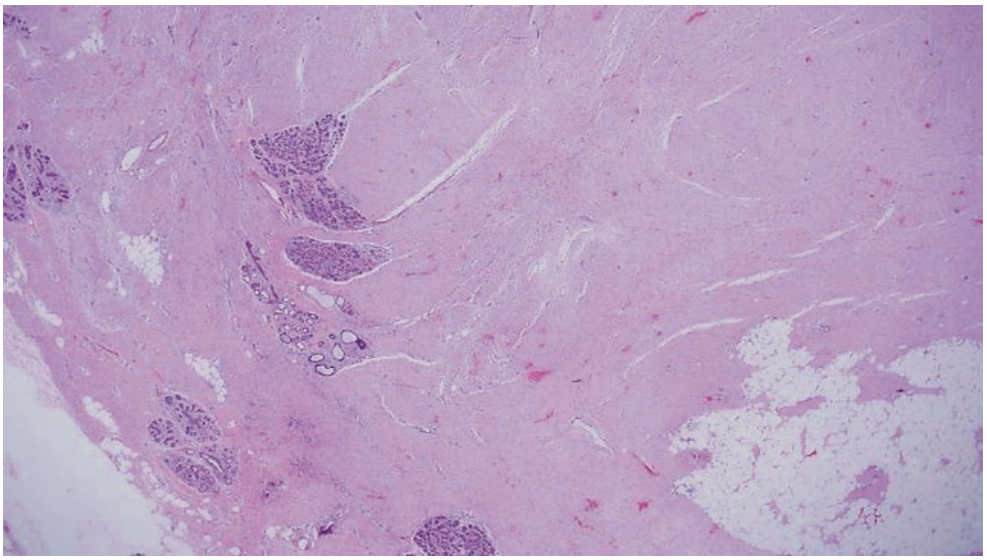

Fig. 11.18 Fibromatosis of breast. Low magnification shows long, intersecting, sweeping fascicles of collagenised tissue, extending around residual breast lobules

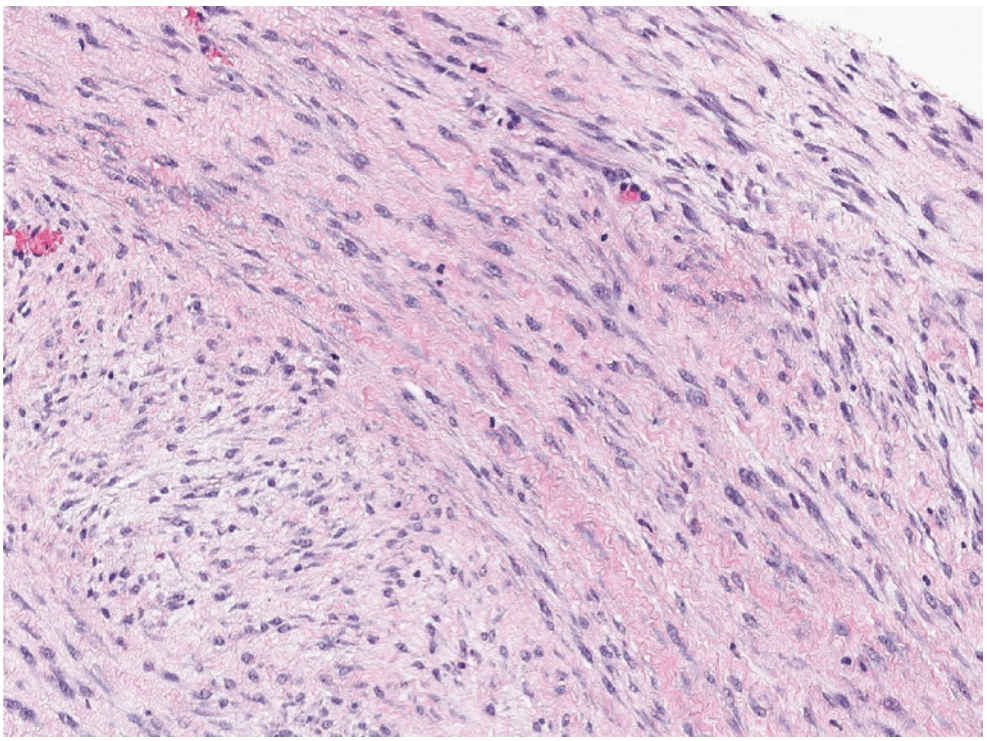

Fig. 11.19 Fibromatosis. Intersecting bands of spindle cells within a collagenous stroma show minimal nuclear atypia, with elongated, stretched cells containing compressed nuclei

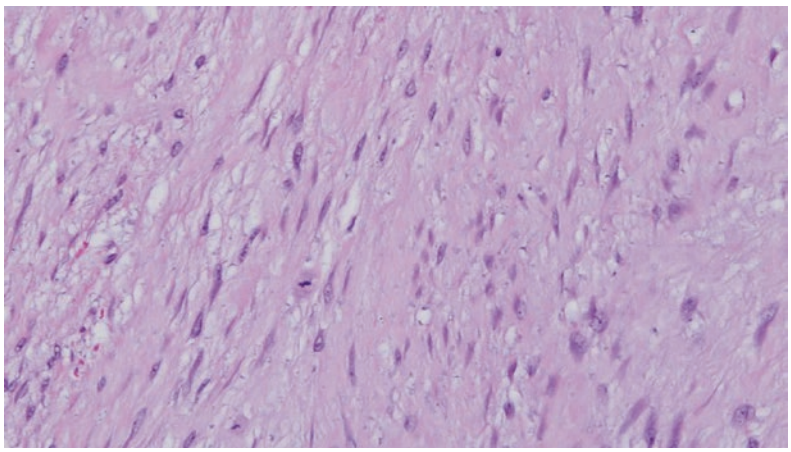

Fig. 11.20 Fibromatosis. High magnification shows the spindle cell nuclei to have slender shapes with narrow, tapered ends, with some nuclei displaying slight waviness. The nuclei are separate from each other, without significant overlapping. An occasional mitosis may be observed

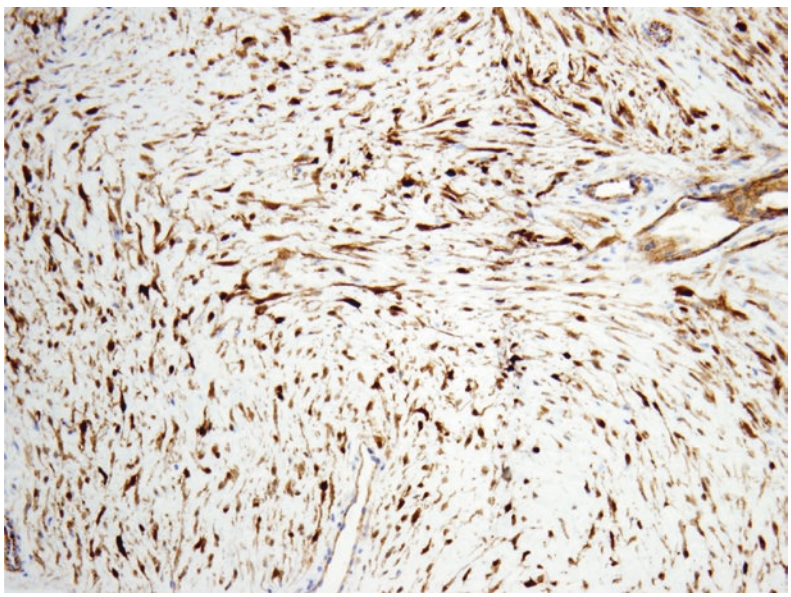

Fig. 11.21 Immunohistochemistry for beta-catenin shows nuclear staining of the spindle cells in fibromatosis. This staining is often used as supportive evidence for the diagnosis, but beta-catenin expression has been reported in other tumours such as metaplastic carcinoma and phyllodes tumours

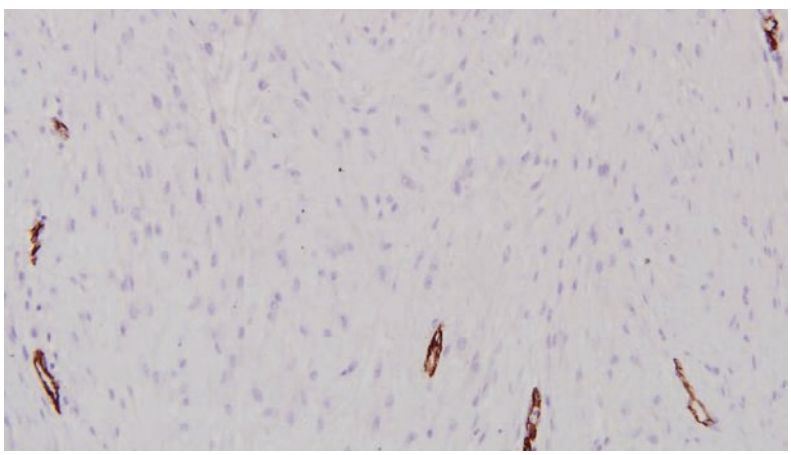

Fig. 11.22 Immunohistochemistry for CD34 is negative in fibromatosis, with only several small, interspersed, thin-walled vessels being highlighted

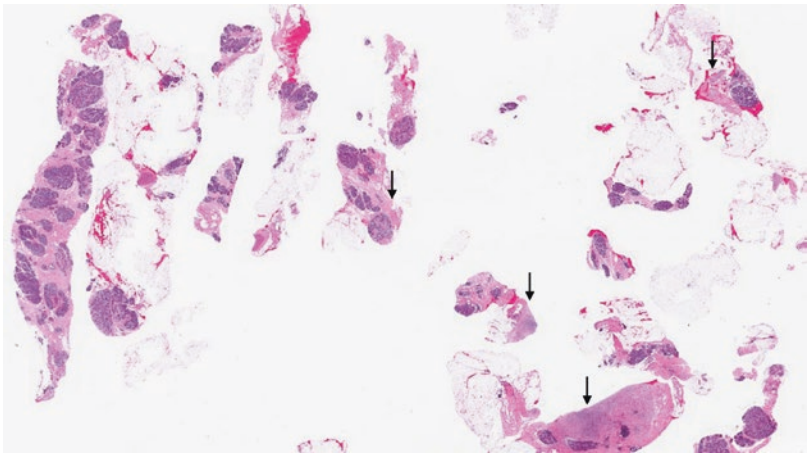

Fig. 11.23 On core biopsy, the diagnosis of fibromatosis is challenging. Radiologically, fibromatosis often forms a stellate mass with spiculations mimicking cancer. Careful assessment of the cores is needed in order to identify the spindle cell proliferation (*arrows*). An immunohistochemical workup may narrow the differential diagnostic spectrum and suggest the diagnosis, but complete excision is usually required for confirmation

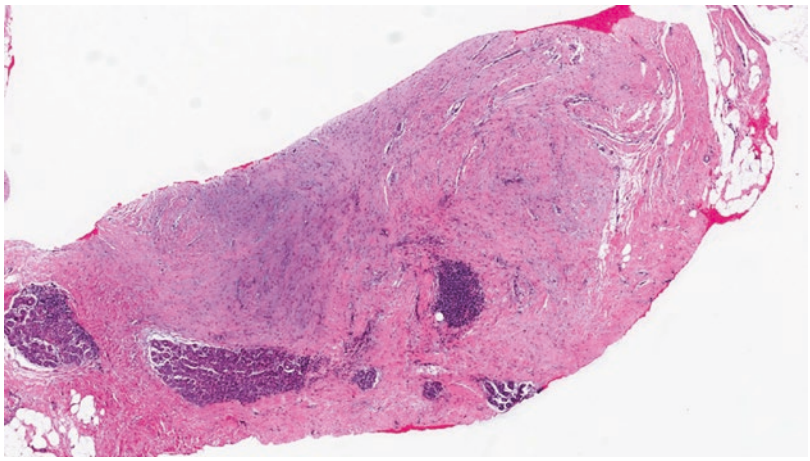

Fig. 11.24 Fibromatosis on core biopsy. The spindle cell process has low cellularity, with a few chronic inflammatory cell infiltrates

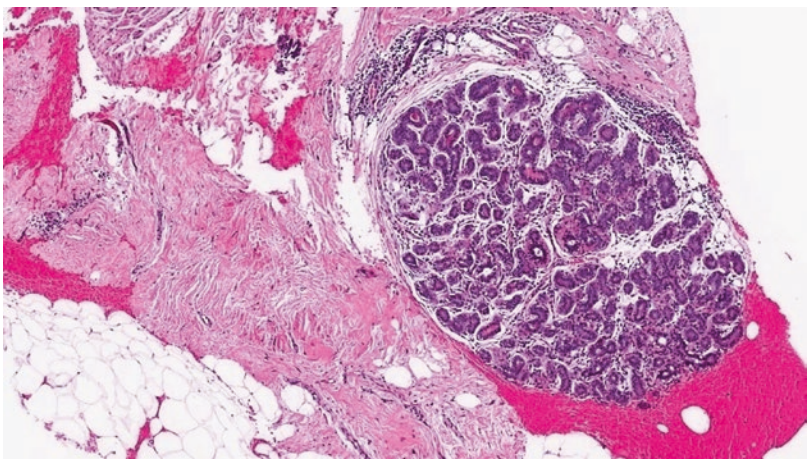

Fig. 11.25 Fibromatosis on core biopsy. A dense, fibrocollagenous process is seen partially encircling a breast lobule

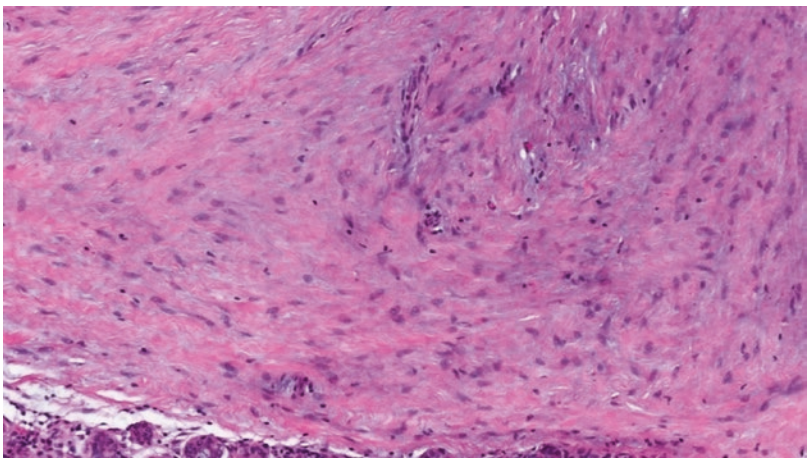

Fig. 11.26 Fibromatosis on core biopsy. High magnification shows slender, elongated, and slightly wavy nuclei with tapered ends. Cytoplasmic outlines are indistinct

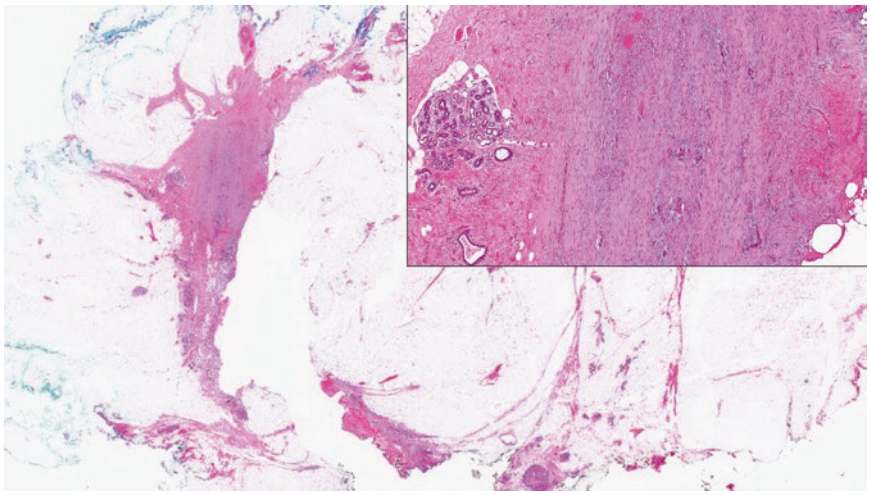

Fig. 11.27 Excision biopsy shows the stellate outlines of the lesion at low magnification. With the history of a prior core biopsy, a differential that needs to be excluded is fibrous scarring, but this excision was performed within a week after the core biopsy, and histologically the reparative process would comprise relatively fresh granulation rather than a fibrous-like lesion. *Inset* shows a higher magnification of the spindle cell lesion, which resembles the observations on the core biopsies. Correlation with the core biopsy findings is important in finalising the diagnosis

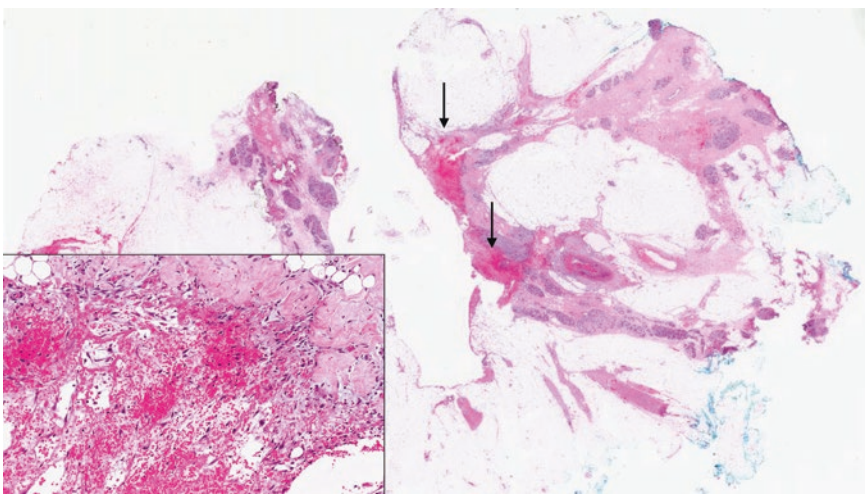

Fig. 11.28 Excision specimen of fibromatosis, with the previous biopsy site identified as an area of haemorrhage and granulation (*arrows*). *Inset* shows fibrin and blood, with granulation representing tissue reaction to the previous biopsy

Differential Diagnosis

Fibrous Scarring

Reparative granulation in the immediate postoperative or post-biopsy period may resemble nodular fasciitis, but more remote instrumentation can lead to fibrous organisation that can mimic fibromatosis (Figs. 11.29 and 11.30). A clinical history and histological evidence of prior instrumentation (such as foreign-body-type giant cells and haemosiderin deposits) are useful in reaching the correct diagnosis.

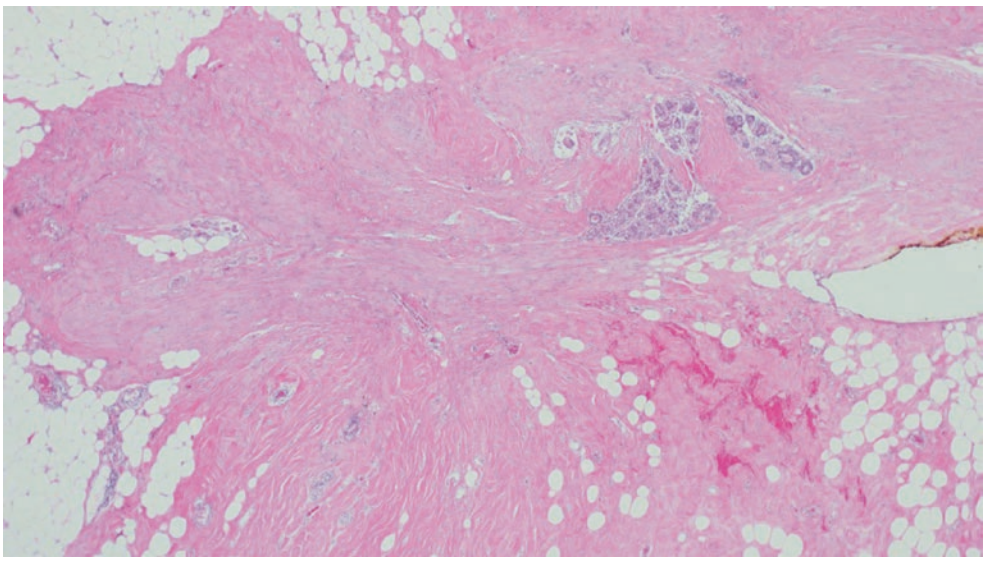

Fig. 11.29 Fibrous scar resembling fibromatosis. At low magnification, there is a somewhat stellate fibrous lesion with focal haemorrhage. Previous stereotactic core biopsy was performed close to 7 weeks prior to this excision

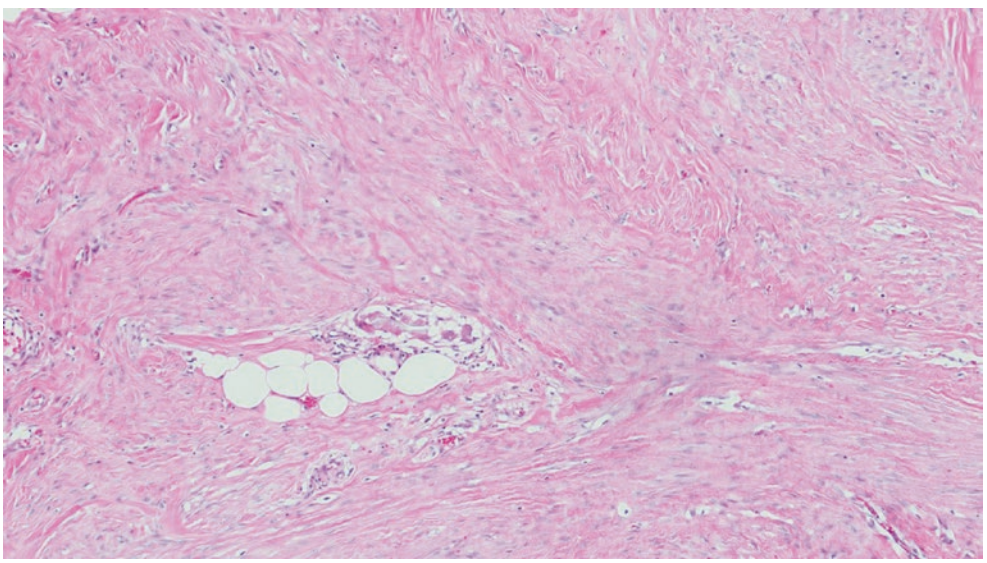

Fig. 11.30 Fibrous scar resembling fibromatosis. A few foreign-body-type, multinucleated giant cells are seen amid the fibrosis. A history of previous biopsy is useful in reaching the correct diagnosis. Correlation with the radiological appearance is also important, as fibromatosis presents as a stellate lesion or as an architectural distortion on imaging, whereas a fibrous scar is consequent to instrumentation, which may have been performed for other reasons such as calcifications or a mass. The organised fibrosis reflects tissue injury that was more remote, which can be temporally compared with when the biopsy was performed

Myoid Hamartoma

Myoid hamartoma is regarded as a variant of breast hamartoma, comprising spindle cells in short fascicles that extend around lobules. The spindle cells are histologically bland and show smooth muscle differentiation, which may be verified with desmin and smooth muscle markers on immunohistochemistry (Figs. 11.31, 11.32, and 11.33) [6].

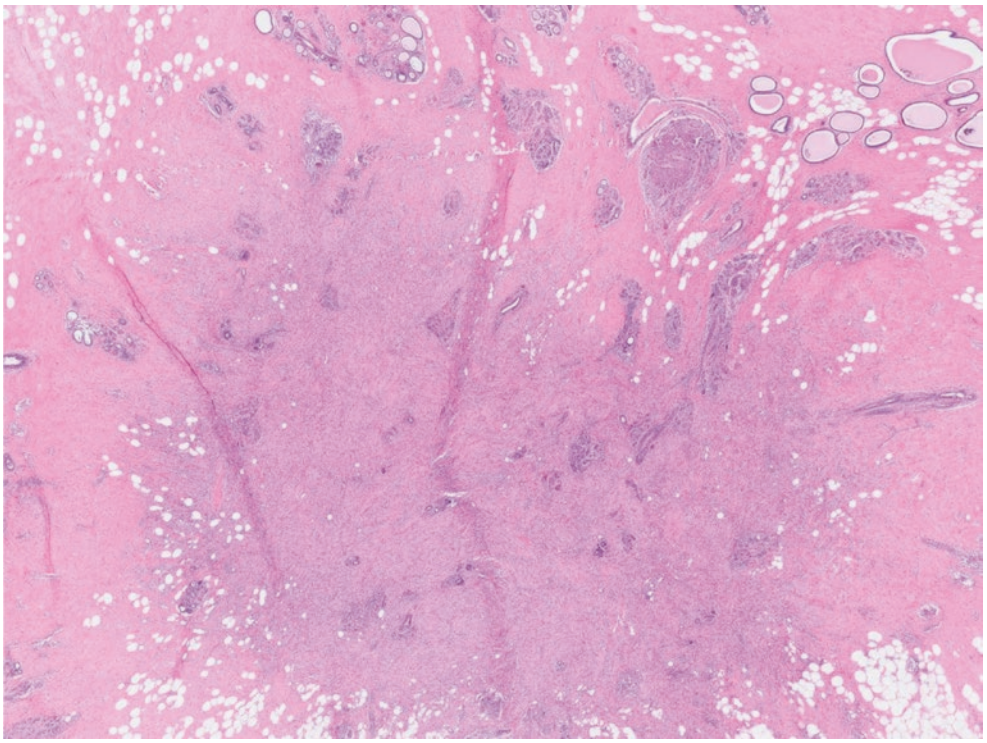

Fig. 11.31 Myoid hamartoma. Low magnification shows a spindle cell lesion incorporating breast lobules, especially towards its periphery

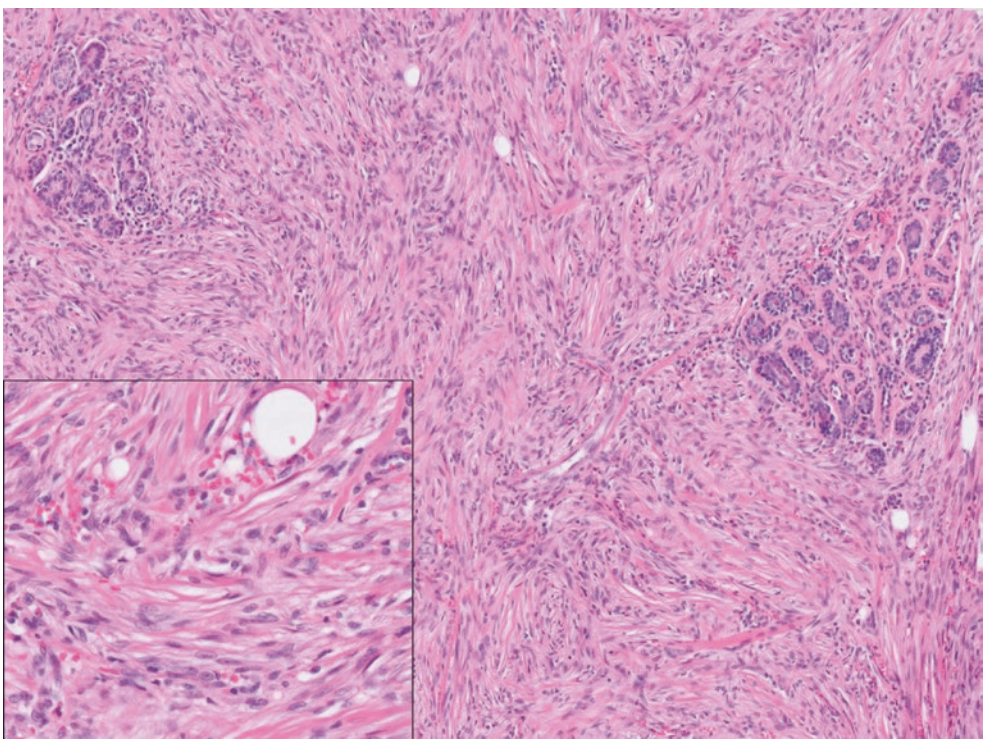

Fig. 11.32 Myoid hamartoma. Spindle cells in short fascicles and vague storiforming, extending around breast lobules. *Inset* shows high magnification of the spindle cells with ovoid-to-elongated, banal nuclei. No mitoses are found

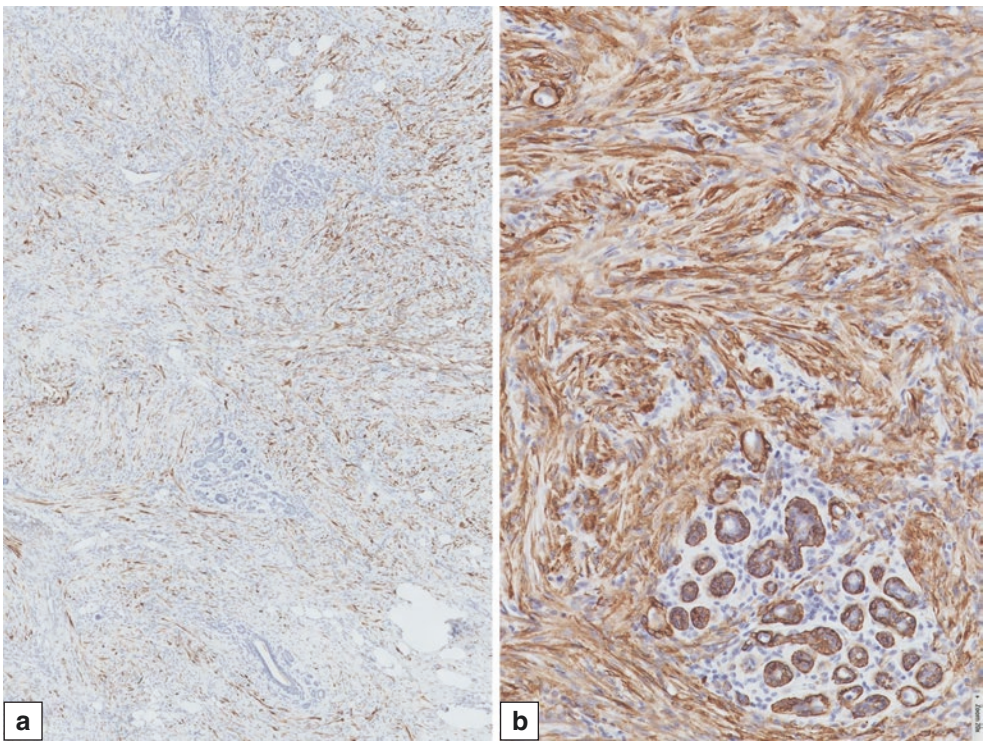

Fig. 11.33 Myoid hamartoma. Immunohistochemistry shows positive reactivity of the spindle cells for desmin (**a**) and SMA (**b**), corroborating a smooth muscle origin. Epithelial markers including high molecular weight keratins are negative

Fibromatosis-Like Metaplastic Carcinoma

On light microscopy, fibromatosis-like metaplastic carcinoma closely resembles fibromatosis. The presence of histological transitioning to more epithelioid and squamous foci and the coexistence with ductal carcinoma in situ are clues to metaplastic carcinoma, which also can be corroborated with positive keratin immunostaining.

Fibrosarcoma

Fibrosarcoma is a more cellular tumour than fibromatosis, with a greater degree of cytological atypia and mitotic activity. Fibrosarcoma is very rare in the breast; when observed, it may be part of a dermatofibrosarcoma with secondary involvement of the breast, or it may be associated with a borderline or malignant phyllodes tumour.

Lipomatous Myofibroblastoma

The intermingling of adipocytes with spindle cells in lipomatous myofibroblastoma can mimic fibromatosis extending among adipose tissue [7]. The general circumscription of myofibroblastoma and its CD34 positivity differentiate it from fibromatosis (Figs. 11.34, 11.35, 11.36, 11.37, 11.38, 11.39, 11.40, 11.41, 11.42, 11.43, and 11.44). Monosomy of chromosome 13q14 and 16q helps corroborate the diagnosis of myofibroblastoma.

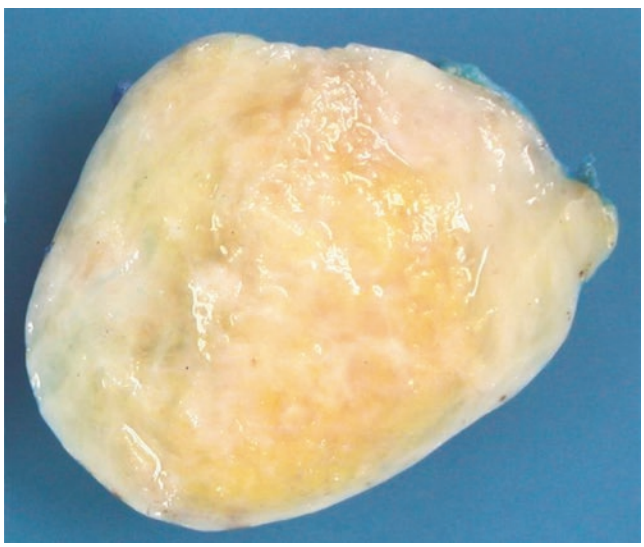

Fig. 11.34 Myofibroblastoma. Gross appearance shows a well-circumscribed border with a cut surface that is yellowish white. Some of the yellowish areas correspond to adipose; the more streaky, whitish zones comprise lesional myofibroblasts and fibroblasts within a collagenous background

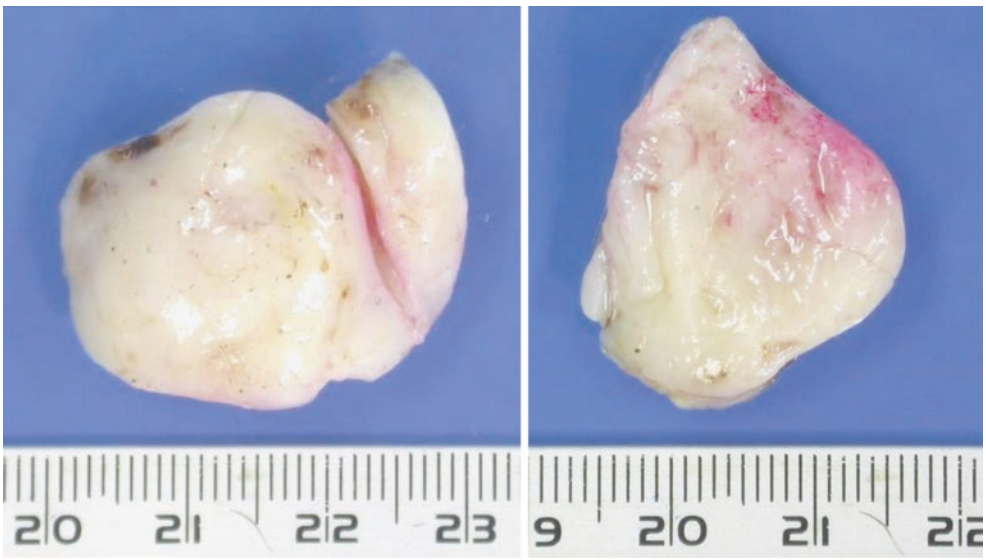

Fig. 11.35 Myofibroblastoma. A lobulated appearance resembling a fibroadenoma can be seen. Cut section shows a whitish appearance with slightly rubbery consistency and a few linear indentations

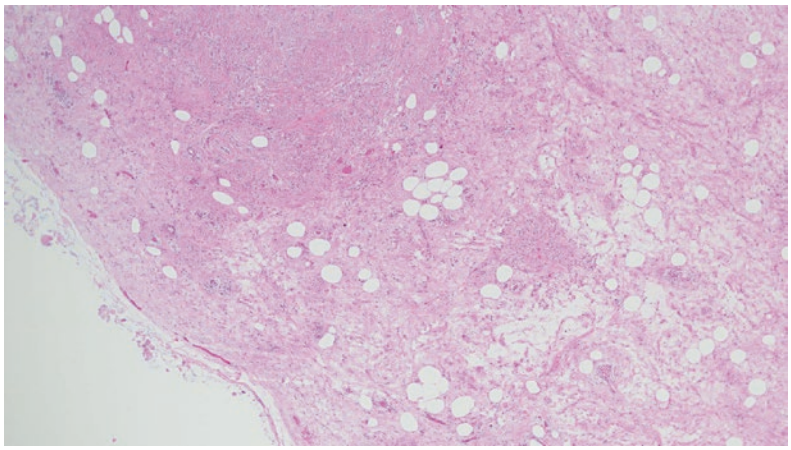

Fig. 11.36 Myofibroblastoma. Low-magnification view shows a well-circumscribed border. Scattered adipocytes are seen among pink, collagenous stroma that contains bland spindle cells. Variable cellularity and oedema are seen

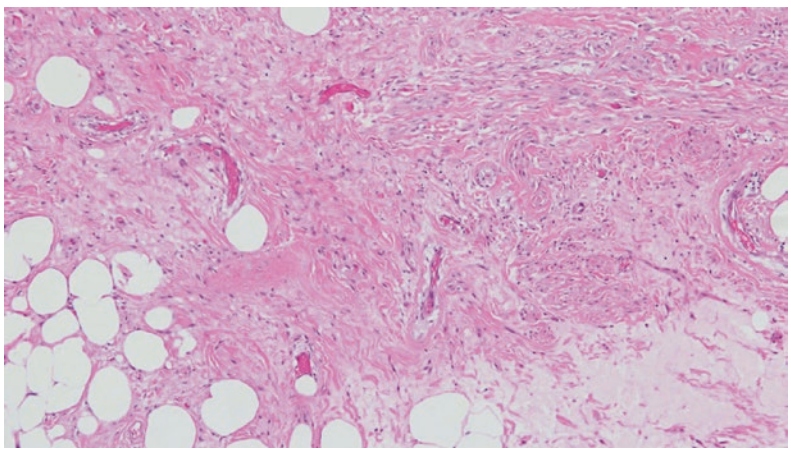

Fig. 11.37 Myofibroblastoma. Spindle cells with ovoid-to-elongated nuclei are seen with pink collagen. Several adipocytes are noted

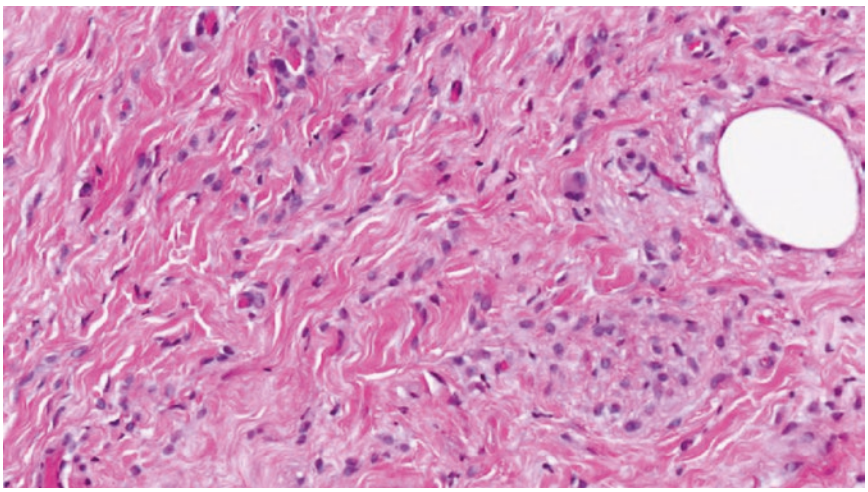

Fig. 11.38 Myofibroblastoma. Ropy, pink collagen fibres are seen among the spindle cells with ovoid nuclei. Some of the spindle cells appear relatively plump and are aligned in a vaguely linear fashion, which can mimic an invasive lobular carcinoma of classic type, especially when nuclear reactivity for oestrogen receptor is seen (which can be encountered in myofibroblastoma). Immunohistochemistry confirms the absence of epithelial differentiation

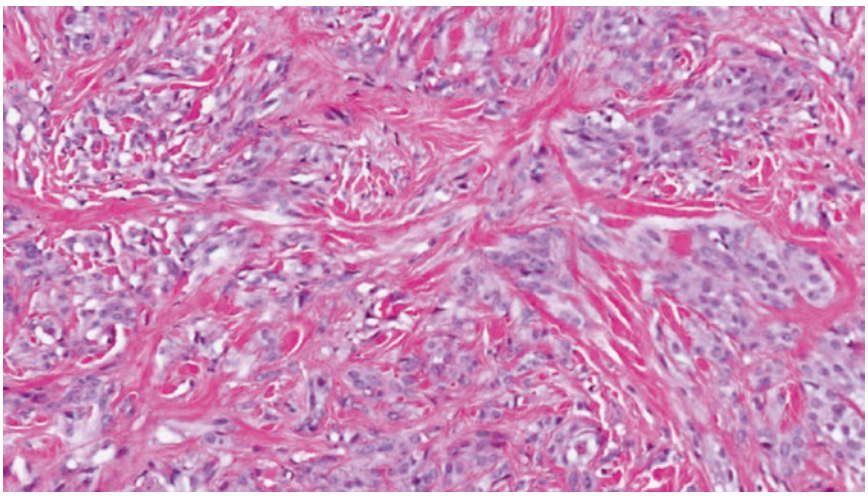

Fig. 11.39 Myofibroblastoma. Some of the epithelioid spindle cells can be aggregated into bundles resembling an epithelial process

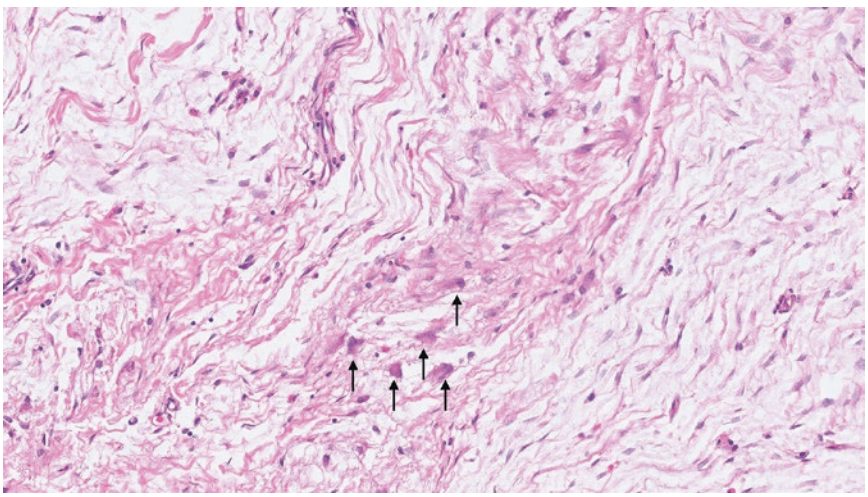

Fig. 11.40 Myofibroblastoma. Occasional individually dispersed epithelioid cells are present (*arrows*)

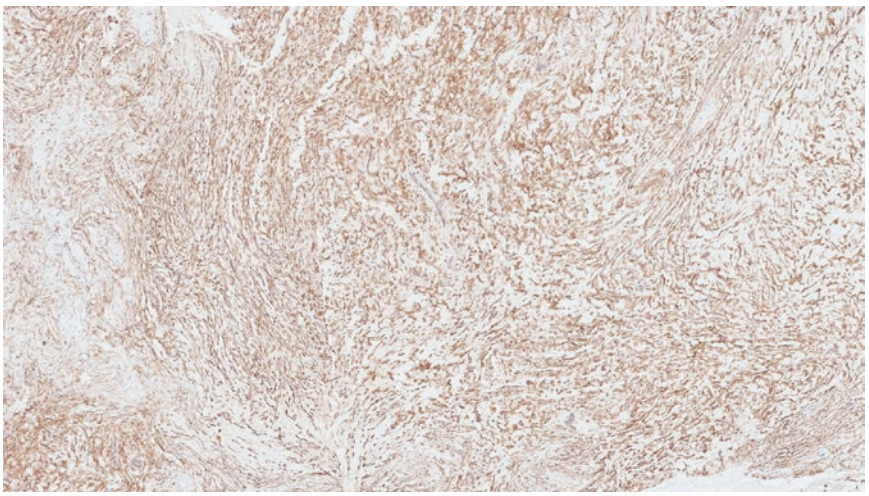

Fig. 11.41 Myofibroblastoma. Diffuse CD34 immunohistochemical positivity in the spindle cells

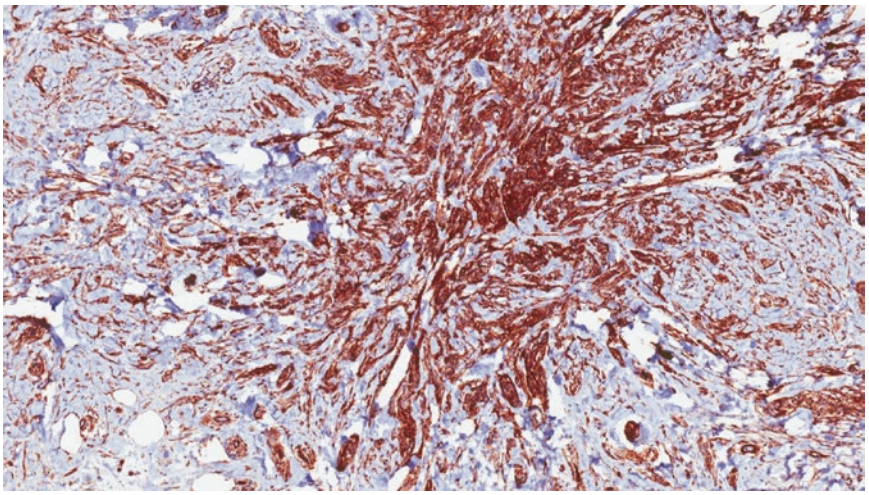

Fig. 11.42 Myofibroblastoma. CD34 immunohistochemistry shows diffuse reactivity of the spindle cells

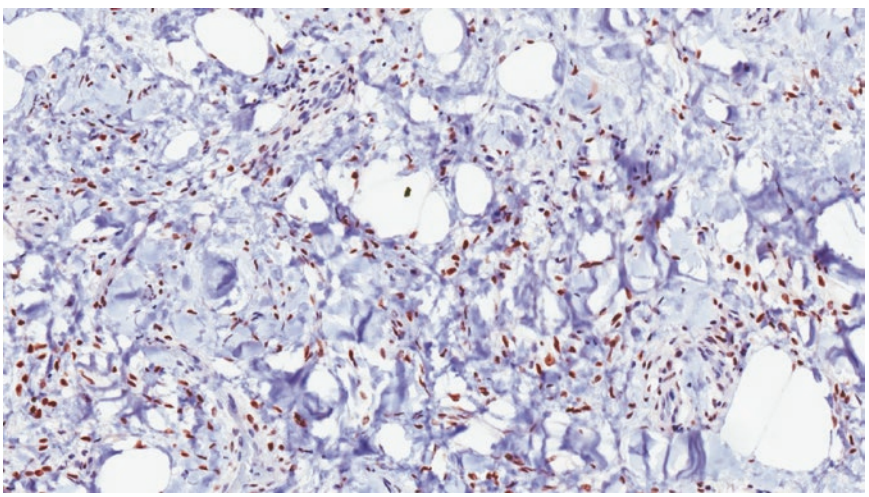

Fig. 11.43 Myofibroblastoma. Oestrogen receptor can be expressed in the spindle nuclei of myofibroblastoma. This appearance can resemble positively stained invasive lobular carcinoma cells. Circumscription of the lesion, absence of lobular neoplasia, and lack of keratin immunopositivity point away from carcinoma

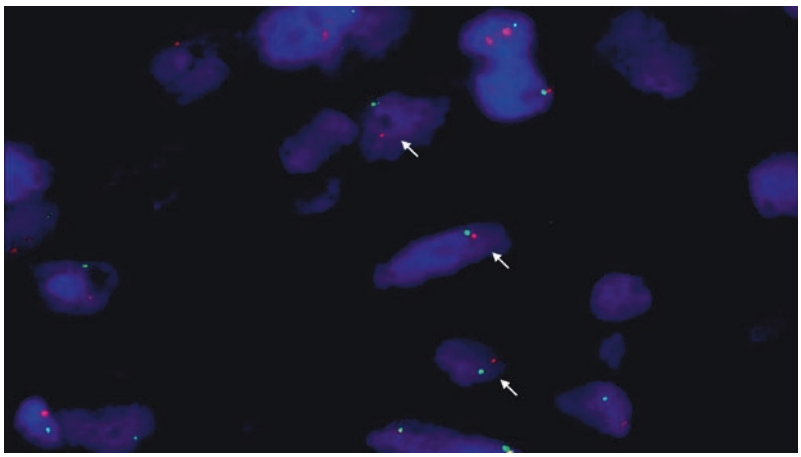

Fig. 11.44 Myofibroblastoma. On fluorescence in situ hybridisation (FISH), the LSI RB1 probe is labelled with SpectrumOrange fluorophore and is specific for the RB1 gene at 13q14. The control probe LSI 13q34 is labelled with SpectrumGreen fluorophore, and the probe is located near the telomere region of the q arm at 13q34. FISH signals show a one red and one green pattern, indicating monosomy 13 with loss of *RB1* gene (*arrows*) (Courtesy of Cytogenetics Laboratory, SGH Pathology)

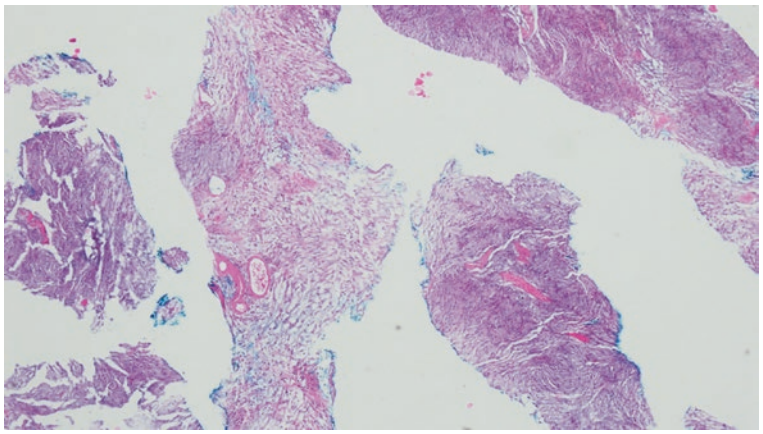

Fig. 11.45 Schwannoma. Core biopsy of a breast lump in an elderly man shows a spindle cell lesion with oedematous and myxoid zones among more cellular areas, representing the Antoni B and Antoni A appearances of a schwannoma

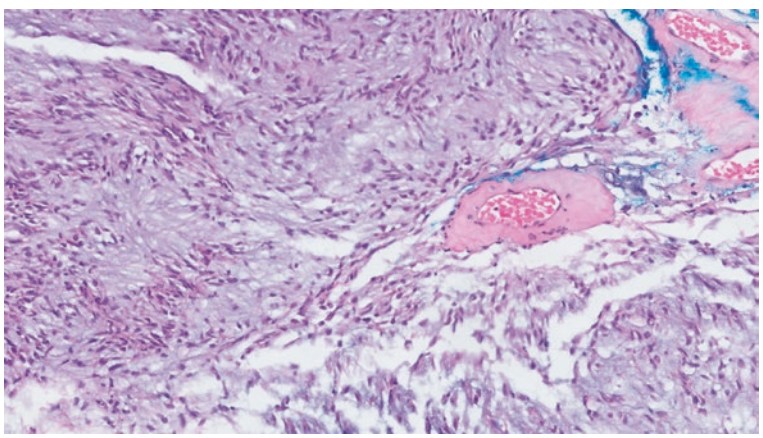

Fig. 11.46 Schwannoma. Higher magnification shows palisading of the spindle cell nuclei with interspersed hyalinised vessels

Neural Tumours

Neurofibroma and schwannoma (Figs. 11.45, 11.46, and 11.47) may rarely present as breast lumps, usually in the skin overlying the breast. Intraparenchymal lesions can also be encountered. These lesions stain immunohistochemically with S100.

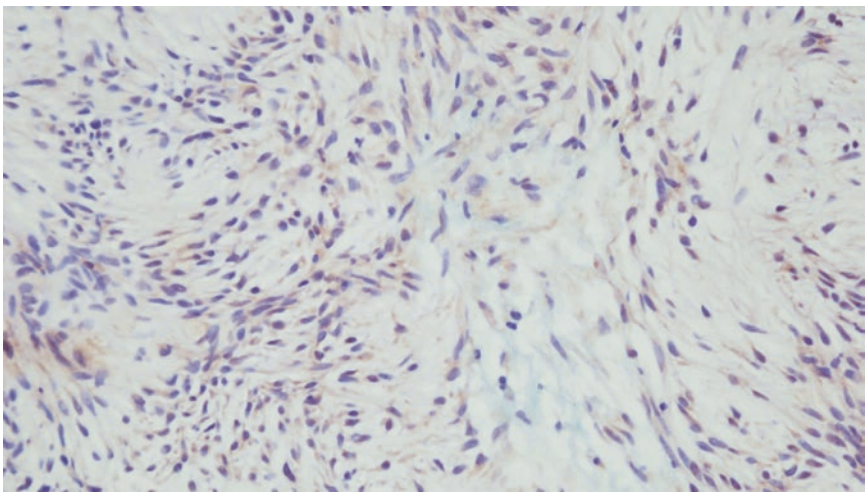

Fig. 11.47 Schwannoma. Immunohistochemistry for S100 shows faint cytoplasmic reactivity in some spindle cells

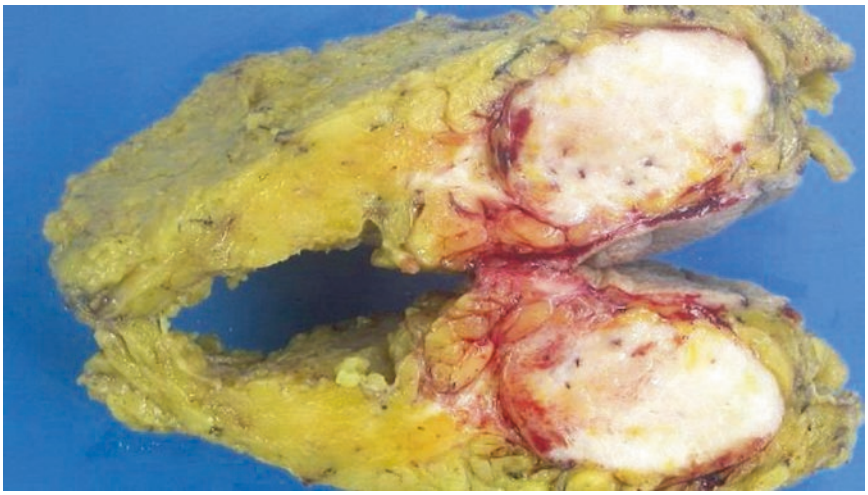

Fig. 11.48 Fibromatosis-like metaplastic carcinoma. Grossly, the whitish tumour shows a relatively circumscribed boundary

Prognosis and Therapy Considerations

Fibromatosis may locally recur in about 20–30 % of cases, usually consequent to incomplete resection. Correlation between positive surgical margins and recurrence, however, is not always direct, as some cases with positive margins do not recur, whereas some with negative margins may recur. Spontaneous resolution has been reported.

Fibromatosis-Like Metaplastic Carcinoma

Definition

Fibromatosis-like metaplastic carcinoma is a histologically low-grade spindle cell form of metaplastic carcinoma that usually expresses epithelial keratins diffusely and may disclose focal squamous differentiation [8].

Clinical and Epidemiological Features

Fibromatosis-like metaplastic carcinoma is clinicoradiologically similar to the more common breast cancers; it presents as a palpable breast mass or is mammographically detected.

Imaging Features

Radiologically, it typically presents as a spiculated, ill-defined breast mass on mammography, though some may be well defined.

Pathologic Features

Macroscopic Pathology

Macroscopically, the tumour may have circumscribed contours with a whitish, fibrous to fleshy appearance (Fig. 11.48).

Microscopic Pathology

Comprising interlacing fascicles of spindle cells with low-grade nuclear atypia and scattered but usually few mitoses, the tumour shows infiltration at the periphery among benign breast lobules and adipose (Figs. 11.49, 11.50, 11.51, and 11.52). Its bland histology often leads to an initial benign impression. There may be focal squamous differentiation or plumper epithelioid cells, which are clues to the correct diagnosis. An association with papillomas and complex sclerosing lesions is reported [9]. Immunohistochemistry is needed to confirm the presence of epithelial differentiation (Figs. 11.53 and 11.54). Hormone receptors and c-erbB-2 are negative.

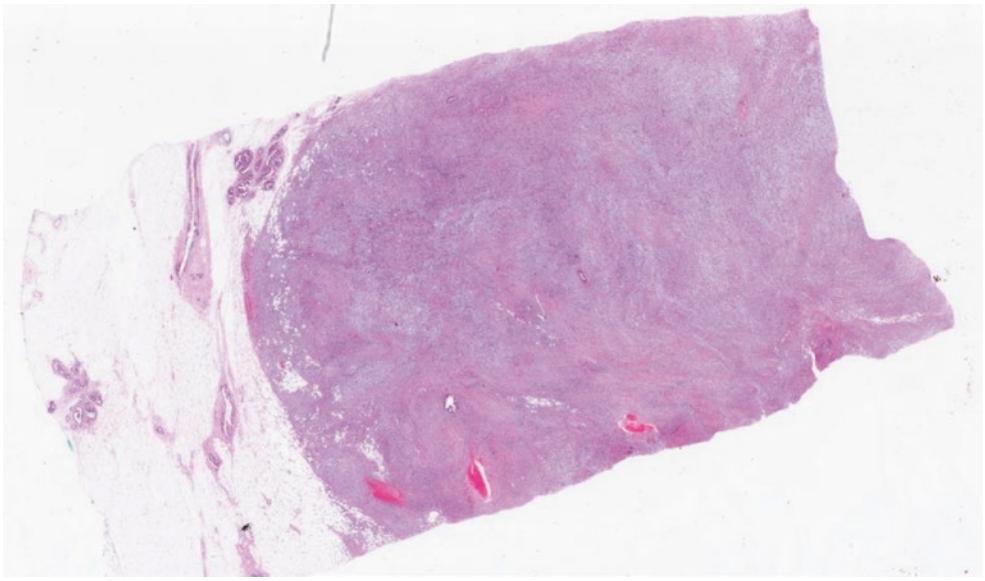

Fig. 11.49 Fibromatosis-like metaplastic carcinoma. At low magnification, the tumour seems to have a relatively circumscribed border, but the presence of entrapped adipocytes can be visualised at the tumour periphery

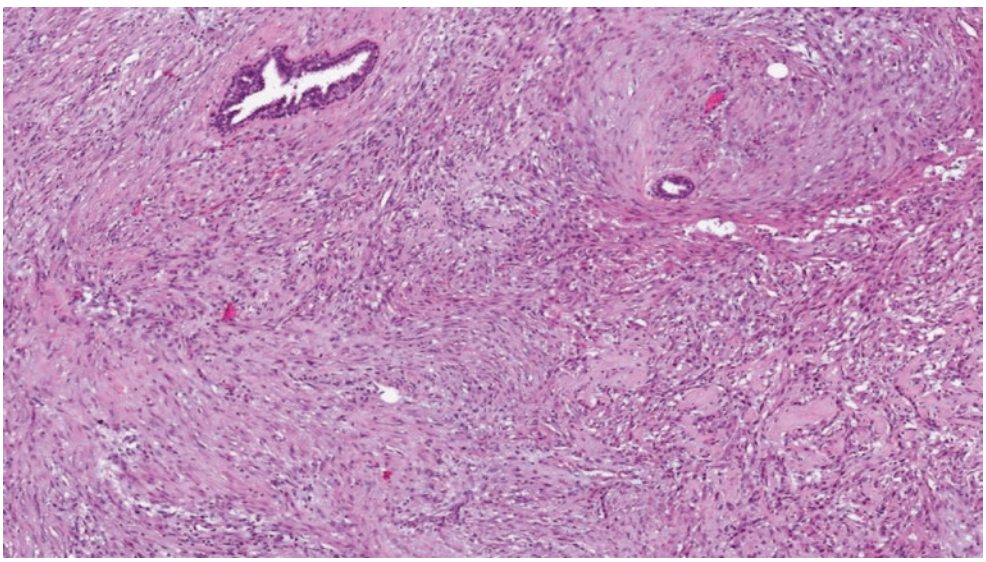

Fig. 11.50 Fibromatosis-like metaplastic carcinoma. Spindle cells interweave in short fascicles and surround benign ducts. In contrast to fibromatosis, this tumour shows areas of increased cellularity, where the spindle nuclei are more closely approximated and overlap. Nuclear atypia tends to remain mostly modest

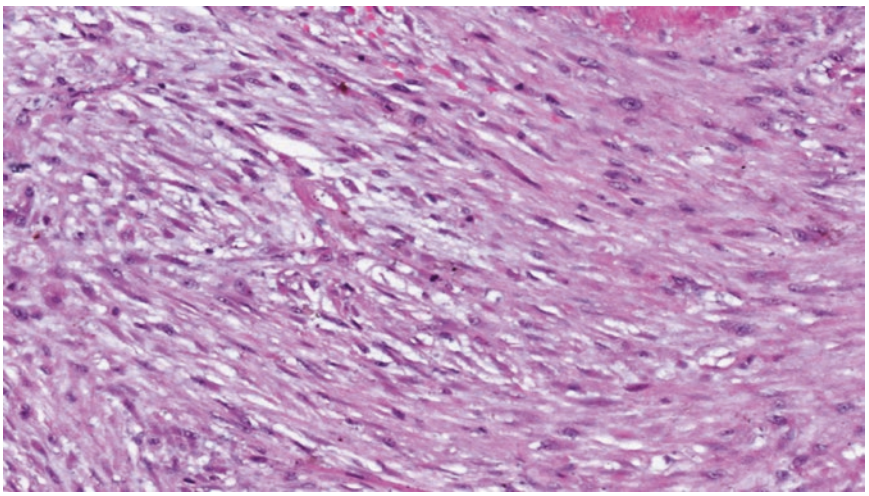

Fig. 11.51 Fibromatosis-like metaplastic carcinoma. At high magnification, a greater degree of nuclear variation may be seen, with scattered mitoses, but there are no high-grade nuclear alterations in this tumour

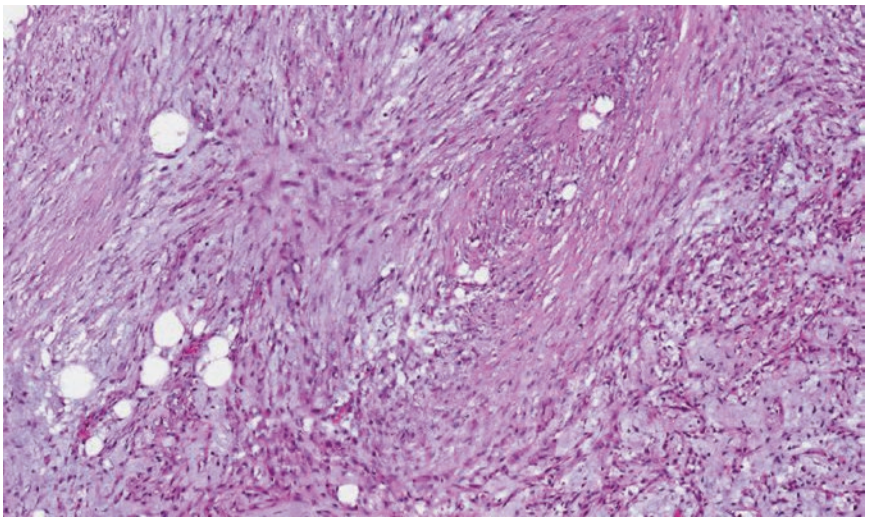

Fig. 11.52 Fibromatosis-like metaplastic carcinoma. Histologically, sheets of spindle cells are arranged in an interlacing pattern with a focal semblance of storiforming. In the *right lower field*, there are irregular nests of cells that have an anastomosing, net-like appearance. The presence of more aggregated epithelioid and squamoid cells distinguish it from fibromatosis and should raise suspicion of metaplastic carcinoma

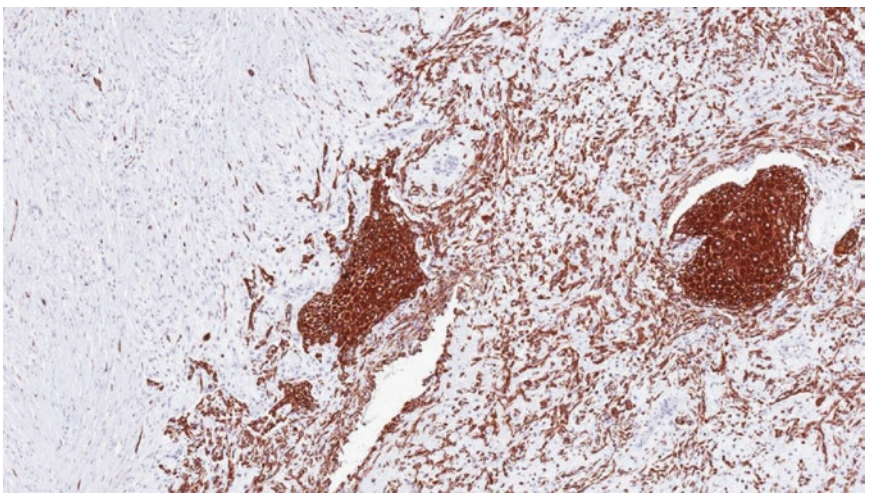

Fig. 11.53 Fibromatosis-like metaplastic carcinoma. MNF116 immunohistochemistry shows diffuse positivity, accentuating the subtle anastomosing network of more aggregated cells observed on light microscopy. In addition, larger, solid islands of pavemented squamous-like cells are unveiled, which are also decorated by MNF116

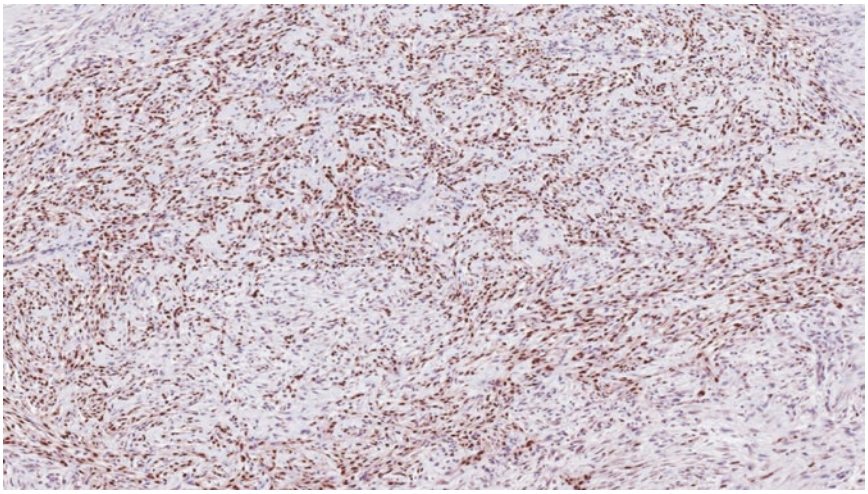

Fig. 11.54 Fibromatosis-like metaplastic carcinoma. Immunohistochemistry for p63 discloses diffuse nuclear positivity

Differential Diagnosis

Fibromatosis

The main differential is fibromatosis, which differs from fibromatosis-like metaplastic carcinoma by the absence of squamous and epithelioid foci and the lack of keratin expression on immunohistochemistry. Beta-catenin, which is positive in the nuclei of fibromatosis, is not a definitive distinguishing marker; it has been reported to be expressed in metaplastic carcinoma, though it is often focal in distribution [10].

Spindle Cell Metaplastic Carcinoma

Spindle cell metaplastic carcinoma shows a greater degree of cytological atypia than fibromatosis-like metaplastic carcinoma, with frequent squamous and epithelioid foci. It overlaps histologically with spindle squamous cell carcinoma and myoepithelial carcinoma.

Prognosis and Therapy Considerations

Fibromatosis-like metaplastic carcinoma has a more favourable prognosis than other types of metaplastic breast carcinoma. It can locally recur, but metastases are infrequent. Recent molecular studies suggest that it has low genomic instability, unlike metaplastic carcinomas in general [11].

Spindle Cell Metaplastic Carcinoma

Definition

Spindle cell metaplastic carcinoma is a breast carcinoma showing a predominant spindle cell morphology. It overlaps with spindle squamous cell carcinoma and myoepithelial carcinoma, both of which are classified under the rubric of spindle cell metaplastic carcinoma [12].

Clinical and Epidemiological Features

Metaplastic carcinoma is uncommon, accounting for less than 1 % of all breast cancers. Spindle cell metaplastic carcinoma constitutes a morphological subtype of the heterogeneous family of metaplastic breast carcinomas.

Imaging Features

On imaging, metaplastic carcinoma tends to be seen as lobulated, well-defined masses. The margins can demonstrate both well-defined and ill-defined borders with spiculations. Sonography may show cystic areas within the masses, which are due to necrosis or haemorrhage. The masses usually grow rapidly and tend to be large at the time of imaging.

Pathologic Features

Macroscopic Pathology

Gross appearances may resemble those of conventional invasive ductal carcinoma, but some spindle cell metaplastic carcinomas have circumscribed outlines with whitish-grey, fleshy cut surface (Fig. 11.55).

Fig. 11.55 Spindle cell metaplastic carcinoma. The tumour shows ill-defined borders and has a greyish-beige cut surface

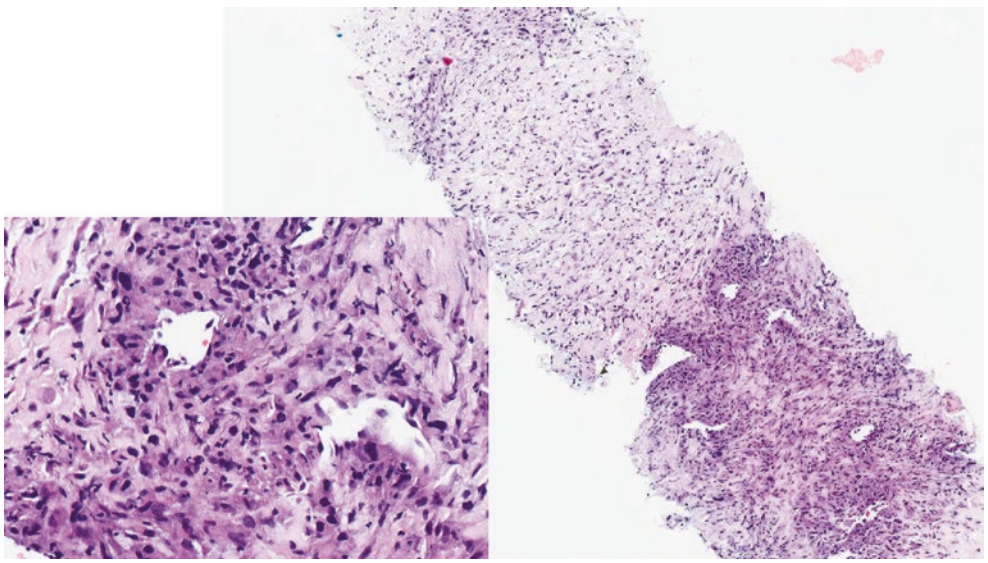

Fig. 11.56 Malignant spindle cell tumour on core biopsy, showing variable cellularity with pleomorphic spindle cells. *Inset* shows plump epithelioid and spindle cells with marked nuclear pleomorphism with hyperchromasia. The presence of keratin immunopositivity may favour a diagnosis of spindle cell metaplastic carcinoma, but it is important to note that focal keratin staining may be encountered in malignant phyllodes tumours and sarcomas, especially those with epithelioid morphology

Microscopic Pathology

Malignant spindle cells arranged in interlacing fascicles permeate around and efface residual ducts and lobules, with irregular extensions into surrounding adipose. Mitoses and necrosis are present. Squamoid and squamous foci with keratinisation, and ductal carcinoma in situ, can be seen (Figs. 11.56, 11.57, 11.58, 11.59, 11.60, 11.61, and 11.62). Immunohistochemistry confirms the presence of keratin expression, although this may be patchy, requiring assessment on different tumour blocks, especially if there is no accompanying ductal carcinoma in situ to support a metaplastic carcinoma origin. A panel of antibodies to keratins is recommended, owing to different antibody sensitivities and specificities (Figs. 11.63 and 11.64) [13, 14].

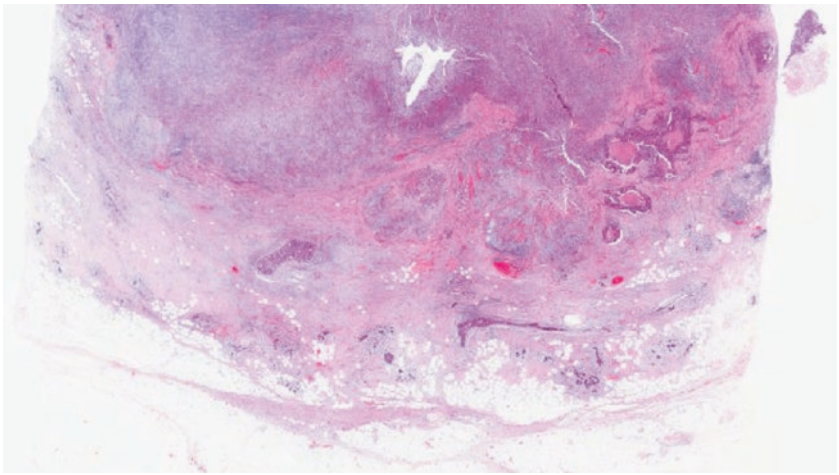

Fig. 11.57 Spindle cell metaplastic carcinoma. Excision of the case with the malignant spindle cell tumour on core biopsy (Fig. 11.56). At low magnification, cohesive aggregates of tumour cells with central necrosis (*right field*) indicate epithelial differentiation. Ductal carcinoma in situ is also present, though it is difficult to discern at this magnification

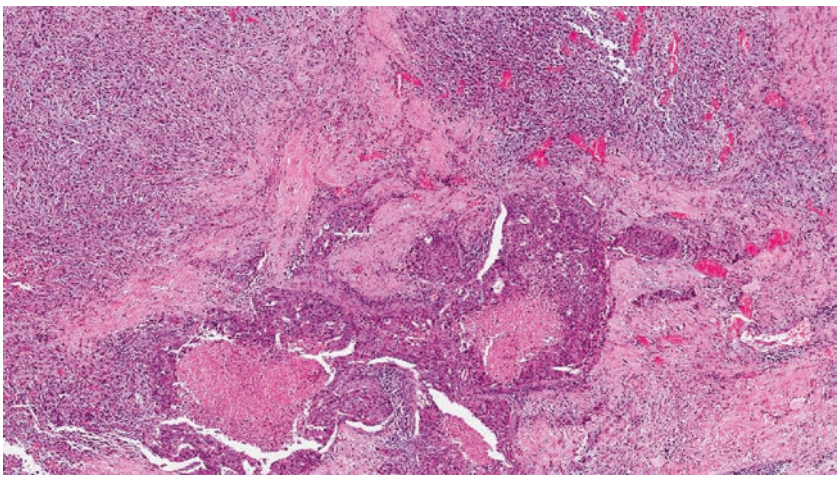

Fig. 11.58 Spindle cell metaplastic carcinoma. The presence of focal epithelial differentiation is observed as confluent, malignant epithelial islands with central amorphous necrosis. Malignant spindle cells surround and merge with these epithelial islands. The finding of ductal carcinoma in situ in a malignant spindle cell tumour supports the diagnosis of metaplastic carcinoma

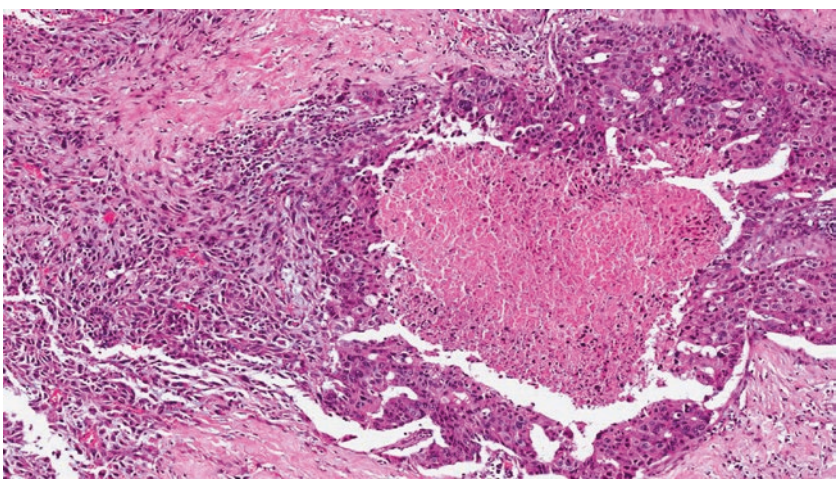

Fig. 11.59 Spindle cell metaplastic carcinoma. Higher magnification shows the malignant epithelial island transitioning to high-grade abnormal spindle cells

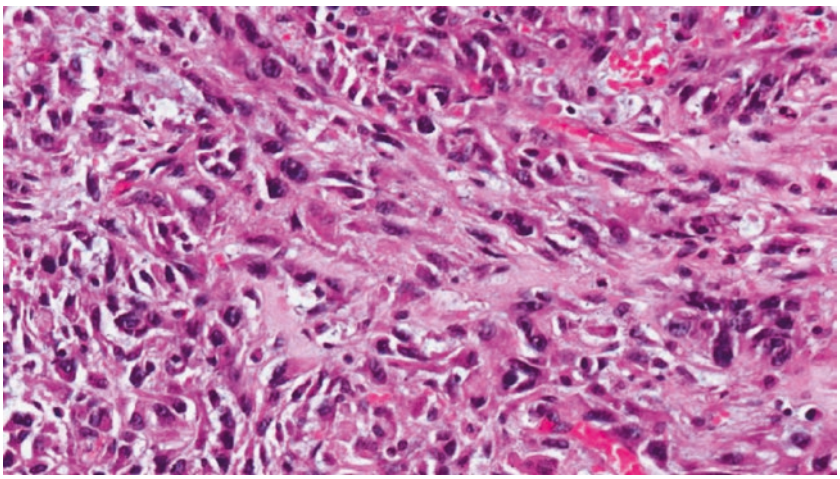

Fig. 11.60 Spindle cell metaplastic carcinoma. High-grade malignant spindle and epithelioid cells are seen forming a large part of the tumour

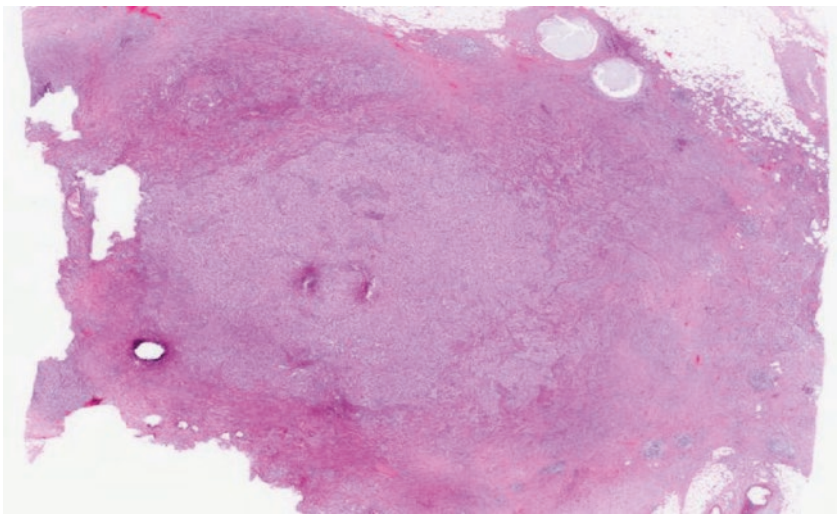

Fig. 11.61 Spindle cell metaplastic carcinoma. This tumour shows percolation into surrounding adipose

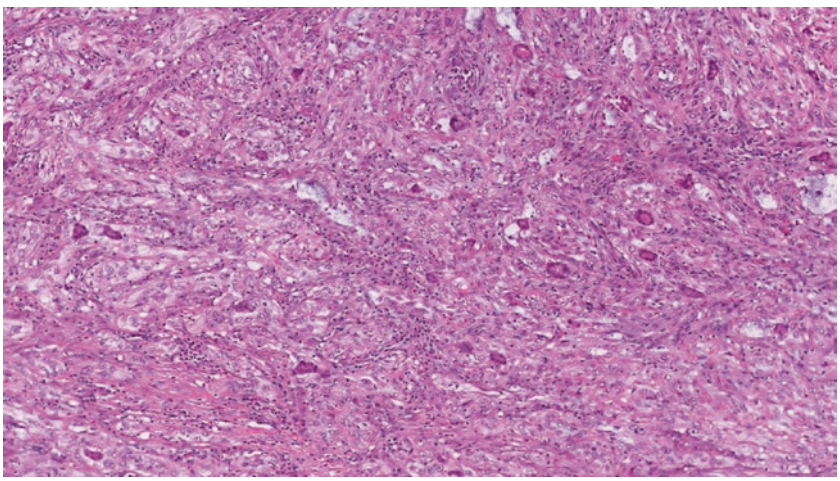

Fig. 11.62 Spindle cell metaplastic carcinoma. Abnormal spindle cells swirl around small tubules, appearing to arise from the outer border, suggesting the possibility that the malignant spindle cells are derived from a myoepithelial origin. Carcinomas of myoepithelial derivation are classified as metaplastic spindle cell carcinoma, as there is substantial histological and immunophenotypic overlap

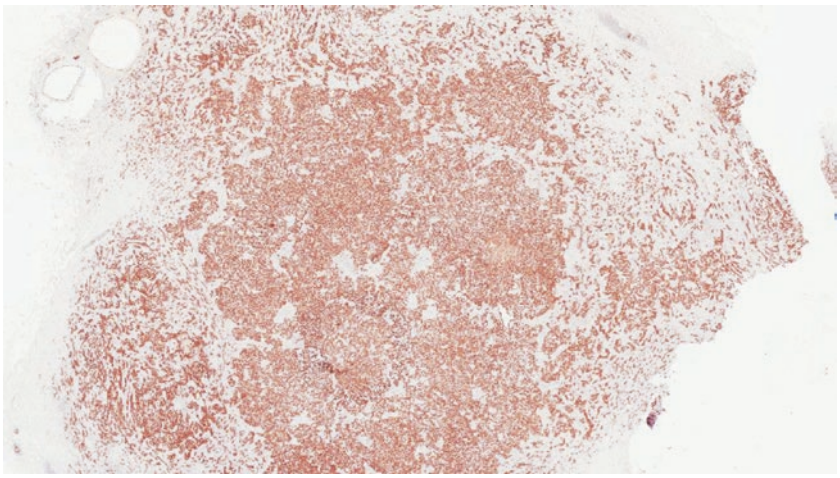

Fig. 11.63 Spindle cell metaplastic carcinoma. Immunohistochemistry for CK14, a high molecular weight cytokeratin, shows diffuse reactivity of the tumour cells, with accentuation of aggregated anastomosing and confluent tumour groups

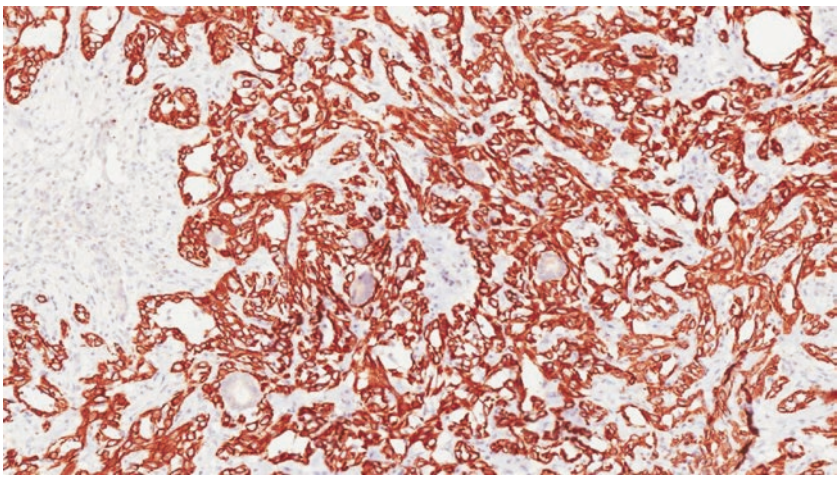

Fig. 11.64 Spindle cell metaplastic carcinoma. Higher magnification of CK14-positive tumour cells shows a net-like interlacing pattern of tumour cells

Differential Diagnosis

Metaplastic Carcinoma with Mesenchymal Differentiation

In this category of metaplastic carcinoma, malignant osteoid, chondroid, and chondromyxoid elements are present. Liposarcoma is an uncommon heterologous component in metaplastic carcinoma, being more commonly observed in malignant phyllodes tumours (Figs. 11.65, 11.66, 11.67, 11.68, 11.69, 11.70, and 11.71) [15].

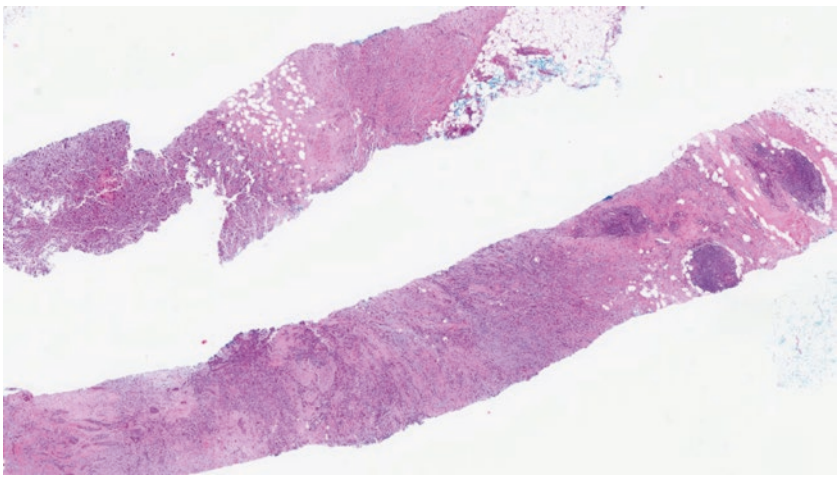

Fig. 11.65 Metaplastic carcinoma with mesenchymal differentiation. Core biopsy of the breast tumour shows a malignant spindle cell process with hypercellular tumour zones interspersed with fibrous areas. At low magnification, the tumour merely shows sheets of tumour cells

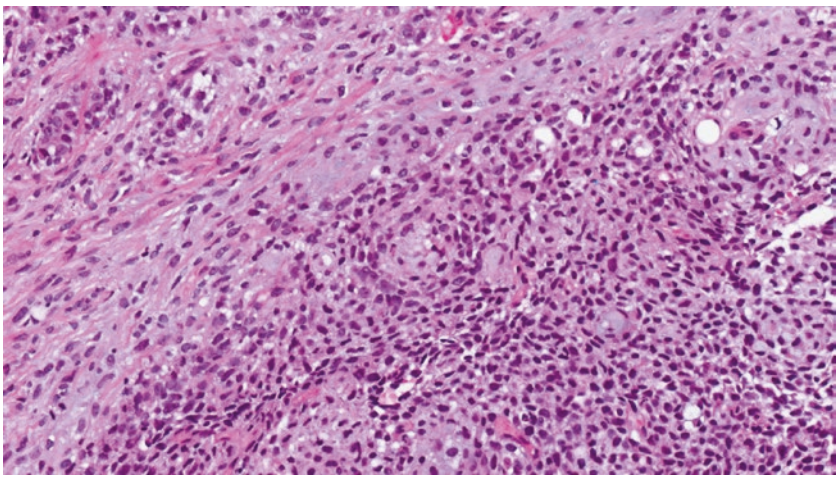

Fig. 11.66 Metaplastic carcinoma with mesenchymal differentiation. The tumour shows vaguely cohesive and anastomosing groups of tumour cells amid myxoid matrix

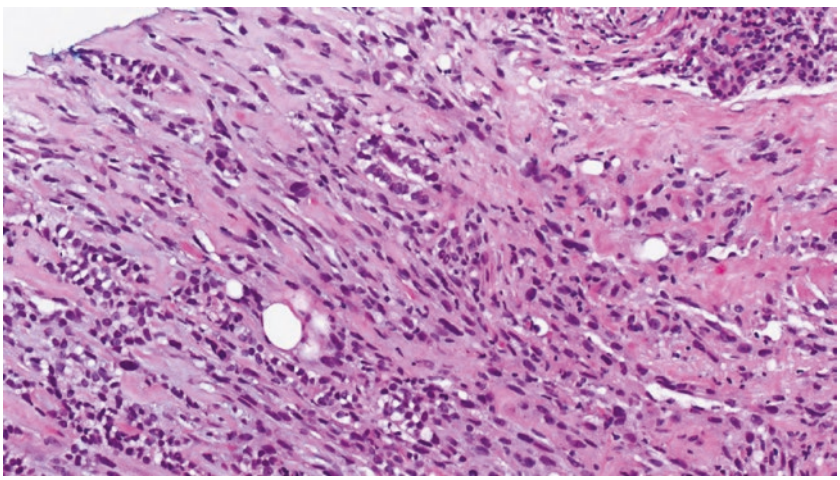

Fig. 11.67 Metaplastic carcinoma with mesenchymal differentiation. Elsewhere, the tumour consists of elongated malignant spindle cells that blend with more trabecular groups

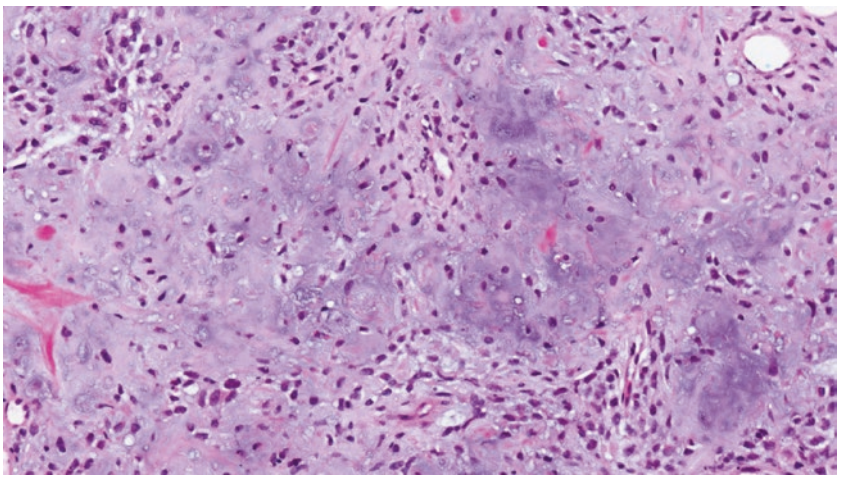

Fig. 11.68 Metaplastic carcinoma with mesenchymal differentiation. Higher magnification reveals chondromyxoid material among abnormal spindle cells with hyperchromatic nuclei

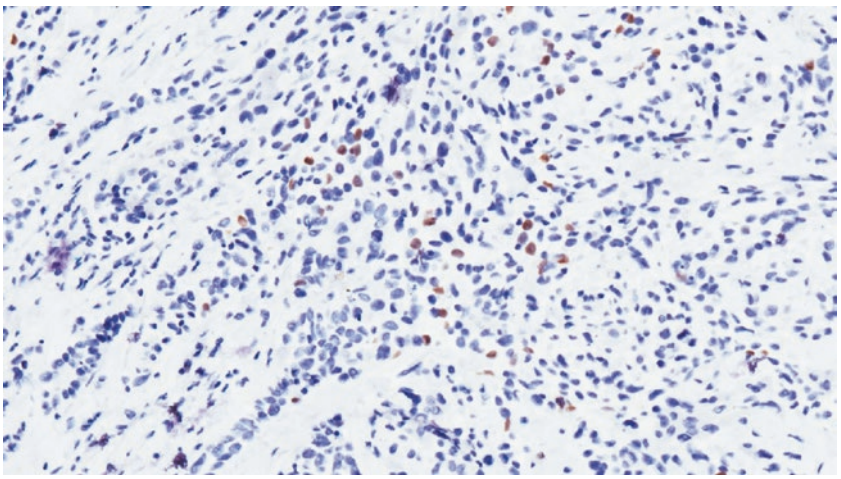

Fig. 11.69 Metaplastic carcinoma with mesenchymal differentiation. Immunohistochemistry for p63 shows patchy nuclear positivity. As immunostaining for p63 and keratins may be patchy and focal, a panel of antibodies is recommended rather than relying on a single marker

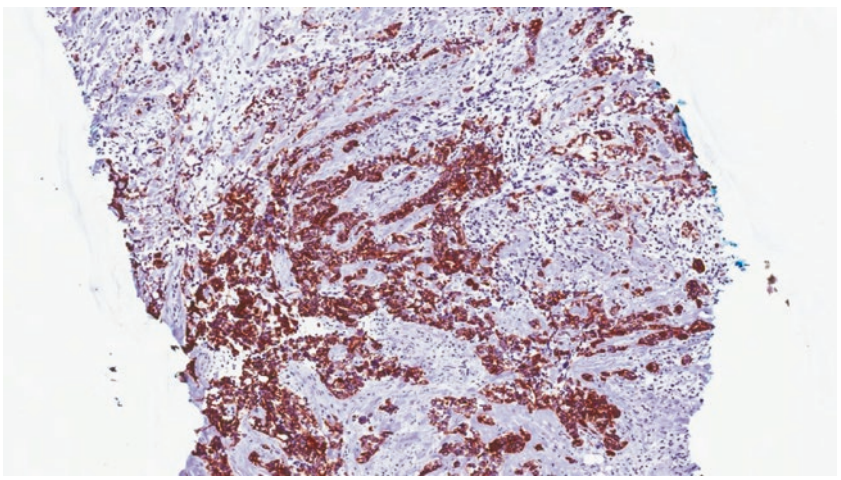

Fig. 11.70 Metaplastic carcinoma with mesenchymal differentiation. MNF116 immunohistochemistry accentuates the invasive aggregates of malignant epithelial cells

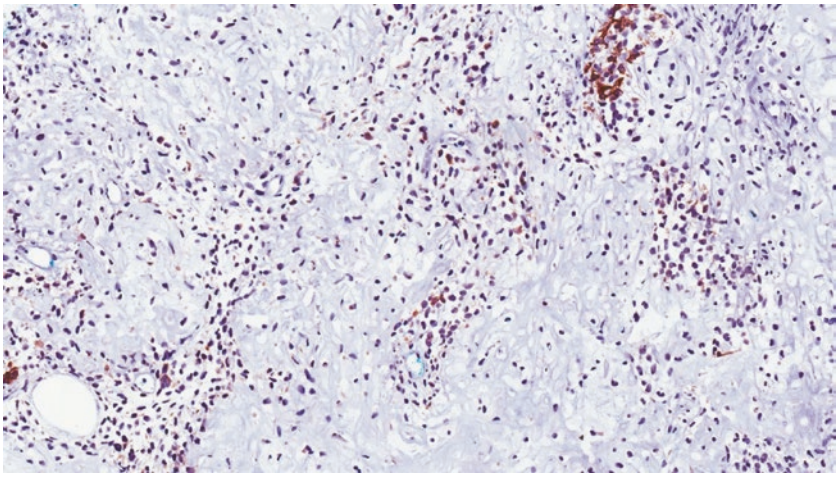

Fig. 11.71 Metaplastic carcinoma with mesenchymal differentiation. More patchy reactivity for MNF116 is observed in the chondromyxoid zones

Malignant Phyllodes Tumour

The sarcomatous component of a malignant phyllodes tumour may be morphologically indistinguishable from spindle cell metaplastic carcinoma. Adequate sampling is required to identify characteristic phyllodal leafy fronds. Though diffuse keratin staining of the malignant spindle cells favours metaplastic carcinoma, focal keratin staining, as well as p63 and p40 staining, has been described in malignant phyllodes tumours [14, 16].

Sarcoma

High-grade sarcoma may be microscopically indistinguishable from spindle cell metaplastic carcinoma. It is a diagnosis of exclusion, after metaplastic carcinoma and malignant phyllodes tumour have been ruled out [17–19].

Prognosis and Therapy Considerations

Spindle cell metaplastic carcinoma is frequently triple-negative, with no expression of hormone receptors and c-erbB-2, resulting in limited therapeutic options apart from chemotherapy, though some reports indicate that it has a lower response rate than other forms of triple-negative disease [12]. Spindle cell metaplastic carcinoma has a propensity to distantly metastasise without axillary nodal involvement.

Phyllodes Tumour with Stromal Overgrowth

Definition

These phyllodes tumours have stromal expansion that exceeds one low-power field (×4 microscope objective, ×10 eyepiece), without accompanying epithelial elements. This phenomenon is usually seen in phyllodes tumours of borderline or malignant grades.

Clinical and Epidemiological Features

Phyllodes tumours occur in older women in the fifth decade of life and beyond. They are usually clinically symptomatic as breast lumps with recent rapid growth. Large tumours may erode through the skin.

Imaging Features

Imaging reveals a well-defined oval or gently lobulated, inhomogeneous mass, which is usually indistinguishable from fibroadenoma. It does not calcify like fibroadenomas, and several cleft-like, cystic spaces may be seen on sonography. A rapidly growing fibroadenoma-like mass should be evaluated carefully to exclude a phyllodes tumour. Ill-defined margins are suggestive of malignant grade.

Pathologic Features

Macroscopic Pathology

These tumours may achieve large sizes exceeding 10 cm, with whitish, whorled cut surfaces, myxoid degeneration, and yellowish necrotic zones (Fig. 11.72). A fibrous capsule is usually present but does not translate to microscopic circumscription.

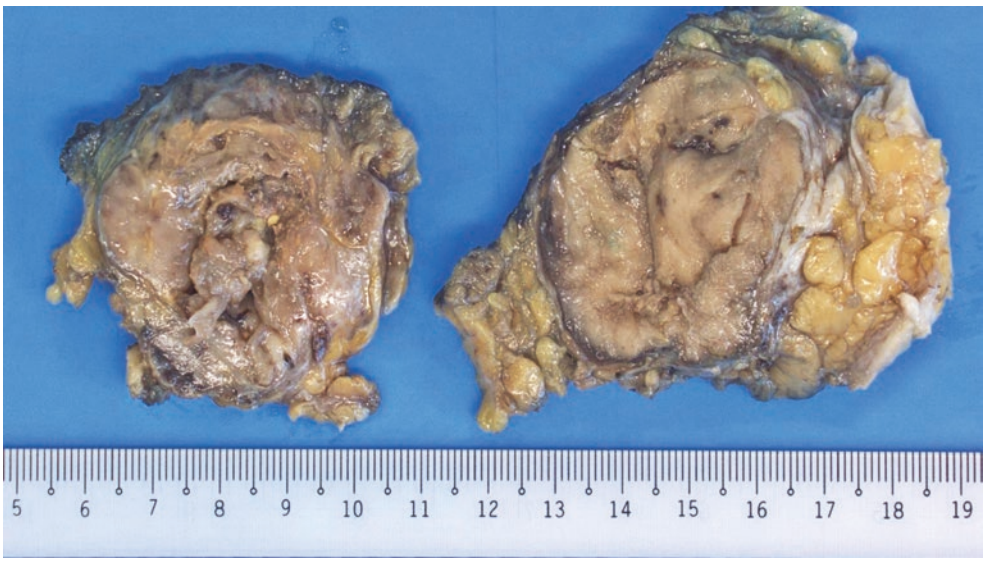

Fig. 11.72 Excision specimen of a malignant phyllodes tumour, showing a greyish-brown appearance with elongated, curvilinear clefts giving a broad, fronded appearance. Areas of haemorrhage and focal yellowish necrosis are present. The tumour borders seem relatively circumscribed, with bosselated contours

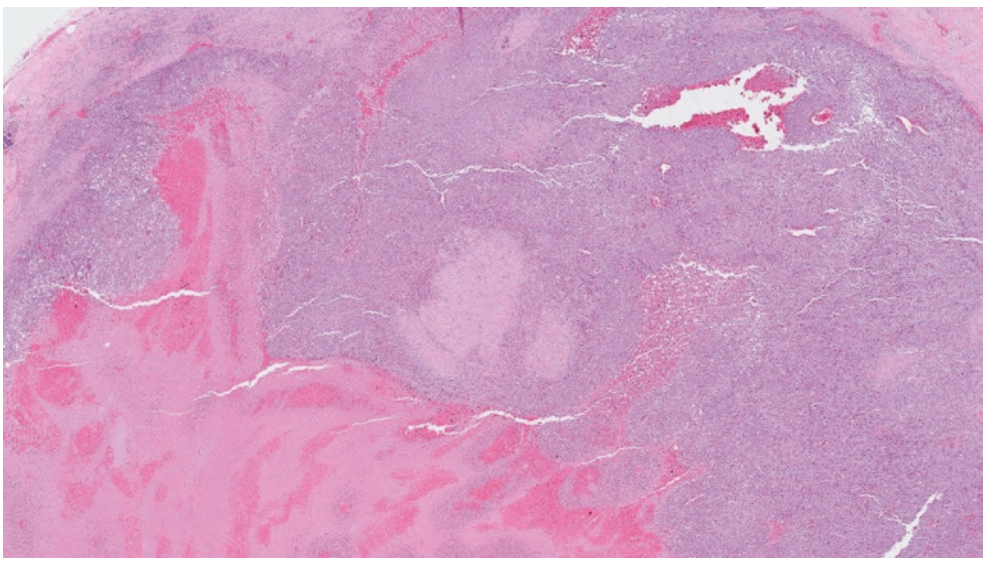

Fig. 11.73 Malignant phyllodes tumour. At low magnification, the tumour consists of hypercellular sheets of tumour cells with areas of haemorrhagic necrosis. Although the borders seem circumscribed grossly, there is no fibrous capsule separating tumour from surrounding tissue microscopically; there are areas in which tumour cells appear to extend into surrounding tissue

Microscopic Pathology

Phyllodes tumours with stromal overgrowth show expanses of stroma only, devoid of epithelial elements. In borderline tumours, the stromal overgrowth usually takes the form of low-grade spindle cells, which may mimic nodular fasciitis, fibromatosis, and other low-grade spindle cell neoplasms if characteristic phyllodal fronds are absent. For malignant phyllodes tumours with high-grade sarcomatous overgrowth (Figs. 11.73, 11.74, 11.75, 11.76, 11.77, and 11.78), there is marked nuclear pleomorphism with high mitotic activity and occasional malignant heterologous elements. Immunohistochemistry is useful in excluding metaplastic carcinoma, though caution must be exercised in interpreting keratin and p63/p40 immunostains because of their presence in malignant phyllodes tumours [14–16]. CD34 is useful, as it can be expressed in phyllodes tumours but is infrequent in metaplastic carcinoma [13].

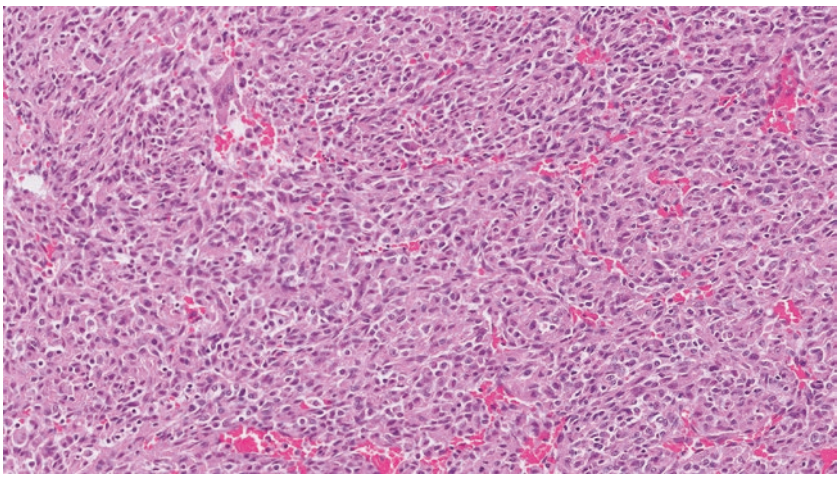

Fig. 11.74 Malignant phyllodes tumour. Higher magnification shows plump epithelioid and spindle cells that are closely packed, with scattered microhaemorrhages. An osteoclastic-type, multinucleated giant cell is noted

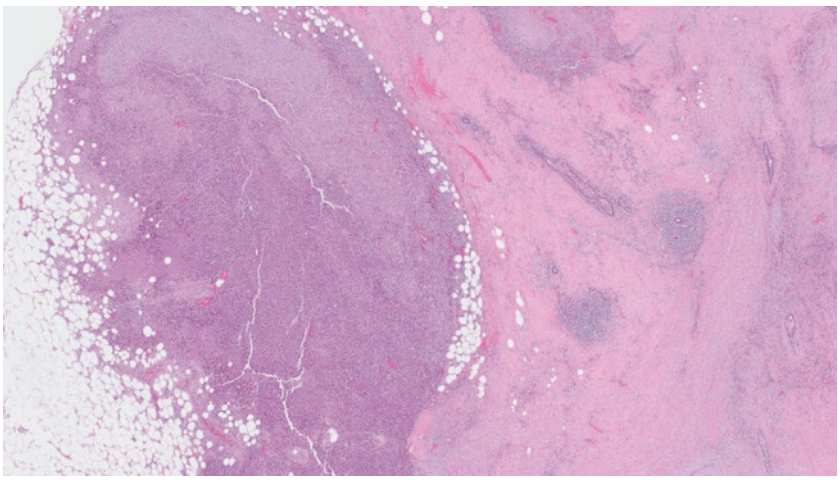

Fig. 11.75 Malignant phyllodes tumour. Sheets of tumour cells are percolating irregularly into the fat. No obvious stromal fronds with accompanying epithelium are present

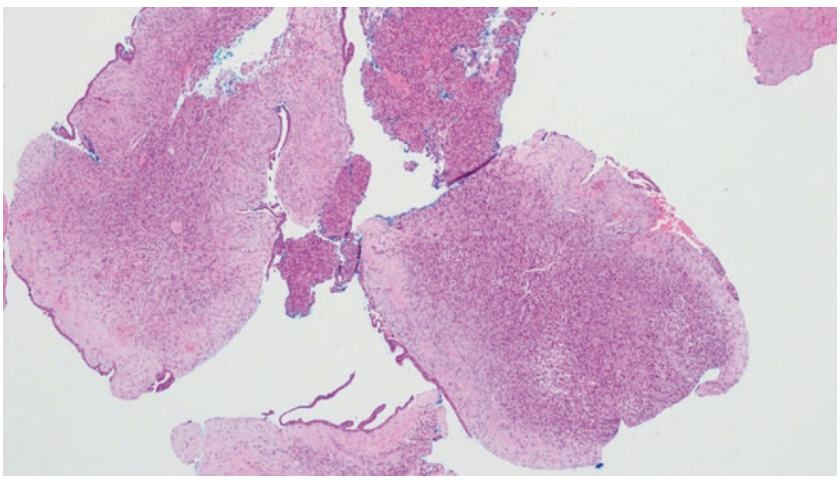

Fig. 11.76 Malignant phyllodes tumour. Review of the previous core biopsy of the tumour shown in Figs. 11.72, 11.73, 11.74, and 11.75 disclosed phyllodal fronds with hypercellular stroma, which could not be found in the subsequent mastectomy

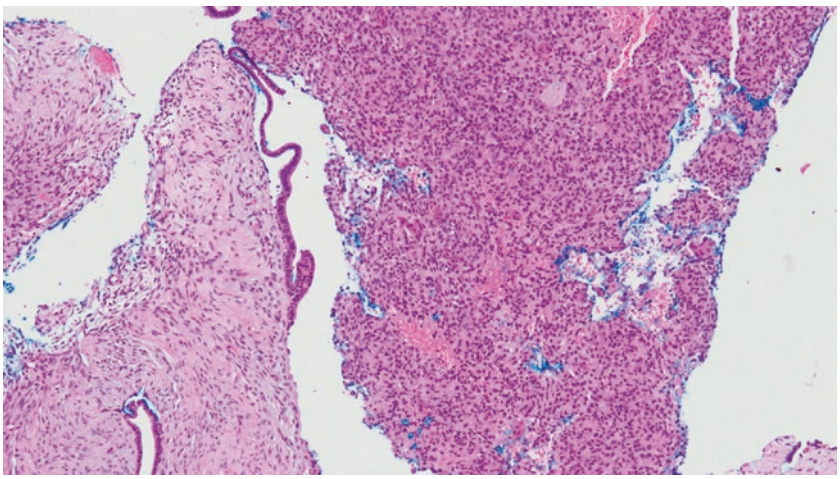

Fig. 11.77 Malignant phyllodes tumour on core biopsy. Elongated stretches of epithelium are seen in conjunction with hypercellular malignant stroma

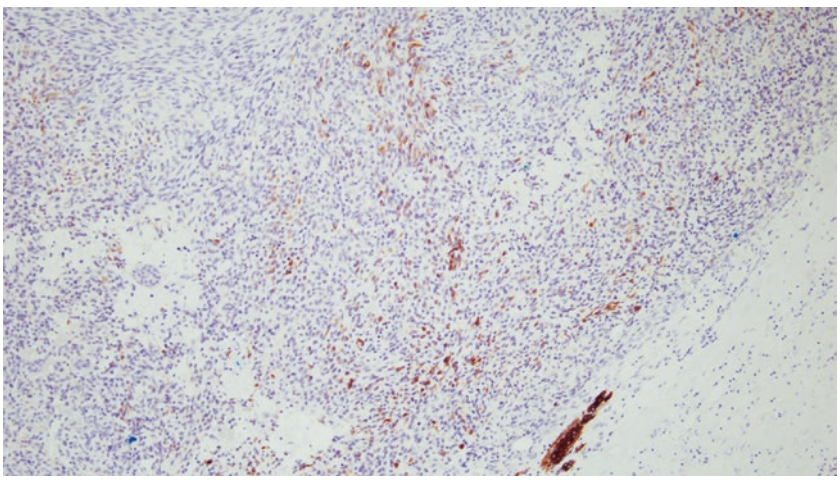

Fig. 11.78 Malignant phyllodes tumour. Cam5.2 immunohistochemistry shows focal reactivity of the spindle tumour cells. Based on the light microscopy, without the presence of characteristic phyllodal fronds, a firm diagnosis of phyllodes tumour cannot be made. The three key differentials of a malignant spindle cell tumour in the breast are metaplastic carcinoma, malignant phyllodes tumour, and sarcoma. Keratin positivity favours metaplastic carcinoma, but it has been described in both malignant phyllodes tumour and sarcoma. Focal positivity for keratin is demonstrated in this malignant phyllodes tumour. Additionally, keratin reactivity in metaplastic carcinoma may also be focal, compounding the difficulty in making the diagnosis

Differential Diagnosis

Depending on whether the stromal overgrowth features low-grade or high-grade cytological features, corresponding differential diagnostic considerations apply; these considerations are discussed above and in the figure legends.

Prognosis and Therapy Considerations

Borderline and malignant phyllodes tumours have a higher likelihood of recurrence than benign phyllodes tumours, with the malignant category potentially metastasising and leading to death. Complete surgical removal remains the current treatment of choice, though the extent of margin clearance is still controversial [15].

Dermatofibrosarcoma Protuberans

Definition

Dermatofibrosarcoma protuberans is a tumour that arises in the dermal skin but may secondarily involve the breast parenchyma, mimicking a primary spindle cell lesion of the breast.

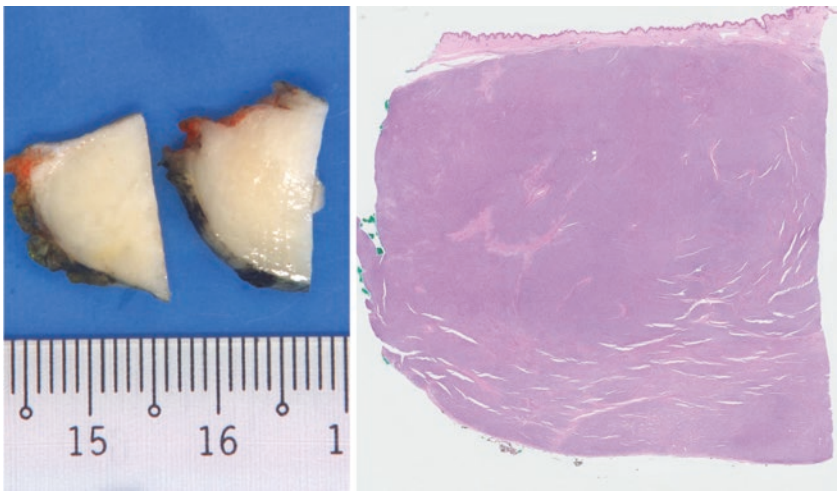

Fig. 11.79 Dermatofibrosarcoma protuberans. The gross appearance is whitish, glistening, and smooth. On low magnification, the tumour is close to the epidermis and arises in the dermis with deep extension. The appearance is uniformly hypercellular, with a few irregular, fibrous areas

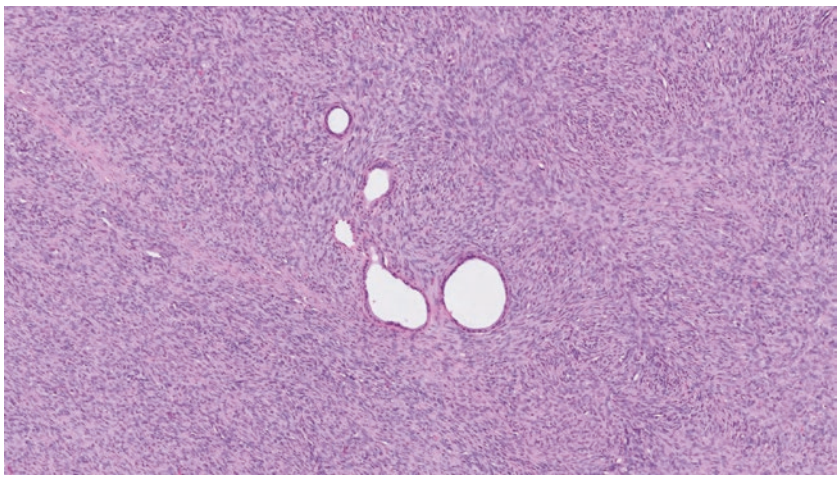

Fig. 11.80 Dermatofibrosarcoma protuberans. Hypercellular sheets of spindle cells encircle residual ducts

Clinical and Epidemiological Features

Dermatofibrosarcoma protuberans usually presents as a lump in the skin of the breast, with tethering to the skin; it potentially mimics carcinoma. Pain has been reported. Rarely, it can occur in the breast parenchyma without visible skin attachment [20].

Imaging Features

Imaging typically shows a superficial mass in the subcutaneous tissue adjacent to the dermis. The mass is often round or oval and shows variable internal echogenicity on sonography. Margins are usually well defined, but they can also be poorly defined, with a hyperechoic rim on ultrasound evaluation.

Pathologic Features

Macroscopic Pathology

Grossly, there is a whitish, firm mass without encapsulation, which can be fibrous or slightly myxoid, attached to the overlying skin (Fig. 11.79). A reddish-brown to bluish coloration may be observed, depending on the amount of haemorrhage or melanin pigment.

Microscopic Pathology

Dermatofibrosarcoma protuberans consists of a monomorphous proliferation of spindle cells with elongated, hyperchromatic nuclei and scattered mitoses. A short, storiform, and intersecting fascicular pattern is present. Infiltration of surrounding tissue is seen, with permeation into fat in a lace-like, intercalated manner (Figs. 11.80, 11.81, 11.82, and 11.83). Immunohistochemically, there is positive staining for CD34, with negative reactivity for factor XIIIa.

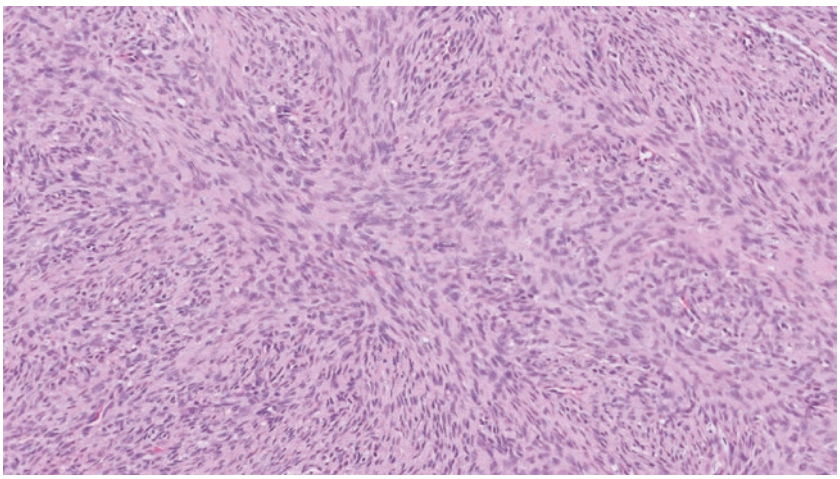

Fig. 11.81 Dermatofibrosarcoma protuberans. Higher magnification shows fascicles of spindle cells with ovoid to spindle nuclei that generally demonstrate mild atypia

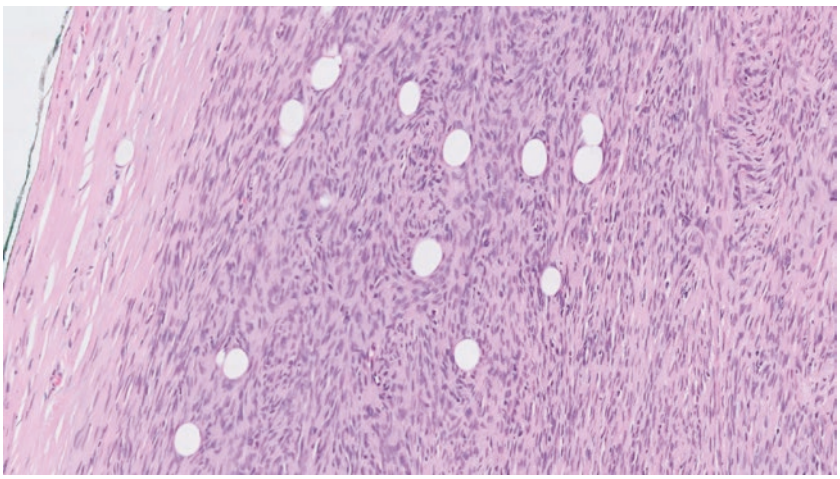

Fig. 11.82 Dermatofibrosarcoma protuberans. Neoplastic spindle cells entrap fat in their midst

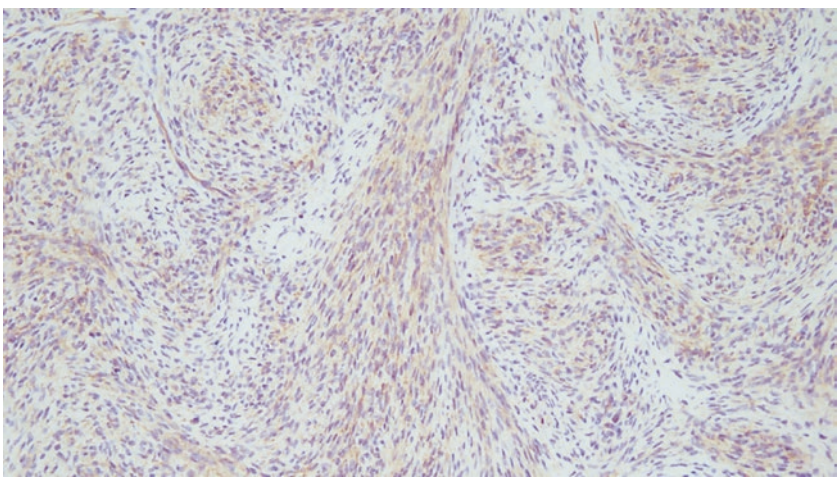

Fig. 11.83 Dermatofibrosarcoma protuberans. Immunohistochemical reactivity for CD34 is frequently positive, though in this case the staining intensity is relatively weak

Differential Diagnosis

Dermatofibroma

The dermatofibroma is usually confined to the upper dermis, though occasionally it can extend into the deep dermis and subcutis. There are accompanying foamy histiocytes, sometimes including Touton giant cells and haemosiderin deposits. A prominent storiform pattern is absent. There is no atypia, and mitoses are rare. In contrast to dermatofibrosarcoma protuberans, the dermatofibroma is CD34 negative and factor XIIIa positive. Stromelysin 3, which is positive in dermatofibroma but negative in dermatofibrosarcoma protuberans, may also be useful [21].

Phyllodes Tumour with Stromal Overgrowth

Stromal overgrowth in phyllodes tumour may resemble dermatofibrosarcoma protuberans, especially when CD34 positivity is demonstrated. Demonstration of phyllodal fronds helps to clinch the correct diagnosis.

Fibromatosis

Dermatofibrosarcoma protuberans is more cellular, has a storiform pattern with spindle cells harbouring hyperchromatic nuclei, and is diffusely CD34 positive.

Fibromatosis-Like Metaplastic Carcinoma

Dermatofibrosarcoma protuberans is hypercellular and has a "bluish" appearance at low magnification, whereas fibromatosis-like metaplastic carcinoma is often less cellular. Immunohistochemical positivity for keratins confirms metaplastic carcinoma.

Prognosis and Therapy Considerations

Because of its infiltrative nature, dermatofibrosarcoma protuberans is reported to recur locally in up to 50% of cases [20]. Complete excision with negative margins of 2–3 cm clearance is the mainstay of treatment.

Sarcoma

Definition

Primary breast sarcoma is uncommon and encompasses a heterogeneous group of tumours, of which angiosarcoma is the most common [17].

Clinical and Epidemiological Features

Patients present with a breast lump or a radiologically detected mass. Patients with angiosarcoma may have a prior history of radiation, and the overlying skin can be discoloured.

Imaging Features

Sarcoma usually presents as an ill-defined and lobulated mass. It shows variable internal echogenicity on sonography and may appear heterogeneously hyperechoic.

Pathologic Features

Macroscopic Pathology

Grossly, sarcomas show fleshy, whitish appearances with ill-defined outlines (Fig. 11.84). Angiosarcomas are haemorrhagic, and there may be blood clots.

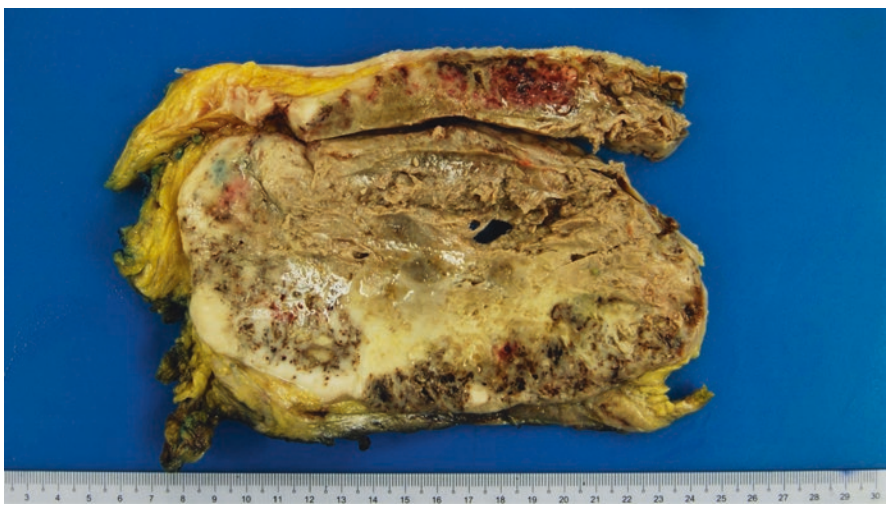

Fig. 11.84 Breast osteosarcoma. This large, necrotic tumour shows haemorrhagic and fibrotic areas. Primary sarcoma of the breast is extremely rare and is a diagnosis of exclusion, after metaplastic carcinoma and malignant phyllodes tumour are excluded

Microscopic Pathology

Spindle cells of varying degrees of anaplasia are present. For angiosarcomas, vascular spaces can be observed among the spindle cells or may occur as intracytoplasmic lumens containing red blood cells. Malignant osteoid is seen in osteosarcoma (Figs. 11.85 and 11.86), myxochondroid elements in chondrosarcoma, and rhabdomyoblasts in rhabdomyosarcoma (Figs. 11.87, 11.88, 11.89, 11.90, and 11.91). Lineage such as smooth muscle and neural differentiation may also be demonstrated by immunohistochemistry. Granulocytic sarcoma is an extramedullary tumour-forming collection of myeloid leukaemic cells (Figs. 11.92, 11.93, and 11.94).

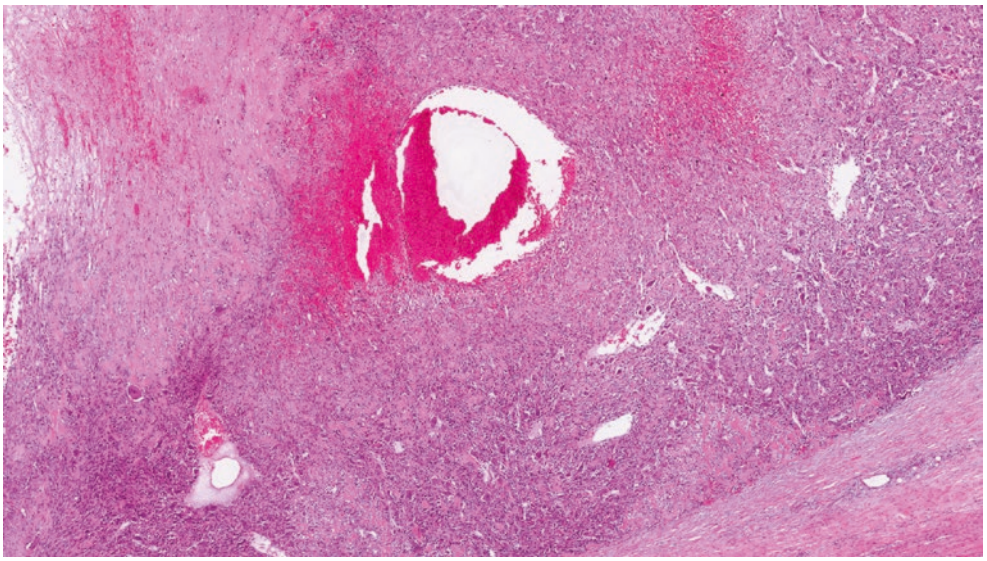

Fig. 11.85 Breast osteosarcoma. Sheets of malignant spindle cells are present, with a few ectatic, thin-walled vessels and an area of haemorrhage

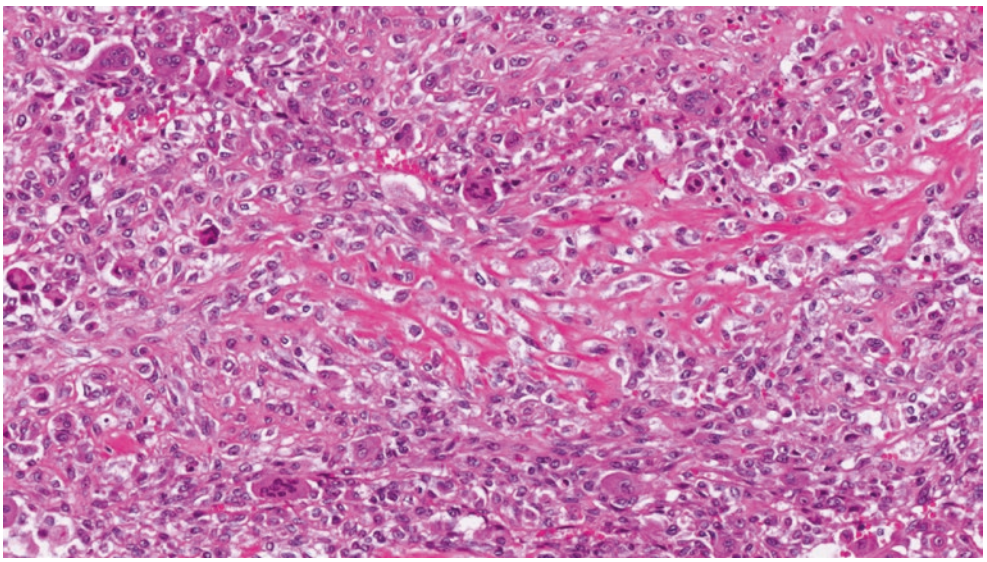

Fig. 11.86 Breast osteosarcoma. Spindle and epithelioid malignant cells show pink, lace-like material consistent with osteoid. Osteoclastic giant cells are noted

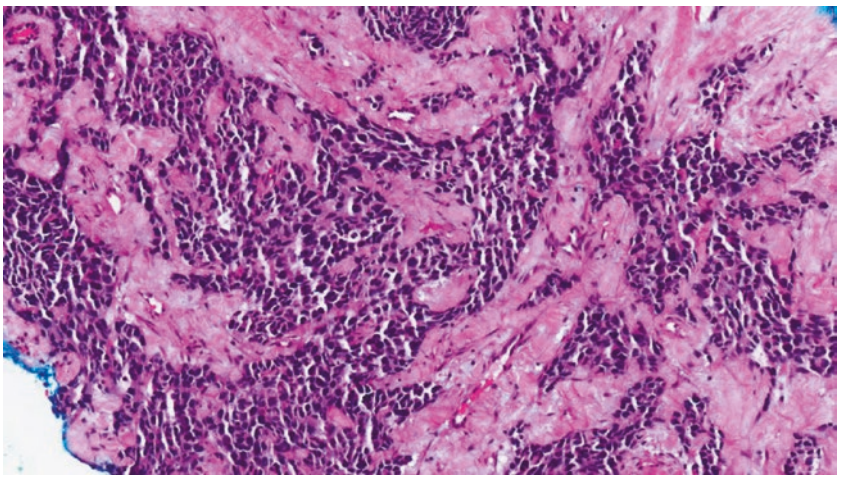

Fig. 11.87 Rhabdomyosarcoma metastatic to the breast in a young girl who was previously diagnosed with nasal rhabdomyosarcoma. Histologically, there are anastomosing aggregates of cells with hyperchromatic nuclei and thin, pink cytoplasmic rims. The nested pattern mimics carcinoma

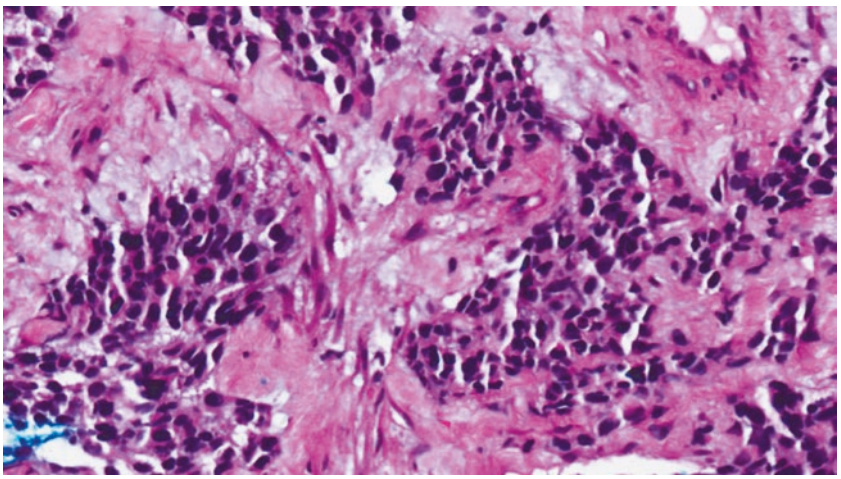

Fig. 11.88 Metastatic rhabdomyosarcoma. At high magnification, tumour cells show moderately pleomorphic nuclei with vaguely discernible pink, cytoplasmic rims

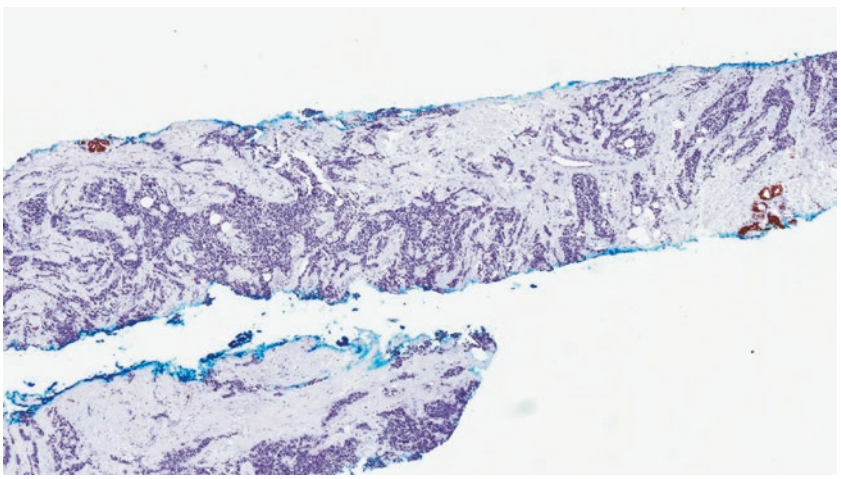

Fig. 11.89 Metastatic rhabdomyosarcoma. Immunohistochemistry for MNF116 is negative in this tumour. Tumour cells invade the breast parenchyma between benign breast lobules and are positively displayed by the broad-spectrum keratin stain

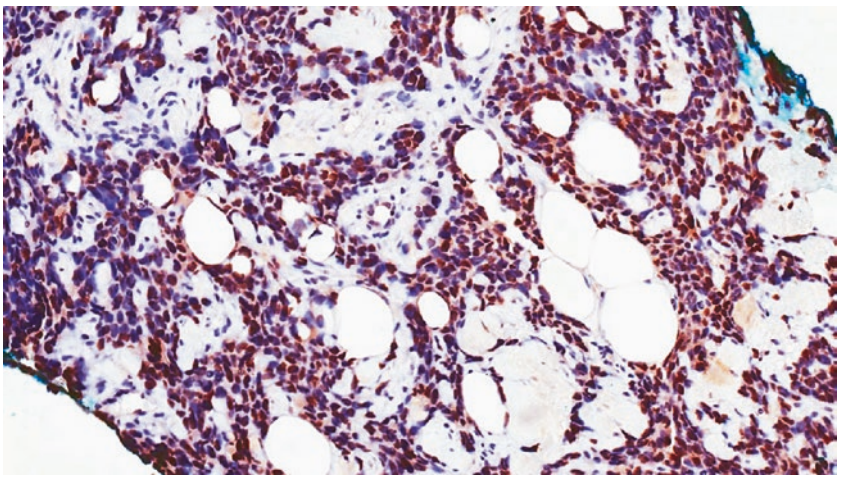

Fig. 11.90 Metastatic rhabdomyosarcoma. MyoD1 immunohistochemistry shows positive nuclear staining in the majority of tumour cells

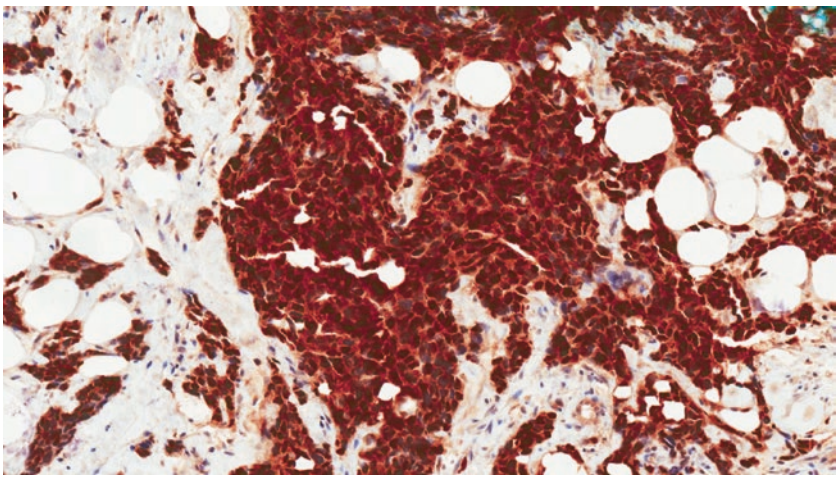

Fig. 11.91 Metastatic rhabdomyosarcoma. Myogenin is diffusely highlighted in tumour cells on immunohistochemistry

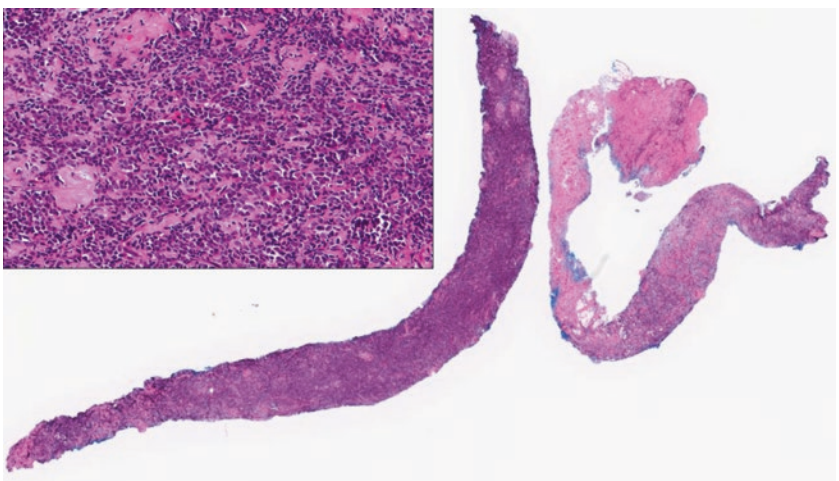

Fig. 11.92 Granulocytic sarcoma. Core biopsy of a breast mass shows a diffuse infiltrate of hyperchromatic tumour cells, which on higher magnification (*inset*) shows a semblance of compartmentalisation. Although "sarcoma" may be a misnomer (this tumour is derived from haemopoietic cells), its histological appearance may resemble sarcomas arising from a mesenchymal origin

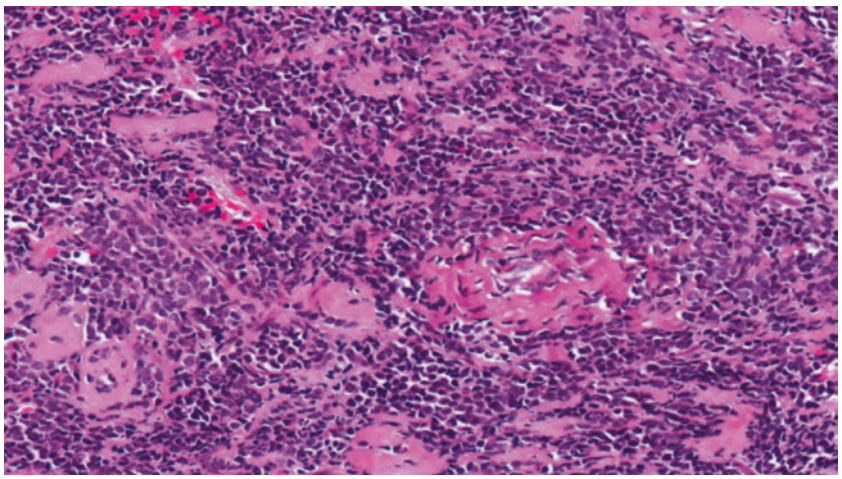

Fig. 11.93 Granulocytic sarcoma. High magnification shows tumour cells with ovoid nuclei with irregular nuclear contours

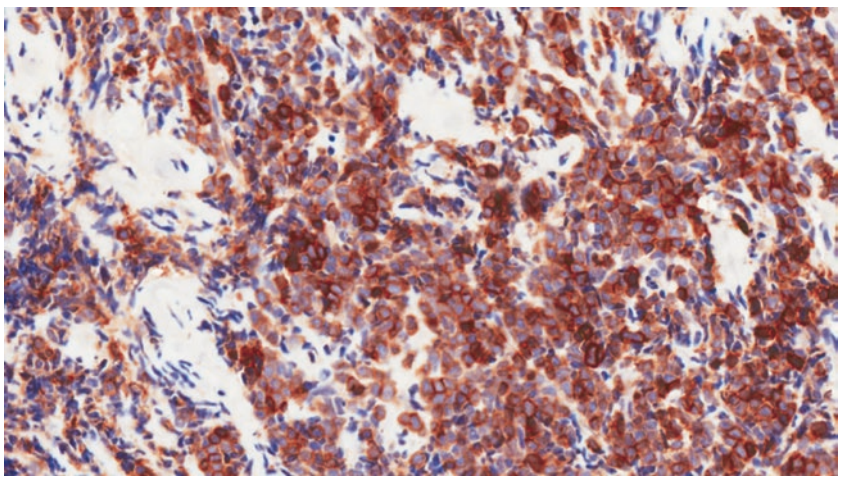

Fig. 11.94 Granulocytic sarcoma. Immunohistochemistry for CD117 shows cytoplasmic reactivity of tumour cells

Differential Diagnosis

Metaplastic Carcinoma

This is a key differential diagnosis, and clues are the presence of more conventional invasive carcinoma components or identification of ductal carcinoma in situ. In their absence, immunohistochemical demonstration of keratin expression by sarcomatoid cells enables the diagnosis.

Malignant Phyllodes Tumour

Diagnosis of sarcoma warrants exclusion of a malignant phyllodes tumour, which (though rare) is more common than primary breast sarcoma. Heterologous elements of liposarcoma, osteosarcoma, chondrosarcoma, or rhabdomyosarcoma can be encountered in malignant phyllodes tumours. Diligent sampling of the tumour to locate the typical phyllodal fronds is needed.

Metastatic Sarcoma to the Breast

Uncommonly, primary sarcomas originating elsewhere in the body may metastasise to the breast. Appropriate clinical history and clinicoradiological workup are useful.

Prognosis and Therapy Considerations

Breast sarcoma in general tends to have a poorer prognosis than breast carcinoma, though the prognosis may depend on the specific histological subtype. Complete surgical resection with negative margins is the main therapeutic modality. A multidisciplinary management approach is needed, with possible targeted treatment for angiosarcoma (Table 11.1) [17].

Table 11.1 Comparison of clinicopathological features of key spindle cell lesions of the breast

	Nodular fasciitis	Fibrous scar	Fibromatosis	Fibromatosis-like metaplastic carcinoma	Spindle cell metaplastic carcinoma	Phyllodes tumour	Sarcoma
Clinical information	Rapid growth Tissue plane usually subcutis or chest wall rather than breast parenchyma	Prior instrumentation or tissue injury	Rare association with breast implants	Clinicoradiologically similar to breast carcinoma, may be radiologically circumscribed	Symptomatic or radiologically detected breast mass	Usually large lump, may have history of recent rapid growth	Symptomatic or radiologically detected breast mass. May have past diagnosis of sarcoma if metastatic in origin
Histological pattern	"Feathery" tissue culture-like appearance with red cell extravasation and chronic inflammation	Depending on duration between tissue injury and biopsy, changes range from reactive granulation to collagenous fibrosis. Haemosiderin deposits may be present	Intersecting fascicles of spindle cells with wavy nuclei, minimal atypia, and scant mitoses	Intersecting fascicles of spindle cells with modest nuclear atypia and low mitotic activity Squamous and epithelioid foci may be present May be associated with papilloma, complex sclerosing lesion	Spindle cells with nuclear pleomorphism and mitoses. Squamous foci, DCIS may be present	Spindle cells with variable nuclear atypia The presence of stromal fronds with accompanying stromal hypercellularity is characteristic	Spindle cell morphology with wide-ranging appearances depending on the lineage
Keratins	Negative	Negative	Negative	Positive	Positive (a wide antibody panel may be needed)	Negative, but may sometimes show focal positivity	Mostly negative but can be focally positive
Beta-catenin	Negative	Negative	Positive	May be positive	May be positive	Negative, but aberrant expression is reported	May be positive in fibrosarcoma
CD34	Negative	Negative	Negative	Negative	Negative	Often positive, inverse correlation with grade	Negative

DCIS ductal carcinoma in situ

References

1. Polat P, Kantarci M, Alper F, Gursan N, Suma S, Okur A. Nodular fasciitis of the breast and knee in the same patient. Am J Roentgenol. 2002;178:1426–8.
2. Son YM, Nahm JH, Moon HJ, Kim MJ, Kim EK. Imaging findings for malignancy-mimicking nodular fasciitis of the breast and a review of previous imaging studies. Acta Radiol Short Rep. 2013;2:2047981613512830.
3. Brogi E. Benign and malignant spindle cell lesions of the breast. Semin Diagn Pathol. 2004;21:57–64.
4. Gocht A, Bösmüller HC, Bässler R, Tavassoli FA, Moinfar F, Katenkamp D, et al. Breast tumors with myofibroblastic differentiation: clinico-pathological observations in myofibroblastoma and myofibrosarcoma. Pathol Res Pract. 1999;195:1–10.
5. Taccagni G, Rovere E, Masullo M, Christensen L, Eyden B. Myofibrosarcoma of the breast: review of the literature on myofibroblastic tumors and criteria for defining myofibroblastic differentiation. Am J Surg Pathol. 1997;21:489–96.
6. Mizuta N, Sakaguchi K, Mizuta M, Imai A, Nakatsukasa K, Morita M, et al. Myoid hamartoma of the breast that proved difficult to diagnose: a case report. World J Surg Oncol. 2012;10:12.
7. Magro G, Longo FR, Salvatorelli L, Vasquez E, Vecchio GM. Lipomatous myofibroblastoma of the breast: case report with diagnostic and histogenetic considerations. Pathologica. 2014;106:36–40.
8. Dwyer JB, Clark BZ. Low-grade fibromatosis-like spindle cell carcinoma of the breast. Arch Pathol Lab Med. 2015;139:552–7.
9. Gobbi H, Simpson JF, Jensen RA, Olson SJ, Page DL. Metaplastic spindle cell breast tumors arising within papillomas, complex sclerosing lesions, and nipple adenomas. Mod Pathol. 2003;16:893–901.
10. Lacroix-Triki M, Geyer FC, Lambros MB, Savage K, Ellis IO, Lee AH, Reis-Filho JS. β-catenin/Wnt signalling pathway in fibromatosis, metaplastic carcinomas and phyllodes tumours of the breast. Mod Pathol. 2010;23:1438–48.
11. Takano EA, Hunter SM, Campbell IG, Fox SB. Low-grade fibromatosis-like spindle cell carcinomas of the breast are molecularly exiguous. J Clin Pathol. 2015;68:362–7.

12. Reis-Filho JS, Lakhani SR, Gobbi H, Sneige N. Metaplastic carcinoma. In: Lakhani SR, Ellis IO, Schnitt SJ, Tan PH, van de Vijver MJ, editors. WHO classification of tumours of the breast. Lyon: IARC Press; 2012. p. 48–52.
13. Rakha EA, Aleskandarany MA, Lee AH, Ellis IO. An approach to the diagnosis of spindle cell lesions of the breast. Histopathology. 2016;68:33–44.
14. Chia Y, Thike AA, Cheok PY, Chong LY, Tse GM, Tan PH. Stromal keratin expression in phyllodes tumours of the breast: a comparison with other spindle cell breast lesions. J Clin Pathol. 2012;65:339–47.
15. Tan BY, Acs G, Apple SK, Badve S, Bleiweiss IJ, Brogi E, et al. Phyllodes tumours of the breast: a consensus review. Histopathology. 2016;68:5–21.
16. Cimino-Mathews A, Sharma R, Illei PB, Vang R, Argani P. A subset of malignant phyllodes tumors express p63 and p40: a diagnostic pitfall in breast core needle biopsies. Am J Surg Pathol. 2014;38:1689–96.
17. Lim SZ, Ong KW, Tan BK, Selvarajan S, Tan PH. Sarcoma of the breast: an update on a rare entity. J Clin Pathol. 2016;69:373–81.
18. Schnitt SJ. Spindle cell lesions of the breast. Surg Pathol. 2009;2:375–90.
19. McMenamin ME, DeSchryver K, Fletcher CDM. Fibrous lesions of the breast. A review. Int J Surg Pathol. 2000;8:99–108.
20. Lee SJ, Mahoney MC, Shaughnessy E. Dermatofibrosarcoma protuberans of the breast: imaging features and review of the literature. AJR Am J Roentgenol. 2009;193:W64–9.
21. Cribier B, Noacco G, Peltre B, Grosshans E. Stromelysin 3 expression: a useful marker for the differential diagnosis dermatofibroma versus dermatofibrosarcoma protuberans. J Am Acad Dermatol. 2002;46:408–13.

Invasive Carcinoma

12

Most breast malignancies arise from epithelial cells of terminal ductal lobular units and are categorised as carcinomas [1–3]. Invasive or infiltrative carcinoma refers to a proliferation of neoplastic cells with penetration through the basement membrane of ducts and lobular units into the breast stroma. Breast carcinoma, although often discussed as a single disease, actually constitutes a diverse group of tumours that differ in clinical presentation, imaging features, histopathologic appearance, expression of biologic markers, and clinical behaviour. Several histological subtypes of invasive breast carcinoma have been recognised based on a wide range of criteria, including cell type, architectural features, type and location of secretions, and biomarker profiles. The WHO classification of breast tumours recognises 21 different histologic types of breast cancer with distinct morphologic features [1]:

- Invasive ductal carcinoma (invasive carcinoma no special type, invasive carcinoma not otherwise specified)
- Invasive lobular carcinoma
- Tubular carcinoma
- Invasive cribriform carcinoma
- Mucinous carcinoma
- Carcinoma with medullary features
- Carcinoma with apocrine differentiation
- Carcinoma with signet-ring cell differentiation
- Invasive micropapillary carcinoma
- Metaplastic carcinoma
- Carcinoma with neuroendocrine features
- Secretory carcinoma
- Invasive papillary carcinoma
- Acinic cell carcinoma
- Mucoepidermoid carcinoma
- Polymorphous carcinoma
- Oncocytic carcinoma
- Lipid-rich carcinoma
- Glycogen-rich clear-cell carcinoma
- Sebaceous carcinoma
- Salivary gland/skin adnexal-type tumours

Invasive breast cancers are broadly classified into invasive carcinomas with special morphologic types and invasive carcinomas without any special morphologic features. When an invasive carcinoma does not have any special histologic features, the terms *invasive or infiltrative ductal carcinoma*, *invasive carcinoma no special type*, or *invasive carcinoma not otherwise specified* are used. Some special types of breast carcinomas have relevant prognostic implications, and it is clinically important to recognise them. Others have unique morphologic features but have no special biologic behaviour associated with the special morphology. Mucinous carcinoma is described in Chap. 6; invasive lobular carcinoma is detailed in Chap. 10; invasive papillary and micropapillary carcinomas are included in Chap. 4. Some of the vanishingly rare subtypes are not specifically described.

Invasive Ductal Carcinoma (Invasive Carcinoma No Special Type, Invasive Carcinoma Not Otherwise Specified)

Definition

Invasive ductal carcinoma or infiltrative ductal carcinoma is defined as an invasive breast cancer with histologic features that do not fit any of the special types of breast cancer. Therefore, the diagnosis of invasive ductal carcinoma is based on the exclusion of other special types of breast cancers [1–3].

Clinical and Epidemiological Features

Invasive ductal carcinoma constitutes 45–75 % of all invasive breast carcinomas and comprises a heterogeneous group of tumours. The main reason for the wide incidence range reported in the literature is that many breast cancers show focal components of special types of breast carcinoma [4–7].

P.H. Tan, A.A. Sahin, *Atlas of Differential Diagnosis in Breast Pathology*, Atlas of Anatomic Pathology,
DOI 10.1007/978-1-4939-6697-4_12

Many invasive carcinomas show a mixture of growth patterns, and some experts recognise a mixed invasive ductal and special-type carcinoma category. The amount of special-type carcinoma that is required for a tumour to be categorised into a mixed category is not well established in the literature. For tumours with excellent prognosis, such as tubular carcinoma or invasive cribriform carcinoma, more than 90 % of the tumour must be special type in order to classify it as such. In the case of other types of special carcinomas, however, there are no established criteria for designating a tumour as a mixed category or simply classifying it as an invasive ductal carcinoma. The term "ductal" does not imply that these tumours arise from ducts; rather, it indicates that these tumours commonly show ductal differentiation.

There are no specific clinical features that distinguish invasive carcinoma of no special type from other types of invasive breast cancer. Invasive ductal carcinoma occurs in a wide age range [1]. Although it can occur at any age, it is more common in the fifth and sixth decades. In most series, the average age is 55–60 years. The incidence decreases after age 80. A painless, palpable mass is the most common presentation. Nipple discharge or retraction, skin fixation, or oedema can be seen in advanced cases. Some patients present with redness of the breast skin (inflammatory breast carcinoma) (Fig. 12.1). The average tumour size at the time of diagnosis is about 2 cm. Patients diagnosed from screening mammography tend to have smaller lesions [8].

Imaging Features

Invasive ductal carcinomas most commonly present as masses on radiology. Because of its infiltrative growth pattern, it usually appears irregular and lobulated on mammography, in contrast to benign mass-forming lesions, which tend to be round or oval (Fig. 12.2). Margins of the mass are typically irregular, with spiculated borders corresponding to an invasive growth pattern on histologic evaluation (Fig. 12.3). Microcalcifications (grouped, clustered, or segmental in appearance) are commonly found on mammography (Fig. 12.4). Microcalcifications are more frequently associated with the in situ carcinoma component of the tumour, though the stroma of invasive carcinoma or necrosis within the invasive carcinoma can also show microcalcifications. Ultrasound typically reveals an irregular mass with indistinct margins and inhomogeneous echo texture with

Fig. 12.1 Inflammatory breast carcinoma shows reddened skin over the breast, which may feel warm. Histologically, it corresponds to the presence of dermal lymphovascular emboli (Courtesy of Dr. Benita Tan)

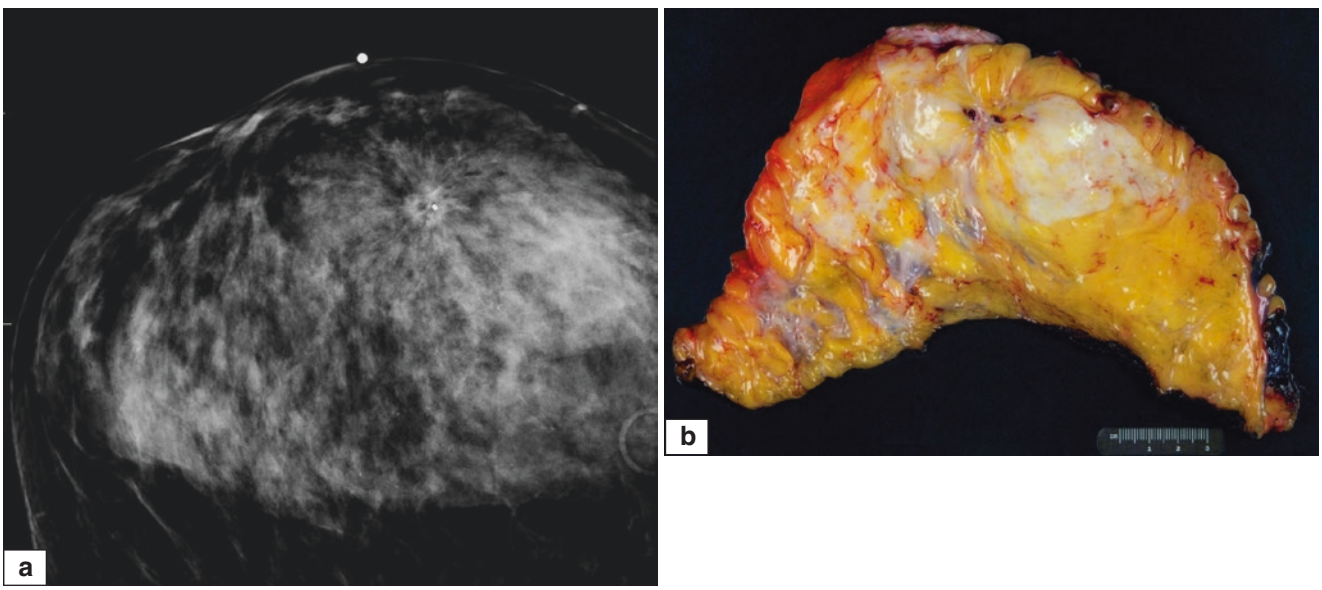

Fig. 12.2 Invasive ductal carcinoma. Radiographic and gross features. (**a**) Mammogram shows a radiodense mass with irregular, infiltrating borders. (**b**) Mastectomy specimen shows a grey-white mass invading the fatty breast parenchyma

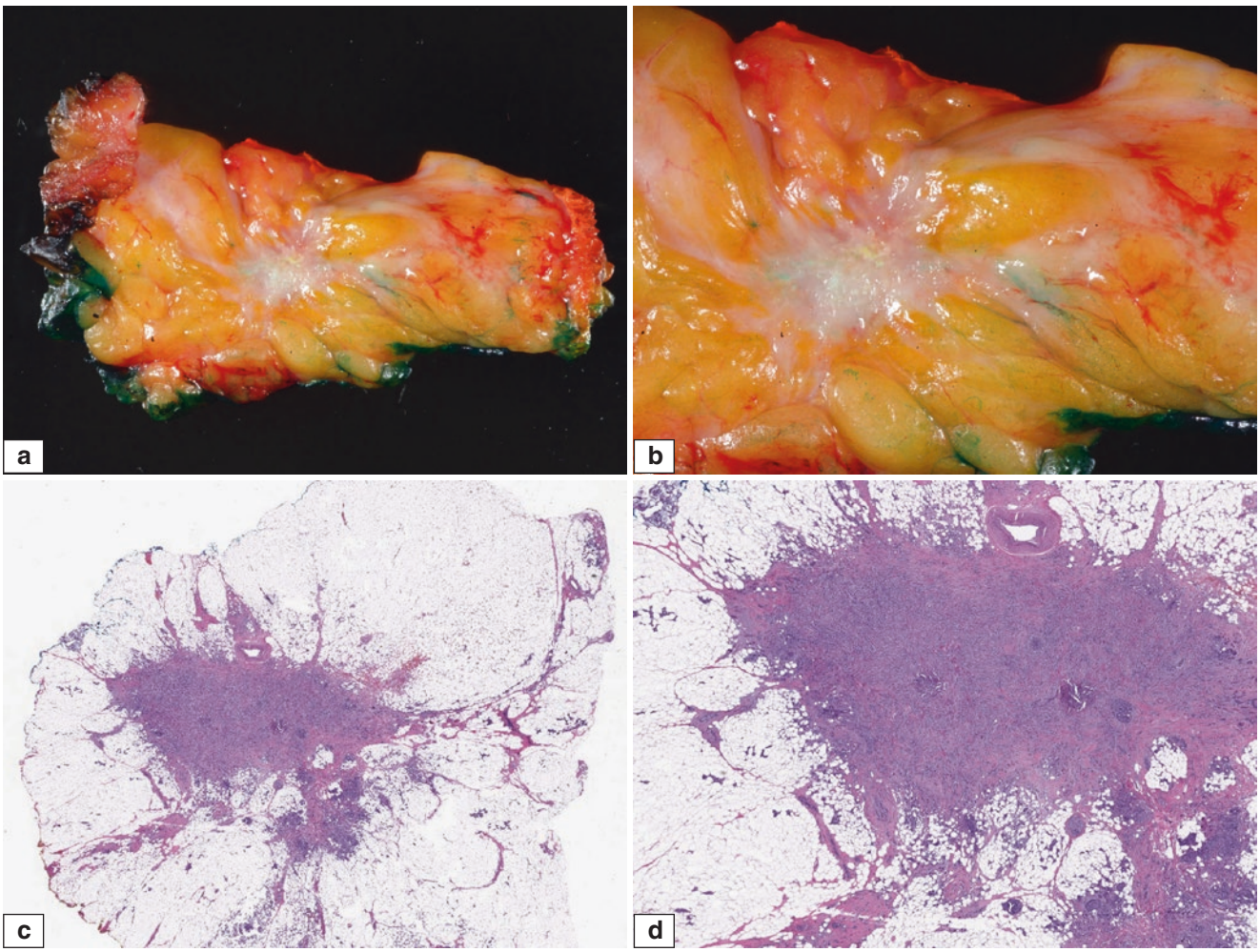

Fig. 12.3 Invasive ductal carcinoma. Gross and microscopic features. (**a**, **b**) Strands of grey-white tissue infiltrate the adipose tissue. (**c**, **d**) Histologic sections of the tumour show tumour cells growing into adipose tissue with associated fingerlike projections corresponding to the infiltrative gross appearance

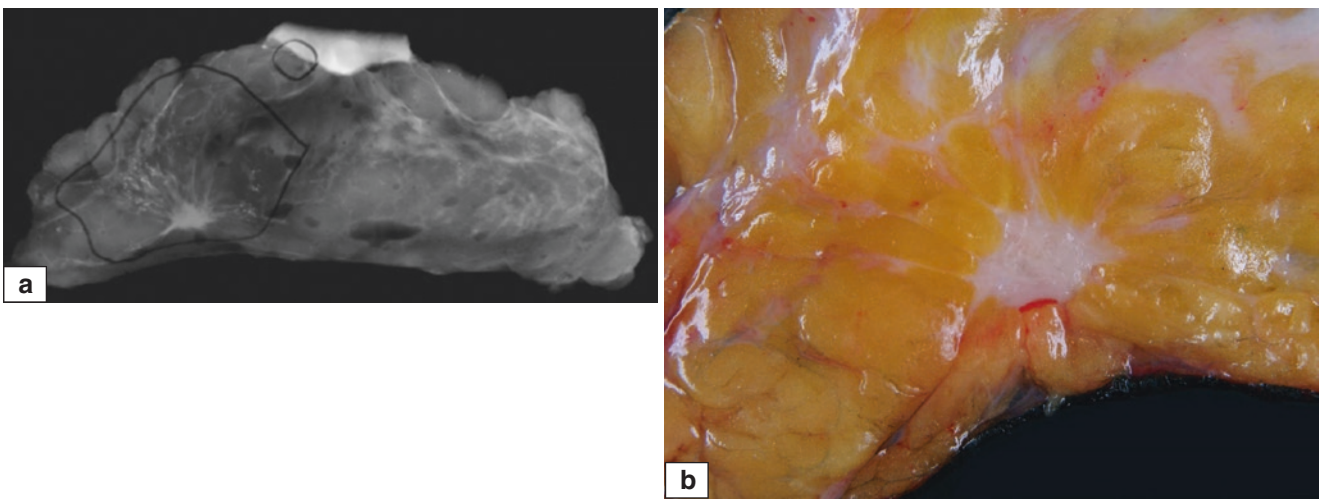

Fig. 12.4 Invasive ductal carcinoma. Radiographic and gross features. (**a**) X-ray of an irregular tumour mass associated with a large area of microcalcifications. (**b**) Corresponding irregular grey-white mass with white, fibrous streaks indicating tumour extension

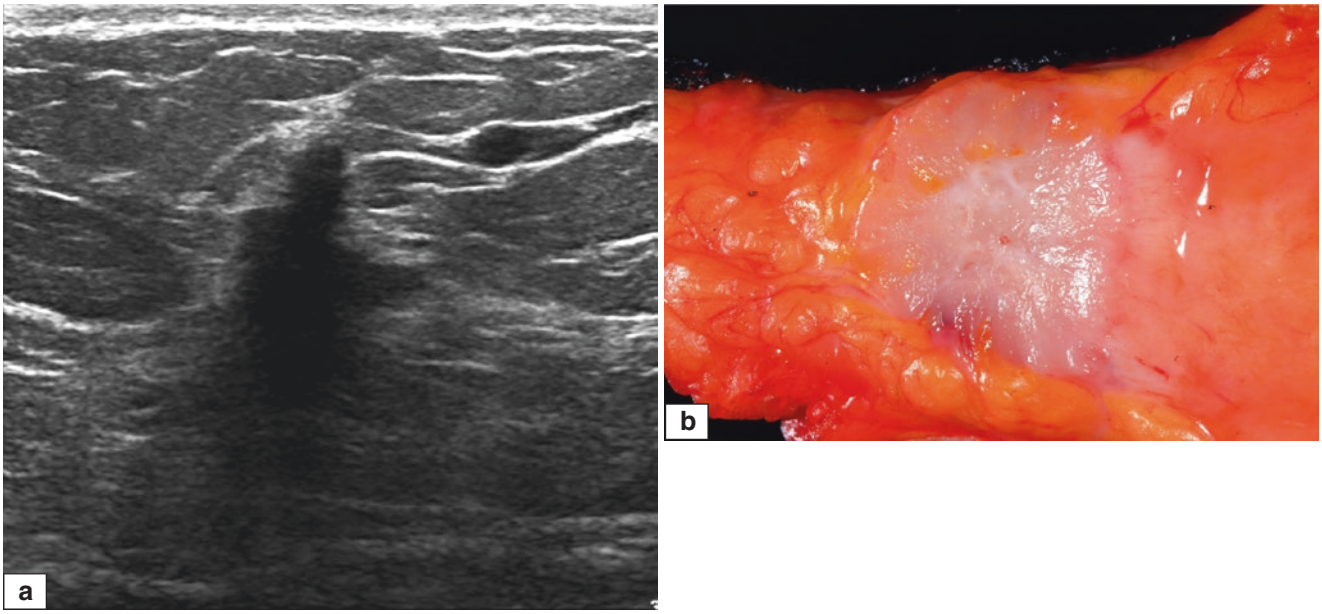

Fig. 12.5 Invasive ductal carcinoma. Sonographic and gross features. (**a**) Tumour appears as a hypoechoic mass with posterior shadowing. (**b**) Corresponding excised specimen shows an irregular mass

acoustic shadowing (Fig. 12.5) [9]. On MRI, invasive carcinoma usually appears as an irregular mass with enhancement kinetics that show a suspicious rapid wash-in and wash-out pattern. Several other functional MRI techniques are also applied to improve the diagnostic evaluation.

Pathologic Features

Macroscopic Pathology

Most invasive ductal carcinomas form solid masses with ill-defined margins and infiltrative edges (Fig. 12.6) or are round and circumscribed with pushing margins (Fig. 12.7). Some tumours have contours with a mixture of these patterns (Fig. 12.8). The consistency and colour of the lesion vary based on the amount of stroma present within the tumour. Invasive carcinomas with an abundant stromal component appear more grey-white and tend to be firm on palpation. In contrast, tumours with less stroma appear tan or yellow and are softer (Fig. 12.9). Certain tumours appear red-brown, not only because of dense cellularity but also because of other morphologic features such as papillary growth pattern and intratumoural haemorrhage (Fig. 12.10). These tumours typically have a concave cut surface as a distinguishing feature, in contrast to benign lesions such as fibroadenomas, which have convex, bulging cut sections (Fig. 12.11). Cystic change can rarely be present and is usually due to tumour necrosis (Figs. 12.12 and 12.13).

Because the tumour size is an important prognostic factor of breast cancer, macroscopic evaluation of tumour size is essential, with careful measurement expressed in three dimensions. Dimensions of smaller tumours are confirmed microscopically. Satellite tumour nodules may be present (Fig. 12.14).

Microscopic Pathology

The microscopic appearance of invasive ductal carcinoma is highly variable [1–3]. The degree of tumour cellularity, growth pattern, extent of associated in situ carcinoma component, degree of cytologic atypia, mitotic activity, amount of stroma, presence or absence of necrosis, and the presence and amount of lymphocytic infiltrate in the stroma and among tumour cells all vary significantly in different tumours. Some of these features may even differ in different areas of the same tumour [10–13]. Tumour cells may show varying degrees of gland formation (Fig. 12.15); may form nests, cords, or trabeculae; or may grow in solid sheets. Necrosis may be present and can be extensive, potentially leading to pseudocyst formation. The appearance of malignant cells varies significantly. Some tumours have minimal cellular atypia and pleomorphism; the tumour cells are small and uniform, similar to the cells of normal duct epithelium. In other tumours, there can be marked cellular atypia and pleomorphism, with tumour cells that have enlarged, hyperchromatic nuclei (Fig. 12.16). The degree of mitotic activity varies significantly, from abundant and easily identified to almost none. Focal mucin production (both intracellular and extracellular) can sometimes be seen. Squamoid, clear-cell, and apocrine differentiation are other histologic findings that can be observed. Similar to tumour cells, the stroma may display marked variation in its amount, composition, and distribution. The amount of

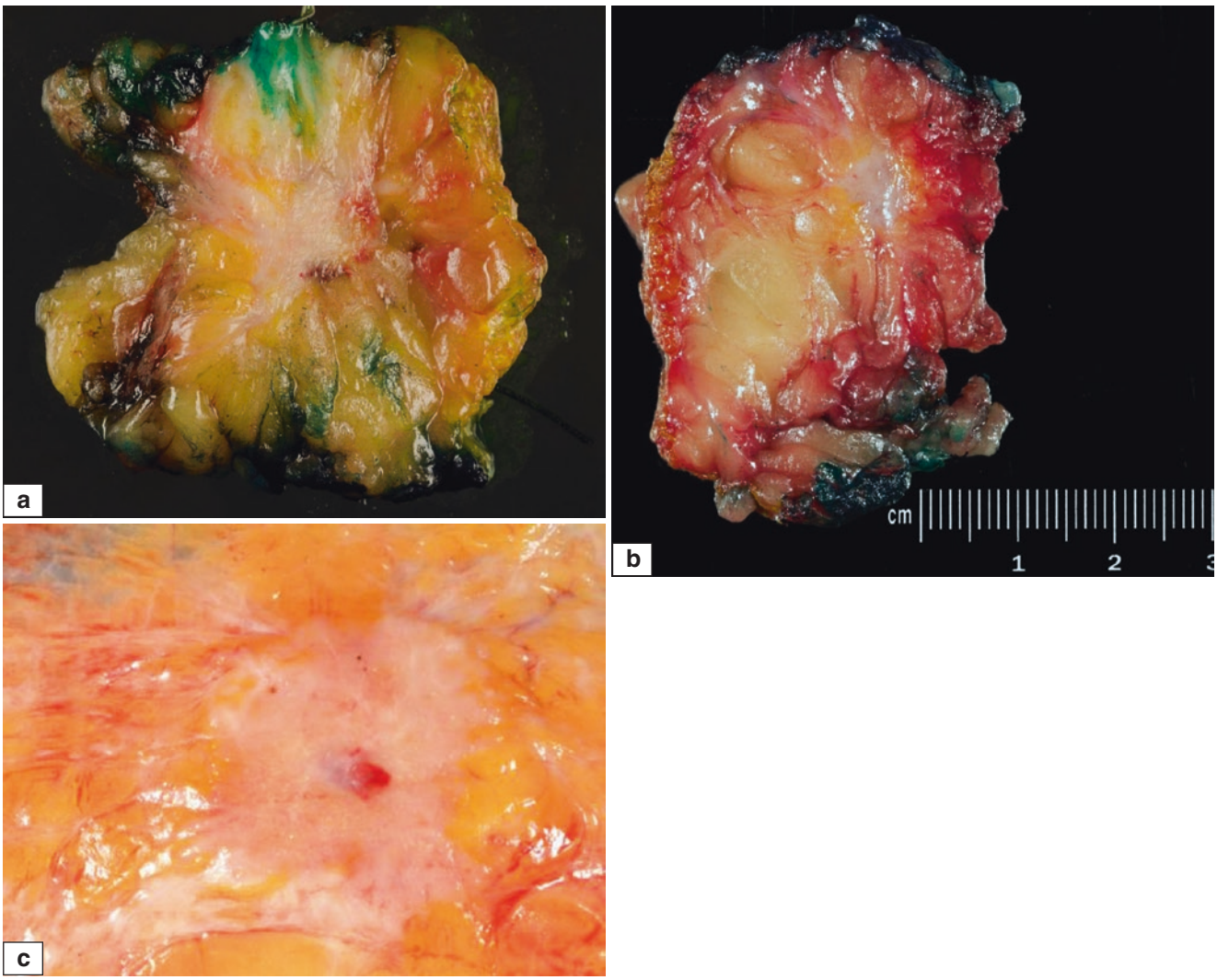

Fig. 12.6 Invasive ductal carcinoma. Gross features. (**a–c**) Different examples of invasive ductal carcinoma showing typical infiltrative margins

stroma can range from none to abundant (Fig. 12.17). Some tumours have large amounts of dense, hyalinised stroma resulting in a very firm consistency, termed *scirrhous carcinoma*. In some tumours, the stroma consists of only collagen, whereas others are cellular and include fibroblasts and myofibroblasts (Fig. 12.18). Elastosis can be present. Stromal distribution throughout the tumour is also variable. Tumour cells may proliferate around the central sclerotic stromal component, but in other tumours, the stroma is uniformly distributed (Figs. 12.19 and 12.20). Calcifications can be detected in more than half of the cases. Additionally, the amount of lymphoplasmacytic infiltrate in tumour and stroma varies considerably, from moderate or marked to none (Fig. 12.21). Recent studies have suggested that the amount of lymphoplasmacytic infiltrate may have a prognostic and potentially predictive value, particularly in triple-negative and c-erbB-2-overexpressing breast cancers [14]. Osteoclast-like giant cells or giant-cell granulomas are rarely seen in the stroma. With adequate sampling of the tumour, an in situ carcinoma component can be identified in most cases of invasive ductal carcinomas (Fig. 12.22). The in situ component is most often ductal, but rarely it can be lobular. When ductal carcinoma in situ (DCIS) is identified, its grade is usually similar to that of the invasive component. The presence of lymphovascular invasion should be carefully evaluated in all invasive ductal carcinomas, preferably at the peripheral aspect of the tumour (Fig. 12.23) [15, 16]. Retraction artefacts that are commonly seen around clusters of tumour should not be confused with true lymphovascular space invasion. Unless a tumour embolus is identified in a large blood vessel, it is not recommended to try to distinguish small capillaries from lymphatics. Perineural invasion occasionally may be seen, but this finding is not of prognostic significance (Fig. 12.24) [17].

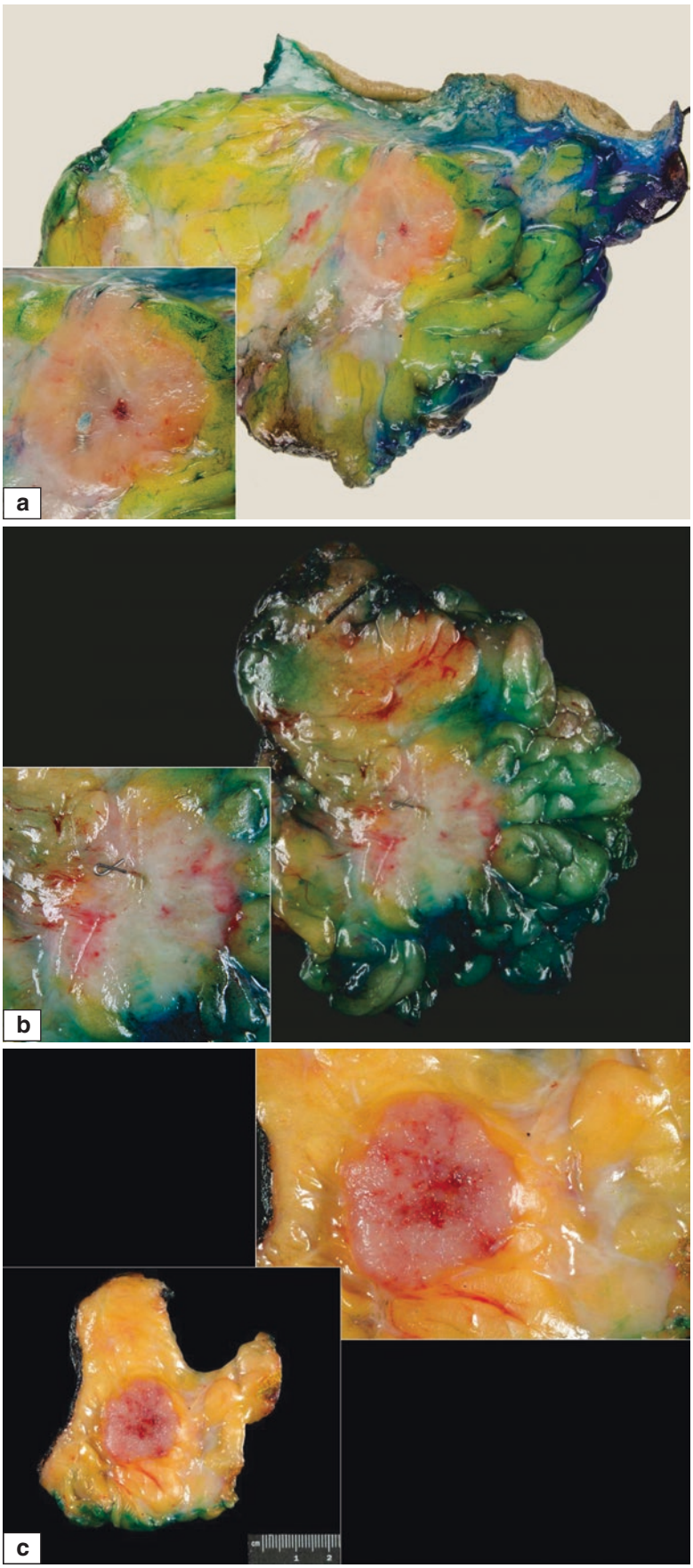

Fig. 12.7 Invasive ductal carcinoma. Gross features. (**a–c**) Tumour examples presenting with well-defined margins and pushing edges

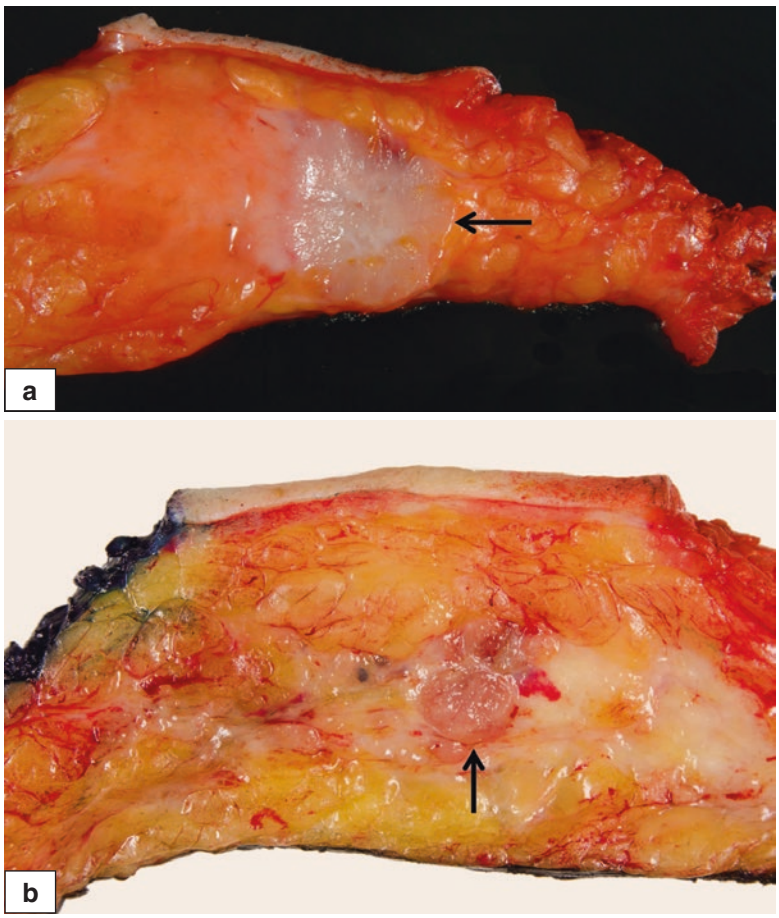

Fig. 12.8 Invasive ductal carcinoma. Gross features. (**a**, **b**) Examples showing both well-circumscribed (*arrow*) and infiltrative (*opposite side*) growth patterns in the same tumour

Grading of Invasive Ductal Carcinoma

Grading of invasive ductal carcinoma of the breast has been shown to be a robust predictor of clinical outcome [18–24]. Providing a grade for all newly diagnosed breast cancers has been recommended by several different breast cancer practice guidelines, including the College of American Pathologists (CAP), American Society of Clinical Oncology (ASCO) and the American Joint Committee on Cancer (AJCC). Several different grading systems using either nuclear features, architectural growth pattern, or a combination of these have been proposed [18, 21, 24]. The most widely used grading system is the Nottingham histologic grading, which was modified by Elston and Ellis [18] to include precise definitions. In this grading system, three tumour characteristics—tubule formation, nuclear pleomorphism, and mitotic count—are evaluated using defined criteria (Table 12.1). Each characteristic is assessed separately and given a score of 1–3, with the values being added to reach a final score of 3–9. Final grading is assigned based on this score, as shown in Table 12.2. The relative importance of the components of this grading system is uncertain, but it is essential to apply the histologic criteria strictly. The subjective nature of histologic grading and interobserver agreement rates have been extensively studied in the literature [19, 20]. Technical factors such as quality of tissue fixation, preservation, and section preparation are recognised as some of the main problems that contribute to poor interobserver reproducibility. Therefore, the well-defined guidelines recommended by the College of American Pathologists for tissue handling should be followed.

Several studies have evaluated the concordance rates of breast cancer grading on core needle biopsy and excision [25, 26]. Most studies show good concordance when there is adequate tumour on core needle biopsy. Tumour heterogeneity is a main concern when determining the grade of breast cancer on small samples. Reported studies suggest that a histologic grade can be reliably assessed from core needle biopsies in most cases. In clinical practice, the core needle biopsy specimen will be the only sample available for patients who are undergoing neoadjuvant therapies. Recent molecular studies emphasise the importance of histologic grading, as breast cancers with different grades show distinct molecular profiles at genomic, transcriptomic, and proteomic levels [13, 21].

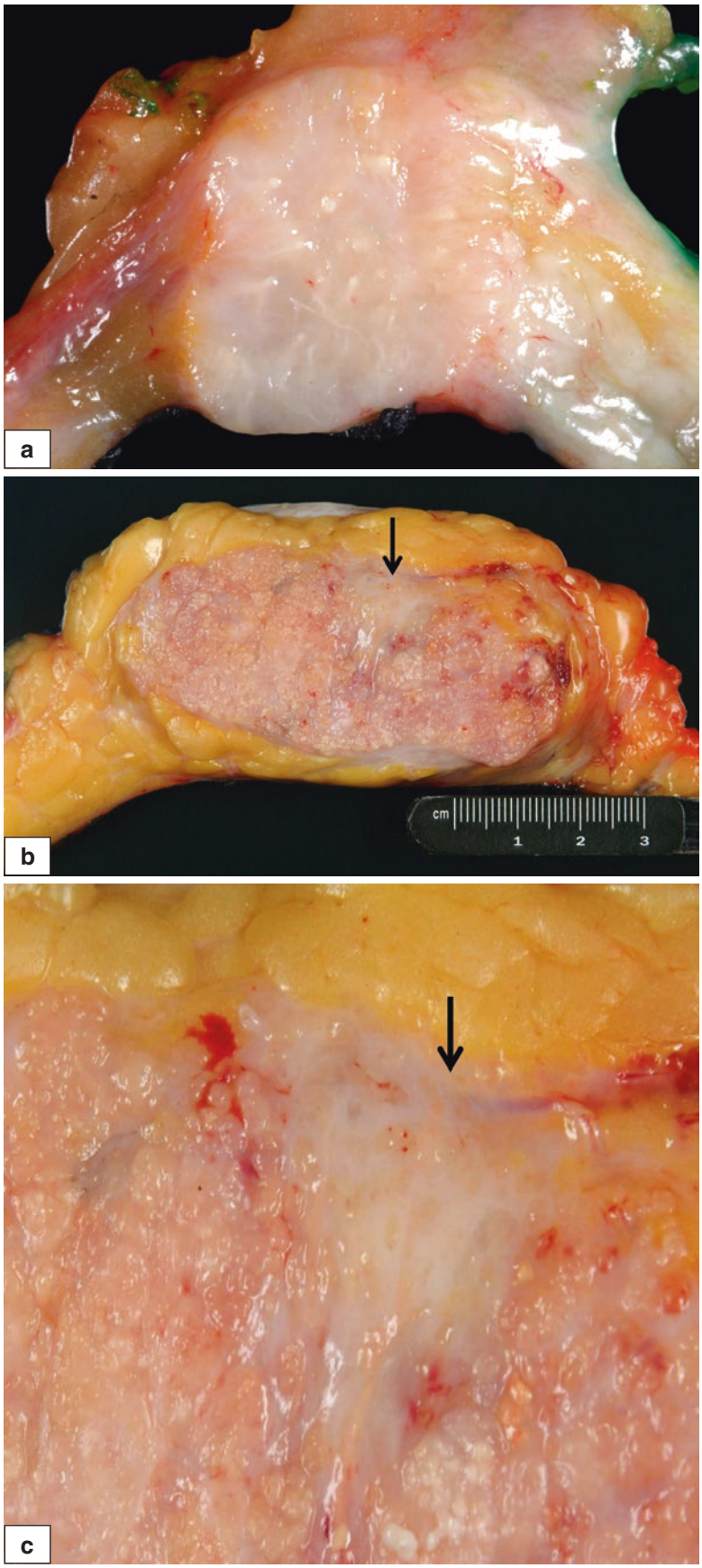

Fig. 12.9 Invasive ductal carcinoma. Gross features. (**a**) The white appearance of this tumour is due to extensive stromal fibrosis. (**b**) The grey-tan appearance of this large invasive tumour is due to high tumour cellularity and scant stroma. (**c**) Close-up of the tumour in (**b**) shows a white area indicating abundant stromal fibrosis (*arrow*) in a background of nodular tumour growth

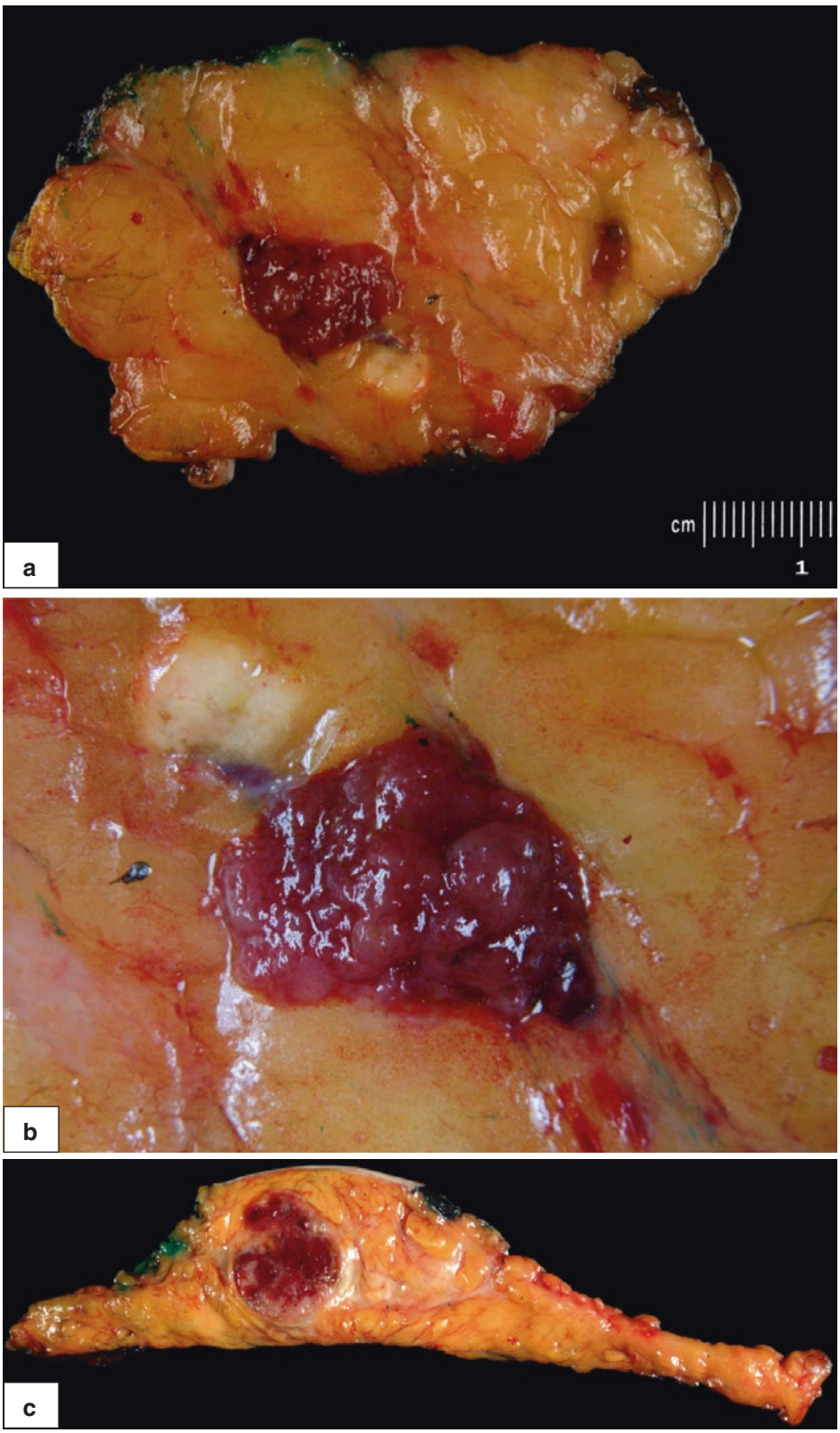

Fig. 12.10 Invasive ductal carcinoma. Gross features. (**a**) Invasive carcinoma with high tumour cellularity on histology, shows prominent papillary growth and a red-brown appearance. (**b**) Higher magnification of (**a**). (**c**) The red-brown colour of this intracystic tumour is due to intratumoural haemorrhage

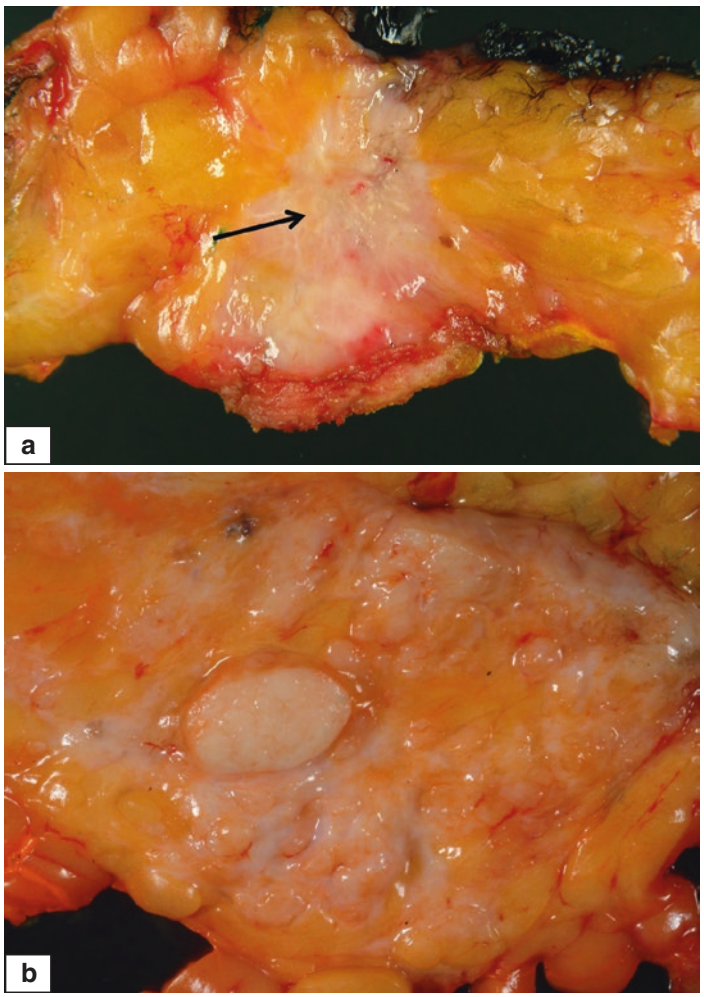

Fig. 12.11 Comparison of gross features of invasive ductal carcinoma and fibroadenoma. (**a**) Cut section of invasive ductal carcinoma is typically concave with central indentation. Yellow-white fibrous strands extending into and retracting the surrounding tissue result in a concave appearance with central indentation (*arrow*). (**b**) In contrast, the cut section of a fibroadenoma is bulging

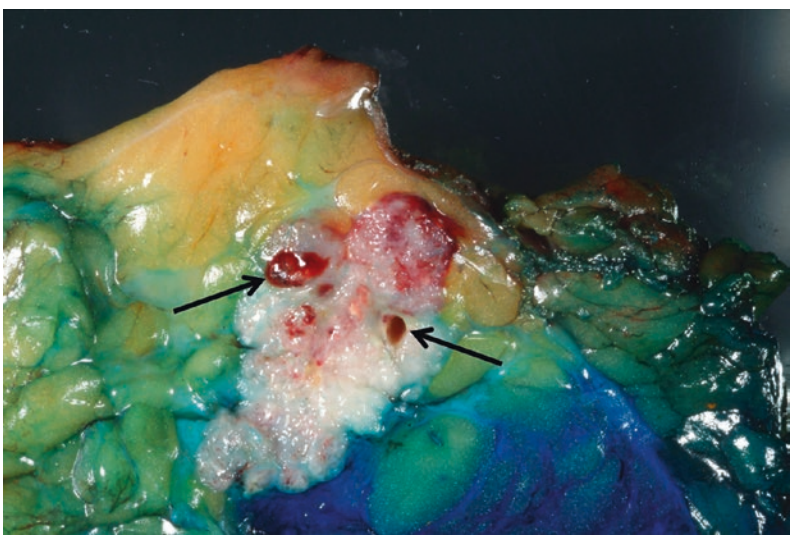

Fig. 12.12 Invasive ductal carcinoma. Gross features. Example of tumour with areas of haemorrhage and necrosis leading to cystic spaces (*arrows*)

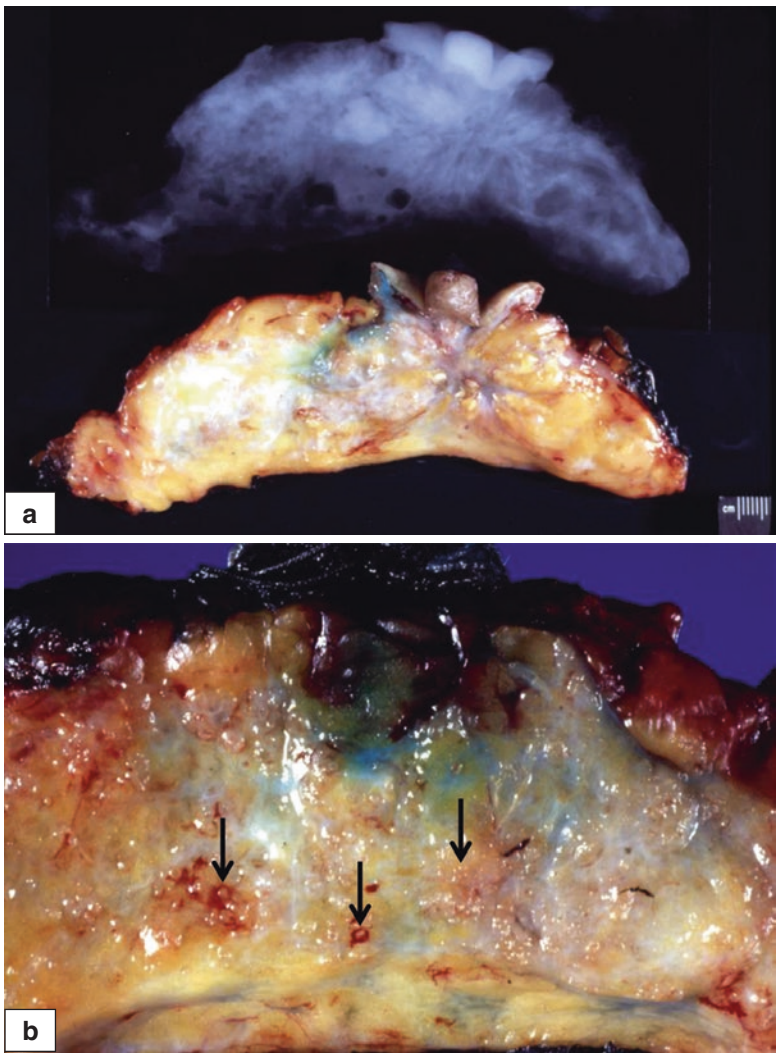

Fig. 12.13 Invasive ductal carcinoma. Radiographic and gross features. (**a**) X-ray of invasive ductal carcinoma in a section of a total mastectomy and its corresponding gross specimen showing an irregular grey-white mass replacing almost the entire breast parenchyma, involving the subareolar region. (**b**) Higher magnification shows a nodular growth pattern with areas of punctate necrosis (*arrows*)

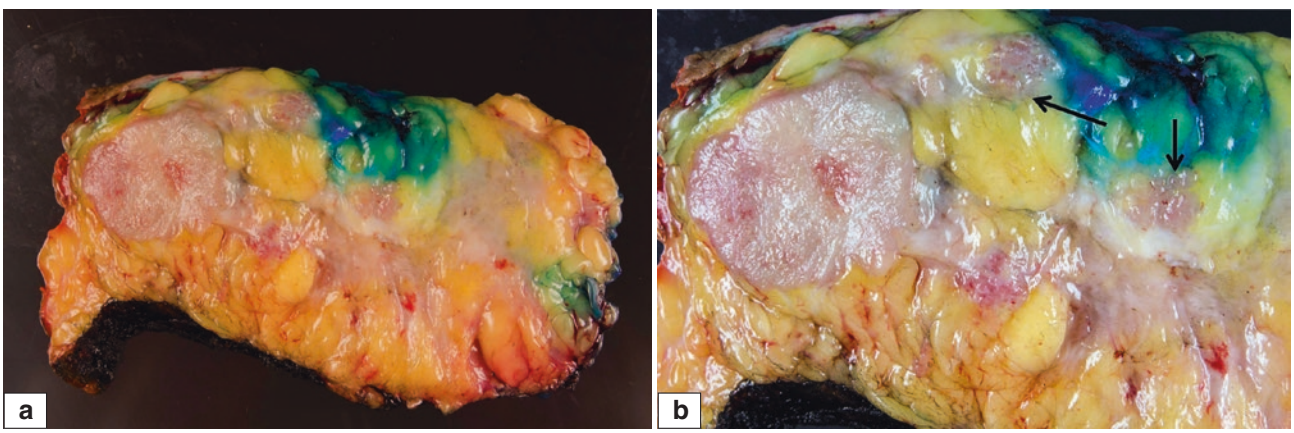

Fig. 12.14 Invasive ductal carcinoma. Gross features. (**a**, **b**) Invasive ductal carcinoma with satellite nodules (*arrows*)

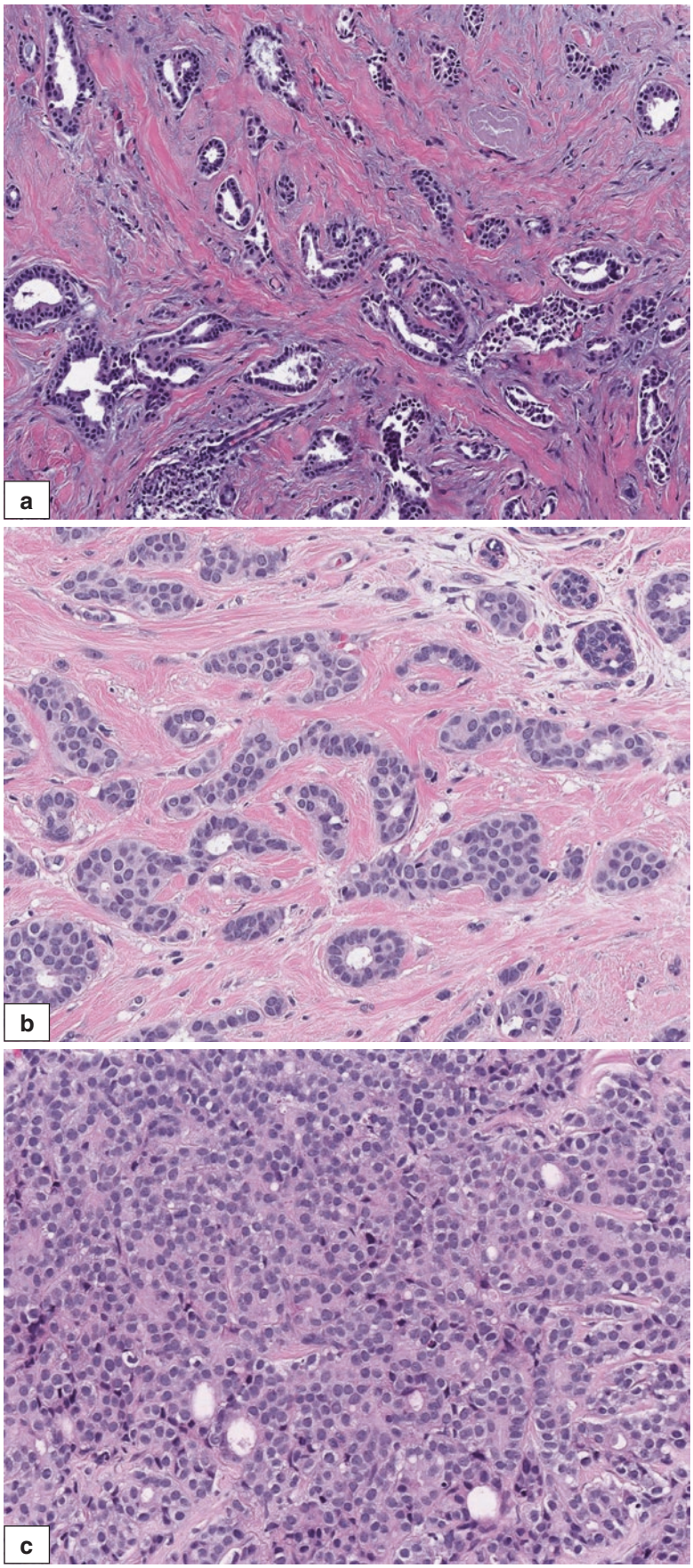

Fig. 12.15 Invasive ductal carcinoma. Microscopic features. Three different invasive ductal carcinoma cases show more than 75 % glandular differentiation (**a**) compared with 30 % (**b**) and less than 10 % (**c**)

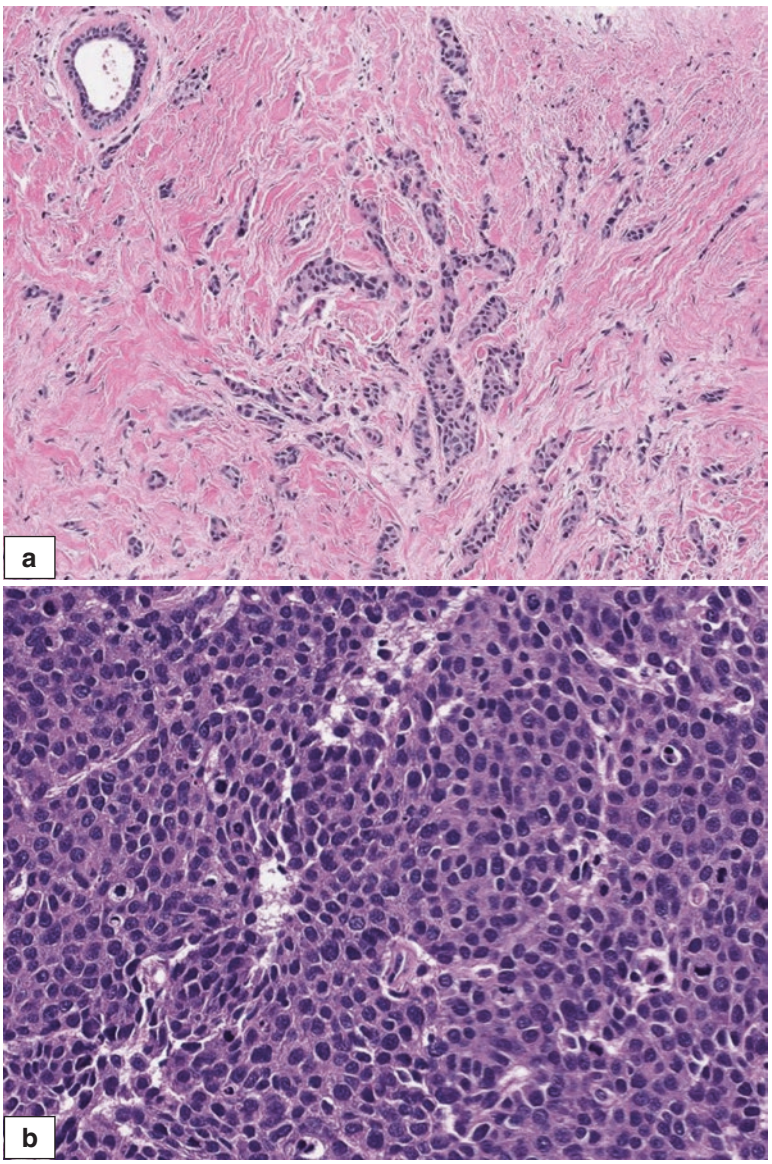

Fig. 12.16 Invasive ductal carcinoma. Microscopic features. (**a**) Low-grade tumour composed of uniform tumour cells having small nuclei, which are similar to adjacent normal ductal cells. (**b**) High-grade tumour with a solid growth pattern and moderate to marked nuclear atypia characterized by significant variation in nuclear size and shape

Immunohistochemistry Features

Invasive ductal carcinoma cells are typically positive for cytokeratin 7. Luminal type cytokeratins (cytokeratin 7/8, 18, and 19) are positive in most tumours, whereas basal cytokeratins (cytokeratin 5/6 and 14) are positive in only a small subset of breast carcinomas. Nearly all invasive ductal carcinomas are negative for cytokeratin 20, and they are positive for epithelial membrane antigen and E-cadherin. Gross cystic disease fluid protein 15 (GCDFP-15) and mammaglobin are reported to be positive in 50–70 % of invasive ductal carcinomas [27, 28]. GATA3 expression is closely related to the molecular typing of breast cancer, and it is present in 90 % of invasive ductal carcinomas. It is expressed in almost 100 % of oestrogen-positive tumours, although at lower levels in oestrogen receptor-negative and triple-negative breast cancers (Fig. 12.25) [29]. Similarly, FOXA1, a member of the forkhead transcription factor family, is associated with oestrogen receptor expression. Studies have shown that FOXA1 is an excellent breast carcinoma marker, but its utility is limited in the triple-negative subtype [30]. Two thirds of invasive ductal breast carcinomas are positive for oestrogen and progesterone receptors. In addition to being prognostic markers, these receptors also predict the likelihood of response to endocrine therapy [31]. In current clinical practice, about 15 %–20 % of invasive ductal carcinomas show c-erbB-2 (HER2/neu) protein overexpression or gene amplification, correlating with high-grade carcinomas (Fig. 12.26). The primary clinical use of c-erbB-2 is to predict the likelihood of response to c-erbB-2-targeted therapy [32].

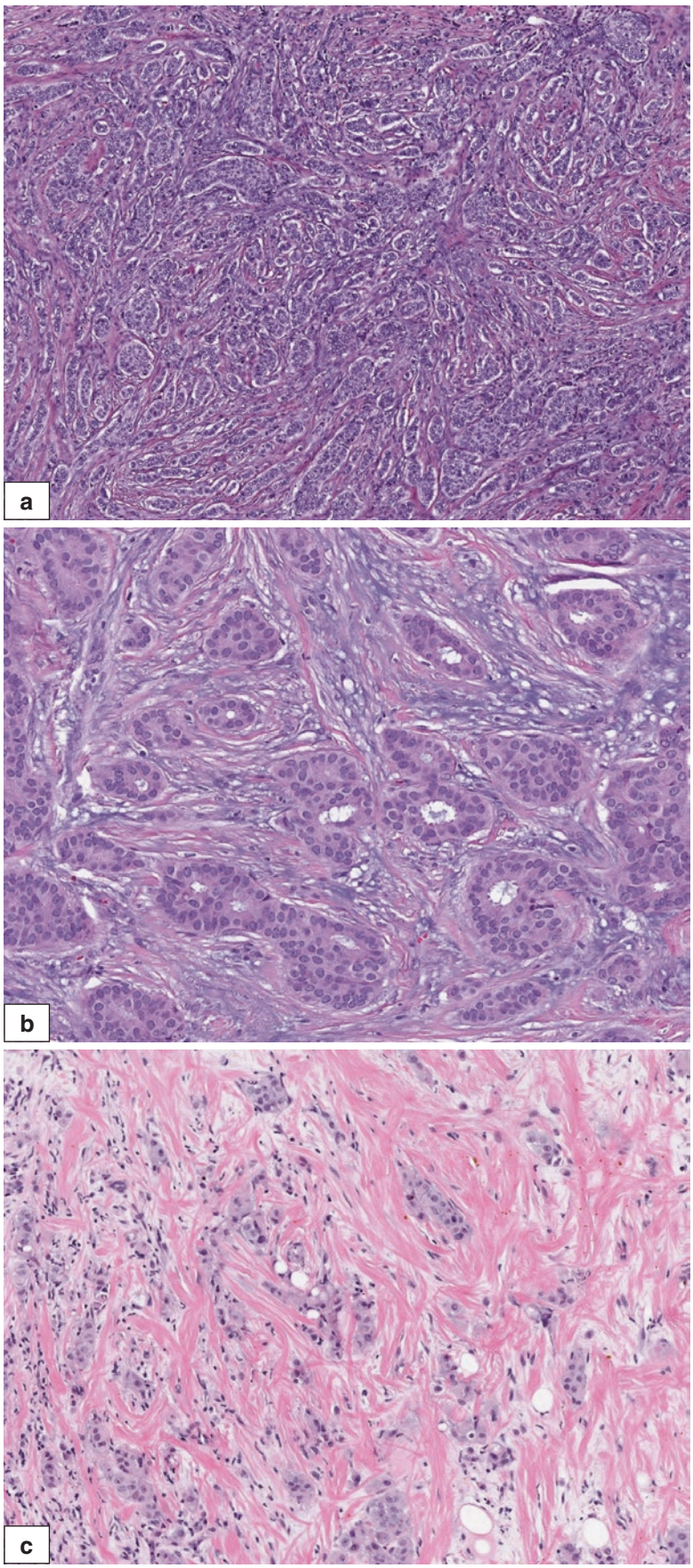

Fig. 12.17 Invasive ductal carcinoma. Microscopic features. (**a**) Invasive carcinoma with minimal stromal component. (**b**) Tumour showing a moderate amount of stroma. (**c**) Invasive tumour with abundant, fibrous, collagenised stroma

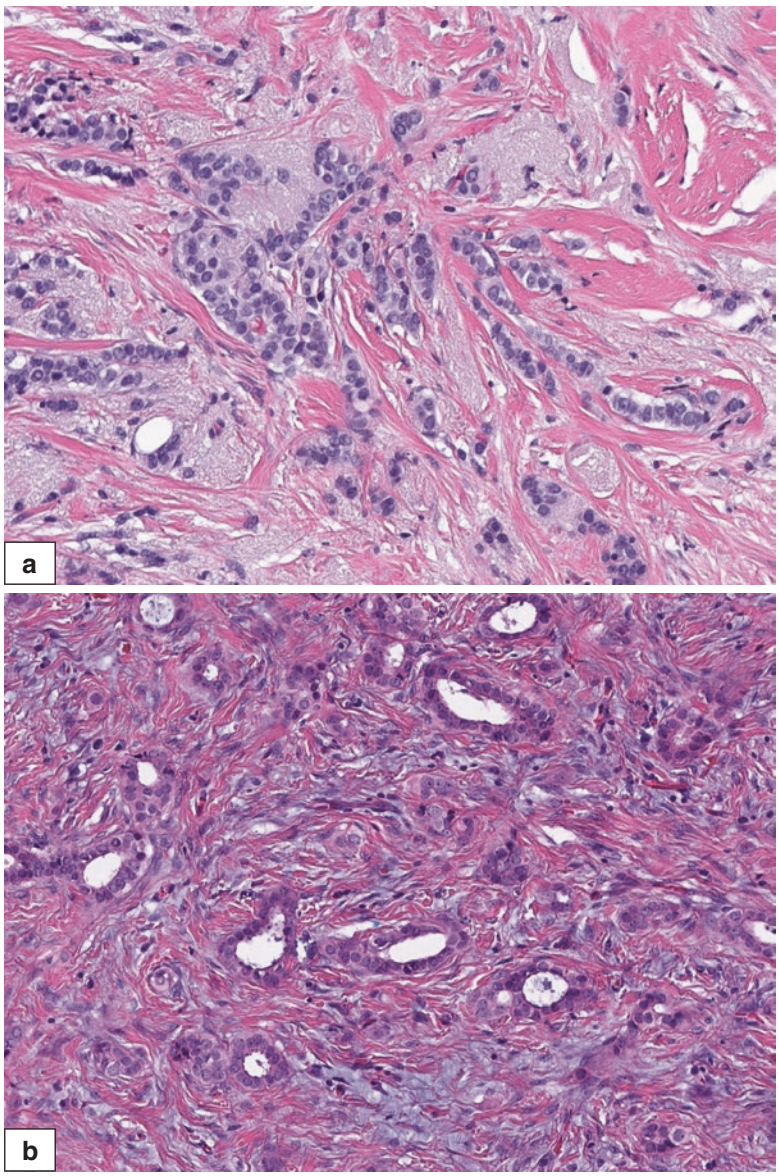

Fig. 12.18 Invasive ductal carcinoma. Microscopic features. (**a**) The stroma of this invasive tumour consists predominantly of collagen bundles without a cellular component. (**b**) Highly cellular stroma, in contrast to (**a**)

Molecular Classification

Over the past two decades, the advent of genomic technologies has allowed molecular characterisation of breast cancer and supported the concept that invasive ductal carcinoma is not a single tumour type but a collection of biologically and clinically different tumours arising from the breast epithelium. Based on high-throughput gene expression analysis, four different molecular types of breast carcinoma were originally described: luminal A, luminal B, basal-like, and c-erbB-2 positive [33–36]. Recent studies have identified several additional distinct subtypes of breast carcinomas, including claudin low, interferon rich, and molecular apocrine. Furthermore, six subtypes of basal-like carcinoma (basal-like1, basal-like2, immunomodulatory, luminal androgen receptor, mesenchymal-like, and mesenchymal stem-like) have been described. Multiple independent studies have demonstrated a significant association between these molecular classes of invasive ductal carcinomas and histologic grade, clinical behaviour, and response to systemic therapy [37–39]. Luminal A tumours account for 50 % of invasive breast cancers and generally correspond to low- to intermediate-grade, oestrogen receptor-positive, c-erbB-2-negative tumours with low proliferation. They include a wide range of low-grade invasive carcinomas, including classic lobular, tubular, and mucinous carcinomas. Luminal B tumours comprise 20 % of invasive breast cancers and correspond to intermediate- to high-grade, oestrogen receptor-positive tumours with a high proliferation rate; c-erbB-2 expression is variable (positive or negative) [36]. The c-erbB-2-positive molecular subclass includes generally high-grade carcinomas, which are mostly but not always c-erbB-2-positive by conventional immunohistochemical

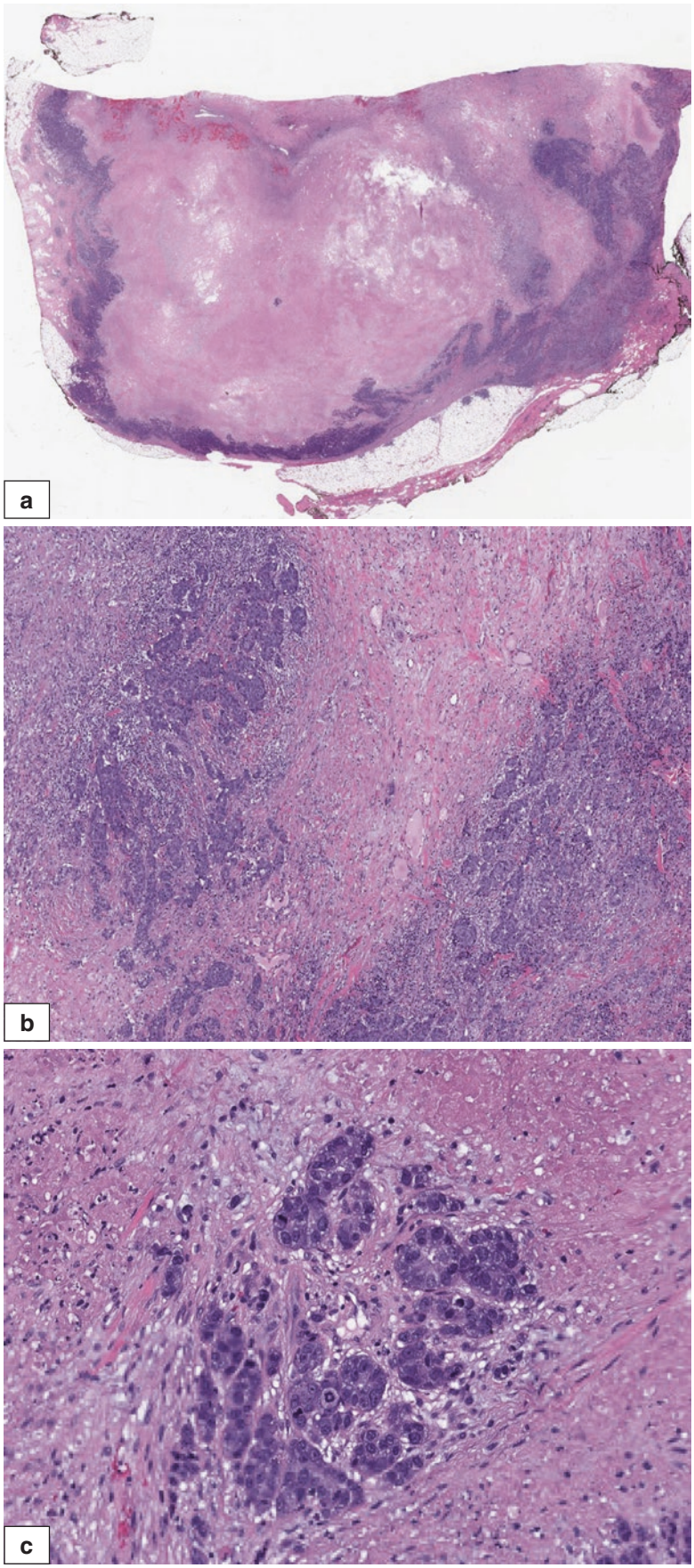

Fig. 12.19 Invasive ductal carcinoma. Microscopic features. (**a**) Low magnification of the tumour, showing a central, sclerotic area with tumour cells radiating outwards. (**b**) Medium magnification of the periphery of the same tumour. (**c**) High magnification of tumour in the sclerotic centre

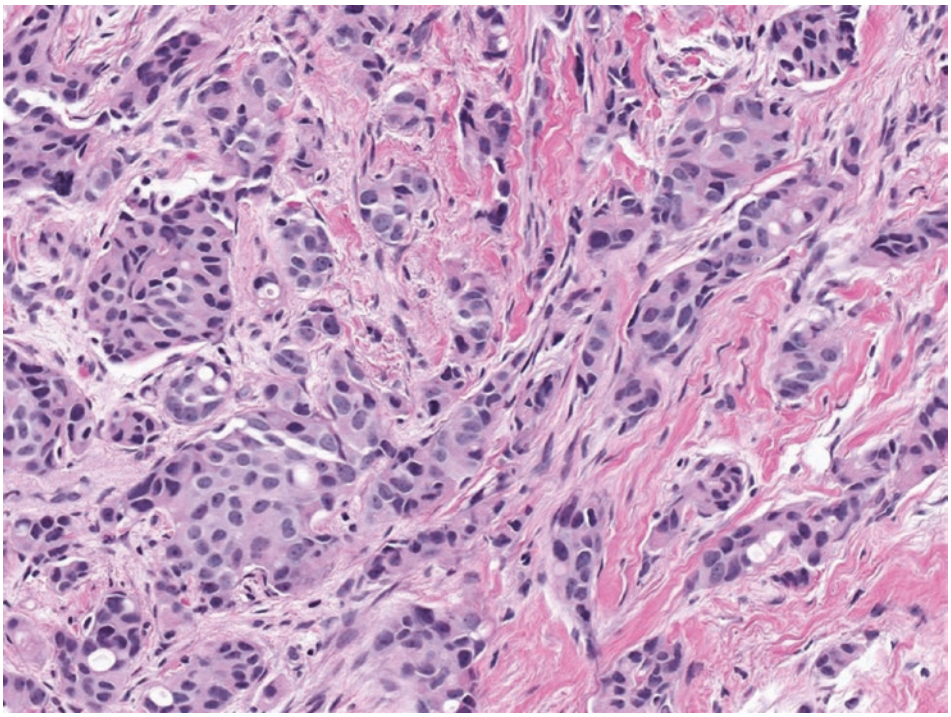

Fig. 12.20 Invasive ductal carcinoma. Microscopic features. Uniform distribution of sclerosis, unlike Fig. 12.19

and gene amplification analyses. This group accounts for 15 % of all invasive breast cancers. They are usually negative for oestrogen and progesterone receptors, Ki-67 expression is high, and *TP53* mutation is common. These tumours are more likely to have lymph node metastasis and poor prognosis. Basal-like carcinomas account for 15 % of all invasive carcinomas and include oestrogen receptor-negative and c-erbB-2-negative tumours; they are typically high-grade cancers with high proliferation rates. They express basal epithelial markers such as cytokeratins 5/6, 14, and 17. Subsets of these tumours also show mesenchymal differentiation as evidenced by spindle cell morphology and positivity for vimentin.

In clinical practice, immunohistochemical classification based on the expression of oestrogen and progesterone receptors, c-erbB-2 overexpression, and evaluation of proliferation markers is applied as a surrogate for molecular subtypes. Invasive ductal carcinomas are classified into four categories: oestrogen receptor-positive low proliferation, oestrogen receptor-positive high proliferation, c-erbB-2 positive, and triple-negative. These four categories roughly correspond to the molecular subtypes. The importance of these markers has been shown in multiple studies, and recently it has been proposed that these biomarkers should be included in the staging of breast cancer [40].

Differential Diagnosis

The differential diagnosis of invasive ductal carcinoma includes malignant tumours such as special types of invasive breast cancers, metastatic carcinomas, non-invasive carcinomas, and benign lesions such as sclerosing adenosis and radial scar.

Invasive ductal carcinoma should be distinguished from special types of invasive carcinomas, especially those associated with exceptionally favourable prognoses, including tubular, invasive cribriform, and mucinous carcinomas. Invasive ductal carcinoma with extensive tubule formation may mimic tubular carcinoma. The diagnosis of tubular carcinoma should be restricted to tumours that show tubule formation in more than 90 % of the tumour. In tubular carcinoma, tubules are lined by a single layer of low-grade tumour cells. In contrast, well-differentiated invasive ductal carcinomas with extensive tubular differentiation show tubules that are lined by more than one layer of cells which typically show nuclear atypia. Metastatic carcinomas may mimic invasive ductal carcinoma. The presence of DCIS is good evidence for establishing the diagnosis of primary breast cancer. It is important to remember that some metastatic tumours may show a nested growth pattern mimicking in situ ductal carcinoma. Clinical history and immunohistochemical stains can be used to establish the primary versus metastatic nature of the tumour.

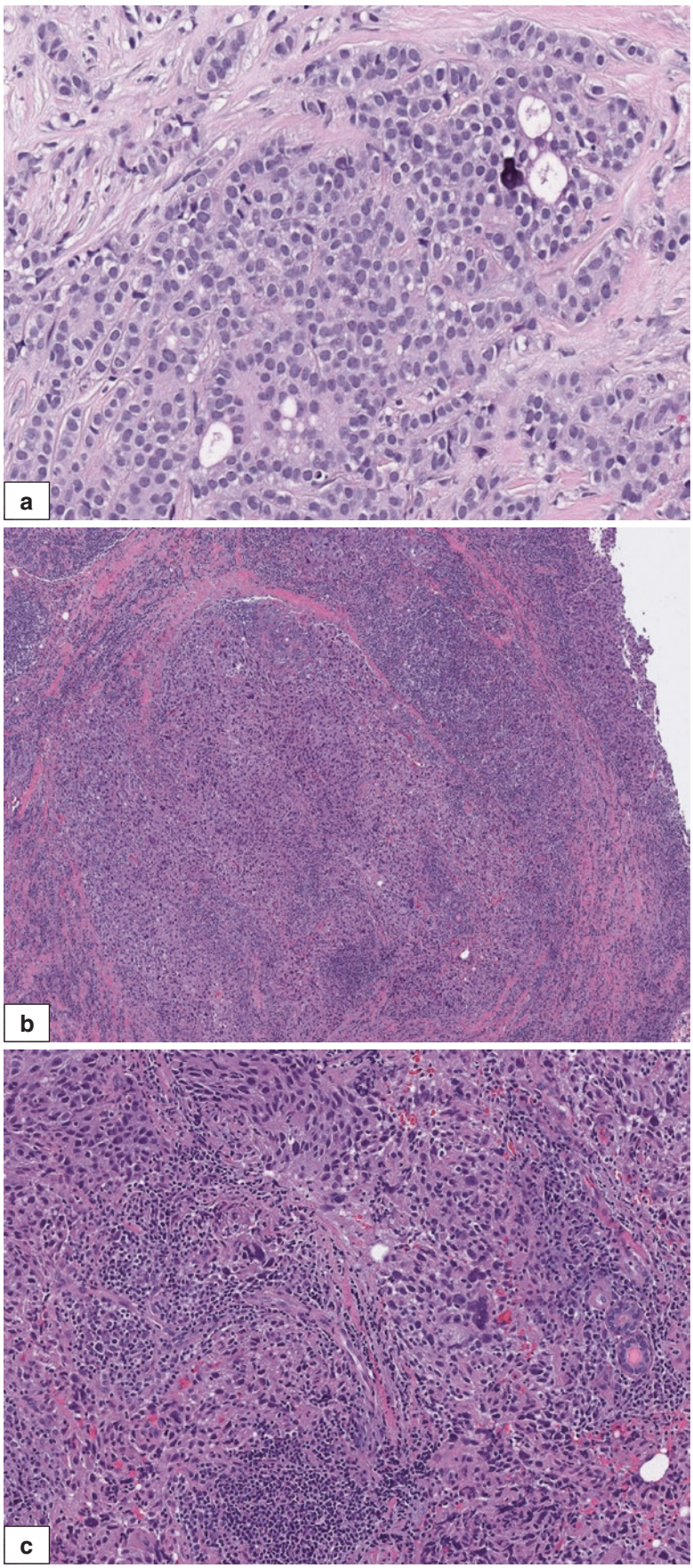

Fig. 12.21 Invasive ductal carcinoma. Microscopic features. (**a**) Invasive carcinoma with no tumour-infiltrating lymphocytes. (**b**) Invasive carcinoma with extensive lymphocyte infiltration. (**c**) Higher magnification of (**b**)

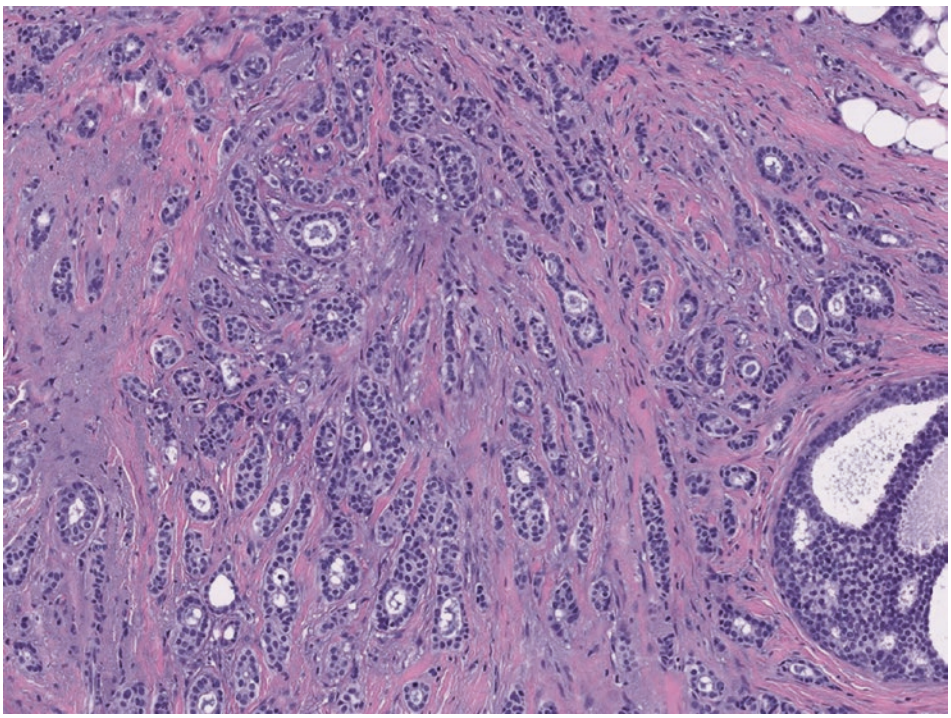

Fig. 12.22 Invasive ductal carcinoma. Microscopic features. Invasive carcinoma with associated in situ ductal carcinoma component (*right lower field*). The nuclear grade is similar in both components though this may be difficult to appreciate at this magnification

In situ ductal carcinomas involving pre-existing lesions with infiltrative margins such as sclerosing adenosis may mimic invasive ductal carcinoma. This is a particularly major diagnostic pitfall when only a small biopsy sample is available. The demonstration of intact myoepithelial cells or intact basement membranes will establish the in situ nature of the ductal carcinoma. Similarly, benign lesions with infiltrative growth patterns may mimic invasive carcinoma (*see* Chap. 5).

Prognosis and Therapy Considerations

The prognosis for invasive ductal carcinoma depends on the stage of the disease and biomarker expression. Staging includes tumour size, lymph node status, and the presence or absence of distant metastasis. Therapy depends on the stage and involves a multimodality approach including surgery, radiation, and systemic therapy. Recently, targeted therapy and immunotherapy approaches have been integrated into clinical practice [41].

Invasive Breast Carcinoma, Special Types

Definition

Special types of breast carcinomas are defined based on specific morphologic features which may be associated with distinct biologic behaviour. These tumours collectively constitute approximately 25–30 % of all invasive breast cancers. Probably the most important special types of invasive carcinoma include tubular and invasive cribriform carcinomas, as well as mucinous carcinomas (*see* Chap. 6); these types are uniformly associated with good clinical outcomes [1, 2, 42].

Tubular Carcinoma

Definition

Tubular carcinoma is a well-differentiated invasive carcinoma composed almost completely of tubules, which are lined by a single layer of low-grade tumour cells and have open lumens.

Clinical and Epidemiological Features

Tubular carcinoma accounts for 2–10 % of all invasive breast cancers in published series. The wide range of reported incidence reflects variations of histologic criteria (percentage of tubules required) to establish this diagnosis and inclusion of patients' data from screening programmes, in which the incidence of tubular carcinoma is much higher. Tubular carcinoma accounts for up to 25 % of carcinomas detected by mammographic screening, whereas it is less than 5 % of breast cancers in unscreened populations [43, 44].

Although tubular carcinoma has been reported in a wide age range (25–80 years), the average age is 60 years, which is slightly older than that of invasive ductal carcinoma. Most

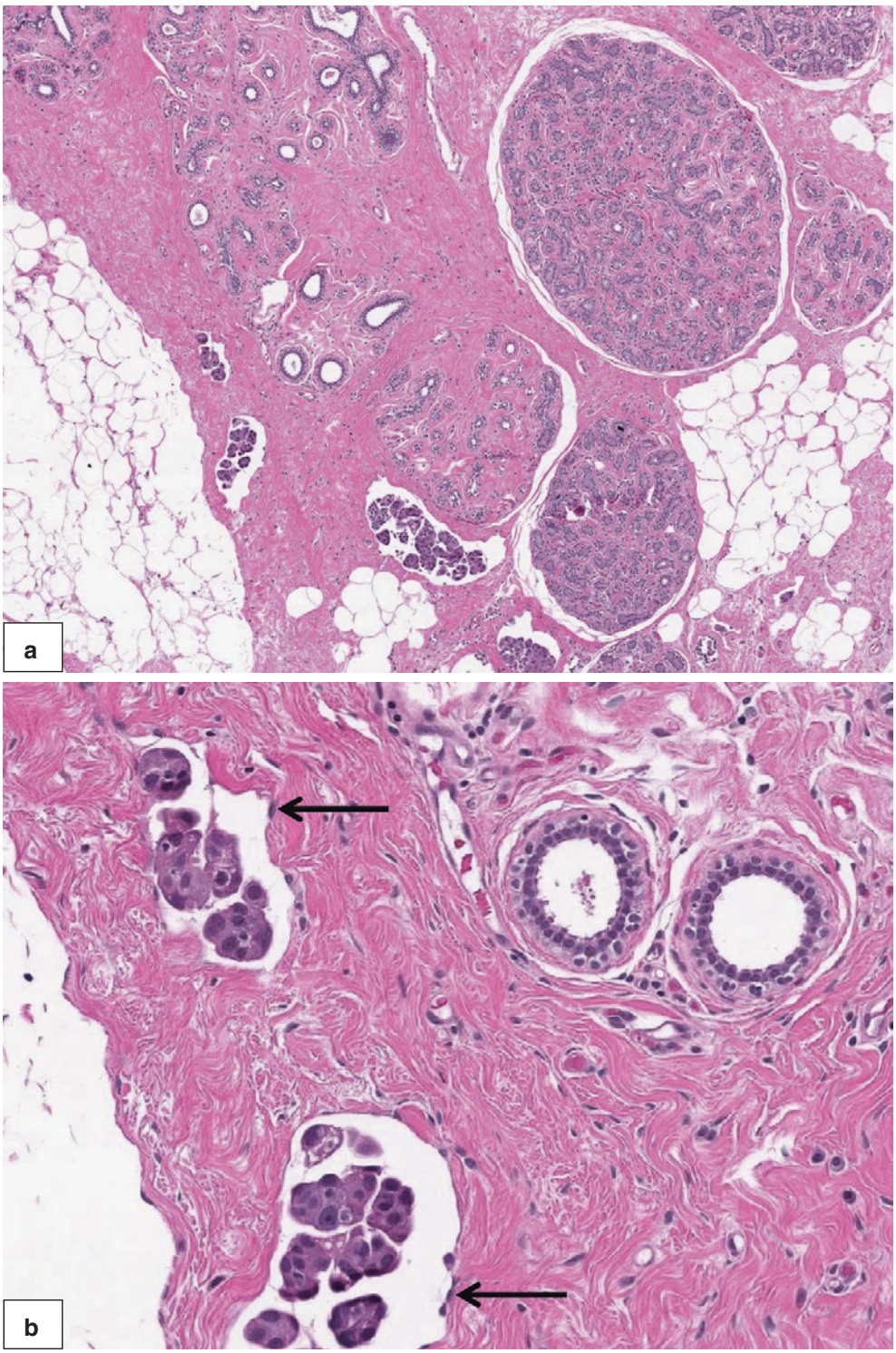

Fig. 12.23 Invasive ductal carcinoma. Microscopic features. (**a**) Lymphovascular space invasion of ductal carcinoma. Clusters of carcinoma cells are seen in endothelium-lined spaces away from the invasive carcinoma. (**b**) Higher magnification shows the flattened endothelial cells lining the spaces (*arrows*)

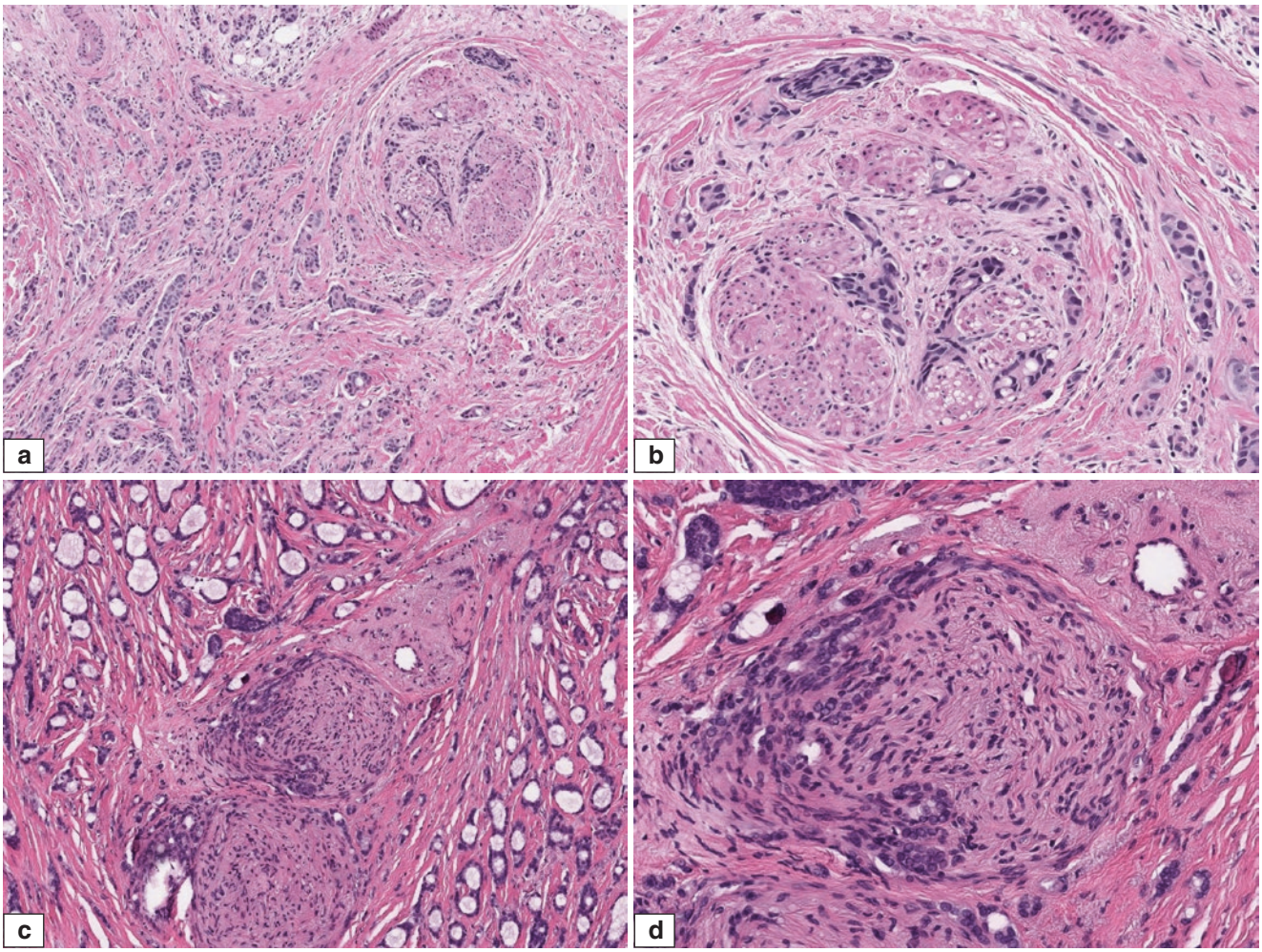

Fig. 12.24 Invasive ductal carcinoma. Microscopic features. Lower (**a**) and higher (**b**) magnification of invasive carcinoma showing perineural invasion. Lower (**c**) and higher (**d**) magnification of another example of perineural invasion. Note that the malignant glands surround and indent the nerve

patients present with either a palpable mass or mammographic abnormality [44, 45]. Tubular carcinoma has also been documented in males. About 10–20 % of patients have been reported with multifocal tubular carcinomas growing as separate foci in one or more quadrants.

Imaging Features

Most tubular carcinomas present as irregularly shaped masses with spiculated margins and central density (Fig. 12.27a). In most cases, the spicules are longer than the diameter of the central lesion. Microcalcifications are present in half of the cases. Mammographic findings may overlap with radial scar. Sonography reveals ill-defined and hypoechoic masses, with posterior acoustic shadowing seen in the majority of cases [45].

Pathologic Features

Macroscopic Pathology

Most tubular carcinomas are less than 2 cm. Mammographically identified tumours tend to be less than 1 cm. They form grey-white, stellate nodules (Fig. 12.27b).

Microscopic Pathology

Microscopically, these tumours are characterised by a haphazard proliferation of angulated, oval, or elongated tubules with open lumens (Fig. 12.27c, d). The tubules have angulated contours with tapering ends and are lined by a single layer of epithelium without a peripheral myoepithelial cell layer (Fig. 12.28). The nuclear grade is generally low. However, focal nuclear atypia and enlargement (nuclear

Table 12.1 Grading of invasive ductal carcinoma

Score	1	2	3
Tubule formation	>75 %	10–75 %	<10 %
	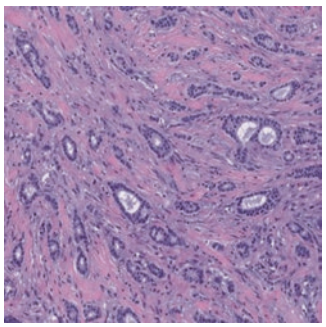	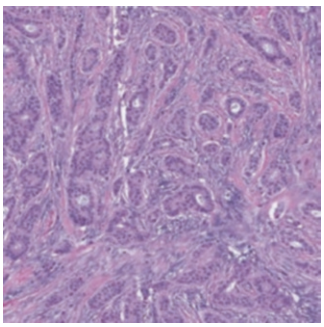	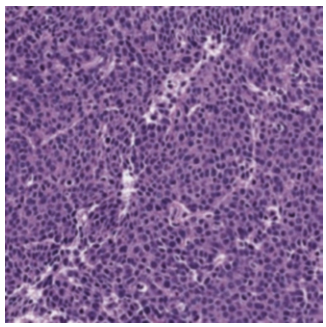
Nuclear pleomorphism	Uniform	Moderate variation	Marked variation
	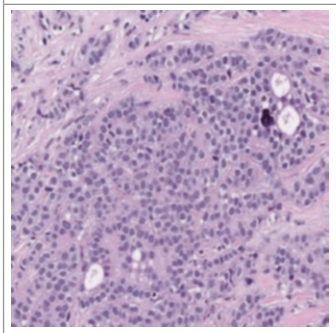	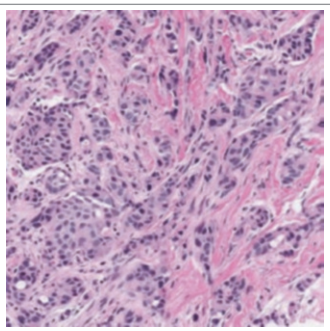	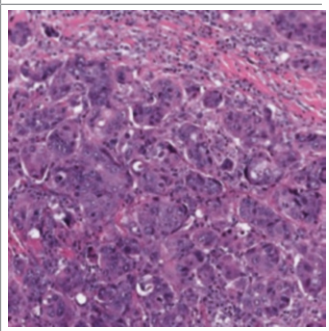
Mitotic count*	Rare	Occasional	Abundant
	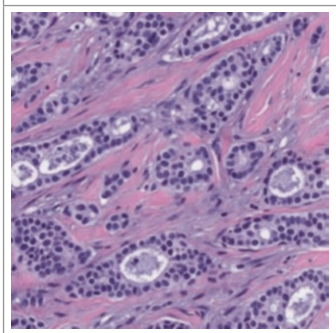	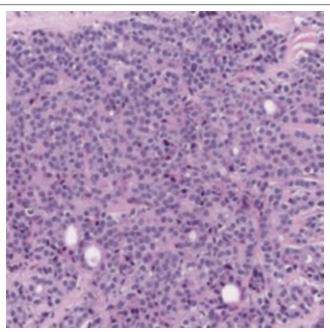	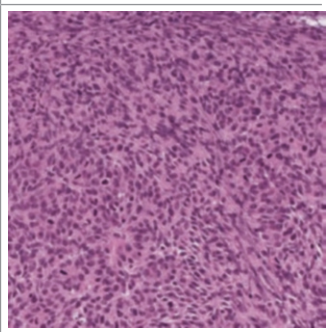

*Mitotic count scores should be calibrated against the microscope high power field diameter

Table 12.2 Histological grade scoring

Grade	Summary score
Grade 1 (well differentiated)	3–5
Grade 2 (moderately differentiated)	6–7
Grade 3 (poorly differentiated)	8–9

pleomorphism score of 2) may be allowed when tubular architecture is present throughout the tumour. The tumour cells have small nuclei, which resemble adjacent normal ductal epithelium. Individual tumour cells may form apical cytoplasmic snouts. Mitoses are very scant and difficult to find. The stroma can be fibrotic or elastotic. Infiltration of tubules into fat at the periphery of the tumour is commonly seen and is a helpful diagnostic clue in establishing the diagnosis. Concomitant occurrence of in situ carcinomas and epithelial proliferative breast lesions such as lobular neoplasia, flat epithelial atypia, and columnar cell change is common (Figs. 12.29 and 12.30) [46]. In almost all cases, the associated DCIS is low-grade and has cribriform or micropapillary patterns. Microcalcifications can be associated with either concomitant in situ carcinomas or epithelial proliferative lesions. Secretory material in neoplastic tubules can undergo calcifications.

When the tumour has areas of invasive lobular and tubular carcinoma in different proportions, it is referred to as tubulolobular carcinoma; multifocality is more frequent in tubulolobular carcinoma than in pure tubular carcinoma (Fig. 12.31) [47].

The percentage of the tubular carcinoma component that is required to designate a tumour as pure tubular carcinoma has been controversial in the literature. The WHO classification recommends that the diagnosis of tubular carcinoma is reserved for tumours showing more than 90 % tubule forma-

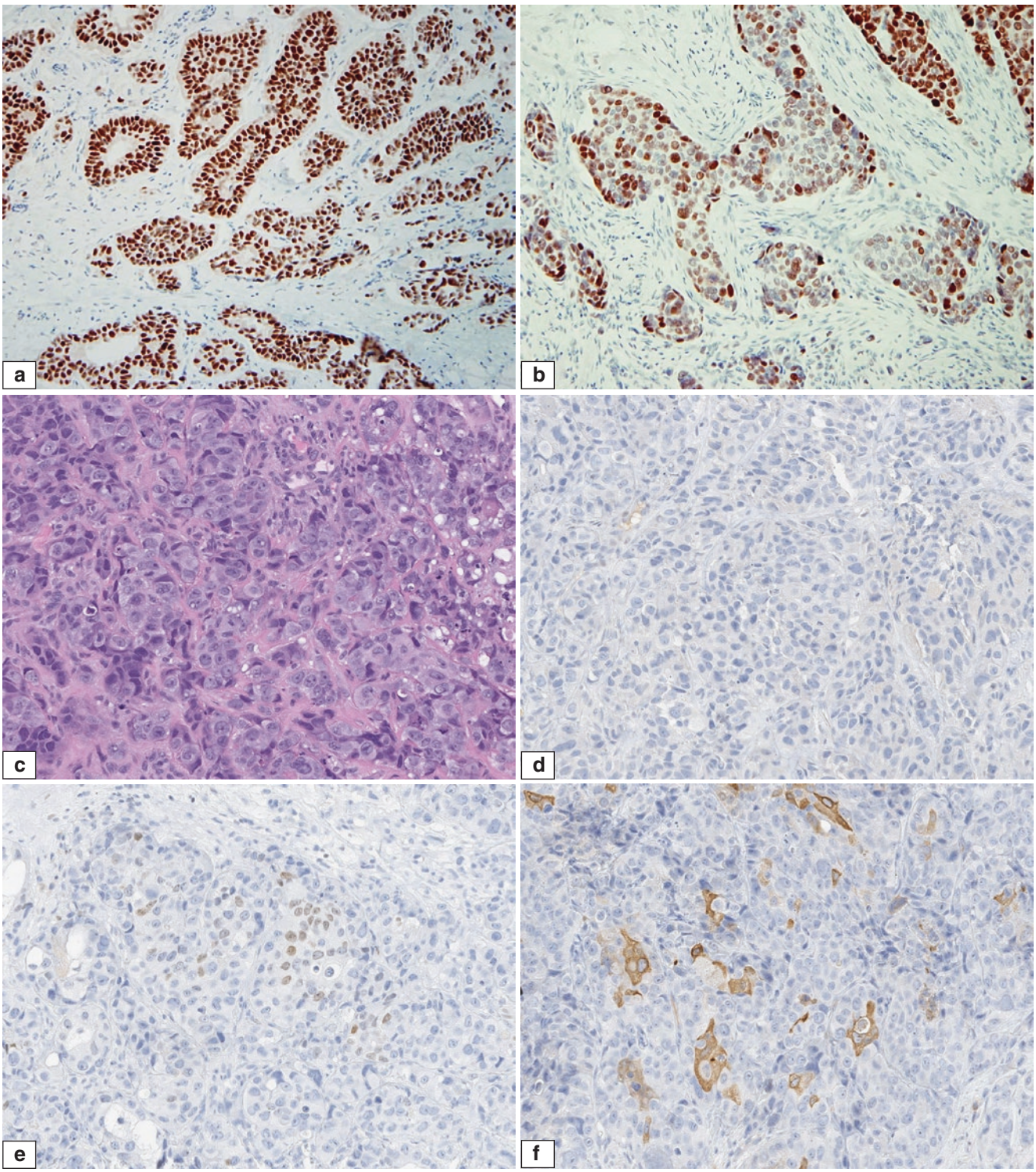

Fig. 12.25 Invasive ductal carcinoma. Immunohistochemical features. Strong positivity for oestrogen receptor in a low-grade invasive ductal carcinoma (**a**). Diffuse positivity for GATA-3 (**b**) in the same tumour. High-grade invasive carcinoma (**c**). The same case shown in (**c**) is negative for oestrogen receptor (**d**) and focally positive for GATA-3 (**e**) and gross cystic disease fluid protein 15 (**f**)

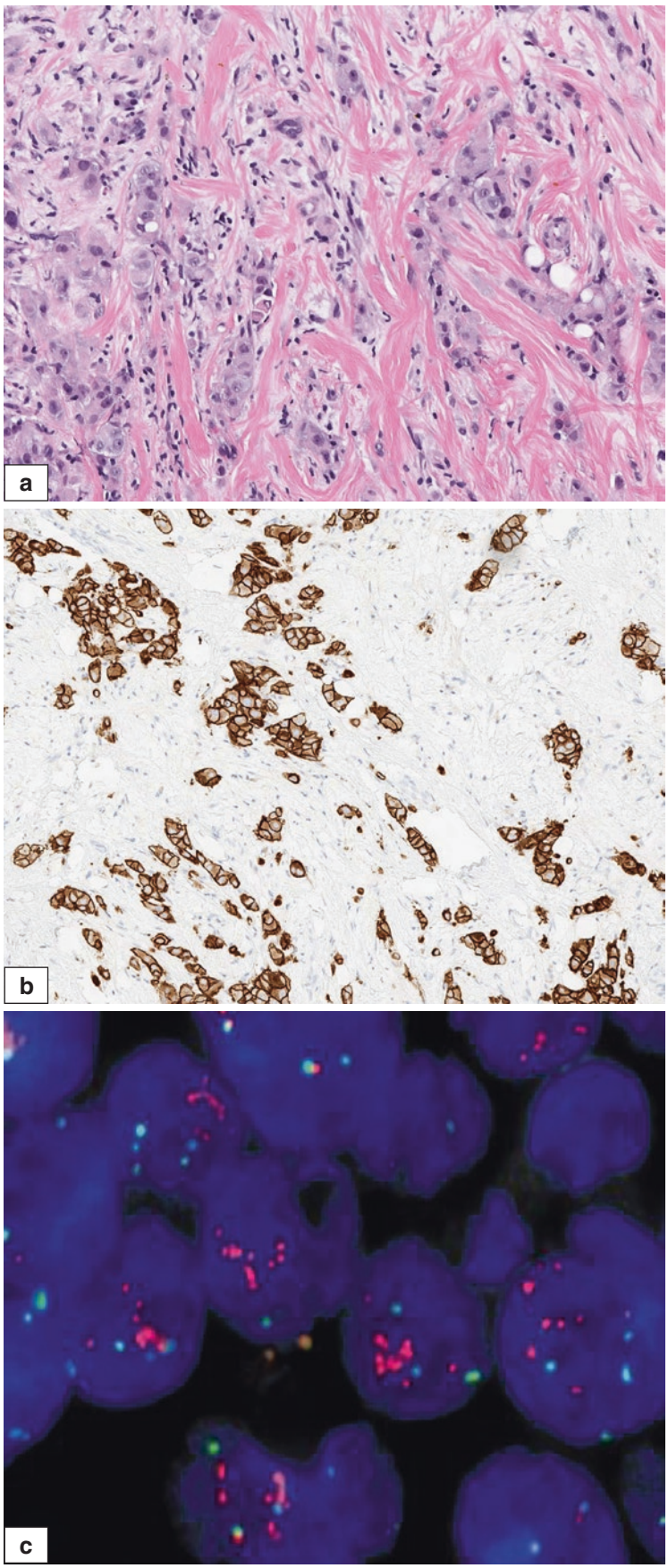

Fig. 12.26 Invasive ductal carcinoma. Immunohistochemical features. (**a**) H&E section of a (poorly differentiated) invasive ductal carcinoma. (**b**) Invasive carcinoma shows strong (3+) membrane staining for c-erbB-2. (**c**) Corresponding fluorescence in situ hybridisation shows increased c-erbB-2 gene copy number (red signals represent the number of c-erbB-2 gene copies and green signals correspond to CEP17)

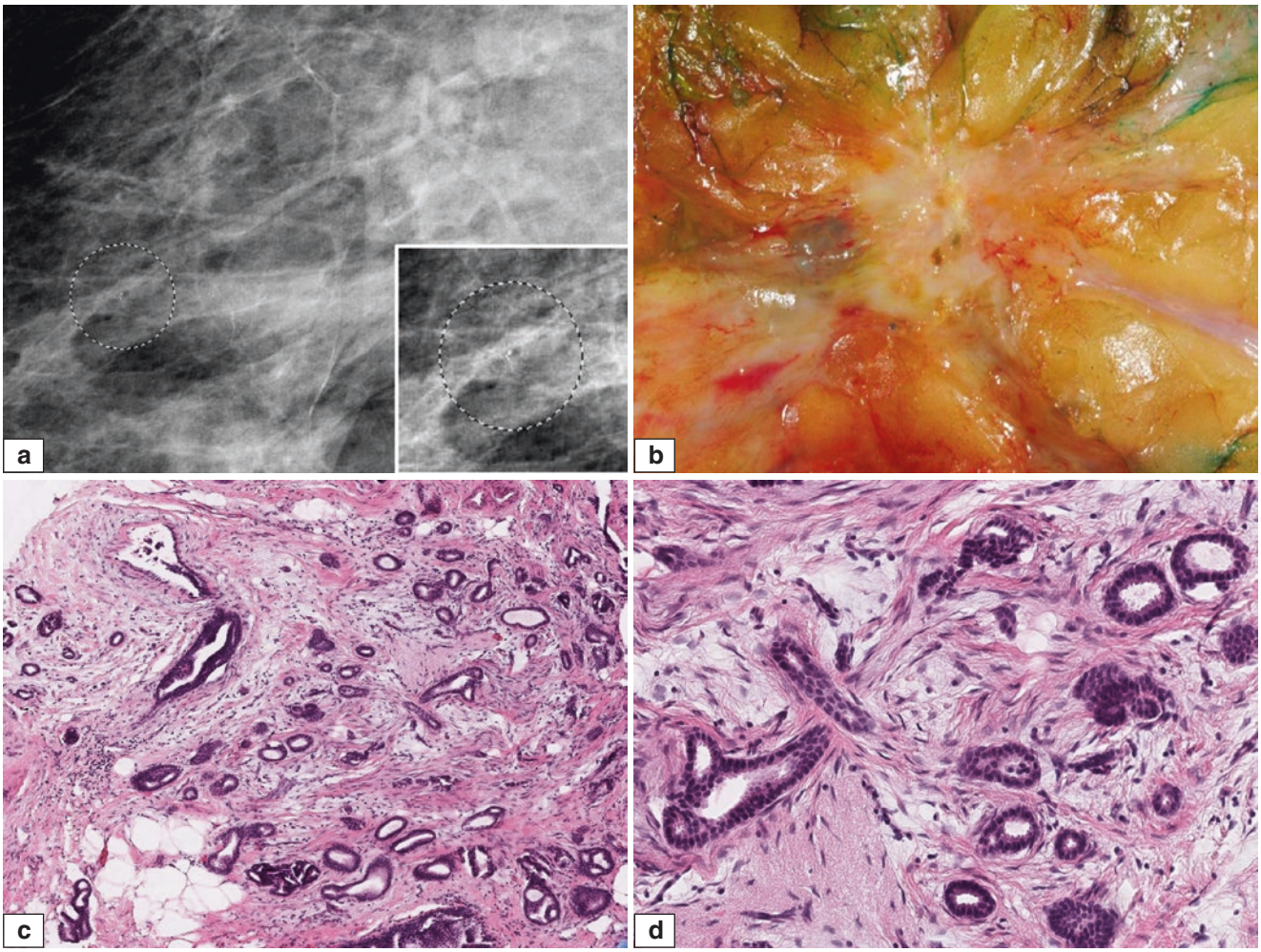

Fig. 12.27 Tubular carcinoma. Radiographic, gross, and microscopic features. (**a**) Mammogram shows an irregular mass with spiculated margins (*circled*). (**b**) Excision of the same mass shows a grey-white tumour with irregular margins. (**c**) Microscopically, the same tumour is composed of well-formed tubules. (**d**) At higher magnification, it is seen that the tubules are lined by a single layer of cells having uniform morphologic features

tion. Tumours showing 50–90 % tubular differentiation are classified as mixed, and those with less than 50 % are classified as invasive ductal carcinomas. Although the diagnosis of tubular carcinoma can be suggested from a needle core biopsy, the actual classification should be reserved to the final review of the entire lesion, to ensure that a non-tubular carcinoma component is not present. The great majority of tubular carcinomas are positive for oestrogen and progesterone receptors and negative for c-erbB-2 overexpression (luminal A type tumours) (Fig. 12.32).

Differential Diagnosis

The differential diagnosis includes benign, small, glandular proliferations of the breast, and invasive carcinomas with tubular growth pattern. The absence of myoepithelial cells in tubules is the hallmark of tubular carcinoma, in contrast to benign small glandular proliferations (Fig. 12.33). Myoepithelial cells may be highlighted by immunohistochemical markers such as smooth muscle actin, smooth muscle myosin, or p63. (For detailed discussion, *see* Chap. 5). Microglandular adenosis is another benign lesion that may mimic tubular carcinoma (Fig. 12.34). Although the lack of a myoepithelial layer in microglandular adenosis glands is a major pitfall, their small and round shapes, in contrast to the angulated and irregular shapes of tubular carcinoma glands, are helpful in distinguishing the two entities. Cells lining microglandular adenosis glands are positive for S100 and negative for oestrogen and progesterone receptors and for epithelial membrane antigen (EMA); tubular carcinoma cells are almost always positive for hormone receptors and EMA. Other malignant tumours that mimic tubular carcinoma include well-differentiated invasive ductal carcinoma

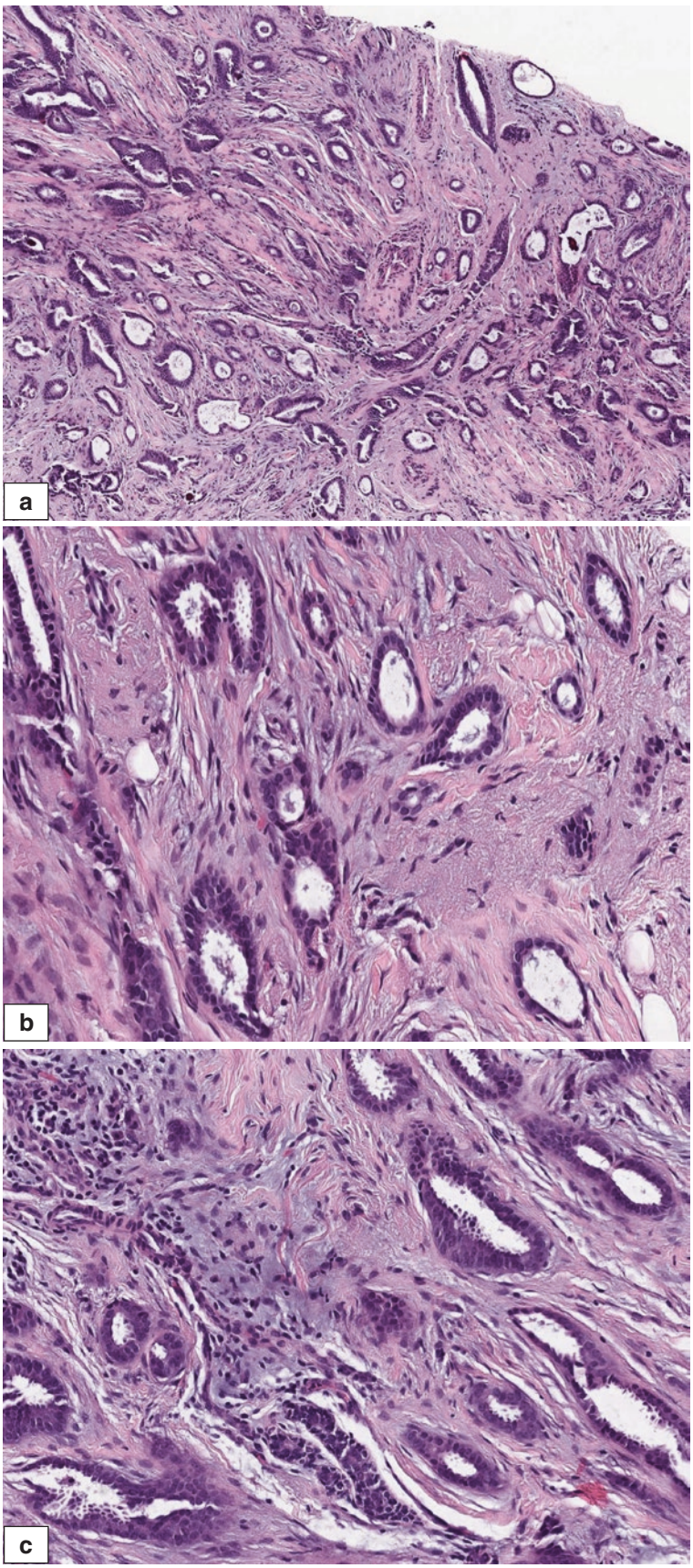

Fig. 12.28 Tubular carcinoma. Microscopic features. (**a**) Low magnification of an infiltrative growth pattern having characteristic open tubules. (**b**) On medium magnification, some tubules show characteristic teardrop shapes. (**c**) High magnification shows apical snouts of the luminal aspects of some of the cells lining the tubules

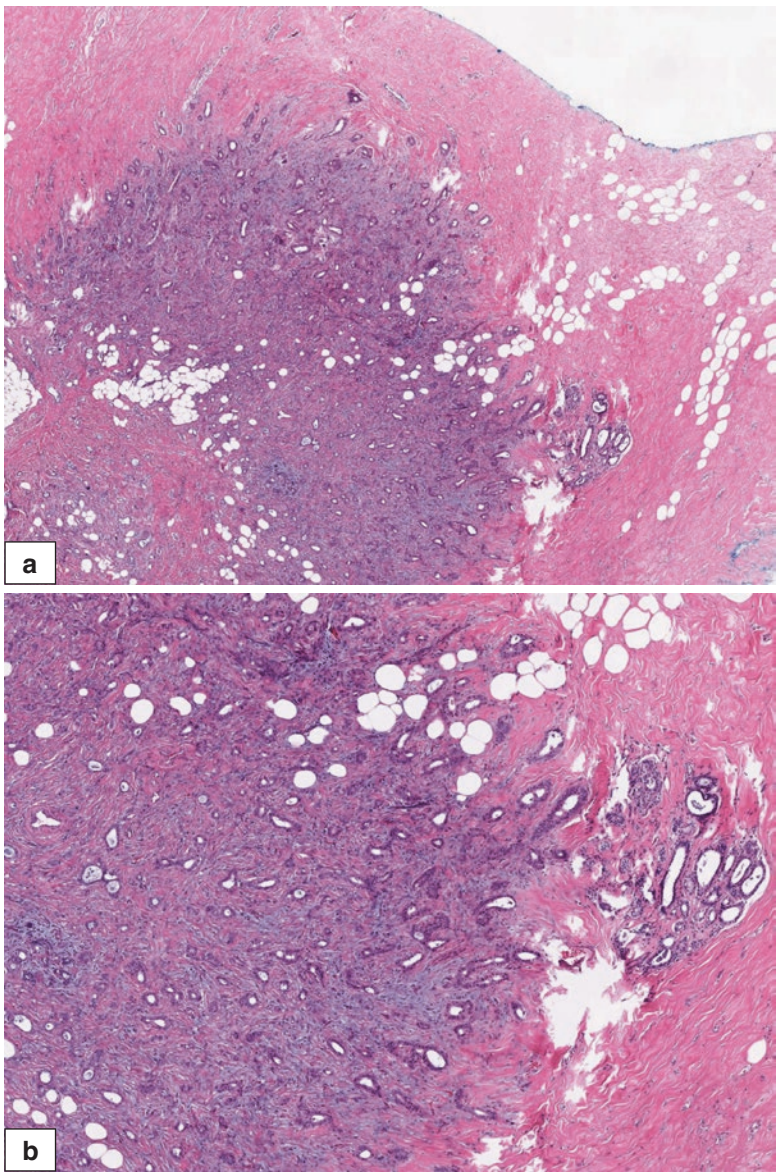

Fig. 12.29 Tubular carcinoma. Microscopic features. (**a**) Low magnification of tubular carcinoma, showing an invasive growth pattern. The entire tumour displays tubular structures. (**b**) Higher magnification of the same tumour shows hypercellular stroma

and low-grade adenosquamous carcinoma. Tubular carcinoma is not synonymous with invasive ductal carcinoma grade 1. Well-differentiated invasive ductal carcinomas have tubules lined by multiple cell layers, display areas of non-tubular growth pattern, and can have more nuclear atypia. Low-grade adenosquamous carcinoma may have well-formed tubules lined by low-grade tumour cells mimicking tubular carcinoma, but when sampled adequately, these tumours show solid nests and squamous differentiation even if they are focal. Adenosquamous carcinoma cells are typically negative for oestrogen and progesterone receptors; this negativity can assist in the differential diagnosis.

Prognosis and Therapy Considerations

Tubular carcinoma generally has a low incidence of metastases to axillary lymph nodes and low recurrence rates, leading to a favourable prognosis [48, 49]. The prognosis of mixed tumours is worse than that of pure tubular carcinoma. The incidence of axillary metastases in tubular carcinoma ranges from 0 to 10% in reported series, and the most important predictor of metastases is tumour size. In patients whose tubular carcinoma is less than 1 cm, the incidence of axillary metastasis is so low that some authors have suggested that axillary lymph node surgery can be omitted, but other authors have shown that axillary lymph node metastases can occur

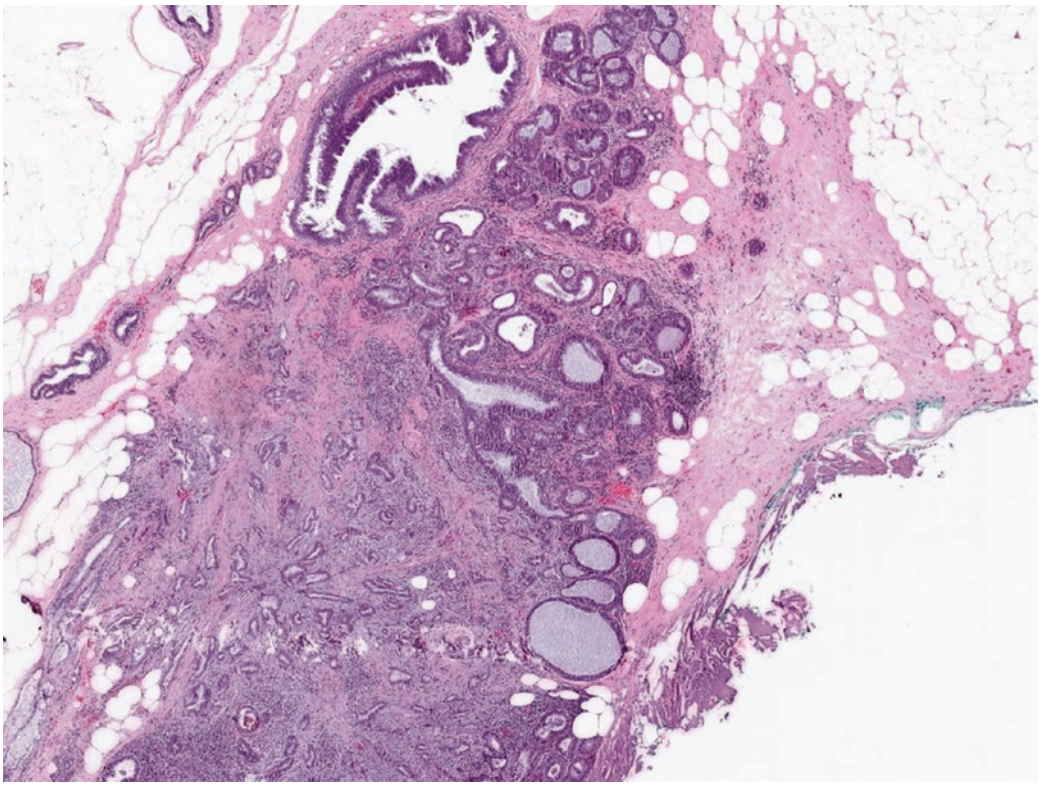

Fig. 12.30 Tubular carcinoma. Microscopic features. The presence of premalignant/high-risk lesions is common adjacent to tubular carcinoma; columnar cell change and atypical ductal hyperplasia are seen here next to the tubular carcinoma

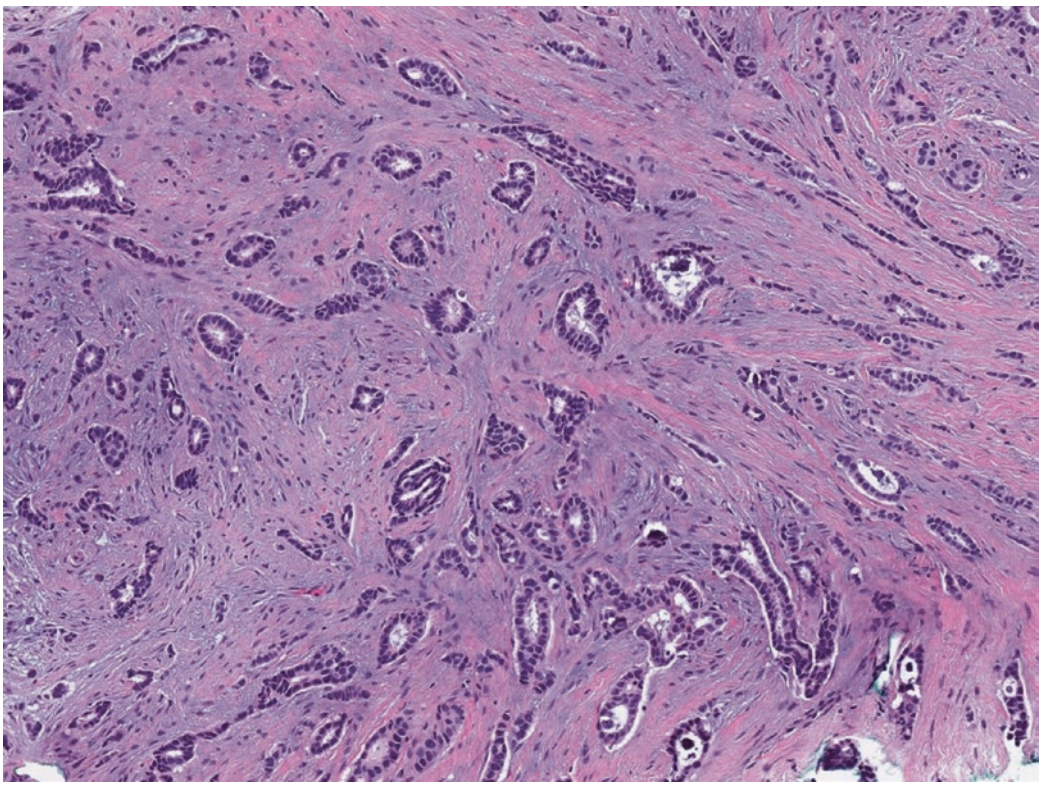

Fig. 12.31 Tubulolobular carcinoma. Microscopic features. This invasive carcinoma is composed predominantly of open tubules and focal, single-cell growth patterns

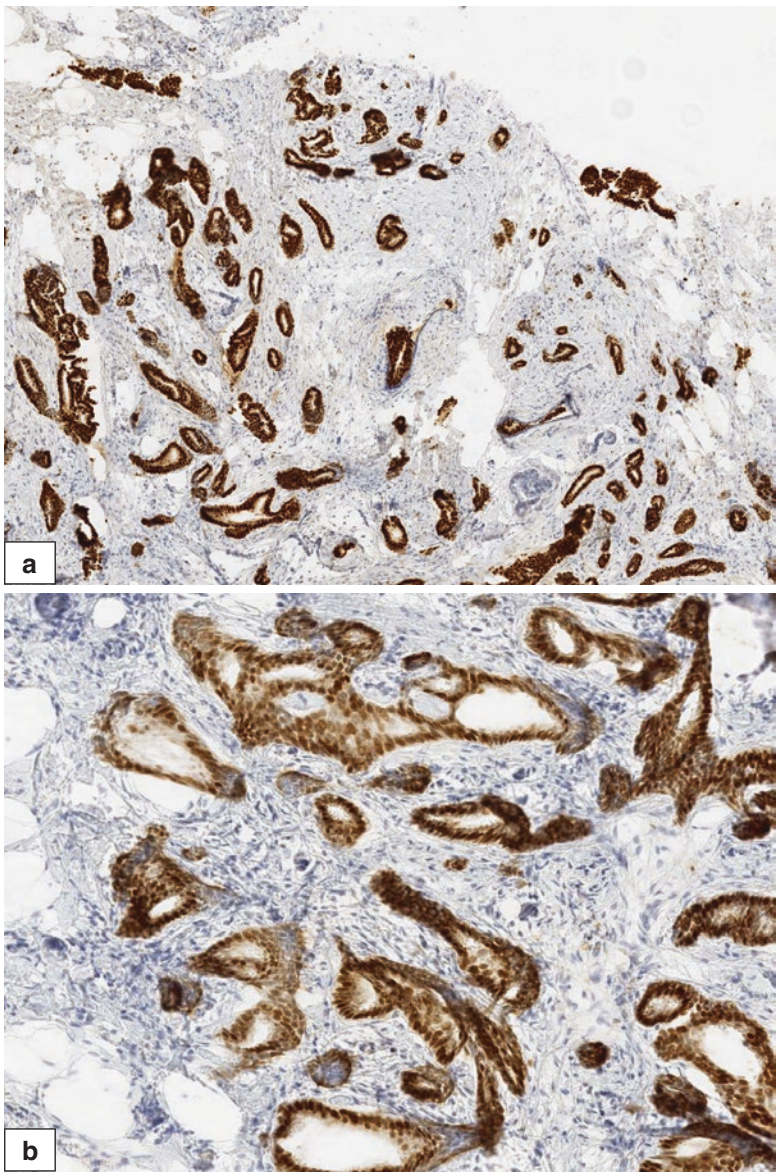

Fig. 12.32 Tubular carcinoma. Immunohistochemical features. Invasive carcinoma cells show diffuse strong positivity for oestrogen receptor (**a**) and progesterone receptor (**b**)

even with tumours less than 1 cm in size. In most cases, metastases also show a tubular carcinoma growth pattern, and only one to three lymph nodes are involved in almost all cases. The standard therapy protocol is segmental resection with sentinel lymph node dissection, followed by radiation therapy. Because the great majority of tubular carcinomas are positive for oestrogen and progesterone receptors, adjuvant hormonal therapy can be administered.

Invasive Cribriform Carcinoma

Definition

Invasive cribriform carcinoma is an invasive, well-differentiated carcinoma with a cribriform growth pattern similar to that of cribriform ductal carcinoma in situ (DCIS).

Clinical and Epidemiological Features

Invasive cribriform carcinoma is rare, representing 0.8–3.5 % of all invasive cancers. This tumour is closely related to tubular carcinoma, and a mixed tubular and invasive cribriform pattern is commonly seen. Because both tumours are associated with excellent prognosis, distinguishing these two components is less critical than verifying that invasive carcinoma not otherwise specified is not present [50]. To be designated as an invasive cribriform carcinoma, more than 90 % of the tumour must display a cribriform pattern. If an invasive carcinoma displays only tubules and cribriform islands, classification as either tubular or invasive cribriform carcinoma depends on which pattern predominates. Invasive cribriform carcinoma has been reported in a wide age range (20–90 years), with the average age in the mid-50s in most reported series [50, 51].

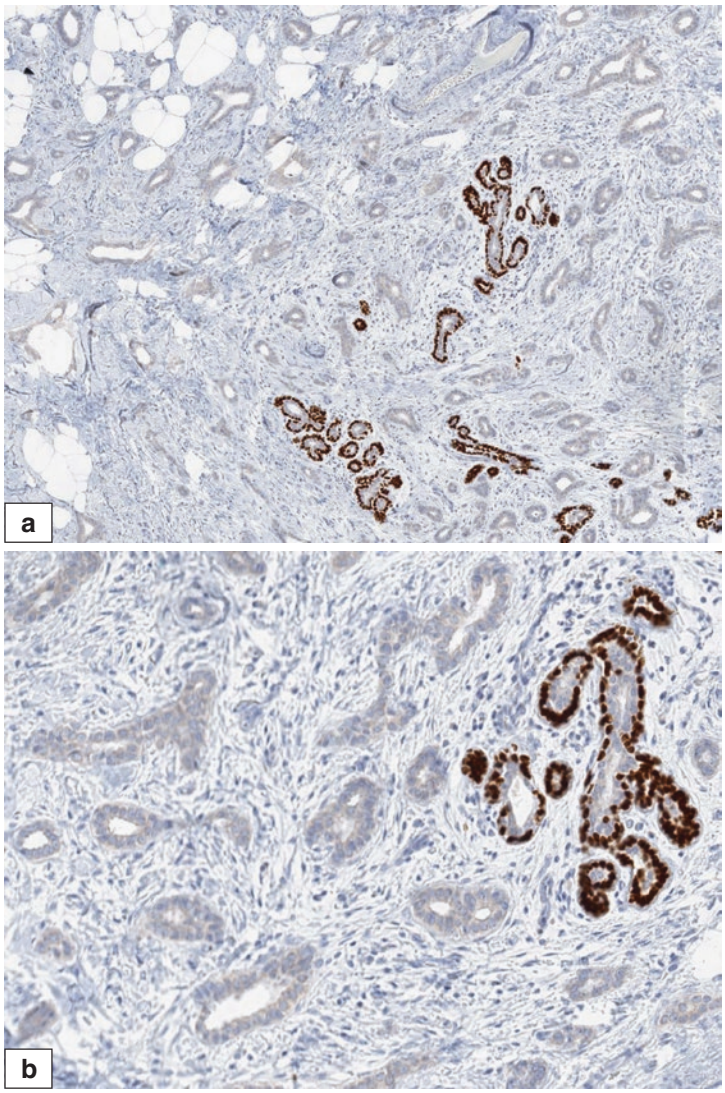

Fig. 12.33 Tubular carcinoma. Immunohistochemical features. (**a**) Immunohistochemical staining for p63. Tubular carcinoma glands lack staining, but entrapped normal ductal structures show strong positivity, indicating an intact myoepithelial layer in benign ducts. (**b**) Higher magnification of (**a**), showing detail

Imaging Features

Mammographic features of invasive cribriform carcinomas are similar to those of other invasive breast cancers. Most lesions present as spiculated masses, with or without microcalcifications. Not uncommonly, they can also present as fairly well-circumscribed masses with a regular shape. Multifocal tumours have been reported in up to 20 % of cases in some series.

Pathologic Features

Macroscopic Pathology

No specific macroscopic features associated with invasive cribriform carcinoma have been described. In most cases, lesions form stellate masses with infiltrative margins (Fig. 12.35).

Microscopic Pathology

Microscopically, invasive cribriform carcinoma is characterised by islands of uniform tumour cells with a cribriform appearance similar to that seen in cribriform DCIS. The tumour nests of invasive cribriform carcinoma usually have irregular borders and show clear-cut stromal invasion, in contrast to the rounded, smooth borders of in situ cribriform carcinoma (Figs. 12.36, 12.37, and 12.38). The nests of invasive cribriform carcinoma lack myoepithelial cells, the presence of which defines in situ cribriform carcinoma. Concomitant in situ carcinoma components, which frequently display cribriform patterns, are present in more than two thirds of the cases. Calcifications can be seen in neoplastic glands. Tumour cells are usually cuboidal to columnar, have low-grade to intermediate-grade nuclei, and typically

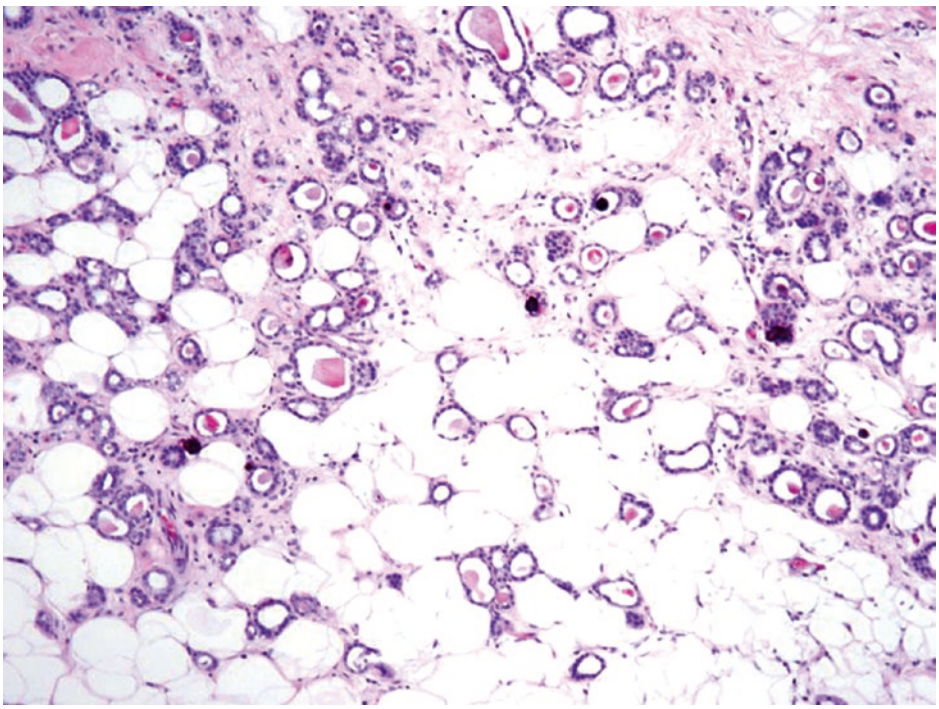

Fig. 12.34 Microglandular adenosis. Histologic features. Small glandular proliferation with an infiltrative pattern may mimic tubular carcinoma. Note the lack of cellular stroma and the round shape of glands, in contrast to the cellular stroma and angulated glands found in tubular carcinoma

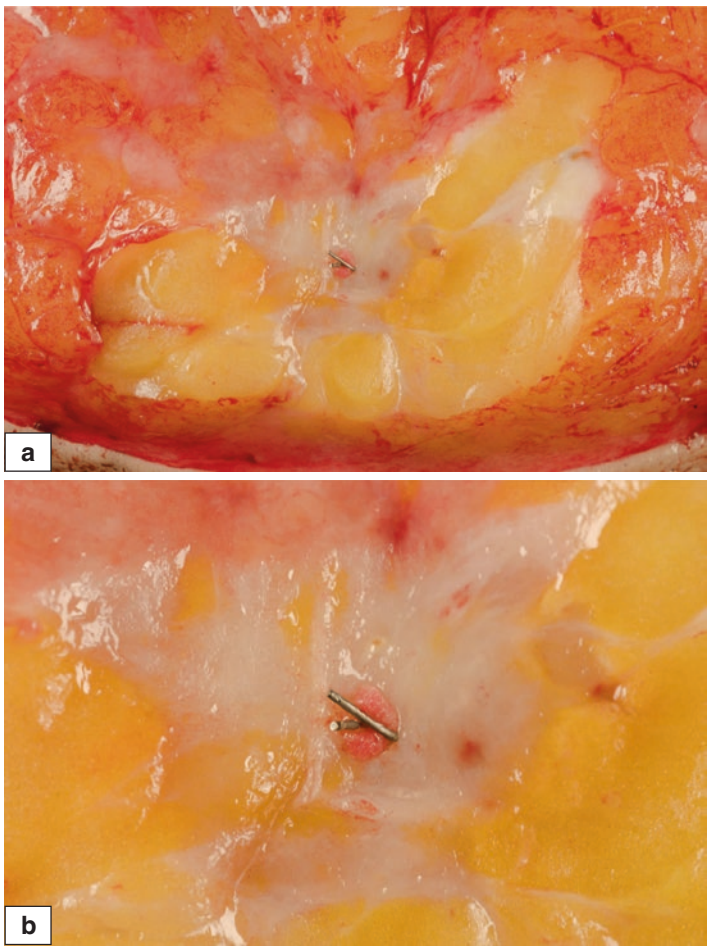

Fig. 12.35 Invasive cribriform carcinoma. Gross features. (**a**, **b**) Tumour with infiltrative edges. Note the biopsy clip in the centre

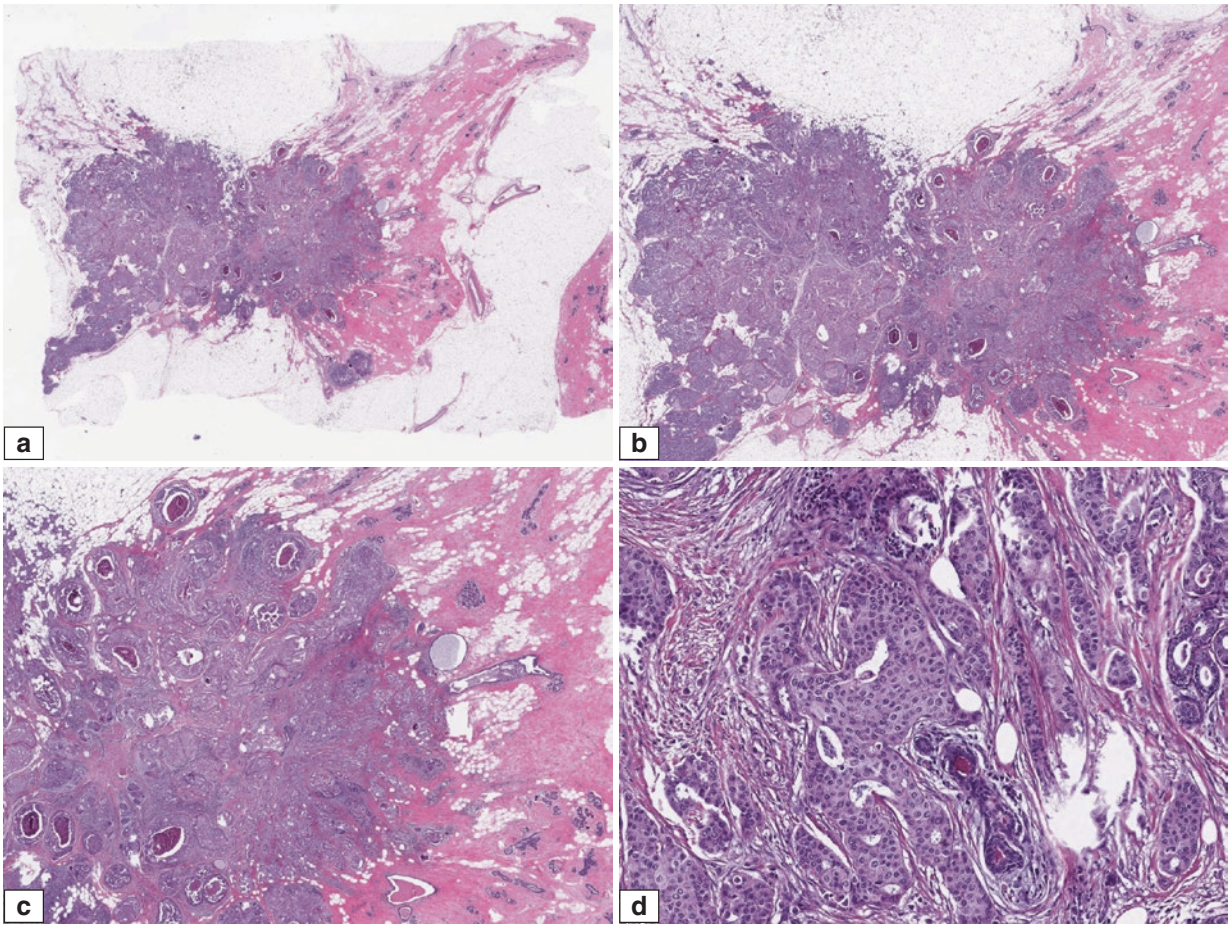

Fig. 12.36 Invasive cribriform carcinoma. Microscopic features. (**a–d**) Invasive carcinoma composed of cribriform structures with an infiltrative growth pattern. Low to high magnification of the same case

have amphophilic cytoplasm. Minor areas of tubular differentiation are commonly seen. Mitotic figures are rare. The associated stroma usually appears cellular and reactive, which can be helpful in establishing the invasive nature, as in situ cribriform carcinomas usually do not have reactive-appearing stroma. Invasive cribriform carcinoma is the most common type of breast cancer associated with stromal or intraluminal osteoclast-like giant cells (Figs. 12.39 and 12.40). These cells have been described in many different histologic types of breast cancer and are thought to be histiocytic in origin, though they are not associated with a known biologic behaviour.

Similar to other well-differentiated breast cancers, invasive cribriform carcinomas are consistently positive for oestrogen and progesterone receptors and negative for c-erbB-2 overexpression (luminal A type tumours).

Differential Diagnosis

Invasive cribriform carcinoma should be differentiated from cribriform DCIS and other invasive carcinomas such as invasive ductal carcinoma and adenoid cystic carcinoma.

Although both in situ and invasive cribriform carcinomas have the same cribriform growth pattern, the nests of invasive cribriform carcinoma show more infiltrative edges. If the infiltrative edge is not present on a small biopsy specimen, the invasive nature of cribriform nests in invasive cribriform carcinoma can be confirmed by the absence of surrounding myoepithelial cells on immunohistochemistry. Invasive ductal carcinomas may have areas of cribriform growth pattern mimicking invasive cribriform carcinoma, but the tumour should almost totally show a cribriform pattern in order to be classified as invasive cribriform carcinoma.

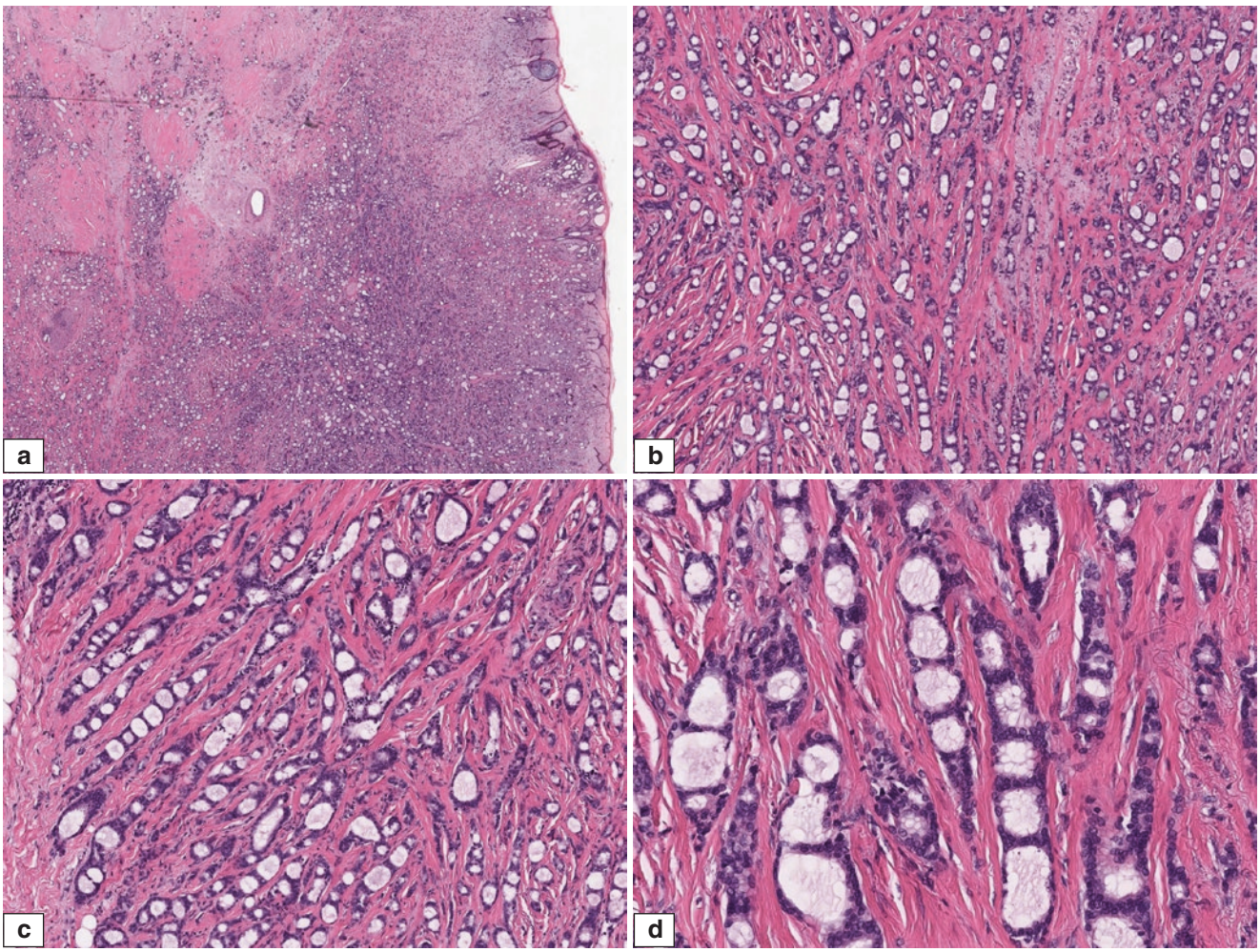

Fig. 12.37 Invasive cribriform carcinoma. Microscopic features. (**a–d**) Invasive carcinoma composed entirely of structures with a cribriform pattern. Low to high magnification of the same case

Adenoid cystic carcinoma can be differentiated from invasive cribriform carcinoma on the basis of its typical dual cell proliferation (Fig. 12.41). Cribriform spaces of adenoid cystic carcinoma characteristically contain material resembling basement membrane, whereas spaces in invasive cribriform carcinoma are often empty. Furthermore, immunohistochemical staining for oestrogen and progesterone receptors will be helpful in this differential diagnosis. Adenoid cystic carcinomas are positive for cKIT and p63 and negative for oestrogen and progesterone receptors; invasive cribriform carcinomas are almost always positive for oestrogen receptor and negative for cKIT and p63 (Fig. 12.42) [52].

Collagenous spherulosis may superficially resemble invasive cribriform carcinoma, but this is usually a focal lesion with a lobulocentric growth pattern. Typically, the cribriform spaces contain basement membrane-like material (Fig. 12.43).

Prognosis and Therapy Considerations

The clinical behaviour of invasive cribriform carcinoma is very similar to that of tubular carcinoma, with a lower incidence of nodal metastases than for invasive ductal carcinoma [50]. Segmental resection with or without radiotherapy and sentinel lymph node sampling are considered standard treatment. Patients with small, pure invasive cribriform carcinomas have an excellent prognosis, and some authors question the need for radiation therapy after complete excision.

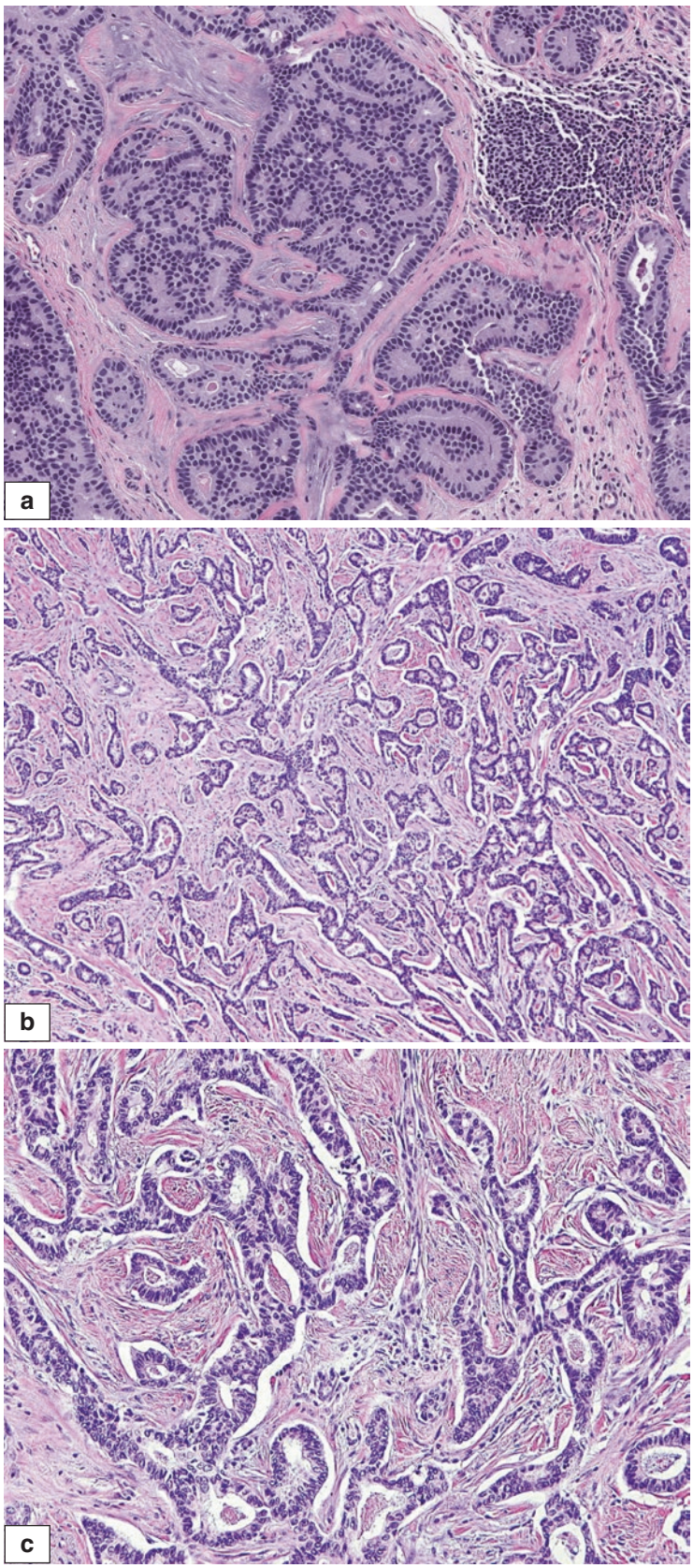

Fig. 12.38 Invasive cribriform carcinoma. Microscopic features. (**a**) Invasive carcinoma composed of large nests of uniform cells with cribriform patterns mimicking in situ cribriform carcinoma. The irregular, angulated edges of the nests indicate the invasive nature of the tumour. (**b**, **c**) Elongated cords and anastomosing islands of tumour cells show a cribriform growth pattern

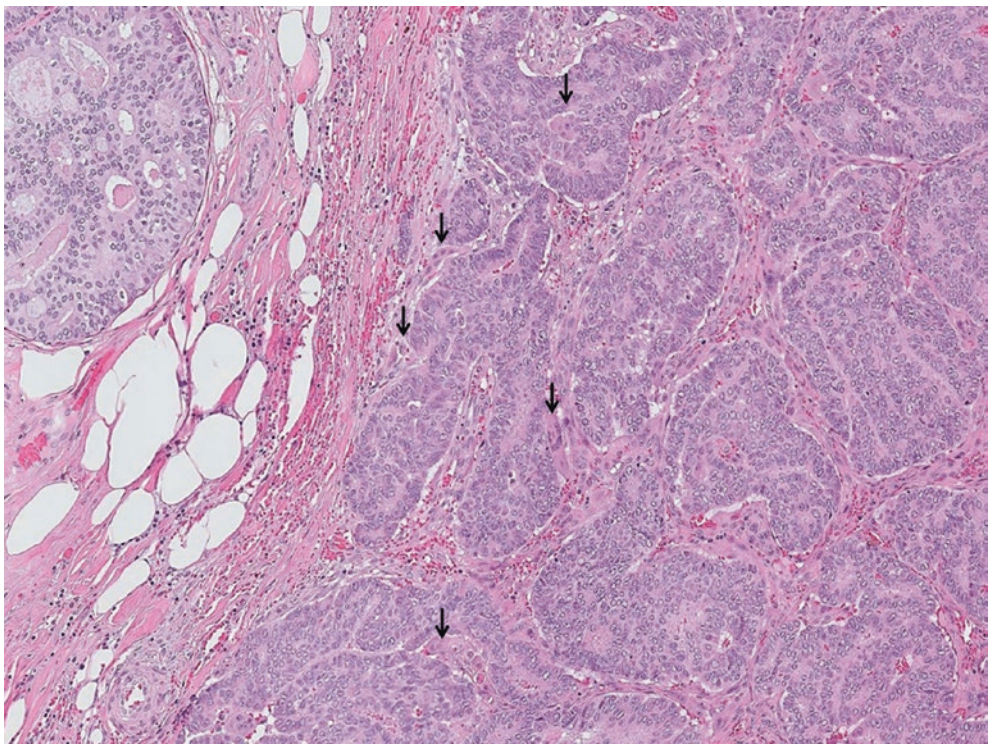

Fig. 12.39 Invasive cribriform carcinoma with osteoclast-like giant cells. Invasive carcinoma comprising irregular cribriform glands is seen within the congested stroma. Scattered osteoclast-like giant cells (*arrows*) are seen among the invading cribriform islands. Cribriform ductal carcinoma in situ (DCIS) is present in the *left upper field*

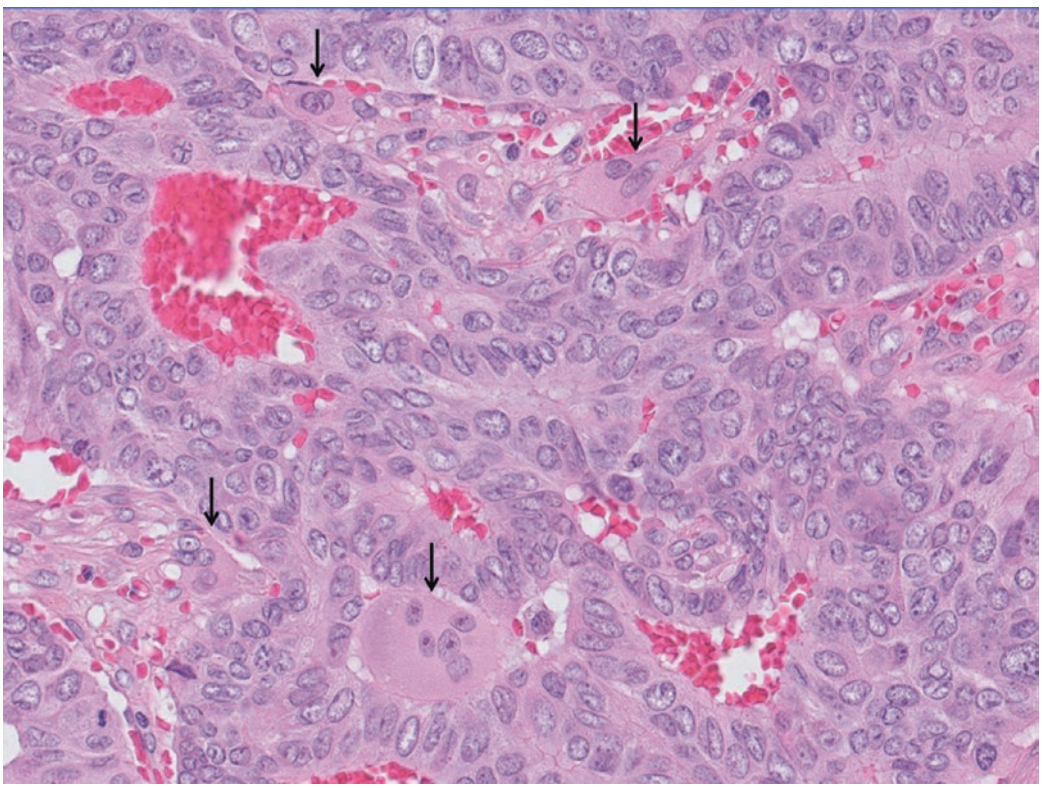

Fig. 12.40 Invasive cribriform carcinoma with osteoclast-like giant cells. High magnification shows the osteoclast-like multinucleated giant cells (*arrows*) among the invasive cribriform islands

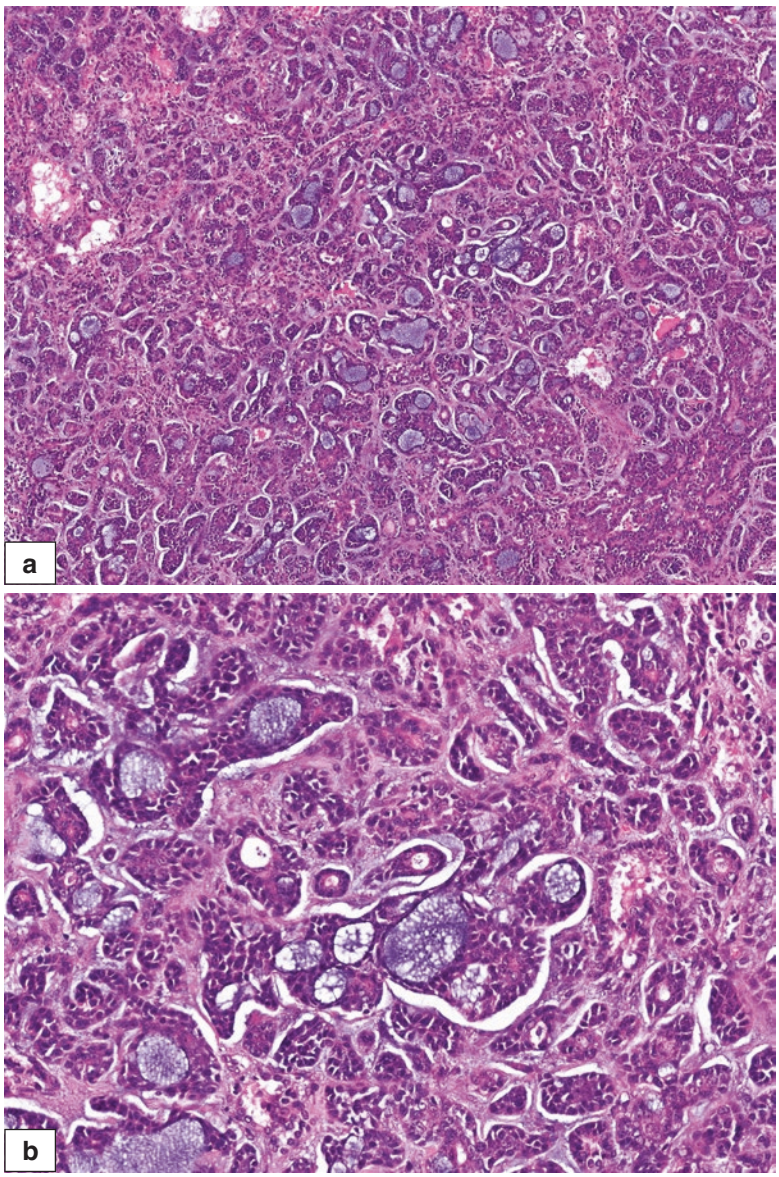

Fig. 12.41 Adenoid cystic carcinoma. Microscopic features. (**a**, **b**) The cribriform architectural pattern of adenoid cystic carcinoma may mimic invasive cribriform carcinoma. Adenoid cystic carcinoma glands contain basement membrane-like material, whereas cribriform carcinoma glands are usually empty

Carcinoma with Medullary Features

Definition

As the histological characteristics of classic medullary carcinoma are difficult to reproducibly define and recognise, the WHO Working Group recommends classifying these tumours as carcinomas with medullary features, a term that incorporates tumours previously categorised as medullary carcinoma, atypical medullary carcinoma, and invasive carcinoma with medullary features [53].

Clinical and Epidemiological Features

Classic medullary carcinomas account for less than 1% of breast carcinomas. Studies that report higher rates likely included atypical forms and invasive carcinomas with medullary features. Patients tend to be younger and may present with palpable lumps. Some tumours are mammographically detected.

Imaging Features

These tumours are often circumscribed and may radiologically mimic a benign lesion (Fig. 12.44). Intralesional cystic components due to tumour necrosis may be seen.

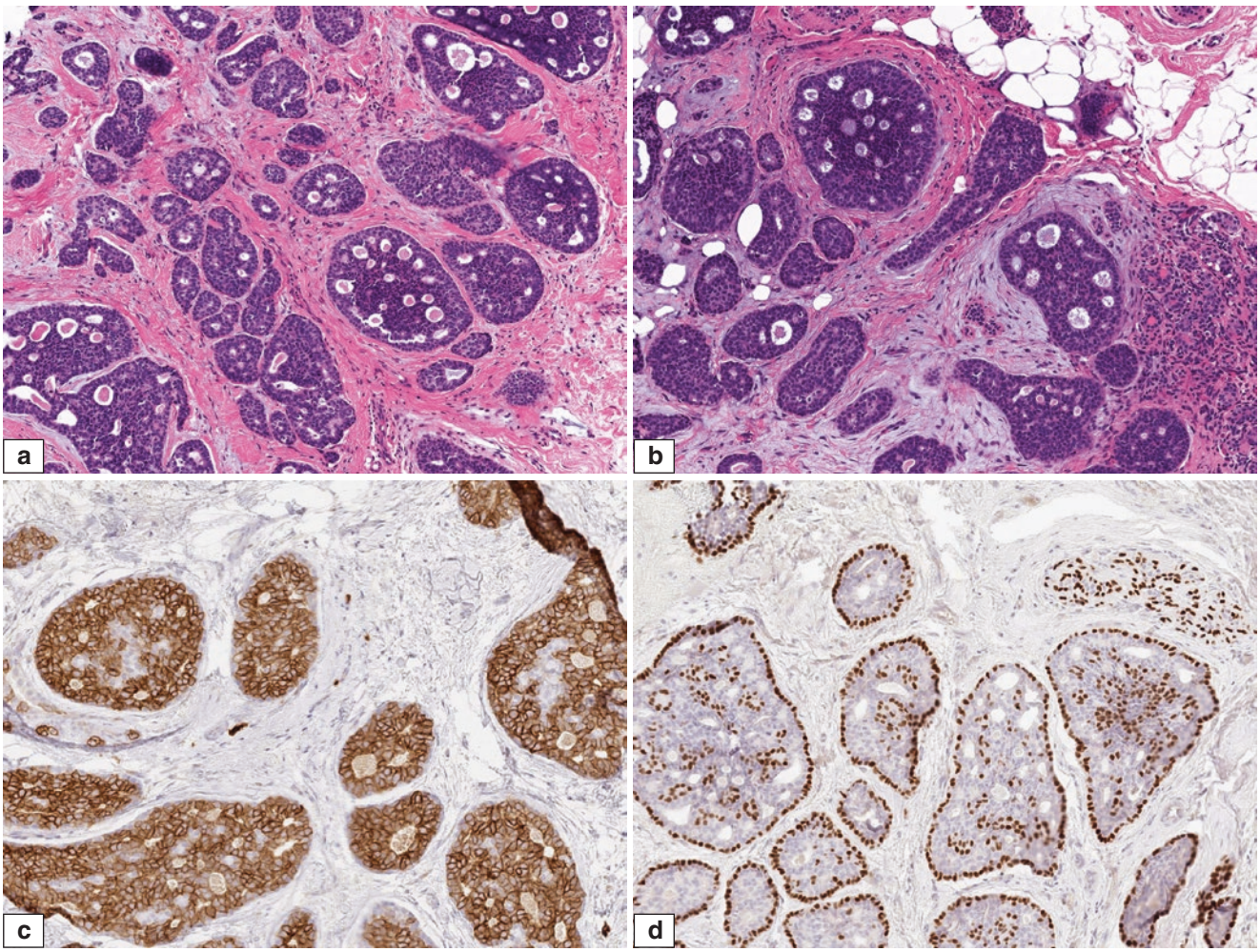

Fig. 12.42 Adenoid cystic carcinoma. Histologic and immunohistochemical features. (**a**, **b**) H&E staining of adenoid cystic carcinoma shows a cribriform pattern. (**c**) Tumour cells are diffusely positive for cKIT. (**d**) p63 staining highlights the presence of two cell populations in cribriform structures

Pathologic Features

Macroscopic Pathology

Carcinomas with medullary features are macroscopically circumscribed, soft, fleshy tumours (Fig. 12.45). Cystic degeneration, necrosis, and haemorrhage may be seen (Figs. 12.46 and 12.47).

Microscopic Pathology

The histological hallmark is the presence of a prominent lymphoplasmacytic infiltrate intermingling with high-grade carcinoma cells in a sheetlike growth pattern with little intervening stroma. Apart from the heavy lymphoplasmacytic infiltrate and high nuclear grade, classic medullary carcinoma shows microscopic circumscription, syncytial architecture in more than 75 % of the tumour, and absence of tubular differentiation. Mitoses, necrosis, and bizarre giant cells may be observed. In atypical medullary carcinoma (Figs. 12.48, 12.49, 12.50, 12.51, 12.52, 12.53, 12.54, 12.55, 12.56, and 12.57) and invasive carcinoma with medullary features (Figs. 12.58, 12.59, and 12.60), only some of these histological parameters are present. As there is interobserver inconsistency in defining the microscopic parameters, many (including the WHO Working Group) have opted for the encompassing diagnosis of carcinoma with medullary features. Receptors (ER, PR, c-erbB-2) are usually negative ("triple-negative"), and these tumours frequently show expression of basal markers and p53 (Figs. 12.61, 12.62, 12.63, and 12.64).

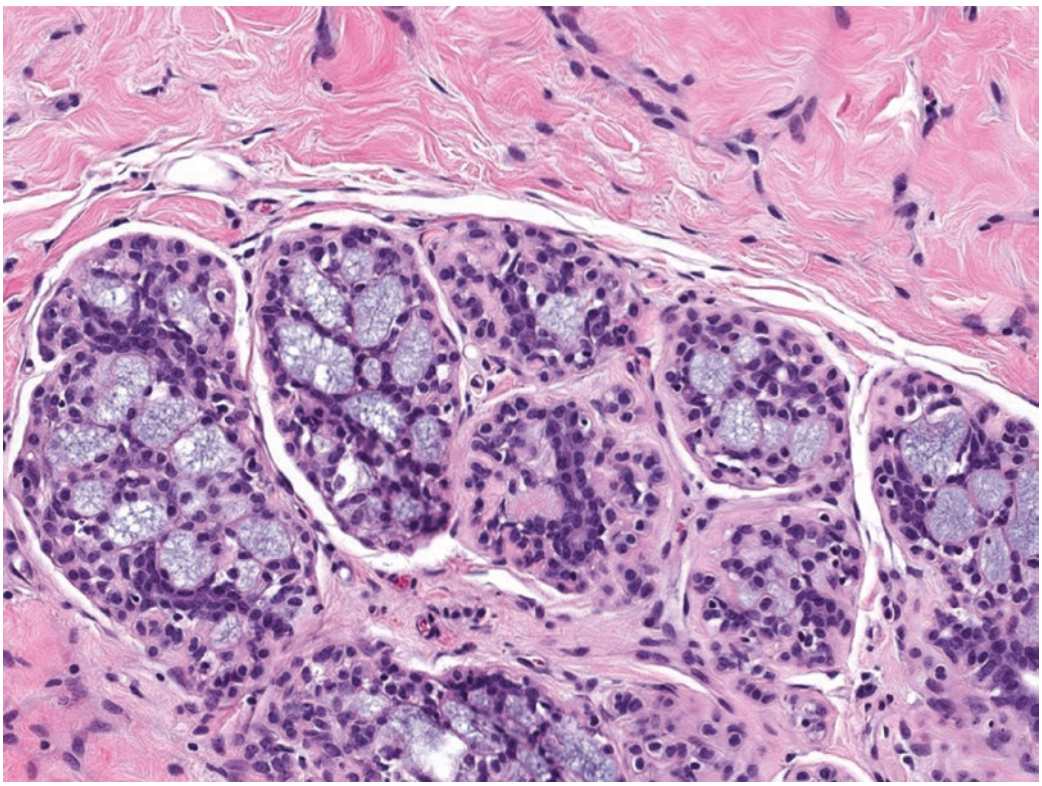

Fig. 12.43 Collagenous spherulosis. Microscopic features. Lobulocentric proliferation of small glandular structures with a cribriform pattern, which may mimic invasive cribriform carcinoma

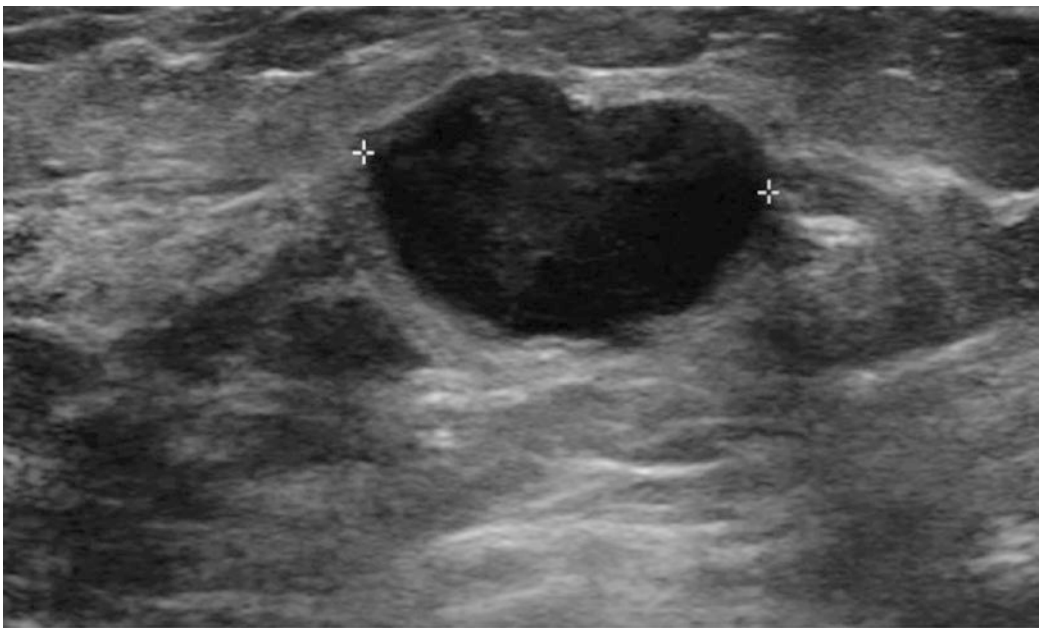

Fig. 12.44 Atypical medullary carcinoma shows a circumscribed, lobulated mass on ultrasonography. This lesion was thought to be possibly a fibroadenoma radiologically (Courtesy of Dr. Lester Leong)

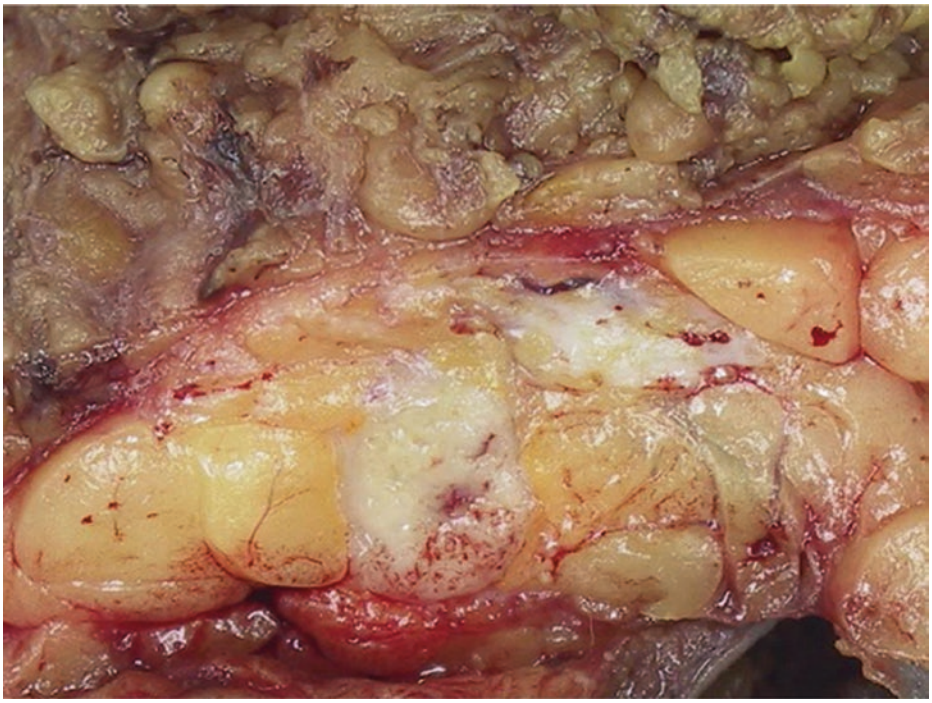

Fig. 12.45 Medullary carcinoma. Grossly, the tumour has circumscribed borders with a whitish cut surface. An area of haemorrhage is present in the central portion from prior needle aspiration

Fig. 12.46 Medullary carcinoma. This tumour has well-circumscribed but unencapsulated borders. There is a fleshy appearance with areas of haemorrhage and necrosis, the latter seen as yellowish foci in the tumour

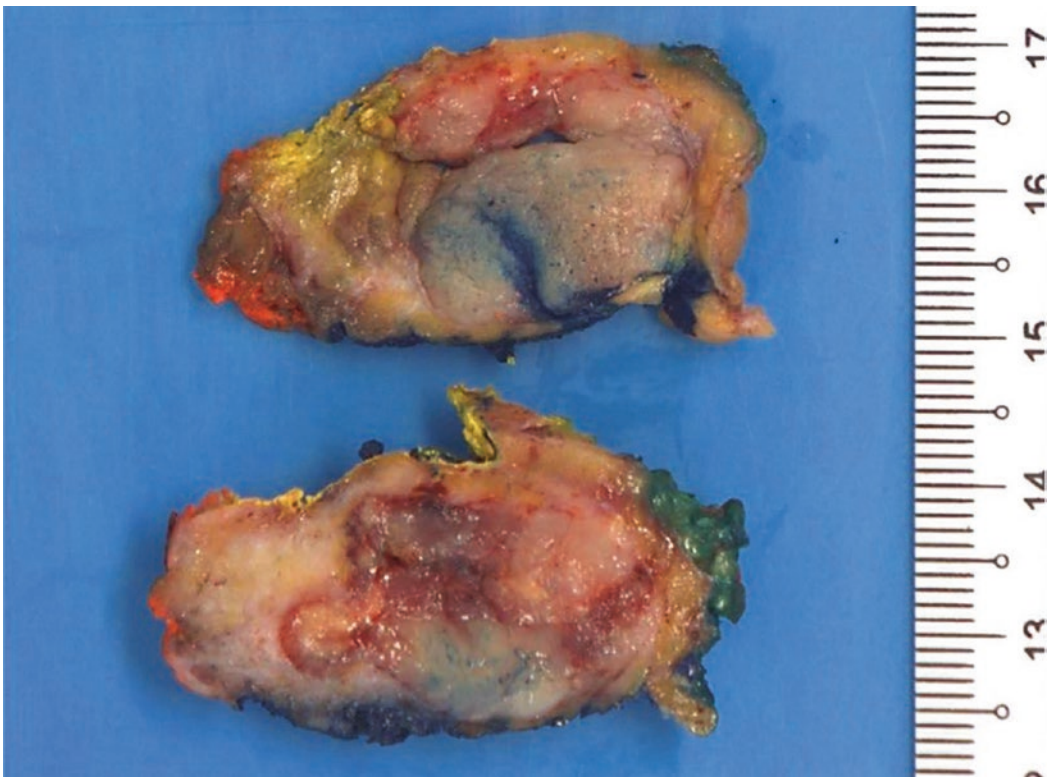

Fig. 12.47 Atypical medullary carcinoma. Excision biopsy shows a soft, fleshy mass with lobulated contours and a rounded nubbin protruding against the adjacent fibrous breast parenchyma

Differential Diagnosis

Malignant Lymphoma

Owing to the heavy lymphoplasmacytic infiltrates, medullary carcinoma may be mistaken for lymphoma and vice versa, especially on limited material from core biopsies. Though cohesion and aggregation of malignant tumour cells are useful clues to carcinoma, some lymphomas may demonstrate artefactual compartmentalisation mimicking carcinoma. In lymphoma, tumour cells tend to harbour irregular nuclear contours with clumpy to vesicular chromatin and ill-defined cytoplasmic borders. Malignant lymphoid cells permeate as diffuse sheets into surrounding parenchyma (Figs. 12.65, 12.66, 12.67, 12.68, 12.69, 12.70, 12.71, and 12.72). Lymphocytic lobulitis and lymphoepithelial lesions with lymphocytes in the breast epithelium can be observed; the latter are more commonly seen in low-grade, marginal zone lymphomas.

Granulocytic Sarcoma

Although there is often a history of myeloid leukaemia, granulocytic sarcoma sometimes may precede the diagnosis of leukaemia. Its occurrence in the breast is exceptionally rare, so it is often not considered among differential diagnoses of a poorly differentiated malignant tumour disposed in diffuse sheets. Marked tumour cell nuclear irregularity and occasional eosinophilic metamyelocytes are helpful clues (Figs. 12.73, 12.74, 12.75, and 12.76). Myeloperoxidase and CD117 immunohistochemistry can aid diagnosis.

Intraparenchymal Lymph Node

A lymph node within the breast parenchyma that has reactive hyperplasia or is involved by carcinoma may resemble medullary carcinoma. Resemblance to a lymph node at low magnification has been suggested as a useful clue for diagnosing classic medullary carcinoma, with its circumscription and dense lymphoid population. A lymph node shows histoanatomic compartments of cortex, medulla, capsule, and sinuses, but some or all of these features may be obscured or effaced when there is involvement by carcinoma. Germinal centre cells with centroblasts and centrocytes may be of potential concern owing to nuclear enlargement, but their confinement within the lymphoid follicles and overall preserved nodal architecture should allow correct interpretation.

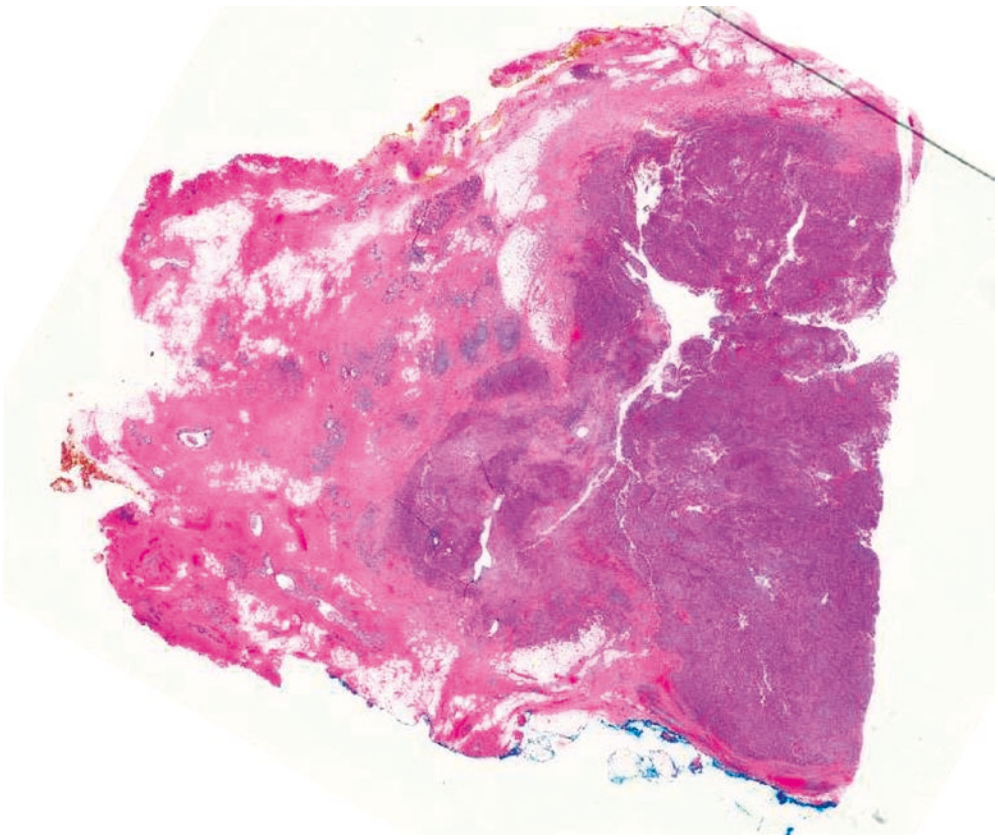

Fig. 12.48 Atypical medullary carcinoma. Scanning magnification shows a relatively circumscribed, lobulated tumour with pushing contours. The histological counterpart of the macroscopic tumour nubbin (Fig. 12.47) is observed protruding out into the surrounding breast parenchyma

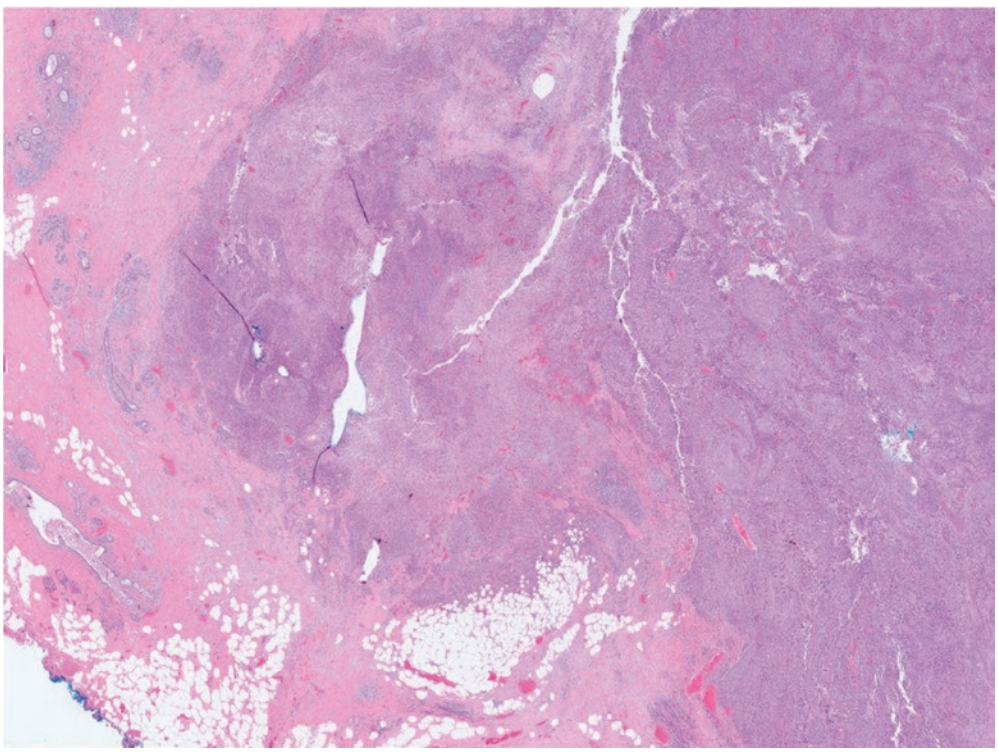

Fig. 12.49 Atypical medullary carcinoma. Closer histological view of the rounded protrusion of the tumour, which has a cellular appearance with paler zones corresponding to the confluent sheets of malignant cells alternating with darker areas represented by the dense inflammatory cells

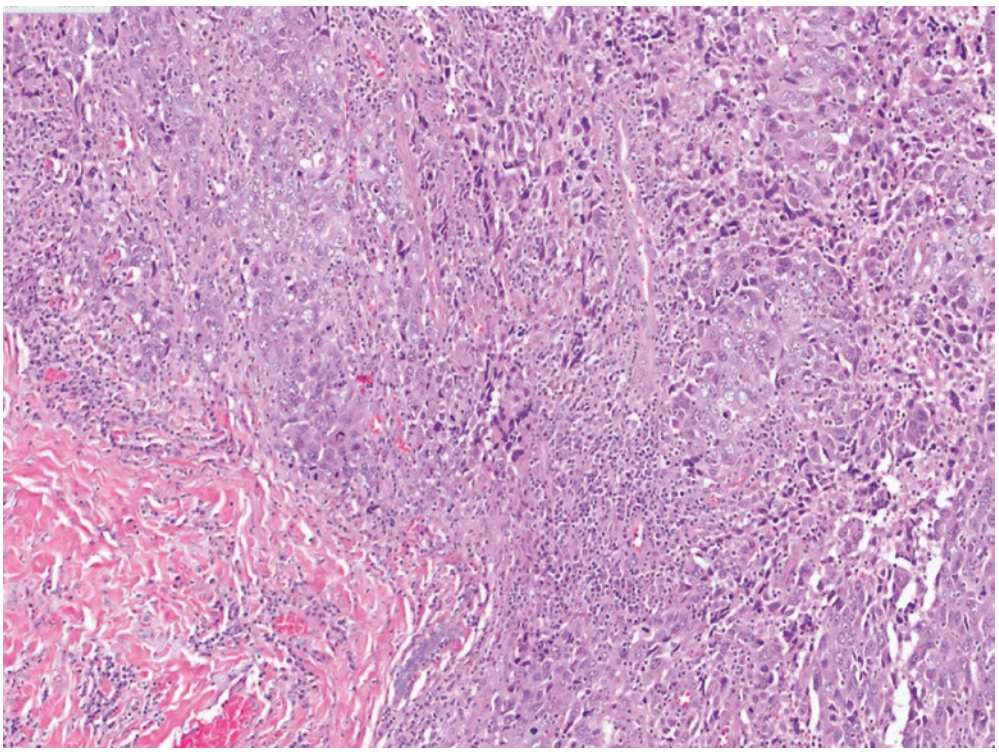

Fig. 12.50 Atypical medullary carcinoma. Broad, anastomosing trabeculae of tumour cells are seen among collections of lymphocytes

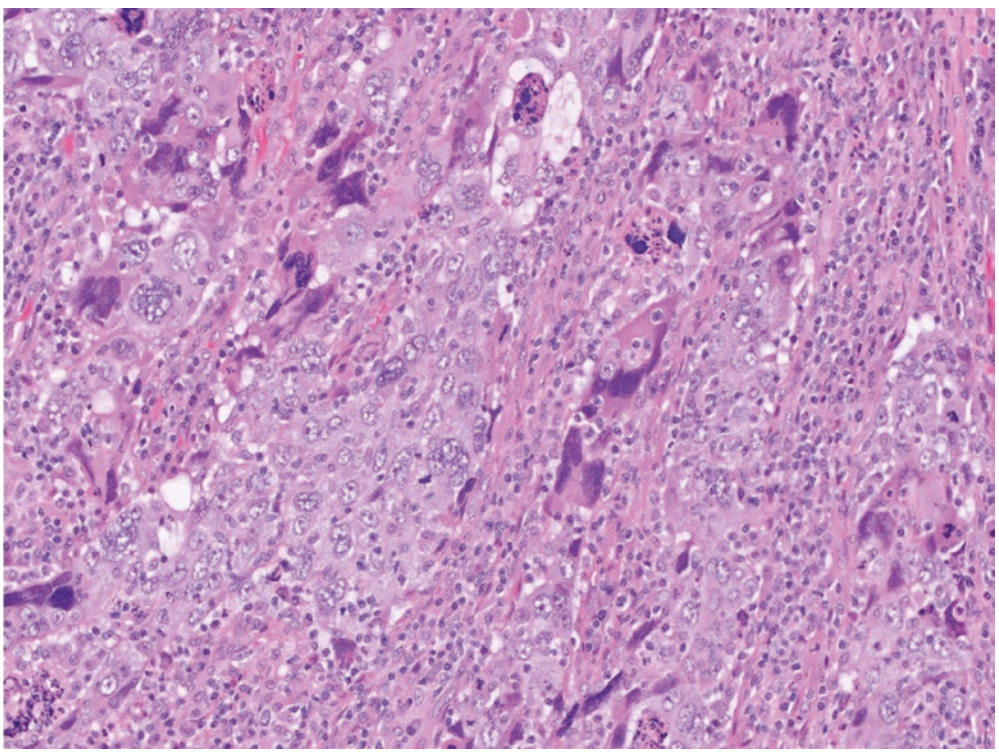

Fig. 12.51 Atypical medullary carcinoma. Bizarre and multinucleated tumour cells are seen among the sheets of malignant cells with markedly pleomorphic vesicular nuclei with prominent nucleoli. Some of the multinucleated tumour giant cells are reminiscent of syncytiotrophoblastic cells, but unlike syncytiotrophoblastic cells, these are negative for hCG and hPL

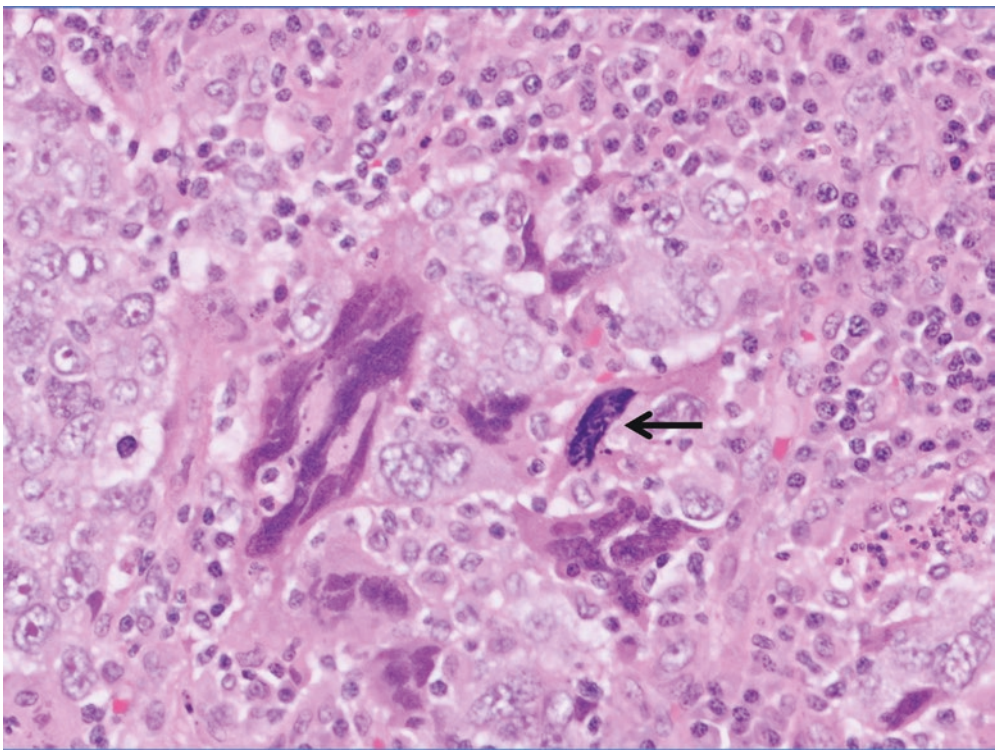

Fig. 12.52 Atypical medullary carcinoma. High magnification of the multinucleated giant cells intermingling with the carcinoma cells. A mitosis is present (*arrow*). Lymphocytes and plasma cells surround malignant cells, with some extending between them

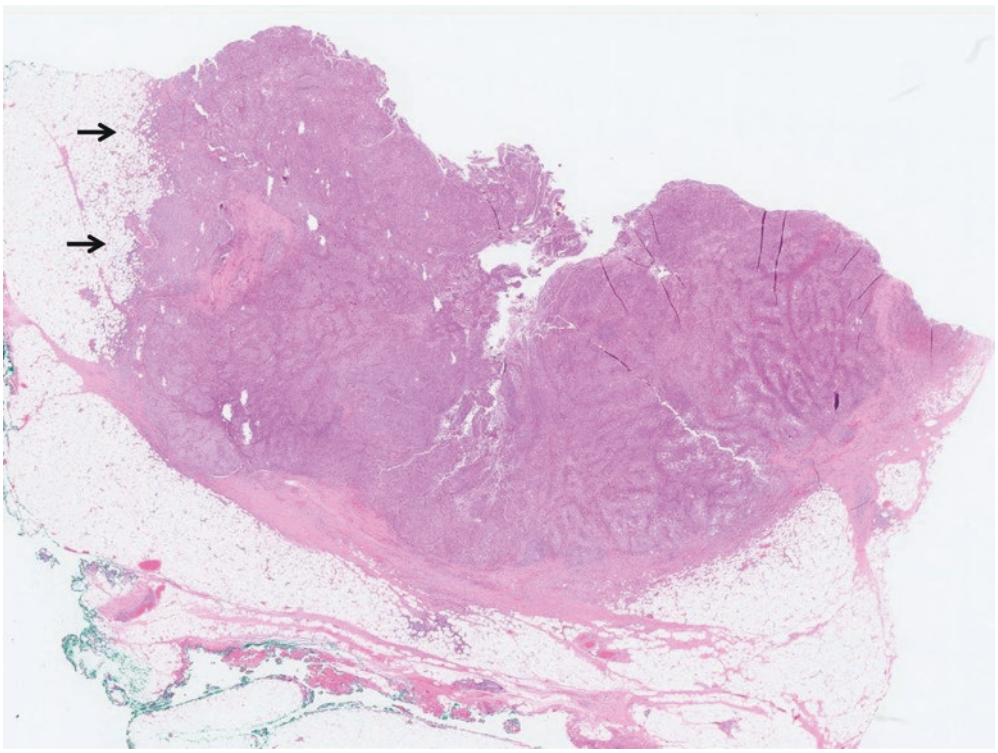

Fig. 12.53 Atypical medullary carcinoma. Low magnification shows partial encapsulation with a fibrous wall, whereas part of the tumour reveals irregular extensions into the surrounding fat (*arrows*)

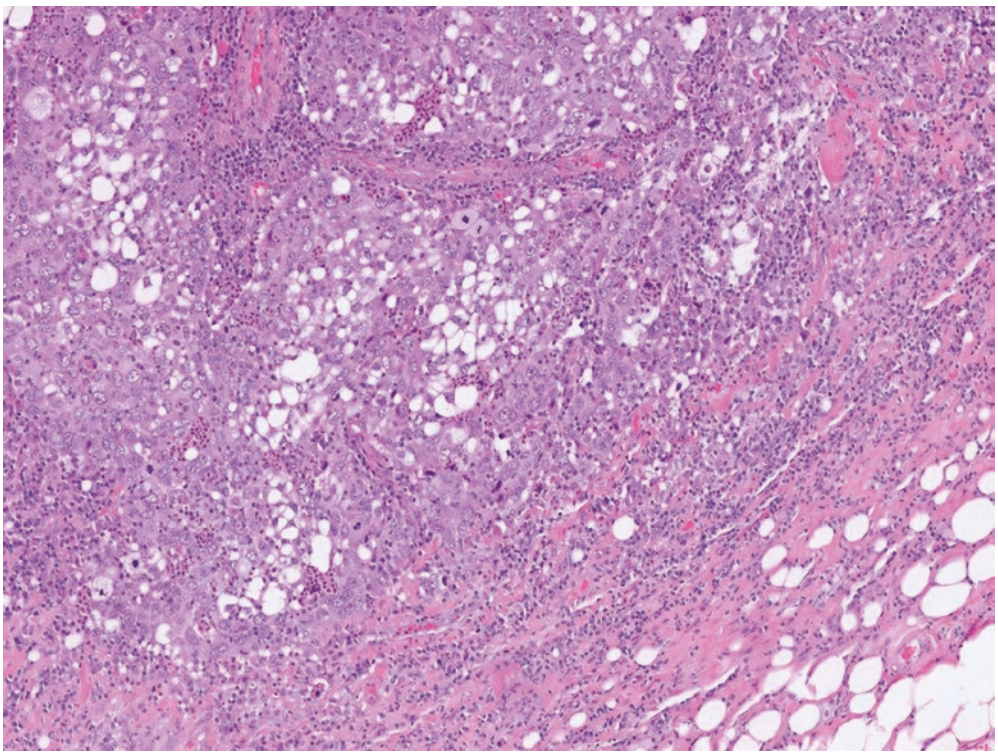

Fig. 12.54 Atypical medullary carcinoma. Some tumour cells show cytoplasmic vacuoles, which are likely degenerative in nature

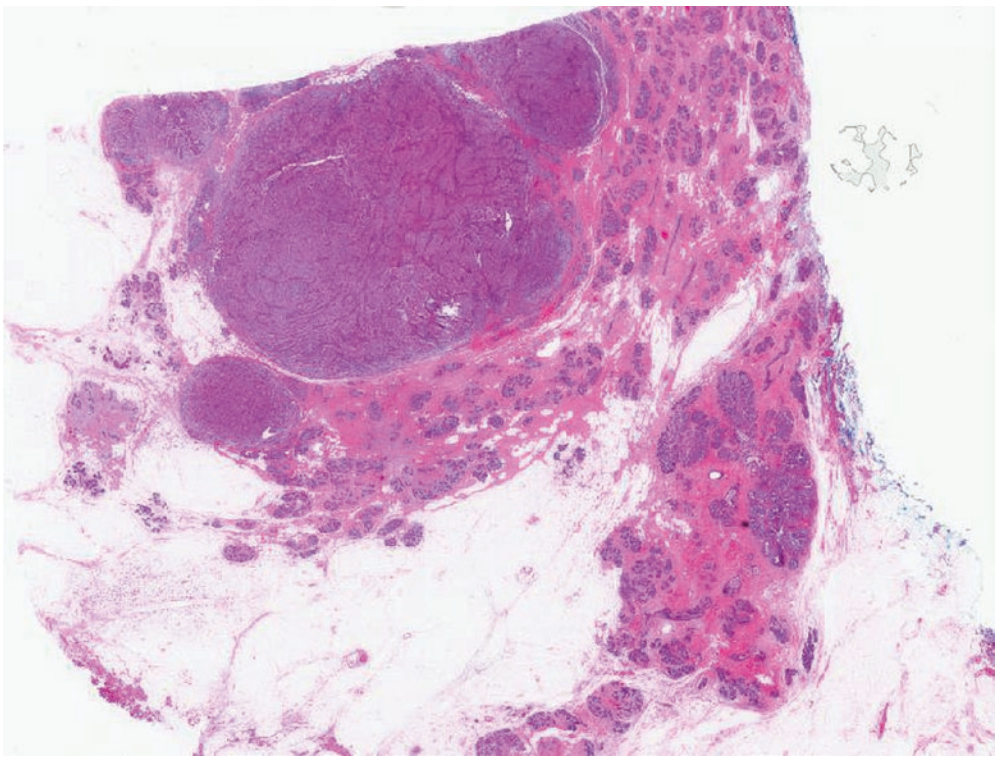

Fig. 12.55 Atypical medullary carcinoma. At low magnification, a slight resemblance to a lymph node is seen. The tumour appears multinodular, with relatively good circumscription. No DCIS is present in the surrounding tissue. Though most medullary carcinomas are not accompanied by DCIS, and its presence is used by some authors as an exclusion criterion for the diagnosis of classic medullary carcinoma, it is possible for DCIS to be rarely encountered in association with medullary carcinoma

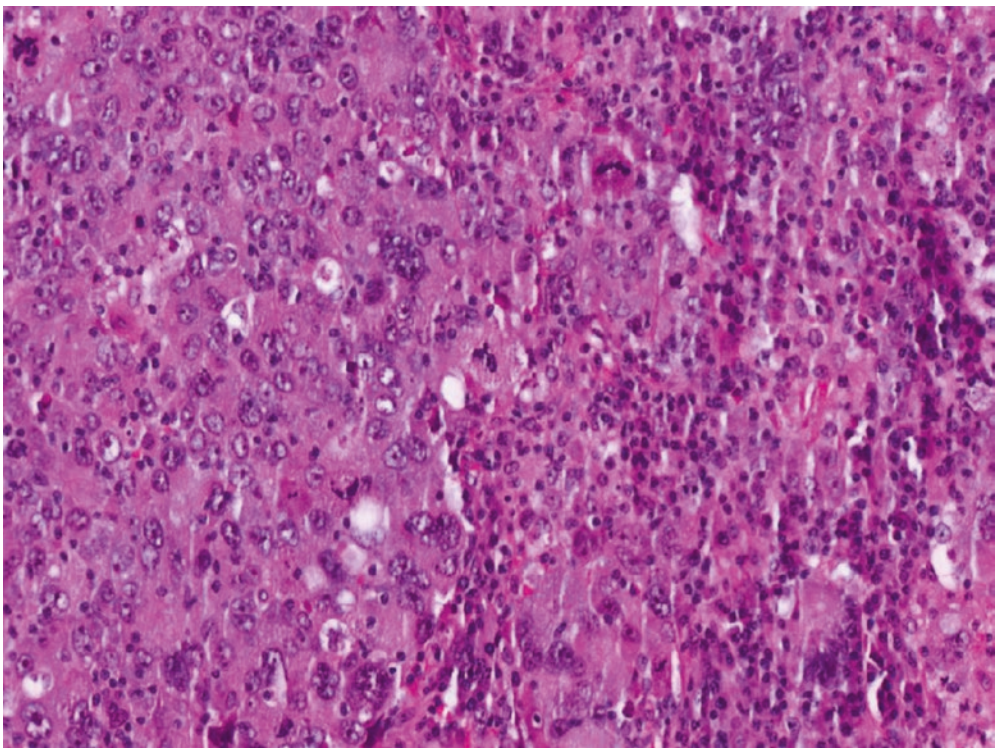

Fig. 12.56 Atypical medullary carcinoma. Syncytial sheets of high-grade carcinoma cells with atypical mitoses are accompanied by lymphoplasmacytic infiltrates within the tumour islands and in the intervening, scant stroma

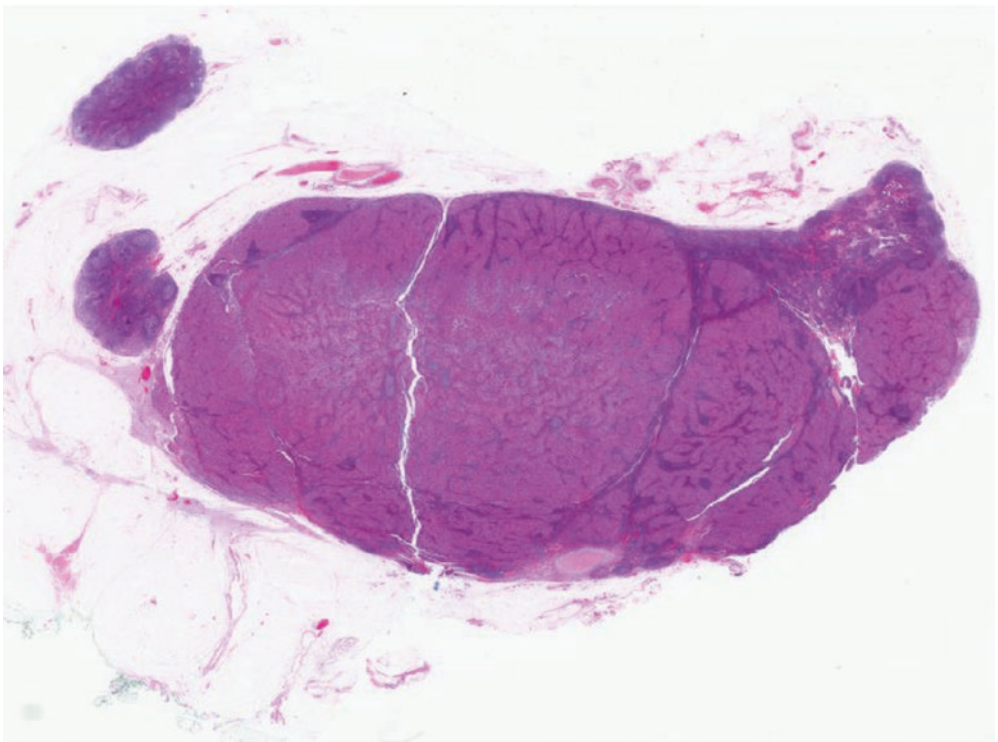

Fig. 12.57 An axillary lymph node showing metastasis from an atypical medullary carcinoma. Anastomosing and coalescent tumour effaces a large portion of the node

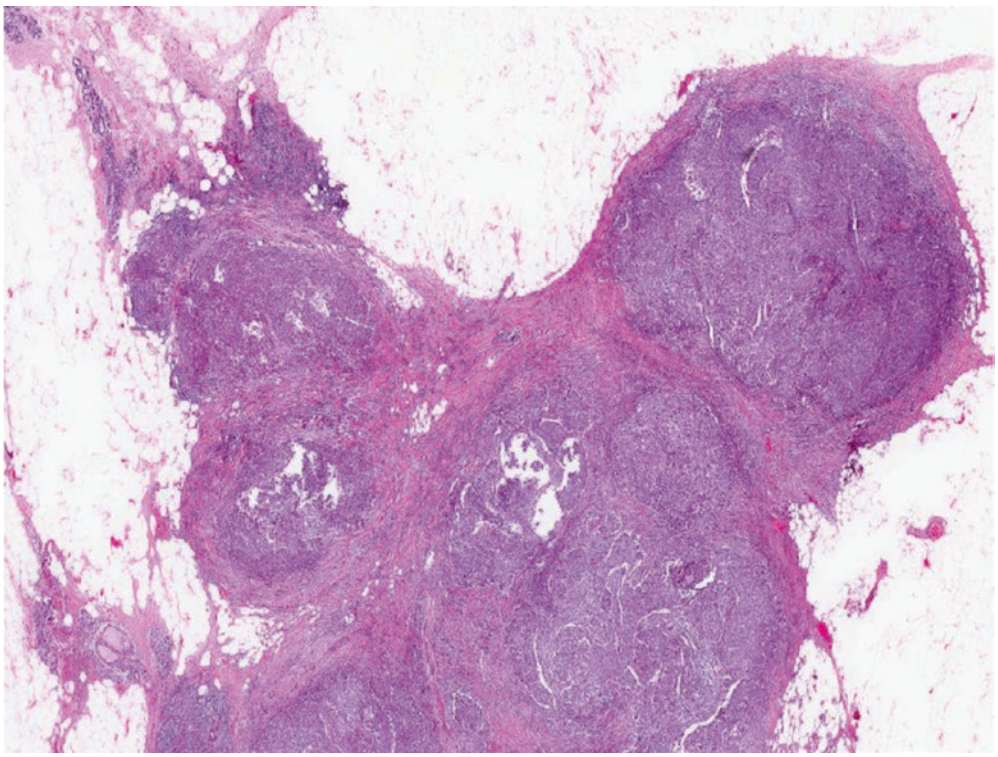

Fig. 12.58 Invasive carcinoma with medullary features. This tumour has a lobulated outline with portions of the tumour extending into adipose. Lymphocytic infiltrates, though present, are less prominent, and there appears to be a greater amount of fibrosis meandering among the tumour islands

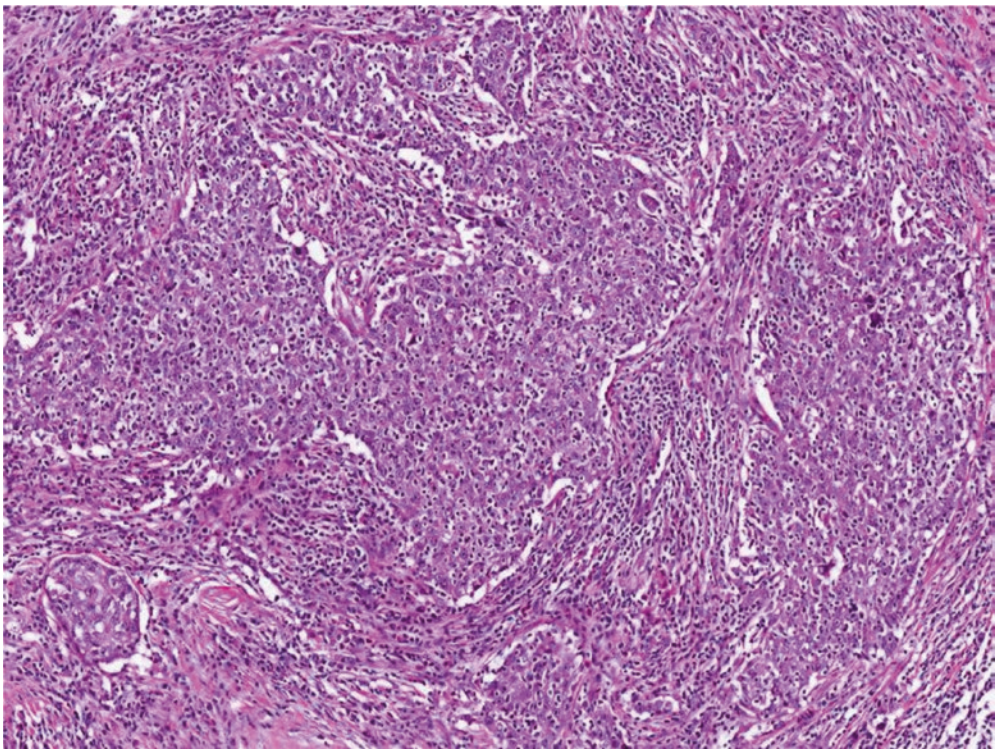

Fig. 12.59 Invasive carcinoma with medullary features. Islands of tumour cells are enveloped by lymphoplasmacytic infiltrates. The interphase between carcinoma islands and the stromal infiltrates is blurred, and many lymphocytes extend into the tumour as well

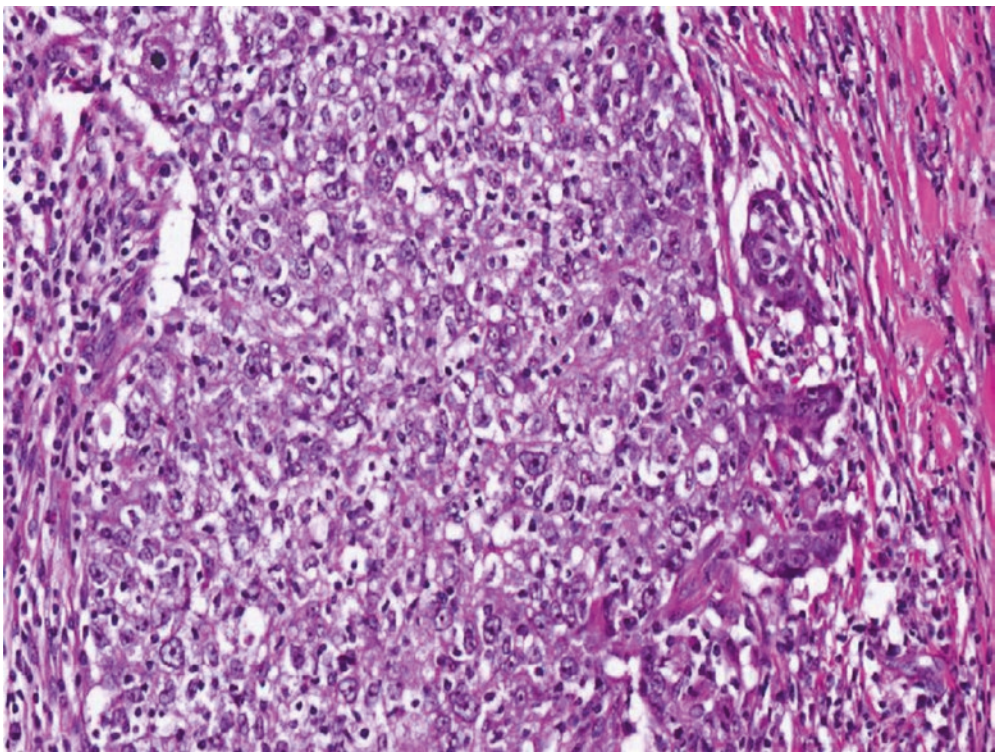

Fig. 12.60 Invasive carcinoma with medullary features. Lymphocytes are seen within the tumour islands (intratumoural lymphocytes), giving an appearance resembling lymphoepithelial carcinoma

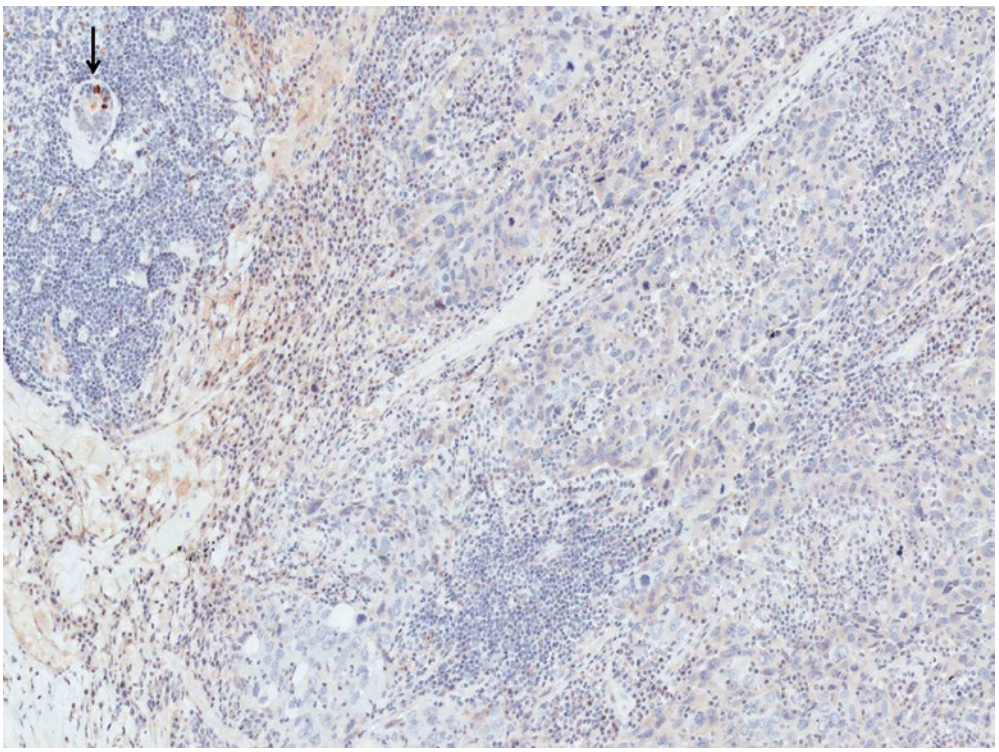

Fig. 12.61 Medullary and medullary-like cancers are usually triple-negative. In this illustration, the tumour cells show negative staining for oestrogen receptor on immunohistochemistry. Note the internal positive control represented by the benign epithelial cell nuclei (*arrow*)

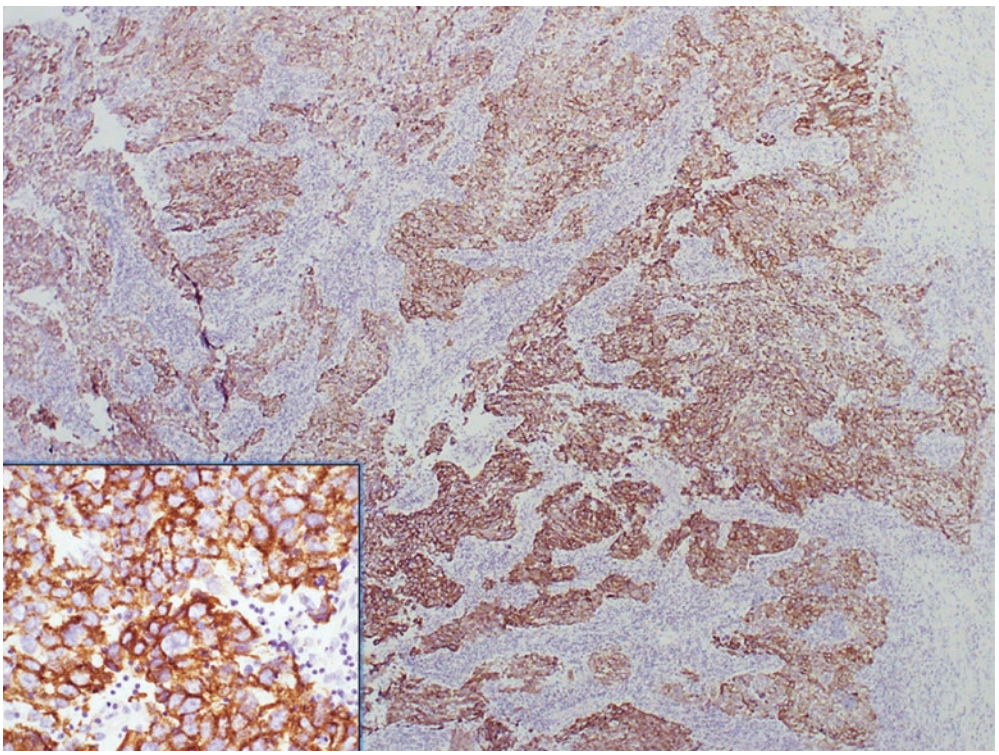

Fig. 12.62 Medullary carcinoma shows positive reactivity of tumour cells for the epithelial marker MNF116, highlighting the anastomosing syncytial trabeculae and irregular islands at low magnification. Inset shows cytoplasmic and membrane positivity of tumour cells for MNF116

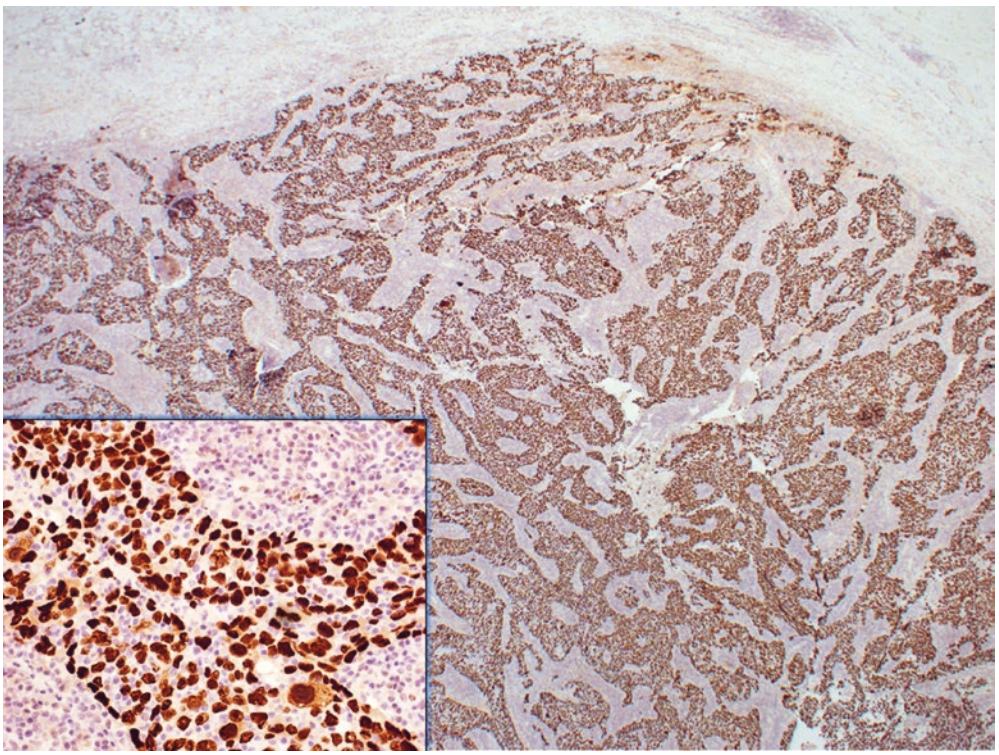

Fig. 12.63 Immunohistochemistry for p53 shows diffuse, intense reactivity of tumour cell nuclei in medullary carcinoma. *Inset* shows a higher magnification of the positively stained nuclei

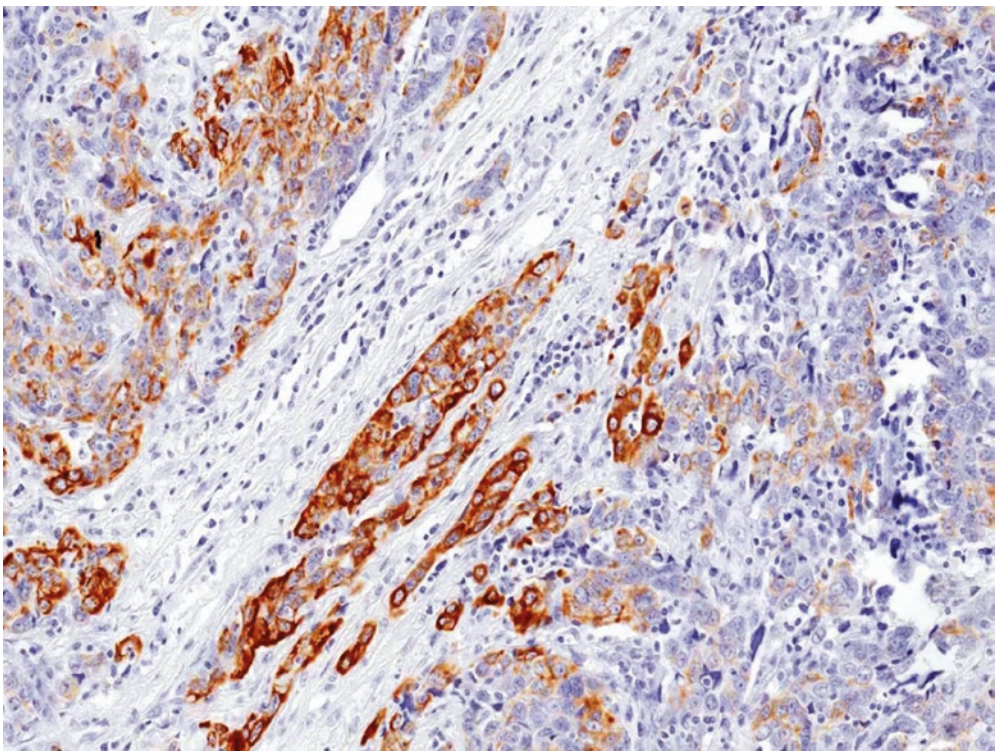

Fig. 12.64 Invasive carcinoma with medullary features. There is positive reactivity for the basal marker CK14 in the tumour cells. Carcinomas with medullary features often express the basal phenotype with expression of basal markers and p63

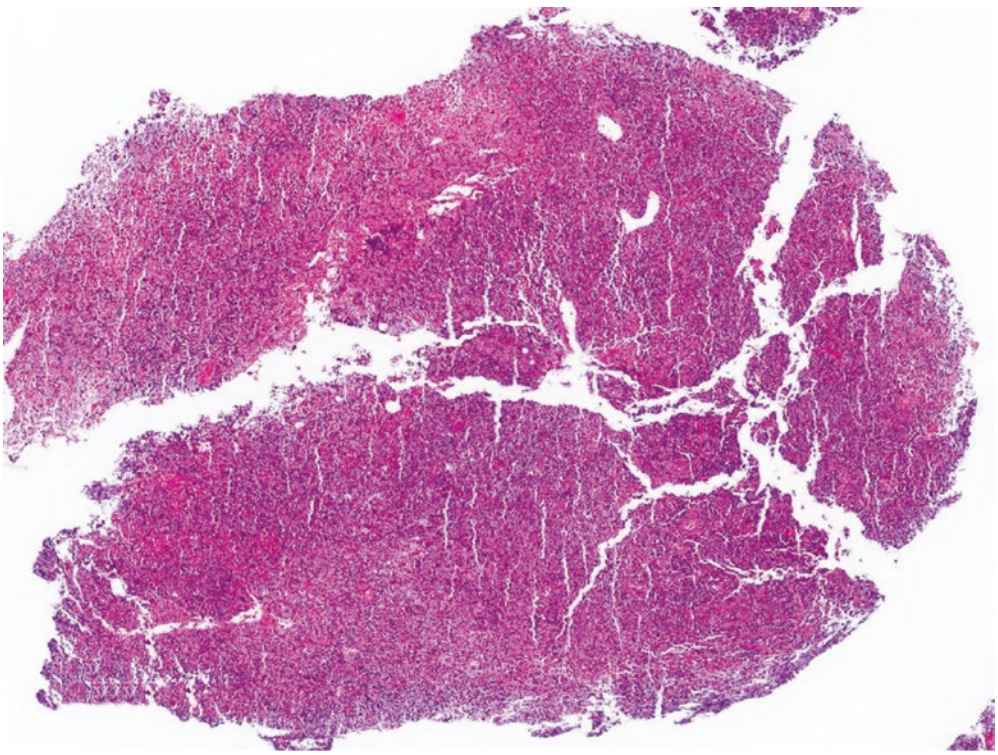

Fig. 12.65 Diffuse large B-cell lymphoma. At low magnification, this incisional biopsy specimen from a breast mass may evoke consideration of a medullary-like carcinoma

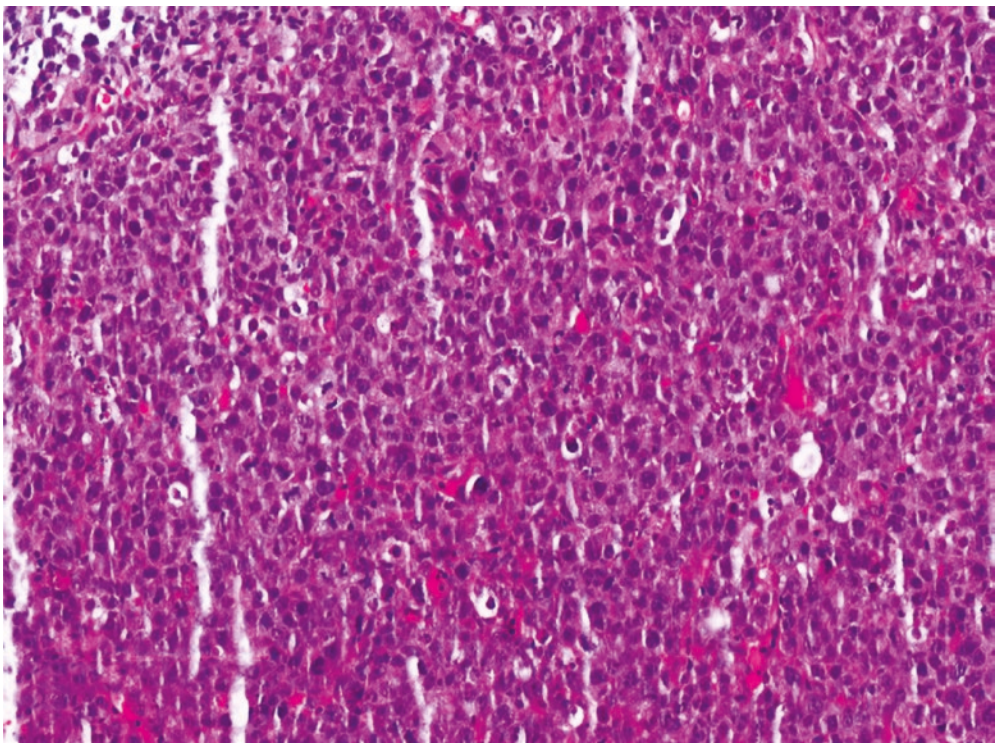

Fig. 12.66 Diffuse large B-cell lymphoma. At higher magnification, tumour cells occur in sheets with vesicular nuclei that have irregular nuclear contours. Mitoses, apoptosis, and karyorrhexis are seen

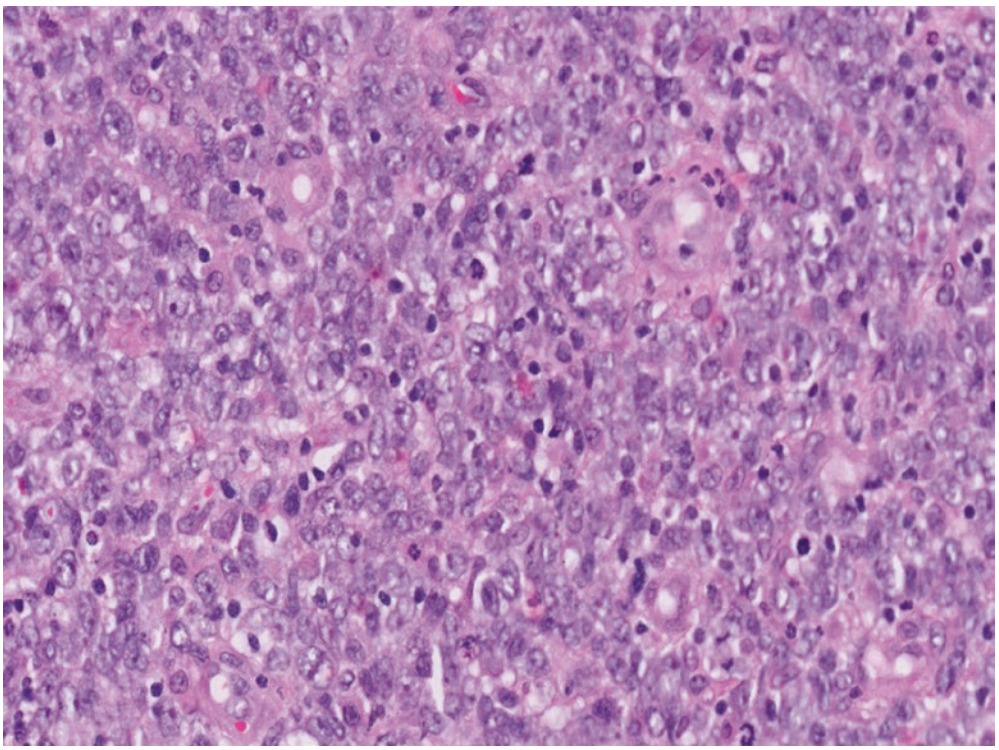

Fig. 12.67 Diffuse large B-cell lymphoma. High magnification shows malignant lymphoid cells with nuclear vesicularity and distinct nucleoli. Some of the nuclei are bent and show grooves. Small admixed lymphocytes with dense nuclei are present

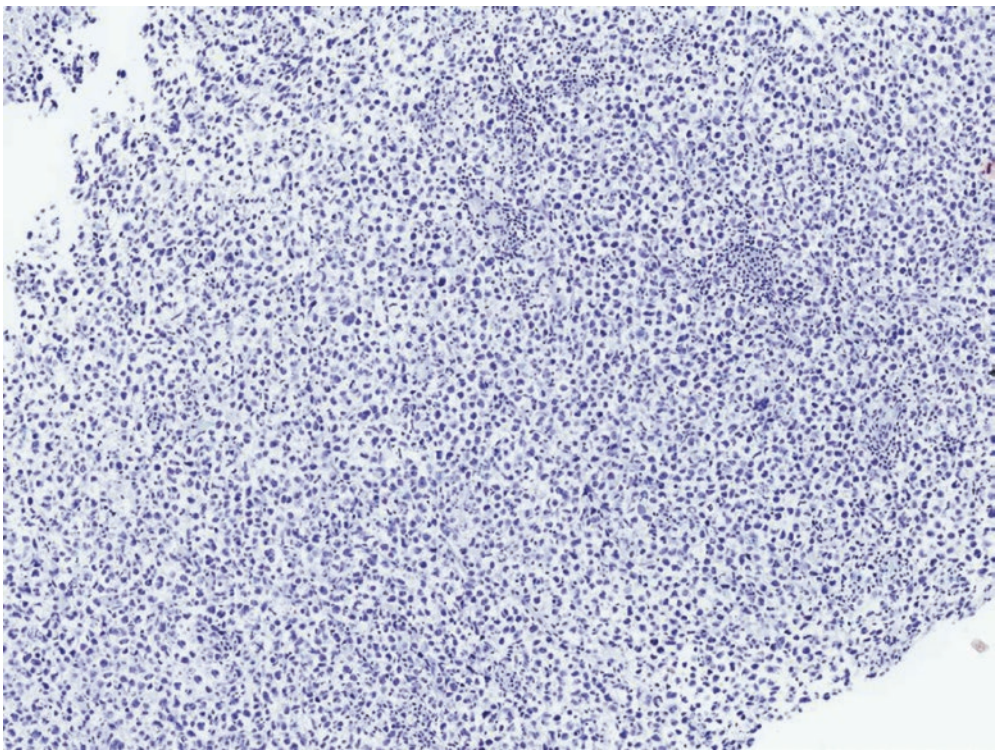

Fig. 12.68 Diffuse large B-cell lymphoma. Immunohistochemistry shows negative staining of the malignant cells for the epithelial marker MNF116

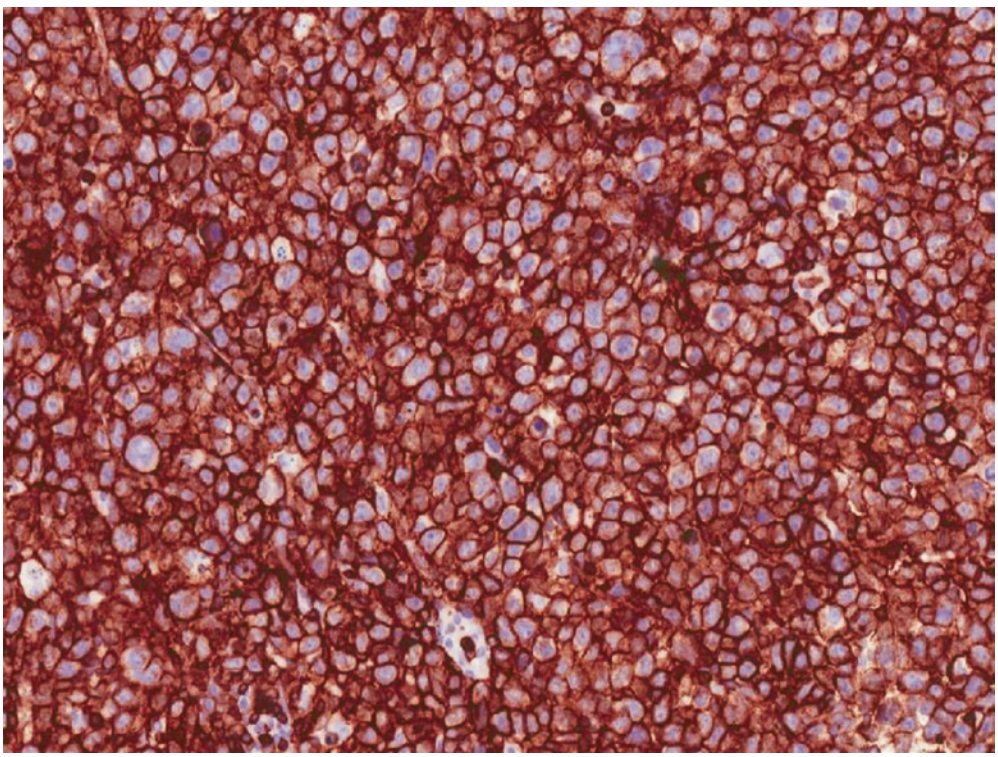

Fig. 12.69 Diffuse large B-cell lymphoma. Diffuse and intense staining of the tumour cells for leukocyte common antigen (LCA) confirms a lymphoid origin

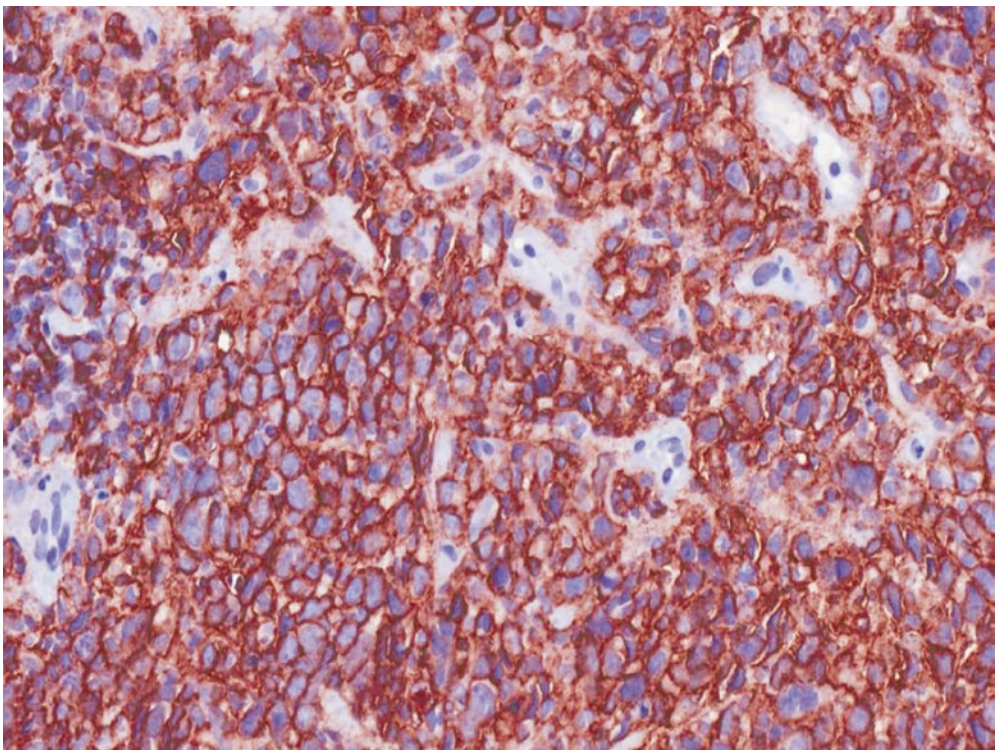

Fig. 12.70 Diffuse large B-cell lymphoma. As with LCA, there is diffuse and strong reactivity for the B-cell marker CD20, indicating a B-cell immunophenotype and supporting the diagnosis of a diffuse large B-cell lymphoma, the commonest type of lymphoma encountered in the breast

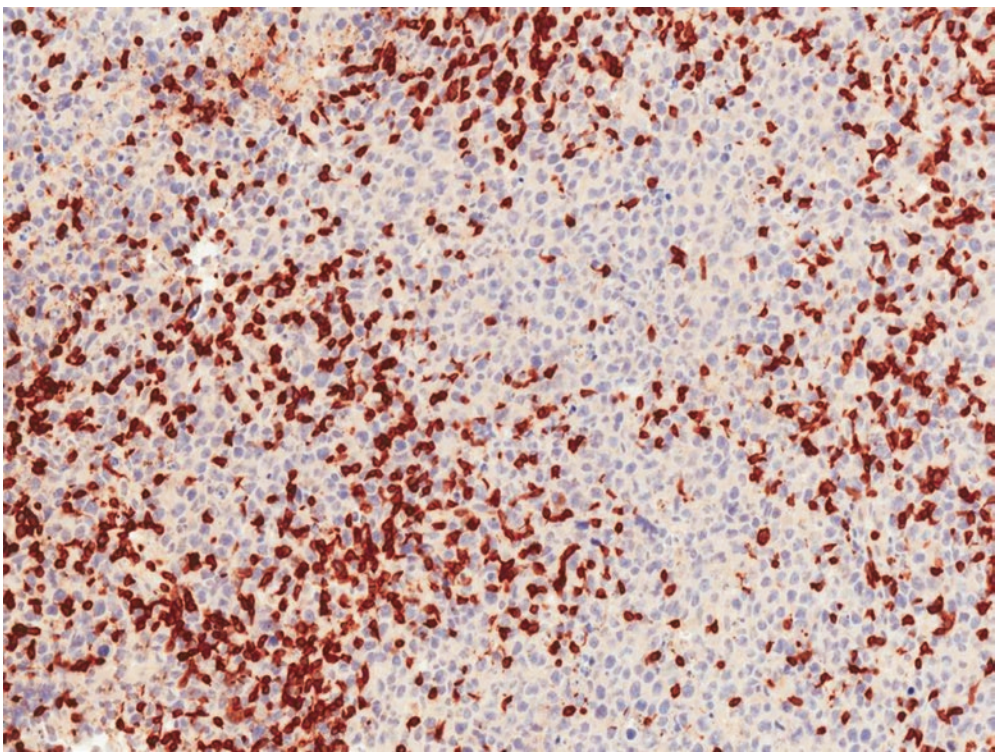

Fig. 12.71 Diffuse large B-cell lymphoma. CD3 immunohistochemistry highlights admixed reactive T cells, which are smaller than the malignant B cells

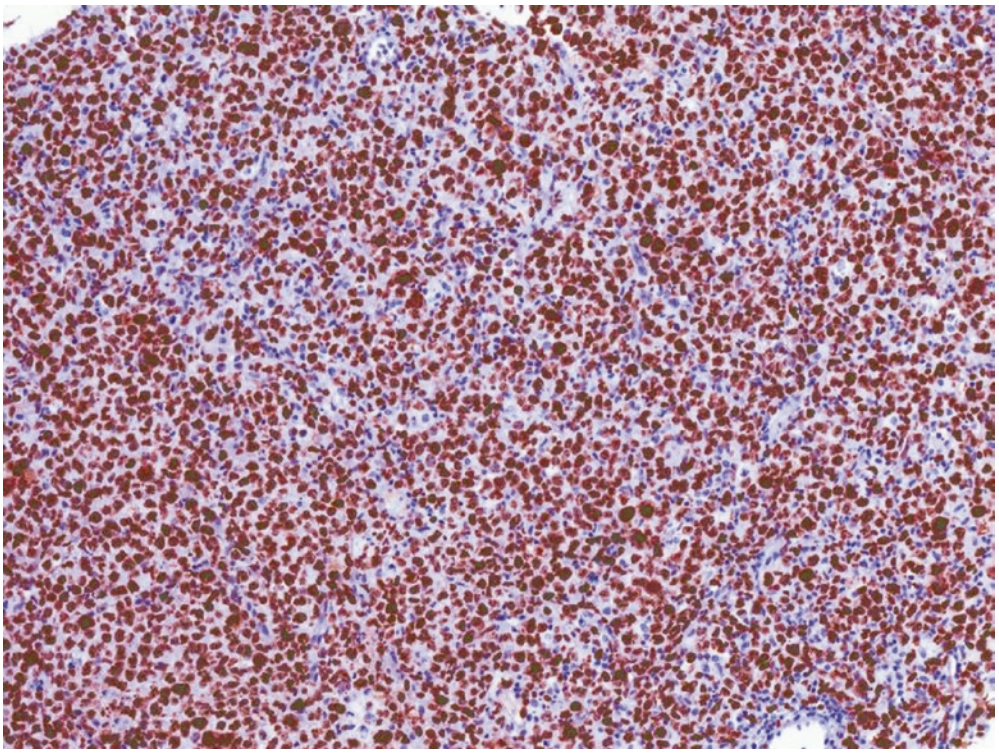

Fig. 12.72 Diffuse large B-cell lymphoma. A high proliferative fraction is seen on Ki67 labelling, as expected in diffuse large B-cell lymphoma

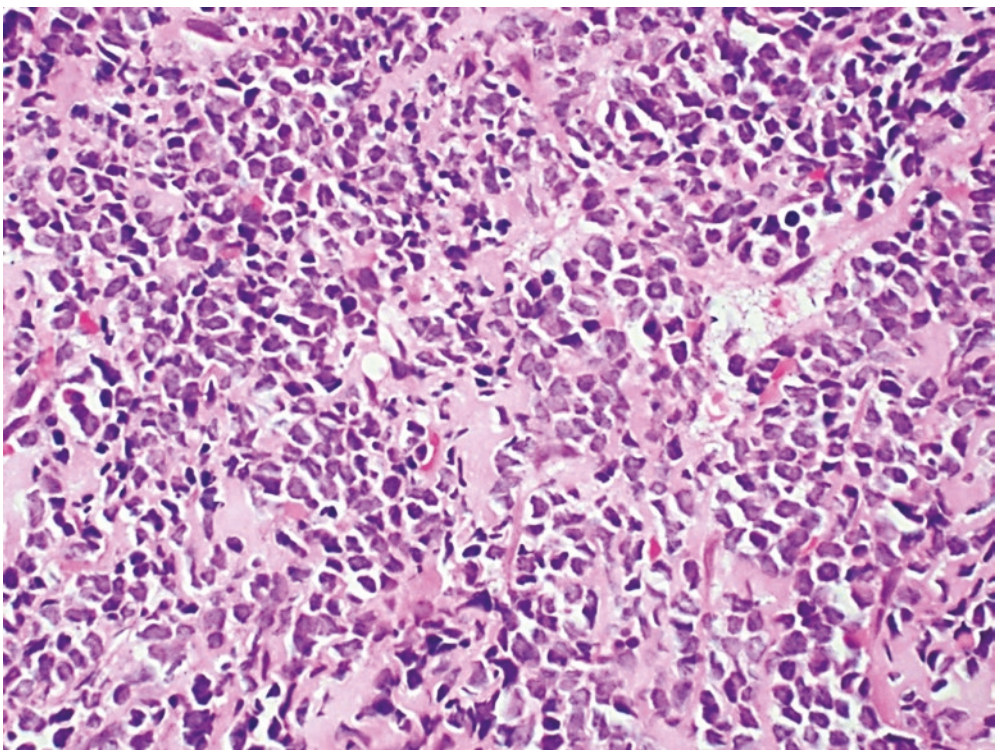

Fig. 12.73 Granulocytic sarcoma consists of diffuse sheets of tumour cells, which may show artefactual aggregation and compartmentalisation by narrow collagen strands separating the groups of malignant cells

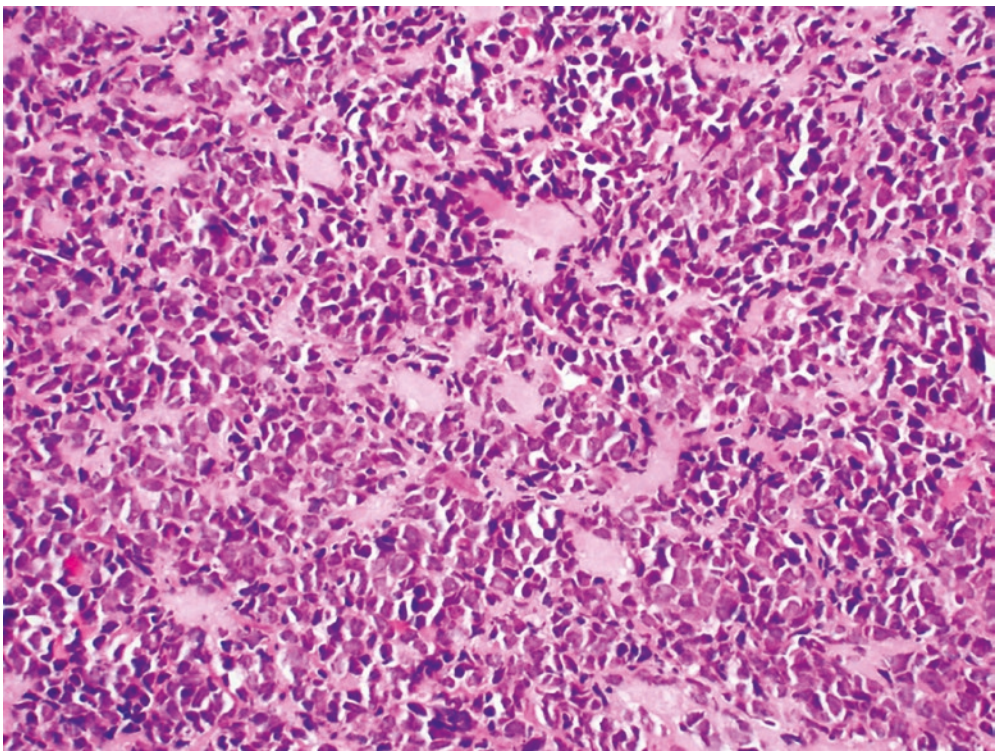

Fig. 12.74 Granulocytic sarcoma. High magnification shows tumour cells with elongated, irregular nuclei and scant cytoplasm. Sometimes, a slightly eosinophilic hue may be observed in the cytoplasm of tumour cells. Eosinophilic metamyelocytes (not seen in this case) may be a helpful clue to the diagnosis

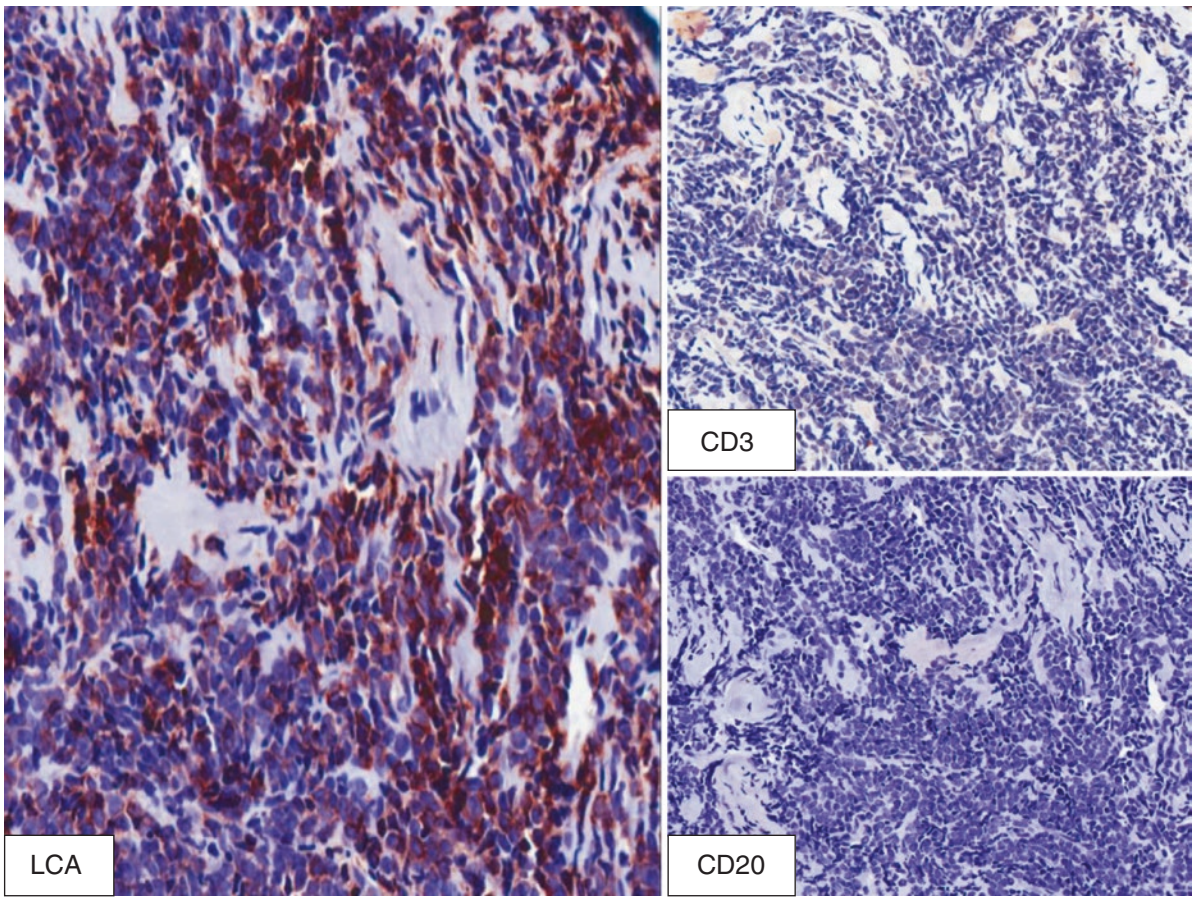

Fig. 12.75 Granulocytic sarcoma. Immunohistochemistry shows patchy reactivity for LCA, but both CD3 (T-cell marker) and CD20 (B-cell marker) are negative in the tumour cells

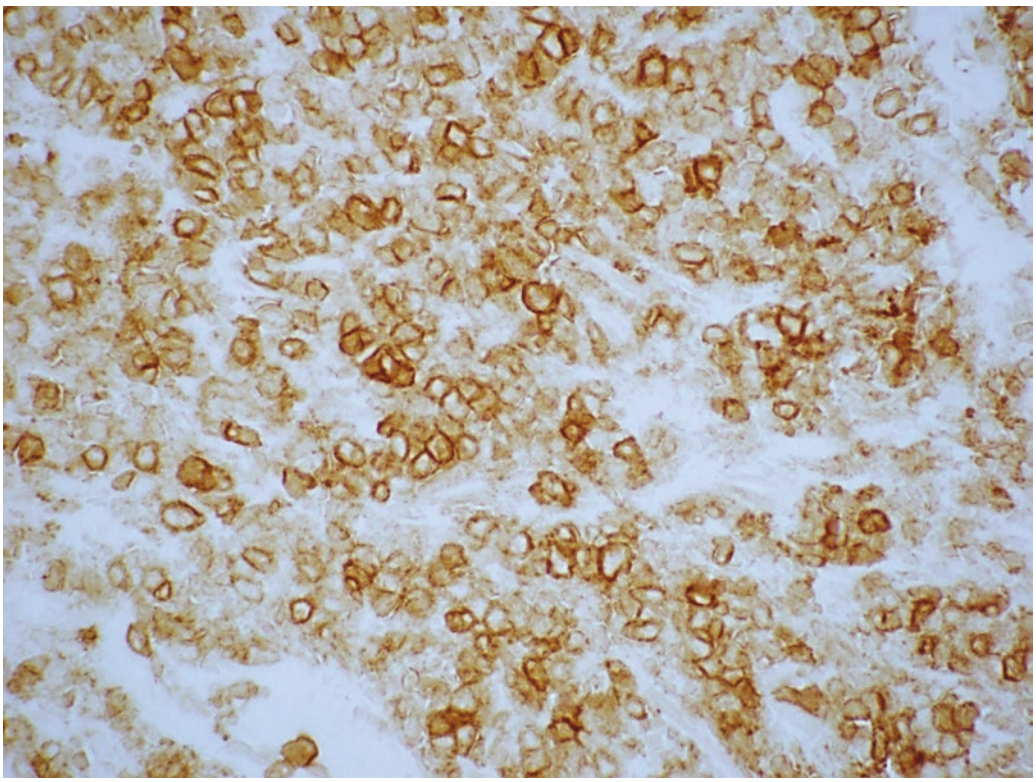

Fig. 12.76 Granulocytic sarcoma shows diffuse staining for CD117

Prognosis and Therapy Considerations

Though originally considered to have a better prognosis than invasive ductal carcinoma, problems with accurately defining classic medullary carcinoma have led to variable reports of its clinical behaviour, with most cases currently being treated as grade 3, triple-negative breast cancers. The presence of lymphoplasmacytic infiltrates, also referred to as tumour-infiltrating lymphocytes, may confer an improved prognosis for these tumours [54]. There is an association between carcinomas with medullary features (including classic medullary carcinoma) and underlying *BRCA1* germline mutations [55].

Metaplastic Carcinoma

Definition

Metaplastic carcinomas are a heterogeneous group of breast tumours characterised by differentiation of neoplastic epithelial elements into squamous, mesenchymal, or mesenchymal-looking components [56]. Several terms have been used to describe metaplastic carcinomas, including *sarcomatoid carcinoma*, *carcinosarcoma*, *carcinoma with pseudosarcomatous stroma*, and *matrix-producing breast carcinoma*. Currently, the WHO 2012 classification [56] divides metaplastic carcinoma into the following descriptive categories:

- Low-grade adenosquamous carcinoma
- Fibromatosis-like metaplastic carcinoma
- Squamous cell carcinoma
- Spindle cell carcinoma
- Carcinoma with mesenchymal differentiation
- Myoepithelial carcinoma

Clinical and Epidemiological Features

Metaplastic carcinomas account for less than 5 % of breast carcinomas, with varying incidence rates depending on definition. Clinical and epidemiological features are similar to those of hormone receptor negative invasive ductal carcinomas which are negative for hormone receptors.

Imaging Features

Metaplastic carcinomas tend to be large, lobulated masses with partially well-defined and ill-defined margins on imaging. Calcific ossifications may be present. Sonography may show cystic areas within the masses that are due to necrosis or haemorrhage (Fig. 12.77).

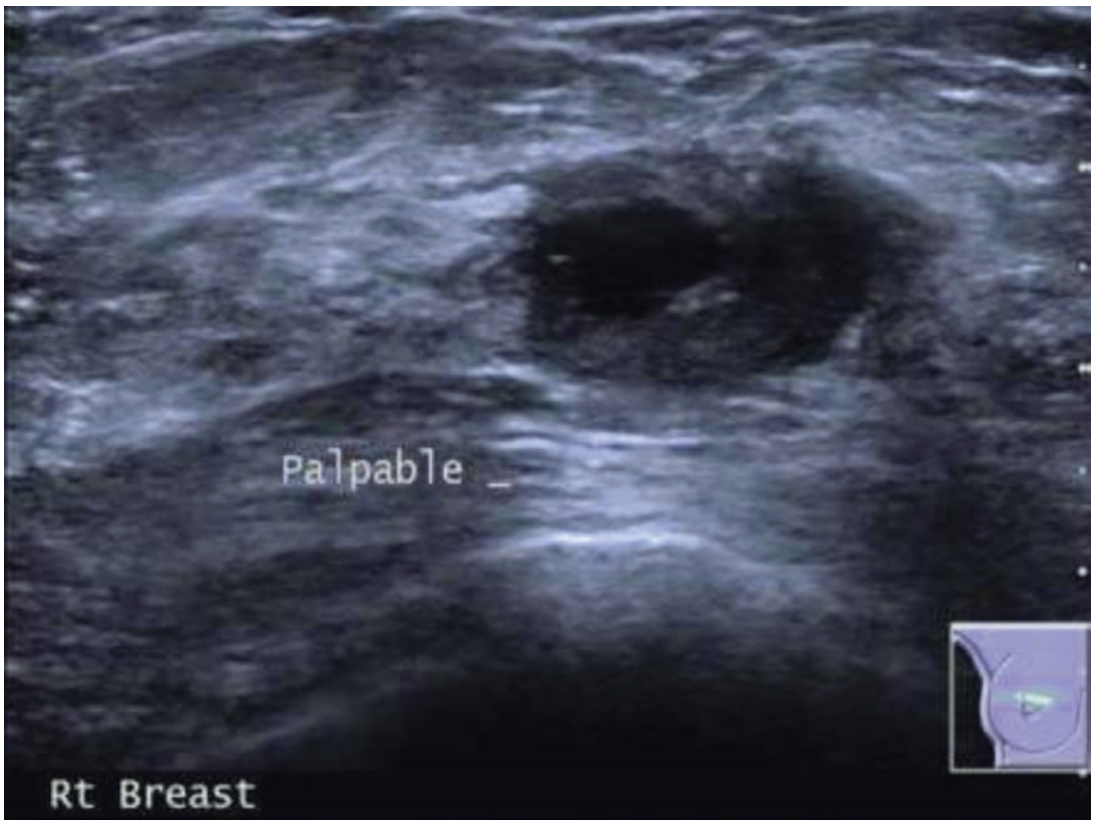

Fig. 12.77 Metaplastic breast carcinoma on ultrasonography shows a slightly ill-defined oval mass measuring 24×19×12 mm at the 12 o'clock position of the right breast, containing a cystic component (Courtesy of Dr. Lester Leong)

Pathologic Features

Macroscopic Pathology

Metaplastic carcinomas appear macroscopically like other invasive breast carcinomas, often displaying irregular borders (Figs. 12.78, 12.79, and 12.80). Some may be grossly circumscribed with central softening, whereas those with squamous differentiation can be cystic.

Microscopic Pathology

Histological appearances depend on the type of metaplastic carcinoma described in the WHO classification.

Low-Grade Adenosquamous Carcinoma

Low-grade adenosquamous carcinoma is composed of small, solid nests and irregular, angulated epithelial tubules associated with squamous differentiation, which may be subtle, appearing as squamous whorls formed by polygonal cells with hardened eosinophilic cytoplasm, or may appear as more obvious squamous islands with keratinisation [57]. These epithelial islands permeate the stroma between breast lobules and may merge with abnormal spindle cells. A lymphocytic infiltrate is often found at the tumour periphery (Figs. 12.81, 12.82, 12.83, 12.84, 12.85, and 12.86). Immunohistochemistry shows positive reactivity of tumour cells for p63 and high-molecular-weight keratins (Figs. 12.87, 12.88, 12.89, and 12.90) [58, 59]. Hormone receptors and c-erbB-2 are usually negative. There is an association with radial sclerosing lesions, papilloma, and adenomyoepithelioma [60–62].

Fibromatosis-Like Metaplastic Carcinoma

Fibromatosis-like metaplastic carcinoma is a histologically and biologically low-grade tumour that closely resembles fibromatosis. It consists of long, intersecting fascicles of spindle cells with banal, slender nuclei within a variably collagenous and myxoid background, extending between breast lobules. Squamous differentiation may be present. High-grade features are absent (Figs. 12.91, 12.92, 12.93, and 12.94). Immunohistochemically, basal keratins and p63 decorate the spindle cells, although this staining may sometimes be focal (Figs. 12.95, 12.96, and 12.97). These tumours are triple-negative.

Squamous Cell Carcinoma (Invasive Carcinoma with Squamous Differentiation)

Invasive squamous cell breast carcinoma is usually of underlying ductal subtype, with variable extent of squamous differentiation featuring pavemented tumour islands with squamous whorls, keratinisation, and intercellular bridges. Extensive squamous differentiation may be associated with cystic degeneration (Figs. 12.98, 12.99, 12.100, 12.101, and 12.102). A desmoplastic stromal response is seen,

sometimes with foreign-body, giant-cell reaction to keratinous debris. Often, squamous components merge with spindle cell elements. The acantholytic variant of squamous cell carcinoma can resemble angiosarcoma. It is noted that medullary carcinoma may sometimes disclose focal squamous areas [56]. Though primary squamous cell carcinoma of the breast has been described, its diagnosis requires exclusion of a primary skin lesion and metastases from elsewhere.

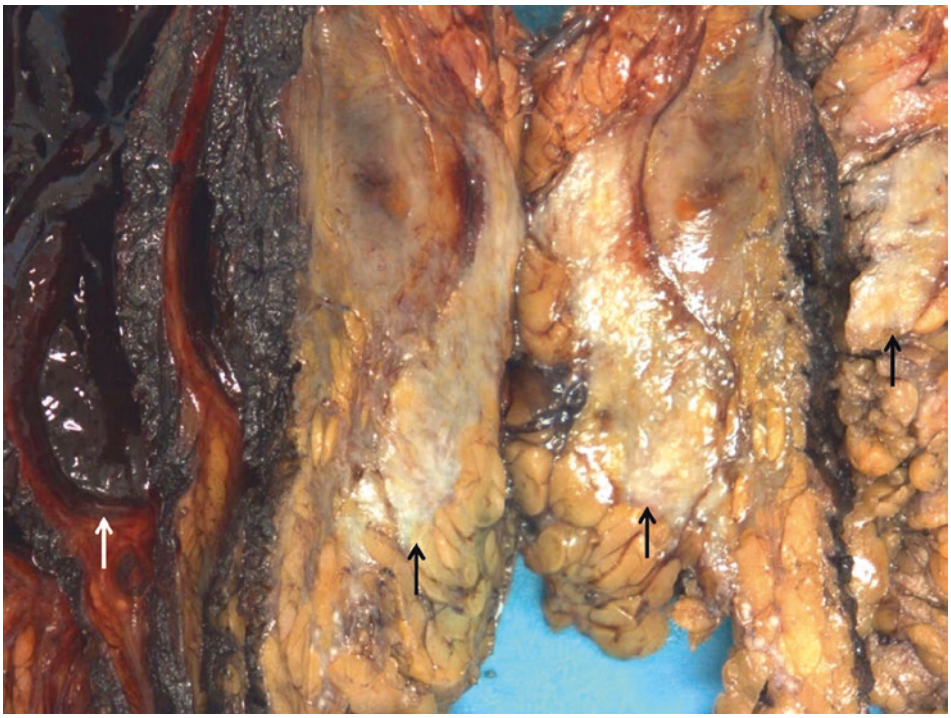

Fig. 12.78 Metaplastic carcinoma with squamous differentiation. Mastectomy specimen sliced to show an irregular, whitish-yellow tumour (*black arrows*), which microscopically demonstrated an invasive ductal carcinoma with squamous differentiation. A haematoma is present in the left field (*white arrow*)

Fig. 12.79 Metaplastic carcinoma. Gross appearance of a metaplastic carcinoma with squamous and chondroid differentiation, involving the nipple and ulcerating through its surface. The cut surface of the tumour has a whitish-yellow, slightly myxoid appearance with areas of haemorrhage and cystic degeneration

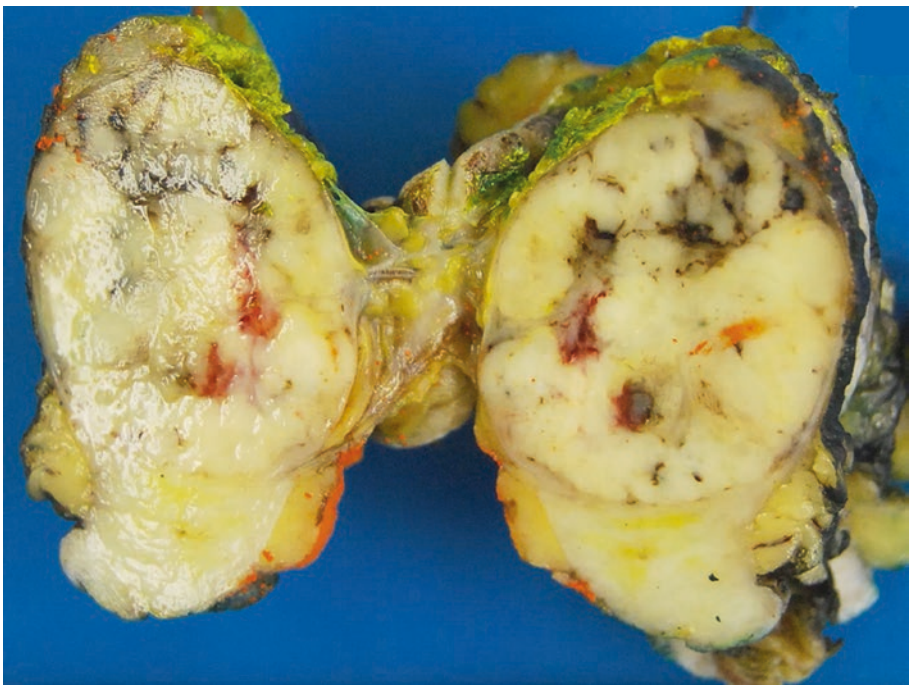

Fig. 12.80 Metaplastic carcinoma. In this circumscribed tumour, which shows chondroid areas histologically, there is a lobulated appearance on cut section, with areas of haemorrhage

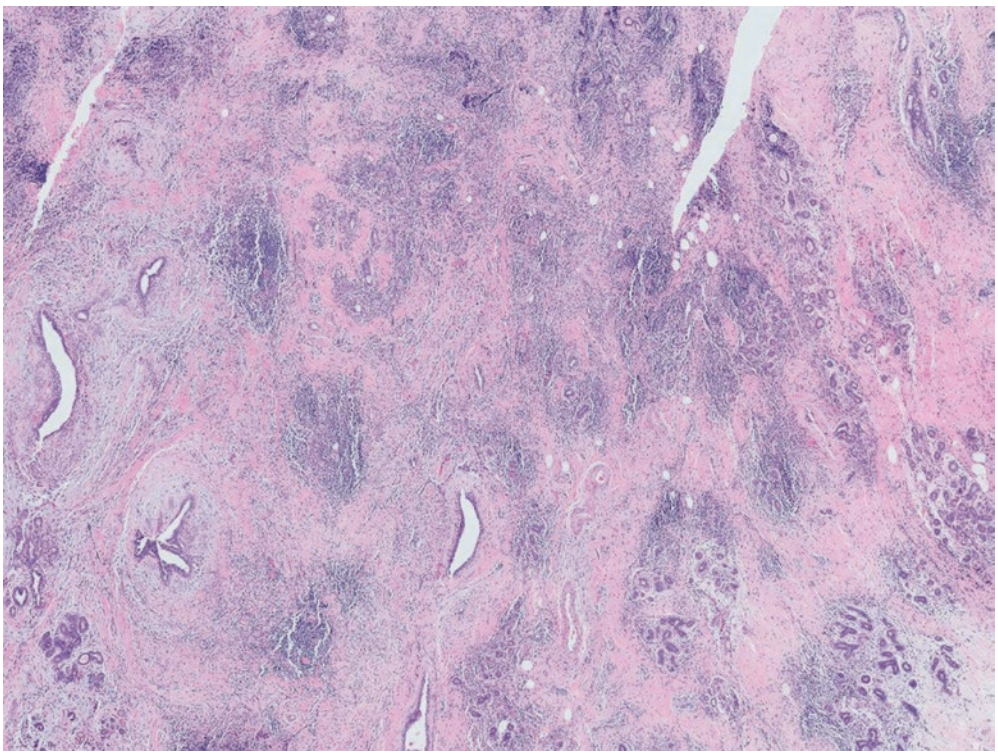

Fig. 12.81 Low-grade adenosquamous carcinoma. Low magnification shows patchy collections of lymphocytes among scattered breast ducts and lobules within fibrosclerotic stroma

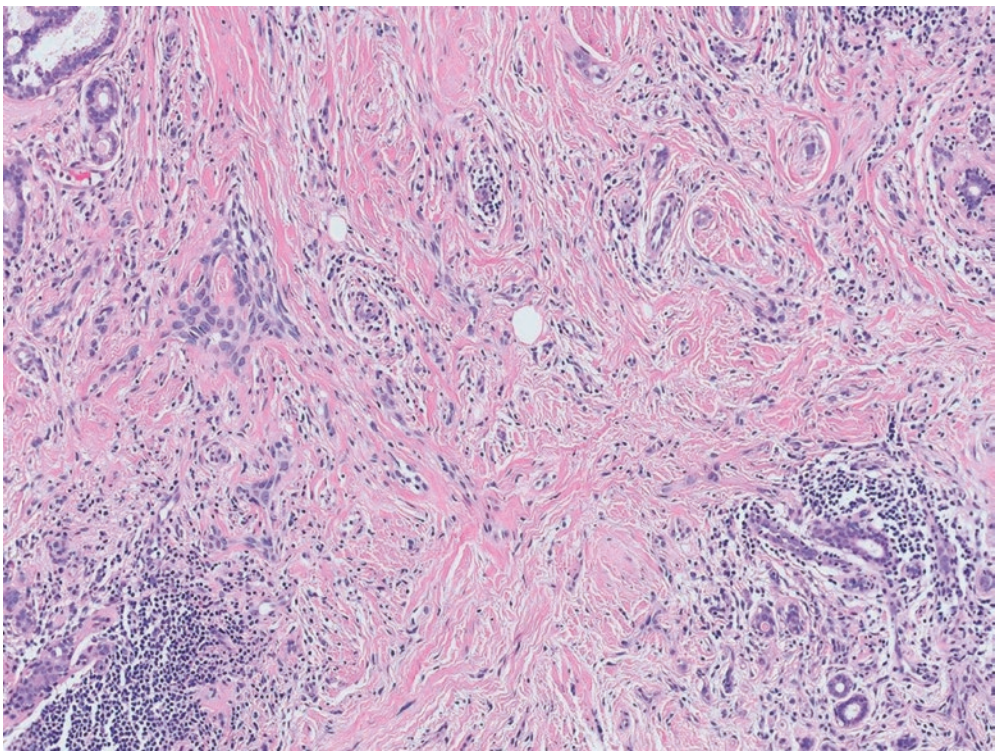

Fig. 12.82 Low-grade adenosquamous carcinoma. Irregular nests and strands of relatively bland epithelial cells are seen within the fibrosclerotic stroma

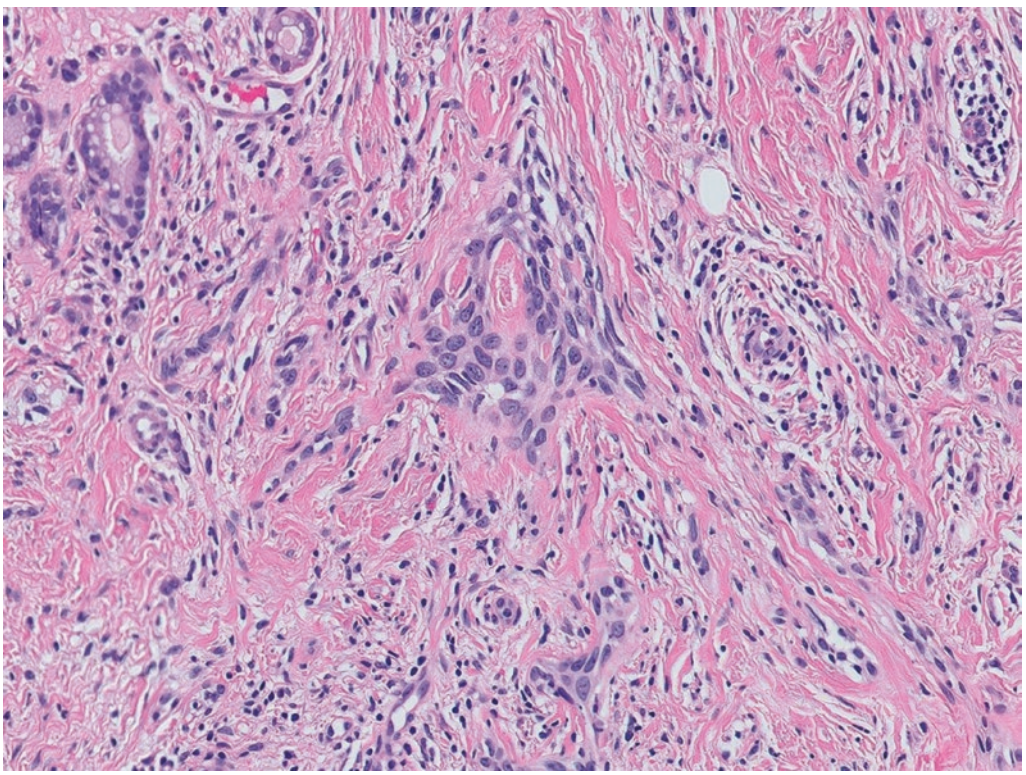

Fig. 12.83 Low-grade adenosquamous carcinoma. Higher magnification of the epithelial islands, which show elongated cells at the periphery of the nests, appearing to merge into the stroma

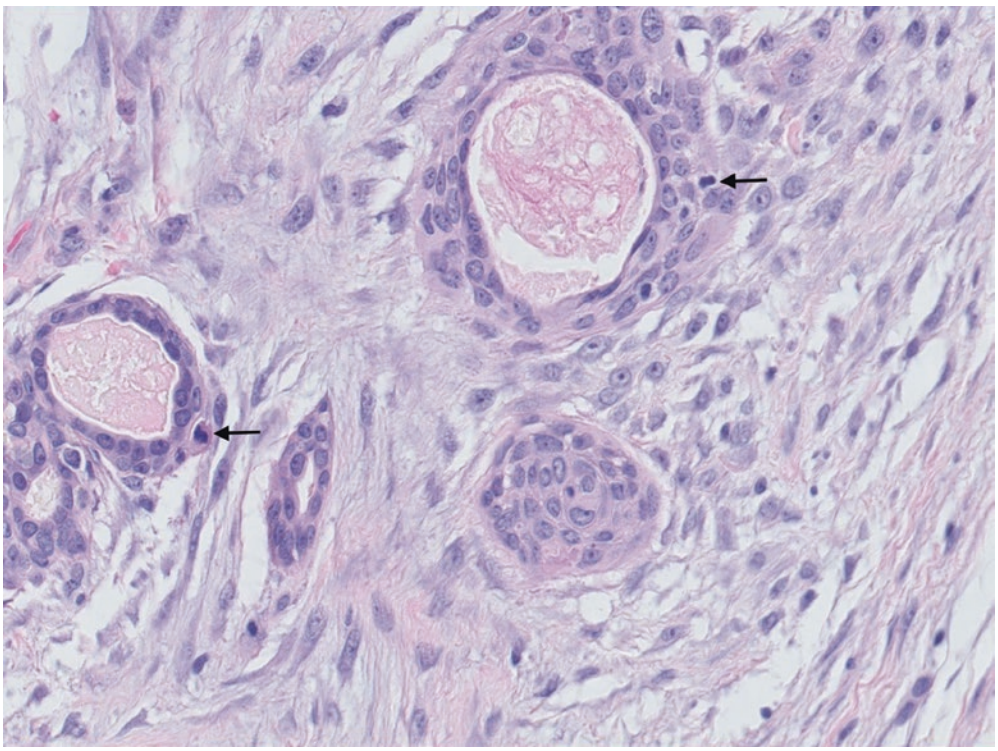

Fig. 12.84 Low-grade adenosquamous carcinoma. A whorled epithelial nest is seen, together with tubules lined by cuboidal and polygonal cells that blend into the surrounding cellular stroma, which contains plump spindle cells. Mitoses are seen (*arrows*). Some of the spindle cells seem to align themselves around the epithelial tubules and nests, giving a whorled lamellar-like appearance

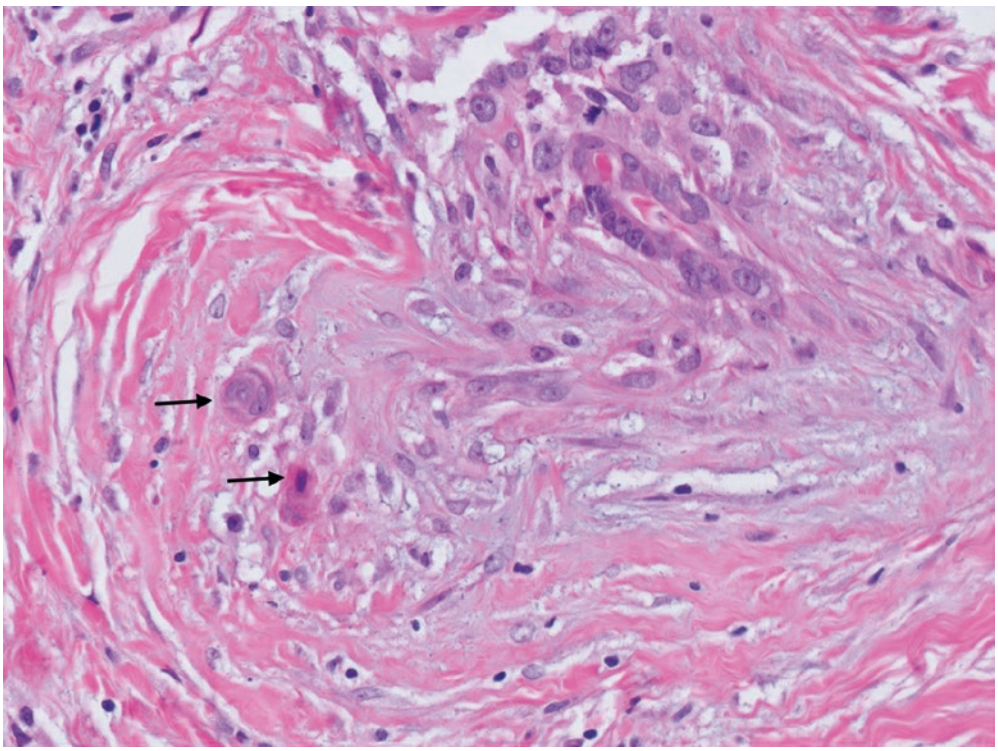

Fig. 12.85 Low-grade adenosquamous carcinoma. Squamoid cells with eosinophilic cytoplasm are observed within the fibrosclerotic stroma (*arrows*). Plump spindle cells are also seen

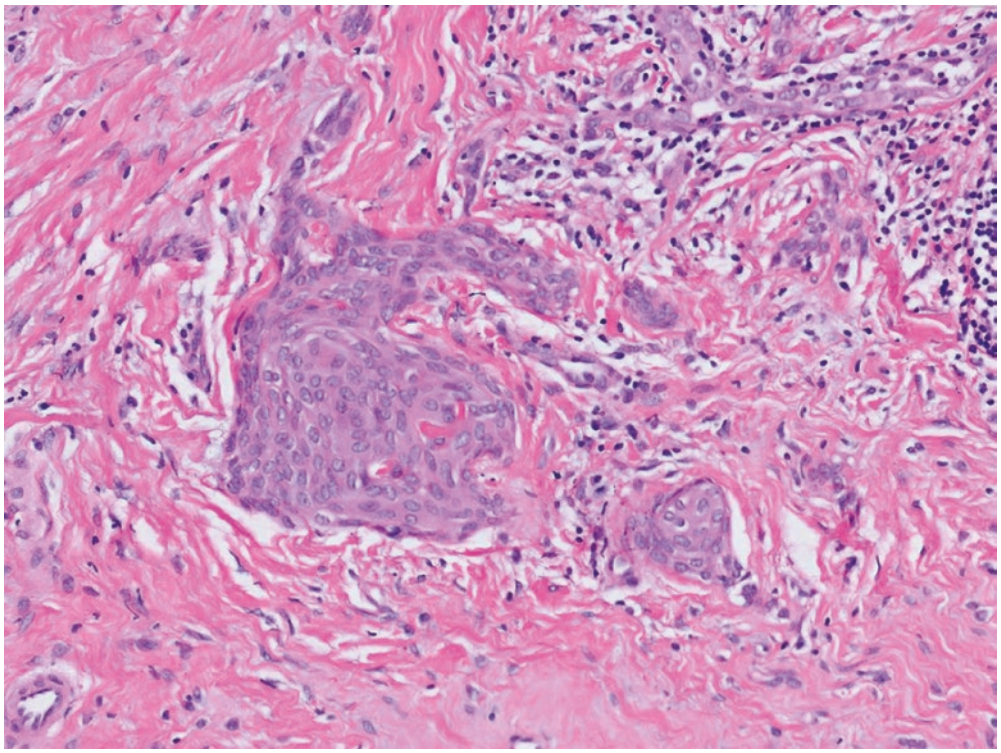

Fig. 12.86 Low-grade adenosquamous carcinoma. Pavemented squamous epithelial islands show irregular borders and tonguelike extensions into the stroma

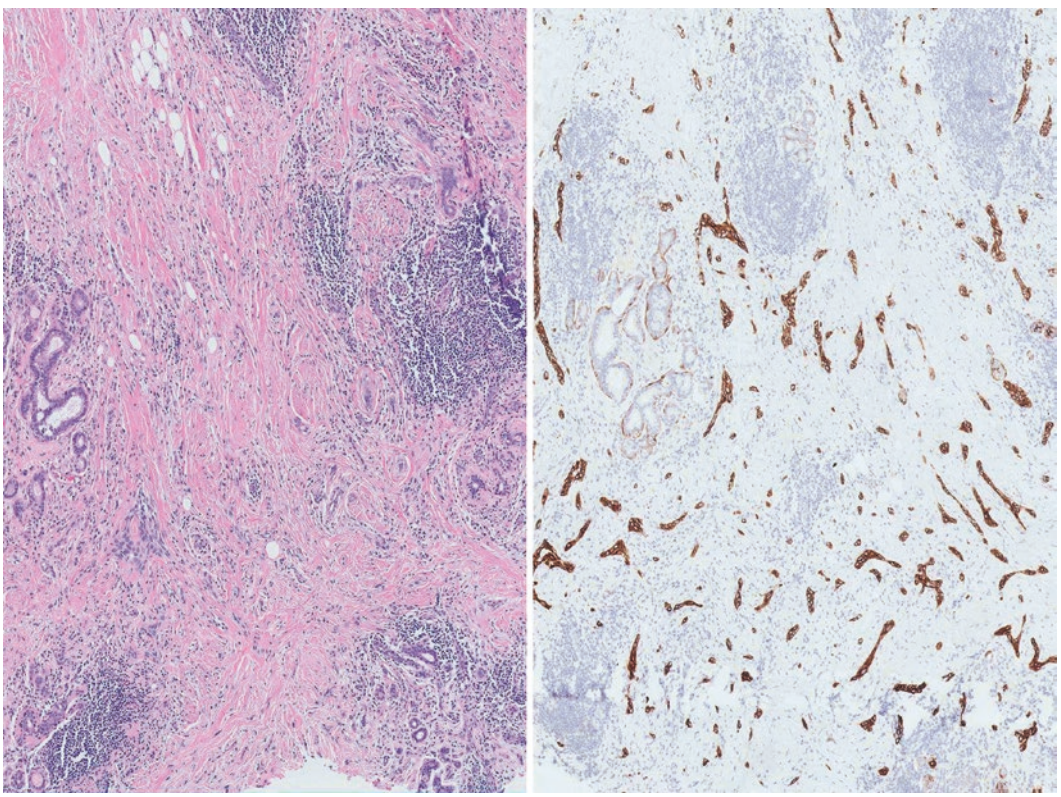

Fig. 12.87 Low-grade adenosquamous carcinoma. Immunohistochemistry with CK5/6 reveals many more epithelial strands and angulated nests than are seen on H&E microscopy, invading the stroma between benign breast lobules

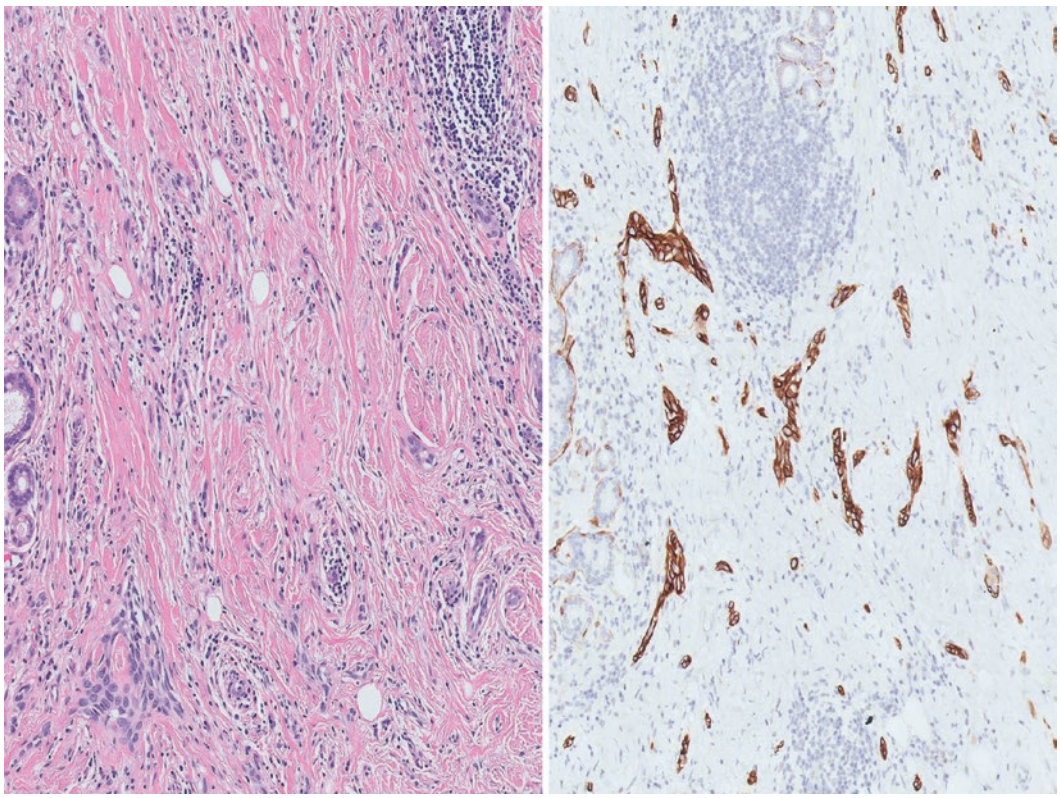

Fig. 12.88 Low-grade adenosquamous carcinoma. Medium magnification shows epithelial nests and cords permeating the stroma, highlighted by CK5/6. Some of the abnormal epithelial nests are difficult to detect, appearing inconspicuous on the H&E section

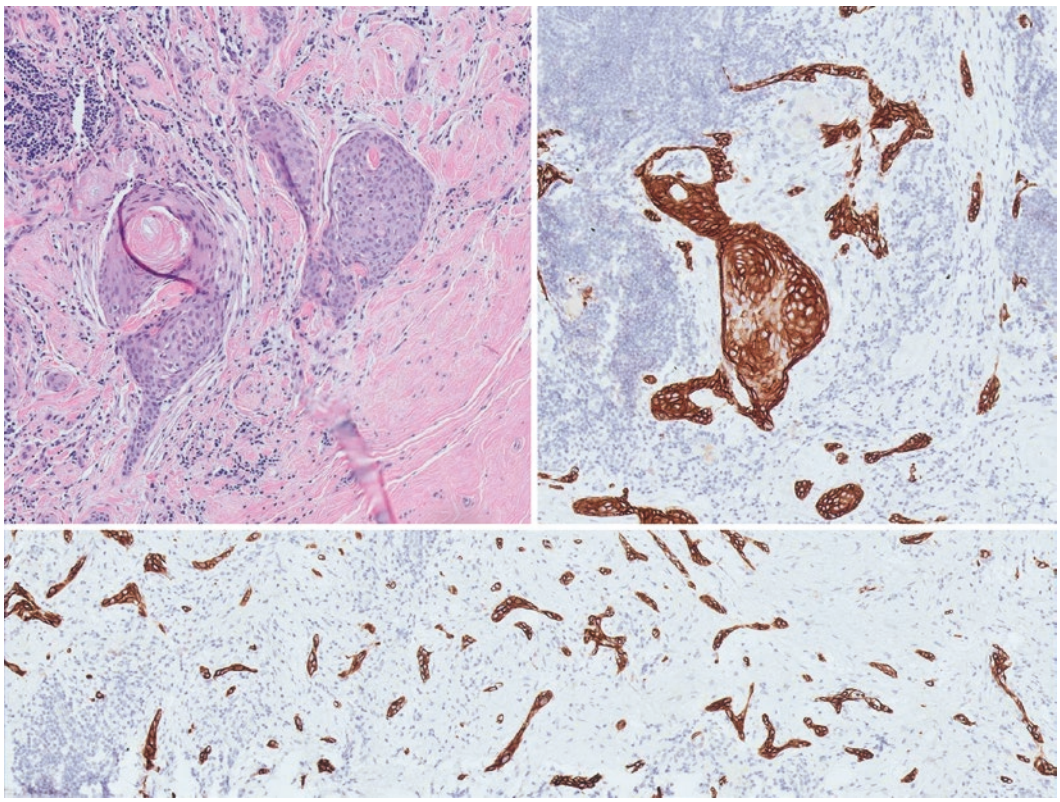

Fig. 12.89 Low-grade adenosquamous carcinoma. Keratinised squamous islands are stained with the high-molecular-weight keratin CK5/6. The lower panel shows the permeative nature of tumour islands stained positively with CK5/6

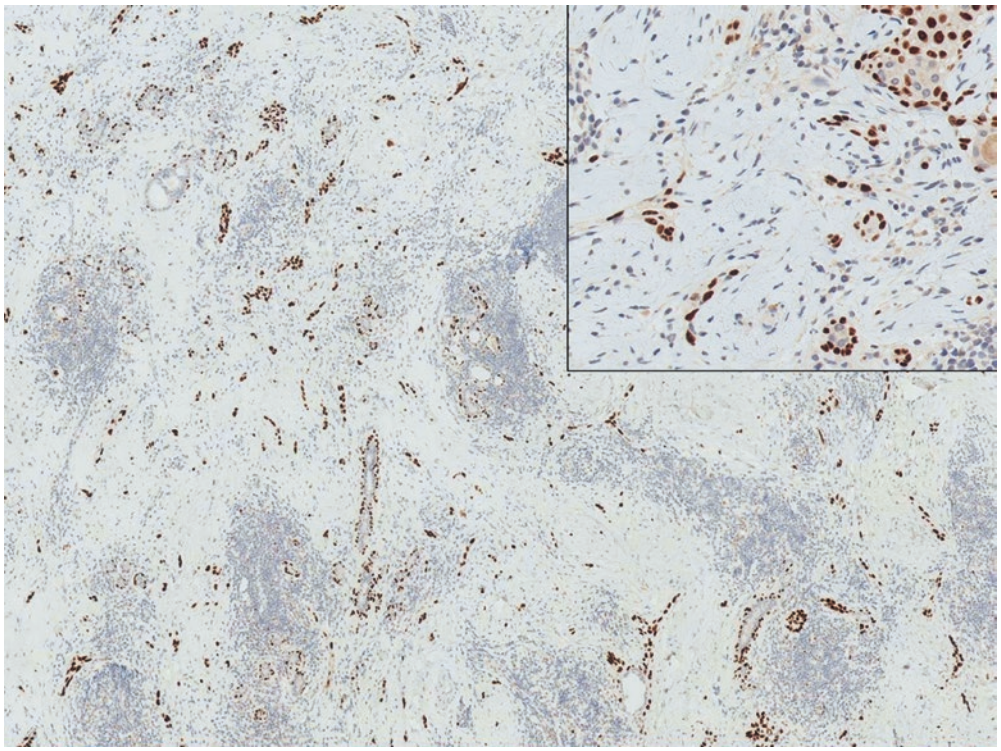

Fig. 12.90 Low-grade adenosquamous carcinoma. Immunohistochemistry for p63 highlights positively staining epithelial nests and spindle cells diffusely infiltrating the interlobular stroma. In contrast, squamoid nests that can be observed in benign conditions such as radial sclerosing lesions are limited to the centre or are contained within the lesion, without significant involvement of, or extension into, adjacent parenchyma

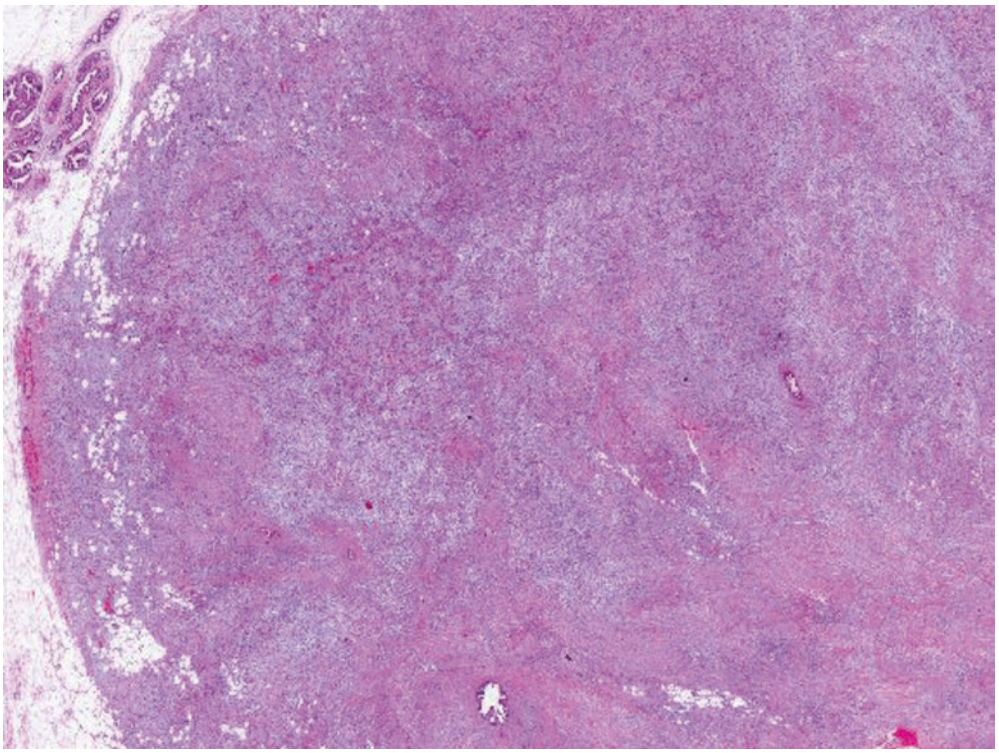

Fig. 12.91 Fibromatosis-like metaplastic carcinoma. Low magnification of the tumour shows a spindle cell neoplasm with entrapped adipocytes at the periphery. A few scattered benign glands are seen within the tumour

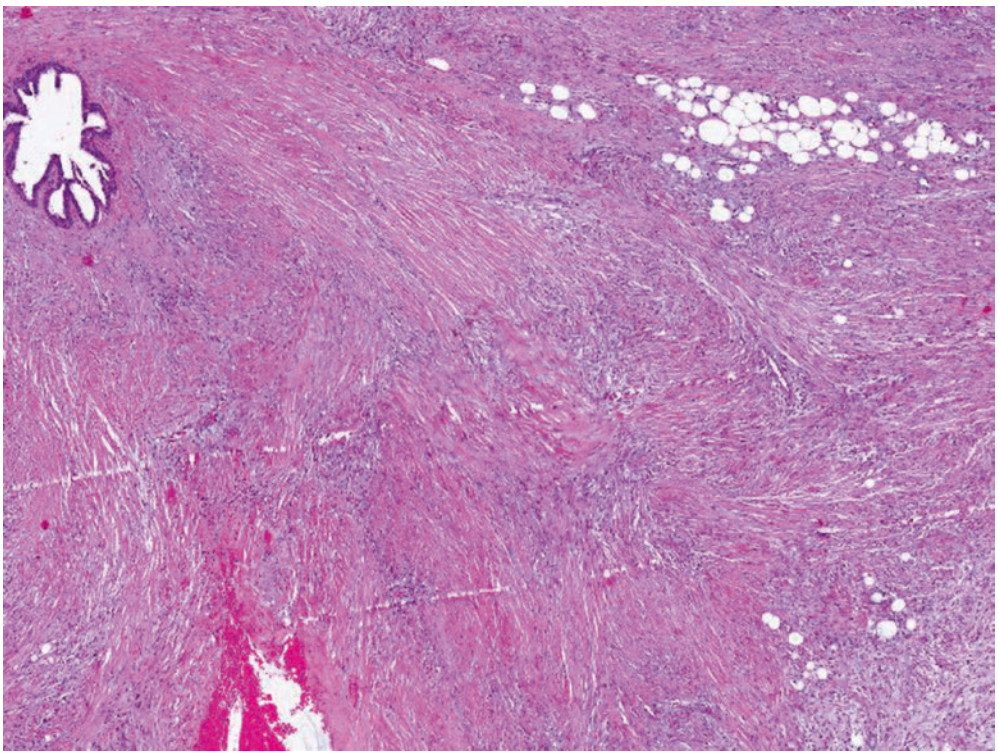

Fig. 12.92 Fibromatosis-like metaplastic carcinoma. Broad, sweeping fascicles of spindle cells are seen within a collagenous background

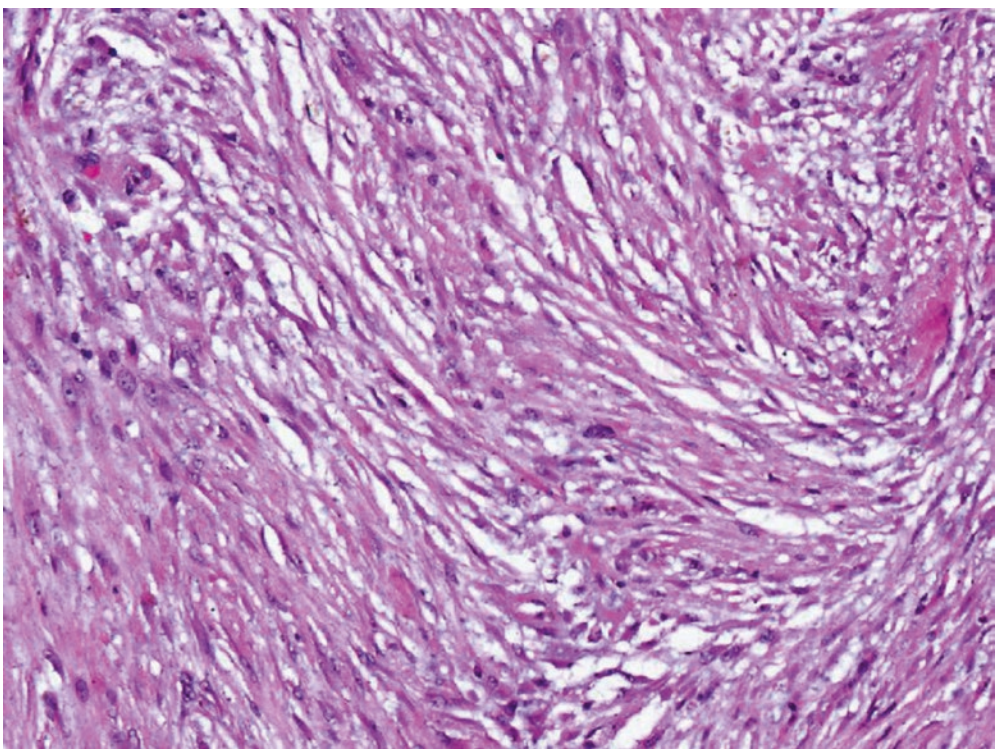

Fig. 12.93 Fibromatosis-like metaplastic carcinoma. Although most of the spindle cells show bland nuclear features, occasional scattered cells may have larger nuclei

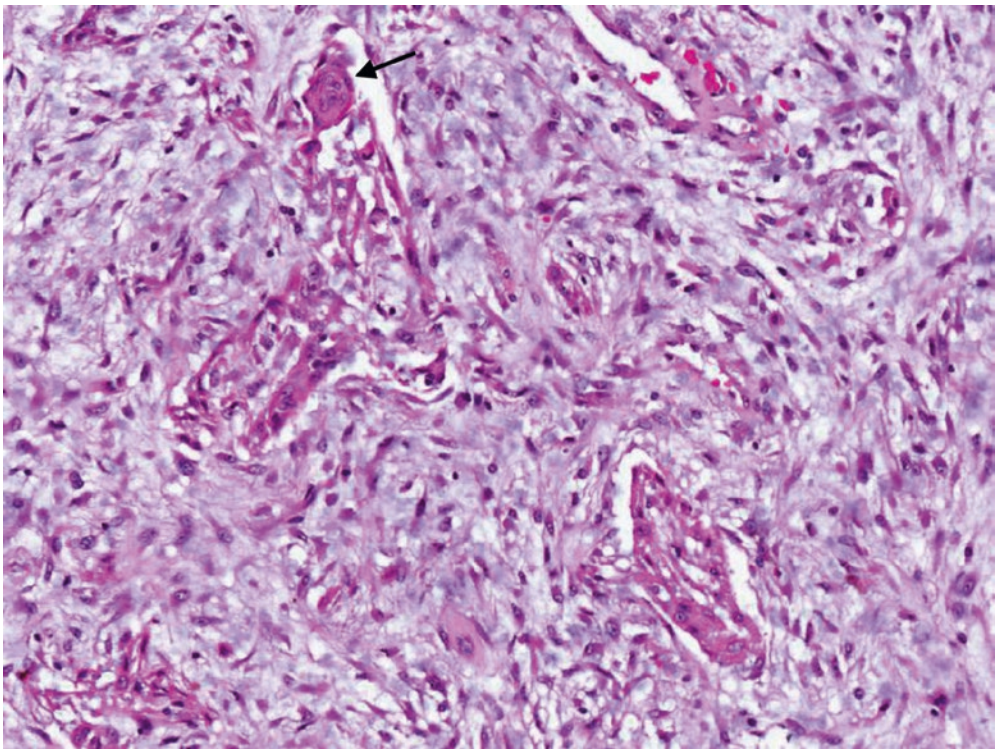

Fig. 12.94 Fibromatosis-like metaplastic carcinoma. More epithelioid nests and a squamous whorl (*arrow*) are seen

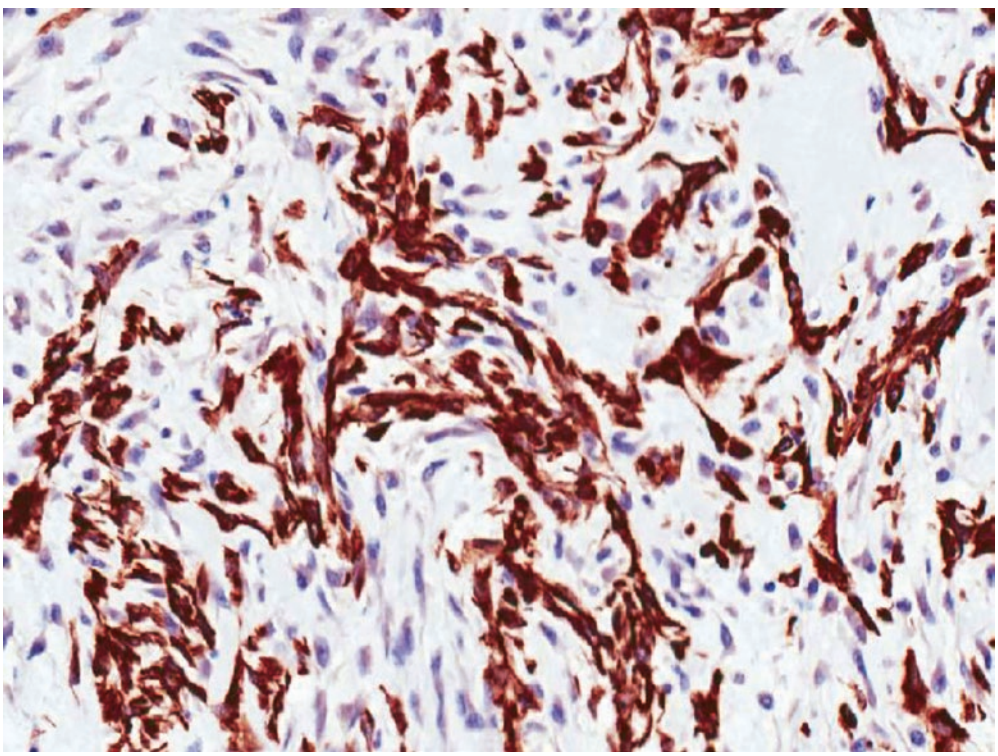

Fig. 12.95 Fibromatosis-like metaplastic carcinoma shows positive immunohistochemical staining of the spindle cells for MNF116

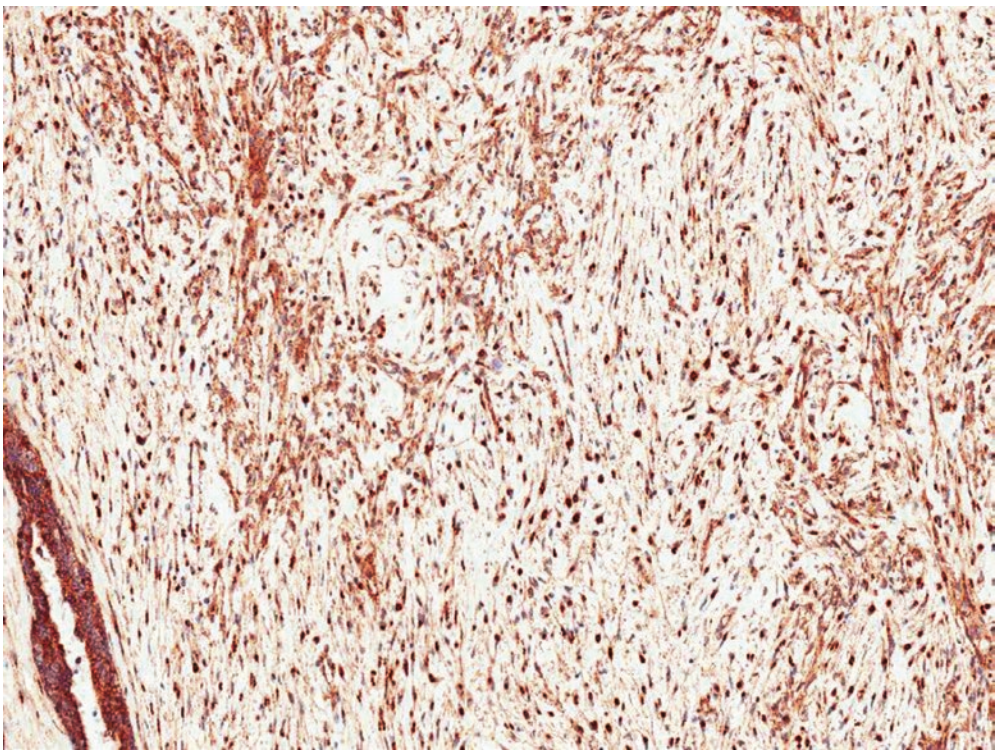

Fig. 12.96 Fibromatosis-like metaplastic carcinoma. Spindle cells show positive cytoplasmic and nuclear staining for beta-catenin, which therefore cannot be relied on as the sole criterion to distinguish the tumour from fibromatosis

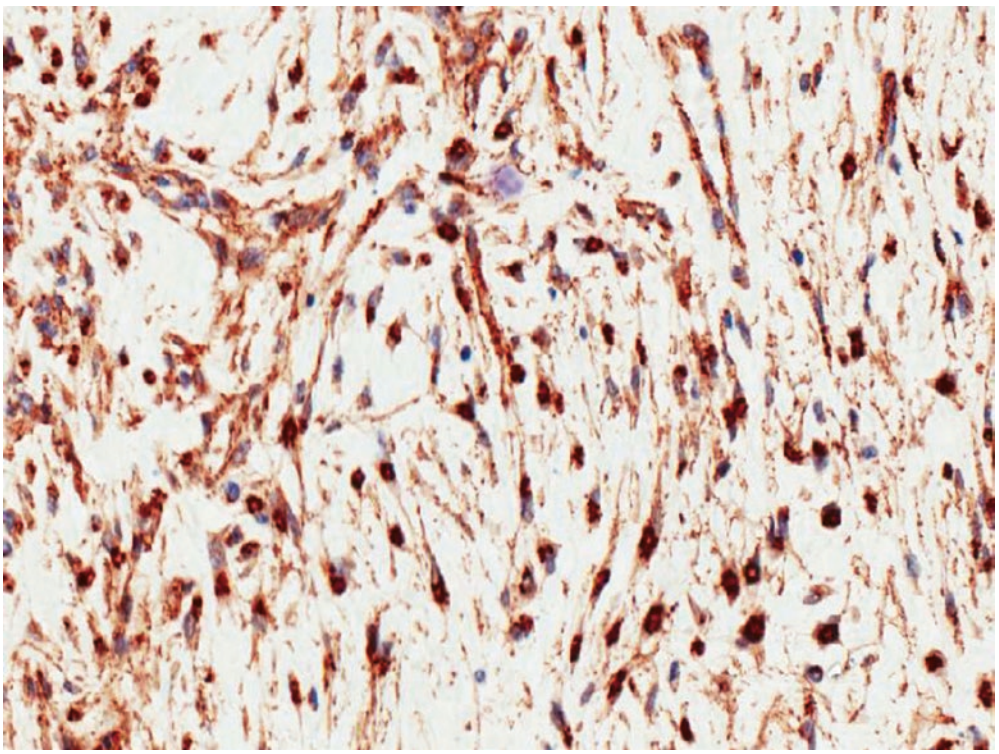

Fig. 12.97 Fibromatosis-like metaplastic carcinoma. High magnification shows nuclear and cytoplasmic staining for beta-catenin

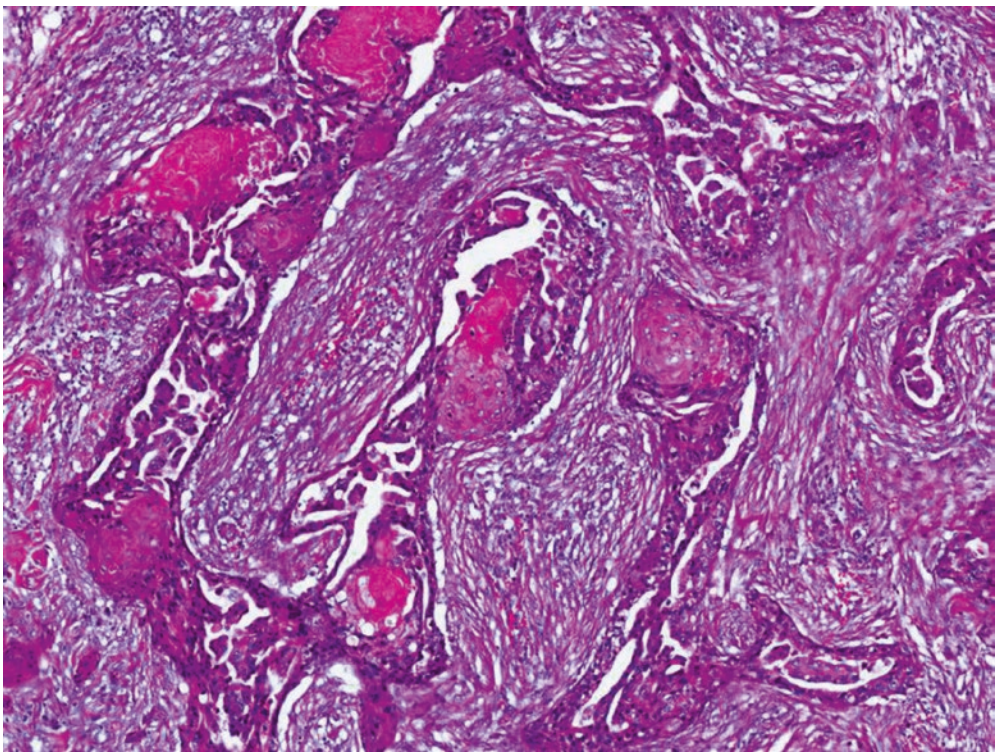

Fig. 12.98 Invasive ductal carcinoma with squamous differentiation. Irregular branching glands show squamous islands. The stroma is desmoplastic

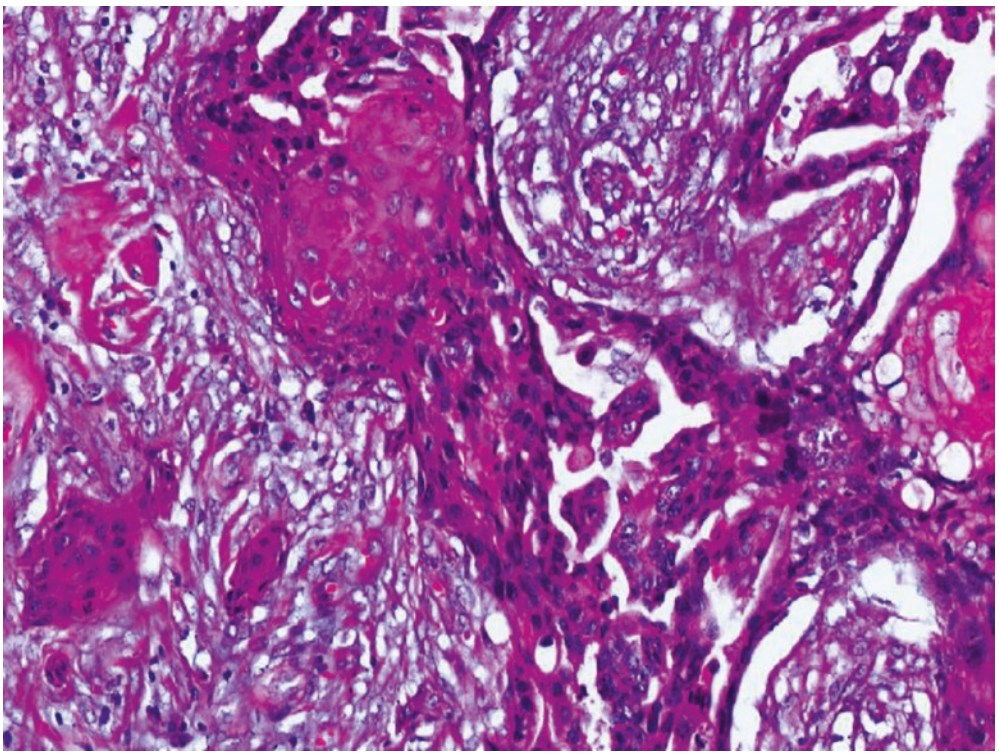

Fig. 12.99 Invasive ductal carcinoma with squamous differentiation. High magnification shows squamous cells with ample pink cytoplasm within malignant glands and also occurring as small nests within desmoplastic stroma

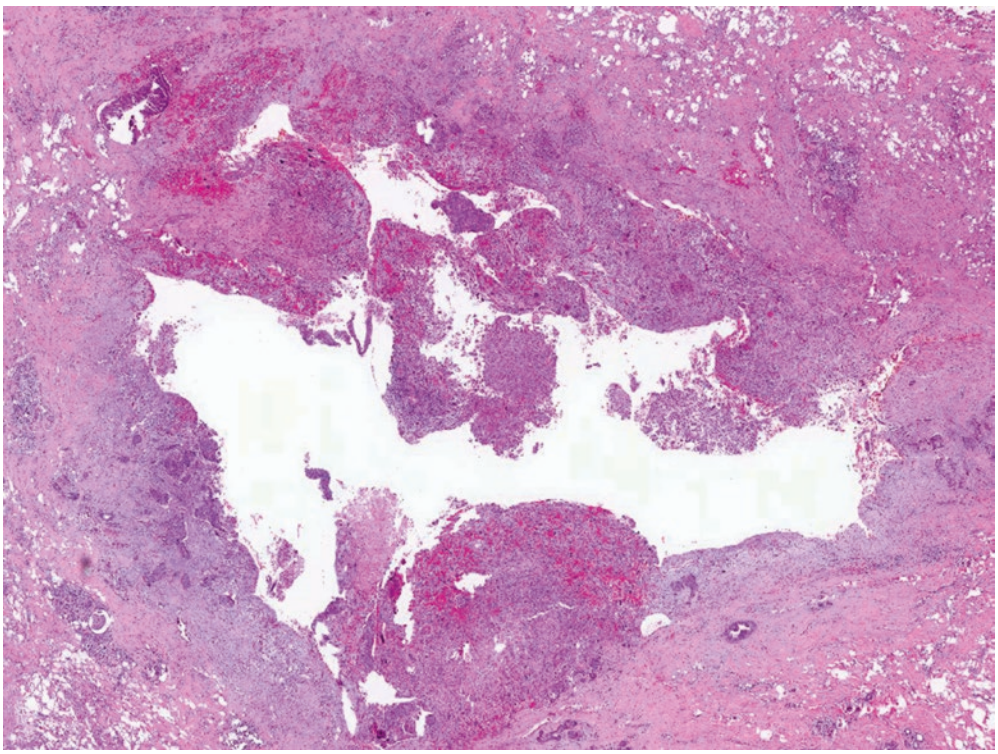

Fig. 12.100 Metaplastic squamous carcinoma shows cystic change. The central part of the tumour shows cystic degeneration. Cellular tumour with haemorrhage is seen in the wall

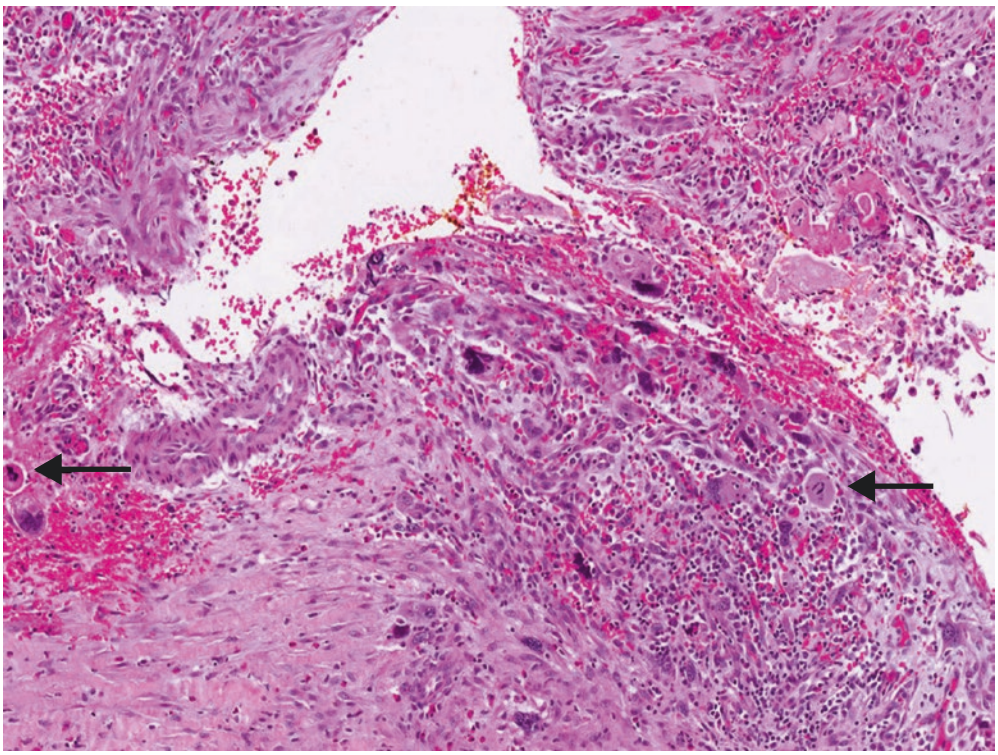

Fig. 12.101 Metaplastic squamous carcinoma shows abnormal spindle and epithelioid cells within the wall, with bizarre hyperchromatic nuclei and discernible mitoses (*arrows*)

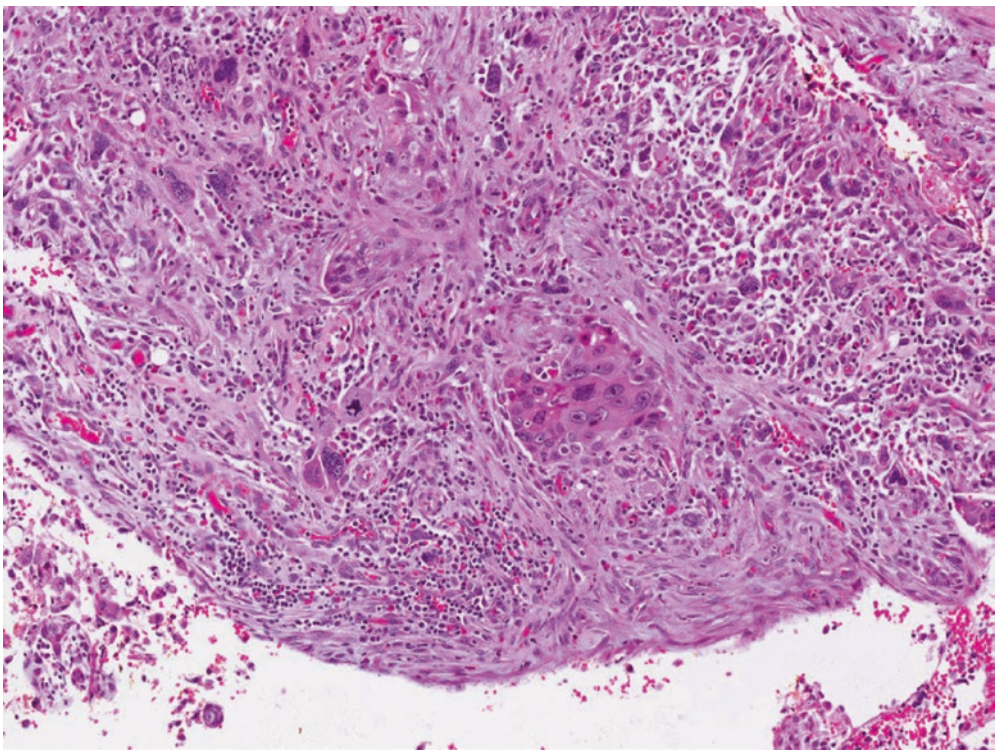

Fig. 12.102 Metaplastic squamous carcinoma shows squamous islands composed of polygonal cells with pleomorphic vesicular nuclei and pink cytoplasm. Bizarre epithelioid tumour cells are also seen

Spindle Cell Carcinoma

This tumour is composed predominantly of malignant spindle cells with moderate to marked nuclear pleomorphism and readily discerned mitoses, arranged in intersecting fascicles and storiform patterns (Figs. 12.103, 12.104, 12.105, and 12.106). Focal squamous differentiation, epithelioid nested foci, and DCIS may be present. Spindle cell carcinoma is histologically indistinguishable from myoepithelial carcinoma, and both tumours are classified in the same category [56, 63]. An inflammatory infiltrate may accompany the malignant spindle cells. Immunohistochemically, p63 and high-molecular-weight keratins are expressed, though this expression may be focal. Presence of DCIS in a malignant spindle cell tumour should strongly favour the diagnosis of spindle cell carcinoma.

Metaplastic Carcinoma with Mesenchymal Differentiation

The mesenchymal component seen in these tumours includes chondroid, osteoid, rhabdomyoid, and (rarely) neuroglial elements (Figs. 12.107, 12.108, and 12.109). Carcinoma is often identifiable, but sometimes the tumour may consist only of malignant mesenchymal tissues. Matrix-producing carcinoma belongs to this category. Like other metaplastic breast carcinomas, these tumours are often triple-negative, expressing p63 and basal keratins.

Mixed Metaplastic Carcinoma

This tumour consists of multiple different elements, all of which should be mentioned and described in the report.

Differential Diagnosis

Syringomatous Tumour

The syringomatous tumour bears close histological resemblance to the low-grade adenosquamous carcinoma [64]. The key difference is the location of the syringomatous tumour in the nipple-areolar region, whereas the low-grade adenosquamous carcinoma occurs within the breast parenchyma.

Radial Sclerosing Lesion

Low-grade adenosquamous carcinoma may be associated with sclerosing lesions, and distinction from a benign radial sclerosing lesion may be challenging, as the latter can also harbour squamoid foci within its midst (Figs. 12.110, 12.111, 12.112, and 12.113). However, low-grade adenosquamous carcinoma shows epithelial nests with squamoid features extending between lobules, beyond the boundaries of the radial sclerosing lesion. Care must be taken in interpreting keratin expression patterns of these lesions [65].

Fibromatosis

The close resemblance between low-grade fibromatosis-like metaplastic carcinoma and fibromatosis causes a diagnostic challenge. The finding of a fibromatosis-like lesion in the breast warrants exclusion of a fibromatosis-like metaplastic carcinoma. Apart from occasional more epithelioid cells and focal squamous areas in fibromatosis-like metaplastic carcinoma, immunohistochemical expression of keratins and p63 is helpful in confirming the diagnosis of carcinoma.

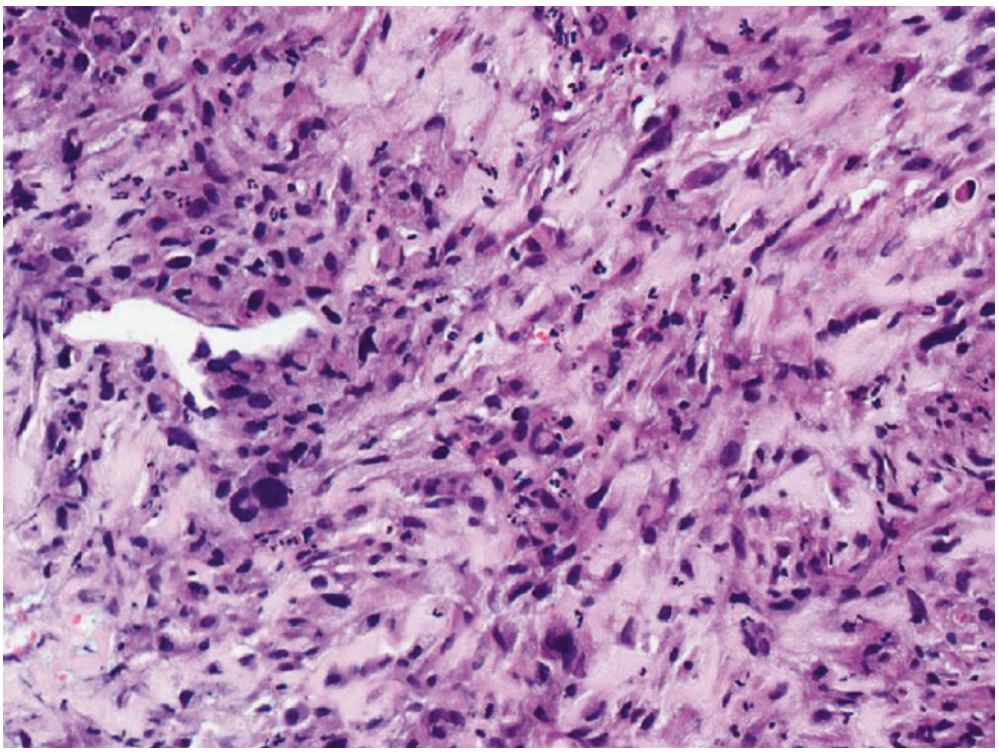

Fig. 12.103 Spindle cell carcinoma. In this tumour, the spindle cells show high nuclear grade features with hyperchromasia and marked pleomorphism

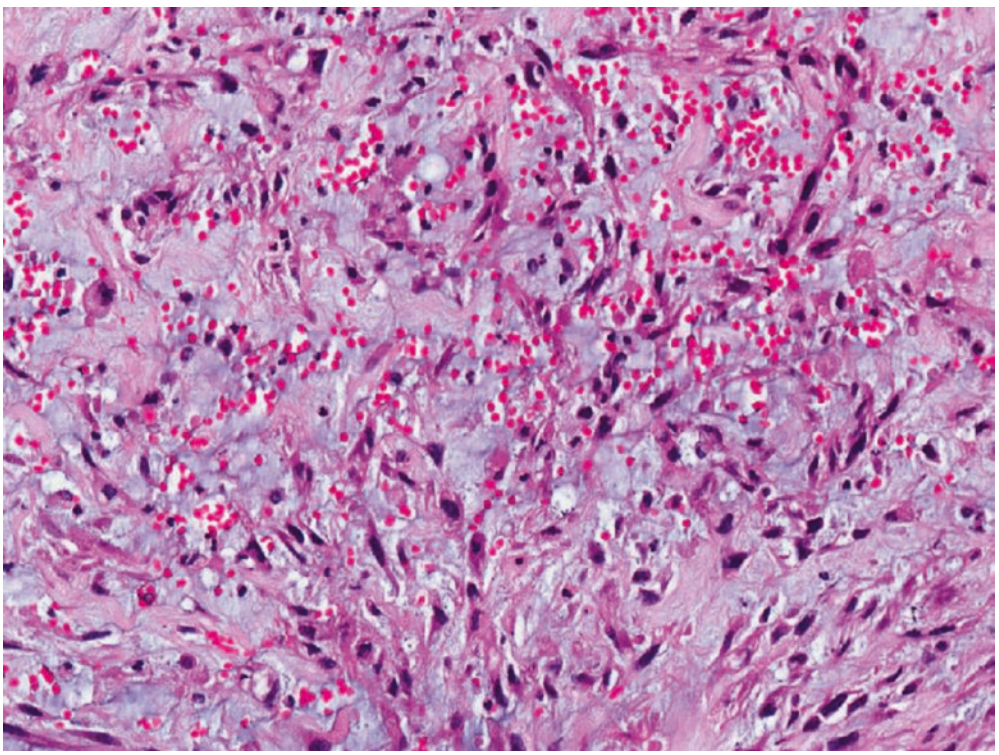

Fig. 12.104 Spindle cell carcinoma shows malignant spindle and epithelioid cells within an oedematous and myxoid stroma

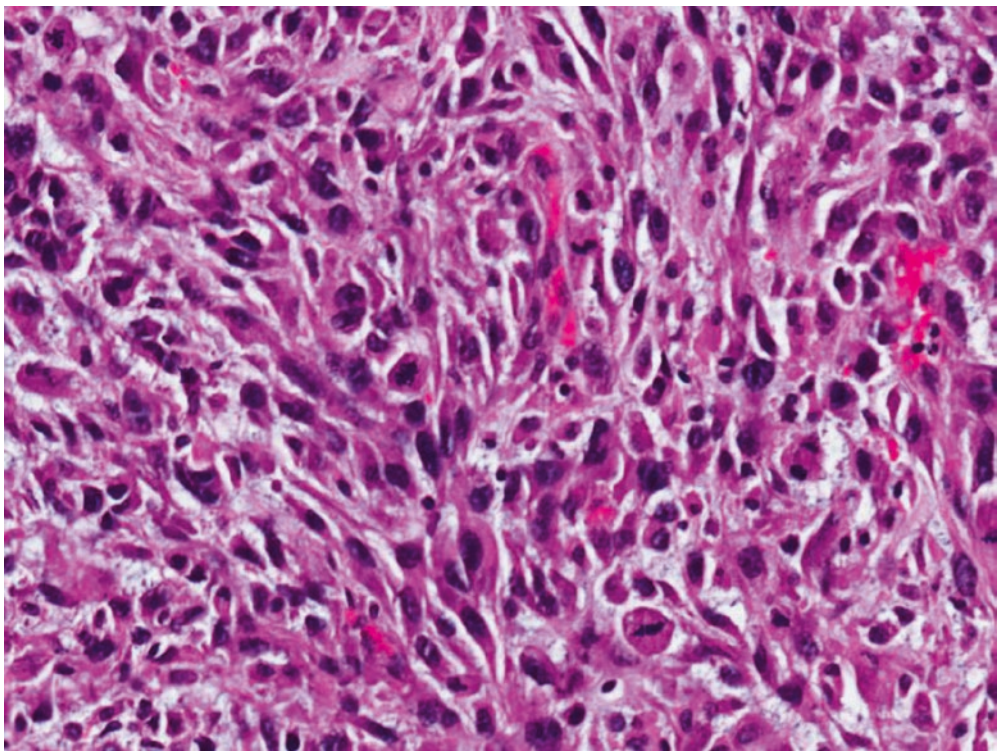

Fig. 12.105 Spindle cell carcinoma. Malignant spindle cells show brisk mitotic activity

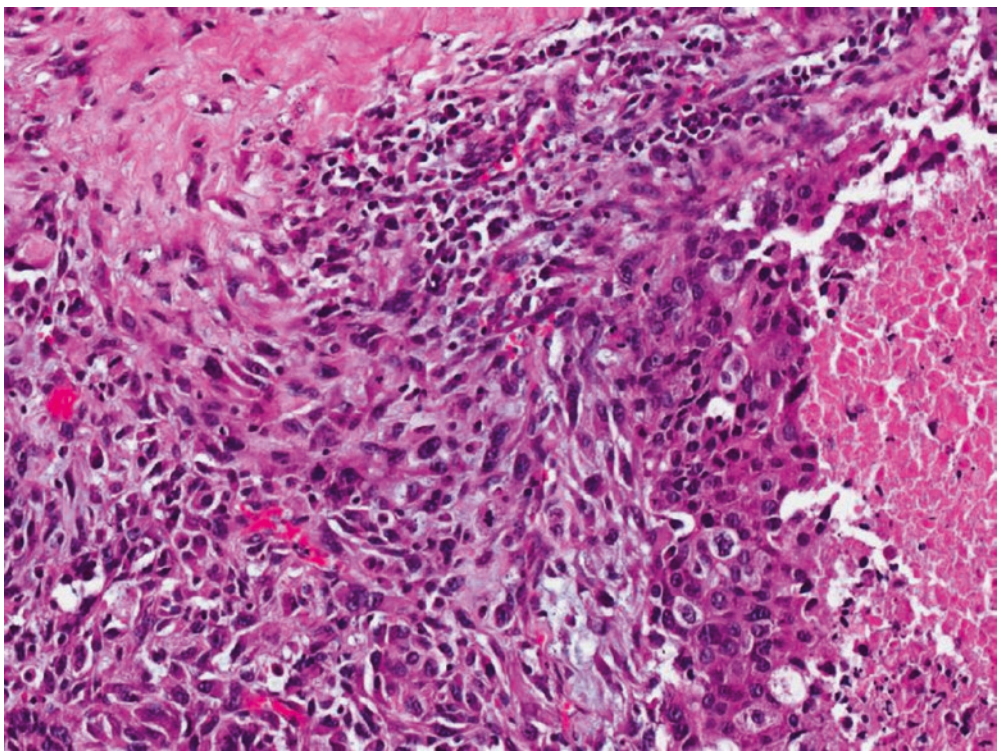

Fig. 12.106 Spindle cell carcinoma. Malignant spindle cells merge with carcinoma islands (right field with necrosis). The presence of unequivocal in situ and/or invasive carcinoma components supports the diagnosis of metaplastic carcinoma in a malignant spindle cell tumour. Immunohistochemistry to demonstrate the expression of keratins can also be used for confirmation

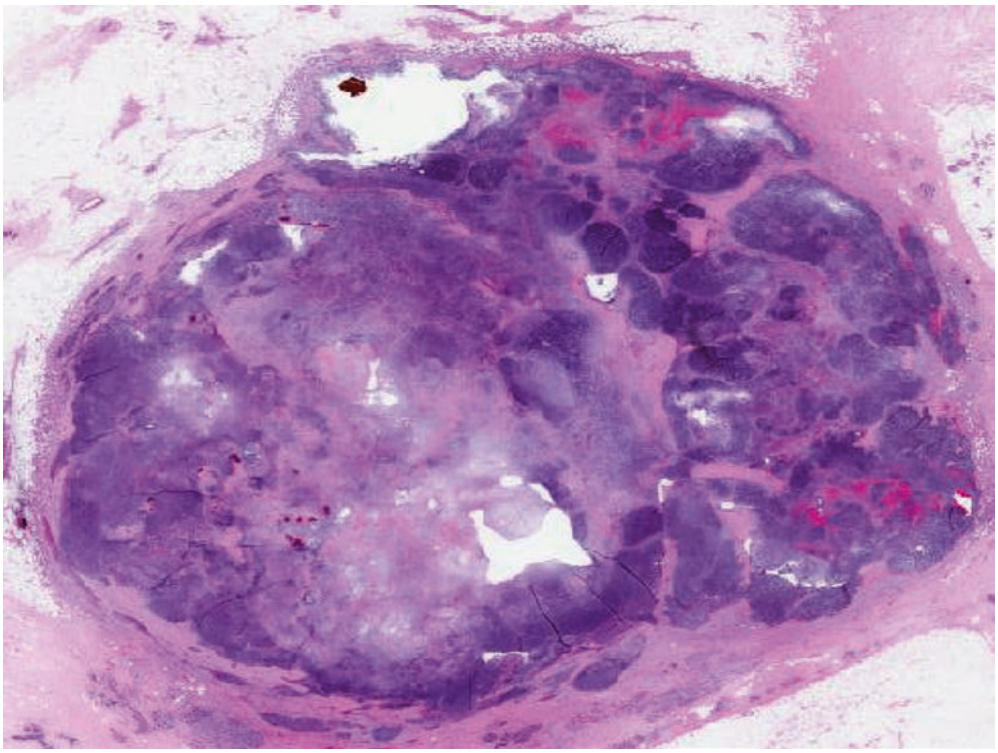

Fig. 12.107 Metaplastic carcinoma with mesenchymal elements and matrix production. At low magnification, the tumour has a relatively rounded appearance with lobulated outlines

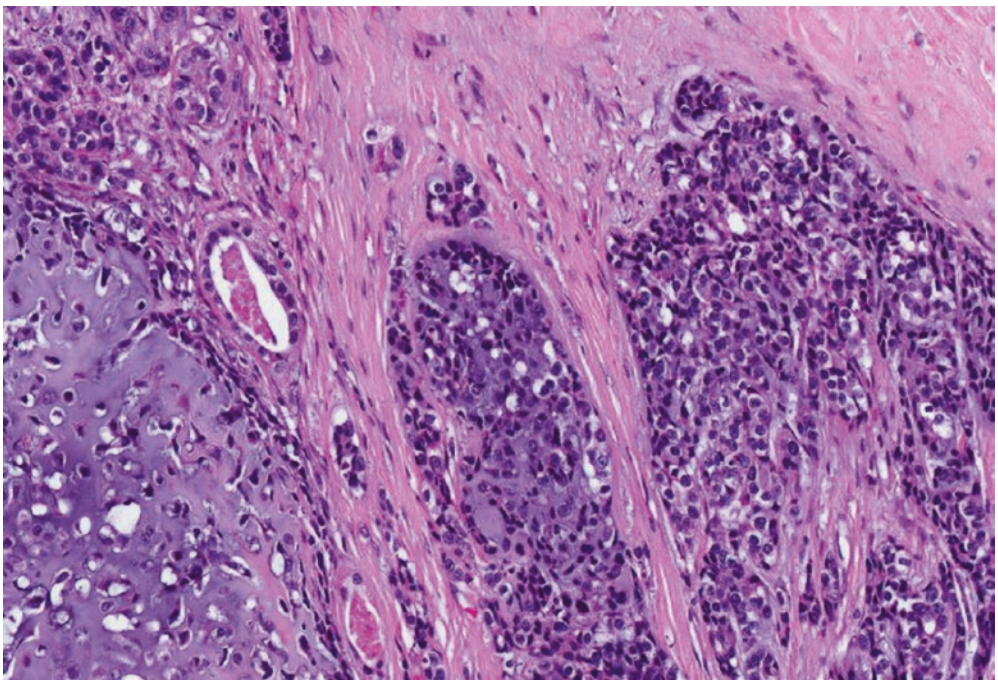

Fig. 12.108 Metaplastic carcinoma with chondroid areas. Anastomosing carcinoma islands (*right field*) are juxtaposed to a chondroid island (*left field*)

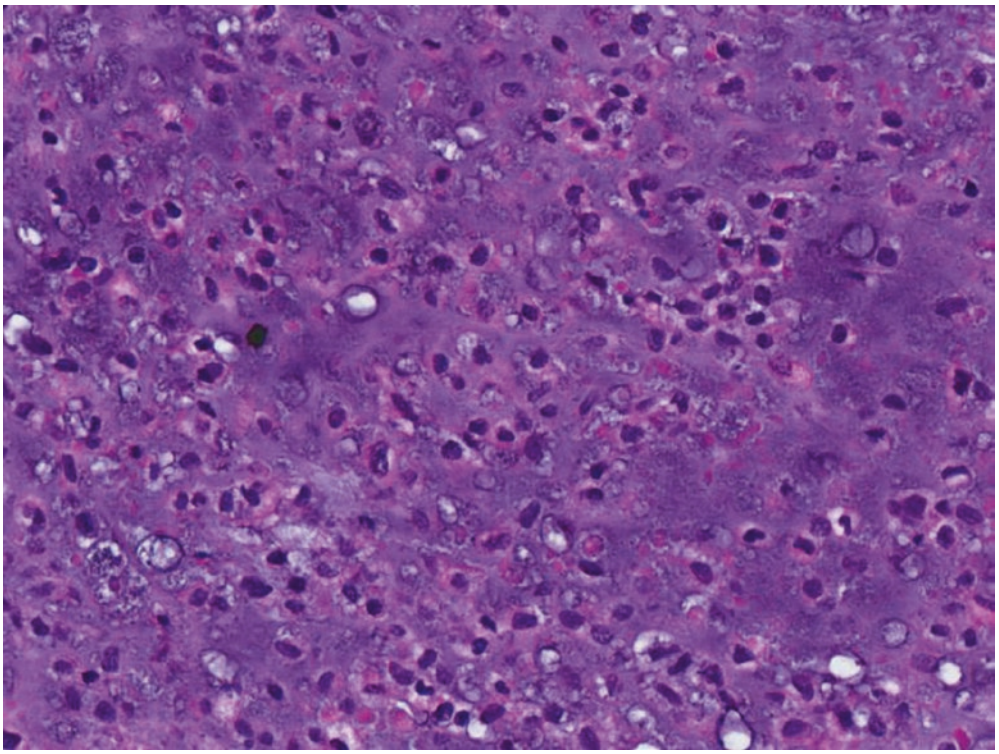

Fig. 12.109 Metaplastic carcinoma with chondroid areas. The chondroid component shows chondroblasts, some occurring within lacunae

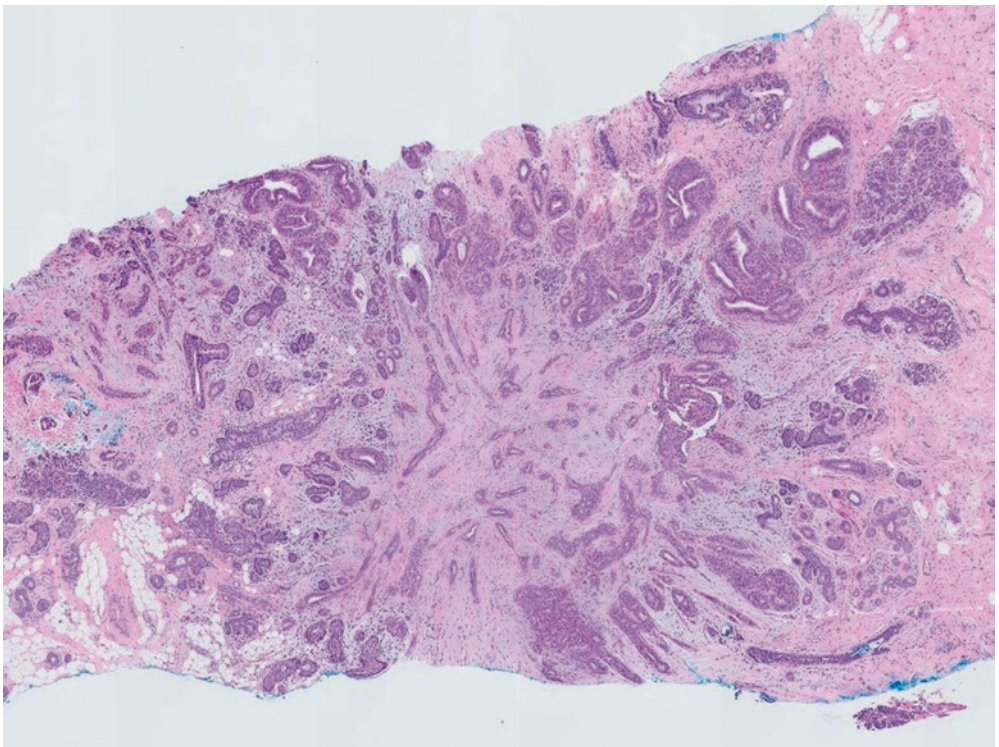

Fig. 12.110 Radial sclerosing lesion on core biopsy. Low magnification shows radiating ducts emanating from a central core, giving a pseudo-infiltrative pattern and mimicking an invasive carcinoma

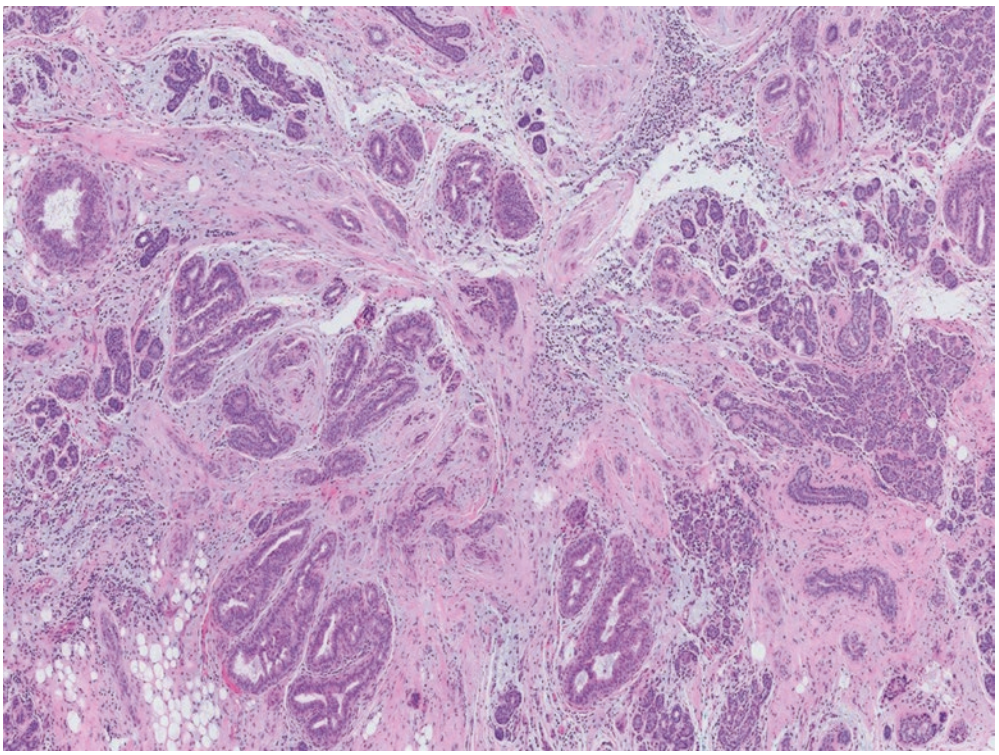

Fig. 12.111 Radial sclerosing lesion shows small epithelial nests in its nidus, associated with mild, chronic inflammation. These islands are confined to the centre and within the periphery of the lesion

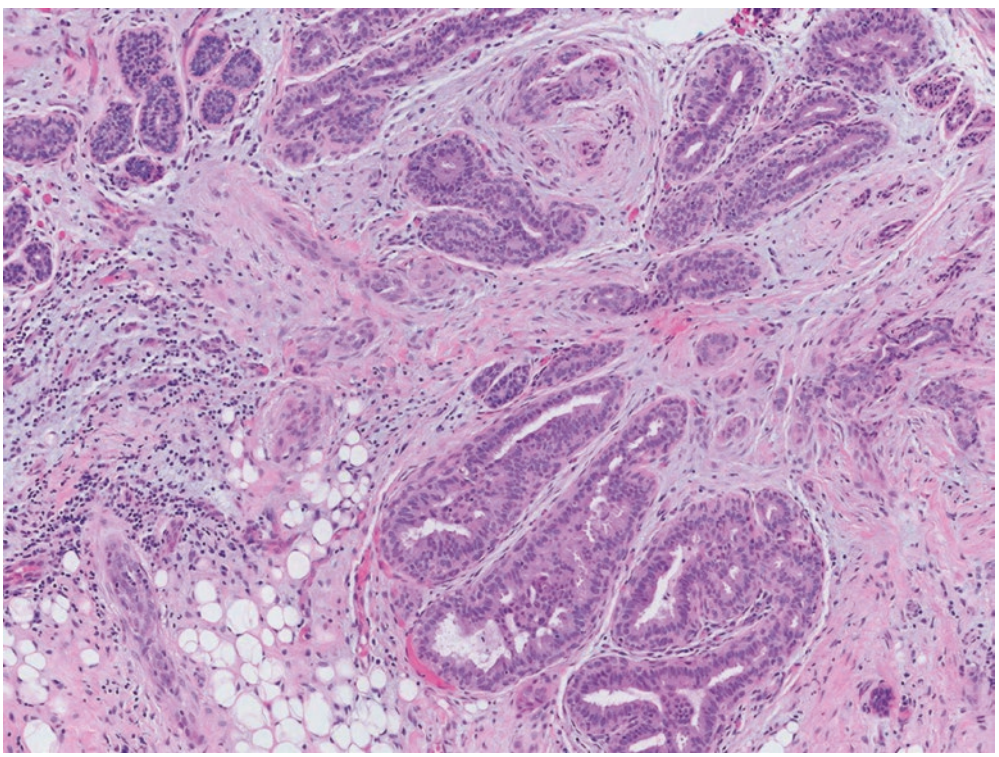

Fig. 12.112 Radial sclerosing lesion. Squamoid nests are seen adjacent to ducts displaying usual ductal hyperplasia. Together with the pseudo-infiltrative pattern, the appearance can be mistaken for low-grade adenosquamous carcinoma, but these squamoid nests are limited to the radial sclerosing lesion and do not show a diffusely permeative nature beyond the general confines of the lesion

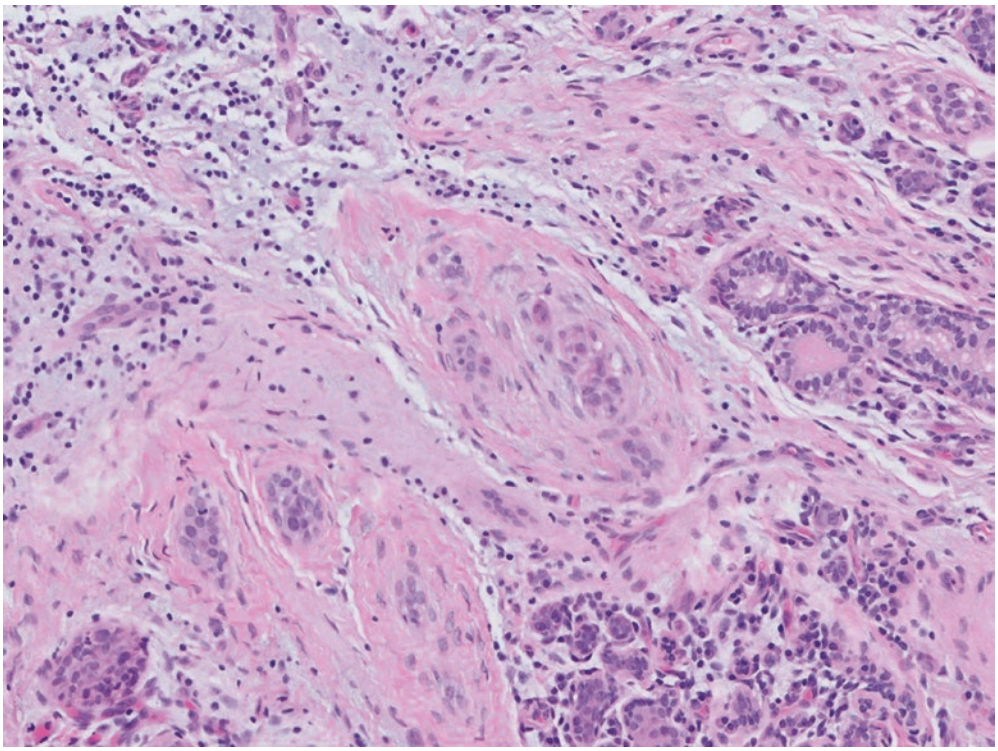

Fig. 12.113 Radial sclerosing lesion. Small nests of epithelial cells are surrounded by spindled stromal cells, accompanied by mild, chronic inflammation

IgG4-Associated Sclerosing Mastitis

IgG4-associated sclerosing mastitis is accompanied by fibrosclerotic stroma with chronic inflammation that features lymphoplasmacytic infiltrates, with the plasma cells expressing predominantly IgG4 (Figs. 12.114 and 12.115). Low-grade adenosquamous carcinoma can also display fibrosclerotic stroma with accompanying lymphocytic aggregates, but plasma cells are not particularly prominent and do not express IgG4. The key difference is the presence of permeative squamoid/squamous nests and tubules in low grade adenosquamous carcinoma.

Pleomorphic Adenoma

The pleomorphic adenoma is a benign epithelial-myoepithelial tumour with histological features similar to its salivary gland counterpart. Due to the presence of chondromyxoid material, it may be mistaken for matrix producing metaplastic carcinoma (Fig. 12.116).

Phyllodes Tumour

Borderline and malignant phyllodes tumour with stromal overgrowth may resemble a spindle cell metaplastic carcinoma. The presence of epithelium-lined stromal fronds and an absence of keratins in the spindle cells indicate a phyllodes tumour. It is important to note that phyllodes tumours, especially the malignant variety, may disclose keratins and p63 in stromal cells on immunohistochemistry, although this phenomenon tends to be patchy and focal [66, 67]. The infrequent though possible occurrence of in situ and invasive carcinoma within a phyllodes tumour may raise further debate on the appropriate categorisation of the tumour in this situation [68].

Breast Sarcoma

Primary breast sarcoma (Figs. 12.117 and 12.118), a rare tumour in the breast, is a diagnosis of exclusion after metaplastic carcinoma and phyllodes tumour have been ruled out [69].

Prognosis and Therapy Considerations

Prognosis depends on the type of metaplastic breast carcinoma, with low-grade adenosquamous and fibromatosis-like metaplastic carcinomas behaving more indolently. Metaplastic carcinomas may not respond to adjuvant chemotherapy and have a worse prognosis than other triple-negative breast cancers. They have a tendency to metastasize to the brain and lung in the absence of axillary nodal involvement [56].

Adenoid Cystic Carcinoma

Definition

Adenoid cystic carcinoma is an uncommon breast malignancy that accounts for less than 0.1 % of all breast carcinomas [70]. It is histologically similar to adenoid cystic carcinoma of the salivary gland, lung, and skin.

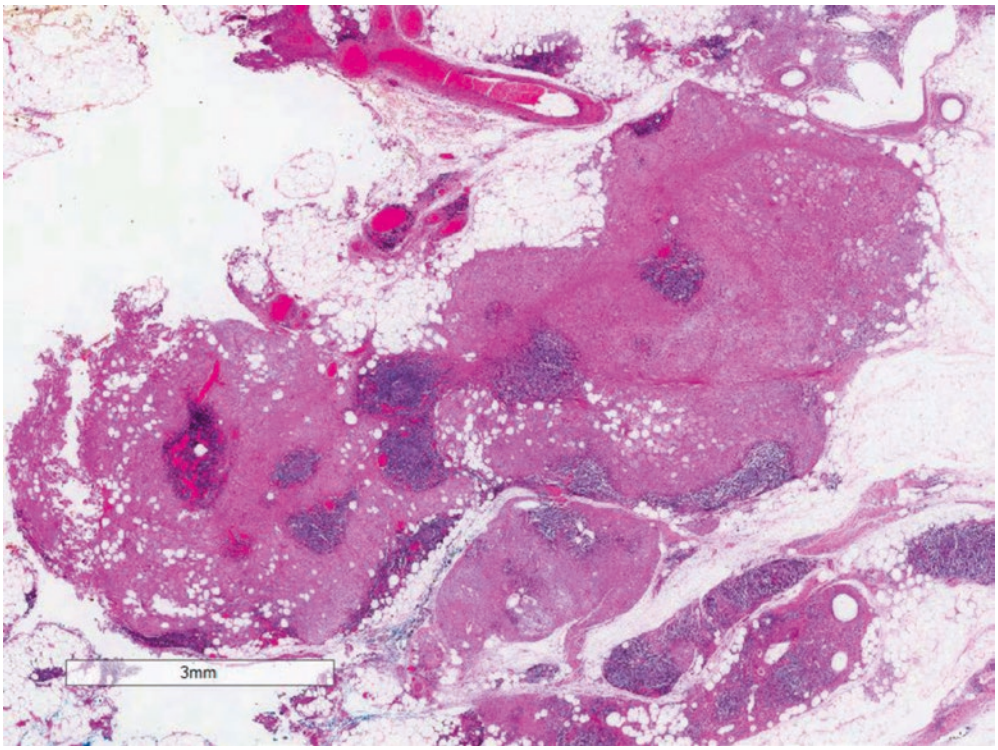

Fig. 12.114 IgG4-associated sclerosing mastitis. Low magnification shows a nodular sclerotic lesion with lymphoid aggregates

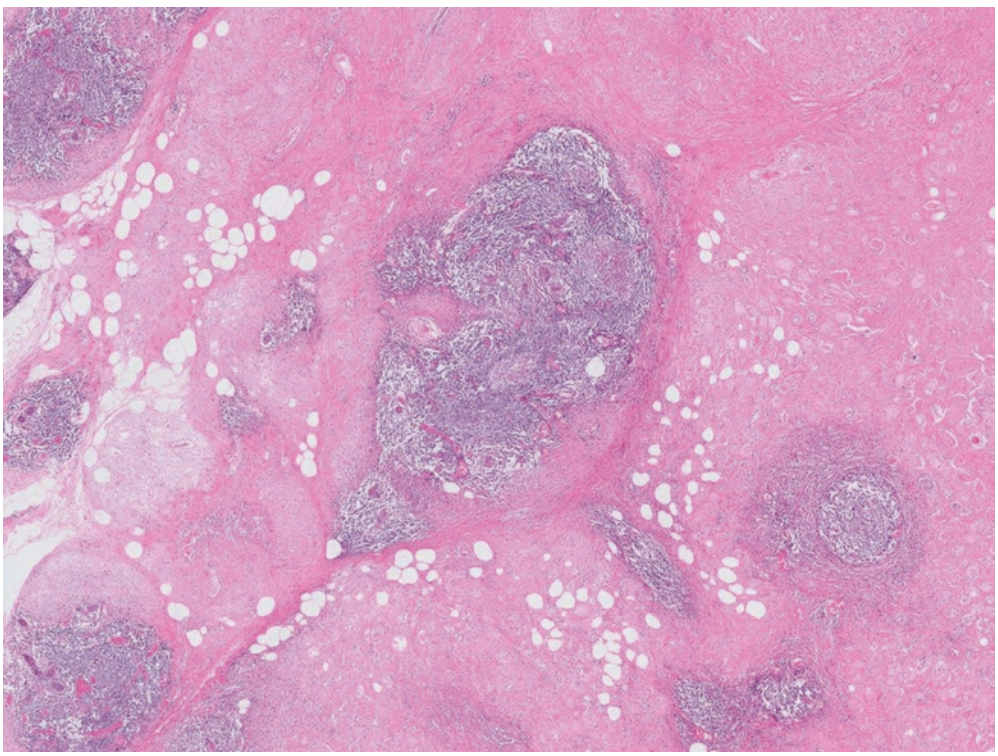

Fig. 12.115 IgG4-associated sclerosing mastitis. Lymphocytic aggregates are prominent in this condition, similar to the lymphoid collections accompanying low-grade adenosquamous carcinoma. In IgG4 disease, however, there is extensive sclerosis of the parenchyma, with effacement of lobules and ducts. Immunohistochemistry confirms the predominance of IgG4-expressing plasma cells among the inflammatory infiltrates

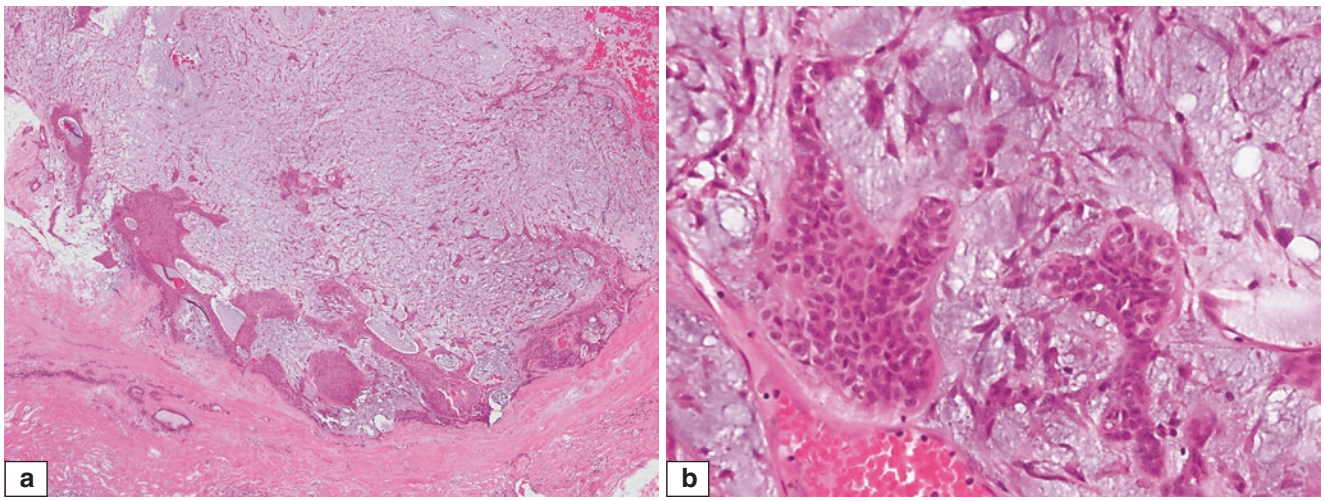

Fig. 12.116 Pleomorphic adenoma. (**a**) Low magnification shows a relatively circumscribed tumour border, with epithelial islands within a myxoid matrix. A few benign ducts are seen in the adjacent breast tissue. (**b**) High magnification shows branching epithelial islands within a myxoid matrix containing slender elongated myoepithelial cells. Presence of mild nuclear atypia and occasional mitotic activity in the epithelial component can raise concern for a matrix producing metaplastic carcinoma, especially in limited samples such as those obtained on core biopsy

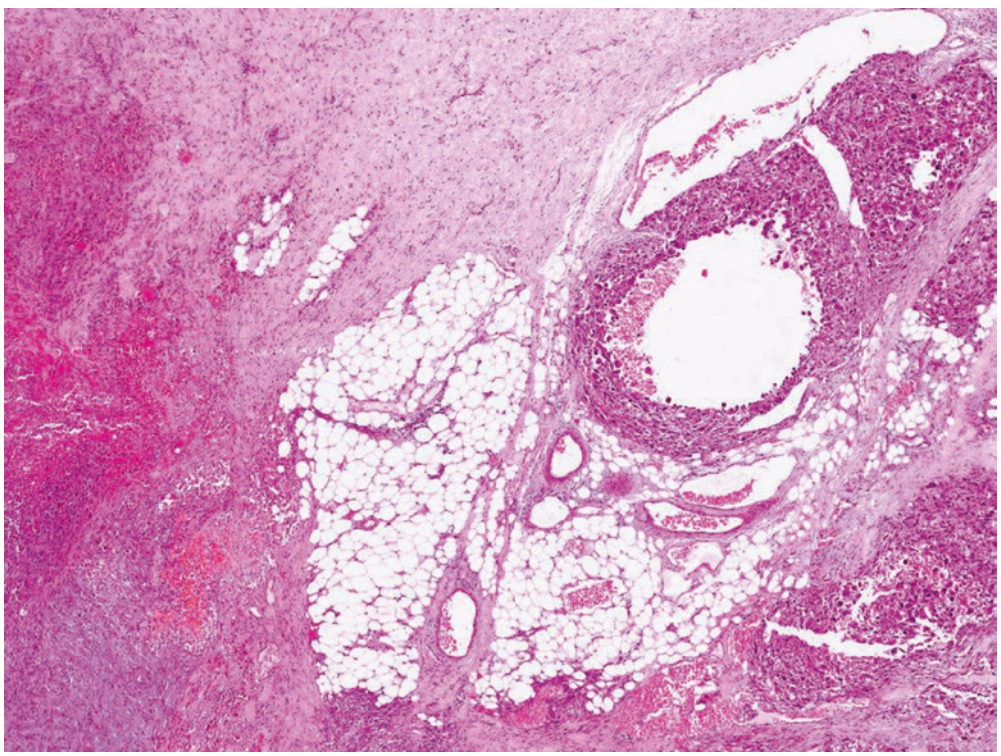

Fig. 12.117 Sarcoma. Sheets of pleomorphic cells are seen invading the fibrofatty breast parenchyma, accompanied by haemorrhage

Clinical and Epidemiological Features

Women ranging from 25 to 80 years of age are affected, with most diagnosed in the postmenopausal years. Symptoms include pain, tenderness, and nipple discharge. Half the tumours reside in a subareolar location.

Imaging Features

Mammography shows either a well-defined lobulated mass or a more ill-defined lesion associated with distortion (Fig. 12.119). Some tumours can be mammographically occult.

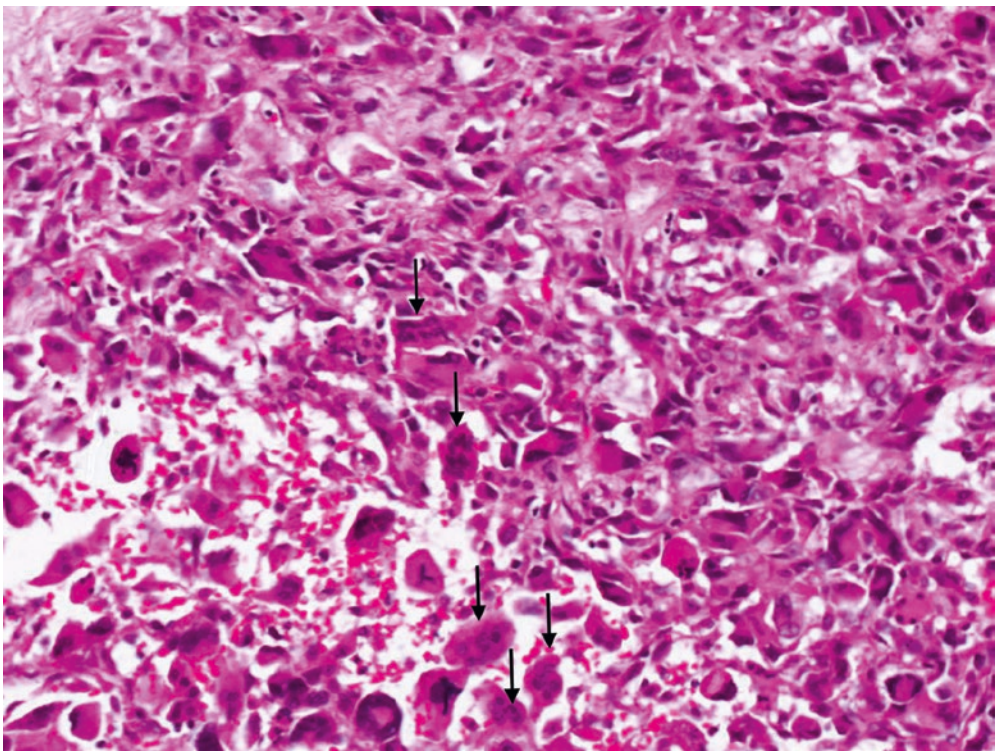

Fig. 12.118 Sarcoma. High magnification shows anaplastic cells with mitoses. A few osteoclastic-type giant cells are also seen (*arrows*). Sarcoma in the breast is a diagnosis of exclusion. Metaplastic carcinoma and malignant phyllodes tumour must be ruled out. In this case, keratins and p63 were negative on immunohistochemistry, and no phyllodal areas were found after thorough sampling

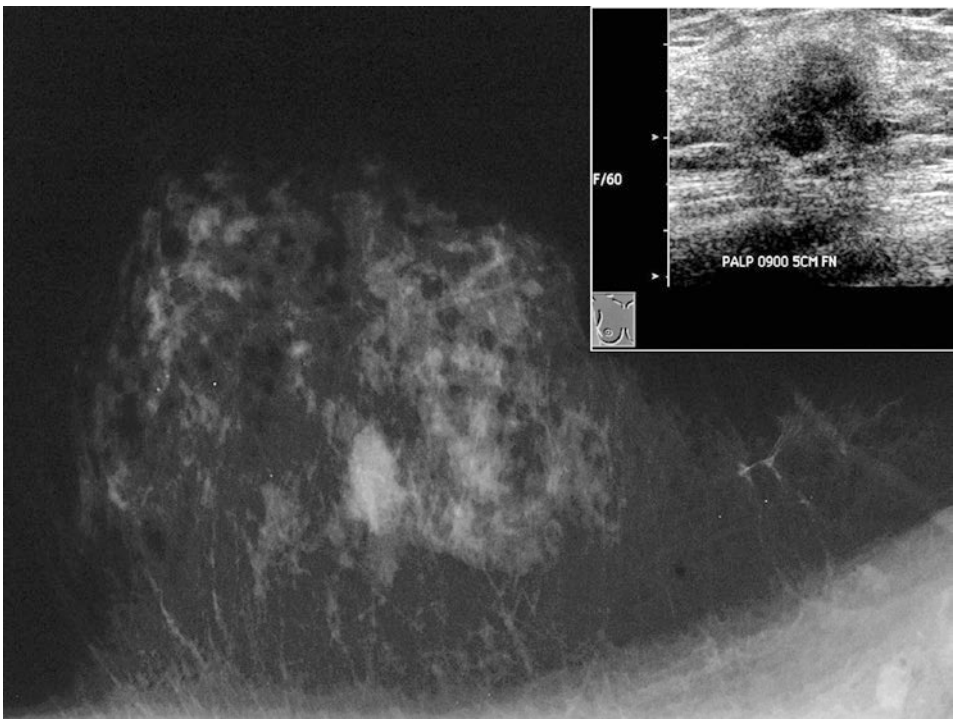

Fig. 12.119 Mammography of adenoid cystic carcinoma. The breast shows an opacity in this right mediolateral oblique view. The opacity has a slightly lobulated appearance. *Inset* shows the ultrasound appearance of the opacity, which is hypoechoic and has posterior acoustic shadows

Pathologic Features

Macroscopic Pathology

Tumours range in size from microscopic to large, symptomatic masses of 12 cm. They may appear greyish-white, circumscribed, and nodular with occasional cystic areas, or they may be less well defined, with irregular borders (Figs. 12.120 and 12.121).

Microscopic Pathology

Adenoid cystic carcinoma is an invasive epithelial–myoepithelial tumour, histologically characterised by large, coalescent, cribriform islands harbouring spaces (pseudolumens) containing watery, basophilic mucopolysaccharides and thicker, eosinophilic basement membrane material, both secreted by myoepithelial cells (Figs. 12.122, 12.123, 12.124, 12.125, and 12.126). True lumens surrounded by luminal epithelial cells are also present. Loose myxoid stroma surrounds the cribriform islands. Tubules, anastomosing trabeculae, and solid nests may also be seen. Squamous and sebaceous metaplasia, and adenomyoepitheliomatous areas, may be observed (Figs. 12.127, 12.128, and 12.129). Some tumours are composed of solid, basaloid nests (Figs. 12.130, 12.131, and 12.132). Immunohistochemically, adenoid cystic carcinoma is most often negative for hormone receptors and c-erbB-2 (triple-negative), with positive staining for p63,

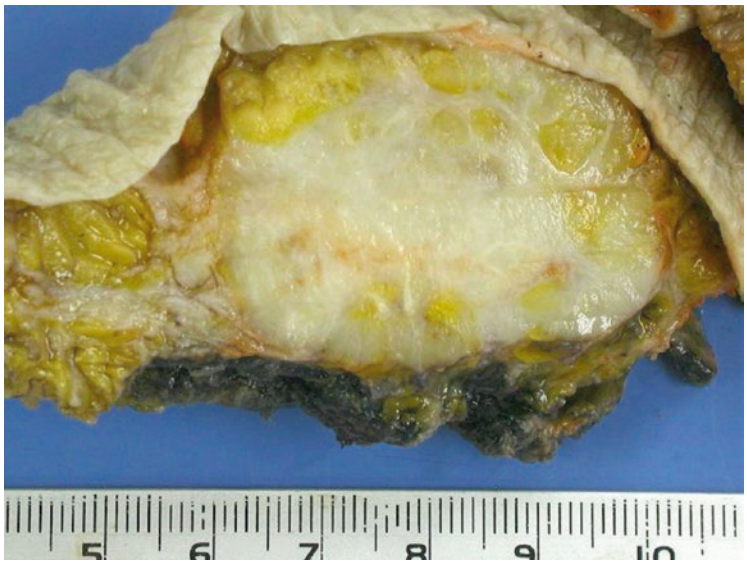

Fig. 12.120 Adenoid cystic carcinoma. Gross appearance shows a whitish-beige tumour with ill-defined borders and some whitish streaks

Fig. 12.121 Adenoid cystic carcinoma. The tumour shows a slightly myxoid quality on its cut surface

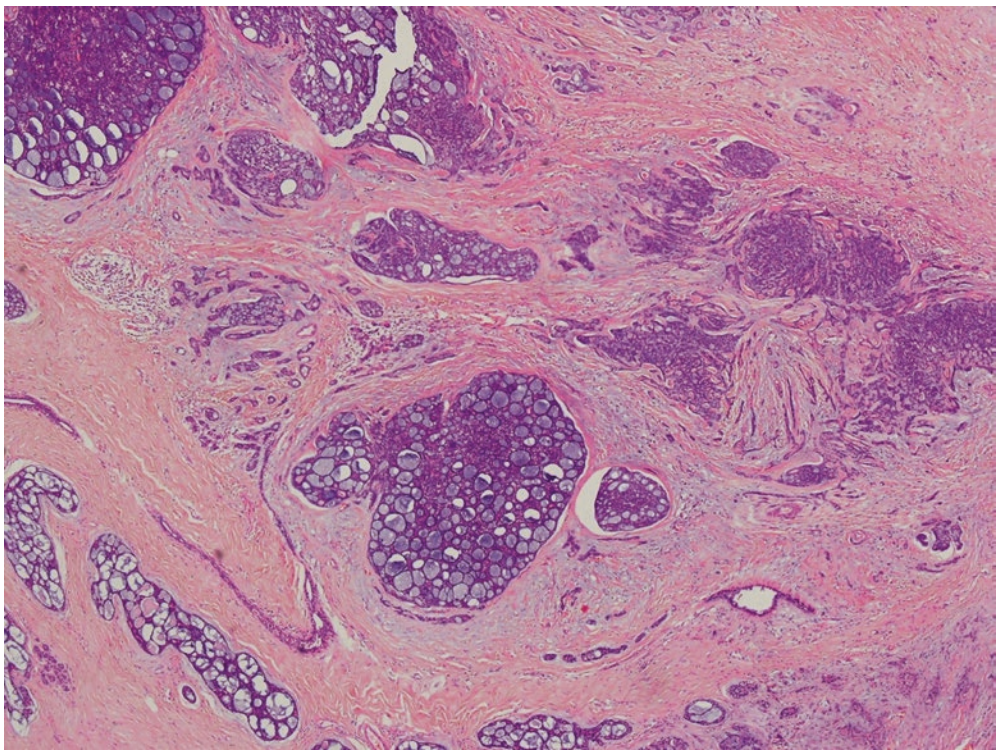

Fig. 12.122 Adenoid cystic carcinoma. At low magnification, cribriform tumour islands with spaces containing both pale, thin, bluish-grey material and more viscid pink substances are present. Smaller nests of irregular tubules and elongated strands of tumour cells are seen within the stroma. The stroma shows a loose, slightly myxoid quality around the large cribriform islands

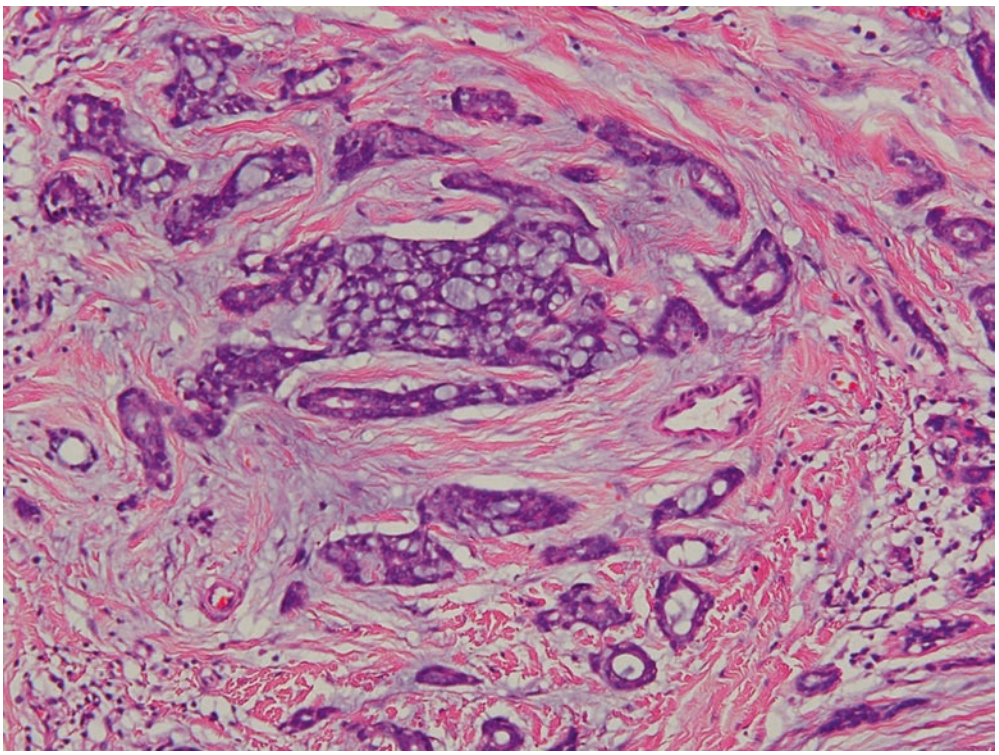

Fig. 12.123 Adenoid cystic carcinoma. Higher magnification shows irregular cribriform contours with tubules within a myxoid matrix. Bluish-grey watery material is seen within several cribriform lumens

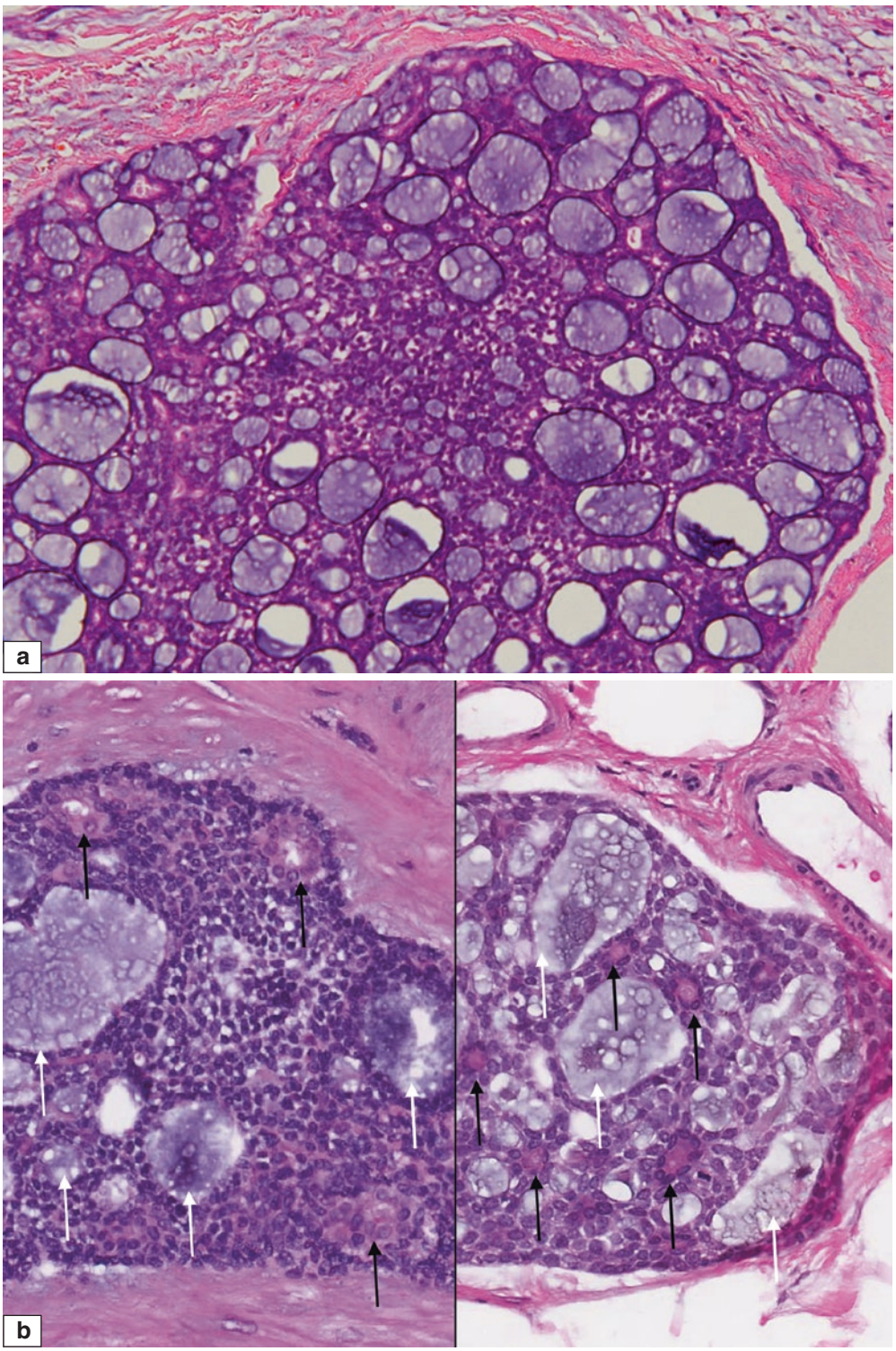

Fig. 12.124 Adenoid cystic carcinoma. (**a**) Adenoid cystic carcinoma shows two types of lumens: pseudolumens, which are lined by myoepithelial-type cells and contain watery, pale bluish-grey material and thicker, pink, basement membrane substance, and true lumens, which are rimmed by luminal-type epithelial cells. The true lumens are less conspicuous than the pseudolumens. (**b**) Pseudolumens containing watery myxoid substance (*white arrows* indicate some pseudolumens) and true lumens lined by cuboidal luminal type epithelial cells (*black arrows*) are present

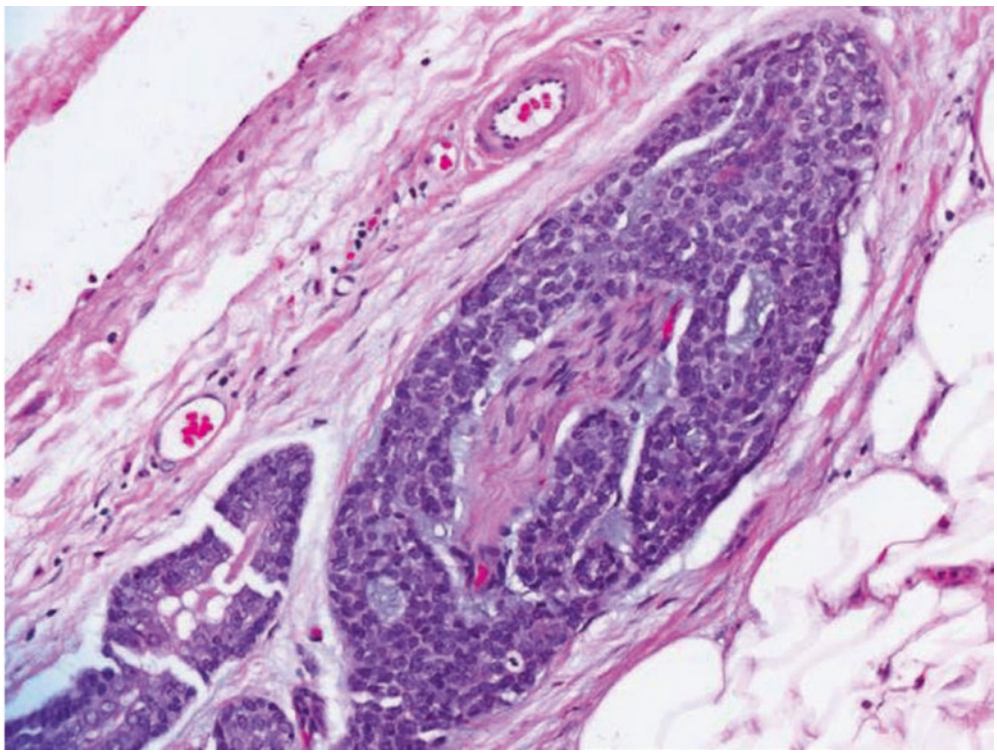

Fig. 12.125 Perineural invasion in adenoid cystic carcinoma. Perineural invasion is encountered in the breast less frequently than in adenoid cystic carcinoma of the salivary gland

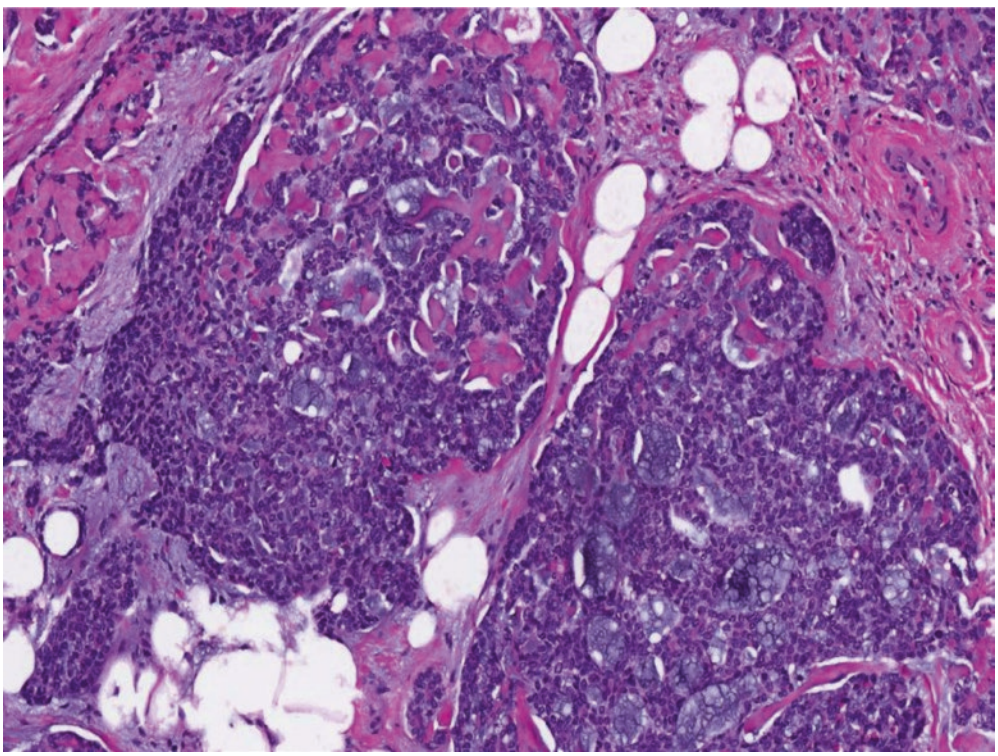

Fig. 12.126 Islands of adenoid cystic carcinoma. Both thin, pale, watery mucopolysaccharide and thick, pink, basement membrane materials are seen

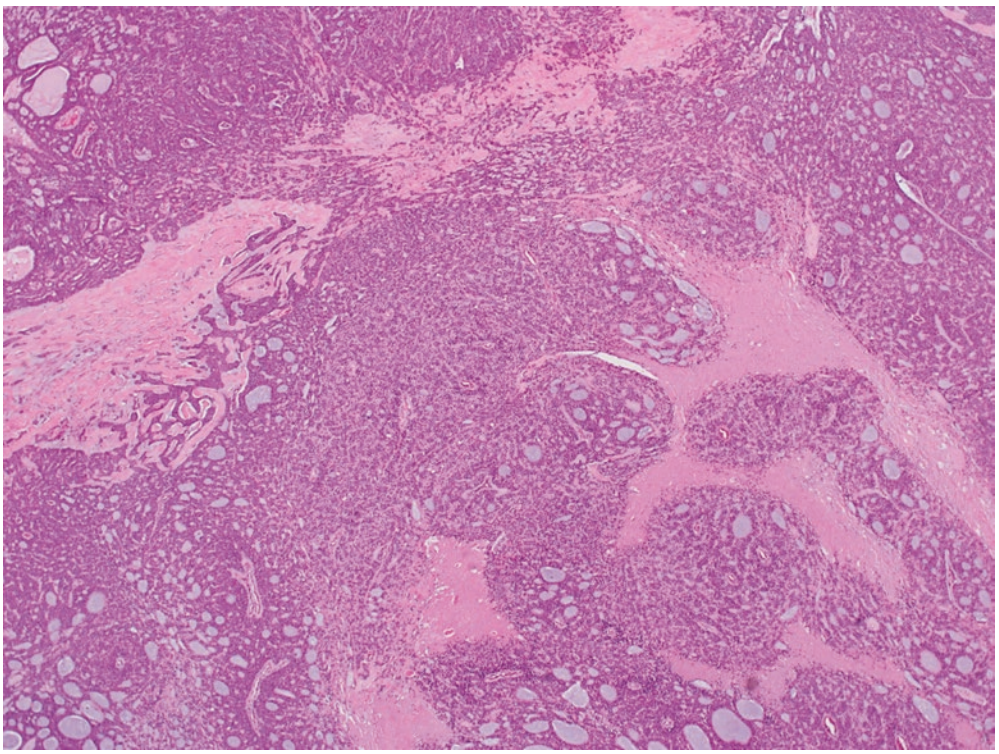

Fig. 12.127 Adenoid cystic carcinoma with a focal adenomyoepitheliomatous area embedded in its midst. At scanning magnification, confluent cribriform islands appear to radiate out from a central tubular zone corresponding to the adenomyoepitheliomatous area

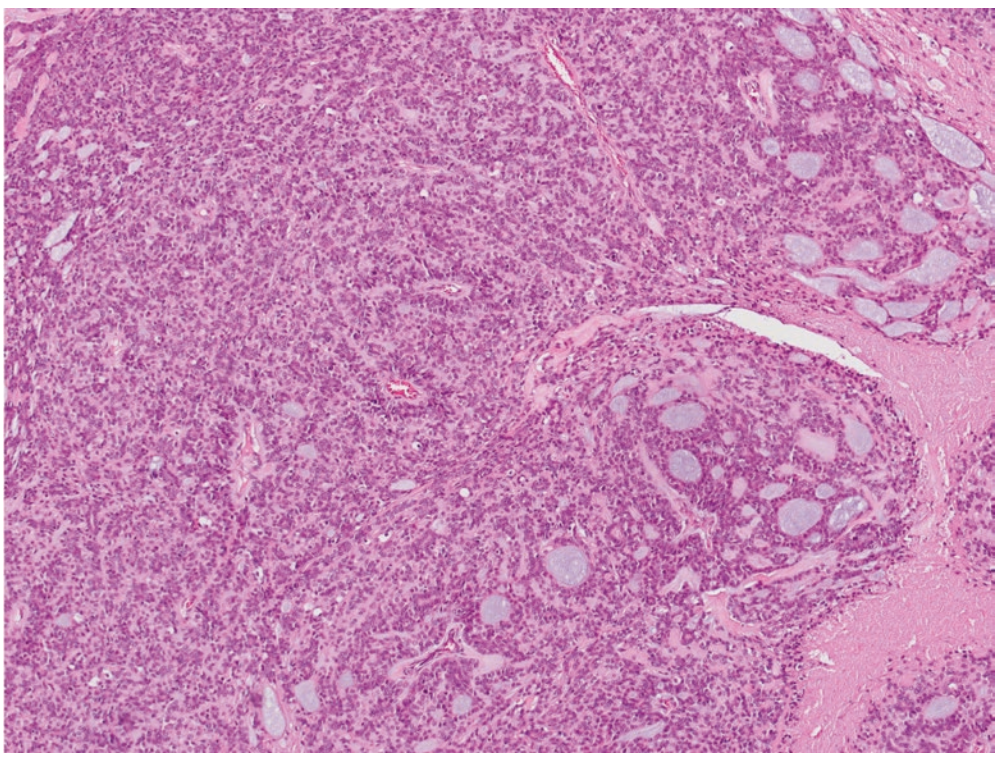

Fig. 12.128 Adenoid cystic carcinoma shows an adenomyoepitheliomatous area in its midst, featuring a lattice of tubules rimmed by a balanced proliferation of both luminal and myoepithelial cells. A gradual transition to recognisable adenoid cystic carcinoma foci with cribriform structures and luminal spaces containing mucopolysaccharides is seen

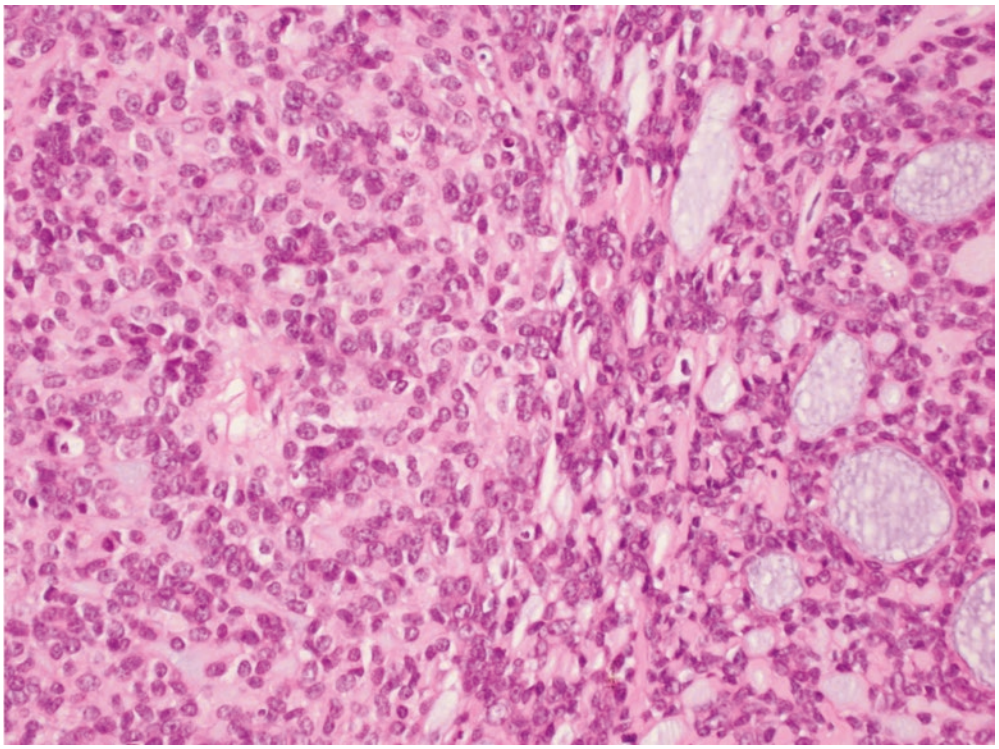

Fig. 12.129 Higher magnification of adenoid cystic carcinoma (*right*) juxtaposed to adenomyoepithelioma areas (*left*)

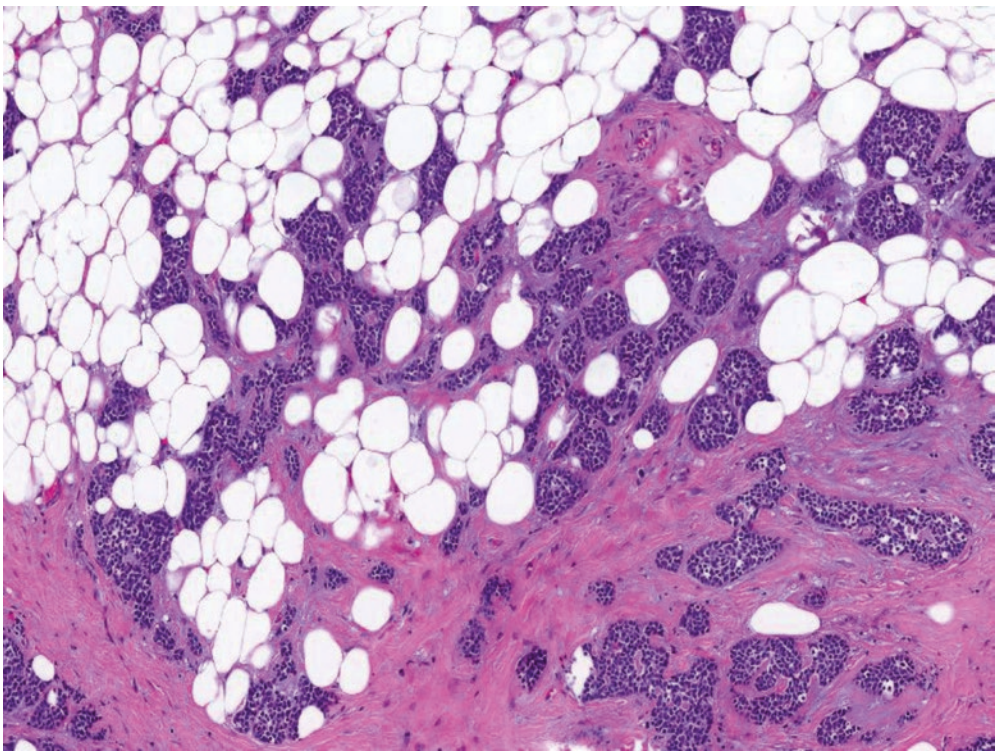

Fig. 12.130 Adenoid cystic carcinoma with solid basaloid features. Small nests and irregular islands of basaloid cells with dense nuclei and scant cytoplasm infiltrate the fibroadipose breast stroma

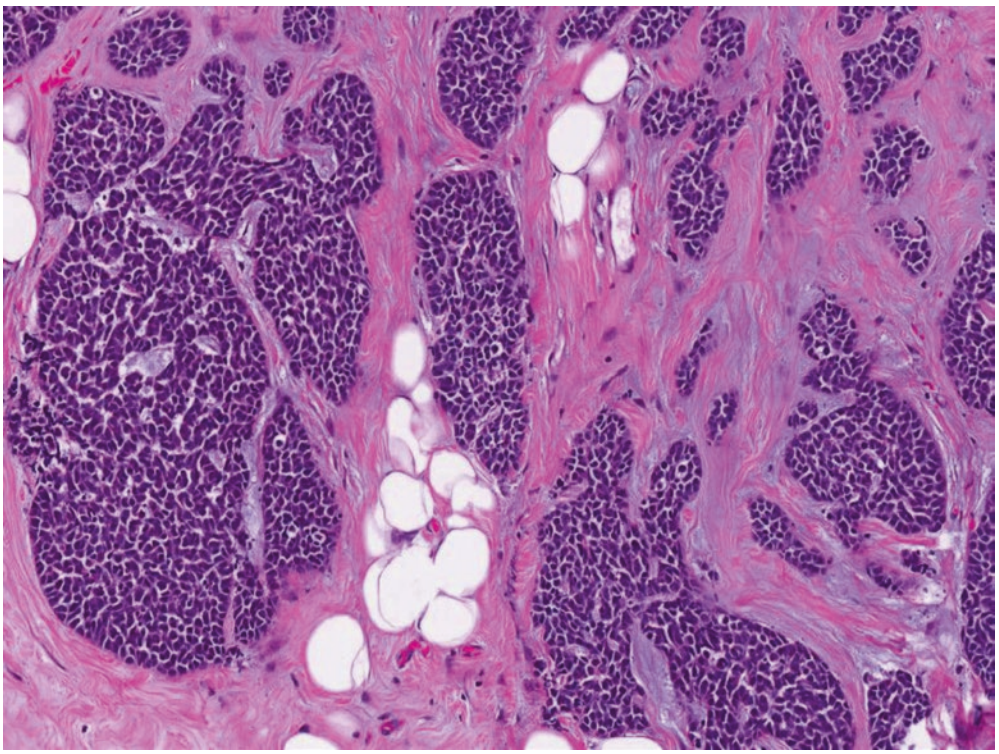

Fig. 12.131 Adenoid cystic carcinoma with solid basaloid features. Irregular tumour islands show some spaces containing myxoid material. A semblance of peripheral regimentation of tumour cells is seen

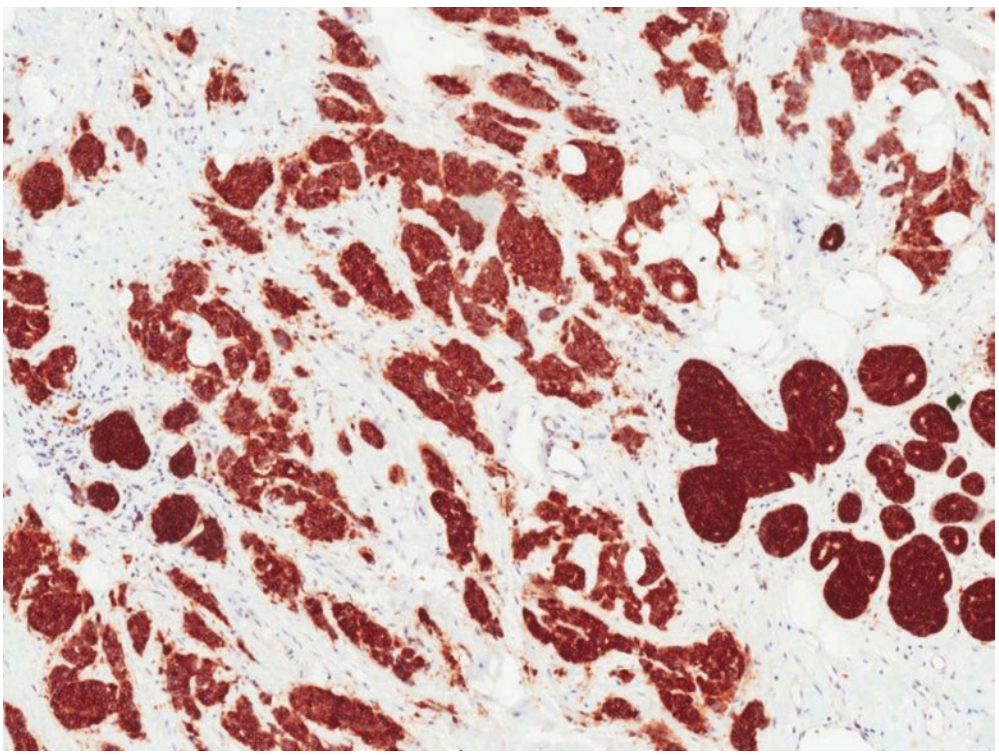

Fig. 12.132 Adenoid cystic carcinoma with solid basaloid features shows diffuse immunohistochemical reactivity for CD117

high-molecular-weight keratins (CK5/6, CK14, CK17), smooth muscle actin (SMA), and SMMHC in the myoepithelial component; CK7 is useful in identifying the luminal epithelial cells, especially in lesions that are predominantly solid or basaloid (Figs. 12.133, 12.134, 12.135, 12.136, 12.137, 12.138, and 12.139). CD117, Cam5.2, and EMA also decorate the luminal cells [71]. Rarely, adenoid cystic carcinoma may coexist with other invasive cancer subtypes (Figs. 12.140 and 12.141). Though it is triple-negative, its mutational burden and repertoire more closely resemble those of salivary gland adenoid cystic carcinoma than those of other triple-negative breast cancers [72]. The translocation t(6;9)(q22-23;p23-24), which generates fusion transcripts involving the genes *MYB* and *NFIB*, is seen in more than 90 % of cases [70].

Differential Diagnosis

Collagenous Spherulosis

Adenoid cystic carcinoma usually presents with a mass, whereas collagenous spherulosis is more often an incidental microscopic lesion discovered in normal breast tissue or in association with other lesions such as usual ductal hyperplasia or intraductal papilloma. Collagenous spherulosis may also be detected as radiological calcifications, which histologically occur within the pseudolumens (Fig. 12.142, 12.143, 12.144, 12.145, and 12.146). It is reported that CD117 is not expressed in collagenous spherulosis [73]. Myoepithelial cells with positive reactivity for p63 and high-molecular-weight keratins rim the pseudolumens of collagenous spherulosis.

Cribriform Ductal Carcinoma In Situ

DCIS with cribriform architecture, which is usually of low to intermediate nuclear grade, resembles adenoid cystic carcinoma (Figs. 12.147, 12.148, 12.149, 12.150, and 12.151). It differs however, in its pure luminal epithelial neoplastic population with diffuse reactivity for oestrogen receptor and diminished or absent staining for high-molecular-weight keratins (Table 12.3). Myoepithelial cells are seen only at the periphery of the cribriform islands, reflecting its non-invasive nature.

Invasive Cribriform Carcinoma

The morphological appearance of invasive cribriform carcinoma is similar to that of cribriform DCIS, but it shows more irregular contours and an absence of rimming myoepithelial cells (Figs. 12.152, 12.153, 12.154, and 12.155). The stroma tends to be desmoplastic, whereas in adenoid cystic carcinoma, the stroma shows myxoid change around the cribriform islands.

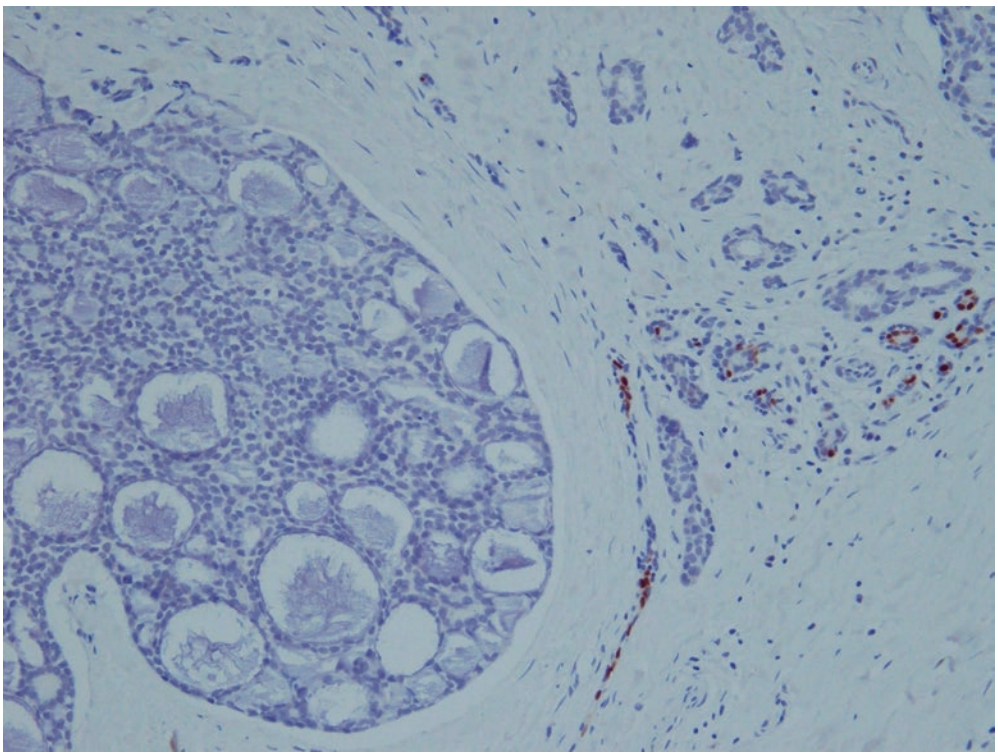

Fig. 12.133 Adenoid cystic carcinoma shows negative staining for oestrogen receptor. (Note the positive internal control with stained nuclei in adjacent breast ductules) Progesterone receptor and c-erbB-2 are also negative (triple-negative)

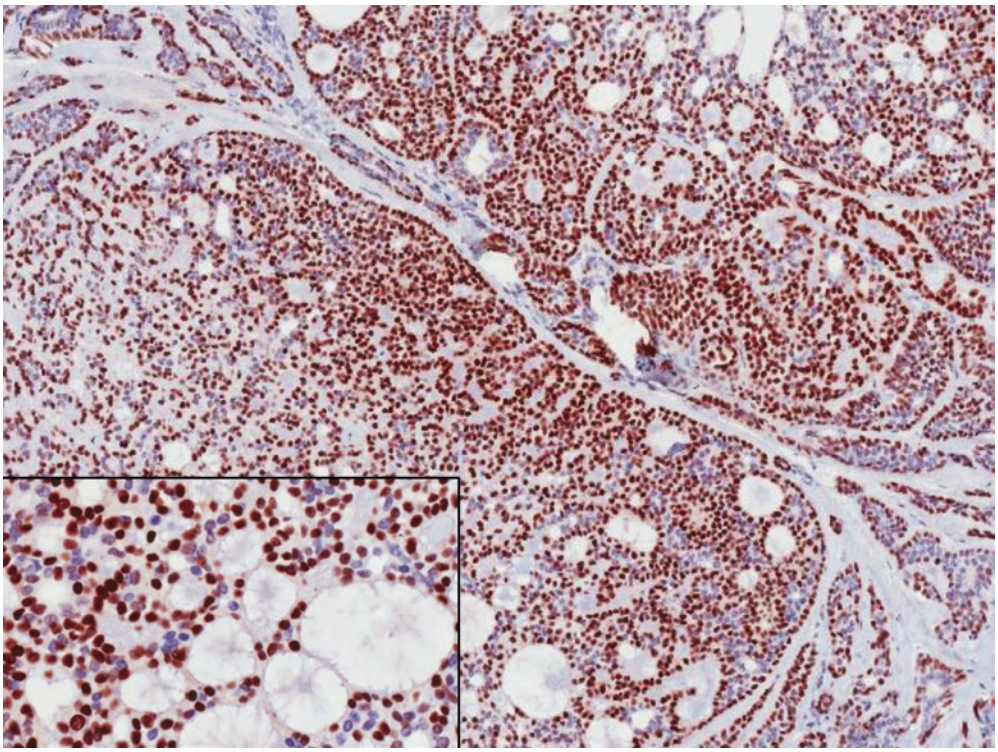

Fig. 12.134 Adenoid cystic carcinoma. Rarely, there may be oestrogen receptor positivity, with tumour cell nuclei being highlighted. *Inset* shows positively stained tumour nuclei rimming pseudolumens containing mucopolysaccharide

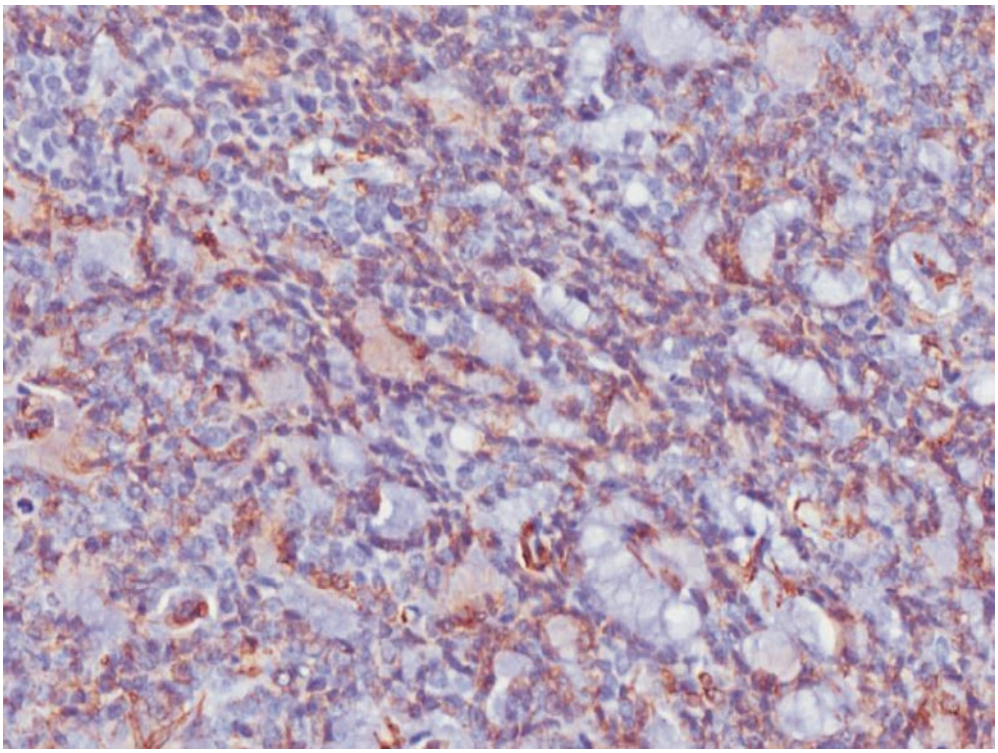

Fig. 12.135 Adenoid cystic carcinoma. Smooth muscle actin (SMA) decorates some of the tumour cells

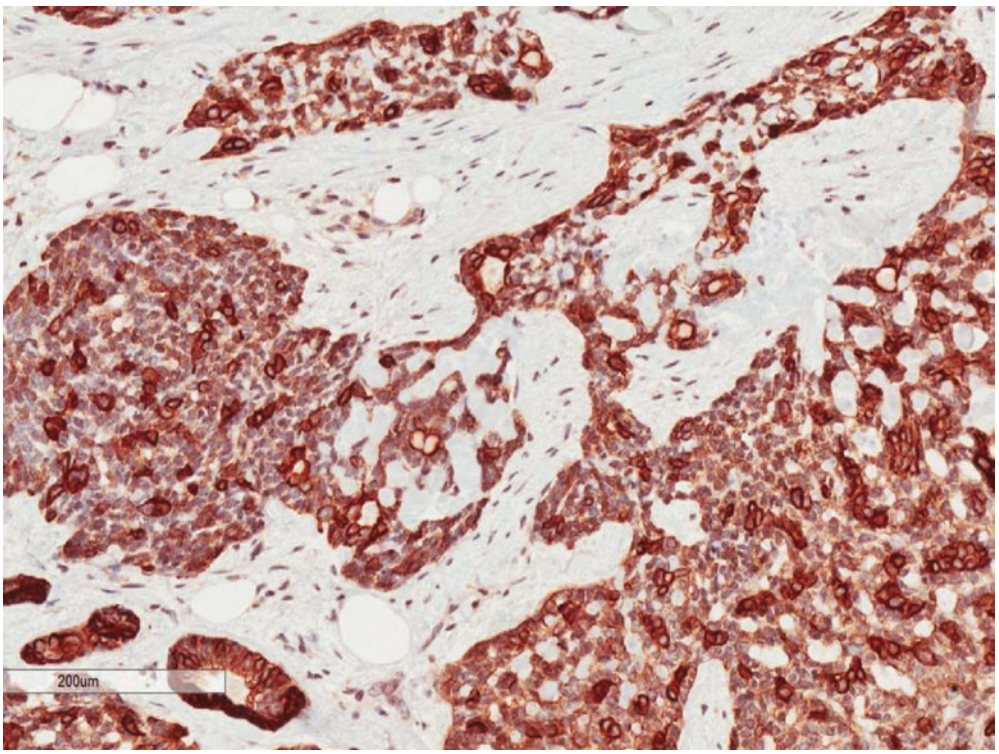

Fig. 12.136 Adenoid cystic carcinoma. CK14 is usually positive, with diffuse reactivity of tumour cells; a few smaller clusters of cells show more intense staining

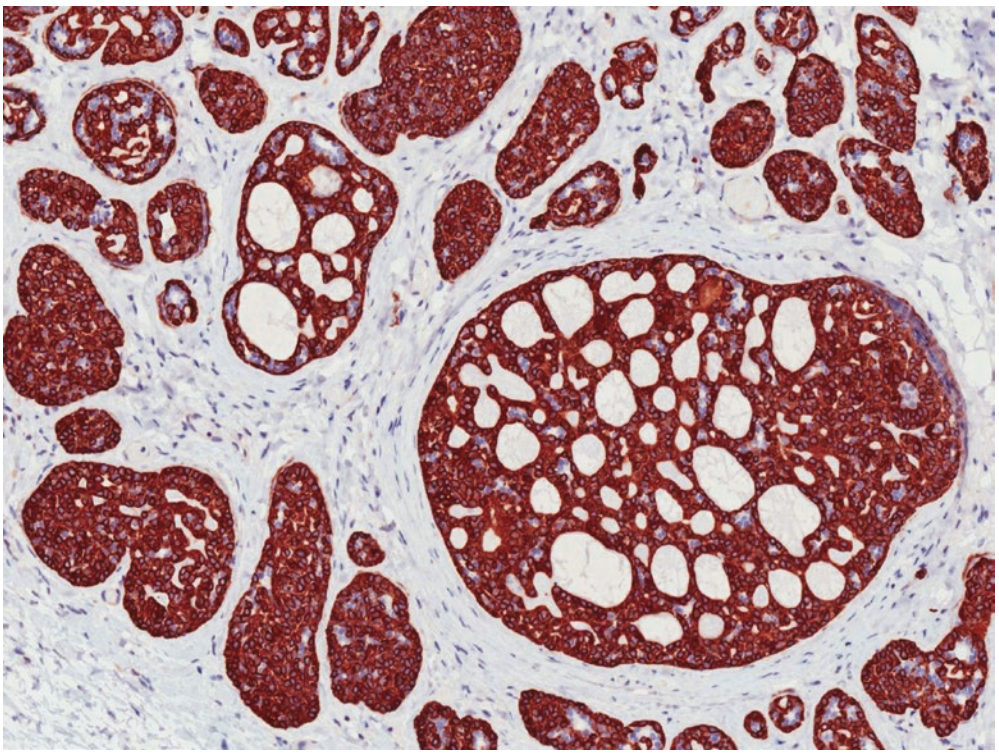

Fig. 12.137 Adenoid cystic carcinoma. CK14 immunohistochemistry stains the myoepithelial cells which comprise the majority of the tumour cell population

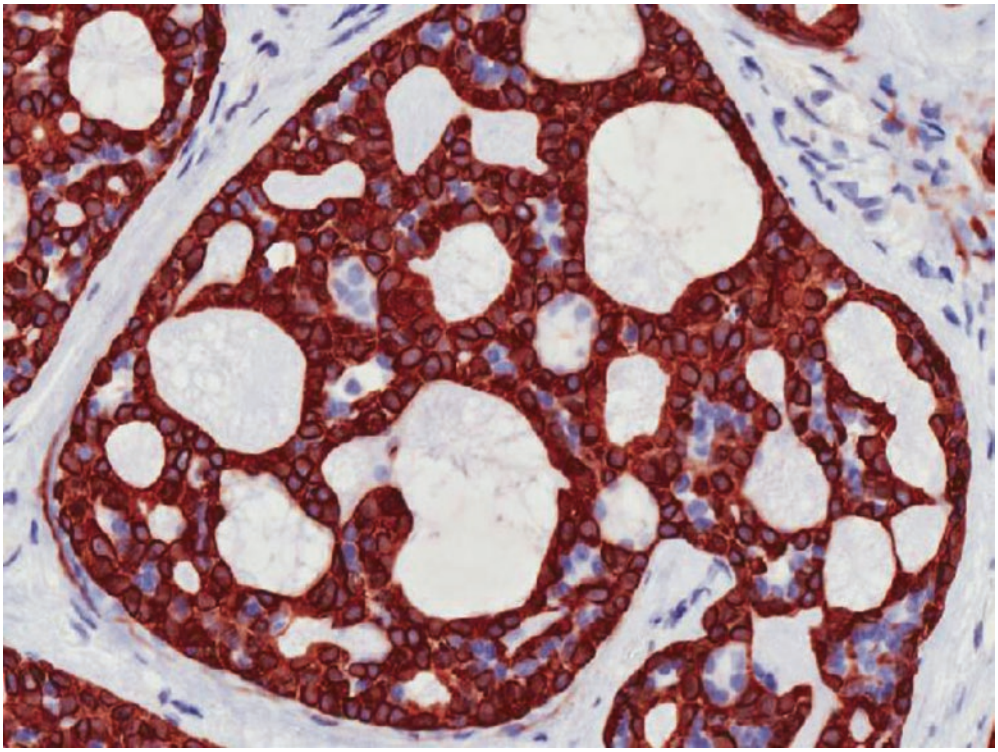

Fig. 12.138 Adenoid cystic carcinoma. High magnification of CK14 immunohistochemistry shows decoration of myoepithelial cells, with negatively stained cells representing luminal cells surrounding true lumens

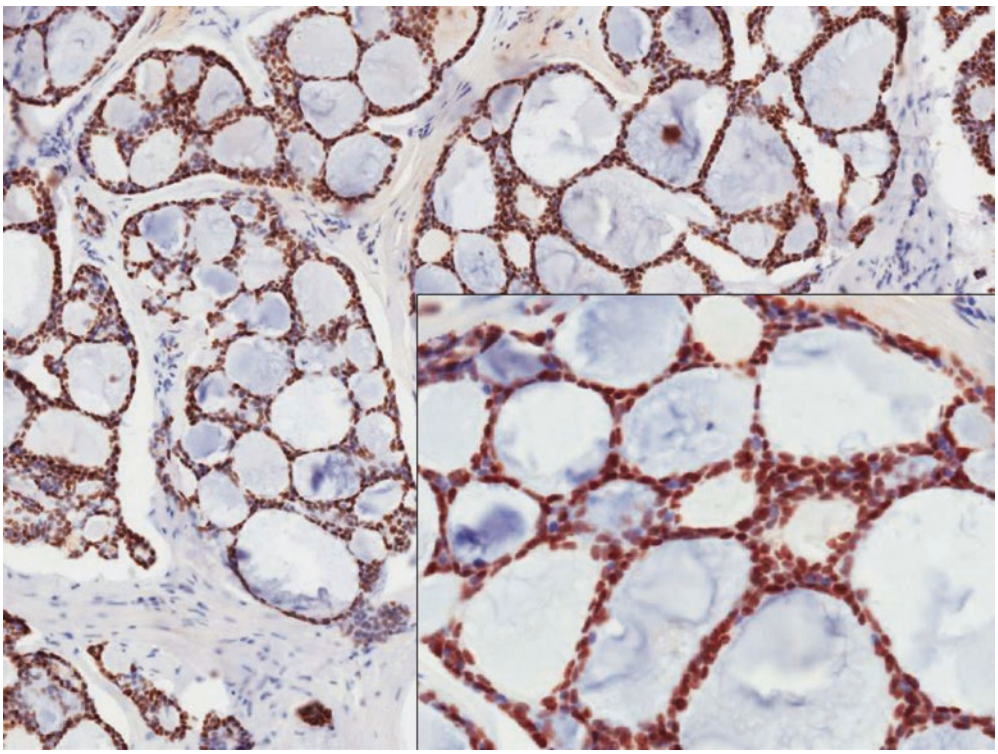

Fig. 12.139 Adenoid cystic carcinoma shows p63 nuclear staining of tumour cells. *Inset* shows higher magnification of the positively stained nuclei

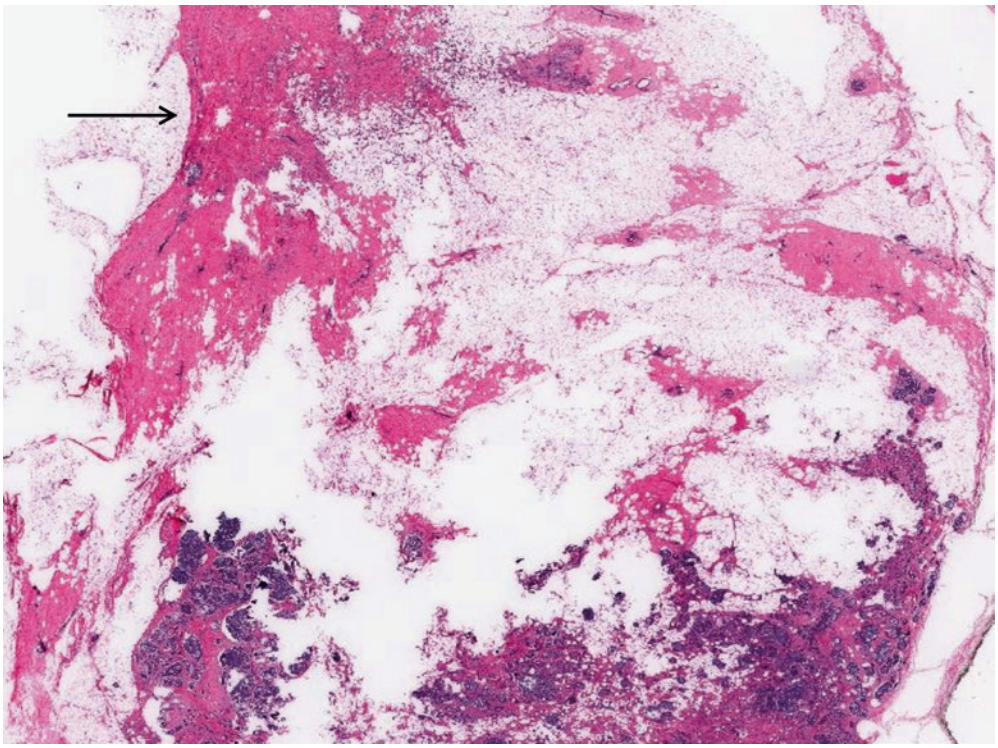

Fig. 12.140 Adenoid cystic carcinoma can coexist with other invasive carcinoma subtypes; in this case, an invasive lobular carcinoma is seen in the upper field (*arrow*), and adenoid cystic carcinoma is present in the lower field

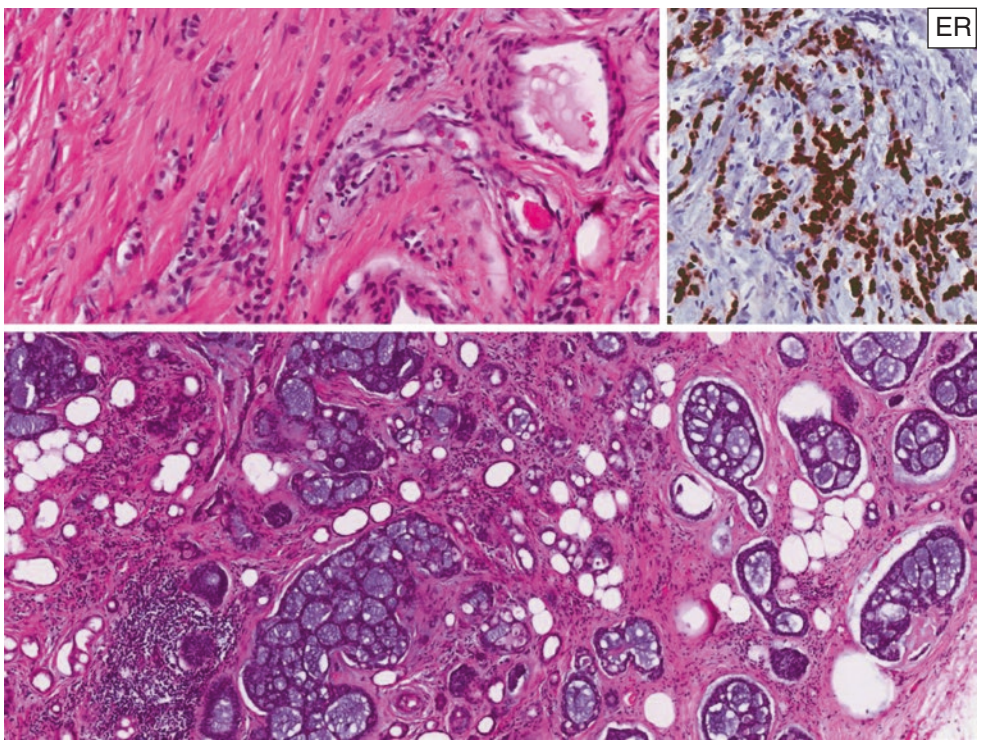

Fig. 12.141 Adenoid cystic carcinoma coexisting with invasive lobular carcinoma. Linear cords of classic invasive lobular carcinoma cells are present within the fibrous stroma, with diffuse oestrogen receptor positivity (*upper half*). Typical histological appearances of cribriform islands in adenoid cystic carcinoma are also observed (*lower half*)

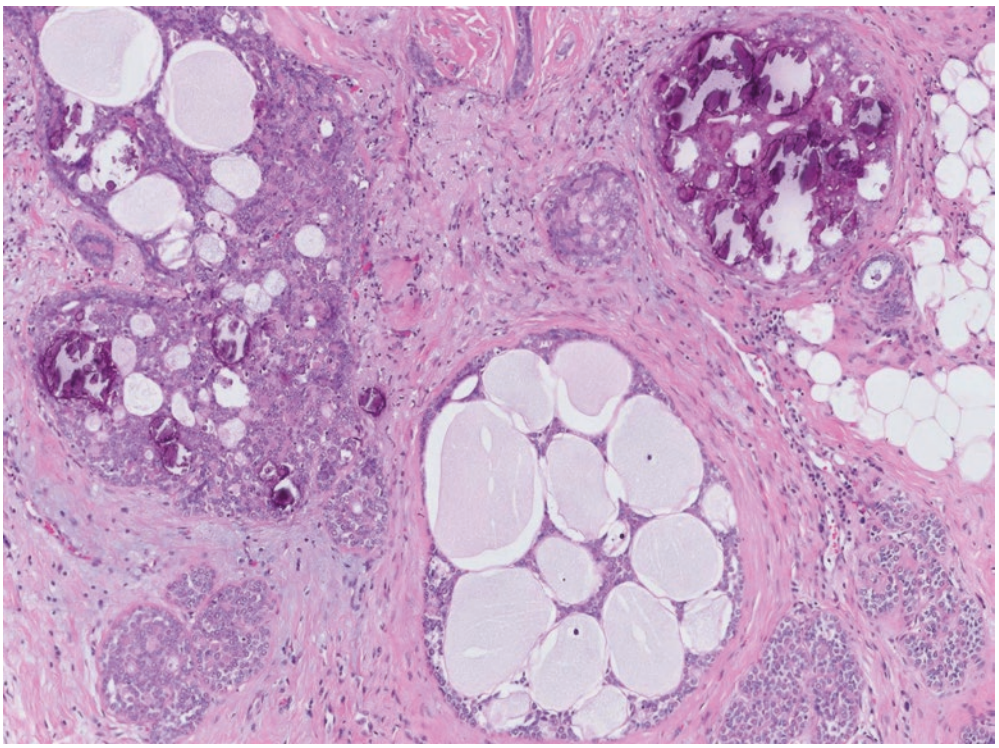

Fig. 12.142 Collagenous spherulosis. Several ducts show a cribriform proliferation with pale, thin material within the spaces, accompanied by calcifications. The pale, thin material has a pink, membranous rim. The intervening stroma shows relatively compact collagen, without any myxoid oedema

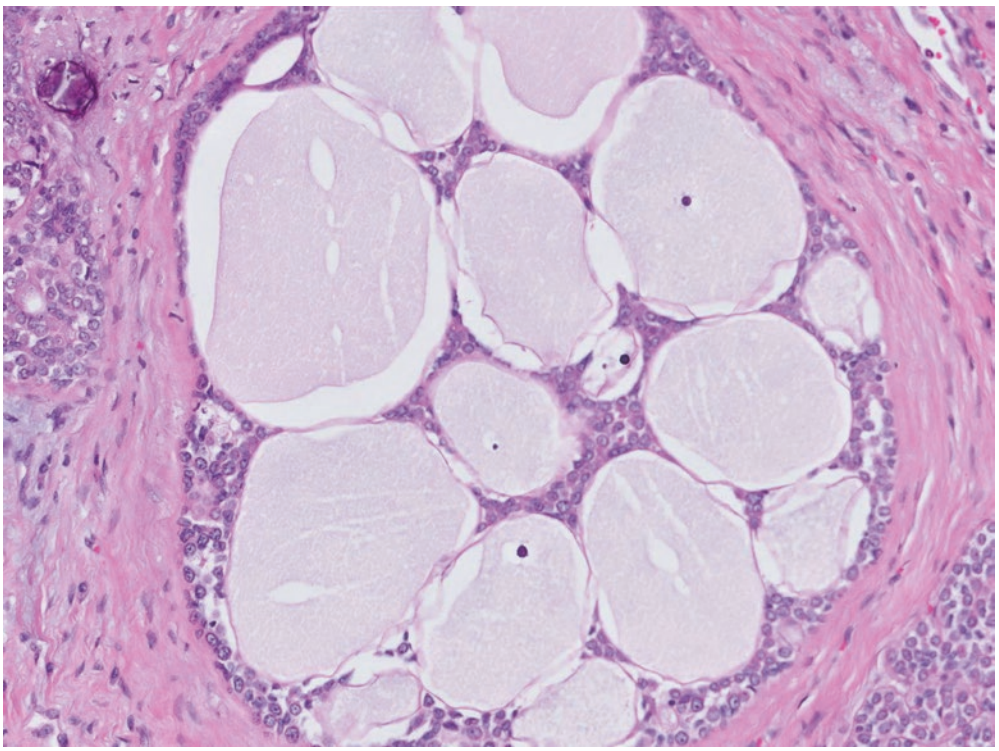

Fig. 12.143 Collagenous spherulosis. Higher magnification shows dilated spaces filled with thin, pale, bluish-grey material and a pink, layered rim

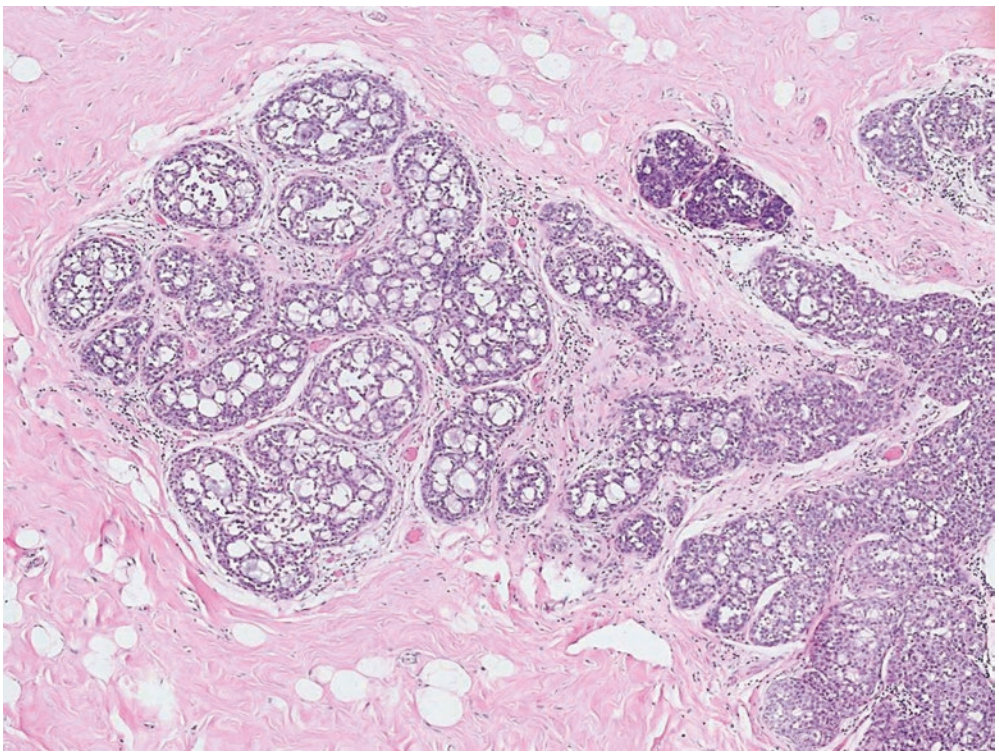

Fig. 12.144 Collagenous spherulosis with lobular neoplasia. When lobular neoplasia colonises ducts with collagenous spherulosis, the resemblance to malignancy is exacerbated. Clues to the correct diagnosis are the presence of adjacent recognisable lobular neoplasia and the usually limited nature of the lesion

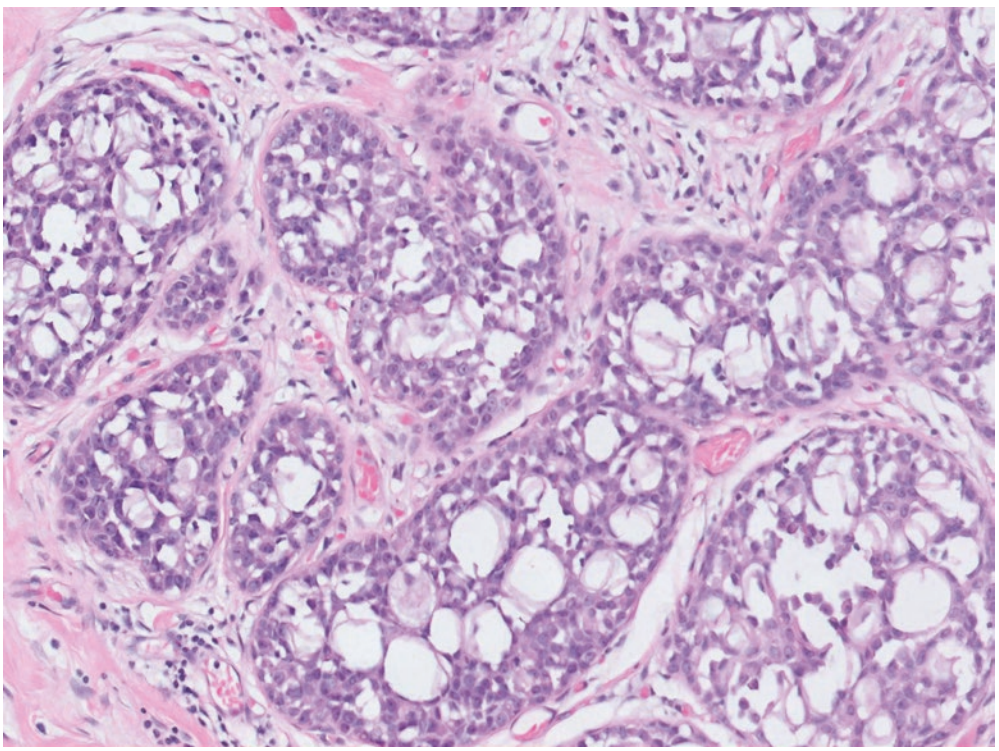

Fig. 12.145 Collagenous spherulosis with lobular neoplasia. At higher magnification, ducts with cribriform spaces show delicate and flimsy, thin, basement membrane strands. Discohesive cells representing lobular neoplastic cells are seen replacing the epithelial cell population

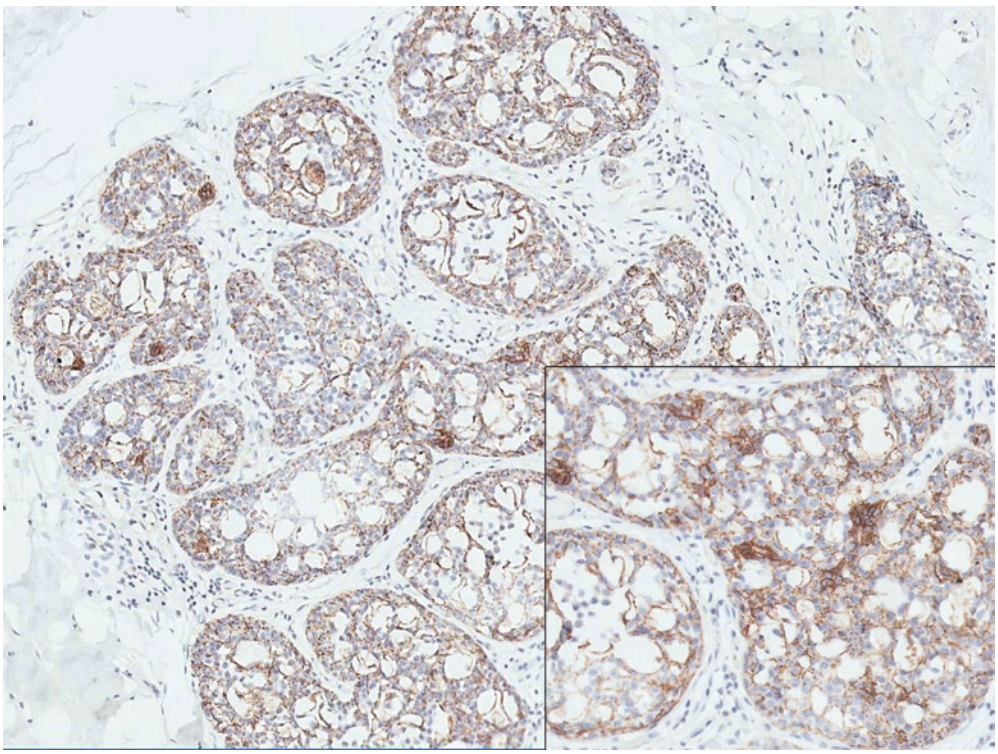

Fig. 12.146 Collagenous spherulosis with lobular neoplasia. E-cadherin immunohistochemistry shows loss of staining in the lobular neoplastic cells; staining is retained in the residual luminal and myoepithelial cells. *Inset* shows the negatively staining lobular neoplastic cells at higher magnification, with small collections of positively reacting epithelial and myoepithelial cells

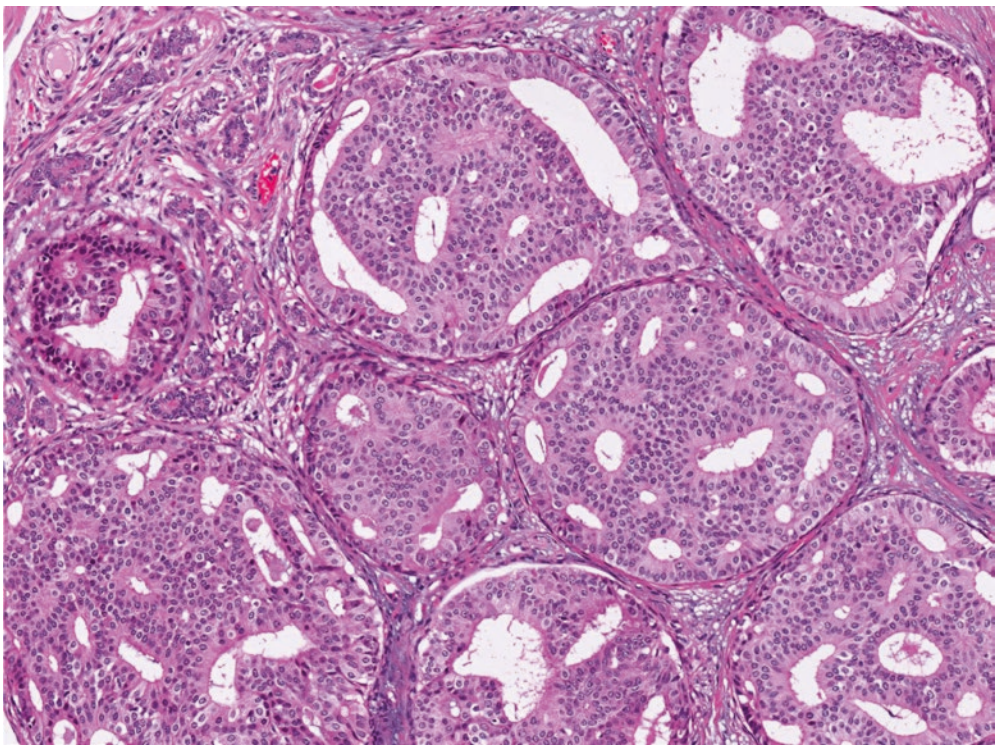

Fig. 12.147 Cribriform DCIS. Expanded ducts with rounded contours show a monotonous epithelial population forming well-defined luminal spaces. The epithelial cells show orientation or polarisation around the luminal spaces

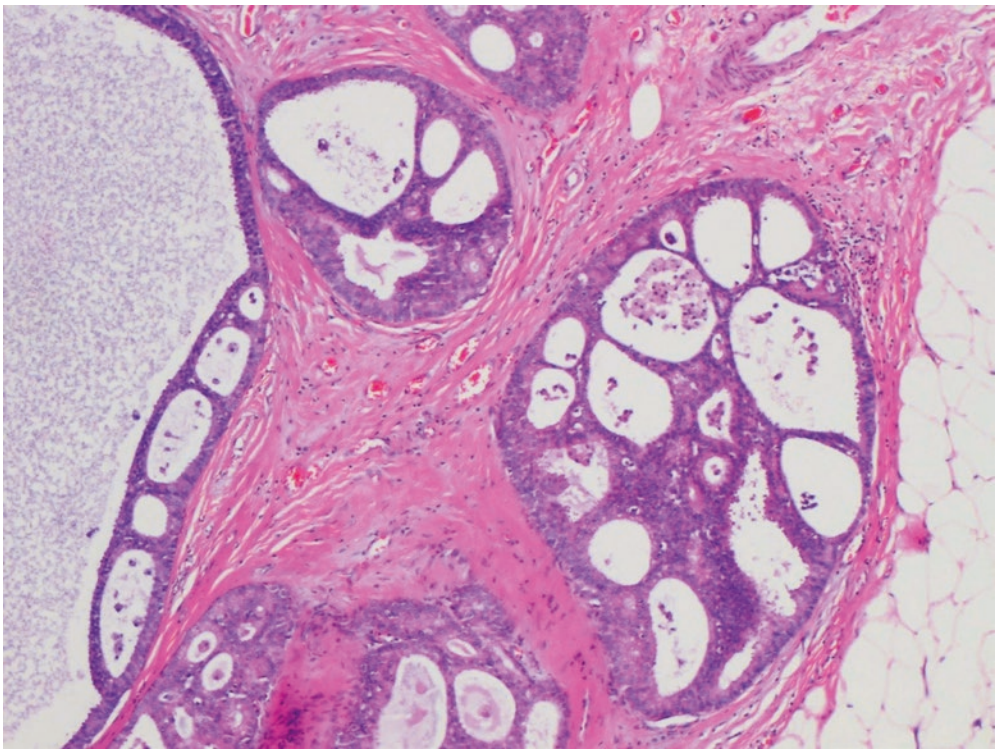

Fig. 12.148 Cribriform DCIS. Expanded ducts show a cribriform architecture with well-defined, punched-out, rounded luminal spaces. Stromal collagen is compact. The cribriform pattern is one of several architectures of DCIS. It has no predictive significance on its own

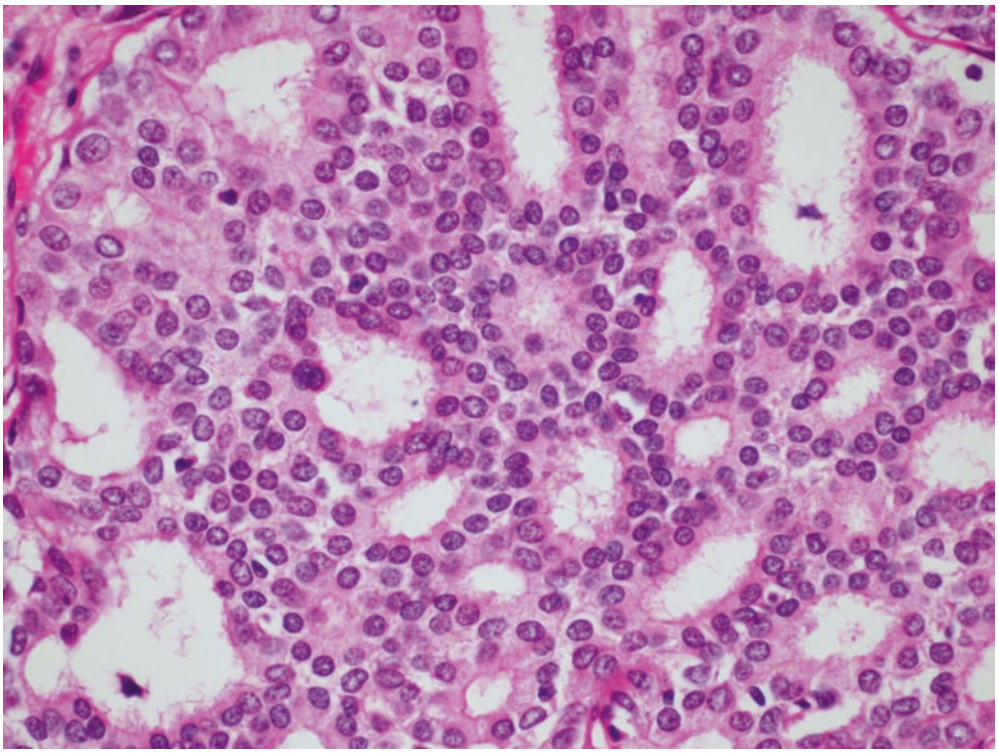

Fig. 12.149 Cribriform DCIS. High magnification shows luminal spaces formed by neoplastic epithelial cells with the apical borders facing the lumens, also referred to as cell polarisation. Cribriform DCIS is often of low to intermediate nuclear grade, but high-grade varieties are also observed. Calcifications are sometimes seen in the luminal spaces, where secretions form the nidus for the psammomatous calcified deposits

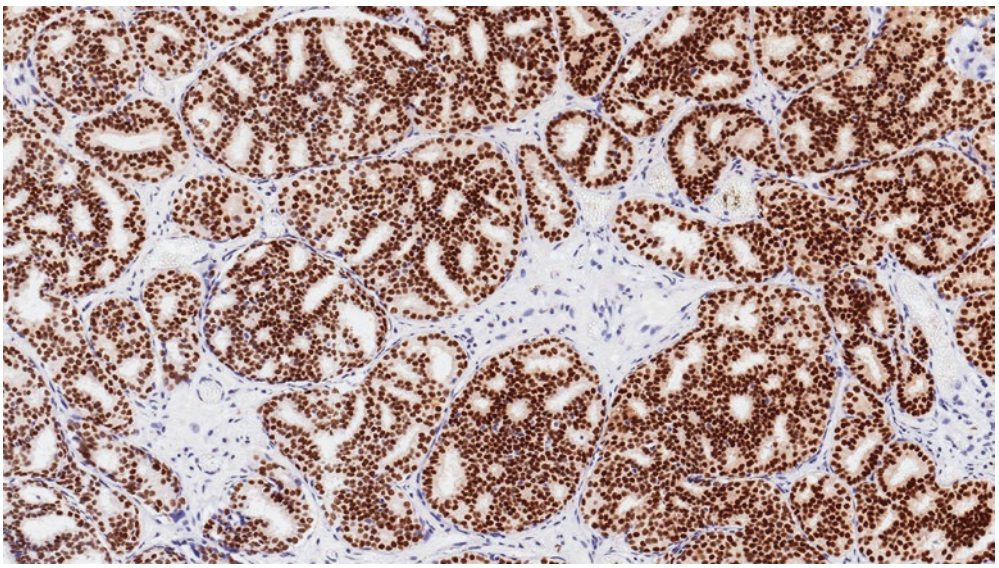

Fig. 12.150 Cribriform DCIS shows diffuse and intense nuclear reactivity for oestrogen receptor on immunohistochemistry

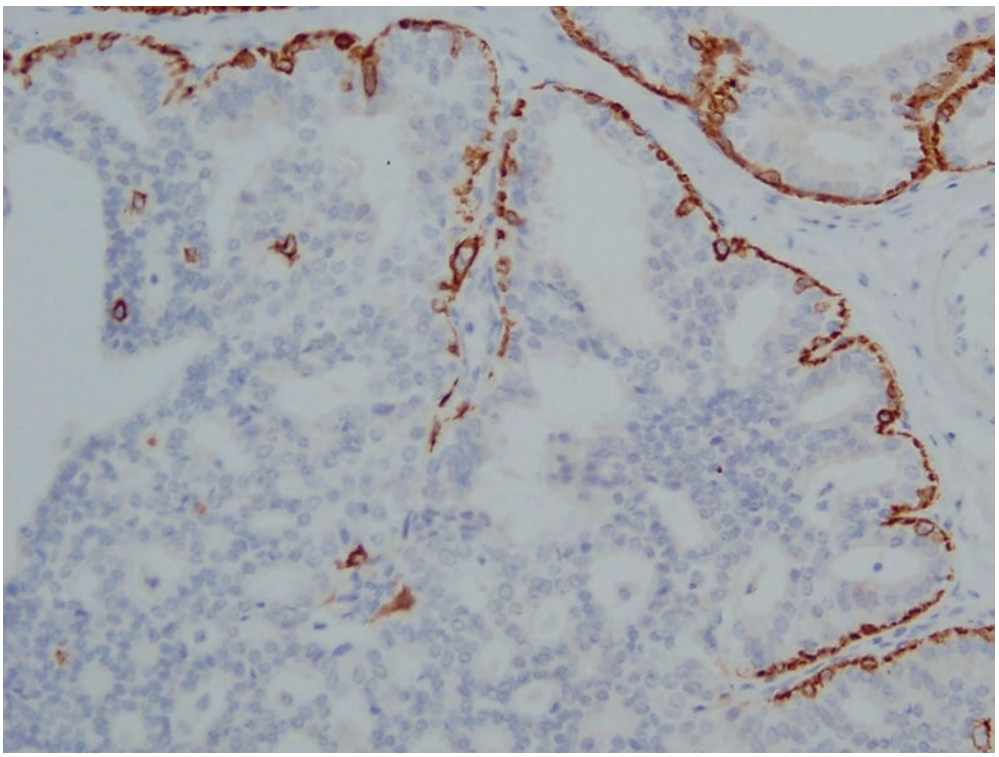

Fig. 12.151 Cribriform DCIS shows preserved myoepithelial cells with immunohistochemical staining for CK14. The neoplastic epithelial cells are negative, reflecting their clonal luminal nature - luminal epithelial cells are negative for high molecular weight keratins such as CK14

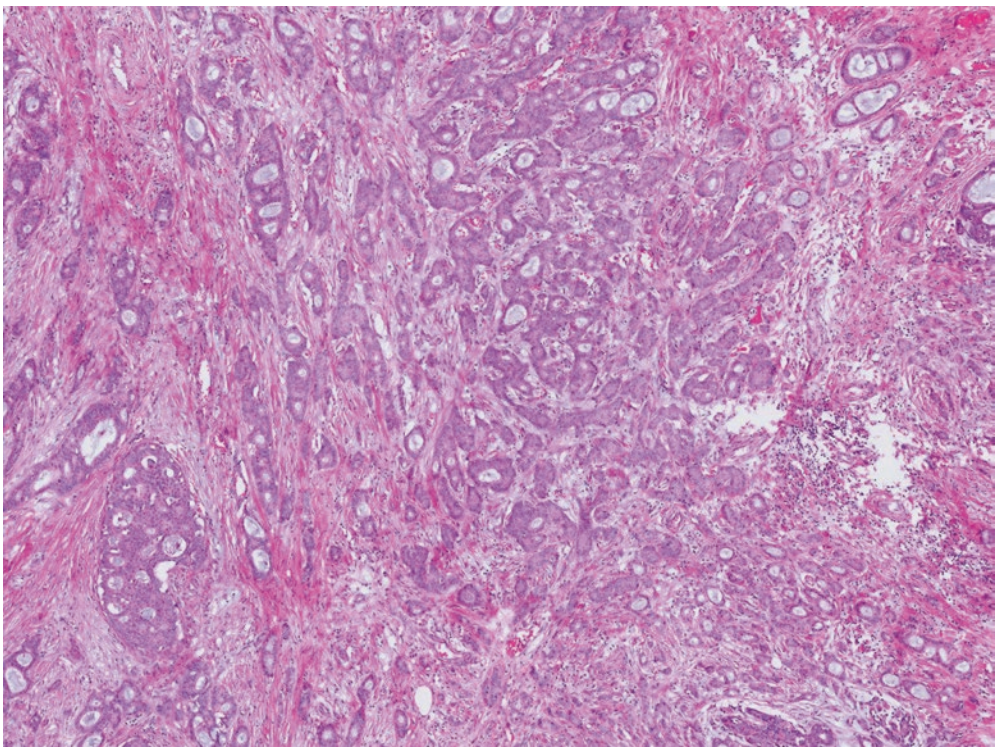

Fig. 12.152 Invasive cribriform carcinoma. In contrast to cribriform DCIS, with its rounded contours of lesional ducts, invasive cribriform carcinoma shows anastomosed cribriform islands with irregular outlines and angulated, tonguelike protrusions into a desmoplastic stroma

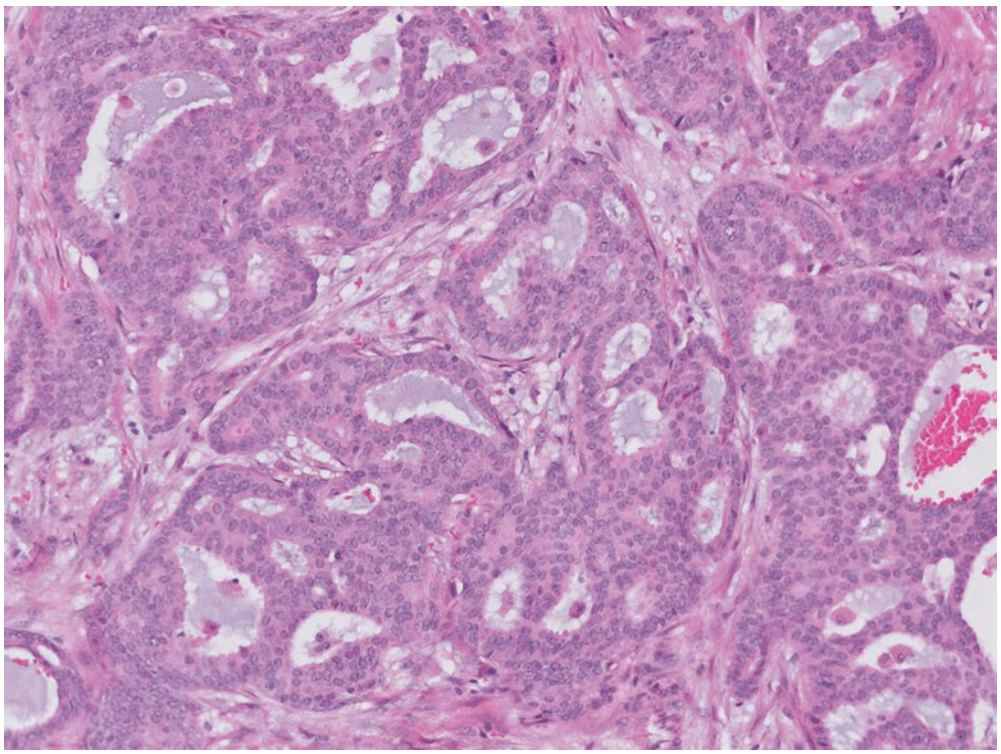

Fig. 12.153 Invasive cribriform carcinoma. Higher magnification shows irregular and confluent cribriform islands invading a loose, desmoplastic stroma

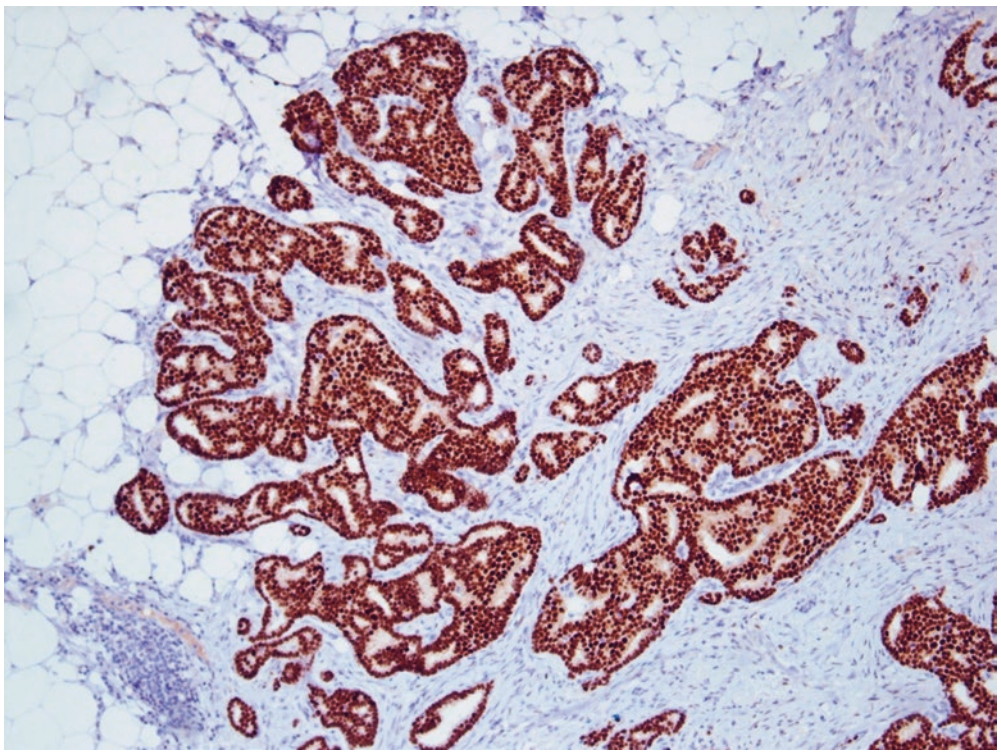

Fig. 12.154 Invasive cribriform carcinoma shows diffuse and intense nuclear reactivity for oestrogen receptor

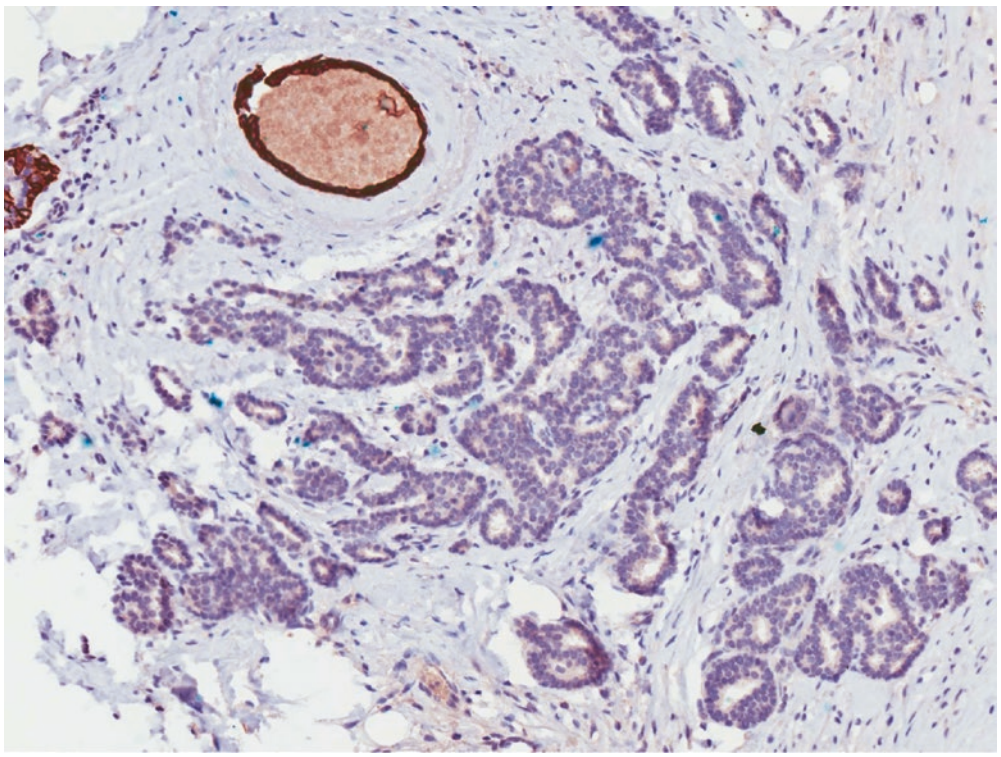

Fig. 12.155 Invasive cribriform carcinoma. CK14 immunohistochemical staining shows an absence of myoepithelial cells around the invasive cribriform islands

Small Cell Carcinoma

The solid variant of adenoid cystic carcinoma with basaloid features may resemble small cell carcinoma. Small cell carcinoma shows nuclear moulding and scant cytoplasm with high nuclear–cytoplasmic ratios, as well as frequent mitoses and karyorrhexis (Fig. 12.156). Immunohistochemically, neuroendocrine differentiation can be demonstrated in small cell carcinoma.

Invasive Carcinoma with Basaloid Features

Invasive carcinoma with basaloid features can resemble the solid variant of adenoid cystic carcinoma, especially when tumour cells show hyperchromatic nuclei with high nuclear–cytoplasmic ratios and produce mucopolysaccharides, as in some forms of matrix-producing carcinomas that are also triple-negative (Figs. 12.157 and 12.158).

Prognosis and Therapy Considerations

Adenoid cystic carcinoma generally has an excellent prognosis. It has been suggested that this tumour can be treated with wide excision alone, but many institutions manage adenoid cystic carcinomas as conventional breast cancers, with adjuvant radiation after excision. The solid variant with basaloid features may be more aggressive in behaviour, with a greater propensity for axillary nodal metastasis [74]. Survival rates are 95 % at 5 years and 90 % at 10 years.

Invasive Carcinomas with Neuroendocrine Differentiation

Definition

These are invasive breast cancers with neuroendocrine differentiation as evidenced by positive reactivity with neuroendocrine markers such as synaptophysin and chromogranin. The WHO classification of breast tumours categorises cancers with neuroendocrine differentiation into three groups: neuroendocrine tumour, well differentiated (carcinoid-like); neuroendocrine carcinoma, poorly differentiated or small cell carcinoma; and invasive carcinoma with neuroendocrine differentiation [75].

Clinical and Epidemiological Features

Patients present with nipple discharge, breast lump, or both. As neuroendocrine expression in breast cancers is not routinely investigated, the incidence is difficult to estimate; various studies have reported that 4–30 % of breast cancers harbour neuroendocrine features. Special types of breast cancers with frequent neuroendocrine expression are the hypercellular (Capella type B) variant of mucinous carcinoma and solid papillary carcinoma (invasive); these are classified under their specific subtypes rather than as invasive carcinoma with neuroendocrine differentiation. (*See* Chaps. 4 and 6).

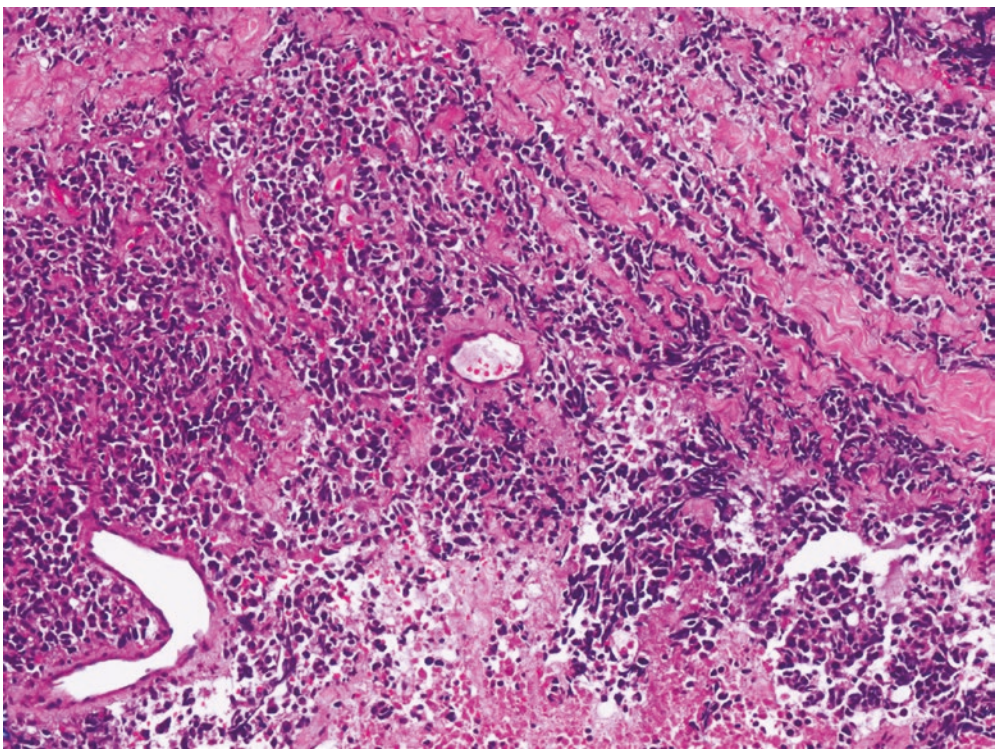

Fig. 12.156 Small cell carcinoma is composed of sheets and cords of tumour cells with hyperchromatic nuclei and scant cytoplasm. Nuclear streaking and necrosis are present. Unlike the basaloid solid variant of adenoid cystic carcinoma, small cell carcinoma invades in sheets with hyperchromatic nuclei that are mitotically active and have discernible nuclear moulding. Necrosis and karyorrhexis are present. On immunohistochemistry, there is often demonstrable neuroendocrine differentiation

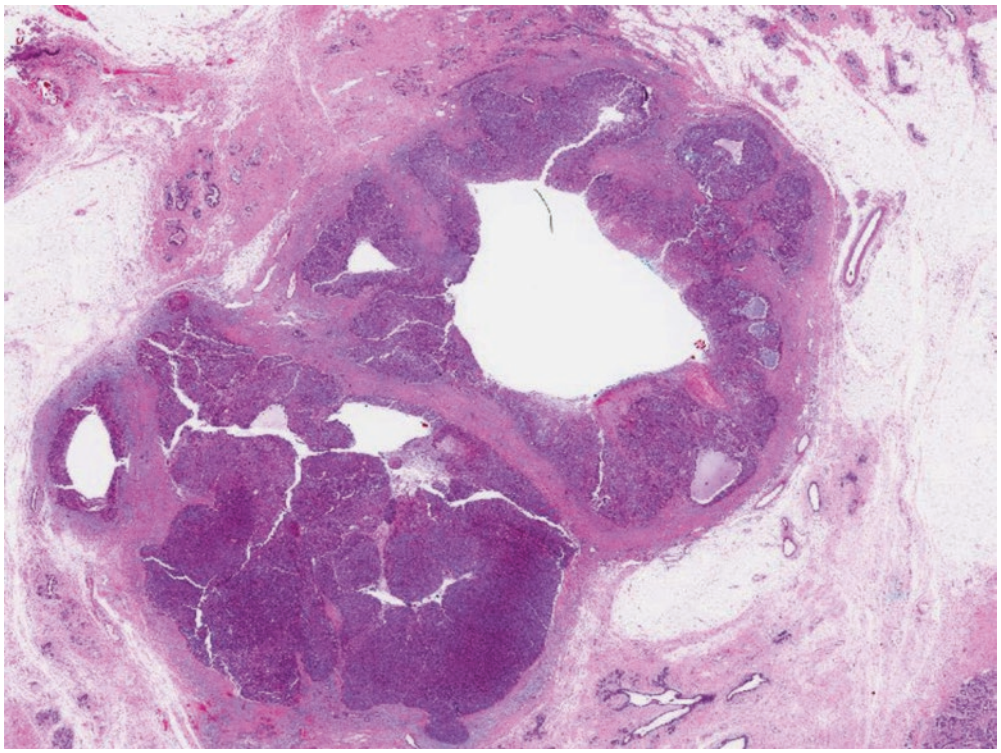

Fig. 12.157 Invasive carcinoma with basaloid features. This lesion can resemble the solid variant of adenoid cystic carcinoma

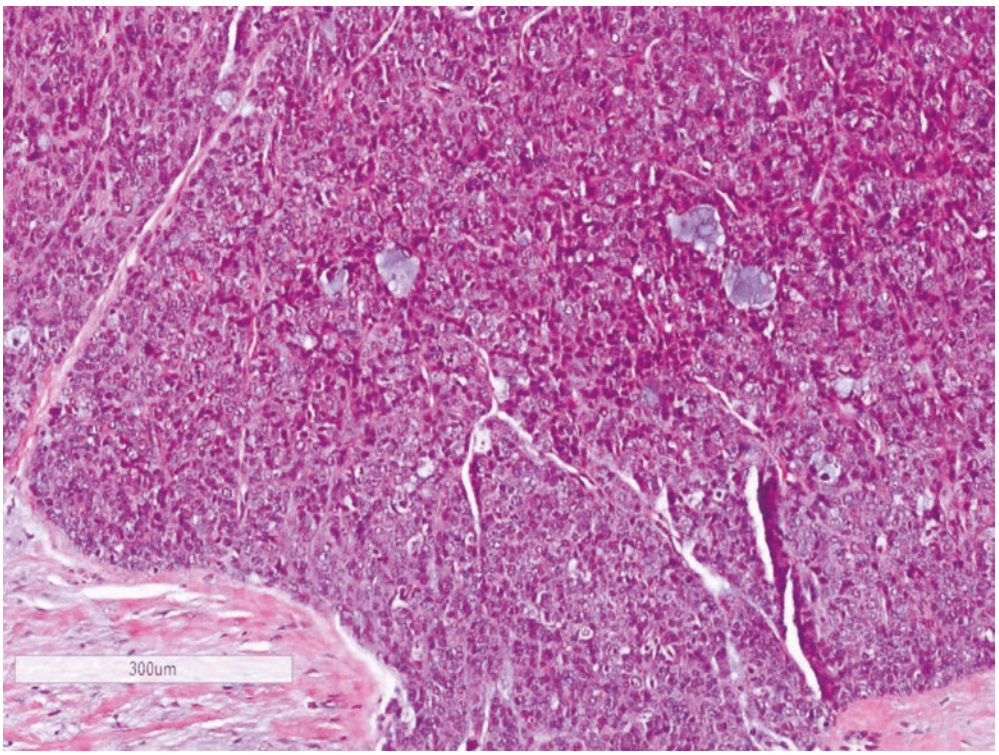

Fig. 12.158 Invasive carcinoma with basaloid features. Some basophilic mucopolysaccharide is seen among the basaloid tumour cells, further mimicking adenoid cystic carcinoma

Imaging Features

These tumours have no unique imaging findings; they generally present as radiologically suspicious masses (Fig. 12.159). Mucinous cancers with neuroendocrine expression have circumscribed, rounded contours and may resemble a benign mass.

Pathologic Features

Macroscopic Pathology

Tumours show greyish-white cut surfaces, with generally infiltrative edges. Some, however, such as mucinous cancers with neuroendocrine differentiation, may appear circumscribed and gelatinous or firm and lobulated.

Microscopic Pathology

Neuroendocrine Tumour, Well Differentiated (Carcinoid-Like)

These invasive carcinomas tend to be of low nuclear grade but sometimes have intermediate nuclear grade features (Fig. 12.160). They resemble the carcinoid tumour occurring in the gastrointestinal tract and lung. Histologically, tumour cells may assume spindle and plasmacytoid appearances, with occasional clear cells.

Neuroendocrine Carcinoma, Poorly Differentiated/ Small Cell Carcinoma

Small cell carcinomas in the breast are morphologically identical to similar tumours of the lung. Tumour cells show high nuclear–cytoplasmic ratios, smoky dense chromatin, nuclear moulding, and brisk mitotic rates. There are areas of necrosis and frequent lymphovascular emboli (Figs. 12.161, 12.162, 12.163, and 12.164). A diagnosis of small cell carcinoma in the breast makes it advisable to exclude a possible metastatic lesion. An in situ component and concurrent invasive carcinoma of ductal or lobular subtype favour a primary breast origin. TTF1 positivity cannot be used to verify a lung origin because this marker is also expressed by many extrapulmonary small cell carcinomas. Large cell neuroendocrine carcinoma, poorly differentiated, can also be encountered, which is usually classified as poorly differentiated invasive breast carcinoma with neuroendocrine differentiation.

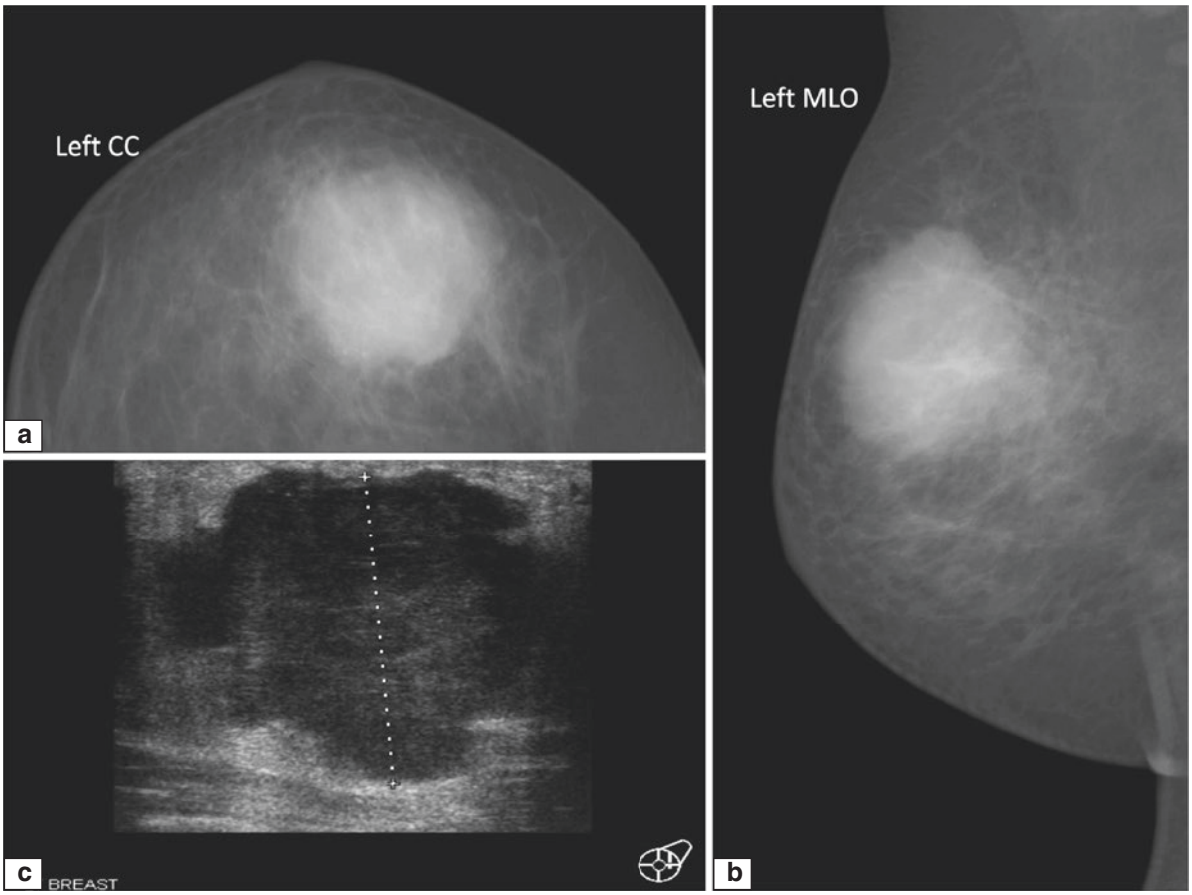

Fig. 12.159 Radiology of small cell carcinoma (poorly differentiated neuroendocrine carcinoma). (**a**, **b**) Mammograms show a large, opaque mass in the left breast, with ultrasound confirming a malignant-appearing, hypoechoic mass with irregular borders (**c**)

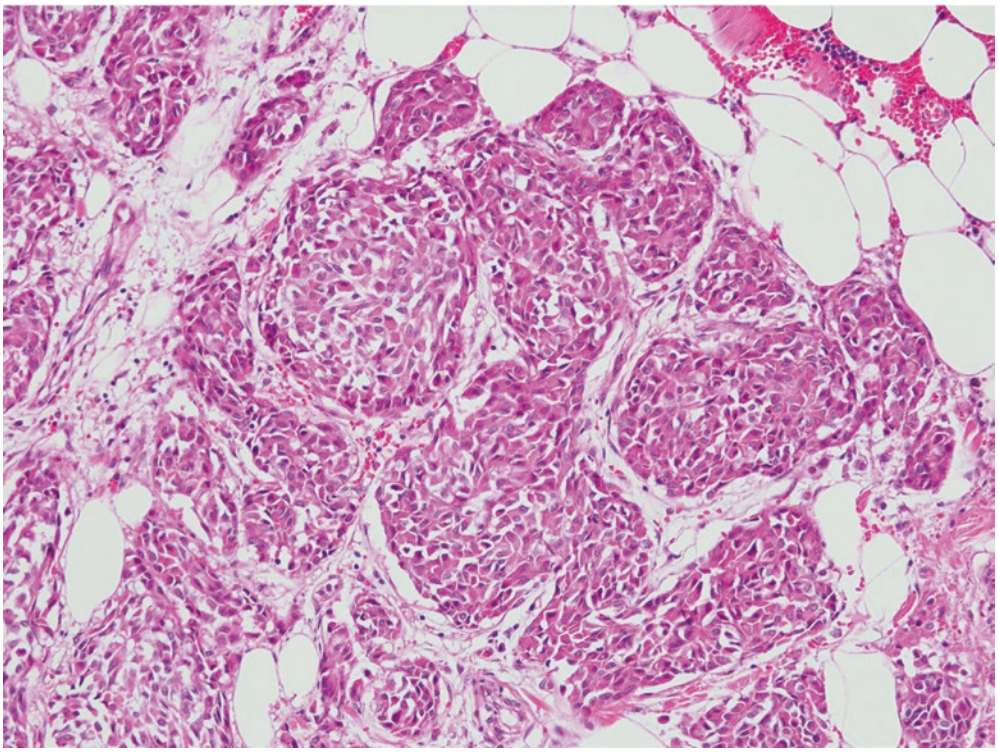

Fig. 12.160 Neuroendocrine tumour, well differentiated (carcinoid-like). This invasive breast carcinoma is composed of rounded nests of tumour cells with spindle and plasmacytoid shapes. The nuclei show mild to focally moderate atypia without obvious mitotic activity. The cytoplasm is eosinophilic

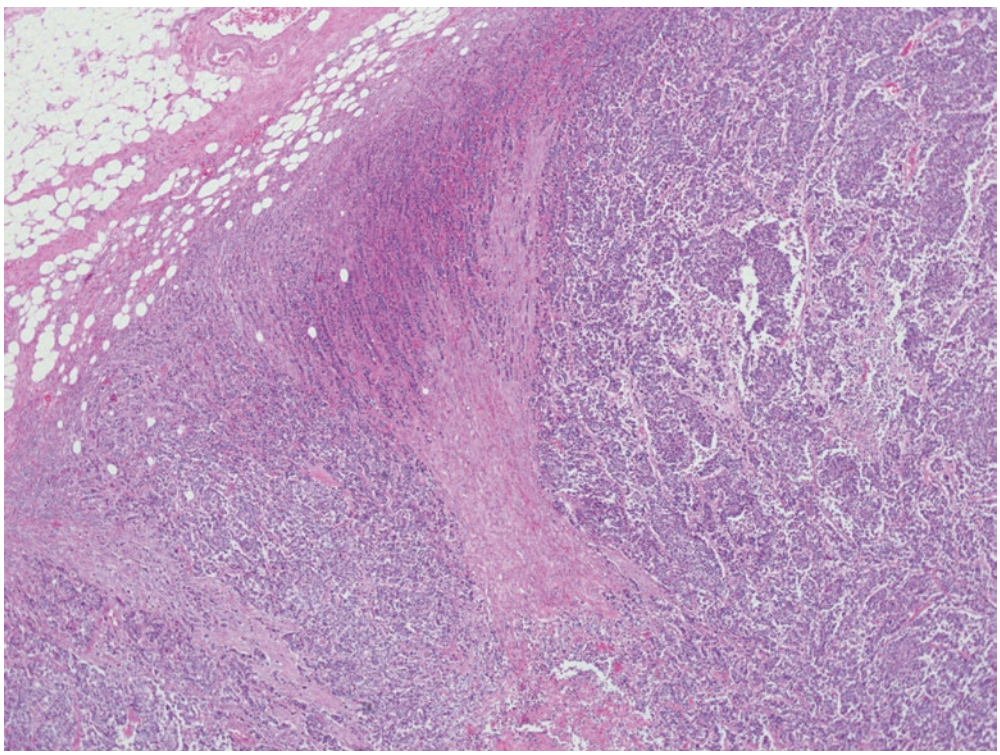

Fig. 12.161 Small cell carcinoma. Solid, irregular nests and narrow trabeculae of tumour cells are seen within a fibrotic stroma

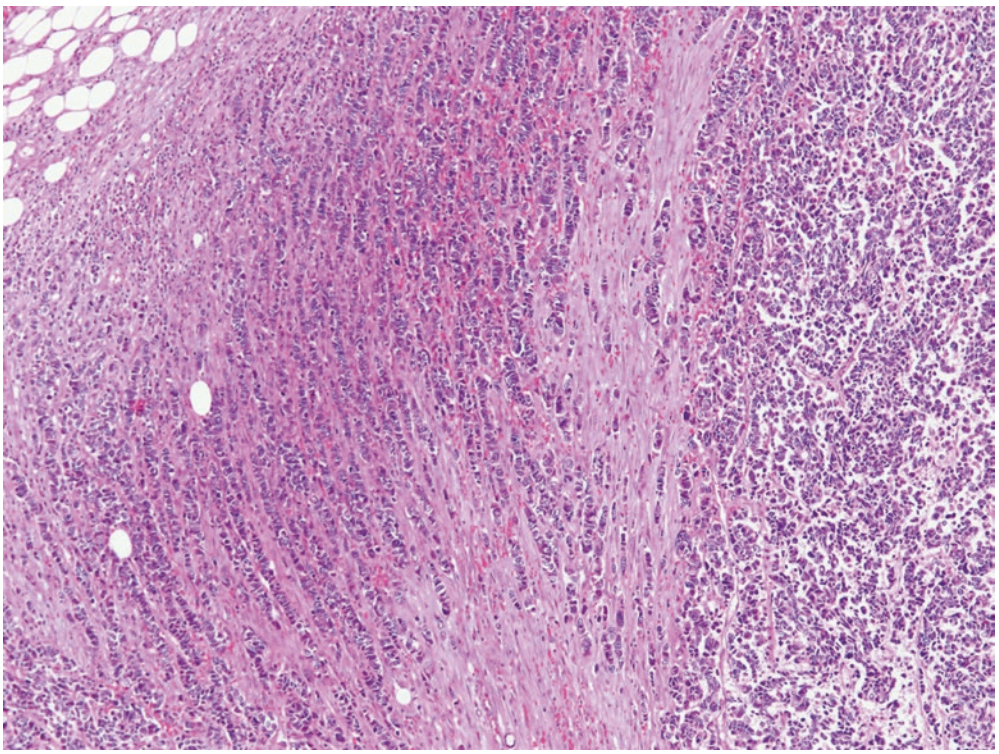

Fig. 12.162 Small cell carcinoma. Linear cords of tumour cells with hyperchromatic nuclei and scant cytoplasm are seen

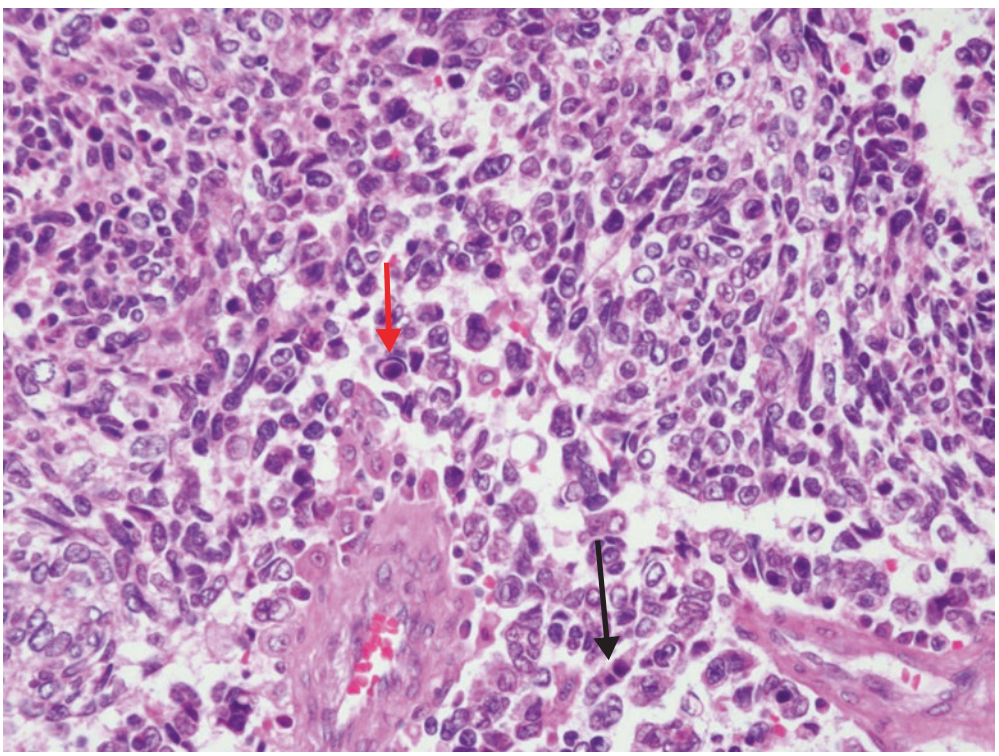

Fig. 12.163 Small cell carcinoma. High magnification shows malignant cells with ovoid or more elongated nuclei and high nuclear–cytoplasmic ratios. Apoptotic nuclei and scattered mitoses are present. A semblance of nuclear moulding (*black arrow*) and cellular cannibalism (*red arrow*) are present

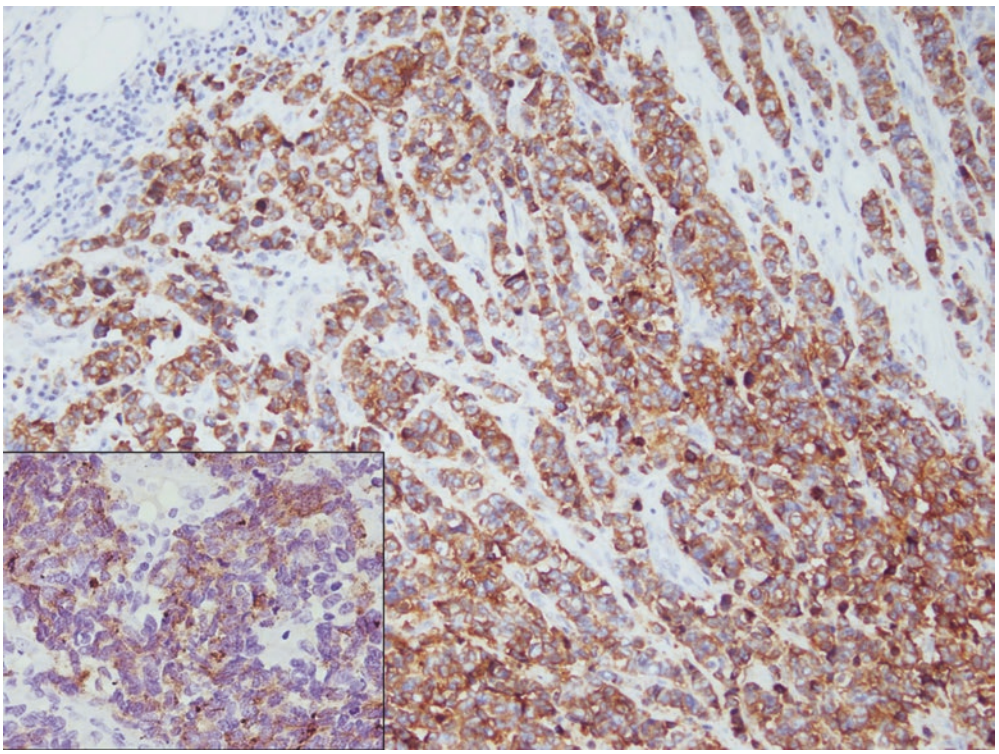

Fig. 12.164 Small cell carcinoma. Immunohistochemistry for synaptophysin shows positive cytoplasmic reactivity indicating neuroendocrine differentiation. *Inset* shows chromogranin expression by tumour cells

Invasive Breast Carcinoma with Neuroendocrine Differentiation

These are invasive carcinomas with special or no special type on histomorphology that are accompanied by neuroendocrine differentiation (Figs. 12.165, 12.166, and 12.167). Variants of mucinous carcinoma and the invasive form of solid papillary carcinoma contribute to a significant proportion of such tumours. Up to 30% of unselected invasive breast cancers may exhibit neuroendocrine marker expression, depending on defining criteria. They are usually positive for oestrogen receptors and negative for c-erbB-2. It is recommended that these should be classified according to the recognisable histological subtype, with a statement mentioning the presence of neuroendocrine expression [76]. Until more conclusive data become available, it appears that there is currently no specific prognostic value in determining neuroendocrine differentiation in conventional invasive breast carcinomas, other than recognising its frequent occurrence in certain special subtypes, whereby its presence may be of diagnostic utility, such as in solid papillary carcinoma.

Differential Diagnosis

Metastatic Well-Differentiated Neuroendocrine Tumour (Carcinoid) and Metastatic Small Cell Carcinoma

Metastatic well-differentiated neuroendocrine tumour (carcinoid) and metastatic small cell carcinoma need to be primarily excluded. An in situ component and concurrent invasive carcinoma of ductal or lobular subtypes favour a primary breast origin. TTF1 positivity cannot be used to verify a metastatic lung origin because this marker is also expressed by extrapulmonary small cell carcinomas. Positive immunohistochemical reactivity for hormone receptors, CK7, GATA3, gross cystic disease fluid protein 15 (GCDFP15), and mammaglobin support a primary breast origin.

Invasive Lobular Carcinoma

Invasive lobular carcinoma, solid variant, may resemble the well-differentiated neuroendocrine tumour (carcinoid) because of the uniform appearance of tumour cells (Fig. 12.168). Immunohistochemistry with E-cadherin (negative/aberrant in invasive lobular carcinoma) and neuroendocrine markers (positive in carcinoid) are discriminatory.

Malignant Lymphoma

Small cell carcinoma of the breast needs to be distinguished from lymphoma. Tumour cells of lymphoma show nuclear irregularity with clumped chromatin, whereas small cell carcinoma tends to have homogeneously dense nuclear hyperchromasia with moulding (Figs. 12.169 and 12.170). Plasmacytoid rims may be observed in malignant lymphoid cells. The proliferative fraction of small cell carcinoma is high; the fraction for small lymphocytic lymphoma is more quiescent.

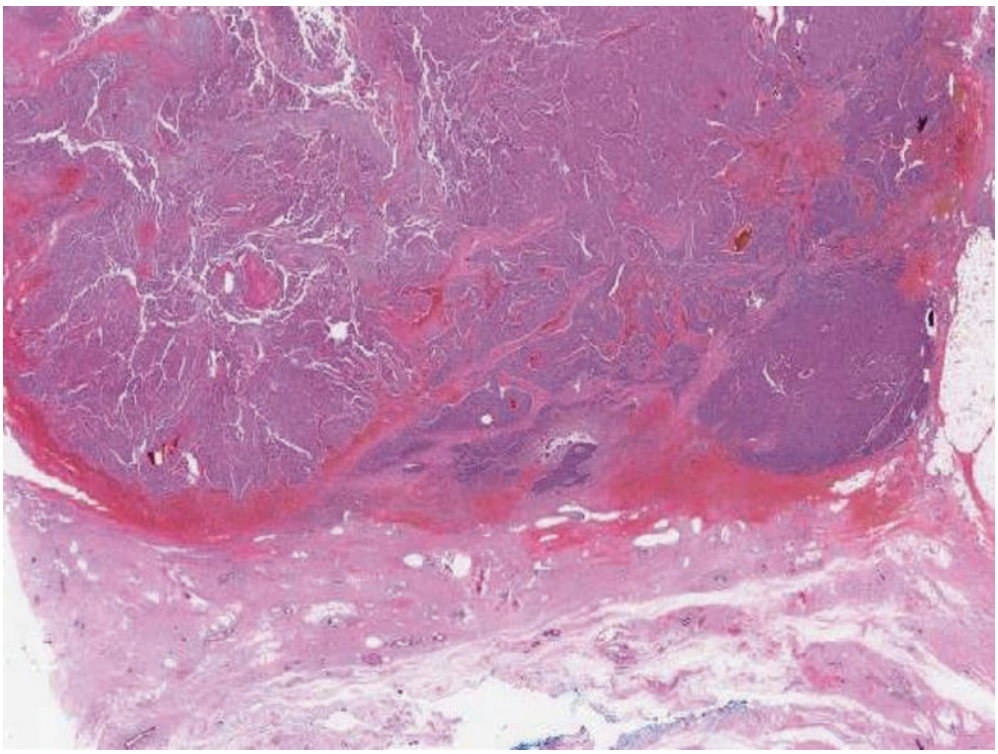

Fig. 12.165 Infiltrative ductal carcinoma with neuroendocrine differentiation. Low magnification shows large sheets of tumour with a pushing border and areas of haemorrhage

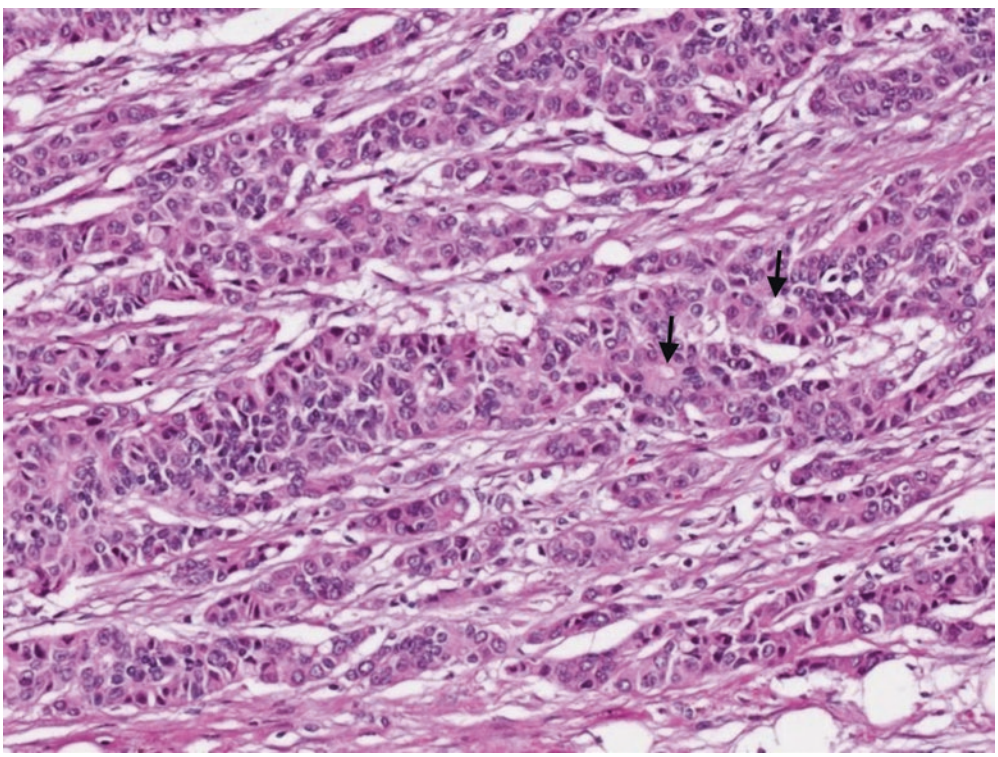

Fig. 12.166 Infiltrative ductal carcinoma with neuroendocrine differentiation. Anastomosing trabeculae of carcinoma cells show focal lumen formation (*arrows*)

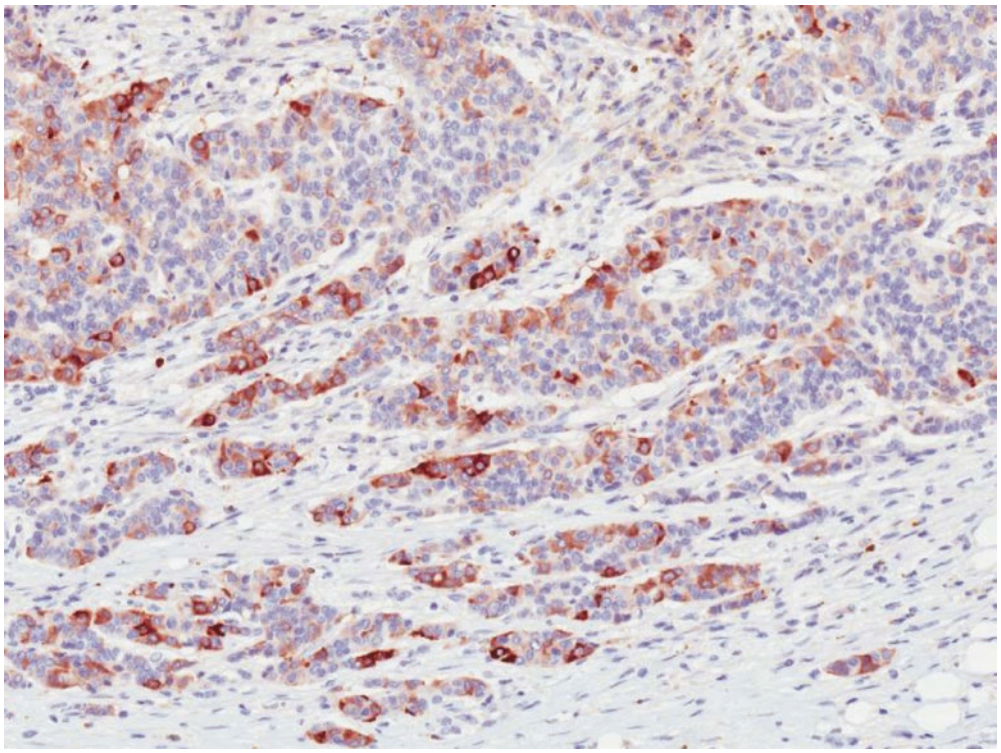

Fig. 12.167 Infiltrative ductal carcinoma with neuroendocrine differentiation. Immunohistochemistry shows synaptophysin positivity in the tumour cells

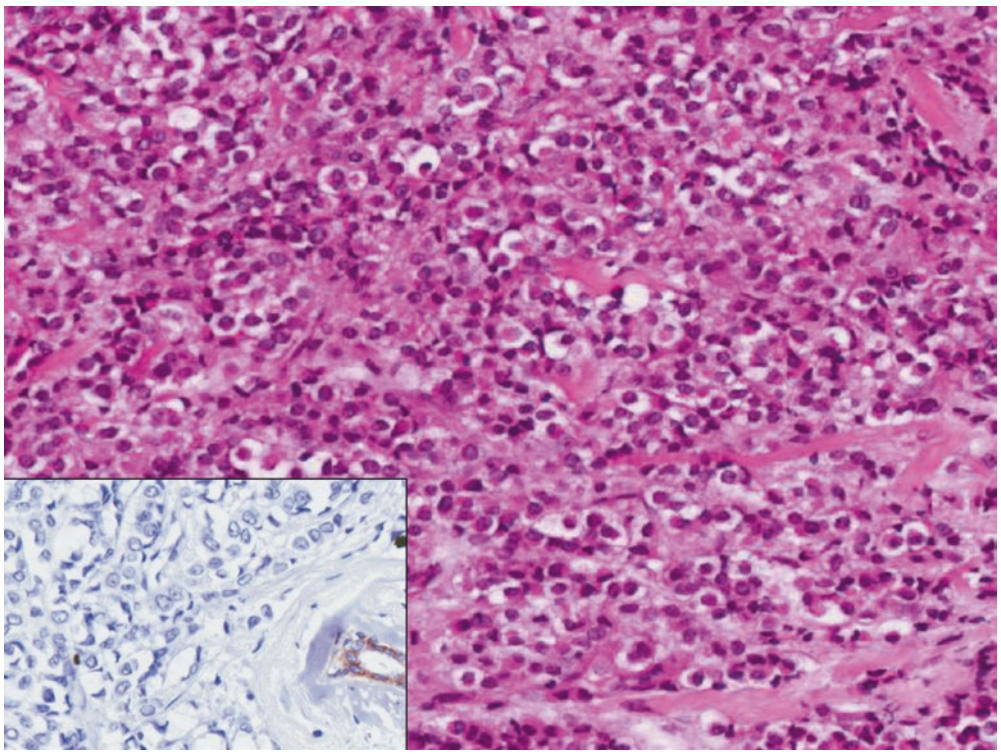

Fig. 12.168 Invasive lobular carcinoma, solid variant, may resemble a well-differentiated neuroendocrine tumour with the uniform cells arranged in an organoid fashion. The presence of more conventional patterns of invasive lobular carcinoma, together with the absence of E-cadherin immunostaining, is useful in making the correct diagnosis. *Inset* shows E-cadherin immunohistochemistry, which is negative in the tumour cells; an internal positive control of a benign duct is seen in comparison

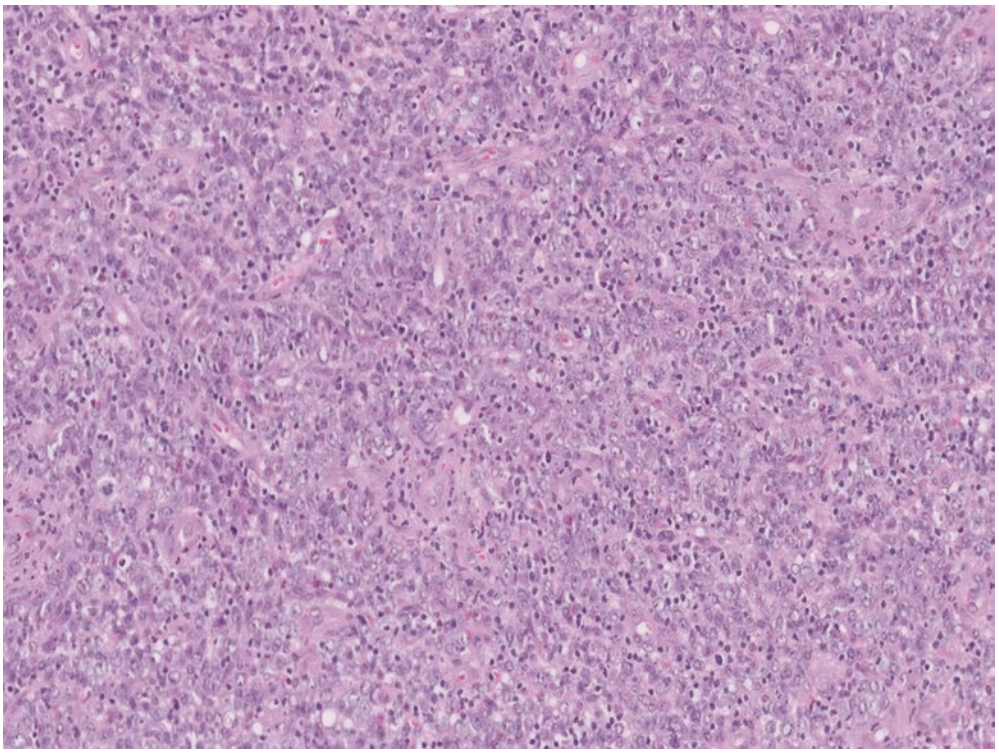

Fig. 12.169 Malignant lymphoma. This diffuse large B-cell lymphoma shows patternless sheets of abnormal lymphoid cells, which may resemble poorly differentiated neuroendocrine carcinoma. Scattered lymphocytes with dense, dark nuclei are seen among the malignant lymphoid cells

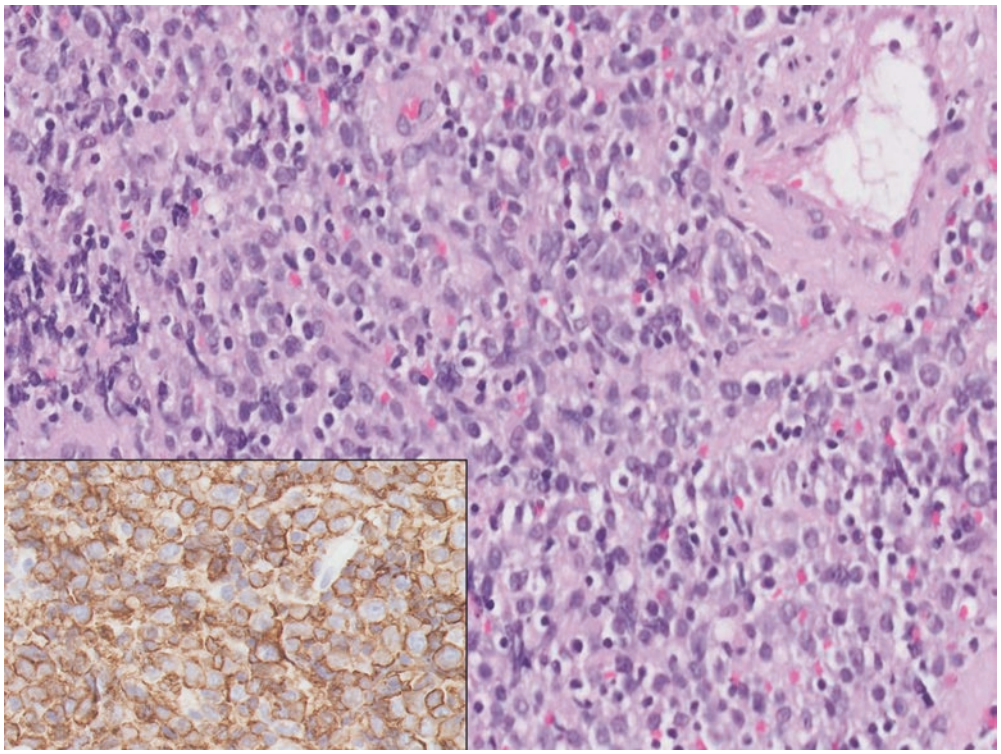

Fig. 12.170 Malignant lymphoma. High magnification shows the abnormal lymphoid cells with vesicular nuclei, distinct nucleoli, and irregular nuclear contours. *Inset* shows positive staining of the lymphoid cells for CD20, a B-cell marker indicating a B-cell immunophenotype of the diffuse large cell lymphoma

Exceptionally Rare Types and Variants

Definition

These rarely encountered histological subtypes of invasive breast carcinoma include secretory carcinoma, acinic carcinoma, and even rarer subtypes such as mucoepidermoid, oncocytic, polymorphous, lipid-rich, glycogen-rich, and sebaceous carcinoma [75]. These tumours are graded using conventional parameters of the degree of nuclear pleomorphism, tubule formation, and mitotic activity.

Secretory Carcinoma

Definition

Secretory carcinoma is a rare, low-grade, translocation-associated invasive carcinoma that shows solid, microcystic, and tubular architectures. A synonym is *juvenile breast carcinoma*.

Clinical and Epidemiological Features

Secretory carcinoma accounts for less than 0.15 % of all breast cancers, affecting both males and females. The median age of presentation is 25 years (range, 3–87 years). Clinically, these tumours are well circumscribed and may be mobile. They are often located near the areola, especially in men and children.

Imaging Features

Radiological findings are of a malignant breast mass.

Pathologic Features

Macroscopic Pathology

Secretory carcinoma shows a grey-white to yellow-tan colour on cut sections (Fig. 12.171). Tumour size averages 3 cm, with a range from 0.5 to 12 cm.

Microscopic Pathology

A combination of patterns is observed in most tumours, composed primarily of microcystic, solid, and tubular appearances (Figs. 12.172, 12.173, 12.174, 12.175, 12.176, 12.177, 12.178, 12.179, and 12.180). In the microcystic pattern, small cysts mimicking thyroid follicles can merge into solid islands. Neoplastic tubules contain luminal secretions. A characteristic feature is the production of intracellular and extracellular secretory material. The tumour may demonstrate pushing borders, though frankly invasive foci are frequent. Sclerotic tissue can be seen in the centre of the lesion. Tumour cells are polygonal with granular eosinophilic to foamy cytoplasm; nuclei are generally regular and contain inconspicuous nucleoli. Mitotic activity is minimal. Intracellular and extracellular secretory material stains positively with periodic acid–Schiff (PAS) or Alcian blue. In situ carcinoma, when present, displays similar secretory features, occasionally with necrosis, or it can be of a low-grade type.

On immunohistochemistry, EMA, alpha-lactalbumin, and S100 protein are frequently expressed (Fig. 12.181). Secretory carcinomas are usually triple-negative (ER, PR, c-erbB-2 negative). E-cadherin, keratins 8/18, CD117, and alpha-SMA can be expressed. A diagnostic feature is the characteristic balanced translocation, t(12;15), which creates an *ETV6-NTRK3* gene fusion (Fig. 12.182).

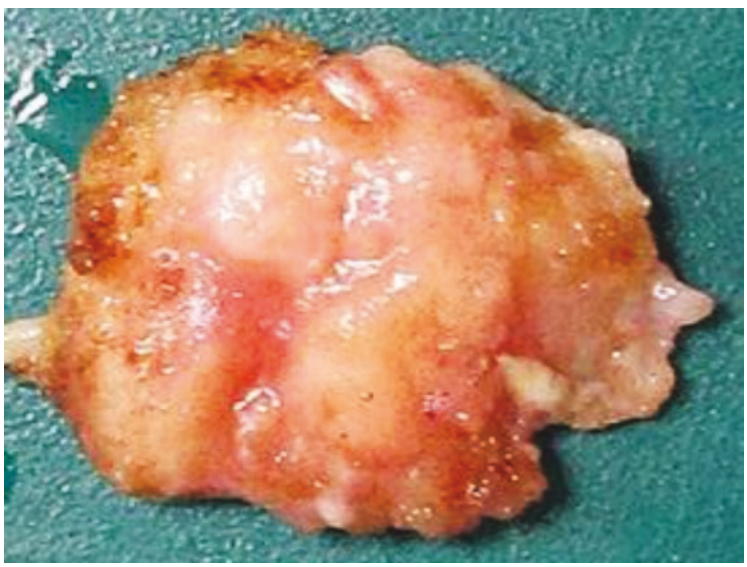

Fig. 12.171 Secretory carcinoma. Macroscopic appearance of an excision biopsy specimen of a secretory carcinoma, showing a slightly lobulated appearance on cut section

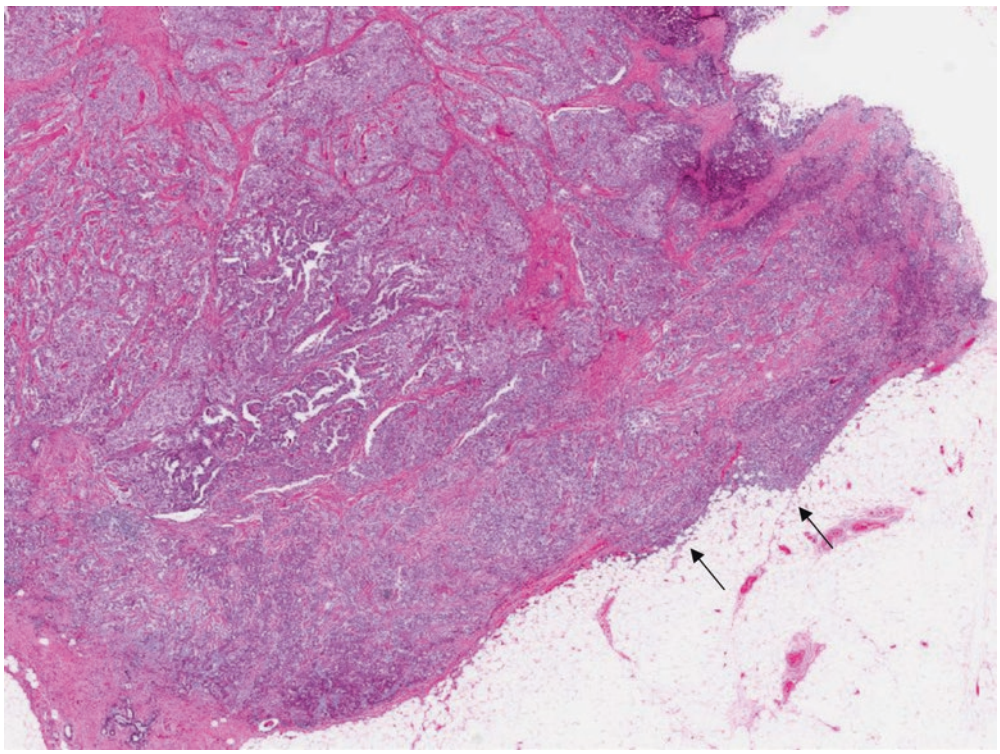

Fig. 12.172 Secretory carcinoma. Low magnification shows a tumour with a partially circumscribed pushing border, with areas where tumour permeates into adjacent adipose (*arrows*)

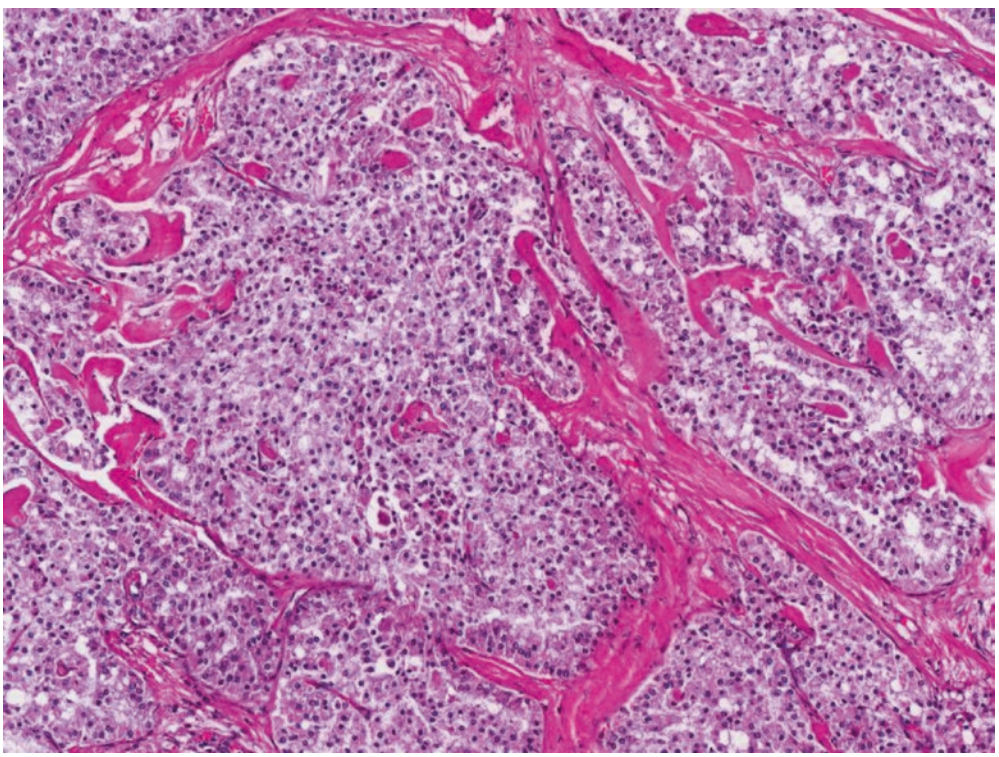

Fig. 12.173 Secretory carcinoma. A predominantly solid pattern is seen with sheets of tumour cells containing pale to pink cytoplasm. There are anastomosed glandular structures (*right upper field*) lined by similar cells with bubbly cytoplasm

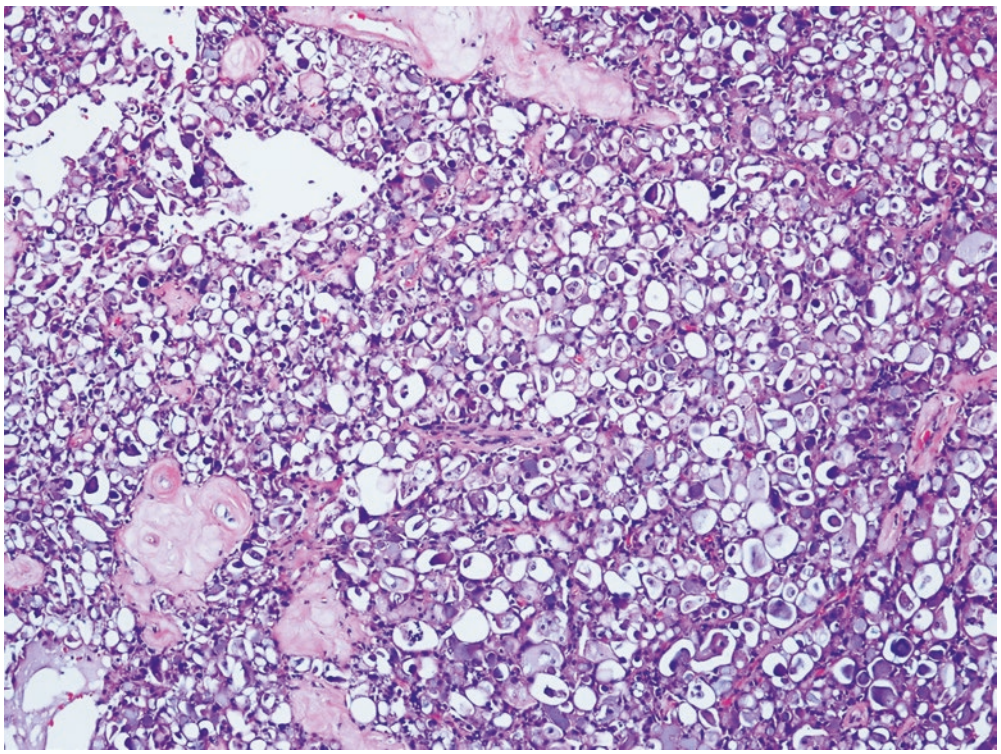

Fig. 12.174 Secretory carcinoma. A microcystic pattern is observed in this tumour, with many small cystic spaces containing pale secretions

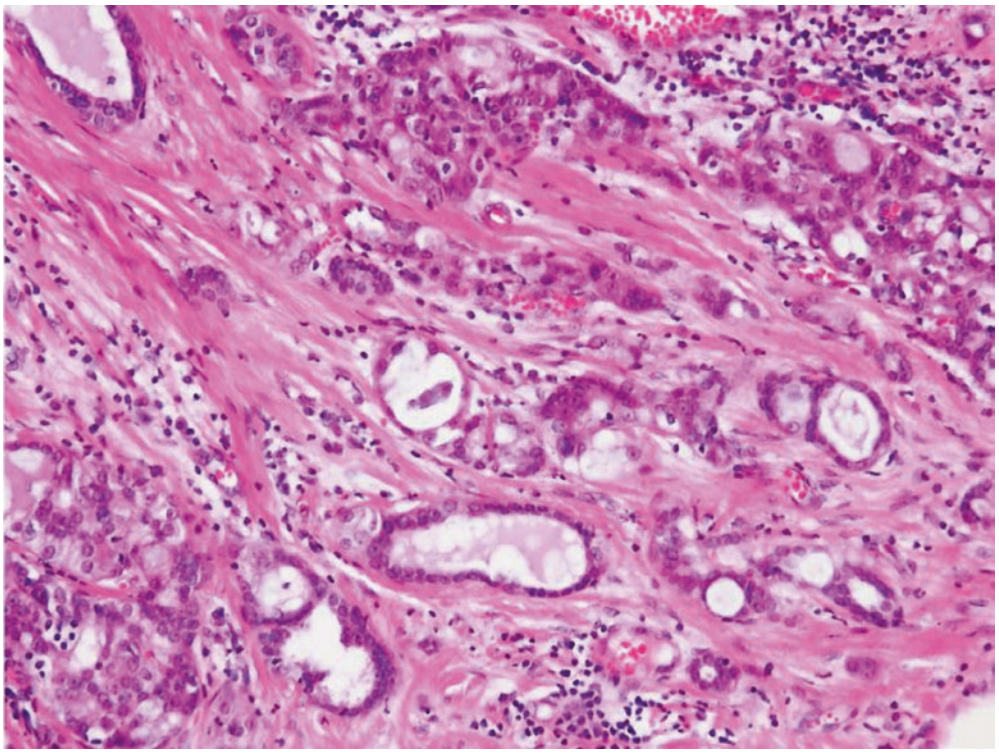

Fig. 12.175 Secretory carcinoma. Tubules lined by cuboidal to flattened cells containing luminal pink and pale secretions can be found among more solid sheets of tumour cells (Courtesy of Dr. Chih Jung Chen)

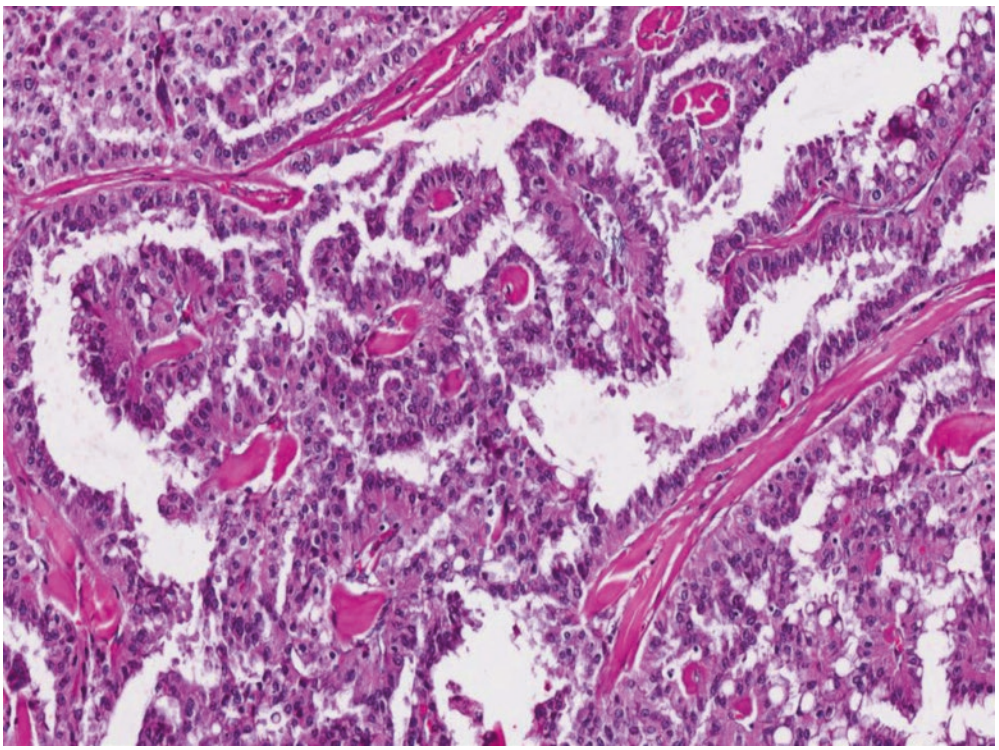

Fig. 12.176 Secretory carcinoma. A papillary architecture with fronds lined by columnar cells with pink cytoplasm and apical cytoplasmic blebs, is seen with hyalinised stroma. Foci where tumour cells contain cytoplasmic vacuoles are present

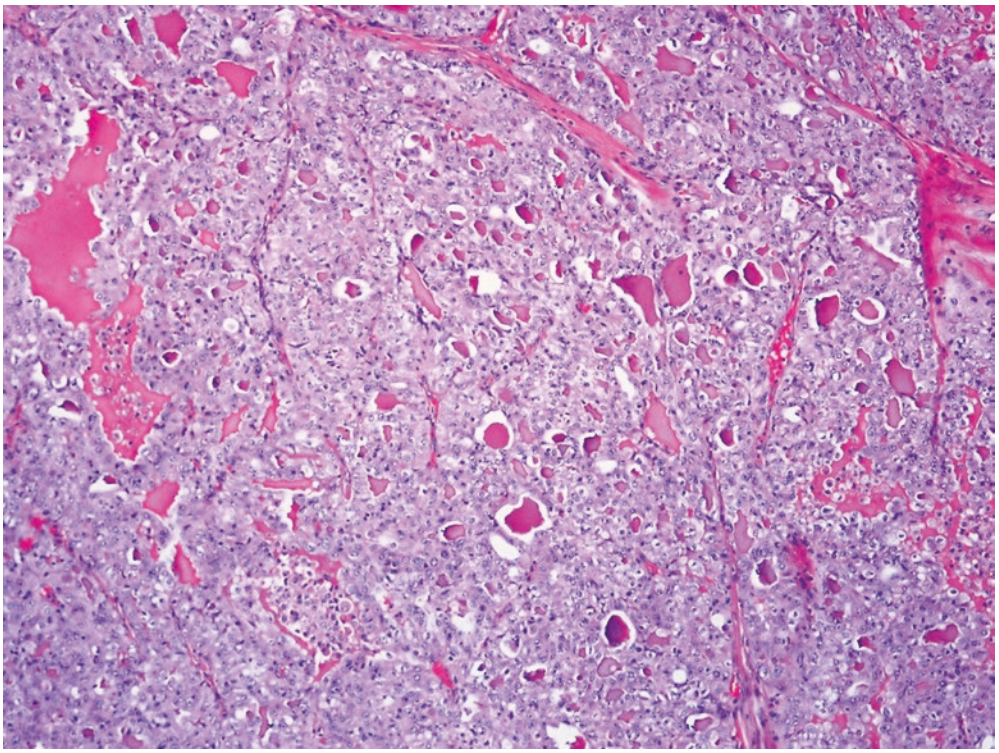

Fig. 12.177 Secretory carcinoma. Pink viscid material resembling colloid is present within spaces lined by tumour cells

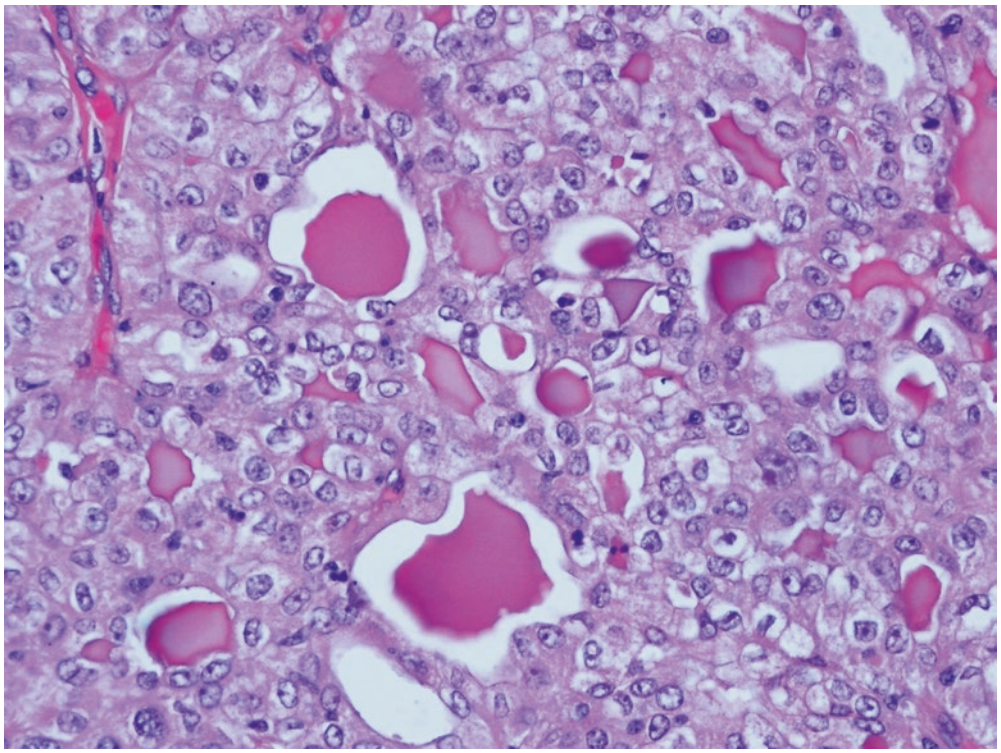

Fig. 12.178 Secretory carcinoma. Characteristic colloid-like viscid pink secretions are observed in spaces among tumour cells. Tumour cells show enlarged vesicular nuclei with occasionally discernible nucleoli

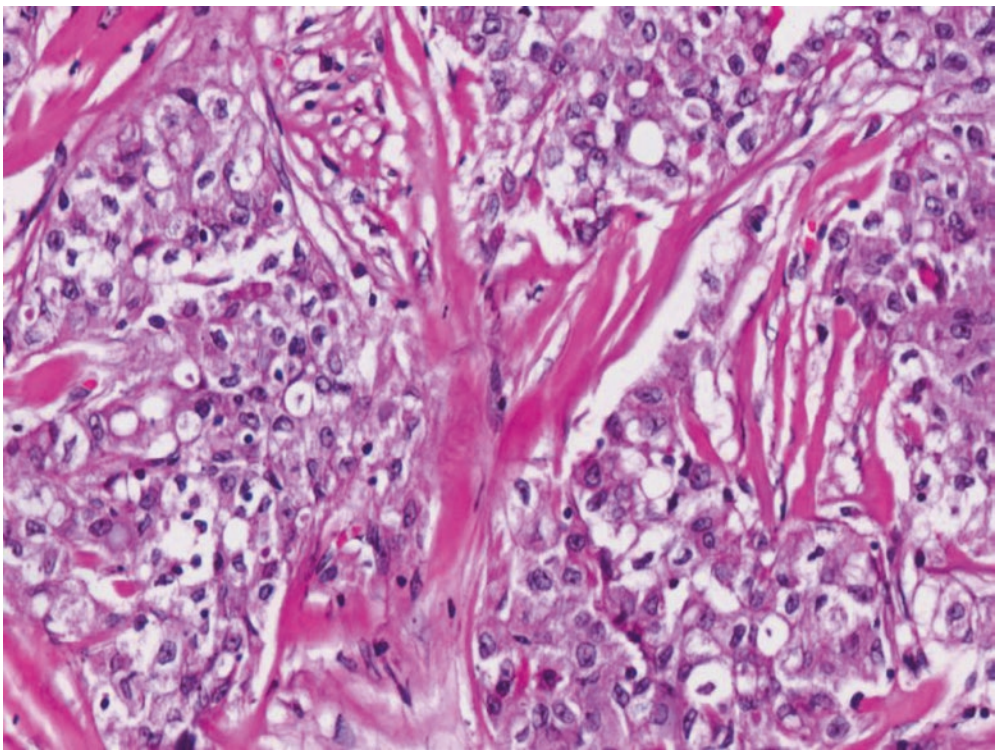

Fig. 12.179 Secretory carcinoma. Intracytoplasmic vacuoles and secretions are seen within tumour cells arranged in solid islands within a collagenous background

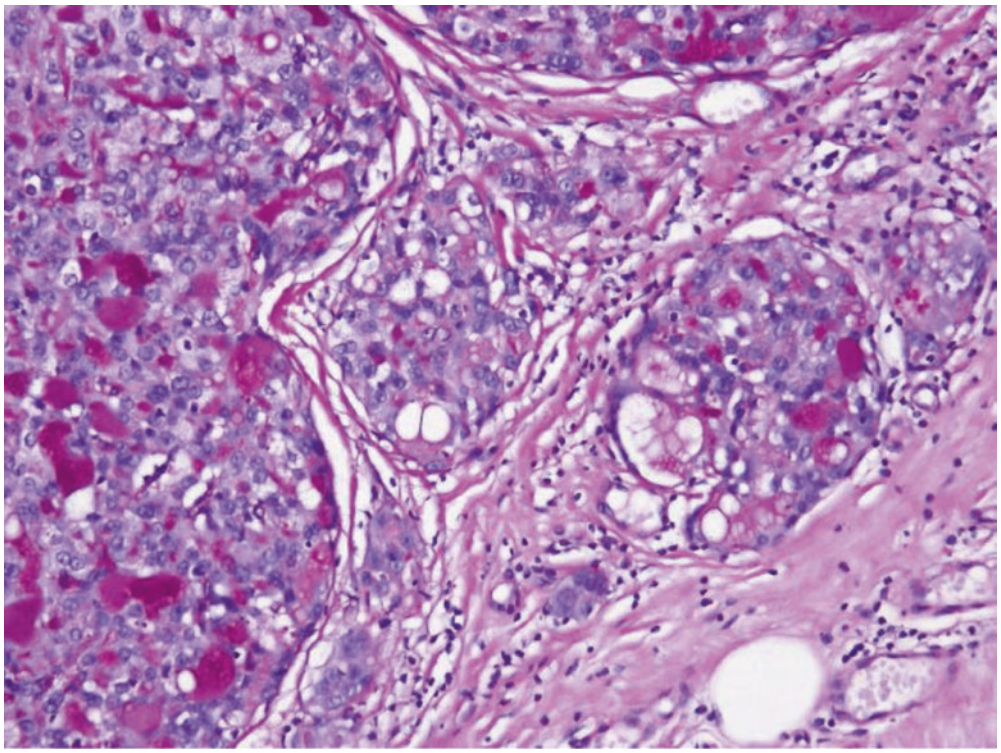

Fig. 12.180 Secretory carcinoma. Secretions stain positively with periodic acid–Schiff

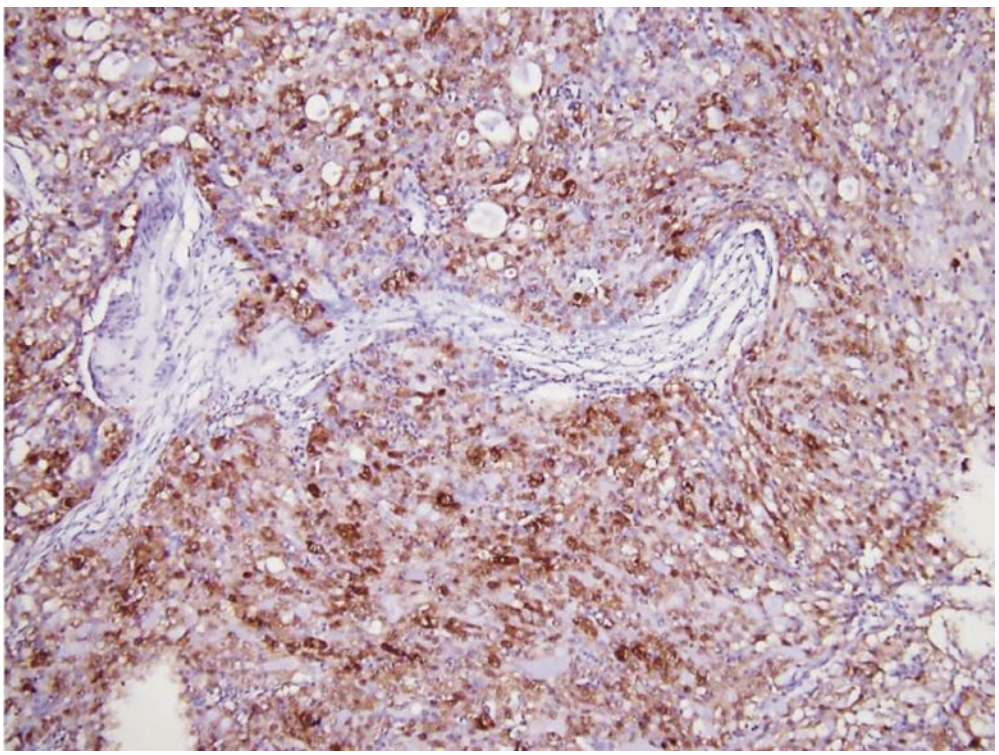

Fig. 12.181 Secretory carcinoma. Immunohistochemistry shows positive reactivity with S100

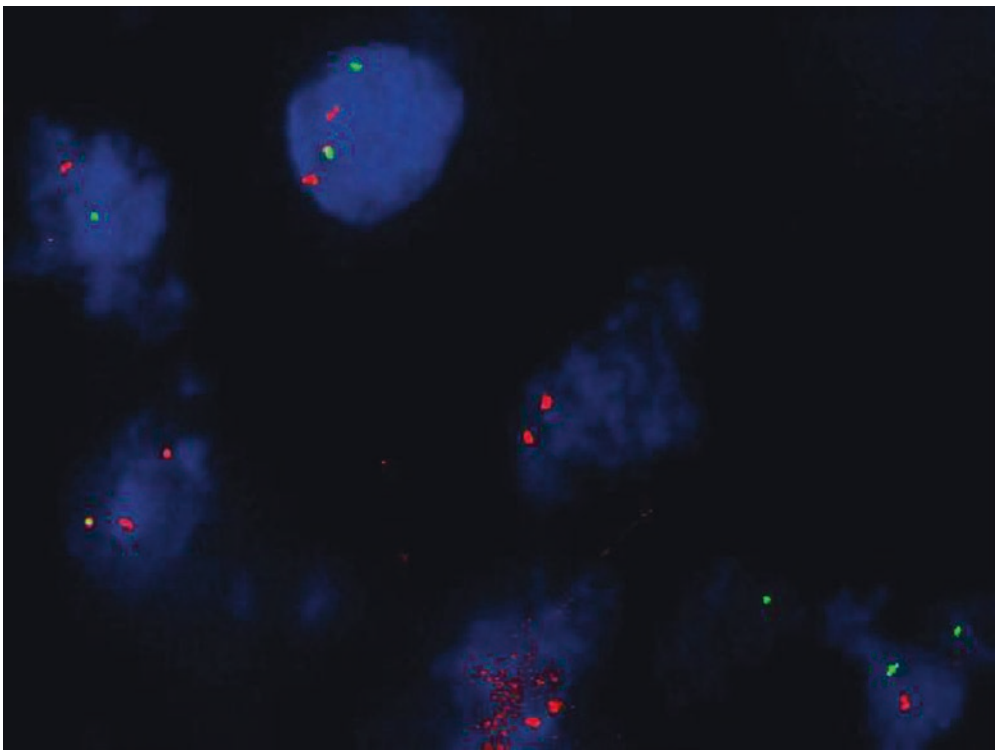

Fig. 12.182 Secretory carcinoma. On interphase fluorescence in situ hybridisation, the fusion (*yellow*) signal or a red signal with a closely associated green signal is the normal *ETV6* gene. (A normal cell will show two fusion signals—i.e. two yellow signals.) The separated red and green signals indicate a disrupted *ETV6* gene. The additional red signal shows that there is an extra copy of the 5′ *ETV6* gene (Courtesy of Cytogenetics Lab, SGH Pathology)

Differential Diagnosis

Acinic Cell Carcinoma

Acinic cell carcinoma consists of acini and solid nests of epithelial cells invading the stroma. Although the expression of S100, lysozyme, and amylase may be similar to secretory carcinoma, a key difference is the absence of the *ETV6-NTRK3* gene rearrangement in acinic cell carcinoma.

Cystic Hypersecretory Carcinoma

Cystic hypersecretory carcinoma, a variant of DCIS with cystic dilatation, micropapillary architecture, and luminal colloid secretions, differs from secretory carcinoma by its in situ nature, the presence of cysts, and a more homogeneous intraductal micropapillary pattern. There may be associated cystic hypersecretory hyperplasia. Invasive carcinoma, when present, tends to be of a poorly differentiated ductal subtype without secretory features [77].

Infiltrative Ductal Carcinoma with Oncocytic Differentiation

Infiltrative ductal carcinoma with oncocytic differentiation may resemble secretory carcinoma when the latter features cells with eosinophilic cytoplasm.

Prognosis and Therapy Considerations

Secretory carcinoma usually has a low-grade clinical course with a favourable prognosis, especially in children and young adults less than 20 years of age. In older patients, a more aggressive course is manifested, and recurrences may arise up to 20 years later [78]. Axillary lymph node metastases rarely involve more than three lymph nodes. Distant metastases are extremely rare.

Acinic Cell Carcinoma

Definition

Acinic cell carcinoma of the breast is similar to acinic cell carcinoma of the parotid gland, showing serous differentiation with zymogen-type cytoplasmic granules.

Clinical and Epidemiological Features

Acinic cell carcinomas of the breast affect women over a wide age range, with a mean of 56 years. Its true incidence is uncertain. Since its initial description in 1996 by Roncaroli et al. [79], fewer than 50 cases have been documented in the literature. Its rare occurrence may be related to lack of recognition, as serous features have been described in some

breast carcinomas that were not specifically designated as acinic cell cancers [80, 81]. Patients present with a breast lump.

Imaging Features

Radiological findings are of a malignant breast mass.

Pathologic Features

Macroscopic Pathology

Acinic cell carcinomas may vary in size from 1 to 5 cm and are grossly similar to other breast carcinomas.

Microscopic Pathology

Histologically, appearances vary from well-differentiated microglandular areas to more solid, less differentiated zones where comedo-type necrosis may be seen (Figs. 12.183, 12.184, 12.185, 12.186, and 12.187). On close microscopic scrutiny, tumour cells have vesicular round to ovoid nuclei, visible nucleoli, and ample amphophilic to eosinophilic cytoplasm that displays distinct granularity. These cytoplasmic granules may be fine and small or large and coarse. They can resemble granules observed in Paneth cells of the intestinal mucosa. Clear-cell appearances have also been encountered, reminiscent of clear-cell carcinoma of renal origin. Mitotic activity is variable and may number up to 15 per 10 high-power fields.

Acinic cell carcinomas of the breast are triple-negative (oestrogen receptor, progesterone receptor, and c-erbB-2 negative). They are positive for lysozyme, alpha-1-antichymotrypsin, salivary gland amylase, EMA, and S100 (Figs. 12.188, 12.189, and 12.190). Immunohistochemistry for these markers may assist in diagnosis. On electron microscopy, cells show zymogen-like granules.

The relationship of acinic cell carcinoma with microglandular adenosis has been discussed, with a few reports of their coexistence. Several authors have suggested a histogenetic link of microglandular adenosis with acinic cell carcinoma [81–85]. On the other hand, it has been stated that there are morphological, immunohistochemical, and ultrastructural differences between these two lesions that prevent a firm conclusion regarding their biological relationship [86].

Differential Diagnosis

Microglandular Adenosis

Microglandular adenosis resembles the small acinar pattern of acinic cell carcinoma (Figs. 12.191 and 12.192). In microglandular adenosis, however, the predominant

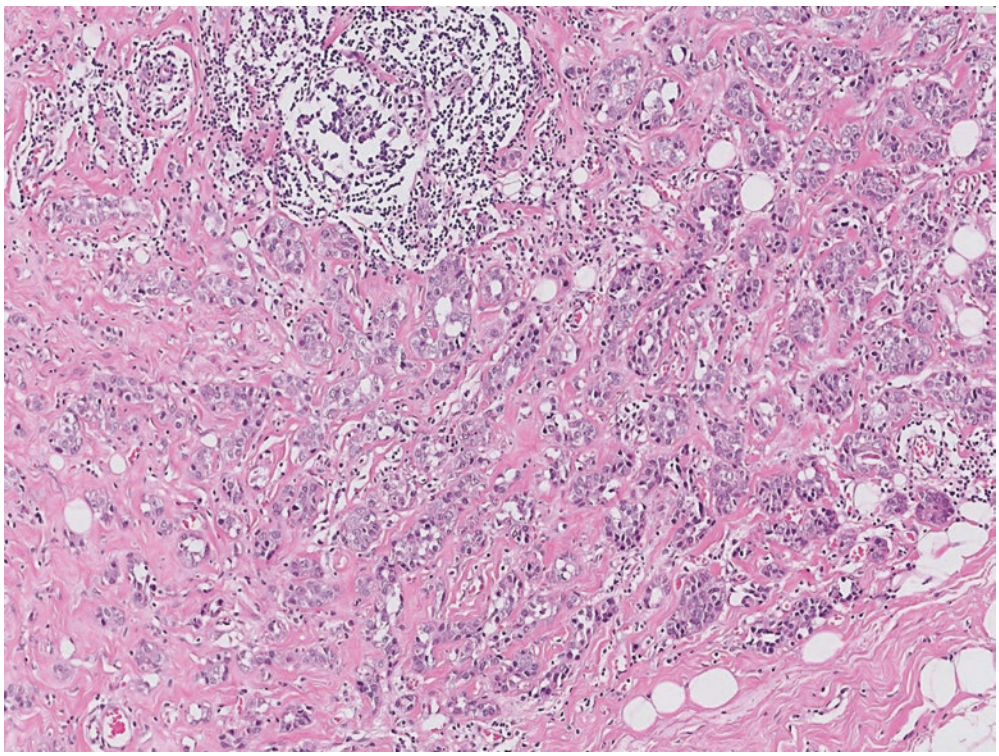

Fig. 12.183 Acinic cell carcinoma. At low magnification, an acinar pattern with haphazardly placed small tumour nests is seen

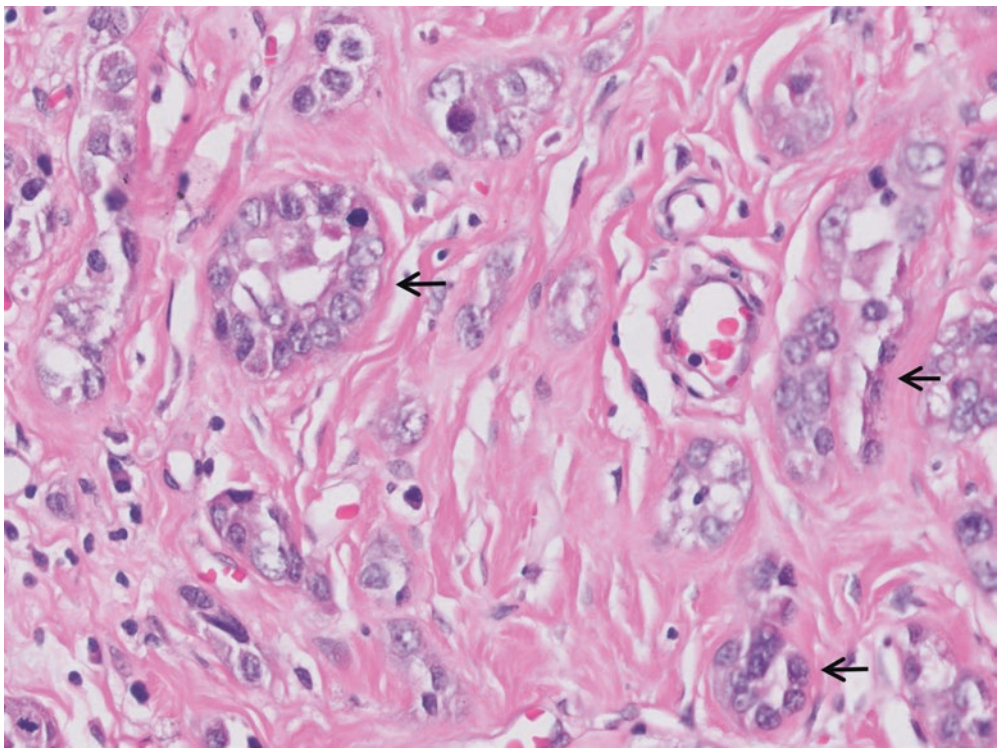

Fig. 12.184 Acinic cell carcinoma. Small solid nests and tubules (*arrows*) composed of cells with enlarged vesicular nuclei and variably discernible nucleoli are seen, with some luminal secretions

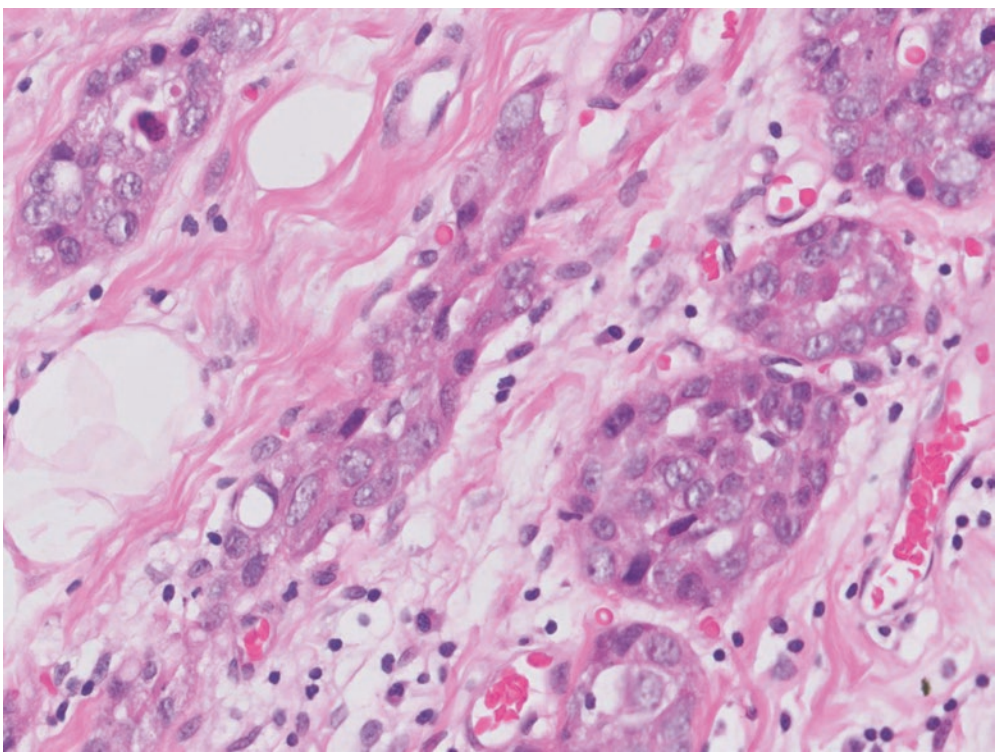

Fig. 12.185 Acinic cell carcinoma. High magnification shows tumour cells with vesicular nuclei and pink to amphophilic granular cytoplasm

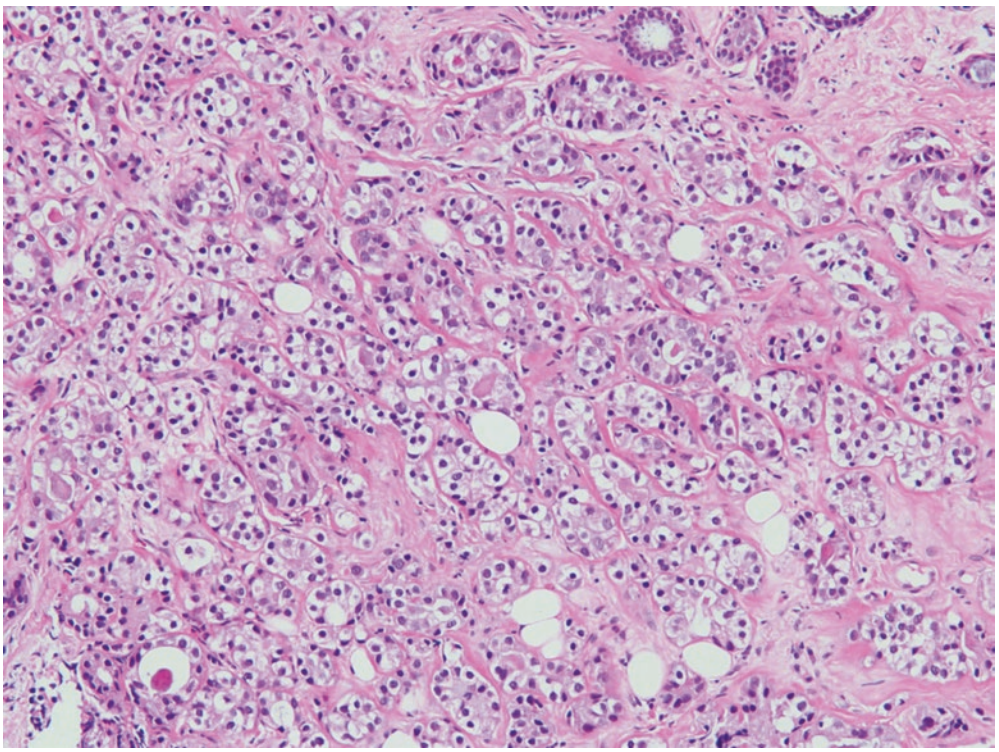

Fig. 12.186 Acinic cell carcinoma. Tumour cells with clear cytoplasm forming small nests can be present

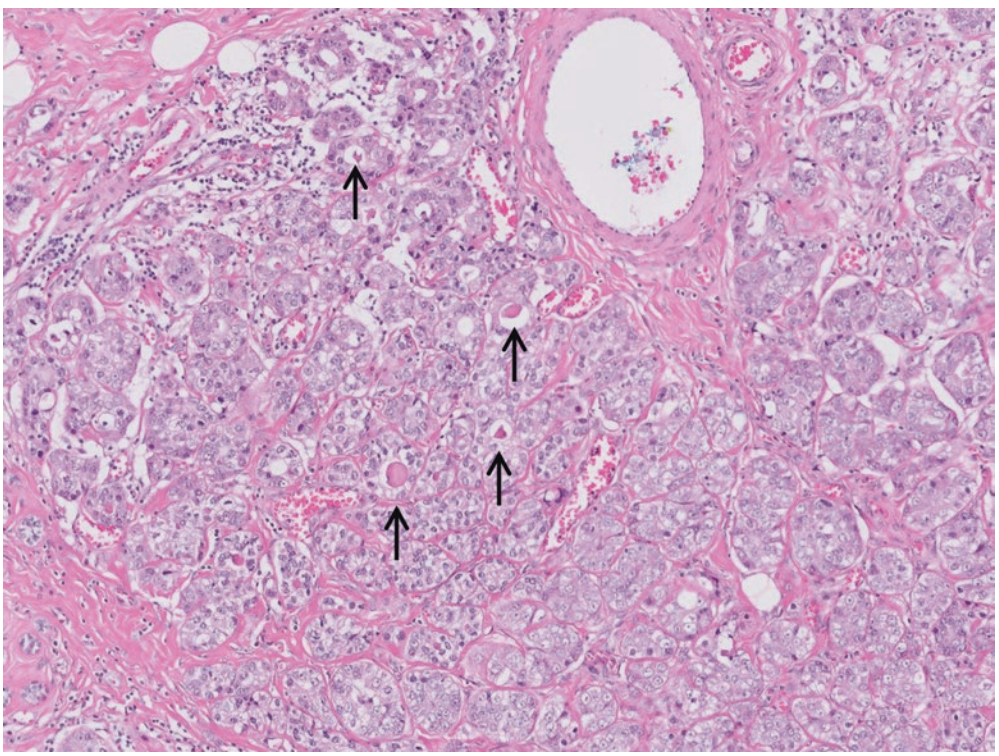

Fig. 12.187 Acinic cell carcinoma. Part of the tumour may feature tubules with luminal colloid-like secretions resembling microglandular adenosis. A histogenetic link is proposed between microglandular adenosis and acinic cell carcinoma

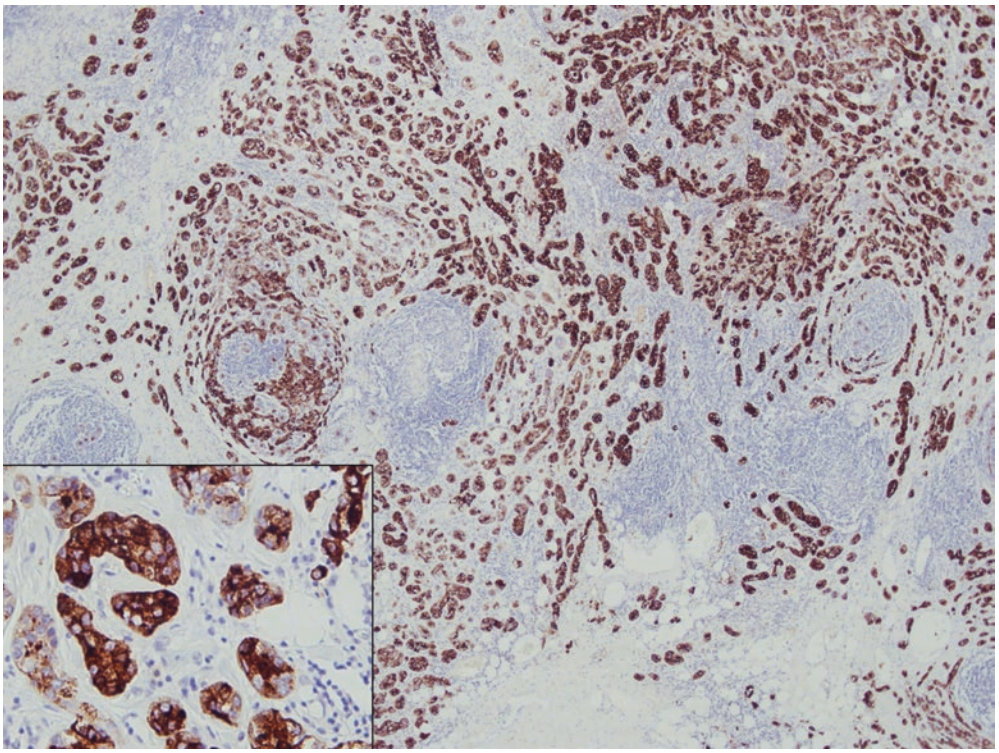

Fig. 12.188 Acinic cell carcinoma. Immunohistochemistry for epithelial membrane antigen (EMA) shows diffuse positive reactivity of tumour cells. *Inset* shows higher magnification of the positively stained tumour cells

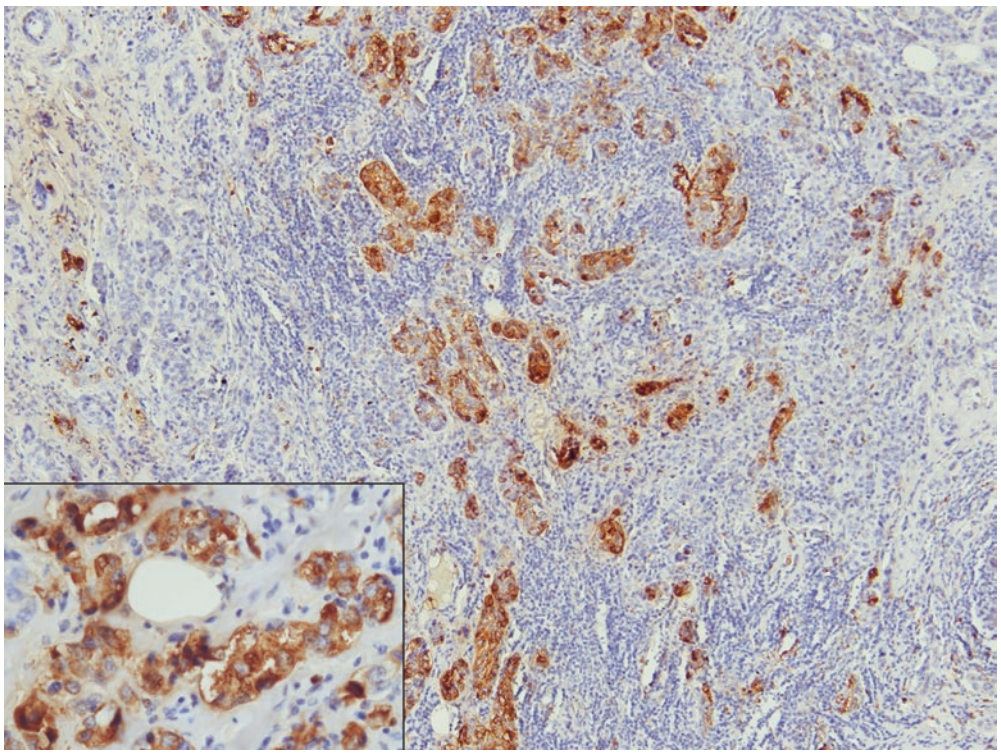

Fig. 12.189 Acinic cell carcinoma. Immunohistochemistry for lysozyme shows positive cytoplasmic reactivity in the tumour cells. *Inset* shows higher magnification of the positively stained tumour cells

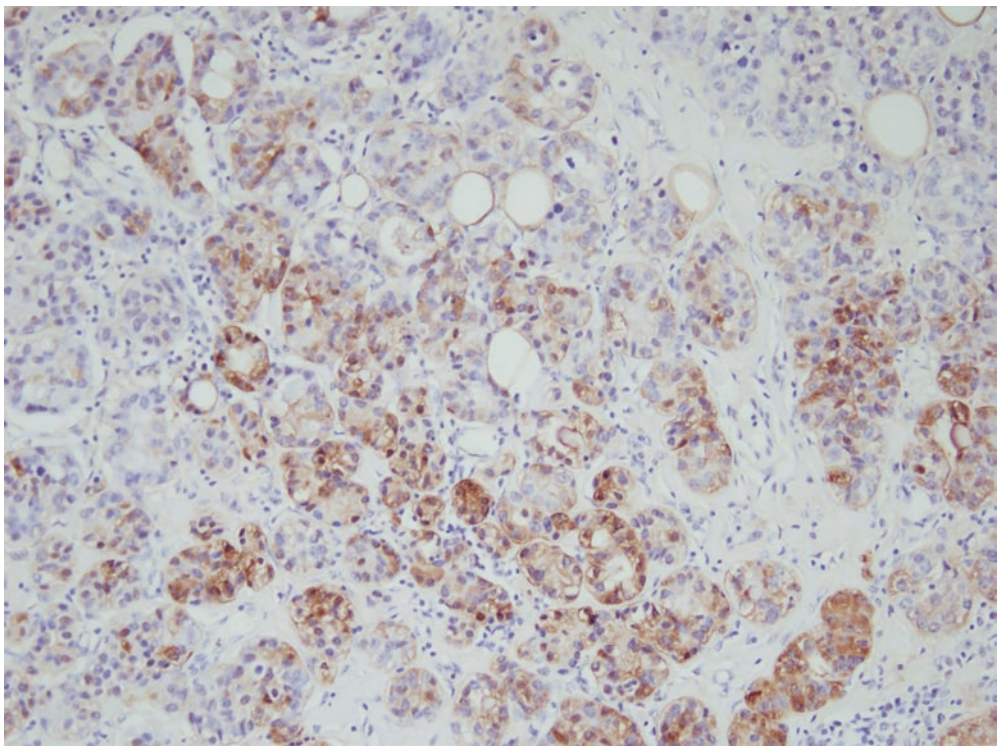

Fig. 12.190 Acinic cell carcinoma. Immunohistochemistry for S100 shows positive cytoplasmic reactivity in tumour cells

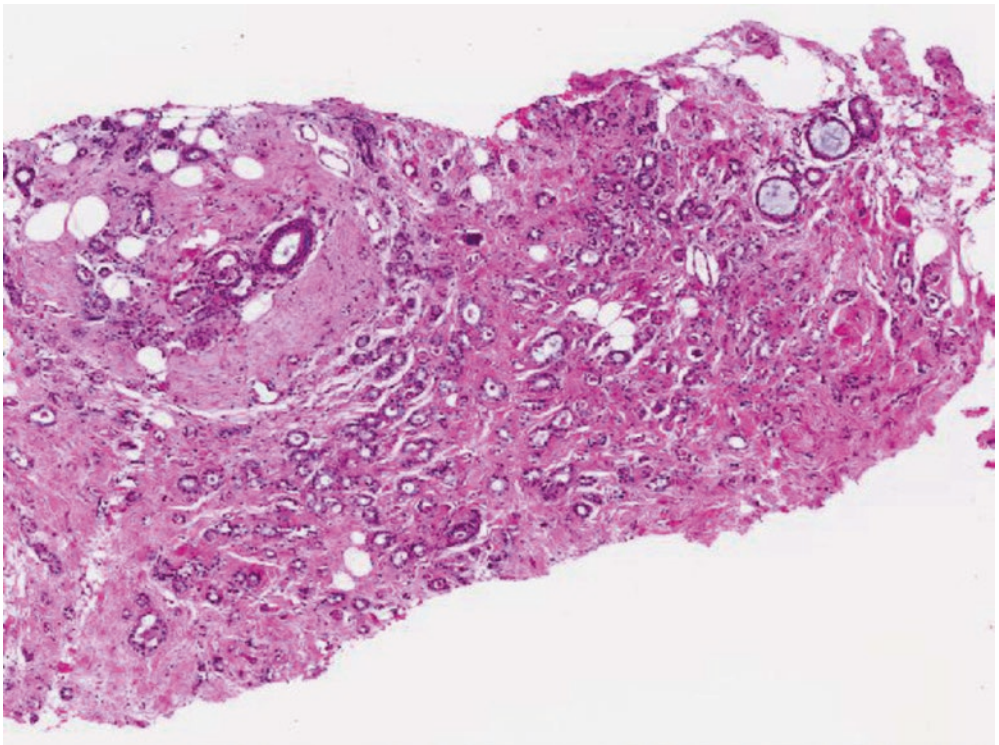

Fig. 12.191 Microglandular adenosis. A core biopsy specimen shows haphazardly placed small tubules with patent lumens containing dollops of pink secretions. When these findings are encountered on core biopsy of the radiological lesion of concern, excision is usually recommended to ensure that there is no atypical component or associated carcinoma

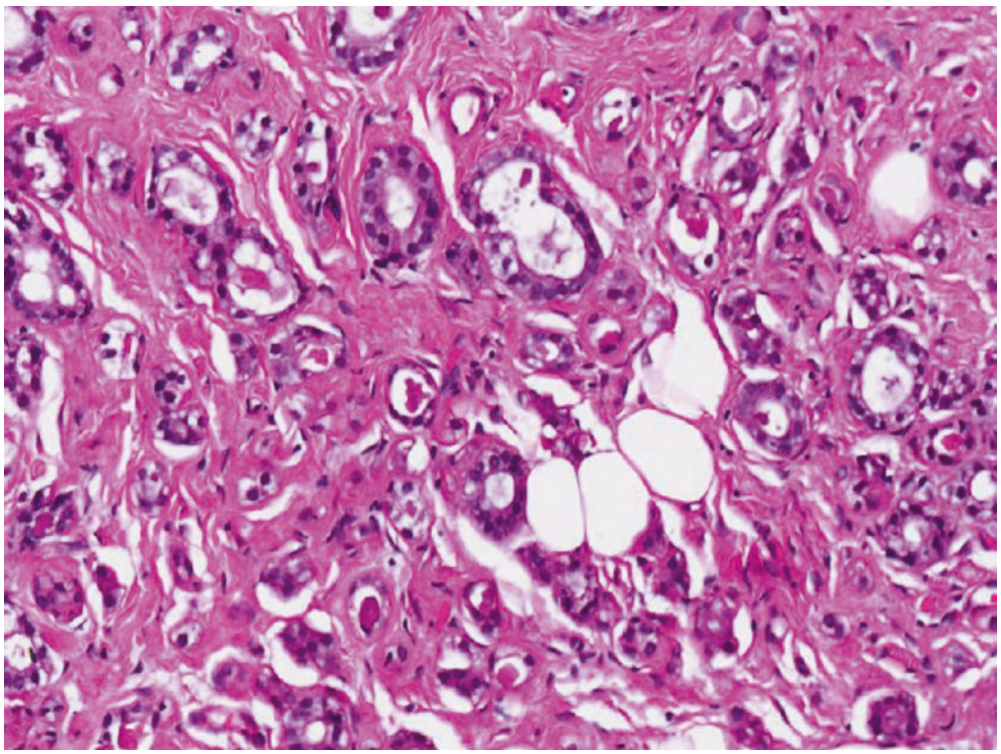

Fig. 12.192 Microglandular adenosis. Tubules with luminal pink, colloid-like secretions are present. In contrast to acinic cell carcinoma, microglandular adenosis has a uniformly small tubular appearance and does not typically harbour solid areas or clear-cell nests. Cytologic atypia is mild in microglandular adenosis, whereas acinic cell carcinoma may display greater nuclear atypia. An intact basement membrane is present around microglandular adenosis, though it is often difficult to demonstrate histologically. Atypical microglandular adenosis with cytologic atypia and abnormal architecture may be challenging to distinguish from acinic cell carcinoma

appearance is of small, rounded tubules with luminal eosinophilic secretions, whereas acinic cell carcinoma tends to have more variable architecture, including solid nests and clear-cell aggregates. A basement membrane sheath may be observed around tubules of microglandular adenosis [87].

Secretory Carcinoma

Secretory carcinoma may resemble acinic cell carcinoma, which can be distinguished using immunohistochemistry and molecular genetics, as acinic cell carcinoma does not display the t(12:15) *ETV6-NTRK3* rearrangement that typifies secretory breast carcinoma [88].

Infiltrative Ductal Carcinoma

Infiltrative ductal carcinoma composed of a nested pattern of invasive tumour cells may resemble acinic cell carcinoma. A third of acinic cell carcinomas are accompanied by infiltrative ductal carcinoma [89].

Prognosis and Therapy Considerations

Acinic cell carcinoma appears to have a favourable behaviour despite its triple negativity. No deaths have been reported directly consequent to the tumour, though its molecular genetics suggest that it may be associated with more aggressive forms of triple-negative disease [90]. Axillary lymph node metastases may be observed.

Table 12.3 Comparison of pathologic features of adenoid cystic carcinoma, collagenous spherulosis, cribriform DCIS, invasive cribriform carcinoma, and small cell carcinoma

Pathologic features	Adenoid cystic carcinoma	Collagenous spherulosis	Cribriform DCIS	Invasive cribriform carcinoma	Small cell carcinoma
Architecture	Cribriform	Cribriform	Cribriform	Cribriform	Solid nests resembling solid basaloid variant of adenoid cystic carcinoma
Contours of lesional islands	Rounded and irregular	Rounded	Rounded	Irregular	Sheets
Cell composition	Epithelial (luminal) -myoepithelial	Epithelial (luminal) -myoepithelial	Luminal epithelial	Luminal epithelial	Neuroendocrine
Secretory material	Watery, basophilic mucopolysaccharides and viscid, eosinophilic basement membrane material	Watery, basophilic mucopolysaccharides and viscid, eosinophilic basement membrane material	If present, pink secretions within lumens; otherwise cribriform lumens are usually empty	If present, pink secretions within lumens; otherwise cribriform lumens are usually empty	No secretions
Calcifications	Not frequent	Sometimes present	Often present	Sometimes present	Usually absent
Stroma	Myxoid	Unremarkable	Usually unremarkable	Desmoplastic	May be desmoplastic
Background	Invades breast parenchyma	Often incidental lesion within usual ductal hyperplasia, papilloma	Expanded lobules	Invades breast parenchyma	Invades breast parenchyma
Immunohistochemistry	CD117, p63, CK5/6, CK14, SMA, S100 positive in tumour cells Triple-negative	p63, CK5/6, CK14, SMA, S100 positive in myoepithelial cells ER patchily positive in the luminal epithelial cells CD117 negative	p63, CK5/6, CK14, SMA, S100 positive in the outer rim of intact myoepithelial cells CD117 variable ER and PR positive in tumour cells	p63, CK5/6, CK14, SMA, S100 negative indicating absence of myoepithelial cells CD117 variable ER & PR positive in tumour cells	Neuroendocrine markers, TTF1 positive Triple-negative CD117 rarely reported [91]

DCIS ductal carcinoma in situ, *ER* oestrogen receptor, *PR* progesterone receptor, *SMA* smooth muscle actin

References

1. Lakhani SR, Schnitt SJ, Tan PH, van de Vijver MJ. WHO classification of tumors of the breast. 4th ed. Lyon: IARC Press; 2012.
2. Tavassoli FA, Eusebi V. Major variants of carcinoma. In: Tavassoli FA, Eusebi V, editors. Tumors of the mammary gland: atlas of tumor pathology. 4th series, fascicle 10. Washington, DC: American Registry of Pathology, Armed Forces Institute of Pathology; 2009. p. 149–72.
3. Hoda SA. Invasive ductal carcinoma: assessment of prognosis with morphologic and biologic markers. In: Hoda SA, Brogi E, Koerner FC, Rosen PP, editors. Rosen's breast pathology. Philadelphia: Lippincott Williams & Wilkins; 2014. p. 413–68.
4. Anderson TJ, Lamb J, Donnan P, Alexander FE, Huggins A, Muir BB, et al. Comparative pathology of breast cancer in a randomised trial of screening. Br J Cancer. 1991;64:108–13.
5. Ellis IO, Galea M, Broughton N, Locker A, Blamey RW, Elston CW. Pathological prognostic factors in breast cancer. II. Histological type. Relationship with survival in a large study with long-term follow-up. Histopathology. 1992;20:479–89.
6. Anderson WF, Pfeiffer RM, Dores GM, Sherman ME. Comparison of age distribution patterns for different histopathologic types of breast carcinoma. Cancer Epidemiol Biomarkers Prev. 2006;15:1899–905.
7. Fisher ER, Gregorio RM, Fisher B, Redmond C, Vellios F, Sommers SC. The pathology of invasive breast cancer. A syllabus derived from findings of the National Surgical Adjuvant Breast Project (protocol no. 4). Cancer. 1975;36:1–85.
8. Sickles EA. Mammographic features of "early" breast cancer. Am J Roentgenol. 1984;143:461–4.
9. Costantini M, Belli P, Bufi E, Asunis AM, Ferra E, Bitti GT. Association between sonographic appearances of breast cancers and their histopathologic features and biomarkers. J Clin Ultrasound. 2016;44:26–33.
10. Jaafar M. Diversity of breast carcinoma: histological subtypes and clinical relevance. Clin Med Insights Pathol. 2015;8:23–31.
11. Viale G. The current state of breast cancer classification. Ann Oncol. 2012;23 Suppl 10:207–10.
12. Weigelt B, Geyer FC, Reis-Filho JS. Histological types of breast cancer: how special are they? Mol Oncol. 2010;4:192–208.
13. Ping Z, Xia Y, Shen T, Parekh V, Siegal GP, Eltoum IE, et al. A microscopic landscape of the invasive breast cancer genome. Sci Rep. 2016;6:27545.
14. Wang K, Xu J, Zhang T, Xue D. Tumor-infiltrating lymphocytes in breast cancer predict the response to chemotherapy and survival outcome: a meta-analysis. Oncotarget. 2016;7(28):44288.
15. Song YJ, Shin SH, Cho JS, Park MH, Yoon JH, Jegal YJ. The role of lymphovascular invasion as a prognostic factor in patients with lymph node-positive operable invasive breast cancer. J Breast Cancer. 2011;14:198–203.
16. de Mascarel I, Bonichon F, Durand M, Mauriac L, MacGrogan G, Soubeyran I, et al. Obvious peritumoral emboli: an elusive prognostic factor reappraised. Multivariate analysis of 1320 node-negative breast cancers. Eur J Cancer. 1998;34:58–65.
17. Karak SG, Quatrano N, Buckley J, Ricci Jr A. Prevalence and significance of perineural invasion in invasive breast carcinoma. Conn Med. 2010;74:17–21.

18. Elston CW, Ellis IO. Pathological prognostic factors in breast cancer, I: the value of histological grade in breast cancer: experience from a large study with long-term follow-up. Histopathology. 1991;19:403–10.
19. Dalton LW, Pinder SE, Elston CE, Ellis IO, Page DL, Dupont WD, Blamey RW. Histologic grading of breast cancer: linkage of patient outcome with level of pathologist agreement. Mod Pathol. 2000;13:730–5.
20. Meyer JS, Alvarez C, Milikowski C, Olson N, Russo I, Russo J, et al. Breast carcinoma malignancy grading by Bloom-Richardson system vs proliferation index: reproducibility of grade and advantages of proliferation index. Mod Pathol. 2005;18:1067–78.
21. Rakha EA, Reis-Filho JS, Baehner F, Dabbs DJ, Decker T, Eusebi V, et al. Breast cancer prognostic classification in the molecular era: the role of histological grade. Breast Cancer Res. 2010;12:207.
22. Fong Y, Evans J, Brook D, Kenkre J, Jarvis P, Gower-Thomas K. The Nottingham Prognostic Index: five- and ten-year data for all-cause survival within a screened population. Ann R Coll Surg Engl. 2015;97:137–9.
23. Ignatiadis M, Sotiriou C. Understanding the molecular basis of histologic grade. Pathobiology. 2008;75:104–11.
24. Papadimitriou M, Kaptanis S, Polymeropoulos E, Mitsopoulos G, Stogiannis D, Caroni C, et al. Nuclear grade plus proliferation grading system for invasive ductal carcinoma of the breast: validation in a tertiary referral hospital cohort. Am J Clin Pathol. 2015;144:837–43.
25. Harris GC, Denley HE, Pinder SE, Lee AH, Ellis IO, Elston CW, Evans A. Correlation of histologic prognostic factors in core biopsies and therapeutic excisions of invasive breast carcinoma. Am J Surg Pathol. 2003;27:11–5.
26. Andrade VP, Gobbi H. Accuracy of typing and grading invasive mammary carcinomas on core needle biopsy compared with the excisional specimen. Virchows Arch. 2004;445:597–602.
27. Zaha DC. Significance of immunohistochemistry in breast cancer. World J Clin Oncol. 2014;5:382–92.
28. Gown AM, Fulton RS, Kandalaft PL. Markers of metastatic carcinoma of breast origin. Histopathology. 2016;68:86–95.
29. Asch-Kendrick R, Cimino-Mathews A. The role of GATA3 in breast carcinomas: a review. Hum Pathol. 2016;48:37–47.
30. Davis DG, Siddiqui MT, Oprea-Ilies G, Stevens K, Osunkoya AO, Cohen C, Li XB. GATA-3 and FOXA1 expression is useful to differentiate breast carcinoma from other carcinomas. Hum Pathol. 2016;47:26–31.
31. Hammond ME, Hayes DF, Dowsett M, Allred DC, Hagerty KL, Badve S, et al. American Society of Clinical Oncology/College of American Pathologists guideline recommendations for immunohistochemical testing of estrogen and progesterone receptors in breast cancer. Arch Pathol Lab Med. 2010;134:907–22.
32. Wolff AC, Hammond ME, Schwartz JN, Hagerty KL, Allred DC, Cote RJ, et al. American Society of Clinical Oncology/College of American Pathologists guideline recommendations for human epidermal growth factor receptor 2 testing in breast cancer. Arch Pathol Lab Med. 2007;131:18–43.
33. Perou CM, Sørlie T, Eisen MB, van de Rijn M, Jeffrey SS, Rees CA, et al. Molecular portraits of human breast tumours. Nature. 2000;406:747–52.
34. Sorlie T, Tibshirani R, Parker J, Hastie T, Marron JS, Nobel A, et al. Repeated observation of breast tumor subtypes in independent gene expression data sets. Proc Natl Acad Sci U S A. 2003;100:8418–23.
35. Prat A, Pineda E, Adamo B, Galván P, Fernández A, Gaba L, et al. Clinical implications of the intrinsic molecular subtypes of breast cancer. Breast. 2015;24 Suppl 2:S26–35.
36. Ades F, Zardavas D, Bozovic-Spasojevic I, Pugliano L, Fumagalli D, de Azambuja E, et al. Luminal B breast cancer: molecular characterization, clinical management, and future perspectives. J Clin Oncol. 2014;32:2794–803.
37. Lehmann BD, Bauer JA, Chen X, Sanders ME, Chakravarthy AB, Shyr Y, Pietenpol JA. Identification of human triple-negative breast cancer subtypes and preclinical models for selection of targeted therapies. J Clin Invest. 2011;121:2750–67.
38. Sabatier R, Finetti P, Guille A, Adelaide J, Chaffanet M, Viens P, et al. Claudin-low breast cancers: clinical, pathological, molecular and prognostic characterization. Mol Cancer. 2014;13:228.
39. Penault-Llorca F, Viale G. Pathological and molecular diagnosis of triple-negative breast cancer: a clinical perspective. Ann Oncol. 2012;23 Suppl 6:19–22.
40. Mittendorf EA, Vila J, Tucker SL, Chavez-MacGregor M, Smith BD, Symmans WF, et al. The Neo-Bioscore update for staging breast cancer treated with neoadjuvant chemotherapy: incorporation of prognostic biologic factors into staging after treatment. JAMA Oncol. 2016;2:929–36.
41. Telli ML, Sledge GW. The future of breast cancer systemic therapy: the next 10 years. J Mol Med (Berl). 2015;93:119–25.
42. Colleoni M, Rotmensz N, Maisonneuve P, Mastropasqua MG, Luini A, Veronesi P, et al. Outcome of special types of luminal breast cancer. Ann Oncol. 2012;23:1428–36.
43. Winchester DJ, Sahin AA, Tucker SL, Singletary SE. Tubular carcinoma of the breast: predicting axillary nodal metastases and recurrence. Ann Surg. 1996;223:342–7.
44. Romano AM, Wages NA, Smolkin M, Fortune KL, Atkins K, Dillon PM. Tubular carcinoma of the breast: institutional and SEER database analysis supporting a unique classification. Breast Dis. 2015;35:103–11.
45. Elson BC, Helvie MA, Frank TS, Wilson TE, Adler DD. Tubular carcinoma of the breast: mode of presentation, mammographic appearance, and frequency of nodal metastases. AJR Am J Roentgenol. 1993;161:1173–6.
46. Rosen PP. Columnar cell hyperplasia is associated with lobular carcinoma in situ and tubular carcinoma. Am J Surg Pathol. 1999;23:1561.
47. Green I, McCormick B, Cranor M, Rosen PP. A comparative study of pure tubular and tubulolobular carcinoma of the breast. Am J Surg Pathol. 1997;21:653–7.
48. Rakha EA, Lee AH, Evans AJ, Menon S, Assad NY, Hodi Z, et al. Tubular carcinoma of the breast: further evidence to support its excellent prognosis. J Clin Oncol. 2010;28:99–104.
49. Dejode M, Sagan C, Campion L, Houvenaeghel G, Giard S, Rodier JF, et al. Pure tubular carcinoma of the breast and sentinel lymph node biopsy: a retrospective multi-institutional study of 234 cases. Eur J Surg Oncol. 2013;39:248–54.
50. Page DL, Dixon JM, Anderson TJ, Lee D, Stewart HJ. Invasive cribriform carcinoma of the breast. Histopathology. 1983;7:525–36.
51. Venable JG, Schwartz AM, Silverberg SG. Infiltrating cribriform carcinoma of the breast: a distinctive clinicopathologic entity. Hum Pathol. 1990;21:333–8.
52. Arpino G, Clark GM, Mohsin S, Bardou VJ, Elledge RM. Adenoid cystic carcinoma of the breast: molecular markers, treatment, and clinical outcome. Cancer. 2000;94:2119–27.
53. Jacquemier J, Reis-Filho JS, Lakhani SR, Rakha E. Carcinomas with medullary features. In: Lakhani SR, Ellis IO, Schnitt SR, Tan PH, van de Vijver MJ, editors. WHO classification of tumours of the breast. 4th ed. Lyon: IARC; 2012. p. 46–7.
54. Marginean F, Rakha EA, Ho BC, Ellis IO, Lee AH. Histological features of medullary carcinoma and prognosis in triple-negative basal-like carcinomas of the breast. Mod Pathol. 2010;23:1357–63.
55. Rakha EA, El-Sheikh SE, Kandil MA, El-Sayed ME, Green AR, Ellis IO. Expression of BRCA1 protein in breast cancer and its prognostic significance. Hum Pathol. 2008;39:857–65.
56. Reis-Filho JS, Lakhani SR, Gobbi H, Sneige N. Metaplastic carcinoma. In: Lakhani SR, Ellis IO, Schnitt SJ, Tan PH, van de Vijver MJ, editors. WHO classification of tumours of the breast. 4th ed. Lyon: IARC; 2012. p. 48–52.

57. Soo K, Tan PH. Low-grade adenosquamous carcinoma of the breast. J Clin Pathol. 2013;66:506–11.
58. Kawaguchi K, Shin SJ. Immunohistochemical staining characteristics of low-grade adenosquamous carcinoma of the breast. Am J Surg Pathol. 2012;36:1009–20.
59. Geyer FC, Lambros MB, Natrajan R, Mehta R, Mackay A, Savage K, et al. Genomic and immunohistochemical analysis of adenosquamous carcinoma of the breast. Mod Pathol. 2010;23: 951–60.
60. Gobbi H, Simpson JF, Jensen RA, Olson SJ, Page DL. Metaplastic spindle cell breast tumors arising within papillomas, complex sclerosing lesions, and nipple adenomas. Mod Pathol. 2003;16: 893–901.
61. Denley H, Pinder SE, Tan PH, Sim CS, Brown R, Barker T, et al. Metaplastic carcinoma of the breast arising within complex sclerosing lesions: a report of five cases. Histopathology. 2000;36: 203–9.
62. Foschini MP, Pizzicannella G, Petersen JL, Eusebi V. Adenomyoepithelioma of the breast associated with low-grade adenosquamous and sarcomatoid carcinomas. Virchows Arch. 1995;427:243–50.
63. Leibl S, Gogg-Kammerer M, Sommersacher A, Denk H, Moinfar F. Metaplastic breast carcinomas: are they of myoepithelial differentiation?: immunohistochemical profile of the sarcomatoid subtype using novel myoepithelial markers. Am J Surg Pathol. 2005;29:347–53.
64. Oo KZ, Xiao PQ. Infiltrating syringomatous adenoma of the nipple: clinical presentation and literature review. Arch Pathol Lab Med. 2009;133:1487–9.
65. Oh EY, Collins LC. Keratin expression patterns in stromal cells of benign sclerosing lesions of the breast: a potential diagnostic pitfall. Arch Pathol Lab Med. 2015;139:1143–8.
66. Chia Y, Thike AA, Cheok PY, Yong-Zheng Chong L, Man-Kit Tse G, Tan PH. Stromal keratin expression in phyllodes tumours of the breast: a comparison with other spindle cell breast lesions. J Clin Pathol. 2012;65:339–47.
67. Cimino-Mathews A, Sharma R, Illei PB, Vang R, Argani P. A subset of malignant phyllodes tumors express p63 and p40: a diagnostic pitfall in breast core needle biopsies. Am J Surg Pathol. 2014;38:1689–96.
68. Sin EI, Wong CY, Yong WS, Ong KW, Madhukumar P, Tan VK, Thike AA, Tan PH, Tan BK. Breast carcinoma and phyllodes tumour: a case series. J Clin Pathol. 2016;69(4):364–9.
69. Lim SZ, Ong KW, Tan BK, Selvarajan S, Tan PH. Sarcoma of the breast: an update on a rare entity. J Clin Pathol. 2016;69: 373–81.
70. Sapina A, Sneige N, Eusebi V. Adenoid cystic carcinoma. In: Lakhani SR, Ellis IO, Schnitt SJ, Tan PH, van de Vijver MJ, editors. WHO classification of tumours of the breast. 4th ed. Lyon: IARC; 2012. p. 56–7.
71. Miyai K, Schwartz MR, Divatia MK, Anton RC, Park YW, Ayala AG, Ro JY. Adenoid cystic carcinoma of breast: recent advances. World J Clin Cases. 2014;2:732–41.
72. Martelotto LG, De Filippo MR, Ng CK, Natrajan R, Fuhrmann L, Cyrta J, et al. Genomic landscape of adenoid cystic carcinoma of the breast. J Pathol. 2015;237:179–89.
73. Reis-Filho JS, Fulford LG, Crebassa B, Carpentier S, Lakhani SR. Collagenous spherulosis in an adenomyoepithelioma of the breast. J Clin Pathol. 2004;57:83–6.
74. Foschini MP, Rizzo A, De Leo A, Laurino L, Sironi M, Rucco V. Solid variant of adenoid cystic carcinoma of the breast: a case series with proposal of a new grading system. Int J Surg Pathol. 2016;24:97–102.
75. Eusebi V, Ichihara S, Vincent-Salomon A, Sneige N, Sapino A. Exceptionally rare types and variants. In: Lakhani SR, Ellis IO, Schnitt SJ, Tan PH, van de Vijver MJ, editors. WHO classification of tumours of the breast. 4th ed. Lyon: IARC; 2012. p. 75–6.
76. Tan PH, Schnitt SJ, van de Vijver MJ, Ellis IO, Lakhani SR. Papillary and neuroendocrine breast lesions: the WHO stance. Histopathology. 2015;66:761–70.
77. Resetkova E, Padula A, Albarraccin CT, Sneige N. Pathologic quiz case: a large, ill-defined cystic breast mass. Arch Pathol Lab Med. 2005;129:e79–80.
78. Wong M, Jara-Lazaro AR, Hui Ng RC, Tiong Lim AS, Cheok PY, Lim TH, et al. ETV6 disruption does not predict indolent clinical behavior in secretory breast carcinoma. Breast J. 2012;18: 604–6.
79. Roncaroli F, Lamovec J, Zidar A, Eusebi V. Acinic cell-like carcinoma of the breast. Virchows Arch. 1996;429:69–74.
80. Inaji H, Koyama H, Higashiyama M, Noguchi S, Yamamoto H, Ishikawa O, et al. Immunohistochemical, ultrastructural and biochemical studies of an amylase-producing breast carcinoma. Virchows Arch A Pathol Anat Histopathol. 1991;419: 29–33.
81. Koenig C, Dadmanesh F, Bratthauer GL, Tavassoli FA. Carcinoma arising in microglandular adenosis: an immunohistochemical analysis of 20 intraepithelial and invasive neoplasms. Int J Surg Pathol. 2000;8:303–15.
82. Kahn R, Holtveg H, Nissen F, Holck S. Are acinic cell carcinoma and microglandular carcinoma of the breast related lesions? Histopathology. 2003;42:195–6.
83. James BA, Cranor ML, Rosen PP. Carcinoma of the breast arising in microglandular adenosis. Am J Clin Pathol. 1993;100: 507–13.
84. Resetkova E, Flanders DJ, Rosen PP. Ten-year follow-up of mammary carcinoma arising in microglandular adenosis treated with breast conservation. Arch Pathol Lab Med. 2003;127:77–80.
85. Shin SJ, Simpson PT, Da Silva L, Janathan J, Reid L, Lakhani SR, et al. Molecular evidence for progression of microglandular adenosis (MGA) to invasive carcinoma. Am J Surg Pathol. 2009;33:496–504.
86. Tavassoli FA, Eusebi V. Tumors of the mammary gland: atlas of tumor pathology. 4th series, fascicle 10. Washington, DC: American Registry of Pathology, Armed Forces Institute of Pathology; 2009.
87. Brogi E. Adenosis and microglandular adenosis. In: Hoda SA, Brogi E, Koerner FC, Rosen PP, editors. Rosen's breast pathology. 4th ed. Philadelphia: Lippincott Williams & Wilkins; 2014. p. 183–212.
88. Reis-Filho JS, Natrajan R, Vatcheva R, Lambros MB, Marchió C, Mahler-Araújo B, et al. Is acinic cell carcinoma a variant of secretory carcinoma? A FISH study using ETV6 'split apart' probes. Histopathology. 2008;52:840–6.
89. Conlon N, Sadri N, Corben AD, Tan LK. Acinic cell carcinoma of breast: morphologic and immunohistochemical review of a rare breast cancer subtype. Hum Pathol. 2016;51:16–24.
90. Guerini-Rocco E, Hodi Z, Piscuoglio S, Ng CK, Rakha EA, Schultheis AM, et al. The repertoire of somatic genetic alterations of acinic cell carcinomas of the breast: an exploratory, hypothesis-generating study. J Pathol. 2015;237:166–78.
91. Yamasaki T, Shimazaki H, Aida S, Tamai S, Tamaki K, Hiraide H, et al. Primary small cell (oat cell) carcinoma of the breast: report of a case and review of the literature. Pathol Int. 2000;50:914–8.

Nipple Lesions

13

The nipple is a pigmented, nodular protuberance on the breast into which lactiferous ducts open. It is rimmed circumferentially by the areola, which is also pigmented. It comprises fibrous connective tissue with bundles of smooth muscle fibres disposed around lactiferous ducts, which contract for milk expression during lactation. The epidermis of the nipple and its surrounding areola consists of stratified squamous epithelium. Sebaceous glands are present in the areola. Skin lesions can therefore occur in the nipple and areolar region.

Squamous Metaplasia of Lactiferous Ducts

Definition

Squamous metaplasia of lactiferous ducts (SMOLD) refers to replacement of lactiferous ductal epithelium by keratinising squamous epithelium, extending deeper than the squamocolumnar junction where lactiferous ducts open onto the nipple skin. SMOLD often occurs in conjunction with subareolar abscesses and fistula formation, secondary to keratin plugs and obstruction, a condition referred to as *Zuska's disease*.

Clinical and Epidemiological Features

Pain, redness, swelling, and purulent discharge from the nipple-areolar region are clinical symptoms. SMOLD mostly occurs in women, but rare cases in men are described [1].

Imaging Features

Imaging reveals mixed solid–cystic masses or abscesses at the superficial periareolar or subareolar region. Fistulous formations to the overlying skin can sometimes be seen on sonography. Dilated ducts may communicate with these inflammatory masses, and there are signs of inflammation such as oedema and increased vascularity in the surrounding breast tissue [2].

Pathologic Features

Macroscopic Pathology

The nipple may be retracted and ulcerated, with necrotic discharge, mimicking malignancy.

Microscopic Pathology

Squamous metaplasia of lactiferous ducts is present, with accompanying keratin plugs, surrounding inflammation, abscess formation, and granulation tissue-lined fistulation of the lactiferous ducts to the areola (Figs. 13.1, 13.2, 13.3, 13.4, 13.5, and 13.6). The nipple epidermis is frequently eroded or ulcerated.

Differential Diagnosis

Squamous Papilloma

In a squamous papilloma, exophytic verrucous projections are covered by benign stratified squamous epithelium (Figs. 13.7, 13.8, 13.9, 13.10, and 13.11). Inflammation is not a key feature, unlike with SMOLD. Keratin formation in a squamous papilloma occurs on the surface, in contrast to SMOLD, in which keratinous plugs are found in the deeper portions of the dilated lactiferous ducts, which have undergone squamous metaplasia.

Squamous Cell Carcinoma, Invasive

Squamous cell carcinoma of the nipple is extremely rare. It can present as an exophytic nipple mass (Fig. 13.12) [3] or as

P.H. Tan, A.A. Sahin, *Atlas of Differential Diagnosis in Breast Pathology*, Atlas of Anatomic Pathology,
DOI 10.1007/978-1-4939-6697-4_13

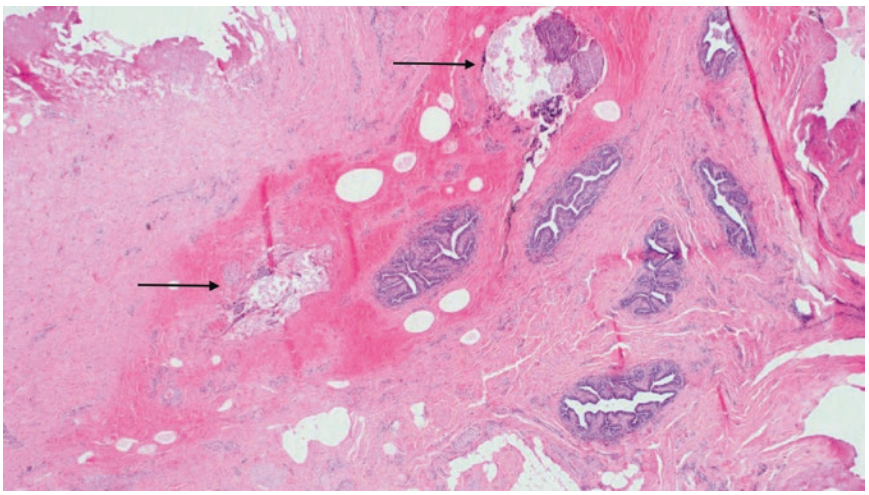

Fig. 13.1 Squamous metaplasia of lactiferous ducts. Microdochectomy specimen shows the profiles of several lactiferous ducts with surrounding haemorrhage. In the upper and mid-fields (*arrows*), there is squamous epithelium with keratinous flakes

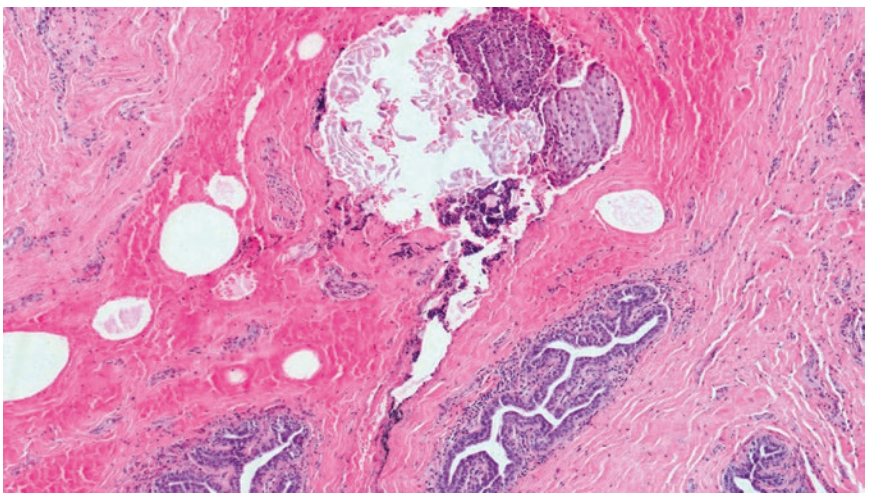

Fig. 13.2 Squamous metaplasia of lactiferous ducts shows accumulation of keratin and surrounding squamous epithelium extending between portions of lactiferous ducts. Periductal chronic inflammation is present

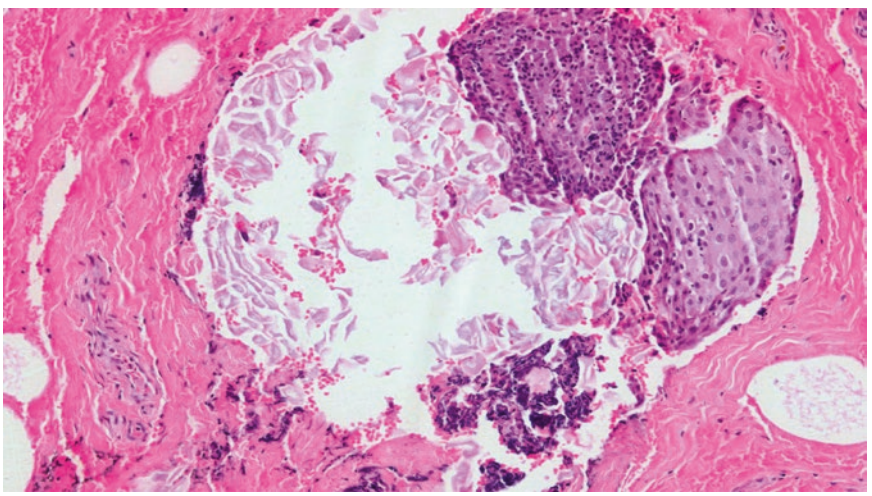

Fig. 13.3 Squamous metaplasia of lactiferous ducts. Keratin plug with squamous epithelium

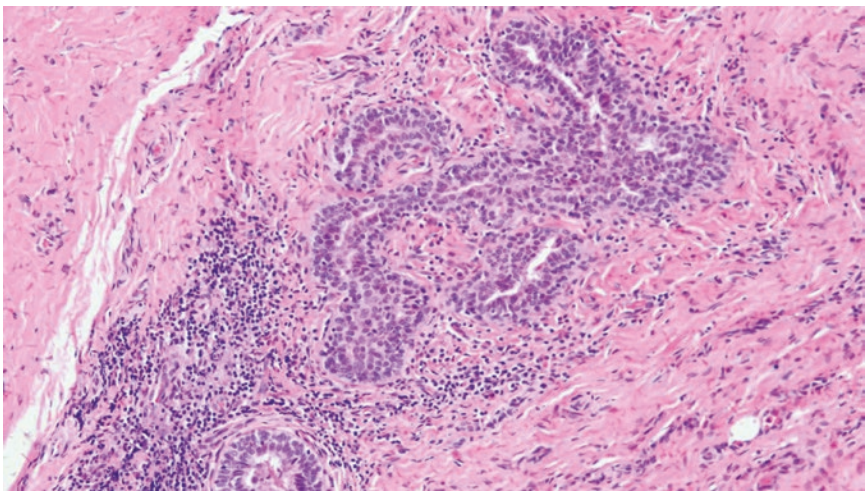

Fig. 13.4 Periductal chronic inflammation along the lactiferous duct in the vicinity of the keratin plug and squamous metaplasia

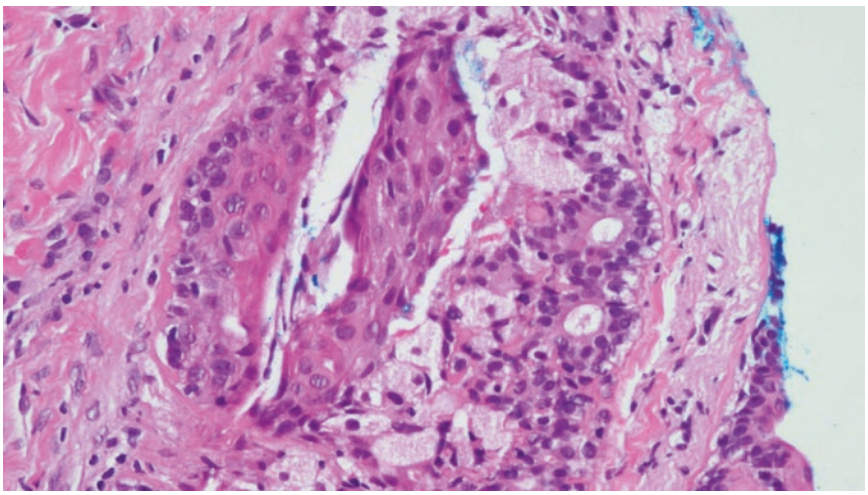

Fig. 13.5 Squamous metaplasia of a lactiferous duct. Pavemented squamous epithelium with polygonal cells containing vesicular nuclei, discernible nucleoli, and pink cytoplasm replaces part of the duct wall. Several foamy histiocytes are also seen

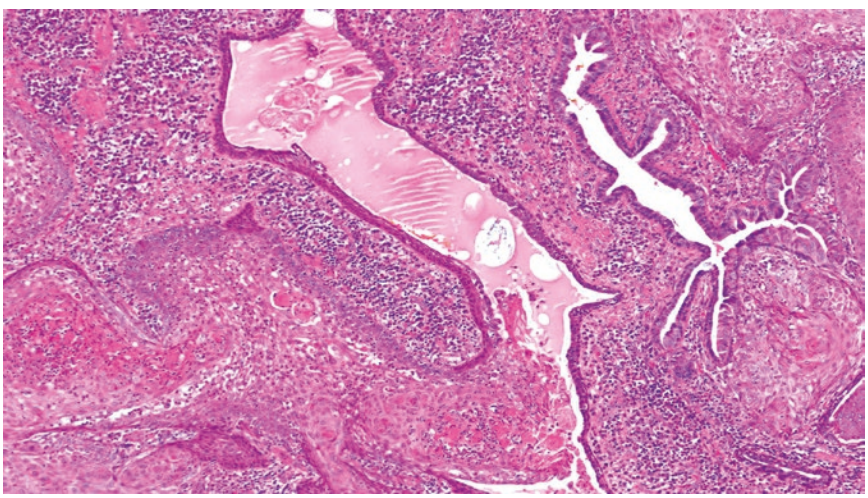

Fig. 13.6 Squamous metaplasia of lactiferous ducts, with part of the duct wall replaced by pavemented squamous epithelium, facing the opposite duct wall of columnar epithelium. Relatively intense chronic inflammation is seen in the periductal stroma

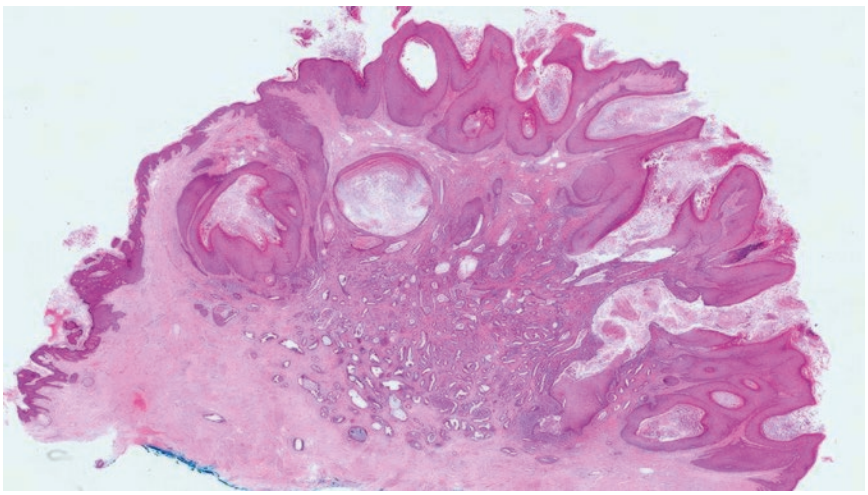

Fig. 13.7 Squamous papilloma overlying a nipple adenoma. At scanning magnification, a verrucous squamous lesion is seen on the nipple surface, featuring exophytic papillomatosis, acanthosis, and hyperkeratosis. A few cysts containing laminated keratin are present. Closely associated with the cysts and occurring within the nipple stroma is a proliferation of closely packed glands constituting the adenoma

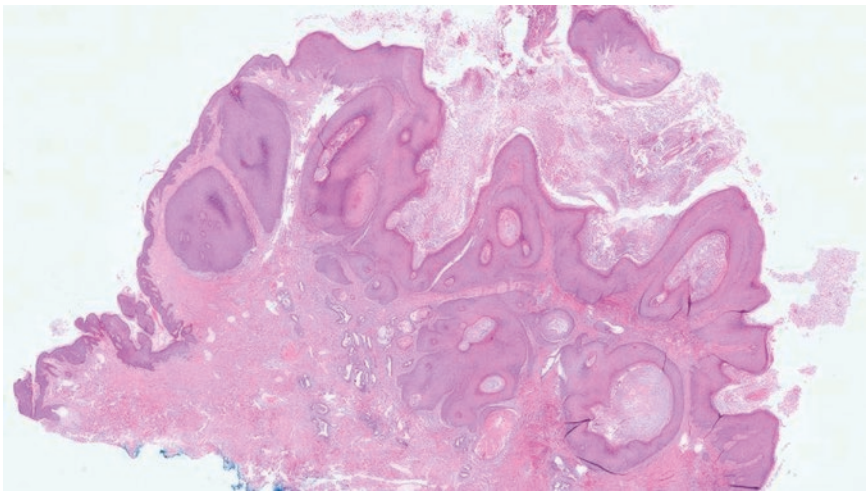

Fig. 13.8 Squamous papilloma overlying a nipple adenoma. Another view of the squamous papilloma with keratin layers and squamous invaginations into the stroma, intermingling with the glands of the adenoma

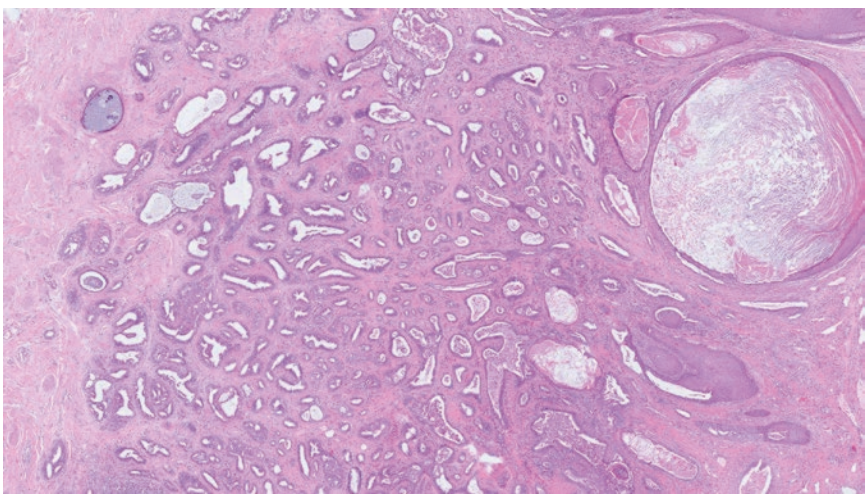

Fig. 13.9 Squamous papilloma overlying a nipple adenoma. The nipple adenoma deep to the nipple squamous papilloma shows crowded glands of varying sizes, some of which are dilated and display luminal epithelial folds. The squamous epithelium merges with the glandular proliferation

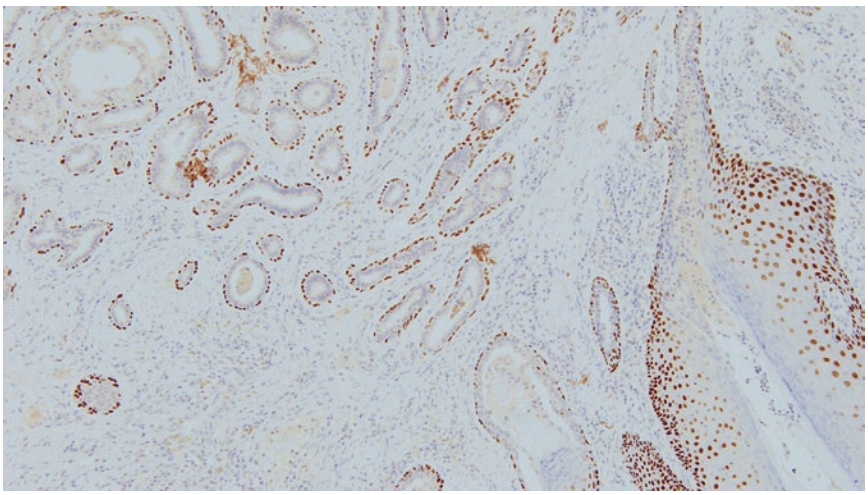

Fig. 13.10 Squamous papilloma with nipple adenoma. Immunohistochemistry for p63 shows positive nuclear staining of the squamous epithelial cells. Myoepithelial cells around glands of the nipple adenoma are also decorated

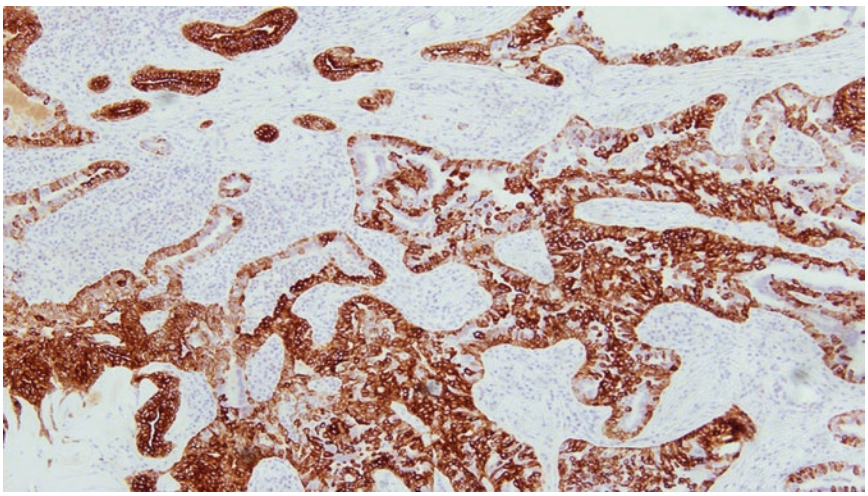

Fig. 13.11 Squamous papilloma with nipple adenoma. The nipple adenoma deep to the squamous papilloma shows usual ductal hyperplasia; the epithelial proliferation shows heterogeneous staining for the high-molecular-weight keratin CK5/6

a scaly lesion [4]. It has been described occurring after radiation treatment for breast carcinomas treated with conservative surgery [5]. Histologically, the superficial portions of the tumour may resemble a squamous papilloma (Fig. 13.13). Reactive atypia of squamous epithelium in Zuska's disease may raise concern for a neoplastic lesion and mimic squamous cell carcinoma. Examination of the deeper portions of the tumour identifies invasive islands (Figs. 13.14, 13.15, and 13.16). Depending on histological grade, keratinisation may or may not be prominent. A well-differentiated squamous cell carcinoma may resemble a keratoacanthoma, but the latter is vanishingly rare, with only one case reported in the nipple [6].

Prognosis and Therapy Considerations

Surgical excision of affected ducts and fistula in Zuska's disease is curative [7].

Nipple Adenoma

Definition

The nipple adenoma is a benign epithelial proliferation centred around the lactiferous ducts, comprising closely arranged tubules with occasional papillary infoldings [8].

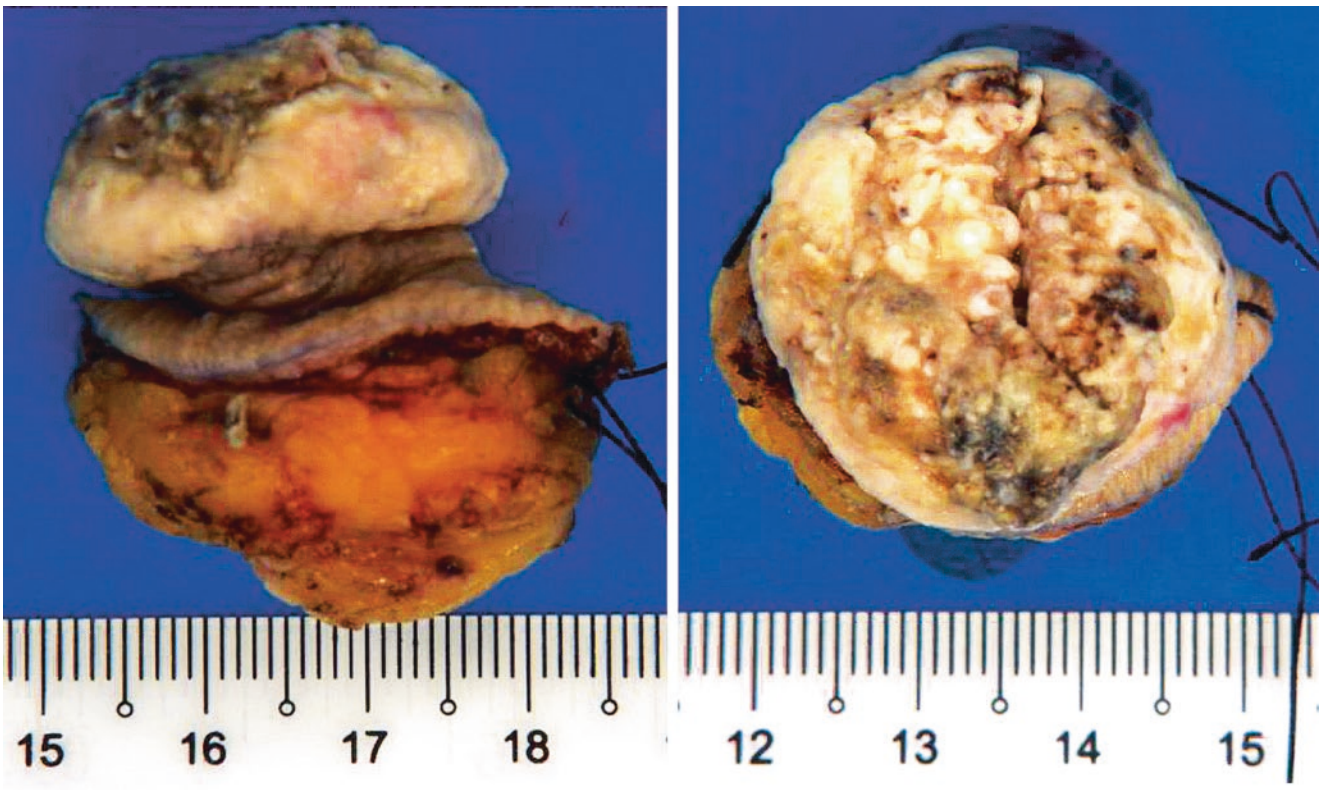

Fig. 13.12 Nipple squamous cell carcinoma, invasive. Gross appearance of the fungating, ulcerated tumour arising from the nipple with overhanging rolled edges. The nipple is completely destroyed by the tumour, leaving an intact areolar rim

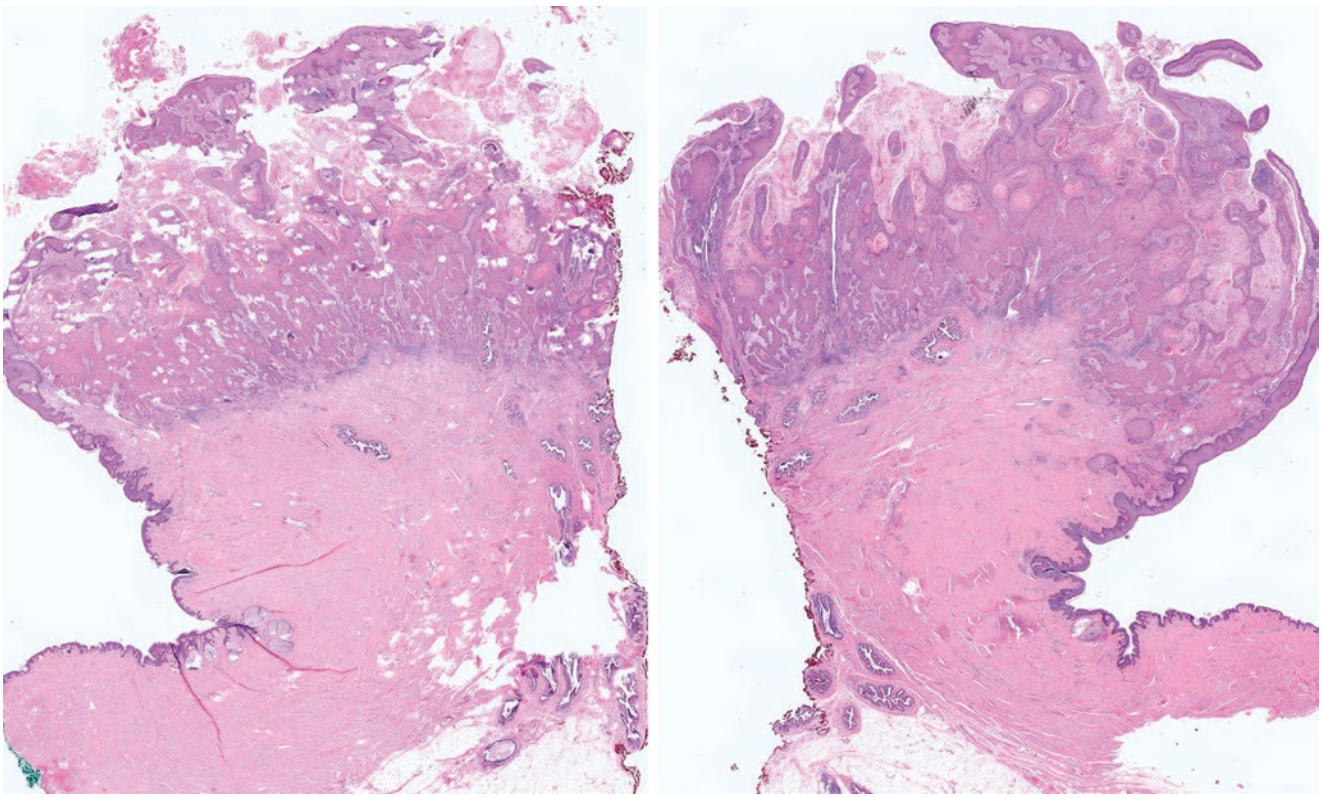

Fig. 13.13 Nipple squamous cell carcinoma, invasive. A hyperkeratotic, verrucous tumour with an exophytic growth pattern may resemble a squamous papilloma at scanning magnification

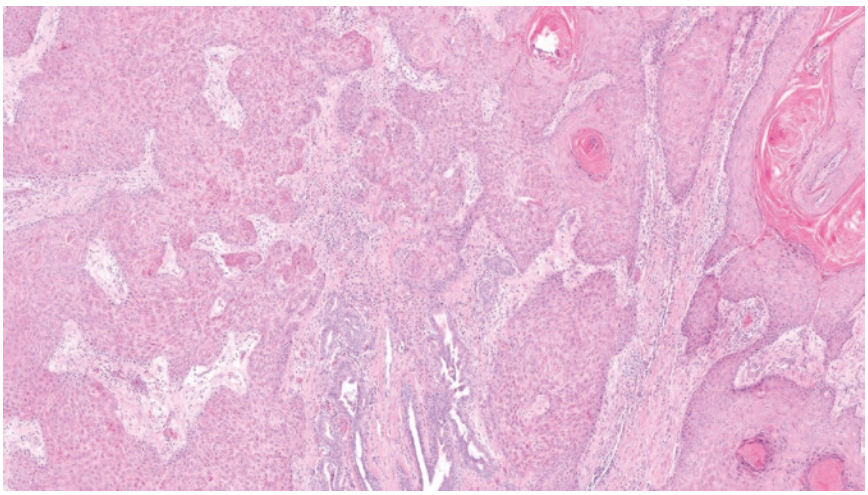

Fig. 13.14 Nipple squamous cell carcinoma, well differentiated, shows anastomosing, confluent islands of squamous cells with keratinisation, surrounding lactiferous ducts. The pavemented squamous islands show irregular tongue-like protrusions into the inflamed fibrotic stroma

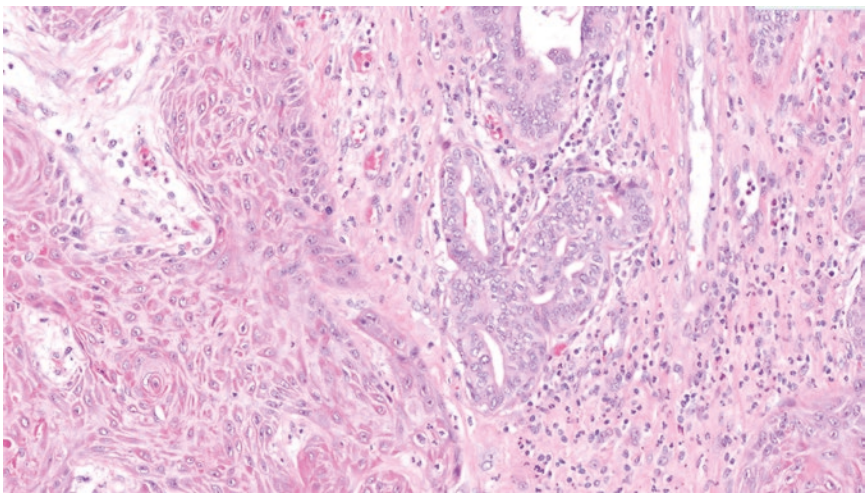

Fig. 13.15 Nipple squamous cell carcinoma, invasive. Tumour islands comprising polygonal cells with vesicular nuclei, distinct nucleoli, pink cytoplasm, intercellular bridges, and occasional mitoses are juxtaposed to benign ducts

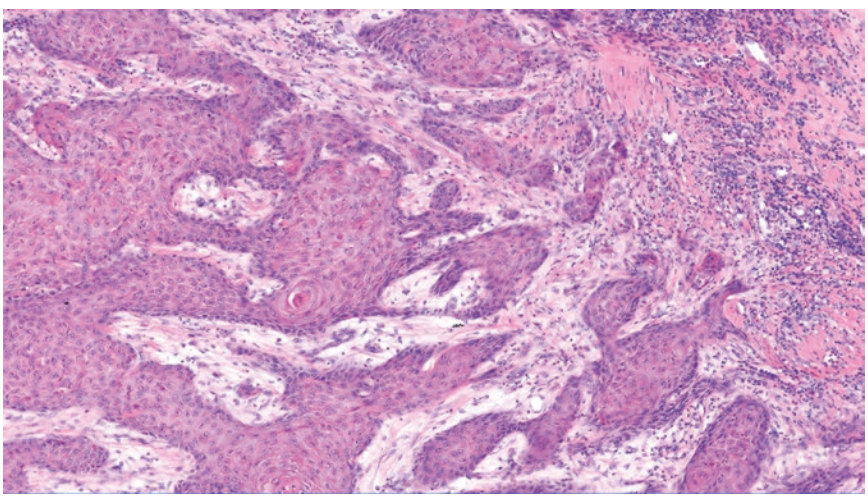

Fig. 13.16 Nipple squamous cell carcinoma, invasive. Irregular tongues of invasive squamous cell carcinoma with occasional squamous whorls are seen within the inflamed stroma

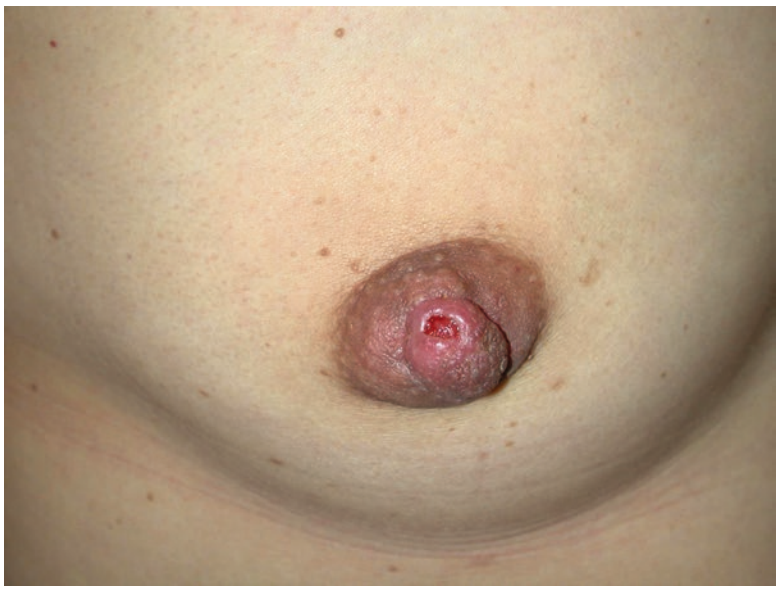

Fig. 13.17 Nipple adenoma. Nipple shows a haemorrhagic erosion. Excision confirmed the presence of a nipple adenoma histologically (Courtesy of Dr. Karen Yap)

Clinical and Epidemiological Features

Nipple adenomas usually occur in adult women over a wide age range, though cases in paediatric patients and men have been described. Clinical symptoms are nipple discharge, erosion (Fig. 13.17), or nodule.

Imaging Features

Nipple adenomas are usually small and are not seen on mammography. They may be detected as well-circumscribed, hypervascular nodules within the nipple on sonography.

Pathologic Features

Macroscopic Pathology

Erosion of the nipple associated with the nipple adenoma may resemble Paget disease. The nipple adenoma can also be macroscopically observed as a nodular lesion in the nipple stroma. Sometimes, no gross abnormalities are discernible.

Microscopic Pathology

Commonly, the histological appearance is that of closely packed tubules with sclerosing adenosis and variable cystic dilatation. Some tubules may demonstrate luminal papillary folds, hence the synonymous term of *florid papillomatosis of the nipple*, though the current preferred terminology is *nipple adenoma*. The myoepithelial layer is preserved. Although the lesion may appear relatively circumscribed at low magnification, no capsule is present, and epithelial nests may stream into the surrounding stroma. Usual ductal hyperplasia can be seen, with occasional necrosis and epithelial mitoses (Figs. 13.18, 13.19, 13.20, 13.21, and 13.22). Increased numbers of Toker cells in the overlying epithelium may lead to confusion with Paget disease [8].

Differential Diagnosis

Intraductal Papilloma

As the nipple adenoma may sometimes feature papillary luminal folds, it can resemble the intraductal papilloma. Conversely, intraductal papilloma can become sclerosed and comprise compressed tubules mimicking nipple adenoma. Whereas nipple adenoma consists predominantly of proliferating glands and tubules, intraductal papilloma shows a lesional core composed of arborescent papillary fronds arising from the walls of lactiferous ducts and projecting into the ductal lumen (Figs. 13.23, 13.24, and 13.25).

Syringomatous Tumour

In contrast to the nipple adenoma which has a rounded configuration at low magnification and comprises closely packed tubules, the syringomatous tumour consists of patent, angulated tubules and epithelial nests with a permeative pattern, located within the stroma and extending into smooth muscle bundles of the nipple and areola. Individual cell keratinisation and squamous whorls may be observed (*see* section "Syringomatous Tumour").

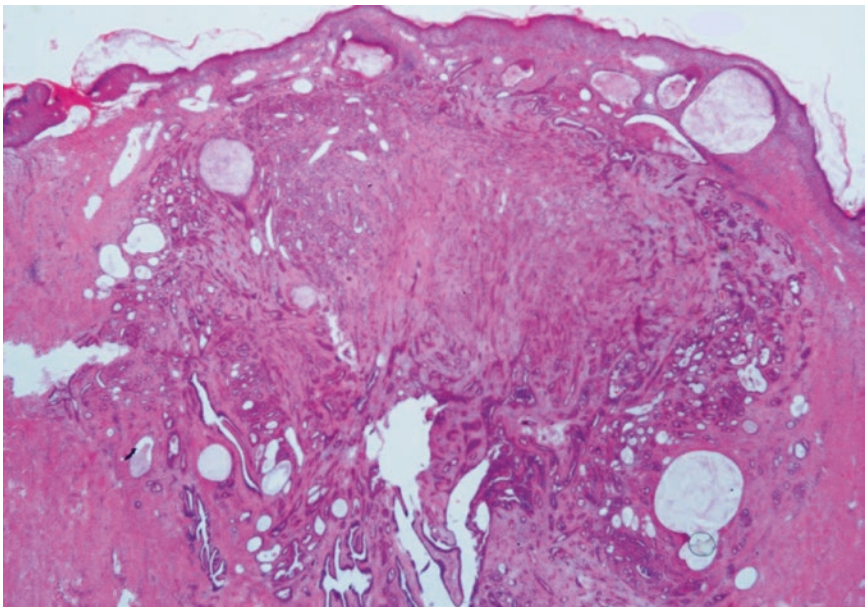

Fig. 13.18 Nipple adenoma. Low magnification shows a proliferation of glands deep to the nipple epidermis, some of which are cystically dilated. Sclerosis is present in part of the adenoma where there is a solidified appearance

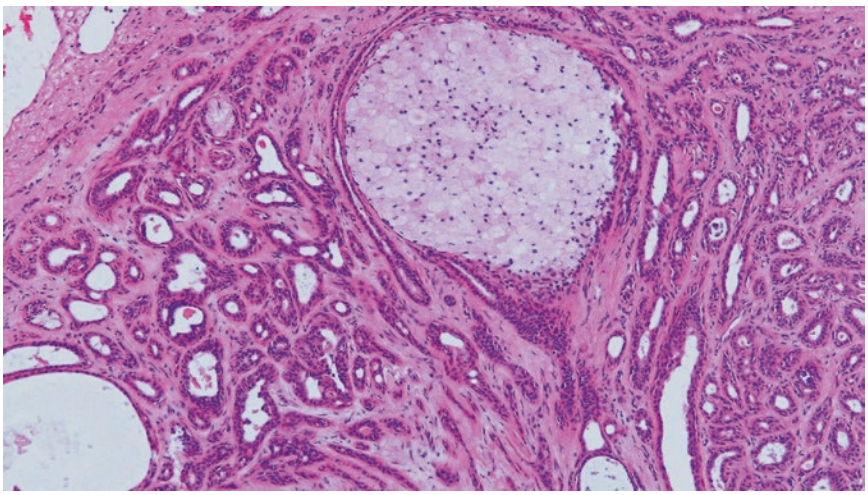

Fig. 13.19 Nipple adenoma. Medium magnification shows bilayered tubules, some of which contain luminal pink secretions. Dilated glands with luminal foam cells are present. The stroma around the glands is fibrotic and hyalinised

Invasive Carcinoma

As the nipple adenoma may incorporate sclerosing adenosis, its pseudo-infiltrative pattern can resemble an invasive process usually of low histological grade. Recognisable bilayered tubules tend to constitute a significant component of the nipple adenoma.

Adnexal-Type Tumours

A variety of adnexal (sweat gland)-type epithelial tumours may arise in the nipple, including the nodular hidradenoma and syringocystadenoma papilliferum. These may be mistaken for nipple adenoma (Figs. 13.26, 13.27, 13.28, 13.29, 13.30, 13.31, and 13.32).

Prognosis and Therapy Considerations

Complete excision is curative. Recurrences may occur if the lesion is incompletely removed.

Syringomatous Tumour

Definition

Syringomatous tumour is an uncommon, locally permeative tumour that shows sweat duct differentiation. These tumours were previously referred to as syringomatous adenoma, but

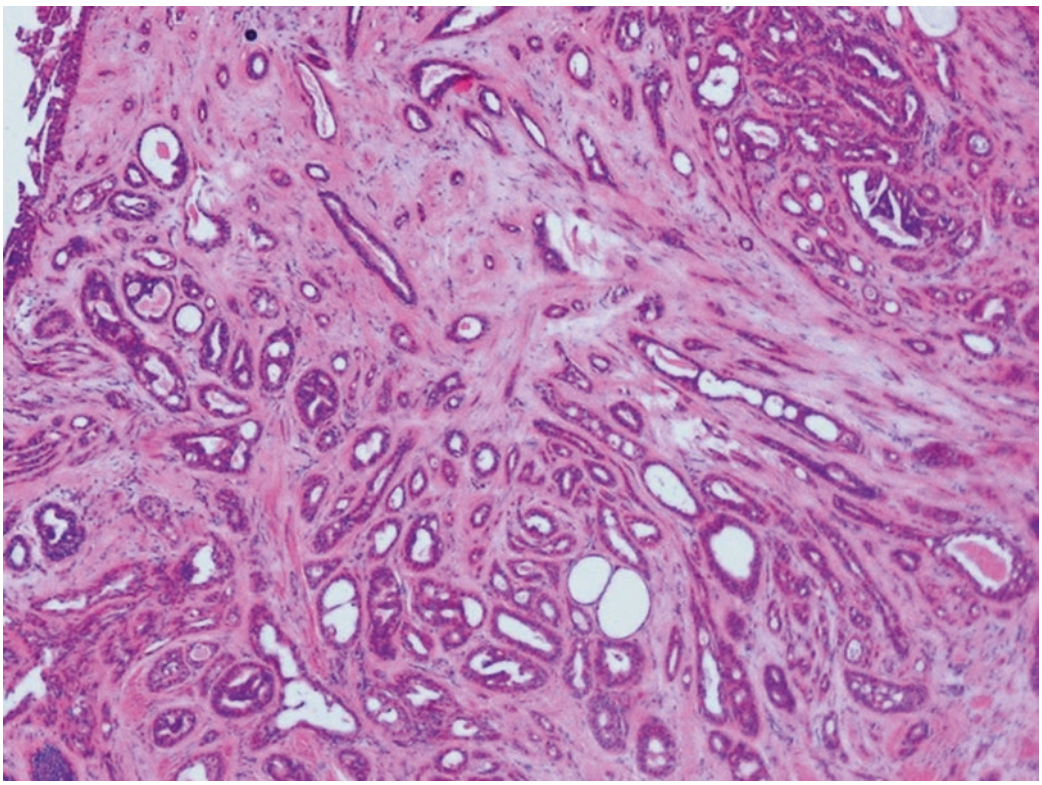

Fig. 13.20 Nipple adenoma. Sclerosing adenosis within a nipple adenoma. The compressed, pseudoinvasive tubules may mimic a low-grade invasive carcinoma. The presence of myoepithelial cells, intact basement membranes and lack of invasion into surrounding tissue support a benign process

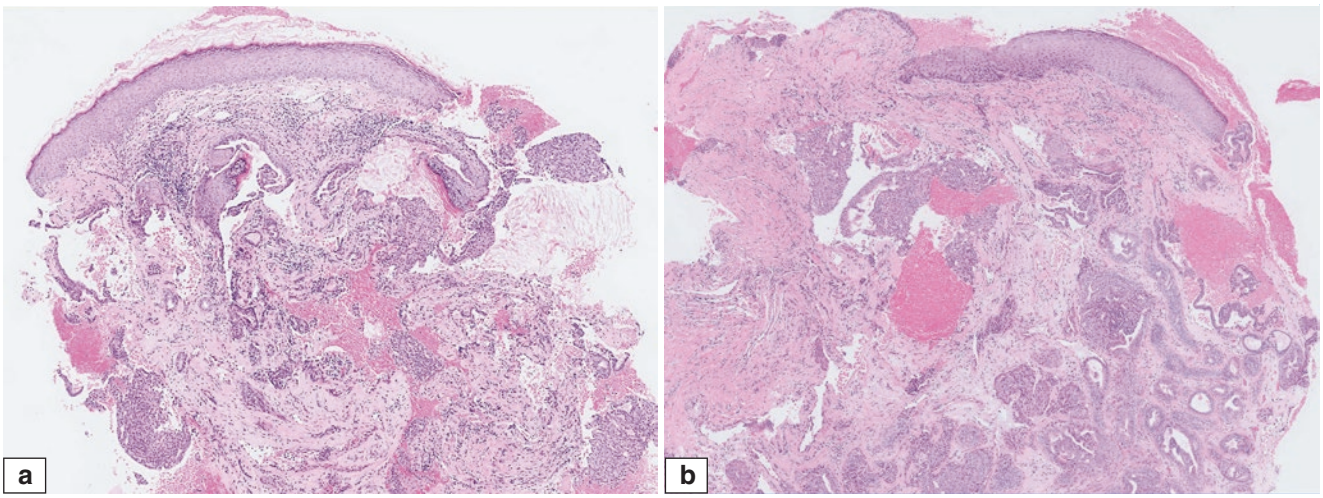

Fig. 13.21 Nipple adenoma. (**a**, **b**) At low magnification, the nipple lesion shows a vaguely rounded configuration, with solid epithelial nests, cystic dilatation of ducts, and luminal projections of epithelium. Communication of the lesion with the nipple epidermis may lead to nipple discharge and the appearance of nipple erosion

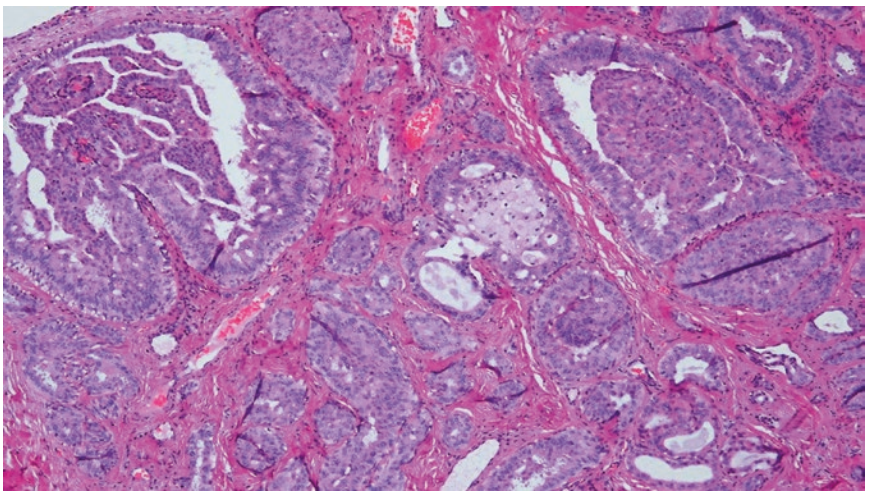

Fig. 13.22 Nipple adenoma. Usual ductal hyperplasia, including luminal papillary infoldings and foamy histiocytes, is present

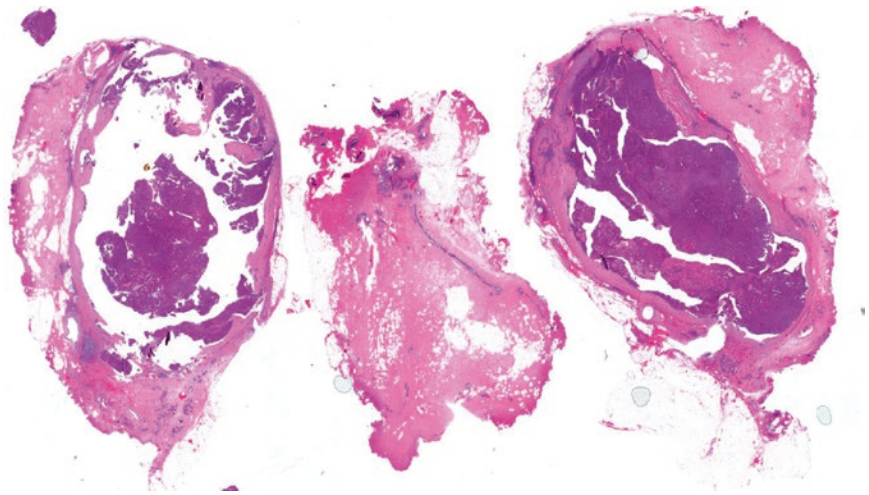

Fig. 13.23 Intraductal papilloma in the retroareolar region, presenting as a nipple-areolar lump. At scanning magnification, the lactiferous duct shows cystic dilatation and a partially solid–cystic epithelial mass

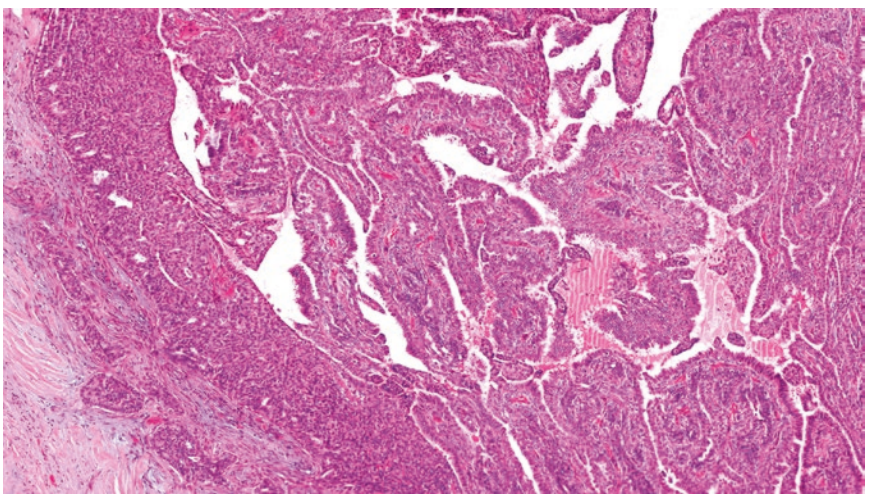

Fig. 13.24 Intraductal papilloma. Medium magnification shows arborescent papillary fronds that are supported by congested fibrovascular septa. The fibrous wall of the cystically dilated duct shows a few entrapped epithelial nests and glands

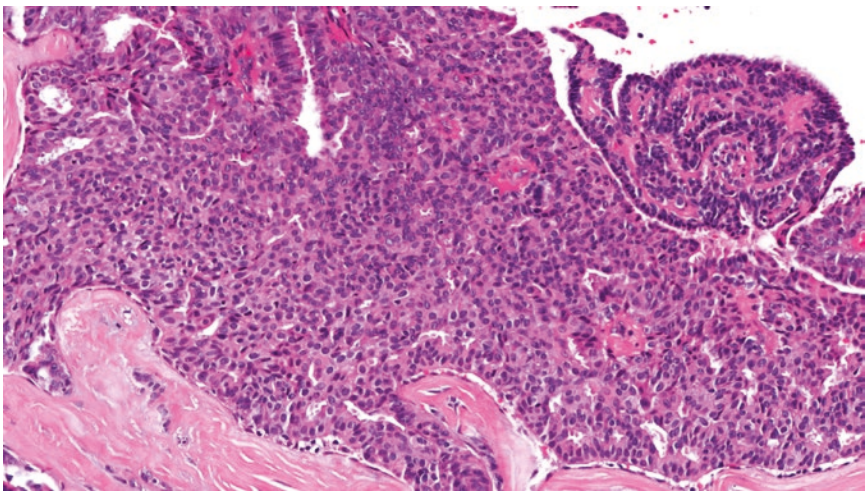

Fig. 13.25 Intraductal papilloma. There is usual ductal hyperplasia with overlapped nuclei of a heterogeneous epithelial population. Irregular slit-like spaces are present

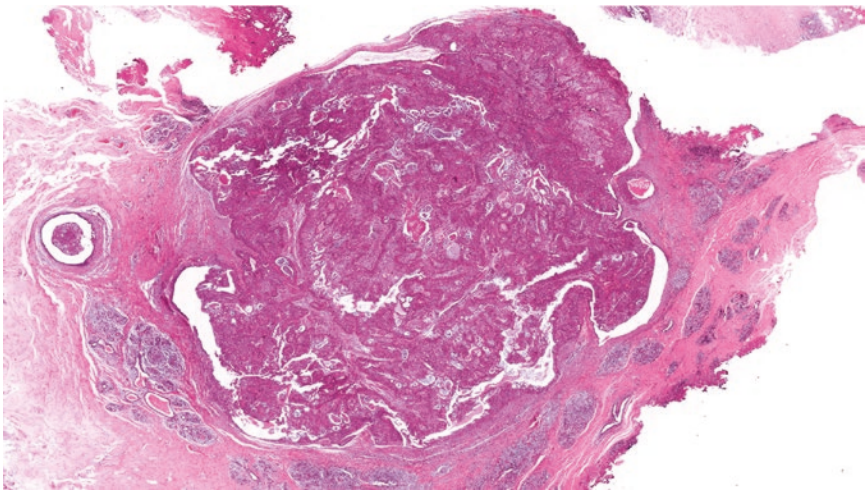

Fig. 13.26 Adnexal-type (eccrine) tumour with a solid–cystic papillary architecture, occurring in the nipple-areolar region and resembling a hidradenoma. Low magnification shows resemblance to an intraductal papillary lesion

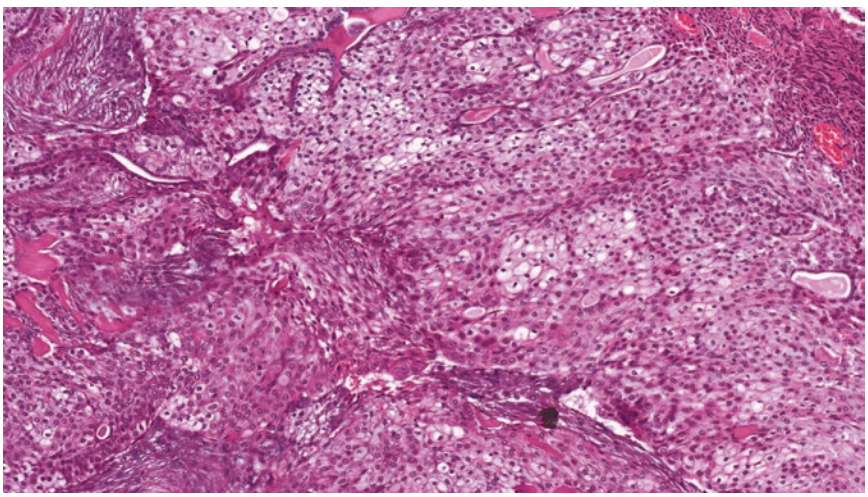

Fig. 13.27 Adnexal-type tumour. Medium magnification shows collections of clear cells interspersed with polygonal cells harbouring pink cytoplasm, which form solid sheets of epithelial cells that are punctuated by ducts lined by flattened epithelium. The ducts contain pink secretions

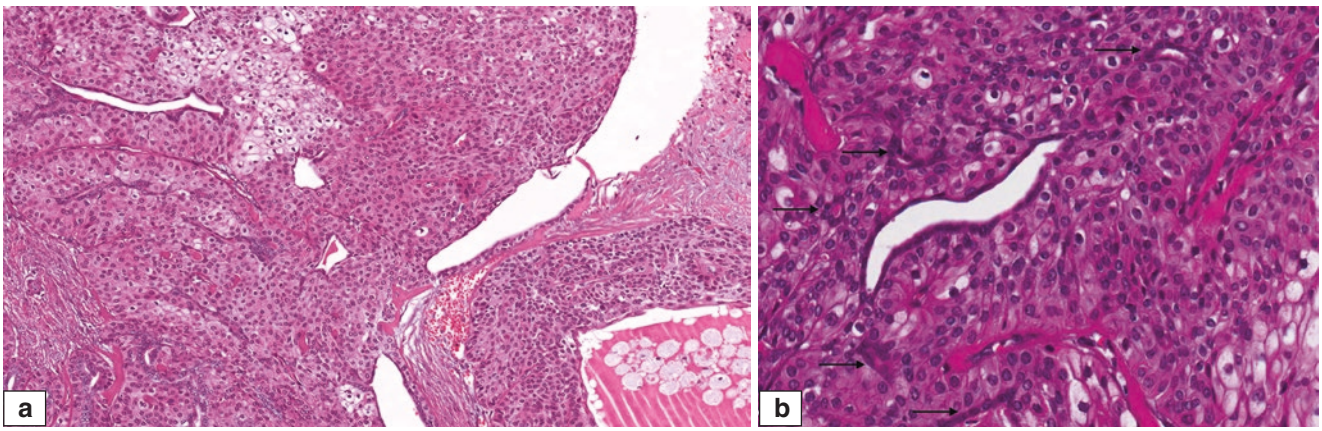

Fig. 13.28 (**a**) Adnexal-type tumour shows pale and pink polygonal cells surrounding elongated duct spaces lined by flattened epithelial cells. (**b**) High magnification of a duct lined by flattened epithelium, surrounded by pavemented epithelial cells with pink and clear cytoplasm. Several smaller, less conspicuous ducts are also seen (*arrows*)

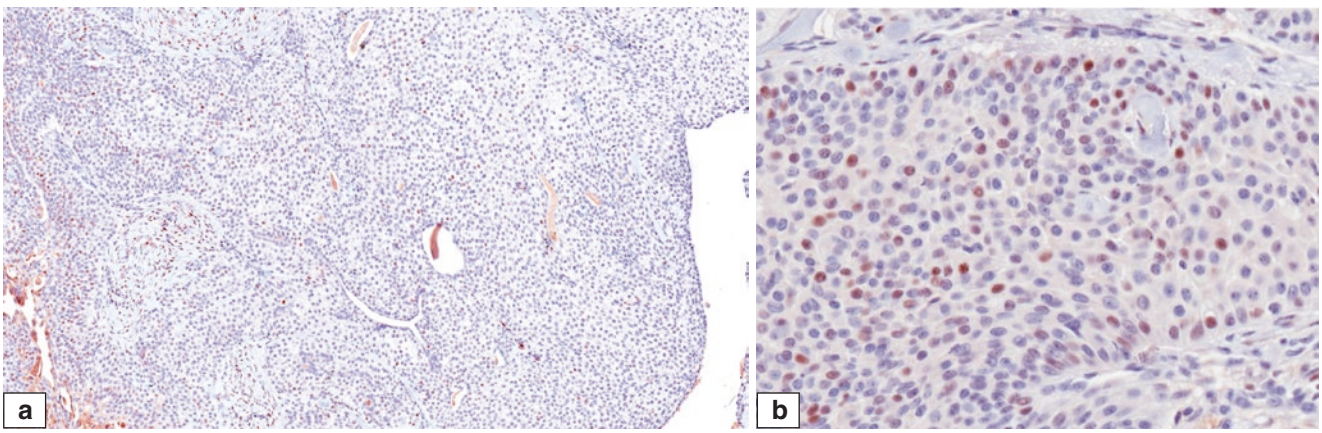

Fig. 13.29 Adnexal-type tumour. (**a**) Immunohistochemistry for oestrogen receptor (ER) is weakly and patchily positive. (**b**) High magnification shows scattered nuclear reactivity of the epithelial cells for ER

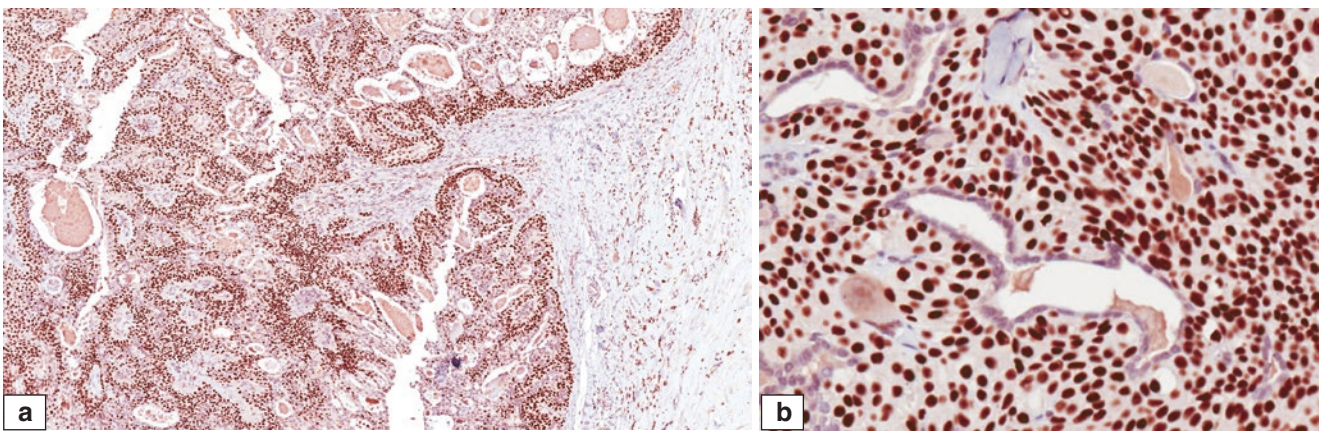

Fig. 13.30 Adnexal-type tumour. (**a**) Immunohistochemistry for p63 shows diffuse positivity of the epithelial cells, with sparing of the ductal lining epithelium. (**b**) High magnification of epithelial nuclei demonstrating intense p63 reactivity, contrasting against the negatively stained ductal epithelium

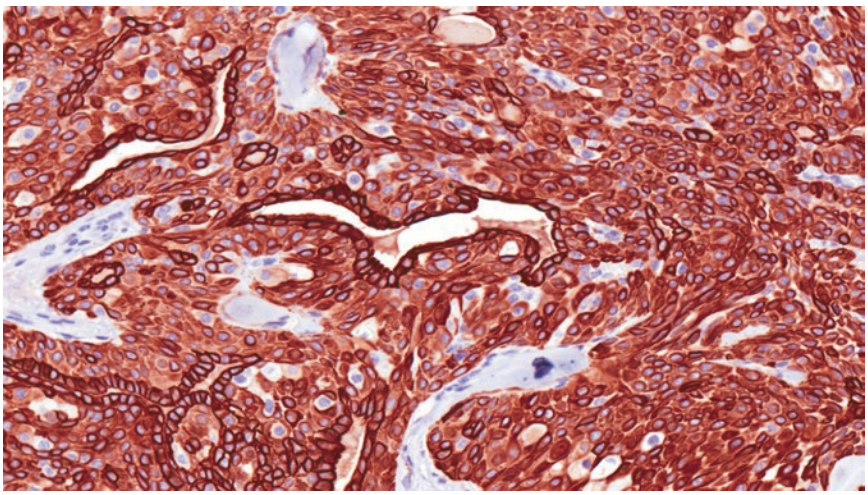

Fig. 13.31 Adnexal-type tumour. CK14 immunohistochemistry shows diffuse staining, with more intense reactivity observed for the ductal epithelium

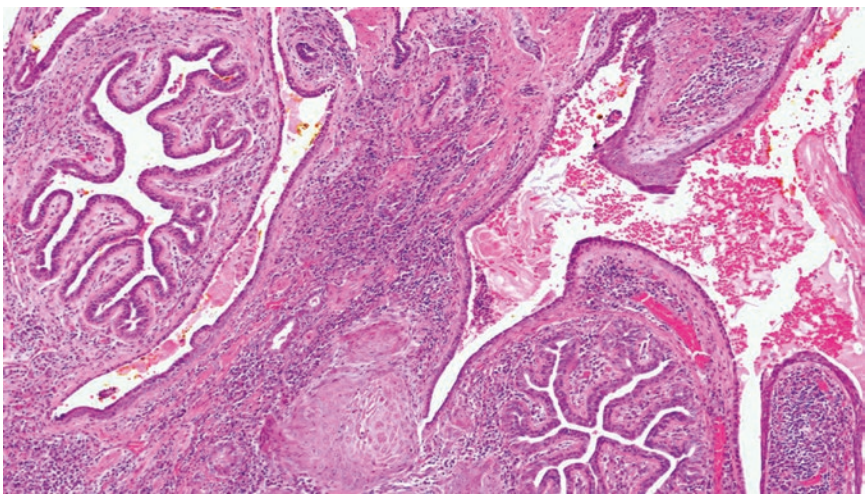

Fig. 13.32 An unusual nipple lesion with some appearances resembling a syringocystadenoma papilliferum with inflamed, broad stromal folds covered by epithelium. Portions of lactiferous ducts cut transversely are seen, as well as islands of squamous epithelium

the term *tumour* is preferred because of its histologic invasive appearance and the propensity for local recurrence.

Clinical and Epidemiological Features

Patients over a wide age range can be affected, clinically presenting with a firm nodule in the nipple-areolar region.

Imaging Features

The tumour has a varied appearance on imaging. It can appear as a spiculated, ill-defined subareolar mass that is indistinguishable from malignancy. It can also be seen as a nonspecific, well-circumscribed subareolar mass. Pleomorphic nipple microcalcifications without a mass and diffuse skin thickening have been reported [9].

Pathologic Features

Macroscopic Pathology

A firm, nodular lesion with ill-defined borders is present in the nipple stroma or the dermis of the nipple-areolar complex.

Microscopic Pathology

Histologically, the syringomatous tumour comprises patent, angulated tubules, epithelial nests, and cords that percolate through the fibrotic stroma and extend into smooth muscle bundles of the nipple and areola. Keratin cysts and squamous

whorls may be observed. The edges of the tumour can be difficult to determine because of its permeative nature. The tubules are often bilayered, with the outer layer of cells staining immunohistochemically with basal and myoepithelial markers; the solid tumour nests are also reactive with these antibodies (Figs. 13.33, 13.34, 13.35, 13.36, 13.37, 13.38, 13.39, and 13.40).

Differential Diagnosis

Low-Grade Adenosquamous Carcinoma

There are close histological and biological similarities between the nipple syringomatous tumour and low-grade adenosquamous carcinoma [10]. The main difference is that low-grade adenosquamous carcinoma occurs in breast parenchyma instead of in the nipple-areolar region (Figs. 13.41, 13.42, and 13.43).

Tubular Carcinoma

The angulated, patent tubules of the syringomatous tumour resemble those of tubular carcinoma, but tubular carcinoma does not demonstrate squamous differentiation. Immunohistochemically, tubular carcinoma shows positive hormone receptor expression and lacks myoepithelial cells, whereas the syringomatous tumour is usually hormone receptor negative and shows positive reactivity for myoepithelial markers (Figs. 13.44, 13.45, and 13.46).

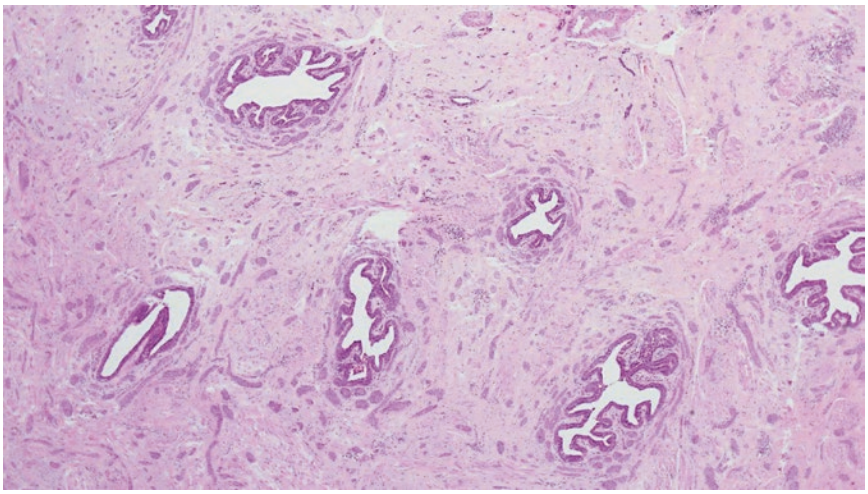

Fig. 13.33 Syringomatous tumour. Epithelial nests and elongated cords extend through the stroma around lactiferous ducts

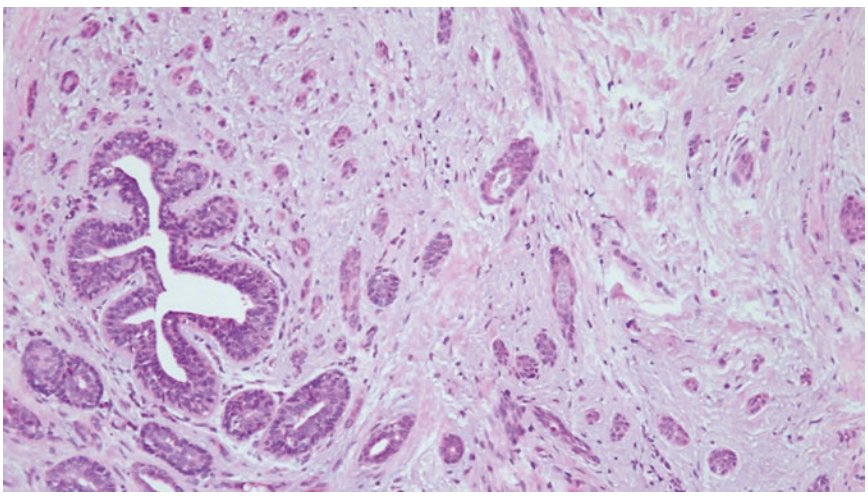

Fig. 13.34 Syringomatous tumour. Small nests and occasional tubules of epithelial cells are seen around a lactiferous duct

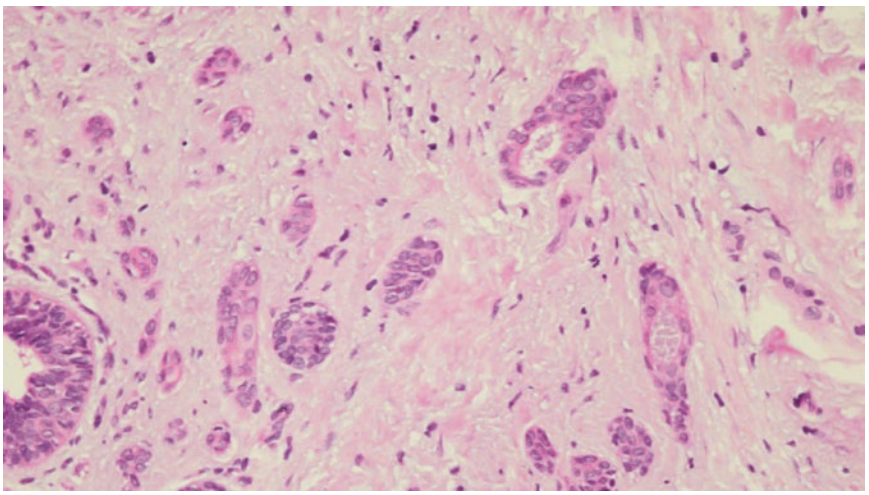

Fig. 13.35 Syringomatous tumour. The epithelial nests and tubules are composed of cells with pink cytoplasm and vesicular nuclei, contrasting against those of the lactiferous ducts. The tubule in the right lower field shows a tapered end. The tubular lumens contain pale, wispy material. A peripheral rim of compressed basal/myoepithelial cells can be discerned

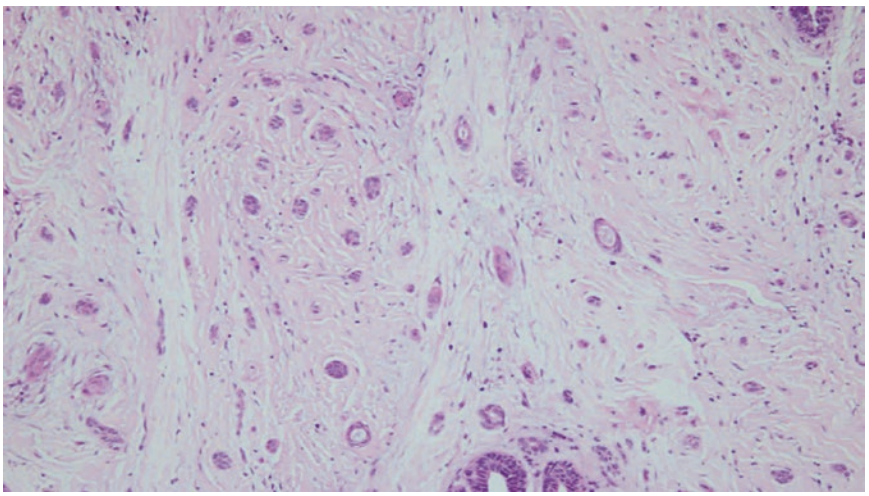

Fig. 13.36 Syringomatous tumour. Epithelial nests and tubules permeate the stroma and nipple-areolar smooth muscle bundles

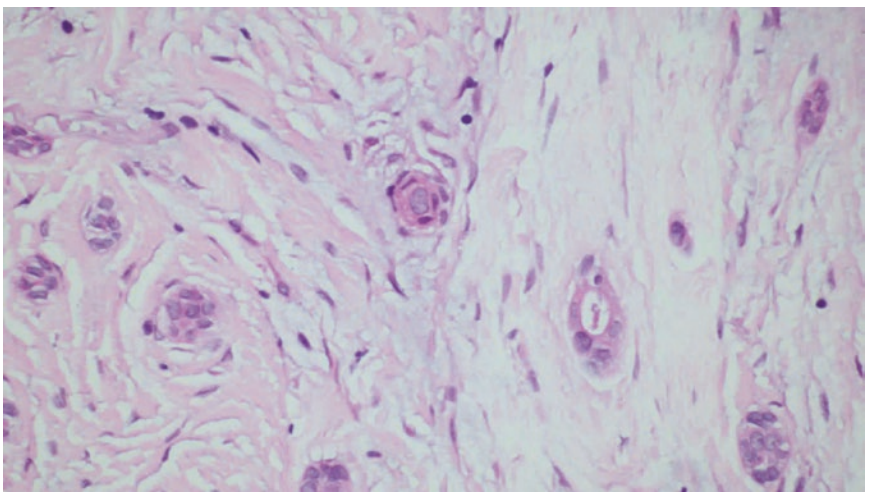

Fig. 13.37 Syringomatous tumour. High magnification shows small epithelial nests with a whorl-like appearance, composed of polygonal cells with pink cytoplasm and vesicular nuclei. A small tubule with a teardrop shape is seen

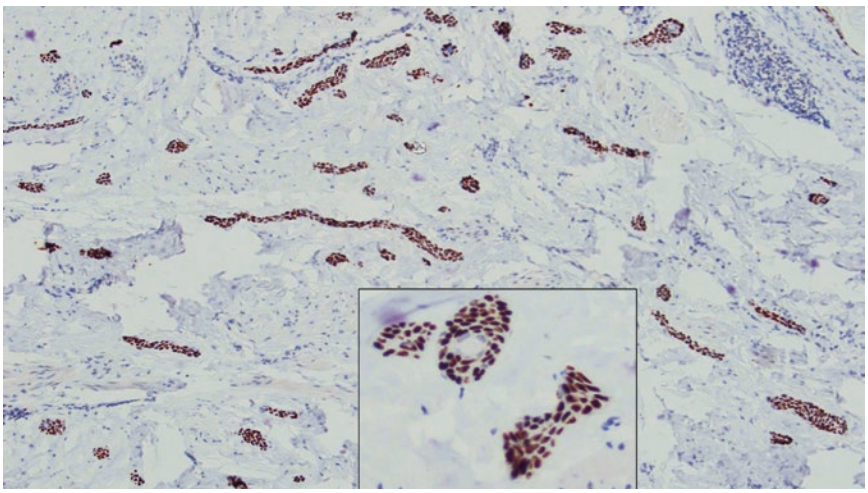

Fig. 13.38 Syringomatous tumour. Immunohistochemistry for p63 shows positive staining of the lesional cells. Inset shows high magnification of tubules and epithelial nests, which are highlighted by p63

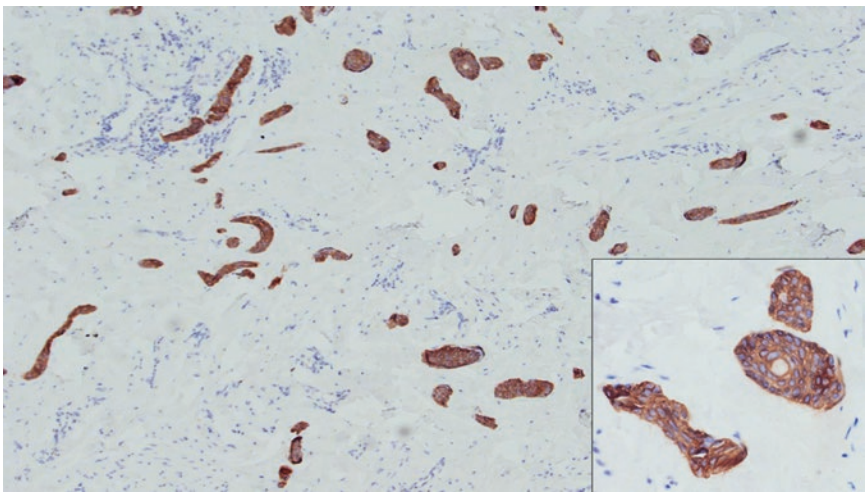

Fig. 13.39 Syringomatous tumour. Immunohistochemistry for the high-molecular-weight keratin CK14 shows positive reactivity of the lesional cells. *Inset* shows cytoplasmic and membrane decoration with CK14

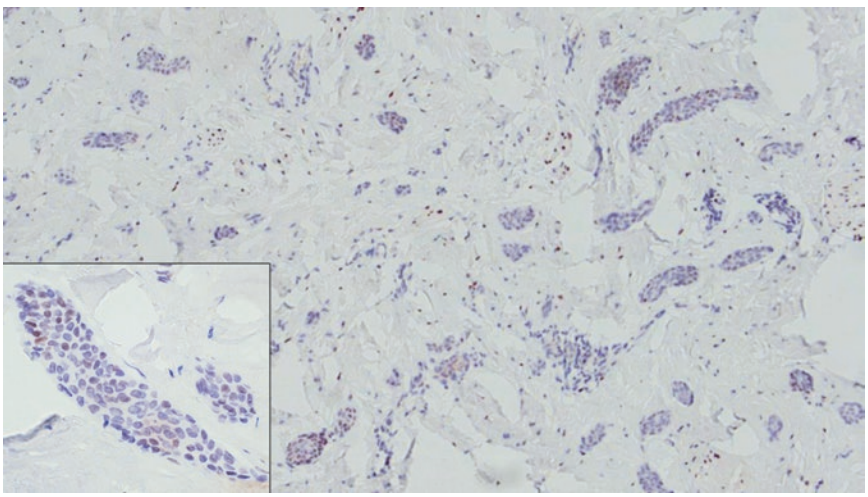

Fig. 13.40 Syringomatous tumour. ER immunohistochemistry is usually negative, but in this case, focal, weak staining is observed in a few lesional cells (*inset*)

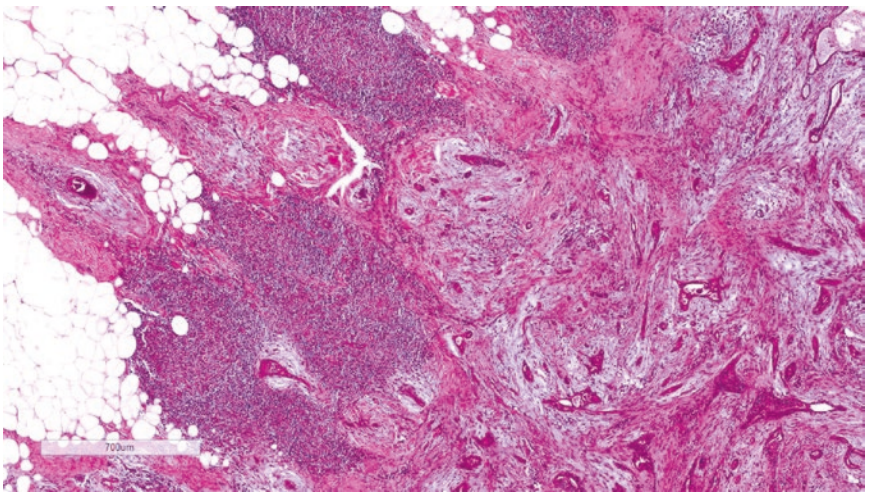

Fig. 13.41 Low-grade adenosquamous carcinoma, a form of metaplastic breast cancer, is located within the breast parenchyma; it shows histological similarity to the nipple syringomatous tumour. At low magnification, low-grade adenosquamous carcinoma shows an infiltrative margin with nests and angulated tubules of epithelial cells disposed within a fibrous stroma. Aggregates of lymphocytes are often observed at the periphery of the tumour, arranged in a pattern that resembles cannonballs

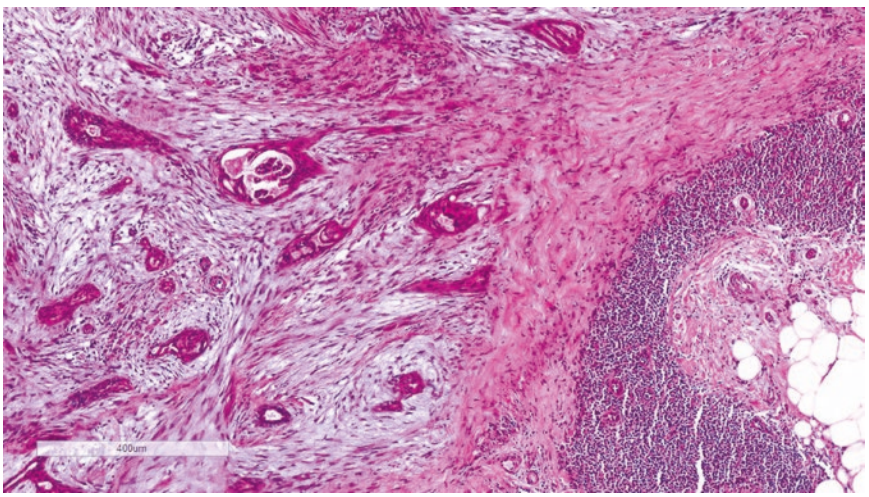

Fig. 13.42 Low-grade adenosquamous carcinoma. A lamellar-like arrangement of stromal spindle cells is noted around the epithelial nests and islands, many of which show tail-like extensions merging with the spindle cell stroma

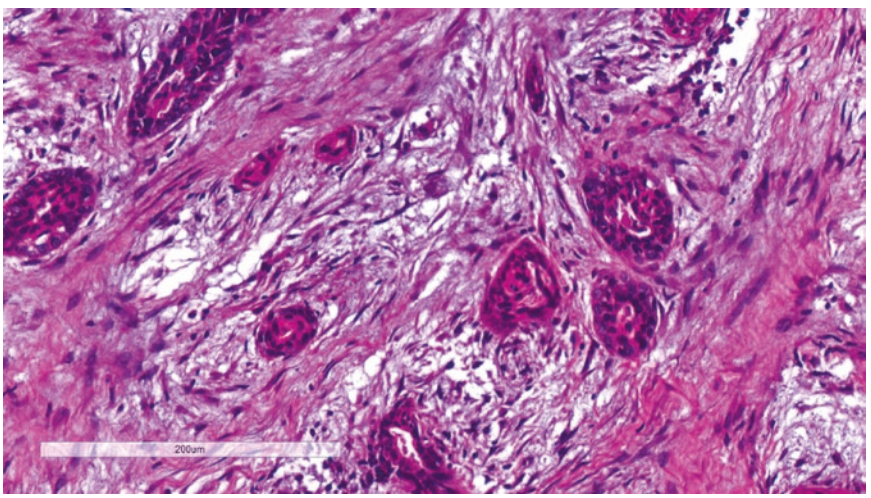

Fig. 13.43 Low-grade adenosquamous carcinoma. Some epithelial nests comprise polygonal cells with pink, eosinophilic cytoplasm, indicating squamoid differentiation. Immunohistochemistry findings are inconsistent and can resemble patterns similar to those of the syringomatous tumour, with positive reactivity for p63 and basal markers, often seen in cells placed at the periphery of the tumour nests

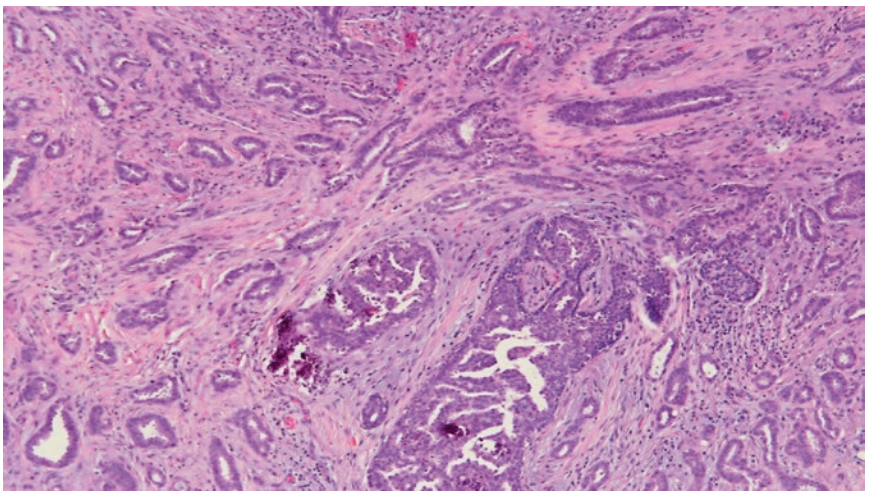

Fig. 13.44 Tubular carcinoma. This special type of invasive breast cancer has an excellent prognosis. It is composed of patent, angulated tubules lined by cuboidal cells, which sometimes disclose apical snouts. The comma-shaped and twisted tubules may resemble those of syringomatous tumour, but unlike the syringomatous tumour, there are no squamoid features and no staining with basal or myoepithelial markers. Low-grade DCIS, present in this case and associated with calcifications, may be encountered in tubular carcinoma

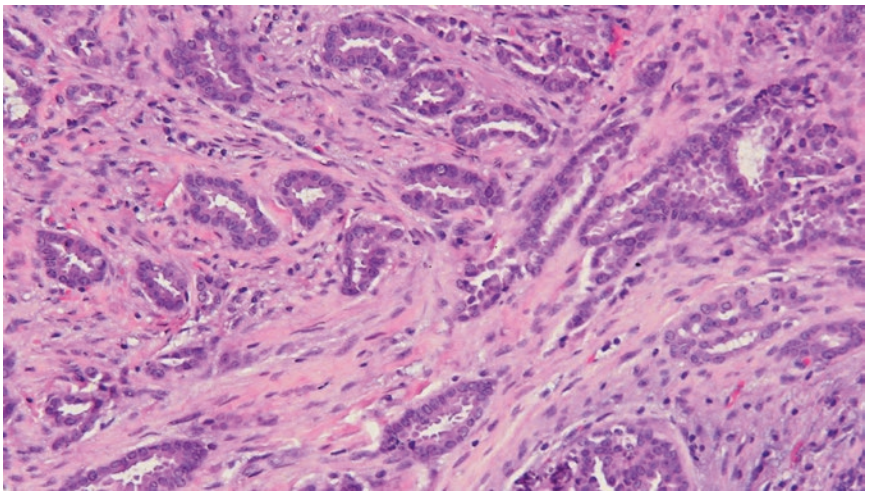

Fig. 13.45 Tubular carcinoma. Patent tubules are haphazardly placed within desmoplastic stroma. The tubules are round, elongated, teardrop shaped and angulated. No myoepithelial cells are present

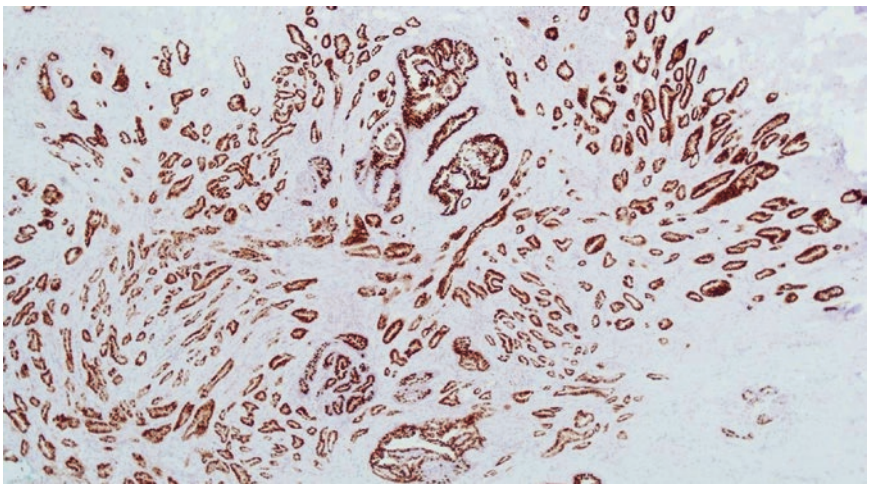

Fig. 13.46 Tubular carcinoma shows diffuse positive nuclear reactivity for oestrogen and progesterone receptors on immunohistochemistry. In contrast, syringomatous tumour is generally negative for hormone receptors and for c-cerbB-2

Prognosis and Therapy Considerations

Wide excision is needed to prevent local recurrence of syringomatous tumour. No metastases have been described to date.

Paget Disease

Definition

Paget disease refers to the presence of malignant glandular cells within the epidermis of the nipple-areolar complex. It is believed to arise from malignant transformation of the intraepidermal portion of lactiferous ducts or from malignant cells migrating into the epidermis from underlying breast carcinoma. Paget disease is associated with underlying in situ and/or invasive ductal carcinoma in a large majority of cases.

Clinical and Epidemiological Features

Paget disease is encountered in about 1–4 % of all breast carcinomas. Clinically presenting as pain, discharge, eczematous rash, itch, or erosion of the nipple (Figs. 13.47, 13.48, and 13.49), it may also be occult and discovered only upon microscopic examination of the nipple in mastectomies performed for breast carcinoma. Paget disease without an underlying in situ or invasive breast carcinoma is rare, reported in 1.4–13 % of all cases of Paget disease [11].

Imaging Features

Nipple changes of Paget disease are commonly nonspecific or normal appearing on imaging. There may be nipple retraction, areolar skin thickening, or dermal microcalcifications. The presence of subareolar microcalcifications or mass is suggestive of an underlying associated malignancy.

Pathologic Features

Macroscopic Pathology

Nipple erythema, roughening, flakiness, erosion, and ulceration can be present (Fig. 13.50). Sometimes the nipple can be completely destroyed, and the changes can extend to the areola and its surrounding skin.

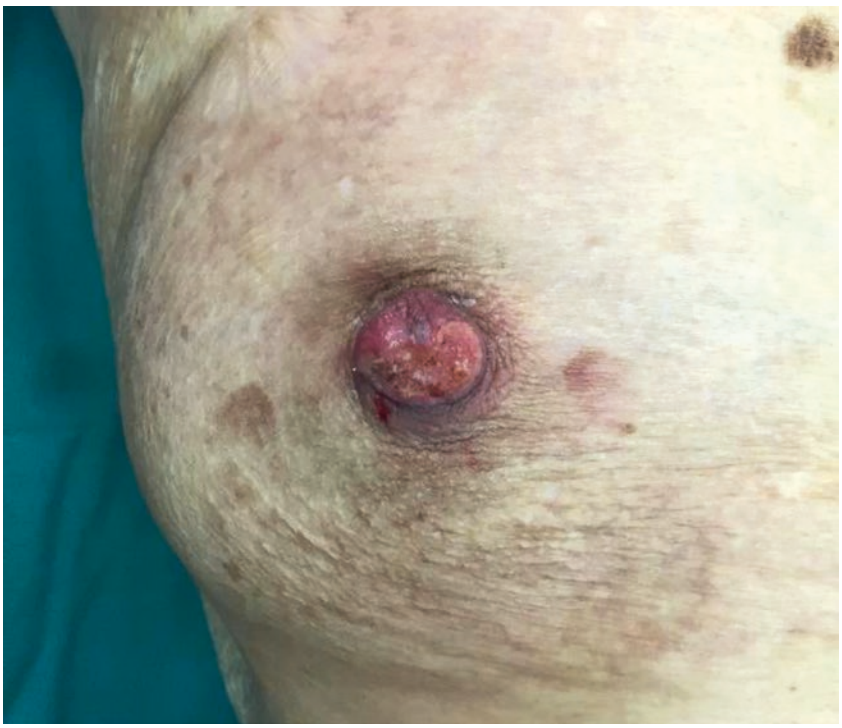

Fig. 13.47 Paget disease of the nipple. The nipple shows a few whitish spots on the slightly raw surface, with focal haemorrhages (Courtesy of Dr. Veronique Tan)

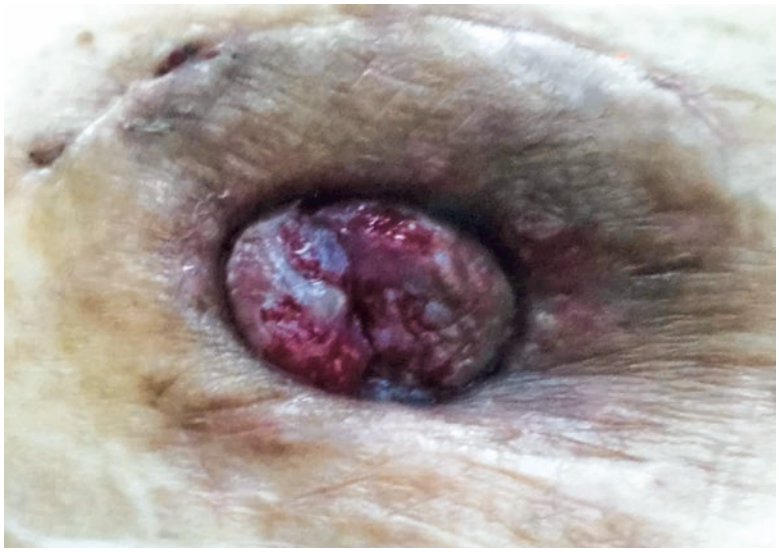

Fig. 13.48 Paget disease of the nipple. A close-up view of the nipple, which is eroded and erythematous. A whitish exudate covers part of the irregular nipple surface. There is also nipple retraction. Subsequent resection showed both invasive and in situ ductal carcinoma accompanying the Paget disease (Courtesy of Dr. Joy Lee)

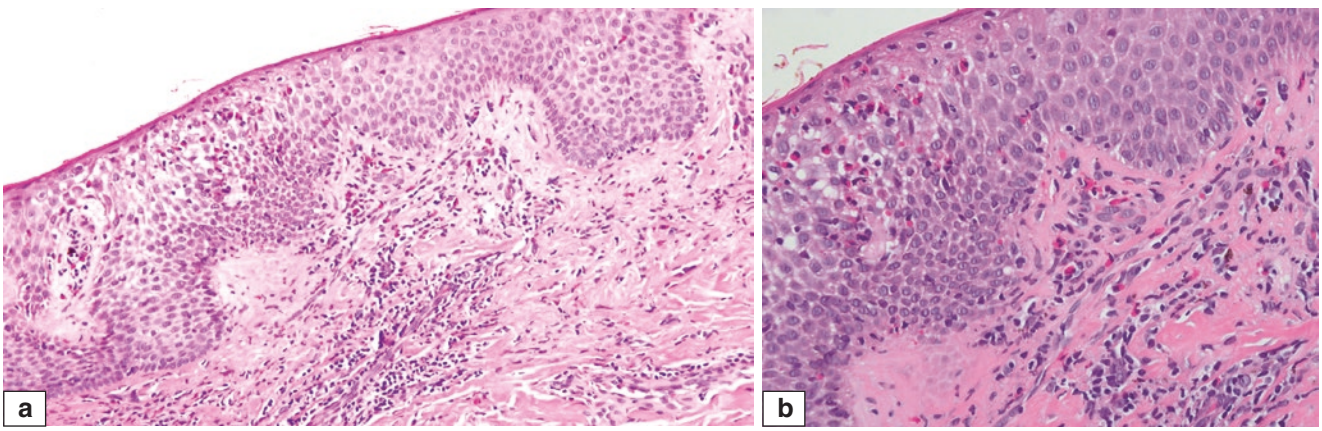

Fig. 13.49 (**a**) Nipple-areolar rash which corresponded histologically to contact allergic dermatitis, with spongiosis, scattered eosinophils, and dermal chronic inflammation. No malignant intraepidermal epithelial cells are present. Clinically, this condition may resemble Paget disease, and careful histological examination is needed to rule it out. (**b**) High magnification shows intraepidermal eosinophils among spongiotic keratinocytes. Several dermal eosinophils are also noted

Microscopic Pathology

Malignant cells punctuate the nipple epidermis in a pagetoid fashion, with cytologically high-grade, abnormal cells placed singly or in clusters among benign epidermal cells (Figs. 13.51, 13.52, 13.53, 13.54, and 13.55). The malignant cells sometimes show gland formation. Ductal carcinoma in situ (DCIS), usually of high nuclear grade, is frequently observed in the underlying lactiferous ducts. Overexpression and amplification of c-erbB-2 are seen in 80–90 % of cases (Figs. 13.56, 13.57, and 13.58). Invasive carcinoma (often of a ductal subtype) is found in 53–60 % of cases [11]. There is an isolated report of Paget disease associated with lobular carcinoma in situ, but this report has been challenged as possibly representing nipple Toker cells rather than Paget cells [12, 13].

Differential Diagnosis

Toker Cells of the Nipple

Toker cells are clear cells in the epidermis of the nipple-areolar region of the breast (Figs. 13.59, 13.60, 13.61, 13.62, and 13.63), which are seen in 9.3–11 % of cases [14–16], though immunohistochemistry for CK7 demonstrates a

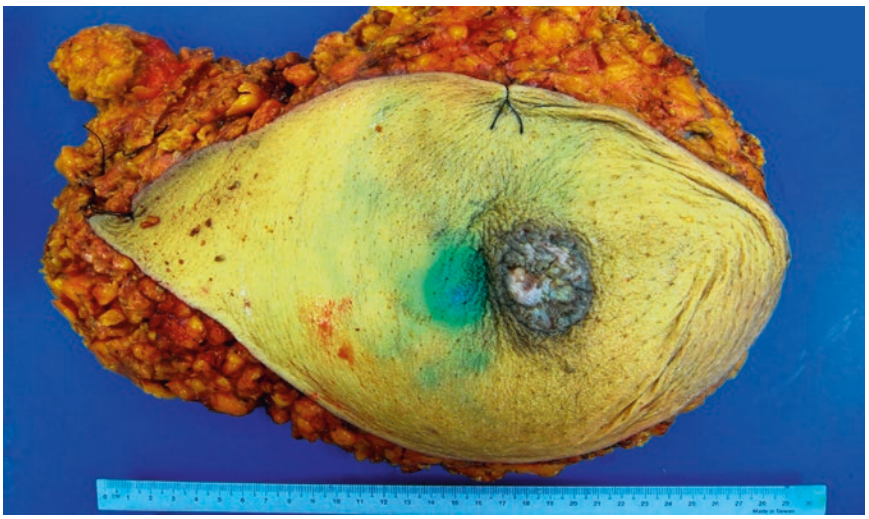

Fig. 13.50 Paget disease. This mastectomy specimen shows an ulcerated, gnarled nipple with rolled, whitish edges, which histologically demonstrated Paget disease. Underlying in situ and invasive ductal carcinoma was present

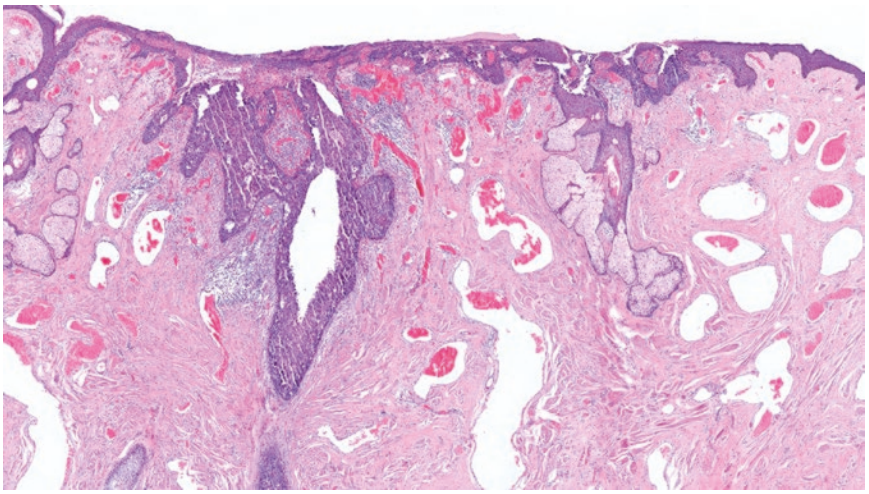

Fig. 13.51 Paget disease. The nipple epidermis is eroded. DCIS is noted in the lactiferous duct

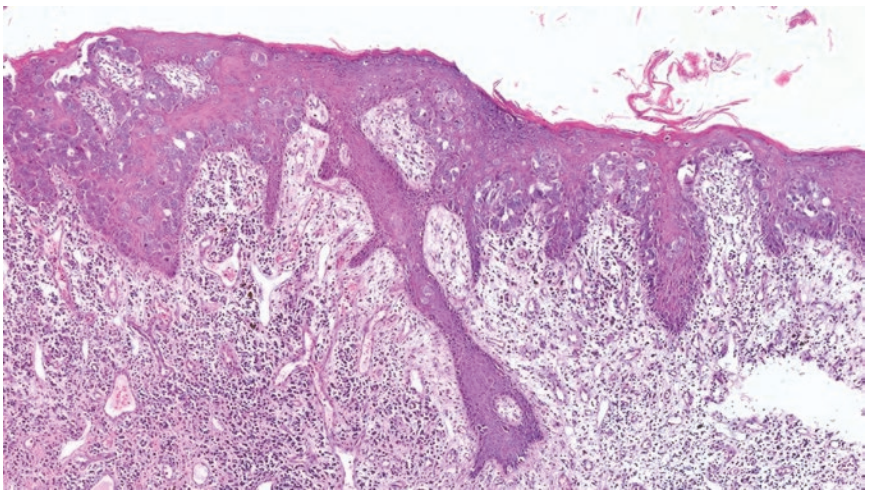

Fig. 13.52 Paget disease. Malignant cells are found within the nipple epidermis, and there is chronic inflammation in the underlying dermis

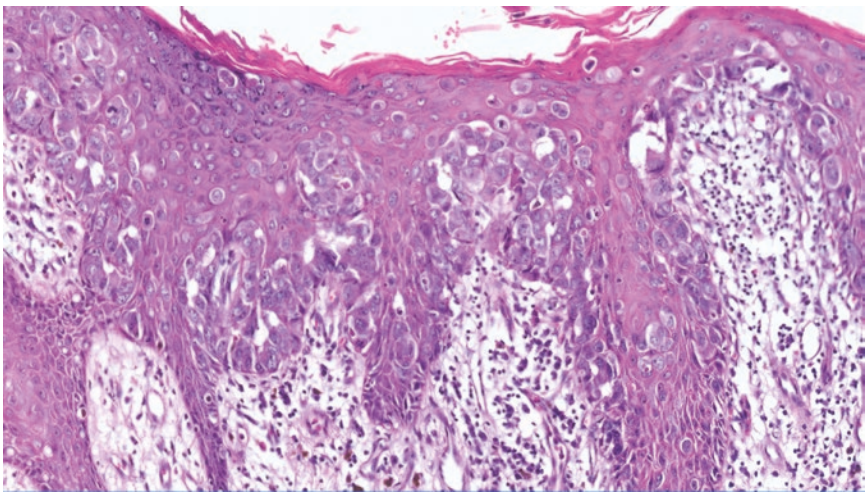

Fig. 13.53 Paget disease. Higher magnification shows malignant Paget cells within the nipple epidermis

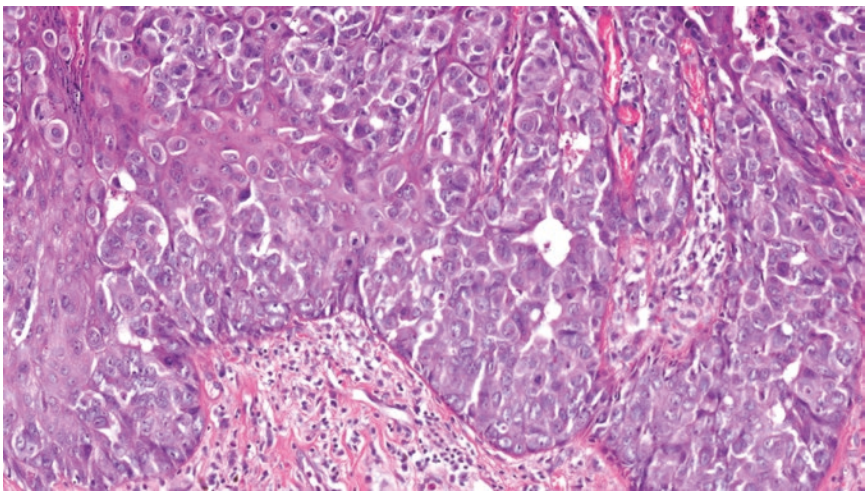

Fig. 13.54 Paget disease. The intraepidermal malignant cells show enlarged vesicular nuclei with distinct nucleoli

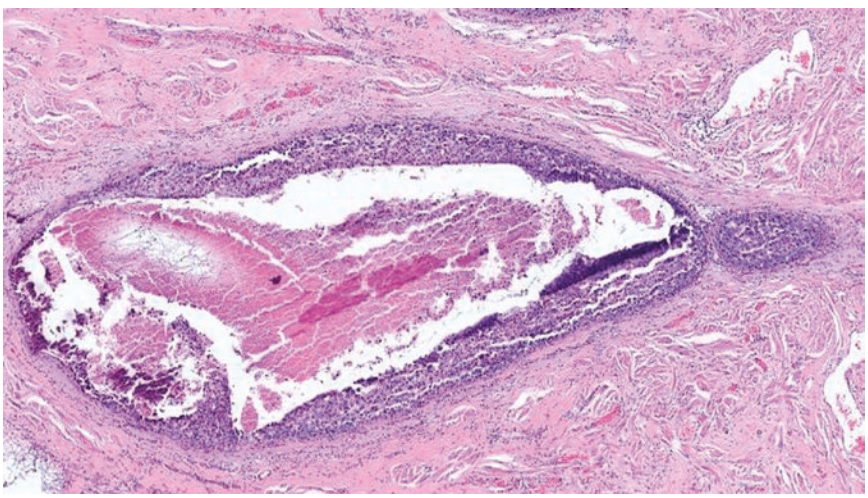

Fig. 13.55 DCIS with necrosis and calcifications is noted along the lactiferous ducts, deep to the nipple displaying Paget disease

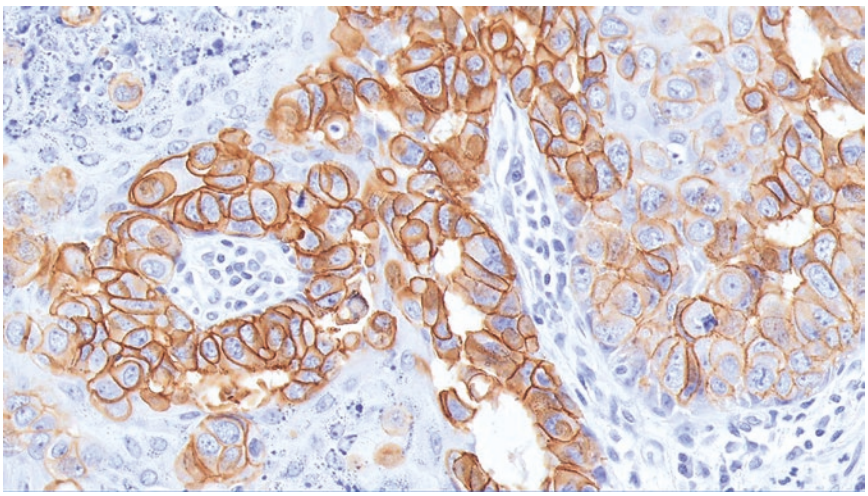

Fig. 13.56 Paget disease. c-cerbB-2 immunohistochemistry is strongly positive (3+) in the majority of the tumour cells

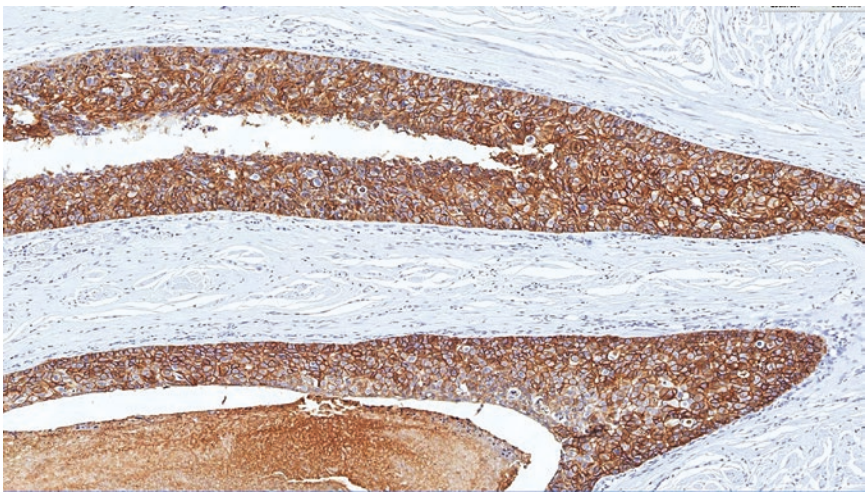

Fig. 13.57 DCIS underlying Paget disease also shows strong c-erbB-2 positivity (3+) on immunohistochemistry

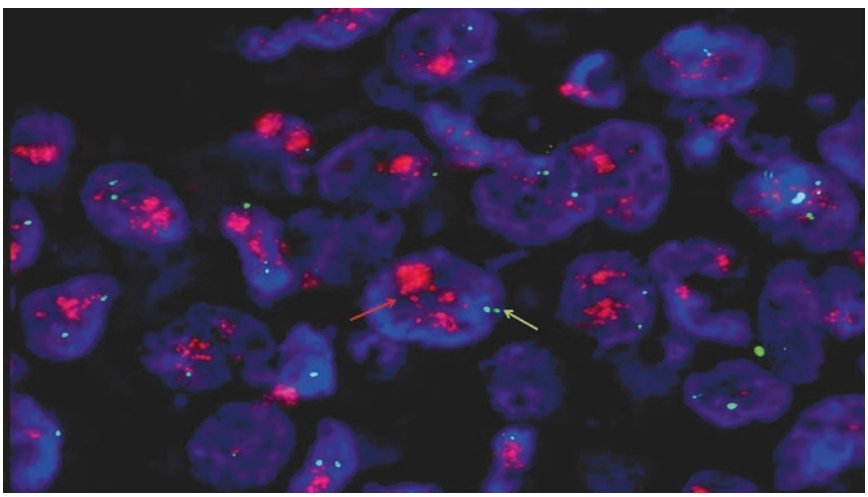

Fig. 13.58 Paget disease of the nipple. Cells hybridised with dual-colour LSI ERBB2 and CEP17 fluorescence in situ hybridisation (FISH) probes show amplification of the *ERBB2* gene (*red arrows*) with normal copy numbers of CEP17 control probe (*green arrow*) (Courtesy of the Cytogenetics Laboratory, SGH Pathology)

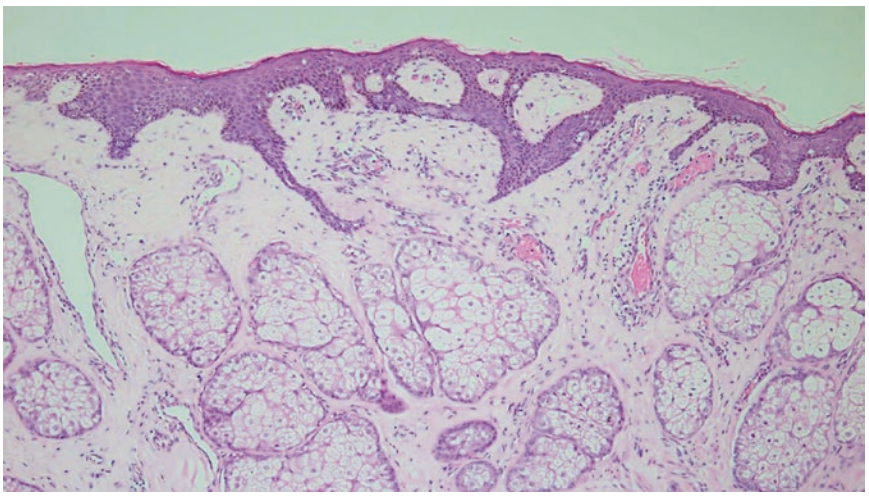

Fig. 13.59 Toker cells of the nipple. At low magnification, several clear cells are seen in the nipple areolar epidermis. Lobules of sebaceous glands are present in the underlying stroma

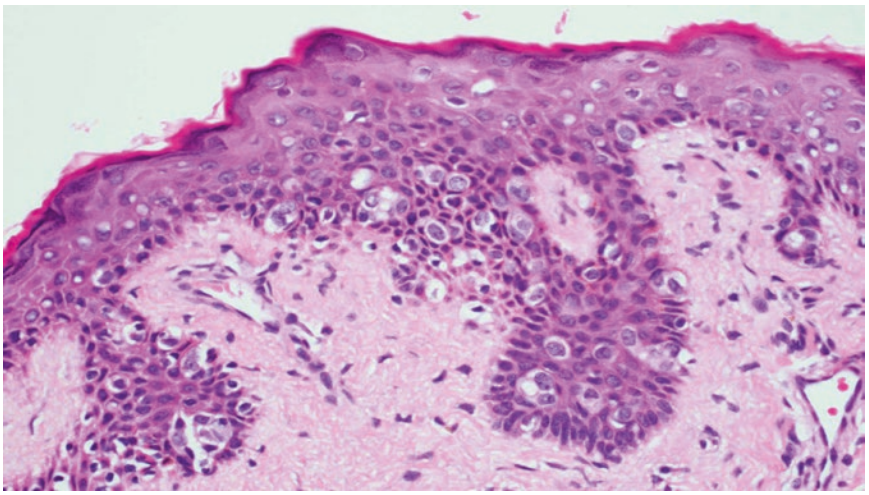

Fig. 13.60 Toker cells of the nipple. Individual and small clusters of pale cells with vesicular nuclei and discernible small nucleoli are present. These resemble Paget cells, although Toker cells are often bland and less pleomorphic than Paget cells, which usually demonstrate high-grade atypia

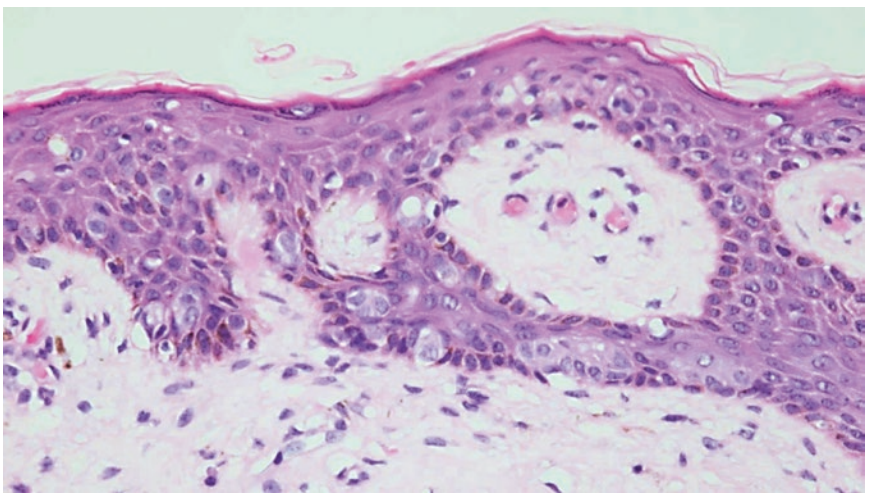

Fig. 13.61 Toker cells of the nipple. Pale cells in the nipple epidermis closely mimic Paget cells. The distinction can be aided with immunohistochemistry; Toker cells are negative for c-erbB-2 and usually positive for ER, in contrast with Paget cells, which are c-erbB-2 positive and ER negative

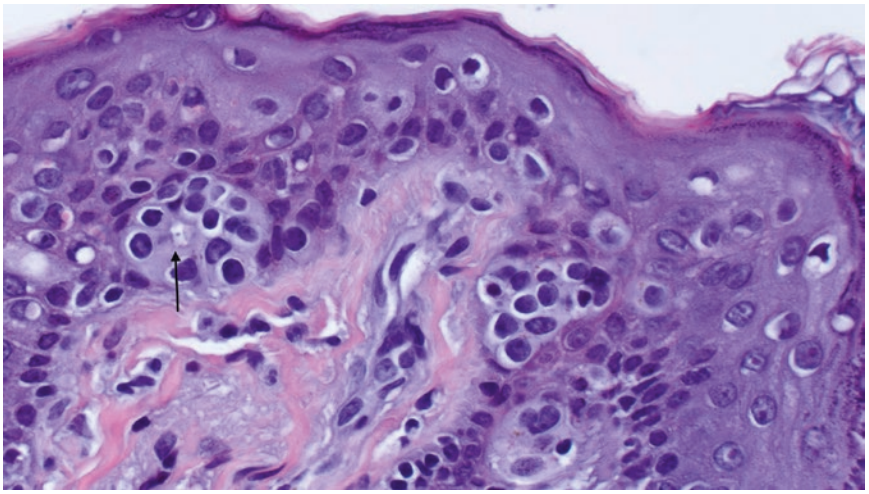

Fig. 13.62 Toker cells. In this example, the Toker cells are clustered, with one cluster disclosing a lumen-like space suggesting gland formation (*arrow*). Some authors refer to these as *Toker cell hyperplasia*, but others prefer to regard these as Toker cells without further qualification (Courtesy of Dr. Timothy Jacobs)

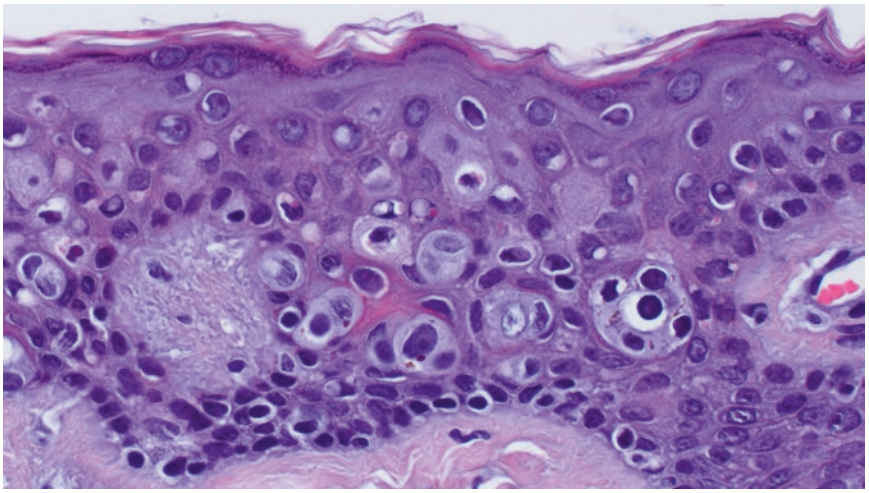

Fig. 13.63 Toker cells of the nipple. Here, a few Toker cells show nuclear enlargement with discernible nucleoli, resembling Paget cells. In such cases, immunohistochemistry is useful in distinguishing Toker cells from Paget cells (Courtesy of Dr. Timothy Jacobs)

much higher prevalence of 88.4 % [17]. Toker cells are believed to be glandular cells of lactiferous ductal origin, though recently it has been suggested that they are developmentally more related to sebaceous glands [16]. The majority of Toker cells are cytologically bland, disappearing after further sections, and do not pose a differential diagnostic concern for Paget disease, but a proportion (27.5 %) can disclose hyperplastic features, with 12.5 % being cytologically atypical [15]. Atypical and hyperplastic Toker cells must be distinguished from Paget cells. Both are CK7 positive. Immunohistochemistry is helpful, with Paget cells being ER/PR negative and c-erbB-2, CD138, and p53 positive, whereas Toker cells show ER/PR positivity with c-erbB-2, CD138, and p53 negativity (Table 13.1; Figs. 13.64, 13.65, 13.66, 13.67, and 13.68). On occasion, Toker cells may disclose weak immunohistochemical reactivity for c-erbB-2 [15]—fluorescence in situ hybridisation may be discriminatory in such cases. Ki67 proliferation index can also be useful, being low in Toker cells [18].

Clear Cells of the Epidermis

Apart from Toker cells, the nipple-areolar epidermis may show other types of benign clear cells, including pagetoid dyskeratosis cells (observed in 40 % of nipples) and "signet-ring" cells (Fig. 13.69), observed in 50.7 % [14, 19]. Both pagetoid dyskeratosis and signet-ring cells are squamous cells that stain with high-molecular-weight keratins and p63, whereas CK7 is negative. Pagetoid dyskeratosis is

Table 13.1 Immunohistochemical comparison between Toker cells, Paget disease, squamous carcinoma in situ, and malignant melanoma

	Toker cells	Paget disease	Squamous CIS	Melanoma
CK7	+	+	–	–
Cam 5.2	+	+	–	–
CK5/6	–	–	+	–
34BE12	–	–	+	–
p63	–	–	+	–
S100	–/+	–/+	–	+
HMB45	–	–	–	+
MelanA	–	–	–	+
ER, PR	+	–/+	–	–
c-erbB-2	–	+	–	–
Ki67	–/low +	+	+	+

CIS carcinoma in situ, *ER* oestrogen receptor, *PR* progesterone receptor

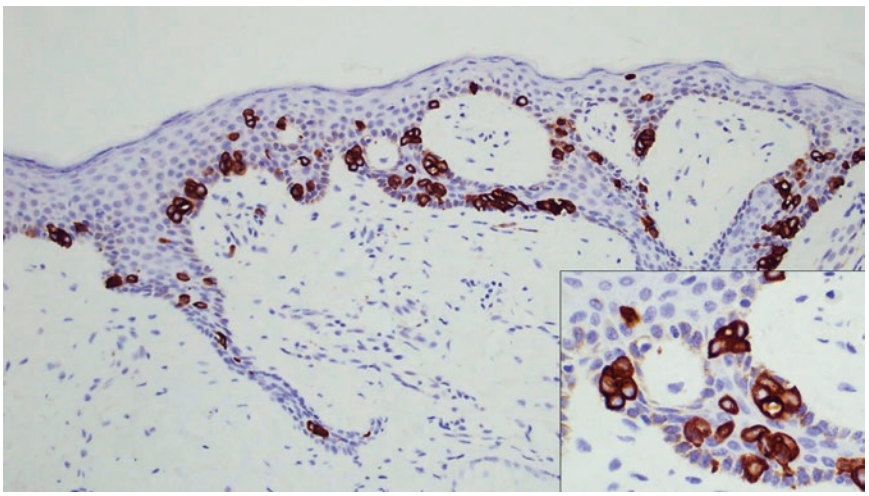

Fig. 13.64 Toker cells of the nipple are CK7 positive; the malignant cells in Paget disease similarly are also CK7 positive. *Inset* shows high magnification of the CK7-positive Toker cells, which can occur in small clusters

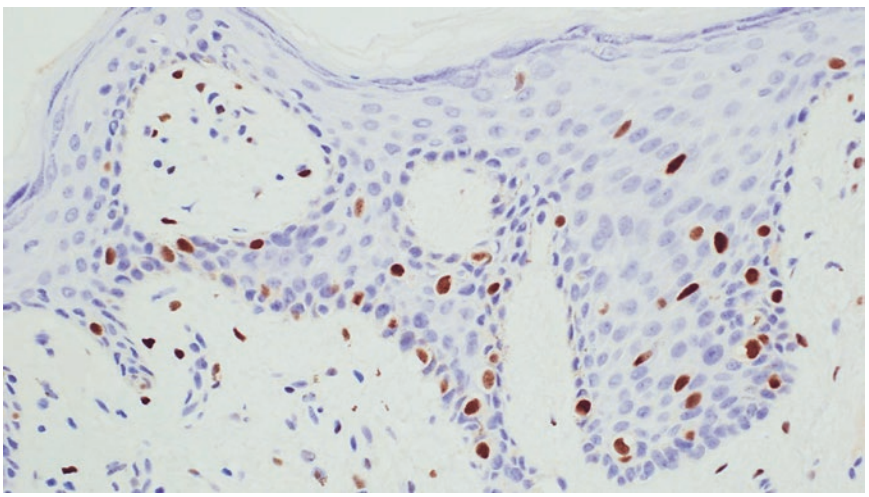

Fig. 13.65 Toker cells of the nipple. Immunohistochemistry shows positive ER staining of the nuclei of Toker cells

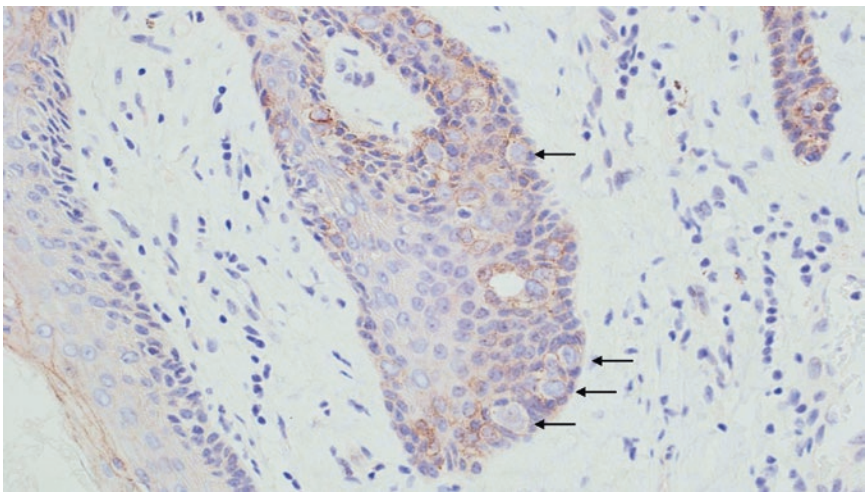

Fig. 13.66 Toker cells of the nipple. c-erbB-2 immunohistochemistry is negative (*arrows* point to several negatively stained Toker cells). Sometimes, there may be equivocal reactivity, in which case FISH may be helpful in ascertaining whether there is amplification of the *c-erbB-2* gene

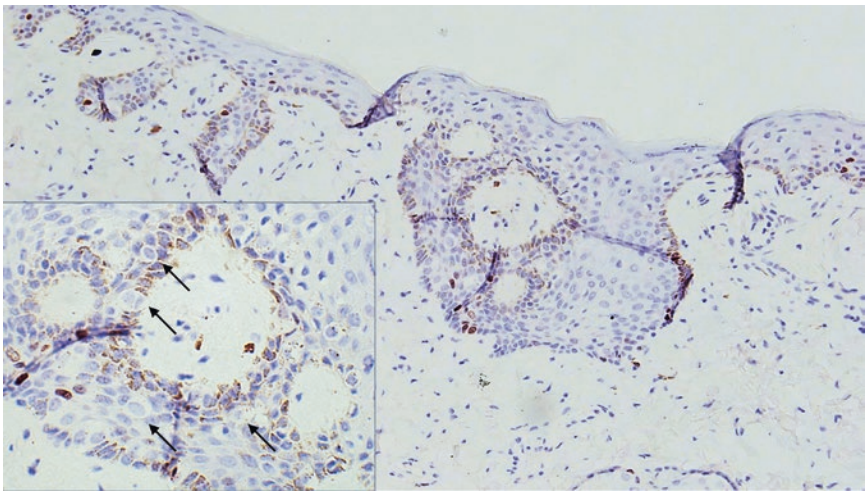

Fig. 13.67 Toker cells of the nipple. Immunohistochemistry for Ki67 shows a low proliferation index, with a few scattered basal epidermal cells disclosing positive nuclear staining, but the Toker cells (*arrows*, *inset*) are negative

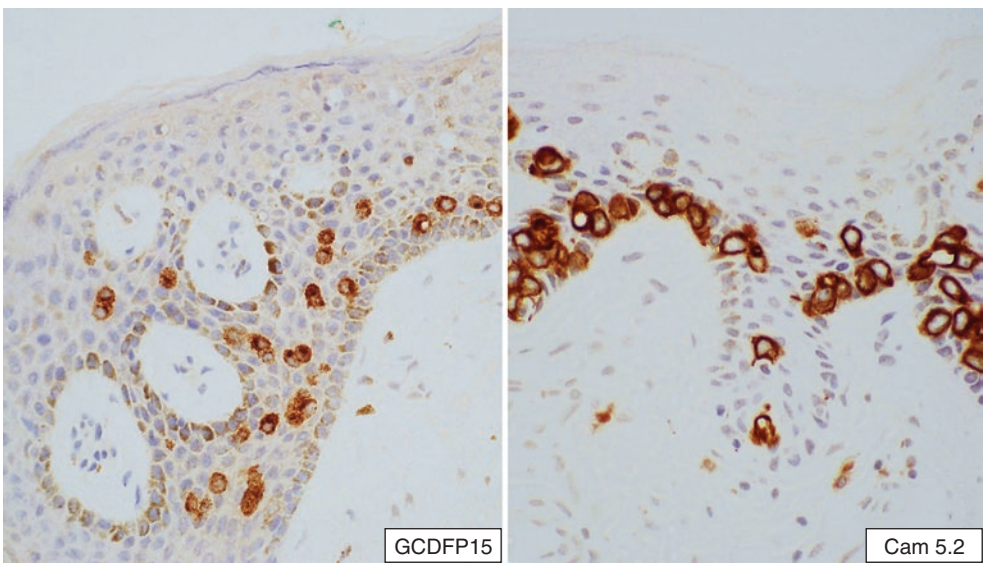

Fig. 13.68 Toker cells of the nipple. Toker cells are positively stained for gross cystic disease fluid protein and low-molecular-weight keratin Cam 5.2

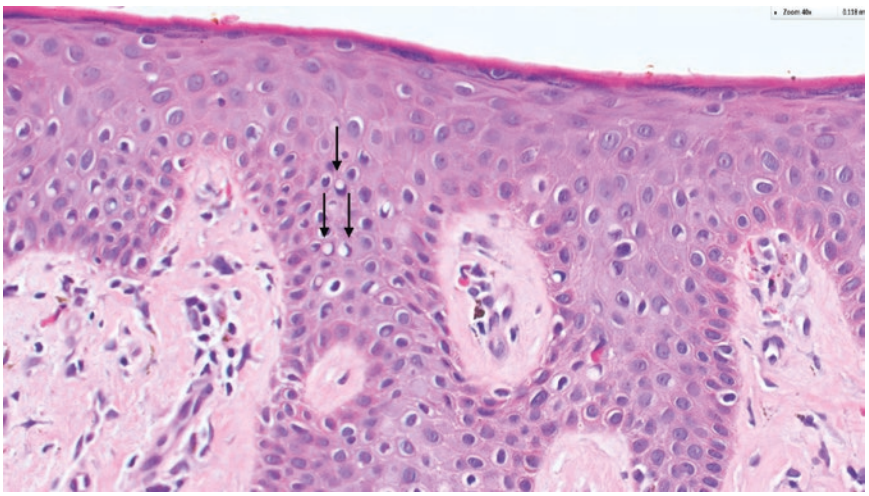

Fig. 13.69 Clear cells of the epidermis. Scattered cells with clear cytoplasm are seen among keratinocytes of the nipple epidermis. A few cells with signet-ring like appearances (*arrows*) are observed, which are likely fixation artefact

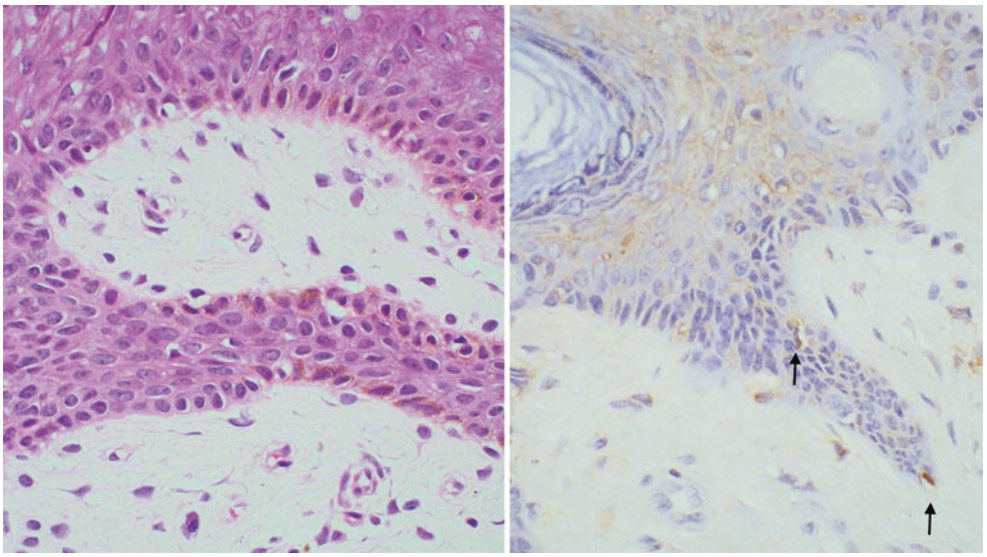

Fig. 13.70 Melanocytes at the dermoepidermal junction. Scattered clear cells seen at the dermoepidermal junction may be of melanocytic origin, with positive reactivity for S100 (*right field*, *arrows*). Melanin pigmentation of some of the basal epidermal cells is also seen

reported to occur secondary to friction [20], whereas signet-ring cells are related to fixation artefact [14]. Clear-cell papulosis, koilocytes, glycogen-rich squamous cells, and melanocytes (Fig. 13.70) may also present morphologically as clear cells within the nipple-areolar epidermis.

Squamous Carcinoma In Situ (Bowen Disease)

Squamous carcinoma in situ is exceedingly rare in the nipple-areolar complex (Figs. 13.71, 13.72, 13.73, and 13.74). Histologically, it may demonstrate individual malignant cells with variably clear cytoplasm within the epidermis closely mimicking Paget disease, or it may comprise full-thickness dysplasia of the epidermis. Immunohistochemistry shows positive staining for high-molecular-weight keratins and p63, while CK7 and c-erbB-2 are negative (Figs. 13.75, 13.76, 13.77, 13.78, and 13.79; Table 13.1).

Malignant Melanoma

Malignant melanoma rarely affects the nipple. Clinicopathologically, it can resemble Paget disease, especially pigmented mammary Paget disease. There may be a history of a long-standing naevus. Pigmented Paget disease is believed to result from local production of melanocyte chemotactic factor by Paget cells at the dermoepidermal junction or from transfer of melanin to the malignant cells [21]. Immunohistochemistry is needed for distinction (Figs. 13.80, 13.81, and 13.82).

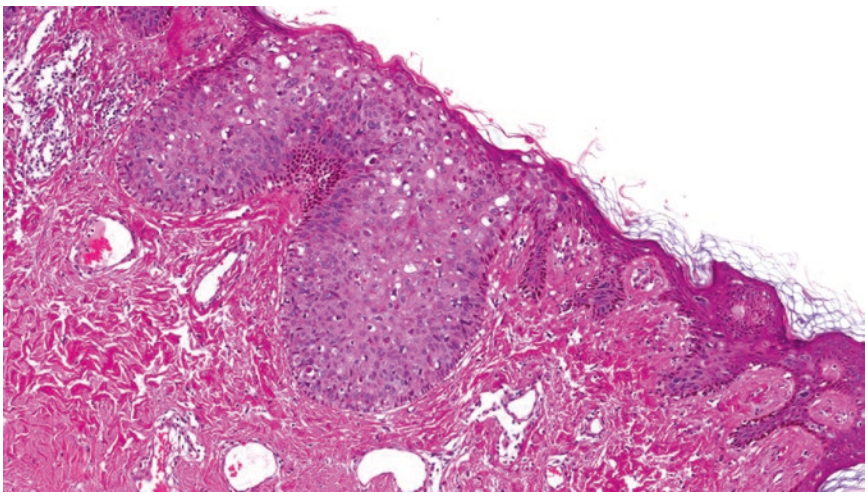

Fig. 13.71 Squamous carcinoma in situ (Bowen disease) of the nipple. The nipple epidermis shows abnormal cells with hyperchromatic nuclei, seen throughout the epidermal thickness

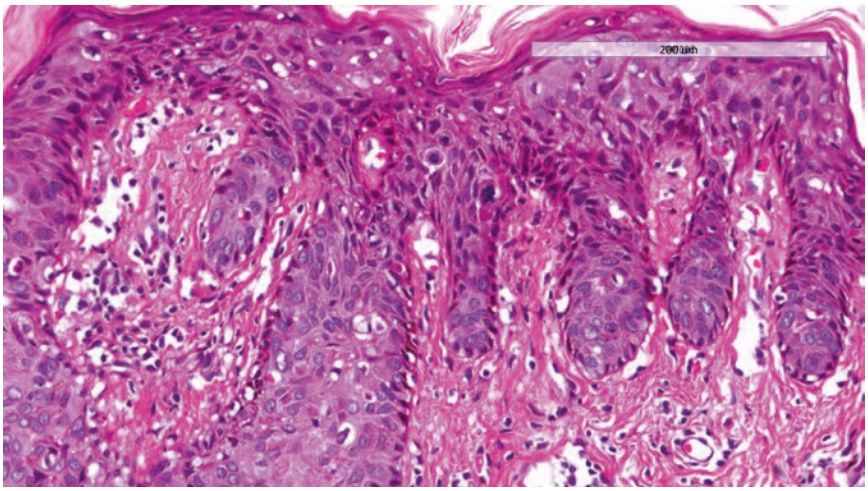

Fig. 13.72 Squamous carcinoma in situ. Higher magnification shows malignant cells with pleomorphic, hyperchromatic nuclei and clear to pink cytoplasm interspersed among normal keratinocytes, mimicking Paget disease

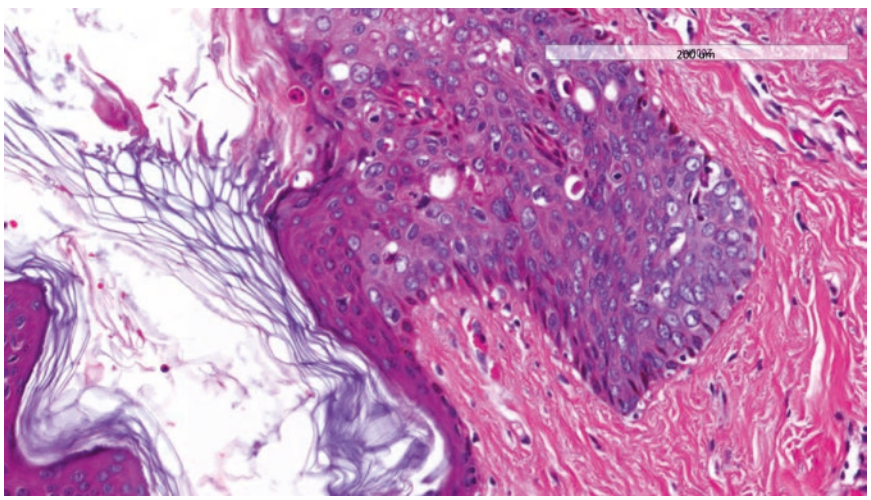

Fig. 13.73 Squamous carcinoma in situ. There is a fairly abrupt transition from normal epidermis to squamous carcinoma in situ, where there is full-thickness replacement by cells with enlarged pleomorphic nuclei. Scattered mitoses are present

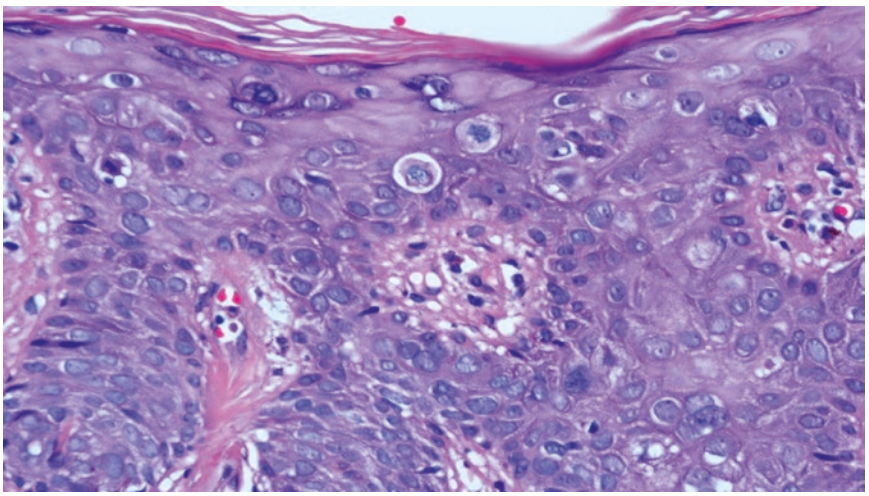

Fig. 13.74 Squamous carcinoma in situ. The malignant squamous cells punctuate the nipple epidermis and stand out with their more ample cytoplasm and larger nuclei. Although full-thickness replacement of the epidermis by malignant cells is often seen in squamous carcinoma in situ, sometimes the malignant cells are dispersed individually and are not found across the entire squamous epidermal width

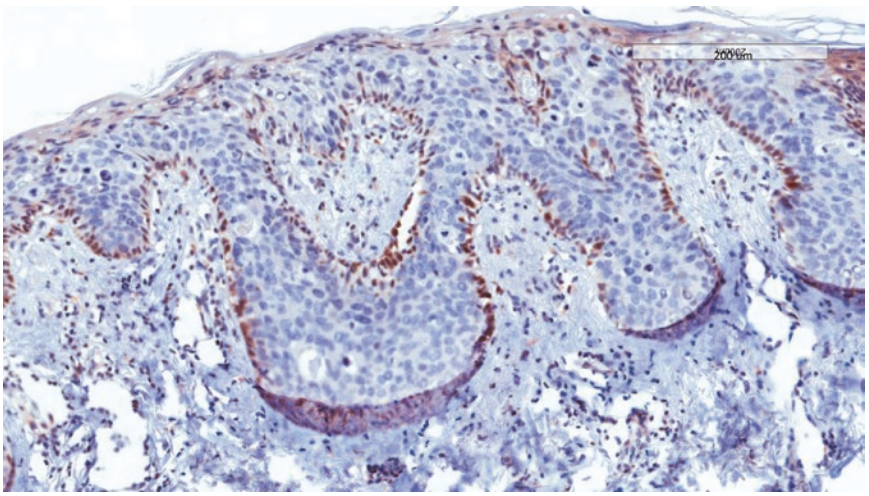

Fig. 13.75 Squamous carcinoma in situ. Immunohistochemistry for c-erbB-2 is negative in the malignant cells. Basal epidermal cells show melanin pigmentation

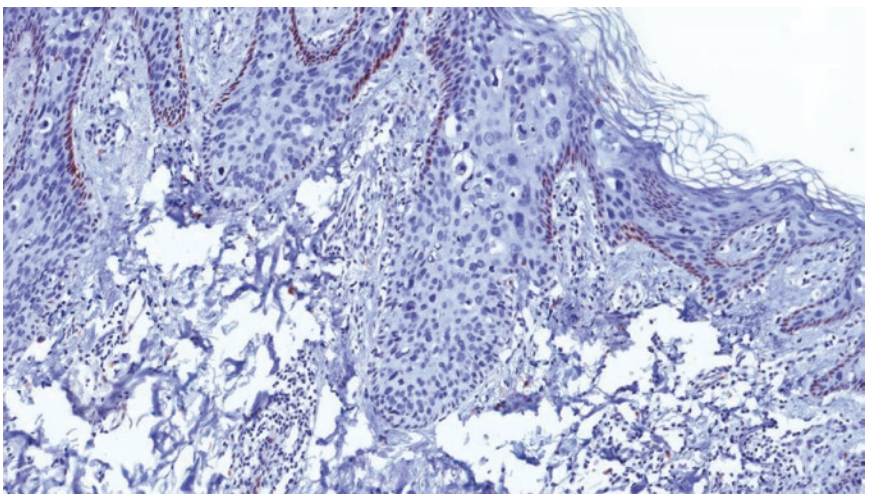

Fig. 13.76 Squamous carcinoma in situ. CK7 immunohistochemistry is negative. In contrast to squamous carcinoma in situ, both c-erbB-2 and CK7 are positive in malignant cells of Paget disease

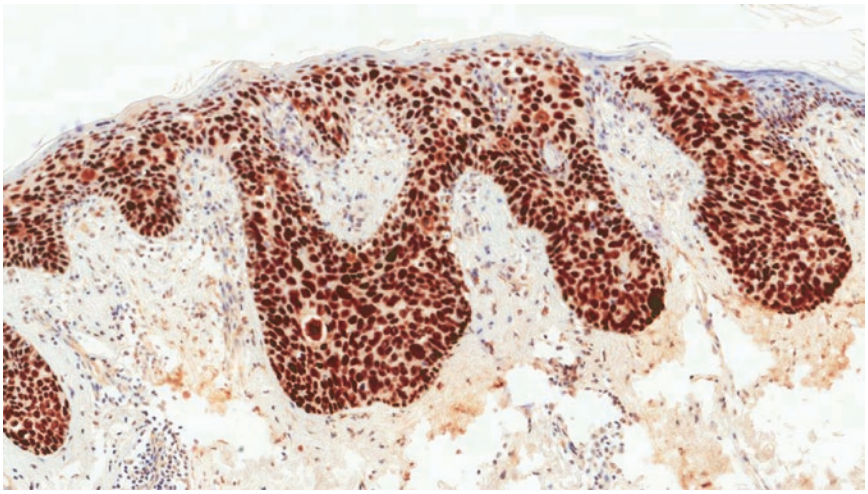

Fig. 13.77 Squamous carcinoma in situ. Immunohistochemistry for p63 shows positive nuclear reactivity of malignant cells within the nipple epidermis

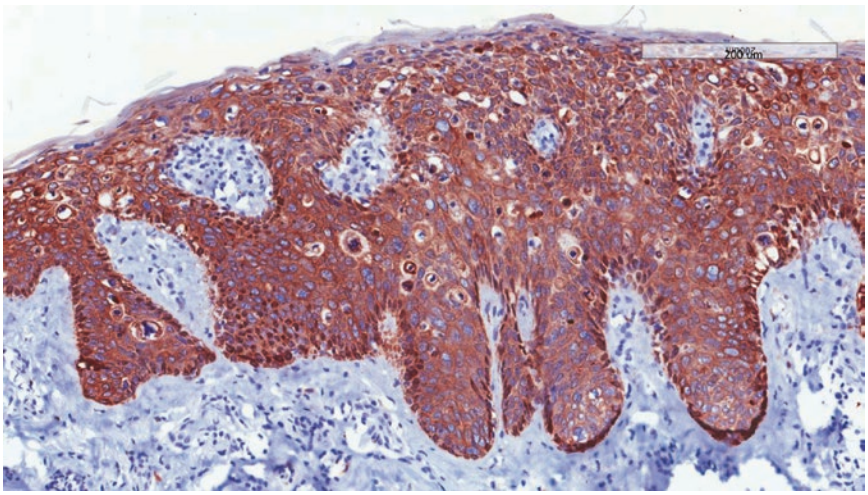

Fig. 13.78 Squamous carcinoma in situ. Immunohistochemistry for the high-molecular-weight keratin 34BE12 shows positive cytoplasmic and membrane staining of the malignant cells. In contrast to squamous carcinoma in situ, both p63 and 34BE12 are negative in malignant cells of Paget disease

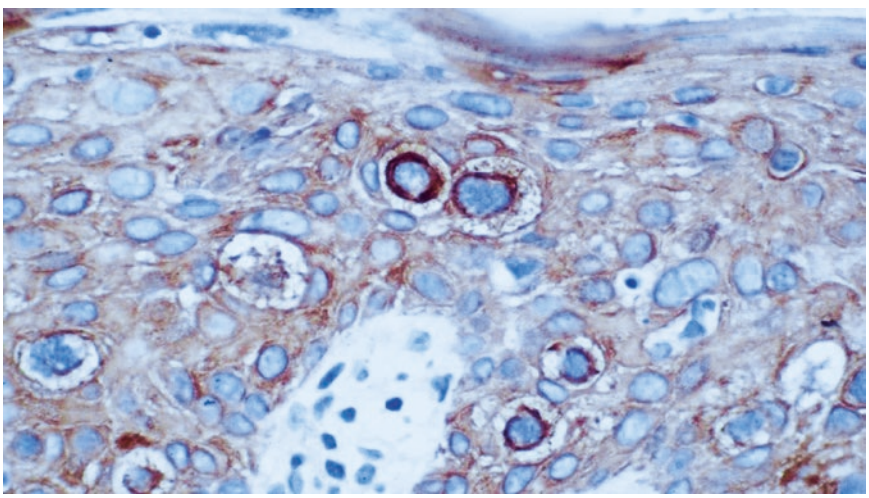

Fig. 13.79 Squamous carcinoma in situ. High magnification of a section stained immunohistochemically for 34BE12 shows cytoplasmic reactivity of the malignant tumour cells

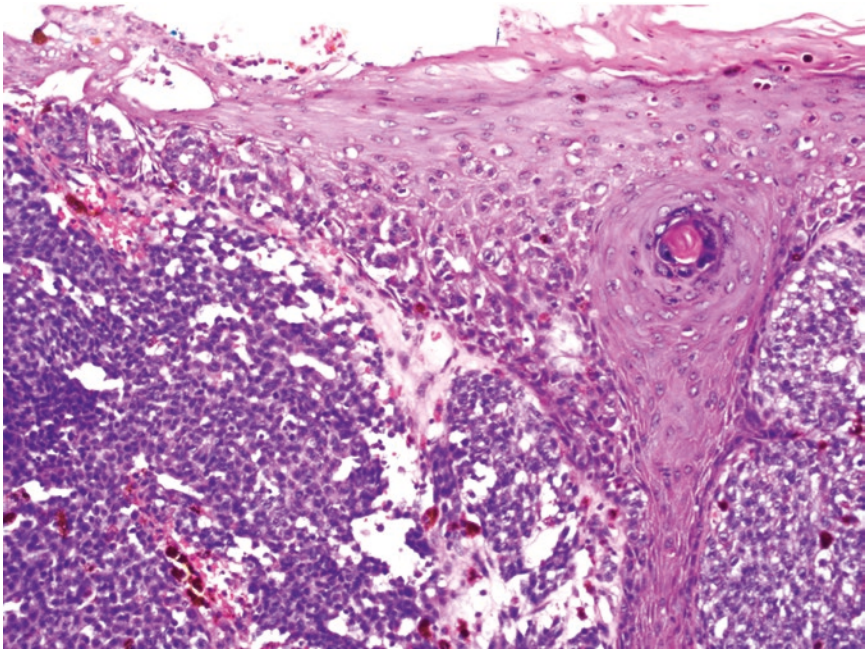

Fig. 13.80 Melanoma involving the nipple epidermis. Sheets of tumour cells are seen in the nipple stroma, with rounded nests of malignant melanoma cells observed in the lower epidermis of the nipple. Brown melanin pigment is noted among the melanoma cells

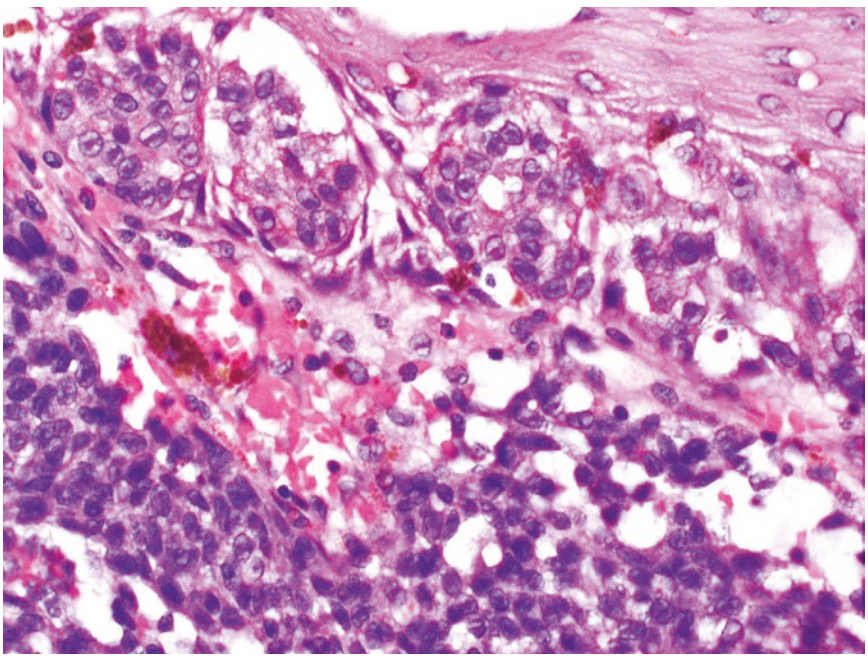

Fig. 13.81 Melanoma involving the nipple epidermis. High magnification of the clusters of melanoma cells in the basal epidermis, accompanied by brown melanin pigment. The tumour cells show enlarged vesicular nuclei with prominent nucleoli and may mimic Paget cells

Prognosis and Therapy Considerations

The prognosis of Paget disease depends on the pathological characteristics of the associated carcinoma. The reported 5-year overall survival is 94–98 % for DCIS and 73–93 % for invasive ductal carcinoma [11]. Direct dermal invasion from Paget disease (Fig. 13.83) has a more favourable outcome than skin invasion from underlying breast carcinoma and must therefore be distinguished from the latter, which represents pT4b disease [22].

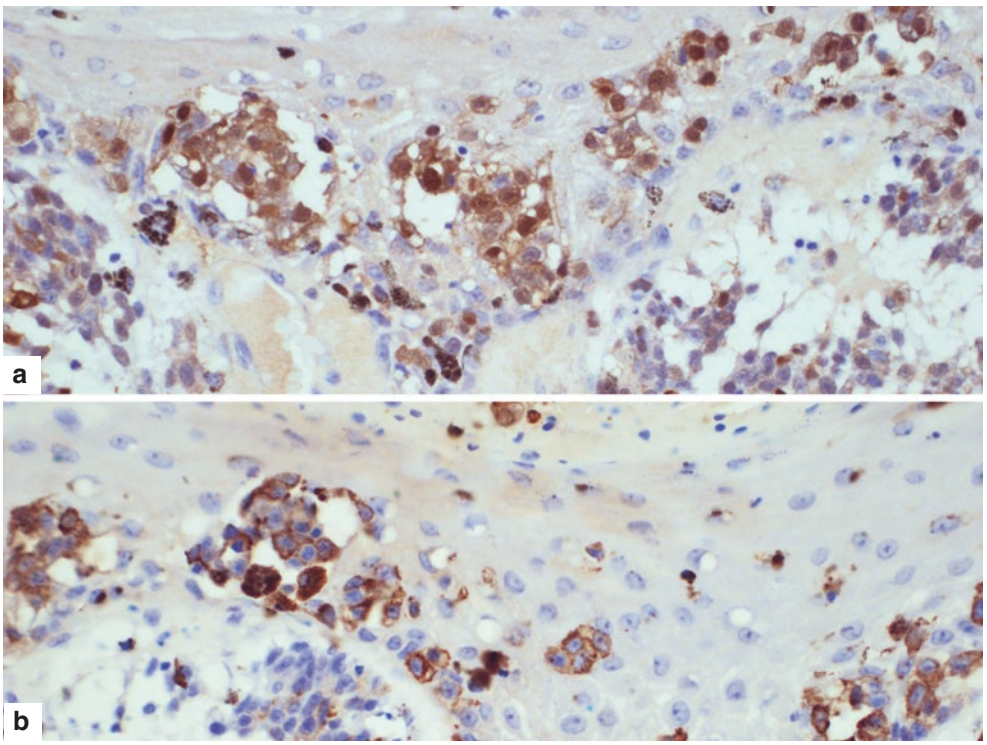

Fig. 13.82 Melanoma involving the nipple epidermis. Immunohistochemistry for S100 (**a**) and HMB45 (**b**) shows positive reactivity of the melanoma cells

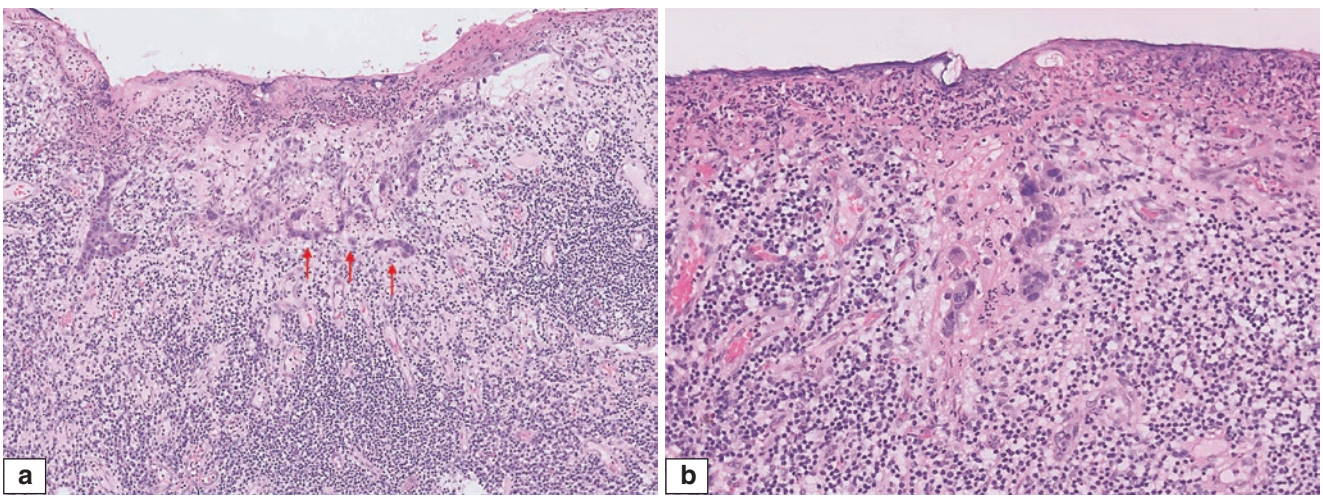

Fig. 13.83 Paget disease with direct dermal invasion. (**a**) The nipple epidermis is eroded, with remnant rete pegs variably harbouring intraepidermal malignant cells. A few small cords and narrow trabeculae of tumour cells are detached from the epidermis, lying within the oedematous inflamed stroma (*red arrows*). (**b**) Higher magnification shows the detached malignant epithelial aggregates within inflamed stroma. The overlying epidermis here is ulcerated. No invasive disease was found in the rest of the mastectomy specimen which contained ductal carcinoma in situ. It may be difficult to distinguish early invasive disease from Paget cells that are still contained within rete pegs that are sectioned at a tangent. What can be helpful is to determine if the detached malignant epithelial island is connected with rete pegs in adjacent levels, in which case invasion is unlikely. Alternatively, immunohistochemistry for high molecular weight keratins or p63 may highlight a peripheral rim of squamous cells around the malignant Paget cells confirming absence of invasion. In this example, assessment is made challenging by the ulceration. However, the presence of individual malignant cells within the inflamed stroma, and persistence of such foci after deeper levels, support the conclusion of direct dermal invasion from Paget disease

References

1. Johnson SP, Kaoutzanis C, Schaub GA. Male Zuska's disease. BMJ Case Rep. 2014;2014. doi: 10.1136/bcr-2013-201922.
2. Lo G, Dessauvagie B, Sterrett G, Bourke AG. Squamous metaplasia of lactiferous ducts (SMOLD). Clin Radiol. 2012;67:e42–6.
3. Pendse AA, O'Connor SM. Primary invasive squamous cell carcinoma of the nipple. Case Rep Pathol. 2015;2015:327487.
4. Sofos SS, Tehrani H, Lymperopoulos N, Constantinides J, James MI. Primary squamous cell carcinoma of the nipple: a diagnosis of suspicion. J Plast Reconstr Aesthet Surg. 2013;66:e315–7.
5. Loveland-Jones CE, Wang F, Bankhead RR, Huang Y, Reilly KJ. Squamous cell carcinoma of the nipple following radiation therapy for ductal carcinoma in situ: a case report. J Med Case Rep. 2010;4:186.
6. Drut R. Solitary keratoacanthoma of the nipple in a male. Case report. J Cutan Pathol. 1976;3:195–8.
7. Passaro ME, Broughan TA, Sebek BA, Esselstyn Jr CB. Lactiferous fistula. J Am Coll Surg. 1994;178:29–32.
8. Eusebi V, Lester S. Nipple adenoma. In: Lakhani SR, Ellis IO, Schnitt SJ, Tan PH, van de Vijver MJ, editors. WHO Classification of tumours of the breast. Lyon: IARC; 2012. p. 150.
9. Kim HM, Park BW, Han SH, Moon HJ, Kwak JY, Kim MJ, Kim EK. Infiltrating syringomatous adenoma presenting as microcalcification in the nipple on screening mammogram: case report and review of the literature of radiologic features. Clin Imaging. 2010;34:462–5.
10. Boecker W, Stenman G, Loening T, Andersson MK, Sinn HP, Barth P, et al. Differentiation and histogenesis of syringomatous tumour of the nipple and low-grade adenosquamous carcinoma: evidence for a common origin. Histopathology. 2014;65:9–23.
11. Shousha S, Eusebi V, Lester S. Paget disease of the nipple. In: Lakahni SR, Ellis IO, Schnitt SJ, Tan PH, van de Vijver MJ, editors. WHO Classification of tumours of the breast. Lyon: IARC; 2012. p. 152–3.
12. Sahoo S, Green I, Rosen PP. Bilateral Paget disease of the nipple associated with lobular carcinoma in situ. Application of immunohistochemistry to a rare finding. Arch Pathol Lab Med. 2002;126:90–2.
13. Fair KP. Bilateral Paget disease of the nipple. Arch Pathol Lab Med. 2002;126:1159.
14. Val-Bernal JF, Diego C, Rodriguez-Villar D, Garijo MF. The nipple-areola complex epidermis: a prospective systematic study in adult autopsies. Am J Dermatopathol. 2010;32:787–93.
15. Di Tommaso L, Franchi G, Destro A, Broglia F, Minuti F, Rahal D, Roncalli M. Toker cells of the breast. Morphological and immunohistochemical characterization of 40 cases. Hum Pathol. 2008;39:1295–300.
16. Saeed D, Shousha S. Toker cells of the nipple are commonly associated with underlying sebaceous glands but not with lactiferous ducts. J Clin Pathol. 2014;67:1010–2.
17. Nofech-Mozes S, Hanna W. Toker cells revisited. Breast J. 2009;15:394–8.
18. Park S, Suh YL. Useful immunohistochemical markers for distinguishing Paget cells from Toker cells. Pathology. 2009;41:640–4.
19. Garijo MF, Val D, Val-Bernal JF. An overview of the pale and clear cells of the nipple epidermis. Histol Histopathol. 2009;24:367–76.
20. Garijo MF, Val D, Val-Bernal JF. Pagetoid dyskeratosis of the nipple epidermis: an incidental finding mimicking Paget's disease of the nipple. APMIS. 2008;116:139–46.
21. Requena L, Sangueza M, Sangueza OP, Kutzner H. Pigmented mammary Paget disease and pigmented epidermotropic metastases from breast carcinoma. Am J Dermatopathol. 2002;24:189–98.
22. Sanders MA, Dominici L, Denison C, Golshan M, Wiecorek T, Lester SC. Paget disease of the breast with invasion from nipple skin into the dermis: an unusual type of skin invasion not associated with an adverse outcome. Arch Pathol Lab Med. 2013;137:72–6.

Male Breast Lesions

14

The structure of the male breast is almost identical to that of the female breast, yet both benign and malignant breast neoplasms are rare in males [1–3]. Until puberty, the male and female breasts are identical, composed of lactiferous ducts and fibrofatty stroma [4]. In males, testosterone levels increase during puberty, causing involution and atrophy of the ducts. In females, both stroma and ducts proliferate and lobular units develop in response to oestrogen and progesterone. The normal adult male breast is composed primarily of a small nipple-areolar complex, subcutaneous adipose tissue, stromal elements, and a few poorly developed ductal structures that end blindly (Fig. 14.1). Cooper ligaments are absent, and terminal ductal lobular unit formation is rare, which explains the rarity of many lesions such as cysts, fibroadenomas, phyllodes tumours, and lobular neoplasia. Most lesions in the male breast are of ductal origin [5, 6].

Gynaecomastia

Definition

Gynaecomastia is the non-neoplastic enlargement of the male breast, resulting from a proliferation of both epithelial and mesenchymal components of the breast.

Clinical and Epidemiological Features

Asymptomatic gynaecomastia is a relatively common, usually self-limited disorder. It is reported in 30–40 % of men [7–14]. The pathophysiology of gynaecomastia is poorly understood [15, 16]. The causes of gynaecomastia development range from benign physiologic processes to rare neoplasms. Proper

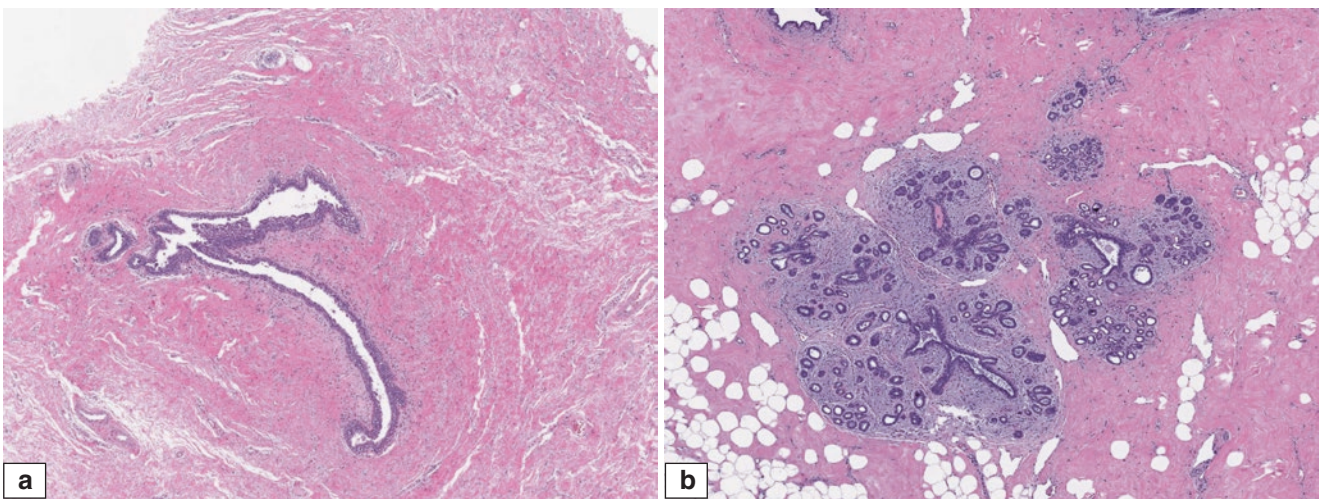

Fig. 14.1 Comparison of male and female breasts. (**a**) Male breast composed predominantly of stromal elements, including fibrous and adipose tissue, with poorly developed ducts and without any lobular units. (**b**) Adult female breast, showing ducts connected to lobular units

P.H. Tan, A.A. Sahin, *Atlas of Differential Diagnosis in Breast Pathology*, Atlas of Anatomic Pathology,
DOI 10.1007/978-1-4939-6697-4_14

identification of the aetiology of the gynaecomastia is important for clinical management [17, 18]. Based on its aetiology, gynaecomastia is classified into three categories: physiologic, secondary, and pharmacologic.

Physiologic gynaecomastia can occur in neonatal, pubertal, and elderly males. Neonatal gynaecomastia, which is the enlargement of breast tissue in newborns due to maternal hormones, usually resolves within several weeks of birth. Pubertal gynaecomastia is common and has a peak incidence at age 13–15 years. It is usually bilateral and is associated with breast tenderness (Fig. 14.2). It is due to hormonal surges during this period and in most cases resolves in a couple of years without any intervention. The incidence of gynaecomastia increases with age, and enlargement of breast tissue is usually due to a hormonal imbalance.

Secondary gynaecomastia can be due to hypogonadism (either congenital or acquired), endocrine disorders such as hyperthyroidism, metabolic disorders such as alcohol-induced liver disease, and chronic renal disease. It can also arise from neoplasms such as testicular tumours associated with increased levels of oestrogen, human chorionic gonadotropin, and prolactin; adrenal cortical tumours; and rarely other solid tumours such as bronchogenic carcinoma and squamous cell carcinoma of the skin [17, 19].

Pharmacologic gynaecomastia appears to be the result of the ingestion of a variety of implicated medications. Exogenous oestrogens, anabolic steroids, digitalis, marijuana, chlorpromazine, and some chemotherapeutic agents and antituberculosis drugs are reported to cause gynaecomastia [9, 19].

Gynaecomastia presents as a soft, mobile breast enlargement behind the nipple. The lesion can vary in size; most commonly it is 2–5 cm. Breast tenderness and pain can occur, but other symptoms such as nipple discharge, bleeding, and skin retraction are usually indicative of an additional pathology such as malignancy [12, 17].

Imaging Features

The imaging features of gynaecomastia depend on the duration of the lesion. In the early development phase, a discrete subareolar mass, corresponding to increased fibroglandular tissue, can be identified on mammography or ultrasound evaluation. Long-standing lesions (usually more than 1 year) are characterised by a dendritic pattern with linear bands of fibroglandular tissue radiating to the periphery. Mammography can show an asymmetric or central subareolar density, and ultrasound evaluation reveals hyperechoic fibroglandular tissue surrounding a central, subareolar hypoechoic area (Fig. 14.3). Microcalcifications are rarely present. Both ultrasound and mammography can be used to identify carcinomas arising in the background of gynaecomastia in males as effectively as they are used in females.

Pathologic Features

Macroscopic Features

The macroscopic features of gynaecomastia are nonspecific. Usually, it appears as ill-defined fibrous tissue with no identifiable discrete nodules (Fig. 14.4).

Microscopic Features

Histologic features vary with the age of the lesion, regardless of its aetiology. In the early phase (also referred to as the *florid phase*), gynaecomastia is characterised by an increased number of ducts embedded within the oedematous myxoid stroma (Figs. 14.5 and 14.6). Varying degrees of intraductal epithelial proliferation are present. Most of the ducts show a branching configuration and are lined by an epithelium of three to four cells thick, without significant cytologic atypia (Fig. 14.7). The epithelial proliferation has

Fig. 14.2 Bilateral gynaecomastia (Courtesy of Dr. Veronique Tan)

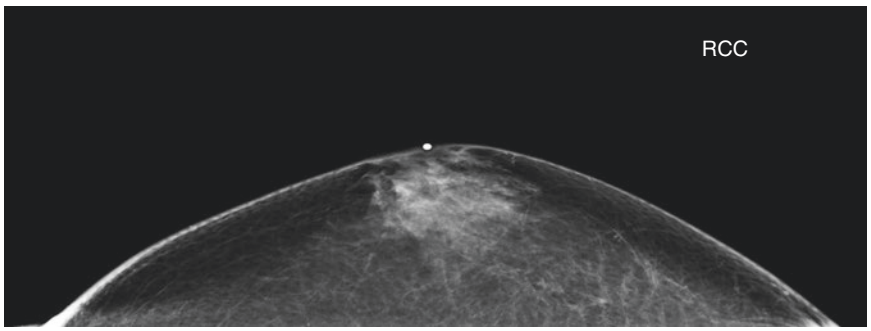

Fig. 14.3 Mammographic image of gynaecomastia. A flame-shaped density containing interspersed fat and ill-defined borders is seen in the subareolar region

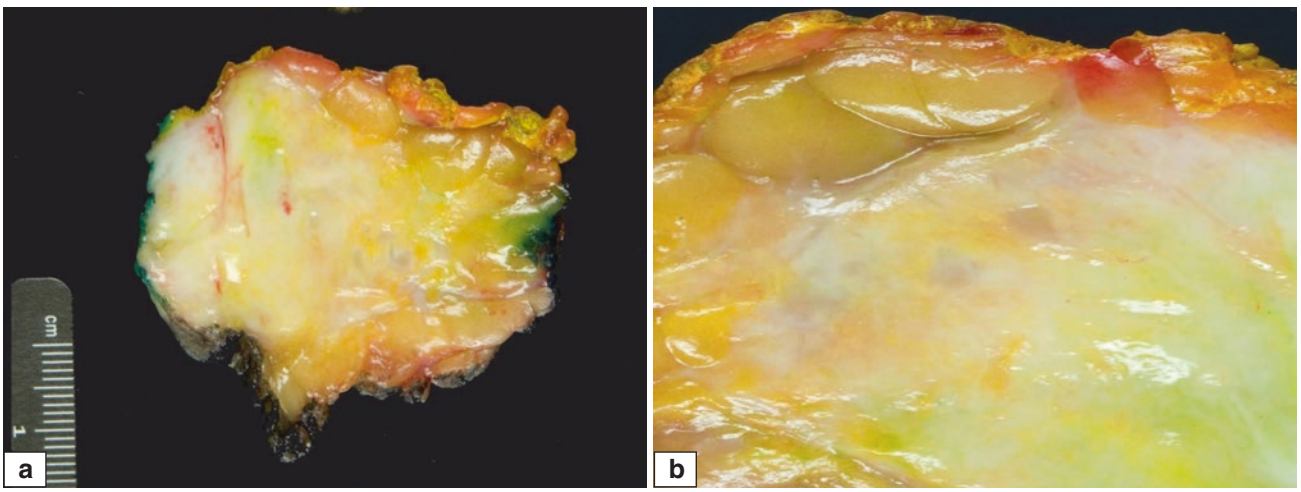

Fig. 14.4 Gross appearance of gynaecomastia. (**a**) Gynaecomastia shows adipose tissue with an ill-defined, grey-white fibrous density. (**b**) The edge of the fibrous density is imperceptible

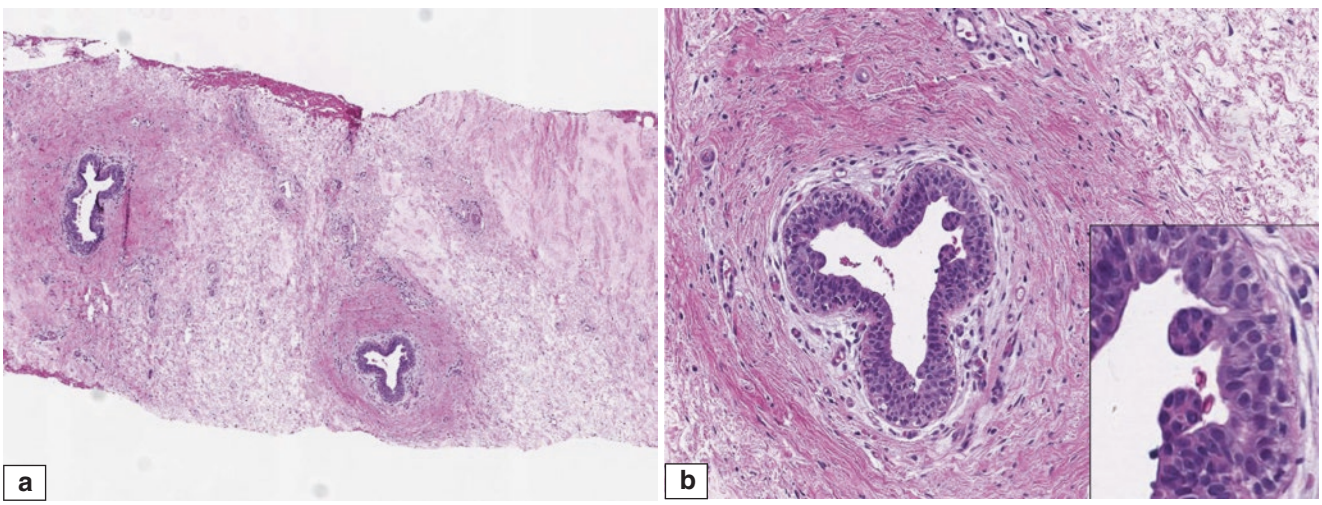

Fig. 14.5 Microscopic features of gynaecomastia. (**a**) Scattered ducts associated with hypercellular stroma. (**b**) The epithelium shows tufting. *Inset* shows high magnification of the epithelial tufts

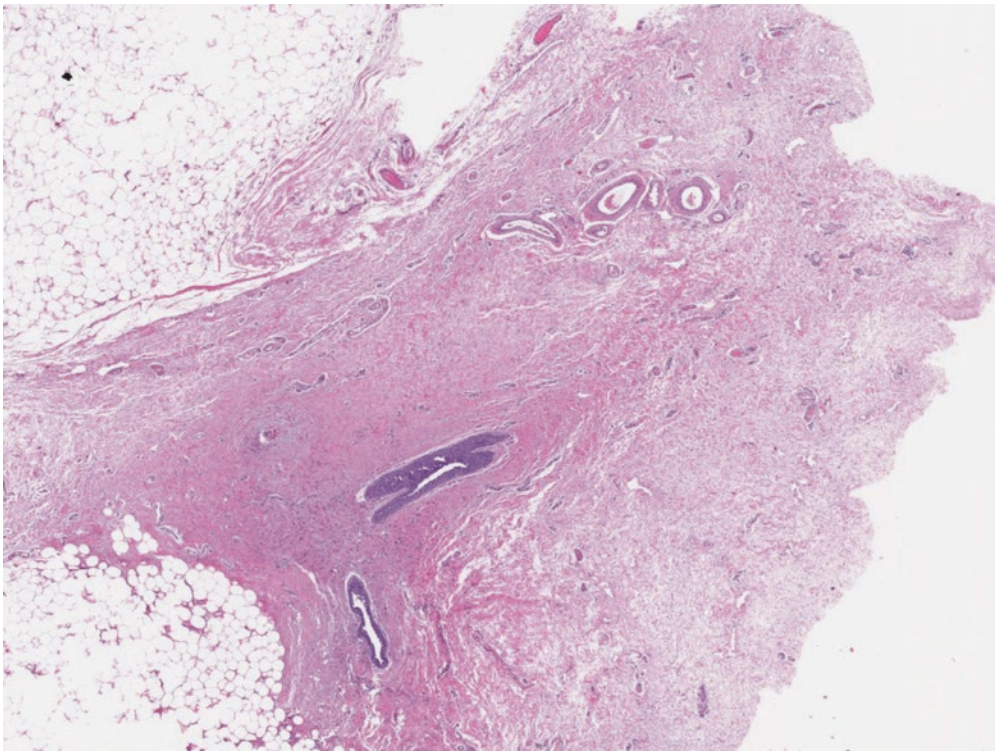

Fig. 14.6 Microscopic features of gynaecomastia. The stroma is densely fibrous and lacks an adipose tissue component

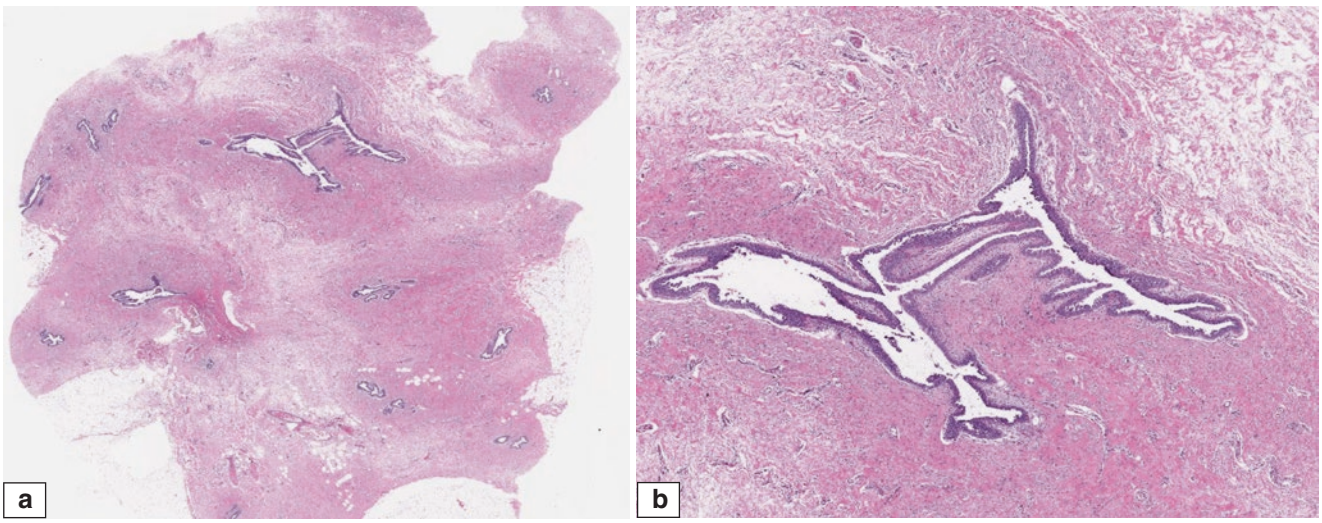

Fig. 14.7 Microscopic features of gynaecomastia. (**a**) Ducts show a branching configuration without marked epithelial thickening. The stroma is hypocellular. (**b**) Higher magnification of a duct without significant epithelial hyperplasia

a characteristic appearance, with tapering tufts protruding into the lumen, resembling a micropapillary architectural pattern (Figs. 14.8 and 14.9). The proliferating epithelial cells forming the luminal protrusions of gynaecomastia are not monomorphic (Figs. 14.10, 14.11, and 14.12). Epithelial hyperplasia may be florid (Fig. 14.13). The stroma around the ducts is usually hypervascular and may contain inflammatory cells (Figs. 14.14 and 14.15). Metaplastic changes such as apocrine and squamous metaplasia can occur in gynaecomastia (Fig. 14.16). Pseudoangiomatous stromal hyperplasia (PASH) can also be present (Fig. 14.17). In the later phase of gynaecomastia (also called the *fibrous phase*),

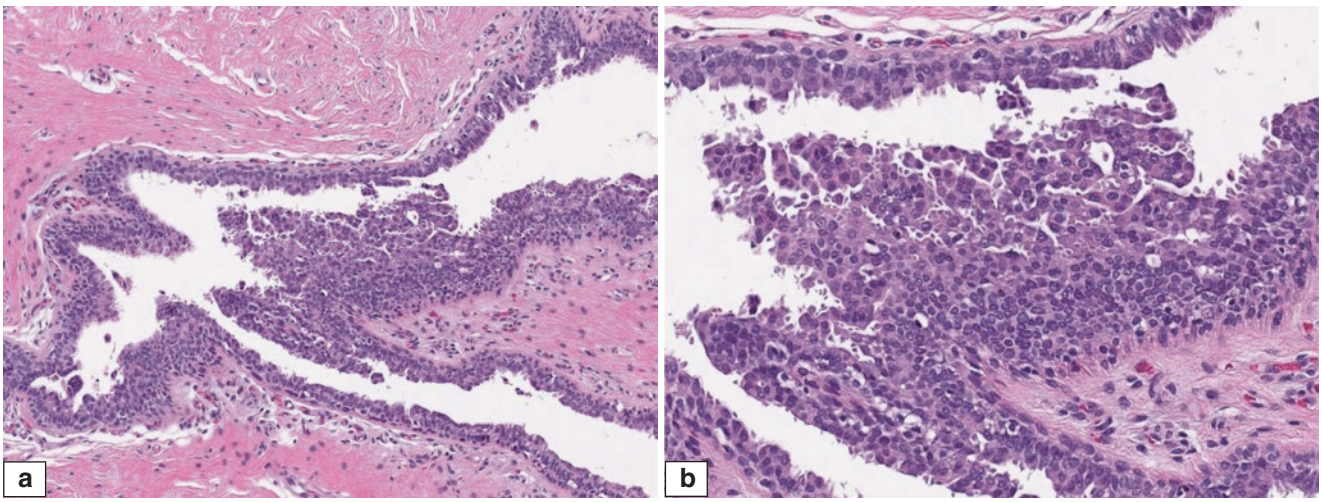

Fig. 14.8 Microscopic features of gynaecomastia. (**a**) Lining epithelium shows marked proliferation. (**b**) Proliferating epithelial cells are polymorphic in appearance

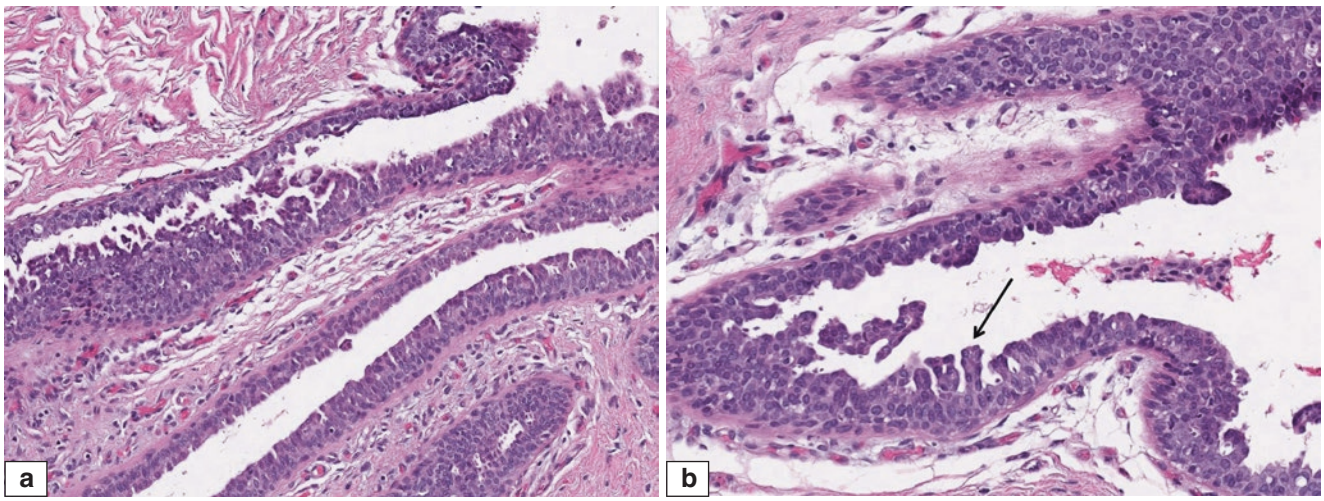

Fig. 14.9 Microscopic features of gynaecomastia. (**a**) Slightly dilated ducts are lined by thickened epithelium showing focal tufting, which may mimic a micropapillary pattern. (**b**) Micropapillary-like tufts are slender and non-rigid and comprise epithelial cells with a heterogeneous appearance (*arrow*)

fibrotic stroma predominates, ductal proliferation is diminished, and the epithelium undergoes atrophy (Fig. 14.18). The ducts are usually lined by flattened epithelium. The periductal stroma is hyalinised.

In rare cases, lobular development can occur; its pathogenesis is unclear. Ductal epithelial cells in gynaecomastia are usually strongly positive for oestrogen, progesterone, and androgen receptors [16, 17]. The presence of a dual cell population in the epithelial hyperplasia can be demonstrated by immunohistochemical stains for myoepithelial markers. Gynaecomastia glands occurring secondary to antiandrogen therapy may show positivity for prostate-specific antigen [20]. This finding should not be misinterpreted as showing a prostate origin for these glands.

Differential Diagnosis

Gynaecomastia must be differentiated from pseudogynaecomastia and benign and malignant breast neoplasms. Pseudogynaecomastia (lipomastia) refers to prominence of the breast due to excessive adipose deposition in subcutaneous tissue without breast glandular proliferation; it usually occurs in elderly, obese males. Physical examination and imaging studies reveal diffuse breast enlargement without subareolar nodules.

The epithelial proliferation seen in the early phase of gynaecomastia can be quite prominent and can mimic in situ carcinoma. The characteristic architectural features of gynaecomastia and the lack of cytologic monotony of in situ

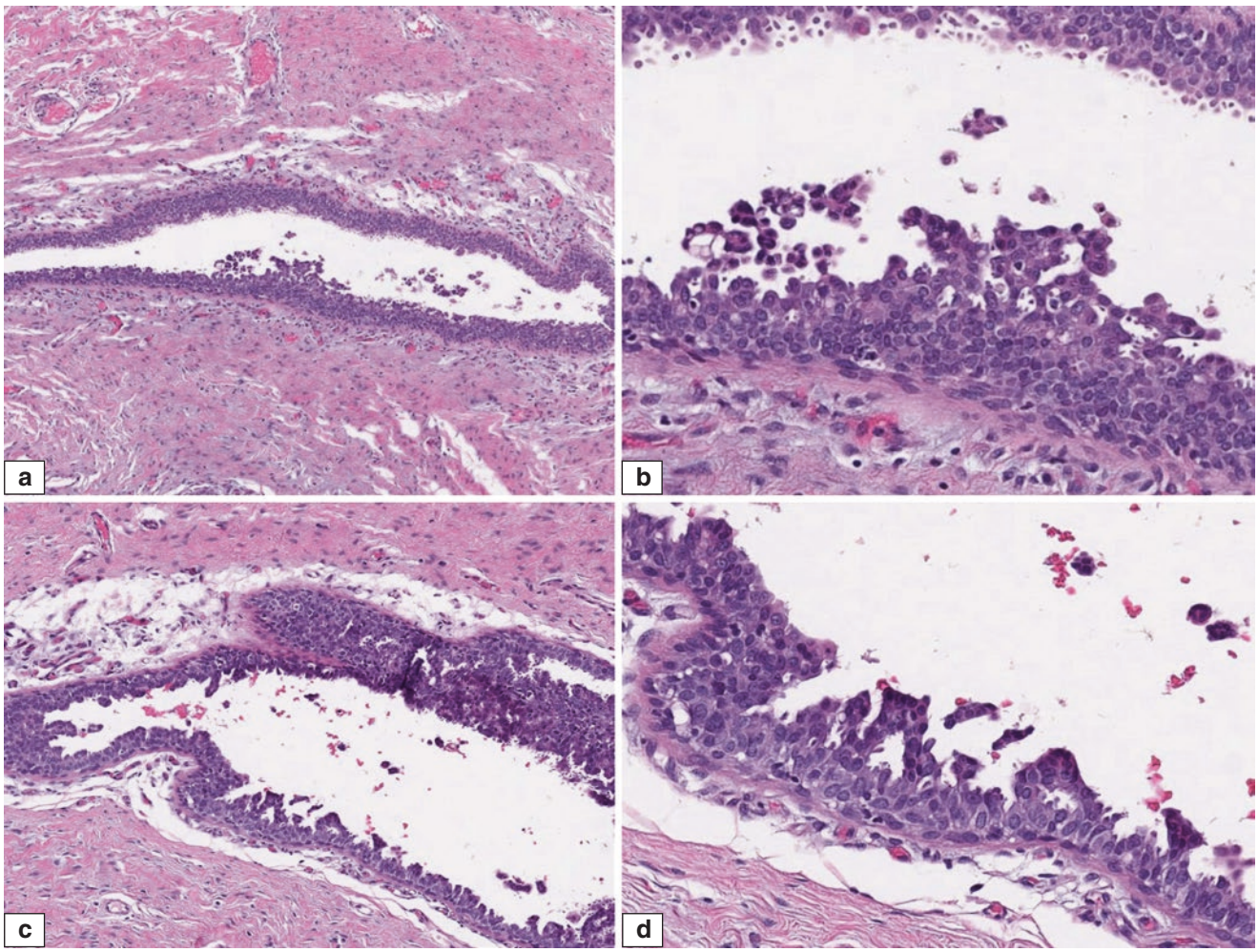

Fig. 14.10 Microscopic features of gynaecomastia. (**a–d**) Lining epithelium shows micropapillary tufts, which are irregularly distributed and tapering near the tips

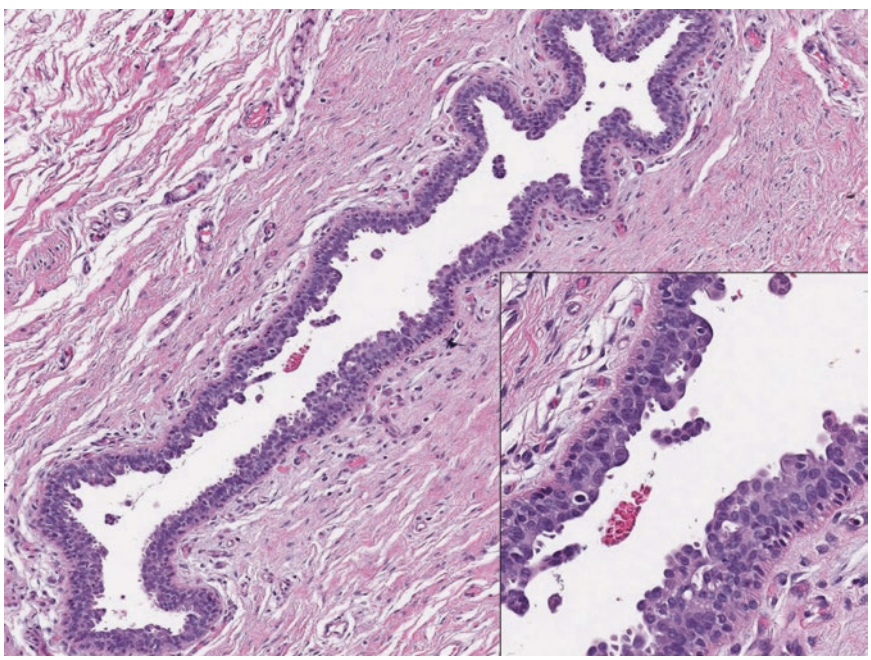

Fig. 14.11 Microscopic features of gynaecomastia. Lining epithelium shows luminal protrusions. *Inset* shows high magnification of the epithelial protrusions into the duct lumen

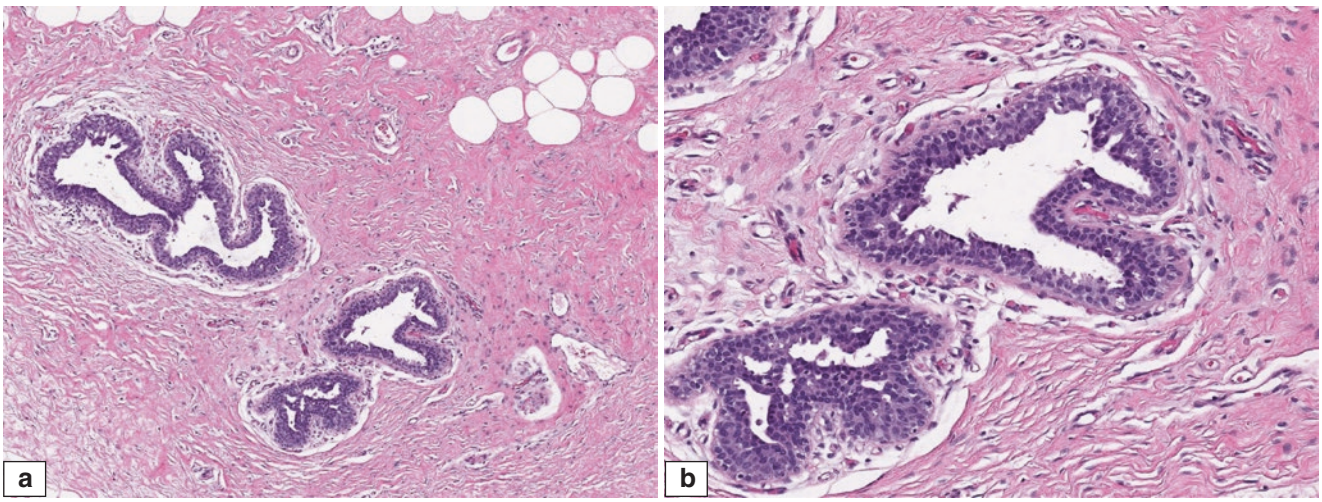

Fig. 14.12 Microscopic features of gynaecomastia. (**a**, **b**) Cellular fibrotic stroma associated with small glands, which are lined by epithelium of three to four cells thick

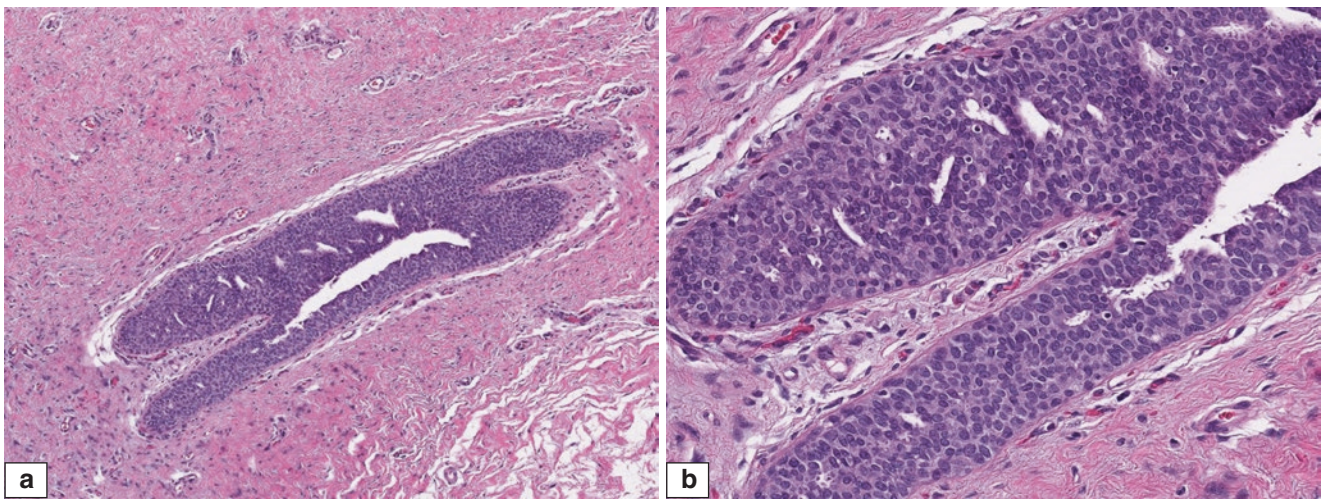

Fig. 14.13 Microscopic features of gynaecomastia. (**a**, **b**) Florid usual ductal hyperplasia almost completely fills the lumen. Based on the polymorphous nature of the epithelium, it is not atypical

ductal carcinoma should be helpful in making the distinction. Atypical ductal hyperplasia is rarely diagnosed in a background of gynaecomastia [21]. Its distinction from usual ductal hyperplasia is based on primarily morphological and adjunctive immunohistochemical features, with atypical ductal hyperplasia often disclosing a cribriform pattern of uniform epithelial cells accompanied by high ER and reduced CK5/6 expression.

Benign breast lesions such as nipple duct adenomas, papillomas, and sclerosing adenosis may occur in the male breast. Histologic criteria for these lesions are the same as in a female breast.

Prognosis and Therapy Considerations

Gynaecomastia reflects an underlying imbalance in the hormonal physiology in which there is an increase in oestrogen relative to androgen action at the breast-tissue level. Similar to female breast development, oestrogen, along with growth hormone and insulin growth factor-1 (IGF-1), is required for breast growth in males. Normally a balance exists between oestrogens and androgens in males. Any pathologic condition or medication that can cause an elevation in the ratio of oestrogen to androgen, either by increasing oestrogen levels or decreasing androgen levels, can induce gynaecomastia [13, 17, 18].

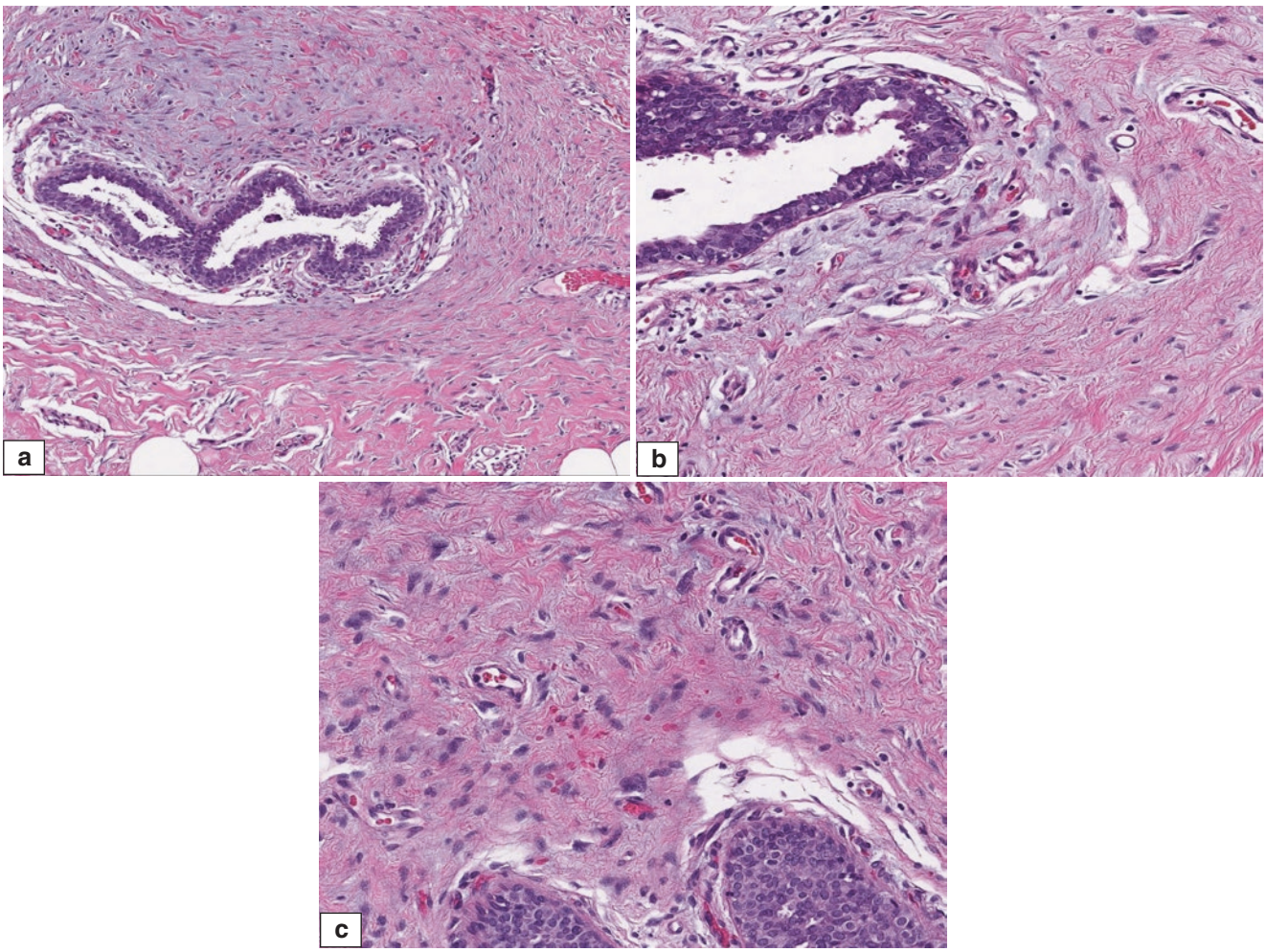

Fig. 14.14 Microscopic features of gynaecomastia. (**a**, **b**) The periductal stroma is oedematous and has myxoid features. (**c**) The stromal cells have variably dense and irregular nuclei admixed with a proliferation of capillaries

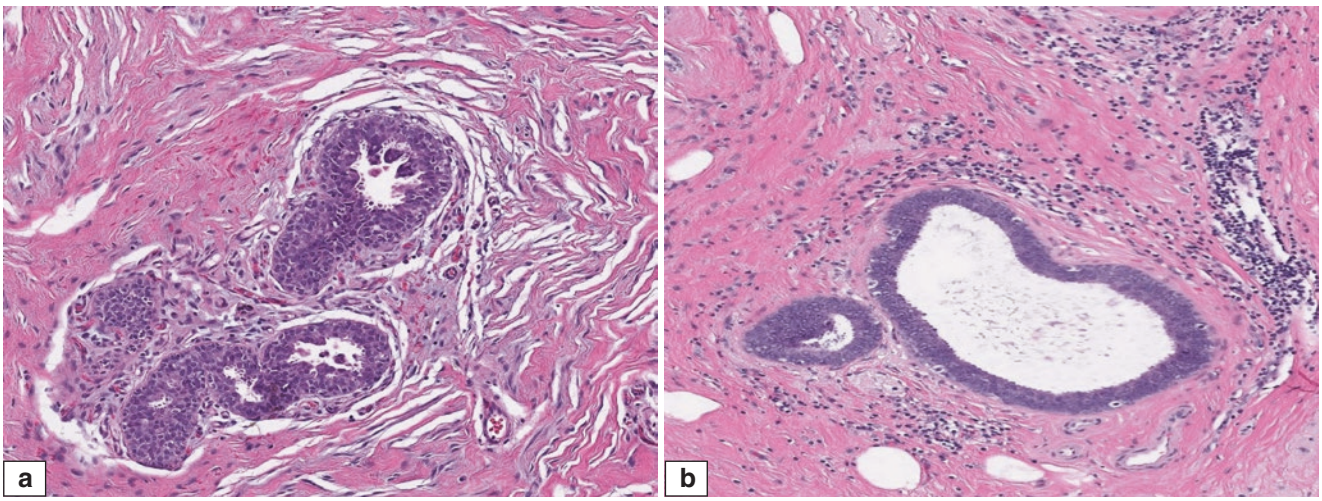

Fig. 14.15 Microscopic features of gynaecomastia. (**a**) The periductal stroma is hypercellular and contains scattered inflammatory cells. (**b**) Prominent periductal inflammatory infiltrate

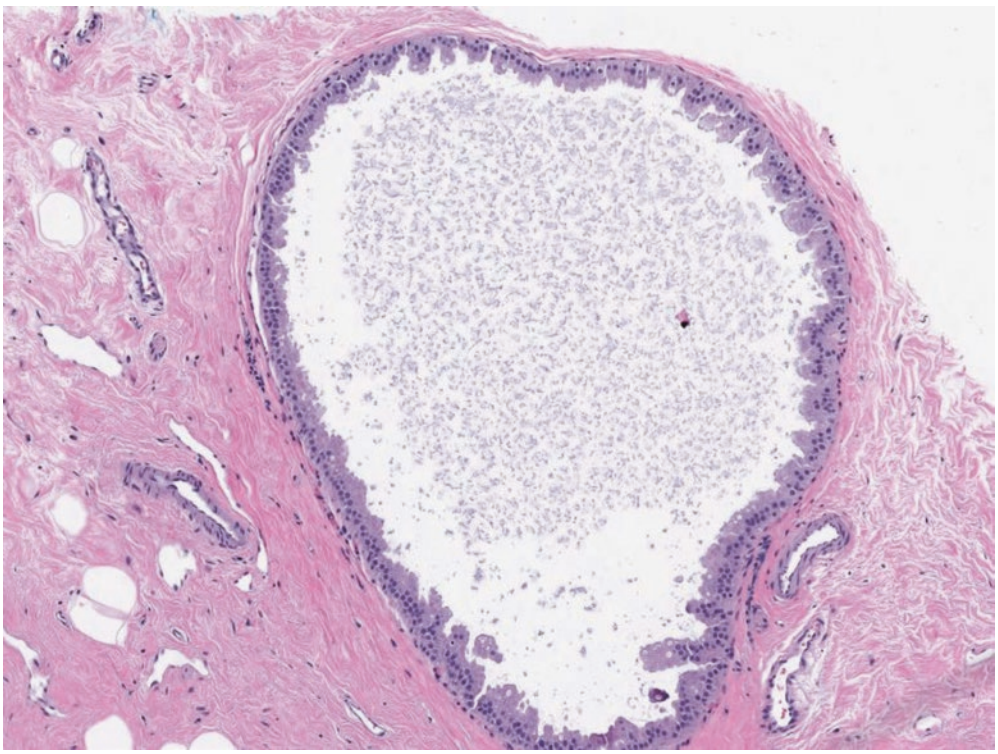

Fig. 14.16 Microscopic features of gynaecomastia. Cystic change with apocrine metaplasia is shown

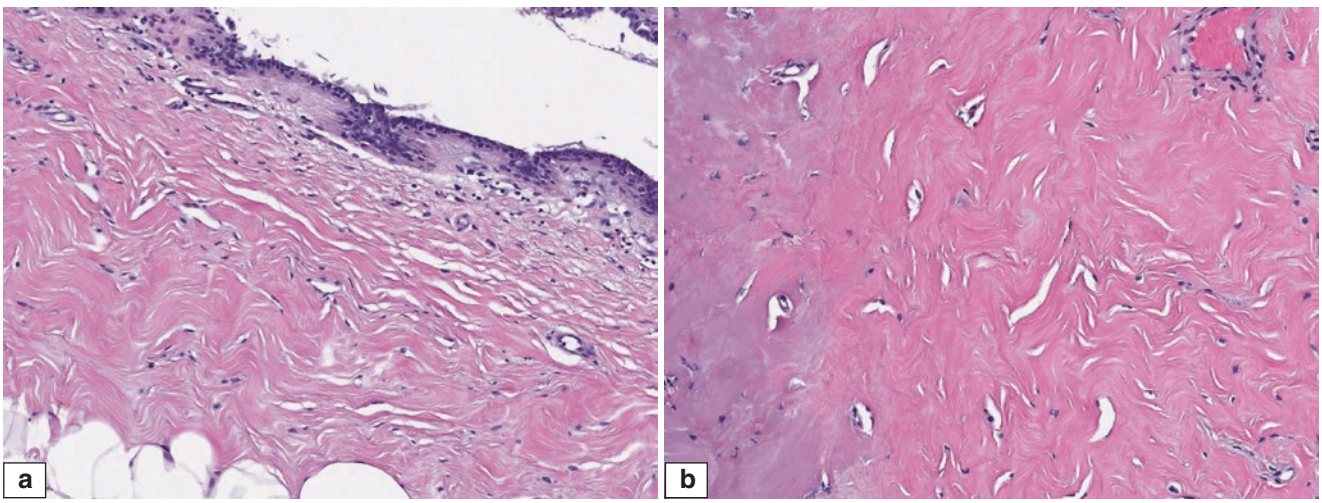

Fig. 14.17 Microscopic features of gynaecomastia. (**a**, **b**) Pseudoangiomatous stromal hyperplasia (PASH) is commonly seen in a background of gynaecomastia

Most cases of gynaecomastia are asymptomatic and patients seek clinical attention for cosmetic concerns. The condition may cause local pain and tenderness, however, and could occasionally be the result of a serious underlying illness or sensitivity to a medication; it may even be inherited. In all ages, if a specific cause of the gynaecomastia is identified, treatment of the underlying cause is warranted, but most cases do not require treatment. Treatment should not be initiated during the initial phase, when the breast hypertrophy may regress. If no underlying cause is discovered, then close observation is appropriate. Surgery to remove the enlarged breast tissue may be necessary if gynaecomastia does not resolve spontaneously or with medical therapy.

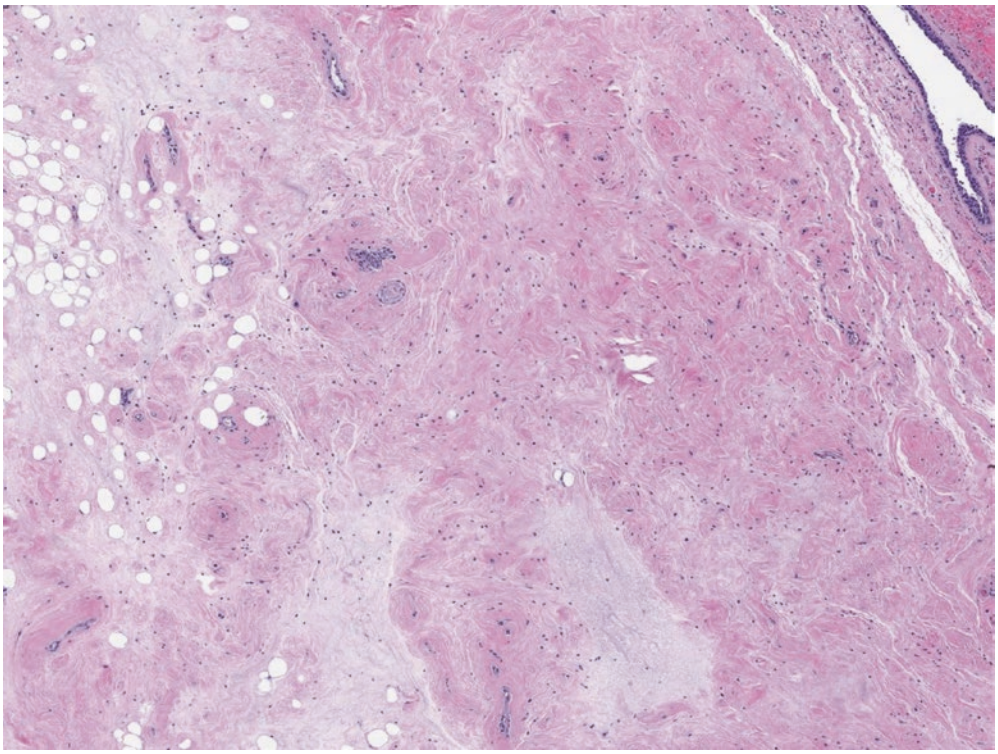

Fig. 14.18 Microscopic features of gynaecomastia. Hypocellular diffuse fibrosis (end stage of gynaecomastia)

Male Breast Cancer

Definition

Male breast cancer is simply breast carcinoma that occurs in the breast tissue of men.

Clinical and Epidemiological Features

Because of its relative rarity, male breast cancer has not been studied as extensively as female breast cancer. Male breast cancer is an uncommon tumour in Western countries, accounting for less than 1 % of all breast cancers and less than 1 % of all malignancies in males. The ratio of male to female breast cancer is approximately 1:100 in the United States. According to the American Cancer Society, an estimated 2240 new cases of male breast cancers occur annually, and approximately 400 men die from breast cancer [22–24]. The incidence rate of male breast cancer is higher in African Americans than in whites, and it is higher in geographic regions where chronic liver disease due to infectious and neoplastic aetiologies is relatively higher than in Western countries [25–30]. In central Africa, breast cancer constitutes 5–6 % of all malignancies in males.

Risk factors for male breast cancer include family history of breast cancer, inherited gene mutations, Klinefelter syndrome, liver disease, increased sources of endogenous and exogenous oestrogen, obesity, occupational and environmental exposures, and radiation [28]. Breast cancer risk is increased if other members of the family have had breast cancer. About one of five men with breast cancer has a close male or female relative with breast cancer. Men with a mutation in the *BRCA2* gene have an increased risk of breast cancer. *BRCA1* mutations can also increase the risk of male breast cancer, but the risk appears to be lower. Mutations in *CHEK2* and *PTEN* genes may be responsible for some male breast cancers [29, 31–34]. Klinefelter syndrome is a congenital condition defined by chromosomal abnormality of XXY. Compared with other men, patients with this syndrome have lower levels of androgens and higher levels of oestrogens; for this reason, they often develop gynaecomastia. Men with Klinefelter syndrome have a 50-fold higher risk of developing breast cancer than men in the general population. Ionising radiation is a known risk factor for female breast cancers, and similarly, the risk of male breast cancer increases with exposure to chest radiation. The liver

plays an important role in sex hormone metabolism by making binding proteins. These binding proteins affect hormonal activity. Men with severe liver disease such as cirrhosis have relatively low levels of androgens and higher levels of oestrogen, which lead to a higher rate of gynaecomastia as well as an increased risk of developing breast cancer. Men with occupational exposures to electromagnetic fields, gasoline fumes, or polyaromatic hydrocarbons have been reported as having a higher risk of developing breast cancer [22, 35].

Although male breast cancer is more common in elderly men, it can occur at any age, even in children. The average age at diagnosis is 65–67 years, which is a decade older than for women with breast cancer [36, 37]. A self-detected and painless breast mass, which is usually located in the retroareolar area, is the most common presenting symptom. Nipple discharge, bleeding, retraction, skin ulceration, and pain can also be present. Most lesions are unilateral. Synchronous bilateral male breast cancer is exceedingly rare.

Imaging Features

Mammography and ultrasonography have been used to differentiate benign lesions from cancer in men who have a breast lesion, but their benefit as a screening tool in males has been controversial [38–40]. Characteristic features of male breast cancer are very similar to those of breast cancer in females; a mass or architectural distortion with irregular margins is the most common presentation (Fig. 14.19). Unlike gynaecomastia, male breast cancer is located eccentrically to the nipple. A density associated with gynaecomastia is typically symmetrical and is described as having a triangular configuration in the early stages and a dendritic pattern in established lesions. Carcinoma may be obscured by background gynaecomastia. Cystic and papillary carcinomas may present as well-circumscribed masses. Calcifications can be identified in up to one third of the cases.

Pathologic Features

The pathologic features of male breast cancer are similar to those of female breast cancer [41, 42].

Macroscopic Features

The gross appearance of male breast cancer is identical to breast cancer in females. A hard, irregular, stellate, grey to white mass associated with yellow streaks is the most common gross appearance (Figs. 14.20 and 14.21).

Microscopic Features

Almost 90–95 % of all male breast carcinomas are invasive. In contrast to females, the frequency of in situ carcinoma is low in men, accounting for approximately 7 % of all male breast cancers; 95 % of these cases consist of ductal carcinoma in situ (DCIS) (Figs. 14.22 and 14.23). Only a few cases of lobular carcinoma in situ have been reported [43]. The most common histologic type of invasive male breast cancer is invasive ductal carcinoma not otherwise

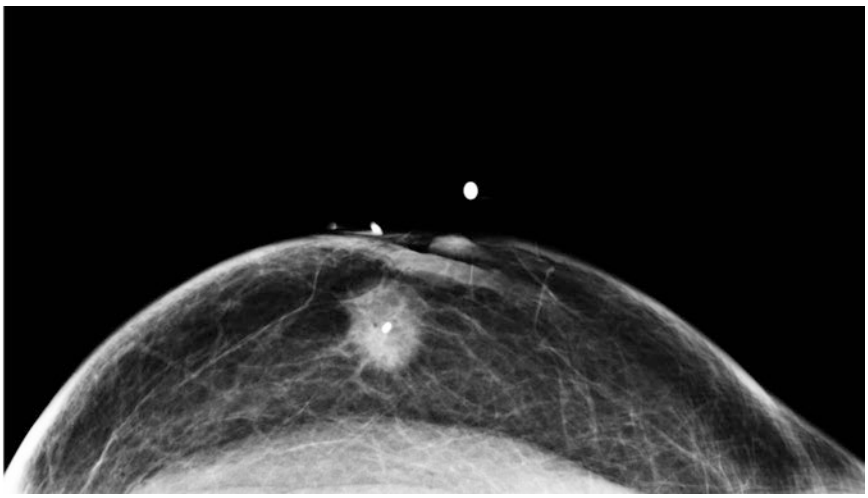

Fig. 14.19 Mammographic appearance of male breast cancer. A 1.8 cm eccentrically located spiculated mass is observed in the retroareolar area

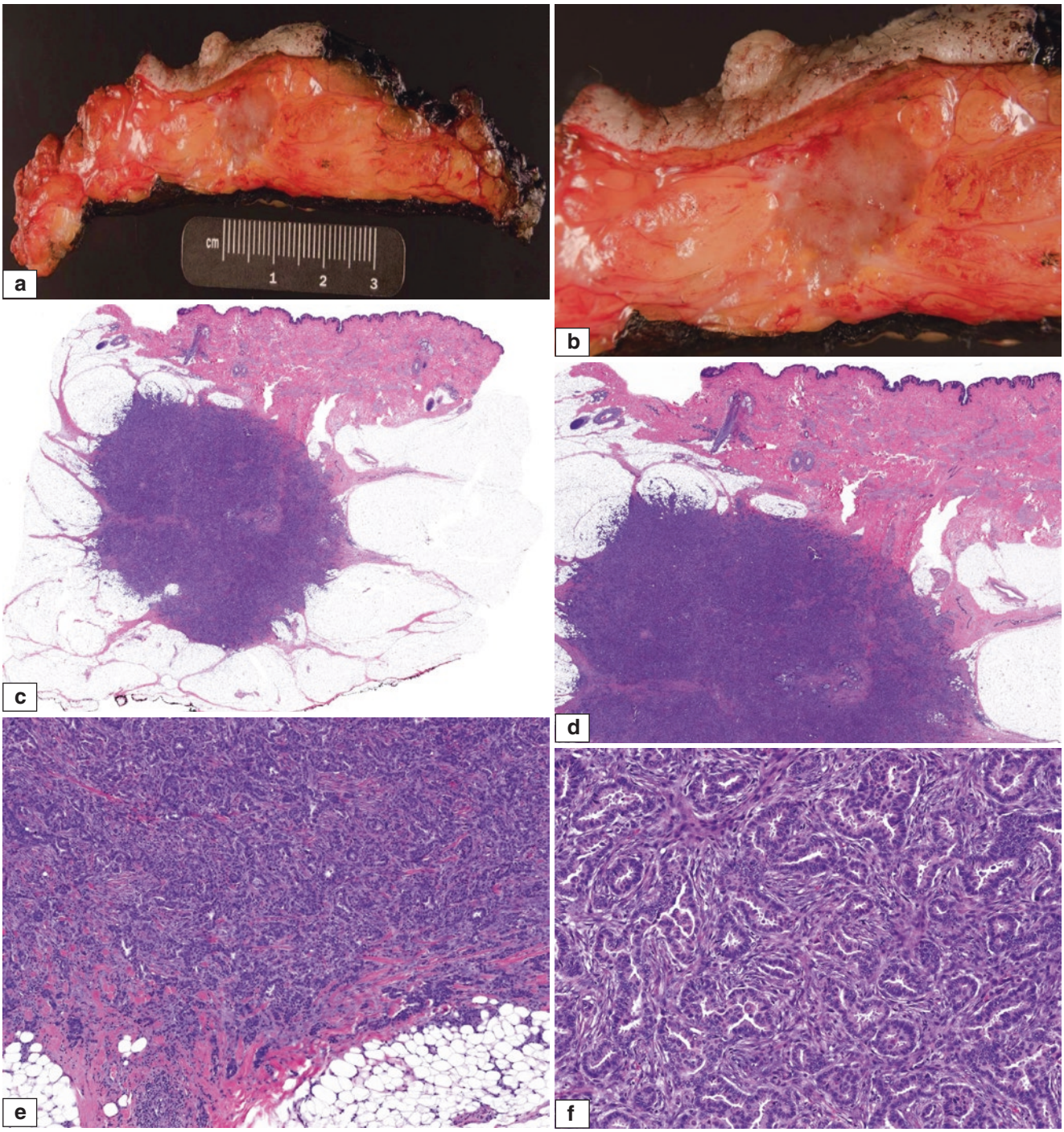

Fig. 14.20 Gross and microscopic features of male breast cancer. (**a**, **b**) Total mastectomy of male breast cancer, showing a well-demarcated tan-grey tumour. (**c**, **d**) Microscopic evaluation shows distinct demarcation of tumour from adjacent stroma, which is predominantly adipose tissue. (**e**, **f**) Higher magnification shows an invasive ductal carcinoma grade 2 (moderately differentiated)

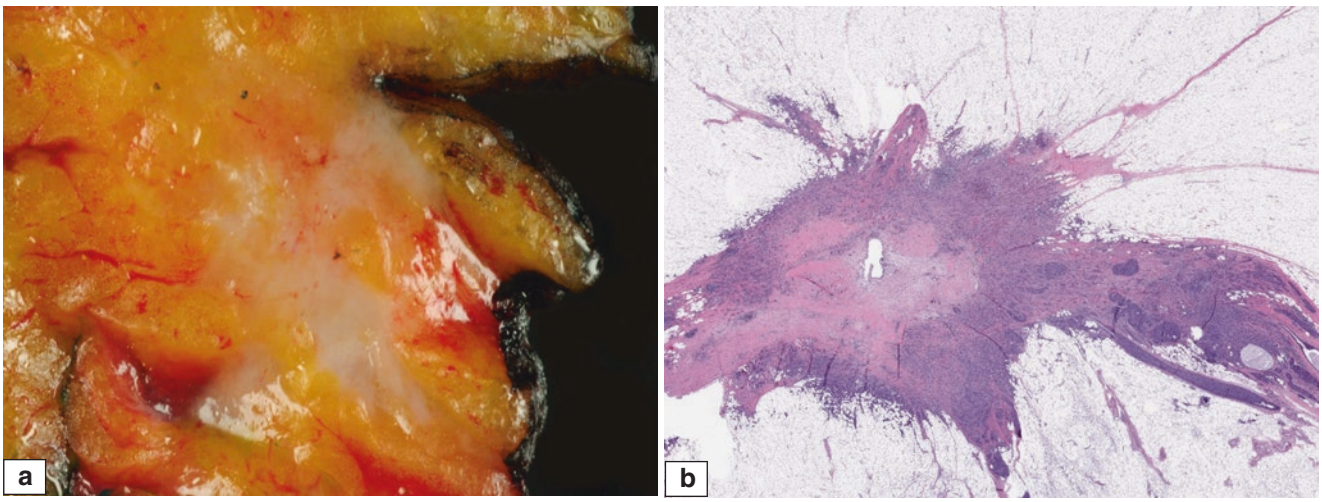

Fig. 14.21 Gross and microscopic features of male breast cancer. (**a**) Resection of tumour shows an irregular mass with infiltrative margins. The adjacent stroma is fibrous. (**b**) Microscopic evaluation shows an invasive carcinoma in a background of fibroadipose tissue

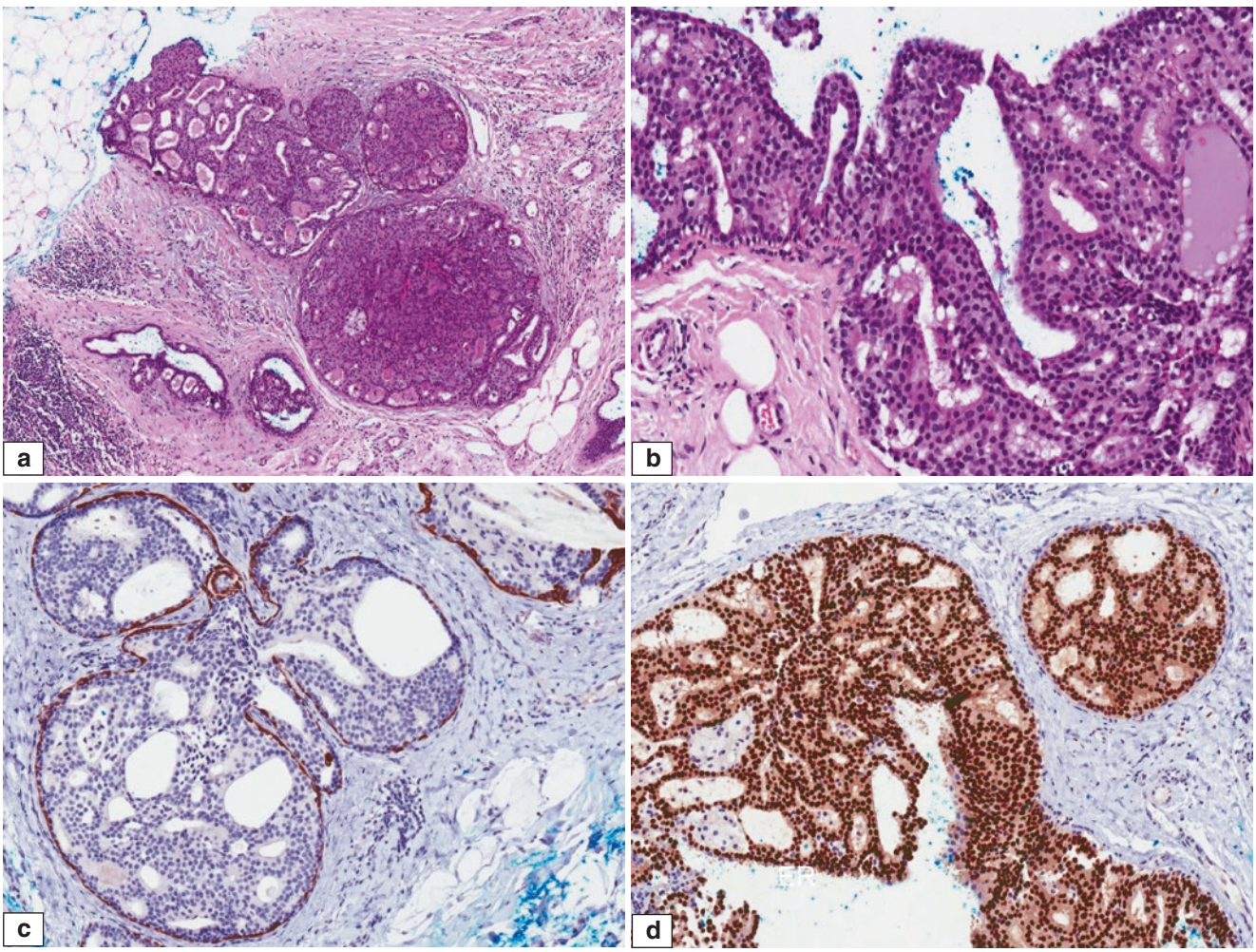

Fig. 14.22 Ductal carcinoma in situ (DCIS) in the male breast. (**a**) Expanded ducts are filled with a monotonous epithelial population with rigid cribriform spaces. Surrounding chronic inflammation is seen. (**b**) High magnification shows a uniform monomorphic population of epithelial cells. (**c**) Immunohistochemistry for CK14 decorates the peripheral myoepithelial population, but the neoplastic epithelial population is negative. (**d**) Diffuse positivity for oestrogen receptor is observed in the DCIS cells

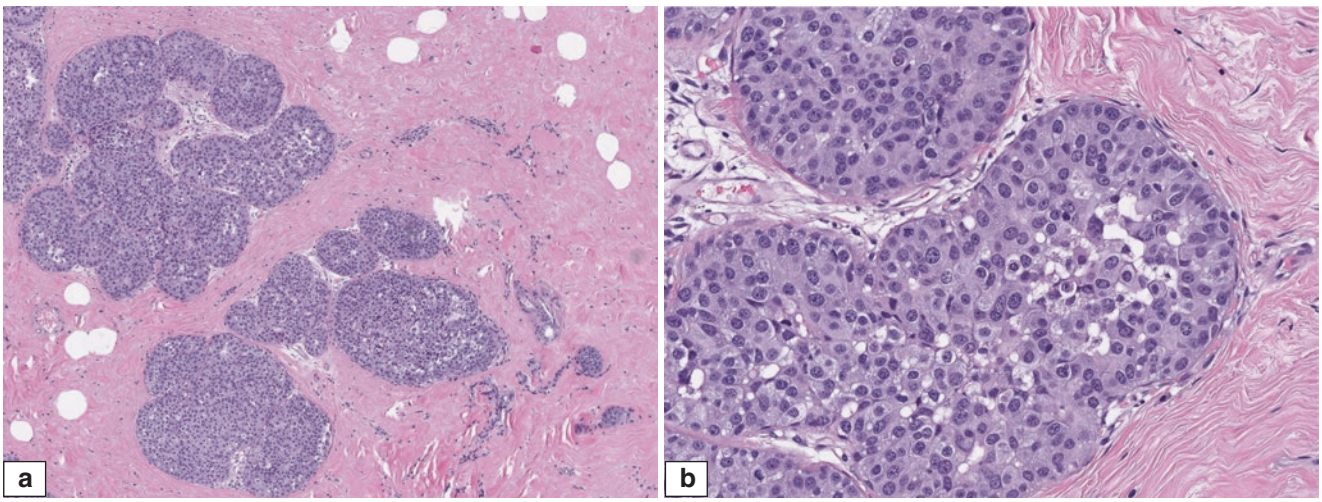

Fig. 14.23 Microscopic features of male breast cancer. (**a**, **b**) Male breast DCIS of intermediate nuclear grade

specified, accounting for 85 % of all cases. All other histologic types of invasive carcinoma have been reported in males [44]. In contrast to female breast cancers, invasive lobular carcinoma is rare in men. Some studies show that invasive papillary carcinomas are relatively more common in males than in females (Fig. 14.24). Similarly, neuroendocrine differentiation is more frequently observed in male breast cancer (Fig. 14.25). The grading system for female breast carcinoma should be used for male breast carcinoma. The majority of invasive male breast carcinomas are moderately or poorly differentiated (histological grades 2 and 3). Well-differentiated (grade 1) invasive carcinomas (including tubular, cribriform, and mucinous carcinomas) can also occur. The growth pattern and cytologic features of male breast cancer are identical to those of female breast cancer. The frequency of an in situ carcinoma component is reported to be lower in males (20–50 %) than in females (60–70 %). Inflammatory breast cancer is also reported in males. Paget disease of the nipple in men is extremely rare [45].

Most breast cancers in men express oestrogen and progesterone receptors. Based on data from the Surveillance, Epidemiology, and End Results (SEER) Program of the National Cancer Institute, the rates of hormone receptor positivity are higher in men than in women, with 90 % oestrogen receptor positivity and 80 % progesterone receptor positivity in male breast cancers, versus 75 % and 65 % in female breast cancers (Fig. 14.26). The expression of androgen receptor has been reported in 50–90 % of male breast cancers. Overexpression and amplification of the c-erbB-2 oncoprotein and gene have been reported to be similar to those found in their female counterparts [46–49].

Differential Diagnosis

Gynaecomastia, papillomas, benign and malignant stromal neoplasms, biphasic tumours (fibroadenoma and phyllodes tumour), reactive conditions such as fat necrosis, and metastatic tumours are the main differential diagnoses for male breast cancer. In most cases, based on clinical examination, imaging features, and preoperative core needle biopsy, a diagnosis can be easily established. Metastases from other solid neoplasms are sometimes difficult to diagnose. Metastatic prostate adenocarcinoma is commonly a diagnostic problem. Patients who receive hormonal therapy for prostatic adenocarcinoma almost always develop gynaecomastia, which may show epithelial proliferations mimicking DCIS. Identification of all criteria required to establish the diagnosis of DCIS is important. Immunohistochemical staining for high-molecular-weight cytokeratins may be helpful because hyperplastic lesions show strong positivity, whereas the expression of high-molecular-weight cytokeratins is significantly diminished or lost completely in DCIS. Myoepithelial markers can be used to establish the invasive versus in situ nature of the ductal carcinoma. Expression of prostate-specific antigen is commonly used to confirm the prostate origin of a metastatic carcinoma. It is a useful marker in males to differentiate primary breast cancer from metastases, but rarely a primary male breast cancer can disclose aberrant expression of prostate-specific antigen. Prostate-specific acid phosphatase has so far not been reported in male breast cancer and can be used to establish the prostate origin of the cancer [50, 51]. Identification of intracytoplasmic mucin supports the diagnosis of breast carcinoma, as prostate carcinomas invariably fail to show any intracytoplasmic mucin.

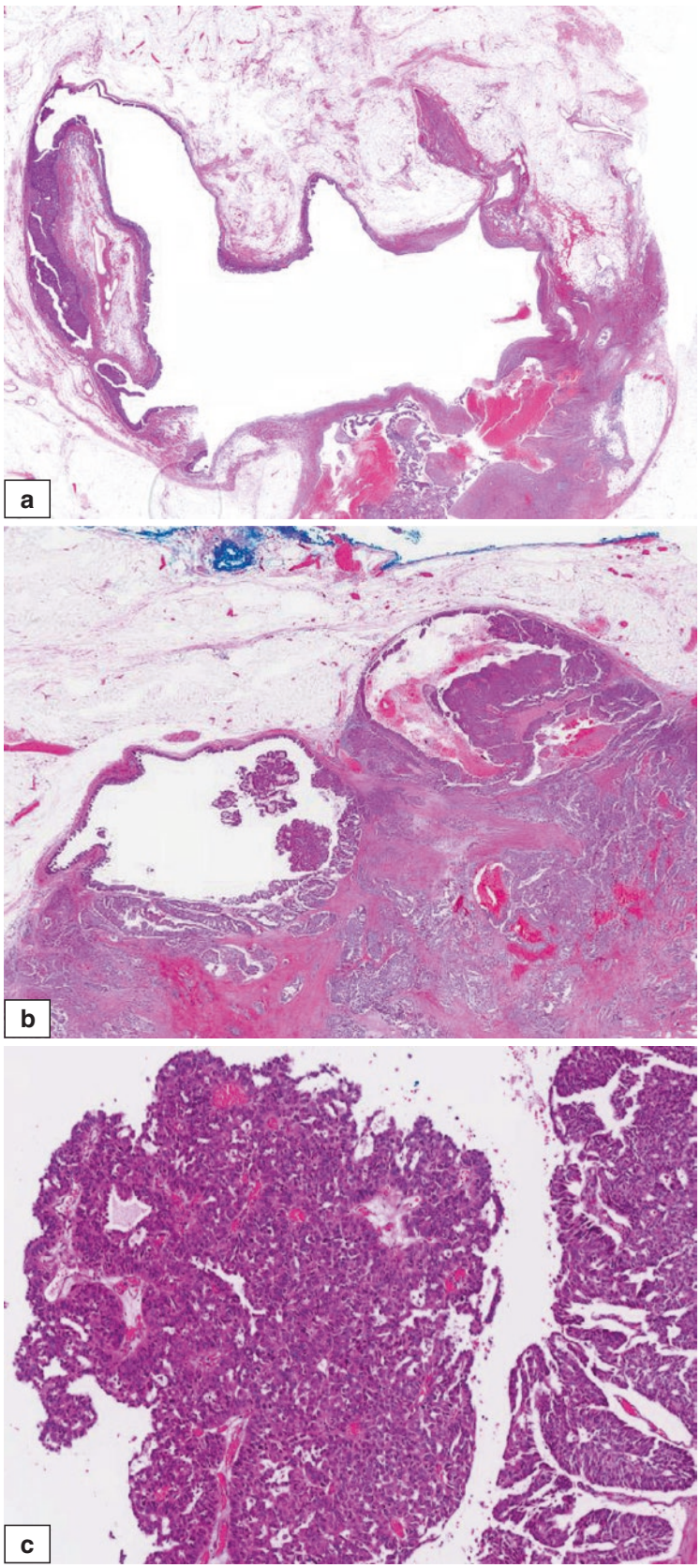

Fig. 14.24 Male breast cancer. (**a**) This tumour shows a cystic component with areas of haemorrhage. (**b**) A solid–cystic appearance is seen, with papillary fronds projecting into the cystic lumens; the surrounding tissue shows invasive tumour islands associated with haemorrhage. (**c**) Higher magnification of the malignant papillary structures, which are observed protruding into the cystic lumen

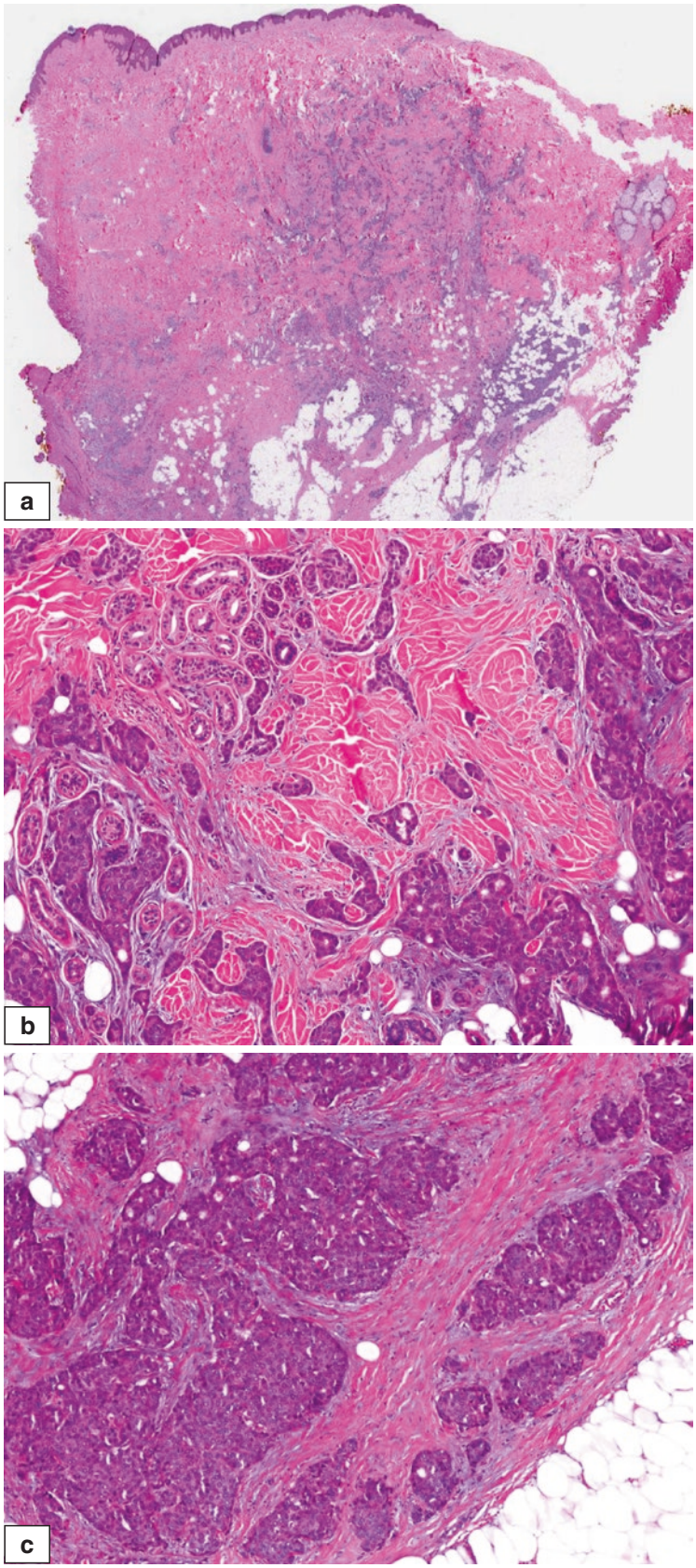

Fig. 14.25 Male breast cancer. (**a**) Low magnification shows an invasive carcinoma forming irregular, anastomosing nests in the dermis and fibrofatty breast parenchyma. (**b**) Invasive tumour islands extend around adnexal structures of the skin. (**c**) Confluent islands of tumour cells are seen in a fibrotic stroma. The tumour cells show eosinophilic cytoplasm. (**d**, **e**) Invasive carcinoma cells show diffuse reactivity for oestrogen receptor (**d**) and synaptophysin (**e**); the latter indicates neuroendocrine differentiation

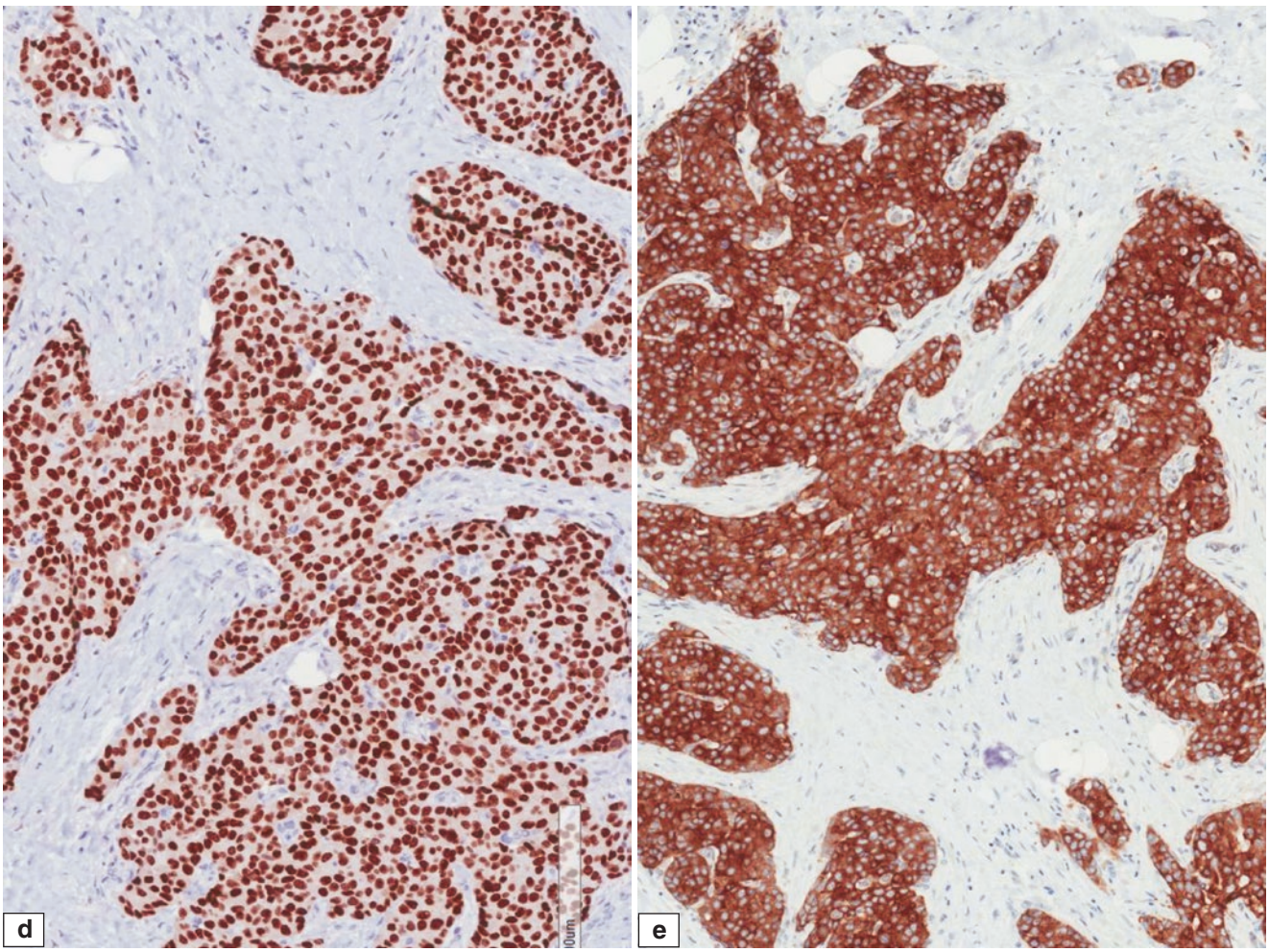

Fig. 14.25 (continued)

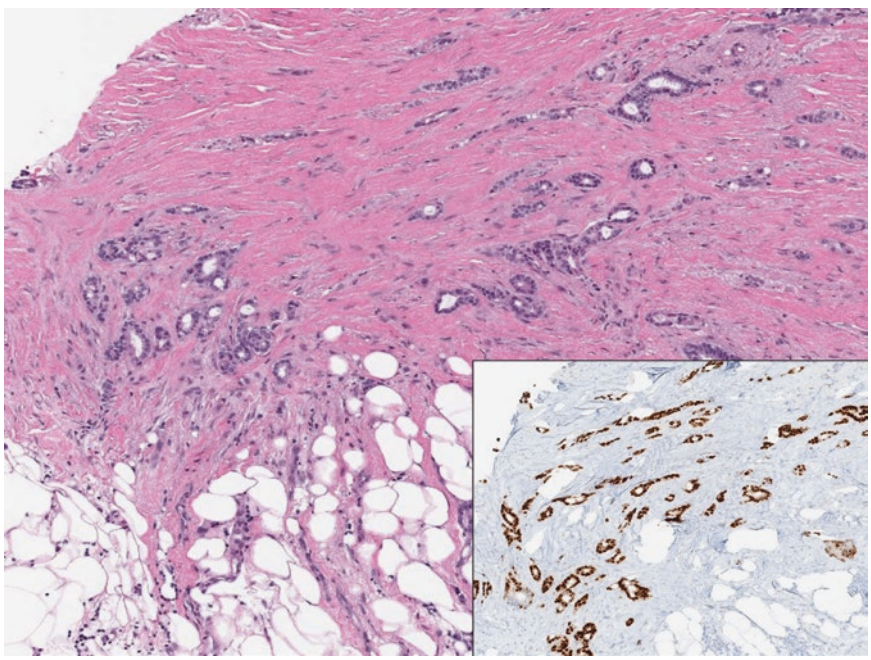

Fig. 14.26 Microscopic features of male breast cancer. Invasive ductal carcinoma. Immunohistochemical staining for oestrogen receptor shows diffuse positivity in the invasive carcinoma cells (*inset*)

Prognosis and Therapy Considerations

The same staging system used for female breast cancer is used for staging male breast cancer [52–55]. Tumour stage defined by tumour size and regional lymph node status is the most important prognostic factor of male breast cancer. Although experience with the sentinel lymph node procedure is relatively limited in male breast cancer, findings suggest that it is as accurate in males as in females [56]. Similar to female breast cancer, in addition to size and stage of the tumour, other biologic factors such as tumour subtype have a clear influence on survival in male breast cancer. Treatment of male breast cancer is the same as for females. It can involve some combination of surgery, radiation, chemotherapy, and hormone or targeted therapy. Since most male breast cancers are hormone receptor-positive, hormone therapy is often used [57].

References

1. Murray MP, Brogi E. Benign proliferative lesions of male breast. In: Hoda SA, Brogi E, Koerner FC, Rosen PR, editors. Rosen's breast pathology. 4th ed. Philadelphia: Lippincott Williams & Wilkins; 2014. p. 957–69.
2. Tavassoli FA, Eusebi V. Tumors of the mammary gland: atlas of tumor pathology. 4th series, fascicle 10. Washington, DC: American Registry of Pathology, Armed Forces Institute of Pathology; 2009.
3. Nguyen C, Kettler MD, Swirsky ME, Miller VI, Scott C, Krause R, Hadro JA. Male breast disease: pictorial review with radiologic-pathologic correlation. Radiographics. 2013;33:763–79.
4. Lemaine V, Simmons P. The adolescent female: breast and reproductive embryology and anatomy. Clin Anat. 2013;26:22–8.
5. Chau A, Jafarian N, Rosa M. Male breast: clinical and imaging evaluations of benign and malignant entities with histologic correlation. Am J Med. 2016;129:776–91.
6. Tangerud Å, Potapenko I, Skjerven HK, Stensrud MJ. Radiologic evaluation of lumps in the male breast. Acta Radiol. 2016;57:809–14.
7. Anderson JA, Gram JB. Male breast at autopsy. Acta Pathol Microbiol Immunol Scand. 1982;90:191–7.
8. Ladizinski B, Lee KC, Nutan FN, Higgins 2nd HW, Federman DG. Gynecomastia: etiologies, clinical presentations, diagnosis, and management. South Med J. 2014;107:44–9.
9. Ersöz H, Onde ME, Terekeci H, Kurtoglu S, Tor H. Causes of gynaecomastia in young adult males and factors associated with idiopathic gynaecomastia. Int J Androl. 2002;25:312–6.
10. Johnson RE, Murad MH. Gynecomastia: pathophysiology, evaluation, and management. Mayo Clin Proc. 2009;84:1010–5.
11. Lapid O, Jolink F, Meijer SL. Pathological findings in gynecomastia: analysis of 5113 breasts. Ann Plast Surg. 2015;74:163–6.
12. Ng AM, Dissanayake D, Metcalf C, Wylie E. Clinical and imaging features of male breast disease, with pathological correlation: a pictorial essay. J Med Imaging Radiat Oncol. 2014;58:189–98.
13. Hong JH, Ha KS, Jung YH, Won HS, An HJ, Lee GJ, et al. Clinical features of male breast cancer: experiences from seven institutions over 20 years. Cancer Res Treat. 2016;48(4):1389.
14. Georgiadis E, Papandreou L, Evangelopoulou C, Aliferis C, Lymberis C, Panitsa C, Batrinos M. Incidence of gynaecomastia in 954 young males and its relationship to somatometric parameters. Ann Hum Biol. 1994;21:579–87.
15. Nordt CA, DiVasta AD. Gynecomastia in adolescents. Curr Opin Pediatr. 2008;20:375–82.
16. Nicolis GL, Modlinger RS, Gabrilove JL. A study of the histopathology of human gynecomastia. J Clin Endocrinol Metab. 1971;32:173–8.
17. Oates SD. Gynecomastia. In: Babiera GV, Skoracki RJ, Esteva FJ, editors. Advanced therapy of breast disease. 3rd ed. Shelton: People's Medical Publishing House–USA; 2012. p. 271–94.
18. Bembo SA, Carlson HE. Gynecomastia: its features, and when and how to treat it. Cleve Clin J Med. 2004;71:511–7.
19. Cuhaci N, Polat SB, Evranos B, Ersoy R, Cakir B. Gynecomastia: clinical evaluation and management. Indian J Endocrinol Metab. 2014;18:150–8.
20. Gatalica Z, Norris BA, Kovatich AJ. Immunohistochemical localization of prostate-specific antigen in ductal epithelium of male breast. Potential diagnostic pitfall in patients with gynecomastia. Appl Immunohistochem Mol Morphol. 2000;8:158–61.
21. Wells JM, Liu Y, Ginter PS, Nguyen MT, Shin SJ. Elucidating encounters of atypical ductal hyperplasia arising in gynaecomastia. Histopathology. 2015;66(3):398–408.
22. Sasco AJ, Lowenfels AB, Pasker-de Jong P. Review article: epidemiology of male breast cancer. A meta-analysis of published case-control studies and discussion of selected aetiological factors. Int J Cancer. 1993;53:538–49.
23. Anderson WF, Jatoi I, Tse J, Rosenberg PS. Male breast cancer: a population-based comparison with female breast cancer. J Clin Oncol. 2010;28:232–9.
24. Giordano SH, Cohen DS, Buzdar AU, Perkins G, Hortobagyi GN. Breast carcinoma in men: a population-based study. Cancer. 2004;101:51–7.
25. Miao H, Verkooijen HM, Chia KS, Bouchardy C, Pukkala E, Laronningen S, et al. Incidence and outcome of male breast cancer: an international population-based study. J Clin Oncol. 2011;29:4381–6.
26. Greif JM, Pezzi CM, Klimberg VS, Bailey L, Zuraek M. Gender differences in breast cancer: analysis of 13,000 breast cancers in men from the National Cancer Data Base. Ann Surg Oncol. 2012;19:3199–204.
27. Ly D, Forman D, Ferlay J, Brinton LA, Cook MB. An international comparison of male and female breast cancer incidence rates. Int J Cancer. 2013;132:1918–26.
28. Ferzoco RM, Ruddy KJ. The epidemiology of male breast cancer. Curr Oncol Rep. 2016;18:1.
29. Masci G, Caruso M, Caruso F, Salvini P, Carnaghi C, Giordano L, et al. Clinicopathological and immunohistochemical characteristics in male breast cancer: a retrospective case series. Oncologist. 2015;20:586–92.
30. Sanguinetti A, Polistena A, Lucchini R, Monacelli M, Galasse S, Avenia S, et al. Male breast cancer, clinical presentation, diagnosis and treatment: twenty years of experience in our Breast Unit. Int J Surg Case Rep. 2016;20S:8–11.
31. Tai YC, Domchek S, Parmigiani G, Chen S. Breast cancer risk among male BRCA1 and BRCA2 mutation carriers. J Natl Cancer Inst. 2007;99:1811–4.
32. Deb S, Wong SQ, Li J, Do H, Weiss J, Byrne D, et al. Mutational profiling of familial male breast cancers reveals similarities with luminal A female breast cancer with rare TP53 mutations. Br J Cancer. 2014;111:2351–60.
33. Silvestri V, Barrowdale D, Mulligan AM, Neuhausen SL, Fox S, Karlan BY, et al. Male breast cancer in BRCA1 and BRCA2 mutation carriers: pathology data from the Consortium of Investigators of Modifiers of BRCA1/2. Breast Cancer Res. 2016;18:15.
34. Deb S, Lakhani SR, Ottini L. Fox SB The cancer genetics and pathology of male breast cancer. Histopathology. 2016;68:110–8.
35. Brinton LA, Richesson DA, Gierach GL, Lacey Jr JV, Park Y, Hollenbeck AR, Schatzkin A. Prospective evaluation of risk

factors for male breast cancer. J Natl Cancer Inst. 2008;100: 1477–81.
36. Chavez-Macgregor M, Clarke CA, Lichtensztajn D, Hortobagyi GN, Giordano SH. Male breast cancer according to tumor subtype and race: a population-based study. Cancer. 2013;119:1611–7.
37. Mathew J, Perkins GH, Stephens T, Middleton LP, Yang WT. Primary breast cancer in men: clinical, imaging, and pathologic findings in 57 patients. AJR Am J Roentgenol. 2008;191:1631–9.
38. Yen PP, Sinha N, Barnes PJ, Butt R, Iles S. Benign and malignant male breast diseases: radiologic and pathologic correlation. Can Assoc Radiol J. 2015;66:198–207.
39. Khalkhali I, Cho J. Male breast cancer imaging. Breast J. 2015; 21:217–8.
40. Carrasco RM, Benito MA, Gomariz EM, Povedano JLR, Paredes MM. Mammography and ultrasound in the evaluation of male breast disease. Eur Radiol. 2010;20:2797–805.
41. Yu XF, Yang HJ, Yu Y, Zou DH, Miao LL. A prognostic analysis of male breast cancer (MBC) compared with post-menopausal female breast cancer (FBC). PLoS One. 2015;10:e0136670.
42. Muir D, Kanthan R, Kanthan SC. Male versus female breast cancers. A population-based comparative immunohistochemical analysis. Arch Pathol Lab Med. 2003;127:36–41.
43. Kao L, Bulkin Y, Fineberg S, Montgomery L, Koenigsberg T. A case report: lobular carcinoma in situ in a male patient with subsequent invasive ductal carcinoma identified on screening breast MRI. J Cancer. 2012;3:226–30.
44. Leone JP, Leone J, Zwenger AO, Iturbe J, Vallejo CT, Leone BA. Prognostic significance of tumor subtypes in male breast cancer: a population-based study. Breast Cancer Res Treat. 2015;152: 601–9.
45. Akita M, Kusunoki N, Nakajima T, Takase S, Maekawa Y, Kajimoto K, Ohno M. Paget's disease of the male breast: a case report. Surg Case Rep. 2015;1:103.
46. Zografos E, Gazouli M, Tsangaris G, Marinos E. The significance of proteomic biomarkers in male breast cancer. Cancer Genomics Proteomics. 2016;13:183–90.
47. Kornegoor R, Verschuur-Maes AH, Buerger H, Hogenes MC, de Bruin PC, Oudejans JJ, et al. Molecular subtyping of male breast cancer by immunohistochemistry. Mod Pathol. 2012;25:398–404.
48. Wenhui Z, Shuo L, Dabei T, Ying P, Zhipeng W, Lei Z, et al. Androgen receptor expression in male breast cancer predicts inferior outcome and poor response to tamoxifen treatment. Eur J Endocrinol. 2014;171:527–33.
49. Leach IH, Ellis IO, Elston CW. c-erb-B-2 expression in male breast carcinoma. J Clin Pathol. 1992;45:942.
50. Kraus TS, Cohen C, Siddiqui MT. Prostate-specific antigen and hormone receptor expression in male and female breast carcinoma. Diagnostic Pathology. 2010;5:63. doi: 1596-5-63.
51. Kidwai N, Gong Y, Sun X, Deshpande CG, Yeldandi AV, Rao MS, Badve S. Expression of androgen receptor and prostate-specific antigen in male breast carcinoma. Breast Cancer Res. 2004;6(1): R18–23.
52. Henriques Abreu M, Henriques Abreu P, Afonso N, Pereira D, Henrique R, Lopesv C. Patterns of recurrence and treatment in male breast cancer: a clue to prognosis? Int J Cancer. 2016;139(8): 1715–20.
53. Abreu MH, Afonso N, Abreu PH, Menezes F, Lopes P, Henrique R, et al. Male breast cancer: looking for better prognostic subgroups. Breast. 2016;26:18–24.
54. Piscuoglio S, Ng CK, Murray MP, Guerini-Rocco E, Martelotto LG, Geyer FC, et al. The genomic landscape of male breast cancers. Clin Cancer Res. 2016;22(16):4045–56.
55. Fentiman IS. Male breast cancer is not congruent with the female disease. Crit Rev Oncol Hematol. 2016;101:119–24.
56. Flynn LW, Park J, Patil SM, Cody 3rd HS, Port ER. Sentinel lymph node biopsy is successful and accurate in male breast carcinoma. J Am Coll Surg. 2008;206:616–21.
57. Khan MH, Allerton R, Pettit L. Hormone therapy for breast cancer in men. Clin Breast Cancer. 2015;15:245–50.

Treatment-Related Changes

15

Changes Related to Neoadjuvant Chemotherapy

Definition

Neoadjuvant, primary, or preoperative chemotherapy refers to the treatment of patients with systemic agents before definitive surgical removal of a tumour. Neoadjuvant chemotherapy was introduced in the early 1970s as the treatment of choice for inoperable, locally advanced breast cancer. This approach resulted in significant responses and downstaging of many tumours, permitting mastectomy in some patients. Gradually, the idea of neoadjuvant chemotherapy was extended to include patients with large but operable early-stage breast cancer, allowing the same possibility of tumour downstaging and breast-conserving surgery. Additionally, several randomised clinical trials and meta-analyses showed similar disease-free and overall survivals for patients who received chemotherapy in either an adjuvant or neoadjuvant setting. Today, based on these findings, neoadjuvant chemotherapy is considered an appropriate treatment option for most patients diagnosed with breast cancer where adjuvant chemotherapy was indicated [1–5]. For patients with inflammatory breast cancer, neoadjuvant therapy is regarded as the standard of care. It is the preferred option for locally advanced breast cancer, and this approach allows both clinicians and patients to have an in vivo assessment of therapeutic efficacy, which can then be used as a surrogate marker to predict long-term survival [6–8]. Additionally, neoadjuvant trials have been increasingly recognised as a promising platform for efficient testing of investigational compounds and experimental targeted therapies. Most of the current neoadjuvant therapy regimens include a combination of cytotoxic agents. In recent years, with the development of targeted therapy options, many different treatment protocols, which include hormonal and target-specific agents, have been used in the neoadjuvant setting. Assessment of the quantity and biology of the residual tumour can provide further prognostic information for patients receiving neoadjuvant therapy. The possibility of collecting tumour samples before, during, and after the neoadjuvant treatment offers a unique translational research opportunity to delineate the biologic actions of the often personalised, targeted compounds in vivo. Identifying response markers provides a valuable platform from which to advance personalised cancer therapy [8].

Clinical Considerations: Pretreatment Assessment

Breast Evaluation

Assessment of the extent of the breast lesion should begin with a careful physical examination including imaging studies (mammography and ultrasound, with MRI in selected patients) as recommended by the National Comprehensive Cancer Network (NCCN) guidelines [9]. An MRI of the breast is more sensitive in determining the extent of the tumour, but it may also overestimate tumour size. An MRI may be performed if another area of concern highlighted by the initial imaging indicates need for further evaluation [10].

According to NCCN guidelines, an image-guided core needle biopsy with placement of an image-detectable marker of the breast abnormality is necessary to confirm the diagnosis (Fig. 15.1) [9]. This biopsy will also provide tissue to assess histopathologic features (documentation of invasion, histologic type, and grade) and biomarkers (oestrogen and progesterone receptors, c-erbB-2, and Ki-67), as well as to demarcate the tumour bed for post-neoadjuvant management. Additional molecular testing on tissue is not the current standard of care in the preoperative setting at this time; it should not routinely be obtained outside of the context of a clinical trial. Many biomarkers are currently under investigation and may become the standard of care in the future, based on the results of further research. Accurate

P.H. Tan, A.A. Sahin, *Atlas of Differential Diagnosis in Breast Pathology*, Atlas of Anatomic Pathology,
DOI 10.1007/978-1-4939-6697-4_15

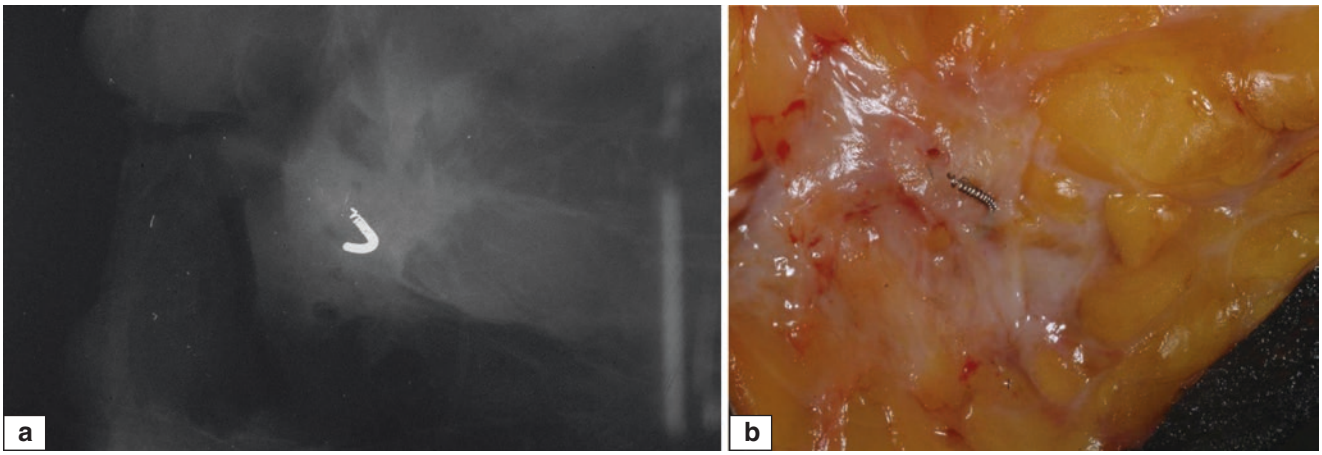

Fig. 15.1 Biopsy clip. (**a**) Specimen X-ray showing clip at the centre of the lesion. (**b**) Gross photograph showing biopsy clip in the centre of the dense, grey-white tumour bed

documentation of the extent of the disease prior to therapy is also very important. If clinical or imaging studies show multiple lesions, biopsy documentation of the additional lesions is recommended.

Axillary Evaluation

Patients being considered for neoadjuvant chemotherapy should undergo a careful physical examination of the axilla, with review of all imaging available, including mammography and ultrasonography [9]. If the clinical or breast imaging results are suspicious for lymphadenopathy, a dedicated axillary ultrasound is recommended for further evaluation [10, 11]. Fine needle aspiration (FNA) or core needle biopsy should be performed on any suspicious-appearing lymph nodes [12]. Placement of a biopsy clip into the biopsied node may improve the accuracy of surgical resection of biopsy-proven metastasis to axillary lymph nodes, allowing a more accurate assessment of pathologic response in the axilla [12].

For patients with clinically node-negative breast cancer at diagnosis, the role of a sentinel lymph node biopsy (SLNB) procedure prior to or following neoadjuvant chemotherapy is controversial [13–15]. One key limitation of SLNB prior to neoadjuvant therapy is that the removal of affected nodes prior to treatment precludes the ability to assess pathologic response. In most centres, performing SLNB after neoadjuvant therapy is preferred for patients with a clinically node-negative axilla at presentation, but it is most important that patient management in this setting must be individualised.

Surgery After Neoadjuvant Systemic Therapy

The aim of surgery after neoadjuvant therapy should be to remove all detectable residual disease with clear margins. In the case of a complete clinical response, the centre of the tumour bed should be removed, including any biopsy clips. Surgical resection volume will be based on preoperative imaging [15].

Evaluation of Breast Specimens After Neoadjuvant Systemic Therapy

Based on clinical and imaging findings, either a segmental resection or total mastectomy may be performed after neoadjuvant systemic therapy. The intention of pathology evaluation of breast specimens after systemic neoadjuvant therapy is to identify the tumour bed, document the response to therapy (including the size, extent, and cellularity of any residual tumour), assess the margins, and review the potential prognostic/predictive markers, if indicated [16, 17].

Accurate, reproducible documentation of pathologic response to neoadjuvant therapy requires the combination of imaging with gross and microscopic findings [17].

Identification of the Residual Tumour/Tumour Bed

Neoadjuvant systemic therapy may produce a variety of physical changes in breast tissue. Residual tumours may look significantly different from an untreated breast cancer. As the stroma of invasive carcinomas after systemic therapy is usually less cellular than that of untreated invasive carcinomas, changes in the previously desmoplastic cellular stroma lead to a softer tumour on palpation, which is more difficult to distinguish from adjacent normal breast parenchyma on gross inspection. In some cases, the tumour shrinks symmetrically, making the identification of residual tumour relatively direct (Fig. 15.2). In some cases, however, the therapeutic response is patchy, and tumours dissipate into scattered nodularity on gross inspection (Figs. 15.3 and 15.4). In these cases, specimen radiography and careful comparison of the imaging studies obtained before and after therapy are essential in order to identify any residual carcinoma (Fig. 15.5) [17].

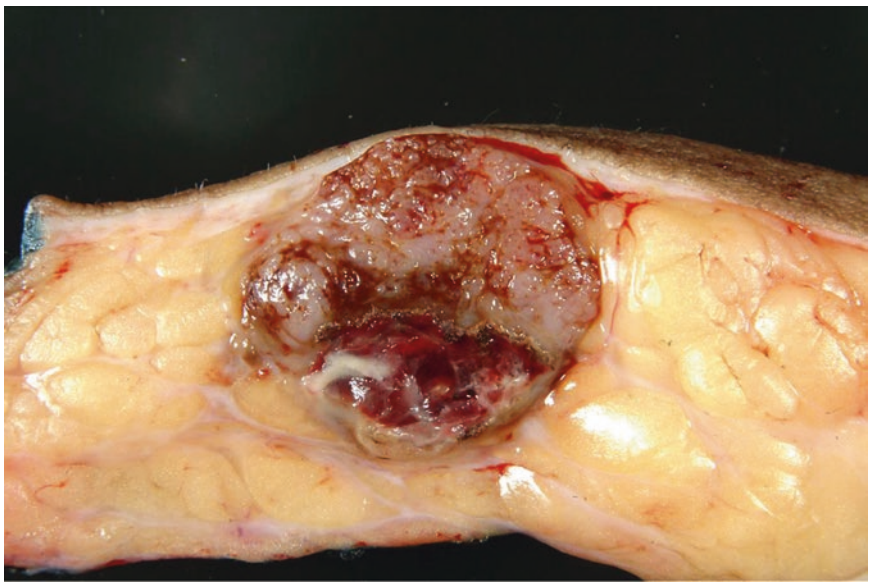

Fig. 15.2 Gross photograph of breast cancer after chemotherapy. A large area of necrosis and haemorrhage is seen in the lower portion of the well-defined tumour. The remaining grey-white portion in the upper part is viable tumour

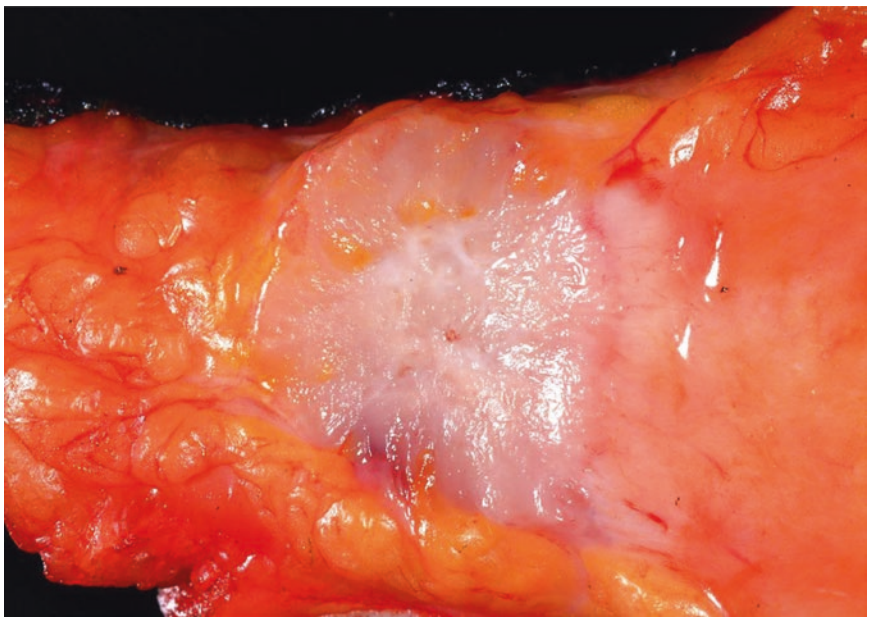

Fig. 15.3 Gross photograph of breast cancer after chemotherapy. This tumour is semi-defined, with still-identifiable borders; viable tumour can be seen as distinct from adjacent normal breast tissue

Histologic Sampling

If the resection specimen is small (e.g., less than 2–3 cm), it is reasonable to submit the entire resected breast tissue for microscopic evaluation. For larger segmental resections and total mastectomy specimens, the number of sections that must be submitted for accurate assessment depends on the size, number, and location of the tumour(s) prior to therapy [17, 18]. At least one to two sections per centimetre of the tumour is recommended if there is a macroscopically evident residual tumour [17, 19, 20]. If no residual tumour is evident on gross inspection of the specimen, the original tumour site (tumour bed) should be identified and sampled extensively [17, 20]. Overly exhaustive random sampling of the entire fibrotic breast parenchyma is not recommended. Obtaining specimen X-rays and carefully comparing imaging findings before and after therapy—including the identification of

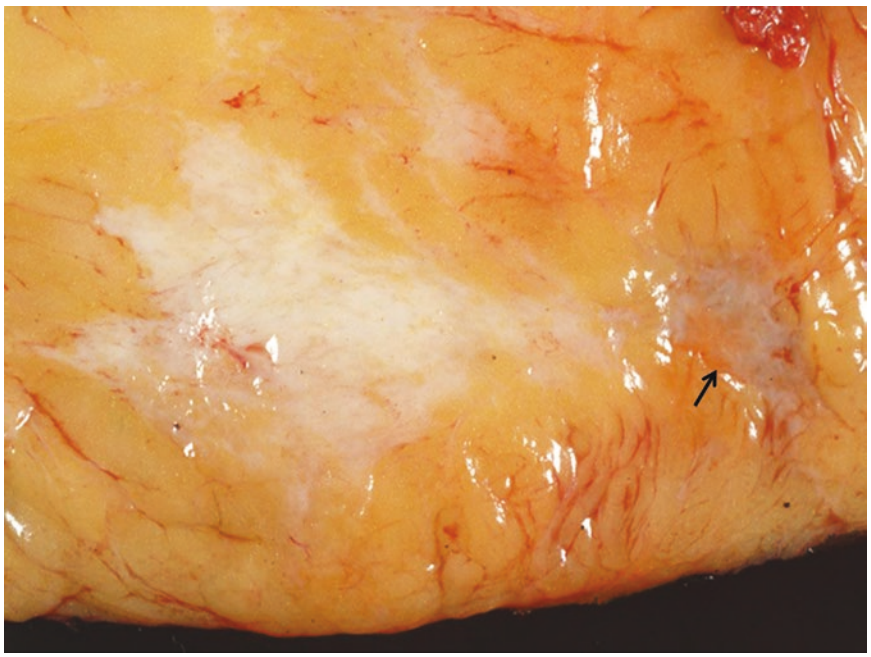

Fig. 15.4 Gross photograph of breast cancer after chemotherapy. Grey-white tissue blends into adjacent breast parenchyma, with ill-defined borders (*arrow*)

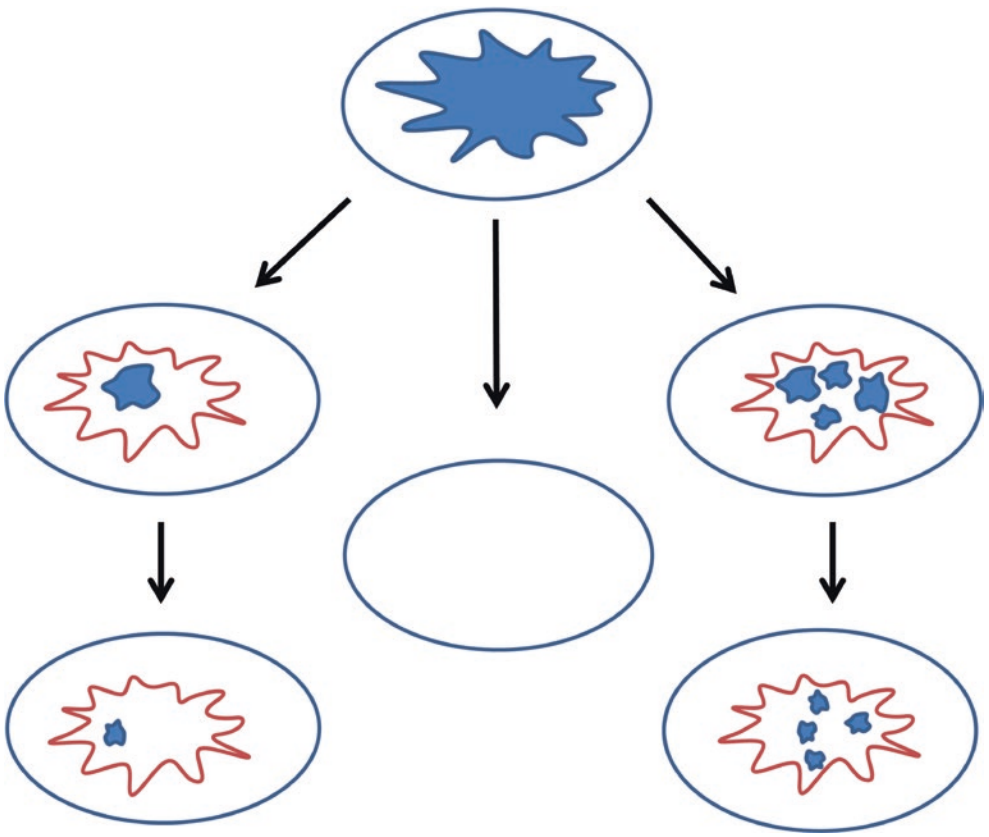

Fig. 15.5 Patterns of response to neoadjuvant therapy. After chemotherapy, tumours can completely disappear (complete pathologic response) (*middle panel*). They can shrink symmetrically (*left panel*), with a single tumour focus getting smaller with each therapy cycle, or they can break into multiple foci covering a similar area to that of the mass before chemotherapy (*right panel*), with each focus being much smaller than the original

biopsy marking clips and other imaging abnormalities such as microcalcifications associated with the tumour site—are critical for the selection of histologic samples. Furthermore, X-ray images of the sliced breast specimen can be used as a map on which paraffin-embedded tissue blocks can be annotated. These maps help the pathologists to reconstruct the extent and location of residual disease during the process of evaluating histopathologic sections prepared from these blocks [17]. This technique is essential, as it provides a more standardised and accurate evaluation of the residual tumour and generally requires processing of fewer tissue blocks than with a random sampling of what appears to be fibrotic breast tissue. Histologic sampling should include grossly visible tumour or tumour bed, as well as the immediately adjacent breast parenchyma. The extent of sampling should be based on the size and extent of the pretreated tumour, using findings from the specimen's radiography. In some cases, additional sampling may be necessary once the initial sections are reviewed, so keeping the sliced specimens in correct order and orientation is critical (Figs. 15.6, 15.7, 15.8, and 15.9) [20, 21].

The recommendation of the American Joint Committee on Cancer (AJCC)/Union for International Cancer Control (UICC) is to measure the largest contiguous focus of invasive carcinoma, excluding intervening fibrotic areas [20, 22]. This approach is appropriate for tumours with symmetrical shrinkage, but it may cause artificial downstaging of the residual tumour size for those tumours showing scattered tumour nests that were an integral part of a single tumour mass before treatment. To consider tumours multifocal, residual tumour foci should be separated by abundant non-neoplastic breast parenchyma or adipose tissue and should be measured independently. In this situation, dimensions from the largest tumour deposit should be used for AJCC staging, with "m" indicating the presence of multiple tumours.

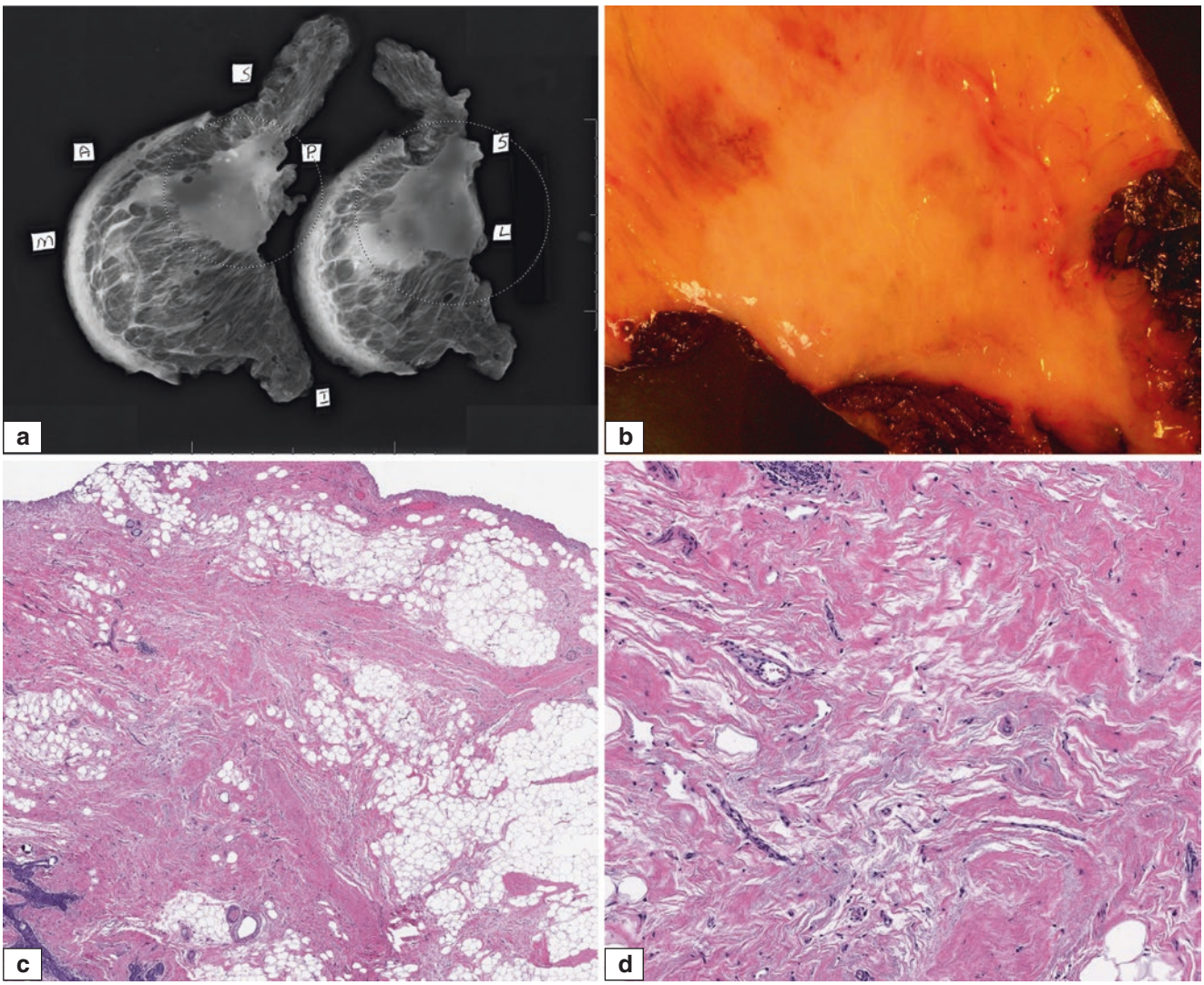

Fig. 15.6 Identification of tumour bed. (**a**) Specimen X-ray of mastectomy slices shows dense, fibrous tumour bed. (**b**) Gross photograph of corresponding fibrous tumour bed. (**c**) H&E-stained section of the fibrous tumour bed consists predominantly of hypocellular stroma with a few residual glandular elements. (**d**) Higher magnification shows hypocellular, dense stroma with prominent vessels in the tumour bed

Histologic Evaluation

The same criteria for evaluating the untreated breast carcinoma should be used for histologic typing of any remaining breast cancer after neoadjuvant therapy. Grading prior to neoadjuvant treatment is a mandatory histopathologic parameter that must be reported for all breast carcinomas. Grading is not a mandatory parameter in the post-therapy evaluation, as systemic therapy may alter the nuclear morphology as well as the mitotic rate, precluding accurate grading [17, 21, 23].

Tumour cellularity often decreases after systemic therapy (Fig. 15.10) [17, 19, 21, 23, 24]. A significant decrease in tumour cellularity has been shown to correlate with better prognosis in multiple studies. Unfortunately, no ideal method of tumour cellularity assessment is currently in use. Tumour cellularity of breast carcinomas often shows great variation even before systemic therapy. Comparing tumour cellularity before and after systemic therapy, to evaluate tumour response, has been proposed [25, 26]. Most tumours treated with neoadjuvant therapy are larger than 2 cm, however, and the extent of tumour sampling prior to systemic therapy varies, as the amount of tissue obtained by different biopsy techniques is significantly different. Also, comparison of tumour cellularity from biopsy material obtained before and after therapy may not always reflect actual tumour cell loss when there are no extreme changes. Therefore, comparison of tumour cellularity on pre-therapy and post-therapy samples is not uniformly reliable.

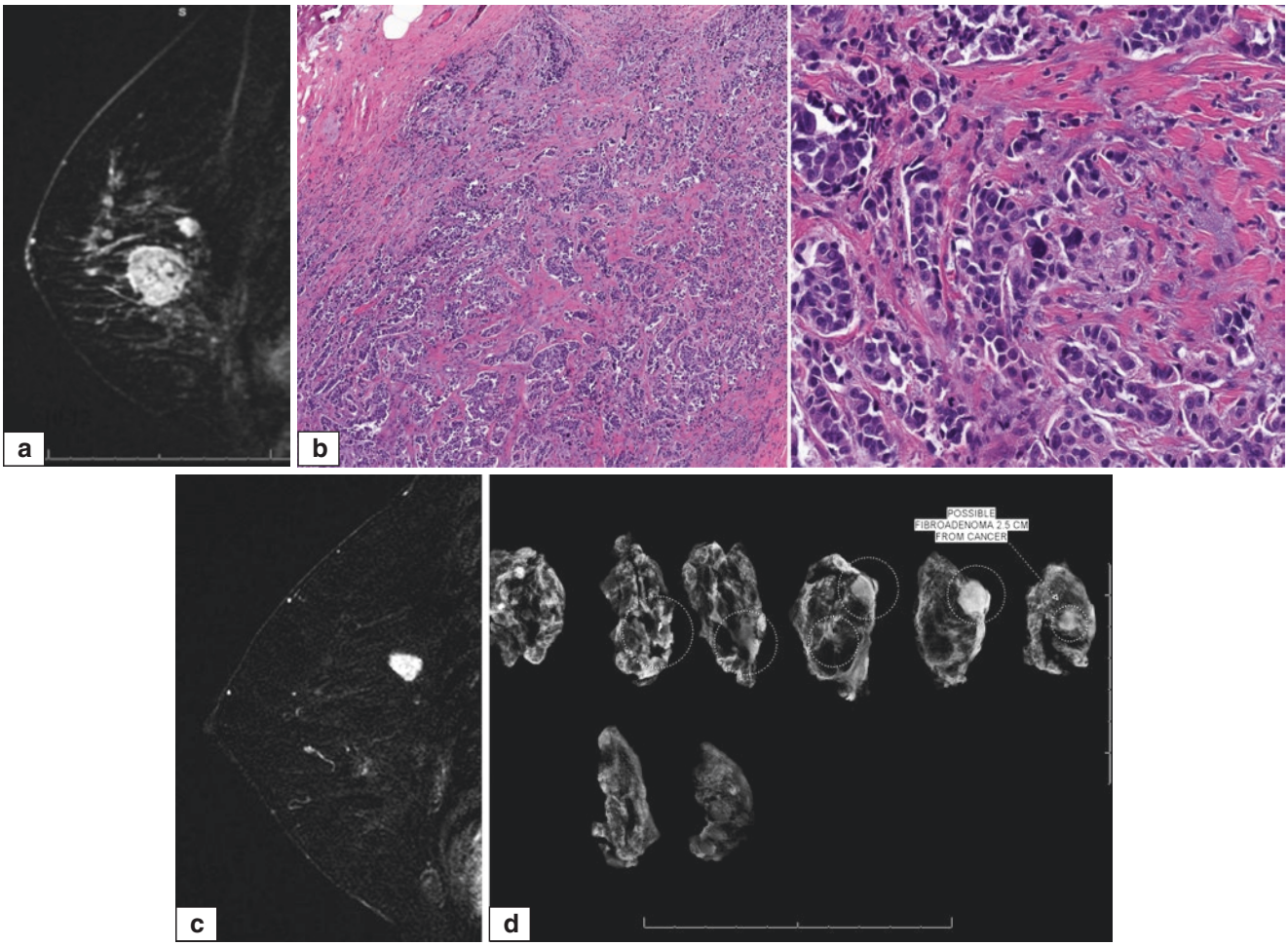

Fig. 15.7 Breast cancer with complete response to chemotherapy. (**a**) Breast MRI shows a large, irregular mass suspicious for invasive carcinoma, next to a smaller lesion with imaging characteristics of a fibroadenoma. (**b**) Core needle biopsy of the larger mass shows an invasive ductal carcinoma. (**c**) Breast MRI of the same patient after 6 months of chemotherapy shows complete disappearance of the large mass; the small lesion remains. (**d**) X-ray of the sliced specimen of the segmental resection. (**e**) Gross photograph of the fibrous tumour bed from the same patient. (**f**) H&E-stained histologic section of the fibrous tumour bed shows dense stroma with inflammatory cells, without any residual invasive carcinoma. (**g**) Note the almost total lack of glandular structures next to the previous biopsy site

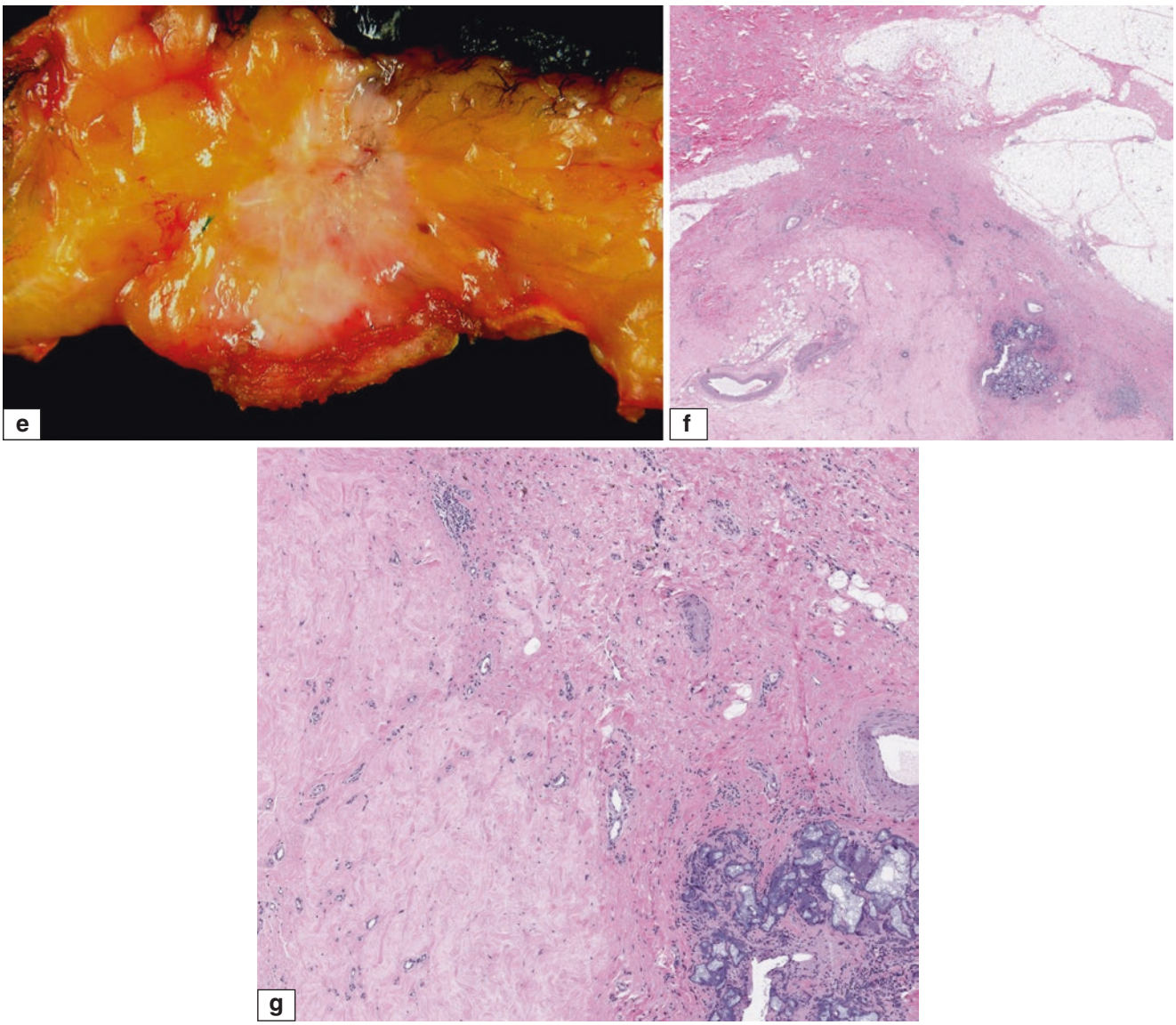

Fig. 15.7 (Continued)

Histologic evaluation should also include assessment of any in situ carcinoma component [17], the presence or absence of lymphovascular invasion, and the margin status (Figs. 15.11 and 15.12). Estimating tumour cellularity may be used to categorise the response to therapy. Depending on the method used, application of strict criteria is recommended [27].

Individual tumour cells show therapy-related changes, including nuclear enlargement, multinucleation, bizarre nuclear shapes, nuclear smudging, cytoplasmic vacuolisation, eosinophilic cytoplasmic change, and apoptosis (Fig. 15.13) [25].

If there is no residual carcinoma, identification of the tumour bed should be confirmed by microscopic evaluation [17]. Histologically, the tumour bed is characterised by hyalinised or fibrous stroma without glandular elements. The stroma is usually infiltrated by histiocytes, lymphocytes, and haemosiderin-laden macrophages. Stromal oedema, elastosis, and myxoid change are commonly observed (Fig. 15.14).

Histologic Changes in the Non-neoplastic Breast Parenchyma

The cytotoxic effect of systemic therapies can also be observed in non-neoplastic breast tissue. Epithelial atypia with nuclear or cytoplasmic enlargement, as well as nuclear hyperchromasia, is commonly seen in both ductal and lobular epithelium, accompanied by sclerosis of basement membranes. These changes should not be confused with residual carcinoma (Fig. 15.15).

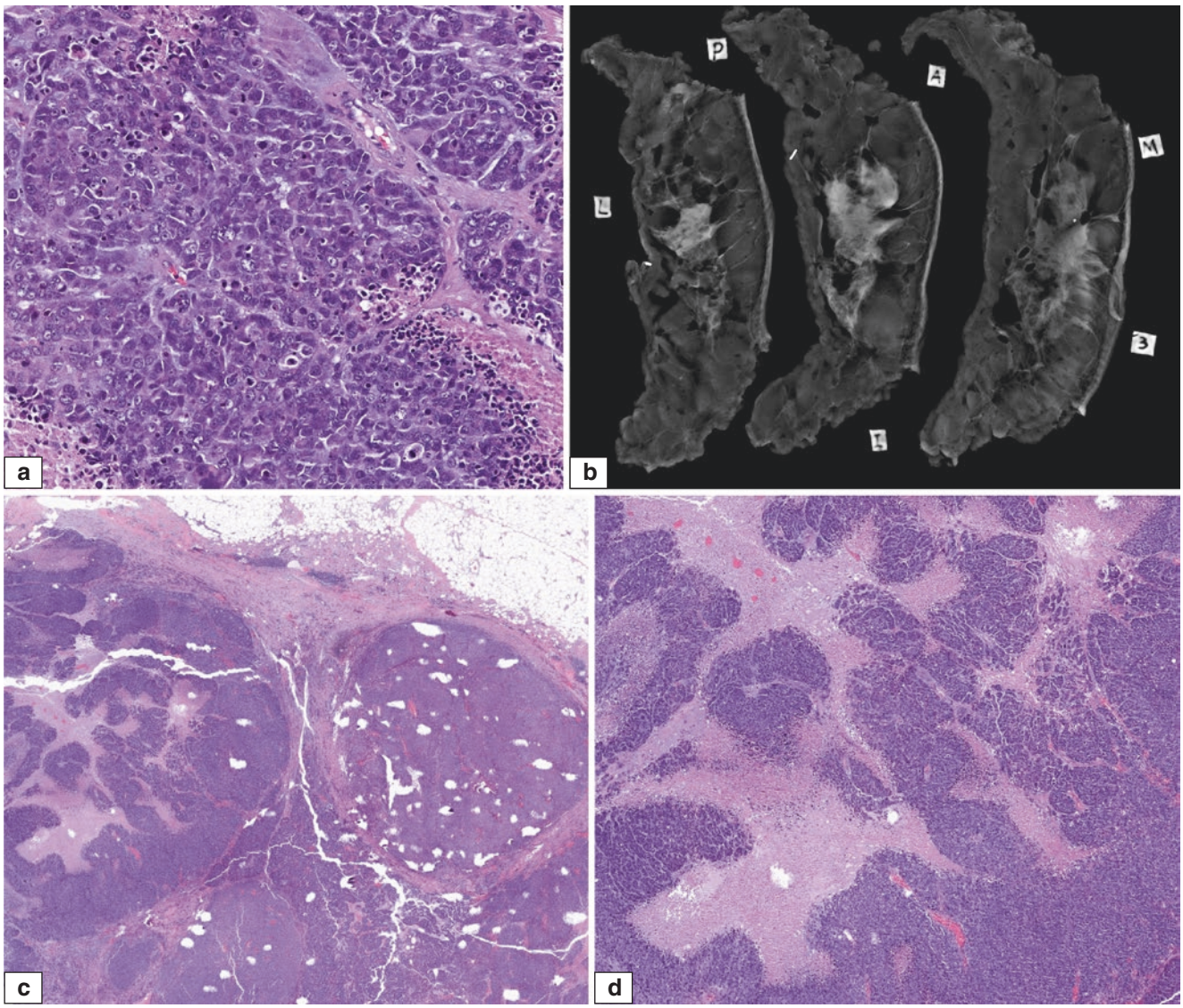

Fig. 15.8 Breast cancer without any response to chemotherapy. (**a**) Core needle biopsy shows solid proliferation of high-grade carcinoma. Tumour cellularity is more than 70%. (**b**) Specimen X-ray of mastectomy shows large tumour with biopsy clip. (**c**, **d**) Histologic sections of tumour after chemotherapy. The tumour cellularity is similar to that of the pre-chemotherapy biopsy (**a**); the presence of geographic necrosis is most likely due to chemotherapy

Histologic Categorisation of Response to Therapy

A number of different classification systems to categorise response to neoadjuvant systemic therapies have been proposed [26–33]. All of these systems recognise two categories: complete pathologic response and no response to therapy. A variable number of categories describing partial levels of response are also recognised. Achievement of complete pathologic response has emerged as an important surrogate end point to determine the efficacy of neoadjuvant systemic therapy and has been correlated with good clinical outcome. Although different definitions of complete pathologic response were used in earlier clinical trials, the current view is that it should now be based on an assessment of residual tumour in both breast and axillary lymph nodes [16, 28]. To define complete pathologic response, all the proposed systems require disappearance of invasive carcinoma in the breast and no metastases in the lymph nodes. The prognostic significance of residual ductal carcinoma in situ (DCIS) after neoadjuvant systemic therapy is controversial. In some categorisation systems, the definition of complete pathologic response includes residual DCIS. Another controversial area is the classification of cases with only lymphovascular tumour emboli (as in Fig. 15.10) with no residual carcinoma in the breast or lymph nodes.

More than ten different classification systems have been proposed, but three systems are currently the most commonly used:

- *Miller–Payne grading* provides five grading categories based on tumour cellularity in the post-neoadjuvant specimen as compared with the pretreatment core biopsy [26].
- *Residual cancer burden* uses size and cellularity of the residual invasive carcinoma, the percentage of residual DCIS, and the tumour burden in lymph nodes (number of lymph nodes with metastases plus the largest size of metastatic carcinoma) to calculate a residual cancer burden index as a continuous score obtained by using a Web calculator; the score is then assigned into one of four classes [30].

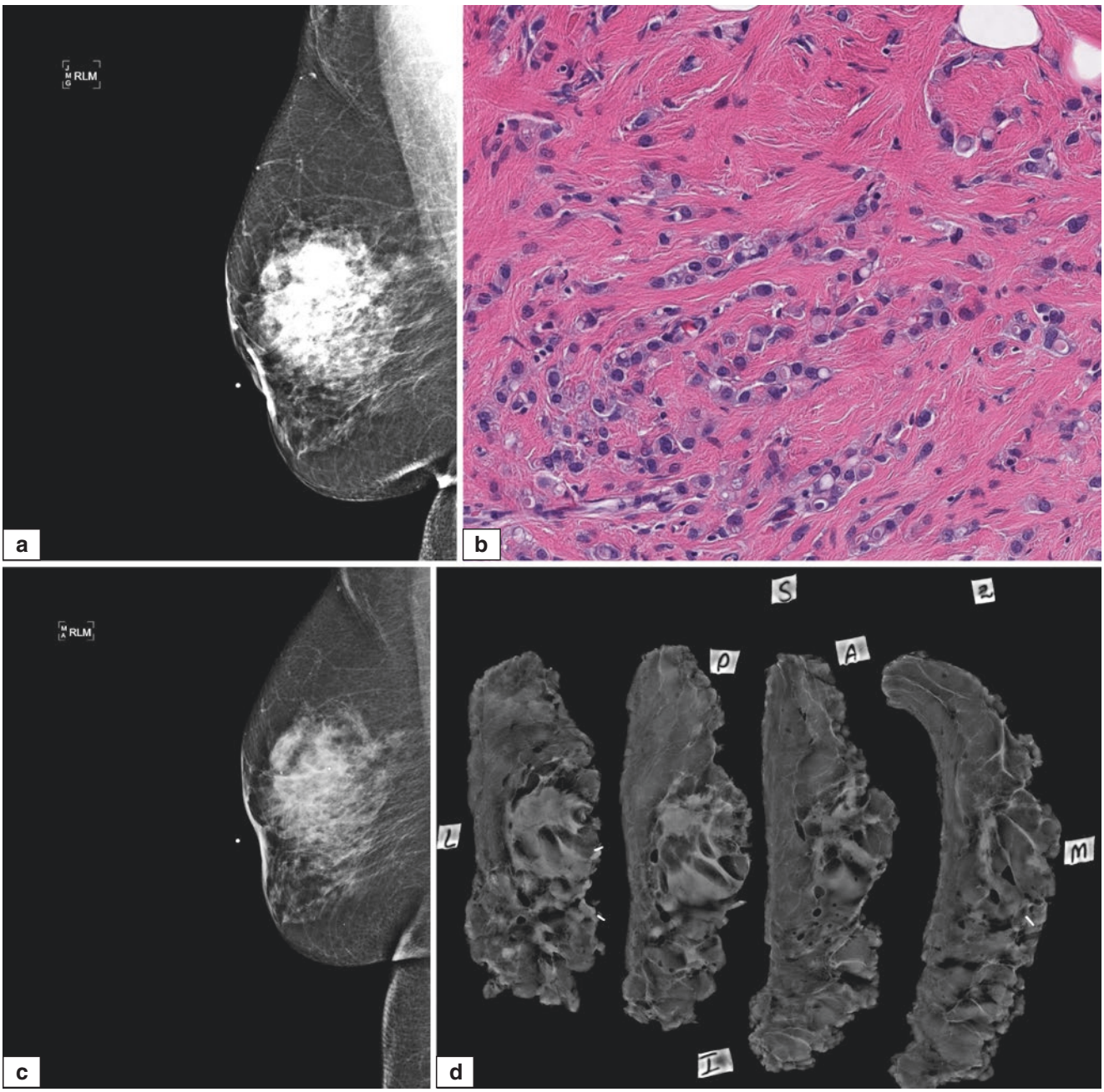

Fig. 15.9 Breast cancer without significant change after chemotherapy. (**a**) Pre-chemotherapy mammogram shows a large, irregular mass in the central portion of the breast. (**b**) Pre-chemotherapy biopsy shows an invasive lobular carcinoma. (**c**) Post-chemotherapy mammogram shows no appreciable change in tumour size. (**d**, **e**) Specimen X-rays of mastectomy slices from the same patient show a well-defined mass involving multiple slices. (**f–j**) H&E-stained histologic sections from different areas of the tumour show invasive lobular carcinoma with varying degrees of cellularity

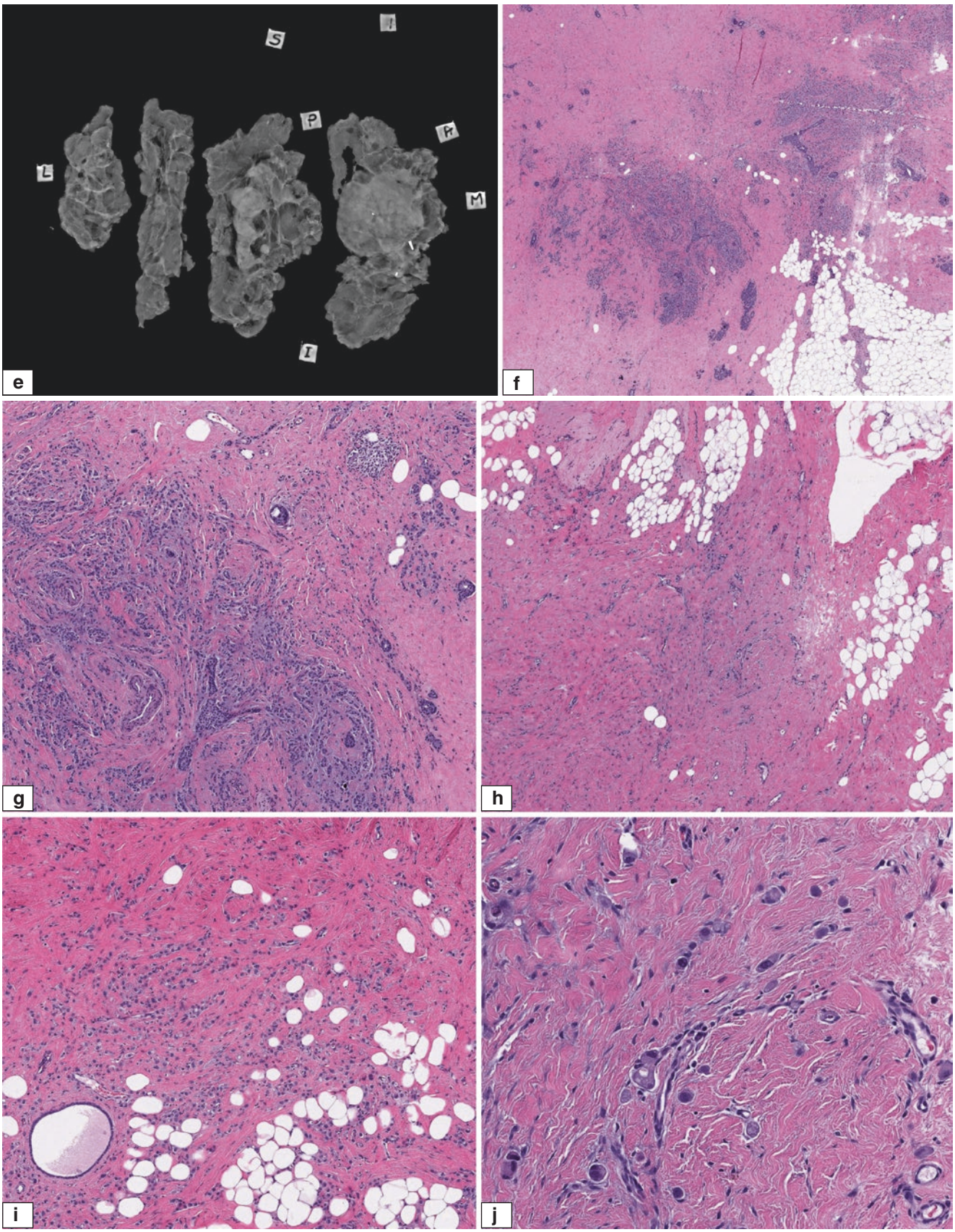

Fig. 15.9 (continued)

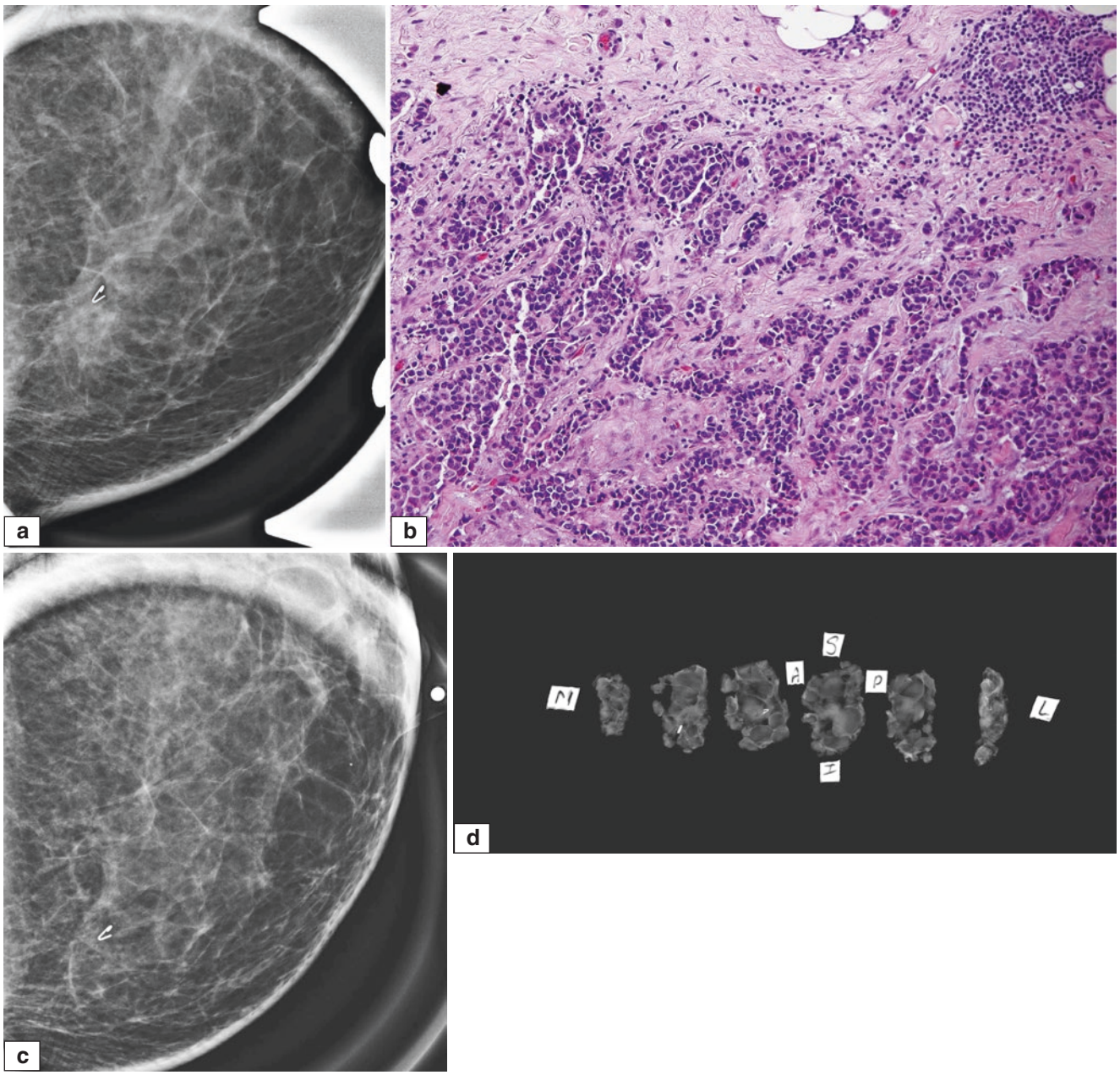

Fig. 15.10 Breast cancer with marked response to chemotherapy. (**a**) Pre-chemotherapy mammogram shows a stellate mass associated with the biopsy clip. (**b**) Needle core biopsy shows an invasive carcinoma with high cellularity. (**c**) Post-chemotherapy mammogram shows a smaller mass associated with the biopsy clip. (**d**) X-ray of segmental resection shows a density associated with the clip. (**e**) H&E-stained histology section shows only scattered residual tumour cells remaining in the fibrous tumour bed which are difficult to spot at this low magnification. (**f**, **g**) Higher magnification of H&E histology sections shows intravascular tumour clusters

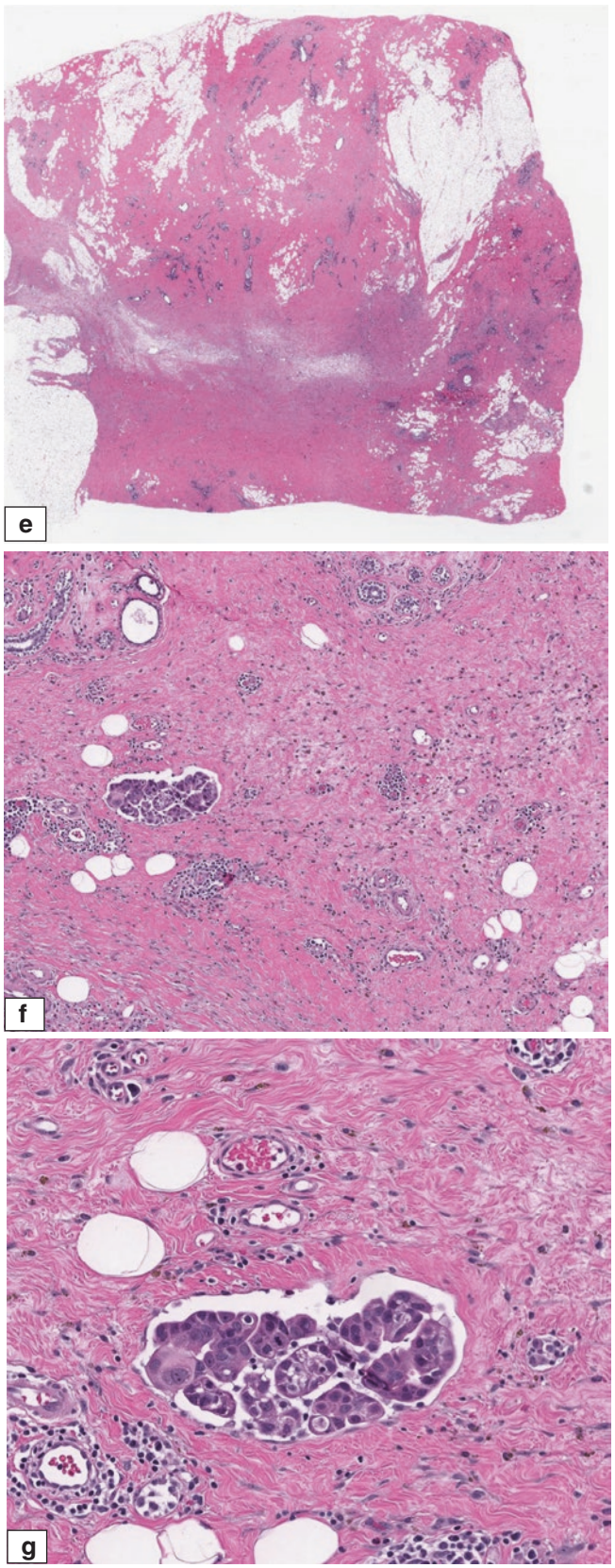

Fig. 15.10 (continued)

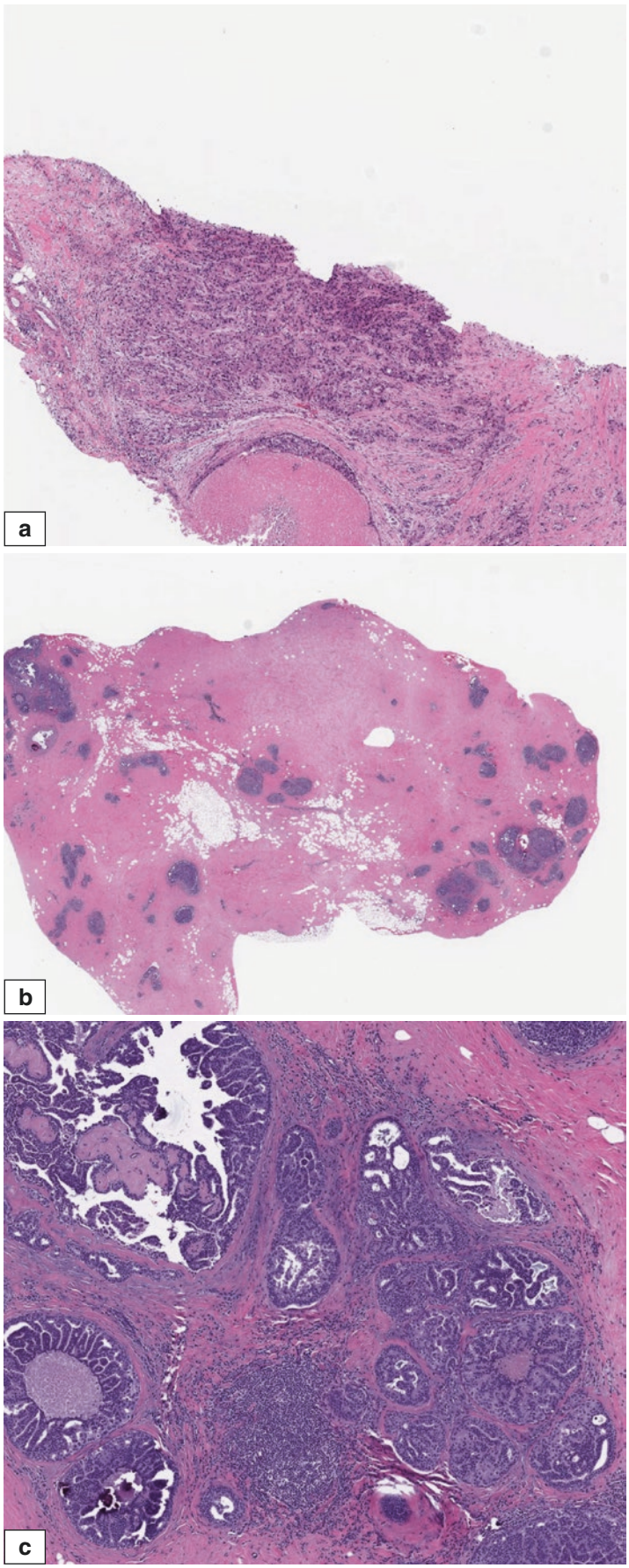

Fig. 15.11 Residual tumour consisting of only DCIS. (**a**) Pretreatment needle core biopsy shows a mixture of invasive and in situ ductal carcinoma. (**b**) Resection after chemotherapy shows dense, fibrous tumour bed with scattered foci of DCIS which are not readily appreciated at this low magnification. (**c**) Higher magnification of DCIS with periductal inflammation and central comedonecrosis

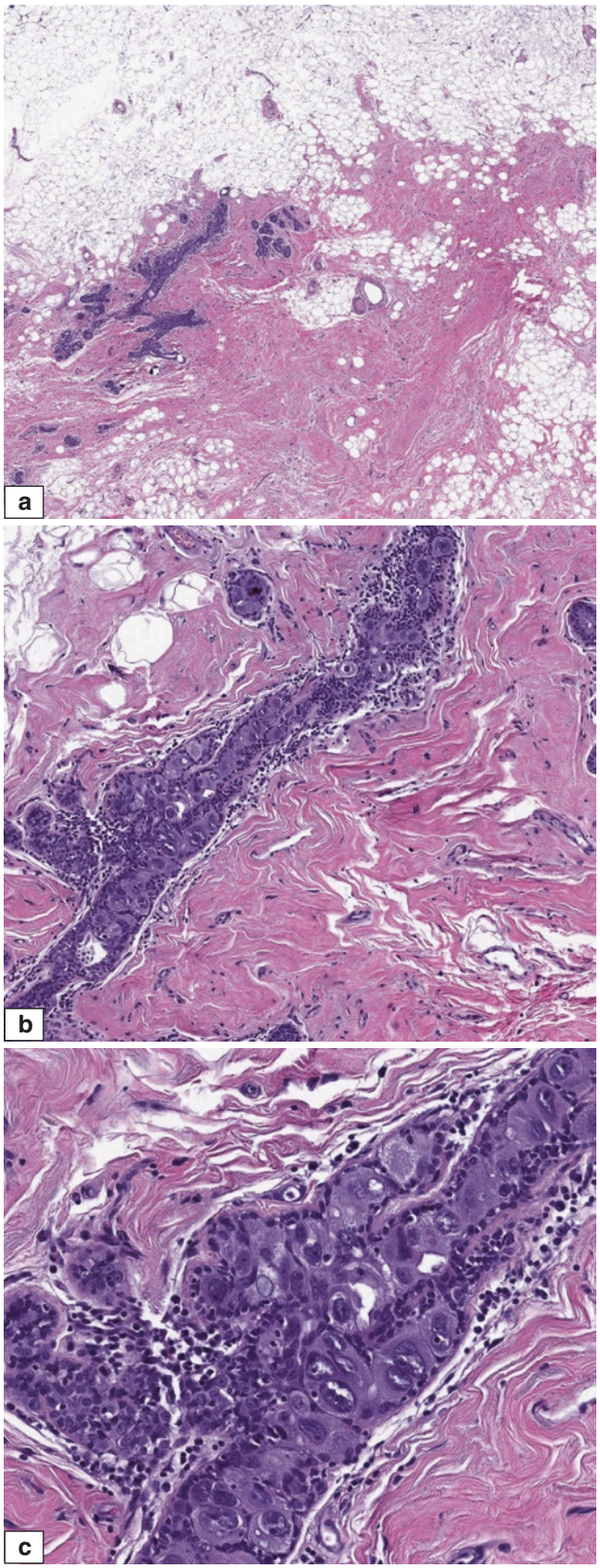

Fig. 15.12 Residual tumour consisting of only DCIS. (**a**–**c**) Series of H&E histologic sections of resection after chemotherapy. The only residual tumour is DCIS in the lobular units. Pleomorphic tumour cells are seen within the duct and ductules. The degree of nuclear atypia may be exaggerated by the chemotherapy

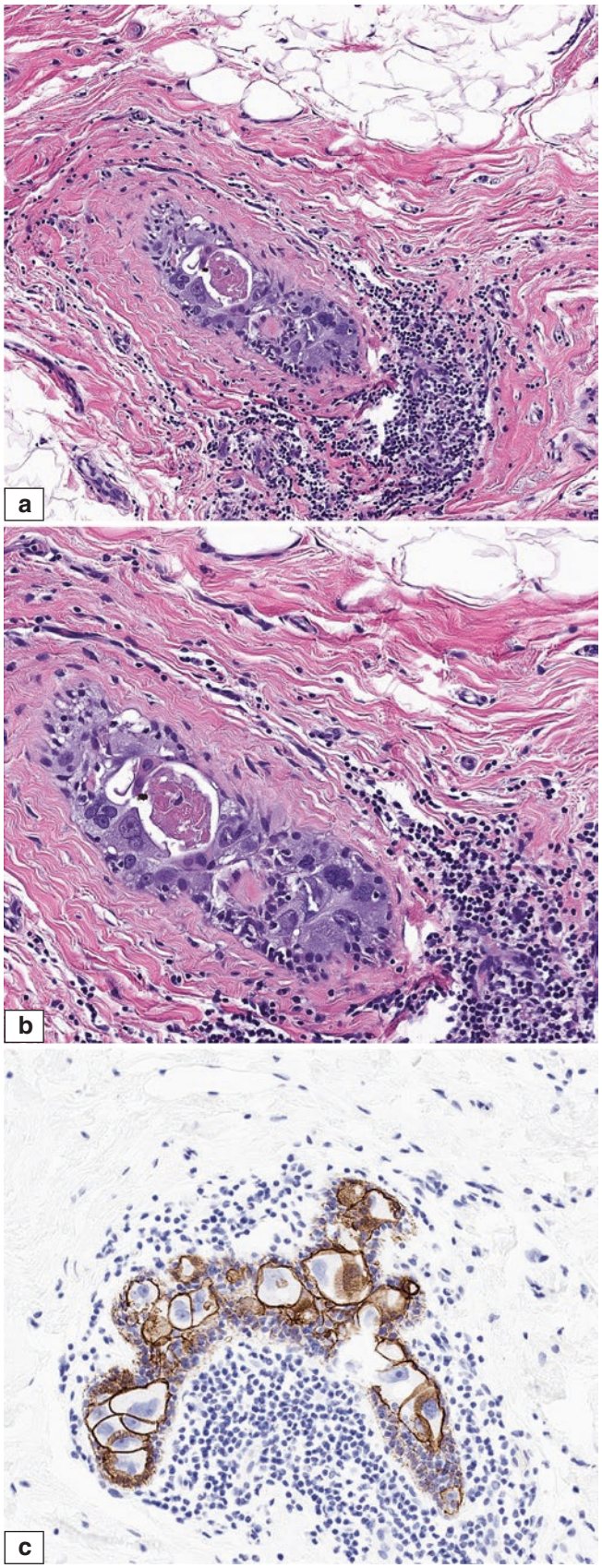

Fig. 15.13 Residual tumour consisting of only DCIS. (**a**–**c**) H&E-stained histologic sections of resection after chemotherapy. Scattered atypical cells may be difficult to identify on lower magnification of H&E sections. In c-erbB-2-positive tumours, immunohistochemistry can be helpful to delineate tumour cells (**c**)

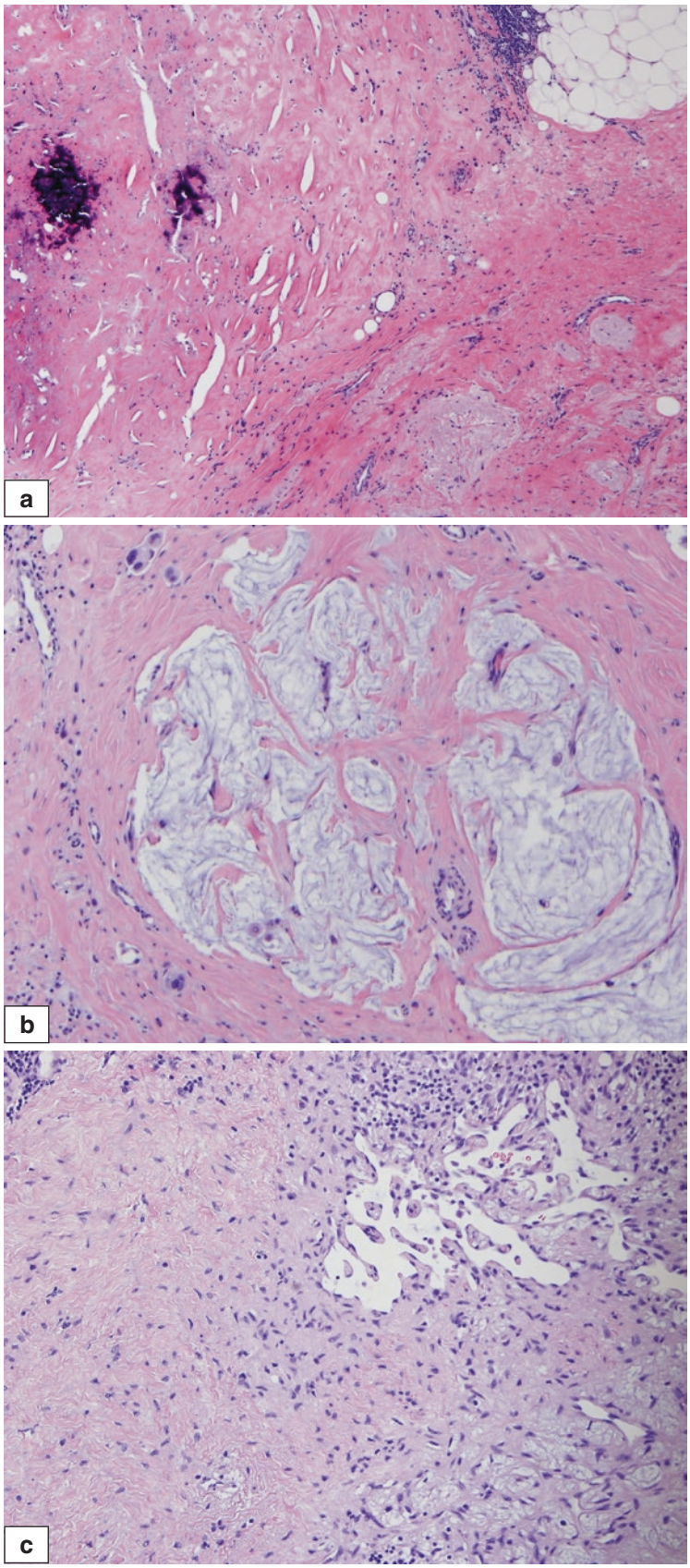

Fig. 15.14 Post-chemotherapy stromal changes. (**a**) Dense stromal fibrosis associated with areas of microcalcification. (**b**) Areas of mucin pools can be seen after chemotherapy. (**c**) Pseudopapillary vascular changes seen after therapy

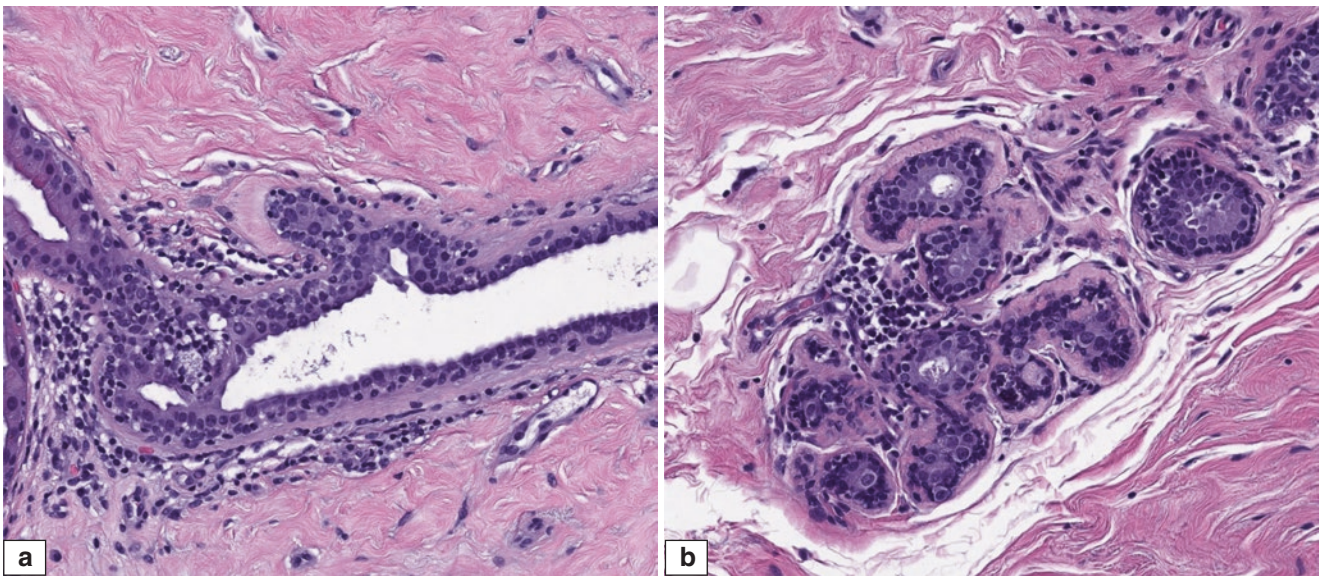

Fig. 15.15 Chemotherapy effect on normal breast epithelium. Cytologic atypia characterised by nuclear enlargement and hyperchromasia can be seen in both ductal (**a**) and lobular (**b**) epithelium

- *Residual disease in the breast and nodes* (modification of the Nottingham Prognostic Index) uses a formula that takes into account tumour size, lymph node stage, and histologic grade after therapy to determine four levels of response [33].

All these systems have been shown to have prognostic significance in certain subsets of patients, but none of them has proved to be superior in predicting clinical outcomes in all subcategories of breast cancer. Communication among multidisciplinary breast cancer team members is the most important factor in deciding which system is most appropriate for their specific type of clinical practice [17].

Histologic Evaluation of Lymph Nodes After Neoadjuvant Therapy

Neoadjuvant therapy affects nodal metastases in a similar manner as the primary tumour. Lymph node metastases may completely disappear after therapy and may show a partial response or no response at all (Figs. 15.16 and 15.17) [34, 35].

Histological appearance of the lymph nodes depends on the size and growth pattern of the metastatic tumour. If the metastatic carcinoma was a solid nodular tumour and showed a complete pathologic response, the node may disclose a large area of fibrosis associated with lymphohistiocytic infiltrate. If the metastatic carcinoma had a more sinusoidal growth pattern, the lymph node architecture may not be altered after therapy or the only evidence of the residual tumour may be a small focus of scarring.

Similar to non-treated breast cancer, the number of positive lymph nodes after therapy is one of the most important prognostic parameters [35]. Any residual tumour cell aggregate, including isolated tumour cells, excludes pathologic complete response. Immunohistochemical staining for cytokeratin is useful in delineating metastatic tumour cells in selected cases where the H&E sections show suspicious cells. Since nodal tumour burden is associated with clinical outcome, the size of the metastasis should be reported in addition to the number of lymph nodes with metastatic carcinoma [36].

Changes Related to Radiation Therapy

The breast may be exposed to radiation therapy either as the primary target of a multidisciplinary therapy protocol or it may be within the radiation field of treatment for other tumours, most commonly mediastinal neoplasms. The radiation effect is the same in both situations, and the extent of changes within the breast varies based on the radiation type, the dosage, and the elapsed time post-radiation as well as individual patient characteristics.

Breast parenchyma may show significant changes due to radiation therapy [37]. It is important to be familiar with the histologic effects as they may mimic neoplastic changes. Radiation effect can be seen in both stromal and epithelial cells (Fig. 15.18). These changes may include the following: collagenisation of intralobular stroma, atrophy of terminal ductal lobular units, thickening of basement membranes, nuclear enlargement, and atypia in stromal fibroblasts and epithelium, all of which can be seen in varying degrees or in combination. Recognition of epithelial atypia as radiation effect in contrast to the possibility of a recurrent tumour is an important differential diagnosis for patients subjected to breast-conserving therapy with adjuvant radiation.

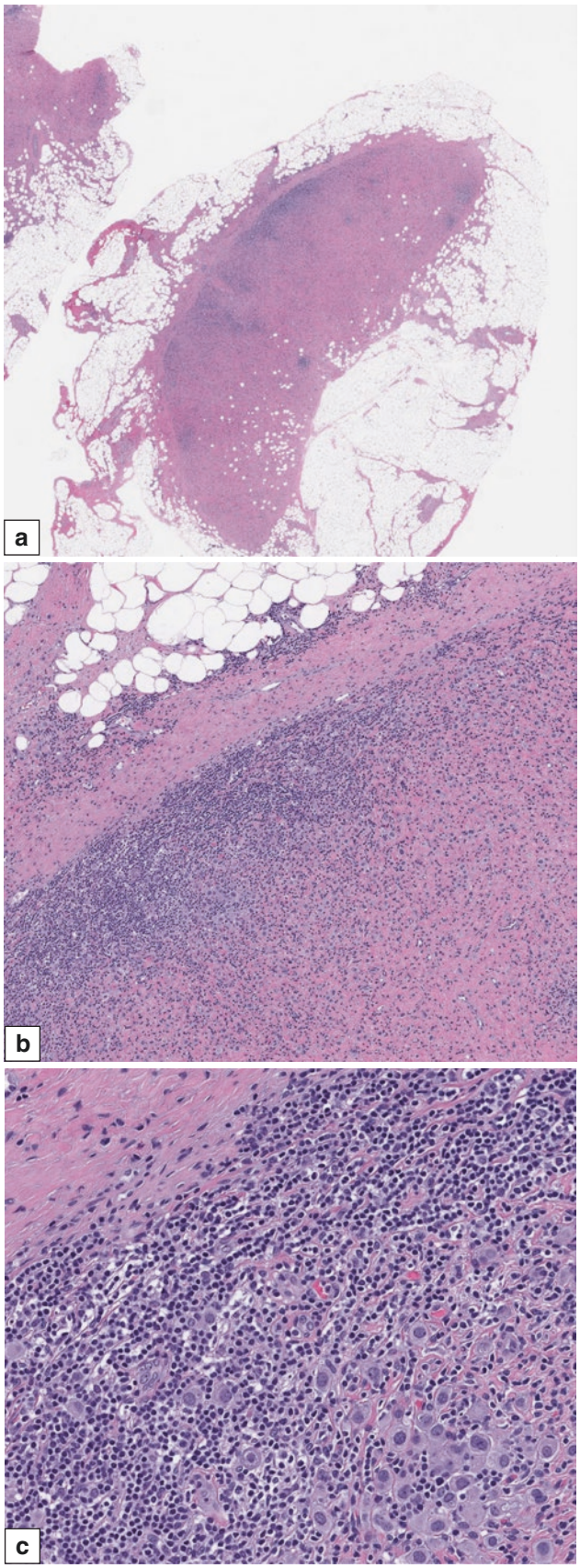

Fig. 15.16 Post-therapy changes in lymph node metastases. (**a**, **b**) Lymph node metastasis of breast cancer after therapy. The lymph node surface is almost completely replaced by metastatic carcinoma with only focal residual lymphoid tissue. (**c**) Higher magnification of (**a**, **b**) shows metastatic carcinoma cells admixed with lymphoid cells

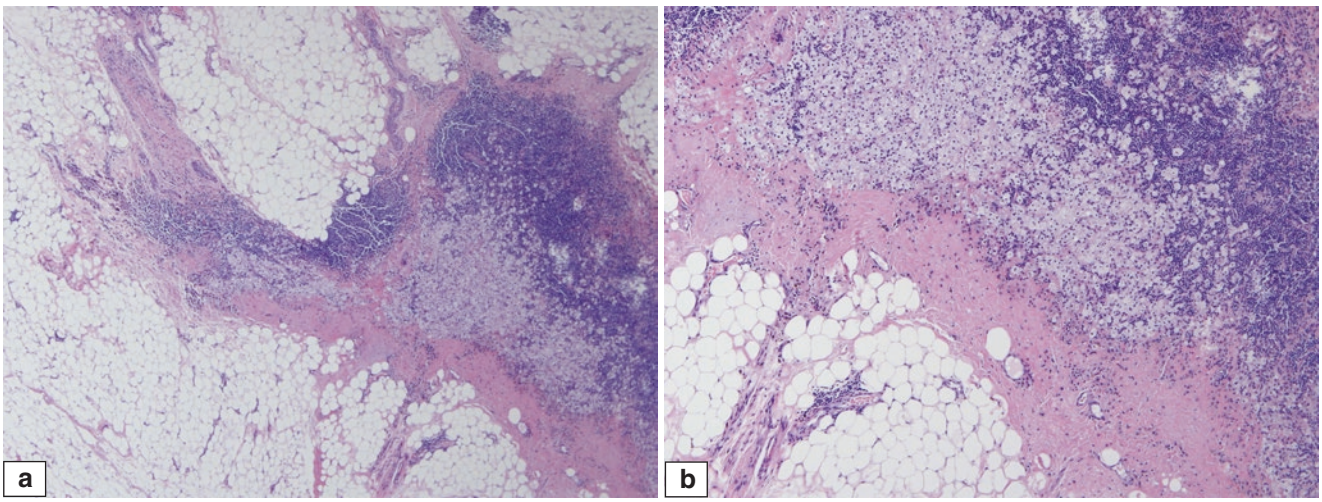

Fig. 15.17 Post-therapy changes in lymph node metastases. (**a**, **b**) Lymph node shows partial replacement by histiocytes without any residual tumour. This focus most likely represents an area of tumour with complete response

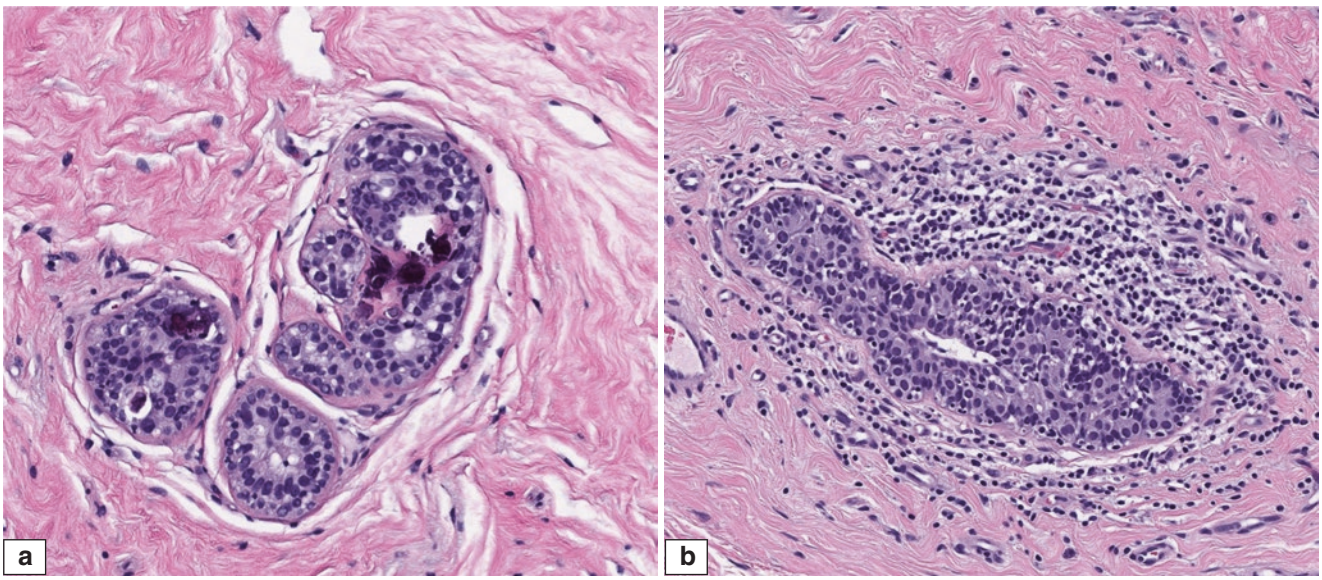

Fig. 15.18 Radiation atypia. (**a**) Microcalcifications in the lobular unit including scattered cells with large nuclei and abundant cytoplasm. Based on nuclear enlargement, in situ carcinoma is a consideration; however, this patient had been through 8 months' post-radiation therapy. The focal nature of the nuclear changes and low nuclear-to-cytoplasmic ratio favour radiation atypia. (**b**) Radiation atypia associated with periductal inflammation

Radiation-induced epithelial atypia in ductal and lobular epithelium can be distinguished from recurrent carcinoma based on a lack of proliferative changes. Radiation atypia usually involves atrophic appearing ductal lobular units and presents as single cells showing nuclear and cytoplasmic enlargement. Cytoplasmic vacuolisation and lack of mitotic activity are also characteristic features of radiation atypia.

All of the listed changes are not specific for radiation but can be observed with chemotherapy. Therefore, instead of diagnosing chemotherapy or radiation therapy changes, our recommendation is to use the term "therapy-related changes".

References

1. Untch M, Konecny GE, Paepke S, von Minckwitz G. Current and future role of neoadjuvant therapy for breast cancer. Breast. 2014;23:526–37.

2. Holmes D, Colfry A, Czerniecki B, Dickson-Witmer D, Francisco Espinel C, Feldman E, et al. Performance and practice guideline for the use of neoadjuvant systemic therapy in the management of breast cancer. Ann Surg Oncol. 2015;22:3184–90.
3. Petrelli F, Cabiddu M, Coinu A, Borgonovo K, Ghilardi M, Lonati V, Barni S. Adjuvant dose-dense chemotherapy in breast cancer: a systematic review and meta-analysis of randomized trials. Breast Cancer Res Treat. 2015;151:251–9.
4. Kaufmann M, von Minckwitz G, Mamounas EP, Cameron D, Carey LA, Cristofanilli M, et al. Recommendations from an international consensus conference on the current status and future of neoadjuvant systemic therapy in primary breast cancer. Ann Surg Oncol. 2012;19:1508–16.
5. Santa-Maria CA, Camp M, Cimino-Mathews A, Harvey S, Wright J, Stearns V. Neoadjuvant therapy for early-stage breast cancer: current practice, controversies, and future directions. Oncology (Williston Park). 2015;29:828–38.
6. Cortazar P, Geyer Jr CE. Pathological complete response in neoadjuvant treatment of breast cancer. Ann Surg Oncol. 2015;22:1441–6.
7. Berruti A, Amoroso V, Gallo F, Bertaglia V, Simoncini E, Pedersini R, et al. Pathologic complete response as a potential surrogate for the clinical outcome in patients with breast cancer after neoadjuvant therapy: a metaregression of 29 randomized prospective studies. J Clin Oncol. 2014;32:3883–91.
8. US Department of Health and Human Services, Food and Drug Administration, Center for Drug Evaluation and Research (CDER). Guidance for industry: pathological complete response in neoadjuvant treatment of high-risk early-stage breast cancer: use as an endpoint to support accelerated approval. 2014.
9. Gradishar WJ, Anderson BO, Balassanian R, Blair SL, Burstein HJ, Cyr A, et al. Invasive breast cancer version 1.2016, NCCN clinical practice guidelines in oncology. J Natl Compr Canc Netw. 2016;14:324–54.
10. Lee CH, Dershaw DD, Kopans D, Evans P, Monsees B, Monticciolo D, et al. Breast cancer screening with imaging: recommendations from the Society of Breast Imaging and the ACR on the use of mammography, breast MRI, breast ultrasound, and other technologies for the detection of clinically occult breast cancer. J Am Coll Radiol. 2010;7:18–27.
11. Dialani V, Chadashvili T, Slanetz PJ. Role of imaging in neoadjuvant therapy for breast cancer. Ann Surg Oncol. 2015;22:1416–24.
12. Feng Y, Huang R, He Y, Lu A, Fan Z, Fan T, et al. Efficacy of physical examination, ultrasound, and ultrasound combined with fine-needle aspiration for axilla staging of primary breast cancer. Breast Cancer Res Treat. 2015;149:761–5.
13. El Hage CH, Headon H, Kasem A, Mokbel K. Refining the performance of sentinel lymph node biopsy post-neoadjuvant chemotherapy in patients with pathologically proven pre-treatment node-positive breast cancer: an update for clinical practice. Anticancer Res. 2016;36:1461–71.
14. Buchholz TA, Mittendorf EA, Hunt KK. Surgical considerations after neoadjuvant chemotherapy: breast conservation therapy. J Natl Cancer Inst Monogr. 2015;51:11–4.
15. Caudle AS, Cupp JA, Kuerer HM. Management of axillary disease. Surg Oncol Clin N Am. 2014;23:473–86.
16. Bossuyt V, Provenzano E, Symmans WF, Boughey JC, Coles C, Curigliano G, et al.; Breast International Group–North American Breast Cancer Group (BIG-NABCG) collaboration. Recommendations for standardized pathological characterization of residual disease for neoadjuvant clinical trials of breast cancer by the BIG-NABCG collaboration. Ann Oncol. 2015;26:1280–91.
17. Provenzano E, Bossuyt V, Viale G, Cameron D, Badve S, Denkert C, et al.; Residual Disease Characterization Working Group of the Breast International Group–North American Breast Cancer Group Collaboration. Standardization of pathologic evaluation and reporting of postneoadjuvant specimens in clinical trials of breast cancer: recommendations from an international working group. Mod Pathol. 2015;28:1185–201.
18. Sahoo S, Dabbs DJ, Bhargawa R. Pathology of neoadjuvant therapeutic response of breast carcinoma. In: Dabbs DJ, editor. Breast pathology. Philadelphia: Elsevier Saunders; 2014. p. 519–35.
19. Leyland-Jones BR, Ambrosone CB, Bartlett J, Ellis MJ, Enos RA, Raji A, et al. Recommendations for collection and handling of specimens from group breast cancer clinical trials. J Clin Oncol. 2008;26:5638–44.
20. Carey LA, Metzger R, Dees EC, Collichio F, Sartor CI, Ollila DW, et al. American Joint Committee on Cancer tumour-node-metastasis stage after neoadjuvant chemotherapy and breast cancer outcome. J Natl Cancer Inst. 2005;97:1137–42.
21. College of American Pathologists. Protocol for the examination of specimens from patients with invasive carcinoma of the breast. 2012. http://www.cap.org/apps/docs/committees/cancer/cancer_protocols/2012/BreastInvasive_12protocol_3100.pdf. Accessed 29 July 2016.
22. Keam B, Im SA, Lim Y, Han SW, Moon HG, Oh DY, et al. Clinical usefulness of AJCC response criteria for neoadjuvant chemotherapy in breast cancer. Ann Surg Oncol. 2013;20:2242–9.
23. Pinder SE, Provenzano E, Earl H, Ellis IO. Laboratory handling and histology reporting of breast specimens from patients who have received neoadjuvant chemotherapy. Histopathology. 2007;50:409–17.
24. Fisher ER, Wang J, Bryant J, Fisher B, Mamounas E, Wolmark N. Pathobiology of preoperative chemotherapy: findings from the National Surgical Adjuvant Breast and Bowel (NSABP) protocol B-18. Cancer. 2002;95:681–95.
25. Sahoo S, Lester SC. Pathology of breast carcinomas after neoadjuvant chemotherapy: an overview with recommendations on specimen processing and reporting. Arch Pathol Lab Med. 2009;133:633–42.
26. Chevallier B, Roche H, Olivier JP, Chollet P, Hurteloup P. Inflammatory breast cancer. Pilot study of intensive induction chemotherapy (FEC-HD) results in a high histologic response rate. Am J Clin Oncol. 1993;16:223–8.
27. Kuroi K, Toi M, Tsuda H, Kurosumi M, Akiyama F. Issues in the assessment of the pathologic effect of primary systemic therapy for breast cancer. Breast Cancer. 2006;13:38–48.
28. Chollet P, Abrial C, Durando X, Thivat E, Tacca O, Mouret-Reynier MA, et al. A new prognostic classification after primary chemotherapy for breast cancer: residual disease in breast and nodes (RDBN). Cancer J. 2008;14:128–32.
29. Sataloff DM, Mason BA, Prestipino AJ, Seinige UL, Lieber CP, Baloch Z. Pathologic response to induction chemotherapy in locally advanced carcinoma of the breast: a determinant of outcome. J Am Coll Surg. 1995;180:297–306.
30. Residual cancer burden calculator. University of Texas MD Anderson Cancer Center, Houston. 2016. http://www3.mdanderson.org/app/medcalc/index.cfm?pagename=jsconvert3. Accessed 30 July 2016.
31. Penault-Llorca F, Abrial C, Raoelfils I, Cayre A, Mouret-Reynier MA, Leheurteur M, et al. Comparison of the prognostic significance of Chevallier and Sataloff's pathologic classifications after neoadjuvant chemotherapy of operable breast cancer. Hum Pathol. 2008;39:1221–8.
32. Ogston KN, Miller ID, Payne S, Hutcheon AW, Sarkar TK, Smith I, et al. A new histological grading system to assess response of breast cancers to primary chemotherapy: prognostic significance and survival. Breast. 2003;12:320–7.
33. Abdel-Fatah TM, Ball G, Lee AH, Pinder S, MacMilan RD, Cornford E, et al. Nottingham Clinico-Pathological Response Index (NPRI) after neoadjuvant chemotherapy (Neo-ACT) accurately predicts clinical outcome in locally advanced breast cancer. Clin Cancer Res. 2015;21:1052–62.

34. Hennessy BT, Hortobagyi GN, Rouzier R, Kuerer H, Sneige N, Buzdar AU, et al. Outcome after pathologic complete eradication of cytologically proven breast cancer axillary node metastases following primary chemotherapy. J Clin Oncol. 2005;23:9304–11.
35. Neuman H, Carey LA, Ollila DW, Livasy C, Calvo BF, Meyer AA, et al. Axillary lymph node count is lower after neoadjuvant chemotherapy. Am J Surg. 2006;191:827–9.
36. Boughey JC, Donohue JH, Jakub JW, Lohse CM, Degnim AC. Number of lymph nodes identified at axillary dissection: effect of neoadjuvant chemotherapy and other factors. Cancer. 2010;116:3322–9.
37. Schnitt SJ, Connolly JL, Harris JR, Cohen RB. Radiation-induced changes in the breast. Hum Pathol. 1984;15:545–50.

Index

P.H. Tan, A.A. Sahin, *Atlas of Differential Diagnosis in Breast Pathology*, Atlas of Anatomic Pathology,
DOI 10.1007/978-1-4939-6697-4